# 8th IAHR EUROPE CONGRESS



## WATER - ACROSS BOUNDARIES

## JUNE 4-7, 2024

## LISBON - PORTUGAL

LNEC - Laboratório Nacional de Engenharia Civil

Editors
Ana Mendonça, Jorge Matos

ISBN 978-972-49-2330-7

IAHR International Association for Hydro-Environment Engineering and Research
Hosted by Spain Water and IWHR, China

Organized by:
LNEC LABORATÓRIO NACIONAL DE ENGENHARIA CIVIL

# Book of Abstracts

## SPONSORS

## SUPPORTERS

# 8th IAHR EUROPE CONGRESS

## WATER - ACROSS BOUNDARIES

## JUNE
4-7, 2024

LISBON - PORTUGAL

LNEC - Laboratório Nacional de Engenharia Civil

IAHR International Association for Hydro-Environment Engineering and Research
Hosted by Spain Water and IWHR, China

Organized by:
LNEC LABORATÓRIO NACIONAL DE ENGENHARIA CIVIL

**Editors**
**Ana Mendonça, Jorge Matos**

# Book of Abstracts

**Legal Notice**
The scientific quality and content of the papers published herein are of the entire responsibility of their authors.
Therefore, the publisher accepts no responsibility or liability whatsoever with regard to the information contained in this publication.
The total or partial reproduction, and any representation of the substantial or partial content of the present publication, by any process or means whatsoever, including copy or transfer, without the express consent of the publisher, is prohibited and constitutes an infringement sanctioned by the Law.

Copyright © LABORATÓRIO NACIONAL DE ENGENHARIA CIVIL, I. P.
Divisão de Divulgação Científica e Técnica
AV DO BRASIL 101 • 1700-066 LISBOA
e-mail: livraria@lnec.pt
www.lnec.pt

Publisher: LNEC

Collection: National and international Meetings

Series: RNI 117

1st. edition: 2024 (pdf)

Descriptors: Water resources management / Hydraulic engineering / Congress
Descritores: Gestão de recursos hídricos / Engenharia hidráulica / Congresso

CDU 626/628.1(063)(4)
ISBN 978-972-49-2330-7
DOI 10.34638/jv1h-bs60

# PREFACE

The 8th Europe Congress of IAHR (International Association for Hydro-Environment Engineering and Research) was held in Lisbon, Portugal, from 4 to 7 June 2024.

The Congress was organised by the IAHR Europe Division and the National Laboratory for Civil Engineering (LNEC), which hosted the conference, together with the Instituto Superior Técnico - University of Lisbon, the Faculty of Engineering - University of Porto and the Lisbon City Council. It was supported by more than 15 sponsors from across the water engineering community.

Under the main theme "Water - Across Boundaries", this edition of the Congress in Lisbon focused on the importance of sharing research, technology and innovation to address unprecedented water challenges and to promote sustainable water engineering. Business as usual practices are no longer tenable. Bringing about the necessary changes is a shared responsibility.

After the review process, over 350 extended abstracts have been accepted for the regular scientific programme of the Congress according to the following themes:

Theme A: Aquifers, rivers, reservoirs and dams

Theme B: Estuaries, coasts and ports

Theme C: Urban water

Theme D: Numerical and experimental methods

Theme E: Climate change and risk mitigation

Theme F: Governance and water resources management

The programme also included four keynote lectures, four master classes, ten special sessions and three technical visits.

On behalf of the organisers of the 8th Europe Congress of IAHR, we would like to thank the speakers and delegates, the members of the Scientific and Organising Committees, the sessions chairs, the conveners of the Master Classes and Special Sessions, as well as the colleagues and volunteers from all the involved institutions.

Helena Alegre
Chair of the Organising Committee
National Laboratory for Civil Engineering (LNEC), Portugal

# COMMITTEES

## Local Organising Committee

**Chair**

Helena Alegre, National Laboratory for Civil Engineering (LNEC), Portugal

**Co-Chairs**

Jorge Matos, Instituto Superior Técnico, University of Lisbon, Portugal
Francisco Taveira Pinto, Faculty of Engineering, University of Porto, Portugal

Ana Mendonça, LNEC, Portugal
Conceição Juana Fortes, LNEC, Portugal
Elsa Alves, LNEC, Portugal
Gonçalo Jesus, LNEC, Portugal
João Fernandes, LNEC, Portugal
Liliana Pinheiro, LNEC, Portugal
Luís Portela, LNEC, Portugal
Maria do Céu Almeida, LNEC, Portugal
Marta Rodrigues, LNEC, Portugal
Rui Capitão, LNEC, Portugal
Teresa Viseu, LNEC, Portugal
Maria João Telhado, Câmara Municipal de Lisboa, Portugal
Pedro Teixeira, Câmara Municipal de Lisboa, Portugal
Elsa Incio, IAHR, Spain

## International Scientific Committee

**Chair**
Jorge **Matos**, Instituto Superior Técnico, University of Lisbon, Portugal

Jochen **Aberle**, Technische Universität Braunschweig, Germany
Soroush **Abolfathi**, University of Warwick, United Kingdom
Claudia **Adduce**, Roma Tre University, Italy
Reza **Ahmadian**, Cardiff University, United Kingdom
Helena **Alegre**, LNEC, Portugal
Maria do Céu **Almeida**, LNEC, Portugal
Elsa **Alves**, LNEC, Portugal
Umberto **Andriolo**, University of Coimbra, Portugal
Alberto **Azevedo**, LNEC, Portugal
Behnam **Balouchi**, Norwegian University of Science and Technology, Norway
Robert **Boes**, ETH Zurich, Switzerland
Elena **Bresci**, University of Firenze, Italy
Maurizio **Brocchini**, Marche Polytechnic University, Italy
Daniel **Bung**, FH Aachen, University of Applied Sciences, Germany
António Heleno **Cardoso**, Instituto Superior Técnico, University of Lisbon, Portugal
José Maria **Carrillo**, Polytechnic University of Cartagena, Spain
Rita **Carvalho**, University of Coimbra, Portugal
Margaret **Chen**, Vrije Universiteit Brussel, Belgium
Ricardo **Cobacho**, Polytechnic University of Valencia, Spain
Carlos **Coelho**, University of Aveiro, Portugal
Florian **Cordier**, EDF R&D LNHE, France
Dídia **Covas**, Instituto Superior Técnico, University of Lisbon, Portugal
Maria da Conceição **Cunha**, Fac. of Science and Technology, Univ. of Coimbra, Portugal
Alan **Cuthbertson**, University of Dundee, United Kingdom
Felice **D'Alessandro**, University of Milan, Italy
Karin de **Bruijn**, Deltares, Delft, Netherlands
Cristiana **Di Cristo**, University of Naples Federico II, Italy
Tomasz **Dysarz**, Poznan University of Life Sciences, Poland
Olivier **Eiff**, Karlsruhe Institute of Technology, Germany
Kamal **El Kadi Abderrezzak**, EDF R&D LNHE, France
Sébastien **Erpicum**, University of Liege, Belgium
Eva **Fenrich**, SystainAbility, Germany
João **Fernandes**, LNEC, Portugal
Tiago **Ferradosa**, Faculty of Engineering, University of Porto, Portugal
David **Ferras**, IHE Delft, Netherlands
Óscar **Ferreira**, University of Algarve, Portugal
Rui **Ferreira**, Instituto Superior Técnico, University of Lisbon, Portugal
Carles **Ferrere-Boix**, Technical University of Catalonia, Spain
Conceição Juana **Fortes**, LNEC, Portugal
Mário **Franca**, Karlsruhe Institute of Technology, Germany
Gabriele **Freni**, University of Enna Kore, Italy
Carlos **Galvão**, Federal University of Campina Grande, Brazil
Pilar **Garcia Navarro**, University of Zaragoza, Spain

Luis **Garrote**, Universidad Politécnica de Madrid, Spain
Carla **Gomes**, Institute of Social Sciences of the University of Lisbon, Portugal
Philippe **Gourbesville**, Polytech Nice Sophia, University of Côte d'Azur, France
Massimo **Greco**, University of Napoli Federico II, Italy
Stefan **Haun**, University of Stuttgart, Germany
Valentin **Heller**, University of Nottingham, United Kingdom
Gonçalo **Jesus**, LNEC, Portugal
Manfred **Kleidorfer**, University Innsbruck, Austria
Katinka **Koll**, TU Braunschweig, Germany
Elpida **Kolokytha**, Aristotle University of Thessaloniki, Greece
Javier **Lara**, University of Cantabria, Spain
João P. **Leitão**, Swiss Federal Institute of Aquatic Science and Technology, Switzerland
Teresa **Leitão**, LNEC, Portugal
Angelo **Leopardi**, University of Cassino and Southern Lazio, Italy
Qiuhua **Liang**, Loughborough University, United Kingdom
João Pedroso de **Lima**, Faculty of Science and Technology, Univ. of Coimbra, Portugal
Anna **Łoboda**, University of Twente, the Netherlands
Amparo **López Jiménez**, Polytechnic University of Valencia, Spain
Dália **Loureiro**, LNEC, Portugal
José Alfeu Sá **Marques**, Faculty of Science and Technology, Univ. of Coimbra, Portugal
Francisco **Martinez-Capel**, Polytechnic University of Valencia, Spain
José Pedro **Matos**, Instituto Superior Técnico, University of Lisbon, Portugal
José Saldanha **Matos**, Instituto Superior Técnico, University of Lisbon, Portugal
Aonghus **McNabola**, Trinity College Dublin, Ireland
Inês **Meireles**, University of Aveiro, Portugal
José Falcão de **Melo**, LNEC, Portugal
Ana **Mendonça**, LNEC, Portugal
Silvia **Meniconi**, University of Perugia, Italy
Antonio **Miglio**, Consultant Engineer, Italy
Daniela **Molinari**, Polytechnic University of Milan, Italy
Michele **Mossa**, Polytechnic University of Bari, Italy
Mohaddeseh Mousavi **Nezhad**, University of Warwick, United Kingdom
Claudio **Neves**, Federal University of Rio de Janeiro, Brazil
Maria da Graça **Neves**, Nova School of Science and Technology, Portugal
Vladimir **Nikora**, University of Aberdeen, United Kingdom
Juliana **Nóbrega**, Federal University of Goiás, Brazil
Michael **Nones**, Institute of Geophysics, Poland
Francisco **Núñez-González**, Polytechnic University of Catalonia, Spain
Indiana A. **Olbert**, University of Galway, Ireland
Rodrigo Proença de **Oliveira**, Instituto Superior Técnico, University of Lisbon, Portugal
Miguel **Ortega-Sánchez**, University of Granada, Spain
Modesto **Pérez-Sánchez**, Polytechnic University of Valencia, Spain
António **Pinheiro**, Instituto Superior Técnico, University of Lisbon, Portugal
Liliana **Pinheiro**, LNEC, Portugal
Dubravka **Pokrajac**, University of Aberdeen, United Kingdom
Cristiano **Poleto**, Federal University of Rio Grande do Sul, Brazil
Maria Manuela **Portela**, Instituto Superior Técnico, University of Lisbon, Portugal

Luís **Portela**, LNEC, Portugal
Elena **Pummer**, Norwegian University of Science and Technology, Norway
Helena **Ramos**, Instituto Superior Técnico, University of Lisbon, Portugal
Roberto **Ranzi**, University of Brescia, Italy
Ana **Ricardo**, Instituto Superior Técnico, University of Lisbon, Portugal
Fernanda **Rocha**, LNEC, Portugal
Marta **Rodrigues**, LNEC, Portugal
Alessandro **Romano**, Roma Tre University, Italy
Maria João **Rosa**, LNEC, Portugal
Paulo Rosa **Santos**, Faculty of Engineering, University of Porto, Portugal
Nils **Rüther**, Technical University of Munich, Deutschland
Maria **Salvetti**, Florence School of Regulation, Italy
Paul **Samuels**, HR Wallingford, UK
Martí **Sánchez Juny**, Technical University of Catalonia,Spain
José Maria **Santos**, School of Agriculture, University of Lisbon, Portugal
Isabella **Schalko**, ETH Zurich, Switzerland
Anton **Schleiss**, École Polytechnique Fédérale de Lausanne, Switzerland
Martin **Schletterer**, TIWAG - Tiroler Wasserkraft AG, Austria
Ana Maria da **Silva**, Queens University, Canada
Sandra **Soares Frazão**, Catholic University of Louvain, Belgium
Jürgen **Stamm**, Dresden University of Technology, Germany
Laura Maria **Stancanelli**, Delft University of Technology, Netherlands
Tibor **Stigter**, IHE Delft, Netherlands
Thorsten **Stoesser**, University College London, United Kingdom
Andrea **Sulis**, University of Sassari, Italy
Rui **Taborda**, Faculty of Science, University of Lisbon, Portugal
Alexandre **Tavares**, University of Coimbra, Portugal
Francisco **Taveira Pinto**, Faculty of Engineering, University of Porto, Portugal
Paulo F. **Teixeira**, Federal University of Rio Grande, Brazil
António Trigo **Teixeira**, Instituto Superior Técnico, University of Lisbon, Portugal
Donatella **Termini**, University of Palermo, Italy
Miguel Ángel **Toledo**, Technical University of Madrid, Spain
Franz **Tscheikner-Gratl**, Norwegian University of Science and Technology, Norway
Manousos **Valyrakis**, Aristotle University of Thessaloniki, Greece
Marcel **van Gent**, Deltares & Delft University of Technology, Netherlands
José Manuel **Vieira**, University of Minho, Portugal
Damien **Violeau**, EDF R&D, France
Teresa **Viseu**, LNEC, Portugal
Liege **Wosiacki**, Advisian, Worley Parsons Group, Brazil
Zhihua **Xie**, Cardiff University, United Kingdom
Taís **Yamasaki**, Durham University, United Kingdom
James **Yang**, Vattenfall R&D, Royal Institute of Technology, Sweden
Eduardo **Yassuda**, Tetra Tech South America, Brazil
Ana C. **Zózimo**, LNEC, Portugal

# IAHR Europe Division Committee

**Chair**
Pawel M. Rowinski, Institute of Geophysics, PAS (IGF PAN), Poland

**Vice-Chair**
Anastasios I. Stamou, National Technical University of Athens (NTUA), Greece

**Past-Chair**
Corrado Gisonni, Università della Campania 'Luigi Vanvitelli', Italy

**Members**
Claudia Adduce, Roma Tre University, Italy
Florian Cordier, Electricité De France, Division R&D, France
Alan J. S. Cuthbertson, University of Dundee, United Kingdom
Benjamin J. Dewals, University of Liege, Belgium
Cristiana Di Cristo, University of Naples Federico II, Italy
Tiago João Fazeres Ferradosa, Faculdade de Engenharia, Universidade do Porto, Portugal
Katinka Koll, Technische Universitaet Braunschweig, Germany
Amparo López Jiménez, Universitat Politècnica de València, Spain
Elena Pummer, Norwegian University of Science and Technology (NTNU), Norway
Nils Rüther, Technical University of Munich (TUM), Germany
Laura Maria Stancanelli, TU Delft, Netherlands

**Co-Opted**
Janek Laanearu, Tallinn University of Technology - Department of Civil Engineering and Architecture, Estonia
Melissa Latella, Euro-Mediterranean Center on Climate Change (CMCC Foundation) - Impacts on Agriculture, Forests and Ecosystem Services (IAFES) Division, Italy
Ana Margarida Lopes Saraiva Alves Bento, CIIMAR - Interdisciplinary Centre of Marine and Environmental Research, Portugal
Cristina Prieto, Fundación I. Hidráulica Ambiental de Cantabria, Spain

**WATER-ACROSS BOUNDARIES**

THEME A: Aquifers, rivers, reservoirs and dams

THEME B: Estuaries, coasts and ports

THEME C: Urban water

THEME D: Numerical and experimental methods

THEME E: Climate change and risk mitigation

THEME F: Governance and water resources management


IAHR International Association for Hydro-Environment Engineering and Research

Hosted by Spain Water and IWHR, China

Taylor & Francis
Taylor & Francis Group




**IAHR members get free or discounted access to these journals and more!**

**Scan here for details:**

# INDEX

## Keynote Lectures


River bars and meanders:from the lab to the real world ..... 3
*Ana Maria da Silva, Professor and Head, Department of Civil Engineering Queen's University, Canada*

Hydro-environment research on climate change adaptation of water infrastructure ..... 5
*Anastasios I. Stamou, Professor and Director of the Department of Water Resources and Environmental Engineering, National Technical University of Athens, Greece*

Challenges in coastal climate change adaptation ..... 7
*Íñigo J. Losada, IHCantabria Research Director; Coastal Engineering Professor, University of Cantabria, Spain*

Challenges and needs to quickly move towards really integrated urban stormwater management ..... 9
*Jean-Luc Bertrand-Krajewski, Professor, INSA Lyon, France*


## Theme A: Aquifers, rivers, reservoirs and dams


A new approach using the IDCM method for discharge prediction in partly vegetated channel flows ..... 13
*Ben Meftah, Mouldi; De Padova, Diana; De Serio, Francesca; Mossa, Michele*

Statistical analyses of key parameters involved in riverbed clogging ..... 15
*Noack, Markus; Aybar Galdos, Alcides*

Fish passes in Portugal: current status, main findings and future directions ..... 17
*Santos, José Maria; Branco, Paulo; Quaresma, Ana; Romão, Filipe; Amaral, Susana; Santos, Marta; Bochechas, Jorge; Telhado, Ana; Godinho, Francisco; Pádua, João; Pinheiro, Paulo; Silva, Ana; Viseu, Teresa; Almeida, Pedro; Ferreira, Teresa; Pinheiro, António*

Eel-friendly fish ladders: navigating challenges for multi-species design ..... 19
*Carcano, Elena; Plymesser, Kathryn*

The Roman soil retention dams – a forgotten technology for water retention in arid climates ..... 21
*Muller, Gerald; Royal, Charlie*

Effects of flow guide walls on sediment flushing in peaking hydropower reservoirs ..... 23
*Tietz, Stefanie; De Cesare, Giovanni; Manso, Pedro; Van Mol, Romain*

Experimenting with riparian vegetation management to enhance the hydraulic and ecological functioning of modified agricultural brooks ..... 25
*Västilä, Kaisa; Huttunen, Kaisa-Leena; Jilbert, Tom; Kuussaari, Mikko; Karttunen, Krister; Wikström, Jani; Valkama, Pasi; Koskiaho, Jari; Aroviita, Jukka*

Evaluation of MAR feasibility in Cyprus based on a co-participative multi-criteria decision analysis ..... 27
*Eisenreich, Sarah; Panagiotou, Constantinos F.; Martins, Tiago; Barouta, Olga; Neophytides, Stelios; Stylianou, Marinos; Stefan, Catalin*

Comparison of IDF curves for mainland Portugal using ground-based and ERA5-Land data ..... 29
*Freitas, Laryssa; Portela, Maria Manuela; Espinosa, Luis Angel; Matos, José*

Inversion of the reaction-diffusion-advection equation for colloidal contaminants utilising the iterative ensemble Kalman filter ..... 31
*Duncan, Liam Andrew; El-Zein, Abbas*

DNN-Enhanced predictive modeling for sediment transport in reservoirs: Riba-Roja case study ..... 33
*Dehghan-Souraki, Danial; Blade, Ernest; Larese, Antonia*

Coping with pulsed flows: evaluating the efficiency of two flow refuges for an Iberian cyprinid ..... 35
*Leite, Renan; Costa, Maria João; Mameri, Daniel; Afonso, Fernando; Pinheiro, António; Santos, José Maria; Boavida, Isabel*

Preliminary results of the monitoring of the insect community in a periurban section of the Manzanares River (Madrid, Spain) ..... 37
*Ibarra Mellado, Sergio; García Sánchez-Colomer, Manuel Ramón; Young Sánchez Mateos, Arturo David; Viejo Montesinos, José Luis*

Use of InSar technology to determine the active portion of a gravel braidplain ..... 39
*Guadagno, Valeria; Del Giudice, Giuseppe; Di Cristo, Cristiana; Di Martire, Diego; Viparelli, Enrica; Leopardi, Angelo*

DAM SAFETY – how a contractual strategy and the involvement of an independent expert can contribute to it ..... 41
*Geisseler, Bettina*

Development of a simple reservoir water level controller ..... 43
*Nogueira, Filipa N.; Pinho, José L.S.*

Stormwater attenuation & enhanced infiltration system to mitigate flood & drought conditions: Part II – rural environment ..... 45
*Stephen D. Thomas; George R. French; Jamie Bates; Joseph A. O'Meara; Matthew P. Dale; Bruno Casal*

Innovative dam design for low-head seawater pumped hydropower storage in the North Sea ..... 47
*Jayasinghe Arachchige, Lasantha; de Vilder, Lucas; Bagas Prasasti, Eksa; Terheiden, Kristina; Geisseler, Bettina; Moll, Roelof; Bricker, Jeremy*

Influence of mowing macrophyte vegetation on water level in a small lowland river in agricultural landscape ..... 49
*Miroslaw-Swiatek, Dorota; Grygoruk, Mateusz; Okruszko, Tomasz; Szporak-Wasilewska, Sylwia*

Effect of flow velocity on eDNA degradation for biodiversity assessment in rivers ..... 51
*Dercksen, Jelle A.; Stancanelli, Laura Maria; Trimbos, Krijn B.; Blom, Astrid*

Temporal development of local scour around bridge abutments under a stepwise hydrograph ..... 53
*Gökmener, Serkan; Gogus, Mustafa; Altan Sakarya, A.Burcu*

Impact of the Grand Ethiopian Renaissance dam in Nile Delta aquifer under different filling scenarios ..... 55
*Kuriqi, Alban; Abd-Elaty, Ismail*

A GIS-MCDA based participatory method to map managed aquifer recharge feasibility in Chiba watershed, CapBon, NE Tunisia ..... 57
*Chekirbane, Anis; Khemiri, Khaoula; Panagiotou, Constantinos F; Stefan, Catalin*

Characterization of large-scale turbulence horizontal coherent structures in ice-covered flows ..... 59
*Gamboa Monge, Cristopher Alexander; Ferreira da Silva, Ana Maria*

Generation of realistic deformed beds in sine-generated meandering streams ..... 61
*Dong, Mengsi; Ferreira da Silva, Ana Maria*

Investigation of the long-term changes in sediment load along a free-flowing transboundary Middle Danube reach ..... 63
*Tamás, Enikő Anna; Djordjevic, Dejana; Mihajlovic, Ljubisa; Abonyi, Csaba; Vujanovic, Aleksandar; Kalocsa, Béla*

Preliminary results for a managed aquifer recharge feasibility index for the southern Portuguese region ..... 65
*Nunes Martins, Tiago; Eira Leitão, Teresa; Panagiotou, Constantinos; Mendes Oliveira, Manuel; Portela, Maria Manuela; Stefan, Catalin*

Pumped storage reconversion in Alto Lindoso hydroelectric power plant in Portugal ..... 67
*Fernandes, Marco; Pinto, Pedro; Osório, Nuno; Noronha, Daniela; Benites, Liliana; Calvo, João*

Impact of partially-covered mixed heighted vegetation on the lateral velocity and discharge of open channel flow ..... 69
*Tang, Xiaonan; Wang, Yibo; Teng, Qinzheng; Yin, Haoxing; Shao, Mingtao*

Swimming behaviours of Atlantic salmon kelts at hydropower dams ..... 71
*Simmons, Olivia M.; Silva, Ana T.; Forseth, Torbjørn; Andreasson, Patrik; Müller, Stephanie; Calles, Olle; Aldvén, David*

Flow and turbulence structure in vertical slot fishway: effect of Reynolds number ..... 73
*Kucukali, Serhat*

Design of Alto Tâmega spillway. From brainstorming to the final functional test ..... 75
*Ramírez, Miguel Ángel; de la Torre, Luis; Chacón, Rafael; Granell, Carlos*

Physical model-based maximization of historical precipitation in the basin with complex topography ..... 77
*Hiraga, Yusuke; Meza, Joaquin*

Modelling managed aquifer recharge in Chiba River basin (Tunisia) with the AQUATOOL decision support system ..... 79
*Ghannem, Syrine; Bergillos, Rafael J.; Chekirbane, Anis; Khemiri, Khaoula; Paredes-Arquiola, Javier; Solera, Abel; Andreu, Joaquín*

Evaluation of flood susceptibility in Cyprus based on a co-participative multi-criteria decision analysis ..... 81
*Panagiotou, Constantinos F.; Feloni, Elissavet; Kountouri, Josefina; Mettas, Christodoulos; Evagorou, Evagoras; Akylas, Evangelos*

Modelling sediment delivery in river catchments: a review ..... 83
*Padulano, Roberta; Latella, Melissa; Caloiero, Tommaso; Costanzo, Carmelina; Costabile, Pierfranco*

Web-based numerical groundwater modelling at the Akrotiri managed aquifer recharge site, Cyprus using the INOWAS platform ..... 85
*Glass, Jana; Panagiotou, Constantinos; Junghanns, Ralf; Stefan, Catalin*

Automatic identification of potential outliers in large data bases of time series based on autoencoders. Application to dam monitoring data ..... 87
*Salazar González, Fernando; Irazábal, Joaquín; Silva-Cancino, Nathalia; Mata, Juan*

Tree-based approaches for imputation of missing precipitation records ..... 89
*Teegavarapu, Ramesh; Nguyen, Thu*

Atlantic salmon (*Salmo salar*) conservation and sustainable hydropower in Norway: new innovative downstream passage solutions ..... 91
*Silva, Ana T.; Forseth, Torbjørn; Albayrak, Ismail; Simmons, Olivia M; Pandey, Kamal; Vetsch, David; Solemslie, Bjørn Winther; Boes, Robert; Calles, Olle; Andreasson, Patrik; Müller, Stephanie; Lillberg, Eric; Baktoft, Henrik; Ø. Gjelland, Karl; Økland, Finn; Pulg, Ulrich; Dahlhaug, Ole Gunnar; Harby, Atle; Aldvén, David*

Retrospective analysis of the structural behavior of Almendra dam after 53 years of its construction ..... 93
*Sigüenza, Alicia; de la Torre, Luis; Pérez, Yolanda; Baena, Carmen; Milla, José*

Sediment transport and deposition processes under various hydrological-hydraulic conditions – HEORES project ..... 95
*Klun, Mateja; Kuzmanić, Tamara; Lebar, Klaudija; Rak, Gašper; Kryžanowski, Andrej; Mikoš, Matjaž; Rusjan, Simon*

Effects of flow restoration on the hydraulic conditions in River Juktån ..... 97
*Höller, J. Bastian; Andersson, Anders G.; Hellström, J. Gunnar I.*

Flow characteristics around a freshwater mussel in a gravel bed flume ..... 99
*Termini, Donatella*

Experimental investigation of flow around spillway ramps with varying spanwise widths towards successful downstream fish passage ..... 101
*Kumahor, Sedem; Aleyasin, Seyed Sobhan; Tachie, Mark F.; Ghamry, Haitham; Katopodis, Christos*

An ecohydraulic approach for 2D hydraulic modelling of a regulated river reach ..... 103
*Niemi, Frida Maria; Andersson, Anders Gustav; Hellström, Johan Gunnar Ingebret*

Effects of weir installed at the bypass entrance of bar rack systems on hydraulic conditions and behavior of downstream migrating fish ..... 105
*Aleyasin, Seyed Sobhan; Fang, Xingjun; Tachie, Mark Francis; Katopodis, Christos; Ghamry, Haitham*

Hydropeaking frequency: implications for fish stranding and river management ..... 107
*Hayes, Daniel S.; Auer, Stefan; Führer, Simon; Greimel, Franz; Tonolla, Diego; Bätz, Nico; Weber, Christine; Unfer, Günther; Zeiringer, Bernhard; Merl, Kevin; Silva, Luiz; Naudascher, Robert; Gorla, Lorenzo; Schmutz, Stefan*

Assessment of restoration success by hydromorphological parameters: lessons learned from a riprap removal ..... 109
*Koll, Katinka; Wunsch, Tobias; Vieweg, Michael*

Evaluation of tree root depth and piezometric level in a historical botanical urban garden in Lisbon city, Portugal ..... 111
*Mendes, Maria Paula; Falcão, Ana Paula; Afonso, Nuno; Esteves, Miguel; Paz, Maria Catarina*

Turbulence thresholds for cyprinids in vertical slot fishways: a laboratory experiment-based analysis ..... 113
*Romao, Filipe; L. Quaresma, Ana; Simão, Joana; Bravo-Córdoba, Francisco; Viseu, Teresa; M. Santos, José; Sanz-Ronda, Francisco; N. Pinheiro, António*

Robust modelling of groundwater in Portugal mainland: exploring the correlation with the NAO Index – a preliminary study ..... 115
*Lourenço, Vanda M.; Lordelo, Maurício; Rodrigues, Paulo C.; Mendes, Maria Paula*

Density currents forming within an array of in-line and emergent cylinders ..... 117
*Brito, Moisés; Ferreira, Rui M.L.; Ricardo, Ana M.*

Gravity currents interacting with a large-scale roughness ..... 119
*Maggi, Maria Rita; Di Lollo, Giovanni; Adduce, Claudia*

TKE budget equation terms of a gravity current approaching a vertical obstacle ..... 121
*Di Lollo, Giovanni; Adduce, Claudia; Brito, Moises; Ricardo, Ana M.; Ferreira, Rui M.L.*

Crato. The most recent multipurpose hydraulic scheme being built in Portugal ..... 123
*Samora, Mario; Alves, Elsa*

A Lagrangian perspective on the characterization of the Agulhas leakage ..... 125
*Busatto, Jacopo; Falcini, Federico; Lacorata, Guglielmo; Adduce, Claudia*

Quantifying the influence of source variability on unsteady buoyant jets ..... 127
*Hetherington, Morgan; Cuthbertson, Alan James Stewart; Dawson, Sue*
Experimental modelling of rock dumping in a Norwegian fjord ..... 129
*Cuthbertson, Alan James Stewart; Neshamar, Otto; Thiem, Oyvind; Davies, Peter; Berntsen, Jarle*
Criticality in gravity currents ..... 131
*Skevington, Edward; Dorrell, Robert*
Dynamics of gravity currents interacting with sediment bed ..... 133
*Maggi, Maria Rita; Negretti, Maria Eletta; Hopfinger, Emil J.*
Flow pattern of a vane-controlled 90º mobile bed lateral diversion in morphological equilibrium ..... 135
*Büyüker, Zehra; Bombar, Gökçen; Cardoso, António Heleno*
Alqueva project – a case of regional development ..... 137
*Vazquez, Jorge*
300 MW Balakot hydropower project – a Himalayan challenge ..... 139
*Roberto, Filipe; Costa, Sérgio Correia; Pinheiro, António; Ribeiro, Raquel*
Evaluation of hydrological dam safety considering flood peak and volume ..... 141
*Requena, Ana I.; Jiménez-Álavarez, Antonio; Garcia, Celia*
Is riverbank vegetation important in river modelling? ..... 143
*Łoboda, Anna; Bomers, Anouk; Duong, Trang Minh*
Dynamics of artificial spawning sites for trout and grayling – novel monitoring approaches based on pit-tagged gravel substrate at the Inn River ..... 145
*Schletterer, Martin; Holzapfel, Patrick; Paster, Michael; Schähle, Zacharias; Zöschg, Hannes; Hauer, Christoph*
The reconstruction of the Gove multipurpose dam and hydropower plant in Angola. Design, construction and operation challenges in the context of changing water and energy needs in the international Cunene River basin ..... 147
*Pereira da Silva, Antonio; Mendes, Carolino*

## Theme B: Estuaries, coasts and ports

Estimation of open channel bathymetry with video images from surface data ..... 151
*Aveiro, Francisco; Abreu, Tiago; Brito, Moisés; Neves, Maria Graça*
Propeller scour confined by a quay wall in waterways ..... 153
*Ferraro, Domenico; Lauria, Agostino; Penna, Nadia; Gaudio, Roberto*
An online, open mesh generation assistant for OPENCoastS using OCSMesh ..... 155
*Martins, Ricardo; Fortunato, André; Oliveira, Anabela; Jesus, Gonçalo; Mani, Soroosh; Myers, Edward; Moghimi, Saeed*
Shallow-water deformation effects of long-period ship-induced waves in estuaries ..... 157
*Dempwolff, León-Carlos; Windt, Christian; Melling, Gregor; Bihs, Hans; Holzwarth, Ingrid; Goseberg, Nils*
Re-analysis of extreme sea state events modelling using a data-driven technique ..... 159
*Goeury, Cédric; Fouquet, Thierry; Bagnis, Tristan; Benoit, Michel; Teles, Maria*
Practical use of smartphone cameras in morphodynamic beach state and rip current risk estimation ..... 161
*Chintam, Venkateswarlu; VV Arun Kumar, Surisetty; Madipally, Ramesh; Baggu, Gireesh; C V, Naidu*
Wave propagation over a sandy beach: preliminary comparisons between wave-resolving model and short range K-band radar ..... 163
*Gaiolini, Mattia; Codjo, Aénor; Colombani, Nicolò; Ferraro, Luciana; Gennarelli, Gianluca; Ludeno, Giovanni; Postacchini, Matteo*
Exploring compound flood hazards: bridging statistics and hydrodynamics in estuaries ..... 165
*Gomez Rave, Dina Vanessa; Urrea Mendez, Diego Armando; Del Jesus Peñil, Manuel*
Nature positive ports and coastal infrastructures ..... 167
*Leblanc, Phil; Gutierrez, Jorge; Rella, Andrew; Jover, Fernando*
Towards technical design guidance for estuarine nature-based solutions ..... 169
*Dunlop, Thomas; Glamore, William; Felder, Stefan*
Influence on a riverine estuary due to an increase in outtake of cooling water ..... 171
*Burman, Anton; Lier, Øyvind; Macchion, Olivier; Jensen, Atle*

Numerical modelling of infragravity waves in a tidal inlet during storm conditions ..... 173
*Mendes, Diogo; Nahon, Alphonse; Martins, Kévin; Fortunato, André; Bertin, Xavier; Mengual, Baptiste; Lavaud, Laura; Pezerat, Marc; Pires-Silva, António*

Reduction of microplastic pollution in shipbuilding industry ..... 175
*Lučin, Ivana; Alvir, Marta; Družeta, Siniša; Lučin, Bože*

Interfacial mixing of the stratified flow in the trapezoidal-shape channel with presence of background vorticity ..... 177
*Laanearu, Janek; Kaur, Katrin; Malcangio, Daniela*

Unbalanced sediment flux caused by tidal pumping and residual circulation in the meso-tidal Yeosu Bay .. 179
*Ha, Ho Kyung; Kim, S.I.; Seo, J.Y.; Park, J.H.; Kim, P.J.*

A new low-Reynolds $k$-$\varepsilon$ turbulence model for shear flow along smooth walls ..... 181
*Aung, Thu Zar; Toorman, Erik*

Enhanced utilisation of tidal range schemes to support migration to Net Zero ..... 183
*Lam, Man-Yue; Ahmadian, Reza*

Faecal indicator organism prediction through machine learning enhanced by dimensionality reduction ..... 185
*Amini, Hossein; Yue Lam, Man; Ahmadian, Reza*

The impact of different lagoon operation procedures on regional water exchange rate ..... 187
*Guo, Bin; Ahmadian, Reza*

Machine learning analysis of elemental variation in sediment cores from Boka Kotorska Bay – Adriatic Sea ..... 189
*Manojlovic, Vaso D; Radomirović, Milena; Tanaskovski, Bojan; Cantaluppi, Chiara; Degetto, Sandro; Stanković, Slavka*

Innovative nature-based solutions for coastal resilience ..... 191
*Proença, Barbara; Gomes, Andreia; Bosnic, Ivana; Rato, Lénia; Bendô, Raylton; Mendes, Diogo; Fonseca, Diogo*

Distributions and migrations of heavy metals at the water-sediment interface in the coastal area of the Yangtze River estuary, China ..... 193
*Zhang, Zhirui; Liu, Shuguang; Lou, Sha; Zhong, Guihui; Zhou, Xiaosheng; Zhou, Feng; Radnaeva, Larisa Dorzhievna; Nikitina, Elena; Fedorova, Irina Viktorovna*

Numerical simulation of combined coastal inundation due to fluvial flood, storm surge and wave induced set-up/runup ..... 195
*Samaras, Achilleas; Karambas, Theofanis*

Monitoring ocean currents with high-frequency radars along the Portuguese Coast: overview and challenges ..... 197
*Lima, Vânia; Lamas, Luísa*

Site investigation for floating solar panels using multi-criteria decision making ..... 199
*Amini, Hossein; Lewis, Jack; Morgan, Dawn; Masters, Ian; Neill, Simon; Dixon, Andrew; Pan, Shunqi; Ahmadian, Reza*

Opportunities and challenges for a dual wave farm proposal in the north-western nearshore of Portugal ... 201
*Clemente, Daniel Pinto; Castro, Jose Victor Ramos; Duarte, Felipe Teixeira; Pinto, Francisco Vilela Taveira; Santos, Paulo Jorge Rosa; Pinto, Francisco Taveira*

Accuracy assessment of UAV-based remote sensing of turbidity in coastal environments during land reclamation ..... 203
*Kieu, Hieu Trung; Pak, Hui Ying; Trinh, Ha Linh; Pang, Dawn Sok Cheng; Khoo, Eugene; LAW, Adrian Wing-Keung*

Using Hall-effect sensor based devices for high-resolution measurements of wave-driven near-bottom water flow in the gulf of Riga ..... 205
*Piho, Laura; Ristolainen, Asko; Parnell, Kevin; Soomere, Tarmo*

Spatial variations in the vulnerability of the shores of the eastern Baltic sea with respect to future extreme water levels ..... 207
*Viigand, Katri; Eelsalu, Maris; Soomere, Tarmo*

Exploring wave energy resource on the Pacific shore of South America ..... 209
*Eelsalu, Maris; Soomere, Tarmo; Aramburo, Darwin; Montoya, Rubén; Osorio, Andrés*

Evaluation of microplastic contamination across an Atlantic coastal area ..... 211
*Morgado, Vanessa; Bettencourt da Silva, Ricardo; Palma, Carla*

Optimisation of sampling uncertainty in vast marine systems: development of methodologies based on Monte Carlo simulations of georeferenced information ..... 213
*Borges, Carlos; Palma, Carla; Bettencourt da Silva, Ricardo J.N.*

Propeller jet induced scouring in presence of a quay wall ..... 215
*Macías-Lezcano, Jesús; Llull, Toni; Aberle, Jochen*

Decomposing alongshore sediment transport into cells and compartments: a case study in the gulf of Riga, the Baltic sea ..... 217
*Jankowski, Mikolaj; Parnell, Kevin; Soomere, Tarmo*

Unveiling WORSICA's role in tracking the dynamics of the Óbidos lagoon ..... 219
*Azevedo, Alberto Carlos; Martins, Ricardo; Oliveira, Anabela; Fortunato, André*

Deep neural network enhanced early warning system for port operations ..... 221
*Pinheiro, Liliana; Fortes, Conceição; Gomes, Andreia*

Construction of the new port of Lajes das Flores ..... 223
*Pereira, Flávio; Leite, Hugo; Robalo, João; Fernandes, Luís*

Assessment of soft coastal protection alternatives for Saint-Louis (Senegal) ..... 225
*Sancho, Francisco Eduardo Ponte; Oliveira, Filipa Simões Brito Ferreira; Nahon, Alphonse Pascal David*

A wave energy assessment for the Moroccan coast ..... 227
*Bernardino, Mariana; Schneider, Magnus; Rusu, Liliana*

HIDRALERTA: emergency response module for coastal wave overtopping and flooding at Praia da Vitória Bay ..... 229
*Fortes, Conceicao Juana; Pinheiro, Liliana; Zózimo, Ana Catarina; Lima, Larize; Serrazina, Vera*

Analytical and numerical modelling of wave dissipation over rigid and flexible vegetation in a flume: drag coefficient calibration ..... 231
*Reis, Rui A.; Fortes, Conceição J.E.M.; Suzuki, Tomohiro*

Influences of climate adaptation measures for coastal flood using system dynamics approach ..... 233
*Perney, Marion Eva Pauline; Moreno, Mauro; Giannino, Francesco; Leone, Mattia Federico*

Energy transfer optimum in waves generated by high mobility subaerial landslides ..... 235
*Parvin, Amir; Abadie, Stephane; El Omari, Kamal; Le Guer, Yves*

A new dimension in satellite altimetry: Insight into the SWOT data for assessing the dynamics of hydrosystems ..... 237
*Zawadzki, Lionel; Gasnier, Nicolas; Fjortoft, Roger; Pottier, Claire; Desroches, Damien; Pena Luque, Santiago; Picot, Nicolas; Barroso, Therese*

Monitoring of coastal infrastructure – example of brine discharge system ..... 239
*Robakiewicz, Małgorzata*

The coastal challenge of climate adaptation: discussion on systemic approaches ..... 241
*Perney, Marion Eva Pauline; Barroca, Bruno; Clemente, Maria Fabrizia; Heinzlef, Charlotte; Leone, Mattia Federico; Thomas, Isabelle; Serre, Damien*

Run-up and overtopping video analysis using timestack methodology ..... 243
*Lemos, Rute Gomes; Carvalho, Miguel; Fortes, Conceição; Andriolo, Umberto*

Where the brazes and San Bernard rivers meet the gulf of Mexico ..... 245
*Stull, Trevor; Ahmari, Habib; Khandaker, Nabila*

CONNECT – local coastal monitoring service for Portugal ..... 247
*Rodrigues, Marta; Fortunato, André B.; Martins, Ricardo J.; Jesus, Gonçalo de; Brito, Ana C.; Oliveira, Anabela; Nahon, Alphonse; Costa, José L.; Alves, Elsa; Korani, Zahra Mardani; Azevedo, Alberto*

Sand waves and sediment recirculation along the main channel at the mouth of the Tagus estuary ..... 249
*Portela, Luís Ivens*

Improving surfability assessment along a submerged detached breakwater at praia da Vagueira, Portugal ..... 251
*Tavares, Pedro Grade Ferreira; Mendonça, Ana; Fortes, Conceição Juana; Bicudo, Pedro*

Investigation of seasonal variation of microplastics and micropollutants in inland terrestrial waters ..... 253
*Baycan, Neval; Pelit, Füsun; Gündüz, Orhan*

Occurrence of microplastic in the Thai aquatic environment ..... 255
*Kurwadkar, Sudarshan; Natalia, Grace; Kitpati Boontanon, Suwanna; Pathomsiri, Somchai*

Optimization tool for the design of climate change robust flood control areas in tidal zones ..... 257
*Salazar, Danitza; Willems, Patrick*

Energy transition in APS ports ..... 259
*Bandeira, Eduardo; Moutinho, Eduardo; Araújo, João*

Adapting coastal and port defence structures to facilitate the energy transition ..... 261
*Calheiros, Tomas; Khalooei-Tafti, Seyed Shahabedin; Ramos, Vitor; Giannini, Gianmaria; Rosa-Santos, Paulo; Taveira-Pinto, Francisco*

Paving the way for greener mobility in small-medium ports ..... 263
*Amado Cruz, Maria Manuel; Barata, Ricardo; Barbosa, Sebastião; Macedo, Joaquim; C. Coelho, Margarida*

Decarbonization and Innovation in the port of Lisbon ..... 265
*dos Santos Sengo, Paula Cristina*

## Theme C: Urban water

A novel IoT-based flood control system with high efficiency in runoff quality and quantity management ..... 269
*Pirouz, Behrouz; Palermo, Stefania Anna; Turco, Michele; Javadi Nejad, Hana; Piro, Patrizia*

A physics-based approach for including sewer network effects in pluvial flood modelling in the absence of drainage network information ..... 271
*Montalvo, Carlos; Reyes-Silva, Julian; Sañudo, Esteban; Cea, Luis; Puertas, Jerónimo*

A numerical ecohydrological model for simulating the hydrological response of multi-layer green roofs to climate forcing ..... 273
*Pumo, Dario; Ippolito, Matteo; Alongi, Francesco; Cannarozzo, Marcella; Mattina, Calogero; Noto, Leonardo*

A comprehensive resilience assessment system for water distribution networks ..... 275
*Carneiro, Joana; Loureiro, Dália; Cabral, Marta; Covas, Dídia*

The effect of selected SuDS on the tailwater urban drainage system: preliminary results ..... 277
*Orsi, Erica; Crispino, Gaetano; Iervolino, Michele; Maietta, Filomena; Gisonni, Corrado*

Nature-based solutions in urban watersheds – the SEE-URBAN-WATER project ..... 279
*Hack, Jochen*

Tackling microplastic pollution with nature-based solutions from urban runoff and wastewater ..... 281
*Calzadilla, Darío; Hernández-Crespo, Carmen; Andrés-Doménech, Ignacio*

Long-term laboratory analysis of the impact of sediment characteristics on the clogging process of permeable asphalt and its hydrological and water quality response ..... 283
*García Haba, Eduardo; Naves, Juan; Hernández-Crespo, Carmen; Goya-Heredia, Angélica; Suárez, Joaquín; Anta, Jose; Andrés-Doménech, Ignacio*

Decentralized management of urban wastewater through the implantation of artificial wetlands for the renaturalization of the Carraixet ravine ..... 285
*Gil Martínez, Enric; Hernández Crespo, Carmen; Rodrigo Santamalia, Mª Eugènia; Asensi Dasi, Enrique Javier; Lidón Cerezuela, Luís; Benedito Durá, Vicent*

Nature-based drainage systems: analysis of ecosystem services in the Manzanares River (Madrid, Spain) 287
*Díaz Redondo, María; Cortés Sánchez, Francisco M.; García Sánchez-Colomer, Manuel Ramón*

Experimental investigations of thin layer surface runoff on natural grassland ..... 289
*Jakobs, Tim; Oberle, Peter; Franca, Mário J.*

An assessment of the potential for wastewater heat recovery in the Zambian food processing industry .... 291
*Murali, Madhu K.; Mancusi-Ungaro, Eleanor; McNabola, Aonghus*

Optimal pump scheduling within a water distribution network by means of a global optimization solver .... 293
*Fecarotta, Oreste; Carravetta, Armando; Montillo, Renato; Morani, Maria Cristina*

Results of a methodology for the measurement of the CSO polutograph in a continental Mediterranean climate region. The Madrid case study ..... 295
*Lastra, Antonio; Pinilla, Alejandro; Botello, Jaime; Ortega, Monica; Ortega, Celia; Ruiz, Laura; Carrasco, Alejandro*

The factors affecting the domestic water consumption in Portugal: an econometric approach ..... 297
*Xavier, António; Antunes, Carla; Costa Freitas, Maria de Belém*

Stormwater attenuation & enhanced infiltration system to mitigate flood & drought conditions: Part I – urban environment ..... 299
*Thomas, Stephen; French, George; Watson, James; O'Meara, Joseph; Dale, Matthew; Casal, Bruno*

From source to receptor: an integrated approach to analyse sediments and particle bound pollutants from urban wet weather discharges ..... 301
*Rojas-Gomez, Karen Lorena; Benisch, Jakob; Helm, Björn; Borchardt, Dietrich; Krebs, Peter*

Unlocking the potential of digital twins in water and wastewater systems: a holistic approach ..... 303
*Moran, Vincent; Besharat, Mohsen; Evans, Barbara; Bartram, James; Ramos, Helena M.*

Critical future demand scenarios for the robust design of water distribution networks ..... 305
*Magini, Roberto; Cunha, Maria da Conceição; Marques, João; Ridolfi, Elena*

Runoff coefficient of green roofs in Trondheim, Norway ..... 307
*Sousa, Vitor; Matos, José Pedro; Meireles, Inês; Bertolin, Chiara*

Methodology for modelling rainwater harvesting with snow – application to Trondheim, Norway ..... 309
*Passanha, Vasco; Silva, Cristina Matos; Bosco, Camillo; Sousa, Vitor; Sivertsen, Edvard*

Modelling the operation of wastewater pumping stations for wet-weather conditions ..... 311
*David, Luís Mesquita; Martins, António; Ataíde, Alexandre; Silva, Osvaldo; Oliveira, Anabela*

Implementation of a real-time decision model for the reduction of pollutant loads discharge in combined sewer overflows. Study case: Madrid ..... 313
*Lastra, Antonio; Carrasco, Alejandro; Ortega, Mónica; Botello, Jaime; Sunyer, David; Villanueva, Ángel*

Water grid: Is electrical energy recovery possible? From the water supply network? From the water distribution network? ..... 315
*Nuc, Francois; Hendrick, Patrick*

Design and experimental validation of a phononic crystal-based solution for improved noise and vibration behavior of ram pumps ..... 317
*Nasraoui, Saber; Ferras, David; Dupont, Capucine*

Green roofs hydrological performance and contribution to urban rainwater management ..... 319
*Mendes, Ana Mafalda; Monteiro, Cristina M.; Santos, Cristina*

Analysis of water-energy consumption and carbon emissions in urban water sectors using Sankey diagrams and GIS mapping ..... 321
*Min, Kyoung Won; Lee, Gyumin; Kim, Hyunjung; Kang, Doosun*

Digitalization for modelling: the importance of data for improving sustainability in water distribution systems ..... 323
*Cuellar, Christian; Perez-Sanchez, Modesto; López-Jiménez, P. Amparo; Sanchez-Romero, Francisco Javier; Ramos, Helena*

Nature-based solutions for urban flooding adaptation in unplanned settlement in Mozambique ..... 325
*Ottaviani, Susanna; Serrao, Livia; Marzadri, Alessandra; Antonio, Alfredo Manhota; Msopela, Amerigo de Stela Vladimir; Chate, Harold Juvenal; Paulino, Wilson Alberto Manguita; Paulino, Edilson; Zolezzi, Guido*

Urban drainage control plan. Modelling the integrated drainage network. A case study in Caneças/ Ramada/Odivelas, Portugal ..... 327
*Raposo, Carlos; Freitas, Susana; Rodrigues, Helder; Caetano, Leonor; Pires, Rita; Teixeira, Filipe*

Modelling and analyses of micro hybrid pumped hydropower storage ..... 329
*Pina, João; Pérez-Sánchez, Modesto; López-Jiménez, P. Amparo; Ramos, Helena M.*

A methodology for assessing water efficiency of office buildings – application to a full-scale case study .. 331
*Vieira, Paula; Poças, Ana; Dias, Patrícia; Pestana, Rita*

Tróia WWTP expantion and retrofit to produce reuse for water ..... 333
*Raposo, Carlos; Guimarães, João*

Energy balances as tools for assessing carbon neutrality in urban water systems ..... 335
*Jorge, Catarina; Almeida, Maria do Céu; Loureiro, Dalia; Cardoso, Maria Adriana; Covas, Dídia*

Impact of seawater inflows into drainage network on water for reuse treatment – case study of the Alvor irrigation system ..... 337
*Oliveira, Paulo Bettencourt; Raposo, Carlos*

Time frequency analysis of anomalies in water distribution networks using pressure wave signals ..... 339
*Cabral, Marta; Matos, José Pedro; Pauseiro, Ana; Covas, Dídia*

Advanced image processing techniques to analyse the air volume variation in pressurized transient flows ..... 341
*Cabral, Marta; Ferreira, João Paulo; Quadrado, Bernardo; Covas, Dídia*

Hydraulic transients in water supply systems with hydropower plants ..... 343
*Covas, Dídia I. C.; Ferreira, João P.; Delgado, João N.; Cabral, Marta; Almeida, António B.*

Hydraulic analyses of a sustainable urban drainage system for highly urbanized areas ..... 345
*Li, James Yiuwah; Joksimovic, Darko; Fan, Celia; Fong, Patelle; Chen, Boji; Dicke;, Bianca*

Water neutral garden calculator ..... 347
*Teh, Tse-Hui; Butler, Adrian; Yousaf, Javid; Rautenberg, Svea; Watson, Carl*

Little catchments on the rooftop – effects of irrigation on water, matter and heat fluxes in green roofs ..... 349
*Helm, Björn; Herr, Laura Elisa; Walter, Richard; Goldberg, Valeri; Freudenberg, Peggy*

The use of hydrants for anomaly detection in the water distribution networks. Preliminary laboratory tests ..... 351
*Maietta, Filomena; Meniconi, Silvia; Capponi, Caterina; Crispino, Gaetano; Gisonni, Corrado; Brunone, Bruno*

Assessing the impact of urbanisation on combined sewer networks: A case study in Thessaloniki, Greece ..... 353
*Zafeirakou, Antigoni; Galiatsatou, Giota; Katsoulea, Anastasia; Gatzioura, Argyro; Nikoletos, Iraklis A.; Kapouniari, Maria*

A comparison between the potential for storm water control of blue roofs: results of field experiments ..... 355
*Gullotta, Aurora; Campisano, Alberto*

Advancing combined sewer network management: the Smart infiltration/inflow Management System (SiiMS) ..... 357
*Timiraos, Míriam; F. Águila, Jesús; Brandón, Óscar; Sobreira, Juan Luis; Garabato, Lucía; Barros, Carlos; Martínez, Alejandro; Díaz, Saul; García, Xela; Blázquez, Gonzalo; Forero, Andrea Camila; Morales, Nicolás*

Flood assessment and risk mitigation in Quelimane, Mozambique ..... 359
*Afonso, Inês; Furlan, Paloma; Manso, Pedro; Vicente, Pedro; Matos, Jorge*

Improved mixed flow model for large-scale multi-shaft pipeline ..... 361
*Lu, Yanqing; Zhou, Ling; Feng, Rui-lin; Xue, Zijian; Hu, Yinying; Chen, Qian-xun*

Comparative analysis of urban rainwater harvesting potentials: case studies of Tijuana, Mexico, Lisbon, Portugal, and Trondheim, Norway ..... 363
*Ocaranza, Laura; Matos Silva, Cristina*

Challenges and opportunities to manage wastewater and rainwater in Lisbon ..... 365
*Fernandes, Miguel; Almeida, Maria do Ceu; Fernandes, Fernando*

Lisbon urban water cycle observatory ..... 367
*Mendes, Rui; Dinis, Rui; Silva, Eduardo*

Reinventing urban water management: the Lisbon Drainage Master Plan (LDMP) ..... 369
*Diniz Vieira, Gonçalo; Silva Ferreira, José; Andrade Gomes, Tiago*

Numerical modelling and experimental verification in time domain of hydraulic rams ..... 371
*Ferras, David; Nasraoui, Saber; Dupont, Capucine*

Protecting Beira City (Mozambique) from frequent floods ..... 373
*Serra, Pedro; Prinsen, Geert; D'Orey, Victória; Pronker, Jenny*

Inclusion of natural areas in a holistic resilience assessment framework ..... 375
*Brito, Rita Salgado; Cardoso, Maria Adriana; Sfetsos, Athanasios; de la Cruz, Alex; Russo, Beniamino*

Climate change impacts on Lisbon floods and the potential benefits of nature-based solutions for adaptation ..... 377
*Antunes Dias, Luís Filipe; Ferrara, Francesco; Rodrigues, Miguel; Mourato, João; Telhado, Maria João; Freitas, Catarina*

AgIR Project Action no. 3 – characterization of wastewater affluent to wastewater treatment plants from hospital units in the municipality of Lisbon ..... 379
*Silva, Dora; Bértolo, Liliana; Cardoso, Eugenia; Bento, Diogo; Pecurto, Catarina; Teixeira, Pedro*

## Theme D: Numerical and experimental methods

Microplastic particles in cohesive sediment mixtures as an additional factor influencing erosion ..... 383
*Haun, Stefan; Ponce, Maria; Htun, Naung Naung; Wieprecht, Silke*

Horizontal wave paddle for wave-current interaction experiments ..... 385
*Muller, Gerald*

Hybrid physically based and machine learning model for streamflow prediction ..... 387
*López-Chacón, Sergio Ricardo; Salazar, Fernando; Bladé, Ernest*

Parameters of flow over a Coanda screen by Particle Image Velocimetry (PIV) measurements ..... 389
*Guachamín Paladines, Katherine Xiomara; García Bermejo, Juan Tomás; Carrillo Sánchez, José María; Castillo Elsitdié, Luis Gerardo*

From hindcast to forecast with distributional neural networks in water demand forecasting ..... 391
*Johnen, Gregor; Niemann, André; Hutwalker, Alexander; Donner, Christoph*

Local analysis of the gas exchange in a step-and-pool configuration via numerical simulation ..... 393
*Peruzzo, Paolo; Durighetto, Nicola; Botter, Gianluca*

Non-hydrostatic Galerkin model with linear/quadratic weighted average pressure ..... 395
*Calvo Gobbetti, Lucas Enrique; De Padova, Diana; Mossa, Michele; Guerra, Gisselle*

Investigation of negatively inclined buoyant jets with RANS and LES numerical simulations ..... 397
*Alvir, Marta; Lučin, Ivana; Sikirica, Ante; Kranjčević, Lado*

Machine learning approach to modelling compound coastal-fluvial flooding..... 399
*Olbert, Agnieszka Indiana; Moradian, Sogol*

Influence of different numerical setups on scour pattern at the initial scour stage next to bridge pier protected with riprap..... 401
*Harasti, Antonija; Gilja, Gordon; Adžaga, Nikola; Žic, Mark*

Modelling the velocity coefficient $\alpha$ for the optimization of discharge estimation by non-contact techniques..... 403
*Alongi, Francesco; Nasello, Carmelo; Mattina, Calogero; Pumo, Dario; Noto, Leonardo Valerio*

A comparative analysis of flow velocities at the outlet structure of Alqueva II pumped storage power plant..... 405
*Oliveira, Adriano; Fernandes, Irene; Viseu, Maria Teresa; Zorn, Marco; Riedelbauch, Stefan*

Parameterization of roughness distribution on floodplains in 2D shallow-water simulations..... 407
*Travert, Jean-Paul; Goeury, Cédric; Bacchi, Vito; Zaoui, Fabrice; Boyaval, Sébastien*

A comparative analysis of deep learning techniques for river flow forecasting in northwest Spain ..... 409
*Farfán-Durán, Juan F.; Cea, Luis*

Why computational fluid dynamics is mandatory in physical modelling of large hydraulic structures: a six-step methodology of integration..... 411
*Sassetti Mendes, Lourenço; Viseu, Teresa; Melo, José F.; Muralha, António*

Hydraulic performance for innovative erosion protection systems ..... 413
*Freitas, Diogo; Molano, Laura; Garcia, Diego; Torres, Ginna*

Hydraulic resistance of near-natural floodplain vegetation: a dataset for validating numerical models using a laboratory scale model..... 415
*Folke, Frederik; Aberle, Jochen*

Surface flow velocity estimations in low-luminosity environments using quinine-based tracer techniques . 417
*Zehsaz, Soheil; de Lima, João L. M. P.; de Lima, M. Isabel P.; Isidoro, Jorge M. G. P.; Martins, Ricardo*

Visualisation and simulation of solute transport in water distribution networks..... 419
*Peng, Zhangjie; Piazza, Stefania; Sonnenwald, Fred; Corredor Garcia, Jesus Leonardo; Freni, Gabriele; Guymer, Ian*

Free surface velocity measurement in highly-transient viscoplastic flows: combining NIR surface detection and PIV techniques ..... 421
*Martínez-Aranda, Sergio; García-Palacín, Ignacio; García-Navarro, Pilar*

Effect of submergence ratio on flow characteristics of rigid vegetation array..... 423
*Haspolat, Emre; Koken, Mete*

Design of a low-head shaft driven contra-rotating reversible pump turbine for pumped hydro storage application..... 425
*Joseph, Melvin; Zangeneh, Mehrdad; Ruiz, Ruben Ansorena; Goseberg, Nils*

Quadrant analysis of flow structures downstream of a bridge pier protected with riprap ..... 427
*Gilja, Gordon; Fliszar, Robert; Harasti, Antonija; Valyrakis, Manousos*

Sensitivity analysis of the distributed hydrological model SWAT to the Curve Number (CN2) parameter..... 429
*Gomes, Kaline Muriel de Figueiredoo; Silva, Jonathan Mota; Saad, Sandra Isay*

Insights from energy dissipation basin downstream of free-falling jets through numerical simulations ..... 431
*Ros-Bernal, Alicia; Carrillo, José M.; García, Juan T.; Castillo, Luis G.*

Numerical simulation of head losses at fish-friendly fine screens..... 433
*Ozbey, Cumhur; Kucukali, Serhat*

Machine learning-based hydropower turbine designs ..... 435
*Sikirica, Ante; Alvir, Marta; Čarija, Zoran; Kranjčević, Lado*

Generalizing hydraulic-based graph neural networks to irregular meshes and time-varying boundary conditions..... 437
*Bentivoglio, Roberto; Isufi, Elvin; Jonkman, Sebastiaan Nicolas; Taormina, Riccardo*

Experimental investigation of flow turbulent structures along pier spacing in open channel..... 439
*Ikani, Nima; H.Pu, Jaan; Cooke, Kavian*

Analysis of flow velocity profile for immobile bed condition next to bridge pier protected with riprap ..... 441
*Gilja, Gordon; Opačak, Luka; Harasti, Antonija; Valyrakis, Manousos*

Machine learning methodologies for leakage flow in a masonry dam (Santa Fe's dam) ..... 443
*Bonet, Enrique; Yubero, Maria Teresa; Sanmiquel, Lluís; Bascompte, Marc*

Innovative Image-based techniques for scour monitoring and measurement around offshore foundations ..... 445
*Bento, Ana Margarida; Fazeres-Ferradosa, Tiago; Chambel, João; Miranda, Filipe; Cabral, Tomás; Rosa-Santos, Paulo; Taveira-Pinto, Francisco*

Experimental prediction of 1-dimensional riverbed deformation using machine learning along the Mogami River, Japan ..... 447
*Yamamoto, Tao; Kazama, So*

Dam break in power-law cross-sections channels with different upstream/downstream widths ..... 449
*Valiani, Alessandro; Caleffi, Valerio*

Sediment scaling effects in physical modelling on erosional and depositional patterns ..... 451
*Siedersleben, Jakob Johannes; Schuster, Marco; Achleitner, Stefan; Aufleger, Markus*

Dike failure experiments. Influence of inflow conditions and soil composition ..... 453
*Jónatas, Ricardo; Amaral, Sílvia; Aleixo, Rui; Palinhos, Marta; Viseu, Teresa; Ferreira, Rui*

A new regulation system for PRS turbines ..... 455
*Picone, Calogero; Sinagra, Marco; Tucciarelli, Tullio*

Cross border cascading hazard scenarios in sava river basin – results of the CROSScade project ..... 457
*Novak, Gorazd; Rak, Gašper; Četina, Matjaž); Žižmond, Jure; Anžlin, Andrej; Kosič, Mirko*

Statistically sound approach to compare oil patterns and assess the accuracy of the forensic findings ..... 459
*Rocha, Ana Catarina; Palma, Carla; Bettencourt da Silva, Ricardo*

Planning and development of burst event field tests in a real water distribution network ..... 461
*Ferreira, Bruno; Caetano, João; Almeida, Soraia; Carriço, Nelson; Covas, Dídia*

AI-Anomaly Project: condition assessment of urban water assets through the detection of cracks based on artificial intelligence methods ..... 463
*Cabral, Marta; Matos, José Pedro; Silva, Ana; Valença, Jónatas; Grau, Isel; Correia, Tiago*

Large eddy simulation in a lateral cavity physical model ..... 465
*Carvalho, Rita; Restrepo, Steven; Ferreira, Rui*

Numerical simulation of a plunging jet. Performance comparison between volume-of fluid and two-phase Euler solvers ..... 467
*Muralha, António; Melo, José F.; Ramos, Helena M.*

Experimental investigation of microplastics entrainment in grid-generated turbulence: effect of size and shape ..... 469
*Shamskhany, Arefeh; Karimpour, Shooka*

Power performance assessment of SC-Darrieus vertical axis water turbine using CFD simulation ..... 471
*Karakaya, Derya; Elçi, Şebnem*

Photogrammetry for flow measurement at the air-water interface of flow past a semi-circular cylinder ..... 473
*Trieu, Hang; Bergström, Per; Hellström, Gunnar; Sjödahl, Mikael*

3D simulation of landslide generated waves with OpenFOAM ..... 475
*Louis-Napoléon, Aurélie; Heinrich, Philippe; Abadie, Stéphane*

Numerical simulation of flow patterns around triple square pier: vortices formation ..... 477
*Ikani, Nima; Pu, Jaan H*

Application of machine learning techniques for the generation of optimal layouts in branched water networks ..... 479
*del Teso, Roberto; Gómez, Elena; Montaña, Álvaro R.; Estruch-Juan, Elvira*

Modified discharge rating curve applicable under strong backwater effects due to nearby reservoirs ..... 481
*Marinheiro, Rui; Matos, José Pedro; Matos, Jorge; Sousa, Vitor Faria e; Meireles, Inês; Mahunguana, Manuel*

Numerical modelling of the Canales dam middle outlet ..... 483
*Castejon Zapata, Maria; Lopez Gomez, David*

Assessing the impacts of simplified methodology and shuttle radar topography mission in inundation map ..... 485
*Salgado, Sérgio Ricardo Toledo; Carvalho, Elsa Maria da Silva; Viseu, Maria Teresa; Oliveira, Othon Fialho*

Physical model tests on slope deformation at mining pit lakes due to wave impact ..... 487
*Heyer, Torsten; Stamm, Jürgen; Raabe, Paul; Dahmen, Dieter*
Optimization of supervised learning chain models for monthly flow prediction ..... 489
*Berbić, Jadran; Ocvirk, Eva*
On the performance assessment of hydro-morphodynamic models: fuzzy logic versus subjective correlation ..... 491
*Schwindt, Sebastian; Grigull, Paul Jacques; Negreiros, Beatriz; Haun, Stefan*
Wake characteristics of flow past circular cylinder with and without helical strakes in open channels ..... 493
*Thakurta, Abhinav; Balachandar, Ram*
Granular cooling of uni-sized particles during jamming process ..... 495
*Mendes, Solange Valente; Aleixo, Rui; Larcher, Michele; Amaral, Sílvia; Ferreira, Rui M.L.*

## Theme E: Climate change and risk mitigation

Exploring the escalating occurrence of heatwaves in Portugal: insights from a validated ERA5-Land dataset from 1980 to 2021 ..... 499
*Espinosa Villalpando, Luis Angel; Portela, Maria Manuela*
Characterization of extreme warm events in the Lisbon region (Portugal) based on ERA5-Land data ..... 501
*Freitas, Laryssa Mariana Moreira; Portela, Maria Manuela; Espinosa, Luis Angel; Matos, José*
Understanding the evolving landscape of droughts in a changing climate: exploring global responses of different drought types ..... 503
*Hosseinzadehtalaei, Parisa; Termonia, Piet; Tabari, Hossein*
The role of governance structure in shaping global risks of compound hot-dry events ..... 505
*Tabari, Hossein*
Water availability analysis along navigable waterways in Flanders using conceptual modelling and time series analysis ..... 507
*Breugelmans, Laurens; Bertels, Daan; Willems, Patrick*
Analysis of historical drought in Lisbon region, in the west of Portugal, using Reconnaissance Drought Index, RDI ..... 509
*Abd-Elhamid, Hany; Zelenakova, Martina; Portela, Maria Manuela; Espinosa, Luis Angel; Oskoui, Issa; Baranczuk, Jacek; Baranczuk, Katarzyna*
Addressing class imbalance problems in data-driven rainfall-runoff modelling ..... 511
*Vilaseca, Federico; Chreties, Christian; Castro, Alberto; Gorgoglione, Angela*
Evaluation of the effects of climate change on flood, case study: Cork, Ireland ..... 513
*Moradian, Sogol; Olbert, Agnieszka Indiana*
Exploring the effectiveness of nature-based solutions through the assessment framework tool implemented within the H2020 PHUSICOS project ..... 515
*Pugliese, Francesco; Ascione, Giuseppe; Giugni, Maurizio*
Effective flood emergency response: rapid deployment solutions ..... 517
*Freitas, Diogo; Molano, Laura; Garcia, Diego; Torres, Ginna*
Enhancing flood exposure analysis of cultural heritage ..... 519
*De Lucia, Claudia; Franceschini, Serena; Francini, Carlo; Castelli, Fabio; Arrighi, Chiara*
Identification of compound flooding hotspots along the Andalusian coastline (Spain) ..... 521
*Del Rosal Salido, Juan; Silva de Santana, Marcus; Bermúdez, María; Ortega-Sánchez, Miguel*
Temporal compounding of hydrological extremes across the Upper Jhelum basin in a changing climate ... 523
*Ansari, Rubina; Casanueva, Ana; Grossi, Giovanna*
River monitoring in extreme low flow using Sentinel-2 and Landsat 9 imagery: the lower Tagus River (Portugal) ..... 525
*Gerardo, Romeu; Pedroso de Lima, Isabel; Pedroso de Lima, João*
SIMPCCe: A software tool for the analysis of reservoir inflows under climate change scenarios ..... 527
*Navas, Salvador; del Jesus, Manuel*
Multivariate models for flood prediction: a glimpse into the future ..... 529
*Urrea Méndez, Diego Armando; Gómez Rave, Dina Vanessa; Navas, Salvador; del Jesus Peñil, Manuel*

Save OceanVille: a risk game enhancing communication among public decision-makers ..... 531
*Merino, Marta*

River-basin restoration hydraulic complexities in some Estonian rivers ..... 533
*Laanearu, Janek*

Simulation of the Brague flood of October 2015 in southeast of France ..... 535
*Cordier, Florian; Davarend, Thibaut; Ah-Woane, Emmanuel; Amama, Zied; Sochinskii, Arkadii; Majdalani, Samer; Moussa, Roger; Delestre, Olivier*

Drought characterization for the Ciénaga Grande de Santa Marta (Colombia) ..... 537
*Cortés, Andrés Felipe; Bateman, Allen; Medina, Vicente*

Regional assessment of climate change impacts. The case of the Ceira River basin, Portugal ..... 539
*Costa, Miguel; Mendes, Juliana; Maia, Rodrigo*

Assessing drought conditions using precipitation values completed with K-Nearest Neighbors (KNN) ..... 541
*Yesilyurt, Sefa Nur; Yildiz, Eyyup; Onusluel Gul, Gulay; Dalkilic, Huseyin Yildirim*

Investigation the impact of fime interval between rainstorms and wave storms to characterize compound events in the NW Mediterranean ..... 543
*Aguilera Vidal, Maria; Jiménez, José.A; Ortego, M.I; Sanuy, Marc*

Urban wastewater infrastructure adaptation strategies: methods and implementation towards climate change resilience ..... 545
*Diogo, Paulo A.; Rodrigues, António C.; Mano, António P.; Miranda, Pedro A.; Santos, Susana; Inocêncio, Paulo; Santos, Ana S.; Broco, Nuno; Coelho, Joana P.*

Hydropower production impacts from climate change future scenarios at the Cabril Dam, Portugal ..... 547
*Diogo, Paulo A.; Rodrigues, António C.; Duarte, Gonçalo A.*

A methodology for climate-proofing inland navigation infrastructure projects: the Seine-Schelde project ... 549
*Lopez-Fabara, Carmen; Elango, Nivedha; De Sutter, Renaat; De Winter, Annick; Serpentier, Frank; Van Waeyenberge, Jeroen; Ratinckx, Peter; Proença, Bárbara*

Prevalence and physical properties of Urban Flood Drifters (UFDs) in extreme floods ..... 551
*Bayón, Arnau; Valero, Daniel; Franca, Mário J.*

A multipurpose alpine lake – modelling supplies and withdrawals in view of climate change ..... 553
*Ruegg, Evanice; De Cesare, Giovanni; Gillioz, Alexandre*

Monitoring surface soil moisture, evapotranspiration, and vegetation greenness from multi-level observations in the UAE dryland ecosystems ..... 555
*Kim, Youngwook; Abdelhamid, Abdalla; Meerasha, Benazir; Kim, Young Ki; Kim, Ashley*

Analysis on spatial return period of extreme rainfall in different regions ..... 557
*Kazama, So; Yanagisawa, Hajime*

Assessing hydrological impacts of urbanization and climate change in Orunia basin, Gdańsk, Poland ..... 559
*Gulshad, Khansa; Szydłowski, Michał*

Impact of climate change on the supply-demand balance of collective irrigation systems. methodological approach ..... 561
*Ferreira, Antónia; Rolim, João; Brandão, Cláudia; Cameira, Maria do Rosario*

Assessment of blue water availability for agriculture in the Mediterranean ..... 563
*Garrote, Luis; Sordo-Ward, Alvaro; Bianucci, Paola*

Fine scale rainfall disaggregation in Greece using RBLRPM ..... 565
*Skroufouta, Sofia; Baltas, Evangelos*

Coastal adaptation strategies for infrastructures: a global to local approach ..... 567
*Lara, Javier; Fernandez, Alberto; Lucio, David; Alvarez de Eulate, Maria; Losada, Inigo*

Mapping inundation of estuarine margins driven by ocean and fluvial forcings ..... 569
*Fortunato, André B.; Freire, Paula; Ana, Rilo; Viseu, Teresa; Rodrigues, Marta*

Flash flood risk assessment in data scarce regions vulnerable to climate change: hydrological lessons learnt from Jordan ..... 571
*Hohmann, Clara; Maus, Christina; Leberke, Hanna; Awad, Ahmad; Hoffmann, Peter; Ziegler, Dörte*

A mechanical-based calibration for a rapid vulnerability assessment of masonry buildings subject to floods ..... 573
*Liguori, Francesco Salvatore; Capparelli, Giovanna; Madeo, Antonio; Versace, Pasquale*

On development of extreme rainfall intensity-duration-frequency relations for urban water infrastructure design in the climate change context ..... 575
*Nguyen, Van Thanh Van*

Anthropogenic disaster vulnerability in European rivers ..... 577
*Rowinski, Pawel M.; Kalinowska, Monika B.; Okruszko, Tomasz; Parasiewicz, Piotr; Jozsa, Vilmos*

Numerical study to quantify the role of morphological parameters in the coastal flooding: Zarautz beach . 579
*Abalia, Aritz; de Santiago, Iñaki; Garnier, Roland; Liria, Pedro; Epelde, Irati; Nieto, Asier; Morichon, Denis*

Evaluation of combined fluvial, coastal and pluvial flooding using a data-driven enhanced physically-based model: a case study in NW Spain..... 581
*Cea, Luis; Figueroa, Carlos A.; Farfán-Durán, Juan F.; Puertas, Jerónimo; Sopelana, Javier*

Assessing compound flooding hazard in estuaries by integrating a climate emulator and a hybrid model ..... 583
*Ortiz-Angulo Cantos, Jared; Camus Braña, Paula; Mendez Incera, Fernando; Castanedo Bárcena, Sonia; Jimenez Tobio, Mirian; Cagigal Gil, Laura; Pérez Díaz, Beatriz*

The Gloria storm January 2020, a state-of-the-art compound event ..... 585
*Llasat-Botija, Montserrat; Llasat, Maria Carmen; Marcos-Matamoros, Raül; Aguilera Vidal, Maria; Sanuy, Marc; Valdemoro, Herminia I; Castán, Salvador; Jimenez, José A.*

Stress test scenarios as a useful addition to a risk approach ..... 587
*de Bruijn, Karin; Slager, Kymo; Van de Hurk, Bart*

Lessons learnt from recent flood disasters in Europe: Indicative cases ..... 589
*Bento, Ana Margarida; Cordier, Florian; Dewals, Benjamin; El Kadi Abderrezzak, Kamal; Ferradosa, Tiago; Gisonni, Corrado; López-Jiménez, P. Amparo; Molinari, Daniela; Pummer, Elena; M. Rowiński, Paweł; Schröter, Kai; Stamou, Anastasios I.*

Probabilistic study of flooding and erosion processes in coastal zones of Andalucía (Spain) for the XXI century ..... 591
*Silva-Santana, Marcus Vinicius; Otiñar, Pedro; Cobos, Manuel; Magaña, Pedro; Millares, Agustín; Gutiérrez, David; Martín, Jorge; Arjona, Pablo; Lira-Loarca, Andrea; Baquerizo, Asunción*

## Theme F: Governance and water resources management

Comparative analysis of river management between France and China ..... 595
*Cao, Yixin; Wantzen, Karl Matthias*

A stakeholder-adapted methodology to identify feasible regions for managed aquifer recharge in the Mijares and Palancia basins (Spain) ..... 597
*Ghannem, Syrine; Bergillos, Rafael J.; Panagiotou, Constantinos F.; Paredes-Arquiola, Javier; Solera, Abel; Andreu, Joaquín*

A Brazilian approach to monitoring water governance and its governance system at different planning levels ..... 599
*Macena da Silva, Maycon Breno; Rios Ribeiro, Márcia Maria*

Multi-level analysis of water governance through the robustness framework ..... 601
*Silva, Maycon Breno Macena da; Veiga, Maria Eduarda Barbosa da; Ribeiro, Márcia Maria Rios; Galvão, Carlos de Oliveira*

A modelling framework and a testbed model for demonstrating novel greenhouse wastewater treatment and nutrient recovery..... 603
*Evans, Barry; Khoury, Mehdi; Vamvakeridou-Lyroudia, Lydia; Chen, Otto; Mustafee, Navonil; Guleria, Tavishi; Broeke, Joep van den; Chen, Albert*

Small reservoir siting 'from scratch': merging GIS-based and participatory approaches in a multi-criteria analysis..... 605
*Arrighi, Chiara; Masi, Matteo; Piragino, Francesco; Castelli, Fabio*

Monitoring the water distribution network and its management optimisation: the Calvagese Della Riviera case study ..... 607
*Azizi Nadian, Hossein; Brunati, Filippo; Peli, Marco; Ranzi, Roberto*

Integrated hydraulic modeling for water level control in the Moëres lowland, using Delft3D-FM coupled with real time control tool..... 609
*Achour, Mohamad; Masson, Eric; Parent, Briz; Blanpain, Olivier*

Sensitivity of water stress indices to climate change in Tuscany (Italy)..... 611
*De Simone, Marco; Arrighi, Chiara; Castelli, Fabio*

Does sampling frequency matter? Comparative analysis of physicochemical quality elements in the Manzanares River (Madrid, Spain) ..... 613
*Cortés Sánchez, Francisco M.; Díaz-Redondo, María; García Sánchez-Colomer, Manuel Ramón*

Integrating hydrological modelling and system dynamics tools for understanding Water-Ecosystems-Food Nexus: hints from the Tarquinia area (Italy) ..... 615
*Yaseen, Marwah; Portoghese, Ivan; Iacobellis, Vito; Vanino, Silvia; Baratella, Valentina; Fabiani, Stefano; Gunacti, Mert Can; Gul, Ali; Barbaros, Filiz; Giordano, Raffaele; Pagano, Alessandro*

A methodological approach for supporting socio-hydrological modelling of a complex Nexus system ..... 617
*Panciera, Claudia; Portoghese, Ivan; Pagano, Alessandro; Giordano, Raffaele; Yesilyurt, Sefa Nur; Gunacti, Mert Can; Cetinkaya, Cem Polat; Onusluel Gul, Gulay; Najar, Mohamed; Lopez, Estrella; Bea, Manuel*

A web-based decision co-creation platform for the circular economy by representing wastewater treatment, the extraction of value-added compounds, biogas, water and nutrients ..... 619
*Khoury, Mehdi; Evans, Barry; Guleria, Tavishi; Van Den Broeke, Joep; Vamvakeridou-Lyroudia, Lydia; Chen, Otto; Mustafee, Navonil; Chen, Albert .S*

Would short term online monitoring improve the WFD-sampling strategy? Subsampling of high frequency data from four watersheds in Saxony..... 621
*Benisch, Jakob; Helm, Björn; Krebs, Peter*

Impact of beaver activity on water resources in the catchment and water quality..... 623
*Zaborowski, Stanisław; Kałuża, Tomasz; Strzeliński, Paweł; Hammerling, Mateusz*

Aggregating opinions of the stakeholders in a fuzzy environment ..... 625
*Bakas, Thomas; Latinopoulos, Dionissis; Papadopoulos, Christofer; KAGALOU, Ifigenia; SPILIOTIS, MIKE*

Water 2.0 | going local – the territorial approach/Portuguese case – Grândola municipality ..... 627
*Varanda, Paulo; Pena, Edídila*

The impact of human activities on the flood risk ..... 629
*Rak, Gašper; Škerjanec, Mateja*

SDGs-EYES: a novel european project to enhance, integrate and monitor water-related SDG indicators ..... 631
*Latella, Melissa; Santini, Monia; Mancini, Marco; Miguel-Lago, Monica; Natali, Stefano; Lazzarini, Michele; Padulano, Roberta*

Water balance modeling of the Nile River behind Aswan High Dam and the future expectation..... 633
*Soliman, Mohamed*

Integrated approach to evaluate the role of floating farming for addressing disaster risk management and nexus between water-food-health-economy-human wellbeing..... 635
*Kumar, Pankaj; Ahsan, Md Nasif; Takahashi, Yasuo; Miwa, Koji*

DPSIR analysis of the closure of water resources in the Axarquía region (southern Spain) ..... 637
*Berbel, Julio; Diaz-cano, Esther; Montilla, Nazaret; Hurtado, Antonio*

Stakeholder-based WEFE system sustainability assessment: a SWOT analysis application on an agricultural mediterranean area..... 639
*Malamataris, Dimitrios; Chatzi, Anna; Babakos, Konstantinos; Pisinaras, Vassilios; Hatzigiannakis, Evangelos; Panagopoulos, Andreas*

Application and testing groundwater sustainability indicators for stressed semi-arid regions ..... 641
*García Salazar, Nicolás; Barreiras, Nuno; Costa, Luís; Monteiro, José Paulo*

The state of european river network connectivity ..... 643
*Leite, Tamara; Duarte, Gonçalo; Segurado, Pedro; Ferreira, Maria Teresa; Branco, Paulo*

Adaptive agreements on benefits sharing for managed aquifer recharge in the Mediterranean region ..... 645
*Conrad, Anika; Heim, Ronjon; Bergillos, Rafael; Andreu, Joaquín; Rohde, Charlotte; Stefan, Catalin; Panagiotou, Constantinos; Chekirbane, Anis; Leitão, Teresa; Ghannem, Syrine; Solera, Abel; Paredes, Javier*

Assessment of the impact of drought management protocol in the Guadalquivir River basin applying hydro-micro-macro-economic modelling ..... 647
*Valle-García, Ángela; Montilla-López, Nazaret M.; Berbel, Julio; Gutiérrez-Martín, Carlos*

The right to the city as lens for a multifaceted analysis of Managed Aquifer Recharge ..... 649
*Alpes, Keyla; L. Craveiro, João; E. Leitão, Teresa*

Water reuse in the context of water planning: challenges of the transnational Guadiana River basin ..... 651
*Sousa, Maria Carolina; Matos, Manuel Victor; Miranda, Ana Catarina; Cardoso, Andreia Saavedra; Fidelis, Teresa*

Uncertainties in hydrological-hydrodynamic catchment flood modeling..... 653
*De Vos, Leon Frederik; Rüther, Nils; Broich, Karl*

Flood analysis in a small catchment following the July 2021 events in Belgium: respective contributions from runoff and overflowing ..... 655
*Soares-Frazao, Sandra; Zech, Yves; Meurice, Robin; Delpierre, Nathan; Gousenbourger, Pierre-Yves*

Performance of water delivery by direct pumping system at farm level: case study of Abu-Gabal Tertiary canal, Egypt ..... 657
*Meleha, Shimaa; Aly, Ahmed; El-Ansary, Ahmed; Soliman, Mohamed*

Indicators to promote sustainable and climate resilient water management at urban natural spaces ..... 659
*Cardoso, Adriana; Fernandes, João Nuno; Barbosa, Ana Estela*

Water demand and usage trends among group water schemes: implication for water conservation ..... 661
*Antwi, Sarpong Hammond; Getty, David; Rolston, Alec; Linnane, Suzanne; Smith, Róisín Dowd*

How can we adapt together? Bridging water management and city planning approaches to climate change ..... 663
*Vinagre, Vítor; Fidélis, Teresa; Luís, Ana*

Impact of implementation of efficiency targets in public water supply ..... 665
*Díaz-Cano Ocaña, Esther; Berbel, Julio; Hurtado, Antonio*

Impacts of the implementation of efficiency targets at river basin scale ..... 667
*Diaz-Cano, Esther; Berbel, Julio; Expósito, Alfonso*

Financing water stewardship: introducing impact investments to address water impacts of food production value chains ..... 669
*Saikkonen, Liisa; Oinonen, Soile; Sojamo, Suvi; Penttilä, Outi; Diaz-Cano, Esther*

The Axarquía (SE Spain) as Living Lab for testing governance innovations aiming at a sustainable management of water resources ..... 671
*Sánchez García, Damián; Sojamo, Suvi*

Occurrence and distribution of Per- and Polyfluoroalkyl substances in San Francisco Bay Area drinking water ..... 673
*Kurwadkar, Sudarshan; Hoffman-Davies, Emma*

On the generalization of image-based river turbidity monitoring in different hydrological conditions ..... 675
*Miglino, Domenico; Saddi, Khim Cathleen; Isgrò, Francesco; Jomaa, Seifeddine; Rode, Michael; Manfreda, Salvatore*

# POSTERS

## Theme A: Aquifers, rivers, reservoirs and dams

Preliminary results of the monitoring of the insect community in a periurban section of the Manzanares River (Madrid, Spain) ..... 679
*Ibarra Mellado, Sergio; García Sánchez-Colomer, Manuel Ramón; Young Sánchez Mateos, Arturo David; Viejo Montesinos, José Luis*

Development of a simple reservoir water level controller ..... 680
*Nogueira, Filipa N.; Pinho, José L.S.*

Stormwater attenuation & enhanced infiltration system to mitigate flood and drought conditions in urban and rural environments: part II ..... 681
*Stephen D. Thomas; George R. French; Jamie Bates; Joseph A. O'Meara; Matthew P. Dale; Bruno Casal*

Impact of beaver activity on water resources in the catchment and water quality ..... 682
*Zaborowski, Stanisław; Kałuża, Tomasz; Strzeliński, Paweł; Hammerling, Mateusz*

Assessment of dam inflow forecasting by blending ensemble NWP rainfall with radar prediction ..... 683
*YU, Wansik; PARK, Jinhyeog; KANG, Shinuk; KIM, Kyoungpil; KIM, Mieun*

Reducing storage volume causes loss of water quality in semi-arid reservoirs and reduces the diversity of benthic macroinvertebrates ..... 684
*Medeiros, Carlinda Railly; Ferreira, Lucianna Marques Rocha; Costa, Laisa Daiana Alcântara; Nóbrega, Rodolfo Bezerra; Cunha, John Elton de Brito Leite; Molozzi, Joseline; Galvão, Carlos de Oliveira*

Streamflow predictions in ungauged basins using remote sensing information and artificial intelligence ... 685
*Kim, Sangdan; Won, Jeongeun; Seo, Jiyu*

Understanding the impacts of river network fragmentation on freshwater fish species ... 686
*Leite, Tamara; Borgwardt, Florian; Branco, Paulo*

Implementation of finite element techniques for the displacement control of constructed dams ... 687
*Yubero, Maria Teresa; Bonet, Enrique; Sanmiquel, Lluis; Bascompte, Marc*

## Theme B: Estuaries, coasts and ports

Assessing shoreline changes using satellite and UAV imagery: a Kinmen coast case study in Taiwan ... 688
*Huang, Wei-Po; Hsu, Jui-Chan; Ye, Chun-Jhen; Lin, Sin-Hong*

Reduction of microplastic pollution in shipbuilding industry ... 689
*Lučin, Ivana; Alvir, Marta; Družeta, Siniša; Lučin, Bože*

Unbalanced sediment flux caused by tidal pumping and residual circulation in the meso-tidal Yeosu Bay ... 690
*Ha, Ho Kyung; Kim, S.I.; Seo, J.Y.; Park, J.H.; Kim, P.J.*

Machine learning analysis of elemental variation in sediment cores from Boka Kotorska Bay – Adriatic Sea ... 691
*Manojlovic, Vaso D; Radomirović, Milena; Tanaskovski, Bojan; Cantaluppi, Chiara; Degetto, Sandro; Stanković, Slavka*

AQUABREAK: An innovative nature-based solution for coastal resilience ... 692
*Proença, Barbara; Gomes, Andreia; Bosnic, Ivana; Rato, Lénia; Bendô, Raylton; Mendes, Diogo; Fonseca, Diogo*

The coastal challenge of climate adaptation: systemic approaches ... 693
*Perney, Marion Eva Pauline; Barroca, Bruno; Clemente, Maria Fabrizia; Heinzlef, Charlotte; Leone, Mattia Federico; Thomas, Isabelle; Serre, Damien*

Occurrence of microplastic in Thai aquatic environment ... 694
*Kurwadkar, Sudarshan; Natalia, Grace; Kitpati Boontanon, Suwanna; Pathomsiri, Somchai*

## Theme C: Urban water

A surrogate-based optimization of urban-roofing strategies for flash flood control ... 695
*Kim, JiHyun; Choi, Suyeon; Panahi, Mahdi; Kim, Yeonjoo*

Decentralized management of urban wastewater through the implantation of artificial wetlands for the renaturalization of the Carraixet ravine ... 696
*Gil Martínez, Enric; Hernández Crespo, Carmen; Rodrigo Santamalia, Mª Eugènia; Asensi Dasi, Enrique Javier; Lidón Cerezuela, Luís; Benedito Durá, Vicent*

Stormwater attenuation & enhanced infiltration system to mitigate flood & drought conditions: part I ... 697
*Thomas, Stephen; French, George; Watson, James; O'Meara, Joseph; Dale, Matthew; Casal, Bruno*

Hydraulic modeling of the wastewater subsystem (SAR) of Serzedo ... 698
*Ribeiro, Vítor; Silva, Carlos; China, Hugo; Carraco dos Reis, Filipe*

Cadastral survey, cleaning, and video inspection of collectors – SAR Lever-Gaia ... 699
*Fonte, André; Nogueira, Pedro; China, Hugo; Carraco dos Reis, Filipe*

Roof-harvested rainwater health risk assessment: a case study in Lagos, Nigeria ... 700
*John, Chukwuemeka; Pu, Jaan*

Roof-top sediment deposition and microbial analysis in various sanitation environments ... 701
*John, Chukwuemeka; Pu, Jaan*

URCA!: climate change scenarios, design storms and participatory approach to improve urban resilience ... 702
*Palla, Anna; Gnecco, Ilaria; Pirlone, Francesca; Grossi, Giovanna; Pezzagno, Michèle; Pietta, Antonella; Dada, Arianna; Maglionico, Marco; Campisano, Alberto Paolo; Piro, Patrizia; Ermini, Ruggero; Fattore, Carmen; Giudicianni, Carlo; Todeschini, Sara; Creaco, Enrico Fortunato*

## Theme D: Numerical and experimental methods

Sensitivity analysis of the distributed hydrological model SWAT to the Curve Number (CN2) parameter ..... 703
*Gomes, Kaline Muriel de Figueiredo; Silva, Jonathan Mota; Saad, Sandra Isay*

Cross border cascading hazard scenarios in Sava River basin – results of the CROSScade project ..... 704
*Novak, Gorazd; Rak, Gašper; Četina, Matjaž); Žižmond, Jure; Anžlin, Andrej; Kosič, Mirko*

Depth determination in coastal regions using a machine learning model and a time series of PlanetScope images ..... 705
*Santos, Rúben; Quartau, Rui*

Impact of the random forest algorithm parameterization on the determination of depth in coastal regions using PlanetScope images ..... 706
*Santos, Rúben; Quartau, Rui*

Statistically sound approach to compare oil patterns and assess the accuracy of the forensic findings ..... 707
*Rocha, Ana Catarina; Palma, Carla; Bettencourt da Silva, Ricardo*

Air characteristics during rapid filling of long distance water transmission pipes ..... 708
*Feng, Rui-lin; Zhou, Ling; Besharat, Mohsen; Lu, Yanqing; Chen, Qian-xun; Hu, Yinying; Li, Yunjie*

The comparison of a mechanistic model with a machine learning model for microplastic modelling in Gediz River basin, Türkiye ..... 709
*Kazanci, Yiğithan; Baycan, Neval; Alyürük, Nefise; Gündüz, Orhan*

## Theme E: Climate change and risk mitigation

Coastal risk assessment and application of the small islands: case study on Green Island and Orchid Island in Taiwan ..... 710
*Ye, Chun Jhen; Huang, Wei Po; Hsu, Jui Chan*

Effective Flood emergency response: rapid deployment solutions ..... 711
*Freitas, Diogo; Molano, Laura; Garcia, Diego; Torres, Ginna*

Dam-break flood risk assessment and response actions within self-rescue zone ..... 712
*de Sousa Lima, Anderson Matheus; de Oliveira Galvão, Carlos*

The evaluation of water supply capability for drought management ..... 713
*Park, Jin Hyeog; Kang, Shin Uk; Choi, Hyun Gu; Yu, Wan Sik*

Cascading effects and scenario risk assessment for damaging geohydrological events ..... 714
*Biondi, Daniela; Bloise, Sara; Versace, Pasquale*

## Theme F: Governance and water resources management

A framework and indicators for global water security assessment ..... 715
*Lee, Joo-Heon; Park, Seo-Yeon; Kim, Young-Jun; Kim, Jong-Suk*

Does sampling frequency matter? Comparative analysis of physicochemical quality elements in the Manzanares River (Madrid, Spain) ..... 716
*Cortés Sánchez, Francisco M.; Díaz-Redondo, María; García Sánchez-Colomer, Manuel Ramón*

Management of electric network failure in mini-hydro plants ..... 717
*Sinagra, Marco; Picone, Calogero; Accetta, Angelo; Pucci, Marcello; Tucciarelli, Tullio*



# Keynote Lectures

# River Bars and Meanders: from the Lab to the Real World

Ana Maria FERREIRA da SILVA

Queen's University, Kingston, ON, Canada
anamaria.dasilva@queensu.ca

ABSTRACT

A stream flowing in alluvium deforms its bed surface so as to form ripples, dunes, bars, etc., and commonly deforms also its channel as a whole so as to create, in plan view, meandering or braiding patterns. One can say that, in general, an alluvial stream undergoes a variety of hydro-morphodynamic processes leading to the emergence of a variety of alluvial forms that can be either bed or plan forms (da Silva and Yalin 2017). This lecture focuses on meandering and related alluvial processes (free alternate bars, for the sake of simplicity henceforth referred to simply as alternate bars).

As is well-known, meandering is the plan form most commonly acquired by rivers, especially in the low-land alluvial plains. Sediments redistributed in meandering streams create localized erosion and deposition zones at the bed and banks (da Silva and Yalin 2017, Leopold et al. 2020), ultimately leading to the progressive plan view evolution of the stream through downstream migration and lateral expansion (Friedkin 1945, Brice 1974, Hooke 1980, da Silva and Yalin 2017). These processes make meandering streams highly dynamic and complex systems, posing great challenges to river engineers and scientists – which explains why various aspects of meandering have been the object of extensive theoretical, experimental and numerical research for many years.

While invaluable, the experimental research on the topic shines light on a larger issue, applicable to many fields, and which can be synthesized in the following sentence: "What we observe in the laboratory is always true, but may not be the total truth". This matter is illustrated in this lecture by focusing on two topics, with the first topic being the initiation of meandering, and the second, the nature of the secondary (or cross-circulatory) motion in meandering streams.

Previous and highly notable large-scale experiments leading to the view that alternate bars are the cause of meandering are juxtaposed against more recent observations and work demonstrating that the initiation of meandering in alluvial streams is not always preceded by the occurrence of alternate bars. A turbulence-based explanation for both the emergence of alternate and the development of an incipient meandering plan form, treating these as two distinct manifestations of the same phenomenon, is briefly outlined.

Secondary motion (i.e. motion in the direction normal to the primary or longitudinal motion) results from an imbalance between cross-sectional net pressure force and centrifugal force, and is an essential feature of the flow in meandering streams. Secondary motion alters the magnitude and direction of boundary shear stress and sediment transport, erosion and depositon of bed and banks, mixing processes, transport of pollutants, and other processes (Baek et al. 2006, Blanckaert 2011, Moncho-Esteve et al. 2017). The classical view on secondary motion is derived from numerous studies on fully developed and relatively deep flow in circular bends (for reviews, see Chang 1988 and da Silva and Yalin 2027), and consists of fluid in the upper layers moving towards the outer bank, and in the lower layers moving towards the inner bank. In cross-sectional view, this motion appears as a single cell, sometimes referred to as primary or center region cell (see e.g. Kang and Sotiropoulos 2011, Moncho-Esteve et al. 2017). Meandering bed deformation has been directly attributed to this type of motion – with it causing the bed material to move from the outer bank to the inner bank and eventually leading to the formation of a "point bar" around the apex at the inner bank, and a laterally adjacent pool.

Does the above "picture" of secondary motion reflect the conditions in real meandering rivers? And can the above explanatiom for bed deformation, primarily derived from laboratory observations in circular channels having rather small values of width-to-depth ratio ($B/h$), truly be generalized to the case of real meandering rivers? This question is pertinent as the values of $B/h$ of large natural meandering streams are very large (often 50-100, say), while the intensity of cross-circulation gradually decreases with increasing values of $B/h$. Is there a threshold value of $B/h$ beyond which the effect of cross-circulatory motion becomes of secondary importance where the bed deformation is concerned? And if yes, what kind of flow and sediment transport mechanisms could then be responsible for the bed deformation? The second part of the lecture deals with these questions.

**References**


Baek KO, Seo IW, Jeong SJ (2006) Evaluation of dispersion coefficients in meandering channels from transient tracer tests, J Hydr Engrg, 132(10), 1021–1032.

Blanckaert K (2011) Hydrodynamic processes in sharp meander bends and their morphological implications, J Geophysical Res: Earth Surface, 116(F1), F01003.

Brice JC (1974) Evolution of meander loops, Geological Society of America Bulletin, 85(4), 581–586.

Chang HH (1988) Fluvial processes in river engineering, Wiley, New York.

da Silva AMF, Yalin MS (2017) Fluvial processes, 2nd edition, IAHR Monograph Series, CRC Press, Taylor & Francis.

Friedkin, JF (1945) A laboratory study of the meandering of alluvial rivers, United States Waterways Experiment Station, Vicksburg, Mississippi.

Hooke JM (1980) Magnitude and distribution of rates of river bank erosion, Earth Surface Processes, 5(2), 143–157.

Kang S, Sotiropoulos F (2011) Flow phenomena and mechanisms in a field-scale experimental meandering channel with a pool-riffle sequence: Insights gained via numerical simulation J Geophysical Res: Earth Surface, 116.

Leopold LB, Wolman MG, Miller JP, Wohl EE (2020) Fluvial processes in geomorphology, Courier Dover Publications.

Moncho-Esteve IJ, Folke F, Garcia-Villalba M, Palau-Salvador G (2017), Influence of the secondary motions on pollutant mixing in a meandering open channel flow, Env Fluid Mech, 17, 695–714.

# Hydro-environment research on climate change adaptation of water infrastructure

Anastasios STAMOU[1]

[1] Laboratory of Applied Hydraulics, Department of Water Resources and Environmental Engineering,

National Technical University of Athens, Greece
stamou@mail.ntua.gr

ABSTRACT

Water Infrastructure (WI) is vulnerable to the effects of Climate Change (CC) that can disrupt its functionality; thus, it needs to be adapted to CC. This adaptation needs to be performed following the EC's Technical Guidelines on "Climate-proofing Infrastructure" in combination with guides that are specific for WI, such as these issued by the Joint Assistance to Support Projects in European Regions (JASPERS). JASPERS' guides focus mainly and in detail on aspects related to climate hazards without examining at the required detail the engineering aspects of the WI, which are often based on the relevant hydro-environment research performed in Universities and Research Institutes, unless these are part of the official EC documents. The effective application of these guides in WI requires the utilization of this research in combination with experts' opinion. In this work, indicative works of the hydro-environment research on WI are presented and discussed in an integrated and systematic manner and suggestions for future research are made.

## 1. Introduction

Water Infrastructure encompassing water supply, wastewater, and stormwater works, ranks among the most significant sectors within the critical infrastructure framework, because it provides essential services to our communities and plays a vital role in maintaining our health and safety by preventing flooding and keeping our water courses clean. Water Infrastructure is vulnerable to the effects of Climate Change (CC) that include acute and chronic events, such as precipitation decrease and droughts, increased frequency of heavy precipitation events and river floods, storm surges, coastal floods and erosion, extreme winds, landslides and sediment erosion, wildfires and heat waves, temperature increase and sea level rise and saline intrusion (Stamou 2022). Aiming at fostering the development of resilient, climate-proof infrastructure, the European Commission released the Technical Guidelines on "Climate-proofing Infrastructure" for the period 2021-2027 (EC 2021). These guidelines, which incorporate both CC mitigation and adaptation strategies and mainstream climate considerations in future investment and development, are principally designed for project developers and experts involved in the infrastructure preparation. Additionally, they serve as a valuable resource for public agencies, implementation partners, investors, stakeholders, and others. Infrastructure development must now incorporate a methodology for its climate proofing, along with any of the limitations identified. Such a methodology is virtually a Climate Risk and Vulnerability Assessment (CRVA) that is an effective tool to: (1) determine the relevant climate hazards to infrastructure via the assessment of vulnerability and risk; and (2) inform the implementation of adaptation measures. In the literature, there exist various approaches for conducting a CRVA for WI; most applications are usually performed in global, continental, national, regional, river basin or city scale that are categorized as "sectoral" addressing the risks to the sector or asset level and "systems approach" assessing the infrastructure as an interconnected network, i.e., accounting for dependencies among infrastructures categories. Very recently, JASPERS (2013) presented two guides for the climate proofing of water and wastewater, and flood and disaster risk management projects. JASPERS' guides are systematic and practical; they are based on EC's Technical Guidelines, the relevant EC official documents, as well as IPCC's reports; for example, IPCC (2021). JASPERS' guides focus mainly and in detail on aspects related to climate hazards without examining at the required detail the engineering aspects of the WI that are based on the relevant hydro-environment research performed in Universities and Research Institutes, unless

these are part of the official EU documents. The effective application of these guides in WI requires the utilization of this research in combination with experts' opinion. There exists a significant number of research works in the literature focusing on the various aspects of WI adaptation to CC, such as the vulnerability, the risk analysis, and the adaptation measures for risk reduction, for example on the use of Nature Based Solutions (NBS) for flood risk reduction. In this work, indicative works of the hydro-environment research on WI are presented and discussed in an integrated and systematic manner and suggestions for future research are made.

## 2. Presentation of the hydro-environment research and discussion

The presentation of the hydro-environment research is performed following a CRVA procedure (Stamou et al., 2014) that is structured around five key steps.

The **description of the WI** is the first step and includes: (1.1) the identification of the main components of the WI and their time scale, and (1.2) the identification of the potential hazards that need to be considered for the WI (or its individual components) and the corresponding climate indicators for each potential hazard. The **CC assessment** that is performed in step 2 includes: (2.1) the selection of appropriate CC scenarios of the current and the potential future climatic (and socio-economic) conditions, and (2.2) the calculation/estimation of the values of the climate indicators for these conditions. The **vulnerability assessment** that is performed in step 3 comprises four analyses: (3.1) the exposure analysis; (3.2) the sensitivity analysis, (3.3) the adaptive capacity analysis; and (3.4) the vulnerability analysis. In the exposure analysis, the hazards that are relevant to the location of the WI system are identified, irrespective of its type, based on the values of the climate indicators (determined in step 2) for the current and future conditions. In the sensitivity analysis, hazards pertinent to the WI system are identified, irrespective of its location, by considering 6 thematic areas. The vulnerability analysis integrates the results from the exposure and sensitivity analyses to identify the potentially significant climate hazards of the WI. These hazards are investigated further in detail to assess their risk (step 4) and to propose adaptation measures (step 5). The **risk assessment** of the WI system includes three analyses: (4.1) the likelihood analysis, (4.2) the impact analysis, and (4.3) the risk analysis. The likelihood analysis looks at how likely the potentially significant climate hazards are expected to occur within the lifespan of the WI network, while the impact analysis looks at the consequences for every potentially significant hazard. The results of the likelihood and impact analyses are combined to formulate the risk matrix that summarizes the results of the risk analysis and identifies the significant climate hazards for the WI system, whose risk must be managed and reduced to an acceptable level. This is performed in the **assessment of adaptation measures**; for each of the significant hazards, targeted adaptation measures are examined and assessed following the procedure described in EC (2021), which involves: (5.1) the identification of the adaptation options, (5.2) their appraisal, and (5.3) their integration into the design and the operation of the WI system to improve its climate resilience.

For each of these five steps indicative research aspects are presented and discussed, including methodologies, and suggestions for future research are made. Some of these suggestions are the identification and standardization of the WI components and the potential climate hazards based on literature and experts' opinion, the quantification of the effects of climate hazards to the WI components via modelling and experimental work, the development of new indicators for all WI works, the setting of limits and the standardization of evaluation procedure of the climate indicators, the construction of maps for indicators at the required scale after proper downscaling of the calculations of climate models, the development of innovative approaches for the measurement of adaptive capacity of WI, the development of methods for combined risk estimation from various climate hazards, the need for NBS acceptance in urban environments and the development of the required relevant tools and others.

**Acknowledgements**

The present work was performed within the framework of the project "Support the upgrading of the operation of the National Network on Climate Change (Climpact)" of the General Secretariat of Research and Technology of Greece under Grant "2023NA11900001".

**References**

IPCC (2021) Annex VI: Climatic Impact-driver and Extreme Indices [Gutiérrez JM, Ranasinghe R, Ruane AC, Vautard R (eds.)]. In Climate Change 2021: The Physical Science Basis. Contribution of Working Group I to the Sixth Assessment Report of the Intergovernmental Panel on Climate Change [Masson-Delmotte V, Zhai P, Pirani A, Connors SL, Péan C, Berger S, Caud N, Chen Y, Goldfarb L, Gomis MI, Huang M, Leitzell K, Lonnoy E, Matthews JBR, Maycock TK, Waterfield T, Yelekçi O, Yu R, Zhou B (eds.)]. Cambridge University Press, Cambridge, and New York, NY, 2205–2214 pp. doi:10.1017/9781009157896.020.

JASPERS (2023) European Investment Bank - Publications Office. https://jaspers.eib.org/. Accessed 20 May 2024.

Stamou A (2022) Towards 'Climate Proof' Infrastructure Projects, Civil Engineering Research Journal, 13(3), 555861.

Stamou A, Mitsopoulos G, Koutroulis A (2024) Proposed Methodology for Climate Change Adaptation of Water Infrastructures in the Mediterranean Region, Environ. Process. 11, 12 (2024). https://doi.org/10.1007/s40710-024-00691-w

# Challenges in Coastal Climate Change Adaptation

Inigo J. LOSADA[1]

[1] Instituto de Hidráulica Ambiental-IHCantabria, Spain
losadai@unican.es

ABSTRACT

Coastal areas are among the regions most threatened by climate change. Their location at the interface between land and sea makes coastal natural and socioeconomic systems especially vulnerable to changes in marine and atmospheric dynamics. Changes in mean or extreme sea levels, wind wave direction and magnitude, seawater temperature, acidification, air temperature, wind and precipitation or river discharge induce a wide range of impacts on coastal ecosystems leading to a loss of ecosystem services and biodiversity as well as impacts on socio-economic systems affecting people, infrastructure, or livelihoods.

Beyond extreme or disaster risk management, and since the first studies on mean sea level rise in the early 1990s, the last two decades have seen significant advances in the analysis of climate change-related risks on the coast. This has allowed us to have initial quantifications of the risks derived from climate change on the coast as well as obtaining the first assessments of the costs of inaction. In addition, a fundamental knowledge base on adaptation and its specific application in the coastal zone has been developed.

However, there are still significant challenges to be addressed if effective adaptation is to be implemented to protect the coastal environment from changing climatic conditions.

Throughout this presentation, the main objective will be to address some of these challenges, showing the current state of knowledge with examples, on the one hand, and, on the other hand, the conceptual and scientific-technical aspects that still need to be addressed to meet our societal needs.

The presentation is not intended to be exhaustive but to show examples in different fields of knowledge in which we have not yet made sufficient progress to address the challenges in question or to significantly reduce the uncertainty in dealing with them.

The different challenges will be organized according to the general IPCC risk analysis framework which states that risk is the result of the interaction of hazard, exposure and vulnerability.

To this end, we will begin by looking at some examples of aspects yet to be addressed when analysing risk components. For example, challenges in: the use of projections of marine dynamics and their impact on the uncertainty of risk analysis; the analysis of compound or cascading processes; the impact of timing in the evaluation of impacts and resilience; the long-term modelling of coastline response to changes in marine dynamics; the joint effect of flooding and erosion, or in other aspects such as characterization of vulnerability and adaptive capacity.

The final part of the talk will be devoted to analyzing specific aspects of the adaptation process. From more conceptual and practical questions to a general analysis of the current state of adaptation in coastal zones.

**References**

Álvarez-Cuesta, M., Toimil, A., Losada, I.J. (2021). Modelling long-term shoreline evolution in highly anthropized coastal areas. Part 2: Assessing the response to climate change. Coastal Engineering 168, 103861.
Magnan, A., Bell R., Duvat V., Ford J., Garschagen M., Haasnoot M., Lacambra C., Losada I.J., Mach K.J., Noblet M., Parthasaranthy D., Sano M., Vincent K., Anisimov A., Hanson S., Jurgilevich A., Nicholls R., Winter G. (2023). The global coastal adaptation imprint. Nature Climate Change 13 (11), 1213-1221
Toimil, A., Losada, I.J., Alvarez-Cuesta, M., Le Cozannet, G. (2023). Demonstrating the value of beaches for adaptation to future coastal flood risk in Australia. Nature Communications 14 (1), 3474.

# Challenges and needs to quickly move towards really integrated urban stormwater management

Jean-Luc BERTRAND-KRAJEWSKI

INSA Lyon, France
jean-luc.bertrand-krajewski@insa-lyn.fr

ABSTRACT

Most of the existing underground urban stormwater infrastructures in developed cities are to a very large extent based on the modern urban sewer systems created in the second half of the 19th century in Europe. Urban stormwater management has substantially evolved during the last decades, from a separate engineering field providing a clearly delimited technical service to cities to an increasingly sophisticated and complex domain, attempting to integrate numerous objectives, functions and issues, requiring combined and interacting contributions of multiples disciplines and stakeholders (engineering sciences, environmental sciences, architecture, urban planning and design, landscape, social sciences, etc.) with the ambition to provide more sustainable and liveable cities. However, this evolution is still not sufficiently implemented as standard practice while new social and environmental constraints, and climate change acceleration, require a much faster adaptation. Promoting innovation and evolution is fundamental to really move towards a true multidisciplinary and integrated approach, and to adapt urban stormwater management to the accelerating climate change. A non-exhaustive and non-hierarchical list of eight issues is tentatively proposed for discussion hereafter: 1) breaking silos, 2) revisit financing, 3) gentrification, 4) social inclusiveness and effectiveness, 5) water culture and meaning, 6) integrating nature, 7) accelerating climate change, and 8) promote innovation.



# Theme A

## Aquifers, rivers, reservoirs and dams

# A new approach using the IDCM method for discharge prediction in partly vegetated channel flows

Mouldi BEN MEFTAH[1], Diana DE PADOVA[1]; Francesca DE SERIO[1], Michele MOSSA[1]

[1] Department of Civil, Environmental, Building Engineering and Chemistry, Polytechnic University of Bari,

Via E. Orabona 4, 70125 Bari, Italy,
mouldi.benmeftah@poliba.it, diana.depadova@poliba.it, francesca.deserio@poliba.it, michele.mossa@poliba.it

ABSTRACT

Predicting flow discharge through vegetated channels is critical to planning and decision-making in river management and restoration as well as in the design and operation of hydraulic structures. An accurate flow discharge estimation in composite channels with mainstreams and vegetated areas remains a very complex issue. In this study, we show how we can predict the total and zonal discharges of partly vegetated channels by adapting the Interacting Divided Channel Method (IDCM), applied with a curved interface approach and with the presence of large-scale roughness elements (not considered in previous studies). The proposed approach was validated by conducting various experiments on a physical model consisting of a very large rectangular channel partially covered by rows of vertical, rigid, circular, and rough steel cylinders representing emergent rigid vegetation. Based on the experimental results as well as data collection from previous studies, the consideration of transverse momentum transfer in terms of apparent shear stress at a curved interface plane has shown improved performance, in predicting flow discharges, with IDCM versus the classical Divided Channel Method (DCM). Furthermore, we have also proposed a series of easily applicable expressions to predict the zonal flows of a partially vegetated channel.

## 1. IDCM adaptation

For compound channels, it was observed in the literature (e.g., Huthoff et al., 2008; Tang, 2019; Pradhan and Khatua, 2020, Singh and Tang, 2020; Ben Meftah and Mossa, 2023) that the shear layer development, due to velocity gradient, at the interface between the main channel and the floodplain generates high turbulence and transverse momentum transfer from the fastest to the slowest flow area. The consideration of this momentum transfer is critical in the estimation of the flow discharge in compound channels. Huthoff et al. (2008) proposed the Interacting Divided Channel Method (IDCM), considering the transverse momentum transfer in terms of apparent shear stress to predict the discharge in a compound channel without vegetation presence. The authors asserted that interface momentum transfer accounting helps to better predict zonal and overall flow discharges in compound channels.

In partly vegetated channels, the flow-hydrodynamic structures show the apparition of one or more main subsections of largest velocity (unobstructed zones), subsections of lowest velocity (obstructed zones), and the development of shear layers at the interface between unobstructed and obstructed subsections (see Figure 1). Since these structures are very similar to those of compound channels, the IDCM is physically adaptable to partly vegetated channels. The novelty of this study is the consideration of both large-scale roughness elements (consisting of vegetation stems) and a curved-division interface plane by applying the IDCM method.

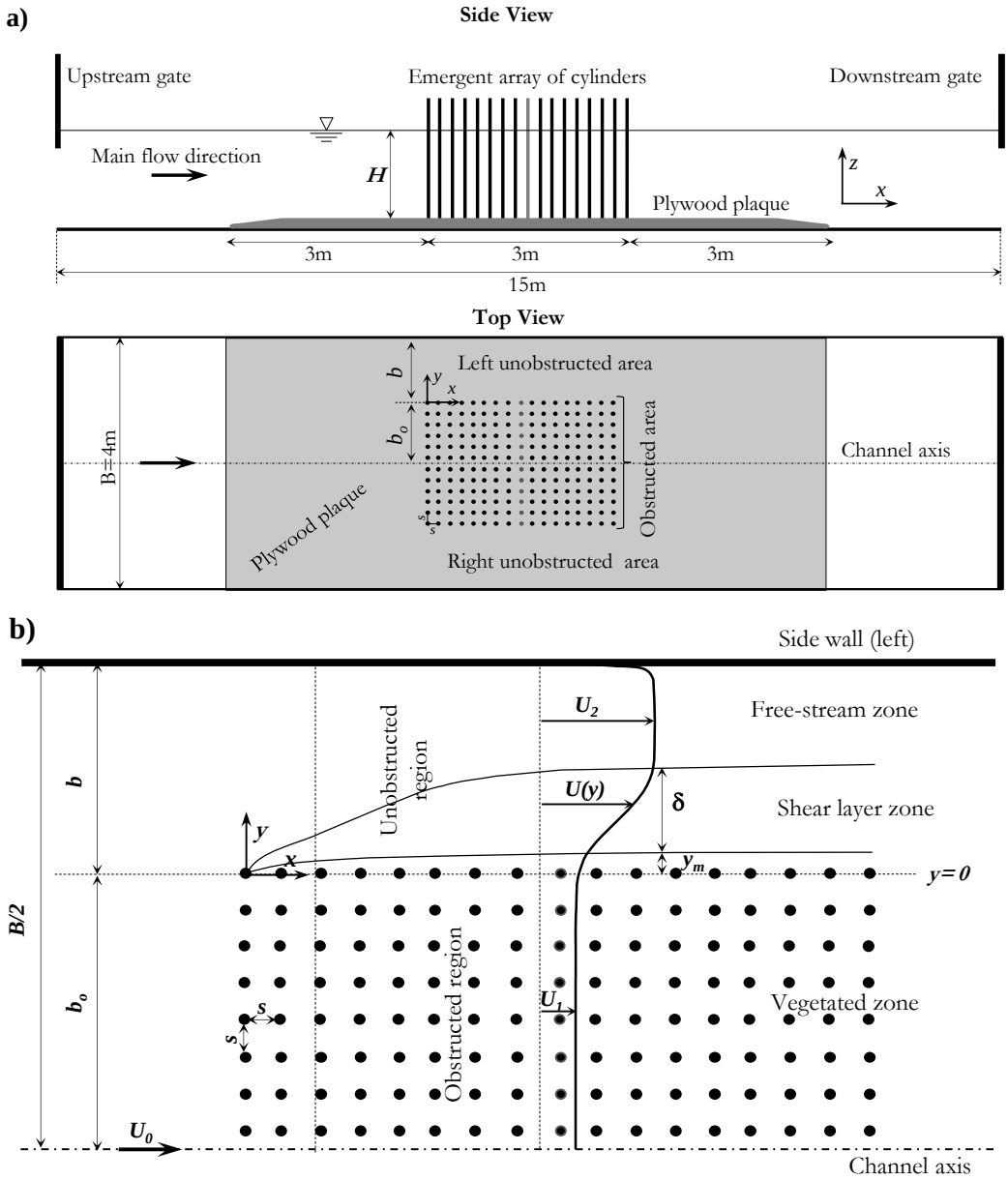



**Fig. 1.** Schematic representation of the laboratory partly vegetated channel: a) side and top views of the channel; and b) flow hydrodynamic structures at the interface with the development of the different flow subsections, where $B$ is the channel width, $b$ is the unobstructed width, $b_o$ is the obstructed width, $H$ is the flow depth, $s$ is the space between cylinders, $U$ is the streamwise velocity, $U_1$ is the flow pore velocity inside the obstructed region, $U_2$ is the free-stream velocity in the unobstructed area, ($x$,$y$,$z$) are the longitudinal, transversal and vertical coordinates, $y_m$ is the effective shear layer origin, and δ is the shear layer width.

**Acknowledgements**

This study was carried out at the Coastal Engineering Laboratory (L.I.C) of the Polytechnic University of Bari, Italy, Department of Civil, Environmental, Building Engineering and Chemistry.

**References**

Ben Meftah M, Mossa M (2023) Discharge Prediction in partly vegetated channel flows: Adaptation of IDCM method with a curved interface and large-scale roughness elements, Journal of Hydrology, 616, 128805. Doi: 10.1016/j.jhydrol.2022.128805

Huthoff W, Roos PC, Augustijn CMA, Hulscher SJMH (2008) Interacting divided channel method for compound channel flow, Journal of Hydraulic Engineering, 134(8), 1158-1165. Doi: 10.1061/(ASCE)0733-9429(2008)134:8(1158)

Pradhan S, Khatua, KK (2020) Momentum transfer coefficients at the adjoining interfaces of a compound channel, Flow Measurement and Instrumentation, 75(10), 101792. Doi: 10.1016/j.flowmeasinst.2020.101792

Singh P, Tang X (2020) Zonal and overall discharge prediction using momentum exchange in smooth and rough asymmetric compound channel flows, Journal of Irrigation and Drainage Engineering, 146(9), 05020003. Doi: 10.1061/(ASCE)IR.1943-4774.0001493

Tang X (2019) Apparent shear stress-based method on an inclined interface plane for predicting discharge in straight compound channels. MethodsX, 6, 1323-1330. Doi: 10.1016/j.flowmeasinst.2019.01.012

# Statistical analyses of key parameters involved in riverbed clogging

Markus NOACK[1], Alcides AYBAR GALDOS[1]

[1] Karlsruhe University of Applied Science, Institute for Applied Research, Germany
markus.noack@h-ka.de
alcides.aybar_galdos@h-ka.de

ABSTRACT

Infiltration and accumulation of fine sediments – riverbed clogging – represents a severe impact on vertical connectivity and hence on interstitial habitats and hyporheic exchange processes. This study investigates functional relationships between a novel field approach to assess riverbed clogging (MultiPAC) and the classical assessment according to the Water Frame Directive (WFD), catchment characteristics and biological data. The resulting unique dataset with subsequent statistical analyses provides promising results toward a quantitative evaluation concept of riverbed clogging.

## 1. Introduction

Riverbed clogging is widely known to interrupt vertical connectivity between groundwater and surface water (Dubuis & DeCesare 2023) and to degrade interstitial habitats for macroinvertebrates and the reproduction of gravel-spawning fish. Moreover, clogging is frequently mentioned as a reason for rivers failing in achieving the demanded 'good ecological status' according to the Water Framework Directive (WFD 2000). However, no standard methods to assess riverbed clogging are available, because of lacking reference values that would allow to assess the deviation to a near-natural condition. Therefore, we applied a multiparameter approach to describe riverbed clogging in the field and performed statistical analyses to derive functional relationships between variables describing clogging and assessments of the WFD (good ecological status, general degradation). The 'general degradation' is a German specific assessment, which mainly indicates hydromorphological impacts and is classified from '1 = high' to '5 = bad' (Lorenz et al. 2004).

## 2. Methods

### *2.1. Multiparameter approach to assess clogging (MultiPAC)*

MultiPAC was developed to detect riverbed clogging based on physical quantitative measurements of the most governing parameters involved in clogging (Negreiros et al. 2023). This includes sediment sampling using the freezecore technique, and the porosity using the water replacement method. Additionally, the VertiCO-method based on a perforated filter pipe and a double packer (Vertical profiles of hydraulic Conductivity and dissolved Oxygen) measures vertical profiles of interstitial dissolved oxygen and hydraulic conductivities.

### *2.2. Statistical Methods*

To analyze functional relationships between selected parameter of MultiPAC and WFD assessment (ecological status, general degradation), we used the multidimensional (MDS), principal component analysis (PCA) and Spearmann correlation (e.g. Holmes & Huber, 2019). In addition, we tried to derive reference values for the different parameters of MultiPAC according to the assessment of the WFD.

## 3. Results

The monitoring with MultiPAC was applied in seven rivers in Germany belonging all to the same river type and all sampling sites are regular WFD-monitoring stations. The seven rivers were chosen based on different

selection criteria including catchment characteristics, results of WFD-monitoring and for some practical reasons such as accessibility. The idea was to cover a wide range of different clogging intensities.

As an exemplary result, Table 1 shows the loading of two components of a PCA (principal component analyses) for different selected parameters of MultiPAC and the ecological status according to the WFD considering all seven rivers. Based on the PCA, the first component explains 62.2% and the second 30.0% of the data variability.

**Table 1.** Loadings of selected parameters of MultiPAC and WFD for two principal components of a PCA.

| | OxySat [%] | FSC < 1mm | Porosity | d84 [mm] | SO | σ_geom | EcolStat |
|---|---|---|---|---|---|---|---|
| Comp 1 | 0.32 | -0.44 | -0.34 | 0.37 | -0.21 | 0.00 | -0.42 |
| Comp 2 | 0.01 | -0.01 | -0.45 | 0.33 | 0.52 | 0.56 | 0.24 |

For the first component, we identified positive correlations for the oxygen saturation (OxySat) and $d_{84}$, while negative correlations are represented by the fine sediment content < 1.0 mm and the ecological status (EcolStat) according to the WFD. The second component shows positive correlations with the sorting coefficient (SO) of the particle size distribution and its geometric standard deviation while the porosity is negatively correlated.

Another exemplary result considers the measured data ranges of MultiPAC in context of the WFD assessment. In Figure 2, the boxplots represent the data range for oxygen saturation (upper 20cm of the riverbed) and the fine sediment content less than 2 mm in contrast to the German WFD assessment ‘general degradation’.

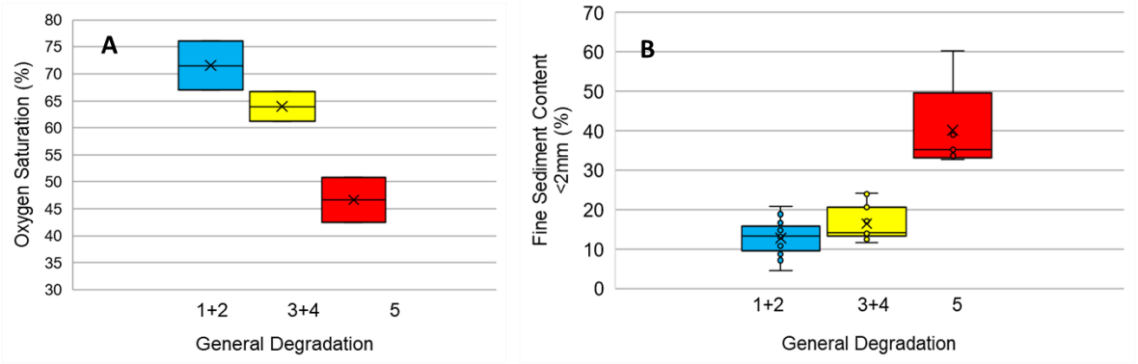



**Fig. 2.** Identified data ranges for A: oxygen saturation (upper 20cm or riverbed) and B: fine sediment content < 2mm against the German WFD assessment ‘general degradation’.

We grouped the seven rivers into three categories (1+2, 3+4 and 5). For both parameters we can observe a clear trend indicating the opportunity to derive reference values, although the difference between the group ‘1+2’ and ‘3+4’ is not very strong.

We are still at the beginning of our analyses and currently we are intensifying the data analyses towards a rivertype-specific evaluation scheme for clogging by including additionally biological data (macroinvertebrates, meiofauna with DNA-analyses) and catchment characteristics (erodibility, hill slope, land use). This leads to a unique dataset that could serve for a quantitative evaluation concept for clogging.

**Acknowledgements**

The authors would like to express appreciation for the support of the sponsors German Federal Environmental Foundation (DBU), Grant Number: AZ 37315.

**References**

Dubuis R, DeCesare G (2023) The clogging of riverbeds: A review of the physical processes. Earth-Science Reviews, 239, 104374. https://doi.org/10.1016/j.earscirev.2023.104374

Lorenz, A., Hering, D., Feld, C.K., Rolauffs, P., 2004. A new method for assessing the impact of hydromorphological degradation on the macroinvertebrate fauna of five German stream types. Hydrobiologia 516, 107–127. https://doi.org/10.1023/B:HYDR.0000025261.79761.b3

Negreiros B, Aybar Galdos A, Seitz L, Noack M, Schwindt S, Wieprecht S, Haun S. (2023) MultiPAC: a multi-parameter approach for assessing riverbed clogging and vertical hyporheic connectivity, River Research and Application, https://doi.org/10.1002/rra.4145.

Holmes, S, Huber, W. 2019. Modern Statistics for Modern Biology, Cambridge University Press. ISBN 9781108705295.

# Fish passes in Portugal: current status, main findings and future directions

José M. SANTOS[1], Paulo BRANCO[1], Ana L. QUARESMA[2], Filipe ROMÃO[2], Susana D. AMARAL[1], Marta SANTO[3], Jorge BOCHECHAS[3], Ana M. TELHADO[4], Francisco GODINHO[5], João PÁDUA[6], Paulo PINHEIRO[7], Ana T. SILVA[8], Teresa VISEU[9], Pedro R. ALMEIDA[10], Teresa FERREIRA[1], António PINHEIRO[2]

[1] Centro de Estudos Florestais (CEF), Instituto Superior de Agronomia, Universidade de Lisboa, Portugal
jmsantos1972@edu.ulisboa.pt
pjbranco@isa.ulisboa.pt
samaral@isa.ulisboa.pt
terferreira@isa.ulisboa.pt

[2] Investigação e Inovação em Engenharia Civil para a Sustentabilidade (CERIS), Instituto Superior Técnico, Universidade de Lisboa, Portugal
analopesquaresma@tecnico.ulisboa.pt
filipe.romao@tecnico.ulisboa.pt
antonio.pinheiro@tecnico.ulisboa.pt

[3] Instituto da Conservação da Natureza e das Florestas (ICNF), Lisboa, Portugal
Marta.Santos@icnf.pt
Jorge.Bochechas@icnf.pt

[4] Agência Portuguesa do Ambiente (APA), Alfragide, Portugal
ana.telhado@apambiente.pt

[5] Conselho Nacional da Água, Lisboa, Portugal
francisco.godinho@sgambiente.gov.pt

[6] EDP Labelec- Estudos, Desenvolvimentos E Atividades Laboratoriais, S.A, Sacavém, Portugal
Joao.Padua@edp.com

[7] AQUALOGUS, Engenharia e Ambiente, Lda., Lisboa, Portugal
ppinheiro@aqualogus.pt

[8] Norwegian Institute for Nature Research, Norway
ana.silva@nina.no

[9] Núcleo de Recursos Hídricos e Estruturas Hidráulicas, Laboratório Nacional de Engenharia Civil, Lisboa, Portugal
tviseu@lnec.pt

[10] MARE – Centro de Ciências do Mar e do Ambiente, Universidade de Évora, Évora, Portugal
pmra@uevora.pt

## ABSTRACT

As in many other countries, river fragmentation by anthropogenic structures in Portugal - with more than 250 large dams and 8000 smaller barriers - has caused fish populations to decline and, in some cases, extirpation of other aquatic organisms unable to effectively disperse between habitats. Mitigating the impacts of river fragmentation on fish movements through the implementation of fishways has thus been an important focus of

rehabilitation efforts for fish, due to their economic, ecological and cultural significance. This study analyses the status of fishway science in Portugal over the past two decades. The main goals were: i) to catalogue the number, type, timing of construction and installation place (e.g., at small barriers, small hydropower plants and dams) of all fishway types, and ii) to resume the main results achieved from ISI Web of Science studies conducted over the different fishway types.

## 1. Main results and conclusions

A total of 95 fishways built from 1950 until the present were identified. Half of the fishways (49.5%) were built before the implementation of the WFD in Portugal (2005), whereas the other half (50.5%) were built thereafter, thus, with no significance between proportions ($\chi2= 0.009$, $P> 0.05$). However, the construction rate of such devices tripled from the pre-WFD period (0.85 fishways/year) to the post-WFD (2.66 fishways/year). Distribution of fishways among the territory is not uniform, since 78.9% of them are located within the northern and central catchments, whereas the remaining 21.1% are in the Mediterranean southern part of the country (Tagus, Sado and Guadiana catchments), where temporary rivers prevail ($\chi2= 23.51$, $P< 0.01$). Fishways were built at different types of instream obstacles, namely SHP (46.3%), small weirs (43.2%) and LHP (10.5%), with significant differences in the proportions between the former and the later ($\chi2= 4,28$, $P< 0.05$). Considering all the hydropower plants (SHP+LHP), 91% of fishways are located in the central and northern river catchments. Regarding fishway design, the pool-type fishway was found to be the most commonly used (n=65, 68.4%), followed by nature-like facilities (n=15, 15.8%), fish locks and combined systems, each accounting for 6.3% (n=6), fish lifts (n=2, 2.1%) and eel passes (only one device, 1.1%). Significant differences between these proportions were found for pool-type fishways when compared to the other designs ($\chi2$ tests, $P< 0.05$) (no test was conducted for lifts and eel passes, due to the very low sample sizes of these facilities). All but one fish locks and lifts were built before the implementation of the WFD (87.5%), particularly during the 70's and 80's of the past century (75%). In contrast, almost all nature-like facilities (n=13, 86.7%) were built after the implementation of the WFD ($\chi2= 4.91$, $P< 0.05$). Literature searched from the ISI WoS and Google Scholar resulted in a total of 36 contributions between 2002-2023, of which 27 were from pool-type fishways (i.e., PaW and VSF designs), 4 from natural fishways, 4 from fish lifts and 1 from fish locks.

Of all the literature that addressed fishways in Portugal, more than three quarters (77.1%) focused on pool-type fishways, which is also the most common type of device (68.4%) found at river obstacles. The same scenario can be found in other European countries and worldwide (Hatry et al., 2013; Larinier, 2008), where pool-type fishways are by far the most used to promote fish passage past obstacles. Natural fishways were the second most abundant fishway type representing 15.8% of all devices in Portugal. This proportion is aligned with the number of ISI-published studies conducted on this type of fishways, i.e. 4 out 36 studies (11.1%). Of these, only 1 concerned the field monitoring of a natural fishway, namely a nature-like bypass channel, and its main conclusions supported the usefulness of these facilities to serve as potential river restoration projects, as they not only provided a migration corridor for the present fish fauna, but also served as habitat for the fish community that would be expected to reside in a local tributary or side-channel. However, neither pool-type fishways nor nature-like facilities are adequate solutions when the goal is to provide fish passage across high obstacles, such as large dams (>15 m). In such cases, fish lifts clearly stand out as the most cost-effective solution (Croze et al., 2008), though they are much less common than the former, with only two devices in the present review (thus representing 2.1%), which is in accordance with global statistics (Noonan et al., 2012).

Future studies should consider increasing the number of field studies to validate the results from experimental assessments, the development of selective fishways as a response to widespread invasions by non-native fish and improving the knowledge of fish swimming ability and energetics to refine criteria for bidirectional fishway construction and retrofitting.

**References**

Croze O, Bau F, Delmouly L (2008) Efficiency of a fish lift for returning Atlantic salmon at a large-scale hydroelectric complex in France, Fisheries Management and Ecology, 15, 467–476.

Hatry C, Binder TR, Thiem JD, Hasler CT, Smokorowski KE, Clarke KD, Katopodis C, Cooke SJ (2013) The status of fishways in Canada: trends identified using the national CanFishPass database. Reviews in Fish Biology and Fisheries, 23, 271–281.

Larinier M (2008) Fish passage experience at small-scale hydro-electric power plants in France, Hydrobiologia, 609, 97–108.

Noonan MJ, Grant JWA, Jackson CD (2012) A quantitative assessment of fish passage efficiency. Fish and Fisheries, 13, 450–464.

# Eel-Friendly Fish Ladders: Navigating Challenges for Multi-Species Design

Elena CARCANO[1], Kathryn PLYMESSER[2]

[1] Dipartimento di Ingegneria ed Architettura, Università degli Studi di Parma, Italy
elena.carcano@unipr.it

[2] Civil Engineering Department, Montana State University, Bozeman, Montana, USA
kathryn.plymesser@montana.edu

ABSTRACT

There are still relatively few examples of eel fishway designs, particularly when considering the coexistence of multiple fish species with varying swimming abilities. Designing effective fishways able to cater eels, with anguilliform morphology and limited swimming capabilities, with different fish species, presents a significant challenge. Moreover, the existing data for eels' swimming abilities is still limited. Henceforth, practical trials to test eels swimming performance in reference to slow species (e.g. *Telestes Muticellus*) is highly encouraged. It is customarily accepted, in Italy, that when eels cohabit with other fishes of poor swimming abilities, a specific passage for eels is not required. This perspective is primarily rooted in practical convenience, advocating for a universal fishway that can accomodate all species, rather than being scientifically substantiated. This analysis aims to compare the available data on eels' swimming capabilities to those of Varions, alternatively named: *Telestes muticellus*, in the context of multi-species fishways. *Telestes Muticellus* is a tiny fish specie with limited swimming abilities but very common in: Northern Italy, Switzerland, and France. This work, starting from a real case of a restored mini-hydro, aims to provide valuable insights and recommendations regarding the design of targetted fishways and to underscore the necessity for comprehensive and scientifically informed approaches so to address challenges associated with fish passages' design.

## 1. Samples' swimming abilities

### *1.1 Eels swimming abilities*

The maximum burst speed quoted for elvers varies from 0.60 m/s to 0.90 m/s. Several studies referring to the swimming performance of elvers have demonstrated their poor abilities to pass laminar flow conditions. When the flow speed equals 0.30 m/s, the specie can cover a distance of 3 m.



**Fig. 1.** European eel (example), detail of related passage and overall passage figure.

### *1.2 Telestes muticellus swimming abilities*

*Telestes muticellus* is the slowest and yet very common fish species sampled in Northern Italy and Switzerland and reaches lengths of 20 cm maximum in 6-7 years. Its average speed is around 0.40 m/s.



**Fig. 2.** Examples: of Telestes Muticellus, two fishways targetted for Telestes Muticellus specie.

## 2. Eels' passages

### *2.1 Traditional fish passages: shortcomings for eels*

According to literature studies traps used in fishways are not generally suitable for catching thin fishes such as eels. Differently from other migratory species, for which upstream movement is due to breeding reasons, the progression of eels upstream is due to colonisation purposes and involves the young samples in particular. Colonisation begins when elvers, around 70 mm of length with an average weight of 0.3 g, enter an estuary. In such a case two cases of migration happen: passive and active migration respectively. Passive migration relies on flow. At the beginning of the migration season elvers do not have an independent and orientated swimming ability as they use tidal currents to move upstream. From March-April, the elvers acquire the ability to swim and crawl, allowing them to make active progress and overtake some obstacles. This phase continues until the end of the summer. Species between 10 and 40 cm are involved in such a path. Pool passes with deep notches or vertical slots and moderate differences in the level between pools can be throdden by this species. On the contrary, the very few studies carried out demonstrated that fish traps used in fishways are not generally suitable for catching thin fishes such as eels. Introducing brushes in the deepest part of the notches can improve the passage of the eel in some types of facilities. Still experimental trials are highly recomended.

### *2.2 Eels passage: ramps as typical example*

Passage facilities in relying on ramps span from 0.20 to 1m of width and associated slopes generally vary from 5% to 45%. The use of a natural substratum to upholster the passage is highly recomended (i.e: pebbles, branches, briars or straw) although such a cover requires more frequent maintenance and must be replaced periodically. Other technical characteristics are generally chosen in relation to the size of the migrants present at site. As a guide to determining the correct location of the passage in reference of an existing obstruction, the resting and assembly areas for the approaching migrants need to be identified. Before installing the permanent facility tests should be carried out on site using a mobile eel trap in order to confirm the optimum location of the entrance. In this study case several eels and vairons species have been sampled. The adopted solution, in absence of a detailed and more reliable literature and previous experiments, is to combine a *bottom ramp* fish passage with a specific *eel slipway* although eels have demonstrated to have slower swimming abilities respect the *Telestes Muticellus* species. Introducing a separate passage for the eels allows to fulfill their specific migration requirements despite a fast and more practical solution which would suggest to rely on only one fish passage properly designed on the slowest sampled specie. In the nutshell, the authors believe that contextual experiments on different fishes swimming abilities are still highly recomended in order to set a unique passage suitable for all species.

**References**

Arai, T., & Chino, N. (2012). Diverse migration strategy between freshwater and seawater habitats in the freshwater eel genus Anguilla. Journal of Fish Biology, 81(2), 442–455

Deleau, M. J. C., White, P. R., Peirson, G., Leighton, T. G., & Kemp, P. S. (2020). The response of anguilliform fish to underwater sound under an experimental setting. River Research and Applications, 36(3), 441–451.

Elvidge, C. K., Ford, M. I., Pratt, T. C., Smokorowski, K. E., Sills, M., Patrick, P. H., & Cooke, S. J. (2018). Behavioural guidance of yellow-stage American eel Anguilla rostrata with a light emitting diode device. Endangered Species Research, 35,

Parker, A. D., Glover, D. C., Finney, S. T., Rogers, P. B., Stewart, J. G., & Simmonds, R. L. (2016). Fish distribution, abundance, and behavioral interactions within a large electric dispersal barrier designed to prevent Asian carp movement. Canadian Journal of Fisheries and Aquatic Sciences, 73(7), 1060–1071.

# The Roman soil retention dams – a forgotten technology for water retention in arid climates

Gerald MULLER[1], Charlie ROYAL[1]

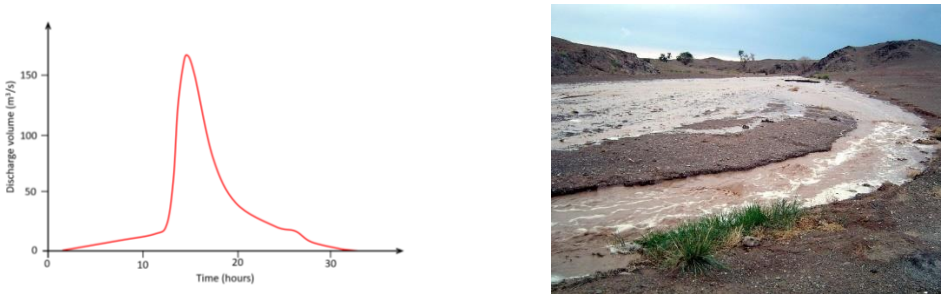
[1] University of Southampton, UK
g.mullere@soton.ac.uk

ABSTRACT

In arid environments, rainfall often occurs in one or two concentrated events per year. This leads to so-called flash floods, rivers which flow in otherwise dry valleys for several hours or days. Today, most of the work on flash floods is aimed at flood management and mitigation. Retaining the water with dams and reservoirs is difficult because of the high sediment load of the flash floods, and because of evaporation. Consequently, the water of the flash floods is lost. In the Roman Empire a very specific solution was developed to address this problem. 2 to 2.5 m high dams were built across dry valleys or wadis to collect the sediment of the flash floods to create farmland. Once the reservoir space had been filled up, the next flash flood would be slowed down so that part of the water could seep into the ground and remain there. Spillways were located at both sides of the dam to maximize the residence time of the water. Today, the technology is only of interest to archaeologists and seems nearly forgotten. It may however be a possibility to reduce water scarcity in arid countries and certainly deserves further development.

## 1. Introduction

Arid and desert zones are characterized by very low precipitation. Often, the complete yearly rainfall is concentrated in one or two short events, Figure 1a shows a typical hydrograph with a duration of only 17 hours. These events cause flash floods, where dry valleys (Wadis in North Africa, Canyons in North America) are suddenly filled with rivers running for hours or several days, Fig. 1b. Today, most of the engineering efforts dealing with flash floods are concerned with flood protection, diversion, and drainage. Very little work seems to be done to utilize this water. The classic solution would be to build dams to capture the water in a reservoir. This however is difficult since (a) the flash floods also transport a large volume of sediment and debris, which fills reservoir up and (b) evaporation quickly reduces the water volume.




(a) (b)

**Fig. 1.** Flash floods, (a) Typical flow hydrograph of a desert flash flood, (b) Flash flood in the Mongolian desert (Source: https://commons.wikimedia.org/w/index.php?curid=8831121),

## 2. Soil retention dams

In the Roman Empire, a different technique for flash flood retention was developed, the soil retention dams which were built in the Provinces of Tripoli (today Libya) and Nabataea (today Israel). These were shallow dams of heights of 2 to 2.5 m built across dry wadis with the aim to capture the sediment to create farmland,

Fig. 2. The dams had spillways on either side of the wadi, so that the flash flood was diverted from the centre of the valley, Vita-Finzi (1961). The sediment accumulated up to the height of the dam, creating farmland and a flood plain where following floods would be slowed down, and the water could seep into the ground.




(a) (b)

**Fig. 2.** Principle of soil retention dams, (a) After construction, (b) Sediment accumulation during flash floods),

The absorption was further increased by the construction of "rubble mounds", gravel filled stone circles of 0.3 to 0.4 m height and 1 to 1.5 m diameters where the water could seep into the ground, and which slow down the flow. The elevation above ground meant that the gravel filter was not blocked by sediment.




(a) (b)

**Fig. 3.** Soil retention dams, (a) Principle, (b) Dams still in use in Avdat / Israel (Photo: Douglas Main, Livescience.com)

Figure 3a shows a retention dam system. The dams and the accumulated sediment form terraces with near horizontal farmland. Due to the reduced gradient and the increased area, a flash flood will be slowed down, and the water can seep into the ground. Excess water is diverted to the spillways on either side of the dam. Several hundred of such dams were built, often as parts of more complex regional water management systems. The remainders of soil retention dams indicate that dams were raised several times, pointing to the success of the technique. In Israel, the remainders of one such a system are apparently still in use, Fig. 3b, Main (2013).

## 3. Discussion

In the Roman Empire, soil retention dams which extend over the full flood plain were built to collect sediment and thereby create farmland in degraded arid Wadis. The collected sediment also acted as water storage, the water from flash floods would be absorbed below the ground, minimizing evaporation. The reported number of such dams points to the success of this technology. Today, soil retention dams appear to be only of interest to archaeologists although some very recent work in Israel indicates the possibility of re-inventing the antique technology, Tepper et al. (2020). In hydraulic engineering the soil retention dams seem to have been completely forgotten. Flash floods are considered as a danger and therefore diverted further downstream and into the sea. Some weir structures bear a resemblance to the Roman dams: check dams cover the width of the stream to reduce the gradient and erosive potential of steep streams. Sand dams are built in rivers to accumulate sand, raising the groundwater level. Sediment basins retain suspended sediment, often for later removal and deposition. The Roman dams combine features of these structures, but they also extend over the full width of the valley, they divert the flow to side spillways, slowing it down further, and the dams of course have the purpose of creating farmland. So, these dams are in fact quite unique, and in a time of increasing water shortage most probably deserve the attention of hydraulic engineers.

**References**

Main, D. (2013). Avdat, Israel. In Photograph. Livescience. https://www.csmonitor.com/Science/2013/0320/Rewriting-Biblical-history-Agriculture-might-be-5-000-years-older-than-believed

Royal C. (2023) An Investigation into the Feasibility of Soil Retention Dams: An Ancient Method for the Cultivation of Land in Arid Regions. Individual project Report. University of Southampton (85 pp)

Tepper, Y., Porat, N., & Bar-Oz, G. (2020). Sustainable farming in the Roman-Byzantine period: Dating an advanced agriculture system near the site of Shivta, Negev Desert, Israel. Journal of Arid Environments, 177.

Vita-Finzi, C. (1961). Roman dams in Tripolitania. Antiquity, 35(137), 14-20.

# Effects of flow guide walls on sediment flushing in peaking hydropower reservoirs.

Stefanie TIETZ[1], Giovanni DE CESARE[2], Pedro MANSO[1,2], Romain VAN MOL[2]

[1] MHYD water and energy solutions, Switzerland
stefanie.tietz@mhyd.group; pedro.manso@mhyd.group

[2] Ecole Polytechnique Fédérale de Lausanne, Switzerland
giovanni.decesare@epfl.ch; pedro.manso@epfl.ch; romain.vanmol@epfl.ch

ABSTRACT

Reservoir sedimentation is known to be a key issue worldwide. One operational measure to deal with sediment accumulations is flushing; however, efficiency is often lacking. The goal of this study is thus to improve the effectiveness and efficiency of flushing operations in short, mountainous reservoirs used for peaking hydropower generation by introducing guide walls into the system. To do so, two purely theoretical topographies with systematically placed guide walls were analysed. The different configurations were compared based on three performance indicators: ratio of evacuated over inflow sediment, as well as local and global bed shear stresses. It was found that even small changes in location and flow alignment of the guide walls may significantly change flow patterns inside the reservoir. In a last step, the methodology was applied to a case study, the Jiji hydropower plant in Burundi, presently under construction, and whose live storage will be paramount to regulate the power network in the country on a daily basis.

## 1. Introduction

Sediment transport is a key issue for the planning, design and sustainable operation of hydraulic infrastructures. If neglected, major accumulations may affect the functioning of the reservoir (Morris et al., 2013) or erosion can lead to potential structural stability problems, to name two examples (E.J. Carlson and P.F. Enger, 1962). However, sedimentation of reservoirs is a natural phenomenon that occurs due to decreasing velocities at reservoir entrances (Morris et al., 2013). This involuntary storage of sediment causes a disequilibrium in the transport regimen of the river, and erosion may occur downstream of the water retaining structure.

Flushing and emptying are two of the operations allowing transfer of sediment along reservoirs and through the dam. In Switzerland, first instances of emptying were conducted in 1960, whereas, flushing is a more recent type of operation gaining momentum in the current millennium (SCD, 2023). The goal of this article is to find ways to improve flushing operations with guide walls that will help guide the sediment charged flow to the bottom outlet.

Ever since the middle of the 20th century, multiple examples of guide walls exist, mainly to stop sediment from entering into water intake structures (E.J. Carlson, 1951; E.J. Carlson and P.F. Enger, 1962; Enger and Dodge, 1954; P.F. Enger and E.G. Carlson, 1962). For those applications, the final solution was found with experiments on a physical model. Only recent projects used a hybrid modelling approach to determine the efficiency of guide walls (Müller et al., 2010). This is because sediment transport and deposition depend on multiple factors such as the geometry of the reservoir, the dam and its appurtenant structures, hydrology, solid transport, reservoir management as well as all other structures influencing the field of flow such as guide walls. Because of the many variables, it is time-consuming and costly to vary them systematically with a physical model, which is where lies the interest of numerical modelling.

The goal of this study is thus to determine which are the effects of guide walls on flushing operations, and how an optimal solution can be identified and characterized for each specific reservoir case.

## 2. Methodology

A stepwise work methodology is implemented to assess the relative strength and weakness of alternative guide wall solutions. First, a theoretical canvas is set, identifying the key parameters representing the main physical features of the problem. Secondly, the main design parameters for guide walls are identified and used to conceive feasible solutions. Then the performance of the different guide wall configurations is assessed by 2D hydraulic computational modelling. Numerical modelling is performed with the HEC-RAS software (USACE

Hydrologic Engineering Center), version 6.3.1. The software uses the St. Venant 2D shallow water equations (Gary W. Brunner, 2016).Three different topographies were analysed; two purely theoretical cases, with guide walls placed systematically and with the third topography the Jiji reservoir in Burundi.
As numerical modelling calculates a high amount of different result variables, it leads to different possibilities for interpretation. In this article, a two phased methodology for performance of guide walls was adapted. First, all wall configurations were visually checked whether they disrupt or decrease bed shear stress continuity and in the affirming case, eliminated from the selection. Then, normalized values of global bed shear stress $\tau$ and ratio of evacuated sediment $R_s$ were analysed. This methodology is not only encompassing the most influential factors for sediment accumulations, but also reflects the current capabilities of the utilized numerical sediment modelling software.

## 3. Results

This was also done for the Jiji case study. The best solutions, identified so far, aim to increase effectiveness of sediment removal in the life storage regions. To do so, they are located in the flood plains of the natural river, outside the main channel, which allows for shear stress continuity. However, it was found that a slight prolongation into the main channel can drastically improve efficiency as it allows to split the flow without significantly decreasing shear stress continuity as is shown on Fig. **1**. It must be noted that the described methodology does not necessarily lead to the most optimal solution but allows to find the best solution among the tested configurations.

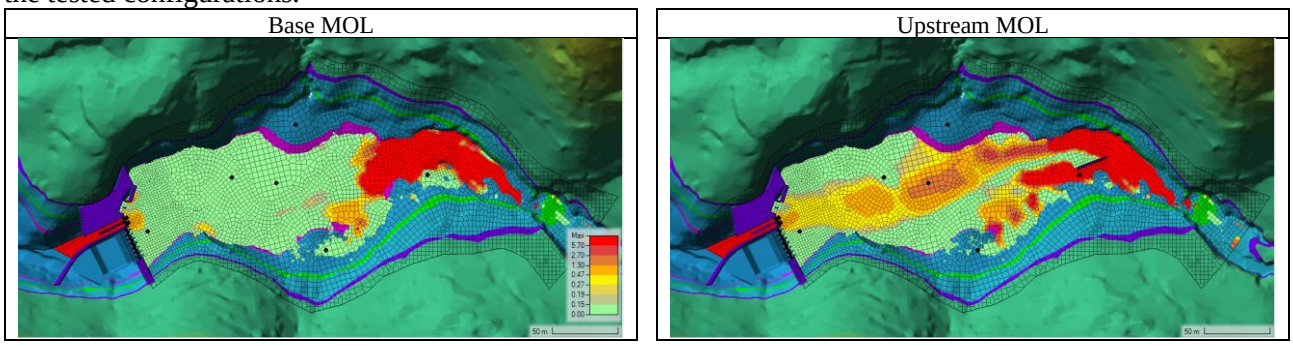



**Fig. 1**. Comparison of bed shear stress for configurations Base (no guide wall) and Upstream at MOL (minimum operation level). Red: shear stresses are sufficient to transport all expected grain sizes. Green: only fine sediment is transported.

## 4. Conclusion

The goal of this work was to analyse the effects of guide walls on flushing operations, considering the effectiveness and the efficiency.
Three different topographies were analysed based on an identical methodology. Two topographies were purely theoretical cases, with guide walls placed systematically. The third topography was a case study of the Jiji reservoir in Burundi. In general, it was shown that even small changes in flow alignment or position of guide walls may have an important impact on shear stress distributions inside the reservoirs.
Truly systematic placement of guide walls may be attempted but will probably remain difficult to implement because of economic or time restraints. However, with an in-depth understanding of flow and shear stress patterns inside a reservoir and engineering experience, key areas for guide walls can be pre-selected to improve the effectiveness of the optimization process.
We thus confirm the usefulness of using 2D numerical modelling to screen guide wall design alternatives during project feasibility stages, before engaging more resources on measurement campaigns for supporting data or physical modelling to reduce uncertainty on guide wall performance.

**Acknowledgements**

The authors would like to thank the Burundi Water and Electricity Production and Distribution Board (REGIDESO) for allowing us to use the Jiji reservoir as a case study, as well as the team from Zutari, in particular Dr Frank Denys, for sharing their data and ideas.

**References**

E.J. Carlson, 1951. Hydraulic Model Studies of Fort Laramie Canal Desilting Basin, North Platte Project (Hydraulic Laboratory Report No. HYD 313). Colo.: Bureau of Reclamation, U.S. Department of the Interior, Denver.
E.J. Carlson, P.F. Enger, 1962. Hydraulic Model Study to Determine a Sediment Control Arrangement for Socorro Main Canal Headworks, San Acacia Diversion Dam, Middle Rio Grande Project, New Mexico (Hydraulic Laboratory Report No. HYD 479). Colo.: Bureau of Reclamation, U.S. Department of the Interior, Denver.
Enger, P.F., Dodge, R.A., 1954. Hydraulic Model Studies of Bartley Diversion Dam; Progress Report No. 3 on General Studies of Headworks and Sluiceway Structures; Missouri River Basin Project, Nebraska (Hydraulic Laboratory Report No. HYD 384). Colo.: Bureau of Reclamation, U.S. Department of the Interior, Denver.
Gary W. Brunner, 2016. HEC-RAS River Analysis System Hydraulic Reference Manual Version 5.0.
Morris, G.L., Annandale, G., Hotchkiss, R., 2013. Reservoir Sedimentation 579–612. https://doi.org/10.1061/9780784408148.ch12
Müller, M., Bieri, M., Boillat, J.-L., Schleiss, A. (Eds.), 2010. Barrage de Lavey – Modélisations physique et numérique des écoulements et du transport solide dans le Rhône. Wasser Energ. Luft.
P.F. Enger, E.G. Carlson, 1962. Hydraulic Model Tests of Bottom and Surface Vanes to Control Sediment Inflow into Canal Headworks (Hydraulic Laboratory Report No. HYD 499). Colo.: Bureau of Reclamation, U.S. Department of the Interior, Denver.
SCD, 2023. DRAFT: Purges et vidanges des retenues - retour d'expérience (Technical Bulletin). Swiss Committee on Dams.

# Experimenting with riparian vegetation management to enhance the hydraulic and ecological functioning of modified agricultural brooks

Kaisa VÄSTILÄ[1], Kaisa-Leena HUTTUNEN[2], Tom JILBERT[3], Mikko KUUSSAARI[4], Krister KARTTUNEN[5], Jani WIKSTRÖM[6], Pasi VALKAMA[7], Jari KOSKIAHO[8], Jukka AROVIITA[9]

[1] Aalto University School of Engineering, Finland
kaisa.vastila@aalto.fi

[1,2,4,5,7,8,9] Finnish Environment Institute, Finland
kaisa.vastila@syke.fi; kaisa-leena.huttunen@syke.fi; mikko.kuussaari@syke.fi; krister.karttunen@syke.fi; pasi.valkama@syke.fi; jari.koskiaho@syke.fi; jukka.aroviita@syke.fi

[3,6] University of Helsinki, Finland
tom.jilbert@helsinki.fi, jani.wikstrom@helsinki.fi

ABSTRACT

There are significant knowledge gaps regarding the potential benefits of holistically planned vegetation management along agricultural brooks and rivers. We found that both the agricultural water management and the riparian plant and beetle diversity benefited from adopting a two-stage channel design with abundantly vegetated floodplains. Benefits for pollinators were gained by sowing flowering species while water quality and flow conveyance could be notably enhanced by mowing ~20-40% of the floodplain area.

## 1. Introduction

The biodiversity and ecosystem services of brooks and small rivers flowing through agricultural areas have deteriorated because of channel modifications, frequent extensive clearing of channel vegetation, and increased loads of suspended sediment (SS) and nutrients (e.g. DeZiel et al. 2019). These same factors influence the flow conveyance and water levels, riverbed siltation, and the fate of dissolved and particulate substances. Farmers are concerned of the potential adverse impacts of vegetation on the water management, including increased risk of flooding and the blockage of sub-surface drainage. Understanding that diverse riparian vegetation is an integral part of healthy brooks and rivers while acknowledging the farmers' concerns, the aim of this contribution is to investigate different practically feasible solutions for achieving more diverse riparian plant communities to enhance both the hydraulic and ecological functioning of modified agricultural brooks.

## 2. Methodology

We conducted field investigations at previously dredged agricultural brooks where part of the channel network had been converted into a nature-based two-stage (compound) channel design consisting of a floodplain excavated on one or both sides of the main (low-flow) channel (e.g. Västilä et al. 2021). The brooks have top widths of up to ~10 m and mean discharges of ~0.06–0.40 $m^3/s$. We assessed the biodiversity effects of two-stage channels (TSCs) compared to conventional dredging, the potential of sowing flower strips on floodplains and channel banks to support pollinators (cf. Pérez-Sánchez et al. 2023), and the influence of partial floodplain vegetation mowing on improving the hydraulic performance and the retention of SS and nutrients.

## 3. Results and discussion

Selective mowing and removal of the clippings on 32% of the TSC floodplain area in late summer resulted in greater relative improvement in flow conveyance during autumn (5–32%) than winter–early spring high flow season (-7–19%) when the vegetative flow resistance was notably lower as the plants were withered and bent (Fig. 1a). The differences between the two years with the same mowed areas are explained by the different mowing methods, resulting in higher stubble and more uncollected clippings in the first year. On the mowed areas, the removal of SS, phosphorus (P) and nitrogen through floodplain deposition was 92%, 67% and 84%

greater, respectively, than on non-mowed areas. Thus, as expected, mowing likely enhanced the supply of particulate substances from the main channel to the floodplain where deposition was supply-limited by the dense, emergent vegetation. Further 31–37% increases in SS and P deposition were achieved by increasing the floodplain inundation frequency through constructing a natural-like rock ramp for raising the water levels.

Riparian plant and invertebrate communities seemed to benefit from the TSC structure having higher taxa richness compared to conventionally dredged ditch sections. This pattern was likely due to the more heterogenous habitat structure (Kędzior & Kosewska 2022) of TSCs with adjacent floodplains and drier ditch banks. Against some earlier studies (DeZiel et al. 2019), our TSCs did not diversify stream channel structure. Consequently, there were no positive effect on benthic invertebrate or diatom diversity. Still the overall effect of TSCs on local biodiversity was clear for all the studied organism groups as the combined taxa richness was clearly higher than for conventional ditches alone (Fig. 1b). Thus, the TSC design can be considered as a step towards biodiversity-friendly farming (Landis 2017).

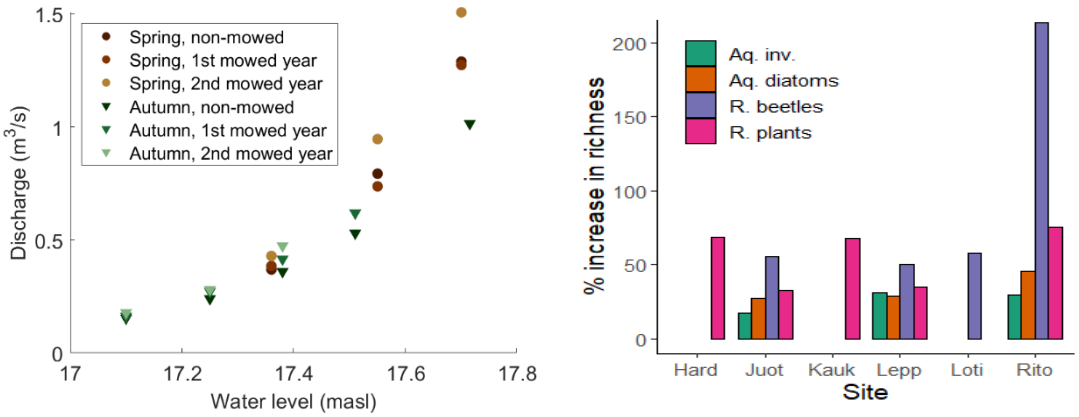



**Fig. 1.** A) The influence of partial mowing of the floodplain vegetation on flow conveyance in two consecutive years. B) catchment-specific increase (%) in taxonomic richness when combining taxa occurring only in a TSC and those occurring in conventional ditch sections.

In our field experiment, sown flower strips established poorly on the floodplain but well on the adjacent drier bank of the TSC. Sown annual plants (e.g. *Phacelia tanacetifolia*) flowered abundantly already during the first summer, and thus pollinators (bumblebees, hoverflies and butterflies) were more abundant on the flower strips than in the control grass strips. During the second and third year, sown perennial plants (e.g. *Leucanthemum vulgare* and *Centaurea jacea*) flowered in increasing abundance whereas the sown annual plants mostly disappeared. In the third year, pollinator abundance was highest in the flower strips on the drier banks and lowest on the grass-sown floodplain areas.

The TSC floodplains could, in certain terms, be included into the field area eligible for Common Agricultural Policy (CAP) support similar to vegetated buffer zones. The new CAP requires maintenance of the floodplain vegetation as well as environmentally sound drainage methods for receiving subsidies for channel maintenance works. Future research should investigate solutions allowing for more woody riparian vegetation and the optimization of vegetation maintenance considering biodiversity, water quality and water management.

**Acknowledgements**

We acknowledge funding from Academy of Finland, Ministries of the Environment and Agriculture and Forestry, Maa- ja vesitekniikan tuki ry, and Salaojituksen tukisäätiö sr. The help of laboratory technician Antti Louhio at Aalto University in constructing equipment for field investigations is appreciated.

**References**

DeZiel (Asmus) B, Krider L., Hansen B, Magner J, Wilson B, Kramer G, Nieber J. (2019) Habitat improvements and fish community response associated with an agricultural two-stage ditch in Mower County, Minnesota, Journal of the American Water Resources Association, 55, 154–188. https://doi.org/10.1111/1752-1688.12713

Kędzior R, Kosewska A (2022) Landscape heterogeneity determines the diversity and life history traits of ground beetles (Coleoptera: Carabidae), Sustainability, 14, 13980. https://doi.org/10.3390/su142113980

Landis DA (2017) Designing agricultural landscapes for biodiversity-based ecosystem services, Basic and Applied Ecology, 18, 1–12. http://dx.doi.org/10.1016/j.baae.2016.07.005

Pérez-Sánchez AJ, Schröder B, Dauber J, Hellwig N (2023) Flower strip effectiveness for pollinating insects in agricultural landscapes depends on established contrast in habitat quality: A meta-analysis, Ecological Solutions and Evidence, 4, e12261. https://doi.org/10.1002/2688-8319.12261

Västilä K, Väisänen S, Koskiaho J, Lehtoranta V, Karttunen K, Kuussaari M, Järvelä J, Koikkalainen K (2021) Agricultural water management using two-stage channels: performance and policy recommendations based on Northern European experiences, Sustainability, 13, 9349. https://doi.org/ 10.3390/su13169349

# Evaluation of MAR feasibility in Cyprus based on a participative multi-criteria decision analysis

Sarah EISENREICH[1], Constantinos F. PANAGIOTOU[2*], Tiago MARTINS[3], Olga BAROUTA[4], Stelios NEOPHYTIDES[2], Marinos STYLIANOU[4], Catalin STEFAN[1]

[1] Research Group INOWAS, Department of Hydrosciences, Technische Universität Dresden, Dresden, Germany
sarah.eisenreich@mailbox.tu-dresden.de, catalin.stefan@tu-dresden.de

[2] Department of Environment and Climate, Eratosthenes Centre of Excellence, Limassol, Cyprus
constantinos.panagiotou@eratosthenes.org.cy, stelios.neophytides@eratosthenes.org.cy

[3] National Laboratory for Civil Engineering, Portugal
tmartins@lnec.pt

[4] Laboratory of Chemical Engineering and Engineering Sustainability, Faculty of Pure and Applied Sciences, Open University of Cyprus, Cyprus
olga.barouta@st.ouc.ac.cy, marinos.stylianou@ouc.ac.cy

ABSTRACT

## 1. Short introduction

Cyprus is an island located at the eastern part of the Mediterranean basin, characterized by semi-arid climatic conditions and limited freshwater resources (Zachariadis, 2010). Combined with the over-exploitation of these resources due to the increasing water consumption among the different sectors, Cyprus possesses the highest Water Exploitation Index among the European countries (EEA, 2023). Excessive amounts of freshwater are abstracted from the groundwater systems to satisfy the water demand, which are continuously deteriorating in terms of quantity and quality.

Coastal aquifers in Cyprus are prone to seawater intrusion due to the inadequate replacement of the abstracted water amounts, urging the national authorities to design water management plans that aim on their gradual restoration. Managed aquifer recharge (MAR) is an environmentally sustainable technology that is currently applied in Cyprus for mitigating the pollution of coastal aquifers due to seawater intrusion. Particularly, treated wastewater is transferred from the exit of wastewater treatment plant stations to recharge ponds through pipeline networks, from where it percolates the unsaturated soil layer until it reaches the aquatic system.

This study focuses on the identification of regions within Cyprus which are feasible for MAR via participative multi-criteria decision analysis (Figure 1).

## 2. Mapping process and preliminary results

Joint discussions with local stakeholders from different water sectors (agriculture, water treatment, supply) have been conducted at different stages of the mapping process to ensure the acceptance of the generated maps from the national authorities. The first stage of the analysis aimed on the identification of the MAR objective (i.e. store groundwater for reuse), water source (i.e., treated wastewater) and recharge technique (i.e., surface spreading method via infiltration ponds) that reflect the needs and geological/morphological specificities of the study area and are expected to contribute to the future planning of MAR implementation in Cyprus.

Next, the parts of the study area which are subjected to implementation constraints (Table 1) were identified and excluded from the feasibility analysis. Particularly: i) geopolitical constraints (the northern part of the island is illegally occupied by the Turkish troops since 1974, and no effective control can be applied by the authorities of the RoC); ii) areas where either no aquifer systems are present, or confined aquifers are present

which do not favor surface spreading methods; iii) drinking water protection zones and iv) land-use land cover types.

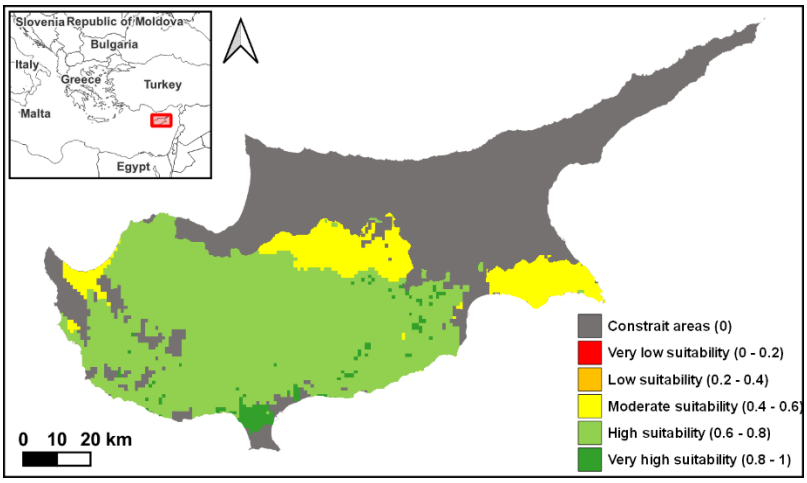



**Fig. 1.** Geographical location of the study area and intrinsic suitability map of the study area.

A number of criteria related to the case study characteristics have been selected that contain information spatially clustered within three thematic layers, namely the intrinsic properties, water available for MAR and water demand of groundwater-dependent ecosystems. In accordance with the participatory approach of AGREEMAR (Martins et al., 2022), a set of weights were assigned to each criterion based on its relevance with the recharge problem, after consulting local stakeholders from the water sector. Preliminary results of the mapping process are shown in Figure 1, particularly the spatial distribution of the intrinsic suitability of the study area. The high scores at the southern part of the island are associated with favorable hydrogeological properties, particularly high aquifer specific yield and aquifer hydraulic conductivity, along with the presence of flat terrains (low terrain slopes), facilitating the implementation of MAR schemes. On the other hand, the low suitability of the eastern coastal regions is partly attributed to the low aquifer geochemistry that is present in that region.

On-going work focuses on the compilation of suitability maps for the remaining thematic layers, water availability and water demand, which are needed for estimating the spatial distribution of MAR feasibility. The results will be discussed with the stakeholders during workshops aiming to validate and improve the generated maps and ensure their usage during the revision/design of water policies related to MAR.

**Acknowledgements**

The AGREEMAR project is funded by National Funding Agencies from Germany (Bundesministerium für Bildung und Forschung – BMBF), Cyprus (Research & Innovation Foundation – RIF), Portugal (Fundação para a Ciência e a Tecnologia – FCT), Spain (Ministerio de Ciencia e Innovación – MCI) and Tunisia (Ministère de l'Enseignement Supérieur et de la Recherche Scientifique – MESRS) under the Partnership for Research and Innovation in the Mediterranean Area (PRIMA). The PRIMA programme is supported under Horizon 2020 by the European Union's Framework for Research and Innovation. Project duration: 1 June 2022 – 31 May 2025.

**References**

Copernicus, "CORINE Land Cover," [Online]. Available: https://land.copernicus.eu/pan-european/corine-land-cover/clc2018. [Accessed June 2023].

EEA, Network, European Environment Agency European Environment Information and Observation, 2023. [Online]. Available: https://www.eea.europa.eu/data-and-maps/data/eea-reference-grids-2/gis-files/cyprus-shapefile. [Accessed June 2023].

EEA, Network, European Environment Agency European Environment Information and Observation, 2023. [Online]. Available: https://www.eea.europa.eu/ims/use-of-freshwater-resources-in-europe-1 [Accessed October 2023]

Martins, T.N., Panagiotou, C.F., Stefan, C., Chkirbene, A. (2022) AGREEMAR Deliverable D2.2. Participative methodology for criteria selection and weighting in MAR site feasibility mapping. Available online at https://www.agreemar.inowas.com/deliverables

Water Development Department Geoportal [Online] Available: https://geoportal-wdd.hub.arcgis.com/ [Accessed June 2023]

Zachariadis T. (2010) Residential Water Scarcity in Cyprus: Impact of Climate Change and Policy Options. Water. 2(4):788-814.

# Comparison of IDF Curves for Mainland Portugal Using Ground-Based and ERA5-Land Data

Laryssa FREITAS[1], Maria Manuela PORTELA[1,2], Luis Angel ESPINOSA[2,3], José MATOS[1,2]

[1] Instituto Superior Técnico, University of Lisbon (IST/UL), Portugal. [2] Civil Engineering Research and Innovation for Sustainability (CERIS), Portugal. [3] Associação do Instituto Superior Técnico para a Investigação e Desenvolvimento (IST-ID), CERIS, Portugal

laryssa.freitas@tecnico.ulisboa.pt (for author 1); maria.manuela.portela@tecnico.ulisboa.pt (for author 2); luis.espinosa@tecnico.ulisboa.pt (for author 3); jose.matos@tecnico.ulisboa.pt (for author 3).

ABSTRACT

This exploratory analysis is focused on mainland Portugal and aims to compare the intensity-duration-frequency (IDF) curves built upon ERA5-Land reanalysis data and the ones established based on ground observations. The results achieved so far clearly indicate that there is still a long way to go before concluding about the feasibility of using reanalysis data to characterize the intensive rainfall in Portugal.

## 1. Introduction

The goal of the study is to compare IDF curves based on ERA5-Land reanalysis data and on ground observations at the eight locations shown in Figure 1. The alphanumeric codes starting with P relate to the centroids of ERA5-Land grid points and the location names (Sezelhe, Deilão, Seia, Muge, Vila Viçosa, Lisboa (IGDL), Santa Clara do Louredo and Estói) refer to rain gauges. The rain gauge assigned to each ERA5-Land grid point was the nearest one with at least 20 years of records. The rainfalls at the rain gauges were provided by the Portuguese meteorological and environmental agencies (IPMA and APA-SNIRH, respectively).

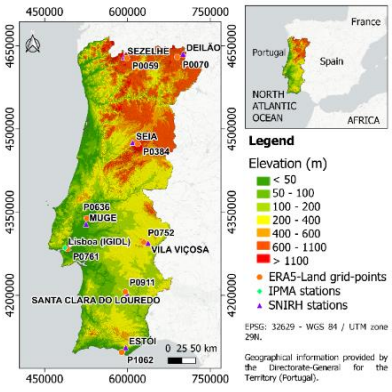



**Fig. 1.** Mainland Portugal elevation map in meters, with the schematic location of the coupled rain gauges and ERA5-Land grid-points.

## 2. Materials and methods

The daily records at the rain gauges had some gaps. Each gap with the duration of 1 day occurring in the rainy season (the only gaps that are relevant when aiming at establishing IDF curves) were filled with the average of the rainfalls in previous and next contiguous days. The annual maximum rainfall samples were obtained for the durations of 24, 48, 72, 96 and 120 hours (1 to 5 days). Their length differed among the rain gauges, as characterized in Table 1.

ERA5-Land has complete hourly values of rainfall during the rainy season which allowed the building of annual maximum rainfall series for the durations of 1, 3, 6, 9, 12, 18, 24, 48, 72, 96 and 120 hours, for the period from Oct/1980 to Sep/2020 (41 hydrological years).

Aiming at comparing IDF curves with those of the reference study from BRANDÃO *et al.* (2001) for some of the locations of Figure 1, two duration intervals were adopted, as considered in that study, namely from 1 to 6 h and from 6 to 120 h. Table 1 summarizes the ERA5-Land grid-points, the closest rain gauges assigned to those points and the identification of the BRANDÃO *et al.* (2001) curves, when applicable. The IDF curves based on ground data can only be compared with the reference ones for durations equal to or higher than 1 day. It is important to highlight that the data sets relate to different periods.

**Table 1.** ERA5-Land grid points, IPMA/ SNIRH rain gauges and IDFs from BRANDÃO *et al.*, 2001.

| ERA5-Land grid-point | | Rain gauge | | BRANDÃO at al. (2001) IDF curve |
|---|---|---|---|---|
| Name | Annual Average rainfall (mm) | Identification (data source; period with records; number of hydrological years with records) | Annual Average rainfall (mm) | |
| P0384 | 54.35 | Seia (SNIRH; Oct/1959 - Sep/1980; 22 years) | 72.35 | Penhas Douradas |
| P0761 | 37.38 | Lisboa (IGDL) (IPMA, Oct/1864 - Sep/2020; 157 years) | 51.48 | Lisboa |
| P0752 | 38.14 | Vila Viçosa (SNIRH, Oct/1946 - Sep/2002; 57 years) | 48.84 | Portalegre |
| P0911 | 38.40 | Santa Clara Louredo (SNIRH; Oct/1980 – Sep/1999; 20 years) | 43.22 | Beja |
| P1062 | 48.01 | Estói (SNIRH; Oct/1983 – Sep/2007; 25 years) | 65.44 | Faro |
| P0070 | 53.57 | Deilão (SNIRH; Oct/1940 – Sep/1997; 58 years) | 45.92 | -- |
| P0059 | 65.54 | Sezelhe (SNIRH; Oct/1949 - Sep/1992; 44 years) | 94.51 | -- |
| P0636 | 37.75 | Muge (SNIRH; Oct/1940 – Sep/2003; 64 years) | 39.95 | -- |

## 3. Results

The results obtained are exemplified in Fig. 2 based on three return periods, RP (50, 100, and 1000 years) and on four coupled ERA5-Land grid points/rain gauges. When available, the IDF curves from the reference study were also represented. Most often, the IDFs based on ERA5-Land underestimate the intensity. Only for Deilão there is a good adjustment between the reanalysis and ground-based curves. A good agreement between IDFs based on ERA5-Land and those proposed in BRANDÃO *et al.* (2001) for the common rainfall durations was only observed in Lisbon (IGDL).

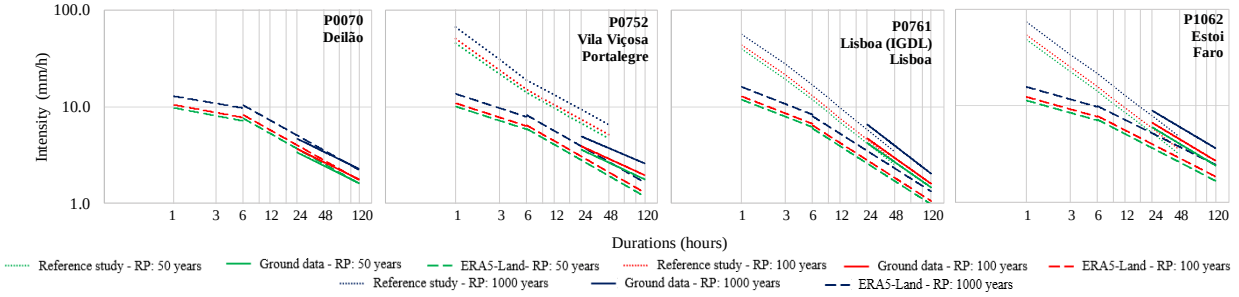



**Fig. 2.** Log-log plots of the IDFs curves for different return periods (RP) and data sets.

The curves of Fig.2 were made dimensionless by dividing the rainfall with a given RP and duration d, $P_d$, by the rainfall with the duration of 24 h and the same RP, $P_{24}$ – Fig. 3. For durations less than 6 h, the comparison with the curves of BRANDÃO *et al.* (2001) seems not to validate the use of ERA5-Land to obtain IDF curves well-adjusted to such small durations, which may be explained by the method used in the reference study to disaggregate daily precipitation data. For durations exceeding 6 h, there can be a good adjustment among IDFs curves, depending on the location.

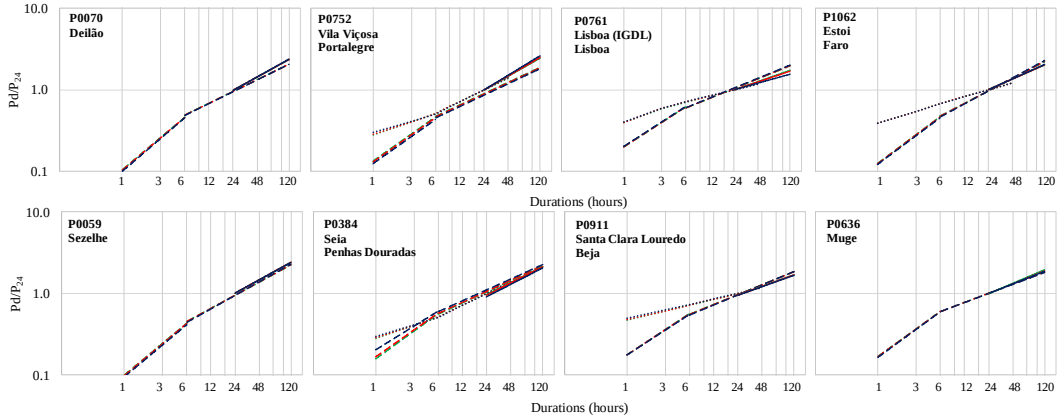



**Fig. 3.** Log-log plots of the dimensionless IDFs curves (the legend is the same as Fig. 2).

**References**

Brandão, C., Rodrigues, R., & Costa, J. P. (2001). Análise de Fenómenos Extremos - Precipitações Intensas em Portugal Continental. Lisboa: Direcção dos Serviços de Recursos Hídricos.

# Inversion of the Reaction-Diffusion-Advection Equation for Colloidal Contaminants Utilising the Iterative Ensemble Kalman Filter

Liam Duncan[1], Abbas El-Zein[1]

[1]University of Sydney, Australia
liam.duncan@sydney.edu.au
abbas.elzein@sydney.edu.au

ABSTRACT

## 1. Introduction and Methods

Recently there has been increased interest in colloidal contamination of groundwater systems because of the emergence of micro and nano plastics and carbon nanotubes as contaminants of interest (Kasel et al., 2013). These contaminants pose a direct threat to ecosystem health and have the potential to remobilise organic contaminants (Wong et al. 2013). Models of colloidal transport facilitate the understanding of the source and extent of historical contamination and enable the design of systems to reduce or prevent future contamination of groundwater systems (Alimi et al. 2021). The transport of colloids in porous media is modelled using a modified form of the reaction diffusion advection equation (RDAE) with the inclusion of kinetic sites for attachment and detachment of colloids at collector sites. Several of the parameters in this equation cannot be measured directly and as such must be estimated using an inversion algorithm.

Local search algorithms, particularly the Levenberg-Marquardt algorithm (LMA) have been utilised extensively in the literature and in commercial software such as HYDRUS, PEST and UCODE to invert the RDAE (Barati et al. 2021). These algorithms typically utilise a gradient descent approach whereby the updated set of estimated parameters are chosen in the opposite direction of the gradient until the minimum is obtained (Simunek et al. 2003). Despite their widespread use, these algorithms don't quantify the uncertainty of parameter estimates (Barati et al. 2021). This uncertainty may develop from the heterogeneity of the soil or from limitations in the precision of experimental techniques. Stochastic algorithms inherently quantify uncertainty through the construction of probability distribution functions for each of the unknown variables (Barati et al. 2021). One such stochastic method receiving attention for its simplicity and computational efficiency is the iterative Ensemble Kalman filter (iEnKF). The iEnKF estimates the posterior distribution of the parameters through linear Gaussian updates of an ensemble of samples from the prior distribution. An advantage of the iEnKF is that it doesn't calculate gradient but uses the covariance of the parameters, model predictions and observational data to update the ensemble (Zhang et al. 2020). This significantly reduces the computational costs associated with calculating gradients especially for high dimensional problems (Evensen 2003). Previous studies have utilised the iEnKF to predict solute transport in aquifers. However, to the best of the authors' knowledge, no such attempt has been made for the more complex equations required to model colloidal contaminants. Therefore, in this study we validate the use of the iEnKF algorithm to find the inverse solution to a form of the RDAE:

$$\frac{\partial C}{\partial t} + \frac{\rho}{\theta}\frac{\partial S}{\partial t} = \alpha_x |v| \frac{\partial^2 C}{\partial x^2} - v\frac{\partial C}{\partial x} \quad (1)$$

where $C$ – concentration of colloids suspended in solution [M.L$^{-3}$], $t$ – time [T], $\rho$ – dry bulk density of the porous media [M.L$^{-3}$], $\theta$ – porosity [-], $S$ is the concentration of colloids attached at collector sites [M.M$^{-1}$] , $\alpha_x$ is the dispersivity [L], $x$ is the distance from the source [L] and $v$ is the pore water velocity [L.T$^{-1}$]. The concentration of colloids attached at collector sites is described by:

$$\frac{\rho}{\theta}\frac{\partial S}{\partial t} = k_a \psi C \quad (2)$$

where $k_a$ - rate of attachment of colloids at collectors [$T^{-1}$], $k_d$ is the rate of detachment [$T^{-1}$] and $\psi$ – blocking function describing the change in attachment rate with depth [-]. In this equation the parameters $\alpha_x$, $k_a$, cannot be measured directly and must be estimated using the iEnKF. To assess the capability of the iEnKF, a synthetic dataset is created by assuming the values of these parameters. Synthetic datasets are preferred to experimental ones in this first stage of validation because the correct parameter values are known and can be compared with the estimations made by the iEnKF.

## 2. Results

Figure 1 presents results generated by the study and shows the successful convergence of the parameter estimates to the correct solution of the synthetic dataset within 20 iterations and the initial and final distribution of these ensembles. The convergence indicates the capability of the iEnKF to provide accurate parameter estimation whilst the final ensemble represents the uncertainty from which measurement of standard deviation and confidence intervals can be assessed with ease.

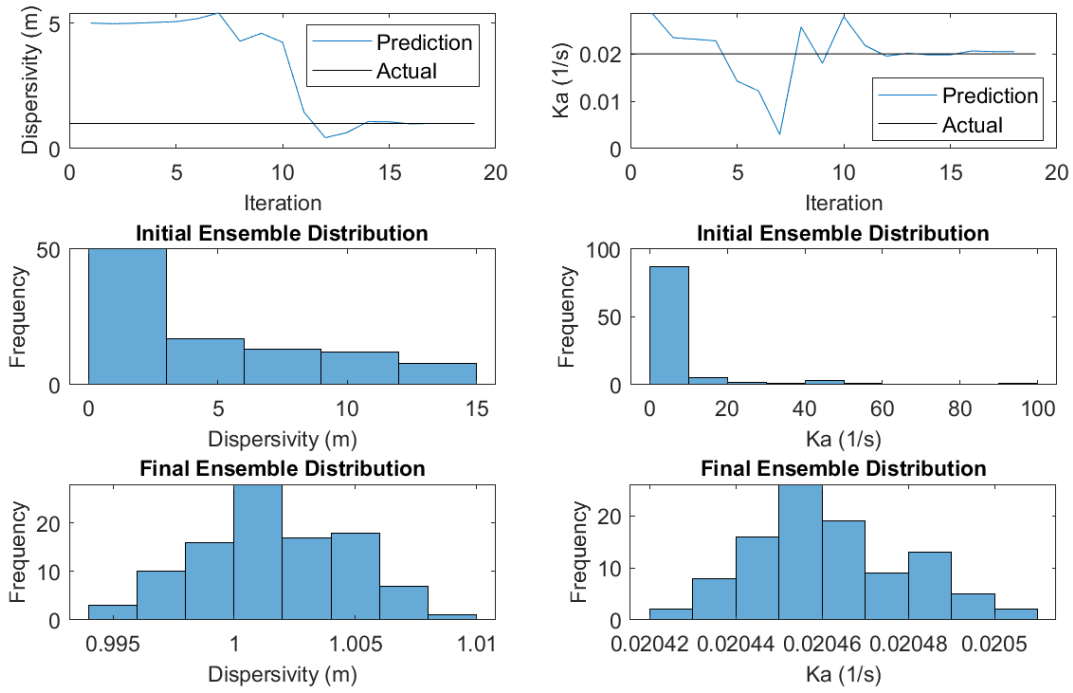



**Fig. 1:** Prediction of Dispersivity ($\alpha_x$) and Attachment Coefficient ($K_a$) using the iEnKF

## 3. Conclusions

The form of the iEnKF presented in this paper is shown to be effective at parameter estimation and uncertainty characterisation of colloidal transport in porous media. The accuracy and computational performance of the iEnKF are similar to those of LMA in inverting the RDAE, with the crucial advantage that the former, unlike the latter, is capable of characterising the uncertainty of estimates.

**References**


Kasel D, Bradford SA, Šimůnek J, Pütz T, Vereecken H, Klumpp E (2013) Limited transport of functionalized multi-walled carbon nanotubes in two natural soils, Environmental Pollution, 180, 152–158

Wong JKH, Lee KK, Tang KHD, Yap PS (2020) Microplastics in the freshwater and terrestrial environments: Prevalence, fates, impacts and sustainable solutions, Science of The Total Environment, 719, 1-15

Alimi OS, Farner JM, Tufenkji N (2021) Exposure of nanoplastics to freeze-thaw leads to aggregation and reduced transport in model groundwater environments, Water Research, 189, 1-9.

Chu X, Li T, Li Z, Yan A, Shen C (2019) Transport of Microplastic Particles in Saturated Porous Media, Water, 11, 1-12

Moghaddam MB, Mazaheri M, Samani JMV (2021) Inverse modeling of contaminant transport for pollution source identification in surface and groundwaters: a review, Groundwater for Sustainable Development, 15, 1-15

Zhang J, Vrugt JA, Shi X, Lin G, Wu L, and Zeng L (2020) Improving Simulation Efficiency of MCMC for Inverse Modeling of Hydrologic Systems With a Kalman-Inspired Proposal Distribution, Water Resources Research, 56, p.1-24

Evensen G (2003) The Ensemble Kalman Filter: theoretical formulation and practical implementation, Ocean Dynamics, 53, 343–367

# DNN-Enhanced Predictive Modeling for Sediment Transport in Reservoirs: Riba-Roja Case Study

Danial DEHGHAN-SOURAKI[1], Ernest BLADE[2], Antonia LARESE[3]

[1,2] Flumen Institute, Polytechnic University of Catalunya (UPC)
danial.dehghan@upc.edu, ernest.blade@upc.edu

[3] University of Padova
antonia.larese@unipd.it

ABSTRACT

## 1. Introduction

The incorporation of Artificial Intelligence (AI) techniques in sediment transport modeling, especially in reservoir contexts, is revolutionizing water resources management and environmental engineering. Sediment deposition and erosion significantly impact reservoirs, crucial for water storage, flood control, and energy generation. Traditional modeling methods often struggle with computational efficiency, accuracy, and managing the complex, dynamic, and nonlinear processes of sediment movement. AI offers a solution by efficiently replicating the Iber sediment transport model, thereby facilitating the demanding calibration process and enhancing sediment transport modeling in the Riba-Roja reservoir [1, 2].

## 2. Methodology

### *2.1. Sediment Transport Model*

The sediment transport module in Iber [3] simulates bedload and suspended sediment transfer. It is based on the hydrodynamic modules' estimated velocity, depth, and turbulent viscosity fields. The depth-averaged turbulent convection-diffusion equation was used to describe suspended sediment motion. The sediment transport model equations can be expressed as below equation [4]:

$$\frac{\partial hC}{\partial t} + \frac{\partial hU_x C}{\partial x} + \frac{\partial hU_y C}{\partial y} = \frac{\partial}{\partial x_j}\left(\left(\Gamma + \frac{\nu_t}{S_{c,t}}\right) h \frac{\partial C}{\partial x_j}\right) + (Er - De) \quad (1)$$

### *2.2. Deep Neural Network Implementation*

Central to this study's focus is the implementation of a Deep Neural Network (DNN). This cutting-edge computational paradigm has been trained to utilize historical sediment transport data as well as pertinent input parameters. Its architecture, characterized by multiple interconnected layers, functions as a mechanism for the extraction of intricate features and, subsequently, regression analysis. A comprehensive optimization process is undertaken, encompassing hyperparameter tuning and architectural refinement, to maximize the DNN's predictive precision. The following is the basic equation for a three-layer DNN regression model:

$$\hat{y} = W_3\left(\sigma\left(W_2\left(\sigma(W_1 X + b_1)\right) + b_2\right)\right) + b_3 \quad (2)$$

In this equation, $\hat{y}$ represents the projected target value, X represents the input features, $W_1$, $W_2$, and $W_3$ represent the weights for each layer in a three-layer network, $b_1$, $b_2$, and $b_3$represent the biases for each layer, and $\sigma$ (sigmoid) represents the activation function applied element-wise to the intermediate layer outputs.

## 3. Case Study: Riba-Roja Reservoir

A prominent case study within the Riba-Roja Reservoir illustrates sediment transport dynamics in action. The basin, which covers an area of 85,000 km$^2$, is home to a network of 107 reservoirs and an irrigated area of around 800,000 acres. The Riba-Roja Reservoir is distinguished by its unique and long structure. The force of sediment discharge, driven by tributaries and natural sources, has substantially affected the geomorphological

terrain of the basin. The Riba-Roja Reservoir's efficient management of sediment transport serves as a reminder of the crucial ecological and economic importance of attentive reservoir management techniques.

## 4. Results and Discussion

Figure 1.a shows that, except for slight anomalies in the first 3 kilometers upstream from the reservoir's head, the projected Accumulated Sediment Volume (ASV) curves closely correspond with the experimental curves across the reservoir. These variations indicate difficulties in reliably estimating sediment transport in this upstream region, most likely due to changing sediment properties, complex hydraulic conditions, or probable measurement errors. Nonetheless, the simulation demonstrates the model's overall ability to reasonably anticipate sediment deposition inside the reservoir, albeit there is still space for improvement, particularly in upstream locations.

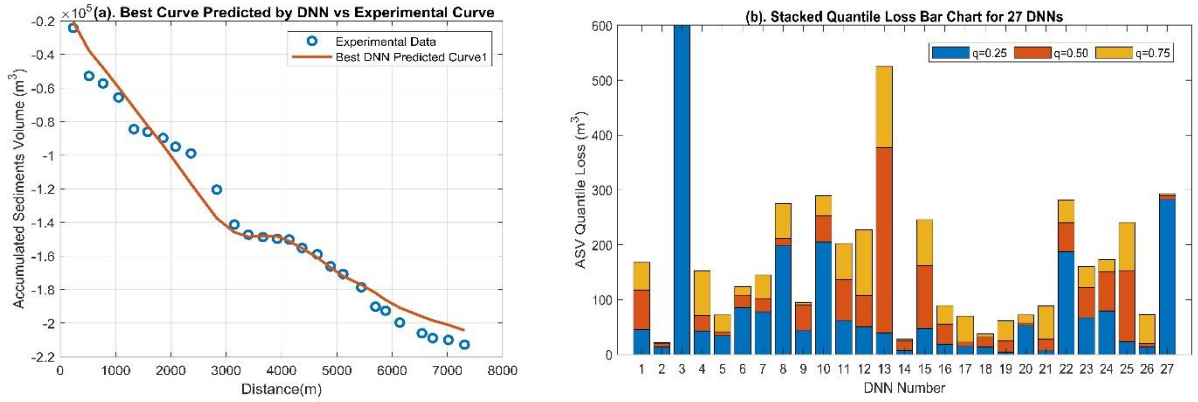



Figure 1. Variations of RMSE error of the global DNN network with the number of test datasets (a) and Individual DNNs quantile loss in ASV values (b)

In Figure 1.b, a stacked bar chart is used in this investigation to analyze the prediction accuracy of 27 DNN models for anticipating ASV curves. The graph shows that, except for DNN model number 3, the majority of quantile loss values, which represent prediction errors, fall outside the middle 50% of the ASV distribution. This divergence in DNN model 3 is caused by an ASV curve discontinuity between points 2 and 3, offering a challenge to model accuracy. Importantly, even the largest quantile loss, found in DNN model 3, remains less than 5% of the actual ASV value, highlighting these models' general ability to closely replicate the genuine ASV curve.

## 5. Conclusion

This study's efforts highlight the significance of sediment transport modeling as a tool for understanding sediment dynamics inside reservoirs. Furthermore, a thorough evaluation of the DNN's predictive skills underlines its potential as a revolutionary tool in sediment transport investigations. Future developments in DNN design, along with careful collection of data, have the potential to improve predictions even more.

**References**

[1] K. Rezaei, B. Pradhan, M. Vadiati, and A. A. Nadiri, “Suspended sediment load prediction using artificial intelligence techniques: comparison between four state-of-the-art artificial neural network techniques,” Arabian Journal of Geosciences, vol. 14, no. 3, p. 215, Feb. 2021, doi: 10.1007/s12517-020-06408-1.
[2] K. Roushangar, S. Shahnazi, and H. M. Azamathulla, “Sediment Transport Modeling through Machine Learning Methods: Review of Current Challenges and Strategies,” 2023, pp. 223–240. doi: 10.1007/978-981-19-7100-6_13.
[3] E. Bladé et al., “Iber: herramienta de simulación numérica del flujo en ríos,” Revista Internacional de Métodos Numéricos para Cálculo y Diseño en Ingeniería, vol. 30, no. 1, pp. 1–10, Jan. 2014, doi: 10.1016/j.rimni.2012.07.004.
[4] L. Cea et al., “IberWQ: new simulation tool for 2D water quality modelling in rivers and shallow estuaries,” Journal of Hydroinformatics, vol. 18, no. 5, pp. 816–830, Sep. 2016, doi: 10.2166/hydro.2016.235.

# Coping with pulsed flows: Evaluating the efficiency of two flow refuges for an Iberian cyprinid

Renan LEITE[1], Maria João COSTA[2], Daniel MAMERI[3], Fernando AFONSO[4], António PINHEIRO[5], José Maria SANTOS[6], Isabel BOAVIDA[7]

[1, 2, 5, 7] Civil Engineering for Research and Innovation for Sustainability, Técnico - University of Lisbon, Lisbon, Portugal, renanleite@edu.ulisboa.pt, mariajcosta@tecnico.ulisboa.pt, antonio.pinheiro@tecnico.ulisboa.pt, isabelboavida@tecnico.ulisboa.pt

[1, 3, 6] Forest Research Centre, Associate Laboratory TERRA, School of Agriculture - University of Lisbon, Lisbon, Portugal, renanleite@edu.ulisboa.pt, dmameri@isa.ulisboa.pt, jmsantos@isa.ulisboa.pt,

[4] CIISA – Centre for Interdisciplinary Research in Animal Health, Faculty of Veterinary Medicine, University of Lisbon, Portugal, fafonso@fmv.ulisboa.pt

[4] Associate Laboratory for Animal and Veterinary Sciences (AL4AnimalS), University of Trás-os-Montes and Alto Douro, Portugal, fafonso@fmv.ulisboa.pt

ABSTRACT

The impacts of artificial pulsed flows associated with hydropower production on the downstream biological and physical processes have been extensively addressed, particularly those affecting fish fauna, causing fish drift and forcing changes in habitat selection. Our knowledge of these impacts in improving habitat enhancement strategies is still limited, especially for cyprinids. The goal of this study was to evaluate the attraction efficiency of two flow-refuges differing in their approaching angles, for the Iberian barbel (*Luciobarbus bocagei*, Steindachner 1864) at an indoor experimental flume. We tested two flow-refuge approaching angles i.e., 45º and 70º, creating distinct hydraulic conditions at the flow-refuge entrance. Two flow events, i.e., a base (BF)- and a pulsed-flow (PF), were tested for each flow-refuge type. To analyse flow-refuge efficiency, we quantified fish individual and group use patterns (absolute frequency and permanence time) at two distinct refuge locations (downstream and inside) and physiological responses (glucose and lactate). The flow field was characterized using an ADV probe. The results showed that the individual frequency of use during the PF events was higher, especially for the45ºangle . Significant differences in the frequency of individual use, inside and downstream of the area of the flow-refuge, among flow events were found. The use in group of the flow-refuge did not show a significant effect in neither inside nor downstream locations of the flow-refuge. There was no statistical evidence that the position of the flow refuge affected the group behavior of *barbels* under PF. Although the PerMANOVA did not show significant results for the overall metrics, the permanence time as an individual uses inside the 45º flow-refuge tends to be higher than the 70º flow-refuge, during PF events. The flow events and the approaching angles tested did not trigger physiological responses in the tested trials. Overall, the 45º flow-refuge tended to be used more often than the 70º. The flow field differed between the two insertion angles. The 45º flow-refuge induced channel narrowing and subsequently creating greater flow uniformity. This enhanced flow homogeneity likely contributed to increase the flow-refuge use by fish. These findings emphasize the critical importance of carefully selecting the insertion angle when designing and installing flow-refuges for cyprinids, particularly in river ecosystems impacted by pulsed flows.

## 1. Introduction

Hydropower is a highly efficient electricity source, responding almost instantly to the market demand by changing the turbine discharges. However, the rapid flow fluctuations due to the high energy demand, i.e.,

hydropeaking, disturb the biological, morphological, and hydrological processes of the downstream river system (Alp et al., 2020), debilitating its ecological integrity. In recent years, the amount of research addressing hydropeaking has grown substantially, and have been mostly focused on salmonids, demonstrating that changing particular features in artificial habitat design can trigger distinct behavioral changes, dictating their efficiency. However, few studies have proposed habitat enhancement solutions to reduce its impacts based on fish behavior (Costa et.al., 2019). To fill this gap of knowledge, the main goal of the present study was to evaluate the use of two types of flow-refuge by *barbels* at an experimental flume, during simulated pulsed flow conditions on movement behavior and stress physiology. An integrated approach was conducted where behavioral metrics and blood physiology were quantified, in addition to the characterization of the hydraulic environment.

## 2. Material and Methods

Fish sampling for the *barbels* took place in the Sorraia River (39.011376 ˚ N, -8.357126 ˚ W), a tributary of the lower Tagus River (central Portugal), in November of 2021, using a low-voltage electrofishing gear and transported in a constantly aerated tank to the laboratory. The experiments were conducted at an indoor flume located at the Hydraulics Laboratory of Instituto Superior Técnico, University of Lisbon. The flume usable area for fish was 6.5 m long x 0.7 m wide, delimited upstream and downstream by perforated metallic panels. The maximum discharge was 60 $L.s^{-1}$ controlled by a downstream flap gate and an upstream sluice gate. The flow-field characterization was performed using an Acoustic Doppler Velocimeter (ADV; Nortek-AS Vectrino 10 MHz).

## 3. Results and Discussion

Overall, the absolute frequency of fish use (mean ± SD) at the 45º flow- refuge was higher than the 70º. Significant differences in the frequency of individual use inside (I_Ins; $\chi 2(3) = 9.7968$, $p= 0.02$) and downstream (I_Down; $\chi 2\ (3) = 11.159$, $p=0.01$) of the area of the flow-refuge, among events were found. The use in group of the flow-refuge, did not show a significant effect in neither inside nor downstream locations of the flow-refuge. The permanence time in the flow-refuge for the *barbels* on the 45º flow-refuge was higher than 70º. Nonetheless, the statistical analysis did not show a significant effect of the flow on permanence time. The physiological analyses were not statistically significant among trials, even though glucose levels were higher in PF70. Lactate levels did not indicate significant differences. As expected, the lowest velocities were observed during BF trials, and they were found in the immediate area downstream of the flow-refuge. The maximum velocities for PF (60 $L.s^{-1}$) found were 0.914 $ms^{-1}$ (PF45) and 0.781 $ms^{-1}$ (PF70). The flow-refuge use indicated that fish behavior changed according to the flow conditions and the insertion angle. Group use frequency did not demonstrate significant differences. This may be understood as a non-disruption of group behavior, meaning that the simulated PF conditions may not have affected the group behavior. According to Costa et al. (2019) findings, the frequency of use in group could be explained by the fact that lower discharge and pressure magnitudes can generate stability in the group behavior. The ADV results demonstrated that the flow-field was changed by such structures (i.e., different velocity ranges within the flume). The 45º flow-refuge was demonstrated to be the most suitable flow-refuge during pulsed flow conditions throughout the study, as it displayed the highest flow-refuge use and permanence time. The absence of physiological adjustments among trials, together with the characterization of the flow-field, suggests that the conditions created were not harsh enough to trigger a stress response. Flume studies may not replicate natural conditions but provide knowledge regarding fish interactions under a controlled environment, which are essential for the development of more efficient solutions and their application in the field. These indirect mitigation measures can be used by cyprinids for flow-refuges during pulsed flows associated with hydropower production. Future studies should consider extended tests with different ramping rates, different ranges of flow rates (higher ones), or even other fish guilds (e.g. water-column species).

**Acknowledgements**

This study received funding from Fundação para a Ciência e a Tecnologia (FCT) through the EcoPeak4Fish project – (PTDC/EAM-AMB/4531/2020). Forest Research Centre (CEF) (UIDB/00239/2020) and Civil Engineering Research and Innovation for Sustainability (CERIS) (UIDB/04625/ 2020) are research unit funded by FCT. Renan Leite was supported by a grant from FCT, given through the River Restoration and Management Doctoral Programme (FLUVIO) Portugal (grant UI/BD/151419/2021).

**References**

Alp A, Akyüz A, Kucukali S. Ecological impact scorecard of small hydropower plants in operation: An integrated approach (2020). Renewable Energy 162:1605-17.

Costa, M. J., Ferreira, M. T., Pinheiro, A. N., & Boavida, I. (2019). The potential of lateral refuges for Iberian barbel under simulated hydropeaking conditions. Ecological Engineering, 127, 567-578.

# Preliminary results of the monitoring of the insect community in a periurban section of the Manzanares River (Madrid, Spain)

Sergio IBARRA MELLADO[1], Manuel Ramón GARCÍA SÁNCHEZ-COLOMER[2], Arturo David YOUNG SÁNCHEZ MATEOS[1], José Luis VIEJO MONTESINOS[1]

[1,3,4] Department of Biology, Faculty of Science, Universidad Autónoma de Madrid (UAM)
sergio.ibarra@estudiante.uam.es
arturo.young@estudiante.uam.es
joseluis.viejo@uam.es
[2] Centre for Studies and Experimentation in Public Works (CEDEX)
manuel.colomer@cedex.es

ABSTRACT

This study evaluates insect communities as part of a monitoring campaign that started in 2023 to assess the recovery of the ecological and hydrological continuity of a section of the Manzanares River (Madrid, Spain).

## 1. Introduction

### *1.1. The Manzanares River restoration project*

The study contributes to the project "Recovery of the fluvial ecosystem Manzanares-Gavia-Bulera. Green and blue infrastructure Metropolitan Forest of Madrid", supported by the Biodiversity Foundation (Ministry for Ecological Transition and the Demographic Challenge), under NextGenerationEU's Recovery, Transformation and Resilience Plan (PRTR). The group responsible for the project is formed by the Madrid City Council, the Centre of Studies and Experimentation of Public Works (CEDEX) and the Conama Foundation.

The study site is an ecologically degraded section of the Manzanares River located on the outskirts of the municipality of Madrid, it is filled with debris dumped during the 1950s. The river is constrained between steep slopes, and its banks are fixed by breakwaters and gabions. Discharges from three large wastewater treatment plants and two storm tanks reach the river through outlets. These large concrete structures disrupt the continuity of the riparian gallery forest. Interventions will be carried out to modify the infrastructure for environmental and ecological restoration.

Insects are key indicators of changes in soil, water, and air quality (Chowdhury et al., 2023). The main advantage of using a group of insects as a bioindicator is that they increase the number and types of environmental responses perceived when studied (Kremen et al., 1994). Nevertheless, insect communities are rarely analyzed. We have developed a novel sampling method to effectively monitor flying insect populations.

### *1.2. Objective*

The goal of this study is to evaluate the recovery of the river ecosystem. We plan on monitoring changes in insect communities in relation to climate and human intervention before, during and after construction work.

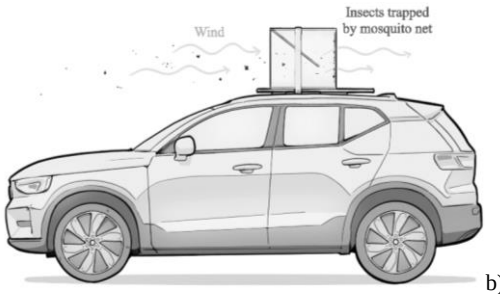
## 2. Methods

We introduce an innovative sampling method: a vehicle-mounted box as a trap for airborne insects. The device is a reinforced acrylic 50 x 50 cm cube strapped onto the roof rack of an SUV Fig. 1a. A tilting acrylic lid opens on its own once the car is in motion allowing air to flow through the box and out of a 2 mm mosquito net on the back pane Fig. 1b. This mesh collects the animals which then are placed into a plastic vial and conserved in a 70% ethanol solution. The main advantage of this system is the ease to infer the number of

insects or biomass per cubic meter of air sampled. This study presents the results of 11 months of sampling before the construction began.



a)



b)

**Fig. 1a, 1b.** Vehicle-mounted insect collector (1a) and mechanism once the car is in motion (1b).

Once a month we drove up and down a concrete road situated at about 15 m from the riverbank until the total distance covered amounted to 10 km. Two 1 x 10 m transects were inspected on foot, identifying epigean invertebrates with the naked eye. These transects are besides two future construction sites. A set of climatic data was gathered each day from a nearby weather station as well as satellite data: NDVI (Normalized Difference Vegetation Index) and Moisture index values for both the riverbank and the two transects.

Flying insects were later identified and classified into three weight classes: heavy, medium & light. If a taxon of interest was found, i.e. black flies or invasive species, they were placed in a separate container. Insects which played an important role as pollinators were separately classified and analyzed.

## 3. Preliminary results

We collected a total of 935 flying insects belonging to 8 different orders, 99 individuals were important pollinators (11%). November was the month with the highest abundance: 440 captures. In August, on the contrary, only 12 insects flew into the trap. Pollinator abundance peaked in April, with 53 captures, more than 50 percent of all pollinators. Individuals of the black fly *Simulium erythrocephalum* were captured in July and November. 21 different invertebrate orders were observed on the plants and soil of the two transects. During the summer diversity dropped, especially in July when only 3 invertebrate orders were detected.

There is a strong correlation between diversity of flying insects and pollinator diversity ($p < 0{,}001$) and flying insect biomass *vs* pollinator biomass ($p < 0{,}001$). Biomass of flying insects is strongly correlated with maximum temperature ($p < 0{,}001$) as well. Diversity and abundance in the transects are inversely correlated to maximum temperature and positively correlated to relative humidity, Moisture index and NDVI values.

## 4. Discussion

The most shocking finding is that insects were more abundant during autumn and winter months (September to January). Our main hypothesis is that air humidity is the limiting factor for small insects but heat benefits heavier flying insects such as bees, wasps, or hoverflies (Syrphidae) which are pollinators and were present independently of air humidity. Black flies are significant for public health as they feed on human blood, can cause allergic reactions and are prone to be a vector of disease (Kim, 1987).

Diversity in ground transects appears to be very dependent on humidity and less so on temperature, plants offer shelter, nourishment, and a humid microclimate to many invertebrates like springtails (Collembola) or snails, and herbaceous vegetation was notably more abundant during the winter months.

We hope to monitor how the construction sites affect these insect populations in the future. Our predictions are that epigean arthropods inhabiting the transects will be negatively impacted by debris from construction work. Dust will affect plant cycles can be which can modify pollinator interactions and numbers.

**References**

Chowdhury S, Dubey VK, Choudhury S, Das A, Jeengar D, Sujatha B, Kumar A, Kumar N, Semwal A & Kumar V (2023) Insects as bioindicator: A hidden gem for environmental monitoring, Frontiers in Environmental Science, 11, 1146052. doi: 10.3389/fenvs.2023.1146052

Kim KC, Merritt RW (Eds.) Black flies, ecology, population management, and annotated world list, University Park, London, 1987. ISBN 0-271-00417-7

Kremen C (1994) Biological inventory using target taxa: a case study of the butterflies of Madagascar, Ecological Applications, 4, 407–422.

# Use of InSar technology to determine the active portion of a gravel braidplain

Valeria GUADAGNO[1], Giuseppe DEL GIUDICE[2], Cristiana DI CRISTO[3], Diego DI MARTIRE[4], Enrica VIPARELLI[5] and Angelo LEOPARDI[6]

[1,6] Università degli Studi di Cassino e del Lazio Meridionale
Cassino (Italy)
valeria.guadagno@unicas.com
a.leopardi@unicas.com

[2,3,4] Università degli Studi di Napoli Federico II
Napoli (Italy)
delgiudi@unina.it
cristiana.dicristo@unina.it
diego.dimartire@unina.it

[5] University of South Carolina, Columbia (United States)
viparell@cec.sc.edu

ABSTRACT

Characterizing width and depth of the active portion of a gravel braidplain, is still an open problem due to scour and fill of the gravel bed during floods. In the present study SAR satellite images are used to identify wet and active widths, as well as the number of active channels. Active width is here defined as the width of the portion of the braidplain where most of sediment transport occurs. The proposed procedure can be useful for bedload transport calculations and predictions of river morphology.

## 1. Introduction

The possibility of using Sentinel-1 SAR images with a resolution of 20 x 4 m, and a time revisiting of 6 days are used to characterize wet and active widths of a gravel bed is explored. The analysis is conducted for a 12 Km long reach of the Trionto River, a braided gravel bed river (Leopold et al., 1957), located in the northern part of Calabria in Southern Italy. We used DInSAR, Differential Interferometry SAR (Gabriel et al., 1989), to analyze data collected over one year (from October 2016 to September 2017). The comparison between images allowed us to identify relatively stable and mobile areas of the braidplain, as indicated in Figure 1, where green dots are indicative of relatively stable (not mobile) areas.




**Fig. 1 –** Interferometric data. The presence of the green PS means that the backscattering of signal is coherent over the 30 acquisitions collected between October 2016 and September 2017 and it is considered representative of a portion of the braidplain where limited sediment motion**.** The lack of a coherent signal that is caused by vegetal cover or water is considered representative of fast changes associated with sediment transport

## 2. Methods and results

The identification of the active portion of the braidplain from interferometric data is done in steps. First vegetation is identified from optical images collected in a dry period and classified as stable part of the study area. Noting that floods of the Trionto River are relatively short and associated with precipitations, it is assumed that the change in Permanent Scatters (PSs) is due to rapid changes caused by sediment transport during floods. A 4x4 m grid was drawn on the study area. Circular buffers with diameters varying between 8 m and 16 m and centers in the centroids of the grid cells were used to identify relatively mobile (few PSs inside the buffer) and stable (many PSs in the buffer) areas. The number of green dots falling in each buffer was normalized by the maximum number of PSs found in a buffer of that size. In this way we obtained mobility maps of the entire braidplains. These maps were converted into binary maps showing stable and not stable parts with the sue of thresholds varying between 0.05 and 0.25. The binary maps for different mobility maps and threshold equal to 0.2 is shown in Figure 2 where blue indicates not stable areas.

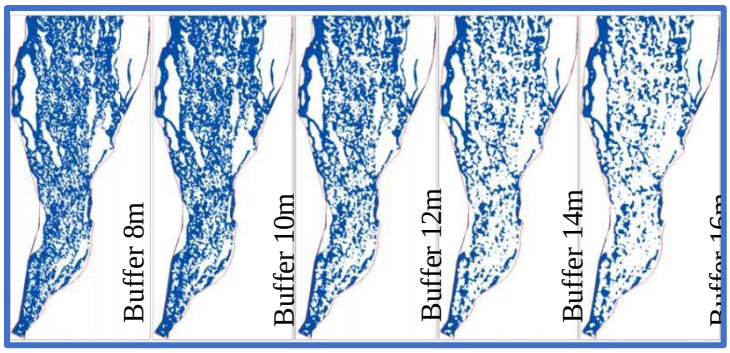



**Fig. 2 –**The stable and unstable portion of the area changes due to the buffer size (Threshold=0.20).

Active channels are identified from the maps of Figure 2 by joining connected elements that are at least 8 m wide. Connected segments that are isolated in the braidplain are not considered to be channels and are therefore eliminated. The result of this channel extraction procedure is presented in Figure 3a. The difference between wet and active widths in section 1 is presented in Figure 3b, while the number of active channels in sections 1-4 is presented in Figure 3c.

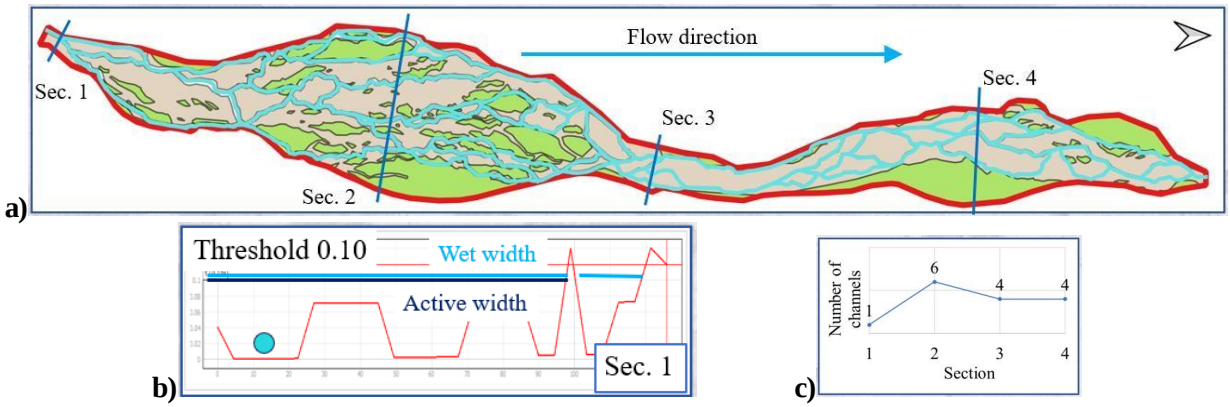



**Fig. 3 –** Results of the channel extraction procedure. a) Active channels. b) Wet and Active width in section 1. c) number of active channels in sections 1-4.

### References

Gabriel, A. K., Goldstein, R. M., & Zebker, H. A. (1989). Mapping small elevation changes over large areas: Differential radar interferometry. Journal of Geophysical Research: Solid Earth, 94(B7), 9183-9191.
Leopold, L.B., Wolman, M.G., 1957. River channel patterns: braided, meandering, and straight. U.S. Geological Survey Professional Paper 282-B, Washington, DC, pp. 39–84.

### Funding

The PhD scholarship of Valeria Guadagno is financed by INPS (Istituto Nazionale di Previdenza Sociale), Italy.

# *DAM SAFETY* - How a Contractual Strategy and the Involvement of an Independent Expert can Contribute to it

Bettina GEISSELER

GEISSELER LAW, Germany

geisseler@geisseler-law.com

(The article is partly based on an article co-written by Michel Lino, ISL Ingénierie, France, Luciano Canale, at that time Scatec, Italy, and Stéphane Giraud, FIDIC Contract Specialist, France [i])

ABSTRACT

Dams and water reservoirs will play an increasingly important role within the energy transition in view of the intended growth of intermittent other power generating "renewables", but as well considering the risks resulting from the severe climate change the world is currently facing.

Dam safety is not only crucial to successfully ensure the long-term sustainability and the multiple benefits of a dam project and water reservoirs, in particular multi-purpose reservoirs, but it is the primary condition for its acceptance by civil society. Dam failures worldwide continue to be too numerous, as well in recent years. The International Commission on Large Dams (ICOLD) has recently issued a "World declaration on Dam Safety" [ii] and declared dam safety the highest priority of the organization.

The paper

1. gives an overview on examples of comprehensive Dam Safety Regulations resulting from compulsory national state regulations respectively worldwide accepted (international) standards;
2. describes potentially diverging perspectives and interests of the major stakeholders of a dam project;
3. proposes as conclusion
   - the early involvement of an independent expert resp. Dam Safety Panel of Experts (DSPoE) by discussing his/her role and tasks and a potential financial impact of his/her (binding?) recommendations,
   - an adapted contractual set-up and contractual provisions to consider dam safety issues during the whole lifecycle of a dam,
   - solutions how to deal with unforeseen underground/ geotechnical or hydrological conditions as the most likely uncertainties during the construction phase: e.g., by establishing a robust geological baseline report commonly agreed upon by both contractual parties (Owner/ Employer and Contractor) and a clear risk attribution to either one of the contractual parties or the use of Alliance Contracts with the purpose of sharing the risks.

## 1. Introduction

ICOLD recently issued a bulletin on statistical analysis of dam failures, i.e., Bulletin 188[iii] . The available data clearly show that most of the dam failures are caused by faulty and insufficient design, related in most cases to geotechnical issues. And: most of the failures on dams built in the 20th century and all failures of dams built after the year 2000 occurred during the 5 first years after construction.

## 2. Compulsory Regulatory Framework

An extensive review of the dam safety regulatory framework in 51 countries, estimated to account for more than 95 percent of the ICOLD's register of world dams, has been carried out by the World Bank in 2018[iv]. A majority of the developed countries have established during the past decades comprehensive Dam Safety

Regulations, which e.g. define, in which intervals the behaviour of a dam during its lifecycle has to be evaluated by the owner or on behalf of the owner by an external expert/ engineering company, whose report has then to be submitted to the supervising state authority. Unfortunately, the existence of such State Regulations is often not the case in developing countries, even in those where large dam projects are currently being designed and constructed. In countries without such regulations, it is up to the Owner (and recommended!) to oblige its Contractor to comply not only with the "state-of-the-art" requirement, but with internationally accepted standards or recommendations of private norming associations such as the DIN norms in Germany or the ICOLD Bulletins.

## 3. Stakeholders and their interests

Dam safety should in no way be sacrificed by cost or time savings considerations. The considerations should be equal, irrespective whether it is a public project (with a state entity as Owner) or a privately developed project, e.g., by means of the build – own – operate – transfer (BOOT) delivery method. All stakeholders involved should have the same interest. But there might be constellations, depending on the contractual set-up and the possibility of one stakeholder to contractually instruct /influence another party, in which the involved parties, e.g., a designer as subcontractor to the Contractor, might be faced with considerations such as the bankability of the project and the request to balance safety aspects with the necessity to deliver a competitive offer.

It is the financing institutions, which generally have an utmost interest that the necessary safety aspects are respected, and which often make the involvement of an independent expert a condition for financing the project. The World Bank has played a pioneer role in this respect [v].

## 4. The independent Expert

To assure that adequate dam safety considerations are respected all the time by all involved parties the early involvement of an independent expert resp. a DSPoE will be the solution. Regardless, whether engaged by the Owner, having the ultimate responsibility for the safety of the plant operated by him, or upon the request of the financing institution, it is crucial, that the expert is independent in his/her opinion and cannot be influenced by the interested parties such as the Owner, Contractor, or Designer. Legally spoken, it is up to the party having engaged the expert to assure that his/ her recommendations will be complied with. An Owner is strongly advised to follow the recommendations. Anyhow, 2 questions remain in this context: (i) shall the state legislation provide for a binding character of the recommendation of an expert in some restricted cases; (ii) who bears the not calculated (financial / time for completion) consequences of the recommendation issued by an expert: will it trigger a Variation (the Contractor will be compensated) or is it within the original Scope of Works without any compensation for the Contractor? Regarding the point of engagement, it seems to be desirable that he/she is already involved at the concept phase (site identification, determination of the type of dam) and stays involved at least until the Final Acceptance which should not be earlier than 5 years after the Provisional Acceptance of the erected dam.

## 5. Contractual set-up

Choosing the adapted contractual set-up is essential: 'Design-Bid-Build' or 'Design-Build Scheme', Turnkey or multi-contracting structure, the use of a Model Agreement such as the FIDIC Emerald Book[vi]? Regarding unforeseen conditions, which in the far most cases are linked to the underground condition, the contractual parties should determine the contractual basis on which they will rely. They can attribute the risk for hindrances due to unforeseen events and the consequences (costs and time for completion) to overcome them to either one of the parties or they can, by means of so-called Alliance Agreements, share those risks, at least above a certain threshold.

---

[i] The mentioned article has been published in HYDROPOWER & DAMS, issue 2, 2023.

[ii] ICOLD, World declaration of dam Safety; Paris, France, October 2019

[iii] ICOLD, Bulletin 188 – Dam failure statistical analysis; Paris, France, 2021

[iv] World Bank (WB): „Laying the foundations"; Washington DC, USA, 2018

[v] WB: 1977–Policy Operational Manual Statement 3.80 „Safety of Dams", repl. by the Policy O.P.4.37, 2010 , superseded by ESS4-Annex 1 on Dam Safety Panels, 2018 ; or WB: Good Practice Note on Dam Safety; Washington DC, USA, April 2021

[vi] https://fidic.org/books/conditions-contract-underground-works-2019-emerald-book

# Development of a Simple Reservoir Water Level Controller

Filipa N. NOGUEIRA[1], José L.S. PINHO[2]

[1,2] CTAC - Center for Territory, Environment and Construction,
Department of Civil Engineering, University of Minho,
4710-057 Braga, Portugal.
filipan@civil.uminho.pt
jpinho@civil.uminho.pt

ABSTRACT

In this work, a simple strategy for water level control in reservoirs is presented. Here, we consider that the reservoirs are controlled by a pump station when rainfall-runoff events cause water level disturbances. This controller reveals to have a good performance, has the advantage of being simple to implement, is fast, is robust in the presence of errors in the weather forecast, may be tuned in order to achieve different speeds of convergence, and allows the changing of the desired reference value during the control process.

## 1. Introduction

The water level in certain reservoirs must be managed under stringent ranges. The increase of the water level can lead to floods and low water levels may disrupt some water uses. Thus, an automatic controller that maintains an adequate water level in reservoirs constitutes an important tool to help the operational management of controlled reservoirs.

Many studies have been made in this context. A distributed linear quadratic Gaussian controller is presented in (Lemos, 2013), and a model predictive controller (MPC) is used in (Maestre, 2015), however, the MPC is in general very time-consuming and highly dependent on the weather forecast quality. A proportional integral derivative (PID) controller is described in (Lacasta, 2014). Although a controller based on PID may lead to an oscillatory signal bringing forth an unstable output and it depends on a suitable value for the integral gain, that may take a long time to obtain in case the process poles are not fast enough.

In this work, we propose a controller for the automatic water pumping in a reservoir, subject to rainfall-runoff inflow disturbances. The controller is based on a state space representation, which makes it very easy to implement, and is considered to be nonlinear, not due to the use of nonlinear design methods, but rather because of the imposition of a positivity constraint on the control variable, which makes it a nonlinear function of the state of the system. It also has the advantage of allowing the change of the desired reference value during the control process and it may be tuned in order to achieve different speeds of convergence. The proposed controller ensures asymptotic reference tracking, independently from the value of the design parameter, and it is robust under the presence of errors in the weather forecast.

## 2. Model and control description

We consider a simple model of a reservoir as illustrated in Fig. 1. The water level is represented by $h(k)$ and is measured in meters, $m$, with respect to a reference datum; the control flow that pumps water out of the system is represented by $Q_c$, whereas the disturbance rainfall-runoff inflow is represented by $Q_d$. Both $Q_c$ and $Q_d$ are measured in $m^3/s$. Mathematically, this model may be described as:

$$h(k+1) = h(k) + BQ_c(k) - B\,Q_d(k), \tag{1}$$

where, $B$=-$T/A$, $A$ is the average storage area ($m^2$), $T$ is the control time step ($s$), $k$ is a positive integer, and $h(k) < 0$.

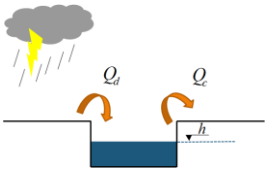



**Fig. 1** Scheme of a water reservoir.

The design of a control law for the automatic water pumping, in order to maintain a desired water level, $h^*$ in the reservoir, can be regarded as an output reference tracking problem. Moreover, it may be proven that when the controller

$$Q_c(k) = \max\left(0, \tilde{Q}_c(k)\right), \tag{2}$$

with

$$\tilde{Q}_c(k) = 0.99\,B^{-1}\left(h^* - h(k)\right) + \hat{Q}_d(k), \tag{3}$$

is applied to the system (1), the water level $h$ converges to the reference value $h^*$.

## 3. Results

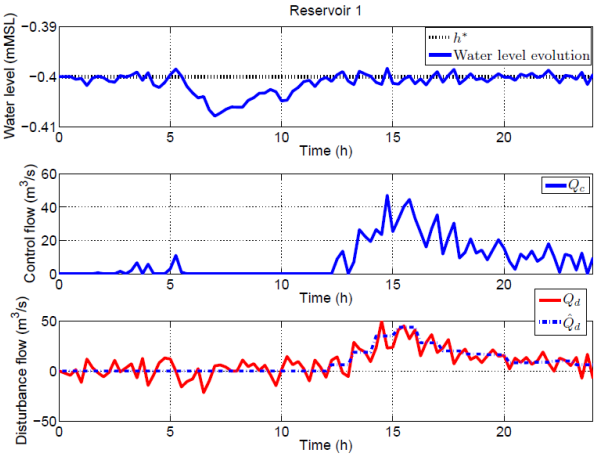



**Fig. 2** The evolution of the water level is illustrated on the top graph, where the dashed black line corresponds to the desired reference value. The pump control flow is represented on the second graph. On the bottom graph the rainfall-runoff inflow, $Q_d$, is marked in solid red line, whereas the estimated disturbance, $\hat{Q}_d$, is marked in dashed blue line.

**Acknowledgements**

This work was financed by FCT / MCTES through national funds (PIDDAC) under the RD Unit The Centre for Territory, Environment, and Construction (CTAC), under reference UIDB / 04047/2020.

**References**

J. M. Lemos, L. F. Pinto, L. M. Rato, M. Rijo, Multivariable and distributed lqg control of a water delivery canal., Irrigation and Drainage Engineering 139(10) (2013) 855–863.

J. M. Maestre, P. J. van Overloop, M. Hashemy, A. Sadowska, E. F. Camacho, Human-in-the-loop model predictive control of an irrigation canal., IEEE control systems 35(4) (2015) 19–29.

A. Lacasta, M. Morales-Hern´andez, P. Brufau, P. Garc´ıa-Navarro, Simulation of pid control applied to irrigation channels., Proceedings of the 12th International Conference on Computing and Control for the Water Industry, Procedia Engineering 70 (2014) 978–987.

# Stormwater Attenuation & Enhanced Infiltration System to Mitigate Flood & Drought Conditions: Part II – Rural Environment

Stephen D. THOMAS[1], George R. FRENCH[1], Jamie BATES[1], Joseph A. O'MEARA[2], Matthew P. DALE[2], Bruno CASAL[3]
stephen.thomas@ogi.co.uk

[1] OGI Groundwater Specialists, Durham, UK
[2] Groundwater Dynamics Ltd, Leamington Spa, UK
[3] Sondagens Casal Lda, Sintra, Portugal

**Abstract**. This paper describes a stormwater attenuation & enhanced infiltration system, specifically designed for a Rural Environment, comprising the construction of attenuation trenches, perforated pipes with gravel surround, integrated with large numbers of drilled vertical infiltrators installed through the base of the trenches.

Combining the pressure head of the collected stormwater in the attenuation trenches, with the negative suction pressure within the unsaturated vadose zone, provides the differential pressure to force the water into the ground via these infiltrators. Furthermore, by installing vertical infiltrators, higher permeable ground strata are often encountered, particularly in anisotropic ground conditions where the horizontal permeability is much greater than the vertical permeability.

Stormwater Attenuation & Enhanced Infiltration Systems (SAEIS) have been used regularly in the UK for many years, both to mitigate flooding, and to provide recharge to groundwater resources. With groundwater resources similarly in decline in Portugal, together with more frequent flooding conditions occurring during intense rainfall, such collection and enhanced infiltration systems would also be most beneficial to the hydrogeology and weather conditions of Portugal.

Mathematical modelling is presented which simulates the water flow through the infiltrator system, and into the unsaturated soil strata. Combining the storage capacity of the attenuation trenches with a large number of infiltrators, produces a highly efficient attenuation and infiltration system that not only mitigates the impact of flooding but has no requirement for ongoing energy consumption.

With stormwater collected, filtered, attenuated, and then infiltrated to the vadose zone, collected stormwater will eventually find its way down to the water table, and so mitigate drought conditions by supplementing the aquifer water resources.

Stormwater attenuation & enhanced infiltration systems (SAEIS) exemplify true low-carbon sustainability, and contribute to the United Nations Department of Economic and Social Affairs for Sustainable Development - Goal 6: *Ensure availability and sustainable management of water and sanitation for all*.

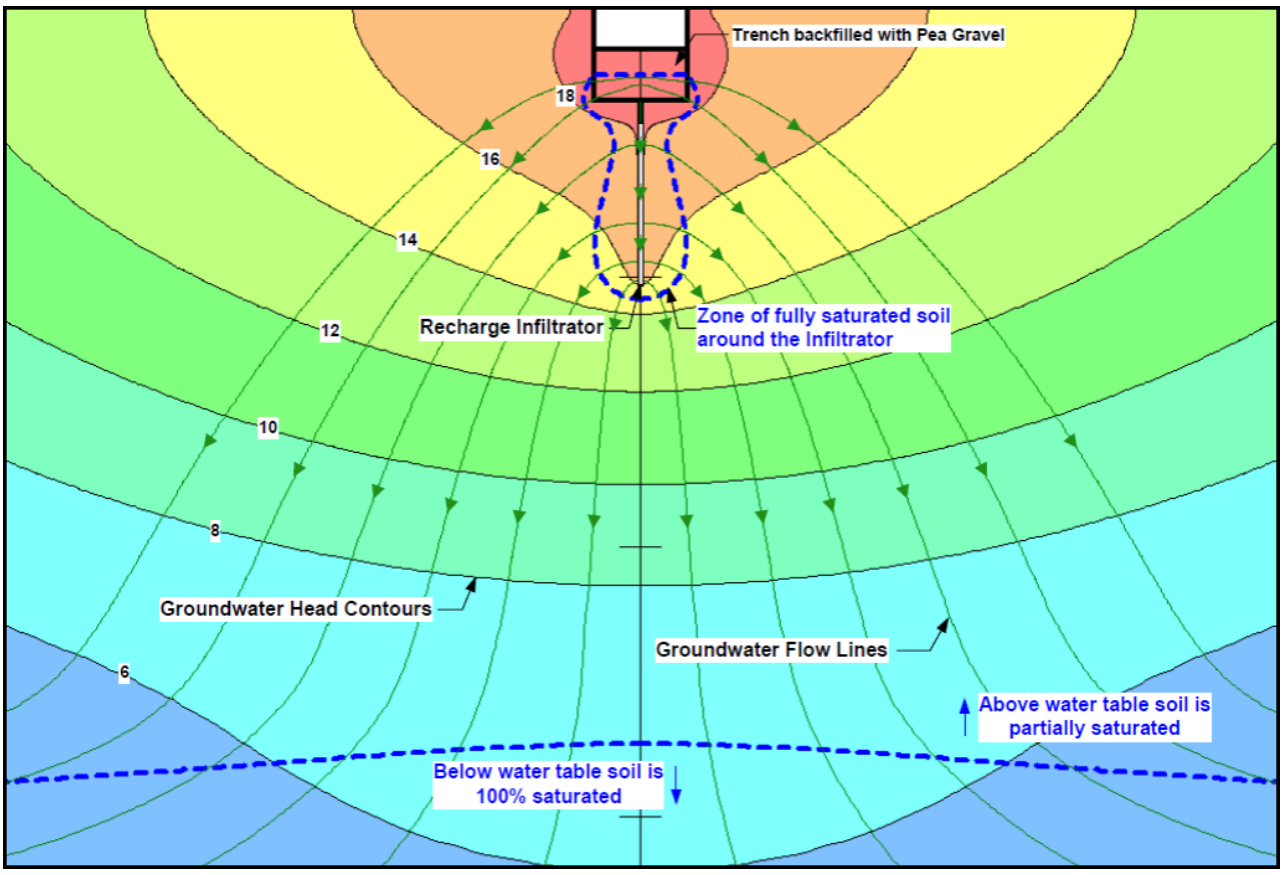



**Fig. 1.** Finite Element modelled head contours & flow lines from a single infiltrator.



**Fig. 2.** The images above depict a test project between Birmingham and Manchester, where a total steady rate of over 2000 m3/day of infiltration to the ground was achieved from 78 infiltration wells.

# Innovative Dam Design for Low-Head Seawater Pumped Hydropower Storage in the North Sea

Lasantha Jayasinghe ARACHCHIGE[1], Lucas de VILDER[1], Eksa Bagas PRASASTI[2], Kristina TERHEIDEN[2], Bettina GEISSELER[3], Roelof MOLL[1], Jeremy BRICKER[4]

[1]Delft University of Technology, The Netherlands; [2]University of Stuttgart (IWS), Germany; [3]Geisseler Law, Germany; [4]University of Michigan, USA

j.a.l.s.jayasinghearachchige@tudelft.nl; l.h.devilder@tudelft.nl; eksa-bagas.prasasti@iws.uni-stuttgart.de kristina.terheiden@iws.uni-stuttgart.de; geisseler@geisseler-law.com; J.R.Moll@tudelft.nl; jeremydb@umich.edu

ABSTRACT

The growing share of renewable, intermittent power sources requires enhanced grid stability through energy storage technologies, among Pumped Hydropower Energy Storage (PHES) is the most mature and environmentally friendly. The ALPHEUS project ("Augmenting Grid Stability Through Low Head Pumped Hydro Energy Utilization and Storage", funded by the EU-Horizon (2020) program) focuses on developing an innovative concept to improve Reversible Pump/Turbine (RPT) technology and adjacent civil structures to make PHES economically viable in shallow seas and coastal environments with flat topography. It aims to find suitable sites, innovative dam design and construction methods, considering environmental, social, and investments costs (profitability for potential operators). Further it aims to assess compatibility and integration with intermittent offshore wind and solar energy sources, for a competitive and sustainable energy storage system, aligning with Europe's 2050 climate-neutral objectives, while augmenting grid stability and flexibility.

**Site Identification and permitting process**

A parametric analysis and GIS study was carried out to identify the potential sites for low-head pumped hydro storage in the North Sea zones of six bordering states (Germany, France, Great Britain, Belgium, The Netherlands, and Denmark). This analysis encompassed an evaluation of the geology, reserved environmental zones, planned and operational wind projects (for the mutual benefit of both installations), maritime routes, navigability, and wave heights/directions, including extreme events. Two potential preliminary sites were identified within the Netherlands' coastal region for detailed assessment and extended the study for optimization (Fig. 1). The permitting process for a potential project will depend on the applicable national laws governing the site, whether the site will be within the Territorial Sea respectively the Exclusive Economic Zone (EEZ) of a country, and the outcome of an Environmental Impact Assessment taking into account the potentially affected reserved areas ((Natura 2000).

**Dam and Powerhouse Design**

One of the key challenges of this project is to develop an innovative and sustainable dam design. Since the project is developed in the sea and working under extreme wave conditions, the research assessed innovative construction mechanisms for handling the equipment, materials, and resources while mitigating risk. At the preliminary stage, several dam construction alternatives were evaluated, for example; Geo containers and Embankment dam concepts.

After assessing possible failure mechanism, construction challenges and various other risks, a caisson (pre-cast) dam with an inner berm (Fig. 2) was selected as the most suitable design. Ongoing analyses are still focused on assessing caisson stability, innovative construction methods, piping prevention, and other potential risks during and after construction.

This pre-cast caisson can limit the onsite-offshore construction and remedy the need to work under challenging wave conditions. However, optimizing the design for minimum construction risk and time requires more than

just a caisson to function as the dam. Combining an inner berm into the caisson can optimize the design to a greater extent. Figures 2 and 3 illustrate the structure of the caisson combined with an inner berm and the schematic diagram of the proposed ring dam with its components. The powerhouse of the PHES as part of the ring dam is optimized according to the site characteristics and especially to the operational characteristics of the emerging technology of contra-rotating, variable speed, reversible pump-turbines (CR-VS-RPT), which have a high efficiency over a wide range of (low) heads and varying discharges. The structural analysis revealed that while the wet method which employs pre-cast caissons for the powerhouse construction incurs slightly greater costs, the dry construction method utilizing a cofferdam offers an efficient alternative due to its increased operational flexibility.

## Energy Storage Capacity

The storage capacity of the project was assessed for two different capacities:20GWh and 2GWh.This storage capacity is highly sensitive to the operating head range, reservoir volume, and diameter. A water depth of approximately 20 m was set as the boundary condition for the preliminary design. The maximum operational head of the plant is limited to 20m, while the lowest operating head is 2m (the average head is 11m) based on the results of the turbine experiments. To achieve the desired storage capacities (20GWh and 2GWh) with this operating head range, it is required to have a dam perimeter of 22km and 7.7km respectively.

## Summary

The site investigations for the potential construction and operation of a PHES in the “Greater North Sea” area clearly illustrate the wide range of local conditions and opportunities. Based on the selected offshore sites, the only possible dam construction would be a caisson dam. The identified high-potential sites are further to be investigated, encompassing innovative design and construction considerations, alongside cost estimation and project viability assessment.

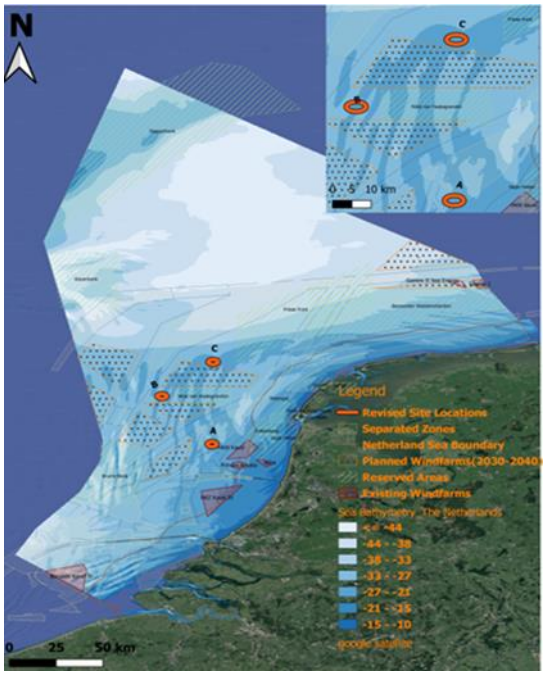



Fig. 1. Potential sites(A,B and C) and offshore reserved areas in the Netherlands.

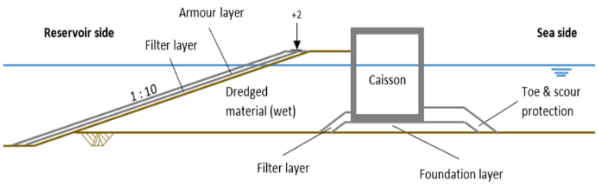



Fig. 2.The proposed structure for the caisson dam and the inner berm

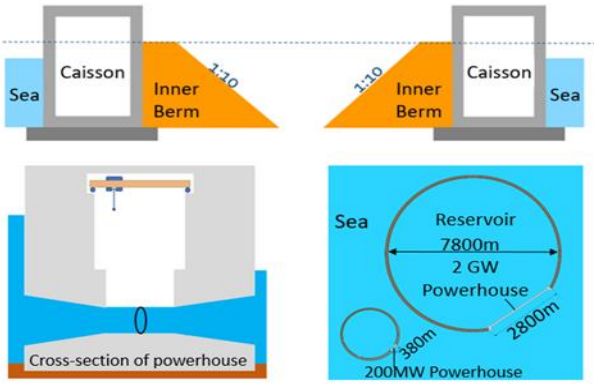



Fig. 3. Schematic drawings of dam and powerhouse general arrangements


### Acknowledgements

This project has received funding from the European Union’s Horizon 2020 research and innovation programme under grant agreement No 883553.


### References


ALPHEUS Stakeholders (2024). ALPHEUS: Augmenting Grid Stability Through Low Head Pumped Hydro Energy Utilization and Storage. https://alpheus-h2020.eu/. Accessed on September 20, 2023

Natura 2000.(2000). Protected Nature. Ministry of Agriculture, Nature and Food Quality,The Netherlands. https://www.natura2000.nl/beschermde-natuur, Accessed on October 30, 2022.

# Influence of mowing macrophyte vegetation on water levels in a small lowland river in the agricultural landscape

Dorota MIROSŁAW-ŚWIĄTEK[1], Mateusz GRYGORUK[1], Sylwia Szporak-Wasilewska[1], Tomasz OKRUSZKO[1]

[1] Warsaw University of Life Sciences – SGGW, Institute of Environmental Engineering, Poland
dorota_miroslaw_swiatek@sggw.edu.pl
mateusz_grygoruk@sggw.edu.pl
sylwia_szporak@sggw.edu.pl
tomasz_okruszko@sggw.edu.pl

ABSTRACT

In a typical lowland agricultural landscape of Europe, dominated by small (+/- 5 m wide and +/- 1 m deep) rivers and adjacent wetlands, processes of the response of these systems to management should be studied to avoid their degradation, yet allowing for successful and sustainable agriculture. One of the purposes of river maintenance works is to reduce the hydraulic roughness of river channels, by mowing vegetation. This action allows for lowering water levels during the peak flows of floods. To reduce negative impacts on the river biodiversity, vegetation mowing can be performed in sections, leaving plants (and even whole patches of macrophytes) in the channel (Bal et al., 2011). The affected river channel level regulates the hydraulic head of adjacent groundwater and affects the status of ecosystems in the valley. In practical modeling applications, assessment of the impact of maintenance measures on adjacent wetlands uses a simplified approach of combining the groundwater flow model with the river flow model through an internal boundary condition value defined as the position of the water table in the river (Grodzka-Łukaszewska et al., 2022). In this study, we proposed an artificial neural networks model (ANN) as a tool in the prediction of the water level, and the effect of vegetation mowing on river flow conditions was taken into account by the flow reduction factor (*k*). The research was made for the river reach (6 km) of the river Upper Biebrza (NE Poland, Fig. 1). The maximum channel width is 8 m and the maximum depth does not exceed 2.5 m. The river is characterized by a slight water slope not exceeding 0.00024 and is very intensively overgrown. Vegetation starts in May and continues until the end of November, reaching its maximum extent in September. This is illustrated by a bankful flow value of 0.96 $m^3/s$ during the non-vegetation period and 0.37 $m^3/s$ in September. Water levels were measured with automatic pressure transducers installed in piezometers located in the stream bed at four cross-sections located along the reach in km 5+946 (RI), 3+556 (RII), 2+548 (RIV), 0+531 (RV) (Fig. 1). The loggers were in continuous operation between 27 June 2018 and 10 June 2021.

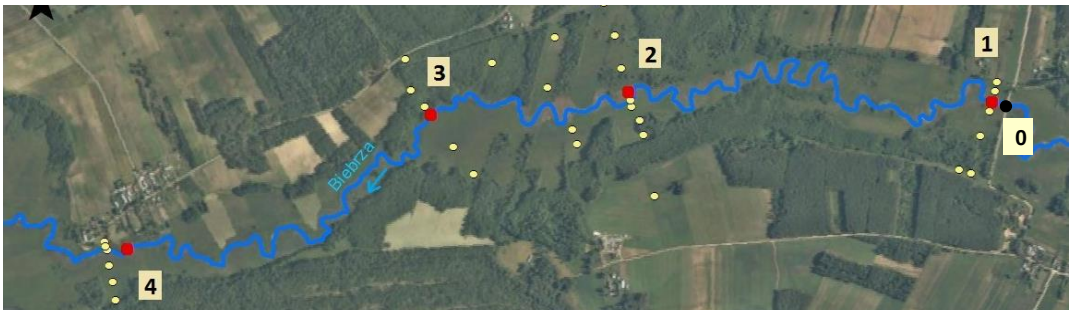



**Fig. 1.** The study reaches and location of monitoring/sampling points (water level dataloggers: 1 – RI, 2 – RII, 3 – RIV, 4 - RV; 0 – gauge Rogożyn Stary).

To determine the relationship between flow (*Q*) and the water level (*WL*), a rating curve was built for the Rogożyn Stary water gauge cross-section (Fig. 1, point 0), both during the free-flow period and due to the strong overgrowth of the river during the vegetation season (Fig. 2). The rating curve was elaborated using direct flow rate measurements. The flow reduction coefficient (*k*) (Fig. 3) was determined based on flow

measurements in the growing season. The end date of taking the coefficient into account was determined based on the vegetation growth phenomenon at the gauge cross-section (gauge Sztabin on the Biebrza River), which has a long record of hydrological observations and is located near to the analyzed river reach.

Based on eight hydrometric measurements taken in the analyzed reach, a linear relationship was found between Manning's roughness coefficient (*n*) and the flow reduction coefficient (*k*). In the literature, the total resistance of vegetated channels ($n_{tot}$) is estimated as a sum of the channel value of Manning's ($n_{ch}$) and vegetation components of Manning's ($n_{veg}$) ($n_{tot} = n_{ch} + n_{veg}$ , (Green et al., 2006)) The vegetation resistance is often estimated by using a blockage coefficient. This can be the amount of the cross-section that is blocked by the vegetation relative to the entire cross-section. Green (2006) found the following exponential relation: $n_{veg} = 0.0432e^{0.0281.BSA}$ (BSA - vegetation plan surface area).

Multi-layer perception (MLP) ANN model was developed using the back-propagation training algorithm to predict water level in river cross-sections RI, RII, RIII, and RV. For the appropriate training of the developed ANN model, the daily water level at cross-section RI (*WL*), flow reduction factor *k*, and information about flow conditions (bankful or overbank flow) were used as input training data. The target-predicted value of the trained ANN model was the corresponding daily water level at cross-sections RII, RIV, RV.

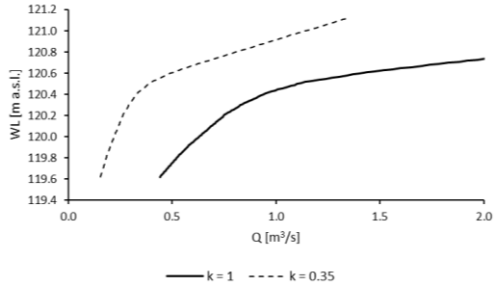



**Fig.2.** Rating curve at Rogozyn Stary gauge (k=1 - non-vegetation period; k = 0.35 - maximum vegetation development (September), k – flow reduction factor

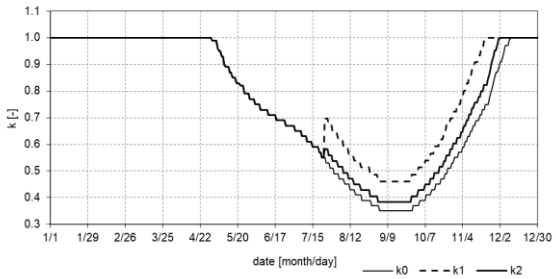



**Fig. 3.** Variation of flow reduction coefficient during the year (k0 - natural channel; river maintenance works scenarios: k1 and k2)

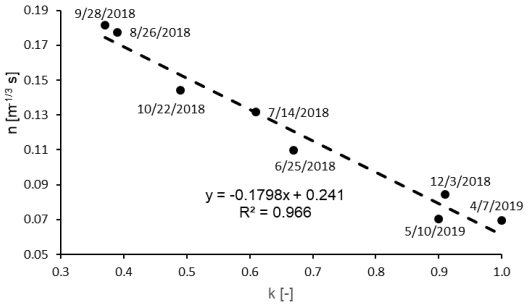



**Fig.4**. Manning's coefficient (n) vs. flow reduction factor (k)

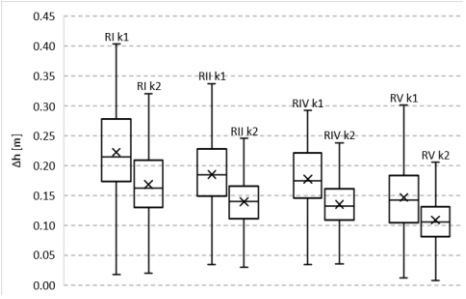



**Fig. 5.** Effect of river maintenance works - distribution of water table lowering in the analyzed cross-sections.

The following two scenarios of maintenance works were implemented in the calculations: *k1* - the vegetation is mown on July 25, and *k2* - the vegetation is mown on July 25, but mowing is limited to leaving some macrophytes in the river. Based on Green's formula and hydrometric measurements (Fig.4) (BSA = 25% in July), the variability of the flow reduction factor *k* was estimated for the adopted maintenance works scenarios. According to the results of Bal's research (Bal et al., 2011), it was assumed that leaving the part of vegetation increases the $n_{tot}$ coefficient by 18% on average compared to the total mowing variant. The developed ANN model was used to predict the position of the water table in the period 6/27/2018 – 6/10/2021 in which scenarios *k1* or *k2* of maintenance works are performed every year on July 25. Figure 5 shows the range of variability of the lowering of the water table in the RI, RII, RIV, and RV cross-sections, related to the position of the water table in natural conditions without maintenance works (*k0*). Full mowing of vegetation (*k1*) reduces, on average, the water table by 25 cm, and leaving some vegetation (*k2*) reduces the average water table by 10 cm. In the future, the developed model will be combined with a groundwater model to estimate the impact of river maintenance works on wetlands adjacent to the river.

**References**


Bal, C. et al., 2011. How do macrophyte distribution patterns affect hydraulic resistances? Ecol. Eng. 37(3): 529–33.

Green, J.C., 2006. Effect of macrophyte spatial variability on channel resistance. Adv. Water Resour. 29, 426–438.

Grodzka-Łukaszewska M, Sinicyn G, Grygoruk M, Mirosław-Świątek D, Kardel I, Okruszko T. 2022. The role of the river in the functioning of marginal fen: a case study from the Biebrza Wetlands. PeerJ 10:e13418 https://doi.org/10.7717/peerj.13418.

# Effect of flow velocity on eDNA degradation for biodiversity assessment in rivers

Jelle A. DERCKSEN[1], Laura Maria STANCANELLI[1], Krijn B. TRIMBOS[2], Astrid BLOM[1]

[1] Faculty of Civil Engineering and Geosciences, Delft University of Technology, the Netherlands
[2] Institute of Environmental Sciences, Leiden University, the Netherlands
j.a.dercksen@tudelft.nl

ABSTRACT

Given the decline in biodiversity and the increase in restoration efforts, high-throughput biomonitoring methods for fluvial systems have become key. The detection of environmental DNA is a promising technique to meet these needs. This research aims to investigate the interaction between flow velocity in fluvial systems and eDNA detectability. To this end, a set of laboratory experiments were conducted. Zebrafish eDNA was introduced into an annular flume, and four tests were conducted, each lasting seven days and having a different flow velocity. eDNA concentrations decreased with time, but in the case of the highest flow velocity run, initially an increase in detectable eDNA concentration was noted. Mechanisms responsible for the initial increase in detectable eDNA could influence eDNA-based species abundance estimates in field scenarios.

## 1. Introduction

Biodiversity has declined significantly in fluvial systems (e.g. Strayer and Dudgeon, 2010). Simultaneously, the value generated by biodiversity is increasingly recognized by both the scientific community and policy makers (Friberg et al., 2016). To monitor biodiversity, there is a need for techniques that provide information on species richness and abundance across geographic scales. Traditional biomonitoring techniques fail to meet these requirements due to limited availability of taxonomic experts, hindering biodiversity identification.

A promising alternative to traditional techniques makes use of species-specific snippets of genetic material that are released by their host species, i.e. environmental DNA (eDNA) in various forms. By capturing this material from the subject species' environment (be it from freshwater, soil, or aerial systems) subsequent standardized genetic testing may then indicate the species' presence. This detection method has the capacity to fulfil our biomonitoring needs by processing large quantities of high-resolution biodiversity data in a standardized manner. In lotic systems, i.e. rivers or streams, eDNA may deposit, or be transported downstream (Deiner et al., 2016). As a result, water samples collected in lotic systems may contain eDNA originating locally, or from extensive distances upstream (130 km: Pont et al., 2018). After release, the fate of eDNA is dependent on the state of the eDNA, the rate of degradation, and the flow characteristics of the system (Jane et al., 2015). Until now, eDNA degradation experiments are mostly performed in static water conditions (e.g. Wood et al., 2020), leaving out the potential effects of flow velocity. The objective of this study therefore is to assess the effect of flow velocity on eDNA degradation.

## 2. Method

A set of annular flume experiments was conducted at the Hydraulic Laboratory of Delft University of Technology to observe the degradation of eDNA under conditions of flow (Fig. 1). The flume's rotation is set by choosing angular speeds for both the bottom ($\omega_{bottom}$) and the top ($\omega_{top}$) in opposite directions. This counter-rotating design is intended to minimize the formation of secondary flow cells, a common occurrence in curved systems. As per previous investigations performed in this set-up (Booij, 1994), we adopt a consistent tangential velocity ratio ($\omega_{top}/\omega_{bottom} = 1.8$). The experiment was repeated for four runs, three of which were characterized by different rotation speeds ($\omega_{top}$: 0.35 m/s, 1.05 m/s, 1.80 m/s), and one as a control run (0.00 m/s). Vertical velocity profile measurements were taken using an ADV (Nortek Vectrino) to characterize the hydrodynamics established inside the channel. Each experimental run lasted seven days, and was initiated by adding genetic material to the flume in the form of 60 liters of rearing water from a

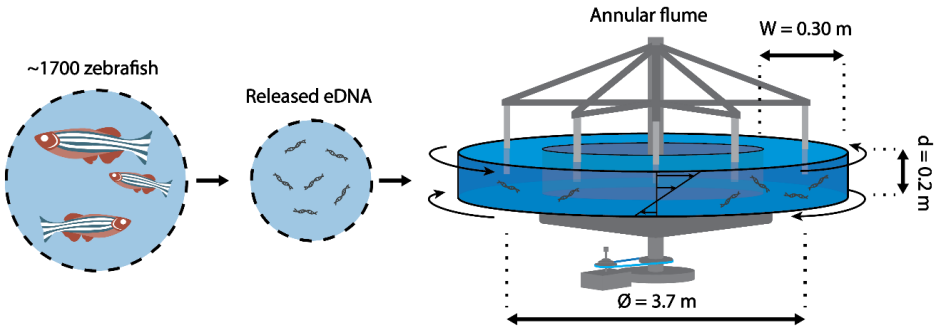



**Fig. 1.** The experimental setup, with the dimensions of the annular flume.

controlled population of 1700 wild-type zebrafish (*Danio rerio*). Water was sampled from the flume in triplicate at ten points in time, and abiotic parameters (temperature, pH, conductivity) were simultaneously measured. Final quantification of water samples was done in duplo by targeting a 73 base pair fragment of the COI gene using the QX200 ddPCR system (Bio-Rad, Hercules, CA).

## 3. Results

Across the experimental runs, eDNA concentrations (number of reads/mL) remained detectable until the final sampling time (168 h, 7 days). eDNA concentrations decreased with time. In the case of the 1.80 m/s run, an increase in detectable eDNA concentrations is observed within the first 48 hours, followed by a more rapid decrease in eDNA concentrations compared to the 0.00 m/s runs (Fig. 2). We speculate that this initial increase in detectable eDNA concentrations may be caused by the fragmentation of eDNA particles. This would result in smaller, and more evenly abundant eDNA particles in the flume, increasing the probability of eDNA detection. In field monitoring scenarios, eDNA particle fragmentation, as described above, could obscure the relation between the population size of a species and the amount of eDNA produced by this population, influencing eDNA-based species abundance estimates.

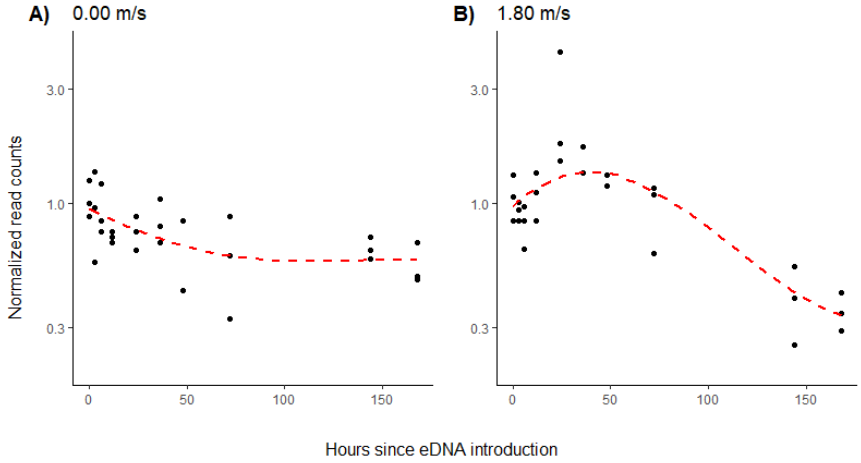



**Fig. 2.** eDNA degradation curves of the experimental runs with tangential velocities of the top lid of A) 0.00 m/s, and B) 1.80 m/s.

**References**

Booij, R. (1994) Measurements of the flow field in a rotating annular flume. Report no. 94-2.

Deiner, K., Fronhofer, E. A., Mächler, E., Walser, J. C., & Altermatt, F. (2016). Environmental DNA reveals that rivers are conveyer belts of biodiversity information. Nature communications, 7(1), 12544.

Friberg, N., Angelopoulos, N. V., Buijse, A. D., Cowx, I. G., Kail, J., Moe, T. F., Moir, H., O'Hare, M. T., Verdonschot, P. F. M., & Wolter, C. (2016). Effective river restoration in the 21st century: from trial and error to novel evidence-based approaches. In Advances in ecological research (Vol. 55, pp. 535-611). Academic Press.

Jane, S. F., Wilcox, T. M., McKelvey, K. S., Young, M. K., Schwartz, M. K., Lowe, W. H., Letcher, B. H., & Whiteley, A. R. (2015). Distance, flow and PCR inhibition: e DNA dynamics in two headwater streams. Molecular ecology resources, 15(1), 216-227.

Pont, D., Rocle, M., Valentini, A., Civade, R., Jean, P., Maire, A., Roset, N., Schabuss, M., Zornig, H., & Dejean, T. (2018). Environmental DNA reveals quantitative patterns of fish biodiversity in large rivers despite its downstream transportation. Scientific reports, 8(1), 10361.

Strayer, D. L., & Dudgeon, D. (2010). Freshwater biodiversity conservation: recent progress and future challenges. Journal of the North American Benthological Society, 29(1), 344-358.

Wood, S. A., Biessy, L., Latchford, J. L., Zaiko, A., von Ammon, U., Audrezet, F., Cristescu, M. E., & Pochon, X. (2020). Release and degradation of environmental DNA and RNA in a marine system. Science of the Total Environment, 704, 135314.

# Temporal Development of Local Scour Around Bridge Abutments under a Stepwise Hydrograph

Serkan GOKMENER[1], Mustafa GOGUS[2], A. Burcu ALTAN SAKARYA[1]

[1] Hydraulics Laboratory, Department of Civil Engineering, Middle East Technical University, Ankara, Turkey
gokmener@metu.edu.tr

[2] Department of Civil Engineering, Çankaya University, Ankara, Turkey
mgogus@cankaya.edu.tr (for author 2)
burcuas@metu.edu.tr (for author 3)

ABSTRACT

In this experimental study, the temporal development of the local scour was investigated around the semi-circular end and rectangular bridge abutments under unsteady-state clear-water approach flow conditions in a rectangular sediment channel. A 6-hour stepwise hydrograph consisting of 3 different successive flow intensities, each applied continuously for 2 hours, was used to get unsteady-state approach flow conditions. During the experiments, 6 different abutment lengths with constant width were tested. Bed profiles around the abutments were recorded with a measurement device every 15 minutes to examine the temporal development of the local scour around the abutments. Effects of the abutment length and shape, flow intensity and test duration on the scour depths around abutments along with those at the front, upstream and downstream faces of the abutment were also examined. Based on experimental results, it was observed that flow intensity is the most critical parameter in scour development and the maximum scour depth was always recorded at the front noses of the abutments. In addition, for a given abutment length, flow conditions and test duration, the scour depths were always observed greater for the rectangular abutments than those for semi-circular end abutments.

## 1. Introduction

In the literature, several studies were conducted to estimate the maximum scour depths around bridge elements such as piers and abutments. However, these studies mainly focused on predicting equilibrium scour depth for steady-state flow conditions. Contrary to laboratory studies conducted under steady flow conditions, bridge failures generally occur during flood events under unsteady flow conditions (Gökmener, 2023). Furthermore, it is revealed that the maximum scour depths under flood events are much smaller than predictions for equilibrium scour depths under steady flow conditions (Borghei et al., 2012). According to Hager and Unger (2010), steady approaches overestimate the maximum scour depth by approximately 30%. Although several studies have been conducted over the last decades to predict the scour depth around bridge elements under unsteady approach flow conditions, these studies have mainly focused on piers. Despite this, Gjunsburgs et al. (2021) proposed a semi-analytical model based on the bed sediment movement equation to predict the scour depth around vertical-wall abutments located on floodplains and Gokmener & Gogus (2022) experimentally investigated the temporal development of scour depth around semi-circular end abutments under unsteady clear-water flow conditions, there are still gaps in the literature on the scour formation around abutments under unsteady flow conditions. The aim of this study is to investigate the temporal development of scour depths around bridge abutments under unsteady flow conditions with varying abutment shapes and lengths.

## 2. Experimental Setup

Experiments were conducted in a rectangular sediment channel with a bed slope of $S_0$=0.001 (Fig. 1.). Non-cohesive uniform sand with a median diameter size of $d_{50}$=1.5 mm and a geometric standard deviation of particle size distribution, $\sigma_g$=1.29 were tested as erodible bed material. A pump from a water tank with a constant head provided the required discharge to the experimental setup. A control gate was set at the end of the channel to regulate the flow depth and intensity.

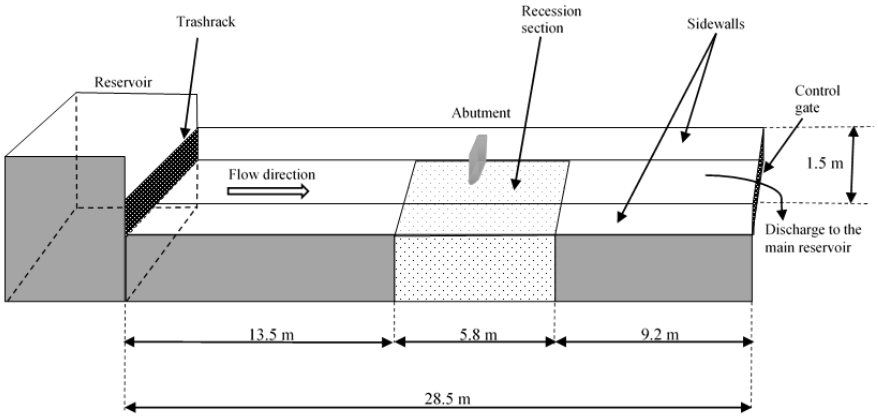



Fig. 1. Sketch of the experimental setup (Gogus et al., 2023)

Semi-circular end and rectangular abutments of lengths, $L_a$= 15,20, 25, 30, 35, and 40 cm, having a constant width of $B_a$=10 cm were tested during the experiments. A 6-hour stepwise hydrograph with a constant discharge of 0.0678 $m^3/s$, consisting of 3 different successive flow intensities as $U/U_c$=0.7 (y=17.4 cm), $U/U_c$=0.8 (y=15.2 cm) and $U/U_c$=0.9 (y=13.5 cm) respectively each applied continuously for 2 hours, were applied to get unsteady flow conditions. The variations on the erodible bed material around the abutment were measured by an acoustic measuring device every 15 minutes at 24 points.

## 3. Results

Based on experimental results, the scour depths at the upstream, downstream and front noses of an abutment increased with increasing time and flow intensity for a given abutment length. Maximum scour depths always occurred at the front nose of the abutment regardless of the abutment length at any flow intensity tested. Since the longer abutments cause greater horseshoe vortex and increased bed shear stress zones compared to shorter ones (Koken and Gogus, 2015), as the lengths of the abutments increased for a given time and flow intensity, greater scour depths obtained around the abutment. Moreover, for the shorter abutment lengths tested, $L_a \leq$ 25 cm, the scour depths started to form at higher flow intensities. Furthermore, around the short abutments, $L_a/y<1$, negligible scour depths were observed for flow intensities less than 0.9. The rectangular abutments for a given length and test duration tend to create greater scour depths than semi-circular end ones due to the blunt nature of the rectangular abutments that lead to greater scour depths. In addition, for the abutments of lengths $L_a \geq$ 30 cm, the maximum scour depths were recorded as 30% greater for the rectangular abutments than for semi-circular end ones. This indication is consistent with Melville's (1992) study that presented the abutment shape factor values for the maximum scour depth around semi-circular and rectangular abutments as 0.75 and 1, respectively. However, for the other abutment lengths tested, the maximum scour depths around the rectangular abutments were measured much greater than 30% than those of semi-circular end ones.

## 4. Conclusion

In this study, the effect of flow intensity, abutment length and temporal variation on the development of local scour around bridge abutments were experimentally investigated under unsteady clear-water flow conditions. Experimental results indicated that flow intensity is the most significant parameter affecting scour development. Also, the greatest scour depths were obtained for the longest rectangular abutment length tested.

**References**

Borghei SM, Kabiri- Samani A, Banihashem SA (2012) Influence of unsteady flow hydrograph shape on local scouring around bridge pier, Proceedings of the Institution of Civil Engineers-Water Management, 165(9), 473-480

Gjunsburgs B, Radzevičius A, Šadzevičius R, Skominas R (2021) Scours evolution at bridge abutments under unsteady flow events, Iranian Journal of Science and Technology, Transactions of Civil Engineering, 45, 1951-1957

Gogus M, Daskin S, Gokmener S (2023) Effects of collars on local scour around semi-circular end bridge abutments, Proceedings of the Institution of Civil Engineers-Water Management, Ahead of Print, 1-11

Gokmener S, Gogus M (2022) Local scour evolution around semi-circular end bridge abutment in quasi-unsteady condition, Proceedings of the Institution of Civil Engineers-Water Management, 175(4), 163-177

Gökmener S (2023) Effects of Flow Intensity and Collars on Scour Depths Around Bridge Abutments, PhD Dissertation, Middle East Technical University, Ankara, Turkey

Hager WH, Unger J (2010) Bridge pier scour under flood waves, Journal of Hydraulic Engineering, 136(10), 842-847

Koken M, Gogus M (2015) Effect of spur dike length on the horseshoe vortex system and the bed shear stress distribution, Journal of Hydraulic Research, 53(2), 196-206

Melville BW (1992) Local scour at bridge abutments, Journal of Hydraulic Engineering, 118(4), 615-631

# Impact of the Grand Ethiopian Renaissance Dam in Nile Delta Aquifer under Different Filling Scenarios

Alban KURIQI[1], Ismail ABD-ELATY [2]

[1] CERIS, Instituto Superior Técnico, Universidade de Lisboa, Av. RoviscoPais 1, 1049-001, Lisbon, Portugal
alban.kuriqi@tecnico.ulisboa.pt

[2] Department of Water and Water Structures Engineering, Faculty of Engineering, Zagazig University, Zagazig 44519, Egypt
Eng_abdelaty006@yahoo.com

ABSTRACT

This study explores the profound impact of the Grand Ethiopian Renaissance Dam (GERD) in the Nile Delta aquifer under different potential filling scenarios, particularly under minimum and normal flow conditions, alongside the anticipated repercussions involving declining groundwater levels and increasing saltwater intrusion. The study involved three distinct scenarios, each simulating the filling of the GERD reservoir at different elevations: 600 m, 621 m, and 645 m above mean sea level (amsl). These scenarios were denoted as follows: Scenario #1 with a storage volume of 17 billion cubic meters (BCM), Scenario #2 with 37.30 BCM, and Scenario #3 with 74 BCM. In addition, these scenarios considered a collective sea level rise (SLR) of 25 cm and a reduction in the River Nile's hydrographs by 17 BCM, 20.30 BCM, and 36.70 BCM, respectively. This reduction was linked to an incremental increase in abstraction well rates, set at 25%, 50%, and 100%, respectively. The study's findings revealed that introducing a 25 cm SLR, coupled with GERD reservoir filling at 600 m, 621 m, and 645 m AMSL, particularly during the filling phases, could significantly impact the groundwater resources within the Nile Delta. Notably, these impacts were observed in alterations to the quality of freshwater within the Nile Delta. Specifically, the aquifer's salinity increased by 4.47% for Scenario #1, 11.48% for Scenario #2, and a substantial 29.99% for Scenario #3. The construction and operation of GERD hold the potential to usher in a significant reduction in the Nile River's flow, particularly during the crucial filling stages of its reservoir. This decline will, in turn, have a cascading effect on the groundwater recharge in the Nile Delta aquifer. Forecasts point towards expected land subsidence in the Nile Delta area, with projections ranging from 52 mm for the first filling scenario to a staggering 260 mm for the third.

## 1. Introduction

As Egypt faces an uncertain future marked by the dual challenges of population growth and the impacts of climate change, the strain on its water resources is set to intensify. Water scarcity looms as a threat, further exacerbated by the impending operation of the Grand Ethiopian Renaissance Dam (GERD) (Wheeler et al., 2020). Water supplies in arid and semi-arid regions are critical for agriculture, industrial and domestic activities (Santana et al., 2020). Egypt is an arid region with limited water supplies; the average rainfall ranges between 50 to 200 mm per year (El-Rawy et al., 2020). Future overpopulation and climate change will influence and increase the water stress in Egypt, reducing the human water supply and increasing the water shortage (Sowers et al., 2011). This study investigates the impact of different operation scenarios of the Grand Ethiopian Renaissance Dam (GERD) on the Nile River water supply for minimum and normal flow conditions.

## 2. Methodology

This study assesses the impact of Sea Level Rise (SLR) and reduced natural flow due to the Grand Ethiopian Renaissance Dam (GERD) on water budget and salinity, employing the SEAWAT model (Abd-Elaty et al., 2024). Three filling scenarios were examined for the GERD reservoir at elevations of 600 m, 621 m, and 645 m above mean sea level (AMSL), corresponding to storage volumes of 17 billion cubic meters (BCM) (Scenario #1), 37.30 BCM (Scenario #2), and 74 BCM (Scenario #3). These scenarios incorporate a combined SLR of 25 cm and increased abstraction rates of 25%, 50%, and 100%, respectively.

## 3. Results

The research results revealed that as pumping rates increased, both the SLR and the GERD reservoir experienced heightened filling, particularly noticeable during the filling phases. This phenomenon was observed to have significant implications for groundwater resources within the Nile Delta. Specifically, the filling of the GERD reservoir was found to potentially modify the freshwater dynamics, resulting in a respective increase in aquifer salinity by 4.47%, 11.48%, and 29.99% across three distinct scenarios (Figure 1).

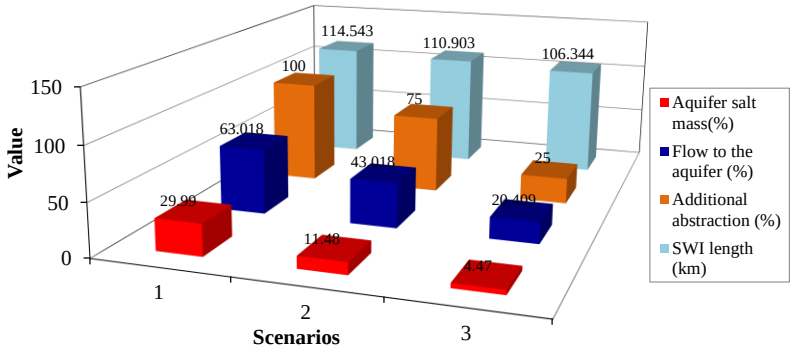



**Fig. 1.** Nile Delta groundwater alteration under different filling scenarios.

The approach and outcomes delineated in this investigation offer valuable insights for evaluating and contrasting the effects of SLR alongside new upper dam initiatives on downstream water budgets and salinity in analogous coastal zones. Notably, these shifts are not uniform across the region, with the eastern and western parts of the Nile Delta bearing the brunt of declining groundwater levels and experiencing more pronounced land subsidence. The accelerated intrusion of seawater and the deteriorating quality of groundwater in the Nile Delta aquifer are of great concern. These findings underscore the urgency of assessing the impact of dam projects on water resources in downstream countries. By shedding light on the complex interplay of factors, this study aims to inform future policy and planning decisions for a sustainable water future in the region.

**Acknowledgements**

Alban Kuriqi is grateful for the Foundation for Science and Technology's support through funding UIDB/04625/2020 from the research unit CERIS.

**References**

Abd-Elaty, I, Kuriqi, A, Pugliese, L, & Ahmed, A (2024) Shoreline subsurface dams to protect coastal aquifers from sea level rise and saltwater intrusion. *Applied Water Science*, 14(3), 1-12.
El-Rawy M, Abdalla F, El Alfy M (2020) Water Resources in Egypt. In: Hamimi Z, El-Barkooky A, Martínez Frías J, Fritz H, Abd El-Rahman Y (eds). The Geology of Egypt. *Springer International Publishing, Cham*. pp 687-711.
Santana CS, Montalván Olivares DM, Silva VHC, Luzardo FHM, Velasco FG, de Jesus RM (2020) Assessment of water resources pollution associated with mining activity in a semi-arid region. *Journal of Environmental Management* 273:111148.
Sowers J, Vengosh A, Weinthal E (2011) Climate change, water resources, and the politics of adaptation in the Middle East and North *Africa. Climatic Change* 104:599-627.
Wheeler, K. G, Jeuland, M, Hall, J. W, Zagona, E, & Whittington, D (2020) Understanding and managing new risks on the Nile with the Grand Ethiopian Renaissance Dam. *Nature Communications*, 11(1), 5222.

# A GIS-MCDA based participatory method to map Managed Aquifer Recharge feasibility in Chiba watershed, CapBon, NE Tunisia

Anis CHEKIRBANE[1], Khaoula KHEMIRI[1], Constantinos F. PANAGIOTOU[2], Catalin STEFAN[3]

[1] National Agronomic Institute of Tunisia (INAT), Carthage University, Tunis, Tunisia

anis.chkirbene@inat.ucar.tn

khaoula.khemiri@inat.ucar.tn

[2] Department of Environment and Climate, ERATOSTHENES Centre of Excellence, Cyprus

constantinos.panagiotou@eratosthenes.org.cy

[3] Research Group INOWAS, Department of Hydrosciences, Technische Universität Dresden, Dresden, Germany

catalin.stefan@tu-dresden.de

ABSTRACT

## 1. Introduction

Managed Aquifer Recharge (MAR) is the purposeful recharge of water to aquifers for subsequent recovery or environmental benefit achieved through various schemes (Dillon et al, 2019). Suitability and feasibility mapping for MAR is recently gaining more attention because of its potential in producing comprehensive maps easily interpreted and used by policy makers. In front of the diverse existing methodologies, an innovative adapted approach was developed in the framework of AGREEMAR project to generate MAR feasibility maps within a participatory approach. Stakeholders were identified and they were involved in MAR suitability mapping process (Fig.1).




**Fig. 1.** General concept of MAR site suitability mapping

## 2. Methodology

Following the mentioned methodology, a GIS-based multi-criteria decision analysis (MCDA) was applied to establish the MAR feasibility in Chiba watershed in CapBon peninsula, NE of Tunisia. The MAR typologies for Chiba basin were determined based on a participative approach after consulting the key stakeholders from general, regional, and local scales. An online questionnaire was used and revealed that in addition to the general goal of integrated water resources management (IWRM), the main two MAR objectives for the study region are (i) improvement of groundwater quality and (ii) long term storage of groundwater. Stakeholders were also able to define the most suitable MAR scheme: infiltration ponds and basins; soil aquifer treatment (SAT) using treated wastewater and dam water release. Concerning constraints, only land use was considered, especially dense urban areas, forests, and protected zones where MAR can't be applied. Relevant criteria were selected after consulting stakeholders during in-person meetings. The most relevant physical criteria were selected in a way that fulfil the complete coverage of the watershed and in respect to the thematic of intrinsic site suitability, recharge water availability and water demand. A special attention was paid to the temporal aspect of the data such the annual rainfall distribution or crop water demand. Weights of each criterion were determined based

on the developed participatory approach in AGREEMAR project (Martin et al, 2022). MAR feasibility maps were obtained using weighted linear combination (WLC) by the mean of ArcGIS software.

The feasibility maps were developed following weighted assessments by stakeholders during in person workshop in the National Agronomic Institute of Tunisia (INAT).

## 3. Results

The resulting maps are similar for both dry and wet season. Zones where MAR is feasible and highly feasible are basically located near the coastal region where intrinsic site characteristics are mostly suitable, conventional and non-conventional water resources for recharge water are available and agricultural and ecosystem demand are high. The high feasibility areas close to the water supply network reflects the importance of the water availability thematic (weight coefficient ≈ 50%). Low feasibility zones are located in the upstream part of the watershed where the intrinsic characteristics are unsuitable (e.g., slope is exceeding 20°) and recharge water is rare (Fig.2).

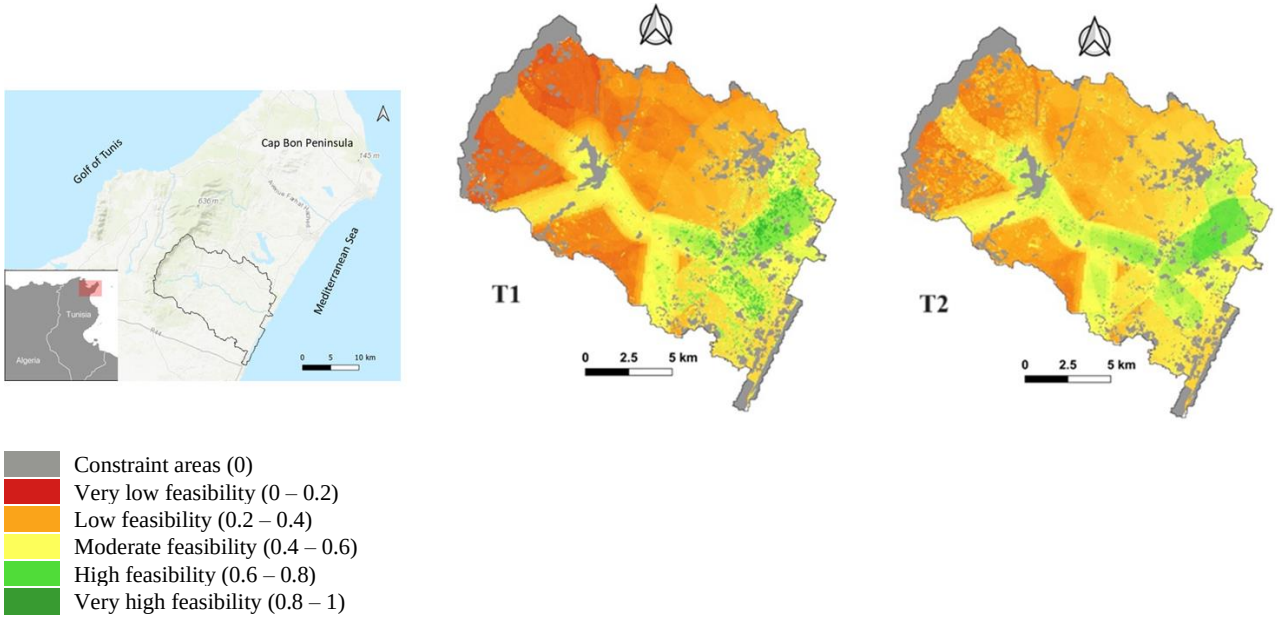



**Fig. 2.** MAR feasibility maps of Chiba watershed in Tunisia during dry (T1) and wet (T2) seasons

## 4. Conclusion

The MAR feasibility maps of Chiba watershed were obtained using a comprehensive methodology that integrates expert-based knowledge and stakeholders' participation. Considering the MAR objectives/typology of Chiba watershed, the most relevant MAR scheme could be infiltration basins and SAT near the coastal region to mitigate seawater intrusion using treated wastewater from Korba WWTP. However, in the dam region, water release and check dams can be efficiently used to long term storage of groundwater. These maps are expected to be used by the water policy makers and water authorities for licensing the implementation of sustainable water management strategies (such as MAR), not only in Chiba watershed, but also across the entire Mediterranean region.

**Acknowledgements**

The AGREEMAR project is funded by National Funding Agencies from Germany (Bundesministerium für Bildung und Forschung – BMBF), Cyprus (Research & Innovation Foundation – RIF), Portugal (Fundação para a Ciência e a Tecnologia – FCT), Spain (Ministerio de Ciencia e Innovación – MCI) and Tunisia (Ministère de l'Enseignement Supérieur et de la Recherche Scientifique – MESRS) under the Partnership for Research and Innovation in the Mediterranean Area (PRIMA). The PRIMA programme is supported under Horizon 2020 by the European Union's Framework for Research and Innovation. Project duration: 1 June 2022 – 31 May 2025.

**References**

Martins TN, Panagiotou CF, Stefan C, Chkirbene, A (2022) AGREEMAR Deliverable D2.2. Participative methodology for criteria selection and weighting in MAR site feasibility mapping. Available online at https://www.agreemar.inowas.com/deliverables.

Dillon P, Stuyfzand P, Grischek T, Lluria, M, Pyne R, Jain RC., ... & Sapiano, M (2019) Sixty years of global progress in managed aquifer recharge. *Hydrogeology journal*, 27(1), 1-30.

# Characterization of Large-Scale Turbulence Horizontal Coherent Structures in Ice-Covered Flows

Cristopher GAMBOA MONGE[1], Ana Maria FERREIRA DA SILVA[2]

[1,2] Queen's University, Kingston, ON, Canada
c.gamboamonge@queensu.ca
anamaria.dasilva@queensu.ca

ABSTRACT

Large-scale coherent turbulence structures encompass the largest conglomerations of eddies rotating vertically (around horizontal axes) or horizontally (around vertical axes). This study centers on large-scale horizontal coherent structures (LSHCSs). Despite their relevance in sediment transport, pollutant dispersion, and fluvial configurations, LSHCSs remain unexplored within ice-covered scenarios. This work aims to address this gap by investigating LSHCSs' scales and life-cycle under such conditions. The approach involves instantaneous flow velocity measurements in a flume using a 2D Micro Acoustic Doppler Velocity (ADV) meter. The simulated ice-cover consisted of extruded polystyrene with mesh; smooth concrete served as streambed. Low-pass filters and Continuous Wavelet Transform (CWT) were used to estimate the characteristic scales of LSHCSs. This study highlights the significant effect of ice-covers on the characteristic scales of LSHCSs, resulting in a reduction of approximately 14% compared to its equivalent open-channel condition. This finding is relevant as it suggests that in scenarios with a movable bed, the length scale of the related bed and plan forms is likely to also be impacted.

## 1. Introduction

Turbulent coherent structures are a well-known feature of open-channels and river flows. They exist at various spatial and temporal scales, from near-wall (small-scale) to large-scale coherent structures extending throughout the body of the fluid (da Silva and Yalin, 2017). Large-scale horizontal coherent structures (LSHCSs) have been the object of several studies, primarily focusing on structures originating at river irregularities, such as sudden changes in direction and bifurcations, as well as in compound channels. A few works have also considered the characteristic scales and dynamics of LSHCSs in rectilinear channels (for a review, see da Silva and Yalin, 2017). In the latter case, LSHCSs originate near the banks and towards the free surface where the horizontal shear stress is largest (Yalin, 1992), then evolve into horizontal disks as they are transported downstream by the flow, and finally disintegrate after reaching a size comparable to the flow width.

While previous research has focused on the internal structure of vertical turbulence in ice-covered channels, there has been no investigation into how ice-covers affect the characteristic scales and dynamics of LSHCSs. The aim of this work is to explore potential differences between the time and length scales of LSHCSs in rectilinear laboratory streams with a free surface and those with a simulated ice-cover.

## 2. Experimental set-up and hydraulic conditions

Two tests, T1S2 and T2S2, were conducted in an 11 m x 0.382 m flume with 0.41 m high glass walls at the Queen's University Water Research Laboratory. To ensure smooth water entry to the flume, a ramp with flow straighteners was mounted in the entrance chamber. The bed was smooth concrete with a slope $S$ = 0.00061.

Instantaneous and time-averaged flow velocities were measured in a uniform open-channel flow (T1S2) and its equivalent covered flow (T2S2). The simulated ice-cover consisted of four consecutive sheets of floating polystyrene. The hydraulic conditions in the tests were as summarized in Table 1. Here $Q$ is flow rate, $h$ is flow depth, $R_h$ is hydraulic radius, $u_{av}$ is average longitudinal flow velocity, $u_*$ is shear velocity, $Re$ is flow Reynolds number, $Fr$ is Froude number, $Re_*$ is roughness Reynolds number, $B/h$ is width-to-depth ratio.

**Table 1**. Summary of hydraulic conditions of the present tests ($B$ = 0.382 m; $S$ = 0.00061).

| Test | $Q$ x10$^3$ (m$^3$ s$^{-1}$) | $h$ (m) | $R_h$ (m) | $u_{av}$ (m s$^{-1}$) | $u_*$ (m s$^{-1}$) | $Re$ | $Fr$ | $Re_*$ | $B/h$ |
|---|---|---|---|---|---|---|---|---|---|
| 1S2 | 5.53 | 0.0500 | 0.0396 | 0.2897 | 0.0173 | 14485 | 0.41 | 3.46 | 7.64 |
| 2S2 | 5.30 | 0.0603 | 0.0260 | 0.2300 | 0.0190 | 13870 | 0.30 | 3.80 | 6.33 |

In test T1S2, flow velocity measurements (FVM) were carried out at 13 equidistant points over the flow depth at the flume centreline, 5.5 m downstream of the entrance. Subsequently, additional 28 FVM were gathered, extending into 7 transverse locations (4 FVM each) towards the right-hand flume wall. This data collection scheme was mirrored towards the left-hand flume wall, resulting in a total 69 FVM for T1S2. In test T2S2, 18 FVM were evenly distributed over the flow depth at the flume centreline, with an additional point taken at each of the same transverse locations described for T1S2, bringing the total FVM for T2S2 to 87. These FVM were obtained using a side-looking 16-MHz 2D SontekTM Micro-ADV, operating at a frequency of 25 Hz, with a sampling duration of 180 seconds.

## 3. Data processing

In the following, the term *length scale* ($\lambda$) represents the streamwise distance a LSHCS travels from its origin to complete disintegration, while *time scale* ($T$) denotes the duration of their journey (Franca, 2015). Following Taylor time-space conversions, these characteristic scales are related as $\lambda = T \cdot u_{av}$ (Yalin, 1992). To determine $\lambda$ and $T$ from the present velocity measurements, the instantaneous velocity records were analyzed using the moving average smoothing (MAS) and the Continuous Wavelet Transform (CWT) (Kanani, 2015).

## 4. Results and discussion

Sample results of application of CWT and MAS to velocity signals at 2.5 cm from the bed surface and at the centreline in both tests are shown in Fig. 1. Analysis of the CWT Power (CWTP) in the frequency-time domain and corresponding Global Wavelet Spectrum (GWS) reveal dominant frequency components of 0.05 and 0.1109 Hz for T1S2 and 0.0833 Hz for T2S2. These findings align with results from MAS technique.

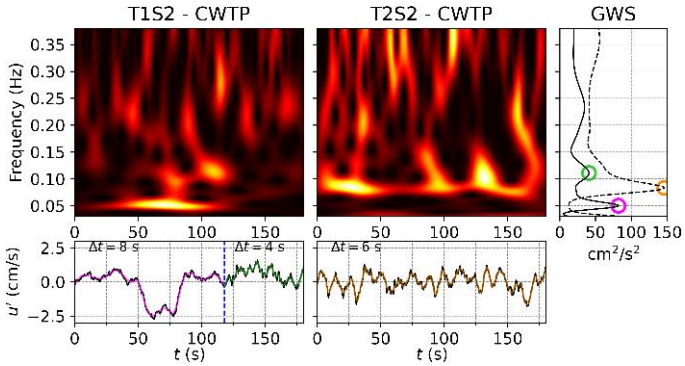



**Fig. 1**. Sample results of CWT Power contour plots, corresponding GWS and filtered oscillograms of $u'$.

As evidenced in Fig. 1, a velocity signal reflects the characteristic scales of successive coherent events within the signal duration. Therefore, to assess the significance of LSHCSs on river morphology and morphodynamics, average characteristic scales are crucial. To this end, the probability density function of the characteristic scales identified in all records was produced for T1S2 and T2S2, yielding for the LSHCSs average time scales $T$ of 13.8 s (T1S2) and 15.0 s (T2S2). These time scales correspond to average length scales of $\lambda = 10.5B$ (T1S2) and $\lambda = 9.0B$ (T2S2).

## 5. Conclusions

Despite the smaller $T$ observed for T1S2 compared to T2S2, the real implications differ due to the dependency of the distance travelled on the average flow velocity. Specifically, the $u_{av}$ in T1S2 is greater than that in T2S2, leading to a 14% reduction in $\lambda$ for the ice-covered flow compared to its equivalent open-channel condition.

**Acknowledgements**

This work was supported by NSERC (Natural Sciences and Eng. Res. Council of Canada) through a Discovery Grant to the 2nd author.

**References**

da Silva AMF, Yalin MS (2017) Fluvial processes, IAHR Monograph Series, CRC Press, 2nd edition.
Franca MJ (2015) Detection and construction of large-scale coherent flow structures in gravel-bed rivers, Earth Surf Process Landf, 40, 93-104.
Kanani A, da Silva AMF (2015) Application of continuous wavelet transform to the study of large-scale coherent structures, Environ Fluid Mech, 15, 1293-1319.
Yalin MS (1992) River mechanics, Pergamon Press, Oxford.

# Generation of realistic deformed beds in sine-generated meandering streams

Mengsi DONG[1], Ana Maria FERREIRA DA SILVA[2]

[1,2] Queen's University, Kingston, ON, Canada
mengsi.dong1@queensu.ca
anamaria.dasilva@queensu.ca

ABSTRACT

It is widely recognized that the physics of meandering flows and processes can best be explored by invoking idealized streams (or 'models') when conducting both experimental and numerical studies. This work deals with the question of how to idealize the geometry of meandering streams, and more specifically on how to generate idealized and yet realistic meandering beds for streams whose channel centerlines follow sine-generated curves. A numerical model is developed to create realistic beds on the basis of established geometric characteristics of deformed beds. The performance of the model is assessed by applying it to the experimental results by various authors, and involving channels with varying sinuosity. The results illustrate that the deformed beds generated by the present model are in satisfactory agreement with the real beds.

## 1. Introduction

As is well-known, meandering is by far the plan shape most frequently acquired by natural streams, especially in the lowland alluvial plains (da Silva and Ebrahimi, 2017). Meandering streams play a major role in the socioeconomic and cultural development of their regions, by being a source of water supply, a means for inland navigating, and providing fertile land for agriculture, among other functions. Given their scientific and practical significance, meandering streams have been the object of extensive and sustained research for many years. Yet, as evidenced by the recent literature, many aspects of the mechanics of meandering flows remain unclear. On the other hand, hydrodynamic numerical models are increasingly being used to explore such aspects. An understanding of the internal structure of meandering flows can be achieved by applying such models to simulate the flow in specific rivers or streams. However, because the meandering geometry varies considerably from stream to stream, establishing and formulating the defining, all-compassing characteristics of meandering flows can most appropriately be achieved by investigating the flow in abstract idealized meandering streams (or 'stream models').

The matter of idealization of the plan shape of meandering streams has been dealt with by Leopold and Langbein (1966), who proposed the well-known sine-generated curve to represent the centerline of regular streams; and Kinoshita (1961), who proposed the Kinoshita curve to represent that of irregular streams. These have since become the most popular means of expressing the path of meandering streams. By contrast, no work so far has dealt with the idealization of the bed in meandering streams, and as a result no satisfactory method exists for the generation of idealized and yet realistic bed topographies. This paper, where a model to generate idealized bed topographies is introduced, is an attempt to address this matter.

## 2. Proposed Model

The present model is developed by taking into account the main characteristics of meandering deformed beds as derived from a multitude of experiments conducted by various authors as summarized by da Silva and Ebrahimi (2017). It is assumed that the flow width does not vary in downstream direction; the flow rate is constant; the stream centerline follows a sine-generated curve and thus the idealized streams are strictly periodic.

As is well known, meandering bed topography consists of laterally adjacent erosion-deposition zones, occurring once per half-channel length. For the conditions specified above, each erosion-deposition zone has the length $L/2$, where $L$ – meander wavelength. These zones shift upstream as the channel sinuosity increases

(see da Silva and Ebrahimi, 2017). Additionally, due to the periodicity of the stream, the volumes of erosion and deposition between any two consecutive cross sections are equal. Finally, it is known that the cross-sectional bed profiles can be adequately described by an exponential function. Accordingly, the present model is based on the following exponential form to express the cross-sectional bed profiles:

$$h_{av} - \Delta z_b = [h_{av} - (\Delta z_b)_c]e^{\alpha n} = h_c e^{\alpha n} \tag{1}$$

where $h$ – flow depth, $h_{av}$ – average flow depth, $\Delta z_b$ – difference between the local bed surface elevation of the deformed bed at any time $t$ and the bed surface elevation of the flat initial bed, $n$ – transversal coordinate measured from centerline, and $\alpha$ – unknown to be determined. Note that the subscript $c$ indicates centerline; and $\Delta z_b > 0$ implies deposition, while $\Delta z_b < 0$ implies erosion. The combination of Eq. (1) with the mathematical expression of equality of erosion and deposition volumes yields an algebraic equation for $\alpha$ from which this can be determined. Because $\alpha$ varies in downstream direction, this algebraic equation must be solved at every different cross-section. Owing to length limitations, the detailed derivations are not included here.

## 3. Results

As an example of the results of the present model, this is used here to produce an idealized version of the deformed bed resulting from one of the mobile bed experiments by da Silva and El-Tahawy (Run 2: $\theta_0 = 70^o$, $B = 0.4$m, $D = 0.65$mm, $h_{av} = 7.3$cm, where $\theta_0$ – initial deflection angle of the sine-generated curve, $B$ – flow width and $D$ – average grain size of the bed material). The measured and idealized bed topographies are displayed in Figs. 1a and 1b, respectively, showing contour-plots of $\Delta z_b/h_{av}$. Fig. 1c supplements the just mentioned figures, by showing the difference between idealized and experimental values of $\Delta z_b/h_{av}$. Clearly, the present model is not able to reproduce all features of the deformed bed, but it very adequately captures its main (defining) characteristics. Application of the present model to additional examples (not included here) has yielded equally satisfactory results.

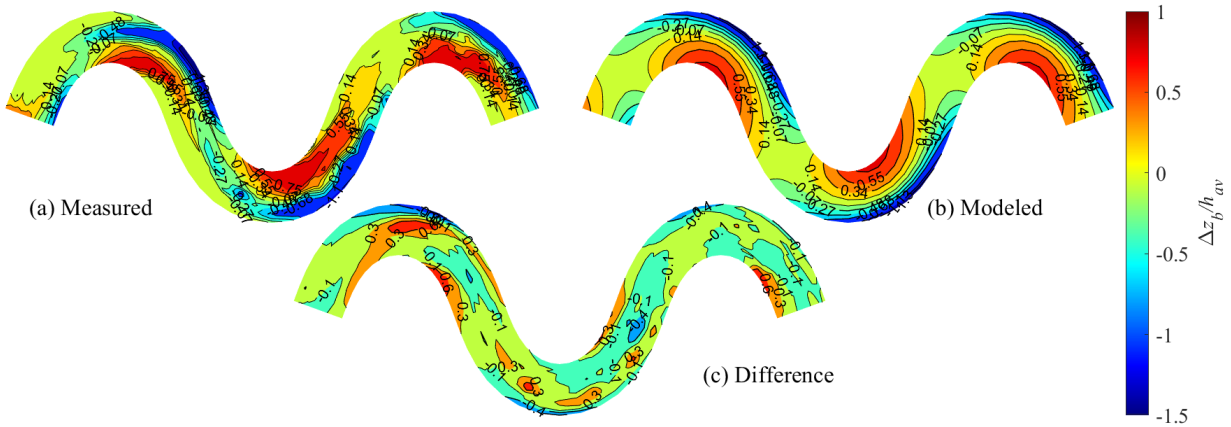



**Fig. 1.** Bed elevation contour-plot (flow from left to right) (a) Measured; (b) Modeled; (c) Difference $((\Delta z_b/h_{av})_{Modeled} - (\Delta z_b/h_{av})_{Measured})$.

## 4. Conclusions

The present mathematical model for the generation of idealized and yet realistic deformed beds in sine-generated streams was found to produce satisfactory results. As expected, the model does not reproduce all features of the bed, such as random irregularities or bed forms superimposed on the bed (dunes, ripples), but it adequately captures the overall characteristics of the bed of meandering streams.

**Acknowledgements**

This work was supported by the Natural Sciences and Engineering Research Council of Canada (NSERC) through a Discovery Grant provided to the second author and the Leaders Create Grant.

**References**

da Silva AMF, El-Tahawy T (2008) On the location in flow plan of erosion-deposition zones in sine-generated meandering streams. J. Hydraulic Res., 46(1), 49-60.
da Silva AMF, Ebrahimi M (2017) Meandering morphodynamics: insights from laboratory and numerical experiments and beyond. J. Hydraulic Eng., 60th Anniversary Paper, 143(9): 03117005, 1-13.
Leopold LB, Langbein WB (1966) River meanders. Sci. Am., 214(6), 60–70.
Kinoshita R (1961) Investigation of channel deformation in Ishikari River. Rep. of Bureau of Resources, Dept. of Science and Technology, Tokyo.

# Investigation of the long-term changes in sediment load along a free-flowing transboundary Middle Danube reach

Dejana ĐORĐEVIĆ[1], Enikő Anna TAMÁS[2], Ljubiša MIHAJLOVIĆ[3], Csaba ABONYI[4], Aleksandar VUJANOVIĆ[5], Béla KALOCSA[6]

[1] Faculty of Civil Engineering, University of Belgrade, Serbia
dejana@grf.bg.ac.rs
[2] Faculty of Water Sciences, University of Public Service, Baja, Hungary
tamas.eniko.anna@uni-nke.hu
[3]Directorate for Inland Waterways, Ministry of Construction, Transport and Infrastructure, Belgrade, Serbia
ljmihajlovic@plovput.rs
[4] Lower Danube Valley Water Authority, Baja, Hungary
abonyics@gmail.com
[5] Saobraćajni Institut CIP d.o.o., Belgrade, Serbia
acavujanovic@yahoo.com
[6] Palustris Co., Baja, Hungary
kalocsa.bela@gmail.com

ABSTRACT

The presented study aims at the indirect estimation of the long-term sediment transport along the sand-bed reach of the free-flowing Middle Danube River based on the surveillance cross-sections' data. A decreasing trend in water levels and an increasing trend in cross-sectional areas are persistent, while longitudinal changes in long-term sediment transport rates indicate the existence of both degrading and aggrading riverbed reaches.

## 1. Introduction

The study targets to indirectly estimate the average multiannual sediment transport. Previously, the analyses of the time series of water levels and discharges for the period between 1950 and 2019 for the entire free-flowing alluvial reach of the Danube River was done for a total of ten gauging stations (Tamás et al, 2021), showing a severe reduction in water levels, which was suspected to origin from riverbed erosion. As sediment monitoring is scarce along the study reach, the estimation of sediment transport changes is based in the present study on bathymetric data collected by the Directorate for Inland Waterways (Plovput) in Serbia, the former Environmental and Water Management Research Institute (VITUKI), and the Lower-Danube-Valley Water Directorate (LDVWD) in Hungary. Similar analyses were carried out by eg. Rákóczi and Sass (2001), or Tang et al. (2021). The research question is if it is possible to assess sediment transport characteristics along the reach with no large tributaries between Baja gauging station (Hungary) and the confluence of the Drava River (Serbia) based on the bathymetry results of the regularly surveyed cross-sections (Đorđević et al. 2023).

## 2. Materials and methods

Bathymetric data were obtained from the databases of Plovput, VITUKI and LDVWD for 23 surveillance cross-sections in Hungary and 46 in Serbia. Estimation of sediment transport is based on two pairs of consecutive surveys, 25 years apart (1996, 1997 and 2021, 2022), and it was done by determining and comparing the areas of cross-sections. Calculated differences in cross-sectional areas were used to determine channel volumes between each pair of cross-sections along the study reach (sr):

$$\forall_{sr,}(t)=0.5(A_i(t)+A_{i+1}(t))\,\Delta x, \quad i=1, 68 \qquad (1)$$

The long-term sediment transport between two cross-sections is thus

$$Q_{s,i} = \frac{\forall_{sr,i}(t_1)-\forall_{sr,i}(t_2)}{\Delta t}\rho_s(1-\lambda) = \frac{\Delta\forall_{sr,i}}{\Delta t}\rho_s(1-\lambda), \quad i=1, 68 \qquad (2)$$

where $\rho_s$ is sediment particle density and $\lambda$ is the porosity of the bed material.

## 3. Results

First the analysis of rates of change in the cross-sectional area ($A$) between two successive surveys ($\Delta A/\Delta t$) was done. Results are presented for four typical gauging stations (Fig. 1., based on all bathymetric surveys).

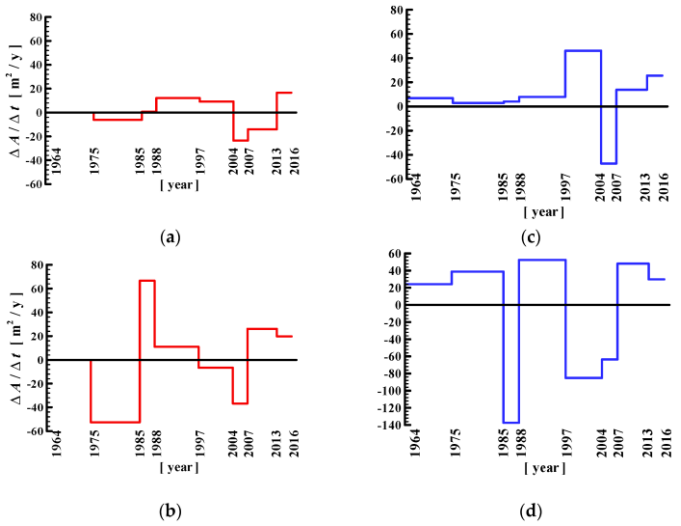



**Fig. 1:** Rate of change in the cross-sectional area in (**a**) Baja; (**b**) Mohács; (**c**) Bezdan; and (**d**) Apatin according to available bathymetric surveys. Red color is used for GSs on the Hungarian, and blue color for GSs on the Serbian side.

Cross-sectional area increased in 52 cross-sections (75%), while it decreased in 17 cross-sections (25%). Then, the longitudinal profiles of $A$ were used to estimate the 25-year long-term sediment transport (Fig. 2.). The largest multiannual sediment transport rate ($Q_s$) is around $65 \cdot 10^3$ t/year, while the most intensive degradation of the riverbed is approximately $45 \cdot 10^3$ t/year. Generally, there is a continuous uptake of sediments from the riverbed (incision), and uptake rates are between $10 \cdot 10^3$ t/year and $25 \cdot 10^3$ t/year.

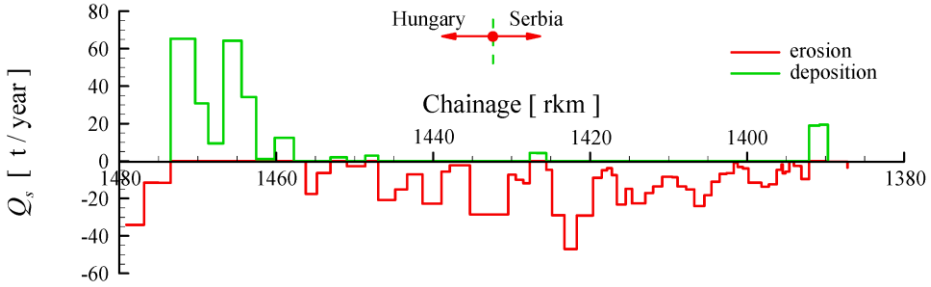



**Fig. 2:** 25 years changes in sediment transport along the study reach (Đorđević et al. 2023)

## 4. Conclusions

It is proven that it is possible to investigate long-term sediment transport rates based on bathymetric surveys. Along the study reach of the Danube the maximum (local) value of the positive sediment transport (aggradation) in the last 25 years is approximately 30% greater than the maximum absolute value of the negative transport (degradation). In 86% of the study reach the long-term sediment transport for the studied period is negative. Thus, sediment balance changes also prove that decreasing water levels are a good indicator of an ongoing severe riverbed erosion process.

**Acknowledgements**

The authors are grateful for the provision of data from the institutions of both countries, Plovput in Serbia and LDVWD in Hungary.

**References**

Đorđević D, Tamás EA, Mihajlović Lj, Abonyi Cs, Vujanović A, Kalocsa B (2013): Estimation of Changes in Sediment Transport along the Free-Flowing Middle Danube River Reach. *Appl. Sci.* 2023, *13*, 10513.

Rákóczi L, Sass J (2001): A Főmeder és az ágrendszerek medermorfológiai-, üledék- és hordalékviszonyainak alakulása. VITUKI Rt., Hungary. Available online: http://www.szigetkoz.biz/monitoring/MTA2001/sass.htm (accessed on 3 March 2023).

Tamás EA, Đorđević D, Kalocsa B, Vujanović A (2021): Hydrological indicators of the riverbed incision along the free-flowing Danube River reach from Budapest to Slankamen relevant for the lateral connectivity between the river channel and floodplains. In Proceedings of the 43rd IAD Conference Rivers and Floodplains in the Anthropocene—Upcoming Challenges in the Danube River Basin, Neuburg, Germany; pp. 62–69.

Tang M, Jun Xu Y, Xu W, Wang B, Cheng H (2021): Three-decadal erosion and deposition of channel bed in the Lower Atchafalaya River, the largest distributary of the Mississippi River. Geomorphology, 380, 107638

# Preliminary results for a Managed Aquifer Recharge feasibility index for the southern Portuguese region

Tiago N. MARTINS[1], Teresa E. LEITÃO[1], Constantinos F. PANAGIOTOU[2], Manuel M. OLIVEIRA[1], Maria Manuela PORTELA[3], Catalin STEFAN[4]

[1] National Laboratory for Civil Engineering, Portugal
tmartins@lnec.pt, tleitao@lnec.pt, moliveira@lnec.pt
[2] ERATOSTHENES Centre of Excellence, Department of Environment and Climate, Cyprus
constantinos.panagiotou@eratosthenes.org.cy
[3] CERIS, Instituto Superior Técnico – University of Lisbon, Portugal
maria.manuela.portela@tecnico.ulisboa.pt
[4] Research Group INOWAS, Institute for Groundwater Management, Technische Universität Dresden, Germany
catalin.stefan@tu-dresden.de

ABSTRACT

## 1. Introduction and methodology

Managed Aquifer Recharge (MAR), the process of purposefully increase groundwater (GW) infiltration to achieve both environmental and economic benefits (Alley et al., 2022), has been broadly implemented throughout the world (Stefan & Ansems, 2018) but is yet to gain traction in regions such as Portugal. MAR is one of the elements that comprise groundwater governance and management (UN-Water, 2022) and it is a complementary mitigation measure to cope with water scarcity scenarios.

To ease the implementation of MAR, an integrated water resources management inspired mapping methodology that relies on the concept of multi-criteria decision analysis (MCDA) was developed within the framework of AGREEMAR project and also as part of a PhD research. As explained in detail in Martins et al. (2022), the methodology follows the workflow presented in Fig.1 and was tested in several Mediterranean case studies, such as the Portuguese river basin districts of Sado e Mira (PTRH6) and Guadiana (PTRH7).

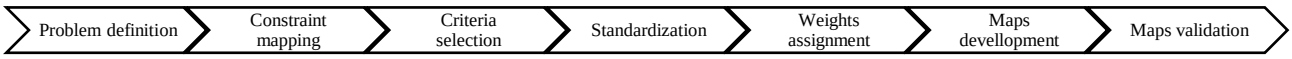



**Fig. 1.** General concept of MAR feasibility mapping process (adapted from Martins et al. 2022)

This MCDA approach considers the clustering of criteria in three different pillars: (1) intrinsic suitability based on the characteristics of the area where it is going to be implemented, (2) surface water available for MAR and (3) need for that type of intervention based on water demand (Panagiotou et al. 2022). The feasibility MAR index ($FI_{MAR}$) is computed using the following equation:

$$FI_{MAR} = \sum(Thematic_W \times \sum(Criteria_W \times Criteria_S)) = \sum(Thematic_W \times Thematic_S), \quad (1)$$

where $Thematic_W$ refers to the specific thematic weighting coefficient and $Thematic_S$ is the standardized thematic map computed from the weighted ($Criteria_W$) summation of the standardized criteria maps ($Criteria_S$). Standardization was conducted by converting all original criteria maps into a scale ranging from 0 to 1.

An innovative aspect is that the procedure heavily relies on the contributions of the stakeholders. For the Portuguese (PT) case study, a questionnaire was deployed targeting stakeholders, including the main representatives of the economic sectors that can benefit from MAR, and specialists (researchers, hydrologists, hydrogeologists) aiming to collect spatial information on the three main pillars: (1) what is seen as the main objective for MAR in the region [i.e., GW storage to mitigate water scarcity], (2) which are the most relevant criteria in terms of the MAR objective and (3) what is the relative degree of importance of each pillar with respect to the selected MAR objective. In total 28 criteria maps were considered in the present analysis.

The resulting weighted feasibility index that was classified in a scale [0, 1] divided into 0.2 intervals classified from "Very low feasibility for MAR" (]0, 0.2]) to "very high MAR feasibility"]0.8, 1]). Zero refers to the exclusion areas where MAR cannot be implemented due to legal restrictions (e.g., wellhead protection areas) or lack of space (e.g., dense urban areas).

## 2. Results and conclusions

Although the implementation of MCDA is widely used to identify suitable regions for the implementation of MAR schemes, the generated maps often rely solely on intrinsic characteristics of the study area (suitability mapping). Subsequently, these maps neglect additional information that is needed for the design of successful MAR systems, such as surface water availability and water demand, but also economic and social criteria that may constrain MAR. All of these other components have been integrated in this study.

The spatial distribution of the $FI_{MAR}$ is presented in Fig. 2, suggesting that about 73% of the study area has moderate feasibility and 21% has high feasibility for general MAR implementation. It is important to note that 49% of the total thematic weight was attributed to the intrinsic site suitability, followed by water availability (35%). As a result, the more feasible areas are strongly related with geologically suitable areas such as sedimentary aquifer systems in the Sado river basin, followed by high water availability areas surrounding the Alqueva system network. These preliminary results were well accepted by the main project stakeholder (APA Alentejo) in the context of the validation process.

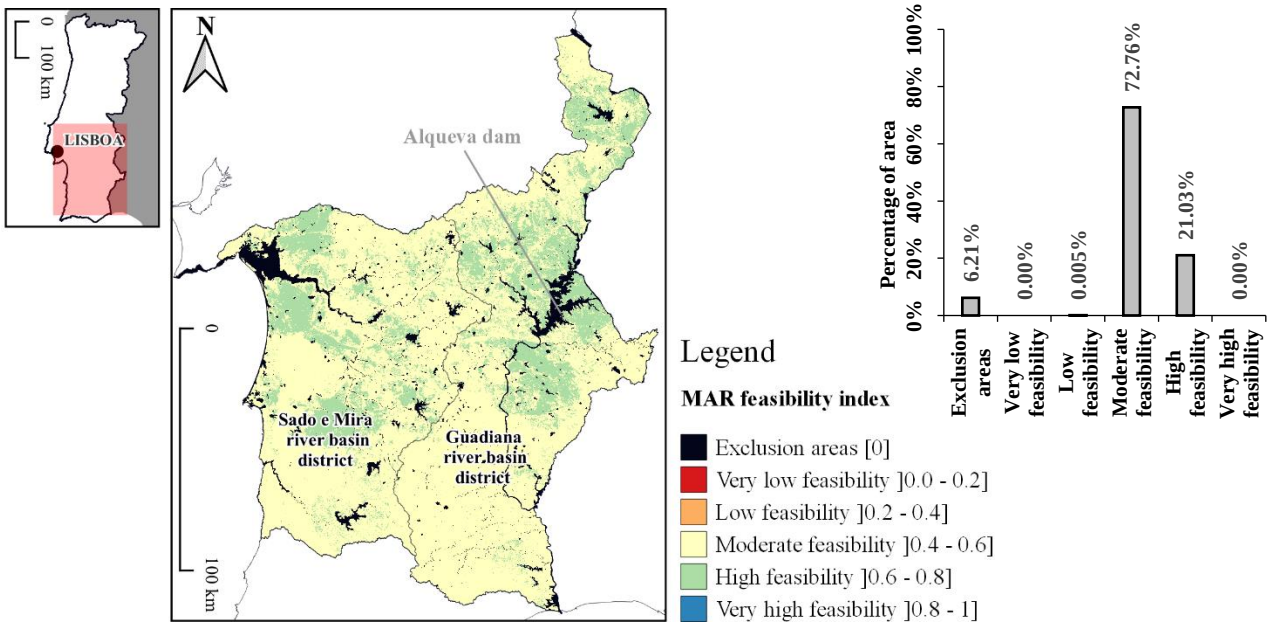



**Fig. 2.** Preliminary results for the computation of MAR feasibility index for the Portuguese case study

In the Portuguese case study, the focus was to provide a new layer of geographical information to support the water management decision-making process in already fresh water stressed regions. It is expected that by addressing and integrating the main stakeholders' concerns this methodology can expand its reach and be easily adopted or adapted as needed in other regions.

**Acknowledgements**

The authors thank APA Alentejo for providing necessary data for criteria characterization. Tiago N. Martins thanks the *Fundação para a Ciência e Tecnologia* (FCT), Portugal, for the Ph.D. grant PD/BD/135590/2018. The AGREEMAR project is funded under the Partnership for Research and Innovation in the Mediterranean Area (PRIMA), supported under Horizon 2020 by the EU's Framework for Research and Innovation, and by the National Funding Agencies (https://doi.org/10.54499/PRIMA/0004/2021).

**References**

Alley W, Dillon P, Zheng Y (2022) Basic Concepts of Managed Aquifer Recharge, in Managed Aquifer Recharge: Overview and Governance. IAH Special Publication. ISBN 978-1-3999-2814-4

Martins TN, Panagiotou CF, Stefan C, Chkirbene A (2022) AGREEMAR Deliverable D2.2. Participative methodology for criteria selection and weighting in MAR site feasibility mapping. Available online at https://www.agreemar.inowas.com/deliverables.

Panagiotou CF, Chkirbene A, Stefan C, Martins TN, Leitão TE (2022) AGREEMAR Deliverable D2.1: Matrix of feasibility criteria for managed aquifer recharge. Available online at https://www.agreemar.inowas.com/deliverables.

Stefan C, Ansems N (2018) Web-based global inventory of managed aquifer recharge applications. Sustainable Water Resources Management, 4(2), 153–162. https://doi.org/10.1007/s40899-017-0212-6

UN Water (Ed.). (2022). The United Nations World Water Development Report 2022: Groundwater making the invisible visible. UNESCO. Available online at https://unesdoc.unesco.org/ark:/48223/pf0000380721

# Pumped storage reconversion in Alto Lindoso hydroelectric power plant in Portugal

Marco FERNANDES[1], Pedro PINTO[2], Nuno OSÓRIO[3], Daniela NORONHA[4], Liliana BENITES[5], João CALVO[6]

[1,2,3,4,5,6] EDP Produção, Portugal

[1,2,3,4] marco.fernandes@edp.com, pedro.pinto@edp.com, nuno.osorio@edp.com, daniela.noronha@edp.com

[5,6] lilianabenites.carvalho@edp.com, joao.calvo@edp.com

## ABSTRACT

The Alto Lindoso dam is located in the Lima river in the north of Portugal, near the border with Spain, right after the confluence of the Castro Laboreiro river with the Lima river itself. The construction of the Alto Lindoso power plant, which started its operation in 1992, was motivated not only by the production of electrical energy, but also as security for the electrical grid as it was able to quickly replace thermal power plant groups that could eventually fail. Taking this into account, it was decided to incorporate high power groups, taking advantage of the existing gross head (288 m) and a high flow rate.

In the past years, Portugal created the Roadmap for Carbon Neutrality 2050 (Roteiro para a Neutralidade Carbónica 2050, 2019), which establishes the vision and trajectories for Portugal to achieve the same number of emissions and removals of carbon dioxide and other greenhouse gases (GHGs) from the atmosphere. It also published the National Energy and Climate Plan 2030 (Plano Nacional de Energia e Clima 2030, 2020), which constitutes the main instrument of national energy and climate policy for the 2021-2030 decade. These instruments translate the focus of Portugal on trying to accomplish the most ambitious objectives of the Paris Agreement.

The EDP group's vision embodies a global plan of decarbonization and electrification of the economy, presenting a strategy focused on accelerating the energy transition in all its platforms and geographies where it is present. On the Generation platform, in Portugal, EDP Produção is responsible for its execution.

The reconversion of one Alto Lindoso generator group to a reversible group is a pumped storage project (Fig. 1) that will bring more flexibility to the electrical production system by adding a pumping capacity, representing around 8 % of the Portuguese pumping power in 2027. The reconverted Alto Lindoso group will allow water to be pumped from the Touvedo reservoir, taking advantage of the opportunities of excess renewable energy in the system, storing it in the Alto Lindoso reservoir to be turbined later in periods of renewable energy scarcity. It is expected that the reconversion will allow an average annual increase in electricity production in Alto Lindoso above 75 % (≈ 600 GWh).

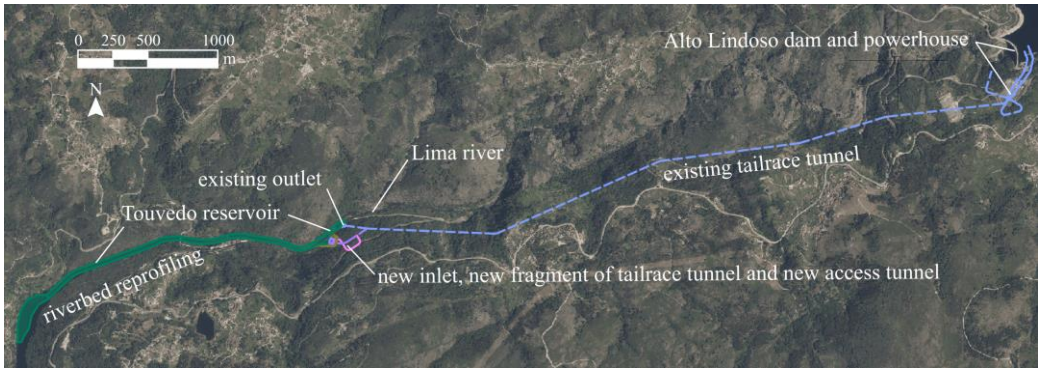



**Fig. 1.** Overview of the pumped storage reconversion of Alto Lindoso project.

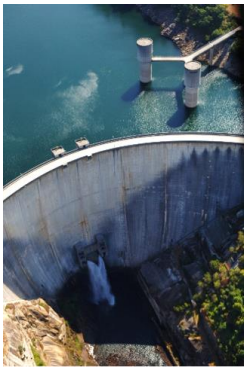


**Fig. 2.** Alto Lindoso dam.

## 1. The Alto Lindoso and Touvedo hydraulic power plants

The Alto Lindoso dam (Fig. 2) is a dome-type, double-curved concrete dam, with a height of 110 m and a crest 297 m long. The reservoir created by the dam, which extends across Portuguese and Spanish territory, receives the inflows from the upstream basin partly regulated by the Spanish dams of Las Conchas and Salas. It has a total capacity of 379 hm³ whereas the useful volume is equal to 347.9 hm³. The dam is complemented by a waterway that consists of two short hydraulic headrace tunnels that feed two turbine groups of 317 MW each, located in an underground powerhouse, in a cave, and a long tailrace tunnel that returns the turbined water to the Lima river, at the Touvedo reservoir head. The Touvedo dam, of gravity-type, was built due to the need of modulation of the high flow turbined by the Alto Lindoso power plant (2 × 125 m³/s), temporarily storing the water in its reservoir and returning it to the natural course of the river with values not exceeding 100 m³/s to avoid sudden and high amplitude variations of the river level. It is equipped with one Kaplan group of 22 MW.

## 2. The Alto Lindoso reconversion project

To create the necessary conditions so that it is possible to pump water from the reservoir of Touvedo to the reservoir of Alto Lindoso, using it to produce energy it in a later period, one main change must occur in the powerhouse (Fig. 3), where one of the turbine groups (the Group I) has to be replaced by a pump-turbine group, consequently implying other adaptations and installation of new equipment that is necessary to allow the inversion of the group and the consumption of energy from the power grid. It should be noted, though, that this change can only occur because the placement of the existing group is compatible with this replacement without many civil works modifications within the powerhouse. The turbine elevation as well as the current spiral case, the draft tube and the generator shaft are to be maintained. Thorough studies were developed concerning unit speed, submergence studies and hydraulic transients.

It is also necessary to make other changes to enable pumping in Alto Lindoso, namely in the tailrace zone (Fig. 4), because the existing tailrace outlet is not compatible with the new flow direction. Changes could be made to the existing outlet, but it would be an expensive and challenging task and would imply that Alto Lindoso couldn't produce energy during several years. Since that is not a desirable solution, it was decided to create a new inlet (Fig. 5), that will work as outlet in turbine operation, nearby the existing one and a short new tailrace tunnel that will connect to the existing one. This option will reduce the Alto Lindoso generation interruption to less than one year during the construction phase. To guarantee that the pumped flow is fed to the new inlet structure, the riverbed inside the upper part of the Touvedo reservoir must be reprofiled along ≈ 2 km (Fig. 1, Fig. 4).

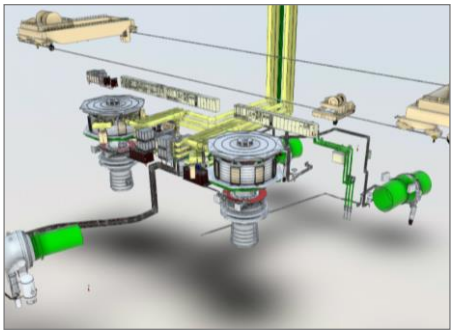


**Fig. 3.** BIM model of the existing equipment in Alto Lindoso powerhouse without the representation of civil construction elements.

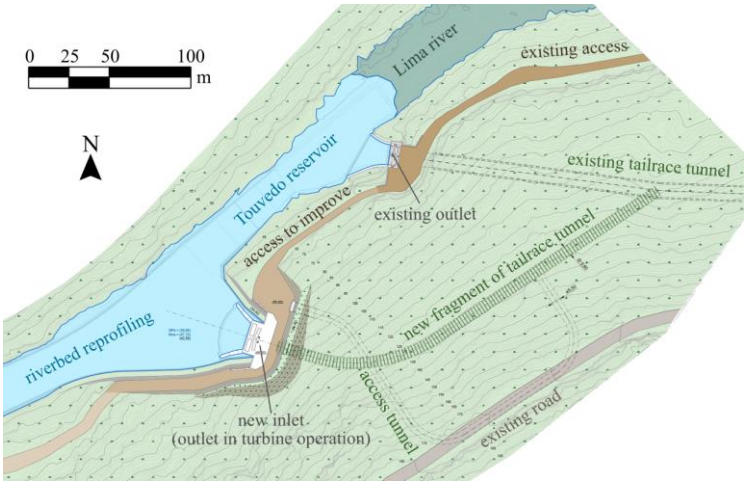



**Fig. 4.** Plan of the tailrace outlet zone representing the existing and new elements.

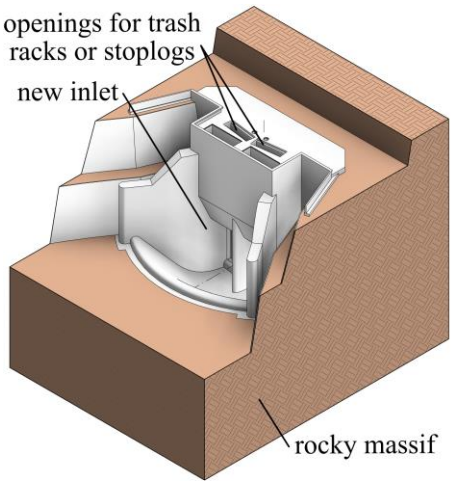



**Fig. 5.** New inlet structure.

**References**

Anexo à Resolução do Conselho de Ministros n.º 107/2019: Roteiro para a Neutralidade Carbónica 2050 – Estratégia de Longo Prazo para a Neutralidade Carbónica da Economia Portuguesa em 2050 (2019) Diário da República n.º 123/2019, Série I de 2019-07-01, 3208-3299, https://diariodarepublica.pt/dr/detalhe/resolucao-conselho-ministros/107-2019-122777644

Anexo à Resolução do Conselho de Ministros n.º 53/2020: Plano Nacional Energia e Clima 2030 (2020) Diário da República n.º 133/2020, Série I de 2020-07-10, 2-158, https://diariodarepublica.pt/dr/detalhe/resolucao-conselho-ministros/53-2020-137618093

# Impact of partially-covered mixed heighted vegetation on the lateral velocity and discharge of open channel flow

Xiaonan TANG[1], Yibo WANG[1], Qinzheng TENG[1], Haoxing YIN[1], Mingtao SHAO[1]

[1] Department of Civil Engineering, Xi'an Jiaotong-Liverpool University, Suzhou, China
Xiao.Tang@xjtlu.edu.cn;

Yibo.Wang2101@student.xjtlu.edu.cn

tengqinzheng20@mails.ucas.ac.cn

Haoxing.Yin21@student.xjtlu.edu.cn

Mingtao.Shao21@student.xjtlu.edu.cn

ABSTRACT

Vegetation of various heights commonly co-exists along natural rivers and wetlands, where sediment, ecological environment, and habit biodiversity are drawing increasing attention in the research in eco-environment and river restoration. In the past, many researchers studied the impact of vegetation on the flow, such as velocity, flow resistance and Reynolds stresses. Due to the extreme complex of interaction between vegetation and flow, previous studies mainly focus on the unform vegetation through flow in open-channels. However, in natural rivers, vegetation of various heights often co-exists and grows along the river bank. In this regard, it is not yet understood about flow characteristics in such flow conditions, i.e. flow with a mixing array of short and tall vegetation along a channel. This paper is to perform a novel experimental study on a water flume, which is partially covered by a mixed vegetation of different heights along one side of the channel, in order to understand the effect of vegetation on the lateral distribution of velocity and discharge. Two different heights of dowels, 5 cm and 10 cm, were used in the water flume of Xi'an Jiaotong-Liverpool University (XJTLU) to represent the short and tall rigid vegetation respectively. Experiments under two flow depths were undertaken to represent different submergence ratios of vegetation, and velocities at various locations were measured by a micro propeller velocimetry.

Experimental results show that the vegetation will significantly reduce the velocity, resulting the low velocity in the vegetated zone and a large transition zone between the vegetated and non-vegetated zones. Due to the retarding effect of vegetation, the velocity profile in the vegetated zone differentiates from the one in the non-vegetated zone, where the logarithmic velocity profile does not hold in this case. The results also show that the discharge in the vegetated zone is much lower (almost one quarter) than that in the non-vegetated zone given the same width.

## 1. Introduction

Aquatic vegetation plays an important role in different ecosystems, including rivers, lakes, swamps and wetlands. Fish, amphibians, and other animals all require aquatic vegetation as their habitats, which is due to the aquatic vegetation can provide an area with slower flow rates. The effect of aquatic vegetation on water flow is reflected in many aspects, such as velocity, flow resistance and Reynolds stresses, which provided complex flow characteristics.

## 2. Experimental setting

In this study, the bed slope of the flume was fixed at 0.003 and the full length of bed is 20m. The water depth is controlled by the inlet pump and tailgate, while the volume flow rate is measured with the electromagnetic flowmeter. Aquatic vegetation simulated by dowels of 6.35m in diameter and two heights of 5cm and 10cm covers a 4.7m long flume section, starting 8.4m away from the flume entrance and maintaining for 4.3m. The

dowels were installed into the perforated board to denote the rigid aquatic vegetations. In Fig.1, the green line segments denote the vegetation.

## 3. Preliminary results

For the sake of brevity, the analysis of velocity is based on the four zones, as shown in Fig.1. The VZ1 and VZ2 are in the vegetated zone, each having one quart of channel width, while FZ1 and FZ2 are in the free zone of flow (i.e. non-vegetated zone). The lateral distribution of depth-averaged velocity(Ud) is shown in Figure 3, where U is the overall velocity of the cross-section. Dimensionless method can enhance the features of data, making analysis easier. It is evident that the mixed vegetations have resistance to the flow. In the vegetated zone, the Ud distributes from 0.6U to 0.8U while in the free flow zone, the Ud increased to over 1.4U. The maximum of Ud occurred at the 10th point, reached twice of U, 25.25cm away from the origin. In addition, the wall also had an impact on the fluid, but this effect did not dominate.

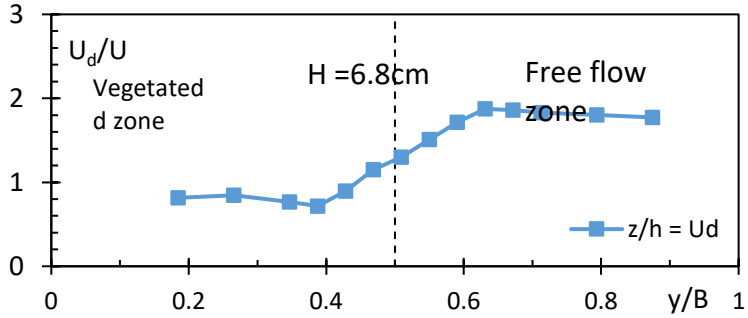



**Fig. 1.** Lateral distribution of depth-averaged velocity (Ud)

## 4. Conclusions

By organizing and analyzing the experimental data mentioned above, we can conclude the impact of mixed vegetation on water flow velocity and flow discharge. The impact is reflected in many aspects, and we can draw the following conclusions.

(1) Mixed vegetation can significantly reduce the incoming flow velocity. In the water channel, the water flow velocity in the vegetated zone was about half that in the free flow zone. The water flow near the outer side had a lower flow velocity due to the influence of wall friction.

(2) Rigid vegetation did not change the trend of flow velocity with depth, and regardless of the region, there was a trend of flow velocity increasing first and then decreasing with depth from deep to shallow.

(3) The influence of composite vegetation on flow velocity was also reflected in flow rate. The flow rate in vegetation areas was about half of that in free flow areas, which was similar to the relationship between depth average velocity.

**References**

Liu D, Diplas P, Fairbanks JD,Hodges, CC (2008) An experimental study of flow through rigid vegetation, Journal of Geophysical Research: Earth Surface, 113.

Nepf H M, Vivoni E R (2000) Flow structure in depth-limited, vegetated flow, Journal of Geophysical Research - Oceans, 105(C12), 28547-28557.

Nezu I, Sanjou M (2008) Turburence structure and coherent motion in vegetated canopy open-channel flows, Journal of Hydro-Environment Research, 2(2), 62-90.

Tang X, Knight DW, Sterling M (2011) Analytical model of streamwise velocity in vegetated channels, Proceedings of the ICE: Engineering and Computational Mechanics, 164 (2): 91-102.

Tang X, Rahimi H, Singh P, Yuan S, Lu C (2023) Analytical modelling of mean velocity profile through two-layered fully submerged vegetation, Journal of Hydraulic Engineering, 149(2): 04022041

Tang X, Rahimi HR, Guan Y, Wang Y (2021) Hydraulic characteristics of open-channel flow with partially-placed double layer vegetation, Environmental Fluid Mechanics, 21(2): 317–342

Rahimi HR, Tang X, Singh P, Li M, Alaghmand S (2020) Open channel flow within and above a layered vegetation: Experiments and first-order closure modeling, Advances in Water Resources, 137(3), 103527

# Swimming behaviours of Atlantic salmon kelts at hydropower dams

Olivia M. SIMMONS[1], Ana T. SILVA[2], Torbjørn FORSETH[3], Patrik ANDREASSON[4], Stephanie MÜLLER[5], Olle CALLES[6], David ALDVÉN[7]

[1,2,3] Norwegian Institute for Nature Research, Norway
olivia.simmons@nina.no
ana.silva@nina.no
torbjorn.forseth@nina.no
[4,5,7] Vattenfall Research and Development, Älvkarleby Laboratory, Sweden
patrik.andreasson@vattenfall.com
stephanie.mueller@vattenfall.com
david.aldven@vattenfall.com
[4] Department of Wildlife, Fish, and Environmental Studies, Swedish University of Agricultural Sciences, Sweden
[6,7] Department of Environmental and Life Sciences, River Ecology and Management Research Group RivEM, Karlstad University, Sweden
olle.calles@kau.se

ABSTRACT

Atlantic salmon kelts must navigate past dams in hydropower-regulated rivers to complete their migrations. Yet, hydropower dams can block their passage and cause delays during migration. Here, we present the results of a field study to understand passage performance and swimming speeds of kelts upstream of a hydropower dam in relation to varying hydraulic conditions. To do so, we used movement data from kelts tagged with acoustic transmitters and hydraulic data from CFD models. We found that as dam operations changed over the study period, the hydraulic conditions in the river also changed. Changes in these conditions acted as a navigation cue for kelts to find a safe route past the dam. Kelt swimming speed increased with body length, and they swam faster as water velocity increased, but slower as turbulence intensity increased.

## 1. Introduction

Hydropower production is growing in importance as the global demand for green energy increases. Yet, hydropower dams sever river connectivity, with negative impacts on migratory fish (Belletti et al., 2020). One such species is the Atlantic salmon (*Salmo salar*), which undertakes several long-distance migrations during its life cycle (Forseth et al., 2017). Though passage solutions have been developed for downstream migrating juveniles and upstream migrating adults, little focus has been paid to downstream migrating adults, known as 'kelts' (Simmons et al., *in review*). Even when there are routes available for kelts to pass dams, they can experience delays while searching for those routes or waiting for the right conditions (Babin et al., 2021). These delays can negatively affect their fitness (Baktoft et al., 2020). Thus, developing downstream passage solutions for kelts is of crucial importance.

Hydraulic conditions, such as flow velocity and turbulence, impact swimming performance for migrating fish (Silva et al., 2020). However, hydropower dams alter the natural hydraulic conditions of a river, which can then impact the way fish behave (Renöfält et al., 2010). The effect of varying hydraulic conditions in regulated rivers has not been previously studied for Atlantic salmon kelts. Therefore, we aimed to better understand kelt swimming behaviour at a hydropower dam by (1) evaluating passage performance, (2) assessing swimming depth preferences, and (3) examining swimming speeds in relation to dam operations and hydraulic conditions. Obtaining better knowledge of kelt swimming behaviour at dams is the first step towards developing efficient and safe downstream passage solutions.

## 2. Methods

Forty-eight kelts were tagged with acoustic transmitters containing pressure sensors upstream of the Bjørset dam in the River Orkla, central Norway (Fig.1; Baktoft et al., 2020). The dam has four spillways with top-opening gates. Migrating kelts could either pass by one of the spillways or by a pipe that crossed the dam. An array of twenty-four autonomous acoustic receivers were deployed upstream of the dam to record the position of the tagged kelts every 2.5 seconds. This data was then used to estimate each kelt's trajectory in the river.

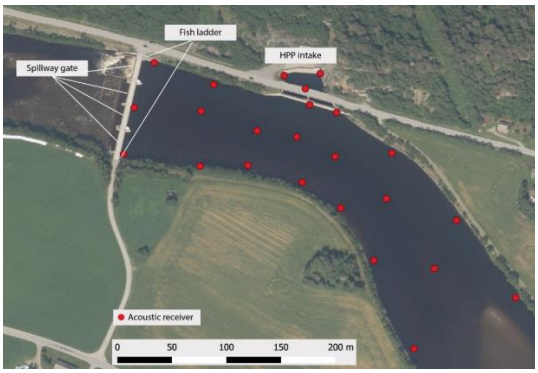



**Fig. 1.** Overview of the study area, with the location of the acoustic receivers marked with red (Baktoft et al., 2020).

The kelts experienced varying hydraulic conditions resulting from the different operational activities of the hydropower plant. Based on the operational activities and concomitant variations in flow discharge, four different scenarios were modelled via computational fluid dynamics (CFD) models. The first scenario represented the period when all spillway gates were closed and kelts could only pass the dam via the pipe. The second scenario represented the next period, when one gate was opened approximately 40%, allowing approximately 8 $m^3s^{-1}$ to discharge past the dam. The third and fourth scenarios represented a further opening of the same gate, to 60% and 70%, respectively, allowing a discharge of 22.3 and 38.4 $m^3s^{-1}$ past the dam. Flow velocity, turbulence kinetic energy, and turbulence intensity were simulated for each scenario using the pimpleFoam utility of the OpenFOAM platform.

## 3. Results

Only one kelt passed the dam during the first scenario, when all the spillway gates were still closed. 75% of the kelts passed the dam within two days of the gate opening, suggesting that the kelts were able to detect that a new passage route was available to them. It is likely they used cues from the changing hydraulic conditions to do so. While swimming upstream of the dam, the kelts tended to be surface-oriented. The hydraulic conditions affected kelt swimming speeds at the dam. Generally, swimming speed increased with kelt body size. Such results indicate the importance of early gate openings at the dam and the effects of altered hydraulic conditions on swimming performance for kelts. This knowledge could be used to improve downstream passage solutions for kelts.

**Acknowledgements**

This work was supported by the Kelt2Sea project funded by the Norwegian Research Centre for Hydropower Technology – HydroCen (RCN project no. 257588).

**References**

Babin AB, Ndong M, Haralampides K, Peake S, Jones R, Curry RA, Linnansaari T (2021) Overwintering and migration behaviour of post-spawned Atlantic salmon *Salmo salar* in a large hydropower-regulated river and reservoir, Journal of Fish Biology, 99(3):856–874. https://doi.org/10.1111/jfb.14768

Baktoft H, Gjelland KØ, Szabo-Meszaros M, Silva AT, Riha M, Økland F, Alfredsen K, Forseth T (2020) Can energy depletion of wild Atlantic salmon kelts negotiating hydropower facilities lead to reduced survival?, Sustainability, 12(18):7341. https://doi.org/10.3390/su12187341

Belletti B, Garcia de Leaniz C, Jones J, Bizzi S, Börger L, Segura G, Castelletti A, van de Bund W, Aarestrup K, Barry J, et al. (2020) More than one million barriers fragment Europe's rivers, Nature, 588(7838):436–441. https://doi.org/10.1038/s41586-020-3005-2

Forseth T, Barlaup BT, Finstad B, Fiske P, Gjøsæter H, Falkegård M, Hindar A, Mo TA, Rikardsen AH, Thorstad EB, et al. (2017) The major threats to Atlantic salmon in Norway, ICES Journal of Marine Sciences, 74(6):1496–1513. https://doi.org/10.1093/icesjms/fsx020

Renöfält BM, Jansson R, Nilsson C (2010) Effects of hydropower generation and opportunities for environmental flow management in Swedish riverine ecosystems, Freshwater Biology, 55(1):49–67. https://doi.org/10.1111/j.1365-2427.2009.02241.x

Silva AT, Bærum KM, Hedger RD, Baktoft H, Fjeldstad H-P, Gjelland KØ, Økland F, Forseth T (2020) The effects of hydrodynamics on the three-dimensional downstream migratory movement of Atlantic salmon, Science of the Total Environment, 705:135773. https://doi.org/10.1016/j.scitotenv.2019.135773

Simmons OM, Aldvén D, Forseth T, Müller S, Calles O, Andreasson P, Silva A. (*in review*) An overview of kelt migration in regulated rivers: Status, knowledge gaps, and future directions towards safe downstream passage. Reviews in Fisheries Science and Aquaculture.

# Flow and Turbulence Structure in Vertical Slot Fishway: Effect of Reynolds number

Serhat KUCUKALI

[1] Hacettepe University, Civil Engineering Department, Hydraulics Division, Turkey
kucukali78@gmail.com

ABSTRACT

A pilot study has been carried out at the Vertical Slot Fishway (VSF) of the Çataloluk Small Hydropower Plant (SHP), which is located in the Ceyhan River Basin in Tekir River in Turkey. 3D velocities and turbulence quantities were collected at several points in the pool with Acoustic Doppler Velocimeter (ADV) for various discharges at the Cataloluk fish passage. The pool depth was measured continuously throughout the year by using an Ultrasonic Distance Sensor (UDS). The UDS monitoring data revealed that pool depth is highly variable during operation. The study characterizes the flow and turbulence in a vertical slot fishway for different discharges and pool depths. The study presents measurements of the velocity components in three directions, covering a range of Reynolds numbers between $6.6x10^5$ and $1.1x10^6$. The monitoring data revealed that the flow velocities were not changed considerably with the increase of Reynolds number, but the velocity fluctuations increased considerably in the pool with the increase of Reynolds number. The findings of the study showed that the increasing and decreasing discharge may have an impact on the passability of the vertical slot fishway regarding the variation in turbulent kinetic energy.

## 1. Introduction

Vertical slot fishways (VSF) are widely utilized technical fish passes on a global scale. A notable advantage of VSF is reported as that its hydraulics is unaffected by changes in discharge or water level in the pools (DWA, 2014). Werner and Seegner (2023) have studied the change of discharge effect on VFSs due to climate change impact. The 1:2 scale physical model study of Werner and Saenger (2023) has shown that with the increase of VSF discharge from 51 L/s to 77 L/s; the maximum measured local velocity increased from 1.22 m/s to 1.30 m/s and the energy dissipation per unit volume increased by a factor of two. Furthermore, Focht and Heneka (2023) studied the different velocity fluctuation patterns in VSF. This study aims to investigate the effect of discharge on maximum local velocity and velocity fluctuations by using in-situ measurements. The results can have important implications for the influence of the discharge on fish passibility.

## 2. Prototype Measurements

The flow structure of a VSF was investigated at the Cataloluk Small Hydropower Plant on the Tekir River, located in the Ceyhan River Basin of Turkey. The width of the fish pass was 1.4 m, the length was 1.85 m, the width of the slot was 0.22 m, and the bed slope of the pool where the ADV measurements were taken was 7% (Kucukali et al., 2023). An Acoustic Doppler Velocimeter, ADV (10-MHz Nortek Vectrino) was used to measure the three-dimensional instantaneous velocity fields. The turbulence quantities were collected at 100 Hz frequency during a sampling time of 30 seconds. Considering the averages of velocity fluctuations, it would have been better to have a longer sampling duration with ADV; but, in our case, it is risky to sample for a longer duration due to possible variation of headwater level. Hydraulic conditions tend to have repeating patterns. Accordingly, a representative basin is selected for the flow and turbulence measurements. From the 3D ADV measurements, the local mean resultant velocity $V_{res}$ can be calculated using Eq. (1)

$$V_{res} = \frac{\sum_{i=1}^{n} V_i}{n} \quad \text{in which} \quad V = \sqrt{u^2 + v^2 + w^2} \tag{1}$$

where n is the number of velocity samples. The spatially-averaged resultant velocity $\langle V_{res} \rangle$ is obtained by numerically integrating the local $V_{res}$ values through the horizontal plane. From the time series of the velocity measurements, the root-mean-square of the turbulent fluctuation velocities in the longitudinal u', lateral v', and vertical w' directions, respectively, were calculated at each measurement point. Then, the turbulent kinetic energy per unit mass *TKE* is computed from Eq. (2)

$$TKE = \frac{1}{2}(\overline{u'^2} + \overline{v'^2} + \overline{w'^2}) \quad (2)$$

The pool depth (i.e. water level) was continuously monitored throughout the year by using an Ultrasonic Distance Sensor (UDS) which has a sampling rate of 1Hz at the representative pool of the fish passage with Nivus i-series and Nivus GPRS data logger. 30-minute time-averaged pool depths are recorded.

## 3. Results and Discussion

The UDS monitoring data showed that the pool depth is highly variable during operation which can have important implications for fish passage design (Kucukali et al., 2023). The ADV data revealed that the flow velocities were not changed considerably with the increase in discharge (Table 1). This result is consistent with the study of Tarrade et al. (2011) and Werner and Saenger (2023) that who found a discharge variation resulted in a variation in the water level and had little influence on the flow characteristics and topology in VSF. On the other hand, in our study, *TKE* increased considerably in the pool with the increase in discharge (Table 1) and higher *TKE* values may hamper fish passage because most fish avoid high TKE regions (Gao et al., 2016).

**Table 1.** The flow conditions in the pool that ADV measurements were taken at the VSF

| | | | |
|---|---|---|---|
| $d_p$ (m) | 0.59 | 0.73 | 1.19 |
| $Q$ ($m^3/s$) | 0.145 | 0.183 | 0.329 |
| $Re_j$ | 6.6E+05 | 8.3E+05 | 1.5E+06 |
| $Fr_j$ | 0.46 | 0.43 | 0.37 |
| $\langle V_{res} \rangle$ (m/s) | 0.40 | 0.45 | 0.49 |
| $\langle TKE \rangle$ ($m^2/s^2$) | 0.036 | 0.049 | 0.063 |
| $(V_{res})_{max}$ (m/s) | 1.40 | 1.53 | 1.57 |
| $(TKE)_{max}$ ($m^2/s^2$) | 0.142 | 0.218 | 0.236 |

Notes: $d_p$=average pool depth, $Q$=discharge, $Re_j$= Jet Reynolds number, $Fr_j$= Jet Froude number, $\langle V_{res} \rangle$=spatially-averaged resultant velocity, $\langle TKE \rangle$=spatially-averaged turbulent kinetic energy, $(V_{res})_{max}$=maximum local resultant velocity, $(TKE)_{max}$=maximum local turbulent kinetic energy

**Acknowledgments**

This work is supported by the Scientific and Technical Research Council of Turkey under the Scientific and Technological Research Projects Funding Program (1001 TUBITAK) grant with agreement number 117M151.

**References**

DWA (2014). Fischaufstiegsanlagen und Fischpassierbare Bauwerke—Gestaltung, Bemessung, Qualitätssicherung; Deutsche Vereinigung für Wasserwirtschaft: Hennef, Germany. (In German).

Focht L, Heneka P (2023). Providing defined velocity fluctuations in ecohydraulic flumes using rotatable fins, Proceedings of 40th IAHR World Congress, 1208-1215, Vienna, Austria.

Gao Z, Anderson HI, Dai H, Jiang F, and Zhao L (2016). A new Eulerian–Lagrangian agent method to model fish paths in a vertical slot fishway, Ecological Engineering 88: 217–225.

Kucukali S, Alp A, Albayrak I (2023). Retrofitting vertical slot fish pass with brush blocks: hydraulics performance, Water, 15(6):1155. https://doi.org/10.3390/w15061155

Tarrade L, Pineau G, Calluaud, D, Texier A, David L, Larinier M, (2011). Detailed experimental study of hydrodynamic turbulent flows generated in vertical slot fishways, Environ. Fluid Mech, 11, 1–21.

Werner P, Saenger N (2023). Experimental impact analysis of climate change on vertical slot passes, Proceedings of 40th IAHR World Congress, 3065-3071, Vienna, Austria.

# Design of Alto Tâmega Spillway. From brainstorming to the final functional test

Miguel Ángel RAMÍREZ[1], Luis DE LA TORRE[2], Rafael CHACON[3], Alberto DUQUE[4]

[1,2,3] Upper Tâmega Hydroelectric Project & Global Technical Services, IBERDROLA, Spain
mrru@iberdrola.es
ltab@iberdrola.es
rchacon@iberdrola.es

[4] Civil Engineer, GRANELL INGENIEROS, Spain
adc@granellingenieros.com

ABSTRACT

The Alto Tâmega Dam is a concrete double-curved arch dam with a maximum height of 104,5 m. This dam creates a reservoir with a capacity of 131,71 $Hm^3$ for the top water level.

The floods are relieved through two lateral spillways, with the intake structure on the abutments of the dam. Both spillways are made up of two independent open channels controlled by floodgates, which run along both banks and are excavated in the rock ending in a ski jump terminal structure.

The spillways are designed for a recurrence period of 10.000 years corresponding to a total flow of 1.826,75 $m^3/s$, with 913,37 $m^3/s$ being discharged in each of four channels, for the maximum water level.

To analyse the performance of the channels, studies were carried out in a reduced model and in a numerical model that allow to verify the discharge conditions along the length of channels and optimize the shapes of the outlet structures.

Once the correct behaviour of the channels has been verified, the spillways go through different design phases until the final tests once built. This communication will show the results of the different studies in a physical and numerical model, and the results of final real test.

## 1. Introduction

The Upper Tâmega Hydroelectric Project, with a total installed capacity of 1.158 MW, is located in the Tâmega River, a right tributary of the Douro River, in the north region of Portugal, and includes, among other elements, the construction of three dams: Alto Tâmega, Daivões and Gouvães.

Alto Tâmega Dam, the highest dam of the Upper Tâmega Hydroelectric Project, is a double curvature arch dam with 104,5 m high above foundation. The dam is provided of two spillways designed with a total discharge capacity of 1.826,75 $m^3/s$ (10.000 year flood).

Initially, the Alto Tâmega spillway was designed with two tunnel spillways and ski jump structures. The main one was designed with a controlled crest followed by a tunnel with free flow behaviour in all ranges of discharges up to 1510 $m^3/s$ and a ski jump terminal structure. The auxiliary one, with a maximum discharge capacity of 300 $m^3/s$, consisted of a pressure tunnel with a submersed intake controlled with a Taintor gate downstream.

An evaluation of the hydraulic behaviour, including a physical model test and additional studies, concluded an unsatisfactory performance of the initial solution. Therefore, a new solution was designed with two surface spillways located in the abutments with the same total discharge capacity of the initial solution. Both spillways comprise of two open channels with a controlled crest intake and ski jump terminal structure.

## 2. Design Phases

Empirical formulae were used during the pre-design of the spillway to determine the discharge capacity, the levels in channels, over-elevated sections, flow rate compression in changes of gradient and launching courses. The aeration efficiency was also checked throughout the canals, with the purpose of assessing the cavitation risk (cavitation rate and concentration of air in the flow rate).

A subsequent analysis was conducted with CFD, using the FLOW 3D software, before the assessment with the physical model. The works at the supply point were assessed first, with the purpose of maximising their discharge capacity, reducing unstable points until the suitable pillar geometry was reached, optimisation of excavated sections in approximation surfaces and determination of the position for the Bradley profile and most suitable supply. Up to 20 different models in CFD were required and, when the satisfactory geometry was achieved, the physical model was modified, altering the previous scale model for the tunnel spillway solution described above.

The main features of the spillway designs for each solution adopted, the reason behind their choice, the optimisation process using Computational Fluid Dynamics (CFD) and physical model tests, specifically the alterations in the energy dissipation structures as well as the analysis of the behaviour in the final real test are the main aspects assessed in the different design phases of the Alto Tâmega dam spillway design.



**Fig. 1.** The Alto Tâmega dam spillways in the final construction stage.

Different challenges had to be faced by the designer team during the construction phase. As shown in figure 1, it involved the construction of two mega structures in a river valley, as well as the right spillway runs over the top of a rockslide on the right margin that occurred during the construction of the power plant foundations. Finally, the Alto Tâmega dam spillways will be tested in a real test during winter 2024.

**Acknowledgements**

António, Muralha e Elsa, Alves, Reserchers of the Laboratorio Nacional de Engenharia Civil in Portugal for developing all the necessary works for the tests on the scale model made in the facilities that this laboratory has in Lisbon.

**References**

Félix Hernando, Arantzazu Arnáez, Miguel Ángel Ramírez (2017). The Upper Tâmega Hydroelectric Scheme. Hydraulic Design and Optimisation of Alto Tâmega Spillway

# Physical model-based maximization of historical precipitation in the basin with complex topography

Yusuke HIRAGA[1], Joaquin MEZA [2]

[1] Department of Civil Engineering, Tohoku University, Sendai, Japan
yusuke.hiraga.c3@tohoku.ac.jp

[2] Department of Civil Engineering, Universidad Técnica Federico Santa María, Valparaiso, Chile
joaquin.meza@usm.cl

ABSTRACT

In basins where extreme floods have caused significant damages, Probable Maximum Precipitation (PMP) estimate is important for flood risk management. Conventionally, PMP has been estimated using the statistical approach in many regions of the world due to its applicability for sparsely-gauged basins. However, for complex terrain such as Andes Mountain Range, the statistical method may not be appropriate since it cannot deal with non-linear orographic effects and precipitation observations are usually not dense. This study used the model-based PMP estimation approach to maximize the target historical precipitation over the Maipo River Basin, Chile. This study further deals with the recently raised questions on the model-based PMP estimation: (1) How can one estimate PMP with the range (not deterministically)? (2) How can one evaluate the frequency of the estimated PMP? Overall, this study will be useful basis on the next generation model-based PMP estimation, especially for basins with complex topography, dominated by Atmospheric Rivers.

## 1 Introduction

Flood disaster-related risk has increasingly become a global concern. Chile, located in South Ameica, is not an exception and has experienced several flood disasters in recent years, such as 2017 and 2021. Probable Maximum Precipitation (PMP) and Probable Maximum Flood (PMF) approaches are widely used for estimating design precipitation and floods to achieve flood management. PMP is defined as the theoretical maximum precipitation for a given duration under possible meteorological conditions [1]. Several approaches have been proposed to rigorously estimate PMP, including the statistical approach [2], storm maximization approach [3], and numerical model-based approach [4,5]. Numerical model-based approach maximizes precipitation depths by numerically solving the nonlinear governing equations of the regional atmospheric processes over the complex terrain. In recent years, numerical model-based approach has been drawing considerable attention due to its potential to overcome the major limitations in the traditional PMP estimation. Despite its benefits, none of previous works attempted to estimate PMP using numerical weather models for South America, harvoring the Andes Mountain Range. Thus, the objective of this study was to estimate maximum precipitation for the target storm events, using a numerical weather model. Furthermore, this study deals with the recently raised questions on the model-based PMP estimation: (1) How can one estimate PMP with the range (not deterministically)? (2) How can one evaluate the frequency of the estimated PMP?.

## 2 Materials and methods

This study used the Weather Research and Forecasting (WRF) model to simulate and maximize the target 72-hr precipitation events. This study used the Climate Forecast System Reanalysis (CFSR) dataset as initial and boundary conditions of the WRF model. Figure 1 shows the 2-way nesting domain of the WRF model with the resolutions of 36km, 12km, and 4km. This study first simulates the target 72-hr precipitation events with various combinations of physical parameters. Then, this study maximizes the simulated precipitation based on the moisture optimization method [5] and atmospheric boundary condition shifting (ABCS) method [5].

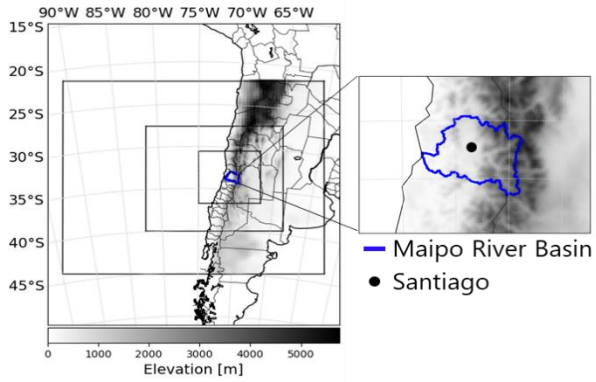



**Fig. 1. Maipo River Basin and WRF model domains**

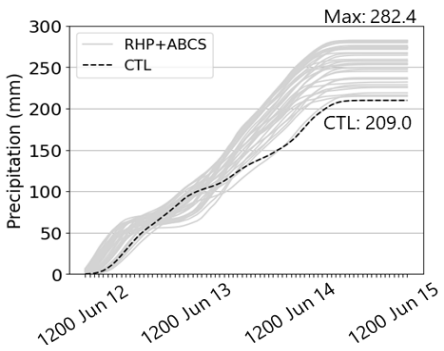



**Fig. 2. Precipitation maximization by means of moisture optimization and ABCS methods**

## 3 Results and discussion

Figure 2 shows the precipitation maximization result for the target precipitation event (UTC 1200 12th June-UTC 1200 15th June, 2000). By combining the Relative Humidity (RH) perturbation method and ABCS method, one can generate ensemble patterns of the target precipitation, leading to the maximum estimate with its range as in Figure 2. The maximum precipitation depth (282.4 mm; 35.1 % increase from CTL) was obtained by shifting atmospheric boundary condition to 1.5 degree south and increasing RH with β=1.3. Figure 3 shows the spatial distributions of the differences in (a) Integrated water Vapor Transport (IVT) and (b) 72-hr precipitation between the maximum case and CTL case. Figure 3 shows that the maximization procedure increased the IVT over the basin in which the IVT field shows the corresponding change to 1.5 degree south shifting. As a result of the IVT increase over the entire basin, precipitation increased in most parts of the basin. Our further analysis shows that the time series of precipitation difference and IVT difference over the basin between the maximum case and CTL case were highly correlated each other: $R^2$=0.85 ($p<0.01$). This high significant relationship between IVT and precipitation is consistent with the previous studies on extreme precipitation mechanisms in Chile. Although it is not presented here in this paper, the frequency of the maximum precipitation was estimated based on the long-term record of the basin-average IVT. Furthermore, the estimated maximum precipitation was compared to the conventional statistical method-based PMP values in the Maipo River Basin. Overall, this study is the first attempt to maximize historical precipitation using a numerical model-based approach in South America.

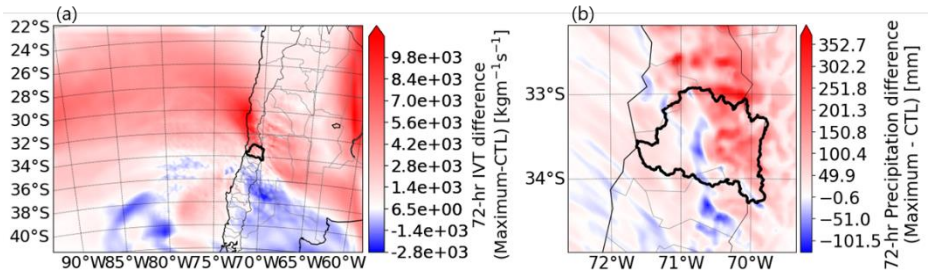



**Fig. 3. Difference in (a) 72-hr IVT and (b) precipitation between the maximum case and CTL**

**Acknowledgments**

This study was supported by JSPS KAKENHI Grant Number 23K19131 (Grant-in-Aid for Young Scientists (Start-up), Yusuke Hiraga).

**References**

[1] WMO. 2009. Manual on estimation of Probable Maximum Precipitation (PMP), WMO-No. 1045.
[2] Hershfield, D.M. 1961. Estimating the probable maximum precipitation. J. Hydraul. Div. 87, 99–116.
[3] Hansen, E.M., Fenn, D.D., Corrigan, P., Vogel, J.L., Schreiner, L.C., Stodt, R.W. 1994. Probable maximum precipitation -Pacific Northwest states: Columbia River (including portions of Canada), Snake River and Pacific coastal drainages. NWS Hydrometeorological Rep. 57, 353.
[4] Ohara, N., Kavvas, M.L., Kure, S., Chen, Z., Jang, S., Tan, E. 2011. Physically based estimation of maximum precipitation over American River Watershed, California. J. Hydrol. Eng. 16, 351–361.
[5] Hiraga, Y., Iseri, Y., Warner, M.D., Frans, C.D., Duren, A.M., England, J.F., Kavvas, M.L. 2021. Estimation of Long-duration Maximum Precipitation during a winter season for large basins dominated by Atmospheric Rivers using a Numerical Weather Model. J. Hydrol. 598, 126224.
[6] Koutsoyiannis, D. 1999. A probabilistic view of Hershfield's method for estimating probable maximum precipitation. Water resources research, 35(4), 1313-1322.

# Modelling Managed Aquifer Recharge in the Chiba River basin (Tunisia) with the AQUATOOL Decision Support System

Syrine GHANNEM[1], Rafael J. BERGILLOS[1], Anis CHEKIRBANE[2], Khaoula KHEMIRI[2], Javier PAREDES-ARQUIOLA[1], Abel SOLERA[1] and Joaquín ANDREU[1]

[1] Research Institute of Water and Environmental Engineering (IIAMA), Universitat Politècnica de València, Valencia, Spain
sghanne@upv.es, rbermec@upv.es, jparedea@upv.es, asolera@upv.es, ximoand@upv.es
[2] National Institute of Agronomy, University of Carthage, Tunis 1082, Tunisia
a.chkirbene@ecopark.rnrt.tn, khemiri.khaoula@gmail.com

ABSTRACT

Water scarcity is one of the most pressing global challenges of the 21st century (Morante-Carballo et al., 2022). It is a challenge that extends beyond geographical boundaries and socio-economic disparities, affecting both developed and developing countries. The imbalance between the supply of fresh water and the growing demand of a rapidly expanding population is striking. Due to the effects of climate change, the Mediterranean region is increasingly subject to prolonged droughts and irregular rainfall, further exacerbating water scarcity problems (Ferragina, 2010). Such challenges are compounded by the overexploitation of aquifers, a practice that has accelerated due to the intensification of agricultural, industrial, and domestic water use. The over-pumping of aquifers not only depletes groundwater reserves but also leads to detrimental consequences, including land subsidence and the intrusion of saline water into freshwater aquifers (Taft, 2015; Tzanakakis et al., 2023).

To address the pressing need for a sustainable and resilient water future, it is imperative to explore innovative approaches. Among these approaches, the conjunctive use of ground and surface water emerges as a pivotal strategy. It ensures a reliable supply of water for irrigation, which in turn improves crop yields. It also prevents groundwater depletion caused by extensive pumping (Sabale et al., 2023). The practice of conjunctive water use helps to recover infiltrated water, which has escaped from the unlined canal. This practice is a critical component for Managed Aquifer Recharge (MAR), offering multifaceted benefits by replenishing aquifers, optimizing water storage, and bolstering water availability (Dillon et al., 2019).

The objective of this work is to model MAR alternatives within the Chiba River basin. The focus is to maintain a reliable water supply, capable of meeting the demand of the various sectors while contributing to aquifer recovery. The Chiba River basin is situated in close proximity to the town of Korba in the Nabeul governorate, on the eastern side of the Cap-Bon peninsula in northwest Tunisia. Covering an area of approximately 230.23 km², this basin has suffered from water and soil degradation due to massive agricultural activities and uncontrolled urban sprawl. The average annual rainfall is around 460 mm (Figure 1).

The proposed methodology includes the development of a water resource management model, using the SIMGES module of the AQUATOOL Decision Support System (Andreu et al., 1996). SIMGES stands as a versatile model designed for simulating the management of basins and intricate water resource systems. It encompasses various components, including surface and underground elements for regulation and storage, intake, transport, consumption/utilization, and artificial recharge. Figure 2 illustrates the model's topology developed using the AQUATOOL SIMGES tool.

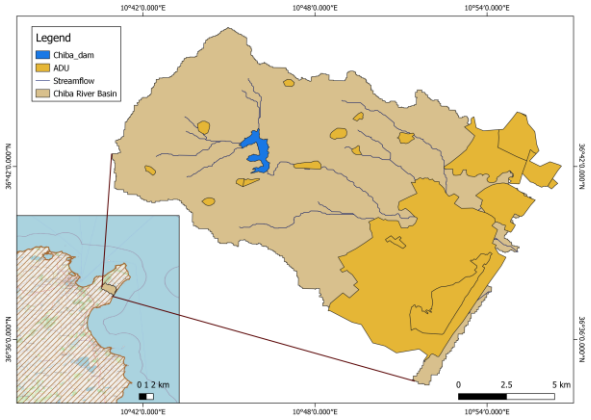



**Fig. 1.** Location of the Chiba River Basin

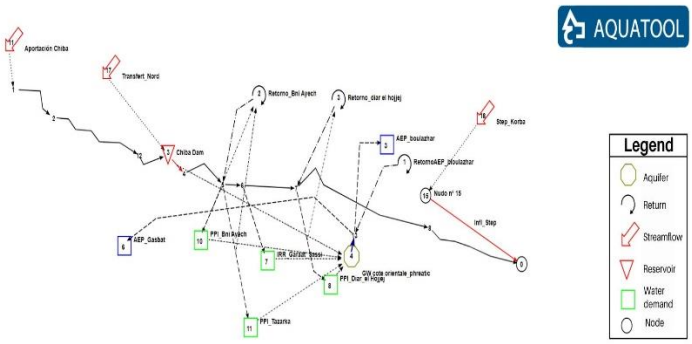



**Fig. 2.** SIMGES modelling scheme for the Chiba basin

Four scenarios were simulated to analyze the evolution of the Cote oriental aquifer and reliability of agricultural water demands in the Chiba river basin. The first scenario represents the current baseline, without MAR. The second scenario examines the effects of the Korba wastewater treatment plant, i.e. the basic scenario (scenario 1) + the use of treated water. In this case, treated water sourced from the Korba wastewater treatment plant is introduced. It is directly employed for artificial aquifer recharge, equivalent to direct aquifer infiltration. Scenario 3 prioritizes direct aquifer recharge from the Chiba reservoir, which means direct infiltration from the Chiba dam is assumed as the primary action, with meeting the region's water demand as a secondary priority. If necessary, other water transfers are assumed to be utilized to offset any water demand deficit after prioritizing aquifer recharge. In the fourth scenario, an operating rule was defined to allow aquifer recharge only during periods of excess water availability in the Chiba reservoir.

The results indicate that when evaluating the average monthly net recharge (infiltration minus pumping) in the aquifer, scenario 2 demonstrates a notable increase in aquifer recharge by 12%. However, in scenario 3, where direct aquifer recharge from the Chiba reservoir is prioritized, the aquifer experiences an increase in recharge. Nevertheless, this increase results in a water supply deficit for all agricultural water demands in the region, posing a significant challenge since the region relies predominantly on agricultural activities. In contrast, in scenario 4, where an operating rule is included in the Chiba reservoir to recharge only during periods of water excess, the aquifer does not exhibit a significant increase in monthly net recharge. This can be attributed to the fact that the availability of water from the Chiba reservoir does not consistently exceed the water demand in the region. Therefore, the viability of using Chiba reservoir's water for aquifer recharge relies primarily on the presence of excess water in the region. This work highlights the potential of water resources management models (like AQUATOOL) to jointly analyze the evolution of the piezometric levels in aquifers and supply to water demands, and optimize MAR solutions to mitigate aquifer overexploitation and water security issues in Mediterranean regions.

**Acknowledgements**

This work has been supported by the Spanish Ministry of Science and Innovation (MCIN) and Spanish Research Agency (AEI) through the research project AGREEMAR (PCI2022-133001), which is funded by European Union NextGeneration EU/PRTR. (MCIN/AEI/10.13039/501100011033). RB was partly funded by MCIN/AEI/10.13039/501100011033 through Juan de la Cierva-Incorporación program (IJC2019-038848-I).

**References**

Andreu, J., Capilla, J., & Sanchís, E. (1996). AQUATOOL, a generalized decision-support system for water-resources planning and operational management. Journal of Hydrology, 177(3-4), 269-291.
Dillon, P., Stuyfzand, P., Grischek, T., Lluria, M., Pyne, R. D. G., Jain, R. C., ... & Sapiano, M. (2019). Sixty years of global progress in managed aquifer recharge. Hydrogeology journal, 27(1), 1-30.
Ferragina, E. (2010). The water issue in the Mediterranean. Environment and Sustainable Development in the Mediterranean, 53-77.
Morante-Carballo, F., Montalván-Burbano, N., Quiñonez-Barzola, X., Jaya-Montalvo, M., & Carrión-Mero, P. (2022). What do we know about water scarcity in semi-arid zones? A global analysis and research trends. Water, 14(17), 2685.
Sabale, R., Venkatesh, B., & Jose, M. (2023). Sustainable water resource management through conjunctive use of groundwater and surface water: A review. Innovative Infrastructure Solutions, 8(1), 17.
Taft, H. L. (2015). Water scarcity: Global challenges for agriculture. In Food, Energy, and Water (pp. 395-429). Elsevier.
Tzanakakis, V. A., Capodaglio, A. G., & Angelakis, A. N. (2023). Insights into Global Water Reuse Opportunities. Sustainability, 15(17), 13007.

# Evaluation of flood susceptibility in Cyprus based on a co-participative multi-criteria decision analysis

Constantinos F. PANAGIOTOU[1*], Elissavet FELONI[2], Josefina KOUNTOURI[1,3], Christodoulos METTAS[1,3], Evagoras EVAGOROU[1,3], Evangelos AKYLAS[1,3]

[1] Eratosthenes Centre of Excellence, Limassol, Cyprus
constantinos.panagiotou@eratosthenes.org.cy, josefina.kountouri@eratosthenes.org.cy, christodoulos.mettas@eratosthenes.org.cy, evagoras.evagorou@eratosthenes.org.cy

[2] National Technical University of Athens, Athens, Greece
feloni@chi.civil.ntua.gr

[3] Cyprus University of Technology, Limassol, Cyprus
evangelos.akylas@cut.ac.cy

ABSTRACT

This study presents the framework under evaluating flood susceptibility in Cyprus using a co-participative multi-criteria decision analysis approach. Cyprus, facing challenges from its semi-arid climate and limited freshwater resources, experiences distinct climatic and diverse rainfall patterns conducive to flooding, particularly in lowland areas due to intensified precipitation events. Collaborative efforts with local stakeholders, including experts and community leaders, guide the mapping process, ensuring validation by national authorities and incorporating diverse perspectives. Initial analysis identifies parameters crucial for understanding flood phenomena, informing future flood prevention strategies. Ongoing work focuses on compiling additional parameters and validating results through stakeholder workshops, integrating historical flood events to refine policy decisions for effective flood management.

## 1. Short introduction

Cyprus, situated in the eastern Mediterranean, faces unique challenges due to its semi-arid climate and limited freshwater resources (Zachariadis, 2010). Characterized by extensive, hot and dry summers and cold, wet winters, the island's climate exacerbates the risk of flooding, particularly in the lowland areas. The island boasts a well-established drainage network, comprising 70 main watersheds, with 47 under the jurisdiction of the Government of the Republic of Cyprus (RoC) (WDD, 2023). Rainfall events in Cyprus exhibit strong spatial variability, mostly occurring over the Troodos and Pentadaktylos mountain ranges, whereas low precipitation rates are observed in the eastern plains and coastal areas. Despite a decline in rainfall frequency, there has been a notable increase in the intensity of precipitation events, heightening the susceptibility to floods (CEA, 2021). Given these challenges, understanding and mapping flood susceptibility are crucial for devising effective mitigation strategies. In this context, our study aims to utilize co-participative multi-criteria decision analysis to assess flood susceptibility in the region.

## 2. Mapping Process and Preliminary Results

Collaborative efforts with local stakeholders, including hydrology experts, community leaders, and government representatives responsible for flood risk management policies, are integral to our mapping process. Their involvement ensures the validation of generated maps by national authorities and incorporates diverse perspectives on flooding issues. Experts provide invaluable input in selecting relevant criteria, analyzing data, and interpreting findings based on scientific (Kazakis et al. 2015; Feloni et al. 2019). Our initial analysis focused on identifying parameters crucial to understanding flood phenomena, considering both literature insights and the geological/morphological characteristics of Cyprus. These parameters are essential for informing future flood prevention strategies in the region.

Figure 1 illustrates the study area and the geographical location of Cyprus Island in the Eastern Mediterranean, while Table 1 provides a summary of the selected parameters and their corresponding data sources.

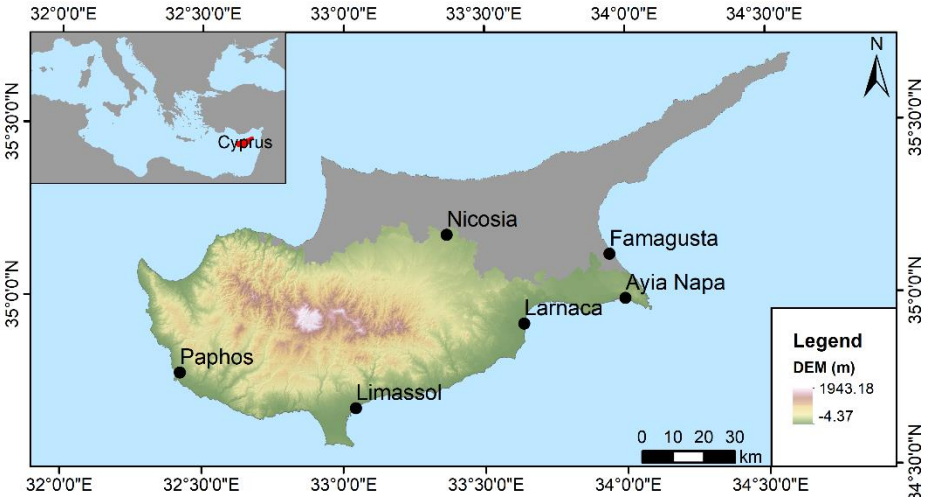



**Fig. 1.** Geographical location of the study area.
The northern part of the island is not considered since it is not subjected under the effective control of the RoC.

**Table 1.** Details of the selected parameters and their standardized scores

| Parameters | Description | Source |
|---|---|---|
| Distance from drainage network [m] | High scores are assigned to areas close to hydrological networks | Water Development Department Geoportal (2023) |
| Terrain elevation [m] | Digital Elevation Model (DEM) with 25m x 25m resolution. High scores are assigned to low elevations (coastal areas/valleys) | Department of Land and Surveys |
| Terrain slope [%] | Derived from the DEM. High scores are assigned to small slopes (flat terrains) | Department of Land and Surveys |
| Hydrogeology [classes] | High scores are given for soil properties that favor surface run-off. | Geology Survey Department |
| Flow accumulation [number of cells] | Derived from DEM | Water Development Department Geoportal (2023) |
| Land use - land cover [classes] | High scores are assigned to urban areas and wetlands, whereas the lowest values are assigned to forests. | CORINE Land Cover (2018) |
| Rainfall intensity [mm/d] | Precipitation data are collected for 90 rainfall stations | Department of Meteorology |

Current efforts are concentrated on compiling the remaining parameters necessary to evaluate the flood susceptibility of the study area. The outcomes will undergo discussion with stakeholders in workshops geared towards validating and improving the generated maps. The inclusion of historical flood events in this discussions aims to ensure their relevance and accuracy in informing revisions or re-designs of water policies pertaining to flood management.

**Acknowledgements**

The authors acknowledge the "EXCELSIOR": ERATOSTHENES: EXcellence Research Centre for Earth Surveillance and Space-Based Monitoring of the Environment H2020 Widespread Teaming project (www.excelsior2020.eu). The "EXCELSIOR" project has received funding from the European Union's Horizon 2020 research and innovation programme under Grant Agreement No 857510, from the Government of the Republic of Cyprus through the Directorate General for the European Programmes, Coordination and Development and the Cyprus University of Technology.

**References**

Cyprus Energy Agency (2021) CLIMATE CHANGE Overview of regional and local trends, policy and governance
Feloni E, Mousadis I, Baltas E (2019) Flood vulnerability assessment using a GIS-based multi-criteria approach – The case of Attica region. Journal of Flood Risk Management
Kazakis N, Kougias I, Patsialis T (2015) Assessment of flood hazard areas at a regional scale using an index-based approach and Analytical Hierarchy Process: Application in Rhodope–Evros region, Greece. Science of The Total Environment, 538, 555–563
Water Development Department Geoportal [Online] Available: https://geoportal-wdd.hub.arcgis.com/ [Accessed June 2023]
Zachariadis T (2010) Residential Water Scarcity in Cyprus: Impact of Climate Change and Policy Options. Water. 2(4):788-814

# Modelling sediment delivery in river catchments: a review

Roberta PADULANO[1], Melissa LATELLA[2], Tommaso CALOIERO[3], Carmelina COSTANZO[4], Gabriele BARBARO[4], Pierfranco COSTABILE[4]

[1] Università degli Studi di Napoli Federico II, Italy
roberta.padulano@unina.it

[2] CMCC Foundation – Euro-Mediterranean Center on Climate Change, Italy
melissa.latella@cmcc.it

[3] National Research Council of Italy, Institute for Agriculture and Forest Systems in the Mediterranean (CNR-ISAFOM), Italy
tommaso.caloiero@isafom.cnr.it

[4] Department of Environmental Engineering, University of Calabria, Italy
carmen.costanzo@unical.it
pierfranco.costabile@unical.it

ABSTRACT

Sediment delivery represents the link between soil erosion within catchments and sediment yield in river networks. It is often estimated using the sediment delivery ratio (SDR) or other lumped parameter models. However, its proper quantification remains challenging due to the complex interplay of factors like lithology, geomorphology, weather, and land cover. Although empirical models have traditionally been used and sometimes adapted to provide spatially distributed estimation, advancements in catchment-scale modelling and remote sensing have expanded estimation capabilities, especially in recent years. This work aims to quantitatively analyse a list of 1,478 studies on sediment delivery modelling derived from Elsevier's Scopus database and published from 1960 to 2023. These studies are classified based on spatial and temporal scales, modelling approaches and processes considered. The findings will provide a comprehensive overview of the state of sediment yield modelling, offering insights into which factors have been considered and which models and approaches have been preferred so far. Here, an overview of the adopted framework is introduced, while the outcomes are still under examinations.

## 1. Introduction

Sediment delivery can be defined as the linkage between on-site soil erosion within a catchment and the off-site sediment yield within the river network or at the basin outlet. From a conceptual perspective, sediment delivery is commonly quantified through the sediment delivery ratio (SDR), namely the ratio of sediment delivered (SD) at the catchment outlet (t km$^{-2}$ yr.$^{-1}$) to gross erosion (SE) within the basin (t km$^{-2}$ yr.$^{-1}$)

$$SDR = \frac{SD}{SE} \quad (1)$$

This definition first appeared in 1949 (Brown, 1949), when some regions of the world started addressing this aspect of sediment management (Walling, 1983). In other countries, this research interest emerged later. For instance, the first evidence of this topic in China dates to the 1970s (Wu et al., 2018).

The amount of sediment delivery depends on several factors, such as lithology (sediment size, soil texture, cohesion and organic content), the geomorphological configuration of the catchment (slope, slope length and basin shape) and its connectivity (Fryirs 2013), namely the presence of pathways or obstacles. It is influenced by weather and climate conditions, like rainfall intensity, favouring or hampering soil particle detachment and transport. Finally, it is also modulated by land cover and use and, in particular, the presence of vegetation.

Since feedback among these factors is highly complex, sediment delivery is often assumed as a black-box concept and estimated in a very rough way (de Vente et al., 2007).

A way to estimate sediment delivery relies on modelling rainfall-induced sediment detachment (i.e. erosion) separately from overland flow and, consequently, computing sediment delivery rate as the lesser of the two or through a sediment continuity equation. However, the most common approach consists of developing a lump parameter model, i.e. an empirical relationship calibrated based on observations. Different empirical models have been defined worldwide so far. However, uncertainty related to estimates and measurements, catchment-specific features and incomplete understanding of the delivery processes have jeopardised such attempts, leading to various formulations valid for a limited geographical area or environmental conditions.

The advent of more sophisticated models for soil erosion and other processes at the catchment scale and the spread of remote sensing in topographical applications have improved the spatially distributed estimation of delivery. As a result, the number of available models significantly increased, providing tools often differing from each other only slightly. Thus, this work aims to tackle the challenge of reviewing all the literature concerning sediment delivery and yield modelling produced so far in order to understand which aspects of this process have been considered, the factors generally included in models and the key features of the adopted model. In the following Section, we outline the framework adopted for such a purpose.

## 2. Framework

The review is based on a quantitative approach for browsing and analysing the works concerning sediment delivery and yield.

First, we generated queries to interrogate the Elsevier's Scopus scientific database, obtaining a list of all the journal articles or reviews whose title contains one of the following search words: "sediment & delivery", "sediment & redistribution", or "sediment & yield". Since Scopus has no access to studies before January 1960, we limited our queries to the period 1 January 1960 – 31 December 2023, despite evidence of related previous work (e.g. Brown, 1949).

Second, we removed from the resulting list all the works not concerning erosion processes in catchments (e.g. those about sediment yield in coastal and marine processes or after earthquakes and wildfires). Moreover, we filtered only the works mentioning "model", "regression", "prediction", "relationship", "equation", "simulation", "estimation" and "formula" in their abstract to exclude those studies not focusing on modelling. In total, we obtained a list of 1,478 works.

While the first two steps are already completed, the following are still ongoing. We are analysing the filtered list in order to classify the works according to different aspects. The classification criteria mainly rely on spatial and temporal scales by distinguishing among studies at the sub-catchment, catchment, national, regional or global scale and from hourly to multiyear time spans. Also, we are discriminating the adopted model, the considered processes (e.g. erosion, transport, deposition, infiltration, etc.) and some model features, such as the typology of input data. Finally, we are flagging the works accounting for some particular aspects like vegetation, land use, climate change or the presence of infrastructures.

In the last phase of this review work, we will compute statistics about the examined fields, summarising all the results deriving from such an in-depth classification and providing an overview of the state-of-the-art sediment yield modelling.

The main outcomes will be presented during the Conference.

**References**

Brown CB (1949) Sediment transportation. In: H. Rouse (Ed.) Engineering Hydraulics (New York: Wiley), pp. 769–857.
De Vente J, Poesen J, Arabkhedri M, Verstraeten G.(2007) The sediment delivery problem revisited, Progress in physical geography, 31(2), 155-178.
Fryirs K (2013) (Dis) Connectivity in catchment sediment cascades: a fresh look at the sediment delivery problem, Earth Surface Processes and Landforms, 38(1), 30-46.
Walling DE (1983) The sediment delivery problem, Journal of hydrology, 65(1-3), 209-237.
Wu L, Liu X, Ma XY (2018) Research progress on the watershed sediment delivery ratio, International Journal of Environmental Studies, 75(4), 565-579.

# Web-based numerical groundwater modelling at the Akrotiri Managed Aquifer Recharge Site, Cyprus using the INOWAS platform

Jana GLASS[1], Constantinos PANAGIOTOU [2], Ralf JUNGHANNS[3], Catalin STEFAN[4]

[1,3,4] Technische Universität Dresden, Germany
jana.glass@tu-dresden.de
ralf.junghanns@tu-dresden.de
catalin.stefan@tu-dresden.de

[2] ERATOSTHENES Centre of Excellence (ERATOSTHENES CoE), Cyprus
constantinos.panagiotou@eratosthenes.org.cy

ABSTRACT

Managed aquifer recharge (MAR) combines various solutions for the interim storage of water underground for later usage or environmental benefits which encompasses infiltration basins and wells. Although MAR represents a viable solution for sustainable water resources management, its contribution to safe water supply at global scale is still limited. This is mainly caused by the lack of data on hydrogeological site-specific characteristics, technological costs and associated operational risks such as unpredictable quality and quantity of recharged and recovered water. Proper monitoring of MAR facilities in combination with simulation-based optimization can better describe the risks associated with MAR implementation, provide support for the optimization of operational management and therewith increase the level of public trust.

The INOWAS platform is a compilation of free web-based empirical, analytical and numerical simulation tools for groundwater management tailored at MAR management (www.inowas.com, *Glass et al, 2022*). It includes tools for real-time monitoring and numerical groundwater flow and transport modelling to optimize the performance of MAR systems while satisfying economic and environmental constraints. Numerical models are frequently used to plan, assess and further improve the operational efficiency of MAR facilities, even though the optimal use of the modelling results is hindered, mainly because these models are only accessible to experts, and not frequently actualized and compared to present observation data. The INOWAS platform allows the web-based setup, run, calibration and analysis of numerical groundwater flow and transport models developed in widely used open-source code such as MODFLOW, MT3DMS, SEAWAT, as well as the direct integration of in-situ observation data into the numerical modelling scheme. Model data can be integrated on the INOWAS platform using the GeoJSON upload e.g. for the study area and locations of boundary conditions, the CSV upload for time series data such as pumping and recharge rates over time and the raster upload for the geological data such as top and bottom of layers, hydraulic conductivities and specific storage. Specific parameters such as a constant soil hydraulic parameter or MODFLOW solver package parameters such as the number of inner and outer iterations and the residual and head change criterion can be directly typed into the INOWAS user interface. The calculation of the model can be initiated via the web interface after which the model data is send and calculated on the servers. After the successful finish of the model run, MODFLOW calculation logs and all model files are displayed and can be downloaded. For results visualization, a map of groundwater heads and drawdowns for a selected layer and time step can be displayed as well as cross sections of specific rows and columns. Time series for specific cells and the volumetric flow budget can be visualized in a graph. The calibration functionality offers the analysis of the model statistics (e.g. maximum and minimum absolute residual, normalized root mean squared error), the display of the simulated versus observed heads, the weighted residuals versus simulated heads and the ranked residuals against normal probability. A distinctive tool for scenario management is also implemented to assess the behavior of the groundwater models under different numerical conditions, fostering the scientifically based decision-making for stakeholders.

The applicability of this approach is demonstrated at the MAR facility in Akrotiri, Cyprus, the web-based model development enabling the direct involvement of the stakeholders at different stages of the implementation process, ensuring the acceptance of the simulation results. Since 2016, a portion of the tertiary treated wastewater from Limassol is transferred via pipeline networks to the Kouris delta region of Akrotiri, where it enriches the local aquifer through a series of infiltration ponds. The primary objectives of the MAR facility are to support the water availability for irrigation while reducing seawater intrusion. This study considers the development of a groundwater model on the INOWAS platform to assess the spatio-temporal effect of MAR on the environment taking into account future developments in the area including land use changes, urbanization and climate variability. The basis of the groundwater flow model stems from previous models developed by *Milnes, 2011* and *Papanikos, 2018* in FEFLOW. The model was adapted to the INOWAS platform, actualized and calibrated for a steady state period using recent observation data from January 2019. As a second step, monthly stress periods were added covering the years 2019-2022 to represent inter-annual changes in the groundwater budget and heads. Workshops with the local stakeholders are planned in spring 2024 to discuss the results of the calibrated groundwater flow model, and to co-design case-specific scenarios considering the stakeholders' knowledge and interest.

The open access, web-based INOWAS platform provides a new framework for groundwater modelling, overcoming the typical limitations of desktop-based software including e.g. high licensing fees, software installation, manual updating, system dependence and limited data accessibility (*Glass et al, 2022*). The international collaboration among various user groups including researchers and decision-makers is fostered by the web-based implementation.

**Acknowledgements**

The AGREEMAR project is funded by National Funding Agencies from: Germany (Bundesministerium für Bildung und Forschung – BMBF, grant no. 02WPM1649), Cyprus (Research & Innovation Foundation – RIF, grant no. 0321-0024), Portugal (Fundação para a Ciência e a Tecnologia – FCT, grant no. PRIMA/0004/2021), Spain (Agencia Estatal de Investigación, Ministerio de Ciencia e Innovación – MCI, grant no. PCI2022-133001) and Tunisia (Ministère de l'Enseignement Supérieur et de la Recherche Scientifique – MESRSI, grant no. PRIMA/TN/21/07). The project is funded under the Partnership for Research and Innovation in the Mediterranean Area (PRIMA). The PRIMA Programme is supported under Horizon 2020 by the European Union's Framework for Research and Innovation.

**References**

Glass, J., Junghanns, R., Schlick, R., Stefan, C. (2022) The INOWAS platform: A web-based numerical groundwater modelling approach for groundwater management applications. Environmental Modelling & Software, 155, 105452. http://dx.doi.org/10.1016/j.envsoft.2022.105452

Milnes, E., (2011) Process-based groundwater salinisation risk assessment methodology: Application to the Akrotiri aquifer (Southern Cyprus). Journal of Hydrology 399, 29–47. https://doi.org/10.1016/j.jhydrol.2010.12.032

Papanikos, I. (2018) Update of an existing three-dimensional hydraulic model of flow and contaminants transport based on newer monitoring data, and simulation of new recharge scenarios adapted to the new climatic and management data within the framework of the Discharge Permit issuance process – Contract with EGL 21/2018 Final Report Results.

# Automatic identification of potential outliers in large data bases of time series based on autoencoders. Application to dam monitoring data

Fernando SALAZAR[1], Joaquín IRAZÁBAL[2], Nathalia SILVA-CANCINO[3], Juan MATA[4]

International Centre for Numerical Methods in Engineering (CIMNE), Spain
[1]fsalazar@cimne.upc.edu; [2]jirazabal@cimne.upc.edu; [3]nsilva@cimne.upc.edu

[4] Laboratório Nacional de Engenharia Civil (LNEC), Portugal.
jmata@lnec.pt

ABSTRACT

The development of machine learning techniques has promoted their application in various fields of engineering, including hydraulics and hydrology. Models of this type have been shown to be capable of generating highly accurate and useful predictions in several areas. However, many of the applications are limited to cases in which the available information is abundant and of good quality. Less attention has been paid to situations – common in professional practice – in which the available data has issues such as periods without records, potentially erroneous values or heterogeneous reading frequency. These problems are even more relevant when dealing with relatively large databases, when visual exploration of each of the series is unfeasible. We present the results of the application of autoencoder neural networks for the automatic filtering of potentially anomalous values from a dam monitoring database with several hundred variables.

## 1. Introduction

Machine learning (ML) based predictive models are applied with increasing frequency in the field of hydraulic and hydrological engineering, from floods (López-Chacón *et al*., 2023) to dam response (Mata, 2011, Salazar, 2017) or the discharge capacity of hydraulic structures (Salazar and Crookston, 2019). Many published works show improved performance as compared to conventional methods in terms of speed of calculation, accuracy or ability to capture non-linear effects or interactions. Since these models rely exclusively on data, their usefulness is highly conditioned by the quality and variety of the data available. The vast majority of application examples refer to cases in which the data series are adequate, sufficiently long and of good quality. However, preprocessing methods have been much less studied, which limits the application of these techniques in situations of scarcity or poor quality of data, which frequently occur in practice. This preliminary phase is particularly important during the process of digitizing databases of historical series, as is the case of monitoring systems of many dams: the installation of automatic systems allows increasing the reading frequency and the size of the database, but it requires unifying the previous records, taken manually, with the new ones. Frequently, these databases are made up of dozens or even hundreds of series, which makes detailed visual inspection of each of them inefficient or even unfeasible. In this communication, we present the results of the application of autoencoders, a method based on neural networks, to automatically detect errors in dam monitoring databases in which exploratory analysis is not feasible due to the large number of existing data series.

## 2. Methodology

### *2.1. Autoencoders*

Autoencoders are a type of neural networks whose initial objective is the encoding of the information provided by a large number of sensors to a lower-dimensional latent space, for subsequent reconstruction of the original signal. This technique has been used to detect anomalies in systems such as wind turbines (Feijóo *et al*, 2021): the autoencoder is trained with normal operating data, so that when it is presented with anomalous measurements, the reconstruction fails, allowing a possible deviation to be identified. Following a similar idea,

we trained an autoencoder with all the variables from a dam monitoring database and then applied it to the reconstruction of the original data. The mean absolute error (MAE) between the output of the autoencoder and the original record is computed, which can be considered an abnormality index. Subsequently, all records can be sorted based on their MAE, so that the dam owner can prioritize those with the highest probability of being reading errors or specific anomalies.

### *2.2. Case study*

This technique has been applied to monitoring data from a dam, whose records cover a period of 30 years, with 1,870 variables and 15,721 rows. The procedure for detecting outliers includes the following steps: a) filtering of series with physical meaning, after which 429 variables are kept; b) training of an autoencoder and application to the reconstruction of the original data; c) calculation of the reconstruction MAE for each observation of each series; d) filtering of variables with some observation with MAE greater than a threshold; e) visual review of potentially anomalous data and correction, if applicable.

## 3. Results

Figure 1 shows the plot of the potentially anomalous values. Only variables that have some record with reconstruction MAE above the threshold appear. The same figure shows, as an example, two of the potential outliers identified. The final decision on whether it is a reading error or an anomalous situation must be made by an expert, considering the nature of the sensor and the life history of the dam, but the tool makes that task approachable, thanks to automatic preliminary filtering. We are currently evaluating the ability of other ML-based methods for this purpose, including DBSCAN and Local Outlier Factor (Ferreira *et al*., 2023). In addition, we are exploring options to help understanding the cause of the anomalous vales, such as cluster analysis.

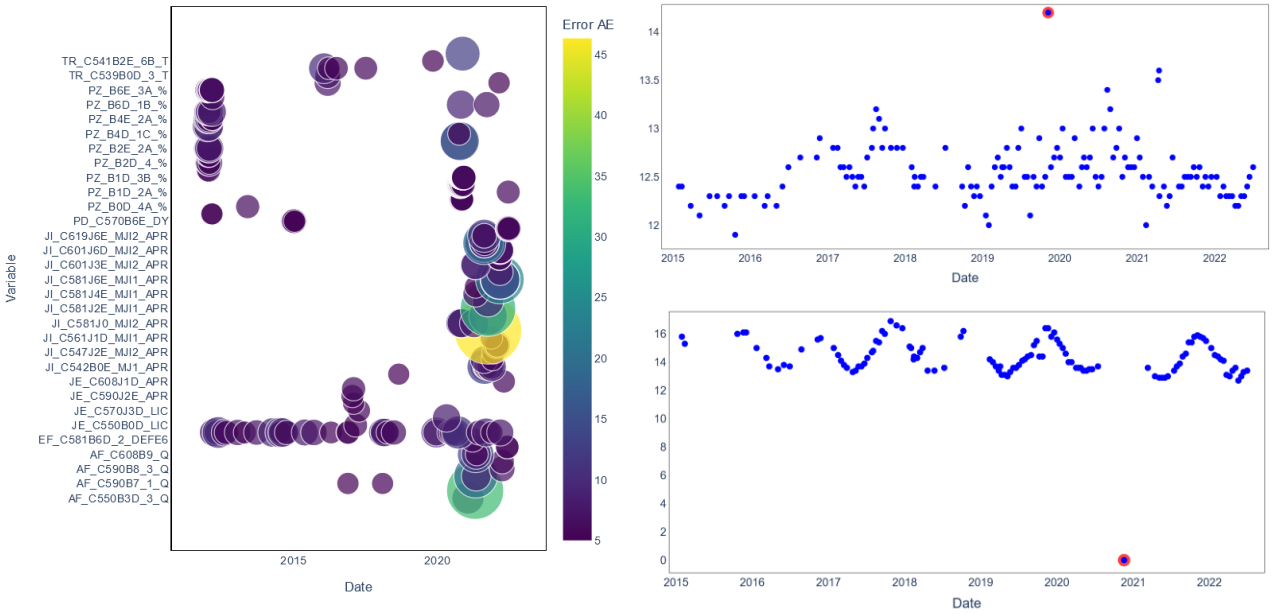



**Fig. 1.** Left: Potential outliers identified (the original plot is interactive). Right: Examples of identified values (highlighted in red) in two of the series.


**Acknowledgements**

This work was developed in the frame of the "DOLMEN" project, funded by the Grant PID2021-122661OB-I00 funded by MCIN/AEI/10.13039/501100011033 and "ERDF A way of making Europe".


**References**


López-Chacón, S. R., Salazar, F., & Bladé, E. (2023). Combining Synthetic and Observed Data to Enhance Machine Learning Model Performance for Streamflow Prediction. *Water*, *15*(11), 2020.

Salazar, F. (2017). A machine learning based methodology for anomaly detection in dam behaviour. PhD Thesis. UPC-Barcelona Tech

Mata, J. (2011). Interpretation of concrete dam behaviour with artificial neural network and multiple linear regression models. *Engineering structures*, *33*(3), 903-910.

Salazar, F., & Crookston, B. M. (2019). A performance comparison of machine learning algorithms for arced labyrinth spillways. *Water*, *11*(3), 544.

Feijóo, M. D. C., Zambrano, Y., Vidal, Y., & Tutivén, C. (2021). Unsupervised damage detection for offshore jacket wind turbine foundations based on an autoencoder neural network. *Sensors*, *21*(10), 3333.

Ferreira, A., Barateiro, J., Mata, J., Tavares de Castro, A. & Cardoso, E. (2023). Automatic outlier detection in sensor data used for structural health monitoring. LNEC Report. ISBN: 978-972-49-2325-3

# Tree-based Approaches for Imputation of Missing Precipitation Records

Ramesh S. V. TEEGAVARAPU[1], Thu NGUYEN[2]

[1,2]Department of Civil Environmental and Geomatics Engineering, Florida Atlantic University, Florida, USA
rteegava@fau.edu

nguyent2018@fau.edu

ABSTRACT

Missing precipitation data is a major issue for many hydrological modeling studies requiring chronologically continuous and error-free data, including climate change and variability. Emerging machine-learning approaches are found to be beneficial for the estimation of missing data. In the current study, missing daily precipitation records are imputed using regression and model tree-based approaches. These approaches are used in a spatial interpolation mode as autocorrelation of the precipitation series at several lags is deemed weak for any temporal interpolation schemes. Missing data at a site is estimated using observations at other sites in a region using the tree-based approaches, which partition the data along with the development of multiple local models for imputation. Daily precipitation data at twenty-two sites in the state of Kentucky are used for the application of the tree-based approaches. Results from this study indicate that tree-based approaches can be used to impute missing precipitation data, with the model tree-based approach providing better estimates than the regression tree method.

## 1. Missing Data Imputation

Missing data imputation is achieved by spatial and temporal interpolation using deterministic and stochastic methods (Teegavarapu, 2013, 2018). Several studies have documented these methods to estimate missing precipitation data at different temporal scales (daily, monthly, etc.). Emerging machine learning methods that are data-driven partition or stratify the data space to develop multiple local models instead of one global model for estimation or prediction. Two approaches and their variants that have been implemented for function approximation are the regression and model trees.

### *1.1. Tree-based Approaches*

A tree-based approach (Quinlan, 1986) implements partitioning or segmenting of the predictor space to create decision spaces based on predictors to arrive at a prediction. In a spatial interpolation mode, the predictors are observations at sites that are used to estimate missing value (i.e., predictand) at a site (i.e., base site). A regression tree partitions the predictor space to obtain the estimate of a predictand using a simple average of values in a specific partition. In contrast, a model tree uses a separate functional relationship relating the predictors and predictand in each partition. Regression tree (RT) and model tree (MT) ( Frank *et al.*, 1998) can be implemented in a pruned or unpruned mode that reduces the possibility of overfitting. Estimates are smoothened or left unsmoothened in instances due to limitations associated with the partitioned predictor spaces.

## 2. Application of Tree-based Approaches

Missing daily precipitation data at twenty-two sites are estimated using RT and MT approaches using historical data and assuming data is missing randomly. Multiple performance measures are used to evaluate both approaches using observed data. The locations of the rain gauging sites in the state of Kentucky, USA, are shown in Fig. 1. A total of 16802 daily precipitation values between the years 1971-2016 are used for the study, with 9200 and 2000 values used for calibration and validation, respectively and the rest of the data are

used for testing. The RT and MT models are developed using Waikato Environment for Knowledge Analysis (WEKA).

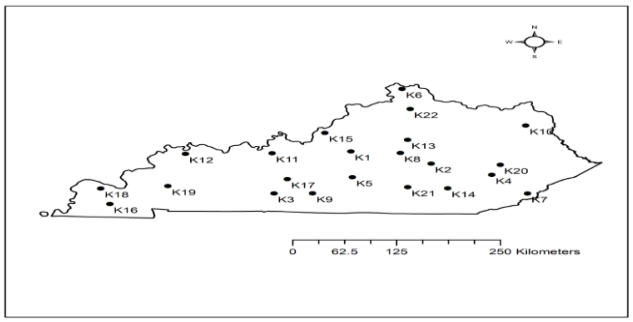



**Fig. 1.** Location of rain gauging sites in Kentucky, USA.

## 3. Results and Analysis

Four variants of RT and MT models which include (1) Model Tree pruned –smoothed (MT(PS)), (2) Model Tree unpruned – unsmoothed (MT(UPUS)), (3) Regression Tree pruned – smoothed (RT(PS)), (4)Regression Tree unpruned – unsmoothed (RT(UPUS)) are developed and evaluated for imputation of missing data. Correlation coefficients (CC) derived based on observed and estimated precipitation values are shown in Fig. 2. CC values indicated that unpruned and unsmoothed variants of MT and RT perform better than pruned and smoothened versions in training. The performances from unpruned and unsmoothed variants can be attributed to overfitting during training. However, in testing, the MT pruned and smoothened variant performs better than the similar variant of the RT model. MT-based models performed better than RT based on multiple performance measures to estimate missing data.

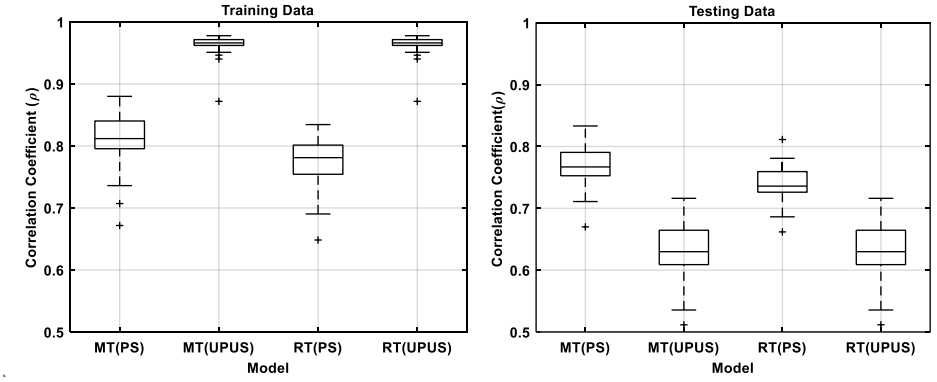



**Fig. 2.** Correlation coefficients based on imputation of missing precipitation at twenty-two sites using different variants of RT and MT for training and testing datasets.

## 4. Conclusions

In this study, regression and model tree-based approaches are developed in spatial interpolation mode to impute missing precipitation data. Preliminary results from the performance evaluation of RT and MT models suggest that the imputation of missing precipitation data is possible with different variants of the tree-based approaches. In general, MT models provided better estimates than those from RT models. Also, the pruned smoothened versions performed better than the unpruned and unsmoothed counterparts, as the latter tend to show overfitting and less generalization capabilities. Further studies are being conducted to develop an ensemble of approaches and correct issues related to under and over-estimating higher-end and lower-end precipitation extremes.

**Acknowledgements**

The precipitation data required for this study was obtained from the Kentucky Agriculture Weather Center.

**References**

Frank E, Wang Y, Inglis S, Holmes G, Witten IH (1998) Using model trees for classification. Machine Learning, 32, 63-76.
James G, Witten D, Hastie T, Tibshirani, R (2021) An Introduction to Statistical Learning with Applications in R, Springer, New York.
Quinlan, JR (1986) Induction of decision trees. Machine Learning, 1(1), 81-106.
Teegavarapu RSV (2013) Floods in Changing Climate: Extreme Precipitation, Cambridge University Press, Cambridge, 286 pp.
Teegavarapu RSV (2018) Trends and Changes in Hydroclimatic Variables: Links to Climate Variability and Change, Elsevier 421 pp.

# Atlantic Salmon (*Salmo Salar*) Conservation and Sustainable Hydropower in Norway: New Innovative Downstream Passage Solutions

Ana T. SILVA[1], Torbjørn FORSETH [2], Ismail ALBAYRAK[3], Olivia M. SIMMONS[4], Kamal PANDEY[5], David VETSCH[6], Bjørn Winther SOLEMSLIE[7], Robert BOES[8], Olle CALLES[9], Patrik ANDREASSON[10], Stephanie MÜLLER[11], Eric LILLBERG[12], Henrik BAKTOFT[13], Karl Ø. GJELLAND[14], Finn Økland[15], Ulrich PULG[16], Ole Gunnar DAHLHAUG [17]; Atle HARBY[18]; David ALDVÉN[19]

[1,2,4,7,14,15] Norwegian Institute for Nature Research, Norway
ana.silva@nina.no; torbjorn.forseth@nina.no: olivia.simmons@nina.no; bjorn.solemslie@nina.no; karl.gjelland@nina.no; finn.okland@nina.no
[3,5,6,8] Laboratory of Hydraulics, Hydrology and Glaciology (VAW), ETH Zurich, Zürich, Switzerland
albayrak@vaw.baug.ethz.ch, boes@vaw.baug.ethz.ch, pandey@vaw.baug.ethz.ch; vetsch@vaw.baug.ethz.ch
[1,10,11,12,19] Vattenfall Research and Development, Älvkarleby Laboratory, Sweden
patrik.andreasson@vattenfall.com; stephanie.mueller@vattenfall.com;
eric.lillberg@vattenfall.com; david.aldven@vattenfall.com
[9,19] Department of Environmental and Life Sciences, Karlstad University, Sweden
olle.calles@kau.se
[13] National Institute of Aquatic Resources, Technical University of Denmark
hba@aqua.dtu.dk
[16]NORCE Norwegian Research Centre AS
ulpu@norceresearch.no>
[17] NTNU-Norwegian University of Science and Technology
ole.g.dahlhaug@ntnu.no>
[18]Sintef Energi
atle.harby@sintef.no

ABSTRACT

The management and conservation of salmonids populations in Norway have become increasingly critical in the face of growing anthropogenic pressures and climate change impacts. Norway, as a major hydropower producer, often has its rivers fragmented by hydropower plants (HPP), which significantly affect aquatic biodiversity. Migratory species such as Atlantic salmon are highly impacted by the presence of HPP. Due to their ecological, economical, and social importance this species is often served as lead species for conservation efforts. In Norway several studies have investigated the behaviour of Atlantic salmon in the presence of HPP. This knowledge is crucial for developing solutions that prioritize the safe and efficient migration of this species ultimately increasing survival rates and safeguarding the ecological health of its populations. While solutions for upstream migration have been well-researched, little information exist on downstream migration of Atlantic salmon. The Safepass, FishFence, FishPath, and Kelt2Sea, herein presented, are among the international initiatives in Norway addressing this issue. These projects were affiliated with or received funding from the HydroCen center, a Norwegian centre dedicated to innovative research on environmentally friendly energy. These efforts are integral to the sustainable management of salmonids in Norway, aligning with the ongoing development of sustainable hydropower sources.

1. **The Safepass project (2015-2019)** The Safepass project aimed to enhance understanding and facilitate safe and efficient Two-ways migration of salmonids and European eel past HPP. It served as a knowledge-building within the hydropower sector, encompassing both laboratory and field investigations conducted in Norway and Sweden. A significant study was conducted in the Mandal River in southern Norway, where the fine-scale swimming behavior of 100 Atlantic salmon smolts (Salmo *salar*) was analyzed using 3D acoustic telemetry and 3D hydraulic modeling. An explanatory model on fish swimming speed and swimming direction for Atlantic salmon smolts was developed. This model highlighted their dependence on hydraulics emphasizing that the direction of water velocity and turbulence, in addition to their magnitude, plays a crucial role (Silva et al., 2020). The model, which accounted for 84% of the swimming direction of salmon smolts in the Mandal River, was successfully re-parameterized to data from the river Orkla, where it also explained 84% of the swimming direction. When subjected to cross-validation, the Mandal model exhibited a reduced

explanatory power of 21% for the swimming direction of salmon smolts in the Orkla site, while the Orkla model explained 26% of the swimming direction in the Mandal site (Szabo-Meszaros & Silva et al. 2021). These findings contributed to the current development of a predictive model for the downstream migratory routes of Atlantic salmon smolts near a hydropower plant, enhancing our ability to support their safe passage.

**2. The FishFence project (2020-2022)** The FishFence project evolved from the research conducted in Mandal during the Safepass project. Its objective was to design and implement a technological solution in the river to prevent the entry of salmon smolts into the turbines. Building upon the scientific insights gained from the Safepass project, a modified angled bar structure, measuring 86 meters in length and 1.5 meters in depth (Figure 1a), was developed in close collaboration with industry partners and the ETH VAW laboratory, taking inspiration from the work from Beck et al. 2020. To assess the effectiveness of this structure in guiding salmon smolts, a 3D acoustic telemetry study was conducted. The FishFence demonstrated an impressive guidance efficiency of approximately 88% (Figure 1b, c).

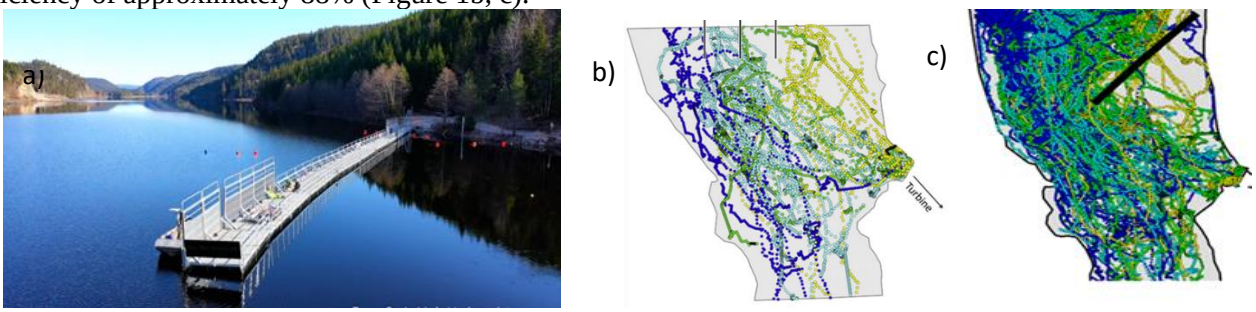



**Fig. 1.** a) Fish guidance fence. Atlantic salmon smolts tracks before (b) and after installation of the guidance fence.

**3. The FishPath project (2021-2026)** FishPath is dedicated to advancing next-generation solutions for redirecting downstream migrating fish away from hydropower intakes and guiding them through secure migration routes. The innovative concept behind this project lies in utilizing knowledge about fish behavior in response to turbulent eddies to create guidance systems that establish alternative migration pathways for fish, circumventing HPP. This interdisciplinary focuses on deepening our comprehension of how eddies affect Atlantic salmon and European eel (*Anguilla anguilla*). FishPath encompasses various live-fish tests and complex hydraulic modeling utilizing computational fluid dynamics (CFD). What also sets this project apart is its holistic approach, examining the relationship between fluid dynamics and fish behavior at different scales, ranging from finely detailed laboratory studies to more natural laboratory settings and, ultimately, real-world river conditions. FishPath involves an international and interdisciplinary team of experts collaborating closely with the Norwegian and Swedish industry.

4. **The Kelt2sea project (2022-2025)** Kelts, have crucial role within fish populations as they can significantly contribute to the spawning stock (Turgeon et al. 2019). Still, little is known about kelts`s downstream migration, and their responses to the hydrodynamics of the surrounding flow. Furthermore, detailed insights into how kelts interact with existing downstream solutions (trash-racks, bypasses, etc) remain scarce. The Kelt2Sea's focal points encompass the study of kelt behavior in response to hydraulics, their interactions with various trash-racks, and their passage through different bypasses. Ultimately, based on data collected from live-fish experiments within the project, a predictive model for downstream migration will be established. This is a pioneer project as no controlled experiments on kelt behavior exist, rendering it unique and of paramount importance for advancing the field of downstream passage solutions. The collaboration between Norway and Sweden University and Industry is integral to this work.

**Acknowledgements** We thank the Research Council of Norway for funding the SafePASS (Project no. 244022) and the FishPath (projects through the ENERGIX program. We also thank the Norwegian Research Centre for Hydropower Technology – HydroCen for funding the Kelt2SEA project and (RCN project no. 257588).

**References** Beck, C., Albayrak, I., Meister, J., & Boes, R. M. (2020). Hydraulic performance of fish guidance structures with curved bars–Part 2: flow fields. Journal of Hydraulic Research, 58(5), 819–830.
Ismail Albayrak, Robert M. Boes, Carl Robert Kriewitz-Byun, Armin Peter & Blake P. Tullis (2020) Fish guidance structures: hydraulic performance and fish guidance efficiencies, Journal of Ecohydraulics, 5:2, 113-131
Silva, A.T.; Bærum, K.M.; Hedger, R.D.; Baktoft, H.; Fjeldstad, H.-P.; Gjelland, K.Ø.; Økland, F.; Forseth, T (2020). The effects of hydrodynamics on the three-dimensional downstream migratory movement of Atlantic salmon. Science of the Total Environment 705, 135773
Szabo-Meszaros, M.; Silva,A.T; Bærum, K.M.; Baktoft, H.; Alfredsen, K.; Hedger, R.D.; Økland, F.; Gjelland, K.Ø.; Fjeldstad, H.-P.; Calles, O (2021) Validation of a Swimming Direction Model for the Downstream Migration of Atlantic Salmon Smolts. Water 13, 1230
Turgeon, K., Turpin, C. and Gregory-Eaves, I. (2019). Dams have varying impacts on fish communities across latitudes: a quantitative synthesis. Ecology Letters, 22:1501-1516

# Retrospective analysis of the structural behaviour of Almendra dam after 53 years of its construction

Alicia SIGÜENZA[1], Luis DE LA TORRE[2], Yolanda PEREZ[3], Carmen BAENA[4], José MILLA[4]

[1,2,3] Operations and Maintenance Hydroelectric Project & Global Technical Services, IBERDROLA, Spain
asiguenza@iberdrola.es
ltab@iberdrola.es
yperez@iberdrola.es

[4] Civil Engineer, GRANELL INGENIEROS, Spain
cmb@granellingenieros.com
jml@granellingenieros.com

ABSTRACT

The Almendra Dam is a double curvature arch dam built on the Tormes River, located in the boundary of Salamanca and Zamora provinces. With a total height above foundation of 202 m and a crest length of 567,23 m, it is currently the highest dam in Spain.

During the summer of 2022, Iberdrola planned an unusual release of nearly 400 $hm^3$ to comply with the Albufeira Convention, an agreement signed by Portugal and Spain governments to regulate the hydro-electric development of the international section of the Duero River. This action would cause the level to drop from 693 m above sea level (current level at that moment) to approximately 670 m. The operation started at the end of the month of September 2022 and finally, it was only necessary to reach the level 684 m.

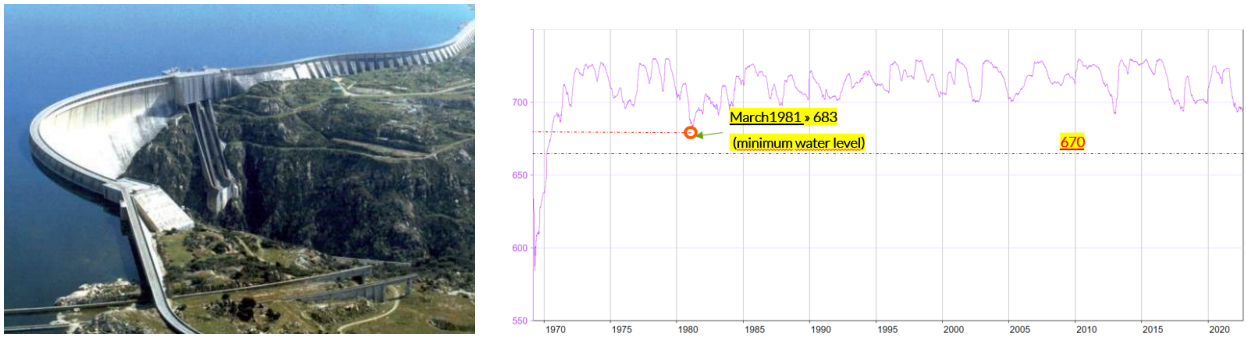



**Fig. 1.** Almendra Dam. Historic reservoir level.

Due to that extraordinary situation, Iberdrola decided to develop a 3D Finite Element Method (FEM) model to anticipate the behaviour of the dam during the discharge.

In order to use this finite element model to contrast the real deformations measured during the process, it was necessary to perform a calibration of the model with the values provided by the monitoring system installed on site and collected during more than 50 years of service of the dam.

## 1. Introduction

The Almendra Dam is located in the Arribes del Duero Natural Park. This dam is part of the "Saltos del Duero hydro-power system" of Iberdrola, together with other infrastructures installed in Aldeadávila, Castro, Ricobayo, Saucelles and Villalcampo, and it dams the water before Tormes river reaches the Duero River.

The Almendra reservoir is one of the largest in Spain with a capacity of 2648.64 $Hm^3$ for the top water level. In this reservoir are placed the water intake of the Villarino Hydro Power Plant, with a head of more than 400 m.

The construction started in 1964 and the filling started before the end of its construction, in 1970. Some technical documents of those years show different details about the dam, construction process, materials, etc. Valuable information is collected in the calculation report signed by COBA entitled "Almendra Dam. Structural Calculation" and dated April 1969. The stress calculations of the dam carried out during the construction phase are developed in that document. Moreover, Iberdrola has a huge amount of data of the monitoring system installed on site retrieved during more than 50 years of service of the dam.

## 2. First FEM Model and calibration process

At the beginning of the work, it was necessary to develop a model with a simple mesh to enable several calculations in order to calibrate different parameters. The main objective of this model was to check the deformations during the exceptional release of water, by comparing real monitoring data and model results. Any remarkable difference between both could require an immediate stop of the operation in progress.

For this reason, it was so important to perform a model where deformation results were realistic, so it could be relied on and used for decision-making. A huge historic data analysis was made in a very short period. Therefore, for this first model, it was decided to choose only the central pendulum data for its calibration.

To understand how the dam was affected by variables like water level and temperature, acting independently or in combination, and see what deformations could be permanent (due to the first filling or due to rheologic effects), all the monitoring data were classified in four different categories depending on their temperature and reservoir level: high temperatures and high reservoir levels, low temperatures and high reservoir levels, high temperatures and low reservoir levels and low temperatures and low reservoir levels.

Through this calibration it was possible to isolate those effects separately and to correct the deformations obtained in the FEM model so that the effect of this extraordinary release could be estimated more rigorously and compared against the monitoring systems data.

## 3. Second FEM Model. Accurate stress and strain analysis.

Once the first model was calibrated and verified with satisfactory results, a second model was developed with a more refined mesh, improved boundary conditions and a more complete calibration work by considering all the pendulums data.

This second model is a more precise tool that enables Iberdrola to make a better forecast and control of the behaviour of the dam in different future situations and to perform an accurate stress-strain analysis under the new approved Technical Safety Standards.

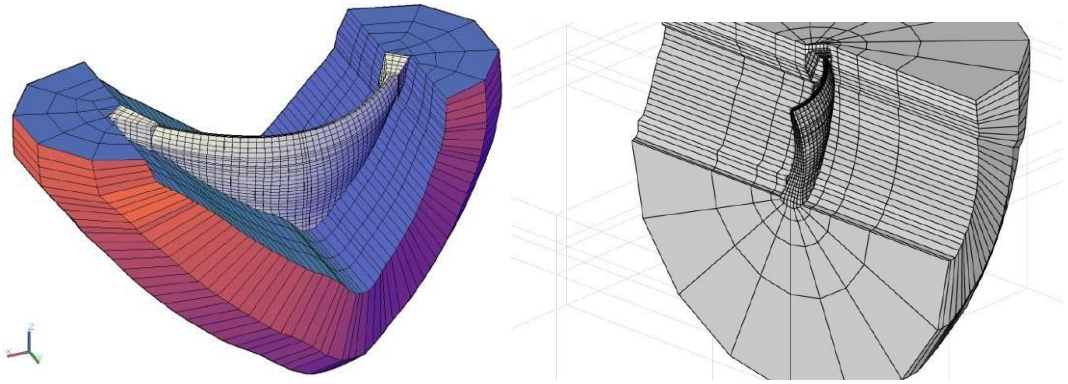


**Fig. 2.** First FEM Model and Second FEM Model.

**Acknowledgements**

Miguel Ángel Ramírez, César Mayoral and Alberto Vaquero of IBERDROLA for their time and effort in preparing the monitoring data used in the model calibration process.

**References**

"Almendra Dam. Structural Calculation" COBA (1969)

# Sediment transport and deposition processes under various hydrological-hydraulic conditions – HEORES project

Mateja KLUN, Tamara KUZMANIĆ, Klaudija LEBAR, Gašper RAK, Andrej KRYŽANOWSKI, Matjaž MIKOŠ, Andrej VIDMAR, Simon RUSJAN

University of Ljubljana, Faculty of Civil and Geodetic Engineering, Slovenia
mateja.klun@fgg.uni-lj.si

ABSTRACT

In the present contribution, Hydro-Ecologically based Operation of run-of-river Reservoirs for Effective Sediment management and energy production (HEORES) project is presented, with the emphasis on the analysis of hydrological and hydraulic conditions and sediment transport and deposition processes in the scope of the project. This part of the project is oriented to two major objectives namely, analysis of the temporal dynamics of HPP reservoir filling with deposited sediments and detailed analysis of hydraulic conditions and related sediment transport/deposition processes.

## 1. Introduction

Sediment transport in the downstream direction with river flow is a natural process. It can be discontinued with natural and artificial reservoirs. Artificial, man-made reservoirs can act as a trap for sediment when are not managed with a respect to sediment transport processes (Kondolf et al., 2014). Aside from disruption of natural sediment cycle and downstream sediment deficit, reservoir sedimentation causes a loss of reservoir storage capacity, hydraulic structures and machinery abrasion, and obstruction of intakes. Sediment connectivity and the balance between sediment entering the reservoirs and sediment passing to the downstream river sections is a key challenge for sustainable reservoir management (Chamoun et al., 2016). Sustainable sediment management enables continuous sediment transport, improving habitat conditions for river ecosystems, as sediment is of a crucial role for the quality of aquatic habitats (Sholtes et al., 2017).

In the view of need for improved sediment management strategies in hydro-power-plant (HPP) reservoirs, project Hydro-Ecologically based Operation of run-of-river Reservoirs for Effective Sediment management and energy production (HEORES) will develop the sediment management plan for the chain of HPP on the lower Sava River with a goal to restore the connectivity along the river course and improve the river channel's habitat role.

## 2. HEORES project

Hydro-Ecologically based Operation of run-of-river Reservoirs for Effective Sediment management and energy production (HEORES) project represents a comprehensive approach considering the specific hydrological and hydraulic conditions of the lower Sava River. It addresses issues of the interdisciplinary, sustainable sediment management strategy, which includes all elements of the natural sedimentation cycle and environmental concerns related to potential sediment pollution.

The 945 km long Sava River is a major drainage basin in Southeastern Europe. It is the biggest tributary of the Danube River. The Sava River catchment area covers 97,713 km$^2$ over four countries, namely, Slovenia, Croatia, Bosnia and Herzegovina, and Serbia. The source of the Sava River is in Slovenia, where it has alpine, torrential characteristics with high temporal dynamics of the flows during high and low flow conditions. As such, in this headwaters part it has a great intake of sediments.

By the construction of run-of-the-river hydro-power-plants (HPP) with limited storage capacity along the Sava River channel the natural dynamics of sediment transport was considerably impacted. More specifically, the sediment got intercepted and deposited within the reservoir volumes. Cascading system on lower Sava River consists of 5 HPP dams, namely HPP Vrhovo, HPP Boštanj, HPP Arto-Blanca, HPP Krško, and HPP Brežice, as shown in Fig. 1. The current operation of this HPPs is based solely on hydrological data, without the consideration of sediment transport processes and their influences on the HPP operations.

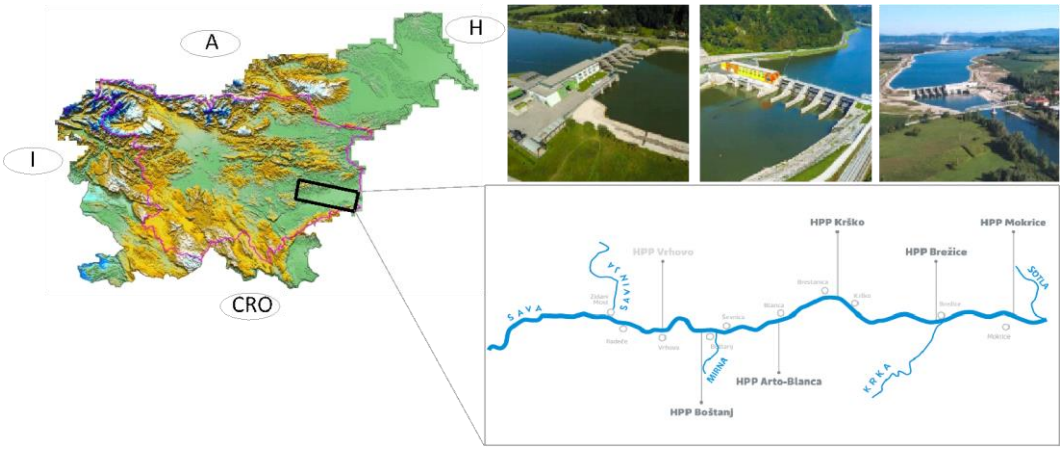



**Fig. 1.** Study area of the lower Sava River.

## 3. Analysis of hydrological and hydraulic conditions and sediment transport and deposition processes

In the scope of the HEORES project, the hydrological and hydraulic conditions, as well as the sediment transport and deposition processes will be detailly analyzed. This part of the project is oriented to two major objectives (O1 and O2), namely, O1 – Analysis of the temporal dynamics of HPP reservoir filling with deposited sediments and O2 – Detailed analysis of hydraulic conditions and related sediment transport/deposition processes.

With the establishment of detailed hydrometric surveys and monitoring it is expected that areas inside the reservoir where intensified sediment deposition is occurring can be identified (hypothesis H1). The monitoring will include series of bathymetric measurements as well as monitoring of hydraulic conditions in the HPP reservoirs during various hydrological conditions and HPP operations, using Acoustic Doppler Profiler (ADP). Suspended sediment is going to be continuously monitored using optical turbidimeter.

Use of the particle size distribution (PSD), which is one of the main sediment characteristics that determines whether it will be transported or deposited under a given hydraulic condition, can help to improve identification of critical sedimentation locations in the reservoirs (hypothesis H2). PSD of coarse-grained sediment will be determined with sieve analysis using sieve shaker. PSD of finer sediments will be determined using optical analyzer. Additionally, particle shape of coarse-grained sediment samples will be analyzed and determined using dynamic image analysis.

**Acknowledgements**

The authors acknowledge that the research is financially supported by the Slovenian Research Agency, research core funding No. P2-0180, and research projects No. L7-50097 and by the HESS d. o. o. Hidroelektrarne na Spodnji Savi.

**References**

Kondolf, G.M., Gao, Y.X., Annandale, G.W., Morris, G.L., Jiang, E., Zhang, J., Cao, Y., Carling, P., Fu, K., Guo, Q., Hotchkiss, R., Peteuil, C., Sumi, T., Wang, H-W., Wang, Z., Wei1, Z., Wu, B., Wu, C., Yang, C.T. (2014) Sustainable sediment management in reservoirs and regulated rivers: Experiences from five continents. Earth's Future, 2, 256–280.

Chamoun, S., De Cesare, G., Schleiss, A.J. (2016) Managing reservoir sedimentation by venting turbidity currents: A review. Internat. J. Sed. Res. 31, 195–204.

Sholtes, J.S., Ubing, C., Randle, T.J., Fripp, J. Cenderelli, D., Baird, D.C. (2017) Managing Infrastructure in the Stream Environment Advisory Committee on Water Information Subcommittee on Sedimentation Environment and Infrastructure Working Group. U.S. Department of the Interior Bureau of Reclamation. https://acwi.gov/sos/pubs/managing_infrastructure_in_the_stream_environment.pdf

# Effects of Flow Restoration on the Hydraulic Conditions in River Juktån

J. Bastian HÖLLER[1], Anders G. ANDERSSON[2], J. Gunnar I. HELLSTRÖM[3]

[1,2,3] Division of Fluid and Experimental Mechanics, Department of Engineering Sciences and Mathematics, Luleå University of Technology, Sweden
bastian.holler@ltu.se
anders.g.andersson@ltu.se
gunnar.hellstrom@ltu.se

## ABSTRACT

Hydropower plays a central role in the plans for future energy supply. In the future renewable energy mix hydropower can be used to regulate intermittent sources like wind- and solar power to meet the electricity demand. Already today 16 % of the world's electricity comes from hydropower (IHA, 2022), with the share being significantly higher in the Northern European countries (Nordic Energy Research, 2021). In Sweden, Hydropower accounts for 45 % of the electricity (SEA, 2022), but most of the plants were built before comprehensive environmental legislation was in place. While hydropower is a renewable and low-emission energy source it has serious implications for the local river ecosystem. One of the phenomena of hydropower plants affecting the ecosystems is the change of the natural river discharge to align the power production with the electricity demand. This altered flow changes the hydraulic habitat in the river and thereby impacts the fauna and flora, for instance by reducing spawning habitats or increasing stranding risks for fish (Burman et al., 2021). Recent EU environmental legislation focusing on the quality of water bodies (EU, 2000) and biodiversity (EU, 2020) led to the necessity to reconsider the effects of existing hydropower plants and implement suitable mitigation measures to protect the ecosystem.

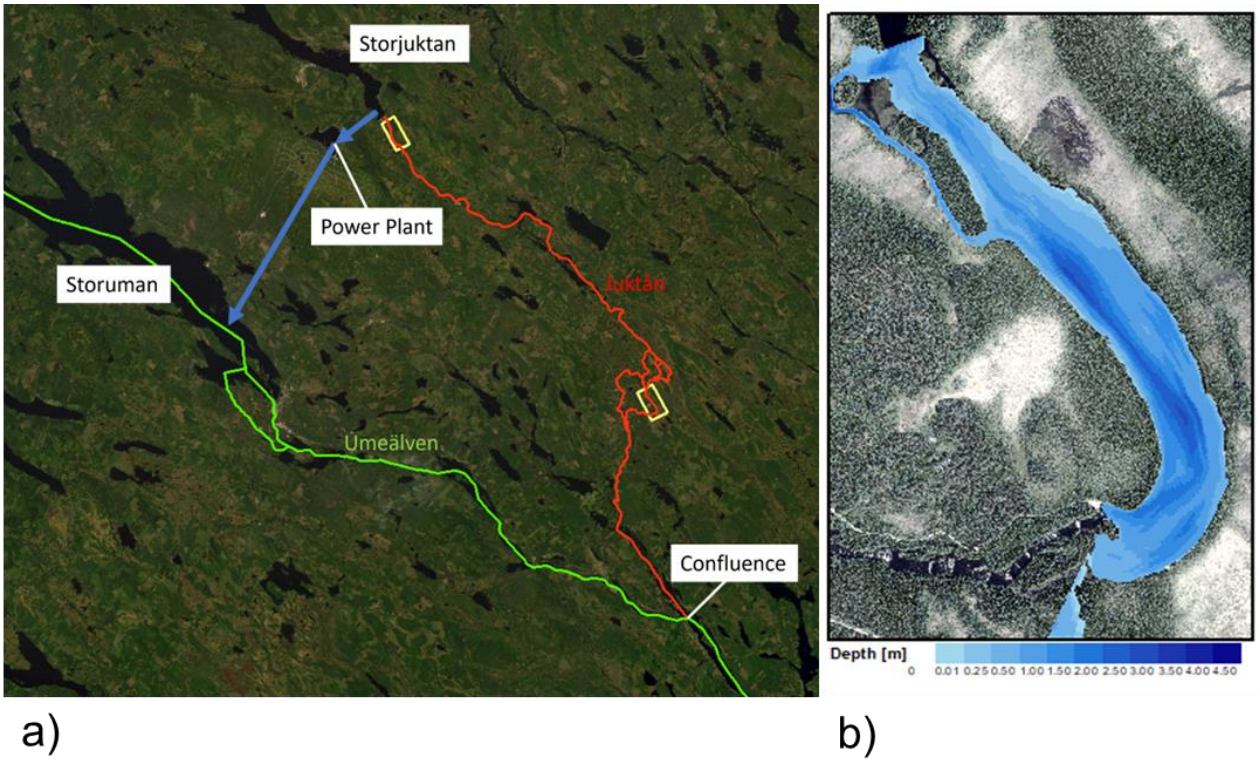



**Fig. 1.** a) Overview of the river system with the diversion of water from Storjuktan to Storuman reservoir and the two study sites (yellow) and b) results of the hydraulic simulation for water depth at one of the study sites

This work will focus on the implementation of mitigation measures in river Juktån, a tributary to Umeälven in Northern Sweden. The majority of the natural discharge in river Juktån is extracted from the riverbed for hydropower production and then discharged directly into the Umeälven through a pipeline, see Fig. 1. The natural riverbed is fed with a base discharge from the Storjuktan reservoir until the confluence with Umeälven ca. 60 km downstream. In a restoration project, the discharge from Storjuktan reservoir into the natural riverbed was adapted with the intention to benefit the ecosystem. While the change of the total annual discharge was negligible, a more natural seasonal discharge pattern was implemented where an increase of discharge in spring was used to imitate the natural spring flood and support the organisms' life cycles. In sections of the river, additional morphological restoration measures were performed. Several small weirs and rock ramps were destroyed to increase connectivity and enable easier access to suitable spawning areas.

In this work, hydraulic modelling was used to investigate the effects of the mitigation measures. Two river stretches were modelled in Delft3D, see Fig. 1. In this case, a two-dimensional numeric solution of the shallow water equations was applied. Field measurements of time-resolved water levels were used to calibrate and validate the models. For both stretches the situation before and after the restoration was modelled and the hydraulic conditions were compared. In one of the stretches, the focus of restoration was to enhance the lateral connectivity and beach vegetation while avoiding increased sediment transport. Here only the discharge was changed. In the other stretch further downstream, extensive instream vegetation should be limited and hydraulic habitats be improved. In this stretch, both hydrologic restoration and the destruction of a weir were realized. Finally, the effectiveness of the implemented mitigation measures was evaluated and the modelled results were compared with observations from the field.

**Acknowledgements**

This research was conducted in the framework of the PhD project *"Digital twins of regulated river reaches with integrated social and economic effects"*, funded by SUN – Natural Resources for Sustainability Transitions. SUN strategic area is initiated by Luleå University of Technology.

**References**

Burman, A. J.; Hedger, R. D.; Hellström, J. G. I.; Andersson, A. G.; Sundt-Hansen, L. (2021) Modelling the downstream longitudinal effects of frequent hydropeaking on the spawning potential and stranding susceptibility of salmonids. Science of the Total Environment, 796, 148999. https://doi.org/10.1016/j.scitotenv.2021.148999.
EU (2000) Directive 2000/60/EC of the European parliament and of the council of 23 October 2000 establishing a framework for Community action in the field of water policy (EU Water Framework Directive).
EU (2020) Bringing nature back into our lives. Biodiversity Strategy for 2030.
IHA (2022) Hydropower status report. Sector trends and insights.
Nordic Energy Research (2021) Renewable energy in the Nordics 2021, Nordic Energy Research: Oslo.
SEA (2022) Energy in Sweden 2022 - an overview.

# Flow Characteristics around a freshwater mussel in a gravel bed flume

Donatella TERMINI[1,2]

[1] Department of Engineering, Italy
donatella.termini@unipa.it

[2] NBFC, National Biodiversity Future Center, Palermo, Italy

ABSTRACT

Mussels are a defined as “ecosystem engineers” capable of affecting the hydrodynamics, passively and actively (Navaratnam et al., 2018; Termini et al., 2023). The generation of larger-scale turbulence around the mussels living on the river bed may also affect the quality of the habitat. Thus, it is extremerly important to know the effects determined to the presence of mussels on flow characteristics. In the present study reports preliminary results on flow and turbulence characteristics around an isolated mussel over a gravel-bed. The presence of mussel enhances the effects determined by the rough-bed on the kinematic characteristics of flow. The analysis is performed on the basis of data collected in a straight laboratory gravel-bed flume both in absence and in presence of an isolated and partially buried mussel (*Unio elongatulus*), aligned with the incoming flow. In order to take into account spatial heterogeneities, the double-averaged velocities are considered for the analysis in the absence of mussel on the bed. Results show that, because of the presence of gravels, in the absence of the mussel, the streamwise velocity profiles show an inflection point with the formation of a mixing layer whose thickness varies passing from the banks to the channel axis. The presence of mussel modifies the shape of the velocity profile with the formation of turbulent flow structures around it. Different effects on the velocity and turbulence fields have been identified in relation with the mussel’s filtrating capacity.

## 1. Experimental apparatus and data

The experimental data were collected in a straight recirculating laboratory flume realized at Hydraulic Laboratory of Department of Engineering of University of Palermo (Italy). The channel is 11 m long, 0.4 m wide and with a rigid transparent banks 0.5 m high (Figure 1).

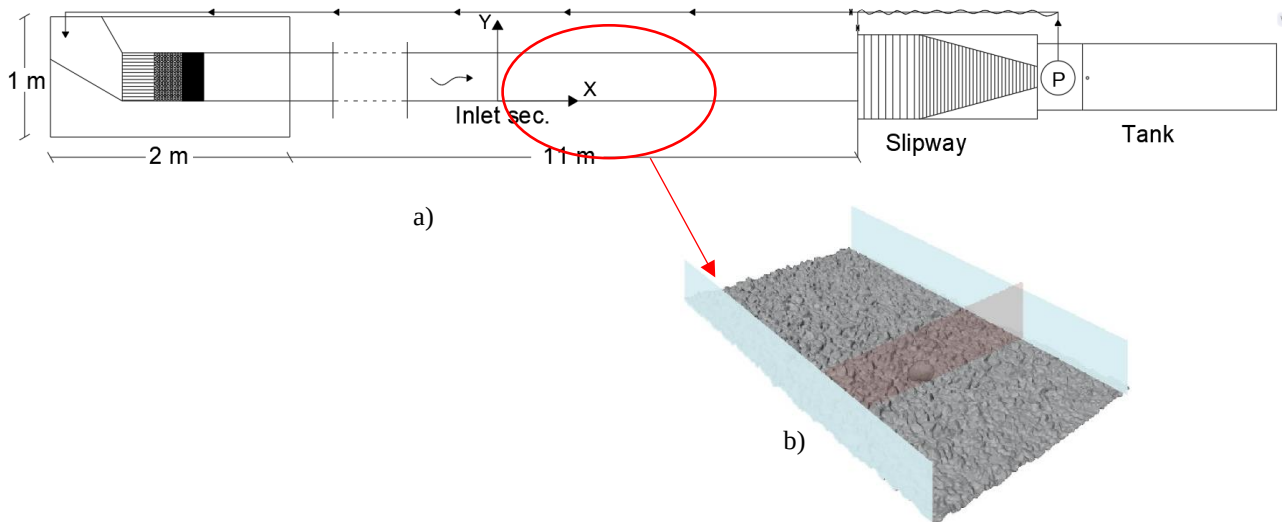



**Fig. 1.** a) Plane view of the channel; b) particular of the bed surface and of the section where the mussel was located

The bed surface was realized of fixed quartz sand in the first entering reach 3.0 m long and of non-uniform gravels ($d_{84}$=1.1 cm) in the remaining part. Three experimental runs were conducted with flow discharge of 0.00765 $m^3/s$. These runs were respectively: 1) in the absence of the mussels, 2) in the presence of a dead mussel, 3) in the presence of a live mussel. In the last two runs the mussel was located in the center of a cross-section located in the central area of the rough-bed channel reach (Figure 1). During each run the 3D instantaneous flow velocity components were measured in a fine grid of selected cross-sections along the channel by using an ultrasonic velocity profiler DOP2000 by Signal Processing s.a.

## 2. Results and conclusion

The instantaneous values have been used to estimate the corresponding time-averaged values. Figure 2 shows as an example the vertical profiles of the longitudinal, transversal and vertical time-averaged velocity components measured around the mussel. It is possible to note that, in the absence of the mussel, because of the presence of gravels the longitudinal velocity component presents low values close to the bed until to form an inflection point (with the formation of a mixing layer) and then gradually increasing as one moves toward the free surface. The presence of mussel, either dead or alive, modifies the shape of velocity profile close to mussel and in the mixing region, determining lower velocity values especially on the right side of the mussel itself. Here, the transversal velocity component changes the sign in the presence of the dead mussel but when the mussel is in live it becomes again positive because of the mussel's syphons filtration. A similar behaviour can be observed for the vertical velocity component. The observed effect determined by the presence of the mussel and by its filtration rate affects both the longitudinal and transversal water fluxes and the turbulent kinetic energy around the mussel itself.

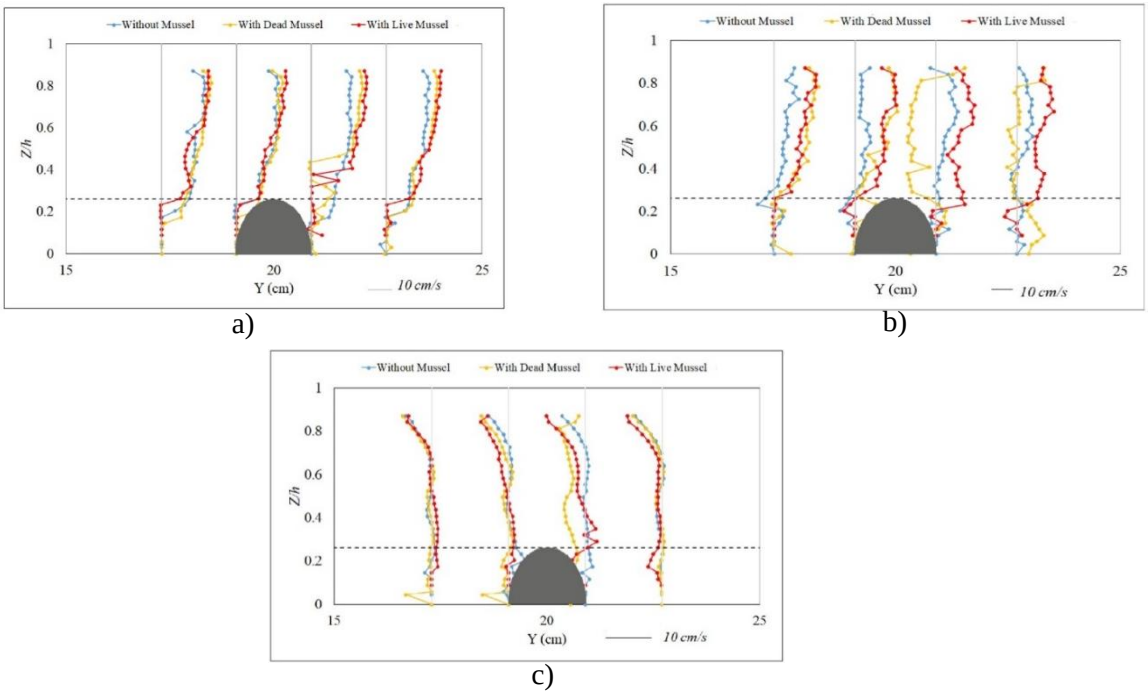



**Fig. 2.** a) vertical profiles of the longitudinal velocity component; b) vertical profiles of the transversal velocity component; c) vertical profiles of the vertical velocity component

It should be noted that the present study has been performed in a controlled environment and by considering a single mussel, not taking into account the complexity of natural ecosystems, both in terms of hydraulic and biotic interactions

**Acknowledgements**

This study was conducted and supported by Italian National Research Programme PRIN 2017, with the project "*ENTERPRISING"*.

**References**

Navaratnam, C. U., Aberle, J., Qin, J., Henry, P. (2018). Influence of Gravel-Bed Porosity and Grain Orientation on Bulk Flow Resistance. HENRY. Hydraulic Engineering Repository. *Water* 2018, 10, 561; DOI:10.3390/w10050561

Termini D., Benistati N., Tosato L., Pilbala A., Modesto V., Fraccarollo L., Manca D., Moramarco T., Riccardi N. (2023). Identification of hydrodynamic changes in rivers by means of freshwater mussels' behavioural response: an experimental investigation". Ecohydrology. 2023;e2544. https://doi.org/10.1002/eco.2544.

# Experimental investigation of flow around spillway ramps with varying spanwise widths towards successful downstream fish passage

Sedem KUMAHOR[1], Mark F. TACHIE[2], Haitham GHAMRY[3], Christos KATOPODIS[4]

[1,2] Department of Mechanical Engineering, University of Manitoba, Winnipeg, Canada
kumahors@myumanitoba.ca, mark.tachie@umanitoba.ca

[3] Department of Fisheries and Oceans Canada, Winnipeg, Canada,
haitham.ghamry@dfo-mpo.gc.ca
[4] Katopodis Ecohydraulics Ltd., Winnipeg, Canada,
katopodisecohydraulics@live.ca

ABSTRACT

An experimental investigation was conducted to elucidate the effects of varying spanwise blockage ratios (10%, 25%, 50%) on the turbulent flow characteristics around a 45º upstream spillway ramp. The experiments were conducted using a particle image velocimetry system and comprehensive analyses were performed to analyze the flow topology. The water depth over the spillway crest was maintained at 0.2*h*, where *h* is the height of the spillway model, and the oncoming flow velocity was maintained at 0.069 m/s for all tested cases. The preliminary results indicate that the flow topology near the bottom wall is significantly dependent on the spanwise blockage ratio of the ramps. However, regardless of the spanwise blockage, a recirculation bubble was consistently observed near the foot of the spillway. Notably, for the 10% blockage case, the recirculation bubble appeared smaller at the foot of the ramp, accompanied by lower magnitudes of turbulent kinetic energy along the test channel, potentially creating a more favorable pathway for downstream migration of fish.

## 1. Introduction

Hydroelectric dams and other anthropogenic barriers on watercourses negatively impact aquatic habitats, disrupting natural flow patterns and altering fish migration cycles (Katopodis & Williams, 2012). While there has been extensive research on upstream migrating fish since the early 20th century, progress in developing fishways for successful downstream passage has been significant. A previous experimental investigation on the turbulent flow around 45º and 30º upstream ramps that spanned the entire width of the standard spillway was performed at various water depths and oncoming flow velocities (Shirinzad et al., 2023). In this study the flow was homogenous in the spanwise direction. The results showed that a distinct recirculation bubble was formed at the foot of the standard 90º spillway model at the lowest water depth (0.2*h* above the crest of the spillway, where *h* is the height of the spillway), while the occurrence of such a bubble is suppressed by the presence of the 45º and 30º ramps. Furthermore, the flow dynamics around the 45º and 30º spillway ramps were similar and this investigation focused on the 45º ramp, since it would be shorter and more economical.

In practical real-world applications at dam sites, constructing a 45º ramp across the entire width of the water channel may not always be feasible. It may be more cost-effective to install the 45º ramp along the banks of the water channel and direct downstream migrating fish toward it. However, this would introduce significant spanwise inhomogeneity around the ramp, influencing the overall effectiveness of the spillway to pass downstream migrating fish. Furthermore, highly three-dimensional turbulent flows around spillways can influence the environmental conditions downstream, including water quality and sediment transport (Kondolf et al., 2014).

The present study seeks to investigate the modifying effects of different spanwise blockage ratios on the turbulent flow around the 45º spillway ramps. To achieve the set objectives, the flow around the 45º ramp was

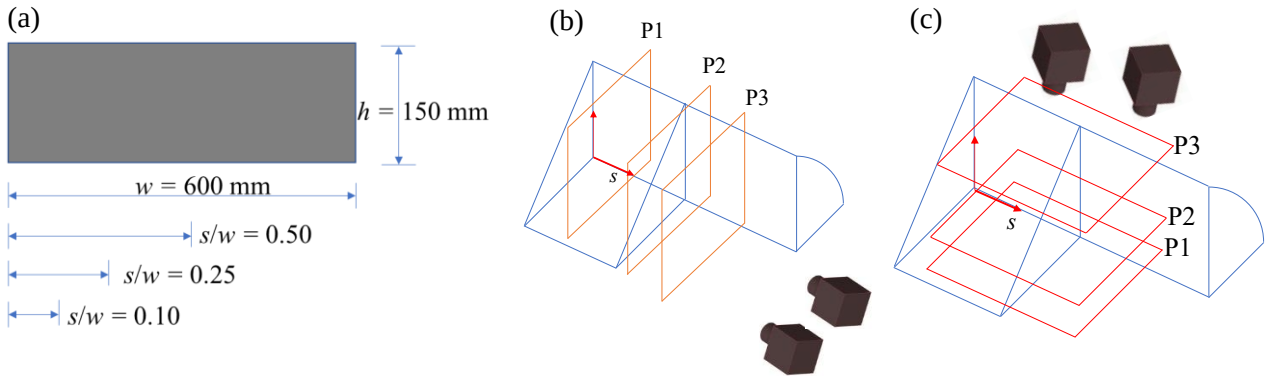



**Figure 1**: Schematic showing (a) front view of the standard 90º spillway (b) measurement positions (P1-P3) in the *x-y* plane and (c) *x-z* plane.

studied at a fixed water depth (0.2*h* above the crest of the spillway) and oncoming flow velocity (0.069 m/s), resulting in Reynolds and Froude numbers of 16500 and 0.08, respectively. Figure 1 shows a schematic of the test cases and camera positions. The spanwise width of the standard 90º spillway was $w$ = 600 mm and the spanwise width of the ramps were varied to achieve $s/w$ = 10%, 25% and 50% blockage (Figure 1(a)).

Velocity measurements were performed at multiple locations (P1-P3) in the streamwise-vertical (*x-y*) and streamwise-spanwise (*x-z*) planes to acquire comprehensive velocity data. In the *x-y* plane, P1, P2 and P3 were located at 0.5*s*, 15 mm from the edge of the ramp and 0.5($w$ – s), respectively. These positions are selected such that a measurement is made over the ramp, at the corner between the ramp and the downstream face, and the mid-point of the remaining water channel width. In the *x-z* plane, P1, P2 and P3 were located at 0.1*h*, 0.4*h* and 1.1*h*, respectively. The heights were selected such that, a location close to the bottom wall where positively thigmotactic fish may be found, within the recirculation zone and above the spillway crest are investigated. A planar particle image velocimetry (PIV) system was used to perform velocity measurements at the three indicated planes (P1-P3). Two cameras were positioned side-by-side on a traverse mechanism which allowed for simultaneous image capture in two fields of view. The PIV system was operated in a double-frame mode to ensure statistically independent samples and facilitate good convergence of turbulence statistics. The sampling rate was set to 3 Hz and a total number of 9000 images were acquired for each test condition, resulting in a total sampling time of 50 minutes per test condition. Velocity vectors were calculated using a GPU-accelerated multi-pass cross-correlation algorithm. The first pass used an interrogation area (IA) of 124 pixels × 124 pixels with 50% overlap and four final passes used an IA of 24 pixels × 24 pixels with 75% overlap. The resulting vector spacing was 0.87 mm (0.0058*h*).

The results indicate that the flow upstream of the ramp is significantly affected by the spanwise aspect ratio, leading to pronounced spanwise inhomogeneity near the bottom wall. Regardless of the spanwise blockage, a recirculation bubble was consistently observed near the foot of the spillway. At 10% blockage, the recirculation bubble appeared to be smaller at the foot of the ramp, accompanied by lower magnitudes of turbulent kinetic energy along the test channel. Based on these findings, the 10% blockage ratio may offer more favorable conditions for fish passage, suggesting that it could be a more suitable configuration to minimize the avoidance of fish navigating the spillway.

In the full paper, a detailed literature review and a complete description of the test facility and measurement procedures will be presented. Mean flow topology, turbulent kinetic energy, one-dimensional profiles and two-point correlation analyses would be performed to elucidate the impact of various ramp blockage ratios on the turbulent flow upstream of the spillway.

**Acknowledgements**

We are grateful to Canada Foundation for Innovation (CFI) for funding for the experimental facility.

**References**

Katopodis, C. & Williams, J. G. (2012). The development of fish passage research in a historical context. *Ecological Eng.*, *48*, 8-18.
Kondolf, G. M. et al. (2014), Sustainable sediment management in reservoirs and regulated rivers: Experiences from five continents, *Earth's Future*, *2*, doi:10.1002/2013EF000184.
Shirinzad, A., Kumahor, S., Tachie, M. F., Ghamry, H., and Katopodis, C. (2023). Investigation of turbulent flows using spillway models aiming to aid downstream migration of fish. *River Research Application*, 1-12 https://doi.org/10.1002/rra.4132

# An Ecohydraulic Approach for 2D Hydraulic Modelling of a Regulated River Reach

Frida M. NIEMI[1], Anders G. ANDERSSON[1], J. Gunnar I. HELLSTRÖM[1]

[1] Division of Fluid and Experimental Mechanics, Luleå University of Technology, Luleå, Sweden
frida.niemi@ltu.se
anders.g.andersson@ltu.se
gunnar.hellstrom@ltu.se

ABSTRACT

With an increase in intermittent energy sources the energy supply becomes more unpredictable. The flexibility of hydropower is predicted to be more utilized to stabilize fluctuations and meet the demand in energy peaks. The increase of hydropeaking, frequent and rapid changes of discharge from the hydropower facilities, can impact the ecology of the river downstream. To capture the dynamics correctly and understand how modelling parameters could influence the hydrodynamics in the river, and in turn impact the habitat quality, this study investigates how sensitive a 2D hydraulic model is for different mesh properties, Manning roughness coefficient and downstream boundary conditions. The study determines how responsive the hydraulic model is to these parameters and how sensitive the results of ecohydraulic variables are in relation to this. Preliminary results show the differences in Manning coefficient for the Neumann gradient downstream boundary condition versus the water level boundary from measurements where the Neumann gradient tend to be more sensitive to changes in Manning numbers than the water level definition.

## 1. Introduction

Capturing the river dynamics in the 2D hydraulic model is essential in order to determine if an area is feasible for fish habitat since the ranges of the preferred hydraulic parameters are narrow and therefore small differences can have a large impact on habitat estimations (Gönczi 1989). One important factor to capture in the model is the roughness of the riverbed due to the influence on the bed shear stress. Manning's roughness formula is commonly used to compensate for the roughness that is not captured by the bathymetry. The mesh properties, in terms of resolution and structure, influences the Manning roughness to compensate for the errors in the discretization of the bathymetry for different meshes such as curvilinear and triangular elements (Bilgili et al. 2023). When changing the friction values, variables such as discharge and depth averaged velocities are affected, however they are also affected by the shape of the mesh elements (Bomers et al. 2019).

The downstream boundary condition when modelling rivers is commonly the Neumann water level gradient or a specified water level from field measurements (Dirichlet condition). With the Neumann water level gradient, the Manning roughness will be changing since the two parameters are dependent on each other. This study investigates the sensitivity of these parameters for a 2D hydraulic model over a regulated river. Mesh properties, bed roughness, downstream boundary and calibration method are evaluated where the sensitivity of various model parameters on the model outcome is assessed by examining the results of depth-averaged velocities, depths, bed shear stress and the hydraulic response for different boundary conditions.

## 2. Study Site & Method

The study site is a regulated river in the northern part of Sweden, a part of Luleälv, located between two hydropower stations. The software used for the hydraulic modelling is Delft3D FM from Deltares, where a hybrid mesh, curvilinear and triangular elements, and a curvilinear mesh is investigated since these have been proven to be most computational efficient and accurate (Bomers et al. 2019, Bilgili et al. 2023). To

calibrate and validate the model, water level measurements from six pressure loggers, with an uncertainty of ±0.1 m in Water Surface Elevation (WSE), is used together with velocity measurements from an acoustic doppler current profiler (Andersson et al. 2022). To decide which Neumann numbers that is most interesting to investigate, a parametric sweep from 1e-07 to 1e-03 was conducted with a constant Manning roughness. The Neumann's that gave reasonable wetted area was below 8e-06 where the estimated value from the water level measurements was 2e-05. Hence, 2e-05, 3e-06, 1e-06 and 8e-07 were chosen for further studies. Then a parametric sweep were performed for a range of relevant Manning coefficients (0.01-0.12).

## 3. Preliminary Results & Conclusions

The result of the parametric sweep of the Manning roughness for the curvilinear mesh is presented in Table 1 where the computational domain were divided into six parts centered around each measurement point. The two presented values for each area represent the initial values obtained from the parametric sweep and the final calibration. The initial values failed to give acceptable water levels and the roughness was adapted after this. The surface levels for the 2e-05 Neumann condition are not presented since no roughness value reached acceptable water levels. Resulting water levels in relation to the measured one of the calibrated models according to Table 1 is presented in Fig.1.

**Table 1.** Manning roughness for the downstream boundaries

| Measurement point: | 1 | 2 | 3 | 4 | 5 | 6 |
|---|---|---|---|---|---|---|
| Neumann 3e-06 | 0.01/0.005 | 0.09/0.05 | 0.10/0.06 | 0.11/0.04 | 0.12/0.10 | 0.12/0.1125 |
| Neumann 1e-06 | 0.01/0.01 | 0.07/0.07 | 0.07/0.07 | 0.07/0.04 | 0.07/0.07 | 0.07/0.075 |
| Neumann 8e-07 | 0.01/0.01 | 0.07/0.04 | 0.07/0.05 | 0.06/0.03 | 0.08/0.07 | 0.08/0.07 |
| Water Level | 0.01/0.01 | 0.08/0.07 | 0.10/0.08 | 0.06/0.01 | 0.11/0.10 | 0.12/0.12 |

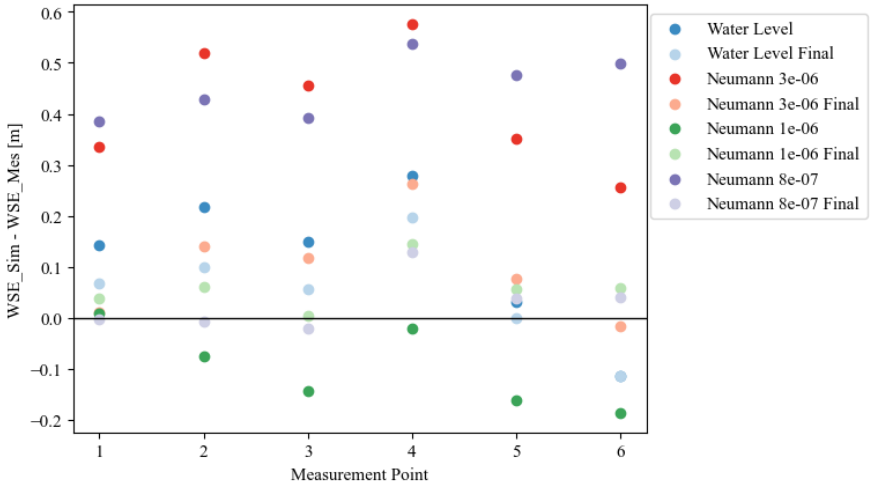



**Fig. 1.** Water levels for the initial and final Manning roughness distribution.

All downstream boundaries give acceptable water levels in the measurement points except in point four. Decreasing the Manning roughness below 0.04 did not change the water levels significant as seen for the water level boundary. Neumann 1e-06 and 3e-06 are most comparable with the water level boundary when comparing the Manning roughness distribution. Another approach on getting an estimation of the Neumann gradient could be to first calibrate the model with the water level boundary condition and then make a parametric sweep of the Neumann gradient. This however is not yet investigated. The models will be compared further by investigating ecohydraulic variables, such as the depth-averaged velocities, bed shear stress and hydraulic response.


### Acknowledgements

This project has received funding from the Swedish Center for Sustainable Hydropower. The center is a competence center that focus on research in the field of environment and society, water construction and turbines.


### References


Andersson, A.G., & Lycksam, H. (2022). Hydraulic Modelling of a Regulated River Reach on Different Scales to Evaluate its Inherent Environmental Conditions. IAHR World Congress, 39, 4189-4195.

Bilgili, E., Bomers, A., van Lente, G.-W., Huthoff, F., & Hulscher, S. J. M. H. (2023). The effect of a local mesh refinement on hydraulic modelling of river meanders. River Research and Applications, 39(5), 832–846.

Bomers, A., Schielen, R.M.J., & Hulscher, S.J.M.H. (2019). The influence of grid shape and grid size on hydraulic river modelling performance. Environmental Fluid Mechanics 19:1237-1294.

Gönczi, A.P. (1989). A study of physical parameters at the spawning sites of the European grayling (Thymallus thymallus L.). Regulated Rivers: Research & Management, 3(1), 221-2247.

# Effects of weir installed at the bypass entrance of bar rack systems on hydraulic conditions and behavior of downstream migrating fish

Seyed Sobhan ALEYASIN[1], Xingjun FANG[2], Mark Francis TACHIE[3], Christos KATOPODIS[4] and Haitham GHAMRY[5]

[1,3]Department of Mechanical Engineering, University of Manitoba, Winnipeg, Manitoba, Canada
aleyasss@myumanitoba.ca, mark.tachie@umanitoba.ca

[2]Institute of Mechanics, Chinese Academy of Sciences, Beijing, People's Republic of China
fangxj@imech.ac.cn

[4]Katopodis Ecohydraulics Ltd., Winnipeg, Manitoba, Canada
katopodisecohydraulics@live.ca

[5]Fisheries and Oceans Canada, Winnipeg, Manitoba, Canada
haitham.ghamry@dfo-mpo.gc.ca

ABSTRACT

The flow field in the bypass of a bar rack system was studied using particle image velocimetry systems to understand the effects of weirs placed at the bypass entrance on hydraulic conditions used to guide fish moving downstream. Three test cases were studied: no weir, triangular weir and arc-shaped weir. Mean velocities, Reynolds stresses and turbulent kinetic energy (*TKE*) are examined. The weirs deflect the flow away from the channel bed and increase the bypass velocity significantly, though remains under the suggested critical value of 1 m/s. There is an increase in the level of Reynolds stresses and *TKE* in the vicinity of the weirs and the shear layers issuing from the weir tips, though *TKE* remains in the most suitable range for fish.

## 1. Introduction

Flow connectivity in freshwater systems is crucial to healthy aquatic ecosystems that support human and aquatic life, biodiversity, and ecological function (Reid et al., 2019). Hydroelectric structures are among the most common anthropogenic barriers to fish migration which include powerhouses with turbine intakes, spillways and bypasses. Since fish passing through turbines may suffer high levels of mortality, safe migration routes are crucial. Bar rack systems are commonly used to safely guide fish downstream and effective bypass design relies on suitable hydraulics (Katopodis and Williams, 2012). The hydraulic conditions associated with the bar rack system depend on various parameters including cross-section area, shape of the bars, bar spacing as well as the width of the bypass. The bypass entrance geometry is critical for generating hydraulic conditions that ensure fish enter and continue moving downstream, rather than swim back upstream. In this study, the impact of the presence of a small obstacle/weir at the inlet of the bypass on the hydraulic conditions is investigated to guide downstream migrating fish more effectively.

## 2. Experimental Setup

The experimental study was performed in a recirculating water channel with the approach velocity of $\boldsymbol{U}_\infty$ = 0.38 m/s. The same bar rack system examined by Fang et al. (2023) was adopted. The bar rack consisted of 16 vertical bars with a bar cross-section of 10 mm × 100 mm, a bar height of 450 mm and a bar spacing of 50 mm. The bars were connected using horizontal bottom and top overlays. The inclination angles of the rack and bars with respect to the approaching flow were $\alpha = 30°$ and $\beta = 45°$, respectively. A bypass with a width of 78 mm was created by installing a vertical plate where the bar racks terminate. The measurements were performed for two weirs, triangular and arc-shaped, installed at the entrance of the bypass as well as a reference configuration (no weir). The triangular weir is a right-angled isosceles triangle with sides of h = 50 mm and a width equal to that of the bypass. The arc-shaped weir has a horizontal side of 65 mm and a maximum height of $h$ = 50 mm. The velocity fields were measured in the mid-span plane of the bypass using two different

configurations of particle image velocimetry (PIV) systems provided by LaVision Inc., namely, two dimensional-two component (2D-2C) PIV and stereo PIV (2D-3C).

## 3. Preliminary Results and Conclusions

The contour plots of streamwise mean velocities, $U/U_\infty$, for the reference case and the triangular weir are presented in Fig. 1. The contour plots of the arc-shaped are qualitatively similar to those of the triangular weir and therefore, due to space limitation are not presented. Figure 1a shows that for the reference case $U/U_\infty \approx$ 1.62 at *x/d* = - 6 and the flow accelerates as it approaches the bypass, leading to the peak value of $U/U_\infty \approx$ 1.95. At the bypass entrance, $U/U_\infty$ > 1.5. The value is consistent with Ducharme's (1972) recommendation for effective guidance for juvenile Atlantic salmon (*Salmo salar*). The effects of weirs on the mean velocity field in the region of *x/h* < -3 are almost negligible. As the flow approaches the weirs, it decelerates due to the blockage effect and deflects away from the bottom wall (Fig. 1b). The lack of recirculation areas upstream of the weirs creates a favorable condition for fish passing over the weirs. Above the weirs, the flow accelerates as it approaches the bypass and reaches $U_{max}$ = 0.95 m/s and 0.97 m/s for the arc-shaped and triangular weirs, respectively. Therefore, $U_{max}$ in the bypass is lower than the 1 m/s threshold recommended in the literature.

The normalized contour plots of streamwise, $\overline{u'u'}/U_{max}^2$, and vertical, $\overline{v'v'}/U_{max}^2$, Reynolds normal stresses are presented in Fig. 2. For the reference case, the variation in the Reynolds stress distribution is negligible and the values are very small. For the weir cases, there is an increase in the level of Reynolds stresses, particularly in the vicinity of the weirs and the shear layers emanating from their trailing edge. Although the distributions of Reynolds stresses are qualitatively similar, the values of $\overline{v'v'}$ are considerably lower than those of $\overline{u'u'}$. The study of turbulent kinetic energy, *TKE*, (not shown) showed that for all cases *TKE* ≤ 0.05 m$^2$/s$^2$, indicating that *TKE* is in the most suitable range for fish to move toward the bypass.

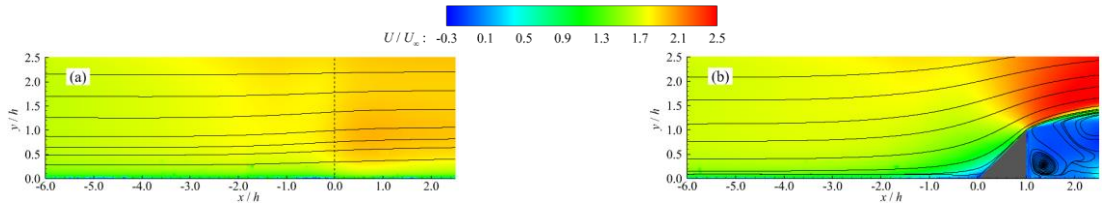



Fig. 1. Contours of streamwise mean velocity for (a) reference case and (b) triangular weir measured at the mid-span plane of the bypass. The mean streamlines are superimposed on the contours. The dashed line in (a) represents the bypass entrance.

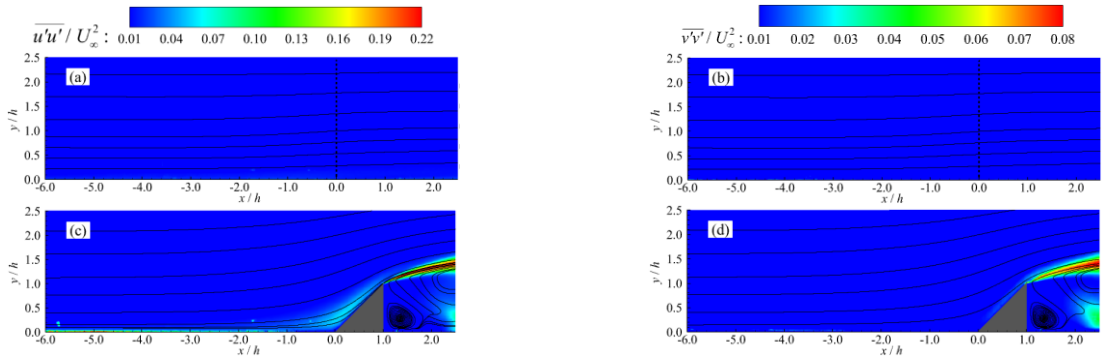



Fig. 2. Contours of streamwise (left) and vertical (right) Reynolds stresses for [(a) and (b)] reference case and [(c) and (d)] triangular weir

In the final paper, the contours of mean velocity, Reynolds stresses and turbulent kinetic energy for all test cases will be presented. Turbulence eddies will also be examined due to their importance on fish behavior. It is observed that the shape of eddies is greatly impacted by the weirs, assisting fish toward the bypass.

**Acknowledgments**

The authors are grateful to the Department of Fisheries and Oceans Canada for funding this research.

**References**

Ducharme, L.J.A. 1972. "Application of louver deflectors for guiding Atlantic salmon" *Journal of the Fisheries Board of Canada* 29 (10): 1397–1404.

Fang, X., M. F. Tachie, C. Katopodis, and H. Ghamry. 2023. "Using PIV to improve bar rack guidance for downstream migrating fish" *Proceeding of the 40th IAHR World Congress*, Vienna, Austria.

Katopodis, C., and J. G. Williams, J.G. 2012. "The development of fish passage research in a historical context" *Ecological Engineering* 48: 8-18.

Reid, A.J., Andrew K. Carlson, Irena F. Creed, Erika J. Eliason, Peter A. Gell, Pieter TJ Johnson, Karen A. Kidd et al. 2019. "Emerging threats and persistent conservation challenges for freshwater biodiversity." *Biological Reviews* 94 (3): 849-873.

# Hydropeaking frequency: implications for fish stranding and river management

Daniel S. HAYES[1], Stefan AUER[2], Simon FÜHRER[3], Franz GREIMEL[4], Diego TONOLLA[5], Nico BÄTZ[6], Christine WEBER[7], Günther UNFER[8], Bernhard ZEIRINGER[9], Kevin MERL[10], Luiz SILVA[11], Robert NAUDASCHER[12], Lorenzo GORLA[13], Stefan SCHMUTZ[14]

[1,2,3,4,8,9,10,14] University of Natural Resources and Life Sciences, Vienna, Department of Water, Atmosphere and Environment, Institute of Hydrobiology and Aquatic Ecosystem Management, Austria
email: daniel.hayes@boku.ac.at

[5] Institute of Natural Resource Sciences, Zurich University of Applied Sciences, Wädenswil, Switzerland

[6,7] Eawag, Swiss Federal Institute of Aquatic Science and Technology, Surface Waters – Research and Management, Kastanienbaum, Switzerland

[11,12] Stocker Lab, Institute of Environmental Engineering, Department of Civil, Environmental and Geomatic Engineering, ETH-Zurich, Zurich, Switzerland

[13] Federal Office for the Environment FOEN, Bern, Switzerland

ABSTRACT

The scientific and management discourse on hydropeaking flow-ecology relationships has largely focused on assessing biotic effects related to flow metrics of single hydropeaking events. The ecological effects of re-occurring peaking have been rarely studied to date, albeit this being a key issue due to the deregulation of the energy market and increased share of volatile energy sources, causing an increase in hydropeaking frequency. Particularly regarding stranding, an increase in hydropeaking frequency might be disastrous, leading to adverse ecological effects ranging from individual organisms and upscaling to entire populations. Therefore, this study endeavors to advance the discourse on hydropeaking frequency, particularly in the context of fish stranding. We explore the effects of stranding due to repeated hydropeaks on both individual fish and their populations. Our synthesis draws from a comprehensive review of both the peer-reviewed and grey literature, enriched with insights from empirical fieldwork and experimental datasets.

## 1. Introduction

The existing research on hydropeaking largely examines the biological impacts of flow intensity parameters like peak magnitude or ramping rate (Moreira et al., 2019). Yet, hydropeaking involves frequent and rapid flow changes, sometimes occurring several times a day, a phenomenon that has been understudied despite its growing relevance due to the rise of intermittent green energy sources like wind and solar, necessitating more frequent hydropeaking to compensate for energy production gaps, a situation exacerbated by the deregulation of energy markets. Increased hydropeaking frequency poses significant risks for fish through stranding, affecting fish populations and communities in hydropeaked rivers (Hayes et al., 2021). Despite this, most studies have focused on the effects of individual peaking events rather than the frequency of hydropeaking. This article seeks to advance the discussion on hydropeaking frequency and its effects on fish stranding, synthesizing current knowledge through the literature, complemented by field and experimental data.

## 2. Results

To explore the cumulative impact of repeated hydropeaking events on fish mortality, we simulated the decline of grayling (*Thymallus thymallus*) larvae across 20 consecutive down-ramping events, based on stranding rates from outdoor flume studies (Auer et al., 2014). Assuming all stranded fish die and react uniformly to each event without considering natural mortality, our model shows that rapid down-ramping rates of 0.5 or 2.9 cm/min could nearly eradicate the larvae population within 18 or 7 events, respectively.

Even slower down-ramping rates of 0.1 or 0.2 cm/min could reduce the population by 66% to 88% after 20 events (Fig. 1a).

Analyzing fish sampling sites from Austrian mountain rivers (Hayes et al., 2021), we found a clear negative correlation between peaking frequency and the 'Fish Index Austria' (Fig. 1b), indicating a significant decline in fish community health with an increase in daily hydropeaking events ($\rho$=0.45, $p<0.001$). Sites experiencing less than one peak per day had an average index score of 2.98 ±0.93 SD, while those with more than one peak per day showed a poorer average score of 4.16 ±0.86 SD. Moreover, almost all sites meeting the Water Framework Directive's good ecological status had fewer than one peak per day.

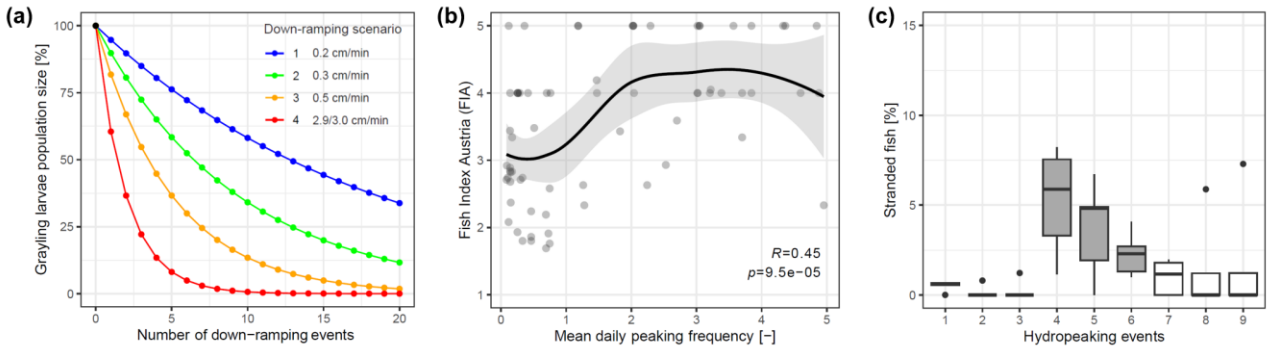



**Fig. 1.** (a) Hypothetical decline of grayling larvae based on mean stranding rates from outdoor flume experiments during the day (Auer et al., 2014), (b) relationship between daily peaking frequency and the 'Fish Index Austria' (1 being best, 5 worst) in Austrian rivers (Hayes et al., 2021), and (c) boxplot of juvenile grayling stranding during nine consecutive hydropeaking events (Auer et al., 2014).

Experimental studies are crucial to determine how stranding risks for fish might change with repeated events. Auer et al. (2014) investigated the stranding of juvenile grayling over nine consecutive hydropeaks within a 24-hour period, structured into three daytime peaks, followed by three nighttime peaks, and concluding with three more peaks the next morning. Initial daytime peaks resulted in minimal stranding, likely due to the fish's larger size (60-75 mm). However, stranding rates increased during the night, but were still lower than in trials with similar ramping patterns. Interestingly, stranding decreased across the nighttime peaks, suggesting the removal of 'weak' fish or an adaptation effect. The subsequent daytime peaks showed lower stranding rates than at night but were higher than the initial daytime rates, indicating potential stress or fatigue from the multiple hydropeaking events (Fig. 1c).

## 3. Discussion

In this study, we aimed to deepen the understanding of how the frequency of hydropeaking events affects fish stranding, integrating recent data and findings. Our review highlights the significant threat that hydropeaking poses to young-of-the-year fish in alpine rivers, with a clear link between more frequent hydropeaking and greater ecological damage to fish communities. Even though experimental data suggests that fish may adapt behaviorally to frequent flow changes, these adaptations cannot compensate for the cumulative effects of stranding due to repeated hydropeaking. Such cumulative effects appear to potentially harm not just individual fish but also populations and ecosystems. Today's hydropeaking mitigating strategies fall short addressing these broader ecological and long-term impacts of hydropeaking. By combining insights on the increased risk of fish stranding with the observed potential for cumulative impacts, we underline the urgent need for comprehensive river management strategies that consider both the frequency of hydropeaking events and their ecological consequences. This holistic perspective is crucial for guiding future research and developing effective mitigation practices to protect riverine ecosystems.

## Acknowledgements

This research was funded in whole, or in part, by the Swiss Federal Office for the Environment [BAFU-442.3-64886/2], the Austrian Science Fund (FWF) [P 34061-B], and the Christian Doppler Research Association.

## References

Auer S, Fohler N, Zeiringer B, Führer S (2014) Experimentelle Untersuchungen zur Schwallproblematik.

Hayes DS, Lautsch E, Unfer G, Greimel F, Zeiringer B, Höller N, Schmutz S (2021) Response of European grayling, *Thymallus thymallus*, to multiple stressors in hydropeaking rivers, Journal of Environmental Management, 292, 112737

Moreira M, Hayes DS, Boavida I, Schletterer M, Schmutz S, Pinheiro A (2019) Ecologically-based criteria for hydropeaking mitigation: A review, Science of the Total Environment, 657, 1508-1522

# Assessment of Restoration Success by Hydromorphological Parameters: Lessons Learned from a Riprap Removal

Katinka KOLLl[1], Tobias WUNSCH[2], Michael VIEWEG[3]

[1] Technische Universität Braunschweig, Leichtweiß-Institute for Hydraulic Engineering and Water Resources, Division for Hydraulic Engineering and River Morphology, Germany
katinka.koll@tu-bs.de

[2] Stadt Braunschweig, Fachbereich Umwelt, Abt. 68.2-Gewaesser- und Bodenschutz, Germany
tobias.wunsch@braunschweig.de

[3] Helmholtz Centre for Environmental Research (UFZ), Department Conservation Biology, Germany
michael.vieweg@ufz.de

ABSTRACT

Hydromorphology is one of the two quality components supporting the evaluation of the ecological quality of a river reach according to the specifications of the European Water Framework Directive (WFD). However, a standard procedure for definition and classification of hydromorphological parameters is still not available. A common definition would allow to compare different restoration projects, and a classification is needed to evaluate the success of a restoration measure. At present, recommended parameters are based on cross-sectional surveys, and a measure is considered as successful if the diversity or variability of considered parameters increased.

A project that was carried out to investigate the development of restoration measures demonstrated the need for an analysing procedure that is applicable for areal data but not depend on cross-sectional data. The results revealed that a high diversity of a hydromorphological parameter does not necessarily indicate a natural state of the river section.

## 1. Introduction

Hydromorphological parameters are hydraulic and morphological parameters, like water depth, water level width and velocity, that are determined as a function of characteristic hydrological events, e.g. annual mean or bankful discharge. Since the implementation of the WFD several suggestions for hydromorphological parameters are published. The data are analysed statistically to check if the diversity or variability of the parameters increased, which commonly is taken as a measure that a restored reach develops towards a natural state. The recommended hydromorphological parameters are based on cross-sectional surveys, however, nowadays field surveys aim to get area data at least for the topography. Thus, the analysing procedures should be applicable for area data.

In the project ‘Wilde Mulde’ (Schulz-Zunkel et al. 2022) the development of river restoration measures was investigated. For three sites the floodplain topography was measured by remote sensing and the river bed was scanned with an echo sounder. A procedure was developed to analyse data gained from areal surveys. It includes selection of the up- and downstream borders of a river reach as well as the determination of the left and right bank position, which is not obvious for natural slip-off banks. Moreover, the data have to be interpolated, and subregions have to be determined, especially when analysing a river bend.

## 2. Study sites

The river Mulde is a meandering lowland gravel bed river in Germany. One of the restoration measures was removing the riprap at the outer bank of a bend over a length of about 600 m to enable lateral erosion (site UG2). Besides the restored reach two reference sites were surveyed to compare the development of the

restoration with the general development of the river. Site UG1 represents a modified river reach with riprap protected banks on both sides. Site UG3 is a natural reach without any protection. The sites are shown in Fig. 1.



**Fig. 1.** Study sites - left: UG1 modified reach, middle: UG2 riprap removal reach, right: UG3 natural reach (views in flow direction).

Data are available from three surveys, one just before restoration and two more in the first and second year after removal of the riprap in UG2.

## 3. Results

As an example for the development of the three sites within the three years of survey the standard deviation of the bed levels is shown in Fig. 2. The irregularly spaced echo sounding data were interpolated to get a 1x1 m spaced grid. The upstream and downstream end of a reach was determined by analysing the change of vectors along the main river course. The remote sensing data were used to determine the positions of the left and right bank. The areas belonging to cut bank and slip-off bank were defined by the mean bed level height and its standard deviation determined in the whole reach.

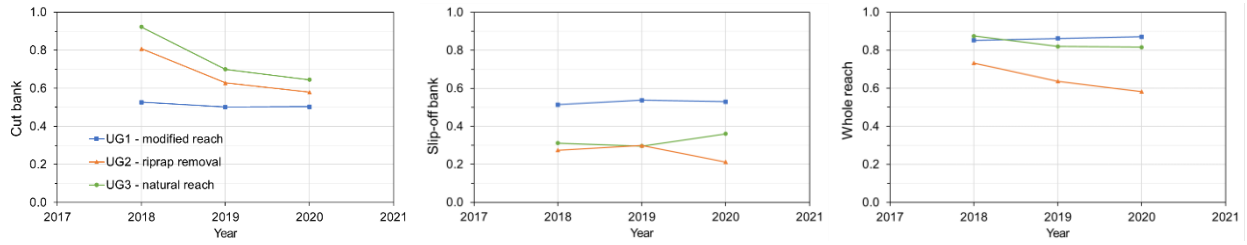



**Fig. 2.** Standard deviation of the bed levels [m] - left: for the cut bank area, middle: for the slip-off bank area, right: for the river reach between left and right bank.

In the cut bank area the standard deviation of the bed levels at the restoration side (UG2) decreased after removing the riprap, which seams to indicate that the measure was not successful. However, this parameter decreased also in the natural reach, which demonstrated that this was a natural process. A flood with almost bankfull discharge, occurring between the surveys of 2018 and 2019, caused erosion and collapse of the unprotected banks. For the slip-off banks the standard deviation at the modified reach was highest. The indication of a natural site by a high variability would lead to the conclusion that the riprap protected bank in UG1 is more natural than the unprotected bank in UG3. The values for the restored and the natural site are close in 2028 and 2019, but deviate in 2020 because the value decreased for the restored site and increased for the natural site. The reason is not clear, yet. For the analysis of the whole reach it is interesting to note that the standard deviations were very similar for the modified and the natural reach and quite constant within the three years of survey. The values for the restored site were lower and decreased with the years. This demonstrates that more sophisticated criteria than simply a higher diversity or variability are needed to evaluate hydromorphological parameters, and specifications of the morphology need to be taken into account. The analysing procedure and detailed results will be presented at the conference.

**Acknowledgements**

The project ‘Wilde Mulde—Restoration of a dynamic riverine landscape in Central Germany’ (funding label: 01LC1322B-F) was funded by the Federal Ministry of Education and Research (BMBF) and the Federal Agency for Nature Conservation (BfN) with funds also from the Federal Ministry for the Environment, Nature Conservation and Nuclear Safety (BMU) in Germany (funding code: 01LC1322C). The BMBF was funding this project as an Initiative for Sustainable Development (FONA).

**References**

Schulz-Zunkel, C., Seele-Dilbat, C., Anlanger, C., Baborowski, M., Bondar-Kunze, E., Brauns, M., Gapinski, C., Gründling, R., Haaren, C. v., Hein, T., Henle, K., Junge, F., Kasperidus, H. D., Koll, K., Kretz, L., Rast, G., Schnauder, I., Scholz, M., Schrenner, H., Dziock, F. (2022). Effective restoration measures in river-floodplain ecosystems: Lessons learned from the ‘Wilde Mulde’ project. International Review of Hydrobiology, 1–13. https://doi.org/10.1002/iroh.202102086

# Evaluation of tree root depth and piezometric level in a historical botanical urban garden in Lisbon city, Portugal

Maria Paula MENDES[1], Ana Paula FALCÃO[1], Nuno AFONSO[1], Miguel ESTEVES[2], Maria Catarina PAZ[3]

[1]CERIS, Instituto Superior Técnico, Universidade de Lisboa, Portugal
mpaulamendes@tecnico.ulisboa.pt
ana.p.falcao@tecnico.ulisboa.pt
nunofafonso@tecnico.ulisboa.pt

[2]CEG, Instituto de Geografía e Ordenamento do territorio, Universidade de Lisboa, Portugal
m.esteves@ciencias.ulisboa.pt

[3]ESTBarreiro, Instituto Politécnico de Setúbal, Portugal
catarina.paz@estbarreiro.ips.pt

ABSTRACT

The Lisbon botanical Garden, dating back to the 19th century, is home to nearly 18,000 of plants species from around the world. As construction work is being planned that involves soil excavation near the garden boundaries, it is crucial to establish whether tree roots can access the groundwater level in the area potentially affected by this work. Given the garden´s natural and historical significance, our research was conducted using non-invasive techniques, such as near-surface geophysics. Specifically, electrical resistivity tomography (ERT) and ground-penetrating radar (GPR) were employed to assess tree root depth and establish the saturated zone, respectively. The applied methodology allowed us to determine that: (1) groundwater levels were higher in May 2021 compared to October 2020, ranging between 3 and 2.7 meters, and 4 and 3 meters, and (2) the mean root system depth is approximately between 2.5 and 3.0 meters. The results obtained will assist in defining mitigation measures and guidelines to prevent the loss of these important species.

## 1. Introduction

Situated in the heart of Lisbon, in the Príncipe Real district, the 1878 Lisbon Botanical Garden is home to an enormous diversity of plants, and it is particularly rich in tropical species from New Zealand, Australia, China, Japan, and South America. Preserving the *in-situ* conditions of certain collections, notably palm trees and cycads, is of utmost importance due to their significance.

Lisbon enjoys a mild Mediterranean climate, characterized by a dry period of five months from May to September. The garden's terrain features rough and irregular relief, a result of its natural geomorphological evolution. A prior survey identified an upper landfill layer, with maximum depth of 13 m, consisting of sandy-clay deposits containing limestone and basalt fragments/blocks, fossil remnants, and various materials (e.g., plastic, wood, bricks). Our study is focused on this layer, as it encompasses the root zone and the upper phreatic zone. These landfill deposits are recharged by precipitation, irrigation water, and seepage from the water and sewage distribution networks.

Electrical resistivity tomography (ERT) is a non-invasive approach that is well-suited for assessing root zone. It relies on the sensitivity of soil resistivity to factors such as moisture content, density, lithology, and the presence root. ERT can provide valuable insights while causing minimal disruption to the site, as indicated in previous studies (Nijland et al., 2009; Octavian et al., 2020; Vanderborght et al., 2013). Ground-penetrating radar (GPR) is another non-invasive technique that proves useful for determining groundwater table, particularly in garden pathways (Essam et al., 2020; Paz et al., 2017). GPR operates by emitting electromagnetic radar pulses within a frequency of 10–1000 MHz to create subsurface images.

In order to determine whether tree roots can access the groundwater table in two plots, we conducted a total of two Electrical Resistivity Tomography (ERT) profiles and three Ground-Penetrating Radar (GPR) profiles on two separate dates: 17 October 2020 and 7 May 2021. This research is of utmost importance in ensuring

the protection of the trees, especially given the construction plans that involve soil excavation near the garden's vicinity. These construction activities could potentially alter the groundwater flow, making the study essential for safeguarding the trees' well-being.

## 2. Results

The three GPR profiles showed that the groundwater levels were higher in May 2021 compared to October 2020, ranging between 3 and 2.7 meters, and 4 and 3 meters, respectively (Fig. 1). These values align with previous studies that utilized piezometers to measure groundwater levels and obtained similar results within this range. The three ERT profiles provided insight into the depth of the root zone, which was found to be approximately between 2.5 and 3.0 meters deep. This implies that nearly all the roots in the two plots can access the water table during the springtime. An example of the ERT profile obtained in October 2020 is depicted in Fig. 1, where the root zone is characterized by higher resistivity values (40 ohm m and 140 ohm m).

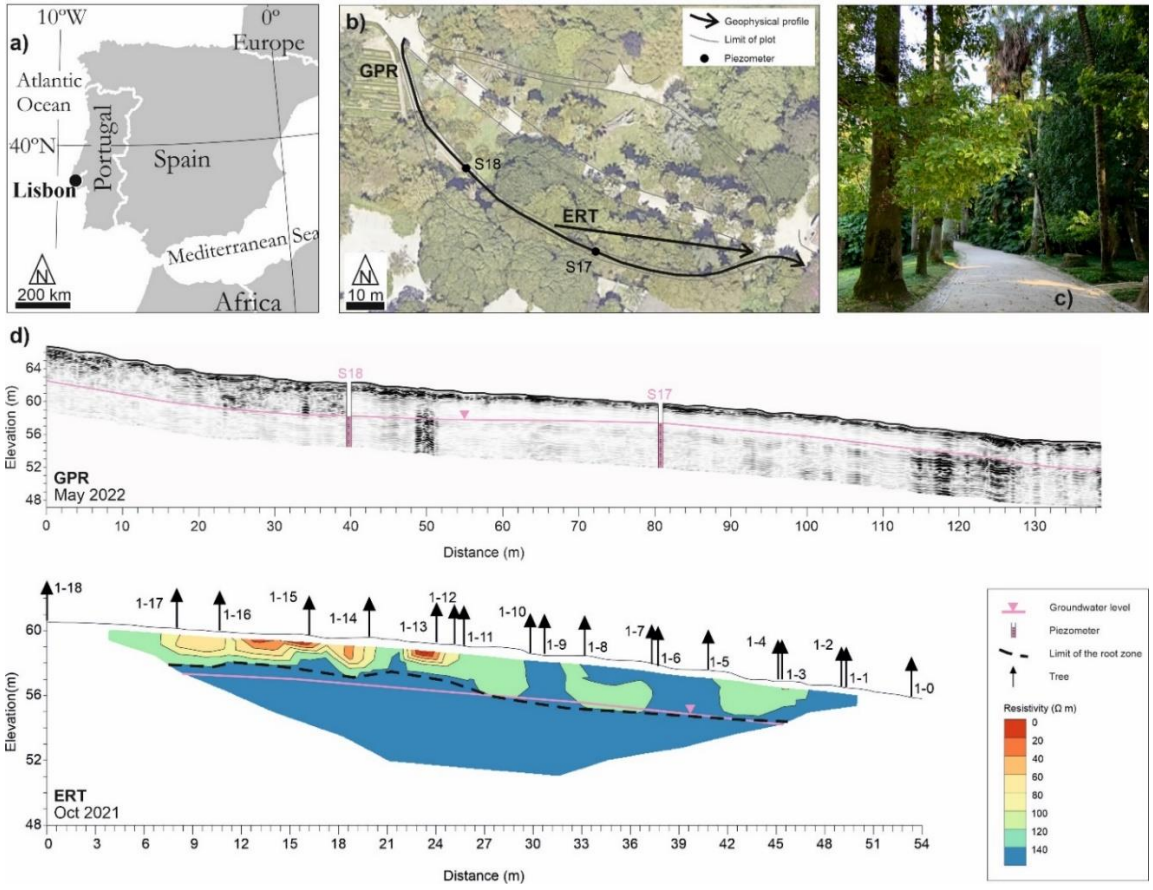



**Fig. 1.** a) Location of Lisbon Botanical Garden; b) detail of Lisbon Botanical Garden with the location of the geophysical profiles; c) example of trees and pathways of the garden; d) ground penetrating radar (GPR) and electrical resistivity tomography (ERT) models.

**Acknowledgements**

M. P. Mendes, A. P. Falcão and N. Afonso acknowledge the Portuguese Foundation for Science and Technology (FCT) and research unit CERIS (UIDB/04625/2020). We are grateful to Instituto Dom Luiz, F.C., for providing the geophysical equipment.

**References**

Essam, D., Ahmed, M., Abouelmagd, A., Soliman, F., 2020. Monitoring temporal variations in groundwater levels in urban areas using ground penetrating radar. Sci. Total Environ. 703, 134986. https://doi.org/https://doi.org/10.1016/j.scitotenv.2019.134986

Nijland, W., Meijde, M. Van Der, Addink, E.A., Jong, S.M. De, 2009. Detecting soil water use by Mediterranean vegetation on rocky soils using electrical resistivity tomography Catena Detection of soil moisture and vegetation water abstraction in a Mediterranean natural area using electrical resistivity tomography. Catena 81, 209–216. https://doi.org/10.1016/j.catena.2010.03.005

Octavian, M., Kuras, O., Pridmore, T., Mooney, S.J., 2020. Potential of geoelectrical methods to monitor root zone processes and structure : A review. Geoderma 365. https://doi.org/10.1016/j.geoderma.2020.114232

Paz, C., Alcalá, F.J., Carvalho, J.M., Ribeiro, L., 2017. Current uses of ground penetrating radar in groundwater-dependent ecosystems research. Sci. Total Environ. 595, 868–885. https://doi.org/https://doi.org/10.1016/j.scitotenv.2017.03.210

Vanderborght, J., Huisman, J.A., van der Kruk, J., Vereecken, H., 2013. Geophysical Methods for Field-Scale Imaging of Root Zone Properties and Processes, in: Soil–Water–Root Processes: Advances in Tomography and Imaging. John Wiley & Sons, Ltd, pp. 247–282. https://doi.org/https://doi.org/10.2136/sssaspecpub61.c12

# Turbulence Thresholds for Cyprinids in Vertical Slot Fishways: A Laboratory Experiment-Based Analysis

Filipe ROMÃO[1], Ana L. QUARESMA[1], Joana SIMÂO[2], Francisco J. BRAVO_CÓRDOBA[3], Teresa VISEU, José M. SANTOS[4], Francisco J. SANZ-RONDA[5], António N. PINHEIRO[1]

[1] CERIS – Civil Engineering for Research and Innovation for Sustainability, Instituto Superior Técnico, University of Lisbon, Portugal
filipe.romao@tecnico.ulisboa.pt, analopesquaresma@tecnico.ulisboa.pt, antonio.pinheiro@tecnico.ulisboa.pt

[2] LNEC – National Laboratory for Civil Engineering, Hydraulics and Environment Department, Water Resources and Hydraulic Structures Department, Lisbon, Portugal
jsimao@lnec.pt, tviseu@lnec.pt

[3] GEA-Ecohidráulica, Centro Tecnológico Agrario y Agroalimentario Itagra.ct, Palencia, Spain
fjbravo@itagra.com

[4] CEF – Forest Research Centre, Associate Laboratory TERRA, School of Agriculture, University of Lisbon, Lisbon, Portugal
jmsantos@isa.ulisboa.pt

[5] GEA-Ecohidráulica, Area of Hydraulics and Hydrology, Department of Agroforestry Engineering, University of Valladolid, Palencia, Spain
jsanz@iaf.uva.es

## ABSTRACT

Cyprinid species fish passage thresholds have been rarely assessed and are vital to update design guidelines. Fish experiments and 3D numerical modelling were used to compare 4 vertical slot fishway configurations set to exceed volumetric dissipated power design guidelines recommendations for cyprinids. This study showed the importance of jointly assessing species-specific thresholds to update fish passage design guidelines.

## 1. Introduction

Restoring river´s longitudinal connectivity is a key issue in the recovery of freshwater ecosystems. In Europe, reducing the environmental impacts of anthropogenic barriers, such as dams and weirs, by attaining effective passage and migration for fish populations is required, to achieve good ecological status on water bodies, according to the Water Framework Directive and Biodiversity Strategy 2030. Fishways are the main mitigation solution used to restore longitudinal connectivity when barrier removal is not an option. The Vertical Slot Fishway (VSF) is considered one of the best technical-type fishways (FAO/DWK, 2002, Clay, 2017). Literature and design guidelines indicate that the volumetric dissipated power ($P_v$) in the pools should be lower than 150 $Wm^{-3}$ for cyprinids species, while commonly the slope ranges around 10% or less for small-scale hydropower facilities (Larinier, 2002; Larinier, 2008). This study main aim was to assess the passage performance of an Iberian cyprinid (*Luciobarbus bocagei*, Steindachner, 1864 - hereafter barbel) in an experimental VSF that exceeded these design recommendations. For this, the passage performance of the barbel was assessed in a prototype fishway set with a slope of 15,2 %, which generated a $P_v > 150$ $Wm^{-3}$ in the pools.

## 2. Methods

### *2.1 Fishway facility and experiments*

A prototype fishway facility was used in the National Laboratory for Civil Engineering (LNEC) at the Hydraulics and Environment Department in Lisbon, Portugal (Fig 1). Two VSF designs were used (Table 1): i) a standard VSF based on design 11 of Rajaratnam et al. (1992) with two distinct flow depths in the pools (VSF_A and VSF_B); ii) the same design transformed in a deep notch (FAO/DVWK, 2002) using a sill, also

with the same two flow depths (DN_A and DN_B). Fish experimental runs were conducted with 100 wild fish during the migration season using PIT Tag telemetry.

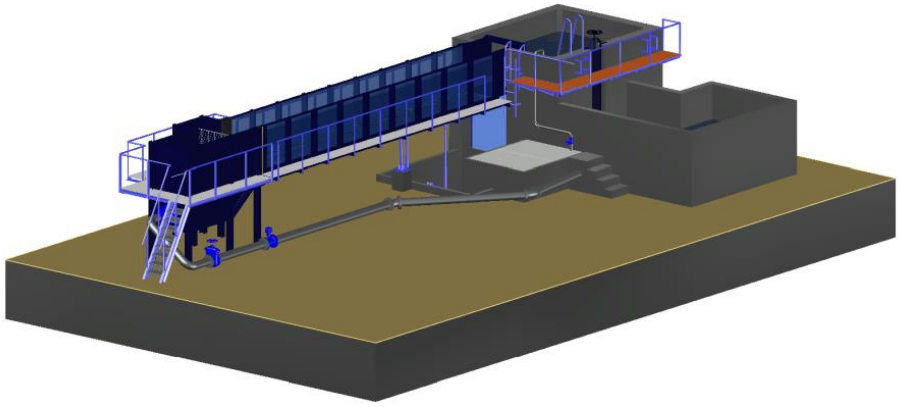


Fig 1. Fishway prototype.

Table 1. Discharge (Q) and pool mean water depth (hm) of each configuration tested.

| Fishway configuration | Q ($l.s^{-1}$) | hm (m) |
|---|---|---|
| VSF_A | 81 | 0,55 |
| VSF_B | 110 | 0,80 |
| DN_A | 71 | 0,55 |
| DN_B | 99 | 0,80 |

*2.2 Hydrodynamic characterization*

FLOW-3D® (v12.0; 2019; https://www.flow3d.com; Flow Science, Inc.) was used to characterize the hydrodynamics of the tested configurations. The calibration of the numerical model was ensured by measurements conducted in the physical facility. The numerical model showed relative differences lower than 6%, when compared to measurements, thus showing that it accurately reproduced the flow fields under analysis.

## 3. Main results and discussion

The configurations tested generated a *Pv* that exceeded literature recommendations by around 25 to 50 %, ranging from 187 $Wm^{-3}$ in DN_B to 222 $Wm^{-3}$ in VSF_A. Numerical model results showed that, although mean and maximum turbulent kinetic energy in the pools are similar, its distribution throughout the pools is considerably different. Larger volumes with magnitudes higher than 0.05 $m^2s^{-2}$ (Silva et al., 2011) were identified in both DN configurations. VSF_A the configuration that presented higher *Pv* in the pools had the smallest volume of water in the pools exceeding 0.05 $m^2s^{-2}$. These findings align with the barbel passage experiments, since fish showed a better performance in VSF_A. A higher number of fish managed to ascend the full facility, accomplishing a lower time to negotiate it when compared to other configurations. Results highlight the need to further investigate cyprinid passage thresholds to improve design guidelines.

**Acknowledgements**

The authors would like to acknowledge the assistance of the staff of LNEC during the fish experiments. Civil Engineering Research and Innovation for Sustainability (CERIS) is a research unit funded by the Fundação para a Ciência e Tecnologia I.P. (FCT), Portugal (UIDB/04625/2020). Forest Research Centre (CEF) is a research unit funded by FCT, Portugal (UIDB/00239/2020). Filipe Romão (https://doi.org/10.54499/2022.03193.CEECIND/CP1713/CT0010) and Ana Quaresma (https://doi.org/10.54499/2022.08169.CEECIND/CP1713/CT0012) are financed by FCT funds.

**References**

Clay, C. H. (2017). Design of fishways and other fish facilities. CRC Press.
FAO/DVWK (2002). Fish Passes: Design, Dimensions, and Monitoring; FAO: Rome, Italy, ISBN 9251048940.
Larinier, M. (2002). Pool fishways, pre-barrages and natural bypass channels. Bulletin Français de la Pêche et de la Pisciculture, 364 (364 supplément), 54–82.
Larinier M. (2008). Fish passage experience at small-scale hydroelectric power plants in France. Hydrobiologia 609: 97-108.
Rajaratman, N., Katopodis, C., Solanki, S. (1992). New designs for vertical slot fishways. Can. J. Civil Eng. 19 (3), 402–414.
Silva, A.T., Santos, J.M., Ferreira, M.T., Pinheiro, A.N., Katopodis, C. (2011). Effects of water velocity and turbulence on the behaviour of Iberian barbel (Luciobarbus bocagei, Steindachner, 1864) in an experimental pool-type fishway. River Res. Appl. 27 (3), 360–373.

# Robust modelling of groundwater in Portugal mainland: Exploring the correlation with the NAO Index - a preliminary study

Vanda LOURENÇO[1], Maurício LORDELO[2], Paulo RODRIGUES[3], Maria Paula MENDES[4]

[1]Dep. Mathematics & NOVA Math, NOVA University of Lisbon, Portugal

[2]Dep. Exact Sciences, State University of Feira de Santana, Brazil

[3]Dep. Statistics & SaLLy, Federal University of Bahia, Brazil

[4]CERIS, Instituto Superior Técnico, University of Lisbon, Portugal

[1]vmml@fct.unl.pt; [2]mslordelo@uefs.br; [3]paulocanas@gmail.com; [4]mpaulamendes@tecnico.ulisboa.pt

ABSTRACT

Effective groundwater management depends on balancing extraction and recharge, particularly as climate uncertainty grows. Understanding the correlation between teleconnection patterns, such as the North Atlantic Oscillation (NAO), and groundwater levels can be a valuable tool for accurate forecasting and adaptation efforts. This study investigates the impact of the NAO index on groundwater levels in the western coastal mainland of Portugal, examining the relationship between the NAO phases and groundwater levels in unconfined detrital aquifers within the Western Meso-Cenozoic Hydrogeological Unit (WU).

Piezometric time series frequently exhibit outliers, typically stemming from irregular and non-recurring events. These outliers not only introduce a carry-over effect on point forecasts but also introduce bias into the estimated model parameters. To address this, we employ traditional modeling techniques like Singular Spectrum Analysis (SSA; Golyandina et al., 2001) and Auto-Regressive Integrate Moving Average models (ARIMA; Newbold, 1983) alongside their robust counterparts—robust SSA (Kazemi et al., 2023) and robust ARIMA (Martin et al., 1983). Here, SSA and robust SSA serve as preprocessing methods for ARIMA and robust ARIMA, respectively.

## 1. Case-study

In 2000, 50% of continental Portugal's urban areas were situated within 13 km of the coastline, an area that accounts for 13% of the total Portuguese land area. The WU experiences significant urban pressures along the coastline, emphasizing the importance of effective groundwater resource management. The Aveiro Quaternary (AQ) Groundwater Body, a vital coastal aquifer system within the WU, boasts an annual groundwater availability of 225 hm3 and exhibits low heterogeneity in its geological medium. This suggests uniform properties in the geological materials, influencing groundwater behavior and availability. This study centers on the readings of nine piezometers, part of the Portuguese Environmental Agency monitoring network and associated with the WU AQ aquifer system. While detailed results for the analysis of nine time series will be presented in subsequent discussions, this extended abstract offers preliminary exploratory findings concentrating on a single time series.

### *1.1. 1Preliminary results*

Results refer to the 143/4 piezometer, located near the coast line and with a depth of 25 m. Both the 143/4 piezometer time series (TS) and the NAO TS consist of 372 monthly measurements recorded from January 1988 to December 2018. Models were fitted using data from 1988-2017. The 12 observations for the year of 2018 were excluded for point forecast validation.

Preliminary robust outlier detection analysis identified 62 outliers in the 143/4 TS, including types such as additive (AO) and level shift (LSO). One of these outliers (LSO) belongs to the validation data. Figure 1

displays the full time series together with the point forecasts for the 12 months of 2018 obtained from all the fitted models. Table 1 presents the forecast errors. Although the results indicate a subtle improvement in forecast accuracy with the implementation of SSA as a prefilter for the ARIMA model, the combination of rSSA with rARIMA demonstrated a more pronounced enhancement. Notably, rSSA-rARIMA outperforms the other methods, even without the calibration of rARIMA (the parameters calibrated in the ARIMA were used here). This suggests the possibility of achieving further enhanced results with calibration in future analyses.

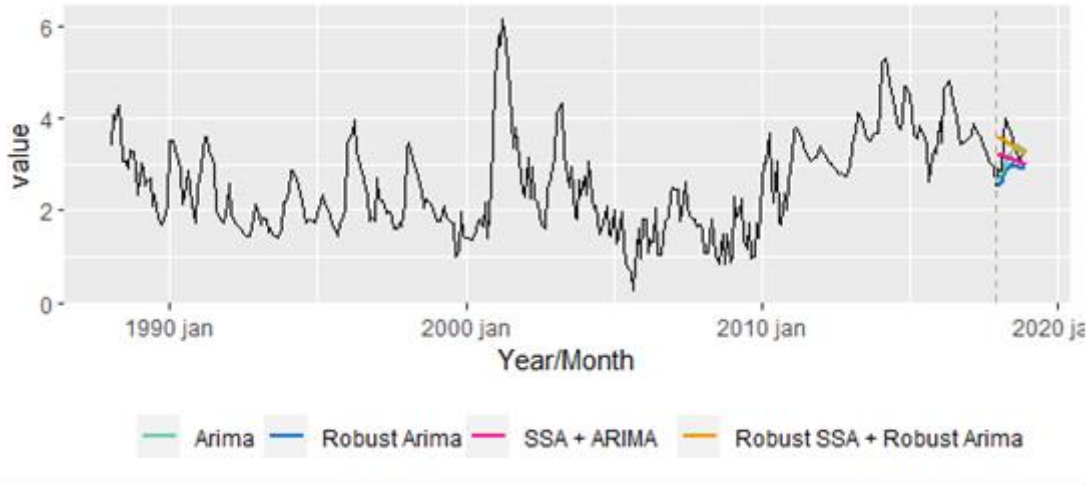



**Fig. 1.** Piezometer 143/4 time series with forecasts from the four fitted models.

**Table 1.** . Comparison of Root Mean Squared Forecast Errors across the four models.

| | **ARIMA** | **R-ARIMA** | **SSA-ARIMA** | **R-SSA + R-ARIMA** |
|---|---|---|---|---|
| RMSFE | 0.4594 | 0.6026 | 0.4339 | 0.3579 |

**Acknowledgements**

M. P. Mendes acknowledges the Portuguese Foundation for Science and Technology (FCT) and research unit CERIS (UIDB/04625/2020). V.M. Lourenço also acknowledges the Portuguese FCT (UIDB/00297/2020; UIDP/00297/2020).

**References**

Golyandina, N., Nekrutkin, V. & Zhigljavsky, A. (2001). Analysis of Time Series Structure: SSA and related techniques. Chapman & Hall, CRC.

Kazemi, M., & Rodrigues, P. C. (2023). Robust singular spectrum analysis: comparison between classical and robust approaches for model fit and forecasting. Computational Statistics, 1--33.

Martin, R. D., Samarov, A. & Vandaele, W. (1983). Robust methods for ARIMA models. In Applied Time Series Analysis of Economic Data (E.Zellner, ed.) 153--177. Washington Bureau of the Census.

Newbold, P. (1983). ARIMA model building and the time series analysis approach to forecasting. Journal of forecasting, 2(1), 23--35

# Density currents forming within an array of in-line and emergent cylinders

Moisés BRITO[1], Rui M.L. FERREIRA[2], Ana M. RICARDO[3]

[1] UNIDEMI, NOVA School of Science and Technology, NOVA University Lisbon, 2829-516 Caparica, Portugal
moisesbrito@fct.unl.pt

[2,3] CERIS, Instituto Superior Técnico, Universidade de Lisboa, Av. Rovisco Pais, 1049-001, Lisboa, Portugal
ruimferreira@tecnico.ulisboa.pt
ana.ricardo@tecnico.ulisboa.pt

## EXTENDED ABSTRACT

In lake-wetland interfaces, density currents have a significant environmental impact and play a relevant role in the transport of nutrients and pollutants. These currents are driven by a hydrostatic imbalance of two adjacent fluids with density variations in temperature, dissolved materials, or suspended compositions, propagate in a predominantly horizontal direction. While the hydrodynamics of density currents propagating over smooth and rough horizontal boundaries is considerably well understood, its interaction with vegetation or other bluff bodies is less studied (Adduce et al, 2012). Addressing an identified research need, the present work is aimed at characterizing the generation and propagation of density currents within an array of vertical cylinders. The research methodology included laboratory and numerical work. The experiments were performed in a horizontal and rectangular cross-section channel with 3.0 m of length, 0.17 m of width and 0.4 m of depth, as represented in Fig.1. The array consisted in 31 lines of three side-by-side bulk cylinders with 2 cm of diameter.

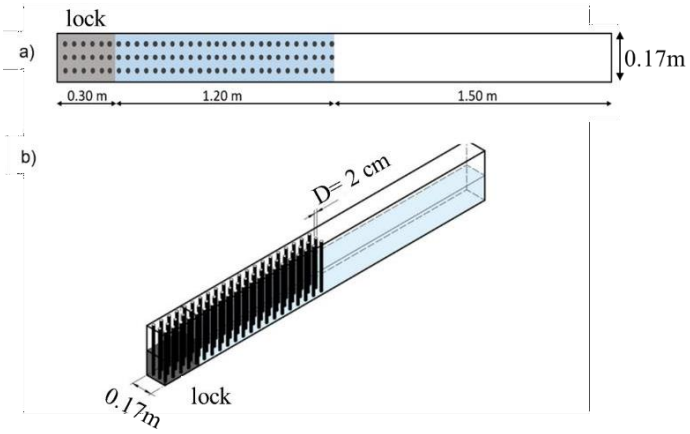



**Fig. 1** Schematic representation of the tested setup: a) top view and b) perspective view.

In the laboratory, tests employing the lock-exchange technique were carried out to generate the density currents with a reduced gravity of 0.09 $ms^{-2}$ e 0.36 $ms^{-2}$. The currents propagation was recorded by a high-speed video camera to obtain density distributions through image analysis techniques. The dense fluid was obtained by a mixture of fresh water and salt while the ambient fluid was obtained by a solution of alcohol and fresh water. The amount of salt and alcohol used were defined in order to attain the target density difference ensuring the match between the refractive index of both fluids (Daviero et al, 2001).

Numerically, the OpenFOAM implementation of LES model with VoF (volume-of-fluid) method to simulate the fluid phase was used. The governing equations are the filtered continuity, Navier-Stokes, and density transport equations for 3D time-dependent and incompressible stratified flows with the Boussinesq approximation. These filtered equations were discretized using the second-order central schemes. Convective

and diffusive terms are handled with an unbounded Gauss linear scheme and scalar transport is calculated using a Gauss-Vanleer scheme. The sub-grid scale (SGS) momentum and mass flux tensors are modeled using the Smagorinsky model. The 3D computational domain aimed at realistically mimicking the laboratory setup was defined with $15h_0$x$0.875h_0$x $h_0$ in streamwise, spanwise and vertical directions, respectively, where $h_0$=0.20 m is the fluid depth. No-slip boundary conditions are imposed for velocity on the cylinders, bottom, and lateral walls, whereas on the top wall a shear-free boundary condition is applied. No-flux conditions are also enforced on all boundaries. The numerical simulations were carried out for four values of reduced gravity, g'= 0.09, 0.18, 0.36 and 0.72 ms$^{-2}$.

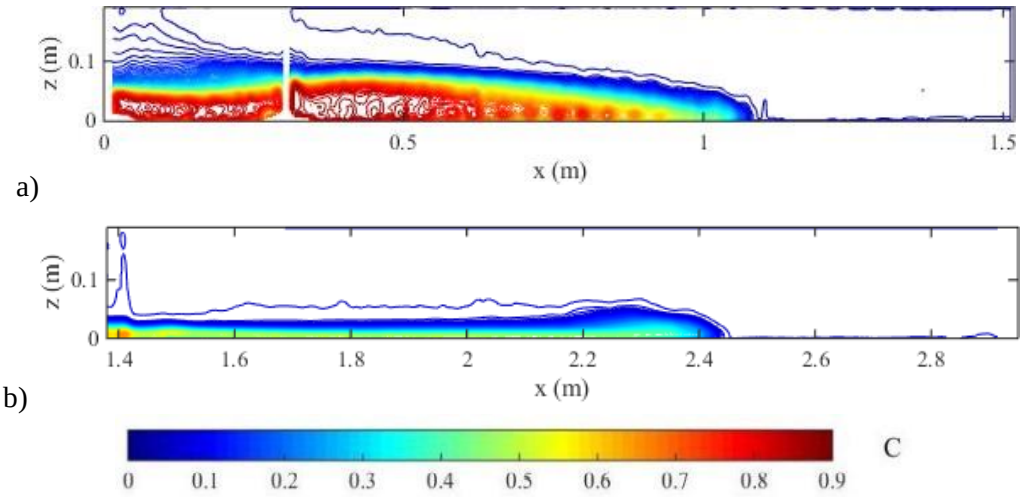



**Fig. 2** Distribution of the current concentration (C) for the laboratory test with $g'$=0.36 ms$^{-2}$ at a) $t$=7 s (current front within the array) and b) $t$=23s (current front in the unobstructed area).

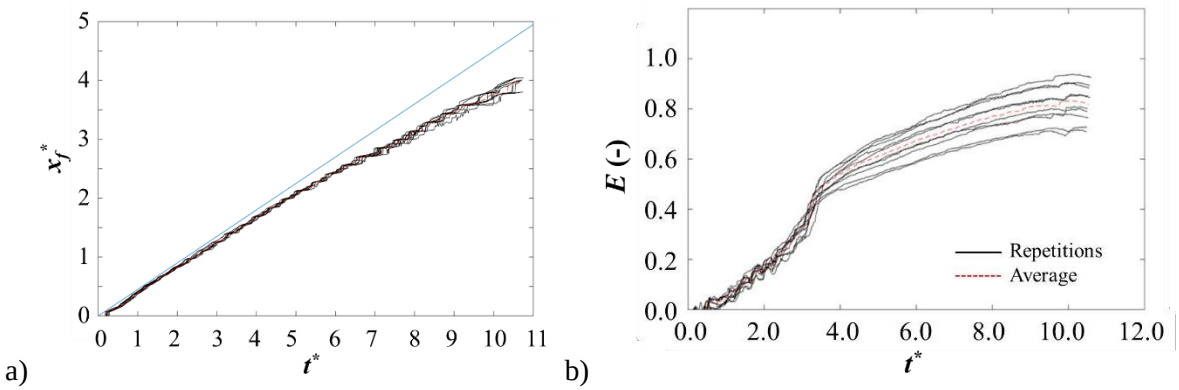



**Fig. 3** a) Non-dimensional position of the current front, $x_f^* = (x_f - x_0)/x_0$, where $x_f$ is the current front position and $x_0 = 0.3$ m is the lock position. b) Entrainment, $E = (V_i - V_0)/V_0$ where $V_i$ is the volume of the dense fluid at the time instant $i$ and $V_0$ is the current initial volume. The data refers to the current within the array for the test with $g'$=0.36 ms$^{-2}$. The non-dimensional time is defined as $t^* = (t \times u_0)/x_0$ where $t$ is the time relative to the lock release and $u_0$ corresponds to the buoyancy velocity.

The results showed that the well-known body-head morphology of a density current over an unobstructed wall was not observed within the array of cylinders (Fig. 2). The drag force created by the array did not impact the initial part of the current propagation as a constant front velocity similar to the Simpson solution (Huppert and Simpson, 1980) for a slumping phase was observed (Fig.3a). The time evolution of the entrainment showed an almost linear increase at an early stage and then the rate of increase was decreasing until the end of the array (Fig. 3b). When the current reached the unobstructed area, it did not have enough kinetic energy to accelerate the front propagation and to continue incorporating ambient fluid, thus entrainment was kept almost constant.

**Acknowledgements**

The presenting author is grateful for the Foundation for Science and Technology's support through funding UIDB/04625/2020 from the research unit CERIS and through the research project PTDC/CTA-OHR/30561/2017.

**References**

Adduce C., Sciortino G, Proietti S (2012) Gravity currents produced by lock ex-changes: experiments and simulations with a two layer shallow-water model with entrainment. J. Hydr. Eng. 138(2), 111-121

Daviero GJ, Roberts PJW, Maile K (2001) Refractive index matching in large-scale stratified experiments. Exp. Fluids 31(2), 119-126.

Huppert HE, Simpson JE (1980) The slumping of gravity currents. Journal of Fluid Mechanics 99 (04), 785-799.

# Gravity currents interacting with a large-scale roughness

Maria Rita MAGGI[1], Giovanni DI LOLLO[2], Claudia ADDUCE[3]

[1] LEGI, UGA/CNRS, UMR 5519, 38000 Grenoble, France
maria-rita.maggi@univ-grenoble-alpes.fr

[2,3] The Department of Civil, Computer Science and Aeronautical Technologies Engineering, Roma Tre University, Rome, Italy
giovanni.dilollo@uniroma3.it
claudia.adduce@uniroma3.it

ABSTRACT

Hydrostatic imbalance of two adjacent fluids with density differences associated with temperature, salinity or sediment concentration gradients often trigger the formation of gravity currents. Such phenomena play a pivotal role in various geophysical and engineering applications, impacting atmospheric, terrestrial, and subaqueous environments (Simpson, 1997). After the influential analysis of Benjamin (1968) many studies examined gravity current flow over a horizontal surface in a uniform ambient. However, in natural environments, the passage of gravity current propagation is often not flat but is rather uneven and the dynamics of the dense flow is strongly controlled by topographic features (Maggi et al., 2023). As a result, the problem of gravity currents propagating through channels obstructed by finite-size patches of obstacles has garnered increasing attention. Surprisingly, despite this growing interest, there has been relatively less emphasis on the experimental analysis of the mixing processes within these currents. In the present study, we investigate experimentally the evolution of bottom-propagating gravity currents in the presence of an array of submerged cylindrical obstacles, using an innovative image analysis technique based on light reflection to evaluate the instantaneous density fields (Adduce et al., 2022).

## 1. Experimental details

The laboratory experiments are carried out in a Perspex tank with a length, height and width of 3 m, 0.3 m and 0.2 m, respectively. Submerged roughness was created by placing an array of rigid plastic cylinders, each with a diameter of 2.5 cm, in a known location to span the entire width of the channel (Fig. 1). The first cylinder was placed at $2.5x_0$ from the lock, with $x_0$=30 cm, in order to ensure that the current approaches the obstacles once it is fully formed and during the slumping phase.

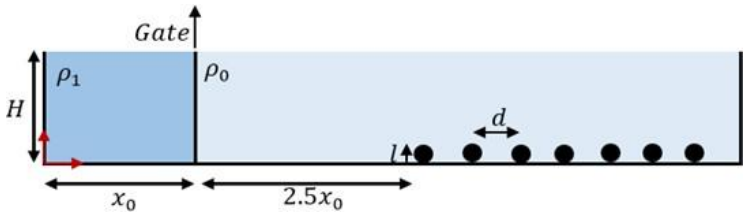



**Fig. 1.** Schematic side-view of the experimental set-up used to perform laboratory experiments

A total of 12 full-depth lock-exchange experiments were conducted and each one was recorded using a digital camera at a frequency of 25 Hz. The primary parameter investigated was the aspect ratio (d/l), which ranged from 4 to 7. Here, d represents the spacing between two obstacles, and l denotes the diameter of the cylinders. All experiments were conducted using the lock-release technique by filling the left and right volumes of the tank to the same water depth (H). The left side of the tank was filled with a saline mixture at density $\rho_1$, while the right side was filled with fresh tap water at a measured density of $\rho_0$ ($\rho_1>\rho_0$). All the experiments were conducted with a constant reduced gravity $g'_0=g\Delta\rho/\rho_0$=0.06 $ms^{-2}$. In order to apply the light attenuation technique and visualize the dense fluid, a controlled quantity of dye was introduced into the

saline water. A calibration method was used to establish the correlation between light intensity and dye concentration for each pixel in the captured images. For a more detailed explanation about the technique used, please refer to Adduce et al. (2022). The dimensionless density field, denoted as $\rho^*$ (x,y,t) is defined as follows:

$$\rho^*(x, y, t)=(\rho(x,y,t)-\rho_0)/\Delta\rho \quad (1)$$

## 2. Discussion

Fig. 2a and 2b depict $\rho^*$ (x,y,t) for the experiments with d/l =4 and d/l =7 and the same initial condition when the current reached $x/x_0$=7, by considering as upper boundary the iso-density threshold ( x, y, t ) = 2% . With d/l =4 (a) the head of the current exhibits a greater dilution compared to the case with d/l =7 (b), and a larger volume of current is observed to be trapped within the bottom roughness. In order to infer the main characteristics of the flow dynamics, depth-averaged density fields were evaluated. Figure 2c-d shows depth-averaged density fields in the plane $x/x_0$ - $t^*$ where $t^*=t/x_0\sqrt{(g_0' H)}$ for the case d/l =4 and d/l =7 respectively. This analysis emphasizes the complex dynamics of the gravity current. It is observed that the formed current front persistently detaches from the upstream face of the obstacle and then plunges towards the interstitial regions through a series of obstacles until the effective buoyancy is depleted. Indeed, as the front surpasses the bottom obstacles, it entrains a portion of the ambient fluid that is trapped in the bottom roughness, leading to a dilution process and a reduction in the buoyancy force of the current. Upon concluding the analysis of this study, it is evident that all the experiments are influenced by the presence of substantial bottom roughness. Additionally, it is observed that a smaller spacing between the obstacles results in a more pronounced influence of roughness on the dynamics of the dense current.

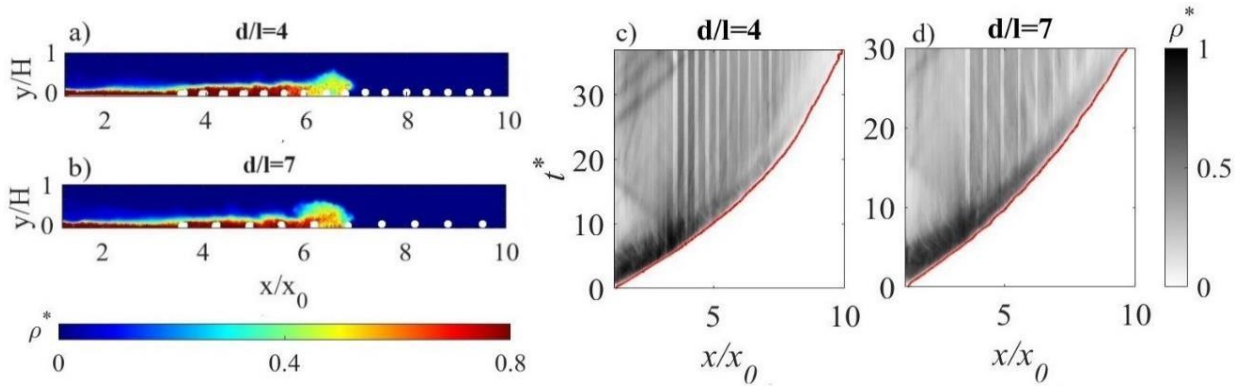



**Fig. 2.** Dimensionless density $\rho^*$ (x,y,t) of the experiments d/l =4 (a) and d/l =7 (b) at $x/x_0$=7. Depth-averaged density fields of the current for the experiments with d/l =4 (c) and d/l =7 (d). The red lines represent the dimensionless front position of the dense flow, while the light gray vertical stripes indicate the presence of the bottom cylinders.

**Acknowledgements**

Funded by European Union - Next Generation EU, project 2022SAFKS4.

**References**

Simpson, J.E., 1997. Gravity currents: In the environment and the laboratory. Cambridge University Press, Cambridge.
Benjamin, T.B., 1968. Gravity currents and related phenomena. J. Fluid Mech. 31, 209–248.
Maggi, M.R., Negretti, M.E., Hopfinger, E.J., Adduce, C., 2023. Turbulence characteristics and mixing properties of gravity currents over complex topography. Physics of Fluids 35.
Adduce, C., Maggi, M. R., and De Falco, M. C. (2022). Non-intrusive density measurements in gravity currents interacting with an obstacle. Acta Geophysica, pages 1–12.

# TKE budget equation terms of a gravity current approaching a vertical obstacle

Giovanni DI LOLLO[1], Claudia ADDUCE[2], Moises BRITO[3], Ana M. RICARDO[4], Rui M.L. FERREIRA[5]

[1,2,] The Department of Civil, Computer Science and Aeronautical Technologies Engineering, Roma Tre University, Italy
giovanni.dilollo@uniroma3.it
claudia.adduce@uniroma3.it

[3] UNIDEMI, Faculdade de Ciencias e Tecnologia, Department of Mechanical and Industrial Engineering, Portugal
moisesbrito@fct.unl.pt

[4,5] CERIS, Istituto Superior Tecnico, Portugal
ana.ricardo@tecnico.ulisboa.pt
ruimferreira@tecnico.ulisboa.pt

ABSTRACT

The terms of the TKE budget equation of a gravity current approaching a vertical cylinder are analyzed experimentally through PIV measurements. The presence of an increasing pressure adverse gradient interferes with the redistribution of TKE in the head of the current, suppressing the transport of TKE from the major production source located at the interface of the two fluids to the rest of the current.

## 1. Introduction

Flows driven by a density gradient, called gravity currents, are present throughout the planet, often spreading pollutants and modifying the environment in which they propagate. Given their impact, it is necessary to understand how gravity currents modify - and are modified by - the different morphologies they may encounter during their path, such as different roughnesses (Maggi et al., 2022) or industrial installations on the seabed (De Falco et al., 2021). The present work aims to interpret the effects that an adverse pressure gradient generated by an obstacle induces on an approaching gravity current, thus providing a first characterization of how the presence of vegetation or human obstacles influences the production and diffusion of turbulent kinetic energy (hereinafter TKE) of these flows, an aspect still little investigated.

## 2. Experimental apparatus

Full lock-released gravity currents are reproduced in a smooth horizontal rectangular channel with a length, height and width of 3 m, 0.4 m and 0.175 m, respectively. An emergent cylinder, mounted vertical at half width of the channel, is placed at 3 $x_0$ from the left side of the channel, with $x_0$=0.3 m is the position of the lock. Given the ratio between the length of the channel and the position of the lock, the current propagates in the slumping phase, even before the impact with the obstacle (Simpson,1999). Instantaneous longitudinal $u$ and vertical $w$ velocity components are measured with a 2D classical P.I.V. along the centerline of the channel, in the refractive index condition. A digital camera with acquisition frequency of 15 Hz records a section upstream the cylinder (Fig.1). The measurements start with the removal of the gate, causing the collapse of the dense fluid (consisting in salt diluted in fresh water) into a mixture of alcohol and fresh water filling the rest of the tank. The height of water column $h_0$=0.2 m is equal for both the volumes. A total of 20 repetitions are performed and analyzed, 10 with the cylinder and 10 without it, to have a base of comparison. All the repetitions have been performed with a constant density gradient $\Delta\rho$=6 kg/m$^3$. The analyses focus on the head of the current, identified as the leading steady part of the current showing the phase during its propagation. The head is followed before the impact with the cylinder, or until the end of section recorded in the undisturbed configuration.

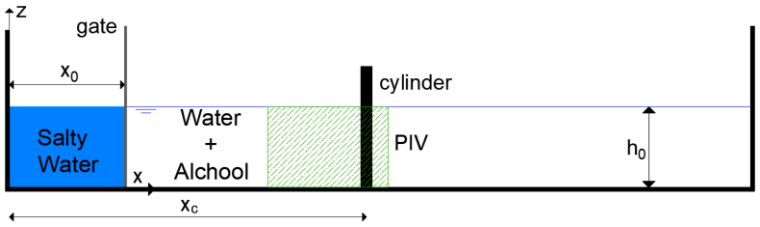



**Fig 1**. Geometry of the channel

## 3. Results

The TKE budget equation is defined as in Dai et al (2023):

$$\underbrace{\frac{\partial\langle k\rangle}{\partial t}}_{K_t} + \underbrace{\langle u_j\rangle\frac{\partial\langle k\rangle}{\partial x_j}}_{C} = \underbrace{-\langle\rho' u'_3\rangle}_{B} \underbrace{-\langle u'_i u'_j\rangle\frac{\partial\langle u_j\rangle}{\partial x_j}}_{P} - \frac{\partial}{\partial x_j}\left(\underbrace{\frac{1}{2}\langle u'_i u'_i u'_j\rangle}_{T} + \underbrace{\langle p' u'_j\rangle}_{TP} - \underbrace{\frac{2}{RE}\left\langle\frac{\partial u'_i}{\partial x_j}u'_i\right\rangle}_{V}\right) - \langle\varepsilon\rangle \tag{1}$$

where $t$ – time [s], $k$= $\langle u'_i\, u'_i\rangle$ – turbulent kinetic energy [m$^2$ s$^{-2}$], $x_i$ – i$^{th}$ Cartesian coordinate [m], $u_i$ – j$^{th}$ velocity components [m s$^{-1}$], $Re$ – Reynolds number, $p$ – pressure [Pa], $\rho$ – density [kg m$^{-3}$]. The symbology $\langle\blacksquare\rangle$ indicates the application of the ensemble average while variables marked with ' are fluctuations on the averaged ones. $K_t$ is TKE variation in time. C, P T, V and ε are the convective rate of change, the production, the diffusion due to Reynolds and viscous stresses and the dissipation of TKE, respectively. B is the buoyancy turbulent fluxes while TP is the diffusion due to pressure. All the terms show a reduction of their intensity inside the head section, excpet for the sum B+DP. Figure 2 shows the maps of TKE production term, with overlapped vectors of TKE fluxes. The current interacting with the cylinder is characterized by almost zero values of P inside the section. At the interface P has higher intensity compared to the undisturbed configuration. The TKE fluxes, in the case of the cylinder, are localized only along the interface layer, the major source of TKE production. Previous study on turbulent flows shown that diffusion due to pressure is generally opposite to turbulent diffusion. In shear layers, however, the two diffusions act in concert, increasing the total diffusion of TKE (Lumley, 1975). This explains the interruption of TKE flows from the interface. Consequently, the failure to redistribute TKE from the major production source causes a reduction in the same in the rest of the current.

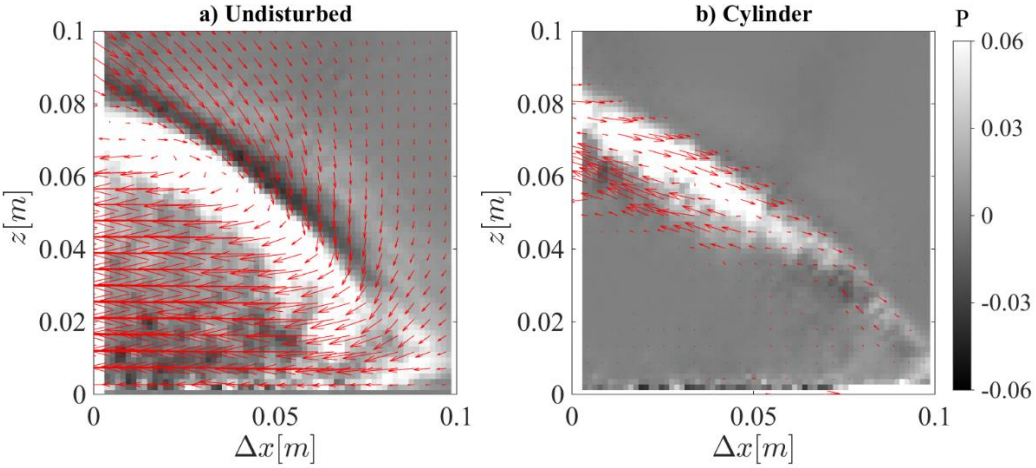



**Fig 2**. Maps of production term for a) undisturbed current and b) current approaching the cylinder. The vectors indicate the TKE fluxes.

**Acknowledgements**

Funded by European Union - Next Generation EU, project 2022SAFKS4

**References**

Dai, A., Huang, Y.L., Wu,C.S., (2023) Energy balance for the collision of gravity currents of equal strengths, Journal of Fluid Mechanics 959

De Falco, M., Adduce, C., Maggi, M., (2021). Gravity currents interacting with a bottom triangular obstacle and implications on entrainment, Advances in Water Resources 154, 103967

Lumley, J. (1975), Prediction methods for turbulent flows, introduction. Lecture series 76

Maggi, M.R., Adduce, C., Negretti, M.E., (2022) Lock-release gravity currents propagating over roughness elements, Environmental Fluid Mechanics, 1-20.

Simpson, J. E. (1999). Gravity currents: In the environment and the laboratory. Cambridge university press.

# Crato. The most recent multipurpose hydraulic scheme being built in Portugal

Mario SAMORA[1]; Elsa ALVES[2]

[1] TPF, Consultores de Engenharia e Arquitetura, S.A., Portugal
mario.samora@tpf.pt
[2] Laboratório Nacional de Engenharia Civil
ealves@lnec.pt

ABSTRACT

## 1. Introduction

The Crato Multipurpose Hydraulic Scheme is a structuring project for the economic and social development and sustainability of the territory of Alto Alentejo in Portugal. It arises from the need for an alternative capable of guaranteeing the resilience of public supply to the populations, even in periods of prolonged droughts. Due to its characteristics, the creation of this strategic storage will also be crucial for the implementation of agricultural techniques included in the Innovation Agenda for Agriculture 2030, with the establishment of a new irrigated area with high levels of water efficiency. The project also intends to contribute to the reconfiguration of energy production in the region, with the installation of floating photovoltaic panels and the production of electricity from a small hydroelectric plant.

Downstream from this new scheme, other irrigation and hydropower schemes already exist in the same catchment area, which raises the issue of water resources sharing at basin level, this being expected to become more frequent as society develops, and climatic changes and oscillations must be dealt with. These matters are presented and discussed in this paper, together with a general description of the scheme's infrastructures.

## 2. The main infrastructures of the Crato Multipurpose Hydraulic Scheme

The main infrastructures of the Crato Multipurpose Hydraulic Scheme (Fig. 1) are the Pisão dam, a small hydroelectric plant, the supply reinforcement system for the Póvoa e Meadas dam from the Pisão reservoir, the irrigation infrastructures to support existing agricultural areas (including irrigation pumping stations, regulation reservoirs and distribution networks, irrigation networks and improvement of agricultural accesses) and a photovoltaic solar plant (150 MW). The Crato Multipurpose Hydraulic Scheme must meet the following uses and consumptions: irrigation of 6770 ha, urban supply (0.83 hm3/year) and ecological flow.

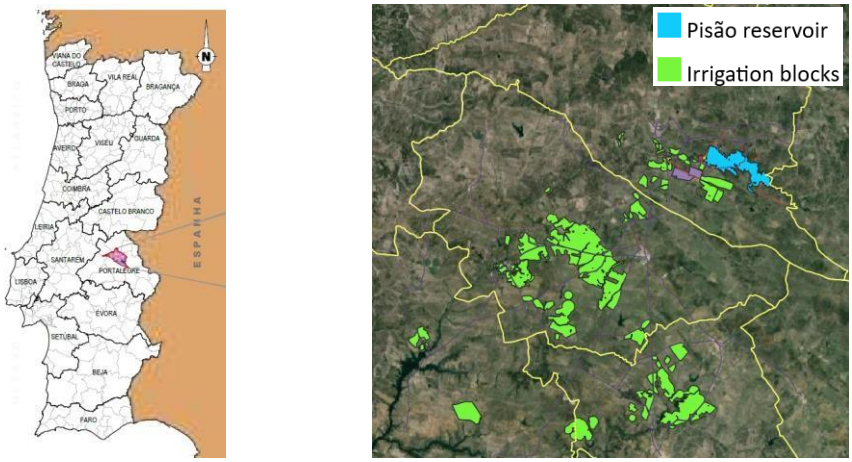



Fig. 1 – Crato Multipurpose Project – location

The Pisão dam, to be constructed on the Seda stream, is an embankment dam, 56 m high and about 1350 m wide, with crest at elevation (252). The spillway is designed for a discharge of 394 $m^3/s$ and is constituted by an approach channel, a labyrinth weir followed by a channel, which ends in a hydraulic jump stilling basin. Downstream of the stilling basin, a tailrace channel is excavated in the natural terrain, with a rockfill-lined bottom and banks protected by gabion walls.

The study of hydraulic performance of the spillway, stilling basin and restitution river channel, was conducted on a hydraulic physical model at 1:40 scale at LNEC (Fig. 2). Downstream of the stilling basin, a mobile bed was used to study erosions. In general, the spillway presents an adequate hydraulic performance for a wide variety of flow conditions. After the hydraulic tests, the protection against erosion of the tailrace channel bed was reinforced.

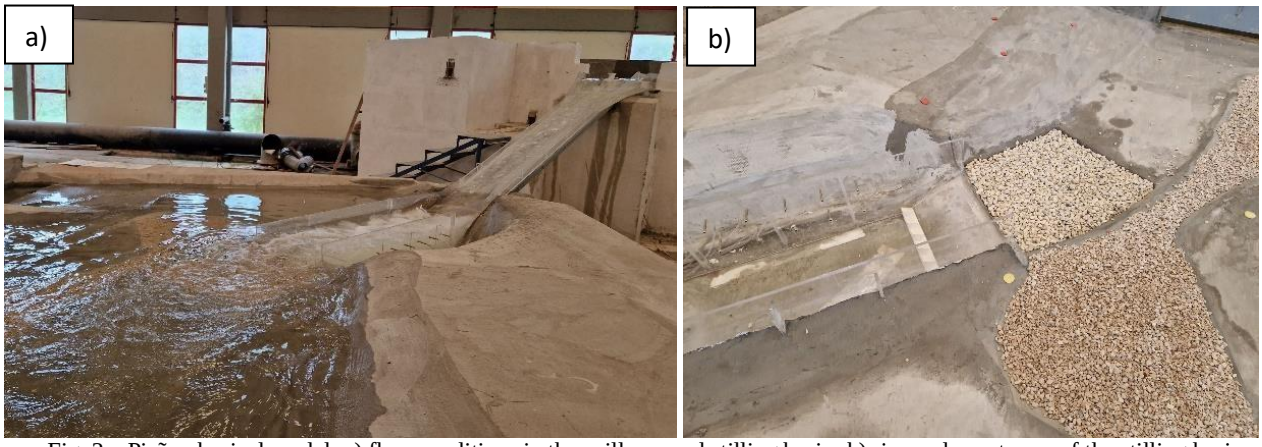


Fig. 2 – Pisão physical model: a) flow conditions in the spillway and stilling basin; b) riprap downstream of the stilling basin

## 3. Challenges of the Crato Multipurpose Scheme

The Pisão dam is the Sorraia river basin, a region with a dry sub-humid climate, with dry and hot summers, and mild and wet winters. The average annual precipitation over the Sorraia basin is 640 mm, producing an average annual runoff of 140 mm. Two large dams, Montargil and Maranhão, were built in the river basin during the second half of the 20th century, as part of the Sorraia Valley Irrigation Plan, which covers an area of 16000 ha. Maranhão dam supplies existing irrigation perimeters, industrial consumptions, and some hydropower plants downstream.

A major challenge of the Crato Multipurpose Hydraulic Scheme is to ensure an efficient water management to satisfy irrigation needs (urban and industrial consumption are priorities) between the different reservoirs existing in the basin. This aspect can be critical in periods of prolonged droughts, including climate change scenarios.

Simulation studies of the exploration of the three main reservoirs of the Sorraia river basin (Pisão, Maranhão and Montargil) proved that there is enough water to meet all needs but, still, restrictions might have to be imposed during long dry spells. So, a management system was studied to ensure that any restrictions needed in exceptional dry periods will be shared by all users in a fair and even way.

# A Lagrangian Perspective on the Characterization of the Agulhas Leakage

Jacopo BUSATTO[1], Federico FALCINI[2], Claudia ADDUCE[3] and Guglielmo LACORATA[4]

[1,2,3,4] Institute of Marine Sciences, National Research Council
federico.falcini@artov.ismar.cnr.it
guglielmo.lacorata@artov.ismar.cnr.it
[1,3] Department of Engineering, Roma Tre University, Italy
jacopo.busatto@uniroma3.it,
claudia.adduce@uniroma3.it

ABSTRACT

This study employs Lagrangian simulations to explore the dynamics of the Agulhas Current region, focusing on mesoscale eddies known as Agulhas Rings. A crucial innovation is the introduction of a rotation index derived from velocity and acceleration vectors, which helps in the identification of trajectories within rotating structures. Trajectory analysis over the Atlantic section reveals distinct outcomes, with trajectories exhibiting stable, high rotation indices indicative of Agulhas Rings and others more linear behaviors. Statistical analysis shows positive rotation indices in trajectories leading to Agulhas Leakage, aligning with the anticyclonic nature of Agulhas Rings. Trajectories with rotation indices consistently above 0.8 resemble stable loops, referring to Agulhas Rings. Further exploration into the temporal aspects of tracer presence within coherent structures is suggested for enhanced predictive capabilities. While the strength of Lagrangian approaches has been solidly assessed, the methodology here presented contributes with valuable insights into Agulhas Current dynamics, highlighting the rotation index's role in predicting trajectory outcomes and distinguishing between anticyclonic and cyclonic structures.

## 1. Introduction

The Agulhas Current (Beal et al., 2006), a swift western boundary current in the southwest Indian Ocean, holds pivotal significance in the global ocean circulation system. Renowned for its role in transporting warm and saline waters from the Indian Ocean to the Atlantic (Agulhas Leakage, see Deruijter el al., 2008, Lutjeharms et al., 2006), the Agulhas Current influences climate patterns, biodiversity, and oceanic heat distribution. Its distinct physical and dynamical properties, marked by mesoscale eddies known as Agulhas Rings, contribute to the complexity of the regional and global circulation.

This study employs Lagrangian simulations (Van Sebille, 2009a, Van Sebille, 2009b) to delve into the dynamics of the Agulhas Current region. Lagrangian turbulence, represented through a kinematic subgrid, and the assumption of stationary, homogeneous, and isotropic turbulence form the basis of our numerical integration process (Palatella el al., 2014, Lacorata et al., 2014, Lacorata et al., 2017, Falcini et al., 2020). The methodology involves a differential equation solver, coupled with spatial and temporal interpolation modules, to handle finite grid Eulerian velocity files. Notably, our spatial resolution of 0.25° proves the ability of capturing the mesoscale activities associated with Agulhas Rings.

## 2. Results

A pivotal aspect of our investigation is the introduction of a rotation index to discern the rotating trajectories. The rotation index, derived from the vectorial product of velocity and acceleration versors, aids in identifying tracers within rotating structures. Through numerical drifters crossing the Atlantic section (10°W,55°S to 20°E,30°S), we evaluate the rotation index for trajectories before and after the cross as:

$$R = \frac{\vec{v}\times\vec{a}}{|\vec{v}||\vec{a}|} = \sin(\alpha) \quad (1)$$

Here $\vec{v}$ is the 2D velocity of the trajectory, $\vec{a}$ its acceleration and α the angle between the two vectors. Two contrasting trajectories illustrate the potential of the rotation index. One trajectory exhibits consistently high rotation indices, indicative of a coherent rotating structure resembling Agulhas Rings. The rotation index remains stable, with values mostly above 0.8, highlighting a structure with a diameter of almost 100 km moving North-Westward. This finding aligns with Casanova et al. (2017), who studied a similar Agulhas Ring with a 30 km radius and a 5-days periodicity (see Figure 1). The second trajectory (not shown in this abstract), despite initial fluctuations, lacks sustained rotation, emphasizing the absence of a rotating structure.

Statistical analysis of trajectory outcomes reveals a notable distinction. Trajectories leading to Agulhas Leakage exhibit dominant positive rotation indices, aligning with the anticyclonic nature of Agulhas Rings. In contrast, trajectories associated with cyclonic structures remain in the retroflection region, eventually joining the South Atlantic and Antarctic Circumpolar Currents.

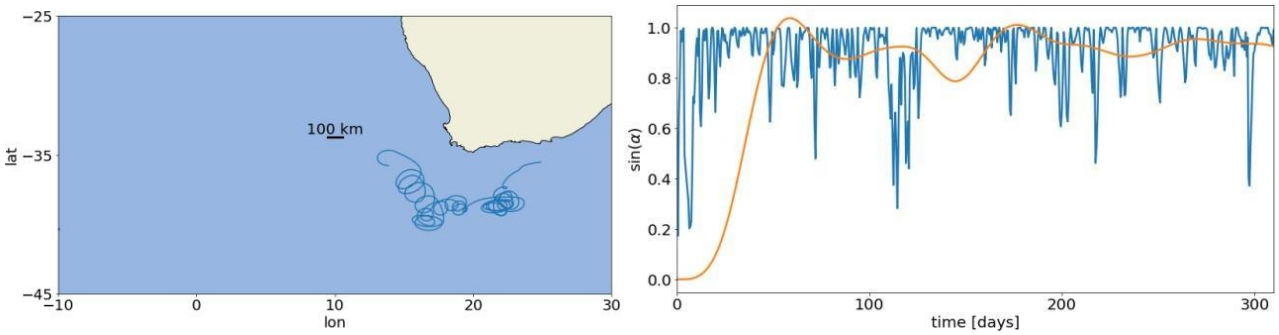



**Fig. 1.** Example trajectory with peculiar rotation index. Left panel shows the trajectory in the South Atlantic. It is trapped inside a coherent anticyclonic structure, for almost 300 days. Right panel shows its rotation index and a low pass filter (yellow line).

## 3. Conclusions

Our study establishes that trajectories with a rotation index consistently above 0.8 align with stable loops resembling Agulhas Rings. These trajectories, characterized by a 50-100 km diameter and a rotation period of approximately 10 days, closely resemble the dimensions and periodicity reported by Casanova et al. (2007). Going further from the usual Lagrangian analysis, the rotation index emerges as a valuable metric for identifying and predicting the behavior of tracers within the Agulhas Current region.

While this study provides a foundation, further exploration into the temporal aspects of tracer presence within coherent structures could enhance the methodology. Investigating the timescales at which tracers remain within these structures could offer nuanced insights into the dynamics of Agulhas Rings and further improve predictive capabilities. In conclusion, this work contributes valuable insights into the dynamics of the Agulhas Current region, shedding light on the role of rotation indices in predicting trajectory outcomes and distinguishing between anti-cyclonic and cyclonic structures, providing an useful tool that empowers the Lagrangian statistical analysis.

**References**

Beal, L. M., T. K. Chereskin, Y. D. Lenn, and S. Elipot, 2006: The Sources and Mixing Characteristics of the Agulhas Current. J. Phys. Oceanogr., 36, 2060–2074, https://doi.org/10.1175/JPO2964.1.

Casanova-Masjoan, M., Pelegrí, J. L., Sangrà, P., Martínez, A., Grisolía-Santos, D., Pérez-Hernández, M. D., and Hernández-Guerra, A. (2017), Characteristics and evolution of an Agulhas ring, J. Geophys. Res. Oceans, 122, 7049– 7065, doi:10.1002/2017JC012969.

De Ruijter, W. P. M. (2008). The Agulhas Current (Maiden: Eos, Transactions American Geophysical Union)

Falcini, F., Corrado, R., Torri M. et al., Seascape connectivity of European anchovy in the Central Mediterranean Sea revealed by weighted Lagrangian backtracking and bio-energetic modeling. Sci Rep 10, 18630 (2020). https://doi.org/10.1038/s41598-020-75680-8

Lacorata, G., Palatella, L., and Santoleri, R. (2014), Lagrangian predictability characteristics of an Ocean Model, J. Geophys. Res. Oceans, 119, 8029– 8038, doi:10.1002/2014JC010313.

Lacorata, G. and Vulpiani, A., Chaotic Lagrangian models for turbulent relative dispersion}, Phys. Rev. E, 95, 4, 2017, American Physical Society, 10.1103/PhysRevE.95.043106, https://link.aps.org/doi/10.1103/PhysRevE.95.043106

Lutjeharms, J. R. E. (2006). The Agulhas Current (Heidelberg: Springer Berlin). doi:https://doi.org/10.1007/3-540-37212-1

Palatella, L., Bignami, F., Falcini, F., Lacorata, G., Lanotte, A. S., and Santoleri, R. (2014), Lagrangian simulations and interannual variability of anchovy egg and larva dispersal in the in the Sicily Channel, J. Geophys. Res. Oceans, 119, 1306– 1323, doi:10.1002/2013JC009384.

van Sebille, E., Biastoch, A., van Leeuwen, P. J., and de Ruijter, W. P. M. (2009a), A weaker Agulhas Current leads to more Agulhas leakage, Geophys. Res. Lett., 36, L03601, doi:10.1029/2008GL036614.

van Sebille, E., Barron, C. N., Biastoch, A., van Leeuwen, P. J., Vossepoel, F. C., and de Ruijter, W. P. M.: Relating Agulhas leakage to the Agulhas Current retroflection location, Ocean Sci., 5, 511–521, https://doi.org/10.5194/os-5-511-2009, 2009b.

# Quantifying the influence of source variability on unsteady buoyant jets

Morgan HETHERINGTON[1], Alan CUTHBERTSON[1], Sue DAWSON[2]

[1] School of Science and Engineering (Civil Engineering), University of Dundee, UK.
a.j.s.cuthbertson@dundee.ac.uk; 140010768@dundee.ac.uk

[2] School of Humanities, Social Sciences and Law (Physical Geography), University of Dundee, UK.
s.dawson@dundee.ac.uk

ABSTRACT

The discharge of domestic and industrial effluents into estuarine or coastal waters (as marine wastewater discharges) or the atmosphere (as industrial emissions), along with naturally-occurring atmospheric discharges (such as volcanic eruptions), are examples of turbulent buoyant jets, where the nature and structure of these discharges intrinsically determine the quality of the surrounding environment (water or air). Understanding and modelling the fundamental behavior of buoyant jets is therefore crucial to minimizing potential environmental and socio-economic impacts associated with these discharges. Well-established, one-dimensional integral model theories have been developed, based on the time-averaged behavior of buoyant jets under the assumption of steady-state source conditions, which are utilized widely for the rapid prediction of ash clouds from volcanic eruptions (Folch et al., 2016) and/or the near-field dilution of effluents discharged into the marine environment (Jirka, 2004). The current study assesses, through scaled laboratory experiments, the limitations associated with these steady-state buoyant jet models by investigating the influence that source variability has on the structure of the unsteady buoyant jets generated and, in particular, their deviation from well-established integral (time-averaged) properties.

## 1. Methods

The scaled laboratory experiments were conducted in a rectangular, acrylic-walled tank with plan-form dimensions 1200mm × 670 mm x 450 mm, and an overall water depth of 870 mm above a false tank bottom. A vertical pipe of internal diameter 18 mm was positioned at the centreline of the tank protruding above the false bottom. The 'effluent' consisted of fresh water of density $\rho_1$ = 1000 kg.m$^{-3}$ (with the addition of fluorescent dye or seeding particles) that was discharged from the pipe exit into a stagnent, homogeneous ambient saline water volume with density $\rho_2$ = 1030 kg.m$^{-3}$, generating a buoyant jet (Fig. 1). The steady-state source flow rate $Q$ was controlled and measured by a valve and ultrasonic flow meter, respectively, while an electronically-controlled solenoid valve was used to control the rate of valve opening and closing, thus generating unsteady pulsed discharges with varing pulse durations (0.5 – 2 s) and frequencies (0.25 – 1 Hz). The resulting vertical buoyant jet and plume dynamics were analysed via image analysis techniques including light-induced fluorescence (LIF) and particle image velocimetry (PIV) to investigate the concentration and velocity fields, and the evolving plume geometry, under steady and unsteady source conditions. Parametric variations were introduced into the experimental runs by changing (a) the source discharge $Q$ and (b) the degree of unsteadiness in the source conditions (i.e. pulse duration and frequency).

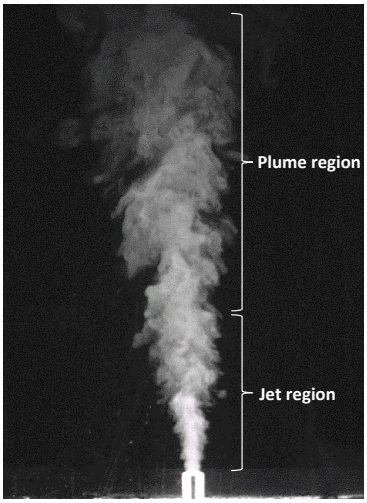



Fig. 1. Dye image of a steady-state buoyant jet discharge.

## 2. Results

Fig. 2 shows the comparison between the time series of non-dimensional concentration $C(z)/C_0$ along the centreline axis of the buoyant jet with increasing vertical distance $z$ from the steady-state (Fig. 2a) and pulsed (Fig. 2b) source conditions (for otherwise identical parametric conditions). Fig. 3 shows the corresponding

time series of vertical centreline velocity $V(z)$ from PIV analysis of instantaneous flow fields generated by steady-state (Fig. 3a) and pulsed (Fig. 3b) source conditions. These results, firstly, illustrate the inherent short-term variability in the concentration and velocity fields for turbulent buoyant jet dynamics, even under steady-state source conditions, although the longer-term, time-averaged behavior is shown to be consistent and in accord with recognized integral properties. By comparison, the unsteady nature of the buoyant jets generated by pulsed source conditions is reflected in the temporal intermittency in the concentration and velocity fields. As a consequence, the long-term, time-averaged behavior of the buoyant jet (particularly close to the source) will also reflect this source intermittency, with an overall reduction in the integral values for the centreline concentrations and velocities compared to steady source conditions. It is also interesting to note that, while the overall concentration distributions $C(z)/C_0$ are relatively similar for steady and intermittent source conditions (during the discharge pulses) (see Fig. 2), the centreline velocities appear to decay more rapidly with distance $z$ for the intermittent source compared to the steady source (Fig. 3). This effect is mainly due to the loss of source momentum flux (during valve closure periods) affecting the residual momentum in the rising buoyant jet, whereas the buoyancy flux continues to act on the less dense, partially mixed effluent plume, meaning that it continues to rise to the free surface at a slower rate and is somewhat detached from the subsequent pulse.

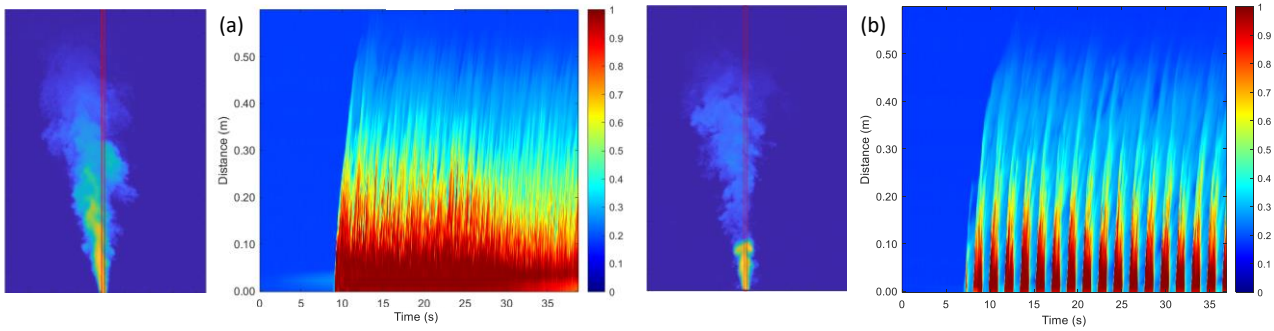



Fig. 2. Instantaneous LIF images showing evolving steady and unsteady buoyant jets, along with the corresponding time series of centreline dye concentration profiles $C(z)/C_0$ for (a) steady-state source conditions ($Q$ = 38.7 l.min$^{-1}$; $\Delta\rho$ = 1000 kg.m$^{-3}$); and (b) unsteady pulsed source conditions (at 1 s intervals, otherwise identical parametric conditions).

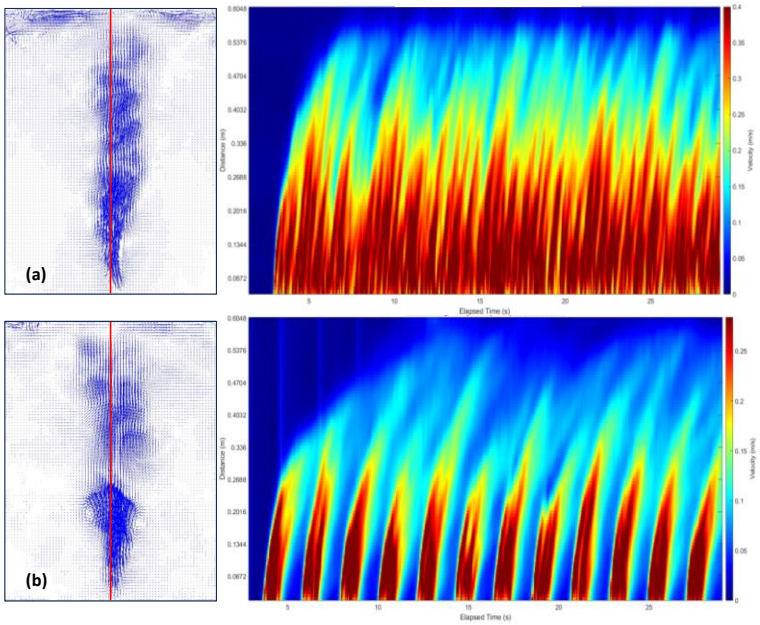



Fig. 3. Instantaneous PIV velocity fields for steady and unsteady buoyant jets, along with corresponding time series of centreline velocity profiles $V(z)$ (m.s$^{-1}$) for (a) steady source conditions (see Fig. 2); and (b) unsteady pulsed source conditions (see Fig. 2).

## Conclusions

The experimental results reveal velocity and concentration profiles of intermittent buoyant jets to differ from steady state assumptions, exhibiting overall reduced integral centreline properties. In addition, unsteady centreline velocity profiles indicate novel features that are not identified in continuous, steady state buoyant jets, such as upper plume detachment from the momentum source. These unsteady buoyant jet results thus indicate deviation from the steady-state assumptions of 1D integral models.

**Acknowledgements**

The authors acknowledge the financial support provided for this project through the Engineering and Physical Sciences Research Council (EPSRC) Doctoral Training Partnership.

**References**

Folch, A., Costa, A., Macedonio G. (2016). FPLUME-1.0: An integral volcanic plume model accounting for ash aggregation, *Geoscientific Model Development*, 9, 431–450. https://doi.org/10.5194/gmd-9-431-2016.

Jirka, G.H. (2004). Integral Model for Turbulent Buoyant Jets in Unbounded Stratified Flows. Part I: Single Round Jet. *Environmental Fluid Mechanics*, 4, 1–56. https://doi.org/10.1023/A:1025583110842.

# Experimental modelling of rock dumping in a Norwegian fjord

Alan CUTHBERTSON[1], Otto NESHAMAR[1], Øyvind THIEM[2], Peter DAVIES[1], Jarle BERNTSEN[3]

[1] School of Science and Engineering (Civil Engineering), University of Dundee, UK.
a.j.s.cuthbertson@dundee.ac.uk; ONeshamar001@dundee.ac.uk
[2] Statens vegvesen, Bergen, Norway.
oyvind.thiem@vegvesen.no
[3] Department of Mathematics, University of Bergen, Norway.
jarleb@uib.no

ABSTRACT

Results are presented from a series of scaled laboratory experiments designed to model the dumping of graded rock masses into a quiescent fjordic water body via either vertical pipes or inclined tunnel shafts. The main environmental concern with this dumping operation relates to the fate of fine suspended particulates present within the rock grain size distribution (GSD), and their potential release into the wider fjord and impact on both wild and farmed salmon stocks. The laboratory experiments therefore consider the dynamic behavior of the graded rock dumps both within the pipes or tunnels, and the particle-laden plumes generated following their release at the pipe/tunnel exit into the water column. Results indicate that hindered fractional settling and size-segregation are the main physical mechanisms controlling rock mass deposition from vertical pipes, while equivalent dumps into inclined pipes behave as particle-laden gravity currents, with a more efficient release of the dumped rock mass (i.e. over shorter time periods) compared to the vertical pipe arrangement. Sequential single-shot mass dumps are also shown, in both dumping arrangements, to control the wider release of fines through re-entrainment processes. Implications for planned full prototype scale dumping operations in natural fjordic water bodies are considered from these idealized, scaled experiments.

## 1. Methods

The scaled laboratory experiments were conducted in a large, rectangular acrylic-walled water tank (Fig. 1b, c) with plan-form dimensions 1 m × 1 m and an overall water depth of 2.5 m. Two proposed rock disposal methods were evaluated in the laboratory arrangement: dumping via vertical pipes or via inclined shaft tunnels (see Fig. 1a). In both cases, the dumped rock masses exit the model pipe/tunnel at a significant depth within the water column, with the expectation that the fines content (typically <1% by weight) will deposit along with coarser rock fragments to the floor of the tank. The main experimental parameters that were varied in the tests were (i) pipe/tunnel orientation (i.e. vertical, 45° and 60° inclined) and geometries (i.e. pipe diameter $D$ and length $L$); (ii) rock dump input masses; and (iii) dumping procedures (i.e. sequential "single-shot" dumps or continuous feed). The main aim of the tests was to understand how these parameters influence fractional settling, mixing and size segregation within the pipe/tunnel, as well as the depositional plume characteristics of the modelled rock dumps (including fines) on exit to the surrounding ambient water volume. The reduced-scale rock fragment GSD was based on matching densimetric Froude numbers for prototype and model settling velocities at the pipe exit, and comprised of seven color-coded melamine particle size classes ($d_s$ = 0.125 – 5 mm) and silica flour ($d_s$ = 25 μm) to represent the fines content.

## 2. Results

Fig. 2 shows a time series image sequence for a single-shot mass input into a vertical pipe, where residual fines from the previous dump (i.e. red particle size class and silica flour) are expelled from the pipe exit as a buoyant puff by the addition of the next mass input at the free surface (Figs. 2a-c). These fines are re-entrained into the fast-settling, coarse particle stream (i.e. cream, blue and green particle size classes) exiting the pipe from the next mass dump (Figs. 2d, e) and deposit to the tank bottom. Size segregation of coloured particle classes occurs along the pipe due to differential settling and turbulent mixing, resulting in progressively finer particle size classes (i.e. yellow, white, black and red particle size classes) depositing

sequentially as particle-laden plumes (i.e. $t$ = 15 → 50 s; Fig. 2f → i), eventually with only the residual fines size classes (i.e. red particles and silica flour) remainng in the pipe (Fig. 2j). The degree of size segregation is controlled primarily by pipe geometry and mass input, with longer/narrower pipes and larger mass inputs promoting increased segregation.

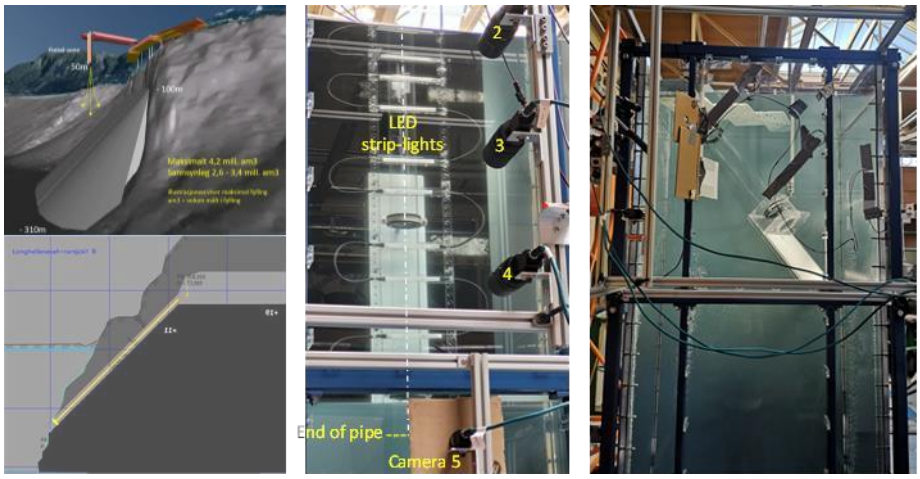



Fig. 1. (a) Schematic diagrams showing rock dumping arrangements via vertical pipelines off floating barge and via inclined disposal shaft from main tunnel. (b), (c) show lab set-up for vertical and inclined (45°) pipes.

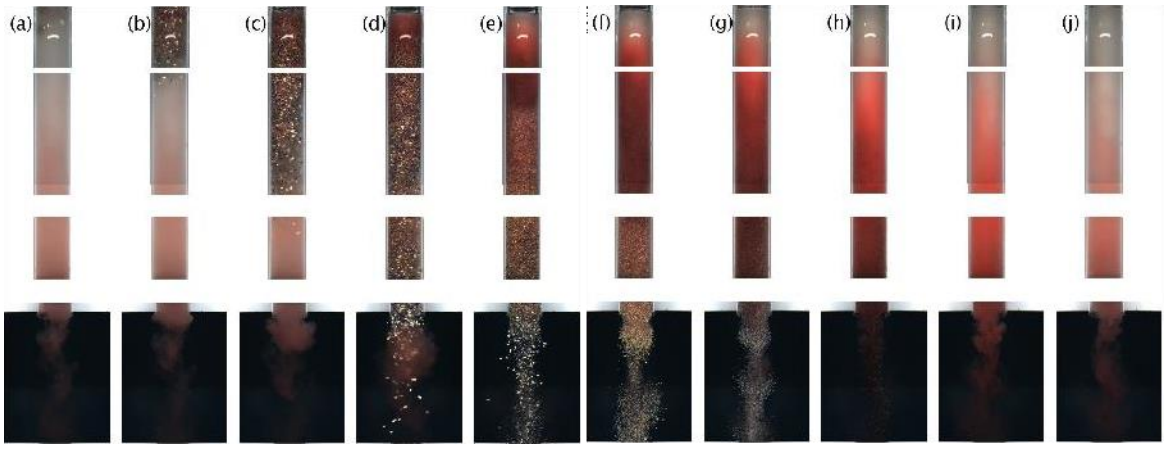



Fig. 2. Time series images of a single-shot dump (mass input = 227g) in vertical pipe ($D$ = 0.046 m; $L$ = 0.6 m) at elapsed times $t$: (a) 0.2 s; (b) 1 s; (c) 3 s; (d) 5 s; (e) 10 s; (f) 15 s; (g) 20 s; (h) 30 s; (i) 50 s; (j) 80 s.

For inclined pipe dumping arrangements, single-shot mass dumps behave as particle-laden gravity currents, propagating down the sloping pipe with well-defined current head and body regions (Fig. 3a-e). The pipe confinement results in alternating acceleration and deceleration of the current front as it transitions between part-bore to full-bore (i.e. plug) flow conditions (Fig. 3a-f), particularly for larger mass inputs and steeper pipe inclinations. In comparison to the vertical pipe, hindered settling and size segregation in the depositing mass are significantly reduced, with only a portion of the fine size classes (i.e. red particles, silica flour) remaining in the pipe over an extended time (i.e. $t \geq$ 6s; Fig. 3h) before again being flushed out at the pipe exit and re-entrained by the next mass input. In this regard, dumping into inclined pipes/tunnels appears more efficient than in vertical pipes, which take considerably longer to empty due to hindered settling and size-segregation.



Fig. 3. Time series images of a single-shot dump (mass input = 227g) into a 45° inclined pipe at elapsed times $t$ after initial mass dump.

**Acknowledgements**

The authors acknowledge the financial support for this project provided by Statens vegvesen as part of an industry-funded project at the University of Dundee.

# Criticality in Gravity Currents

Edward W. G. SKEVINGTON[1], Robert M. DORRELL[1]

[1] University of Hull, England
e.w.skevington@hull.ac.uk
r.dorrell@hull.ac.uk

ABSTRACT

A gravity current is a flow along a horizontal boundary driven by a density difference between the current and the surrounding ambient fluid. Examples include submarine salinity currents, atmospheric cold fronts, turbidity currents, and ventilation flows. Like open channel flows, gravity currents exhibit two flow regimes classified by the motion of long waves: in subcritical flow waves are able to travel both upstream and downstream, that is the waves are faster (in a relative sense) than the current, while in supercritical flow the waves are swept downstream by the current, the current is faster than the waves. In critical flow the upstream directed waves are stationary. Across a stationary hydraulic jump the current slows from supercritical to subcritical, while across a topographic crest a flow may accelerate from subcritical to supercritical. These flow transitions are essential features that need to be identified to understand experimental and environmental flows.

## 1. Standard theory of criticality classification

The classification of subcritical and supercritical flow is straightforward in idealized models, specifically top-hat shallow-water models. Considering two-dimensional flow in $(x, z)$, in these models the velocity of the current takes a constant (in $z$) value $U$ over the range of elevation $0 \leq z - b \leq h$, where $b$ is the bed elevation and $h$ is the depth of the current, dropping to 0 on $z \geq h$. Similarly, the density drops from a constant value of $\rho_c$ within the current to $\rho_0$ above, and we define $R = (\rho_c - \rho_0)/\rho_0$. In such a model criticality can be classified using a Froude number, defined as the ratio of flow velocity to relative wave speed (Baines 1998)

$$Fr_{TH} = |U|/\sqrt{Rgh}. \quad (1)$$

Flow is subcritical for $Fr < 1$, critical for $Fr = 1$, and supercritical for $Fr > 1$. To evaluate the criticality of a real current, a common approach is to approximate the current as a top-hat current. This can be done using the depth defined using the scale of velocity (Ellison Turner, 1959), and then using this depth to define depth averaged velocity and density as

$$h = \left(\int_b^\eta u\, dz\right)^2 / \int_b^\eta u^2\, dz, \quad U = \int_b^\eta u\, dz/h, \quad R = \int_b^\eta \rho - \rho_0\, dz/\rho_0 h. \quad (2)$$

Here, $\eta$ is the upper reaches of the current, $u$ the measured velocity, and $\rho$ the measured density. Then a Froude number is calculated using (1). An alternative Froude number can be defined by using

$$R_{ET} = \int_b^\eta u(\rho - \rho_0)\, dz/\rho_0 hU, \quad Fr_{ET} = |U|/\sqrt{R_{ET} gh}, \quad (3)$$

as done by (Ellison Turner, 1959). To examine the efficacy of these Froude numbers, we consider the salinity current that flows into the Black Sea, see Fig. 1. The data is from (Dorrell et al. 2016), and consists of density and velocity measurements along a submarine channel. There are two sharp drops in the bed elevation at around 2000m and 2350m at which we expect to see a transition to supercritical flow on the downslope. The first slope is followed by a deeply eroded plunge-pool where we expect a hydraulic jump, while the second slope has a much less eroded pool where we expect either a jump or a continuation of supercriticality downstream. Both Froude numbers are larger upstream of the slopes than downstream, but neither is greater than 1 (supercritical) on the first slope and only $Fr_{ET}$ displays a jump transition on the second slope.

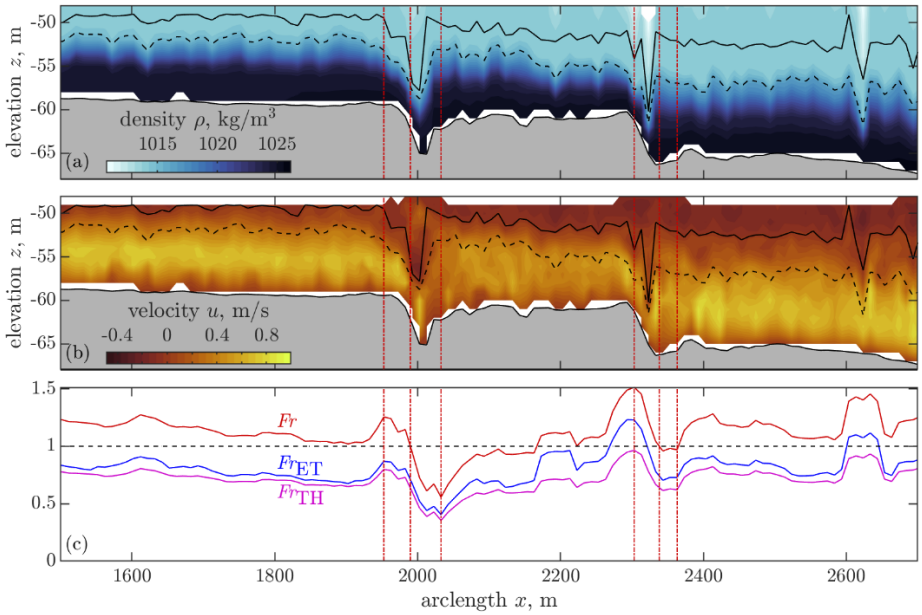



**Fig. 1.** A salinity current in the Black Sea, data from (Dorrell et al. 2016). In (a) and (b) we present the measured density and along-arc velocity fields, with the bed $z \leq b$ shaded in grey, the Ellison-Turner depth $h$ as a dashed line, and the upper reach of the current $\eta$ as a solid line, computed as where velocity vanishes. In (c) we plot the three Froude numbers discussed in the text. Using the flux Froude number $Fr$ we identify regions that may contain hydraulic jumps, and indicate the range and critical point with red dashed lines

## 2. An improved method of classification

There is no fundamental reason why the top-hat shape should be used in shallow-water models, indeed sometimes shape-factors are included in models to account for the profiles of velocity and density present in the flow. Analysis of a model including shape-factors yields the Froude number

$$Fr = |U|/\sqrt{\sigma_{zR} R g h}, \text{ where } \sigma_{zR} = 2\int_b^\eta (z-b)(\rho-\rho_0)\,dz/\rho_0 h^2 R. \quad (4)$$

While $Fr = 1$ at criticality and can be used for criticality classification, it is not the ratio of flow velocity to wave speed. Plotting in Fig. 1, we see that on the first slope we have clear acceleration followed by a hydraulic jump. On the second a jump is weakly detected, subcriticality lasting briefly, but it is possible that supercriticality is maintained and the brief week subcriticality is a result of measurement/processing error.

Substituting for the definitions in (2) and (4), we can rewrite this Froude number as

$$Fr^2 = \int_b^\eta \frac{1}{2}\rho_0 u^2\,dz \Big/ \int_b^\eta (\rho-\rho_0) g (z-b)\,dz. \quad (5)$$

This has a rather elegant interpretation. Due to the Boussinesq assumption, the numerator is the kinetic energy and the denominator is the gravitational potential energy, both integrated over the depth. Consequently, the condition of supercriticality upstream of a hydraulic jump is that kinetic energy exceeds the gravitational potential, identical to the upstream condition derived by (Thorpe, 2010). Downstream, subcriticality implies that the gravitational potential exceeds the kinetic energy.

Extending the analysis to a full three-dimensional flow, (5) is still the appropriate way to classify criticality, however the classification now becomes direction dependent and $u$ should be the projection of velocity in the direction of interest. In particular, across a hydraulic jump $Fr$ will decrease from above to below unity when $\boldsymbol{u}$ is the velocity in the direction normal to the jump. Consequently, we can no longer interpret the numerator of (5) as kinetic energy. Instead we interpret (5) as the ratio of half the momentum flux caused by velocity to the momentum flux caused by pressure. Thus, we term $Fr$ the flux Froude number, and it can be used to classify criticality in real flows, directly using the measured profiles of velocity and density in the model.

**Acknowledgements**

This work was supported by the Turbidites Research Group, University of Leeds (funded by AkerBP, CNOOC, ConocoPhillips, Harbour Energy, Murphy Oil, OMV, Oxy, and PetroChina); and the UK Natural Environment Research Council (R.M.D.).

**References**

Baines PG (1998) Topographic Effects in Stratified Flows, Cambridge University Press, 500 pp.
Dorrell RM, Peakall J, Sumner EJ, Parsons DR, Darby SE, Wynn RB, Özsoy E, Tezcan D (2016) Flow dynamics and mixing processes in hydraulic jump arrays: Implications for channel-lobe transition zones, Marine Geology, 381, 181-193
Ellision TH, Turner JS (1959) Turbulent entrainment in stratified flows, Journal of Fluid Mechanics, 6(3), 423-448
Thorpe SA (2010) Turbulent hydraulic jumps in a stratified shear flow, Journal of Fluid Mechanics, 654, 305-350

# Dynamics of gravity currents interacting with sediments bed

Maria Rita MAGGI[1], Maria Eletta NEGRETTI[2], Emil J. HOPFINGER[3]

[1,2,3] LEGI, UGA/CNRS, UMR 5519, 38000 Grenoble, France
maria-rita.maggi@univ-grenoble-alpes.fr
maria-eletta.negretti@univ-grenoble-alpes.fr
emil.hopfinger@univ-grenoble-alpes.fr

ABSTRACT

The hydrostatic imbalance between two adjacent fluids, characterized by density differences due to temperature, salinity, or sediment concentration gradients, frequently initiates the development of gravity currents. These phenomena play a pivotal role in diverse geophysical and engineering applications, influencing atmospheric, terrestrial, and subaqueous environments (Simpson, 1997). Gravity currents in nature span a wide array of topographical settings. Substantial alterations in topography and seafloor irregularities can be attributed to the influence of these currents. The high velocities near the bed, characteristic of such flows, contribute to their transformative potential. Consequently, rapid morphological alterations may occur in river and estuarine beds due to the passage of these currents, leading to significant sediment transport, erosion, and deposition (Sequeiros et al. 2010). Following Martin et al. (2019) with a linear slope of 7° and a initial stable interface, we investigate the effects of such a current on a sediment bed. It is shown how sediment entrainment develops until reaching an equilibrium state of maximum entrainment capacity. The observed bedforms are discussed.

## 1. Experimental details

Experiments involving a continuously supplied gravity current on a sediment bed were conducted in a Perspex tank, as depicted schematically in Fig. 1a. The channel's initial section is horizontal, followed by a linear slope ($\theta$=7°) that facilitates flow acceleration. The initial shear layer interface remains stable, leading to a pronounced acceleration of the current until it reaches a critical point. Subsequently, the current decelerates as Kelvin-Helmholtz instabilities set in (see Martin et al., 2019). The buoyancy-driven flow was induced using saline solutions ($\Delta\rho = \rho_1-\rho_0$=5 kg/m³), with a flow rate per unit width of $q_0$=64 cm²/s, and a total water depth of $H_0$=18±0.5 cm. To establish an initial condition with a large overall Richardson number, the gate on the horizontal portion was positioned 160cm upstream from the ridge.

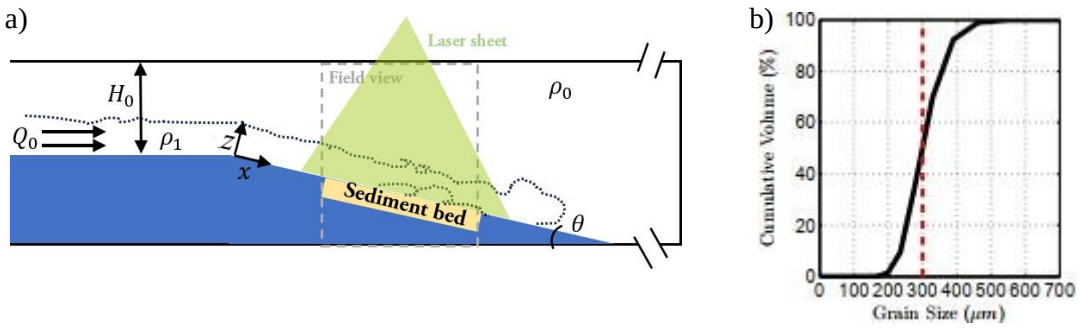



**Fig. 1.** a) Schematic side-view of the experimental set-up used to perform laboratory experiments. b) Particle size distribution curve, including the median grain diameter.

The sediment bed, starting 10cm downstream from the ridge, spans 75cm in length and is 4cm deep. The sediments consist of polystyrene particles with a density of $\rho_s$ = 1040 kg/m³ and a diameter of $d_{50}$ = 300µm. Particle size distributions were analyzed using a Spraytec laser particle size analyzer (Fig. 1b). For Particle Image Velocimetry (PIV) measurements, a CCD camera (1200 × 1600 pixels) captured experimental images at a frequency of 22 Hz. Further procedural details regarding PIV can be found in Martin et al. (2019).

## 2. Discussion

In Figure 2a, profiles of the averaged streamwise velocity <u> and Reynolds stress <u'w'> are presented at x=60cm on the sediment bottom. Here, u' and w' denote the temporal fluctuations of the velocity components, defined as u' = u - <u> and w' = w - <w>, respectively, where the operator <·> represents time-averaging. The temporal average is considered only for the steady flow regime. The figure illustrates that the maximum value reached by <u> is 8.6 cm/s, and the height at which this maximum velocity occurs is influenced by both interfacial drag and the bottom topography. The maximum value reached by Reynolds stress is 0.44 $cm^2/s^2$, corresponding to 5% of <u> and and decreases toward the bed to approach the friction velocity. Figure 2b presents the Hovmöller diagram illustrating the bed elevation anomaly. The figure depicts periodic bed forms (waves) that clearly propagate downstream. Towards the conclusion of the experiment, the amplitude of these bed forms measures 4±2mm (see Fig. 2c), and the wavelength is 13cm. After completing the analysis in this study, our bed form measurements, coupled with accurate velocity data, would enhance our understanding of the formation of ripple-like beds. A future analysis concerns the definition of sediment entrainment criteria using the available data from Garcia et al. (1993), with the aim of predicting sediment entrainment for the present experimental conditions, considering that the change in sediment flux of a dense bottom current flowing over a sediment bed can be written as: d(CUh)/dx= E-D where E is entrainment of sediment from the bed load (sediment layer) and D is deposit. It is generally accepted that $D = C_b w_s$, where $C_b$ is a near bed sediment concentration, taken at 0.05h with h the flow thickness, and $w_s$ is the fall velocity. Concerning E, there is less consensus.

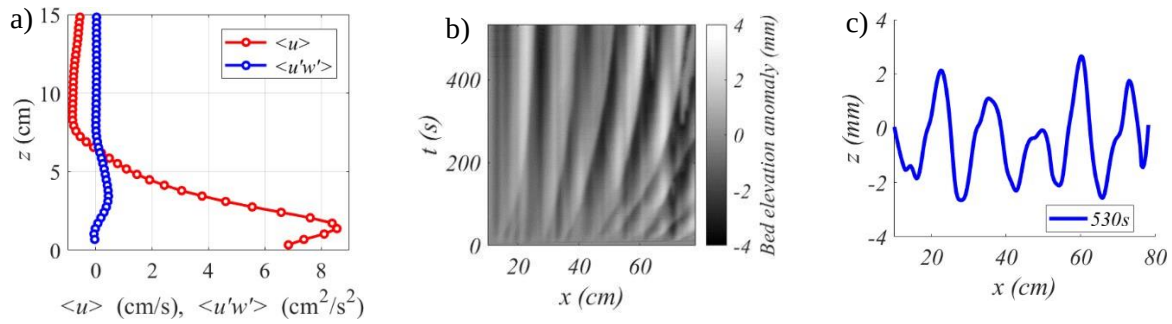



**Fig. 2.** Profiles of the averaged streamwise velocity $< u >$ and of the Reynolds stress <u'w'> determined at x=60cm (a). Hovmöller diagram for the bed elevation anomaly (b). Instantaneous bed elevation anomaly (c).

**References**


Simpson, J.E., 1997. Gravity currents: In the environment and the laboratory. Cambridge University Press, Cambridge.

Sequeiros, O. E., Spinewine, B., Beaubouef, R. T., Sun, T. A. O., Garcia, M. H., & Parker, G. (2010). Bedload transport and bed resistance associated with density and turbidity currents. Sedimentology, 57(6), 1463-1490.

A. Martin, M. E. Negretti, and E. J. Hopfinger, "Development of gravity currents on slopes under different interfacial instability conditions," J. Fluid Mech. 880, 180–208 (2019).

Garcia, M., Parker, G.: Experiments on the entrainment of sediment into suspension by a dense bottom current. Journal of Geophysical Research: Oceans 98(C3), 4793–4807 (1993).

# Flow Pattern of a Vane-controlled 90º Mobile Bed Lateral Diversion in Morphological Equilibrium

Zehra BÜYÜKER[1], Joana BALTAZAR[2], Gökçen BOMBAR[3], António Heleno CARDOSO[4]

[1,3] Civil Engineering Department, İzmir Kâtip Çelebi University, Türkiye
zehra.buyuker@ikcu.edu.tr
gokcen.bombar@ikcu.edu.tr [2]
COBA, Portugal
j.baltazar@cobagroup.com
[4] Civil Engineering Research and Innovation for Sustainability (CERIS), Instituto Superior Técnico, Universidade de Lisboa, Portugal
antonio.cardoso@tecnico.ulisboa.pt

ABSTRACT

Lateral water intakes built in the berms of mobile bed rivers and integrated in urban water supply systems or in diversion channels lead to the occurrence of a phenomenon known as the "Bulle effect". This phenomenon impacts on the sustainability of water diversion systems and leads to intricate engineering problems. Various engineering solutions have been tried to mitigate or solve these problems. The use of submerged vane-fields inserted in the bifurcation zone seems to be one of the most promising solutions. However, there is a considerable gap of knowledge regarding the hydro-morpho-dynamics of vane-controlled mobile-bed water diversions and the design criteria of vane-fields. For the purpose of deepening our understanding of the phenomena involved, an experiment was conducted in a rectangular T-linked channel system which consisted of a main channel and a smaller diversion channel. The flow field and bed morphology were measured after the bifurcation zone reached the equilibrium stage. The results demonstrated a significant reduction in sediment transported from the main channel to the diversion channel thanks to the presence of vanes. More remarkably, the vane-field prevented the diversion channel vortex to start from inside the main channel, contrarily to what has been observed in the absence of vanes.

## 1. Introduction

In many man-made lateral diversions of water from mobile-bed rivers, such as those created for urban water supply or as entrance structures of diversion channels, a phenomenon known as the "Bulle effect" arises. This phenomenon includes the imbalance between the amounts of diverted sediments and water, the sediment diversion being disproportionately higher than the water diversion. This imbalance can lead to significant engineering challenges that must be addressed. To mitigate the Bulle effect and manage the diverted sediment in mobile-bed bifurcations, engineers have been increasingly using submerged vane-fields. These vane-fields are structures designed to influence the flow of water and sediment, with the goal of minimizing sediment accumulation in the diversion entrance and optimizing the performance of water intakes. They are particularly employed in attempts to desilt lateral water intakes, ensuring the efficiency and longevity of these structures. Despite the increasing use of submerged vane-fields, there is still a considerable gap in knowledge regarding the hydro-morpho-dynamics of water diversions and the associated design criteria. Researchers and engineers are actively working to better understand the complex interactions between water flow, sediment transport, and the geometry of diversions. Until to the present, the flow field at uncontrolled mobile bed bifurcations (no vanes present) was mapped in a limited number of studies, whereas studies on the flow field of controlled mobile-bed bifurcations are even scarcer and far from covering the entire domain of pertinent independent variables. Some facts were established though: 1) a separation flow zone occurs along the inner wall of the diversion immediately after the entrance; 2) a diversion channel vortex starting in the main channel bed evolves along the bed of the outer diversion channel wall in the

absence of vanes; 3) a trail vortex is created on top and along the inner row of vanes of the vane field when this is present. The way these organized flow structures interact to reduce the sediment digestion into the diversion channel is still to be established and understood. This knowledge gap highlights the need for further research and the development of comprehensive design guidelines to address the specific challenges posed by sediment diversion in mobile-bed rivers. Efforts to fill this knowledge gap may include field studies, laboratory experiments, and numerical modeling to analyze the behavior of water and sediment in diversified hydraulic conditions. It is the purpose of the present experimental study to understand the physics of the involved phenomena and to gather reliable data for the future training of pertinent CFD models.

## 2. Methods

The experiment was conducted in a rectangular T-linked channel system (Fig. 1) composed of a 9.28 m long (net length), 0.68 m wide, and 0.40 m deep rectangular main channel and a 2.0 m long, 0.26 m wide, and 0.40 m deep rectangular diversion channel. The diversion channel was connected to the main channel through the diversion angle of $\theta$ = 90°, with no bed discordance. The vane field was composed of six arrays of two vanes and acted parallel to the main channel axis; the individual vanes were skewed 10º towards the same axis.

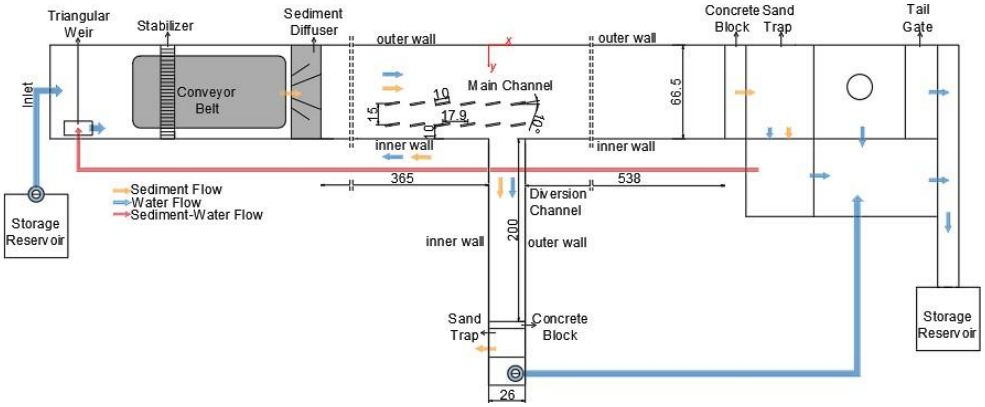



**Fig. 1.** Experimental set-up

The bed of the channels was covered with uniform sand; water and sand were recirculated through independent circuits until the equilibrium stage was reached. The equilibrium bed was surveyed with a Micro-Echo-Sounder and the flow field was measured in a dense grid of points with a robust ADV probe.

## 3. Results

The presence of the recirculation zone near the diversion channel entrance, along its inner wall, became evident. The vane-field induced a trail vortex system spanning along its entire length and extending downstream. This vortex system effectively deviated a significant portion of the main channel bed particles from the diversion entrance. It achieved this by excavating a scour trench between the inner row of the vane-field and the main-channel inner wall, both upstream and downstream of the diversion channel, including its entrance. Particularly noteworthy was the ability of the vane-field to prevent the formation of the diversion channel vortex from inside the main channel, a phenomenon previously documented to occur in the absence of vanes in the same experimental setup for similar flow conditions. The results showed why the amount of sand sucked from the main channel by the diversion channel vortex decreased in the presence of vanes.

## 4. Conclusion

The flow field and the bed morphology of an equilibrium 90° mobile-bed bifurcation controlled by a vane-field are presented and discussed. The most important finding of this study was that the inhibition of the diversion channel vortex to start from inside the main channel, contrarily to what has been reported in the absence of vanes.

### References


Barkdoll BD, Ettema R, & Odgaard AJ (1995) Sediment control at lateral diversions: Limits and enhancements to vane use, Journal of Hydraulic Engineering, 125(8), 862–870.

Baltazar J, Alves E, Bombar G, & Cardoso AH (2021) Effect of a submerged vane-field on the flow pattern of a movable bed channel with a 90◦ lateral diversion, Water, 13(6), 828.

Gumgum F, Cardoso AH (2022) Optimizing the desilting efficiency of submerged vane fields at lateral diversions, Journal of Hydraulic Engineering, 149(1).

Sruthi TK, Ranjith KB, & Chandra V (2017) Control of sediment entry into an intake canal by using submerged vanes, In Proceedings of the International Conference on Applied Physics and Engineering, Penang, Malaysia, 2–3 November 2016; Mohd, M.J., Mohd, A., Mohd, N.A., Eds.; American Institute of Physics: Melville, NY, USA.

# Alqueva Project - A Case of Regional Development

Jorge VAZQUEZ, Portugal
jvazquez@edia.pt

ABSTRACT

Concerning climate changes, Portugal and especially Alentejo, region where is located the Alqueva Project has a significant vulnerability. In fact, the Alqueva Project area, considering its location and the involving orography, receives very little influence from the fresh and humid Atlantic Ocean winds and is more exposed to the winds coming from the north of Africa and the Sahara Desert. It is agreed that we will have a clear rise of the temperature, more frequent extreme events of warm waves and dry periods with less definition of the seasons, and a probable reduction of precipitation and run-off.

The Guadiana River where Alqueva dam is located, starts in Spain, in Ruidera lagoons, at 1 700m altitude, with 110km making up the border line between Portugal and Spain. The total drainage basin covers 66800km2, having only 17% in Portugal (11580km2), with an average rainfall of 550mm.

Alqueva Dam is the great water origin of the Alqueva Project - the largest national multipurpose hydraulic project centered on an integrated management of a strategic water reserve, that ensures, large scale regional irrigation, domestic and industrial water supply, reducing risk of extreme events (namely droughts and floods) in the country's entire southern region, assuring clean energy production, tourism and ludic uses (Fig.1).

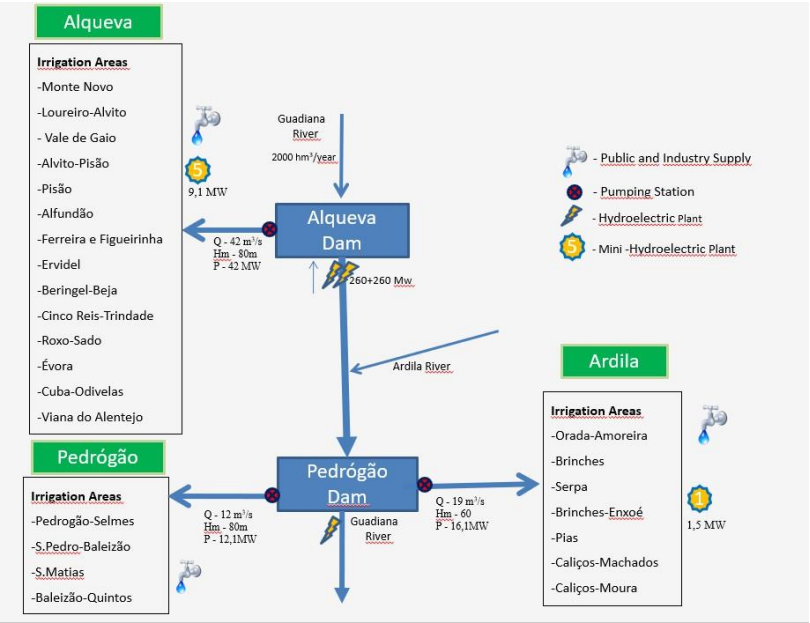



Fig. 1 – Alqueva Multipurpose Project – general diagram

The Alqueva dam has a basin with 55 000km2 and Pedrógão dam, which is located downstream, assuring the reversibility of the system, has a basin of 59 160km2.

Alqueva double curvature arch concrete dam, 96m crest height and 458m crest length, with surface and half-bottom gated spillways (9 800m3/s), is located at Alentejo – region which is one third of the total area of Portugal and one of the most susceptible to desertification zones. The dam allows the creation of a big

4150hm3 storage reservoir with 250km2 inundated area, being the core of the Multipurpose Alqueva Project - comprising a territorial intervention area of more than 10 000km2.

The Alqueva dam (Fig. 2) with a NWL at 152m, has, at the downstream toe, two reversible Hydroelectric Power Stations (Alqueva I and II) – 2 x 260 MW = 520MW.

The first filling of Alqueva dam started in 2002. Meanwhile, an important task of hydraulic circuits construction, crossing the Alentejo territory was executed - integrating approximately 70 reservoirs, weirs and dams, 2 reversible hydro-power plants and 5 mini-hydros, 50 pumping stations, and more than 2.000 km of canals and conduits, creating a robust and structuring network of more than 6.700 water points.

In three years, 2009/10, 2010/11 and 2012/13, a total 0f 14.853hm3 passed downstream of the Alqueva/Pedrogão System. Alqueva discharged for three times, 2010, 2011 and 2013, but severe droughts occurred, namely in 2005, 2012, 2015, 2017 and 2022- clearly identifying the great irregularity of the flow in the Guadiana river - and having been the Alqueva Project crucial to ensure all the water needs in the region



Fig. 2. Alqueva dam

Pedrogão is a concrete gravity dam with a NWL at 84.8m and a crest height and lenght of, respectively, 43 and 448 m, creating an artificial lake with a storage volume of 106hm3-that functions as a balancing water storage for Alqueva reversible hydroelectric power stations - and is located 20km downstream from Alqueva dam, being the first Portuguese dam in compacted concrete.

All these important hydraulic infrastructures involved complex studies and works, following the state-of-the-art, as the case of Alqueva and Pedrógão dams - where National Laboratory (LNEC) played an important role, concerning namely the hydraulic and structural behavior modeling, as all the dams monitoring.

An important program of compensation and mitigation measures was undertaken such as, between may others, i) the creation of a new Luz Village and Luz Museum-intervention inherent to the submersion of the old Village and implying a construction of a new Village and the preservation of collective memories, and ii)the Noudar Park, created as a compensatory measure and to preserve habitats such as those that were submerged by the construction of Alqueva dam, occupying an area of 1000 ha, in a scenario of great natural beauty.

Meanwhile, a central maintenance and monitoring management system was implemented, including remote control, where all maintenance and safety, activities and issues are defined, scheduled, assigned to teams, and recorded. This allows for a much more optimized intervention, and on time, minimizing outage periods, allowing permanent water balances, improving overall efficiency, and resulting in better use.

The guarantee of the ecologic flows downstream of the Project is another commitment we are engaged with, to assure the sustainability of the river biodiversity and ecosystems related. These flows are discharged at Pedrogão dam mini-hidro (10MW) - this dam having a fish elevator passage.

After 15 years of operation and less than 10 years of the first phase conclusion, it can be said that the Alqueva Projet is a success, allowing not only the socioeconomic upgrading of the region, but also creating new challenges, concerning namely the impact of the climate changes and the need to guarantee its sustainability.

Answering these new challenges, a group of actions are ongoing to increase the benefit, to improve the hydraulic and energy efficiency and to ensure that environmental values are protected, including, namely, new hydraulic circuits to allow the availability of water in other potential desertification zones, the installation of photovoltaic plants and a requalification program concerning the water quality and biodiversity improvement.

In this presentation, we summarize the main information concerning the Alqueva Project and its management and operation challenges.

# 300 MW Balakot Hydropower Project – A Himalayan Challenge

Filipe ROBERTO[1], António PINHEIRO[2], Raquel RIBEIRO[3], Sérgio COSTA[4]

[1,3,4] Aqualogus, Engenharia e Ambiente, Portugal
froberto@aqualogus.com
rribeiro@aqualogus.com
scosta@aqualogus.com
[2] Instituto Superior Técnico, Portugal
antonio.pinheiro@tecnico.ulisboa.pt

ABSTRACT

## 1. Introduction

The 300 MW Balakot project is a run-of-river hydropower scheme to be situated on the Kunhar River within the picturesque Kaghan Valley, Mansehra district, nestled in the Khyber Pakhtunkhwa province of the Pakistani Himalayas (Fig. 1). As an integral part of Pakistan's shift towards renewable energy initiatives, the project intends to bolster the region's energy capacity, anticipating the expected rise in energy demand, taking advantage of the abundant local hydropower resources in a sustainable and economically efficient manner.

This paper aims to outline the essential components of project while highlighting the challenges faced by AQUALOGUS due to difficult geological, seismic and sediment transport characteristics of the site.

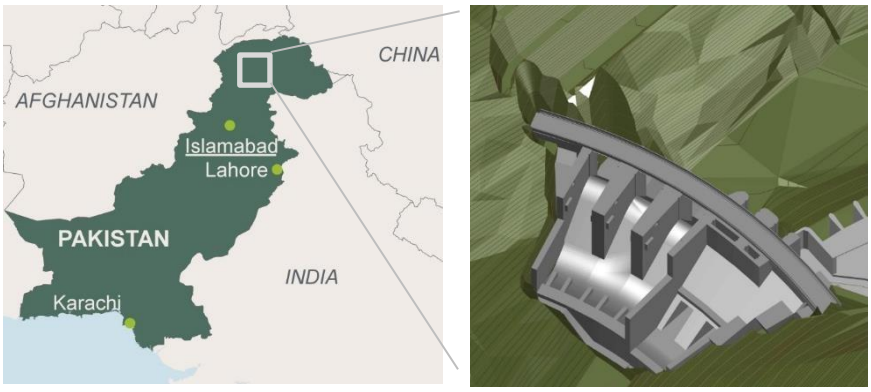



**Figure 1 –** Balakot dam location and overview.

## 2. The 300 MW Balakot Hydropower Project

The Balakot hydropower project comprises several key components, starring a gravity concrete dam standing at a maximum height of 58 m above its foundation with a crest length of 130 m (Fig. 2). On the left bank of the dam, a gated controlled water intake structure heads the intake tunnel – a structure with a circular cross-section boasting an 8.00 m internal diameter and extending over a length of 9100 m. The heart of the project is a cavern-based hydroelectric power station consisting of two cells: a main cell, which is approximately 34 m in height, 20 m in width, and 71 m in length, housing three vertical-axis Francis turbines(Fig. 2); and, adjacent to the main cell, a secondary cavern dedicated to generators and a substation, measuring approximately 20 m high, 14 m wide, and 88 m long. To promote the water return to the river, a circular

cross-section low pressure tunnel was envisaged, featuring an 8.00 m internal diameter and spanning a length of 1515 m.

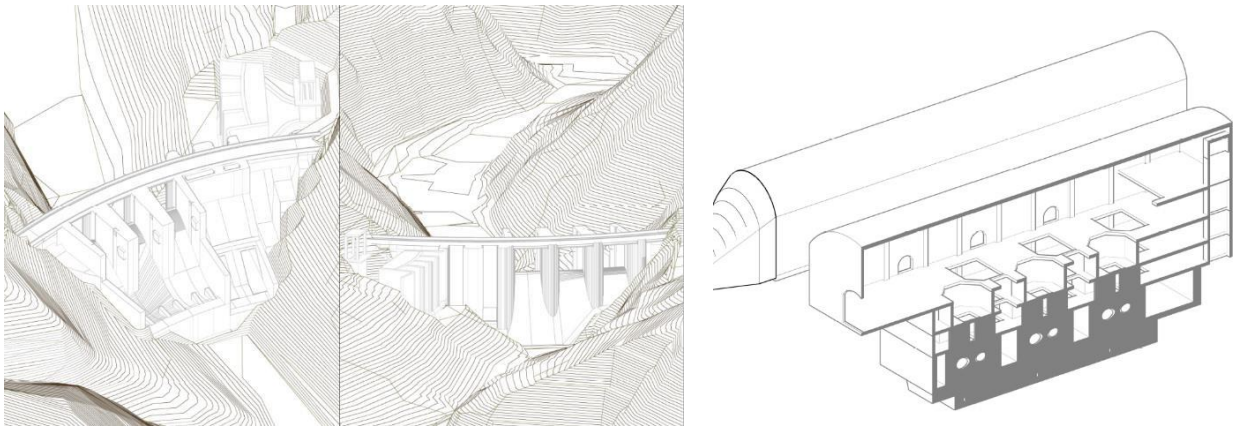


**Figure 2 –** Balakot dam downstream and upstream view (left) and powerhouse main cavern section cut (right).

As a noteworthy addition, a sediment bypass tunnel was designed on the right bank, upstream from the dam. This 650 m long tunnel features an arched cross-section, measuring 7.50 m wide and 8.00 m . The tunnel serves a dual purpose: it plays a crucial role in transporting sediments downstream during flushing operations and assumes a significant function during the construction phase when it serves as the primary river diversion structure.

The Balakot hydropower scheme, with a gross head of 229.00 m and a net head of 217.60 m, will have an installed capacity of 300 MW, with an estimated average annual production (over 50 years) of 1143 GWh.

## 3. The Himalayan Challenge

In addition to the typical technical challenges associated with the design of such structures, the planning and design of the Balakot hydropower project faced additional complexities due to its challenging location. The Himalayas, formed by the collision between the Indo-Australian and Eurasian tectonic plates according to modern plate tectonics theory, are known for their highly active seismicity, both in terms of frequency and intensity. This seismological context presented significant challenges for structural design, requiring the use of calculation methods that differ from the traditional approaches used for large dam design around the world, primarily due to the magnitude of the maximum expected earthquake (characterized by horizontal accelerations around 0.9g).

Furthermore, the orographic and geological features of the region, shaped by the Himalayan formation process and the significant seismic activity it experiences, make the stability of the reservoir's slopes a critical design constraint. Creating a reservoir under these conditions demanded an assessment of the potential consequences of landslides into the reservoir. Consequently, a thorough slope mapping was conducted to pinpoint the most critical potential landslide areas. This procedure was then followed by an in-depth analysis of the mechanisms governing wave generation and propagation within the reservoir, driven by the potential sliding of these masses, and the subsequent implications for the dam safety assessment.

Another substantial set of challenges stems from the high altitude of the region. Although the crest of the Balakot dam is at an elevation of only 1292 m, its catchment area extends to elevations exceeding 4400 m. Approximately 80 to 90% of the upstream catchment area of the Balakot dam is covered with snow during the winter months (typically from January to May), with near-complete thaw during the warmer seasons. These particular conditions have a profound impact not only on the river Kunhar's flow regime, but also on the sediments production and transport along the river. The specificity of these conditions required a dedicated study of the phenomenon and the implementation of specific sediment management measures and procedures.

The paper aims to address the complex seismic stability design of the dam, it will provide detailed information on the geological survey of the riverbanks surrounding the future reservoir area and present the results of the induced reservoir wave simulation, and additionally, it will outline the key features and design aspects of the sediment management.

# Evaluation of hydrological dam safety considering flood peak and volume

Ana I. REQUENA[1], Antonio JIMÉNEZ-ÁLVAREZ[1] and Celia GARCÍA[1]

[1] Centre of Hydrographic Studies of the Centre for Studies and Experimentation of Public Works (CEDEX), Spain
ana.i.requena@cedex.es; antonio.jimenez@cedex.es; celia.garcia@cedex.es

ABSTRACT

Floods are defined by variables such as peak and volume, being relevant to jointly consider them for evaluating hydrological dam safety. This study assesses deterministic and probabilistic methods to characterise floods by comparing the maximum water level reached at the reservoir for a given return period. A Spanish case study with reservoir configurations synthetically generated from real reservoirs is used in the assessment. The study examines annual and seasonal flood frequency analysis. The former is performed considering a routing method with and without spillway gates; the latter does not consider spillway gates and accounts for fixed and random initial water levels at the reservoir. Results confirm that deterministic methods provide greater maximum water levels than probabilistic methods, and that annual analysis provides greater maximum water levels than seasonal analysis when accounting for seasonal variability in the initial water level at the reservoir. Findings allow providing steps for assessing hydrological dam safety that are included in a national handbook.

## 1. Introduction

Floods are extreme events defined by variables such as peak and volume, and therefore it is relevant to jointly consider them for evaluating hydrological dam safety. Floods may be studied using (simpler) deterministic methods that do not consider statistical dependence between variables, or probabilistic methods that do consider it. The *flood peak method* and the *flood peak – volume method* are deterministic methods. The former uses the peak quantile for the studied return period to determine the maximum water level at the reservoir through the outflow curve. The flood peak – volume method uses both peak and volume quantiles to define a design hydrograph that is routed through the reservoir to obtain the maximum water level.

The *regression method* and the (*regional) copula method* are probabilistic methods. The regression method is an alternative approach to the bivariate joint distribution function of peak and volume that provides a simpler way to represent statistical dependence between variables (Mediero et al., 2010). The (regional) copula method is based on a statistical technique where the bivariate joint distribution function is obtained through the characterisation of the statistical dependence between variables (via the copula) and the marginal distribution functions. The use of probabilistic methods entails interpreting the return period based on the risk of dam overtopping, i.e., as the inverse of the probability of exceeding a given maximum water level (Mediero et al., 2010; Requena et al., 2013), requiring the generation of a great number of synthetic hydrographs to be routed through the reservoir to obtain the maximum water level for the studied return period.

The aim of the study is to evaluate hydrological dam safety by assessing deterministic and probabilistic methods to characterise floods by comparing the maximum water level reached at the reservoir for a given return period. The approach is applied to a Spanish case study where reservoir configurations are synthetically generated from existing reservoirs to consider a greater number of case studies. The study focuses on annual flood frequency analysis by considering a routing method with and without spillway gates. Additionally, seasonal flood frequency analysis (Jiménez-Álvarez and Mediero, 2014b) is also studied without considering spillway gates by accounting for fixed and random initial water levels at the reservoir. The latter is performed on a synthetic case study based on a reservoir for which water level records and operating rules are available.

## 2. Methodology

(i) Definition of homogeneous regions and fit of regional GEV distributions for peak and volume (Jiménez-Álvarez and Mediero, 2014a). Confidence intervals are considered in the annual analysis.

(ii) Generation of 50 000 peak – volume pairs by probabilistic methods for the annual (e.g., Fig. 1) and seasonal analysis. Also, peak – volume pairs associated with quantiles for a set of 255 return periods are obtained regarding the flood peak – volume method for the seasonal analysis.

(iii) Assignment of hydrograph shape to peak – volume pairs using the gamma density function.

(iv) Routing of hydrographs through the reservoir: the annual analysis considers a routing method with spillway gates and initial water level at the normal maximum level, and a routing method without spillway gates and initial water level at the spillway crest. The seasonal analysis does not consider spillway gates and accounts for three types of initial water levels: annual fixed (as the spillway crest level), seasonal fixed (as seasonal maximum water levels established by the operating rules), and seasonal random (as a random water level obtained from the seasonal distribution function of initial water levels at the reservoir).

(v) Estimation of the maximum water level for the studied return period ($T$ = 1000 years) for each method and type of initial water level. The value is interpolated from the annual distribution function of maximum water levels, which is obtained by combining the seasonal distribution functions for the seasonal analysis.

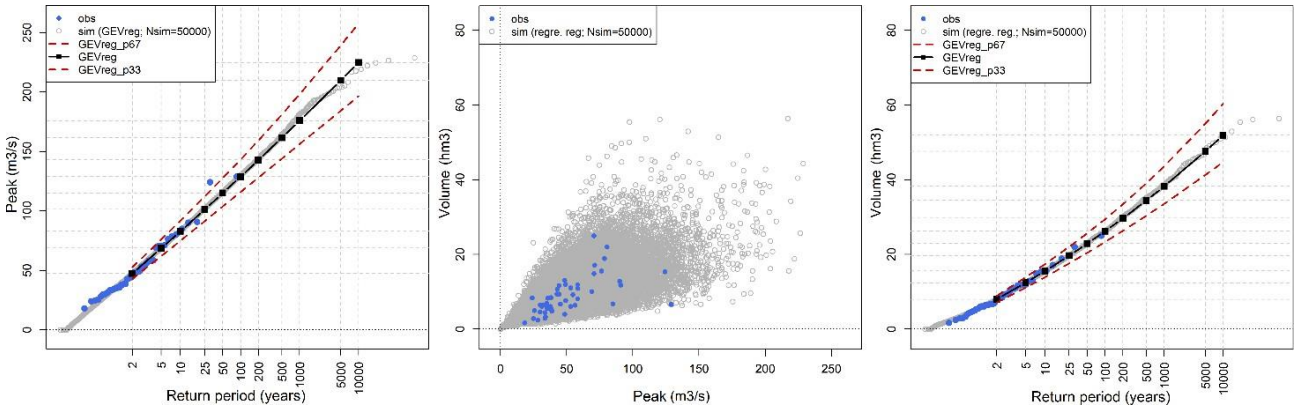



**Fig. 1.** Generation of peak – volume pairs by the regression method showing observed and simulated values: (left panel) regional fit of the GEV distribution for the peak; (central panel) peak – volume pairs; (right panel) regional fit of the GEV distribution for the volume.

## 3. Results and Conclusions

Results confirm that for a given type of initial water level at the reservoir, the maximum water level is obtained by the flood peak method, followed by the flood peak – volume method, and by probabilistic methods. Reservoirs with low storage capacity have associated great uncertainty, being that and the associated maximum water level comparable for all methods. Reservoirs with large storage capacity have associated a lower maximum water level and less uncertainty (and variability for probabilistic methods) regardless of the method accounting for hydrograph routing used. For a given method, the maximum water level for the annual analysis is greater than that for the seasonal analysis when accounting for seasonal variability in the initial water level at the reservoir.

Dam safety is verified when the estimated maximum water level is less than the admissible value. As a result, the proposed sequence of methods for evaluating hydrological dam safety is as follows: (i) flood peak method; (ii) flood peak – volume method with annual fixed initial water level; (iii) flood peak – volume method with seasonal fixed initial water level (if seasonal freeboards exist); (iv) probabilistic methods with annual fixed initial water level; (v) probabilistic methods with seasonal fixed initial water level (if seasonal freeboards exist); and (vi) probabilistic methods with seasonal random initial water level (if possible to obtain the seasonal distribution functions of initial water levels at the reservoir). As the complexity advances, the steps obtain less conservative maximum water levels; except for step (iii) where the value may be less than for step (iv). Findings are accounted for elaborating a national handbook for assessing hydrological dam safety in Spain.

**References**

Jiménez-Álvarez A, Mediero L (2014a) Tratamiento conjunto del caudal y el volumen para la estimación de hidrogramas de diseño de presas, Ingeniería Civil, 174, 33-49.

Jiménez-Álvarez A, Mediero L (2014b) Caracterización del comportamiento estadístico de los caudales máximos estacionales en la España peninsular. Propuesta metodológica para su cálculo, Ingeniería Civil, 174, 51-72.

Mediero L, Jiménez-Álvarez A, Garrote L (2010) Design flood hydrographs from the relationship between flood peak and volume, Hydrology and Earth System Sciences, 14(12), 2495-2505.

Requena AI, Mediero L, Garrote L (2013) A bivariate return period based on copulas for hydrologic dam design: accounting for reservoir routing in risk estimation, Hydrology and Earth System Sciences, 17(8), 3023-3038.

# Is riverbank vegetation important in river modelling?

Anna Maria ŁOBODA[1], Anouk BOMERS[2], Trang Minh DUONG[3]

[1,2,3] University of Twente, Department of Civil Engineering and Management, Enschede, the Netherlands
a.m.loboda@itwente.nl
a.bomers@itwente.nl
t.m.duong@itwente.nl
[3] IHE Delft Institute for Water Education, Delft, The Netherlands
[3] Deltares, Delft, The Netherlands

ABSTRACT

Vegetation as one of the fundamental river system components modifies river processes at various scales, and thus, it plays an important role in effective river engineering and management. To expand knowledge in this research field, this study aimed to investigate the effect of riverbank and floodplain vegetation on the rising water level considering various vegetation coverage. To achieve this objective, the process-based numerical model Delft3D Flexible Mesh was used to simulate the hydrodynamics of the Meuse River, the Netherlands, as a case study. Various static riverbank vegetation scenarios were implemented to represent seasonal changes in vegetation roughness. Moreover, additional scenario with changes in floodplain vegetation was applied to check the importance of this area during rising water levels and flood events.

## 1. Introduction

The interplays between river flows and vegetation are complex and interconnected (Sukhodolov, 2015). Vegetation, one of fundamental river system components, modifies flow patterns, which shape river processes, e.g., sedimentation, erosion, and nutrient retention (Haslam, 1978; Franklin et al., 2008; Sun et al., 2010). Achieving effective flood risk management demands a comprehensive understanding of the complex processes underlying mutual interactions, particularly the intricate interplay between hydraulic dynamics and biotic elements, presenting persistent challenges in research (Nikora, 2010; Nepf, 2012). In the past, conventional thinking held that vegetation would diminish discharge capacity by intensifying flow resistance, consequently elevating flood risks during periods of high flow. However, the perspective of perceiving plants only in a negative way has changed and engineers have shifted their approach to vegetation, acknowledging its substantial environmental advantages for aquatic ecosystems (Sun et al., 2010). It was crucial to recognize that such vegetation plays a pivotal role in the environment, serving as a tool for implementing nature-based solutions in river engineering and management (Shields Jr. et al., 2017). Present challenges involve finding a balance in predicting channel resistance in the presence of vegetation, considering both ecological management and flood control (Nepf, 2012). Nevertheless, accurately predicting processes in rivers with vegetated banks, such as vegetation-induced turbulence, requires extended studies on the seasonality of vegetation due to its dynamic nature.

## 2. Methods

### *2.1. Study area and hydrodynamic model*

This study delved into the exploration of the Meuse River, a prominent waterway in the Netherlands. The study obtained the segment of the river extending from the Eijsden grens (upstream) to the Maaseik gauging station (downstream). The analysis employed computations derived from the hydrodynamic model within the Delft3D Flexible Mesh software (D-Flow FM 2D model of the Meuse River; Deltares, 2022). Through numerical simulations, the research illustrated the influence of riverbank and floodplain vegetation on water levels both, before and during flood occurrences. The Eijsden grens and Maaseik gauging stations served as

reference points, establishing boundary conditions for the model by providing discharge and water level values. These parameters, including initial water level, referred to real-world conditions from the July 2021 flood event.

### *2.2. Roughness*

Concerning the implementation of modifications in vegetation, 6 scenarios were devised, including four scenarios for riverbank vegetation, one scenario for riverbank and floodplain vegetation and one reference scenario (model validated on real data from July 2021) with roughness values included using a trachytope roughness approach. The subsequent 5 scenarios featured adjustments in the roughness values along riverbanks or on the riverbanks and floodplain (Fig. 1a,b) to simulate diverse conditions of vegetation coverage, ranging from low vegetation density and height to the representation of high density and maximum height for the specific vegetation.

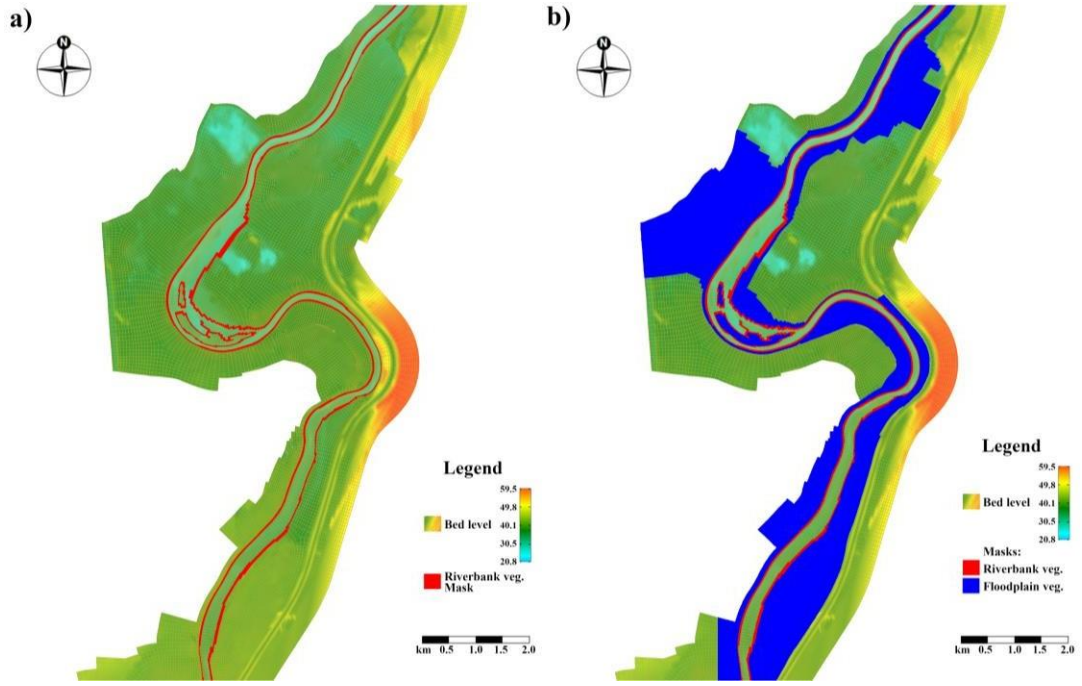



**Fig. 1.** Exemplary area of roughness masks, where changes were implemented on riverbanks (a) and on floodplains (b).

## 3. Preliminary results

The model results depicted scenarios of water level involving five distinct variants of the riverbank roughness map (including variant zero – reference scenario) for selected cross sections. The findings did not reveal significant differences in water levels during the flooding event following alterations made along the riverbanks (Fig. 1a), whereas changes implemented in the roughness of floodplain area (additional 6$^{th}$ scenario, Fig. 1b) showed that vegetation is an important component of the river system during flood event. Regarding the riverbank outcomes, slight disparities in water level values were observed before the flood event showing that riverbank may have an impact on discharges in the range that the floodplains start to inundate. Thus, further studies require to focus on the investigation of the effect on water levels and inundation extents for discharges when overbank flow starts to occur.

**References**

Deltares (2022) https://publicwiki.deltares.nl/display/RWS6GEN/Maas

Franklin P, Dunbar M, Whitehead P (2008) Flow controls on lowland river macrophytes: a review. Science of the Total Environment, 400, 369–378

Haslam SM (1978) River plants: The macrophytic vegetation of watercourses. Cambridge University Press, 396 pp.

Nepf HM (2012) Hydrodynamics of vegetated channels, Journal of Hydraulic Research, 50, 262-279

Nikora V (2010) Hydrodynamics of aquatic ecosystems: an interface between ecology, biomechanics and environmental fluid mechanics. River research and applications, 26, 367-384

Shields Jr FD, Coulton KG, Nepf H (2017) Representation of vegetation in two-dimensional hydrodynamic models. Journal of Hydraulic Engineering, 143: 02517002

Sukhodolov AN (2015) Field-based research in fluvial hydraulics : potential, paradigms and challenges. Journal of Hydraulic Research, 53, 1–19

Sun X, Shiono K, Rameshwaran P, Chandler JH (2010) Modelling vegetation effects in irregular meandering river. Journal of Hydraulic Research, 48, 775-783

# Dynamics of artificial spawning sites for trout and grayling – novel monitoring approaches based on pit-tagged gravel substrate at the Inn river

Martin SCHLETTERER[1,2], Patrick HOLZAPFEL[3], Michael PASTER[3], Zacharias SCHÄHLE[4], Hannes ZÖSCHG[1,5], Christoph HAUER[3]

[1] Department of Hydropower Engineering, TIWAG-Tiroler Wasserkraft AG, Eduard-Wallnöfer-Platz 2, 6020 Innsbruck, Austria
martin.schletterer@tiwag.at; hannes.zoeschg@tiwag.at
[2] Institute of Hydrobiology and Aquatic Ecosystem Management, University of Natural Resources and Life Sciences, Vienna (BOKU), Gregor-Mendel-Straße 33, 1180 Vienna, Austria
martin.schletterer@boku.ac.at
[3] Christian Doppler Labor für Sedimentforschung und -management, Institut für Wasserbau, Hydraulik und Fließgewässerforschung, Universität für Bodenkultur Wien, Austria
patrick.holzapfel@boku.ac.at; michael.paster@boku.ac.at; christoph.hauer@boku.ac.at
[4] Tiroler Fischereiverband, Meinhardstraße 11, 6020, Innsbruck, Austria
zacharias.schaehle@tiroler-fischereiverband.at
[5] Unit of Hydraulic Engineering, Department of Infrastructure, University of Innsbruck, Technikerstraße 13, 6020 Innsbruck, Austria
hannes.zoeschg@uibk.ac.at

## 1. Introduction

Artificial placement and/or management of spawning gravel is a well-established restoration practice in supply-limited river systems or rivers with anthropogenically induced high sediment transport capacity (Pulg, 2008). Many studies have focused on the biological response to artificial gravel dumping by (i) counting spawners or (ii) monitoring hatching success (see Holzapfel et al., 2023). However, there is a lack of data on how the artificial gravel / reproduction sites develop based on upstream (fine) sediment supply and the given hydrological regime. At our case study site, pit-tagged gravel substrate was artificially deposited at suitable places of a large-scale restoration measure. The aim of these surveys was to quantify the erosion and deposition processes in the entire restoration area and to compare the data with the displacements of the pit-tagged substrate.

## 2. Research area

The case study site, a large widening of the Inn river in Tyrol (Austria), extends over a length of approximately three kilometres between Stams and Rietz. This measure was implemented during two low-water periods (October - April) between 2021 and 2023 as part of the extension project of the Sellrain-Silz hydropower plant. The existing bank protection was largely removed, and the river bed was widened up to 75 meters (Zöschg et al., 2023), which resulted in the formation of a side channel (A1 - between rkm 332.5 and 331.4, Fig. 1), a backwater zone (A2 - between rkm 331.0 and 330.2, Fig. 1), and a natural bank on the orographic right side (A3). These changes allow the river to develop its own dynamics and create ecologically valuable areas, such as shallow water zones as well as gravel and sand banks. In addition, the measure enhances biodiversity and habitat diversity both in water and on land. For instance, the initial aquatic ecological structures, such as wooden structures (coarse woody debris) and islands, provide shelters and new habitats for aquatic biota. On the structured banks beetles, reptiles and birds find dynamic riverine habitats and already in 2023 the successful breeding of little ringed plover (*Charadrius dubius*) and common sandpiper (*Actitis hypoleucos*) was observed.

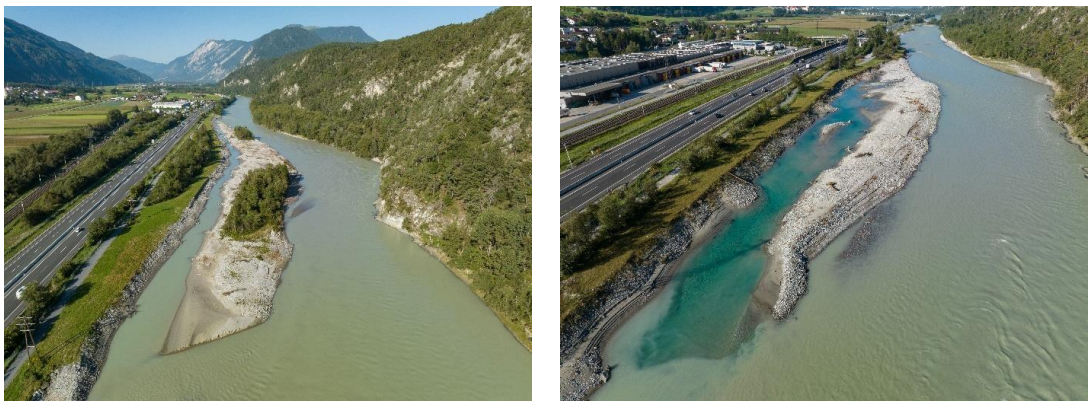


**Fig. 1.** Photos of the Stams-Rietz restoration measure on the Inn river from the UAV flight in September 2023: Left - the side channel A1, right - the back water zone A2 (Photos: droneproject.at)

## 3. Methods

The passive tags were deposited before in spring 2023. In the laboratory stones were drilled and equipped with a tag (Oregon RFID 12 mm HF pit tags). Overall, 210 stones from three different size classes, i.e. (i) 16 mm < b < 22.4 mm; (ii) 22.4 mm < b < 31.5 mm; (iii) 31.5 mm < b < 56 mm, were used (Fig. 2). In the field these stones were admixed with spawning substrate in the side channel and in the main channel. The initial positions of all stones were recorded with a GPS device.




**Fig. 2.** Oregon RFID HF pit tag (source: www.oregonrfid.com) and stones of three different size classes (< 22.4 mm; < 31.5 mm; < 56 mm).

In addition, two photogrammetric surveys using an unmanned aerial vehicle (UAV) were conducted in April 2023, immediately after the completion of the restoration measure, and in September 2023, shortly after a 100-year flood event on this stretch of the river.

## 4. Results & Conclusion

The first results already show some interesting developments of the artificial reproduction sites due to the flood event. On the one hand, how spawning gravel is distributed and if it´s still in position to be suitable for brown trout (*Salmo trutta*) and grayling (*Thymallus thymallus*) reproduction and, on the other hand, the accumulation of fine sediments. Thus, in preliminary conclusion, we highlight that it is not only the onsite suitability and stability which is decisive, but also the superior sediment regime that determines the term ´sustainability´ for spawning restoration measures.

**References**

Holzapfel P, Schähle Z, Schletterer M, Hauer C (2023) Grundlagenuntersuchungen für die Revitalisierung und Erneuerung von Kieslaichplätzen in alpinen Fließgewässern. Österr Wasser- und Abfallw, 75, 405–420, https://doi.org/10.1007/s00506-023-00963-z

Pulg U (2008) Laichplätze der Bachforelle (*Salmo trutta*) in der Moosach – die Bewertung ihrer Funktionsfähigkeit, ihre Degradierung und ihre Restaurierung. PhD thesis Technische Universität München, 175 pp., https://mediatum.ub.tum.de/doc/680304/680304.pdf

Zöschg H, Bacher T, Boschi M, Fey C, Schöber J, Reindl R, Schletterer M, Aufleger M (2023) UAV-based monitoring of sedimentary processes at a large-scale revitalisation of an alpine river – concept and outlook. EGU General Assembly 2023, EGU23-13887, https://doi.org/10.5194/egusphere-egu23-13887

# The reconstruction of the Gove multipurpose dam and hydropower plant in Angola. Design, construction and operation challenges in the context of changing water and energy needs in the international Cunene river basin

António PEREIRA DA SILVA[1], Carolino MENDES[2]

[1] COBA – Engineering and Environmental Consultants, Board Director, Portugal
a.p.silva@cobagroup.com

[2] GABHIC – Gabinete para a Administração das Bacias Hidrográficas do Cunene e Cuvelai, General Director, Angola
carolinomm10@yahoo.com.br

ABSTRACT

This paper focus on the challenges of allocating water resources and operating the large Gove reservoir in Angola, to guarantee the multiple existing uses in the international Cunene basin, in the context of the changing technical, economic, environmental, and social conditions in the region, during almost 50 years of operation from the date of entry in service in 1975.

A description is given of the rehabilitation works of the dam executed between 2008 and 2012, due to the damage that occurred in 1986 and in 1990, and the construction of the hydropower plant. The operation of the reservoir before, during and after rehabilitation, and the compliance to the water resources sharing agreement between Angola and Namibia, are presented. Future perspectives for the operation of the reservoir, at medium and long term, are also given, associated to the increase of water needs, climate change, addition of solar PV, new planned storage reservoirs and hydropower plants downstream.

## 1. The Gove multipurpose development

The Gove dam is located in the Province of Huambo, in Angola, and has the main purpose of river flow regulation and flood control of the Cunene river, and hydropower generation. It is an important strategic water reserve for Angola and Namibia, in a dry region, and its operation is governed by an international water sharing agreement between both countries.

The reservoir at the NWL of (1590.00), has a large storage capacity of $2574 \times 10^6$ m$^3$, about 1.5 times the inflow. The dam (Fig. 1) is a homogeneous embankment, with maximum height of 58 m and a crest length of 1200 m. The hydropower plant, located at the dam toe, has a capacity of 61,8 MW.

## 2. The rehabilitation works

The Gove dam was seriously damaged by war in 1986 and 1990, that put its operation and safety at risk, and at the time emergency repair works were made and the maximum operational water level was lowered.

The rehabilitation design and the powerplant design were developed by COBA between 2002 and 2005, followed by the construction supervision and technical assistance between 2008 and completion in 2012.

The main rehabilitation works included: i) the excavation and reconstruction of the disturbed section of the embankment (Fig. 2), in a maximum height of 24 m, ii) the dam heightening by 1 m, to guarantee the safety freeboard for flood control, due to the revision of the hydrological studies, and iii) the re-establishment of the operation capacity of the intake. The bottom outlet was not repaired and was sealed.

The 61.8 MW hydropower plant was built in the same period and entered service in 2013.



**Fig. 1.** General view of the Gove dam and hydropower plant



**Fig. 2.** Excavation of the dam fill during rehabilitation.

## 3. Water resources and water uses

The catchment area at the dam section is 4 667 km$^2$, only 5% of the total area of the basin (94 891 km$^2$), but contributing with 27% of the total flow. The estimated inflow, based on an historical series of 30 years of monthly flows and using the developed simulation model, is 1 569 hm$^3$/year (49.8 m$^3$/s), with a marked variability between years and between the dry and wet seasons.

Total water needs in the Cunene river basin for water supply and irrigation were estimated at 248.0 hm$^3$/year (7.9 m$^3$/s) at the time of rehabilitation, much lower than the regulation capacity of the Gove reservoir.

## 4. Operation of the Gove reservoir and hydropower plant

The Gove reservoir has been in operation for 49 years, and has been capable of responding to significantly changing water and energy needs and to the maintenance conditions of the structures, namely:

- The initial operation started in 1975, with the main objective of regulation of the Cunene river flows downstream, for regular energy generation at the two existing downstream hydropower plants;
- Operation from 1986/1990, after damage to the dam, with reduced NWL due to safety concerns related to the structural stability of the dam and to the lack of capacity of the spillway;
- Operation during the rehabilitation works, from 2008 to 2012, adopting new safety levels for each excavation stage of the dam body, and defining detailed daily operating rules as to ensure that those maximum levels are respected and simultaneously that same regulation capacity is retained.
- Operation after rehabilitation, in the short term after 2013; regulation downstream of the basin of 35,0 m$^3$/s (1 100 hm$^3$/year), about half the maximum estimated capacity, with remaining capacity used to guarantee energy supply for the city of Huambo (150 GWh/year).
- Long-term operation: Regularization downstream of 70,0 m$^3$/s (2 200 hm$^3$/year), the maximum estimated capacity, and hydropower plant operating connected to the national grid, as a peak powerplant or a reserve, generating mainly in the dry season (135 GWh/year).

The dam and the hydropower plant have been in operation after rehabilitation for 11 years. The analysis of the operation data shows that in the first 4 years priority was given to local energy supply, as envisaged, and afterwards a transition to the long-term operation was adopted, with priority given mainly to flow regulation.

It expected that with further development of irrigation in the Cunene basin, the capacity of flow regularization of Gove will become insufficient to guarantee all water and energy demands. Also, the increase of solar PV generation in the area, new planned water storage and hydropower projects and the effect of climate change will also impact on the future operation of the reservoir.

## 5. Conclusions

The Gove dam is a critical infrastructure, designed with an integrated and long-term perspective of efficient water resources use in a large international basin, guaranteeing reliable water supply and energy generation, and contributing to the economic and social development. Subject to war damage and rehabilitated, it has proven its versatility and resilience by being capable of coping with the changing needs of the region.

Unfortunately, nowadays there are other dams being damaged or destroyed by war and the lessons learned in the Gove rehabilitation can be applied to those structures.

Future challenges include the expected increase of water needs in the region, that will exceed the regulation capacity of the Gove reservoir, and consequently other large hydraulic developments are being planned.



# Theme B

## Estuaries, coasts and ports

# Estimation of open channel bathymetry with video images from surface data

Francisco AVEIRO[1], Tiago ABREU[2], Moisés BRITO[3], Maria Graça NEVES[1]

[1] CERIS, NOVA School of Science and Technology, Universidade NOVA de Lisboa, 2829-516 Caparica, Portugal
f.aveiro@campus.fct.unl.pt
mg.neves@fct.unl.pt

[2] CESAM & ISEP, Polytechnic of Porto, 4249-015 Porto, Portugal
taa@isep.ipp.pt

[3] UNIDEMI, NOVA School of Science and Technology, Universidade NOVA de Lisboa, 2829-516 Caparica, Portugal
moisesbrito@fct.unl.pt

ABSTRACT

This work aims to investigate the reliability of a methodology used for determining bathymetry near seaports through the capture of sea surface images using a video camera in a laboratory channel conducting small-scale experiments. Regular waves are propagated in a fixed horizontal bottom, considering different wave heights and periods. The best results, obtained for the shortest periods and highest wave heights, demonstrate the methodology's usefulness in the laboratory.

## 1. Introduction

Coastal areas, especially those with significant sediment transport, undergo substantial changes in bottom morphology during stormy seasons. Adverse sea conditions make in situ bathymetry monitoring challenging with conventional methods, necessitating alternative solutions. Remote bathymetry detection emerges as a viable option, overcoming limitations imposed by adverse weather and energetic waves. Santos et al. (2022) distinguish between two remote sensing approaches for shallow depths based on imagery. The first relies on the seabed interaction with light radiation, suitable for transparent waters with low turbidity. The second, employed in this study, uses surface wave characteristics to estimate local depth.

## 2. Methodology

Experiments were conducted in a horizontal wave channel at the hydraulic laboratory of NOVA School of Science and Technology | FCT NOVA. The channel, 5 m long with an 8.2 × 25.0 cm² rectangular cross-section of acrylic walls, utilized a piston-type wave maker and a video camera for recording propagating waves. Image orthorectification and timestacks creation followed image acquisition (Umberto, 2019). Bathymetry was inferred based on wave patterns detected in the timestacks, following Santos et al. (2022). Tests covered water depths ($h$) from 6.8 to 15.2 cm, varying wave heights ($H$) between 1.7 and 4.0 cm, and wave periods ($T$) between 0.79 and 1.79 s.

## 3. Results and discussion

Fig. 1 displays a picture of the experiment/flume/camera, a timestack example and the results from a test with $H$ = 3.3 cm and $T$ = 0.75 s. The 7.0 s test, comprising 168 frames, shows $x$-coordinate results along the channel for the vertical coordinate ($z$). Here, $z$ = 0 represents the bottom of the channel and the positions of $x$ between 0 and 3500 mm, respectively, indicate the positions closest to the wave maker and to the camera location. The timestack analysis yielded a median value of $T$ of 0.77 s, close to the linear wave theory dispersion relation's median $T$ value of 0.75 s. Wavelength ($\lambda$) errors were smallest near the camera end ($x \approx 3500$ mm), gradually increasing towards the far end, reaching up to 30%. At the far end of the channel, the errors take values in the order of 5 to 10% in the section from 1800 to 3200 mm, and up to the first 2000 mm this value gradually increases from 10 to 30%. Regarding the $z$ results, as for $\lambda$, it is near the end of the channel closest to the camera where the smallest errors are recorded. In this case, in the last 1250 mm of channel length, the

associated error is of the order of 10%. For the rest of the channel length, *z*-errors became unrealistic due to high errors.

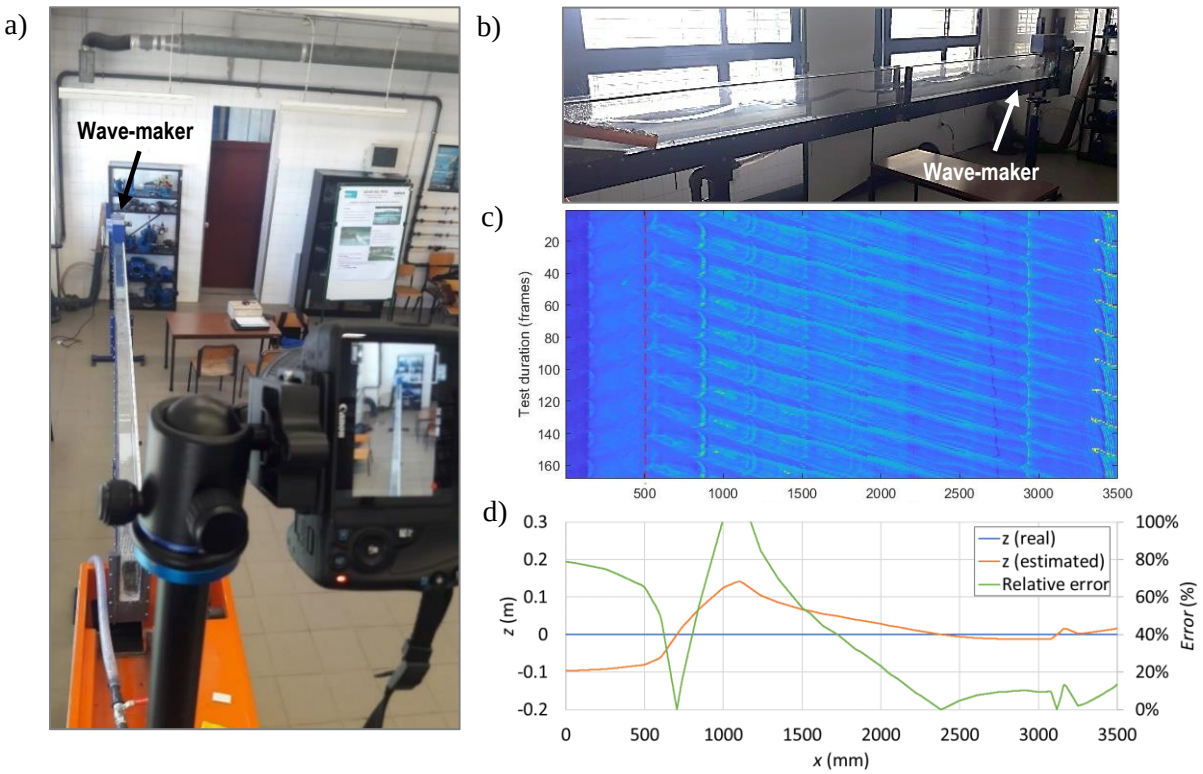



**Fig. 1.** a) and b) Pictures of the experiment/flume/camera. c) Timestack example for a test with *H*=3.3 cm and *T*=0.75 s. d) Real and estimated *z* values and relative error.

## 4. Conclusions

Regular wave conditions with varying characteristics, including different wave heights and periods, were generated in a fixed-bottom open channel flow at NOVA School of Science and Technology | FCT NOVA. A video camera recorded the free surface elevation of shoaling waves, enabling the creation of timestacks for inferring the bathymetry of the experiments. Optimal water depth estimates were achieved for the shortest periods and highest wave heights. Due to the channel's limited dimensions, longer periods resulted in a reduced number of observable waves in an image, diminishing result quality. Overall, the bathymetric estimates demonstrated diminished quality in areas farther from the camera, potentially linked to a decrease in image resolution during the image orthorectification process.

**Acknowledgements**

This study was funded by the PRR – Plano de Recuperação e Resiliência and by the NextGenerationEU funds at University of Aveiro, through the scope of the Agenda for Business Innovation "NEXUS: Pacto de Inovação – Transição Verde e Digital para Transportes, Logística e Mobilidade" (Project nº 53 with the application C645112083-00000059). Thanks to CESAM through the national funds FCT/MCTES (UIDP/50017/2020+UIDB/50017/2020+LA/P/0094/2020). Moisés Brito acknowledge the Portuguese Fundação para a Ciência e a Tecnologia (FCT - MCTES) for its financial support via the project UIDB/00667/2020 and UIDP/00667/2020 (UNIDEMI).

**References**

Santos D, Abreu T, Silva PA, Santos F, Baptista P (2022) Nearshore Bathymetry Retrieval from Wave-Based Inversion for Video Imagery, Remote Sensing, 14(9), 2155

Andriolo U (2019). Nearshore Wave Transformation Domains from Video Imagery. Journal of Marine Science and Engineering, 7(6), 186

# Propeller scour confined by a quay wall in waterways

Domenico FERRARO[1], Agostino LAURIA[2], Nadia PENNA[3], Roberto GAUDIO[4]

[1]Department of Civil Engineering, University of Calabria, 87036 Arcavacata di Rende (CS), Italy
domenico.ferraro@unical.it
nadia.penna@unical.it
roberto.gaudio@unical.it
[2]Department of Engineering for Innovation, University of Salento, 73100 Lecce, Italy
agostino.lauria@unisalento.it

ABSTRACT

The propeller generates a turbulent jet that impacts the seabed or the bottom of a navigation channel, reaching a considerable distance from the propeller itself. The presence of a boundary has a significant impact on the propeller jet development. Tsinker (2012) emphasized the need to consider propeller-induced scour during the design of new port-related structures or when reassessing the performance of existing structures. He noted that all the types of structures could potentially experience scour caused by propellers, especially those designed to withstand horizontal and vertical loads as closed vertical quays and the scour associated with them is generally confined to the area in front of the berth front wall. The still water condition, common in technical literature, is not representative of mooring in navigable channels where a channel flow can influence the scour induced by a propeller jet. In the present work, the scouring process, laterally confined by a quay wall, and induced by the combined effects of the propeller rotation and a water flow running in a laboratory flume was investigated.

## 1. Experimental Campaign

The experimental campaign was carried out at the "*Grandi Modelli Idraulici*" Laboratory of the *Università della Calabria*, Italy, in a 16m-long tilting flume with a 0.985m-wide and 0.8m-deep rectangular cross-section. The 2.5m-long test section was placed 10 m from the channel inlet. In the measurement section a sediment box filled in with uniform fine sand having a median diameter $d_{50}$ = 0.69 (mm) is present. In this study, 3 tests were performed, with their main characteristics summarized in Table 1. The propeller size ($d_p$ = 0.06 m), the number of revolutions ($n$ = 700 rpm), and the position of the hub center of the propeller relative to the undisturbed bottom were kept constant in all the experiments.

**Table 1.** Hydraulic conditions of the laboratory tests. Here, $Q$ is the flow rate, $h_w$ the water depth, $y/d_p$ the dimensionless distance between the propeller and the quay wall, $U$ the mean flow velocity, $Re$=4$RU/\nu$ the Reynolds number, $R$ the hydraulic radius, $\nu$ = $1.31 \cdot 10^{-6}$ m$^2$/s the kinematic viscosity of water at 10°C, $Fr$=$U/(gh_w)^{0.5}$ the Froude number, and $g$ the gravitational acceleration.

| Test | $Q$ (m$^3$/s) | $h_w$ (m) | $y/d_p$ | $U$ (m/s) | $Re$ | $Fr$ |
|---|---|---|---|---|---|---|
| T1 | - | 0.16 | 5.00 | - | - | - |
| T2 | 0.0116 | 0.16 | 5.00 | 0.073 | $3.59 \cdot 10^4$ | 0.067 |
| T3 | 0.0222 | 0.16 | 5.00 | 0.141 | $6.87 \cdot 10^4$ | 0.129 |

### *1.1. Velocity measurement and sampling of the scour hole profiles*

In order to measure the three-dimensional (3D) velocity components an Acoustic Doppler Velocimeter (ADV) was used with a sampling frequency of 100 Hz and a duration of 600 s. Thanks to an automatic traverse system capable of moving a measuring instrument in a 3D space, it was possible to measure the depth of the scour hole several times during the test, maintaining both the flow and the propeller switched on up to the Quasi-Equilibrium Stage (QES) of the scour were achieved (Ferraro *et al.*, 2021, 2022). Finally, once the QES was reached the test was stopped, the flume was dried and the bottom acquired through a high-resolution photogrammetry technique.

### *1.2. Numerical Simulations*

For each test, the acquired QES bathymetry was used as a bottom boundary, whereas the quay wall and propeller geometry were created and added to the simulation in a Computer-Aided Design (CAD) environment. The flow field was simulated by solving the RANSE in 3D with the *k-ω* SST closure model, which includes two new equations in the system, for the turbulent kinetic energy, *k*, and the dissipation of turbulent kinetic energy, *ω*. The equations of motion and the turbulence model were solved numerically using the pimpleDyMFoam solver, embedded in the open-source OpenFoam® C++ libraries.

## 2. Results and Conclusions

### *2.1. QES bathymetry*

In Fig. 1(a), (b), and (c) the QES bathymetry is shown for tests T1, T2, and T3, respectively. From Fig. 1 the effect of the flow intensity, which increases from test T1 to T3, on the scour hole bathymetry is visible. Fig. 1(a) shows a canonical almost symmetrical scour hole and deposition mound, whereas in Figs. 1(b) and (c) the scour hole and deposition mound move downstream, in accordance with the flow direction.

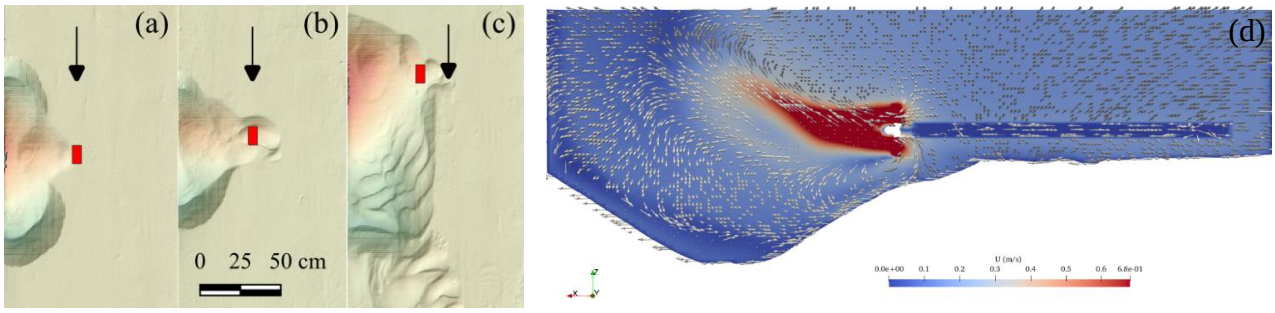



**Fig. 1.** QES bathymetry of Tests T1 (panel a), T2 (panel b), and T3 (panel c). Arrows represent the flow direction, whereas the red rectangle indicates the propeller position. Panel (d) shows the vertical normal slide of the numerical simulation of test T3. Arrows represents the flow velocity direction whereas the colour ramp has a maximum equal to the propeller efflux velocity computed according to Hamill *et al.* (2015).

As the flow intensity grows, the propeller jet deflects downstream, and then the scoured hole moves downstream. An interesting fact is that the scour volume in test T2 is less than T1, as well as that with a higher flow intensity (T3). In the first phase of the scouring process, the propeller jet approaches the bed creating a canonical, initial, scour hole. Once the scour grows, a part of the channel flow creeps below the jet, owing to the Coandă effect. The Creeping Flow (CF) is not strong enough to move the sediments, creating a buffer zone between the jet and the bed sediments, with the consequent reduction of the scour hole. On the other hand, the CF in test T3 is capable to move the bed sediments, increasing the scour hole dimensions and the sediment mound. At the QES achievement, the space between the propeller jet and the CF becomes large enough to reduce the CF velocity down to a value below the critical velocity of the bed sediments. The above speculations are supported by the observation of the flow field in the numerical simulation. In Fig. 1(d) the vertical normal slide at the propeller axis position of the numerical simulation of test T3 is shown. From Fig. 1(d), it is possible to note the vertical deflection of the propeller jet operated by the flow intrusion, owing to the Coandă effect, inside the scour hole. The CF does not allow the jet to spread in both vertical directions, but only upward, reducing the scour induced by the propeller jet in favour of that induced by the CF.

In conclusion, the experimental campaign highlights the effect of the flow intensity and the transversal propeller jet on an erodible bed. The results show a reduction in the scour hole in the test with a low flow intensity, owing to the buffer zone created behind the propeller jet. Numerical simulations clearly support the speculation about the buffer zone, showing lower confinement of the propeller jet owing to creeping flow between the propeller jet and the scoured bed.

**Acknowledgements**

The present work was financed with funds POC Research and Innovation 2014-2020 *Attraction and International Mobility* (AIM) and by the "SILA" Project PONa3_00341, "*Integrated System of Laboratories for the Environment*".

**References**

Ferraro D, Lauria A, Penna N, Gaudio R (2021) Temporal development of unconfined propeller scour in waterways. Physics of Fluids. 33(9).
Ferraro D, Lauria A, Penna N, Gaudio R (2022). Unconfined propeller scour in waterways: The role of flow intensity. Physics of Fluids. 34(9).
Hamill GA, Kee C, Ryan D, (2015) Three-dimension efflux velocity characteristics of marine propeller jets. In: Proc. ICE Marit. Eng. 168(2). 62-75.
Tsinker G (2012) Marine Structures Engineering: Specialized applications. Springer Science & Business Media.

# An online, open mesh generation assistant for OPENCoastS using OCSMesh

Ricardo MARTINS[1], André B. FORTUNATO[1], Anabela OLIVEIRA[1], Gonçalo JESUS[1], Soroosh MANI[2], Edward MYERS[2], Saeed MOGHIMI[2]

[1] Laboratório Nacional de Engenharia Civil, Av. Brasil, 101, 1700-066 Lisbon, Portugal
rjmartins@lnec.pt, afortunato@lnec.pt, aoliveira@lnec.pt, gjesus@lnec.pt

[2] Coast Survey Development Laboratory, National Ocean Service, NOAA, Silver Spring, 9 MD 20910, USA
soroosh.mani@noaa.gov, edward.myers@noaa.gov, saeed.moghimi@noaa.gov

ABSTRACT

The flexibility provided by unstructured grids is a major advantage for coastal ocean modeling. The drawback is the difficulty in generating good quality unstructured grids, and the steep learning curve to use grid generators. In addition, the grid generation procedure requires the availability of bathymetry and coastline data for the system of interest. Finding and processing these data can be a major burden on modelers. This abstract describes an open, online grid generator web assistant that overcomes these problems, greatly simplifying the process of mesh generation for beginner and intermediate users. The grid generator builds both horizontal and vertical grids.

## 1. Introduction

OPENCoastS (opencoasts.ncg.ingrid.pt) is an on-demand web platform service that allows any user to create and manage operational forecast systems for coastal hydrodynamics and water quality (Oliveira et al., 2019). While a forecast system can be set up in a few minutes using this platform, providing the unstructured grid for the user's domain has proven to be difficult to overcome by many users. Hence, developing tools to help users generate unstructured meshes can greatly improve the usability of the platform. Although these tools were created for this platform and model (SCHISM, Zhang et al., 2016), they can be used by other models based on triangular unstructured grids.

## 2. Mesh generator

The assistant is developed in Python and is included in the OPENCoastS platform. The mesh generation is run by OCSMesh (Mani et al., 2021), a Python package developed by NOAA for processing topobathymetry data, i.e., digital elevation model (DEM) into georeferenced unstructured meshes, and generate simulation domain and element-size function, using the JIGSAW (Engwirda, 2014) meshing engine library. Other scripts (developed in Fortran and Python) were used for mesh analysis and improvement. The grid generation procedure follows eight steps described below (Fig. 1).

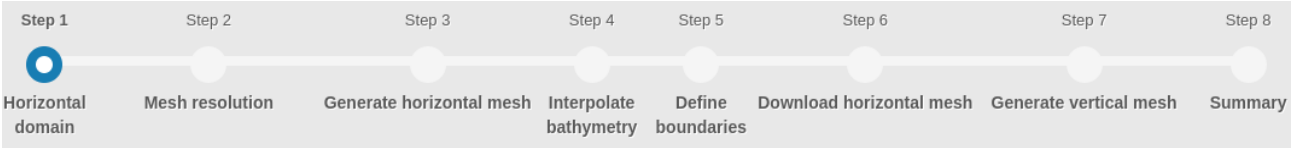



**Fig. 1.** Step workflow for mesh generation

In Step 1, the user defines a region of interest on the map, and provides the bathymetric data or selects from the available bathymetry sources (GEBCO/EMODNET/SRTM 1-arcsec). The land limits can be defined using existing coastlines provided by the grid generator (EMODNET or OpenStreetMaps). As an alternative, the user can provide a maximum elevation, and the grid generator extracts the corresponding isobath from the Digital Elevation Model. The open boundaries are defined within a WebGIS, by defining circular or straight lines on a map (Fig. 2). The domain can then be saved as a json file, to be reused later.

In Step 2, users define the spatially varying mesh resolution. Several criteria can be applied, such as providing the grid's global minimum and maximum resolutions, defining constant resolutions between two isobaths or within a user-defined polygon, or imposing linear increases of resolution with the distance to an isobath. The result of these criteria can be previewed on a map.

Using the domain and grid resolution defined in the previous steps, an horizontal grid is generated in Step 3 using JIGSAW. The grid generated can be visualized on the WebGIS (Fig. 2), and additional scripts can be used to improve the grid (e.g., NICEGRID, Fortunato et al., 2011). The bathymetry is interpolated in Step 4 (Fig. 2), using the bathymetric sources and order defined in Step 1.

Boundaries are defined in Step 5. Users can provide a threshold depth, above which the node will be considered part of a closed boundary. As an alternative, open boundaries can be defined through consecutive pairs of nodes selected on a map (Fig. 2). In this step, users can also impose a minimum depth at elements containing an open boundary node, in order to prevent drying of those elements during the simulations. At this stage, the horizontal grid is ready, and can be downloaded in any EPSG coordinate system in Step 6.

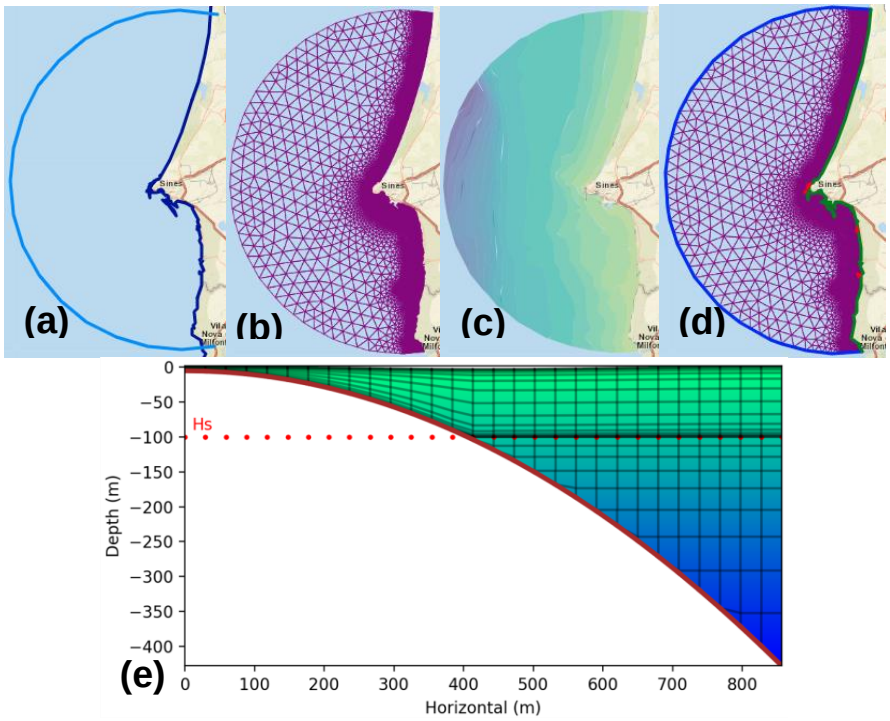



**Fig. 2.** Results from step 1 (a), step 3 (b), step 4 (c), step 5 (d) and step 7 (e) of a mesh generation for the Sines harbor (Portugal)

Step 7 allows users to generate the vertical grid for SCHISM's 3D simulations. These grids can combine Z-levels in the deeper portion of the domain, with bottom-following S layers at the surface (Fig. 2). Finally, users can submit the horizontal grid to be stored in OPENCoastS (Step 8).

From the feedback from beta testers, this tool has proven to be very powerful, helping users to easily build meshes from their domains and speeding up their forecast deployments. Because the mesh assistant can generate very large meshes, the number of grid nodes in OPENCoastS was arbitrarily limited to 175000 to avoid overloading the available cloud resources. Future work consists in optimizing the tool.

**Acknowledgements**

We acknowledge Darren Engwirda for the JIGSAW code, and all the team from LNEC for the development of OPENCoastS and the scripts required for this assistant.

**References**

Fortunato AB, Bruneau N, Azevedo A, Araújo MAVC, Oliveira A (2011) Automatic improvement of unstructured grids for coastal simulations, J. Coast. Res. Special Issue, 64: 1028-1032

Mani S, Calzada JR, Moghimi S, Zhang YJ, Myers E, Pe'eri S (2021) OCSMesh: a data-driven automated unstructured mesh generation software for coastal ocean modeling, NOAA Technical Memorandum NOS CS; 47

Engwirda D (2014) Locally optimal Delaunay-refinement and optimisation-based mesh generation.

Oliveira A, Fortunato AB, Rogeiro J, Teixeira J, Azevedo A, Lavaud L, Bertin X, Gomes J, David M, Pina J, Rodrigues M, Lopes P (2019). OPENCoastS: An open-access service for the automatic generation of coastal forecast systems, Environmental Modelling & Software, 124: 104585

# Shallow-Water Deformation Effects of Long-Period Ship-Induced Waves in Estuaries

León-Carlos DEMPWOLFF[1], Christian WINDT[1],Gregor MELLING[2], Hans BIHS[3], Ingrid HOLZWARTH[2], Nils GOSEBERG[1,4]

[1] Leichtweiß Institut, Technische Universität Braunschweig, Germany
l.dempwolff@tu-braunschweig.de

[2]Federal Waterways Engineering and Research Institute, Germany
[3]Norwegian University of Science and Technology, Norway
[4]Coastal Research Center, Germany

ABSTRACT

## 1. Motivation

In confined maritime channels frequented by large vessels, in particular in estuaries which serve as access routes to seaports, ship-induced waves have become an increasingly important hydrodynamic loading factor due to the ever increasing dimensions of the vessels in operation. Of particular significance is the potential for greater damage associated with the extended wavelength of the long-period primary wave system, distinguishing it from natural hydrodynamic forces. While the mechanics of primary wave generation, driven by Bernoulli's conservation law, are well-established, its behavior as it enters shallow-water areas, such as tidal mudflats or groin fields, remains less understood (Dempwolff et al. 2022a). Field observations indicate that these shallow-water effects play a crucial role in the ship-induced damage potential and can lead to large hydrodynamic loads even in distance to the navigation fairways (Muscalus and Haas 2022; Scarpa et al. 2019). The detrimental effects comprise damage to civil works, morphodynamic changes, and deterioration of ecological habitats alike. Hence, this study seeks to investigate the intricacies of these shallow-water effects, with the goal of advancing understanding and offering valuable insights for the efficient management and mitigation of potential damage in maritime environments.

## 2. Methods

To bridge the knowledge gap, numerical methods grounded in shallow water theory serve as a viable means for predicting and comprehending deformation effects. REEF3D::SFLOW is such a model that has recently been extended with a free surface pressure term to represent ship wave generation and has been validated for the prediction of long-period ship-induced waves (Dempwolff et al. 2022b). The numerical model relies on depth-integrated versions of the Navier-Stokes equations, thereby providing an efficient way to simulate large computational domains, that incorporate extended shallow-water areas (Wang et al. 2020). In contrast to field measurements, numerical methods provide exact control over the waterway bathymetry, allowing the analysis of simplified conceptual channel cross-sections. Unlike, experimental methods, REEF3D::SFLOW affords a swift and cost-effective approach to investigate numerous variations in bathymetric parameters.

## 3. Investigation

Existing field data indicates that the distance between a ship sailing line and shallow water areas are largely governing the resulting wave loads performed (Melling et al. 2020). Similarly, shoaling occurring when primary waves propagate over these shallow areas further intensify the resulting loads (Parnell et al. 2015). However, even though these processes are qualitatively well understood an extended analysis of the underlying functional relationships has not been performed. Therefore, these parameters are examined in detail using the shallow-water-equation solver REEF3D::SFLOW to simulate ship passages in multiple conceptual waterway cross-section as presented by means of example in Fig. 1.

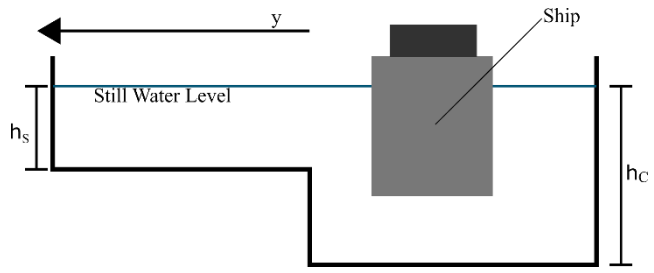



**Fig. 1** Conceptual channel geometry that allows the examination of parametric influences on primary wave loads.

## 4. Results

The results provide valuable insights into the propagation and deformation of long-period ship induced-waves. Fig. 2 indicates the influence of the water depth of the shallow water area on the deformation of the ship-induced primary wave z. The knowledge on these functional relationships helps to improve process understanding and further contributes to establish a knowledge base on ship-waves near waterway banks ultimately improving the engineering guidance and complementing case specific numerical analysis. In doing so, this study aims to facilitate more informed decision-making processes on navigation control and waterway design, ensuring the preservation of the structural integrity of coastal infrastructure and the delicate ecosystems that surround shipping lanes.

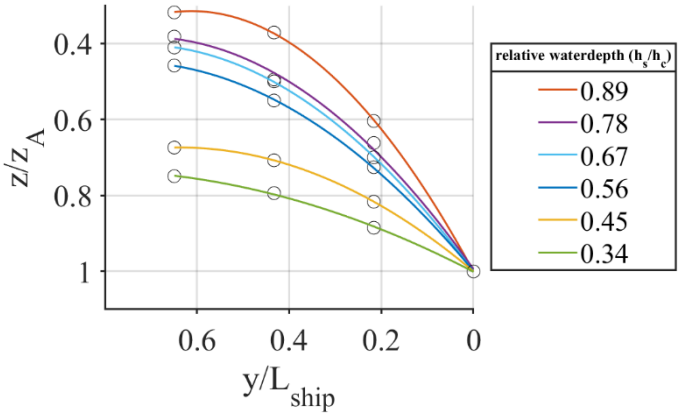



**Fig. 2** Dampening of the primary wave height while propagating over the shallow-water area. Expressed in means of the local wave height z normalized with the wave height at the channel margin. The length of the ship is usd to normalize the propagation distance.

### References

Dempwolff, L.-C., G. Melling, C. Windt, O. Lojek, T. Martin, I. Holzwarth, H. Bihs, and N. Goseberg. 2022a. "Loads and effects of ship-generated, drawdown waves in confined waterways - A review of current knowledge and methods." *Journal of Coastal and Hydraulic Structures*, 2: 46. https://doi.org/10.48438/jchs.2022.0013.

Dempwolff, L.-C., C. Windt, G. Melling, T. Martin, H. Bihs, I. Holzwarth, and N. Goseberg. 2022b. "The influence of the hull representation for modelling of primary ship waves with a shallow-water equation solver." *Ocean Engineering*, 266: 113163. https://doi.org/10.1016/j.oceaneng.2022.113163.

Melling, G., H. Jansch, B. Kondziella, K. Uliczka, and B. Gätje. 2020. "Evaluation of optimised groyne designs in response to long-period ship wave loads at Juelssand in the Lower Elbe Estuary." *Die Küste*, 89: 28. German Coastal Engineering Research Council (KFKI). https://doi.org/10.18171/1.089103.

Muscalus, A. C., and K. A. Haas. 2022. "Vessel wake contributions to erosion at exposed and sheltered shorelines near a tidal shipping channel." *Coastal Engineering*, 104220. https://doi.org/10.1016/j.coastaleng.2022.104220.

Parnell, K. E., T. Soomere, L. Zaggia, A. Rodin, G. Lorenzetti, J. Rapaglia, and G. M. Scarpa. 2015. "Ship-induced solitary Riemann waves of depression in Venice Lagoon." *Physics Letters A*, 379 (6): 555–559. https://doi.org/10.1016/j.physleta.2014.12.004.

Scarpa, G. M., L. Zaggia, G. Manfè, G. Lorenzetti, K. Parnell, T. Soomere, J. Rapaglia, and E. Molinaroli. 2019. "The effects of ship wakes in the Venice Lagoon and implications for the sustainability of shipping in coastal waters." *Sci Rep*, 9 (1): 19014. https://doi.org/10.1038/s41598-019-55238-z.

Wang, W., T. Martin, A. Kamath, and H. Bihs. 2020. "An improved depth-averaged nonhydrostatic shallow water model with quadratic pressure approximation." *Int J Numer Meth Fluids*, 92 (8): 803–824. https://doi.org/10.1002/fld.4807.

# Re-Analysis of Extreme Sea State Events Modelling Using a Data-Driven Technique

Tristan BAGNIS[1], Michel BENOIT[1,2], Thierry FOUQUET[1], Cedric GOEURY[1,2], Maria TELES[1]

[1] National Laboratory for Hydraulics and Environment (LNHE), EDF R&D, Chatou, France

thierry.fouquet@edf.fr , cedric.goeury@edf.fr

[2] LHSV, Ecole des Ponts, EDF R&D, Chatou, France

ABSTRACT

With the objective of answering marine and coastal engineering needs, sea state databases are created by hindcast simulations over long periods. The wave hindcast ANEMOC-3 database, built using the spectral model TOMAWAC for wave generation and propagation and the hydrodynamic circulation model TELEMAC-2D for tidal water levels and currents calculation, covers a period of 45 years from 1979 to 2023. During the calibration of the database, the numerical results must be consistent with past observational data (in situ or satellite measurements). Among other things, this process relies on calibration to determine "empirical adequacy". In particular, the calibration aims at simulating a series of reference events by adjusting some uncertain physically-based parameters until the agreement with available data reaches a satisfactory level. The objective of this work is to implement an efficient calibration algorithm, capable of processing measurements optimally, and to estimate the partially known parameters in the numerical model.

## 1. Introduction

Many problems in science and engineering require the estimation of unknown or uncertain parameters that will produce a solution that best fits a finite set of measurements. Modelling of marine flows and waves is no exception. Hindcast wave databases are sophisticated computer-based simulations providing complete time series of wave parameters and/or full wave spectra with a fine spatial resolution. They are powerful tools for a range of applications, including marine engineering, coastal infrastructure design, offshore operations, wave power assessment and environmental studies. By providing a detailed understanding of past sea states over several decades, they help researchers and professionals make informed decisions and predictions related to ocean environments and their impact on various activities. In this framework, EDF R&D LNHE together with the Cerema developed the hindcast wave database ANEMOC about 16 years ago with the main interest devoted to the French coastal areas of the Atlantic Ocean, English Channel and North Sea (Benoit *et al.*, 2008). With the significant advances in the means of observing continental waters, the ability to exchange data as computational results has become a growing need. Data assimilation algorithms for integrating observation data into real cases are now increasingly applied to hydraulic problems with two main objectives: optimizing model parameters and improving hydraulic and wave simulation and forecasting. The objective of this work is to implement an efficient calibration algorithm, based on data assimilation, to best estimate partially known parameters of the source and sink terms in the wave model (namely wind generation and white capping dissipation coefficients).

## 2. Optimal Calibration using variational data assimilation 3D-VAR

A variational data assimilation algorithm is here used for inverse parameter estimation from observations (here wave buoy data) and numerical results. On the one hand, observations are not perfect. On the other hand, one may have a first guess for the parameters (physical knowledge, previous simulations, etc.), but the latter is uncertain. To find the best compromise between measurements errors and parameters first guess errors, the optimization takes the form of a minimization problem, for the function defined as follows:

$$J(\mathbf{X}) = \frac{1}{2}(\mathbf{X}-\mathbf{X_b})^{\mathbf{T}}\mathrm{B}^{-1}(\mathbf{X}-\mathbf{X_b}) + \frac{1}{2}\big(\mathbf{Y}-\mathcal{H}(\mathcal{M}(\mathbf{X}))\big)^{\mathbf{T}}\mathrm{R}^{-1}\big(\mathbf{Y}-\mathcal{H}(\mathcal{M}(\mathbf{X}))\big)$$

where $\mathbf{Y}$ is the observation vector, $\mathcal{M}$ the numerical model, $\mathcal{H}$ an operator from the simulation to the observation space, $\mathbf{X}$ the set of unknown parameters and $\mathbf{X}_\mathrm{b}$ a background knowledge (or first guess) of the parameters. The background and observation errors are represented by error covariance matrices, respectively

denoted B and R. This formulation of the optimal search of control vector **X** is known as the traditional variational data assimilation cost function, called 3D-VAR.

## 3. ANEMOC hindcast wave numerical database application

The hindcast database ANEMOC is built from simulations with the TOMAWAC model (Benoit et al., 1996) and provides sea-state conditions over the Atlantic Ocean. It has been updated several times and now covers the period from 1979 to 2023. It is composed of computations over two nested meshes. The first mesh, called "oceanic", covers the most of the Atlantic Ocean. It has a relatively coarse spatial resolution with a minimum element size of approximately 20 km along the European coastline. Its main purpose is to make computations for providing boundary conditions to the other (finer) mesh, the "coastal" mesh. This latter one has an element size of under 1 km along the French coastline. The results presented hereafter concern the oceanic domain only. TOMAWAC solves the wave action balance equation with energy source/dissipation processes modelled with semi-empirical parameterizations. The physical processes considered in the numerical model are described in Teles *et al*. (2022). In this work, the focus is done on wind generation (wind coefficient $\beta_m$ and $\alpha$ of the Janssen's model (Janssen, 1991)) and white-capping dissipation parametrization (white-capping coefficients $C_{mout3}$ to $C_{mout6}$ from the Komen *et al*. (1984) model). The numerical model gives hourly output of wave parameters such as spectral significant wave height $H_{m0}$. The capability of ANEMOC to model regular and extreme sea states is here evaluated based on buoy measurements during the one-month period of February 2014, as several very intense storms occurred over the northern part of the Atlantic Ocean over this time frame.

This study has been carried out following the Application Programming Interface (API) framework described by Goeury *et al.* (2022). First of all, the identification of the most influential input parameters by sensitivity analysis has been led to target the calibration parameters. In this work, a polynomial chaos expansion has been carried out to estimate Sobol's sensitivity indices. Among all model parameters, the wind coefficient $\beta_m$ of the Janssen's model is one of the most influencing variables. Consequently, as a first application, the calibration of the model is focused on this parameter. Fig. 1 displays the results of calibration over the one-month period. The result emphasises the efficiency of the inverse parameter estimation with simulated wave height much closer to the buoy measurements after calibration.

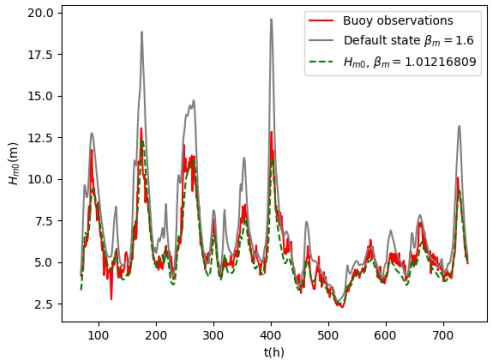



**Fig. 1.** Calibration results at Ouessant buoy (offshore French Britany coastline)

## 4. Outlooks

The data-driven algorithm deployed here could be extended to (i) different numerical models (larger and/or more refined area covering for instance the European coastline), (ii) test alternative parameterizations of the physical sink and source processes in the wave model to better reproduce extreme events, (iii) integrate more observation data (remote sensing altimeter data, for instance), or (iv) correct the simulated wave spectra using observations.

**References**

Benoit M., Marcos F., Becq F. (1996). Development of a third generation shallow water wave model with unstructured spatial meshing. In Proc. 25th Int. Conf. on Coastal Eng. (ICCE'1996), 2-6 September 1996, Orlando (FL, USA), pp. 465-478.

Benoit M., Lafon F., Goasguen G. (2008). Constitution et exploitation d'une base de données d'états de mer le long des côtes françaises par simulation numérique sur 23 ans. Base ANEMOC en Atlantique – Manche – Mer du Nord. European Journal of Environmental and Civil Engineering, Vol. 12/1-2, pp. 35-50.

Goeury C., Audouin Y., Zaoui F. (2022). Interoperability and computational framework for simulating open channel hydraulics: Application to sensitivity analysis and calibration of Gironde Estuary model, Environmental Modelling & Software, Vol. 148, 105243.

Janssen P. (1991) Quasi-linear theory of wind-wave generation applied to wave forecasting. Journal of Physical Oceanography, Vol 21, pp. 1631-1642.

Komen G.J., Hasselmann S., Hasselmann K. (1984). On the existence of a fully developed wind-sea spectrum. Journal of Physical Oceanography, Vol. 14, pp 1271–1285.

Teles M., Weiss M., Benoit M. (2022). Assessment of the ANEMOC-3 sea state hindcast database for modelling a series of energetic winter storms along the French coast. XVII[èmes] Journées Nationales Génie Côtier – Génie Civil, Chatou, France, pp 171-182. DOI:10.5150/jngcgc.2022.019

# Practical Use of Smartphone cameras in Morphodynamic Beach state and Rip current risk estimation

Ch VENKATESWARLU[1] *, Surisetty V V Arun KUMAR[2], M RAMESH[3], B GIREESH[1], C V NAIDU[1]

[1]Department of Meteorology and Oceanography, Andhra University, Visakhapatnam
[2]Space Applications Centre, Ahmedabad
[3]National Centre for Earth Science Studies, Thiruvananthapuram
* venkyocean@gmail.com

ABSTRACT

The present study focuses on detection and analysis of rip currents through a low-cost smartphone-based beach monitoring system (SBMS) by taking the advantage of multiple in-built cameras and on-board memory. The famous tourist destination, Rama Krishna (RK) beach, in East coast of India has been chosen for the study, as it is experiencing high number of drownings (525 causalities since 2006). Videos of 20-minute duration were collected covering different time frames of 2022 and an open-source Quantitative Coastal Imaging Toolbox (QCIT) toolbox has been used to process the videos. Rectified Timex images are generated and utilised to analyse the morphodynamic changes of the beach. Several rip currents have been observed along the coast, with strongest being maximum length of 242 m with a width of 55 m. Beach modal states have been computed to determine the rip current hazard associated with it. Sequential transect data indicated the existence of waves at infra-gravity motions within the rip current channels. During the study period, the beach is dominated by Transverse Bar and Rip (TBR) beach type, which is known for its rip current danger. Rhodamine dye experiments have been conducted to practically measure the strength of the rip currents using video data and field data synergistically. The study is first of its kind in exploring the potential application of low-cost smartphones to scientifically monitor rip currents at any beach. Our study would help in further extending this work for beach sites and can be applied to projects where limited funds are available. We suggest to apply this methodology as a preliminary study before setting up permanent video monitoring station.

# Wave propagation over a sandy beach: preliminary comparisons between wave-resolving model and short range K-band radar

Mattia GAIOLINI[1], Aénor CODJO[2], Nicolò COLOMBANI[1], Luciana FERRARO[3], Gianluca GENNARELLI[4], Giovanni LUDENO[4], Matteo POSTACCHINI[1]

[1] Polytechnic University of Marche, Ancona, Italy
m.gaiolini@univpm.it; n.colombani@staff.univpm.it; m.postacchini@staff.univpm.it

[2] ENSEEIHT, Toulouse, France
aenor.codjo@etu.inp-n7.fr

[3] Institute of Marine Sciences, National Research Council, Napoli, Italy
luciana.ferraro@cnr.it

[4] Institute for Electromagnetic Sensing of the Environment, National Research Council, Napoli, Italy
gennarelli.g@irea.cnr.it; ludeno.g@irea.cnr.it

ABSTRACT

This study focuses on the analysis of the wave propagation and consequent inundation affecting the beach area near the Volturno pine forest (Southern Italy). To this aim, a wave-resolving model (FUNWAVE-TVD) and a short range (SR) K-band radar are used, and their qualitative results are compared, with the purpose of showing the SRK-band radar potential in reconstructing the wave field in the nearshore area.

## 1. Materials and methods

The monitored site pertains to the Volturno pine forest, part of Castel Volturno Nature Reserve (Campania, Italy), bounded by the Volturno River to the northwest and the Regi Lagni canal to the southeast (Fig. 1a). To simulate the wave propagation to the coast, the FUNWAVE-TVD solver was used (Shi et al., 2016). This involved bathymetry setup, definition of the starting wave characteristics, generation of specific inputs, data analysis, validation, and post-processing. For the wave generation, an irregular wavemaker was utilized.

The radar signal processing pipeline here exploited consists of two main steps: 1) imaging from the SRK-band radar (Fig. 1b); 2) bathymetry and surface current estimation. In the first step, spatial-domain beamforming is implemented to obtain a focused image of the scene from the baseband raw radar signals (Schmid et al., 2012). At the second stage, the temporal sequence of focused radar images is processed to retrieve information about the bathymetry and sea surface current fields. To achieve this goal, the dispersion relation characterizing the sea wave spectrum is used (Ludeno et al., 2023, Postacchini et al., 2023).




**Fig. 1.** *a)* Area of interest and model domain. *b)* SRK-band radar recording on the beach of Castel Volturno. *c)* Bathymetry data from various sources.

## 2. Numerical setup and preliminary results

To model realistic sea wave conditions, environmental data like wind direction, wave period, and significant wave height are essential. To this end, sea-state data provided by both Ponza buoy (~80 km far from the test site) and Copernicus program were used. Specifically, to ensure the use of Copernicus data as offshore boundary conditions for the model, some Copernicus wave parameters relevant to the buoy location were compared to those collected by the buoy over a 2-year period (June 2021 to June 2023), obtaining high values of the determination coefficient, especially for mean period ($R^2$=0.80) and significant height ($R^2$=0.92).

Subsequently, a 4 km long and 2 km wide area was defined. Bathymetric data from various sources were retrieved, including EMODnet, two surveys performed in 2013 within the AMICA project (Sorgente et al., 2020), and a Digital Terrain Model (DTM) obtained from LiDAR campaign in 2007-2008. Such data were merged into a single dataset prioritizing accurate elevation values and creating a unified interpolated bathymetry dataset for subsequent simulation use (Fig. 1c).

FUNWAVE- TVD was then run using Copernicus data during SRK-band radar field campaign, using a smaller domain (500m×500m), for a preliminary qualitative comparison between numerical results and reconstructed data. The depth-averaged current velocity in the longshore direction is shown in Fig.2a, where a southward current is evident in the nearshore location (lower part). The SRK-band radar estimates confirm a prevalently southward longshore current in the nearshore area (black arrows in Fig.2b).

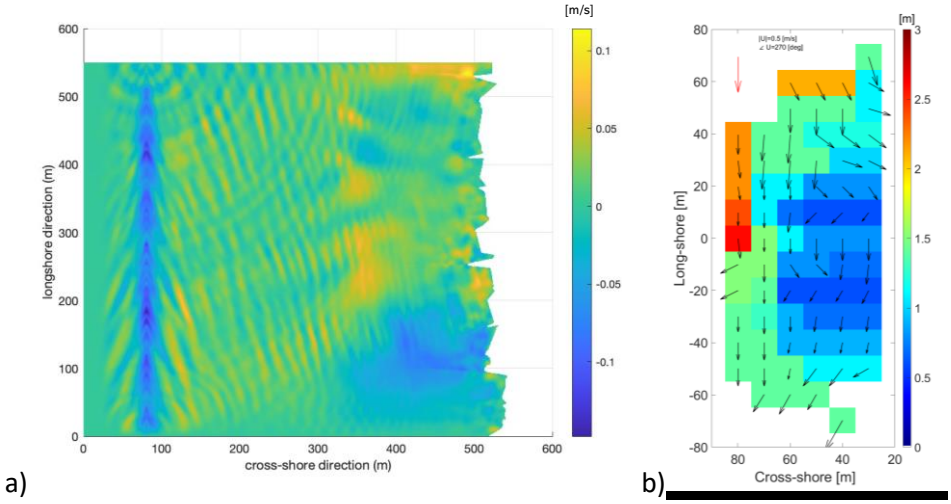



**Fig. 2.** *a)* Longshore depth-averaged modelled velocity [m/s]. *b)* Surface current [m/s] and bathymetry fields from SRK-band radar.

## 3. Conclusions and outlook

This study aims to assess the performance of SRK-band radar estimates of nearshore hydrodynamics through sea wave propagation simulations using FUNWAVE-TVD software. Significant groundwork has been laid, including bathymetry setup, sea-state data processing, and preliminary comparison between numerical results and radar observations. Further results on such comparison will be provided at the conference.

**References**


Ludeno G, Catapano I, Soldovieri F, Gennarelli G (2023). Retrieval of Sea Surface Currents and Directional Wave Spectra by 24 GHz FMCW MIMO Radar, IEEE Transactions on Geoscience and Remote Sensing, 61, 1-13.

Postacchini M, Melito L, Ludeno G (2023) Nearshore Observations and Modeling: Synergy for Coastal Flooding Prediction, Journal of Marine Science and Engineering, 11(8), 1504.

Schmid CM, Feger R, Pfeffer C, Stelzer A (2012) Motion compensation and efficient array design for TDMA FMCW MIMO radar systems, in Proc. 6th Eur. Conf. Antennas Propag. (EUCAP), Mar. 2012, pp. 1746–17

Shi F, Kirby J, Tehranirad B, Harris J, Choi YK, Malej M (2016) FUNWAVE-TVD Fully Nonlinear Boussinesq Wave Model with TVD Solver - Documentation and User's Manual (Version 3.0).

Sorgente R, Di Maio A, Pessini F, Ribotti A, Bonomo S, Perilli A, ... Ferraro L (2020). Impact of freshwater inflow from the Volturno river on coastal circulation. Frontiers in Marine Science, 7, 293.

# Exploring Compound Flood Hazards: Bridging Statistics and Hydrodynamics in Estuaries

Dina GOMEZ RAVE[1], Diego URREA MÉNDEZ[1], Manuel del JESUS[1]

[1] IHCantabria – Instituto de Hidráulica Ambiental de la Universidad de Cantabria. Santander, España.
dinavanesa.gomez@unican.es
diego.urrea@unican.es
manuel.deljesus@unican.es

ABSTRACT

This study presents a robust framework for analysing compound flooding events in estuarine regions, where the interaction between freshwater and coastal waters creates a complex scenario for flood hazards. Traditional risk assessments tend to overlook the interconnected nature of flood drivers, potentially yielding inaccurate risk evaluations. Here, our methodology comprises a two-step process that seamlessly integrates statistical and hydrodynamic models to estimate the joint probability of compound events and their associated hazards. To ground our findings, we focus on the Santoña estuarine ecosystem in Northern Spain, offering a practical demonstration of our approach, and leveraging the interactions between six distinct flooding drivers. Through this case study, we shed light on the nuanced dynamics of compound flooding, illustrating how these insights could inform more accurate risk assessments and enhance flood management strategies. Our findings indicate that the multivariate approach outperforms the traditional univariate assessment method in terms of comprehensiveness, generating results more compatible with observations.

## 1. Introduction

Compound flooding in coastal regions is a widely recognized hazard that has the potential to be intensified due to global warming. Specifically, within estuarine and deltaic ecosystems, inundation dynamics become even more intricate due to the interplay of oceanographic, hydrological, and meteorological factors. The co-occurrence of these phenomena in space and time can exacerbate the local extent, depth, or duration of flooding (Couasnon et al., 2020). Despite their significant dependence, traditional flood analyses typically simulate these processes independently, primarily due to the complexity of their interactions and computational limitations.

Within this context, multivariate statistical models based on copulas have proven to be a viable alternative for addressing limitations of conventional approaches. They offer a holistic procedure for stochastically deriving joint boundary conditions, while accounting for multivariate and spatial dependencies (Bevacqua et al., 2019). Nevertheless, despite the extensive combination of statistical and hydraulic models, their use remains relatively infrequent in academic literature (Olbert et al, 2023). Through the integration of statistical analysis and hydrodynamic models, the potential for enhancing flood impact assessments lies in the improved accuracy of extreme water level estimates (Moftakhari et al., 2019). It enables a comprehensive exploration of a broad spectrum of consequences associated with flood hazard, offering critical insights for flood management practitioners and policymakers.

Here, we characterize the joint return period of compound flooding events in the Santoña Estuary (Cantabria, Spain) by accounting for interactions and dependency structures among six different pluvial, fluvial, and coastal variables. By conducting a case study in the Santoña Estuary (Cantabria, Spain), we analyze the interactions and dependency structures among six different pluvial, fluvial, and coastal variables to characterize the joint return period. Subsequently, we perform hydrodynamic simulations to assess the extent of coastal/fluvial inundation and water depth, providing proxies for the potential risk of compound flooding.

## 2. Methodology

Our methodology tackles compound flood hazards through two linked approaches. Firstly, it addresses the statistical interdependency among flood drivers, employing flexible vine copula structures to assess the joint return period and multivariate design events. Secondly, it incorporates hydrodynamic modeling to account for the physical compounding effects within flood scenarios, ensuring a comprehensive evaluation of the associated risks.

- **Multivariate characterization**: The first component involves a thorough investigation of the statistical interdependencies among drivers: storm surge, significant wave height, wave peak period, sea wind, fluvial discharge, and precipitation. By employing Archimedean and Elliptical copulas in vine-tree constructions, we effectively capture the strength and dependency structures. Based on the Kendall Return Period (KRP) hazard scenario, we calculate the corresponding critical layer and determine the multivariate design events for 100 years return period.
- **Hydrodynamic Modeling:** The second component focuses on hydrodynamic simulations, using a two-dimensional model to explicitly account for the maximum flood extents and inundation depths. This phase is essential for understanding the physical manifestations of compound flooding and assessing flood risk effectively.

## 3. RESULTS

The process of defining compound events, represented as an iso-hyper-surface that distinguishes between safe and hazardous occurrences within the multivariate framework, facilitates the identification of the most likely design events. These events, characterized by their highest probability density, encompass the inherent variability of these critical incidents and the parameterization of their multivariate nature. This information serves as the primary input for conducting hydrodynamic simulations, which delve into the intricate nonlinear interactions among the six drivers, allowing for an understanding of the physical manifestations of compound flooding scenarios.

The integration of both methodologies enables us to estimate the characteristics of flooding associated with compound events in a robust manner. The analysis demonstrates that the multivariate approach surpasses the traditional univariate assessment method in terms of comprehensiveness, since the results obtained are more in line to informal observations of flood processes in different regions. It bridges the gap between statistical analysis and hydrodynamic modeling, providing a comprehensive understanding of the compound nature of flood hazards. This research contributes to improved flood management strategies, particularly in low-lying coastal areas vulnerable to compound flooding. Consequently, the statistical-hydrodynamic methodology proposed in this study represents an effective approach to evaluating flood risk in estuarine areas, offering actionable insights for mitigating and managing flood risks effectively.

**References**

Bevacqua, E., D. Maraun, M. I. Vousdoukas, E. Voukouvalas, M. Vrac, L. Mentaschi, and M. Widmann. 2019. “Higher Probability of Compound Flooding from Precipitation and Storm Surge in Europe Under Anthropogenic Climate Change.” Science Advances 5 (9): eaaw5531. https://doi.org/10.1126/sciadv.aaw5531.

Couasnon, Anaïs, Dirk Eilander, Sanne Muis, Ted I. E. Veldkamp, Ivan D. Haigh, Thomas Wahl, Hessel C. Winsemius, and Philip J. Ward. 2020. “Measuring Compound Flood Potential from River Discharge and Storm Surge Extremes at the Global Scale.” Natural Hazards and Earth System Sciences 20 (2): 489–504. https://doi.org/10.5194/nhess-20-489-2020.

Moftakhari, Hamed, Jochen E. Schubert, Amir AghaKouchak, Richard A. Matthew, and Brett F. Sanders. 2019. “Linking Statistical and Hydrodynamic Modeling for Compound Flood Hazard Assessment in Tidal Channels and Estuaries.” Advances in Water Resources 128 (June): 28–38. https://doi.org/10.1016/j.advwatres.2019.04.009.

Olbert, Agnieszka I., Sogol Moradian, Stephen Nash, Joanne Comer, Bartosz Kazmierczak, Roger A. Falconer, and Michael Hartnett. 2023. “Combined Statistical and Hydrodynamic Modelling of Compound Flooding in Coastal Areas - Methodology and Application.” Journal of Hydrology 620 (May): 129383. https://doi.org/10.1016/j.jhydrol.2023.129383.

# Nature Positive Ports and Coastal Infrastructures

Phil LEBLANC[1], Jorge GUTIÉRREZ[1], Andrew RELLA[2]

[1] ECOncrete, Spain
phil@econcretetech.com, jorge@econcretetech.com

[2] ECOncrete, USA
andrew@econcrete.us

ABSTRACT

The construction of climate resilient and nature inclusive maritime infrastructure require innovative technologies and materials, and novel design considerations beyond the mandatory industry standards. In recent years, there has been a growing interest among ports and coastal stakeholders and engineers to integrate ecologically-engineered-structural solutions into the designs of port and coastal infrastructures. .

In this context, ECOncrete has partnered with several ports globally to demonstrate how eco-engineering technology can be used as Nature-Inclusive Design (NID) solution to promote the creation of diverse marine habitats as an integral part of Port coastal and marine infrastructure to increase their ecological value and mitigate impacts.

The goal of these projects is to catalyze a fundamental change in best practices for the design and construction of ports and coastal defenses where infrastructures are intentionally designed and actively used to promote marine biodiversity, address environmental compensation requirements, and support the restoration of coastal and marine ecosystem health and services.

## 1. Introduction

Increasingly, the permitting and construction of port and coastal infrastructures requires the integration of compensation measures to reduce potential ecological impacts and create opportunities to enhance and restore marine biodiversity. Consequently, there has been a growing interest by stakeholders to integrate NID solutions into the designs and construction of port infrastructure projects (Huib de Vriend, et al. 2014, King et al. 2021, Sella et al. 2022). Port and coastal engineers are exploring how eco-engineered materials and technology can provide design solutions to address not only structural and engineering requirements of port and coastal infrastructures but also the need to promote native marine habitats, increase biodiversity and restore local coastal ecosystems.

Artificial structures have different physical, chemical, and biological characteristics than the natural habitats they replace, often resulting in a reduction, or complete removal of intertidal and shallow subtidal ecosystems (Glasby, et al. 2007). At the same time, artificial hard substrates associated with port infrastructure offer a newly constructed habitat and, if designed correctly, can provide an opportunity for biodiversity enhancements. Structures can be designed with environmentally sensitive materials and additional complexity to support increased settlement, refuge, and feeding opportunities for a wide range of marine organisms.

## 2. Nature Positive Ports and Coastal Infrastructure projects

In 2021, under the Blue Economy Incubator program, a pilot project was launched at the Port of San Diego in California (USA) to demonstrate an innovative design of an ecologically-engineered interlocking regularly placed, multidirectional, water retaining single layer concrete armor unit, the Coastalock, which is designed to create well-defined local ecosystems that mimic natural rock pools which ultimately provide structural, ecological, and community engagement benefits, including carbon sequestration and regeneration of local

marine biodiversity and high hydraulic stability. The results from the ongoing biological monitoring show development towards a richer, more diverse community compared to adjacent control rocks.



**Fig. 1.** Coastalock armor units installed in Port of San Diego (USA) (left) and colonization of the Coastalock units 14 months after installation (center and right)

In 2022, the Living Ports' project, in which the Port of Vigo (Spain), Cardama Shipyard, the Technical University of Denmark (DTU) and ECOncrete are partnering, was launched after the award funding from the European Commission's (Horizon 2020 Fast Track to Innovation). The Living Ports project has already been deployed at the Port of Vigo as a solution for 310 m² of ecologically enhanced quaywall as well as 100 Coastalock armor units, which provide stabilization and subtidal and intertidal marine habitats at an exposed coastal revetment. The project also features a moored underwater observatory that provides the public interactive access to observe the marine life developing on the ecologically engineered quaywall. Biological monitoring is conducted by DTU, and for the first time, underwater sound reduction due to marine life growing on concrete is studied.



**Fig. 2.** Underwater observatory (left) and ecologically enhanced quaywalls in the Port of Vigo (Spain) with marine life colonization 4 months after the installation (center and right)

With these port-based projects, ECOncrete aims to provide examples of nature-inclusive design for coastal protection and sustainable port infrastructure, which can be applied to urban, natural, and working waterfronts around the world. These projects are designed to catalyze a fundamental change in best practices for the design and construction of ports by moving away from obsolete 'grey' infrastructure towards innovative nature-positive 'blue' infrastructure with associated structural, environmental, and socioeconomic benefits.

**References**


De Vriend et al. (2014). 'Building with nature': the new Dutch approach to coastal and river works. Proceedings of the Institution of Civil Engineers - Civil Engineering 2014 167:1, 18-24.

King et al. (2021). Engineering with Nature: Supporting Mission Resilience and Infrastructure Value at Department of Defense Installations. Engineer Research and Development Center (U.S.)

Sella et al. (2022). "Design, production, and validation of the biological and structural performance of an ecologically engineered concrete block mattress: A Nature-Inclusive Design for shoreline and offshore construction". Integrated environmental assessment and management 18.1: 148-162. 202.

Glasby et al. (2007). Nonindigenous biota on artificial structures: could habitat creation facilitate biological invasions?. Mar Biol 151, 887–895

# Towards technical design guidance for estuarine Nature-based Solutions

Thomas DUNLOP[1], William GLAMORE[2], Stefan FELDER[3]

[1,2,3] Water Research Laboratory, School of Civil and Environmental Engineering, UNSW Sydney, Australia

t.dunlop@unsw.edu.au

w.glamore@wrl.unsw.edu.au

s.felder@unsw.edu.au

ABSTRACT

In estuaries, Nature-based solutions (NbS) have the potential to support ecosystem restoration, reduce flood risk and erosion, and provide a myriad of social and environmental co-benefits. However, a lack of design standards, uncertainty in performance, and reliability concerns, have become barriers towards the widespread implementation of NbS. In this study, a review of existing NbS design guidelines, in conjunction with a literature review of intertidal NbS, revealed that technical content balancing ecology with engineering is currently missing in design guidelines. A conceptual approach to integrating ecology and engineering within design guidelines was subsequently proposed. This conceptual approach focuses on the critical thresholds and parameter relationships associated with four key stages of NbS development, namely establishment, growth, recovery and mortality, and functionality. Technical guidance is presented that enables practitioners to overcome deficits in design details, for improved project implementation in the short, medium, and long-term. This guidance advises practitioners of the necessary site-specific and experimental data that are to be collected to improve model predictions of NbS success across the project lifecycle.

## 1. Introduction

The ongoing climate and biodiversity crises have led to a growing interest in the use of Nature-based Solutions (NbS) in estuaries to mitigate the impacts of flood risk and shoreline erosion, while providing a self-sustaining ecosystem. However, to enable the implementation of NbS, practitioners require technical design guidance like the standards and manuals consulted for traditional restoration and engineering projects. The aim of such design guidance is to provide a quantitative understanding of how NbS will respond to ongoing environmental change and how changes to ecosystem growth will impact the capacity of the solution to reduce erosion and mitigate flood risk. In this study, a review of existing NbS design guidelines was undertaken (Dunlop et al., 2023). A conceptual approach towards a technical NbS design guideline was proposed (Dunlop et al., 2023), and the application of this approach to predictive numerical models is outlined. The level of site-specific detail required by practitioners across the NbS lifecycle to improve predictions is discussed.

## 2. Methods

### *2.1. Design Guideline Review*

A literature search for broad guidelines aimed at practitioners for the design and implementation of estuarine NbS was conducted. This search encapsulated books, reports, and industry standards, as well as ecological guidelines of intertidal ecosystems, to provide a comprehensive collection of NbS guidelines in the intertidal zone of estuaries. More than 50 NbS guidelines were reviewed to understand whether these guidelines adequately considered the technical aspects needed by practitioners for NbS design purposes.

### *2.2. Conceptual Approach Development*

Following the outcomes of the design guideline review, a conceptual approach to NbS design was proposed that balances the ecology requirements for ecosystem establishment, growth, mortality, and recovery, with the

engineering values of a functional shoreline defence. This approach was informed by the research presented in academic manuscripts on four prominent estuarine intertidal NbS, namely: seagrass, oyster reefs, mangroves, and saltmarsh.

### *2.3. Numerical Modelling*

This conceptual approach was implemented in a coupled Python and Delft3D Flow-FM model to predict the biophysical changes and shoreline protection functionality of mangrove and oyster reef ecosystems when exposed to varying hydrodynamic and morphological conditions. The modelling and validation of these predictions is ongoing, with the accuracy of site-specific detail explored for different estuarine contexts.

## 3. Results and Concluding Remarks

The critical review of NbS design guidelines revealed a lack of technical data that balanced ecology and engineering in design, instead focusing on guiding principles, case studies, and frameworks for implementation that can help decision makers approach and deliver NbS projects. The conceptual approach towards an integrated design guideline aimed to provide this missing quantitative guidance and is based on four key stages of the NbS lifecycle that can be considered in design (Fig. 1).

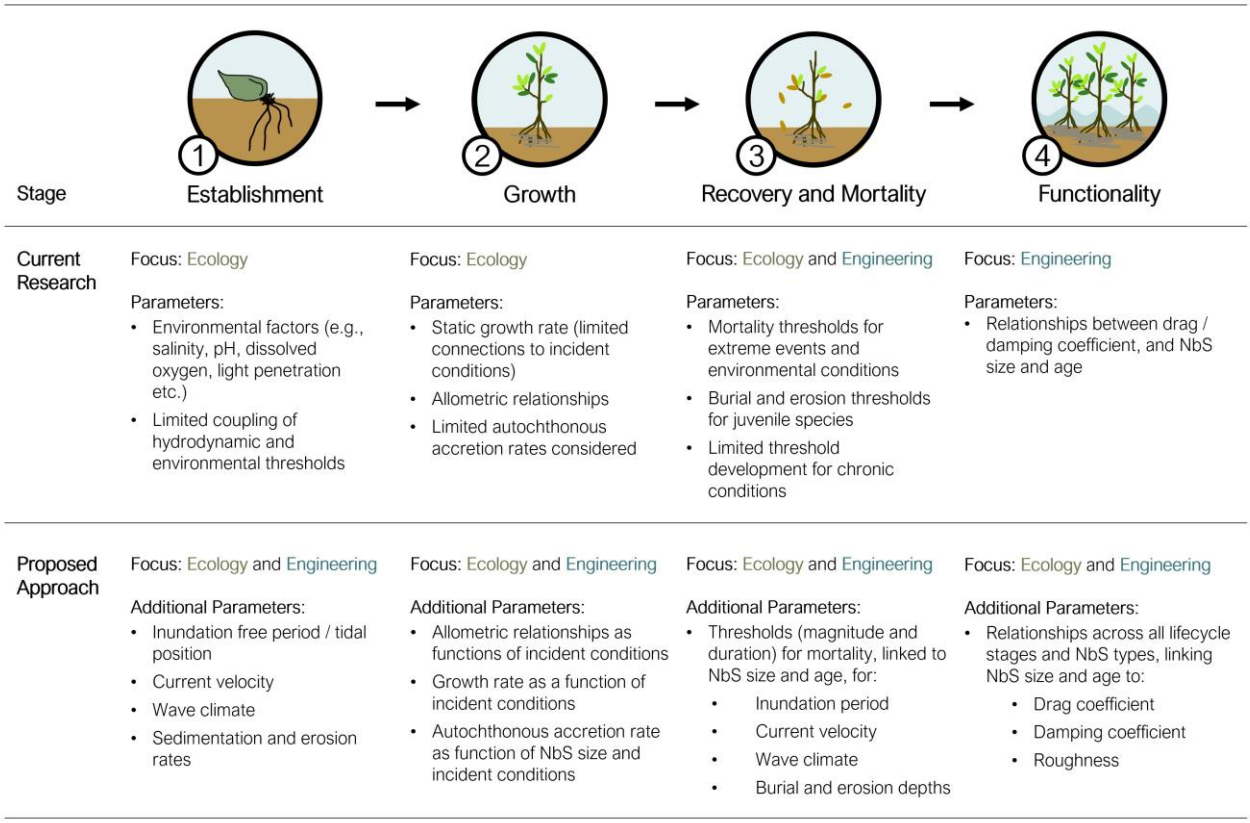



**Fig. 1.** Four stages of a conceptual approach towards a technical design guideline that comprises ecology and engineering (top), with the current research focus from existing guidelines (middle) compared to the focus and parameters of the proposed approach (bottom) (Dunlop et al., 2023).

When this approach is applied to a coupled model with a biogeomorphic feedback loop, the response of the NbS at each stage of the lifecycle to changing hydrodynamic conditions can be quantified, and the time taken for NbS to grow to a sufficient stage for shoreline protection can be predicted. These outcomes provide practitioners with a quantitative understanding of how intertidal NbS will respond to ongoing environmental change and can help inform the choice of whether to implement NbS over conventional shoreline protection measures. The implementation of this approach within a numerical model also demonstrates the impact of site-specific data, highlighting to practitioners the influence of some variables to the accuracy of predictions, and the need for further studies to improve decision-making.

**References**

Dunlop T, Glamore W, Felder S (2023) Restoring Estuarine Ecosystems Using Nature-based Solutions: Towards an Integrated Eco-Engineering Design Guideline, Science of the Total Environment, 873, 162362

# Influence on a Riverine Estuary due to an Increase in Outtake of Cooling Water

Anton BURMAN[1], Olivier MACCHION[1], Øyvind LIER[1], Atle JENSEN[2]

[1] Norconsult Sweden AB, Sweden
anton.burman@norconsult.com,
olivier.macchion@norconsult.com
oyvind.lier@norconsult.com
[2] University of Oslo, Norway
atlej@math.uio.no

ABSTRACT

The operating conditions of a power plant in northern Sweden is going to change in the future. In this work we present a 3D modelling approach where we investigate several future operating conditions. To validate the model, CTD measurements were performed monthly for one year. The model was able to capture the complex dynamics of the estuary.

## 1. Background and problem formulation

Örnsköldsvik is a major city with approximately 50 000 residents on the shore of the Baltic Sea. The history of Örnsköldsvik is closely connected with the heavy industries in the region, mostly related to the forestry and paper production in the area. The power plant uses sea water to provide district cooling as well as cooling water for the adjacent industries. One such industry is FlagshipONE, which is going to produce electrofuel (Naturvårdsverket, 2023). To ensure that they can continue to meet the future needs of the public, Övik Energi is keen to determine the maximum amount of additional water that can be safely extracted from the nearby sea without potentially disrupting the intricate estuarine dynamics of the neighboring bay or interfering with the power plant's operation.

## 2. Measurements and estuary overview

Conductivity, salinity, and depth (CTD) measurements were performed with one-month intervals throughout one year. These measurements were used for validation of the numerical model. The location of the CTD measurements is plotted as red markers in Fig 1. The river Moälven, flowing into the estuary, and the narrow strait are marked by magenta markers in Fig 1. These magenta markers also correspond to the boundary conditions of the model. These two features are the main defining geometrical features of the flow in the estuary. Additionally, the bathymetry of the bay can also be seen in Fig 1. In the strait, an acoustic doppler current profiler (ADCP) was placed. The ADCP performed current measurements with 30 second intervalls throughout the year in the entire water column. The estuary's flow dynamics exhibit seasonality, characterized by an upsurge in seawater inflow propelled by rising density disparities between river freshwater and seawater, this effect is extra profound during the spring flood. In the strait there is a significant threshold which gives rise to a halo- and thermo-cline. This sharp gradient in temperature, which provides consistent cold water throughout the year, is used by the power plant to obtain cooling water for their operations.

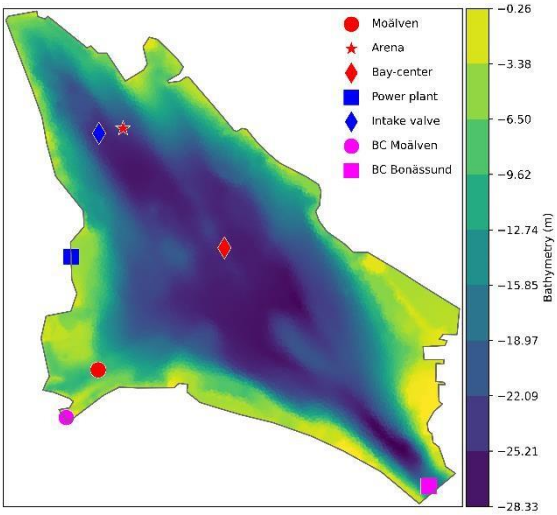



**Fig 1.** Bathymetry and points of interest in the estuary.

## 3. Numerical model and future scenarios

The 3D model was made using DHI's MIKE3 solver. To capture the dynamics of the previously mentioned clines, a temperature/salinity model was employed. A validation case was set up using the current day operation, which was an outtake of 333 l/s through a vent on the bottom of the bay (see the blue point labeled "Intake" in Fig. 1). At the location "Power plant", the heated water is released into the surface water of the bay. The CTD measurements (taken at the three red points in Fig. 1) were extrapolated to cover the entire domain, providing suitable initial conditions. A timestep of 0.1 s was chosen, for larger timesteps the simulation proved unstable. A simulation time of five days was adequate to achieve steady state. The mesh consisted of 20,938 elements horizontally and 60 layers vertically (a combination of z- and σ-layers). Once the model had been validated, six future scenarios were defined. These scenarios involved varying the cooling water outtake from 650 l/s to 10,000 l/s. An outtake of 650 liters per second equates to a doubling of the present operational parameters. The selection of the remaining 5 scenarios was designed to encompass a broad spectrum of potential future operating conditions.

## 4. Results and discussion

### *4.1. Validation*

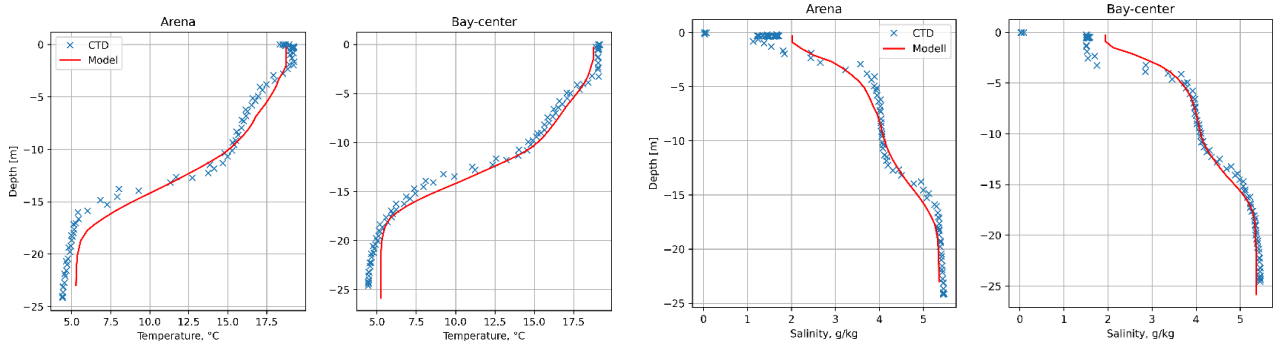



**Fig 2.** Validation of numerical model in two points in the estuary: (left) temperature; (right) salinity.

Profiles for salinity and temperature have been plotted for two relevant points in Fig 2. The model exhibits a good correlation with the measured temperature and salinity. The clines exist in three layers, which have been captured accurately by the model. A mesh study was conducted to determine the necessary vertical resolution to accurately capture this phenomenon. Coarser meshes were unable to capture the sharp gradients.

### *4.2. Future scenarios*

The salinity and temperature profiles were evaluated in the water column above the outtake valve for all future scenarios. The corresponding profiles for all scenarios are shown in Fig 3. As seen, the temperature remains stable in the lower parts of the cline unless the outtake exceeds 2,000 l/s. Once the outtake is above 5,000 l/s, the temperature is increased and may potentially affect the operation of the power plant. This temperature increase (and salinity decrease) results from a mixing effect where fresh, warm surface water is drawn downward into the cline. This effect becomes noticeable once the outtake exceeds 2,000 l/s. This localized effect will be explored in greater detail in the conference proceedings.

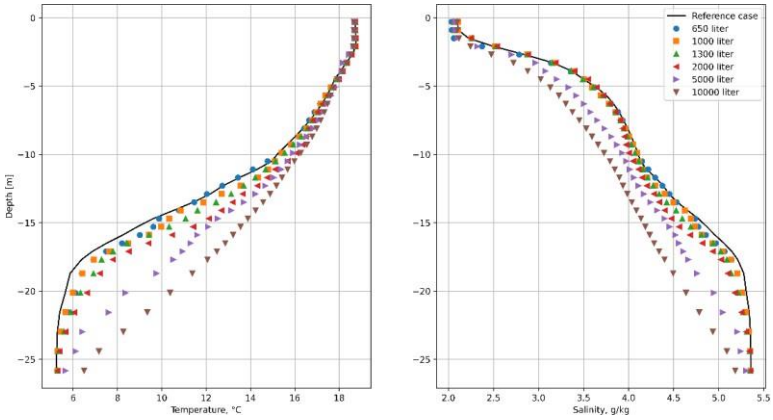



**Fig 3.** Profiles in the water column at the outtake location: (left) temperature; (right) salinity.

**Acknowledgements**

The authors would like to thank Örnsköldsviks Energi for their cooperation and willingness to publish the results herein.

**References**

Naturvårdsverket (2023), FlagshipONE producerar elektrobränsle för sjöfart, https://www.naturvardsverket.se/amnesomraden/klimatomstallningen/klimatklivet/resultat-i-olika-branscher-2022/flagshipone-producerar-elektrobransle-for-sjofart/

# Numerical modelling of infragravity waves in a tidal inlet during storm conditions

Diogo MENDES[1], Alphonse NAHON[2], Kévin MARTINS[3], André B. FORTUNATO[2], Xavier BERTIN[3], Baptiste MENGUAL[4], Laura LAVAUD[4], Marc PEZERAT[5], António A. PIRES-SILVA[1]

[1] CERIS, Instituto Superior Técnico, Portugal
diogo.silva.mendes@tecnico.ulisboa.pt; antonio.pires.silva@tecnico.ulisboa.pt
[2] National Laboratory for Civil Engineering, Portugal
anahon@lnec.pt; afortunato@lnec.pt
[3] UMR 7266 LIENSs, CNRS—La Rochelle Université, France
kmartins@univ-lr.fr; xbertin@univ-lr.fr
[4] BW-CGC (Benoit Waeles - Consultant Génie Côtier), France
baptiste.mengual@bw-cgc.fr; laura.lavaud@bw-cgc.fr
[5] SHOM, France
marc.pezerat@shom.fr

ABSTRACT

During storm conditions, infragravity (IG) waves with periods between 25 s and 300 s can dominate the sea-surface oscillations near the shoreline. Through processes like wave run-up, overwash and wave overtopping, IG waves can hence become major drivers of coastal hazards. Although IG dynamics are relatively well understood in open beaches, their contribution of the hydro-sedimentary dynamics of more complex coastal settings, such as tidal inlets characterized by their ebb and flood deltas connected through a transitional channel, is not well understood. Here, we assess the performance of the widely used XBeach numerical model to predict IG wave dynamics through a comparison against field observations collected on an ephemeral tidal inlet (Albufeira Lagoon) during storm Leslie (2018). XBeach accurately predicted the observed IG significant wave heights reaching up to 1 m over a 2-day period. This performance is assessed at both the nearby beaches and the flood-delta.

## 1. Introduction

During storm conditions, coastal hydrodynamics change mainly due to due to incident short waves, with periods between 4 s and 20 s. The width of the surf zone increases relative to mild wave conditions, which has important implications for swash dynamics, wave set-up and the generation and dissipation of infragravity (IG) waves, with periods between 25 s and 300 s, near the shoreline (e.g., Fiedler *et al*., 2015).

The morphology of tidal inlets is usually more complex than open sandy beaches, where the flood delta is connected to the ebb delta by a transitional channel. This morphological complexity modifies the wave and current patterns, and their interaction. Moreover, field observations during storm conditions in these coastal environments are scarce in the literature. Therefore, the performance of a numerical model to forecast the IG wave dynamics in a tidal inlet during such conditions remains poorly understood.

Here, we use the XBeach numerical model to forecast IG dynamics at the Albufeira Lagoon tidal inlet during storm Leslie (2018). The assessment was performed against field observations specifically collected during this event, covering a region extending from the surf zone to the inner lagoon (Bertin *et al.*, 2019).

## 2. XBeach model application

XBeach is applied in surfbeat mode over a 2DH domain. The grid resolution ranged between 30 m offshore and inside the lagoon and 3 m near the inlet channel. Offshore wave conditions were obtained from a hindcast

simulation with the WWIII model implemented as described in Mengual *et al*. (2022). The tidal level was specified based on the 6-min recorded time series by a tidal gauge located about 20 km north of the study site.

After several sensitivity simulations, we used the *roelvink_daly* formulation (Daly *et al*., 2012) to compute short wave dissipation by depth-induced breaking. The free model parameters were specified as follows: *gamma* = 0.40; *gamma2* = 0.30; *alpha* = 1.5. Regarding bottom friction, the accurate representation of tidal currents at the flood delta required a Manning friction coefficient $n$ = 0.028 $m^{-1/3}s$ with a maximum friction coefficient of 0.0077. Both short wave dissipation by depth-induced breaking and bottom friction impact IG characteristics, thereby contributing to the generation or dissipation of IG waves.

## 3. Results and discussion

Fig. 1. displays the comparison between simulated and observed significant IG wave height (Hm0,ig). In general, the overall agreement both at the nearby beach (left) and at the flood-delta (right) is very good. This can be assessed by the values of error metrics (Bias and RMSE) that are within the range published in the literature (Bertin and Olabarrieta, 2016). The adequate reproduction of Hm0,ig time series suggests an accurate simulation of short-wave transformation, which affect the generation and dissipation of IG waves.

In more details, the model accurately captures the observed decay of Hm0,ig that occurs at the flood-delta (right) between high-tide and mid-tide (i.e. during ebb). This suggests the interaction between incoming infragravity waves and tidal currents is well reproduced by XBeach during storm events. Moreover, the model simulates the correct value of Hm0,ig at the nearby beach (left), with a slight underestimation during the maximum observed Hm0,ig value (at 4am on 14 October).

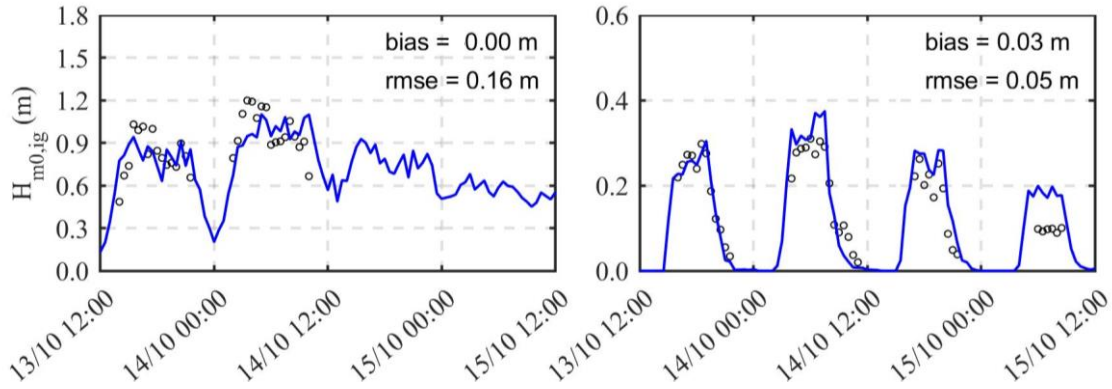



**Fig. 1.** Comparison between simulated (lines) and observed (circles) significant IG height on the nearby beach (left) and at the flood-delta (right). Bias and root-mean square error metrics are also shown.

Overall, the small differences between simulated and observed values of Hm0,ig, both at the nearby beaches and at the flood-delta, supports the use of XBeach to forecast the morphological evolution of this ephemeral tidal inlet during storm conditions.

**Acknowledgements**

The first author acknowledges Foundation for Science and Technology's (FCT) support through funding UIDB/04625/2020 from the research unit CERIS. This research was carried out in the scope of the collaborative project INLEX, funded by the French ANR and the FCT (project 40791ZC).

**References**

Bertin X, Mendes D, Martins K, Fortunato AB, Lavaud L (2019) The Closure of a Shallow Tidal Inlet Promoted by Infragravity Waves. Geophys Res Lett 46, 6804–6810

Bertin X, Olabarrieta M (2016) Relevance of infragravity waves in a wave-dominated inlet. J Geophys Res Oceans 121, 5418–5435.

Daly C, Roelvink D, van Dongeren A, van Thiel de Vries J, McCall R (2012) Validation of an advective-deterministic approach to short wave breaking in a surf-beat model. Coastal Eng 60, 69-83

Fiedler JW, Brodie KL, McNinch JE, Guza RT (2015) Observations of runup and energy flux on a low-slope beach with high-energy, long-period ocean swell. Geophys Res Lett 42, 9933–9941

Mengual B, Bertin X, Place F, Pezerat M, Coulombier T, Mendes D, Fortunato AB (2022) Wave-current interactions at the Tagus Estuary Mouth (Portugal) under storm wave conditions. Ocean Model 175, 102035

# Reduction of microplastic pollution in shipbuilding industry

Ivana LUČIN[1], Marta ALVIR[1], Siniša DRUŽETA[1], Bože LUČIN[2]

[1] Faculty of Engineering, University of Rijeka, Croatia
ilucin@riteh.hr, malvir@riteh.hr, sinisa.druzeta@riteh.hr

[2] FlowTech d.o.o, Rijeka, Croatia
boze.lucin@gmail.com

ABSTRACT

Microplastic pollution in the marine environment has been given increasing attention due to its negative impact on marine organisms. The problem is that these particles can ultimately enter the human body through the food chain causing serious health problems. Shipyards have been previously identified as a cause of microplastic pollution due to antifouling hull paintings. However, what was not identified is that an increasing amount of ship systems are now made out of plastic pipes. This increases the number of operations that produce the plastic debris. Traditionally, plastic pipes are cut, prepared, and installed on the ship. These operations are conducted in the immediate vicinity of the sea which makes it easy for microplastic particles to become airborne and then deposited in the sea. This aspect of the shipbuilding process requires additional attention through the quantification of plastic debris produced during these operations. Quantification methods need to be established in future research.

## 1. Microplastic pollution of marine environment

Microplastic particles have been identified as a large problem in marine environment because they can be colonized by microorganisms, including pathogens and harmful algal bloom species (Amaral-Zettler et al., 2020). The main problem is that these particles can travel long distances and can be ingested by marine organisms. The ingestion of these particles can pose a considerable threat to marine organisms (Guzzetti et al., 2018) causing severe problems. Through the food chain, it can ultimately be ingested by human, negatively affecting their health.

### *1.1. Shipyards as the source of microplastic pollution*

Shipyards have been identified as the source of pollution due to the emission of ultrafine particles due to operational activities (López et al. 2022). Paint fragments (Gaylarde et al., 2021) used for antifouling coating have been identified as a considerable contribution of microplastic in the marine environment. What has previously not been considered are plastic particles that are produced during cutting and preparation activities with plastic pipes. In the work by Luo et al., 2022 it has been identified that cutting PVC pipes can produce a considerable amount of microplastic particles. However, this has not been conducted specifically for pipes used in shipbuilding and shipbuilding activities so additional investigations are needed for exact pollution quantification. Only after this, it can be expected that regular monitoring of microplastic pollution and strategies to reduce it will be implemented in shipbuilding industry since they are currently not implemented.

## 2. Adaptation of existing practices

It is a practice in the shipbuilding industry that operations with plastic pipes are mostly conducted on ships. This makes it easy for plastic particles to become airborne and then deposited on the sea. Novel 3D modeling strategies can be adopted to reduce cutting operations (Lučin et al., 2023) and cutting and preparation activities with plastic pipes can be mitigated in a more controlled environment, i.e. warehouse. The warehouse needs to be designed in a way to capture microplastic particles so they can be properly deposited and not transported by air, clothing, or shoes. An additional benefit is that expanding of pre-outfitting stage by mitigating operations to warehouses can reduce operational costs (Kunkera et al., 2022). However, for the industry to

adopt these strategies exact calculations regarding investments needed, exact reduction of costs and time, and reduced negative environmental impact are needed.

### *2.1. Research challenges*

Various case studies have been conducted by measuring microplastics in harbors (Romeo et al., 2015), beach sediments (Stolte et al., 2015), and marinas (Sparks and Awe, 2022). In general, the main problem with microplastic measurements is that it is difficult to determine the main contributor to microplastic pollution. An additional problem is that there are a lot of different microplastic detection methods (Sharma et al., 2022) making results from different studies not comparable.

Regarding the quantification of the negative impact of cutting operations, additional research is needed. To the authors' knowledge, only one paper (Luo et al., 2022) investigated the amount of particles by cutting pipes in the open area. A more controlled environment is needed where airborne particles would also be collected and quantified. It is important to note that in shipbuilding additional preparation of pipe endings is needed, which also produces a considerable amount of plastic particles. In this work rough estimation of plastic debris quantity is presented for various pipes commonly used in the shipbuilding. The estimation is based on known pipe properties and pipe ending machining required by the manufacturer. Reduction of plastic debris is then estimated based on novel 3D modelling strategy with reduced number of cutting operations. It must be noted that not all plastic debris that is created during pipe ending preparation will be microplastic particles. Therefore, in future work it is required to conduct experimental investigations for various pipe sizes and pipe materials with equipment used in shipbuilding to recreate as much as possible real operating conditions.

## 3. Conclusion

Although novel legislations are continuously being imposed, industry adaptation to novel ecological demands can require substantial amount of time. This can be due to considerable investments or time needed for implementing novel procedures. In the case of shipbuilding, 3D modelling strategies of ship systems can be adopted which would reduce cutting operations. Furthermore, cutting and preparation of plastic pipes can be conducted in warehouses with appropriate solutions for microplastic particles capturing. However, motivation for implementation of these solutions without exact quantification of benefits is questionable. Therefore, tight collaboration between industry and scientists can help identify solutions which are beneficial both from ecological and from economical perspective. Such solutions can help speed up the industry adjustment to more sustainable operation which is a necessity due to rapid increase in ecological problems. Scientists need to establish proper quantification methods so industry can see exact impact they are having on the environment and how implementing novel solutions can help contribute to the reduction of negative impact.

**References**


Amaral-Zettler, L. A., Zettler, E. R., Mincer, T. J. (2020). Ecology of the plastisphere. Nature Reviews Microbiology, 18(3), 139-151.

Guzzetti, E., Sureda, A., Tejada, S., & Faggio, C. (2018). Microplastic in marine organism: Environmental and toxicological effects. Environmental toxicology and pharmacology, 64, 164-171.

López, M., Lilao, A.L., Ribalta, C., Martínez, Y., Piña, N., Ballesteros, A., Fito, C., Koehler, K., Newton, A., Monfort, E. and Viana, M., (2022). Particle release from refit operations in shipyards: Exposure, toxicity and environmental implications. Science of the Total Environment, 804, 150216.

Gaylarde, C. C., Neto, J. A. B., & da Fonseca, E. M. (2021). Paint fragments as polluting microplastics: A brief review. Marine Pollution Bulletin, 162, 111847.

Luo, Y., Al Amin, M., Gibson, C. T., Chuah, C., Tang, Y., Naidu, R., & Fang, C. (2022). Raman imaging of microplastics and nanoplastics generated by cutting PVC pipe. Environmental Pollution, 298, 118857.

Lučin, B., Čarija, Z., Alvir, M., & Lučin, I. (2023). Strategies for Green Shipbuilding Design and Production Practices Focused on Reducing Microplastic Pollution Generated during Installation of Plastic Pipes. Journal of Marine Science and Engineering, 11(5), 983.

Kunkera, Z., Opetuk, T., Hadžić, N., & Tošanović, N. (2022). Using Digital Twin in a Shipbuilding Project. Applied Sciences, 12(24), 12721.

Romeo, Teresa, Michela D'Alessandro, Valentina Esposito, Gianfranco Scotti, Daniela Berto, Malgorzata Formalewicz, Seta Noventa et al. (2015). Environmental quality assessment of Grand Harbour (Valletta, Maltese Islands): a case study of a busy harbour in the Central Mediterranean Sea. Environmental monitoring and assessment 187 1-21.

Stolte, A., Forster, S., Gerdts, G., & Schubert, H. (2015). Microplastic concentrations in beach sediments along the German Baltic coast. Marine Pollution Bulletin, 99(1-2), 216-229.

Sparks, C., & Awe, A. (2022). Concentrations and risk assessment of metals and microplastics from antifouling paint particles in the coastal sediment of a marina in Simon's Town, South Africa. Environmental Science and Pollution Research, 29(40), 59996-60011.

Baruah, A., Sharma, A., Sharma, S., & Nagraik, R. (2022). An insight into different microplastic detection methods. International Journal of Environmental Science and Technology, 19(6), 5721-5730

# Interfacial mixing of the stratified flow in the trapezoidal-shape channel with presence of background vorticity

Janek LAANEARU[1], Katrin KAUR[2], Daniela MALCANGIO[3]

[1,2] Tallinn University of Technology, Ehitajate tee 5, 19086 Tallinn, Estonia
janek.laanearu@taltech.ee
katrin.kaur@taltech.ee
[3] Polytechnic University of Bari, Via Edoardo Orabona 4, 70125 Bari, Italy
daniela.malcangio@poliba.it

ABSTRACT

The dynamics of gravity current developing along a channel with a trapezoidal-shape cross-section is numerically investigated using the computational fluid dynamics modelling approach. The numerical modelling results are qualitatively compared with the observed stratified-flow dynamics characteristics, gained from a series of large-scale experiments of the uni- and bi-directional flows across a submerged, trapezoidal, sill obstruction with presence of background vorticity. Measured velocity and density profiles are used at the channel cross-sections to observe internal-flow dynamics under a range of parametric forcing conditions, related to fluid properties, fluxes and sill conditions. The computational domain of the numerical study is a scaled version of the trapezoidal stratified-flow flume used for the experimental study (Adduce et al., 2019).

## 1. Introduction

The experimental program was conducted in a large-scale facility (Coriolis Platform II) at Laboratoire des E ´ coulements "Ge´ophysiques et Industriels (LEGI) in Grenoble. For the experimental study, a 13 m diameter and 1.2 m deep circular tank was used. The anti-clockwise direction at a constant angular velocity Ω of the water tank was used to simulate the Coriolis effects on the stratified-flow dynamics in the trapezoidal-shape channel (De Falco et al., 2021). The experiments were conducted under different angular velocity conditions and at different fresh-water inflow rates while keeping the salt-water flow constant. The experimental measurements focused on obtaining the velocity and density fields in different planes of the channel. A particular aim of the Grenoble's experimental study was to understand more thoroughly the stratified-flow turbulent fluxes within the interfacial shear layer under presence of the background vorticity. The experiments demonstrated that the interfacial mixing, associated with the transfer of mass and momentum between the superimposed layers was related to the parametric forcing conditions, such as variable saline and freshwater volume fluxes; density differences; sill obstruction submergence depths; angular speed of the flume. In some cases, strong vertical entrainment was observed at the density interface, while, in other circumstances, interfacial waves were first formed at the interface; the interfacial instabilities (e.g. Kelvin–Helmholtz or Holmboe instabilities) providing an additional mechanism for vertical mixing across the density interface. The numerical framework of the dynamics of gravity current due to saltwater intrusion into ambient freshwater in the submerged and obstructed channel has been previously introduced in Laanearu et al (2021) and Kaur et al (2022).

## 2. Modelling

To interpret the observed dynamics of the stratified-flow development in the channel, the Computational Fluid Dynamics (CFD) modeling approach was employed. A three-dimensional computational domain geometry was created based on a scaled version of the experimental apparatus; the trapezoidal-shape channel part of the Grenoble's facility. Numerical simulations of the stratified flow were conducted using a solver of OpenFOAM v1906 (OpenCFD Ltd.): *interMixingFoam*. The flow regime was turbulent, and the freshwater and saltwater layers were considered to be incompressible, isothermal and Newtonian fluids. For the air-water interface

presence, the Volume of Fluid (VOF) method (Hirt and Nichols, 1981) was also considered. To investigate the resulting internal-flow dynamics numerically, the CFD simulations were undertaken, using fixed saline and freshwater volume fluxes; density differences; sill obstruction submergence depths; angular speed of the trapezoidal channel. The numerical model validation was conducted based on the non-rotating experimental results. The rotational case of the stratified flow in the trapezoidal-shape channel was conducted under the same geometrical and grid conditions but using the non-zero angular speed of the computational domain volume elements. The standard $k$-$\varepsilon$ model (Launder and Spalding, 1972; Launder and Sharma, 1974) was adopted in the numerical modelling approach, where the turbulent kinetic energy $k$ and eddy viscosity $\varepsilon$ were determined according to the performance of the RANS model for the one-phase flow, such as water is.

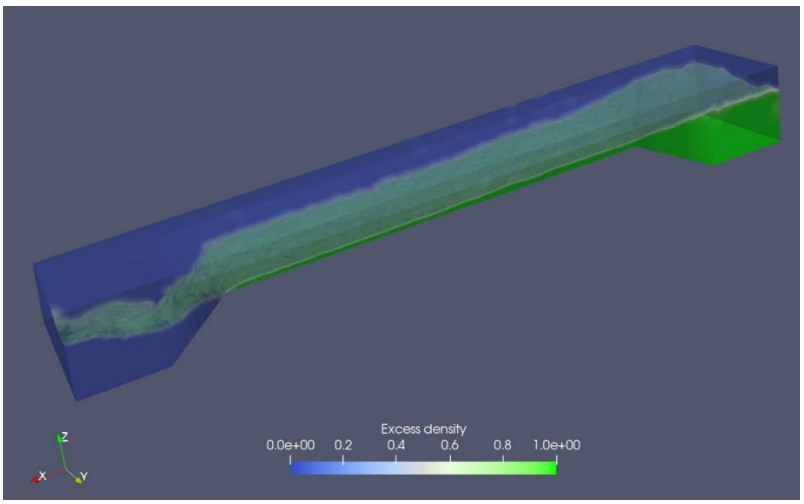



**Fig. 1.** CFD simulation of stratified flow along the trapezoidal channel: saltwater intrusion into ambient freshwater with presence of background vorticity.

## 3. Concluding remarks

The dynamics of stratified-flow dynamics of the trapezoidal-chape cross-section channel is numerically investigated using the CFD model. The numerical modelling results demonstrate qualitatively similar behavior of the observed stratified-flow dynamics, gained from a series of large-scale experiments of the uni- and bi-directional flows in the channel with presence of background vorticity. To interpret the observed dynamics of the stratified-flow development, the CFD modeling was developed using the specific computational-domain grid-development methodology. Comparison is made also for simulated flow fields under conditions of varying diffusivity between the salt- and freshwater masses. It is found that the saltwater intruding into stationary freshwater layer produces more diffusion in the numerical simulations that in the experiments. While the bi-directional flow of fresh and saltwater produces more similar behavior. Therefore, the robustness of the model under varied turbulent diffusion conditions should be assessed in future analysis.

**Acknowledgements**

This research has received funding from the Estonian Research Council, under grant PRG1487, and the Tallinn University of Technology, under grants SSGF21002 and SS19046. The authors acknowledge the assistance and input of the TalTech HPC division.

**References**

Adduce C, De Falco MC, Cuthbertson A, Laanearu J, Malcangio D, Kaur K, Negretti E, Sommeria J, Valrha T, Viboud S (2019). The Dynamics of Bi-Directional Exchange Flows: Implications for Morphodynamic Change within Estuaries, Proceedings of the HYDRALAB+ Joint User Meeting. (1−9). Bucharest, Romania: HYDRALAB+ Joint User Meeting.

De Falco MC, Adduce C, Cuthbertson A, Negretti ME, Laanearu J, Malcangio D, Sommeria J (2021) Experimental study of uni- and bi-directional exchange flows in a large-scale rotating trapezoidal channel, Physics of Fluids, 33, 036602.

Laanearu J, Kaur K, Malcangio D, Cuthbertson A, Adduce C, De Falco MC, Negretti E, Sommeria J (2021). Numerical modelling of the bottom gravity current in an obstructed channel with trapezoidal cross-section, 6th IAHR Europe Congress Warsaw Poland 2020, Polish Academy of Sciences, 247−248.

Kaur K, Malcangio D, Laanearu J (2022). Numerical study of turbulence characteristics of bidirectional flow through a trapezoidal channel, 7th IAHR Europe Congress, September 7-9, 2022, Athens, Greece.

Hirt CW, Nichols BD (1981) Volume of fluid (VOF) method for the dynamics of free boundaries, Journal of Computational Physics, 39(1), 201-225.

Launder BE, Spalding DB (1972). Lectures in mathematical models of turbulence. London: Academic Press.

Launder BE, Sharma BI (1974). Application of the energy dissipation model of turbulence to the calculation of flow near a spinning disc." Lett. Heat Mass Trans. 1(2), 131–137.

# Unbalanced sediment flux caused by tidal pumping and residual circulation in the meso-tidal Yeosu Bay

H.K. HA[1], S.I. KIM[1], J.Y. SEO[1], J.H. PARK[1], P.J. KIM[2]

[1] Department of Ocean Sciences, Inha University, Incheon, Republic of Korea
hahk@inha.ac.kr

[2] Underwater Survey Technology 21, Incheon, Republic of Korea

ABSTRACT

In the western (M1) and eastern (M2) channels of Yeosu Bay, two mooring systems with acoustic Doppler current profilers were installed to investigate the transport processes of suspended sediments. Over the mooring period, the currents (M1: -1.10–0.80 m $s^{-1}$; M2: -0.85–0.85 m $s^{-1}$) were mainly dominated by ebb tides. Two-layered residual currents developed by the freshwater discharge at M2 (< 0.24 m $s^{-1}$) were higher than that at M1 (< 0.16 m $s^{-1}$). Even if the same current-induced shear stress as M2 was applied to the bed, M1 could be resuspended with higher SSC (max: 233 mg $l^{-1}$) to reach the water surface. This is because the bed sediments at M1 have relatively low cohesive sediment (mud) content and shell fragments. These differences in current and sediment resuspension created an unbalanced sediment flux. The seaward sediment flux at M1 was mainly driven by tidal pumping, whereas the landward flux at M2 was mainly driven by residual currents. Although the sediment fluxes tended to be compensated and balanced mutually by tidal cycles over the entire period, the sediment flux at M2 was about twice higher than that at M1. Suspended sediments exhibited an influx pattern into the bay.

## 1. Introduction

A bay is the primary connection between ocean and continent and a transition zone where various physical, chemical, and biological processes are complicatedly combined. Unbalanced sediment transport in the bay causes dredging issues related to undesirable sedimentation in port navigation waterways. It can also determine the distribution of pollutants and nutrients in water bodies, which can affect water quality and the benthic ecosystems. Sediment transport is influenced by hydrodynamic factors such as residual circulation, tidal currents, river discharges, and waves. The combination of these factors, each with different characteristics, could create heterogeneity in the sediment distribution in the bay. In estuarine sediment dynamics, the predominant mechanisms of sediment transport reveal different site-specific configurations (e.g., shape, slope, and bathymetry). Thus, they remain a challenging research topic. A more comprehensive investigation is necessary to comprehend these factors' impact on sediment transport. This study aims (1) to understand the unbalanced sediment flux by tidal pumping and residual circulation and (2) to reveal the sediment resuspension mechanism in the meso-tidal bay.

## 2. Study area

Yeosu Bay is a semi-enclosed embayment surrounded by Namhae Island and Yeosu Peninsula, Korea (Fig. 1). The bay mouth is open to the south, allowing free exchange with the open ocean. The Seomjin River is an estuary system with a mean discharge of 120 $m^3$ $s^{-1}$ (Kang et al., 2020). The maximum tidal range is 2.9 m and 1.1 m for spring and neap tides, respectively. The maximum current is 0.60 m $s^{-1}$ and 0.65 m $s^{-1}$ during the flood and ebb, respectively. Surface sediments were predominantly composed of sandy mud (including shell fragments) in M1 and mud in M2.

## 3. Materials and methods

Two mooring systems with acoustic Doppler current profilers (ADCPs) were installed in the western (M1) and eastern (M2) channels of Yeosu Bay to investigate the transport mechanism of suspended sediments. Ship-borne surveys were performed across the channel. Echo intensity derived from ADCP was converted to the suspended sediment concentration (SSC) by calibrating with water samples. Suspended sediment flux ($F$, kg m$^{-2}$ s$^{-1}$) at mooring stations was calculated, and tidal-averaged $F$ ($\overline{F}$) was decomposed into tidal ($\overline{\overline{U} \cdot \overline{SSC}}$) and residual ($\overline{U' \cdot \mathrm{SSC}'}$) mechanisms as follows:

$$F = U(z) \cdot SSC(z) \quad (1)$$

$$\overline{F} = \overline{\overline{U} \cdot \overline{SSC}} + \overline{U' \cdot SSC'} \quad (2)$$

where $U$ is along-channel current velocity (m s$^{-1}$), and $z$ is depth (m). The prime and overbar notations indicate longer and shorter timescales than the tidal cycles determined by 36-h low- and high-pass filters, respectively. The depth-integrated $\overline{F}$ was represented as total along-channel sediment flux.

## 4. Results and discussion

Residual currents at both M1 and M2 usually exhibited that the surface and bottom currents flowed toward the seaward and landward, respectively. The zero-crossing depths of residual currents were frequently changed with relative importance among tide, wind, and freshwater discharge. Two-layered residual currents developed by the freshwater discharge at M2 (< 0.24 m s$^{-1}$) were higher than that at M1 (< 0.16 m s$^{-1}$). Even if the same current-induced shear stress as M2 was applied to the bed, sediment at M1 could be resuspended with higher SSC (max: 233 mg l$^{-1}$) to reach the water surface compared to that at M2. These differences in current and sediment resuspension created the unbalanced sediment flux. At M1, the residual current was slightly positive (landward direction), whereas the seaward sediment flux was dominant owing to ebb-dominated tidal pumping (88%). At M2, meanwhile, residual currents (73%) dominated landward sediment flux. Although they tended to be mutually compensated and balanced by tidal cycles, the sediment flux in M2 (~0.81 ton m$^{-1}$ day$^{-1}$) was about twice higher than that in M1 (~0.42 ton m$^{-1}$ day$^{-1}$)(Fig. 1).

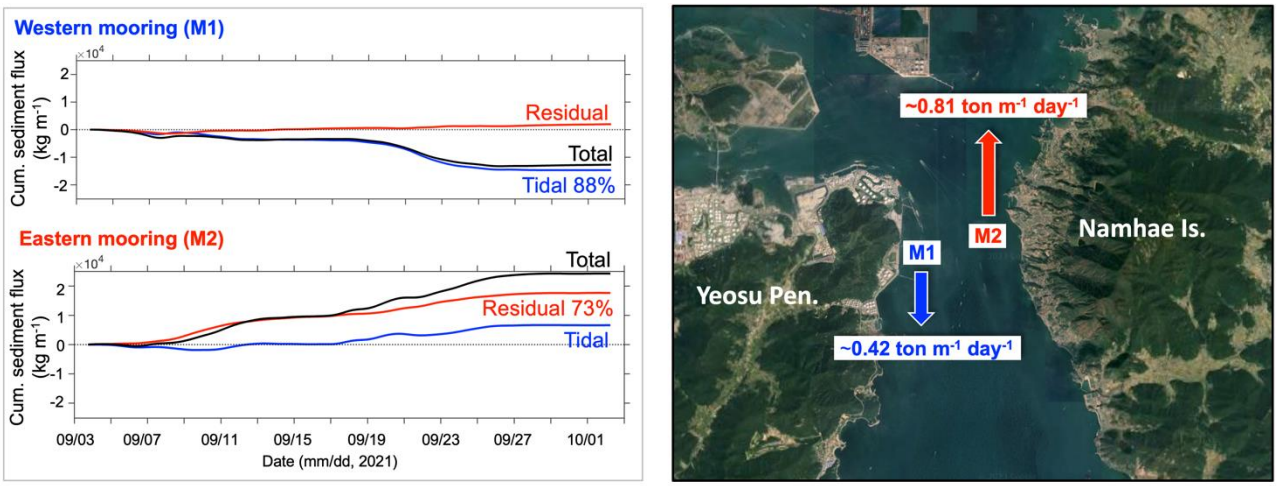



**Fig. 1.** (Left) the time series of cumulative sediment fluxes; (Right) the net sediment fluxes at M1 and M2.

## 5. Conclusions

*In-situ* moorings were installed to investigate the sediment dynamics in the meso-tidal bay. The difference in mechanisms driving sediment transport at two mooring stations resulted in an unbalanced sediment flux. The seaward sediment flux at M1 was mainly driven by tidal pumping (88%), whereas the landward flux at M2 was mainly driven by residual currents (73%). This highlights the important roles of tidal pumping and residual circulation in controlling the sediment transport in the meso-tidal bay systems.

# A new low-Reynolds $k-\varepsilon$ turbulence model for shear flow along smooth walls

Thuzar AUNG[1], Erik TOORMAN[1]

[1]Hydraulics and Geotechnics, KU Leuven, Belgium
thuzar.aung@kuleuven.be
erik.toorman@kuleuven.be

ABSTRACT

In a open channel flow with very high sediment concentrations (>1g/l), the flow exhibits modulation of turbulence due to fluid-particle interactions and particle-particle interactions. Low-Reynolds effects by two- and four-way coupling of sediment-turbulence interactions lead to turbulence damping and energy dissipation in the inner boundary layer (IBL). As a result, the IBL thickens in the presence of particles near the bottom. In large-scale applications, the IBL thickness where low-Reynolds modifications to turbulence occur is not resolved. The numerical simulation of total sediment transport in practical scale applications is typically done by solving suspended transport in the water column, ignoring the IBL thickness and imposing bottom boundary conditions applicable only to clear water. The unresolved processes within the IBL have to be incorporated by the adaptation of near-bottom boundary conditions such that the IBL layer can be bridged with adapted wall functions. To achieve this, a new low-Reynolds turbulence model is necessary to be developed to define new boundary conditions for sediment-laden flow. Therefore, a new low-Reynolds $k-\varepsilon$ turbulence model is constructed with analytical profiles approximating the DNS data and validated in a 1DV model for clear water. New analytical damping functions are defined in terms of the turbulent Reynolds number $v_t^+$, defined as the ratio of eddy viscosity to effective kinematic viscosity of the suspension.

**Model Development**

In the basic equations for the conventional low-Reynolds version of the $k-\varepsilon$ turbulence model, the conservation of turbulent kinetic energy (TKE) $k$ and turbulent dissipation rate $\varepsilon$ are defined as:

$$\frac{\partial k}{\partial \mathrm{t}}+U_i\frac{\partial k}{\partial \mathrm{x}_i}=\frac{\partial}{\partial \mathrm{x}_i}\left(\left(\nu+\frac{\nu_t}{\sigma_\mathrm{k}}\right)\frac{\partial k}{\partial \mathrm{x}_i}\right)+P-\varepsilon \tag{1}$$

$$\frac{\partial \varepsilon}{\partial t}+U_i\frac{\partial \varepsilon}{\partial \mathrm{x}_i}=\frac{\partial}{\partial \mathrm{x}_i}\left(\left(\nu+\frac{\nu_t}{\sigma_\varepsilon}\right)\frac{\partial \varepsilon}{\partial \mathrm{x}_i}\right)+\frac{f_1c_1P-f_2c_2\varepsilon}{T_t} \tag{2}$$

where: $P=\nu_t\left(\frac{\partial U_i}{\partial x_j}+\frac{\partial U_j}{\partial x_i}\right)\frac{\partial U_i}{\partial x_j}$ is shear production, $T_t=\frac{k}{\varepsilon}$ is turbulent timescale, $U_i$ = Reynolds-averaged flow velocity, $\nu$ = kinematic viscosity, $\nu_t$= turbulent eddy viscosity, $c_1$= 1.44, $c_2$ = 1.92, $\sigma_\varepsilon$ = 1.3 (Rodi, 1980), $\sigma_k$ is defined by a low-Reynolds closure, and $f_1$, $f_2$ = low-Reynolds damping functions. The eddy viscosity $\nu_t$ is defined as:

$$\nu_t=f_\mu c_\mu\frac{k^2}{\varepsilon} \tag{3}$$

where $c_\mu$ = 0.09 (Rodi, 1980), $f_\mu$ = a low-Reynolds damping function.
In order to generate data for the damping functions, various online available DNS data sets at $\mathrm{Re}_*$=180-10000 for steady channel flow are utilized. All parameters and functions are plotted as a function of the turbulent Reynolds number $v_t^+$, defined as the ratio of Reynolds stress to viscous stress, which reduces to the ratio of eddy viscosity to kinematic viscosity (Toorman, 2000). For clear water, the fluid viscosity $\nu$ is used, whereas, in sediment-laden flow, this is replaced with the effective mixture viscosity $\nu_e$.

First, $f_\mu$ is computed from Eq.(3) using the $k$ and $\varepsilon$ profiles. The DNS data support that $f_2=1/f_T$, in which the realizable timescale factor $f_T$ is defined in terms of $v_t^+$ according to (Toorman, 2000). By defining $f_1=f_P/f_T$, $f_P$ is derived from Eq.(2). $\sigma_k$ is computed from the second term in the right-hand side of Eq.(1) being equal to the sum of pressure diffusion and turbulent transport. The resulting profiles of $f_\mu, f_1, f_2, f_P, f_T$ **and** $\sigma_k$ provide the necessary DNS-based data set to formulate approximated analytical closures. The DNS data clearly show Reynolds number dependence, i.e. the peak of TKE in the transient region increases with Reynolds number. Therefore the $\mathbf{Re_*=2000}$ DNS data (Hoyas et al., 2006) is selected. Then, the analytical functions of $f_\mu, f_P$ **and** $\sigma_k$ are formulated in terms of $v_t^+$ to provide a best fit to the DNS-derived profiles. The damping functions $f_\mu, f_1, f_2, f_P, f_T$ **and** $\sigma_k$ follow their respective asymptotes in the laminar and turbulent regions, reaching unity in the fully-developed turbulent region.

### Numerical Implementation

The new-low Reynolds $k-\varepsilon$ turbulence model is implemented in a 1DV numerical model and validated with the $\mathrm{Re_*}=4000$ DNS data (Bernardini et al., 2014). Figure.1 provides comparison between nondimensionalized profiles of velocity, eddy viscosity, turbulent kinetic energy and turbulent dissipation rate. The results are in good agreement with each other. The implemented new low-Reynolds model can capture the correct shape of all profiles in general, except for the $y^+<0.1$ region. The turbulent kinetic energy of the 1DV model deviates from the DNS data for $y^+>2000$. This can be explained by the fact that damping functions are calibrated and produced based on the $\mathrm{Re_*}=2000$ DNS data which cannot capture the Reynolds number dependence effect in the TKE profile.

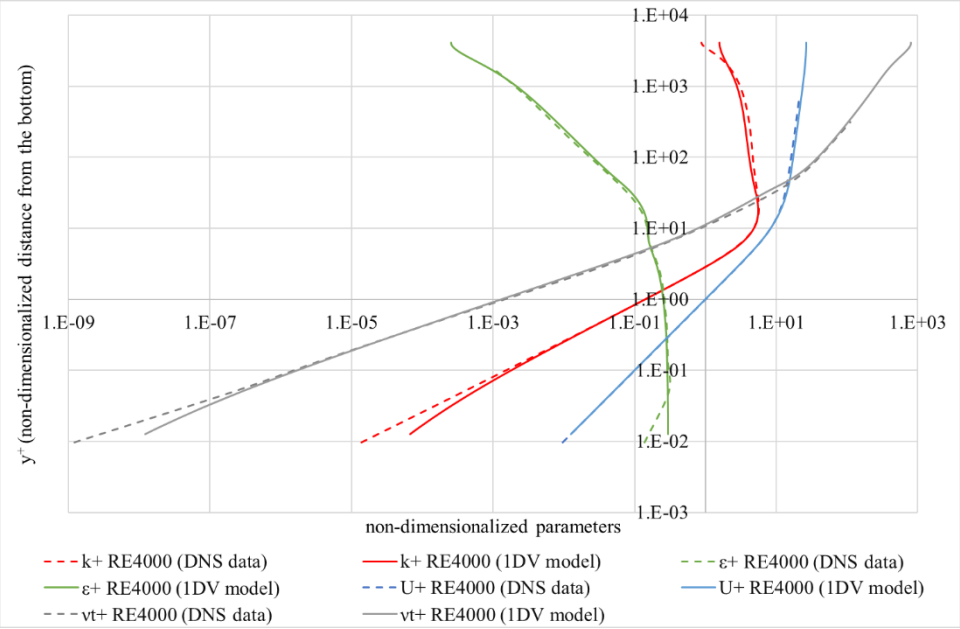



**Fig. 1.** Comparison of non-dimensionalized parameters (turbulent kinetic energy $k^+$, turbulent dissipation rate $\varepsilon^+$, velocity $U^+$, eddy viscosity $\nu_t^+$) of $\mathrm{Re_*}=4000$ (DNS data) and $\mathrm{Re_*}=4000$ (1DV model)

## Conclusion

A new low-Reynolds $k-\varepsilon$ turbulence model for wall-bounded shear flows has been developed, allowing analytical reconstruction of the profiles of velocity, eddy viscosity, turbulent kinetic energy and turbulent dissipation rate. The analytical solution consists of damping functions based on the turbulent Reynolds number $v_t^+$. The damping functions of the new model are developed and calibrated using a DNS dataset at $\mathrm{Re_*}=2000$. The model has successfully been implemented into a numerical code and validated using a $\mathrm{Re_*}=4000$ DNS dataset. The model will be adapted and validated for sediment-laden flow in future work.

#### References


Bernardini M, Pirozzoli S, Orlandi P (2014) Velocity statistics in turbulent channel flow up to RE* = 4000, J. Fluid Mechanics, 742, 171-191

Hoyas S, Jimenez J (2006) Scaling of the velocity fluctuations in turbulent channels up to RE* = 2003, Physics of Fluids, 18, 011702

Rodi W (1980) Turbulence models and their application in hydraulics, IAHR State-of-the-Art Paper

Toorman E (2000) Analysis of near-wall turbulence modelling with $k-\varepsilon$ models, Report HYD/ET/00/COSINUS2, Hydraulics Laboratory, KU Leuven

# Enhanced utilisation of tidal range schemes to support migration to Net Zero

Man Yue LAM[1], Reza AHMADIAN[1]

[1] School of Engineering, Cardiff University, Queen's Buildings, 5 The Parade, Cardiff, UK, CF24 3AA
lamM7@cardiff.ac.uk
AhmadianR@cardiff.ac.uk

ABSTRACT

Tidal Range Schemes (TRSs) are dispatchable energy sources critical for balancing electricity demand and supply. To support transition to Net Zero, a novel objective function, namely the renewable function, is proposed to reflect the proportion of electricity demand provided by renewable energy sources. The renewable function was applied to optimise a TRS in South Wales, UK, and its results were compared to energy and revenue optimised results. The revenue and renewable optimised TRSs generated more energy at the times when more energy was needed, giving higher total revenue and renewable function values respectively, at the expense of production less energy. Such an effect was more visible in revenue optimisation compared to renewable optimisation. Nevertheless, renewable optimisation may become important when the renewable energy supply is more volatile, and more testing under volatile renewables will be conducted in future.

## 1. Background

To alleviate global climate change and achieve the Net Zero emission target, an energy transition from traditional fossil fuel energy to renewable energy is needed. However, some renewable energy sources, e.g. wind and solar, are intermittent and non-dispatchable. To balance energy supply and demand, optimisation of dispatchable renewable energy sources is required. For Tidal Range Schemes (TRSs), revenue optimisation (Harcourt et al., 2019) was conducted to maximise the revenue obtained from the generated electricity. The price of electricity in revenue optimisation is a surrogate function representing the imbalance between energy supply and demand. Nevertheless, electricity price does not reflect the proportion of electricity supplied by renewable energy sources and does not consider regional differences in electricity demand. This research proposes a novel objective function to reflect the proportion of electricity demand provided by renewable energy sources.

## 2. Methodology and initial results

Optimisations were conducted for a proposed TRS in South Wales, UK, with a 0D-model and Genetic Algorithm (GA) method (Xue et al., 2020) with an objective function $f = \int_T V(t)P(t)dt$ where $V(t)$ is a value function; $P(t)$ is the power output; $t$ is time; $T$ is the period within which the optimisation is conducted. In energy optimisation, $V(t) = 1$ for $0 \leq t \leq T$. In revenue optimisation, $V(t)$ is the electricity price $Pr(t)$ (Harcourt et al., 2019). This research proposes a novel renewable energy ratio $R(t) = D(t)/S_R\ (t)$, where $D(t)$ is energy demand and $S_R(t)$ is energy supplied by renewables other than the TRS under study. $R(t)$ reflects the proportion of electricity demand supplied by renewable energy sources, and the optimisations conducted with $V(t) = R(t)$ is defined as renewable optimisation, with the objective function $f_R = \int_T R(t)P(t)dt$ defined as the renewable function. Energy, revenue, and renewable optimisations of the TRS without pumping were conducted for the tidal elevation data in year 2018. A flexible Every Half-tidal cycle and Next (EHN) approach (Xue et al., 2020) was used to include the change in tidal range throughout the year. The optimisations were conducted with $Pr(t)$ and $R(t)$ for year 2018 and year 2023 (without changing the tidal data to year 2023) for comparison as shown in Figure 1. Figure 2 shows the normalized renewable energy ratio $R_n(t)$ and electricity price $Pr_n(t)$, where $R_n(t) = R(t)/\bar{R}$ and $Pr_n(t) = Pr(t)/\overline{Pr}$; $\bar{R}$ and $\overline{Pr}$ are the

mean renewable energy ratio and the mean electricity price, as well as the power output from the optimised TRS. The renewable or revenue optimisations shifted the power generation of the TRS to periods when the value functions were higher. Such shifts were more obvious in the revenue optimisation as confirmed by the correlation coefficients in Table 1. The observation was likely to be resulted from the fact that $R_n(t)$ varied less frequently (i.e. less volatile) than $Pr_n(t)$. Table 2 shows that the revenue and renewable optimisations gave higher total revenue and renewable function values respectively, at the expense of production less energy. The impact of using $R(t)$ in TRS operation is expected to increase when the renewable energy supply becomes more volatile. More testing will be conducted in future to test this claim.

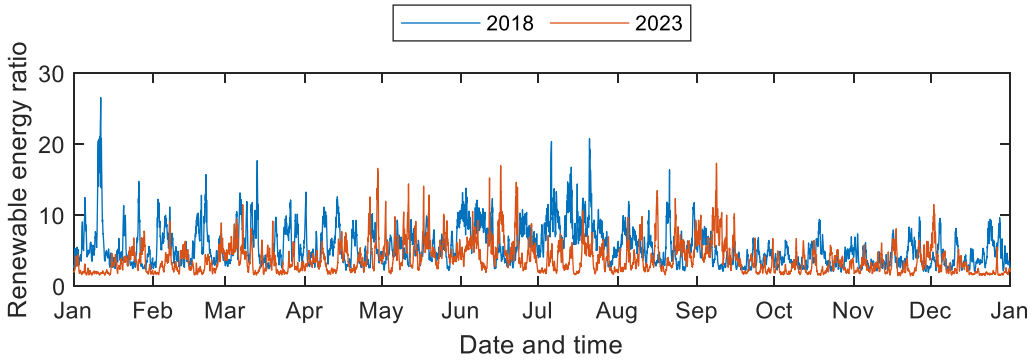



**Fig. 1.** The electricity value function $R(t)$ in year 2018 and 2023 estimated with the data from an electricity company ELEXON.

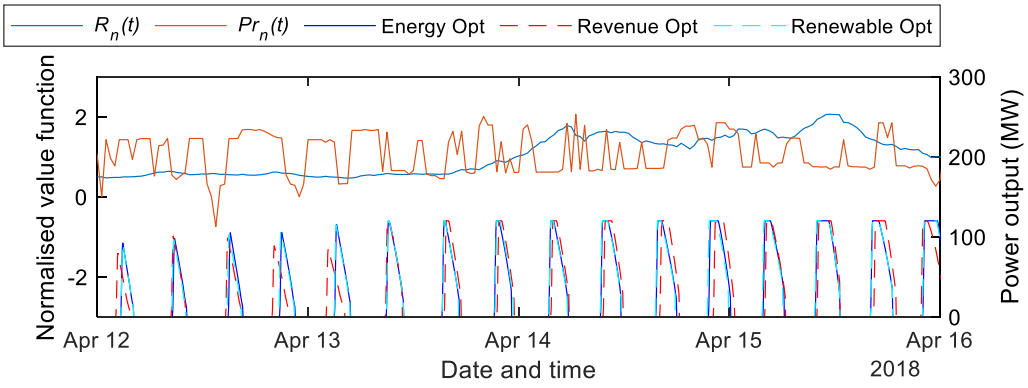



**Fig. 2.** The normalized electricity value functions $R_n(t)$ and $Pr_n(t)$ for year 2023 and the power outputs $P(t)$ from the energy, revenue, and renewable optimisations with twelve 5 m turbines.

**Table 1.** Correlation coefficient with the energy optimised power outputs $P(t)$

| Year for $Pr(t)$ and $R(t)$ | Revenue Optimisation Output | Renewable Optimisation Output |
|---|---|---|
| **2018** | **0.9072** | **0.9852** |
| **2023** | **0.8303** | **0.9845** |

**Table 2.** Energy, revenue, and renewable function with respect to the values obtained from the energy optimisation with prices and renewable energy ratios for 2018 and 2023 respectively

| Year for $Pr(t)$ and $R(t)$ | Revenue Optimisation | | | Renewable Optimisation | | |
|---|---|---|---|---|---|---|
| | Energy | Revenue | Renewable function | Energy | Revenue | Renewable function |
| **2018** | **0.985** | **1.033** | **0.987** | **0.999** | **1.000** | **1.002** |
| **2023** | **0.959** | **1.059** | **0.970** | **1.000** | **0.999** | **1.002** |

**Acknowledgements**

The study is carried out as a part of the TARGET (TidAl Range schemes as configurable Grid-scale Energy sTorage facilities) project, EP/W027879/1, which is financed by the EPSRC (Engineering and Physical Sciences Research Council).

**References**

Xue J, Ahmadian R, Jones O (2020) Genetic Algorithm in tidal range schemes' optimization, Energy, 200, article 117496
Harcourt F, Angeloudis A, Piggott MD (2019) Utilising the flexible generation potential of tidal range power plants to optimise economic value, Applied Energy, 237, 873–884

# Faecal Indicator Organism prediction through machine learning enhanced by dimensionality reduction

Hossein AMINI[1], Man Yue LAM[1], Reza AHMADIAN[1]

[1] School of Engineering, Cardiff University, Wales, United Kingdom
aminih@cardiff.ac.uk
lamm7@cardiff.ac.uk
Ahmadianr@cardiff.ac.uk

ABSTRACT

Water quality is a critical research area with significant social and environmental implications, necessitating collaborative efforts among researchers, policymakers, and the public. This study explores dimensionality reduction techniques and machine learning algorithms for predicting faecal indicator organisms (FIOs) such as *E. coli* and *Enterococci*. Principal component analysis (PCA) served as the dimensionality reduction model, and the prediction accuracy of the dimension-reduced variables was tested with a linear regression model. The analysis reveals that four principal components capture approximately 80% of the data variability. Other machine learning algorithms, such as K-Nearest Neighbors (KNN), eXtreme Gradient Boosting (XGBoost), and CatBoost, will be tested in future.

## 1. Introduction

Faecal Indicator Organisms (FIOs) are widely used as a sign of high pathogens and potential risk to public health in water bodies. Various directives, including the EU revised Bathing Water Directive, require monitoring of FIOs to ensure the safety of bathers. While process based FIO modelling provides critical information for water quality management, they are time consuming and resource intensive, making them less suitable for early warning systems. Data-driven Artificial Intelligence (AI) models, together with the emerging sensor technology (Akoumianaki et al., 2020), were suggested for early-warning models which could warn the immediate and short-term FIO exceedance events based on hydrologic and climatic data (Herrig et al., 2019). For AI models, identifying critical environmental variables governing FIO concentration is important. Rothenhebera and Jones 2018 found that tide and sediment are critical for estuarine and freshwater *Enterococci* concentrations. Lam and Ahmadian (2023) developed an AI model to predict FIOs at Swansea Bay, UK. Yet, their model requires data pre-treatment to remove correlated input variables. Dimensionality reduction models, e.g. Principal component analysis (PCA), remove the need for such a pre-treatment.

## 2. Materials and methods

The ability of PCA to reduce the number of variables needed to predict FIO concentration is tested. PCA is a technique to reduce a large set of input variables to a smaller set that is more important to predict the output variables. Specifically, PCA transforms an M-dimensional input data set, **X**, which may have correlated variables, into a new and smaller set, **Y**, of linearly uncorrelated variables referred to as Principal Components (PCs) (Johnson et al., 2007). PCA reduces the dimensionality of the problem while retaining as much as possible of the variance information contained in the original data set **X**.

The input data set **X** and the output data set in this study were the initial input and output data sets in Lam and Ahmadian (2023). The input and output data sets contained 204 environmental variables and *E Coli* and *Enterococci* concentrations measured at Swansea Bay, UK. PCs were identified with PCA and the explainability of PCA was investigated. The trade-off between modelling accuracy and the number of PCs used can be studied by models such as ridge regression, LASSO regression, and basic linear regression. In this abstract, basic linear regression was applied.

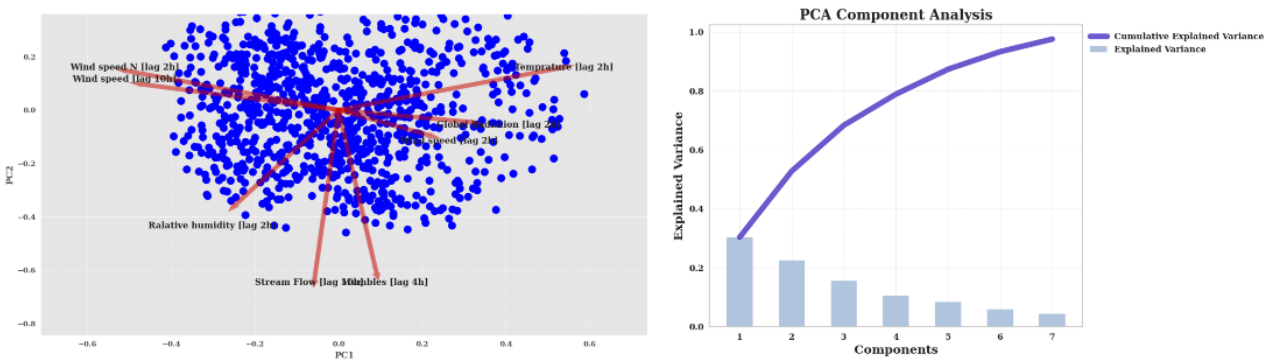



**Fig. 1.** Bi plot and Scree plot; variable importance to every PC and variance explained by each PC

The significance of the factors and explained variance are shown by a visual examination of the biplot for the first two PCs and scree plot (Figure 1). The biplot's data points stand in for observations, and the feature vectors, represented by length and direction, respectively, show how important the observations are and how they correlate with the PCs. For PC1, Global radiation, Wind speed with a time lag of 2h, and temperature are positively strongly correlated with the PC2 while the other wind speeds are negatively more correlated with PC2. Also, Stream Flow and tide at Mumbles are mostly correlated with PC1 but negatively. In the Scree plot, the PCs are represented in the x-axis, and the cumulative explained variance is shown on the y-axis. The first four PCs account for more than 80% of the variation, indicating effective dimensionality reduction. The PCA was capable of identifying critical variables governing FIO concentrations.

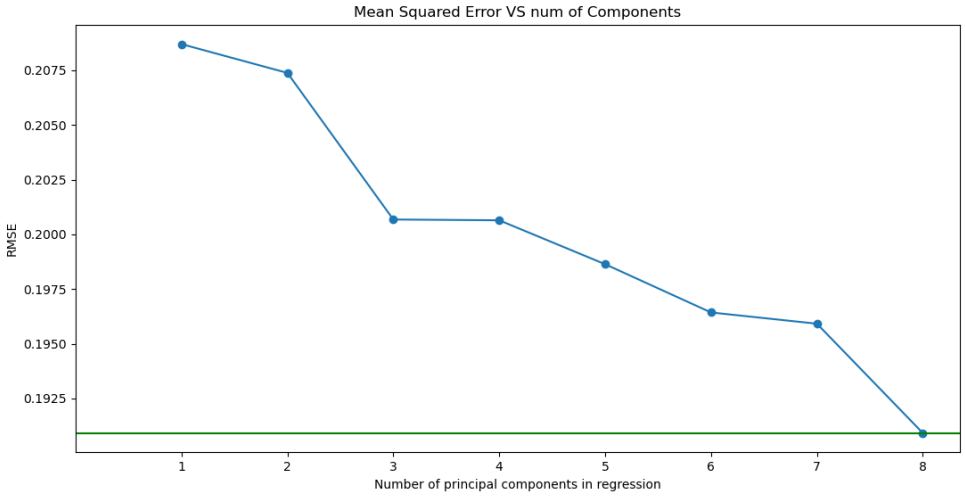



**Fig. 2.** Mean Squared Error Versus Number of Components

Figure 2 shows the root mean squared error (RMSE) obtained from the linear regressions with an increasing number of PCs. RMSE=0.2 was obtained from using 3 or 4 PCs, which is not far from RMSE=0.19 for using all 8 PCs, meaning that FIO can be still predicted with 4 features removed. The reduction of variables supports computationally efficient FIO predictions yet retaining the best possible model accuracy.

**References**

Akoumianaki, I., Pagaling, E., Coull, M., Avery, L., & Potts, J. (2020). Review of monitoring techniques and sampling strategies to identify the most significant sources of faecal indicator organisms (FIO) within a catchment. CRW2018_14.

Herrig, I., Seis, W., Fischer, H., Regnery, J., Manz, W., Reifferscheid, G., & Böer, S. (2019). Prediction of fecal indicator organism concentrations in rivers: the shifting role of environmental factors under varying flow conditions. *Environ. Sci. Eur.*, 31(1), 59

Johnson, G. W., Ehrlich, R., Full, W., & Ramos, S. (2007). Principal Component Analysis and receptor models in environmental forensics, In: *Introduction to environmental forensics* (Eds Murphy, B.L. and Morrison, R.D.). Academic Press., pp. 207-272.

Lam, M.Y., & Ahmadian, R. (2023). Predicting Fecal-Indicator Organisms in Coastal Waters Using a Complex Nonlinear Artificial Intelligence Model. *J. Environ. Eng.*, ASCE, 149(2), 04022093.

Rothenheber, D., & Jones, S. (2018). Enterococcal concentrations in a coastal ecosystem are a function of fecal source input, environmental conditions, and environmental sources. *Appl. Environ. Microbiol.*, 84(17), e01038-18

# The impact of different lagoon operation procedures on regional water exchange rate

Bin GUO[1], Reza AHMADIAN[1]

[1] School of Engineering, Cardiff University, Queen's Buildings, The Parade, Cardiff, UK, CF24 3AA
Guob2@cardiff.ac.uk
AhmadianR@cardiff.ac.uk

ABSTRACT

The operation of a tidal lagoon enables a substantial exchange of water between the impounded basin and the external coastal areas, leading to alterations in water exchange and tidal flushing. It is imperative to comprehend the influence of tidal lagoons on water renewal for effective environmental impact assessment and optimal design, particularly designing the location of turbines and sluice gates, and development of such projects. In this study, the impact of various operational procedures of the Swansea Bay lagoon (SBL) on regional water exchange and renewal capacity was investigated. The numerical model TELEMAC-2D was refined to simulate the operation of SBL, with an examination of water exchange processes through the modelling of changes in a tracer within a control domain with different operational procedures. The findings indicate that the unidirectional generation (one-way generation) displayed a greater ability to renew water compared to bidirectional generation (two-way generation) while bi-directional generation is considered more favourable in terms of other environmental impacts. The incorporation of a pumping function within the same operational framework had only a minimal effect on improving the water exchange.

## 1. Introduction

The functioning of a Tidal Range System (TRS) involves the containment of a significant amount of water, resulting in a difference in water level across the impoundment wall. This potential energy, resulting from the head difference, is then converted into kinetic energy through the use of turbines. The physical effects of a tidal lagoon on tidal levels, currents, water exchange, and the transport of solutes and sediment can have a notable impact on water quality, particularly within the enclosed region of aTRS. In order to reduce adverse environmental and ecological impacts, it is imperative to thoroughly understand the hydro-environmental consequences of the proposed lagoon site and address any anticipated concerns.

The design of a tidal lagoon can be tailored to operation in different modes, taking into account regional tidal characteristics, environmental considerations, the capacity to connect to the national power grid, and cost constraints. An ideal operational scheme should strike a balance between electricity generation and environmental impacts, finding a compromise that allows for sustainable energy production without compromising the integrity of the ecosystem. Previous studies on operational schemes have primarily focused on power output, with limited attention given to the hydrodynamic effects and environmental assessments at a broader level. This research aims to investigate the cumulative environmental impacts of various operational procedures for a lagoon by calculating the rate of tracer exchange under different conditions, thus providing a more comprehensive understanding of water renewal processes.

## 2. Methodology

Swansea Bay Lagoon is an extensively researched tidal lagoon situated on the South Wales coast within the Bristol Channel. The proposed project by Tidal Lagoon Swansea Bay (TLSB) Plc involved an embankment spanning 9.5 km and creating an impounded area of 11.5 km$^2$. Despite the termination of this proposal, it remains a valuable source for benchmarking purposes due to its comprehensive research and potential for investigating water exchange rates.

A depth-averaged hydrodynamic model, specifically TELEMAC-2D, has been employed to simulate the functioning of SBL. Various operational procedures, comprising one-way generation and two-way generation, have been implemented on SBL scenarios, with and without the inclusion of pumping functions (Guo et al., 2020).

In order to assess the impact of a tidal lagoons operation on the duration that takes for water inside the impoundment to be renewed, a non-buoyant, mass-conservative tracer concentration was released and monitored within a control area encompassing the tidal lagoon (Guillou et al., 2020). A residual tracer function was employed to represent the remaining tracer within the investigated domain, as outlined below:

$$r(t) = \frac{\int_{\Omega} h(x,y,t) \cdot T(x,y,t) d\Omega}{\int_{\Omega} h(x,y,t_0) \cdot T(x,y,t_0) d\Omega}, \qquad [1]$$

where $x$, $y$ are the spatial coordinates; $t_0$ is the initial time of tracer releasing; $h$ is the water depth and $T$ is the tracer concentration. In this particular study, the tracer substance was initially introduced into the SBL domain at low-water level for spring tide, and subsequently observed over a period of time to ascertain the variations in its concentration over time.

## 3. Results

The concentration of the tracer in the lagoon impoundment area was monitored continuously over a period of time, as illustrated in Fig. 1. This analysis provided valuable insights into the flushing characteristics of the tracer within the lagoon under different operational procedures. The findings revealed that the tracer concentration decreased at a faster rate during ebb-only generation in comparison to two-way operation. After approximately 3-4 tidal cycles, the tracer concentration reached only 10% of its initial value. This can be attributed to the significant volume of water exchange that takes place during ebb-only generation, as well as the subsequent flooding filling stage. In contrast, during two-way operation, the tracer concentration initially experienced a noticeable decline, followed by a gradual decrease over time. It took more than 11 days for the tracer concentration to reach 10% of its initial value. However, the residual value of the tracer remained relatively stable over a longer period and decreased gradually as it approached zero.

Both operational procedures demonstrated improved tidal flushing when pumping was incorporated. However, it is worth noting that two-way generation, with its bidirectional nature, has a particularly influential impact on the flushing characteristics. This might be because the introduction of pumping with two-way generation enables a greater exchange of water within the basin, not only during ebb tides but also during flood tides. Nevertheless, the long-term impact of the pumping mechanism on enhancing water circulation within the identical operational structure was found to be minimal.

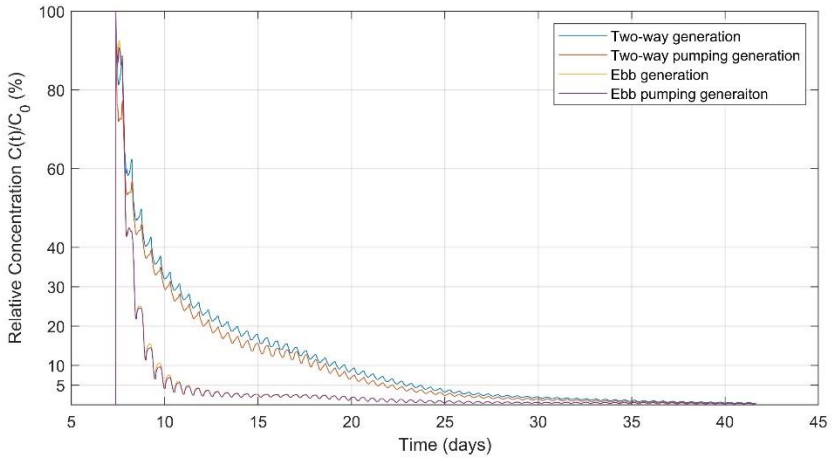



**Fig. 1.** Concentration variations of tracer released in SBL basin with different operation schemes.

**References**

Guo B, Ahmadian R, Falconer RA (2021) Refined hydro-environmental modelling for tidal energy generation: West Somerset Lagoon case study, Renewable Energy, 179, 2104-23.

Guillou N, Thiébot J, Chapalain G (2019) Turbines' effects on water renewal within a marine tidal stream energy site, Energy, 189, 116113.

# Machine Learning Analysis of Elemental Variation in Sediment Cores of the Boka Kotorska Bay – Adriatic Sea

Vaso MANOJLOVIĆ[1], Milena RADOMIROVIĆ[1], Bojan TANASKOVSKI[2], Chiara CANTALUPPI[3], Sandro DEGETTO[3], Slavka STANKOVIĆ[1]

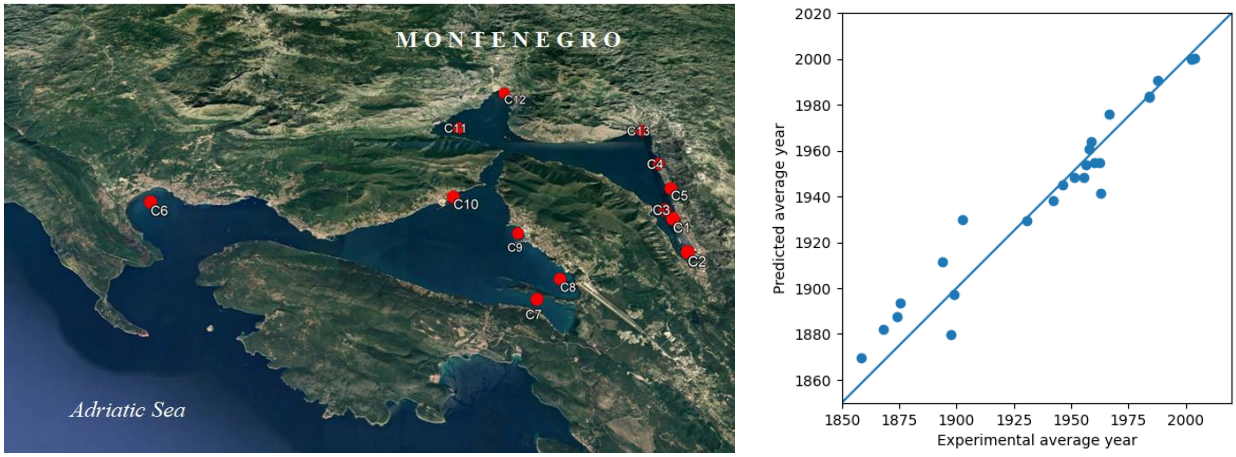
[1] University of Belgrade, Faculty of Technology and Metallurgy, Serbia
v.manojlovic@tmf.bg.ac.rs; mradomirovic@tmf.bg.ac.rs; slavka@tmf.bg.ac.rs
[2] Military Technical Institute, Serbia,bojantanaskovski@yahoo.com
[3] Italian National Research Council, Italy, chiara.cantaluppi@cnr.it; sandro.degetto@alice.it

ABSTRACT

Marine sediments represent a crucial component of coastal ecosystems and serve as indicators of environmental change (Richir et al., 2021). Reflexive human-environmental interactions have intervened and deteriorated pristine nature of sediments, particularly during the 20$^{th}$ century. Through the analysis of sediment cores with the application of statistical and numerical model simulations, it is possible to ascertain the occurrence and magnitude of events caused by anthropogenic factors. Trace element contamination, which is directly related to numerous human activities and perturbations, has been a serious environmental issue in coastal areas, as well as, in river basins, since the 1980s (Dendievel et al., 2020; Mikac et al., 2022). Demography, urban development, regional economy and global production have greatly contributed to the ongoing changes that have led to the deterioration of the aquatic-sediment system, which implies a significant impact on ecosystem functioning, potentially affecting human health (Tanaskovski et al., 2016; Perošević et al., 2018; Radomirović et al., 2021). Information regarding the trajectories and source area of elements and their anthropogenic inputs within the ecosystem cannot be deduced without determining the mineral composition, origin and properties that affect the complex biogeochemical and sedimentological composition of bottom marine sediments (Spagnoli et al., 2021; Mikac et al., 2022).

The Boka Kotorska Bay is situated on the eastern coast of the southern Adriatic in Montenegro. The geology of the catchment area of the Bay (Dolenc et al., 1998; Rivaro et al., 2004) with river inflows (Rivaro et al., 2011) has a significant influence on most elements in the coastal region of the southeastern Adriatic. This paper presents data obtained by the analysis of 13 sediment cores (C1-C13) collected from the coastal areas of the Bay in 2005 (C1-C5) and 2007 (C6-C13) (Fig. 1a) using a core sampler with an inner diameter of 8.2 cm. After sampling, the cores were carefully sliced in 9 to 15 sections, with a total of 181 sections obtained from all core samples. Here, we proposed the integration of a predictive machine learning approach to investigate depositional changes in down-core chemistry and elemental variations in undated sediment cores in the Boka Kotorska Bay. Using the energy dispersive X-ray fluorescence spectroscopy (ED-XRF), major (Al, Ca, Cl, Fe, K, Mg, Mn, Na, P, S), minor and trace elements (As, Ba, Br, Cd, Ce, Cr, Cs, Cu, Ga, Hg, I, La, Nb, Nd, Ni, Pb, Rb, Sb, Sn, Sr, Th, U, V, Y, Zn, Zr) were quantified. High-resolution gamma-ray spectrometry was used for the determination of activity concentrations of radionuclides ($^{137}$Cs, $^{210}$Pb). Concentration profiles of the analyzed elements in sediment cores demonstrated their temporal distribution pattern at different section depths. Covering various aspects relevant to analysis of geochemical data, the predictive modeling performance included an experimental dataset composed of the following variables: sampling dates and locations with corresponding coordinates, average section depths of analyzed sediment cores, average section ages of dated cores, and elemental content of each layer of the analyzed sediment cores. The Extra Trees (Extremely Randomized Trees) Regression method was employed in this research to predict the average age of sections in undated sediment cores based on the different elemental distribution ((major (>1 wt. %), minor (1-0.1 wt. %) and trace (0.1 wt. %)) and other related features used for predictive modeling. Using the results

of $^{137}Cs$ and $^{210}Pb$ dating, elemental composition of sedimentary layers, and machine learning model predictions, an approximate 95-year record of element deposition in sediment cores was determined. Therefore, the proposed methodology demonstrated the utility of machine learning for the interpretation of geochemical data.




a) b)

**Fig. 1**. a) Sampling sites in the Boka Kotorska Bay, Adriatic Sea; b) The relationship between the experimentally obtained values (outputs) and calculated parameters using the obtained model (target)

The analysis results in Fig. 1b showed the simultaneous relative importance of each of the inputs to the model results ($R^2$ on the test set was 0.93, and the mean absolute error in year units was 8.11), demonstrating the model's excellent predictive ability. An integrated approach and comprehensive analysis examined the geochemical record and ages of sediment cores from the different parts of the Bay, increasing the knowledge of geochemical processes in sedimentary system over the last 100 years. The findings of this work will provide a useful basis for our future research that will address the determination of local background concentrations from uncontaminated core layers, as well as the chronological accumulation and deposition of metals in the sediments of the Boka Kotorska Bay.

**Acknowledgements**

This work was supported by the Ministry of Education, Science and Technological Development of the Republic of Serbia (Contract No. 451-03-47/2023-01/200287)

**References**

Dendievel AM, Mourier B, Dabrin A, Delile H, Coynel A, Gosset A, … Bedell JP (2020) Metal pollution trajectories and mixture risk assessed by combining dated cores and subsurface sediments along a major European river (Rhône River, France), Environment International, 144, 106032.

Dolenc T, Faganeli J, Pirc S (1998) Major, minor and trace elements in surficial sediments from the open Adriatic Sea: a regional study, Geologia Croatica, 51(1), 59–73.

Mikac N, Sondi I, Vdović N, Pikelj K, Ivanić M, Luči M, Bačić N, Furdek Turk M, Škapin DS, Krivokapić S (2023) Origin and history of trace elements accumulation in recent Mediterranean sediments under heavy human impact, A case study of the Boka Kotorska Bay (Southeast Adriatic Sea), Marine Pollution Bulletin, 179, 113702.

Perošević A, Pezo L, Joksimović D, Đurović D, Milašević I, Radomirović M, Stanković S (2018) The impacts of seawater physicochemical parameters and sediment metal contents on trace metal concentrations in mussels—a chemometric approach, Environmental Science and Pollution Research, 25, 28248–28263.

Radomirović M, Tanaskovski B, Pezo L, Ceccotto F, Cantaluppi C, Onjia A, Stanković S (2021) Spatial and temporal distribution of pollution indices in marine surface sediments—A chemometric approach, Environmental Science and Pollution Research, 28(31), 42496–42515.

Richir J, Bray S, McAleese T, Watson GJ (2021) Three decades of trace element sediment contamination: The mining of governmental databases and the need to address hidden sources for clean and healthy seas, Environment International, 149, 106362.

Rivaro P, Ianni C, Massolo S, Ruggieri N, Frache R (2004) Heavy metals in Albanian coastal sediments, Toxicological & Environmental Chemistry, 86(2), 85–97.

Rivaro P, Çullaj A, Frache R, Lagomarsino C, Massolo S, De Mattia MC, Ungaro N (2011) Heavy metals distribution in suspended particulate matter and sediment collected from Vlora bay (Albania): A methodological approach for metal pollution evaluation, Journal of Coastal Research, 270, 54–66.

Spagnoli F, De Marco R, Dinelli E, Frapiccini E, Frontalini F, Giordano P (2021) Sources and metal pollution of sediments from a coastal area of the central western Adriatic Sea (Southern Marche Region, Italy), Applied Sciences, 11(3), 1118.

Tanaskovski B, Jović M, Miličić Lj, Pezo L, Mandić M, Stanković S (2016) The geochemistry model of the surface sediment determined by using ED-XRF technique: a case study of the Boka Kotorska bay, Adriatic Sea, Environmental Science and Pollution Research, 23, 11777–11789.

# Innovative Nature-Based Solutions for Coastal Resilience

Raylton BENDÔ[1], Bárbara Proença[1], Andreia GOMES[1], Ivana BOSNIC[1]; Lénia RATO[1]; Diogo MENDES[2], Diogo FONSECA[1],

[1]HAEDES Portugal, Portugal
raylton.bendo@haedes.eu; barbara.proenca@haedes.eu; andreia.gomes@haedes.eu; ivana.bosnic@haedes.eu; lenia.rato@haedes.eu; diogo.fonseca@haedes.eu
[2] CERIS, Instituto Superior Técnico, Portugal
diogo.silva.mendes@tecnico.ulisboa.pt

ABSTRACT

This work aims to address the feasibility of using nature-based solutions (NBS) by taking advantage of systems of biological organisms integrated in coastal activities to simultaneously promote coastal resilience. Precisely, the solution here presented consists in combining offshore seaweed aquaculture with wave attenuation purposes (AQUABREAK). Several studies on similar solutions have addressed the effectiveness of submerged canopies in reducing wave energy. However, the feasibility of such implementations under storm conditions remains uncertain.

With this study we aim at bridging the gap between the use of submerged canopies and coastal resilience by assessing the performance of a floating seaweed field exposed to high energy conditions. This assessment is accomplished through physical and numerical modelling.

The findings support inferences on relevant design considerations and parameters for adapting NBSs to specific local needs and enable the evaluation of the effectiveness of such systems for coastal resilience.

## 1. Introduction

Coastal protection measures against natural hazards are usually achieved through seawalls and breakwaters, which are rigid structures that require ongoing and expensive maintenance. In addition, these have high initial costs that do not always represent an effective measure, such as the case in Furadouro (Ovar) (Tavares et al. 2021).

Several studies have previously addressed the effectiveness of submerged aquatic canopies in mitigating wave energy. For instance, Mork (1996) documented a wave energy reduction ranging from 70% to 85% across 258-meter-long kelp natural kelp forests. Thus, a seaweed aquaculture field appears as a viable alternative or complement to coastal protection, both in economic and ecological perspectives. However, the documented wave conditions under testing do not allow to understand the effectiveness of such biologically based floating structures to apply them as coastal resilience solutions. Here we aim to discuss this subject and contribute to filling this apparent research gap.

## 2. Methods

This study involved assessing the accuracy of a numerical model in simulating wave dissipation caused by suspended seaweed. The SWASH model was employed to emulate and replicate an experiment conducted in a wave flume to assess the wave reduction capacity of a suspended algae field (Miranda et al., 2024). With this purpose, a one-dimensional wave propagation model was executed in order to replicate the progression of the wave height along the flume. The non-hydrostatic SWASH model, that solves the nonlinear shallow water equation, was used to propagate irregular waves considering their interaction with the floating seaweed patch to simulate the transmission and attenuation of the wave energy. The geometry of the mimicked algae field considered by SWASH is represented by the following parameters: element height ($hv$ = 0.075 m), element equivalent diameter ($dv$ = 0.007 m), and density ($Nv$ = 1600 stems/m$^2$) of the canopy field. The drag coefficient

($C_d$), a numerical input parameter, was calibrated by comparing the numerical results of the wave decay with the physical experiments using a statistical method.

In the numerical model, a 34.0 m long flume was considered, including a 4.0 m sponge layer at the opposite side of the incoming wave generation. A wavemaker boundary was defined in accordance with the target wave conditions varying between 0.04 m and 0.14 m for Hm0 and 1.3 s and 2.6 for peak period. The time step was automatically adjusted according to a Courant number ranging between 0.6 and 0.2. All cases were simulated during 5 min, where only the last 4 min were considered valid for post-processing.

## 3. Results

The evolution of the wave height along the flume is illustrated in **Fig. 1**. The results suggest a good capacity of the numerical model to reproduce the wave propagation and dissipation along the wave flume. Furthermore, the statistical metrics show small errors and a strong correlation coefficient. Namely, the Root Mean Square Percentage Error (RMSPE) is approximately 3.97%, the relative Bias is 0.023, and the correlation coefficient is close to 1. These results indicate that the model can accurately reproduce the wave attenuation phenomenon and that the considered seaweed field is effective in reducing wave heights for 14 simulated conditions.

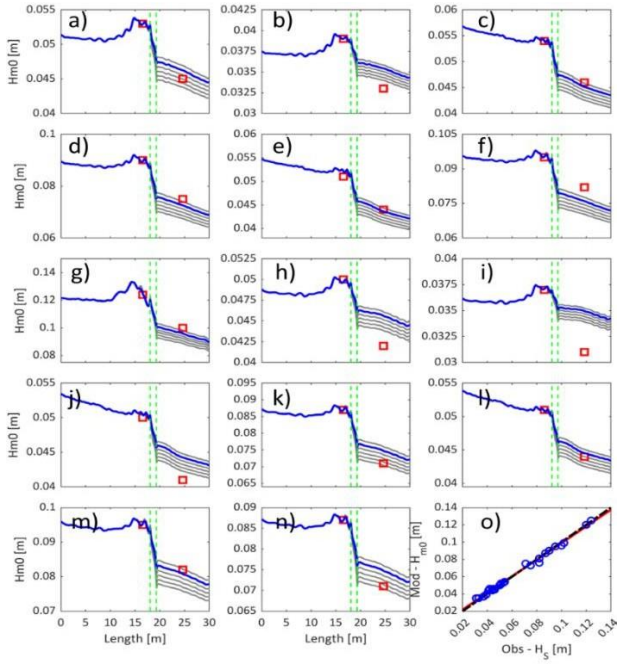



**Fig 1**. (a-n) Comparison between measured (red square) and modelled (continuous line) wave heights ($H_{m0}$), where the offshore wave height $H_0$ was propagated across the flume, including the leading edge of the AQUABREAK, is illustrated for the grey lines for the various Cd combinations. Note that the blue line represents Cd = 1.2, and the green lines signify the presence of AQUABREAK (length = 1.25 m) in the flume; (o) correlation between the modelled (Hm0) and measured significant wave height (Hs).

## 4. Conclusions

NBSs represent innovative approaches to coastal protection using submerged canopies. This study showed that for 14 conditions a seaweed field can be effective in inducing wave attenuation. These results are relevant to support the design features such as the field length and its relative positioning to the coast. These parameters are essential for an optimized wave energy dissipation system and consequent coastal inundation reduction in coastal implementations. In addition, NBSs represent a step toward achieving the EU's $CO_2$ emissions targets.

**Aknowledgements**

This work was performed in the scope of the AQUABREAK - Aquaculture Living Breakwater for Coastal Protection and Sea Decarbonization project, Grant code PT-INNOVATION-0093, funded by the "Blue Growth" Program of the EEA Grants Portugal 2014-2021.

**References**

Miranda, F., Proença, B., Fonseca, D., Haerens, P., Bento, A.M., Siriwardane, S., Pavlou, D., Rosa Santos, P., Taveira Pinto, F. and Fazeres Ferradosa, T. (2024). AquaBreak Project: A Nature-Based Solution Towards Food Demand and Coastal Protection. In Analytical and Experimental Methods in Mechanical and Civil Engineering. DOI: 10.1007/978-3-031-49723-0_7

Mork, M. (1996). The effect of kelp in wave damping. Sarsia, 80(4), 323–327. https://doi.org/10.1080/00364827.1996.10413607

Tavares, A. O., Barros, J. L., Freire, P., Santos, P. P., Perdiz, L. and Fortunato A. B. (2021) A coastal flooding database from 1980 to 2018 for the continental Portuguese coastal zone. Applied Geography, 135, 102534

# Distributions and migrations of heavy metals at the water-sediment interface in the coastal area of the Yangtze River Estuary, China

Zhirui ZHANG[a], Shuguang LIU[a,b], Sha LOU[a,b,*], Guihui ZHONG[a,b], Xiaosheng ZHOU[a], Feng ZHOU[a], Larisa Dorzhievna RADNAEVA[c], Elena NIKITINA[c], Irina Viktorovna FEDOROVA[d]

a Department of Hydraulic Engineering, Tongji University, Shanghai, 200092, China

b Key Laboratory of Yangtze River Water Environment, Ministry of Education, Tongji University, Shanghai, 200092, China

c Laboratory of Chemistry of Natural Systems, Baikal Institute of Nature Management of Siberian branch of the Russian Academy of Sciences, Republic of Buryatia, Russian, Republic of Buryatia

d Institute of Earth Sciences, Saint Petersburg State University, 199034, 7-9 Universitetskaya Embankment, St Petersburg, Russia

* Corresponding author, lousha@tongji.edu.cn

ABSTRACT

The presence of heavy metal pollution in estuaries poses a potential risk to both the water environment and public health. Hydrodynamics at the estuary junction facilitate material exchange and energy transmission within the estuarine system. However, the complexity of estuarine water environments hinders a comprehensive understanding of pollution dynamics in these systems. To this end, field investigations were conducted in September 2022 within the coastal area of the Yangtze River Estuary (YRE). Cd was observed to remain a major contributor to potential ecological risk. As a further step to characterize the water-sediment partitioning of heavy metals in the coastal area of the YRE, indoor water environment column experiments were carried out to elucidate the vertical distribution pattern of heavy metals and the exchange process at the water-sediment interface under hydrodynamics. Based on the actual field survey, the vertical migration of Cd was observed, with horizontally oriented circulation hydrodynamics set up orthogonally. Heavy metal concentrations were collected to determine their vertical gradient distribution over a period of 15 consecutive days. The experimental results were subjected to kinetic and thermodynamic analyses: the kinetic analyses were fitted based on two-constant rate model, Elovich model, the pseudo-first-order kinetic model and the pseudo-second-order kinetic model, which reproduced the interfacial desorption process and proposed a hysteresis mechanism under the influence of hydrodynamic forces. The thermodynamic analysis involved isothermal adsorption fitting at the solid-liquid interface, utilizing data from the steady state of heavy metal distribution during the later observation period, and the variation parameter under hydrodynamic influence were obtained. Finally, the fitted offset after applying hydrodynamic force was modified based on the relative shear flow velocity in the surface sediment. Results in this paper can provide effective information for heavy metal interfacial exchange studies and references for one-dimensional pollutant migration studies.

## 1. Field investigations

Field investigation was carried out at seven sampling points in the Yangtze River estuary in September 2022. Surface sediment samples and water samples were collected respectively. The Geo-accumulation index ($I_{geo}$)and Potential ecological risk index($RI$) of heavy metals investigated were shown in Fig. 1.

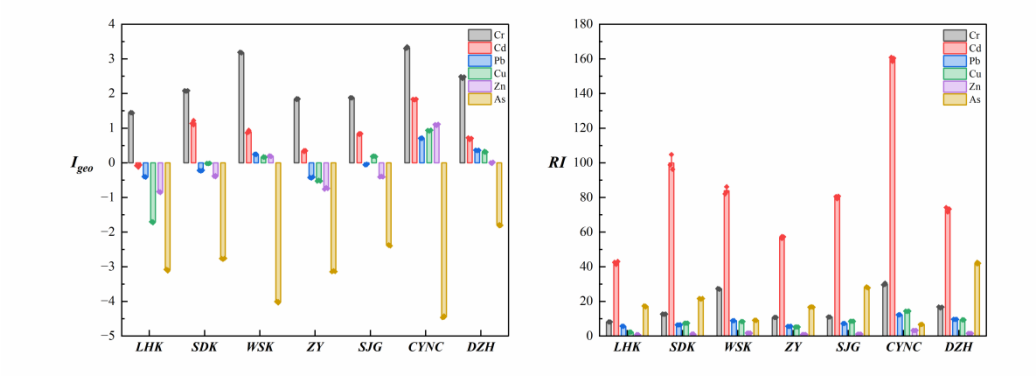



**Fig. 1.** Potential ecological risk index(*RI*) and Geo-accumulation index ($I_{geo}$) of heavy metals in sediments.

## 2. Water environment column experiments

Soil column experiments were conducted at hydrodynamic Laboratory of Tongji University, China. A self-designed soil column device (Fig. 2.) was adopted in the experiments. The soil column was made of acrylic, with the height of 90cm and inner diameter of 8cm. 6 sampling points (S1-S8) were set with the interval of 10cm. The soil column was filled with 30cm fine-grained cohesive sediment (background concentration of Cd: 0.05 μg/L) collected from field investigation in the Yangtze Estuary wetland. Relevant experimental conclusions and analysis results were shown in Fig. 3, 4.

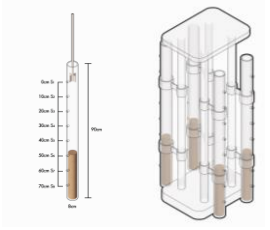


**Fig. 2.** Schematic diagram of hydrodynamic application and schematic of soil column experiments.

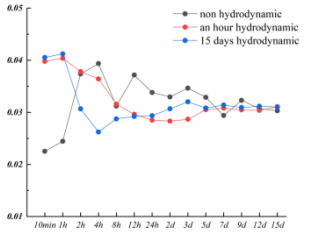



**Fig. 3.** Temporal variation of desorption rate of surface sediments in column experiment.

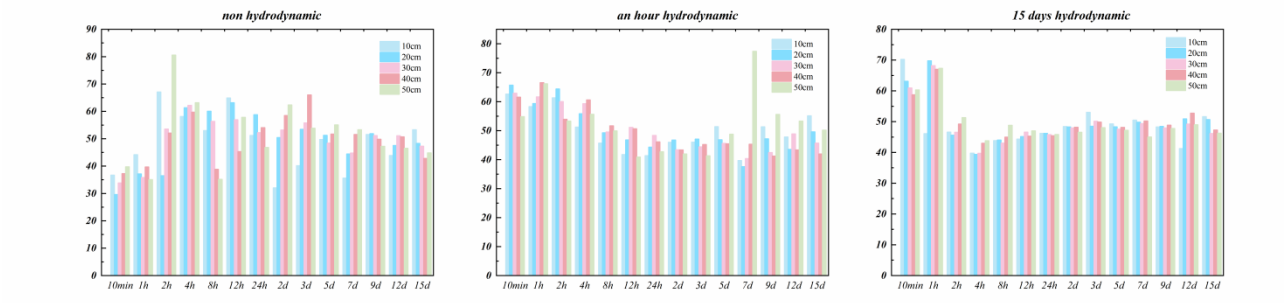



**Fig. 4.** Vertical gradient change of Cd desorption.

**Acknowledgements**

This study was funded by the National Natural Science Foundation of China (42072281, 41602244), Shanghai Science and Technology Innovation Projects (22230712900, 22ZR1464200, 20230742500), Top Discipline Plan of Shanghai Universities-Class I (2022-3-YB-03), and Interdisciplinary Project in Ocean Research of Tongji University (2022-2-YB-01).

**References**

Zhirui Zhang, Sha Lou, Shuguang Liu, Larisa Dorzhievna Radnaeva & Elena Nikitina. (2022). Exchange of Heavy Metal (Cd) at the Sediment-water Interface Affected By Salinity, pH, and Hydrodynamic Based on One-dimensional Soil Column Experiments. (Eds.). The 32nd International Ocean and Polar Engineering Conference.

# Numerical simulation of combined coastal inundation due to fluvial flood, storm surge and wave induced set-up/runup

Achilleas G. SAMARAS[1], Theophanis V. KARAMBAS[2]

[1] Department of Civil Engineering, Democritus University of Thrace, PC 67100, Xanthi, Greece
achsamar@civil.duth.gr

[2] Department of Civil Engineering, Aristotle University of Thessaloniki, PC 54124, Thessaloniki, Greece
karambas@civil.auth.gr

ABSTRACT

In the present work, the numerical simulation of coastal flooding is investigated considering the synergy of fluvial flooding, storm surge and wave induced setup/runup. Two approaches are developed: the first one is based on a linear wave propagation model and a breaking wave induced circulation and setup (based on the Shallow Water Equations), while the second one is based on a higher order Boussinesq-type intra-period nonlinear dispersive wave model which describes the propagation of breaking waves in the surf and swash zone. In order to simulate the wetting-drying process during inundation the dry bed boundary condition (in the two horizontal dimensions) is applied in both SWE and Boussinesq model. The first approach results to the estimation of coastal inundation due to breaking wave setup while the second one to nonlinear wave runup (also including wave setup). In both approaches fluvial flow is also described (applying the "dry bed" boundary condition), resulting in the compound coastal flooding due to synergy of river flow (and overflow), storm surge and wave setup/runup.

This work in considered as the first authors' step in understanding the hydrodynamics of such areas, which is critical for future research on the simulation of coastal morphodynamics under pressures from both the terrestrial and the coastal fields.

## 1. Modelling approach

### *1.1. Linear wave model*

Wave transformation in the nearshore, including the compound wave field near coastal structures, can be simulated satisfactorily by a model based on the hyperbolic-type mild slope equation. Such a model is described in detail by Karambas and Samaras (2017). Breaking wave induced nearshore currents and setup are simulated by solving the depth and shortwave-averaged 2D continuity and momentum equations. Both models are extended in the swash zone according to Karambas and Samaras (2017). Coastal flooding is simulated using the "dry bed" boundary condition according to Militello et al. (2004).

### *1.2. Nonlinear wave model*

An advanced model based on the numerical solution of the higher-order Boussinesq-type equations is used to simulate the propagation of non-breaking and breaking waves, according to Samaras and Karambas (2021). The above mentioned "dry bed" boundary condition, is also applied to simulate wave runup, while it is noted that wave-induced setup is automatically simulated in this type of models.

### *1.3. Storm surge and fluvial flow*

Coastal flooding due storm surge is also simulated by the "dry bed" boundary condition. In both approaches fluvial flow is also described, applying the same boundary condition, resulting in the compound coastal flooding due to synergy of river flow (and overflow), storm surge and wave setup/runup.

## 2. Models Applications

Both the linear and nonlinear wave models described in the previous are applied to predict compound coastal flooding in a beach at a coast in Chalki Island (Greece), with the nonlinear (Boussinesq) model predicting a larger inundation area overall. The latter is expected since simulating wave runup, as done in nonlinear models, results in higher inundation than wave setup which is simulated in linear wave models (which is an important limitation). Figure 1 shows indicative results of the nonlinear wave model (Boussinesq model) due to the synergy of wave setup/runup and river flow/overflow (wave height= 1 m, period= 6 s, river velocity =1 m/s). The incorporation of swash zone hydrodynamics and fluvial flooding is the main advantage of the present approach over the existing ones which are based on linear wave model and a wave induced setup model. Unfortunately no data for the combined wave runup and river flooding hydrodynamics are available.

## 3. Conclusions

A higher order intra-period nonlinear dispersive wave model which describes the propagation of breaking waves in the surf and swash zone.and a linear wave propagation model in combination with a wave induced circulation and setup model can provide useful insights for the simulation of compound flooding in coastal zones comprising highly dynamic areas like river estuaries and natural streams' outlets.

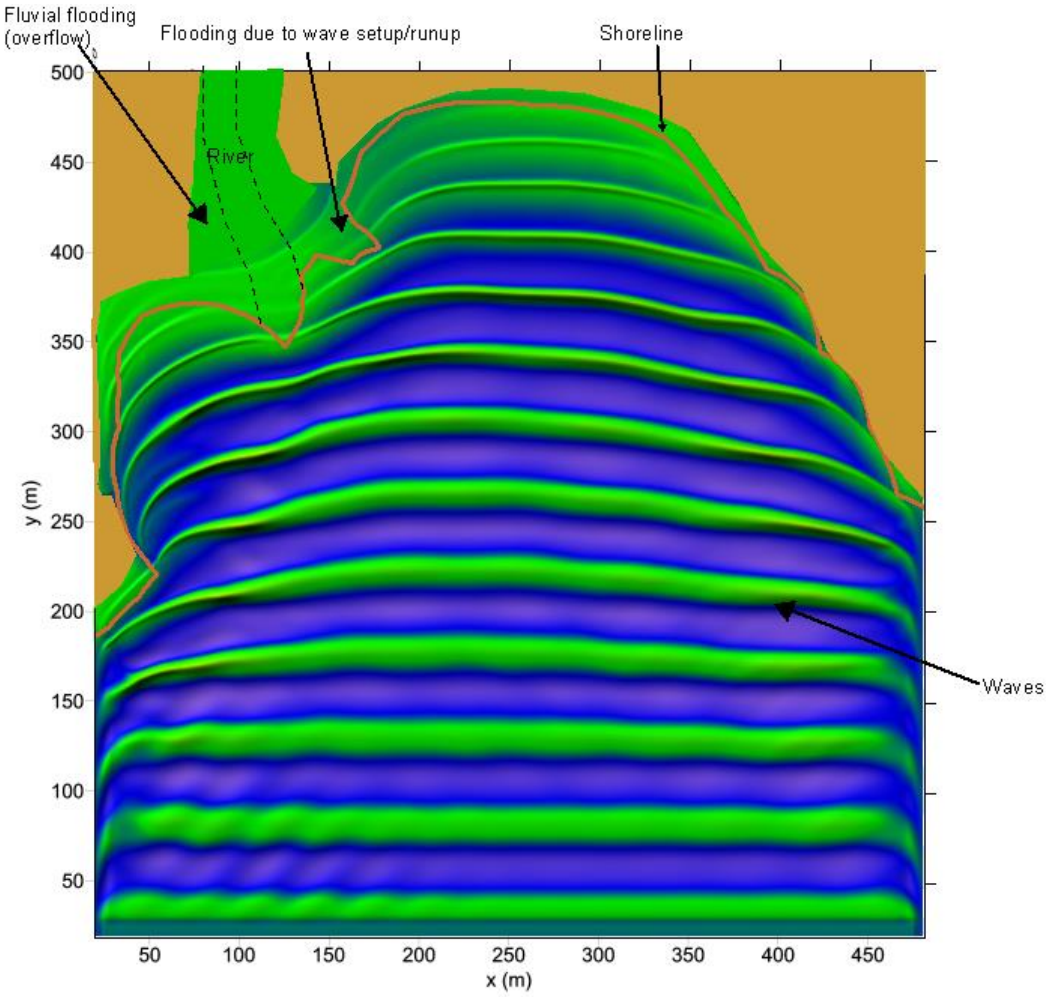



**Fig. 1**. Wave propagation and coastal inundation due to the synergy of wave setup/runup and fluvial flow (nonlinear wave model results). Green colour depicts water level above Mean Water Level.

**References**

Karambas TV, Samaras AG (2017) An integrated numerical model for the design of coastal protection structures, Journal of Marine Science and Engineering 5, 50.

Militello A, Reed CW, Zundel AK, Kraus NC (2004) Two-dimensional depth-averaged circulation model M2D: version 2.0, USACE ERDC Report 1, Technical Documentation and User's Guide, Washington, DC, USA, 134 pp.

Samaras AG, Karambas TV (2021) Modelling the impact of climate change on coastal flooding: Implications for coastal structures design, Journal of Marine Science and Engineering 9, 1008.

# Monitoring Ocean Currents with High-Frequency Radars along the Portuguese Coast: Overview and Challenges

Vânia LIMA[1], Luísa LAMAS[1]

[1] Instituto Hidrográfico, Portugal
vania.lima@hidrografico.pt

luisa.lamas@hidrografico.pt

ABSTRACT

Like many coastal areas worldwide, the Portuguese coastlines are exposed to several challenges such as climate change, sea-level rise, natural hazards, including coastal erosion, storm surges, tsunamis, and maritime and pollution accidents. In that sense, high frequency (HF) radars are extensively employed worldwide for coastal monitoring and measurement of ocean surface currents, waves, and wind. In line with its mission of assuring the permanent monitoring of the Portuguese coastal areas, aiming at a better knowledge of the marine environment and characterization of the coastal currents and wave measurements, the Portuguese Hydrographic Institute started operating the first high-frequency radar stations in 2008.

In this work, we present a review of the lifespan of the Portuguese HF radar network operation, observing and monitoring regional capabilities in the Portuguese coastal areas. We also use in-situ data sets collected during project campaigns, which complement the existing measurements near the coast, making them excellent HFR observation validation sources.

## 1. Introduction and Framework

High frequency (HF) surface wave radar systems are remote sensing detection systems, with extensive application worldwide, which are used to measure ocean surface currents, waves, and wind. Operating in frequencies between 3 and 30 MHz and wavelengths between 10 and 100 m, these systems use electromagnetic waves in the radio waveband, measuring offshore distances of 100 to 200 km, with relatively high spatial (between 1 and 6 km) and temporal resolutions (minimum hourly). The measurement precision of the currents' velocities is around 10 cm/s and 5° in the current direction. Thus, the main product derived from the HF radars is continuous ocean surface currents maps, which is the fundamental purpose and application of most HFR systems.

The present Portuguese national HF radar network comprises 6 CODAR SeaSonde HF radar sites, all managed by the Hydrographic Institute. The HF stations are strategically located along the extensive 940 km of the continental coastline, and include (1) Leça da Palmeira, the northernmost site, (2) São Julião and (3) Cabo Espichel, which cover the Lisbon area, and (4) Sagres, (5) Alfanzina, and (6) Vila Real de Santo António, collectively covering the entire Algarve coastline (Figure 1a). These HF radar stations collect near real-time current, wave and wind data, and Alfanzina is also equipped with a Tsunami detection module.

Currently, the ocean current data from the Portuguese National HF radar network is made continuously available through several services and aggregators. To ensure data accuracy and reliability, the validation of the HF radar data is essential, for which the comparison between HF radar data and in situ measurements, such as drifters and buoys, is crucial. Both methods provide ground truth measurements of ocean surface currents and can be deployed over extended periods of time, complementing the HF radar coverage limitations.

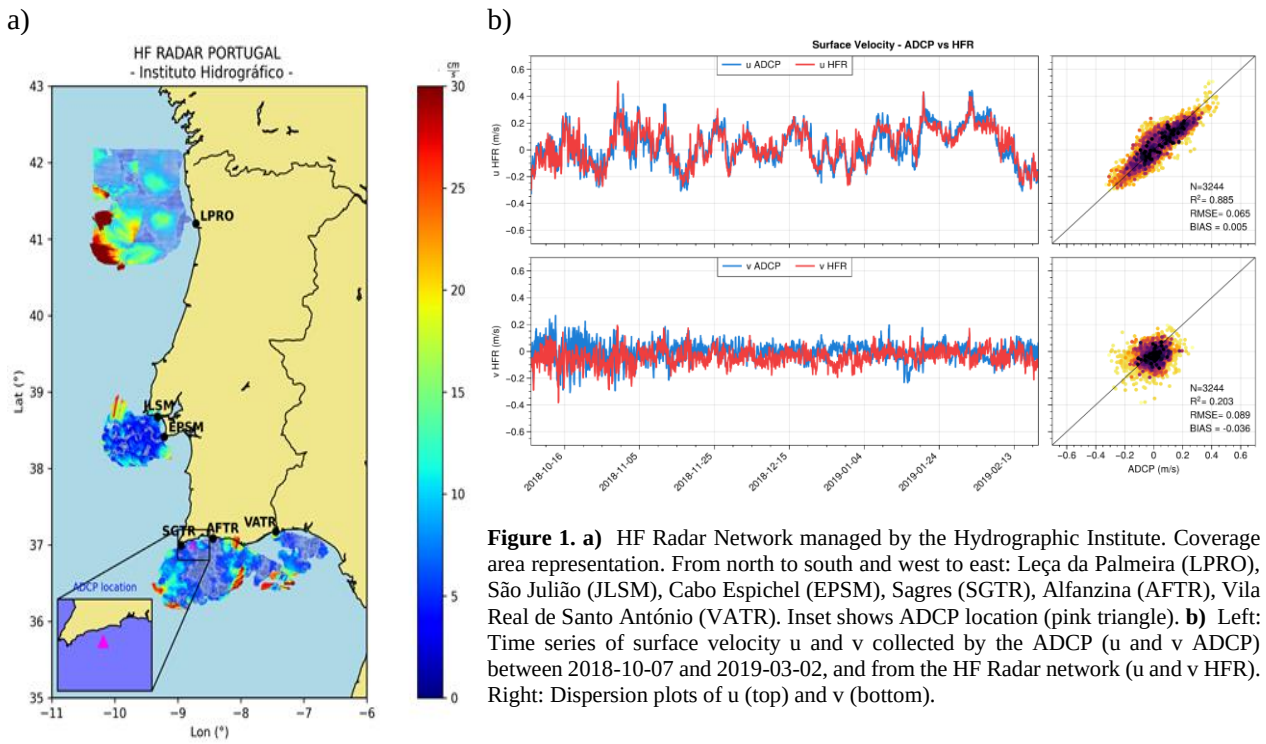



**Figure 1. a)** HF Radar Network managed by the Hydrographic Institute. Coverage area representation. From north to south and west to east: Leça da Palmeira (LPRO), São Julião (JLSM), Cabo Espichel (EPSM), Sagres (SGTR), Alfanzina (AFTR), Vila Real de Santo António (VATR). Inset shows ADCP location (pink triangle). **b)** Left: Time series of surface velocity u and v collected by the ADCP (u and v ADCP) between 2018-10-07 and 2019-03-02, and from the HF Radar network (u and v HFR). Right: Dispersion plots of u (top) and v (bottom).

## Main Results and Conclusions

We carried out a set of measurement comparisons between in-situ instrumentation and HF radars to observe the performance of the HF radar network, proposing improvements based on the presented study.

Comparisons between HFR and ADCP data (Figure 1b) show good agreement for the East-West (u) component of the surface velocity. However, for the North-South (v) component, the HFR does not compare well with the ADCP data: even though the magnitude is similar, the correlation is weak, with an $R^2$ near 0.2. Considering the ADCP location, which is near the coast and close to the HFR baseline, and that the coast is oriented zonally (East-West) might explain the differences between both components, since cross-shore velocities (in this case North-South) tend to be weaker near the coast.

The HF radar observation network contributes to the Portuguese EEZ real-time monitoring and operational forecasting integrated system, MONIZEE (Martins et al., 2010), consisting of a time series spanning over a decade of observed data. Future developments involve the improvement of retrieval algorithms and the installation of new antennas along the Portuguese mainland.

The data provided by the HF radar network, encompassing currents, waves, and wind, is crucial not only for ensuring the effectiveness and safety of maritime operations—such as search and rescue missions and the response to marine pollution incidents—but also for enhancing our understanding of oceanic conditions in coastal regions.

**Acknowledgements**

Vânia Lima is supported by the EU-funded project Blue-Cloud 2026, project number 101094227, and collaborates with JERICO-RI, which has received funding from the European Commission's Horizon 2020 Research and Innovation programme under grant agreements No 871153 and 951799 (projects JERICO-S3 and JERICO-DS, respectively). Luísa Lamas collaborates with project Blue-Cloud 2026.

**References**

Crombie, D. D. (1955). Doppler spectrum of sea echo at 13.56 Mc./s. Nature, 175(4459), 681-682.
Martins, I., Vitorino, J., & Almeida, S. (2010). The Nazaré Canyon observatory (W Portugal) real-time monitoring of a large submarine canyon. In OCEANS'10 IEEE SYDNEY (pp. 1-7). IEEE.

# Site Investigation for Floating Solar Panels Using Multi-Criteria Decision-Making

Hossein AMINI[1], Jack LEWIS[2], Dawn MORGAN[3], Ian MASTERS[3], Simon NEILL[2], Andrew DIXON[4], Shunqi PAN[1], RezaAHMADIAN[1]

[1] Cardiff University, The United Kingdom
aminih@cardiff.ac.uk

[2] Bangor University, The United Kingdom
[3] Swansea University, The United Kingdom
[4] Welsh Water, The United Kingdom

ABSTRACT

Ground-mounted photovoltaics are established as a form of renewable energy conversion. However, limitations on land coverage hinders their development, particularly in urban environments. As a solution, Floating PhotoVoltaics (FPV) technology has been developed for lakes and marine environments. This design can make a significant contribution to an increase in the rollout of solar panels to reduce emissions and contribute to achieving net zero. In this study, the Welsh coast has been investigated for FPV suitability and aims to aid further future devolvement for policymakers and private investors. The study identified several challenges, such as favorable metrological conditions, depth constraints and proximity to existing infrastructure, that need to be addressed before floating solar panels can be widely deployed. However, this study demonstrates that floating solar panels have the potential to be a valuable part of the energy mix in Wales. In this study, we employed Multi-Criteria Decision Making (MCDM) to optimize site selection of FPV along the Welsh coast. The results illustrate the different factors present across the Welsh coast and identify which areas would be able to combat these conditional variables and be able to be deployed, operated and decommissioned effectively.

## 1. Introduction

Global warming, global environmental degradation, and climate change have caused governments and researchers around the globe to seek out alternative and renewable forms of energy conversion. Traditional energy sources have reduced the cost of power generation as technology has improved but in this trade-off, the environment has been degraded significantly (Ahmadian et al., 2010; Manoj Kumar et al., 2022). One of the key drivers causing environmental degradation is the increase in global energy demand which has historically been powered by fossil fuels. However, as a result of international treaties such as the Paris Accord and geopolitical instability.

Governments have been investigating alternative solutions to transition from traditional fossil fuels towards renewable energy sources (Ahmadian et al., 2010; Xue et al., 2019, 2021). There is a range of renewable energy resources but these are dependent on location and availability, however using a combination of different types of renewable energy technologies can be seen as a key solution to respond to energy demand (Gadzanku et al., 2021; Solomin et al., 2021). The most common method for harvesting solar energy is using photovoltaics (PV), the conversion of light energy into electricity. Commercial land-based PV systems have been in operation since the early 1980s. However, the effectiveness and operability of a large solar farm are highly dependent on climate conditions, PV operating temperature, dust, and other debris, and the impact of shadows, whether full or partial. In addition, in order for a solar power plant to be cost-effective and meet electrical demand a large acreage of land is required, on average, 1MW of solar power requires 2.5 acres of land (World Bank, 2019). In many countries, this land could be used more efficiently for agriculture and other industries. Attention

is now focusing on the development of floating photovoltaic (FPV), making use of lakes, reservoirs, and the open sea to site solar farms to optimize land use.

## 2. Material and methods

### *2.1. Study area*

The Welsh coast has a length of around 1400 km (870 miles) and is characterized by scenic views, towns & cities, places of historical interest, and large protected areas such as Pembrokeshire Coast National Park ,Gower Peninsula Area of Outstanding Natural Beauty, Snowdonia National Park, Anglesey Area of Outstanding Natural Beauty ,Cardigan Bay Special Area of Conservation. The Welsh Coast receives on average between 1000-1200 kWh per M2 of Solar Irradiation, which makes it an ideal location when compared to the majority of the rest of the UK. In addition, the are multiple ports, Such as Milford Deep and Anglesey Freeport within Wales currently working on deployment and development on Marine renewable energy devices; as well as the commitment from the Welsh government to produce 100% of its electricity demand by renewable energy by 2035, makes the Welsh Coast an ideal deployment ground for floating Solar(Welsh government, 2023).



**Fig. 1.** Welsh coast, source: google.com/maps.

### *2.2. Methodologies*

In order to fully assess the FPV suitability of the Welsh coast, the most vital resources, like solar irradiation, meteorological conditions, accessibility to the ports, maintenance, etc. must be quantified. To be able to rank the controlling variables and their impact on the overall output of a FPV device, models like Multi-criteria Decision Making (MCDM), Fuzzy-AHP, etc. can be employed to make a good comparison and investigation among different site candidates(Sitorus & Brito-Parada, 2022). In this work, we employed the MCDM methodology to find the importance of each factor on the whole project first and then tried to find the best potential sites in parallel with our own newly developed methodology that performs a similar analysis.

## 3. Results and discussions

One of the key outputs of this work is understanding how to rate/rank different variables influencing the “Floating Solar Panels” project as they are one of the alternatives for the transmission from traditional power sources to renewable sources. Our results show depending on the designing variables which are solar irradiation and stability of structure against wind power and wave conditions, the southern coast is potentially a good place to implement FPV.

**References**


Ahmadian, R., Falconer, R., & Lin, B. (2010). Hydro-environmental modeling of proposed Severn barrage, UK. *Proceedings of the Institution of Civil Engineers - Energy*, *163*(3), 107–117.

Gadzanku, S., Mirletz, H., Lee, N., Daw, J., & Warren, A. (2021). Benefits and critical knowledge gaps in determining the role of floating photovoltaics in the energy-water-food nexus. *Sustainability (Switzerland)*, *13*(8). https://doi.org/10.3390/su13084317

Manoj Kumar, N., Chakraborty, S., Kumar Yadav, S., Singh, J., & Chopra, S. S. (2022). Advancing simulation tools specific to floating solar photovoltaic systems – Comparative analysis of field-measured and simulated energy performance. *Sustainable Energy Technologies and Assessments*, *52*. https://doi.org/10.1016/j.seta.2022.102168

Sitorus, F., & Brito-Parada, P. R. (2022). The selection of renewable energy technologies using a hybrid subjective and objective multiple criteria decision making method. *Expert Systems with Applications*, *206*, 117839. https://doi.org/https://doi.org/10.1016/j.eswa.2022.117839

Solomin, E., Sirotkin, E., Cuce, E., Selvanathan, S. P., & Kumarasamy, S. (2021). Hybrid floating solar plant designs: A review. In *Energies* (Vol. 14, Issue 10). MDPI AG. https://doi.org/10.3390/en14102751

Welsh government. (2023). *Wales aims to meet 100% of its electricity needs from renewable sources by 2035*. https://www.gov.wales/wales-aims-meet-100-its-electricity-needs-renewable-sources-2035

Xue, J., Ahmadian, R., & Falconer, R. A. (2019). Optimising the Operation of Tidal Range Schemes. *Energies*, *12*(15), 2870.

Xue, J., Ahmadian, R., Jones, O., & Falconer, R. A. (2021). Design of tidal range energy generation schemes using a GeneticAlgorithm model. *Appl. Energy*, *286*, 116506.

# Opportunities and challenges for a dual-purpose wave farm proposal in the North-western nearshore of Portugal

Daniel CLEMENTE[1,2], Victor RAMOS[1,2], Felipe TEIXEIRA-DUARTE [1,2], Francisco Vilela TAVEIRA-PINTO[1,2], Paulo ROSA-SANTOS[1,2], Francisco TAVEIRA-PINTO[1,2]

[1] Department of Civil Engineering, Faculty of Engineering of the University of Porto, Rua Dr. Roberto Frias, s/n, 4200-465, Porto, Portugal

[2] Interdisciplinary Centre of Marine and Environmental Research (CIIMAR), Leixões Cruise Terminal, Av. General Norton de Matos s/n, 4450-208, Matosinhos, Portugal

up201009043@edu.fe.up.pt, jvrc@fe.up.pt, felipe.td@gmail.com, up201503164@edu.fe.up.pt, pjrsantos@fe.up.pt, fpinto@fe.up.pt

ABSTRACT

This paper summarizes a recent numerical study on a dual-purpose wave farm for a case study site located in the North-west coast of Portugal: the nearshore area of Esposende. This site not only exhibits a noteworthy wave energy resource for electricity generation, but also suffers from coastal erosion issues, which could be mitigated through the "shielding" effect of a nearshore wave energy farm. The study, carried out with the high-fidelity model SNL-SWAN, analyses distinct park layouts, from orientation to inter-device distance. It compares two standalone bottom-fixed oscillating flap parks, with a total of 150 units, in terms of energy/power output and local wave climate impact. It was found that the alternating configuration, or "W", provided better results than the aligned configuration, or "III". While the orientation outcomes varied, both configurations exhibited a similar increase of Annual Energy Production with greater inter-device distance – up to 316.4 GWh/yr (III) and 341.4 GWh/yr (W). These values refer to the combined farm scenario, as the standalone parks would generally yield even greater energy outputs due to a "shadowing" effect between the parks. In terms of coastal protection, the presence of the farms promotes a reduction of the significant wave heights, in the nearshore area, by up to 31%, although punctual increases were identified (under 7%).

## 1. Introduction

Portugal has significantly invested in renewable energy sources (RES), reaching electricity integration shares of 60% to 90% between 2022 and 2023 (APREN, 2023). To further bolster RES, an auction is underway to allocate a capacity of 10 GW of offshore marine RES by 2030 (XXIII Portuguese Government, 2022). Nevertheless, there is a relevant wave energy resource that can be harnessed in nearshore regions. Furthermore, such an approach enables a dual purpose, as parks composed of several wave energy converters (WECs) can also provide a "shielding" effect to the shoreline by attenuating, through absorption, the incoming waves (Abanades et al., 2018). This is of utmost interest for sensitive areas, such as the Esposende shoreline, in Northwestern Portugal. The area is highly susceptible to complex morpho-hydrodynamics that endanger local communities, such as fishermen, while the local sandbank and ecosystems are classified as vulnerable. Hence, a WEC farm composed of 150 Bottom-fixed Oscillating Flap (B-OF) units of characteristic width *D*, divided into two parks – Farm 1 and Farm 2 (combination designated as Farm 1,2), is proposed to generate renewable electricity from wave action whilst promoting adequate sheltering conditions for the Esposende shoreline.

## 2. Case Study and Numerical Modelling Description

The B-OF parks proposal is shown in Fig. 1. Their geographical positioning attempts to mitigate potential conflicts of marine space use, given the sensitive nature of the Esposende nearshore, and ensure the 8-20 m depth operational range. The two parks are composed of 75 units each, with an individual rating of 3.332 MW and a total installed capacity of about 500 MW. The numerical modelling was carried out with the SNL-SWAN software (WECs modelled as "sheet" obstacles of frequency-dependent transmission coefficient), based on the model setup for a local rehabilitation study (IHRH et al., 2021). A resolution of 3 by 3m was used for the grid,

spanning 1250 and 1300 cells in the cross-shore and longshore directions, respectively, from a starting point at (-58.7, 205.0) km – ETRS89 / Portugal TM06. Eight representative sea-states were obtained through a K-Means clustering analysis of over 270 000 records (1990 to 2020). In terms of study variables, apart from the sea-states, two park layouts – alternating "W" and aligned "III" – were simulated for varying inter-device spacing (1D, 1.25D and 1.5D) and perpendicular alignments with the incoming waves (280º, 295º and 310º).




**Fig. 1.** B-OF farm proposal for Esposende (default park: "W" setup, 1D spacing, and perpendicular to 295º of mean wave direction).

## 3. Results and Discussion

The main results on the Annual Energy Production (AEP) are provided in Table 1. It is perceivable that Farm 1's position is slightly more favourable, in terms of energy absorption, than that of Farm 2. However, there is a significant reduction upon considering the two farms simultaneously, as Farm 1 tends to partially "shadow" Farm 2, thus reducing the latter's absorbed energy. The overall reduction can reach up to 11.57% and is greater for a 1.5D separation, given the larger extension of the "shadowed" region. This also affects more the "III" layout, with front units "shadowing" the lee units more effectively, given the prevailing wave directions. While "W" and "III" yielded lower AEP for a 310º orientation, the highest values were obtained for 280º and 295º, respectively, as a result of the different inter-unit interference patterns under the eight different sea-states. Note that greater spacing entices longer electric cable extensions and travelling distance for maintenance vessels, which may imply additional expenditures. Lastly, "W" farms with 1.5D spacing tended to provide more effective significant wave height $H_s$ reductions (longshore) – up to 31%. This is associated with the greater absorption of wave power, and is lowest for a 310º orientation. However, the mean variations ranged between 4.5% to 7%, with punctual increments in $H_s$ being observed, mostly, in the river mouth area.

**Table 1.** Energy metrics for the worst and best performing farm layouts. The values in brackets are the variation between the sum of standalone farms and the total combined output of both farms.

| AEP (GWh/yr) | "W", 1D, 310º | "W", 1.5D, 280º | "III", 1D, 310º | "III", 1.5D, 295º |
|---|---|---|---|---|
| Farm 1, standalone | 158.07 | 193.15 | 145.14 | 181.66 |
| Farm 2, standalone | 147.18 | 187.68 | 137.31 | 167.64 |
| Farm 1, combined | 157.98 | 192.95 | 145.03 | 181.41 |
| Farm 2, combined | 122.28 | 148.40 | 123.89 | 134.94 |
| Farm 1 + Farm 2, combined | 280.25 (-8.92%) | 341.35 (-11.57%) | 268.91 (-5.03%) | 316.35 (-10.42%) |

**Acknowledgements**

The authors acknowledge funding through the project ATLANTIDA – Platform for the monitoring of the North Atlantic Ocean and tools for the sustainable exploitation of the marine resources, with reference NORTE-01-0145-FEDER-000040, which is co-financed by the European Regional Development Fund (ERDF) through NORTE2020.

**References**

Abanades J, Flor-Blanco G, Flor G, Iglesias, G (2018) Dual wave farms for energy production and coastal protection. Ocean & Coastal Management 160, 18–29.

APREN (2023) Electricity Generation by Energy Sources in Mainland Portugal in 2023 [WWW Document]. APREN - Production. URL https://www.apren.pt/en/renewable-energies/production/ (accessed 7.26.23).

IHRH, Minho University, Esposende City Hall (2021) Risk Characterization Study and Intervention Plan for Protecting the Ofir Sandbank and Cávado Mouth (Intervention Report). Faculty of Engineering of the University of Porto, Esposende, Portugal.

XXIII Portuguese Government (2022) Preliminary proposal of specialized areas and seaports connected to the Nacional Electricity Grid and Transport (No. Decree n.º 11404/2022). Grupo de Trabalho para o planeamento e operacionalização de centros electroprodutores baseados em fontes renováveis de origem ou localização oceânica, Portugal.

# Accuracy Assessment of UAV-based Remote Sensing of Turbidity in Coastal Environments during Land Reclamation

Hieu Trung KIEU[1], Hui Ying PAK[2], Ha Linh TRINH[3], Dawn Sok Cheng PANG[4], Eugene KHOO[5], Adrian Wing-Keung LAW[6]

[1,3,4] Environmental Process Modelling Centre, Nanyang Environment and Water Research Institute, Nanyang Technological University, 50 Nanyang Avenue, Singapore 639798, Singapore
trunghieu.kieu@ntu.edu.sg
halinh.trinh@ntu.edu.sg
dawn.pang@ ntu.edu.sg

[2] Environmental Process Modelling Centre, Nanyang Environment and Water Research Institute, Nanyang Technological University, 50 Nanyang Avenue, Singapore 639798, Singapore
Interdisciplinary Graduate Programme, Graduate College, Nanyang Technological University, 50 Nanyang Avenue, Singapore 639798, Singapore
pakh0001@e.ntu.edu.sg

[5] Engineering and Project Management Division, Maritime and Port Authority of Singapore, Singapore 119963, Singapore
eugene_khoo@mpa.gov.sg

[6] Department of Civil and Environmental Engineering, National University of Singapore, 21 Lower Kent Ridge Rd, Singapore 119077, Singapore
cewklaw@nus.edu.sg

ABSTRACT

## 1. Introduction

Despite the progress in utilizing Unmanned Aerial Vehicles (UAVs) for various applications in recent years, their adoption for regulatory monitoring of turbidity plumes induced by land reclamation operations remains challenging. This difficulty arises from the significantly high spatial resolutions and accuracy required, as well as the wide turbidity ranges with nonlinear reflectance. In addition, uncertainties arising from the complexity of coastal environments must be considered during the processing of the aerial images. In this study, a pilot-scale deployment of UAV-based hyperspectral sensing was carried out to assess the accuracy of turbidity determination (Kieu et al., 2023). Deep machine learning models, namely, Extreme Gradient Boosting (XgBoost) and Deep Neural Network (DNN), were trained using a large dataset collected to address the challenges of achieving higher spatial (sub-metre) resolutions for turbidity determination and better capture the non-linearity of the relationship between the water leaving reflectance and turbidity level. Among these models, the DNN model achieved the highest accuracy with a $R^2$ score of 0.752, demonstrating the current level of accuracy attainable in adopting UAV-based hyperspectral imagery for remotely sensing construction-induced turbidity plumes.

## 2. Materials and methods

The study was conducted at a land reclamation site in the coastal area of Singapore. The UAV system utilised in the study consisted of a DJI hexacopter drone, a push-broom hyperspectral camera for image acquisition, a spectrometer for light calibration, and a GPS module for recording position as shown in Figure 1. A total of four UAV surveys were carried out on 10 November 2021 and 13 January 2022. Each UAV survey covered an area of 150 × 150 $m^2$ and was synchronised with field measurements obtained from a turbidity probe attached to a sampling vessel. The survey planning and image analytics followed the standard framework

described in Trinh et al. (2022). The duration of each UAV flight and field measurements spanned approximately 12 - 14 minutes. The flight altitude was maintained at 60 m above mean sea level, providing a ground resolution of 2 cm/pixel.




**Fig. 1.** (a) UAV-borne hyperspectral system used in this study, (b) DJI Matrice M600 Pro, (c) D-RTK GNSS system, and (d) BaySpec OCI-F hyperspectral imager (Kieu et al., 2023).

## 3. Results

### *3.1. Spectral analysis and band selection for machine learning*

The selection of spectral band for model training employed four feature selection techniques, namely, Pearson F scores, Lasso Coefficient, XGBoost feature score, and sequential forward selection (SFS). Based on the feature selection results, a frequency distribution of all selected spectral bands was plotted. As a result, the ten spectral bands with the highest frequency mostly belong to the red-edge and near-infrared regions and thus they were included in the model training.

### *3.2. Model performance*

This study compared the performance between deep machine learning models, including Extreme Gradient Boosting (XgBoost) and Deep Neural Network (DNN), and simpler Multivariate Linear Regression (MLR) as well as Multivariate Quadratic Regression (MQR) models in terms of turbidity prediction accuracy using the large dataset collected. The results presented in Table 1 illustrate that the two deep machine learning models perform better than the two multivariable regression models across all performance metrics. Between the two machine learning models, the metrics by the DNN model consistently outperforms the XGBoost model and they represent the accuracy that can be achieved at present.

**Table 1.** Prediction performance metrics of MLR, MQR, XGBoost, and DNN models (Kieu et al., 2023)

| Metrics | MLR model | MQR model | XGBoost model | DNN model |
|---|---|---|---|---|
| $R^2$ score | 0.619 | 0.395 | 0.676 | 0.752 |
| RMSE (FNU) | 9.83 | 12.40 | 8.63 | 7.94 |
| MAE (FNU) | 6.88 | 7.85 | 5.48 | 5.23 |
| MPAE (%) | 38.6 | 45.2 | 31.3 | 30.4 |

## 4. Conclusion

We conducted a comprehensive investigation into the utilisation of UAV-based remote sensing with a hyperspectral sensor for monitoring turbidity plumes induced by land reclamation. Machine learning (ML) models were trained using the large dataset collected to better capture the non-linearity of the relationship between the water leaving reflectance and high turbidity level. Performance results indicate that the ML models outperform simpler multivariate linear and quadratic regression models, which justify their adoption for future applications.

**Acknowledgements**

The author would like to acknowledge the support from the Maritime and Port Authority of Singapore (MPA), Surbana Jurong Pte Ltd., and DHI Water & Environment (Singapore) Pte Ltd. in project coordination and data sharing. This work was funded by the Singapore Maritime Institute (SMI) under the research project "UAV-based Remote Sensing of Turbidity in Coastal Waters," grant number SMI-2020-MA-02.

**References**

Trinh HL, Kieu HT, Pak HY, Pang DS, Cokro AA, Law AWK (2022) A Framework for Survey Planning Using Portable Unmanned Aerial Vehicles (pUAVs) in Coastal Hydro-Environment, Remote Sensing, 14(9), 2283.
Kieu HT, Pak HY, Trinh HL, Khoo E, Pang DS, Law AWK (2023) UAV-based remote sensing of turbidity in coastal environment for regulatory monitoring and assessment, Marine Pollution Bulletin, 196, 115482

# Using Hall-effect sensor based devices for high-resolution measurements of wave-driven near-bottom water flow in the Gulf of Riga

Laura PIHO[1], Asko RISTOLAINEN[1], Kevin PARNELL[2], Tarmo SOOMERE[2]

[1] Center for Biorobotics, Tallinn University of Technology, Estonia
laura.piho@taltech.ee
asko.ristolainen@taltech.ee

[2] Laboratory of Wave Engineering, Tallinn University of Technology, Estonia
kevin.parnell@taltech.ee
tarmo.soomere@taltech.ee

ABSTRACT

Field measurements are essential for coastal resource management, protection, validating numerical models and conducting studies related to the climate crisis and associated changes to coastal processes and coastal engineering infrastructure. Such measurements are becoming increasingly important to quantify spatial variability of the impact of short-crested waves on the sedimentary seabed. In Ristolainen et al. (2016) and Ristolainen (2019), a cost-effective device, equipped with a 3D Hall-effect sensor, called a Hydromast, is introduced for high resolution water flow speed and direction estimation. In this work, we present a first-order quantification of spatial variability of wave-driven near-bottom flow both in terms of flow speed and direction in short-crested wave fields based on continuous measurements in the Gulf of Riga (eastern Baltic Sea) over a one-month period using nine Hydromasts.

## 1. The devices

The inspiration for the Hydromast (Fig. 1) comes from a mechanoreceptive organ of the fish called the neuromast that can sense the flow (Bleckmann and Zelick, 2009). The first version of the device was used to characterize near-bed hydrodynamic loads in rivers. The low cost Hydromast (typically under 1,000 € per unit), is equipped with an absolute pressure sensor, 3D Hall sensor, and an inertial measurement unit (IMU). The device has a hollow vibrating mast, covered with copper tape to reduce biofouling. The mast is fixed to a flexible membrane and reacts to vortices and other small fluctuations in the flow (Ristolainen et al., 2019).

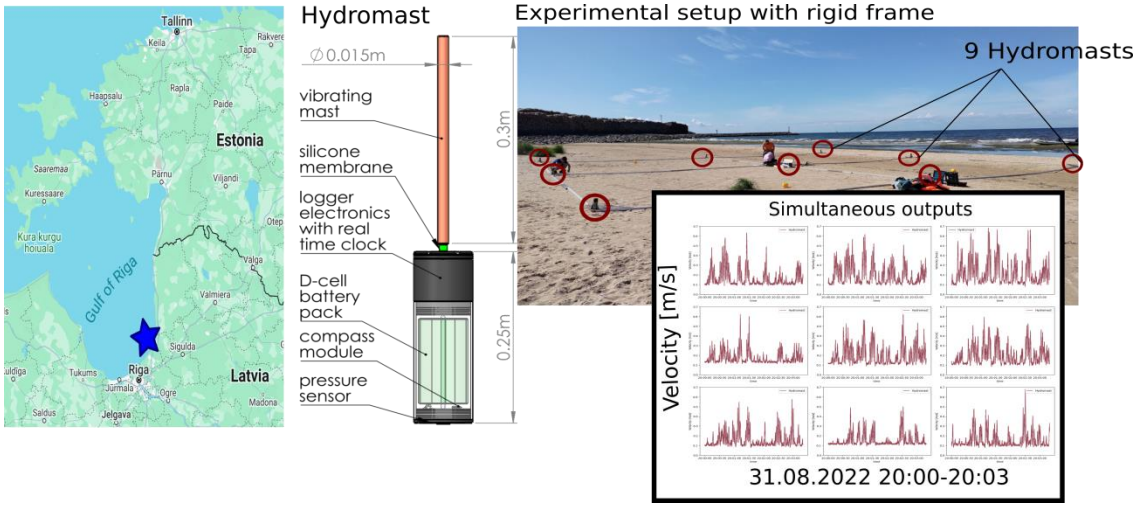



**Fig. 1.** Measurement site in the Gulf of Riga, an overview of Hydromast components, Hydromast placement on the rigid grid for experiments, and the sample output from all 9 devices making simultaneous measurements. (Map retrieved from Google maps, 2. February 2024)

The Hall-effect sensor detects the magnetic field strength from a small magnet installed at the base of the mast inside the flexible membrane. Based on the mast movement due to the water flow, it is possible to estimate both speed and direction of the flow. The device has a limited measurement range of flow speed depending on the mast length, diameter, and weight. In the experiments presented here, 300 mm (about 11.81 in) long and 15 mm (about 0.59 in) diameter masts were used, providing accurate measurements in the range of 0.15–1.1 m/s (maximum tested). Additional information is provided by the IMU (device movement and orientation) and absolute pressure sensor (water depth and pressure fluctuations). The latter allows us to infer additional information about wave height and period.

## 2. The experiments

A one-month long study was conducted near Skulte in the eastern Gulf of Riga (02.08.–08.09.2022). The experimental set-up included an array of nine Hydromasts, mounted on a rigid 20 × 20 m frame with 10 m between the devices, placed at ~3 m depth. All nine devices were continuously measuring for the whole duration (sampling rate 50 Hz). Additionally, an Acoustic Doppler Velocimeter (ADV) (Vector, Nortek) was mounted adjacent to the sensor at the center of the frame. It was set to log data every 30 minutes in 2-minute-long bursts (sampling rate 8 Hz). The ADV and Hydromast records show good agreement in both flow speed and direction (Fig. 2).

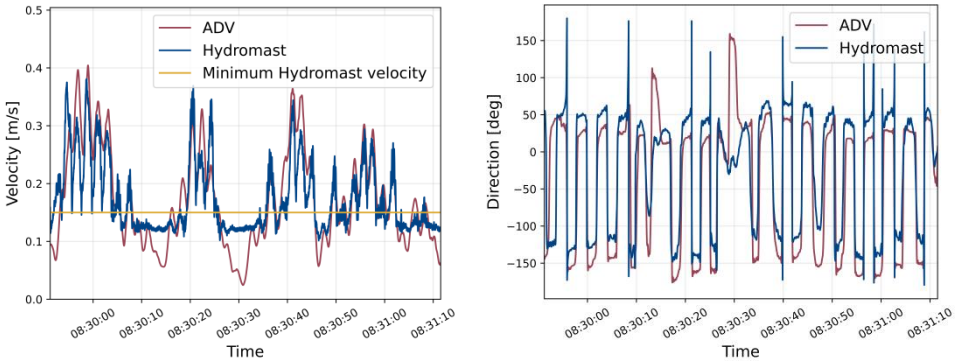



**Fig. 2.** Left: Time aligned Hydromast velocity measurements (Hydromast measurement range 0.15 m/s-1.1 m/s) compared to ADV velocity measurements on 31.08. 2022. Right: Time aligned Hydromast direction measurements compared to ADV on 31.08.2022.

## 3. Results

The described set-up allowed us to quantify wave-driven near-bottom velocity variations in short-crested wave fields (insert to Fig. 1). Further, these in-situ, high-resolution, continuous measurements of local flow properties enabled us to assess associated spatial variations in seabed hydrodynamic loads. The resulting accurate representation of time series of flow speed makes it possible to construct approximations of probability distributions of flow speeds and to build reasonable estimates of occurrence and spatial variability of high speeds that are crucial for the evaluation of the entrainment probability of bottom sediment. We also demonstrate that the resulting data can be used to develop detailed time-frequency characteristics of wave storms and identify signals of various vessels that sail near the measurement site in calm conditions (Rätsep et al., 2021). The low cost of the devices allows wider area coverage over extended periods of time and in extreme environments where the chances of recovering the instruments are reduced.

**Acknowledgements**

The research was co-supported by the Estonian Research Council (grant PRG1129), the European Economic Area (EEA) Financial Mechanism 2014–2021 Baltic Research Program (grant EMP480), and the European Union through H2020 project ILIAD (grant agreement No 101037643).

**References**

Ristolainen A, Tuhtan JA, Kuusik A, Kruusmaa M (2016) Hydromast: a bioinspired flow sensor with accelerometer. In: Biomimetic and Biohybrid Systems. Living Machines 2016, 510–517. https://doi.org/10.1007/978-3-319-42417-0_55

Ristolainen A, Tuhtan JA, Kruusmaa M (2019) Continuous, near-bed current velocity estimation using pressure and inertial sensing. IEEE Sensors Journal, 19 (24), 1558–1748, https://doi.org/10.1109/JSEN.2019.2937954

Bleckmann H, Zelick R (2009) Lateral line system of fish. Integrative Zoology, 4, 13–25. https://doi.org/10.1111/j.1749-4877.2008.00131.x

Rätsep M, Parnell KE, Soomere T, Kruusmaa M, Ristolainen A, Tuhtan JA (2021) Surface vessel localization from wake measurements using an array of pressure sensors in the littoral zone, Ocean Engineering, 233, 109156, https://doi.org/10.1016/j.oceaneng.2021.109156

# Spatial variations in the vulnerability of the shores of the eastern Baltic Sea with respect to future extreme water levels

Katri VIIGAND[1], Maris EELSALU[2], Tarmo SOOMERE[3,4]

[1,2,3] Department of Cybernetics, School of Science, Tallinn University of Technology, Ehitajate tee 5, Estonia
katri.viigand@taltech.ee
maris.eelsalu@taltech.ee
tarmo.soomere@taltech.ee

[4] Estonian Academy of Sciences, Kohtu 6, Tallinn, Estonia

ABSTRACT

Local water level in the microtidal Baltic Sea is shaped by several local drivers, such as the water volume of the entire sea, storm surge and wave-driven effects. These components may appear at varying time and spatial scales. We categorise the shores of Lithuania, Latvia and Estonia in the eastern Baltic Sea (Fig. 1) in terms of their vulnerability with respect to coastal flooding using the likelihood of significantly higher extreme water levels in the future based on the Generalised Extreme Value (GEV) distribution.

## 1. Introduction

Elevated water level is one of the key marine-driven hazards. This hazard, usually expressed in terms of tidal range, is commonly used in the evaluation of coastal vulnerability indices since (Gornitz et al., 1994). This parameter is not applicable for microtidal water bodies, such as the Baltic Sea (Bagdanavičiūtė et al., 2015). This sea, however, may experience large aperiodic water level variations, with a total range >4 m, and changes to the entire sea level up to 80 cm during many weeks. These variations can be characterised in terms of return periods of extreme water levels (EWLs) using a GEV distribution. The shape parameter of this distribution substantially varies along the shores of the Baltic Sea (Soomere et al., 2018). Depending on its sign, the GEV distribution projects different severity of future events. Therefore, this parameter characterises the likelihood of much higher EWLs in the future than observed in the past. It thus provides crucial information about vulnerability of single coastal segments.

## 2. Materials and methods

We explore a 1400 km long coastal stretch of Lithuania, Latvia and Estonia (Fig. 1, right panel) in terms of the likelihood of experiencing significantly higher EWLs in the future based on the GEV distribution. We rely on sea level time series derived from the Rossby Center Ocean (RCO, Meier et al., 2003) model covering years 1961–2005 with a temporal resolution of 6 hours. The dataset is complemented by the hourly output of an early version of RCA4 NEMO model (Hordoir et al., 2013). The coastline of Baltic States was divided into 351 about 3.7 km long sections that correspond to nearshore model cells. For the time series of water level in each such section we evaluate the shape, location and scale parameter of the GEV distribution for water level maxima and minima using the block maxima method and two data subsets (annual maxima and minima, and maxima over 12-month time intervals from July to subsequent June that contain the entire windy season). An ensemble of projections of EWLs and their return periods is developed using both biased and unbiased versions of the method of moments and several versions of the maximum likelihood method.

The shape parameter plays a central role in these projections. If it is negative, the resulting Weibull distribution projects a slow increase in EWLs. A zero shape parameter means that EWLs are governed by a Gumbel distribution that projects faster increase in the EWLs. A positive shape parameter corresponds to a Fréchet distribution that predicts much faster increase in extremes. The presence of various distributions generates different levels of vulnerability of coastal areas with respect to EWLs.

## 3. Results and discussion

The GEV shape parameter based on the RCO data varies substantially along the study area. Moreover, it has a different sign in different coastal segments (Fig. 1, right panel). The entrance and southern part of the Gulf of Riga, the open shores of the West Estonian Archipelago and a part of the Estonian northern coast host an almost zero value of this parameter. In these regions, EWLs and their return periods are expected to behave according to a Gumbel distribution and thus eventually have moderate severity of future floods. The shape parameter is negative along the Lithuania shore and at the open part of Latvia where the EWLs follow a 3-parameter Weibull distribution. The flood-related danger is therefore moderate in these areas in the future. The bayheads of the Gulf of Riga and Gulf of Finland host relatively large positive values of this parameter. It is thus likely that much higher EWLs are possible in these areas in the future according to a Fréchet distribution. This pattern of alongshore variations is evident for the shape parameter evaluated using all above-mentioned approaches, except for the shape parameter found from RCA stormy season data. The spread of single estimates of shape parameter is relatively wide along the Estonian coast where about half of its values are small but positive while another half are also small but negative. As the GEV shape parameter only depends on the asymmetry of the GEV distribution, the presented results are invariant with respect to the global sea level rise, land uplift and subsidence. Even though estimates of this parameter in single locations vary considerably depending on the particular method, its alongshore variations are consistent.

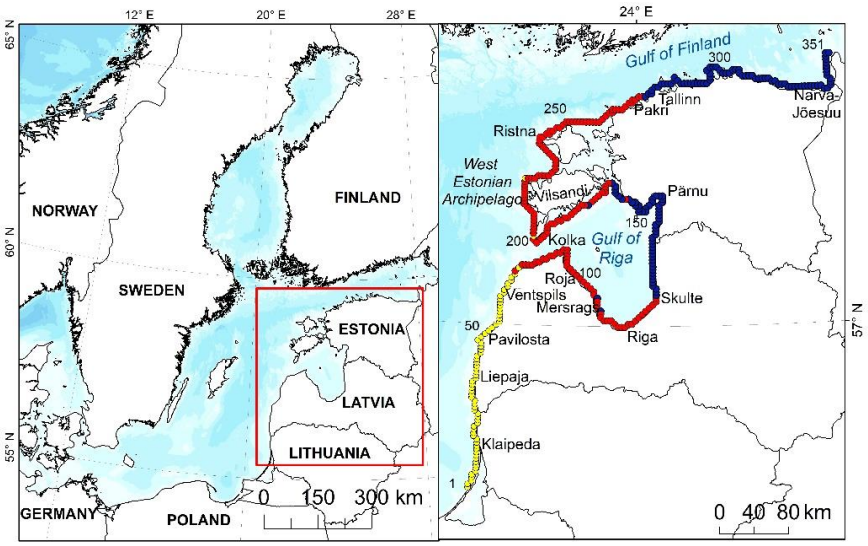



**Fig. 1.** Left panel: Study area in the eastern Baltic Sea. Right panel: Variation in the GEV shape parameter calculated from the 12-month windy season maxima of the RCO model along the coastline of Lithuania, Latvia and Estonia. Blue indicates positive values, red – almost zero values and yellow – negative values of this parameter.

We also present several examples of ensemble-based projections of EWLs once in a few decades. The global sea level rise and changes to water level owing to local land uplift and subsidence enter as linear additives in such projections. The alongshore variation of EWLs with the return period of 50 yr matches well the all-time highest recorded water levels in 14 observation sites. The largest difference is for estimates at Pärnu where local effects and extensive filling of the Gulf of Riga apparently play a role.

**Acknowledgements**

The research was supported by the European Economic Area (EEA) Financial Mechanism 2014–2021 Baltic Research Programme (grant EMP480). The authors are deeply grateful to the Swedish Meteorological and Hydrological Institute for the model data.

**References**

Bagdanavičiūtė I, Kelpšaitė L, Soomere T (2015) Multi-criteria evaluation approach to coastal vulnerability index development in micro-tidal low-lying areas, Ocean & Coastal Management, 104, 124-135, https://doi.org/10.1016/j.ocecoaman.2014.12.011

Gornitz VM, Daniels RC, White TW, Birdwell KR (1994) The development of a coastal vulnerability assessment database, vulnerability to sea-level rise in the U.S. southeast, Journal of Coastal Research, Special Issue 12, 327-338.

Hordoir R, An BW, Haapala J, Dieterich C, Schimanke S, Höglund A, Meier HEM (2013) BaltiX: A 3D Ocean Modelling Configuration for Baltic & North Sea Exchange Analysis, SMHI-Report, Oceanography 48, 115 pp.

Meier HEM, Döscher R, Faxén T (2003) A multiprocessor coupled ice–ocean model for the Baltic Sea: application to salt inflow, Journal of Geophysical Research–Oceans, 108 (C8), 3273, https://doi.org/10.1029/2000JC000521

Soomere T, Eelsalu M, Pindsoo K (2018) Variations in parameters of extreme value distributions of water level along the eastern Baltic Sea coast, Estuarine, Coastal and Shelf Science, 215, 59-68, https://doi.org/10.1016/j.ecss.2018.10.010

# Exploring wave energy resource on the Pacific shore of South America

Maris EELSALU[1], Tarmo SOOMERE[1], Darwin ARAMBURO[2], Rubén D. MONTOYA[3], Andrés F. OSORIO[4,5]

[1] Department of Cybernetics, School of Science, Tallinn University of Technology, Ehitajate tee 5, 19086 Tallinn, Estonia
maris.eelsalu@taltech.ee
tarmo.soomere@taltech.ee

[2] Universidad Tecnológica del Chocó "Diego Luis Córdoba", Grupo de Investigación en Gestión de las Ciencias, Tecnología, Ingeniería y Matemática (GESTEM+B), Grupo de Investigaciones Pedagógicas en el Área de las Matemáticas (INPEMA), Cra. 22 No 18B–10B, Quibdó, Colombia
d-darwin.aramburo@utch.edu.co

[3] Universidad de Medellín, Grupo de Investigación en ingeniería Civil GICI, Grupo de investigación en Calidad del agua y Modelación Hídrica GICAMH, Universidad de Medellín, Carrera 87 N° 30–65, Medellín, Colombia
rdmontoya1@gmail.com

[4] Universidad Nacional de Colombia - Sede Medellín - Facultad de Minas - Departamento de Geociencias y Medio Ambiente - Grupo de investigación OCEANICOS, Cra. 80 No. 65–223 Bloque M2, Medellín 050041, Colombia
efosorioar@unal.edu.co

[5] Center of Excellence in Marine Science, CEMARIN, Colombia
afosorioar@unal.edu.co

ABSTRACT

We analyse the wave energy resource available along the Pacific coast of South America from Panama to the Drake Passage between South America and Antarctica. The wave energy resource to the north of latitude 30°S is almost entirely provided by swells. To the south of 43°S wind-seas predominate among the most energetic wave conditions. The calmest time that contains 1% of the total annual energy flux is 10–20 days. About 50% of the annual energy flux arrives during 100 days with strongest waves. The typical wave height that provides largest contribution to wave energy is 1–1.5 m in the north and increases to 3.5–4 m on the shores of southern Chile. The most energy-containing wave periods are about 10 s in the entire study area.

## 1. Introduction

The eastern coast of the Pacific Ocean is one of the most feasible regions for wave energy harvesting for energy production (Mediavilla and Figueroa, 2017). We analyse systematically spatial and temporal variability in the wave power that approaches the entire western shore of South America. The available wave energy resource depends not only on the formal parameters of the wave climate but also on the persistence of the wave energy flux in terms of wave heights, periods and approach directions over longer time periods from weeks to months, and the possible presence of extreme (possibly damaging) wave conditions. The most desirable areas for energy harvesting feature stable wave conditions with no severe storms.

## 2. Data and methods

Wave power estimations are made using numerically simulated hourly time series of wave properties for 1959–2021 from the European Union Copernicus database (https://cds.climate.copernicus.eu/cdsapp#!/dataset/reanalysis-era5-single-levels?tab=overview) developed using the wave model WAM (Komen et al., 1994) and ERA5 wind information. The analysis is made for a sequence of nearshore grid cells along the western shore of South America from latitude 7°N to 55°S. The longitude of these cells, selected close to the shore at a depth of >50 m, varies from 71 to 82°W. We employ the classic approach to evaluate the scalar wave energy flux $P_S$ from the wave energy $E$ and group speed $c_g$ [m s$^{-1}$] (e.g., Dean and Dalrymple, 1991):

$$P_S = Ec_g = \frac{1}{16}\rho g H_S^2 c_g \quad (1)$$

Here $H_S$ is significant wave height [m], $\rho$ – water density [kg m$^{-3}$], $g$ – acceleration due to gravity [m s$^{-2}$]. The analysis involves three time series: wave energy flux of the entire wave field that involves both swell waves and wind-seas and wave energy flux carried by swell waves and wind-seas.

## 3. Results

The long-term average wave energy flux increases from about 2 kW m$^{-1}$ just to the north of the equator at the Colombian Pacific coast to 20–50 kW m$^{-1}$ in the central and southern Chile and up to 80 kW m$^{-1}$ near the Drake Passage between South America and Antarctica. The wave energy resource to the north of latitude 37°S is almost entirely provided by swells. To the south of 44°S wind-seas predominate among the most energetic wave conditions. The maxima of energy flux by wind-seas up to 20 times exceed the already high average energy flux (Fig. 1) and indicates the presence of extreme wave conditions.

The most frequent wave conditions and situations that are most favourable for wave energy harvesting are greatly different in different segments of the Pacific shore of South America. The typical height of waves that provide the largest contribution to wave energy is about 1–1.5 m in the very north, around 1 m near the equator, gradually increases to the South and reaches 3.5–4 m at the shores of southern Chile. The associated wave periods are almost constant, about 10 s in the entire study area.

The optimal wave conditions for wave energy harvesting in terms of wave fields that provide the largest wave energy flux occur near the equator approximately 60–70 days per year (Fig. 1). In most nearshore areas of Colombia and Ecuador as well as in some coastal segments in Peru and northern Chile, these optimal wave conditions are also the most frequent. Such fairly persistent wave energy flux is an advantageous feature for wave energy harvesting, as it allows for the precise tuning of wave energy converters.

The seasonal variation of monthly mean wave energy flux is commonly from –47% to +32% from the long-term mean. The length of the calmest time that contains 1% of the total annual energy flux is 10–20 days in a year. The 100 calmest days provide about 10% of the annual energy flux. About 50% of the annual energy flux arrives during 100 days with strongest waves. These features signal that wave conditions in the study area, even though highly different in different locations, are generally favourable for energy harvesting.

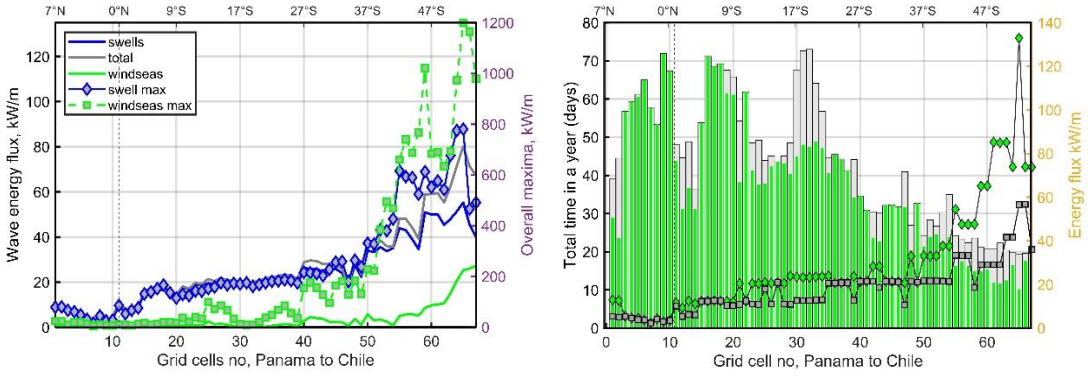



**Fig. 1**. Left panel: long-term average energy flux (kW m$^{-1}$, scale on the left) and energy flux maxima (lines with markers, scale on the right) carried by entire wave fields (grey), swells (blue) and wind-seas (green) in 1959–2021. The upper horizontal scale indicates the latitude of the grid cell while the lower scale indicates the sequential number of the cells. The possible presence of wind-seas wave energy flux extremes ~1000 kW m$^{-1}$ indicates extreme wave conditions that may be dangerous for wave energy converters. Right panel: total time in a year (in days) of mixed wave conditions that provide the best resource to annual wave energy flux (green bars) and mixed wave conditions that occur most frequently (grey bars). The wave energy flux provided by waves corresponding to the best resource is shown using green diamonds and most frequently occurring waves are indicated with grey squares.

**Acknowledgements**

The research was co-supported by the Estonian Research Council (grant PRG1129) and the European Economic Area (EEA) Financial Mechanism 2014–2021 Baltic Research Programme (grant EMP480).

**References**

Dean RG, Dalrymple RA (1991) Water Wave Mechanics for Engineers and Scientists. World Scientific, 292 pp.

Komen GJ, Cavaleri L, Donelan M, Hasselmann K, Hasselmann S, Janssen PAEM (1994) Dynamics and Modelling of Ocean Waves, Cambridge University Press, 532 pp.

Mediavilla DG, Figueroa D (2017) Assessment, sources and predictability of the swell wave power arriving to Chile, Renewable Energy, 114, 108–119. https://doi.org/10.1016/j.renene.2017.03.014

# Evaluation of microplastic contamination across an Atlantic coastal area

Vanessa MORGADO[1,2], Ricardo Bettencourt da SILVA[2], Carla PALMA[1]

[1] Instituto Hidrográfico, Rua das Trinas 49, 1249-093 Lisboa, Portugal
vanessa.morgado@hidrografico.pt
carla.palma@hidrografico.pt

[2] Centro de Química Estrutural, Institute of Molecular Sciences, Departamento de Química e Bioquímica, Faculdade de Ciências, Universidade de Lisboa, Campo Grande, 1749-016 Lisboa, Portugal
rjsilva@fc.ul.pt

ABSTRACT

## 1. Framework

The global recognition of environmental pollution attributed to microplastics is widely acknowledged. Microplastics, which are particles characterised by a non-natural polymeric matrix and range in size from 1 µm to 5 mm, are currently affecting numerous aquatic systems worldwide, including rivers, estuaries, seas, open oceans, and remote regions (Primpke et al., 2022). The significant prevalence of microplastics in the environment has attracted the scientific community's interest in monitoring these contaminants across various aquatic environments and matrices, including ocean floor sediments.

Implementing policies and legislation to control and manage plastic pollution, including microplastics, is crucial for safeguarding the environment, particularly coastal areas. The development of regulations should be informed by the recognised significance and trends of this form of pollution. The true importance and potential sources of this contamination can only be comprehended through the objective characterisation of contamination levels and trends. Consequently, strategies to reduce this contamination can be design and effective implanted aiming at mitigating this issue.

This work has enhanced the objectivity of determining microplastic contamination in sediments by creating a methodology for evaluating the uncertainty associated with these measurements and sampling procedures, namely in sediment samples collected from a 700 km$^2$ area of the Atlantic Ocean coast between Sesimbra and Sines, Portugal.

## 2. Experimental and study area

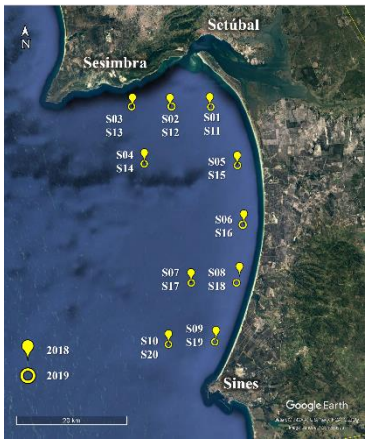



**Fig. 1.** Sampling positions.

In this research, the results were generated based on microplastics analysed from 20 sediment samples collected from a vast oceanic area on the southwest coast of Portugal, bordered by the metropolitan area of Lisbon and the Alentejo region (Figure 1). After sampling, sediment samples were prepared according to the following procedure: i) Sediment sieving to isolate sediment matter with the size range of microplastics; ii) Weighing sieved sediment; iii) Digesting the aliquot using peroxide hydrogen ($H_2O_2$, 30%); iv) Separating the lighter microparticles from the densest matter of the samples using a saturated solution of sodium chloride (NaCl, 99.5%); v) Filtrating the NaCl solution above the settled matter to an adequate filter such as glass fibre membrane (GF/C, 1.2 µm, Ø = 47 mm); vi) Storing filters in closed glass Petri dishes. The suspicious microparticles on the filters were analysed under a stereomicroscope for the identification of their physical characteristics such as size, colour, and shape. The chemical analysis was

performed by the Perkin Elmer spectrometer Spotlight 200i Microscope System or by the PerkinElmer Spectrum Two FTIR enabling the identification of the polymer's chemical composition.

## 3. Synopsis

The present work describes the first bottom-up evaluation of the uncertainty of the quantification of microplastics in environmental sediment samples, taking into account the sampling uncertainty.

The bottom-up evaluation of the uncertainty of microplastics contamination quantification involved the identification and quantification of systematic and random effects affecting the analysis. Different probability density functions were considered to model the identified sources of uncertainty (Morgado et al., 2022) such as the Poisson-Lognormal distribution that derives from the general Poisson distribution for which the distribution parameter ($\lambda$; i.e., mean and variance) follows itself a Lognormal distribution. The Poisson-Lognormal distribution is used to model the random and systematic components that affect the counting of microplastics, using inputs estimated from duplicate sediment analysis and the analysis of sediments spiked with microparticles, respectively. Continuous rectangular and *t*-Student distributions associated with uncertainty components of the sediment sample weighting, such as analytical portion and dry weight determination, were considered. The sampling uncertainty over the vast studied oceanic area was characterised considering the contamination heterogeneity and representativeness of sampling.

Regarding the distribution of the ratio of the number of microplastics per dry mass of sediment, it was modelled by combining the aforementioned distributions and sampling uncertainty components by the Monte Carlo method (MCM), which also allows identifying meaningful variations in microplastic contamination. The developed methodology was implemented in user-friendly MS-Excel spreadsheets used to simulate the probability distribution function of the estimate microplastic contamination of the environmental area. Thus, the distribution percentiles were used to define confidence limits that encloses the true value of the contamination with a 99% probability.

## 4. Results and conclusions

84 microplastics were found in the analysed samples, where PET was the most common polymer found followed by PP. The methodology developed was successfully applied to the quantification of the following types of particles in sediments: i) microplastics, regardless of their physical chemical properties; ii) polyethylene terephthalate (PET); iii) polypropylene (PP); and iv) polyethylene (PE) (Morgado et al., 2023).

This investigation proved that PET microplastics are the predominant polymer type with mean contamination, in 2018 and 2019, between 43 $kg^{-1}$ and 102 $kg^{-1}$, and between 36 $kg^{-1}$ and 85 $kg^{-1}$, for 99% confidence level, respectively. It also unequivocally demonstrates that the contamination level in the studied area did not significantly change between two consecutive years, independent of the polymer types. It was observed that the contamination by PE and PP was equivalent. The comparison of contamination levels was conducted with a 99% confidence level. The collected data pertaining to the environmental area play a crucial role in establishing an objective and binding assessment of microplastic contamination significance (Morgado et al., 2023).

**Acknowledgements**

This work was supported by the Instituto Hidrográfico through the MONIAQUA research program, the Universidade de Lisboa through a PhD Scholarship 2018, and the Operational Program Mar2020 through project "AQUIMAR" (MAR2020 n° MAR-02.01.01-FEAMP-0107), Fundação para a Ciência e a Tecnologia through projects UIDB/00100/2020, UIDP/00100/2020, and LA/P/0056/2020.

**References**

Primpke S, Booth A M, Gerdts, G, Gomiero A, Kögel T, Lusher A, Strand J, Scholz-Böttcher B M, Galgani F, Provencher J, Aliani S, Patankarl S, Vorkamp K (2022) Monitoring of microplastic pollution in the Arctic: Recent developments in polymer identification, quality assurance and control, and data reporting, Arctic Science, 00, 1-22

Morgado V, Palma C, Silva RJNB (2022) Bottom-up evaluation of the uncertainty of the quantification of microplastics contamination in sediment samples, Environment Science and Technology, 56, 11080-11090

Morgado V, Palma C, Silva RJNB (2023) Determination of microplastic contamination levels and trends in vast oceanic sediment areas with uncertainty, Science of the Total Environment, 884, 163612

# Optimisation of Sampling Uncertainty in vast marine systems: development of methodologies based on Monte Carlo Simulations of georeferenced information

Carlos BORGES[1], Carla PALMA[1], Ricardo J.N. BETTENCOURT DA SILVA[2]

[1] Instituto Hidrográfico, Portugal
carlos.borges@hidrografico.pt
carla.palma@hidrografico.pt

[2] Centro de Química Estrutural, Faculdade de Ciências da Universidade de Lisboa, Portugal
rjsilva@ciencias.ulisboa.pt

ABSTRACT

## 1. Introduction

Monitoring has a key role in environmental protection policies, but the interpretation of the obtained results does not usually account for the associated uncertainty. When uncertainty is considered in data analysis, it usually disregards the influence of the uncertainty arising from sampling, which may be the main source of uncertainty. Moreover, classical sampling strategies are not adequate for the assessment of the environmental status of large marine areas and the evaluation of temporal trends due to their seasonality, heterogeneity and size. All these factors, along with the error of positioning, affect the uncertainty of the collected information on the system.

A tool based on Monte Carlo Simulations of georeferenced information was developed to address this issue (Borges et al., 2019; 2021), using user-friendly Microsoft Excel spreadsheets, considering two different situations: a base tool (named "Sampling_Uncertainty) to study areas with a maximum of 20 sampling positions; and an extended tool (named "MegaSampler") to study areas up to 100 sampling points. The tool was produced with the specific purpose of being applied to marine water masses but has already been used in different types of compartments and matrices (e.g., Bettencourt da Silva et al., 2022).

## 2. Modelation Theory

The base modelling involves a four-step approach to obtain estimates of the sampling uncertainty: (1) collection of samples at a defined depth and known GPS coordinates; (2) description of the collected information as a 3D surface ($x$, $y$, $z$), where $x$ and $y$ are GPS coordinates and $z$ the analytical values of the parameter; (3) randomisation of the 3D surface upon inputting the relevant uncertainty components of GPS coordinates and sample analysis; and (4) scanning of the randomised surfaces to model the spatial variation of the parameter upon conversion of the GPS coordinates into Cartesian distances from the point defined as the origin of the referential (Fig. 1.).

Based on the dispersion of simulated values of the studied parameter, the model produces an estimate of the standard deviation, $s$, of results in the sampling circle. The sampling standard deviation, $s_S$, which is independent of the (analytical) repeatability standard deviation, $s_r$, is estimated by Eq. (1).

$$s_S = \sqrt{s^2 - s_r^2} \quad (1)$$

The model allows the simulation of three types of sampling strategies: Single Sampling (SS), by direct application of Eq. (1); Random composite Sampling (RS), by collecting $m$ subsamples in positions randomly selected inside the sampling circle (Eq. (2)); and Linear composite Sampling (LS), by collecting $m$ subsamples, starting from the centre of the sampling circle, obtaining the other ($m$-1) subsamples in a radial line at $d$ meters intervals. For LS, for each radial line to the sampling centre, it is determined the mean, $\bar{z}_h(m;d)$, of $m$ $z_h$ (Eq. (3)).

$$s_S(\mathrm{RS}; m) = \frac{s_S(\mathrm{SS})}{\sqrt{m}} \tag{2}$$

$$the\ s_S(\mathrm{LS}; m; d) = \sqrt{s_{\bar{z}}^2(m; d) - \frac{s_r^2}{m}} \tag{3}$$

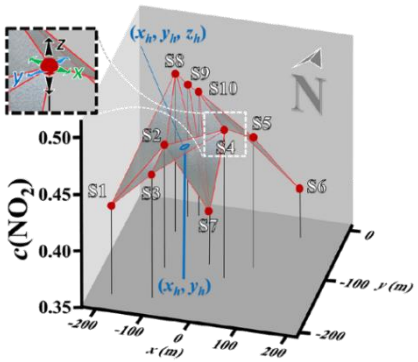



**Fig. 1.** Example of scanning of a 3D randomised surface represented by a combination of various triangular surfaces, applied to nitrite ($NO_2$) concentration estimated from an area with 10 sampling points (S1−S10). The *z-axis* represents the concentration values, $c(NO_2)$. The circle in blue presented in the triangular surface (S2;S3;S4) represents the estimated $NO_2$ concentration, $z_h$, in the geographic coordinates ($x_h$, $y_h$).

The extended model uses the same four-step approach but runs only in the SS mode. To run the model, the sampling area must be separated into different sub-areas (to a maximum of nine) to which the base model is sequentially – and automatically – applied to estimate the sampling uncertainty in the sampling area.

## 3. Results

The developed tool has been applied to two marine systems with different typologies, the Tagus estuary and the Portuguese Continental Platform between Figueira da Foz and Aveiro, and several parameters, namely, nutrients and characteristic oceanic features such as temperature and salinity. The tool's application allowed to obtain estimates of sampling uncertainty for these parameters in the studied systems and also to obtain spatial and density/frequency distributions of the simulated variability (as exemplified in Fig. 2.).

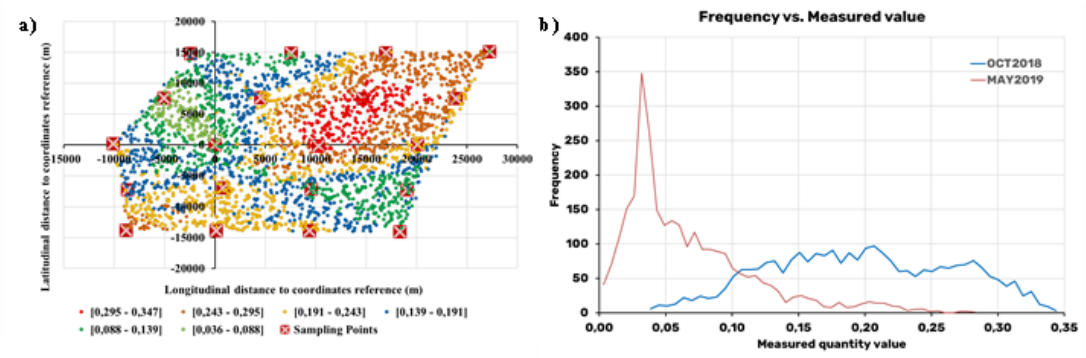



**Fig. 2.** a) Simulated variability of nitrite concentration (µmol $L^{-1}$) on the sampled area of the Portuguese continental platform in October 2018 (spatial variability); b) Frequency distribution plots for the same parameter and area, on two sampling occasions.

From these results, it was also possible to determine if observed temporal trends and parameter correlations, upon incorporation of all uncertainty sources affecting the information, are metrologically significant.

The results obtained also allowed to conclude that the sampling uncertainty is a major contributor to the overall uncertainty and that it is highly dependent on the system´s heterogeneity.

**Acknowledgements**

This work was financed by the Operational Program Mar 2020 through project "AQUIMAR – Caracterização geral de áreas aquícolas para estabelecimento de culturas marinhas" (MAR–02.01.01–FEAMP-0107) and Fundacão para a Ciência e Tecnologia (FCT) through projects UIDB/00100/2020 and UIDP/00100/2020 and Institute of Molecular Sciences through project LA/P/0056/2020.

**References**

Bettencourt da Silva RJN, Argyraki A, Borges C, Palma C, Ramsey MH (2022) Spatial modelling of concentration in topsoil using random and systematic uncertainty components: comparison against established techniques. Analytical Letters, 55 (14), 2199-2219
Borges C, Palma C, Bettencourt da Silva RJN (2019) Optimization of river sampling: application to nutrients distribution in Tagus river estuary, Analytical Chemistry, 91, 5698-5705
Borges C, Palma C, Dadamos T, Bettencourt da Silva RJN (2021) Evaluation of seawater composition in a vast area from the Monte Carlo Simulation of georeferenced information in a Bayesian framework, Chemosphere, 263, 128036

# Propeller jet induced scouring in presence of a quay wall

Jesús MACÍAS-LEZCANO[1], Toni LLULL[1,2], Jochen ABERLE[1]

[1] Leichtweiß-Institute for Hydraulic Engineering and Water Resources, Div. of Hydraulic Engineering and River Morphology, Technische Universität Braunschweig, Germany
j.macias-lezcano@tu-braunschweig.de
jochen.aberle@tu-braunschweig.de

[2] Dept. of Nautical Science and Engineering, Maritime Engineering Laboratory, Universitat Politècnica de Catalunya - Barcelona TECH (UPC), Spain
antoni.llull.marroig@upc.edu

ABSTRACT

In this work, a set of laboratory experiments to study the temporal development of the scour induced by a ship propeller model over a non-cohesive sediment bed is presented. By changing the propeller type, its rotational speed, the bed and wall clearance distances, and the bed-sediment, different boundary conditions were tested. The results show a consistent trend between the measured maximum scour depth and the wall and bed clearance distances. The dependence of the maximum scour depth on the propeller rotational speed is also consistent among the experiments. In addition, the scour geometry is analysed from the relationship between the main dimensions of the scour hole and the eroded volume. The obtained data will be used to derive an equation to estimate the temporal development of the maximum scour depths induced by ship propellers for cases, in which a closed-type quay wall is located in front of the propeller plane.

## 1. Introduction

The highly turbulent jet induced by a rotating propeller has the potential to erode the bed of waterways and in ports. The evolution of the resulting scour depth due to the erosive action of a propeller jet depends on a variety of boundary conditions. The accurate estimation of this depth requires a sound understanding of the scouring process due to ship-induced propeller jets, which is still lacking. In this sense, for decades, laboratory experiments have been performed in order to investigate this phenomenon without the presence of structures that impede the development of the scour (Blaauw & van de Kaa, 1978; Hamill, 1987; Hong et al., 2013; Ferraro et al., 2021). However, the scouring potential of the propeller wash increases if the jet is set under confinement by vertical structures, e.g., quay walls. Some researchers have studied the effect of these vertical quay walls on the scour geometry (Hamill et al., 1999; Yuksel et al., 2019; Llull et al., 2021), and this study aims to extend these studies based on the analysis of a novel experimental campaign.

## 2. Methods

The experiments were carried out in the hydraulic laboratory of the Leichtweiß-Institute for Hydraulic Engineering and Water Resources (LWI) of the Technische Universität Braunschweig. The experiments were performed in a 30 m long, 2 m wide and 0.8 m deep flume that was used as a tank, since the tests were carried out under still water conditions. A sediment recess section (3 m in the spanwise direction, 1m in axial direction of the propeller jet, and 0.5 m deep) was placed against one of the acrylic glass walls of the flume which, at the same time, acted as the quay wall structure. The influence of the sediment size was considered by testing different types of sediment. Most of the experiments were carried out with coarse sand as bed material which had an average grain size of $d_{50}$ = 0.0008 m. These experiments were complemented by two additional sets of experiments using medium sand ($d_{50}$ = 0.0002 m) and fine gravel ($d_{50}$ = 0.0041 m). Also, two physical models of common propeller types (Kaplan P274r propeller and Wageningen B-Series 4.70) consisting of four blades and a diameter of $D_p$ = 0.11 m were used for comparison purposes. The experimental boundary conditions are presented in Table 1.

**Table 1.** Boundary conditions

| Type of propeller | Propeller diameter $D_p$ [m] | Propeller rotational speed $n_p$ [rpm] | Wall clearance distance $X_w/D_p$ [-] | Bed clearance distance $Z_b/D_p$ [-] | Sediment $d_{50}$ [mm] |
|---|---|---|---|---|---|
| Kaplan; Wageningen | 0.11 | 301;594;1188;1339 | 2;3;4;5;6 | 1;1.5 | 0.2;0.8;4.1 |

The temporal evolution of the scour was monitored after predefined time intervals by stopping and resuming the experiments. In selected experiments, the morphology of the whole sand recess was additionally measured by using an array of 16 echosounders (SeaTek). These measurements enabled also to determine the time-evolution of the eroded volume. In other experiments, the scour measurements were performed punctually at locations of interest at the same pre-defined time steps using the bottom detection function of a Vectrino Profiler (Nortek). In all the experiments, Structure-from-Motion photogrammetry technique was used to generate 3D models of the undisturbed bed before the experiment and the scour geometry after completion of the experiment, so that the eroded volume could be computed.

## 3. Results

The results confirmed the dependency of the scour geometry and, specifically, its maximum depth $\varepsilon_{max}$ on the varied boundary conditions. A deeper scour hole was generated as a consequence of smaller bed clearance distances, greater propeller rotational speeds, and a finer sediment size. Contrary to estimates, it was found that the greater the wall clearance distance $X_w$, the greater the maximum scour depth $\varepsilon_{max}$. The scouring mechanism can be divided into two distinct processes. The first is induced by the diffusion of the jet impinging on the bed upstream of the quay wall and is limited by the position of the quay structure. The second one is caused by the propeller jet deflected towards the bed due to the vertical obstruction. A similar trend has already been observed for open quays (Wei, 2018). When $X_w \leq X_{m,u}$, where $X_{m,u}$ is defined as the distance between the propeller face and the maximum scour depth in the unconfined case, a direct proportionality between $\varepsilon_{max}$ and $X_w$ was observed. For the complete set presented in this work, the condition $X_w \leq X_{m,u}$ calculated according to Hamill et al. (1999), was fulfilled. Therefore, it is suggested that the role played by each scouring mechanism for closed-type quays can also be determined by the ratio $X_w/X_{m,u}$. The geometric relationship of the induced scour holes is presented in Fig. 1(a), which shows the relation between the maximum scour depth and its width for different boundary conditions and time steps. The relationship between the eroded volume and the maximum scour depth was also consistent, as shown in Fig. 1(b).

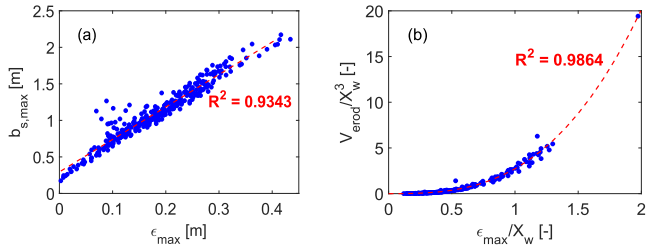



**Fig. 1.** Geometric relationship within the scour hole under free propeller boundary conditions, i.e., without a ship hull, rudder and/or nozzle. **(a)** Linear agreement between width $b_{s,max}$ and depth $\varepsilon_{max}$ of the induced scour holes. **(b)** Power-law dependence between the eroded volume $V_{erod}$ and maximum scour depths $\varepsilon_{max}$.

**Acknowledgements**

The authors thank Mrs. Lina Schulz and Mr. Florian Haselow, who took part in the experimental activity during their B.Sc. theses. This research was carried out within the framework of the project "IHATEC – Innovative Hafentechnologien. Propellerstrahlinduzierte Erosionserscheinigungen" funded by the German Federal Ministry for Digital and Transportation (BMDV).

**References**

Blaauw HG, van de Kaa EJ (1978) Erosion of bottom and sloping banks caused by the screw race of manoeuvring ships, Delft Hydraulics Laboratory, Delft, Netherland, 1-12

Ferraro D, Lauria A, Penna N, Gaudio R (2021) Temporal development of unconfined propeller scour in waterways, Physics of Fluid, 33, 095119

Hamill GA (1987) Characteristics of the screw wash of manoeuvring ship and the resulting bed scour, PhD thesis, Queen´s University of Belfast, Northern Ireland, UK

Hamill GA, Johnston H, Stewart D (1999) Propeller wash scour near quay walls, Journal of Waterway, Port, Coastal and Ocean Engineering, 125:4, 170-175

Hong J, Chiew Y, Cheng N (2013) Scour caused by a propeller jet, Journal of Hydraulic Engineering, 139, 1003-1012

Llull T, Mujal-Colilles A, Gironella X (2021) Twin propeller time-dependent scouring processes, Physical experiments, Ocean Engineering, 236, 109461

Yuksel Y, Tan RI, Celikoglu Y (2019) Determining propeller scour near a quay wall, Ocean Engineering 188, 106331

Wei M (2018) Propeller jet flow and its associated scour hole around open quay structures, PhD thesis, Nanyang Technological University, Singapore

# Decomposing alongshore sediment transport into cells and compartments: a case study in the Gulf of Riga, the Baltic Sea

Mikolaj JANKOWSKI[1], Kevin PARNELL[1], Tarmo SOOMERE[1]

[1] Wave Engineering Laboratory, Department of Cybernetics, School of Science, Tallinn University of Technology, Estonia
mikolaj.jankowski@taltech.ee
kevin.parnell@taltech.ee
tarmo.soomere@taltech.ee

ABSTRACT

The Gulf of Riga's western southern and eastern shores belong to a more than 700 km long interconnected sedimentary coastal system of the eastern Baltic Sea. Even though many shore segments of this water body are relatively straight, the presence of small headlands and even minor changes in the orientation of the coastline together with a two-peak directional system of predominant winds leads to a natural division of this system in numerous fully or partially separated segments. We decompose this system into single sedimentary cells and compartments based on the analysis of wave-driven bulk and net potential sediment transport using high-resolution wave time series and the Coastal Engineering Research Centre (CERC) approach.

## 1. Wave-driven sediment transport and compartments along rapidly developing shores

Wave-driven sediment transport plays a particularly large role in shaping the shores of relatively young water bodies, such as the Baltic Sea, the coasts of which are still in rapid development. This mostly counterclockwise transport may, theoretically, bring sediment grains from the Sambian Peninsula to Pärnu Bay in the Gulf of Riga over a more than 700 km long coastal stretch. Wave-driven transport, estimated at a relatively low resolution of about 5.5 km, involves one major accumulation area near Cape Kolka (north-western Latvia) and one almost impermeable divergence area near Cape Akmenrags on the western coast of Latvia (Soomere and Viška, 2014). These features divide the entire sedimentary system into three major compartments. Two of them are weakly interconnected across Cape Akmenrags while sediment transport from the Baltic proper shores to the interior of the Gulf of Riga has an almost entirely one-way character.

## 2. The task and the methods

This resolution is too low to identify smaller-scale structures of alongshore sediment transport and partially or totally separated sedimentary cells on this coastal stretch. Some indication about their presence can be inferred from frequent divergence areas and temporary reversals of alongshore sediment flux (Viška and Soomere, 2013). These features characterize the interplay of the shape of this gradually straightening coastal stretch, with numerous minor headlands, and the two predominant wind directions in the area.

We make an attempt to decompose the sedimentary system along a semi-isolated part of this coastal stretch in the interior of the Gulf of Riga into partially or totally separated sedimentary cells at a resolution that matches the typical spatial scale of coastal formations. We employ wave time series replicated using a three-level nested SWAN wave model forced by ERA5 wind fields (Giudici et al., 2023). This model is applied to the entire Baltic Sea at a 3 nautical mile (nmi) resolution, to the Gulf of Riga at a 1 nmi resolution, and to the nearshore segments of the Gulf at a resolution down to about 250 m (Najafzadeh et al., 2024). The shoreline of the Gulf of Riga is divided into about 600 m long sectors. It is assumed that seabed is locally plane in the sectors, with isobaths parallel to the shoreline. This assumption, even though not perfect at some locations, makes it possible to adequately evaluate the joint effect of shoaling and refraction to properties of waves that approach the shore at a relatively large angle during their propagation from the nearshore model grid cells to the breaker line. The bulk and net potential sediment transport is evaluated for such segments using the

Coastal Engineering Research Centre (CERC) approach (USACE, 2002) based on time series of wave properties at the breaker line, and applied exactly as in (Viška and Soomere, 2013). As we are interested in sediment flux divergence and convergence areas, the outcome of simulations is invariant with respect to environmental parameters (water salinity, grain size, density, porosity, and availability of fine sediment) and robust with respect to specification of the CERC parameter and breaking index.

## 3. The decomposition

As an example of the output of the study, we present the decomposition of the sedimentary system along the eastern coast of the Gulf of Riga (Fig. 1). Even though this coast is almost straight, small variations in the coastline orientation lead to the presence of several sedimentary cells. While some cells are separated by river mouths, small headlands such as Cape Kurmrags also serve as invisible barriers to sediment transport and thus separators of sedimentary cells with typical length of about 5 km. Extensive variation in the intensity of potential net transport indicate areas prone to erosion (if the net transport increases from the left to the right) and accumulation (if the net transport accordingly decreases).

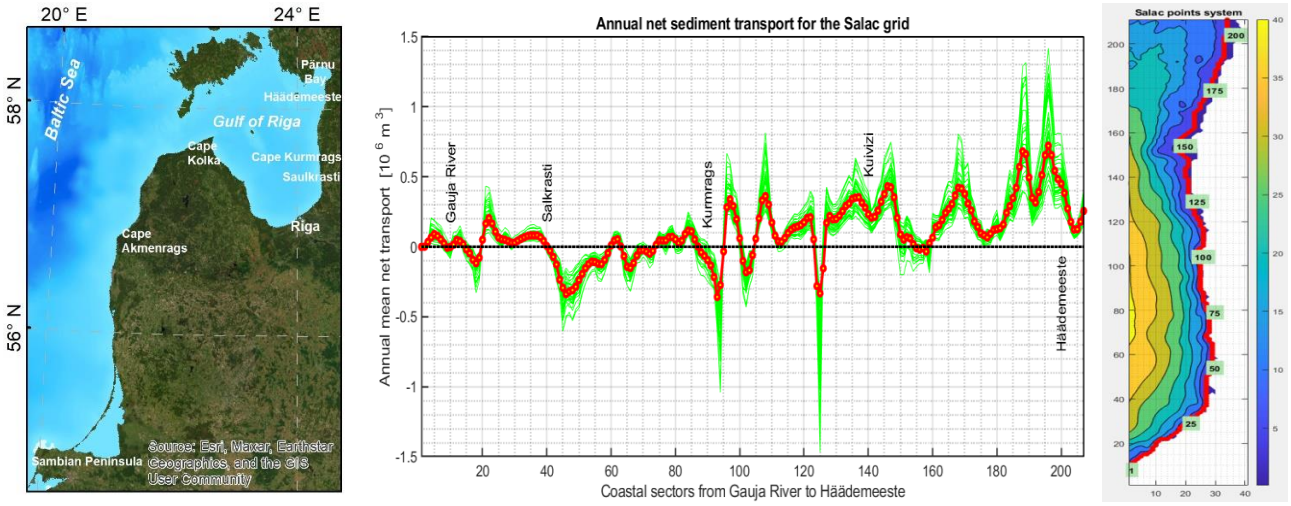



**Fig. 1.** Location scheme of the Gulf of Riga (left panel), simulated potential net sediment transport along an almost straight stretch of the eastern coast of the Gulf of Riga from the mouth of River Gauja (about 10 km to the north of Riga) in Latvia to Häädemeeste township (25 km to the south of Pärnu) in Estonia (middle panel) and the location of grid cells of the wave model in this stretch (right panel). Green lines: potential net sediment transport in single years, red: the average of this transport over 33 years 1990–2022. The length of each coastal sector is about 600 m. The sediment transport zero-downcrossings reflect convergence areas of sediment flux and zero-upcrossings indicate divergence areas. Systematic divergence areas serve as invisible barriers for sediment flux. Coastal segments between such areas (zero-upcrossings) serve as almost isolated sedimentary cells.

## 4. The message

The presented decomposition provides crucial information for managing the coastal area in terms of the location of most probable erosion and accumulation regions. It also indicates how far sediment may be transported from a particular location under the current wind and wave climate. This information is central for closing the sediment budget in this microtidal water body where the cut and fill cycle involves large alongshore excursions of coastal sediment (Eelsalu et al., 2022).


### Acknowledgements

The research was co-supported by the Estonian Research Council (grant PRG1129) and the European Economic Area (EEA) Financial Mechanism 2014–2021 Baltic Research Program (grant EMP480).


### References


Eelsalu M, Parnell KE, Soomere T (2022) Sandy beach evolution in the low-energy microtidal Baltic Sea: attribution of changes to hydrometeorological forcing, Geomorphology, 414, 108383. https://doi.org/10.1016/j.geomorph.2022.108383

Giudici A, Jankowski MZ, Männikus R, Najafzadeh F, Suursaar Ü, Soomere T (2023) A comparison of Baltic Sea wave properties simulated using two modelled wind data sets, Estuarine, Coastal and Shelf Science, 290, 108401. https://doi.org/10.1016/j.ecss.2023.108401

Najafzadeh F, Jankowski MZ, Giudici A, Männikus A, Suursaar Ü, Soomere T, Viška M (2024) Spatiotemporal variability of wave climate in the Gulf of Riga, Oceanologia, 66, early access, https://doi.org/10.1016/j.oceano.2023.11.001.

Soomere T, Viška M (2014) Simulated sediment transport along the eastern coast of the Baltic Sea, Journal of Marine Systems, 129, 96–105. https://doi.org/10.1016/j.jmarsys.2013.02.001

USACE (2002) Coastal Engineering Manual, Department of the Army, U.S. Army Corps of Engineers, Manual No. 1110-2-1100.

Viška M, Soomere T (2013) Simulated and observed reversals of wave-driven alongshore sediment transport at the eastern Baltic Sea coast, Baltica, 26 (2), 145–156. https://doi.org/10.5200/baltica.2013.26.15

# Unveiling WORSICA's Role in Tracking the Dynamics of the Óbidos Lagoon

Alberto AZEVEDO[1], Ricardo MARTINS[2], Anabela OLIVEIRA[3], André B. FORTUNATO[4]

[1,2,3,4] Laboratório Nacional de Engenharia Civil (LNEC), Portugal
[1]aazevedo@lnec.pt ,[2]rjmartins@lnec.pt ,[3] aoliveira@lnec.pt, [4]afortunato@lnec.pt

**Abstract**

Coastal zones necessitate efficient monitoring systems for assessing changes in water presence and area. Utilizing Sentinel-2 multispectral satellite images, the WORSICA web portal introduces advanced water indices (NDWI, MNDWI, AWEI, and AWEIsh) for real-time monitoring of Óbidos Lagoon in Portugal. This platform offers critical insights for sustainable coastal management and risk assessment. Additionally, the integration of the Flood2Topo methodology facilitates topobathymetry retrieval in intertidal zones, enhancing understanding of coastal dynamics. By tracking water levels, identifying flood-prone areas, and evaluating ecological changes, WORSICA aids in formulating effective conservation strategies and sustainable resource management plans. Integration of temporal data improves the accuracy of topobathymetric models, empowering stakeholders to make informed decisions regarding coastal conservation and management. With its integrated features and advanced capabilities, WORSICA emerges as an essential tool for comprehensive coastal monitoring, contributing to long-term preservation of coastal ecosystems and resilience of coastal communities.

## Monitoring of the Óbidos Lagoon

The WORSICA web portal revolutionizes coastal monitoring, granting the research and technical communities' free access to advanced tools for tracking water dynamics. Leveraging the computational resources provided by the INCD (National Distributed Computing Infrastructure in Portugal), WORSICA integrates Sentinel-2 multispectral satellite imagery and state-of-the-art water indices (Calatrava *et al.*, 2023). In the present study, this innovative platform contributes to the real-time monitoring of the Óbidos Lagoon in Portugal (see Fig.1a), providing researchers and stakeholders with vital insights for sustainable coastal management and risk assessment.




a) b)

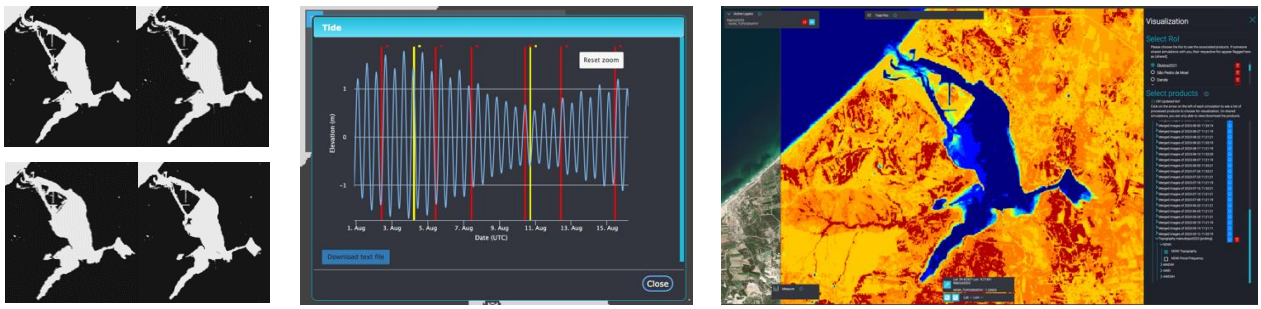
**Fig. 1.** a) Location of the Óbidos lagoon and b) an example of the Sentinel-2 image from October 6, 2023, illustrates the detection of the water-land interface line in the Óbidos lagoon using the NDWI water index

### *1.1. Coastline detection*

WORSICA utilizes advanced water indices derived from Sentinel-2 multispectral satellite imagery, such as NDWI, MNDWI, AWEI, and AWEIsh, to monitor the dynamic evolution of the coastline and water extension of the Óbidos Lagoon in Portugal comprehensively. By leveraging these indices, the platform effectively tracks changes in water levels and area extension, providing crucial insights into coastline dynamics. These indices not only help identify potential flood-prone areas but also contribute significantly to assessing morphodynamic changes at the mouth of the Óbidos Lagoon. Through integrating historical and real-time data, WORSICA enables a comprehensive understanding of the region's coastal evolution, empowering stakeholders to implement informed conservation strategies and sustainable management plans.

### *1.2. Flood2Topo methodology*

Flood2Topo is integrated into WORSICA, employing a methodology that utilizes water indices, the FES2014 tidal model, and other tidal data as inputs (Fassoni-Andrade et al., 2021, 2023). This methodology aims to determine precise topobathymetric information in the intertidal zones by establishing an equivalence between flood frequency and water level exceedance probability. Specific tidal levels are attributed to various coastlines derived from the water indices. Consequently, a topobathymetric model is constructed for the intertidal zones, offering a comprehensive understanding of the lagoon's hydrological characteristics and sediment dynamics. Leveraging temporal variations, WORSICA facilitates the generation of accurate topobathymetric models, empowering stakeholders to make informed decisions regarding coastal conservation and management.




a) b) c)

**Fig. 2.** Example of the Flood2Topo methodology applied to the Óbidos lagoon during the period of study. a) Representation of all water masks retrieved from the water indices (NDWI, MNDWI, AWEI, or AWEIsh); b) tidal levels for each image; c) final topobathymetric model for the study region.

## Conclusions

WORSICA, with its integrated features and advanced capabilities, is an indispensable tool for comprehensive coastal monitoring and management. By leveraging Sentinel-2 multispectral satellite images and innovative water indices, along with the Flood2Topo methodology, the portal provides valuable insights into the dynamic nature of specific coastal regions. However, it has limitations, such as dependency on water levels for defining the water mask from the indices and the inability to use FES2014 data within the lagoon area due to differences in water levels inside and outside the lagoon. Despite these limitations, this holistic approach aids in developing sustainable conservation strategies, effective risk assessment, and decision-making, ensuring the long-term preservation of coastal ecosystems and fostering resilient coastal communities.

#### References

Calatrava, A., Asorey, H., Astalos, J., Azevedo, A., Benincasa, F., Blanquer, I., Bobak, M., Brasileiro, F., Codo, L., del Cano, L., Esteban, B., Ferret, M., Handl, J., Kerzen- macher, T., Kozlov, V., Krenek, A., Martins, R., Pavesio, M., Rubio-Montero, A.J., Sanchez-Ferrero, J., 2023. A survey of the European Open Science Cloud services for expanding the capacity and capabilities of multidisciplinary scientific applications. Distributed, Parallel, and Cluster Computing (cs.DC), 46p. https://doi.org/10.48550/arXiv.2211.07738.

Fassoni-Andrade, A.C, Durand, F., Azevedo, A., Bertin, X., Santos, L.G., Khan, J.U., Testut, L., Moreira, D.M., 2023. Seasonal to interannual variability of the tide in the Amazon estuary, Continental Shelf Research, Volume 255, 2023, 104945, ISSN 0278-4343, https://doi.org/10.1016/j.csr.2023.104945.

Fassoni-Andrade, A. C., Durand, F., Moreira, D., Azevedo, A., dos Santos, V. F., Funi, C., and Laraque, A.: Comprehensive bathymetry and intertidal topography of the Amazon estuary, Earth Syst. Sci. Data, 13, 2275–2291, https://doi.org/10.5194/essd-13-2275-2021, 2021.

# Deep Neural Network Enhanced Early Warning System for Ports Operations

Liliana PINHEIRO[1], Juana FORTES[1], Andreia GOMES[1]

[1]Laboratório Nacional de Engenharia Civil, Portugal
lpinheiro@lnec.pt, jfortes@lnec.pt, ahgomes@lnec.pt

ABSTRACT

Downtime of port terminals results in large economic losses and has a major impact on the overall competitiveness of ports. Early Warning Systems (EWS) are an effective tool to reduce ports' vulnerability by increasing their preparedness and planning capacity to either avoid or efficiently respond to emergency situations.

The SAFEPORT EWS predicts met-ocean variables and their impact on ships (navigating, docking or moored) and port operations daily, Pinheiro et al. (2020), and provides alerts for emergencies and operational constraints. It is currently implemented in six ports, namely: Praia da Vitória, São Roque do Pico and Madalena do Pico, in the Azores archipelago, and Sines, Aveiro and Figueira da Foz, on the west coast of Portugal.

All information provided by this EWS is available in a dedicated website and mobile application. In addition, an alert bulletin is sent by e-mail to interested parties. This provides port stakeholders with a decision support tool for timely implementation of mitigation measures to prevent accidents and economic losses.

This system is now being enhanced with artificial neural network tools to obtain more accurate results from numerical wave propagation models and to allow the use of complex and time-consuming numerical models in an operational framework. As with any EWS, its usefulness depends heavily on its reliability, accuracy, and consistency. Two types of ANN have therefore been developed.

## 1. The Early Warning system

The SAFEPORT EWS follows a series of EWS from the HIDRALERTA platform, which includes three Azorean ports: Praia da Vitória, S. Roque do Pico and Madalena do Pico, (Poseiro, 2019 & Pinheiro et al., 2020), five other ports on the west coast mainland: Sines, Aveiro, Figueira da Foz, Ericeira and Peniche, and three coastal areas: Costa da Caparica, Faro and Quarteira. All the EWS of HIDRALERTA include coastal flooding and/or wave overtopping of coastal structures. Some of the ports in Hidralerta have implemented the SAFEPORT Port Navigation and Operations Alert System for certain vessels.

The system uses available forecasts of regional offshore wind and wave characteristics, together with astronomical tidal data, as inputs to a series of numerical models. These numerical models provide estimates of wave and wind characteristics at all scales, from regional, simulated with multiple nested grids using the SWAN model (Booij et al., 1996), to local, using a non-linear Boussinesq-type model or a linear mild-slope model. The EWS uses DREAMS and BOUSS-WMH to transfer the wave characteristics from the harbour entrance area to the harbour interior. The numerical model DREAMS (Fortes, 2002) is a linear finite element model based on the mild slope equation to simulate the propagation of monochromatic waves. The BOUSS-WHM model, (Pinheiro et al., 2011) is a nonlinear finite element model based on the extended Boussinesq equations derived by Nwogu (1993), capable of simulating the propagation of regular and irregular waves.

Finally, the ship's response to these wave and wind forcings is computed using a 3D panel method hydrodynamic model (Korsemeyer et al. 1988) and a motion equation solver.

Predicted hourly movements and mooring forces are compared with pre-set thresholds. An assessment of the probability of these values being exceeded gives a hazard level. The risk levels depend on the Maximum Breaking Load (MBL) of the mooring lines (OCIMF, 1992). Finally, on the basis of the predicted risk level, emergency situations and the safety of port operations can be foreseen in advance (72 hours) and appropriate warnings are issued.

## 2. Artificial Neural Networks

Two types of ANN were developed for the system. The first type of ANN uses available measured data to train the ANN and then calibrate/correct the numerical results to achieve more accurate predictions.

Three neural networks were trained to evaluate the possibility of improving the accuracy of the forecasts. The Keras open source neural network library, was used to develop the NNs.

Input layer data consists of a 40-year database of offshore wave parameters (Hs, Tz and θ) and wind data (speed and θ), Figure 1. Training data consists of 20-year measured wave characteristics from the Sines 1D wave buoy.

Output layers (one for each NN) consist of the wave parameter at the buoy, Hs, Tz and θ. To train the network 80% of the data was used and 20% was used to test it. The cost function is the mean squared error, mse, of the entire training set. The rectified linear unit (ReLU) activation function is used to introduce non-linearity to the network. The trained networks provided more accurate estimates for all variables and thus can be used to improve the reliability of the EWS.

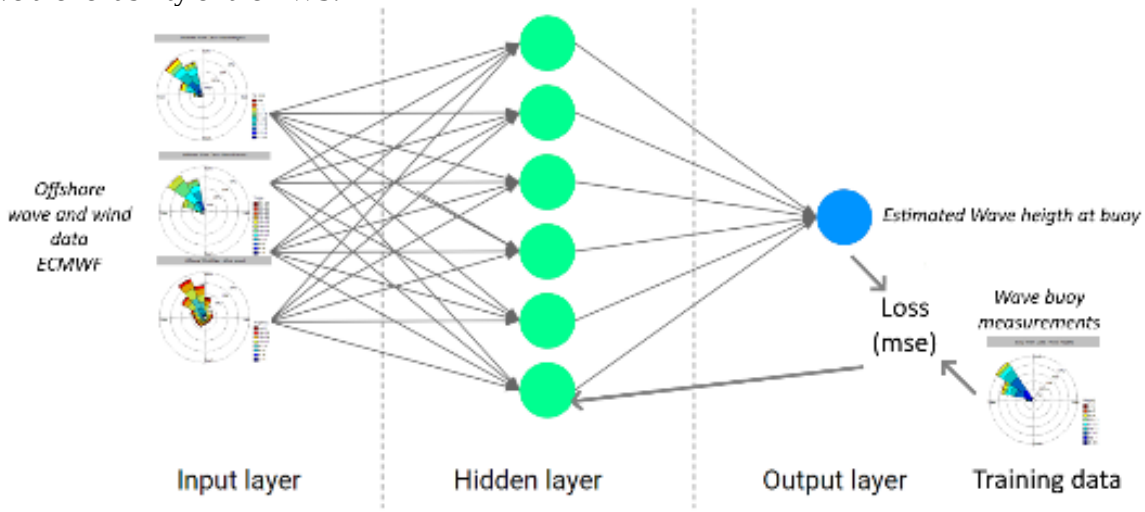



**Fig. 1.** Structure of the Neural Network for the wave height estimation/forecast at the Sines Buoy.

The second type of ANN uses an extensive set of pre-run complex numerical simulations using a Boussinesq-type numerical model for the wave propagation inside the sheltered area of the harbour to train the ANNs. The output of this ANN enables the system to get the same complex hydrodynamic fluid flow in shallow waters sheltered areas and around the 3D ship hull simulations results in the most time effective manner.

Results are extracted at any number of points along the ship's navigation channels, berths and moorings.

Another ANN is trained to reproduce the ship's response to wave and wind forcings using a 3D panel method hydrodynamic model (Korsemeyer et al. 1988) and a motion equation solver. Each specific ship hull and mooring arrangement will be replaced by a specific ANN.

**Acknowledgements**

The authors thank the financial support of LIFE Garachico Project (LIFE20 CCA / ES / 001641), “Fundo Azul” project BlueSafePort (Ref: FA_04_2017_016) - Safety System for Manoeuvring and Moored Ships in Ports and the FCT project To-SeAlert: (Ref. PTDC/EAM-OCE/31207/2017).

**References**

Booij, Holthuijsen, Ris (1996) The SWAN wave model for shallow water. ICCE´96 Orlando, pp. 668-676.

Fortes, C.J.E.M. (2002). Transformações não lineares de ondas em portos. Análise pelo método dos elementos finitos. Tese de doutoramento. Lisboa: IST/DEM.

Korsemeyer, Lee, Newman, Sclavounos (1988): The analysis of wave effects on tension-leg platforms, 7th International Conference on Offshore Mechanics and Arctic Engineering, Houston, Texas, pp. 1-14.

Pinheiro, Fortes, Reis, Santos, Guedes-Soares (2020): Risk Forecast System for Moored Ships. Coastal Engineering Proceedings, (36v), management.37. https://doi.org/10.9753/icce.v36v.management.37

Pinheiro, Fortes, Reis, Santos, Guedes-Soares (2022) Neural Networks For Optimization Of An Early Warning System For Moored Ships In Harbours. Coastal Engineering Proceedings, (36v), management.37.

Pinheiro, Fortes, Santos, Fernandes & Walkley (2011). Boussinesq-type Numerical Model for Wave Propagation Near Shore and Wave Penetration in Harbors. MARTECH 2011 1st International Conference on Maritime Technology and Engineering. Lisboa, 10-12 May.

Pinheiro, Fortes, Santos, Fernandes, (2013). Numerical software package SWAMS – Simulation of Wave Action on Moored Ships. Proc. PIANC 3nd Mediterranean Days of Coastal and Port Engineering, 22 a 24 de maio, Marseille, França.

Poseiro, Gonçalves, Reis, Fortes, (2017) – Early warning systems for coastal risk assessment associated with wave overtopping and flooding. Journal of Waterway, Port, Coastal, and Ocean Engineering.

# Construction of the New Port of Lajes das Flores

Flávio PEREIRA[1], Hugo LEITE[2], João ROBALO[3], Luís FERNANDES[4]

[1] Portos dos Açores, S.A., Portugal

fpereira@portosdosacores.pt

[2,3,4] MSW, Estudos e Projetos de Obras Marítimas, Lda.

hleite@msw-consultores.pt

jrobalo@msw-consultores.pt

lfernandes@msw-consultores.pt

ABSTRACT

The passage of hurricane Lorenzo through the Azores archipelago, in October 2019, caused serious damage to the Port of Lajes das Flores, in Flores Island, which is the island's only commercial port where goods, essential to its population, enter and leave by sea, severely restricting its operations. For this reason, it is both justified and expected a special sensibility with this from the political decision-makers, since the non-operation of this port for days, or even weeks, has serious social and economic impacts in the populations of Flores and Corvo islands, not only in the imports of essential goods and other things, but also in the exports of goods produced there. In order to solve this problem, a lot of resources have been mobilized to Flores Island, expected to be financed by community funds and also by regional funds through a program contract, not only for the chartering of ships and complementary support measures for the populations and companies, but essentially to carry out a series of emergency works to allow the facilities that were still operational to be used. Among those works were several urgent cleaning and clearing operations, as well as the contracts "*Proteção de Emergência ao terrapleno e cais a -5m (ZH)*" (Emergency protection of the embankment and quay at -5m (ZH)) and "*Empreitada de Construção de Ponte-Cais*" (Jetty construction contract), concluded in June 2023 and January 2023, respectively.

In addition, Portos dos Açores, S.A. has contracted the necessary studies and designs for the Construction of the New Port of Lajes das Flores, having the respective detailed design already been completed. The tender for the final contract has also already been launched with a base price of one hundred and seventy-two million euros and an execution time of sixty months, making it the largest maritime construction work ever carried out in the Autonomous Region of Azores. The efforts required to carry out an investment of this magnitude involve a great deal of work, including: topographic surveys (3D), geological and geotechnical studies, Physical Model tests in channel (2D), Simulator Maneuvering Studies, Tridimensional Physical Model tests, all phases of the Detailed Design (with the inherent challenges of dimensioning marine works with a sea disturbance never recorded before), design review procedures, among others. Geotechnical studies and surveys are also underway with the purpose of exploring a new quarry on the island, given the limitation of existing natural resources and the huge volume of rockfill of various sizes required in an intervention of this nature. In terms of project components, the main one is the maritime one, with the construction of the new breakwater, one component rebuilt and the other built as new, with adherent quay, also including general dredging and rehabilitation of the northern and southern sectors of the port, which were also destroyed. On land, it involved the rehabilitation of the port embankment, with the construction of three new buildings (a new multipurpose building to replace the one destroyed in 2019, including the port operations and support for the southern sector of the port, another, to be rebuilt, dedicated to support for the northern sector of the port, and another for the port access gate) and yet another building entirely dedicated to drinking water tanks for supply and firefighting. Across the board, new utilities infrastructures were developed, including the electrical grid, the water supply and firefighting systems, rainwater drainage system, wastewater sewage system, telecommunications, CCTV, access control and, finally, a new infrastructure for fuel pipelines.

Meanwhile, in December 2022, the port of Lajes das Flores was once again hit by a violent storm resulting from Efrain depression, which caused even more damage to the existing breakwater and embankment, leading to a deeper destruction of a section of the breakwater, which significantly degraded the shelter conditions in the port basin and on the newly built jetty, increasing the risk of damage. In this respect, Portos dos Açores, S.A. has, once again, as a matter of total urgency, provided studies and designs for the respective repair works, having already proceeded with the total execution of them (completed in September 2023), which was required to be urgent, swift, started and concluded during the summer period, with the aim of using resources from the region and, to the greatest possible extent, reusable in the definitive work.

In addition to the technical aspects, an investment of this importance and size involves also economic, financial, social and political aspects with high exposure and pressure, among others.

The aim of this communication is to address all these aspects, sharing their challenges, difficulties and achievements from the perspective of the project Owner, the port authority.



**Fig. 1.** Aerial photo of the Port of Lajes das Flores before hurricane Lorenzo



**Fig. 2.** Aerial photo of the Port of Lajes das Flores after being hit by hurricane Lorenzo, in October 2019



**Fig. 3.** Aerial photo of the Port of Lajes das Flores after being hit by a violent storm, resulting from Efrain depression, in December 2022

**References**

Morim de Oliveira, MSW – Estudos e Projetos de Obras Marítimas, Lda. (2023) – "*Projeto de Execução para a Construção do Novo Porto das Lajes das Flores*" (Detailed design for the Construction of the New Port of Lajes das Flores);
Laboratório Nacional de Engenharia Civil - LNEC (2021) – "*Reconstrução do Molhe-Cais do porto das Lajes das Flores – Ensaios em modelo físico bidimensional*" (Rebuilding of the Port of Lajes das Flores' breakwater – Bidimensional Physical Model tests).

# Assessment of soft coastal protection alternatives for Saint-Louis (Senegal)

Francisco SANCHO[1], Filipa S. B. F. OLIVEIRA[1], Alphonse NAHON[1]

[1] Laboratório Nacional de Engenharia Civil, Portugal
fsancho@lnec.pt, foliveira@lnec.pt, anahon@lnec.pt

ABSTRACT

The Barbarie spit (*Langue de Barbarie*) is a 100–400 m-wide West-Africa coastal barrier that has fluctuated in length between 10 and 30 km over the last century (Anthony, 2015). The changes in length reflect the variable position of the Senegal river mouth, where rates of spit growth vary greatly (100 to 700 m/year), depending on variations in wave characteristics, river discharge and river mouth dynamics, combined with barrier-breaching events (Bergsma et al., 2020).

The Barbarie sandy barrier protects the island of Saint-Louis, within the Senegal river delta. Of particular significance is the historic city of Saint-Louis, a UNESCO world heritage city (Anthony, 2015). Coastal erosion can be severe along the 2 km stretch in front of Saint-Louis, with retreat rates of up to 20 m/year (Tavenau et al., 2021). Moreover, the coast in front of the city is home to small-craft fishing activity of high socio-economic implications.

Given the Saint-Louis settings and the Barbarie spit dynamics, the city is at high coastal erosion and flooding risk. So, informed coastal management is necessary, based on the assessment of alternative coastal protection solutions. Given the world-wide success of several soft-management (beach nourishment) interventions, this paper addresses and compares four alternative solutions, consisting of artificial protective offshore islands and shore-attached peninsulas.

## 1. Methodology

ShorelineS (Roelvink et al., 2020) is an open-source, free-form coastline model that can describe most kind of planar coastal transformations based on the relatively simple principles of 1) longshore transport gradient driven changes as a result of coastline curvature and 2) spit formation at high-angle wave incidence (Elghandour and Roelvink, 2020). It relies on a vector-based coastline concept, describing the coastline like a freely moving string of points. An arbitrary number of coastal sections is supported, which can be open or closed, and can interact with each other through relatively straightforward merging and splitting mechanisms. Also, rocky parts or structures may block wave energy and/or interrupt longshore sediment transport. These features allow for developing shoreline undulations and formation of spits, migrating islands, merging of coastal shapes, salients and tombolos.

In this paper, the model is first applied and calibrated with satellite derived shorelines of Barbarie spit (Fig. 1), from 2015 to 2019. Model parameters were set to reproduce the estimated net average littoral drift in this area, as well as the Barbarie spit growth rate. Subsequently, the model is used to assess the medium to long term coastal evolution, forced by the hindcast wave time series. Several options in terms of intervention at the nearshore region seaward of Saint-Louis are assessed, with nourished sand mounds varying in initial number and shape.

## 2. Results and preliminary conclusions

The tested soft-solutions caused the breaching of Langue de Barbarie within less than 3 years of simulation, except for one out of four solutions. These breaches occurred mostly south of Saint-Louis (within 1-3 km away), as can be seen in Fig. 2 for one of the solutions. The breaches are likely caused by shoreline instabilities triggered by the partial and transitional sheltering effect of the interventions. These instabilities and the erosion/accretion patterns at Langue de Barbarie, however, are not restricted southwards of Saint-

Louis. Compared to other locations with less intense longshore sediment transport, the lifetime of the soft solutions sandy mounds appeared to be quite brief (of the order of 3 years).

To conclude, it would be desirable to confirm the present findings by confronting them with those from alternative shoreline evolution models.

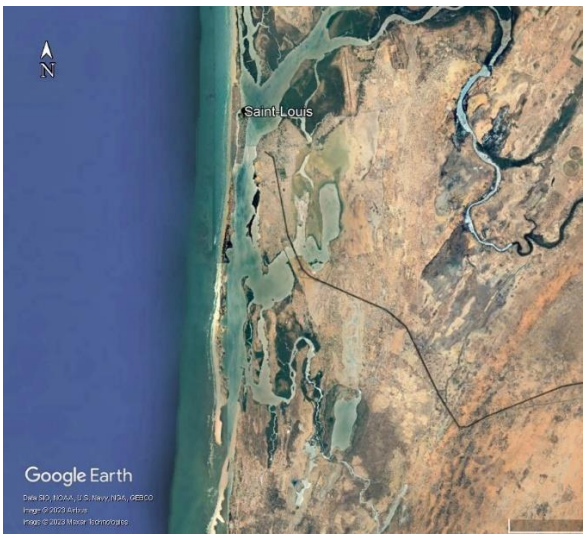



**Fig. 1.** General view of the coast in front of Saint-Louis (Senegal).

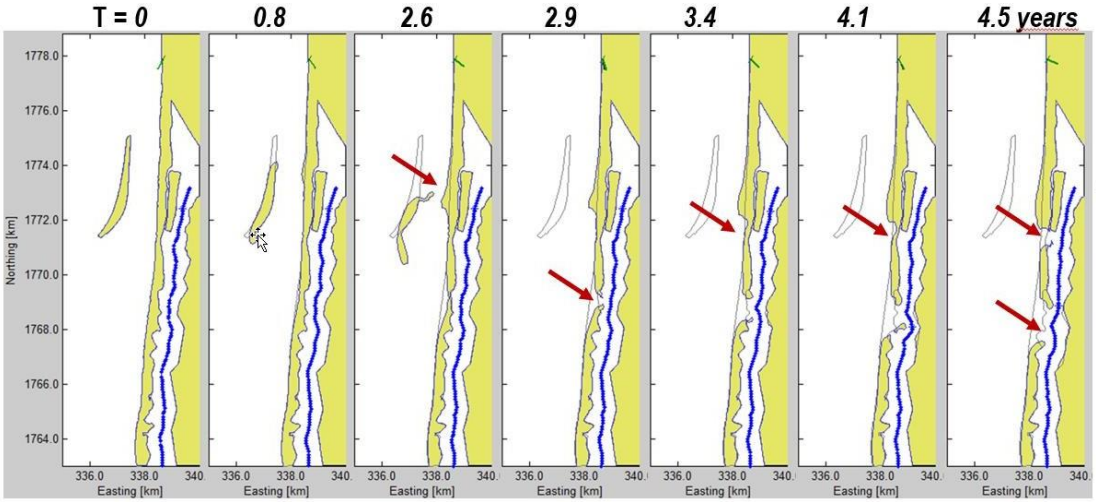



**Fig. 2.** Shoreline evolution after the implementation of an offshore island. (Arrows point to disturbances triggered by the protective solution).

**Acknowledgements**

The authors acknowledge the discussions with the promoters of the study as well as the financing from Programa de Cooperación INTERREG MAC 2014-2020, Proyecto RES-COAST. The use of the ShorelineS model was facilitated by Dano Roelvink, whose collaboration is greatly appreciated, as well as the discussions with Diogo Mendes who helped with model-setup issues. Wave hindcast data used in this study is available at https://zenodo.org/records/8139334 (Samou et al., 2023).

**References**

Anthony, E.J. (2015). Patterns of Sand Spit Development and Their Management Implications on Deltaic, Drift-Aligned Coasts: The Cases of the Senegal and Volta River Delta Spits, West Africa. In: Randazzo, G., Jackson, D., Cooper, J. (eds) Sand and Gravel Spits. Coastal Research Library, vol 12. Springer, Cham. https://doi.org/10.1007/978-3-319-13716-2_2.

Bergsma, E.W.J.; Sadio, M.; Sakho, I., Almar, R., Garlan, T., Gosselin, M. and Gauduin, H., (2020). Sand-spit evolution and inlet dynamics derived from space-borne optical imagery is the Senegal-river inlet closing?. In: Malvárez, G. and Navas, F. (eds.), Proceedings from the International Coastal Symposium (ICS) 2020 (Seville, Spain). Journal of Coastal Research, Special Issue No. 95, pp. 50-54. Coconut Creek (Florida), ISSN 0749-0208.

Roelvink, D., Huisman, B., Elghandour, A., Ghonim, M. and Reyns, J. (2020) Efficient Modeling of Complex Sandy Coastal Evolution at Monthly to Century Time Scales. Front. Mar. Sci. 7:535. doi: 10.3389/fmars.2020.00535.

Samou, M.S., Bertin, X.; Sakho, I.; Lazar, A.; Sadio, M.; Diouf, M.B. (2023). Wave Climate Variability along the Coastlines of Senegal over the Last Four Decades. *Journal Atmosphere* 2023, 14(7), 1142; https://doi.org/10.3390/atmos14071142.

Taveneau, A.; Almar, R.; Bergsma, E.W.J.; Sy, B.A.; Ndour, A.; Sadio, M.; Garlan, T., (2021). Observing and Predicting Coastal Erosion at the Langue de Barbarie Sand Spit around Saint Louis (Senegal,West Africa) through Satellite-Derived Digital Elevation Model and Shoreline. Remote Sens., 13, 2454. https://doi.org/10.3390/rs13132454.

# A wave energy assessment for the Moroccan Coast

Mariana BERNARDINO[1], Magnus SCHNEIDER[1], Liliana RUSU[2]

[1] Centre for Marine Technology and Ocean Engineering, Portugal
mariana.bernardino@centec.ulisboa.pt; magnus.schneider@tecnico.ulisboa.pt

[2] Faculty of Engineering, "Dunarea de Jos" University of Galati, Romania
Liliana.Rusu@ugal.ro

ABSTRACT

An assessment of the wave energy available in the Moroccan coast was performed using SWAN, a third-generation wave model, covering a period of 30 years, from 1991 to 2020. The wave model was forced with 10 m wind data from the new ERA-5 reanalysis and boundary conditions generated by the WAVEWATCH III model, also forced by ERA5. Significant wave height and period and wave energy were analyzed at a regional scale. The mean wave energy density within the domain is estimated to be about 20 kW/h. The most energetic area of the Moroccan coast is located at the center between the cities of Agadir and Essaouira. Five specific locations were evaluated along the coast to determine the most energetic ones. Finally, the performance of six different wave energy converters was assessed for each of the five locations.

## 1. Introduction

As a part of economic and social reforms, Morocco is undergoing an ambitious energy transition that will concentrate efforts on renewable energy sources. Since 90% of Moroccan energy supply is imported (Moreno & Ferreiro, 2018), and the demand of energy in the country is increasing about 5% each year (Costas, 2019), the potential upsides of new energy sources being installed in the country are considerable and encouraging. The global potential offshore wave energy is estimated to be of the same order of magnitude as the world's electrical consumption, (Angelis-Dimakis et al., 2011). Wave models can be used to estimate the relevant parameters needed for and evaluation of the sea state and potential power production, using wind data and boundary conditions.

In this study a 30 year hindcast of the sea state at the Moroccan coast using the SWAN model (Booij et al., 1999), forced with wind data from the ERA-5 database was produced and used to evaluate the wave energy potential in the Moroccan coast. Additionally, the performance of six different wave energy converters was assessed for five different sites along the coast. The results were compared with the relevant studies in this region.

## 2. Data and methods

The area of interest in this work, is the region between the longitudes 5.3° W and 20° W, and between the latitudes 27° N and 37° N, that includes the Moroccan Atlantic coast as well as the Canary Islands and Madeira. The modeling of wave conditions was carried out using SWAN version 1.32AB. The computational grid used spherical coordinates and was built with a spatial resolution of 0.1º, it spans between the coordinates 20º W and 5.3º W and between 27º N and 37.5º N. Bathymetry data was provided by the General Bathymetric Chart of the Oceans (GEBCO) and was adapted to a resolution of 0.05º latitudinally and longitudinally. Wind data was extracted from the ERA-5 (Hersbach & Dee, 2016) dataset with a spatial resolution of 0.25ºx0.25º (about 30km) temporal resolution of six hours. To obtain boundary conditions, the WWIII wave model, was implemented with a resolution of 0.5º by 0.5º over the North Atlantic basin and also forced with ERA5 data.

The SWAN model implementation was calibrated using the available empirical data from three wave buoys, located off the coast of Gran Canaria, off the coast of Cadiz off the coast of Faro, for 2018. Results from the

comparison between significant wave height from the SWAN model and observations, from Gran Canaria can be seen in figure1.

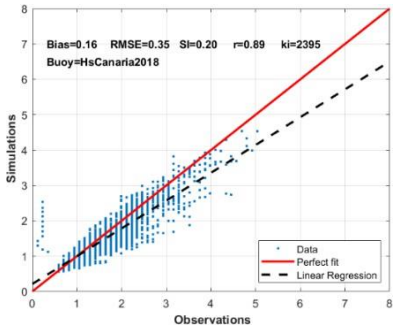



Figure 1- Validation of the SWAN model

The mean power production of the six WEC's that were considered (AquaBuoy, Pelamis, Oceantec, Wavebob, Wave Dragon and Seabased) was calculated using the Power Matrixes of each device, in five specific locations near the coast and the efficiency of each WEC was computed for each location.

Results were compared with previous studies.

## 3. Conclusions

The most energetic locations are around Agadir which is in the center of Morocco's coastline, in the north and south waves are less energetic. The most energetic site is affected by waves with an average energy of 20.7 kW/m and the least energetic site is in the north and shows values of around 9.7kW/m. The Mann-Kendall test confirmed that there is a slight positive trend regarding wave energy.
Compared with other studies, the Moroccan Atlantic coast provides more potential wave energy than its Mediterranean coast, the Cape Verde Islands, and the Canary Is-lands. However, it appears to have less wave energy than the Azores and Madeira Archipelagoes and the Portuguese continental coasts which are located in higher latitudes. Nevertheless, this area holds a large potential for wave energy production. New prototypes for wave energy converters are being produced and these new technologies could impact the feasibility of wave energy production in Morocco.

The performance assessment of the six WEC's showed that Wave Dragon is clearly more powerful than the others with a production of yearly 8 MW, while Wavebob is the least powerful with a yearly production of under 0.5 MW. The most efficient device is the Oceantec with an efficiency over 60% and the least efficient is AquaBuOY with under 10% efficiency.

**References**

Angelis-Dimakis, A. et al., "Methods and tools to evaluate the availability of renewable energy sources," Renewable and Sustainable Energy Reviews, vol. 15, no. 2. 2011. doi: 10.1016/j.rser.2010.09.049.
Booij, N., R. C. Ris, and L. H. Holthuijsen, "A third-generation wave model for coastal regions 1. Model de-scription and validation," J Geophys Res Oceans, vol. 104, no. C4, 1999, doi: 10.1029/98JC02622.
Costas, G., "Energías renovables en Marruecos," Madrid, 2019
Hersbach, H., and Dee, D., "ERA5 reanalysis is in production," ECMWF Newsletter, vol. 47, p. 7, 2016, Accessed: Oct. 13, 2022. [Online]. Available: https://www. ecmwf.int/en/newsletter/147/news/ERA5-reanalysis-production.
Moreno, L., & Ferreiro, A. (2018). Marruecos: la energía se renueva. http://www.fenelec.com

# HIDRALERTA: Emergency Response Module for Coastal Wave Overtopping and Flooding at Praia da Vitória bay

Conceição J.E.M. FORTES[1], Liliana V. PINHEIRO[1], Ana Catarina ZOZIMO[1], Larize LIMA[1], Vera SERRAZINA[1]

[1]National Laboratory for Civil Engineering, Portugal
jfortes@lnec.pt, lpinheiro@lnec.pt, aczozimo@lnec.pt, llima@lnec.pt, vserrazina@lnec.pt

ABSTRACT

The present work describes the developments done so far to the Praia da Vitoria coastal region under the LIFE-GARACHICO project, namely the implementation of module on HIDRALERTA early warning system for emergency response to coastal waver topping and flooding at Praia da Vitória bay.

## 1. Introduction

Macaronesia is made up of 5 archipelagos, including the Canary Islands and the Azores archipelago. Macaronesia islands are especially vulnerable to climate change impacts due to their coastal exposure and abrupt orography. Thus, innovative adaptation measures are needed to protect coastal areas from the impacts of climate change.

The LIFE Garachico project - Coastal Flooding Adaptation To Climate Change Through Flexible Strategies In Macaronesia Urban Area, proposes the development of methodologies for the creation of an effective Flexible Adaptation Strategic Framework for the coastal municipalities of Macaronesia, based on the definition of acceptable levels of risk and specific interventions at the local level, in order to increase the resilience of these areas against current and future extreme coastal events due to climate change. The study cases are Garachico and Puerto de la Cruz, at Tenerife at the Canary Islands, and Praia da Vitória at Terceira Island (Archipelago of the Azores).

The tasks of the project include: implementation of an early warning system (EWS), a set of adaptation measures to reduce the risk of overtopping and flooding, in each of the study cases, and the creation of a manual of technical recommendations. In the case of Praia da Vitória, the EWS implemented is the HIDRALERTA system (Poseiro 2019) and the adaptation measures foreseen are associated with the access and the circulation of urban traffic and pedestrians. Those measures and respective protocols (emergency plans) will be established in case of overtopping and flooding alerts and should be activated by the HIDRALERTA system itself (emergency module system). The Garachico test case will also define the basis of a manual of recommendations based on the experience gathered during the application of their own EWS and adaptation measures.

The present paper describes the development of a new HIDRALERTA module that automatically activates a set of emergency plans (emergency preparedness and response activities), to enhance the response of the authorities to the alert events.

## 2. Study case

Praia da Vitória is in a large bay on the east coast of Terceira Island. It is bordered to the north by Ponta da Má Merenda and to the south by Ponta do Baixio (Fig. 1), which defines a roughly rectangular basin with about 1 km x 2 km. This bay provides excellent conditions for water sports, such as sailing or windsurf. The protection of the bay from severe sea-wave conditions is done by the so-called north and south breakwaters and by the frontal coastal defense at the bay shoreline.

The bay shoreline has a coastal defense 1 km long. Rooted to the coastal defense there is a field of five groines, which are referred to herein as groins 1 to 5, from south to north. Along the main coastal road there is not an intense occupation. There is a building at the root of groin 3, where currently operates a bar. Along the road, there is a promenade. Halfway, there is an outdoor car parking, training machines and a hotel. Two restaurants are located at the north and the south sides of the bay. In some storm situations, there are severe overtopping and flooding situations along the coastal defense, which put in danger traffic, equipment and specially, pedestrians that uses frequently the site. Adaptation measures that involve the control of access and circulation of urban traffic as well as pedestrian will contribute to reduce the risk.




**Fig. 1.** Praia da Vitória.

## 3. The new module of HIDRALETA system

HIDRALERTA is a forecast and early warning system for coastal and port regions capable of predicting emergency situations, as well as carrying out risk assessment. As a forecast and early warning tool, HIDRALERTA enables the identification, in advance, of the occurrence of emergency situations, prompting the responsible entities to adopt measures to avoid loss of lives and minimize damage. The system provides forecasts, 72 hours in advance and with a 3-hour interval, of wave climate characteristics, its consequences (overtopping and flooding) and risk levels associated. It is a modular system: I – Sea-wave characterization, Module II – Overtopping determination, Module III – Risk assessment; Module IV – Alert System.

A prototype for Praia da Vitoria bay has already been developed. Although HIDRALERTA sends alerts to the responsible authorities, it does not indicate the necessary procedures they should perform to reduce the risks in case of emergency situations related with overtopping and flooding events. In that way and considering the adaptative measures related to traffic and pedestrian access and circulation, specific protocols (emergency plans) will be established in close collaboration with the authorities. Those protocols will be implemented into HIDRALERTA as a part of a new module V – Emergency Response Plans. In this new module a set of previously discussed and prepared documents will be stored in a database and will be activated according to the type and level of alert foreseen. Emergency plans and all the relevant information about the occurrences are then sent to the executive authorities (municipality, civil protection, or others). Information provided will be direct, concise, and easy to understand. Emergency plans to be activated must be well identified, so that operatives can follow those measures and protocols in a timely manner.

**Acknowledgements**

The authors thank the financial support of LIFE Garachico Project (LIFE20 CCA / ES / 001641) and the Portuguese Nat. Distri. Comp. Infrastructure INCD for computing resources.

**References**

Fortes, C.J.E.M., Reis, M.T., Pinheiro, L., Poseiro, P., Serrazina, V., Mendonça, A., Smithers, N., Santos, M.I., Barateiro, J., Azevedo, E.B., Salvador, M. & Reis, F.V. (2020). The Hidralerta System: Application to the Ports of Madalena do Pico and São Roque do Pico, Azores, in Journal of Aquatic Ecosystem Health & Management, Doi: 10.1080/14634988.2020.1807295.

Poseiro, P. (2019). Forecast and Early Warning System for Wave Overtopping and Flooding in Coastal and Port Areas: Development of a Model and Risk Assessment (Doctoral Dissertation), IST-UL.

# Analytical and numerical modelling of wave dissipation over rigid and flexible vegetation in a flume: Drag coefficient calibration

Rui A. REIS[1], Conceição J.E.M. FORTES[1], Tomohiro SUZUKI[2]

[1] Hydraulics and Environment Department, National Laboratory for Civil Engineering, Lisbon, Portugal
rreis@lnec.pt

[2] Flanders Hydraulics, Antwerp, Belgium

ABSTRACT

Data of wave dissipation over vegetation fields was collected from laboratory flume experiments, for different vegetation and wave conditions. An analytical model and a numerical model are applied to estimate the wave dissipation obtained in the experiments, through the calibration of the bulk drag coefficient ($C_D$). Results and conclusions will analyse and compare each model behaviour and obtained $C_D$ values.

## 1. Introduction

Coastal vegetation can contribute to protect the coasts from sea wave action, as controlling local biology and morphodynamics. A common way to estimate the wave energy dissipation over vegetation is to use the Mendez and Losada (2004) analytical formulation in combination with the calibrated bulk drag coefficient parameter ($C_D$). However, an excessive range of $C_D$ values is found in the literature related to same Reynolds ($Re$) or Keulegan-Carpenter ($KC$) numbers. This may be due to a lack of universality of the empirical equations proposed and/or limitations of the analytical model. The numerical model SWASH (Zijlema et al., 2011) characterises wave dissipation over vegetation fields (Suzuki et al., 2019, 2022; Reis et al., 2020) considering the influence of the drag, inertia, and porous effects on cylindrical structures. Potentially, SWASH offers enhanced capacities to describe the physical processes involved and to calibrate associated $C_D$ values. Wave dissipation over vegetation data was collected by performing laboratory flume experiments, enabling an ideal control of the study conditions. The analytical formulation and the SWASH numerical model are applied to estimate the wave dissipation obtained in the experiments, through the calibration of the $C_D$.

The objective of this study is to investigate: i) how the analytical and SWASH models can represent the experimental wave dissipation, and ii) the calibrated $C_D$ values obtained from each modelling approach.

## 2. Flume Experiments

Wave flume experiments of wave propagation over artificial vegetation fields were conducted in COI3 wave flume at Portuguese National Laboratory for Civil Engineering (Fig. 1).

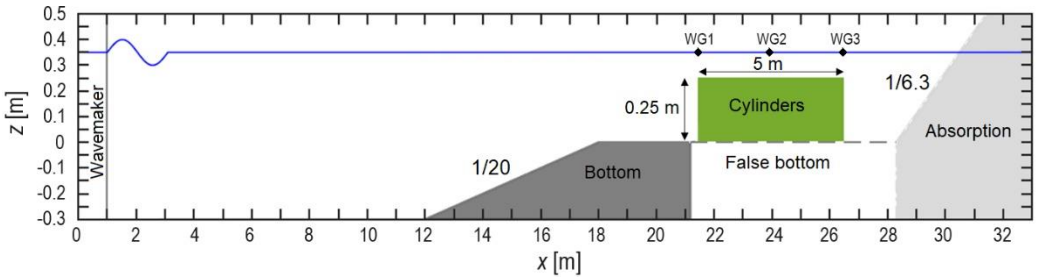



**Fig. 1.** Wave flume layout schematisation.

Vegetation fields were constructed from rigid (flexural rigidity $EI$ = 6.5 N m$^2$) and flexible ($EI$ = 4×10$^{-4}$ N m$^2$) cylinders, regularly distributed with vegetation spatial densities $N_v$ = 220 elm/m$^2$ (N220) and 440 elm/m$^2$ (N440). The cylindrical elements in rigid and flexible vegetation fields had the same

dimensions (diameter $d_v$ = 0.01 m, and length $l_v$ = 0.25 m). The vegetation fields were exposed to non-breaking regular wave conditions with wave periods $T$ = 1.4 s and 2.0 s, and several wave heights ($H$). Two still water depths were tested, $h$ = 0.35 m and 0.25 m, corresponding to submergence ratios ($Sr = l_v/h$) $Sr$ = 0.7 and 1.0. Measurements of the free-surface elevation ($\eta$) were taken using wave gauges (WG) at the edge, middle and back of the vegetation fields (Reis et al., 2024).

## 3. Analytical and Numerical Modelling

Experimental results of wave dissipation over vegetation obtained in the flume tests were modelled using the Mendez and Losada (2004) analytical formulation by calibrating/fitting the parameter $C_D$.

The SWASH model based on the nonlinear shallow water equations is applied to simulate the wave *dissipation by vegetation obtained in the experiments by performing a calibration to the $C_D$. Numerous* numerical simulations are run in order to obtain the final $C_D$ result, corresponding to the best agreement between the numerical and experimental data, for each simulated experimental test condition. The SWASH model was run in nonstationary mode using a regular computational grid. At the boundary of the SWASH domain, the regular waves were generated imposing for each run the respective free-surface elevation ($\eta$) time series measured in the laboratory tests at the front-edge (WG1). A sponge layer was used to simulate the energy dissipation from wave breaking in the tests, that only occurred in the absorption zone at the flume end. Non-hydrostatic pressure was included using the Keller-box numerical scheme, and vertical discretization was considered.

## 4. Main Results and Discussion

Results are analysed for i) the wave dissipation obtained in the experimental tests, ii) the performance of both models to simulate the experimental data (Fig. 2) through the root mean square error (RMSE) and mean relative error (MRE) between the models' and experimental results, iii) empirical relations of the $C_D$ results with the *Re* and *KC* numbers, and iv) differences in the $C_D$ obtained from calibration of both models. Results for different tested vegetation fields and wave conditions will be presented. Preliminary results generally indicate that despite an overall similar estimation of the experimental data is obtained from the two modelling approaches, a difference in the corresponding $C_D$ values is observed.

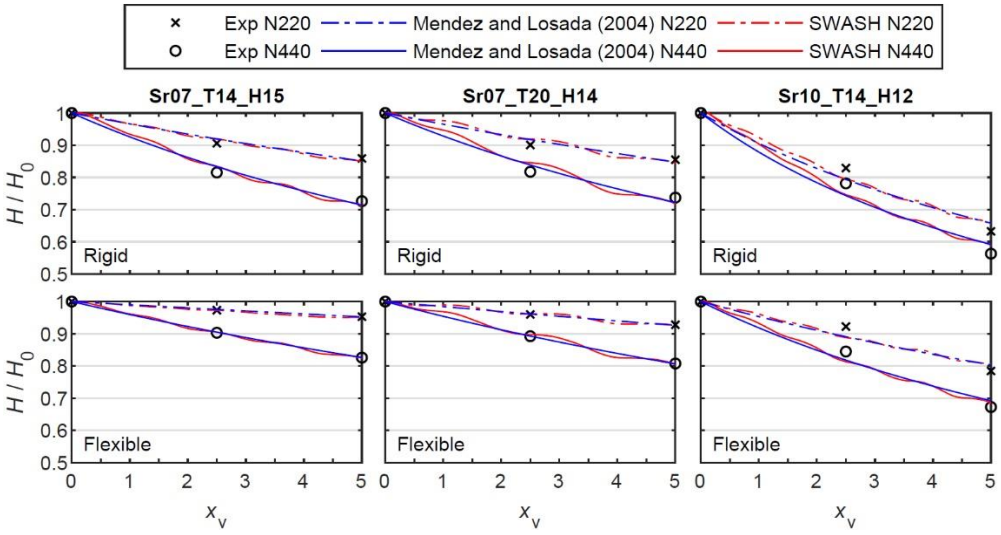



**Fig. 2.** Wave dissipation ($H/H_0$) over the tested vegetation fields: results of both calibrated analytical formulation (Mendez and Losada, 2004) and SWASH model against the experimental data.

**Acknowledgements**

Rui A. Reis acknowledges a PhD fellowship granted by Fundação para a Ciência e a Tecnologia (grant PD/BD/128511/2017).

**References**

Reis, RA, Fortes, CJEM, Rodrigues, JA, Hu, Z, Suzuki, T (2024) Experimental study on drag coefficient of flexible vegetation under non-breaking waves, Ocean Engineering, Volume 296, 2024, 117002

Mendez, F, Losada, I (2004) An empirical model to estimate the propagation of random breaking and nonbreaking waves over vegetation fields, Coastal Engineering, 51, 103–118

Reis, RA, Pires-Silva, AA, Fortes, CJEM, Suzuki, T (2020) Experiences with SWASH on modelling wave propagation over vegetation: Comparisons with lab and field data, Journal of Integrated Coastal Zone Management, 20(2), 145-150

Suzuki, T, Hu, Z, Kumada, K, Phan, L, Zijlema, M (2019) Non-hydrostatic modeling of drag, inertia and porous effects in wave propagation over dense vegetation fields, Coastal Engineering, 149, 49–64

Suzuki, T, Hu, Z, Kumada, K, Phan, L, Zijlema, M (2022) Corrigendum to "Non-hydrostatic modeling of drag, inertia and porous effects in wave propagation over dense vegetation fields" [Coast. Eng. 149 (July 2019) 49–64], Coastal Engineering, 173, 104100

Zijlema, M, Stelling, G, Smit, P (2011) SWASH: An operational public domain code for simulating wave fields and rapidly varied flows in coastal waters. Coastal Engineering, 58(10), 992–1012

# Influences of climate adaptation measures for coastal flood using system dynamics approach

Marion Eva Pauline PERNEY[1,2], Mauro MORENO[3], Francesco GIANNINO[3], Mattia Federico LEONE[1]

[1] Università degli Studi di Napoli Federico II, DiARC, Italy
[2] Université Gustave Eiffel, Lab'Urba, France
marion.perney@unina.it
mattia.leone@unina.it

[3] Università degli Studi di Napoli Federico II, Department of Agricultural Science, Italy
mauro.moreno@unina.it
giannino@unina.it

ABSTRACT

In a global warming context, frequency, and intensity of extreme events are increasing. Human societies are dependent on both environmental and socio-technical systems, and more vulnerable to climate induced impacts. Climate resilient development is the process of implementing greenhouse gas mitigation and adaptation measures to support sustainable development (IPCC, 2023) adjusting the built, social, and ecological environment to minimize the negative impact of events caused by humans and climate change. To assess the relevance of territorial adaptation measures in a dynamic and holistic approach, the use of a System Dynamics approach is developed to represent the influences of technical solutions, both conventional and based on nature, to contrast risk in flood management in the case of coastal cities, with multidisciplinary dimensions, and to assist stakeholders in the identification of possible measures for resilient pathways.

## 1. System dynamics for water management in coastal cities

System dynamics (SD) thinking is an approach that enables the identification of numerous interactions within the various interconnected subsystems that influence the dynamic behavior of the overall system (Sterman, 2000). It allows to view complex systems as interrelated components that affect each other over time. They can be used to represent different policies, strategies, and organizational structures. By experimenting with the model, decision-makers can gain insights into the potential outcomes of various actions.

The coastal system is an open, dynamic, and complex system, a physical meeting point between land, sea and air; it is the space in transition where the terrestrial environment and the marine environment influence each other (Vitale, 2006). In the context of climate change, the Mediterranean region and its cities are characterized by a high degree of vulnerability to climate variations. The Mediterranean basin can be considered a hot spot for changes in most of the key climatic and hydrological components (Lionello, 2012; MedECC, 2020). Phenomena such as floods, water scarcity, droughts, heat waves, coastal erosion and saline intrusion are having an increasingly strong impact on the environment and human activities and water management is a central issue in the Mediterranean region. For these reasons, the field of investigation for developing and testing the tools is the Mediterranean coastal area, which is increasingly vulnerable to the growing impacts of climate change and ongoing socio-cultural and political changes.

## 2. Model framework and objective of the stock and flow model

The model presented is a conceptual framework able to study adaptation and mitigation measures to contrast coastal risks using dynamic tools and methods for assessing the relevance of territorial adaptation measures in urban coastal areas. By examining the literature and studying current practices in three Mediterranean cases, a city model is developed to manage variations in water levels during coastal and fluvial flooding. It

will be calibrated for the specific case of Naples, Italy. Linked to the model, adaptation solutions are presented in a catalogue, which feed the tool with the data collected and help stakeholders to identify possible measures giving information on co-benefices in terms of climate mitigation and Sustainable Development Goals (SDGs) but also adaptations limits and maladaptation drivers.

The objective of the model is to represent the dynamics of surface water absorption as a function of the various urban water management parameters in the case of a coastal city. It considers a compound coastal flood (combination of pluvial and coastal flood) and river flood events, explores Nature Based Solutions, technical architectural and engineering solutions, and employs adaptive responses (management, protection, accommodation, and retreat). The different types of water storage and flows/processes have been identified, as Coastal flow, Surface water, River/ponds, Soil water, groundwater table, city drainage system, harvesting water system. For each of these systems, the model considers a stock of water quantities. Finally, an attempt is made to simulate different scenarios to study the interlink through technical solutions, urban features, and coastal flood water management.

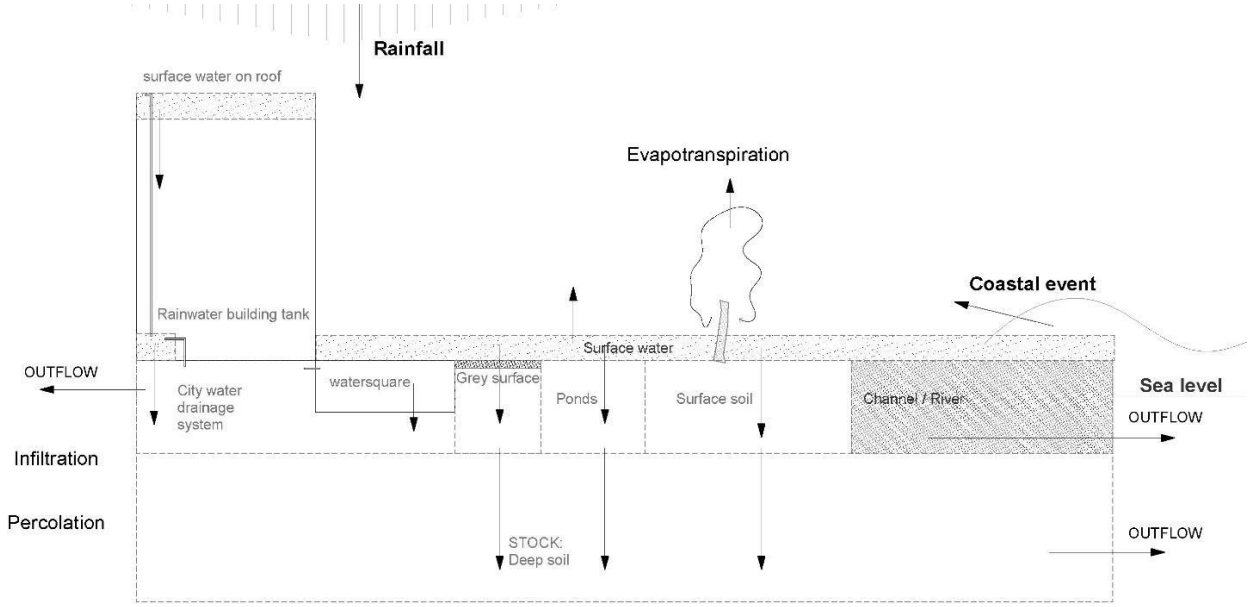



**Fig. 1.** Verbal model of the system dynamics model of water balance in a coastal city.

## 3. Research contribution

The presentation explores SD thinking and tools for dialogue and decision-making on complex and interdisciplinary issues linked to Climate Change Adaptation and Disaster Risk Reduction actions. The quantitative developed stock and flow model contributes to study the climate impacts on coastal cities under a cross-sectorial approach. The whole research, central subject of a PhD thesis and linked to the Horizon Europe project KNOWING, aims at keeping an interdisciplinarity and connections between policy experts, technical services, modelers and urban designers, to promote a strong and effective risk governance framework, based on the promotion of knowledge-based decision-making processes and science-driven strategies and to tackle the issues of the conventionally siloed approach to single hazard, and the distance between “risk science” and “environmental science” communities.

**Acknowledgements**

The project “KNOWING - Framework for defining climate mitigation pathways based on understanding and integrated assessment of climate impacts, adaptation strategies and societal transformation” (2022-2026) is funded by the European Union under the Horizon Europe programme (GA 1011056841).

**References**

IPCC. (2023). Weather and Climate Extreme Events in a Changing Climate. In Climate Change 2021 : The Physical Science Basis. Contribution of Working Group I to the Sixth Assessment Report of the Intergovernmental Panel on Climate Change (1re éd.). Cambridge University Press. https://doi.org/10.1017/9781009157896.

Lionello, P. (2012). The Climate of the Mediterranean Region : From the Past to the Future. Elsevier.

MedECC. (2020). Climate and Environmental Change in the Mediterranean Basin – Current Situation and Risks for the Future. First Mediterranean Assessment Report (Version 1). Zenodo. https://doi.org/10.5281/ZENODO.722482.

Sterman, D. J. (2000). Business Dynamics—Systems Thinking and Modeling for a Complex World. The McGraw-Hill Companies.

Vitale, A. (2006). Ritrovare il mare: Linee guida per gli interventi di riqualificazione della fascia costiera di Napoli. 1-255.

# Energy transfer optimum in waves generated by high mobility subaerial landslides

Amir PARVIN[1], Stéphane ABADIE[1], Kamal EL OMARI[2], Yves LE GUER[1]

[1] Université de Pau et des Pays de l'Adour, E2S-UPPA, France
amir.parvin@univ-pau.fr
stephane.abadie@univ-pau.fr
yves.leguer@univ-pau.fr

[2,] Université de la Réunion, France
kamal.el-omari@univ-reunion.fr

ABSTRACT

## 1. Introduction

In this paper, we study the problem of waves generated by subaerial landslides; a very complex problem involving granular physics, fluid mechanics and wave processes. Recently, a few studies (Bullard et al., 2019; Rauter et al., 2021) proposed a simplification of the generation stage, considering a water slide (i.e., an inviscid liquid with the same density as the reservoir fluid). In these studies, they concentrate on the prediction of the maximum wave amplitude after generation.

In the present paper, we follow the same strategy of simplification, but this time, focus on the energetic transfer processes from the stage of generation, to the end of the main wave transformations.

## 2. Methodology

A RANS multiphase Navier-Stokes VOF simulation (multiphaseInterFoam model) is used for this investigation. This type of model (as soon as the generation stage is simplified), allows a complete description of the energetic processes and gives all the variables necessary for the interpretation. A turbulence model is mandatory for a proper description of the dissipation processes. Here, the k-ω SST modified with a buoyancy term, as proposed by Devolder et al. (2018), is used.

The model is first thoroughly validated, considering all the processes intended to be described. This work points out the importance of a fine tuning of the model for a proper description of the processes. Hence, the time step should be low enough to respect convective and diffusive CFL conditions as described in Rauter et al. (2021). The discretization schemes for convective terms also play a critical role regarding energy dissipation. Finally, with the model set-up proposed, we achieved a correct representation of the dissipation processes, but not perfect, as non negligible numerical dissipation is still present for the most violent wave breaking cases.

The model is then used to conduct a numerical experiment involving a subaerial triangular water slide initially at rest just at the water line. The volume of the slide is gradually increased. The objective is to understand how the slide energy transfers to the free surface and then, how the wave processes (dispersion, breaking) act to shape the final leading wave energy, which is our hazard indicator.

## 3. Results

Fig. 1 shows the two main patterns observed depending on the slide volume. In the right panels, the slide volume is relatively small. The wave breaking is localized and the initial wave clearly disperses with time. Conversely, on the left panels, the initial slide volume is large, the wave generated is equally large and the

breaking is the main factor affecting the subsequent wave dynamics. Note also that the wave does not disperse.

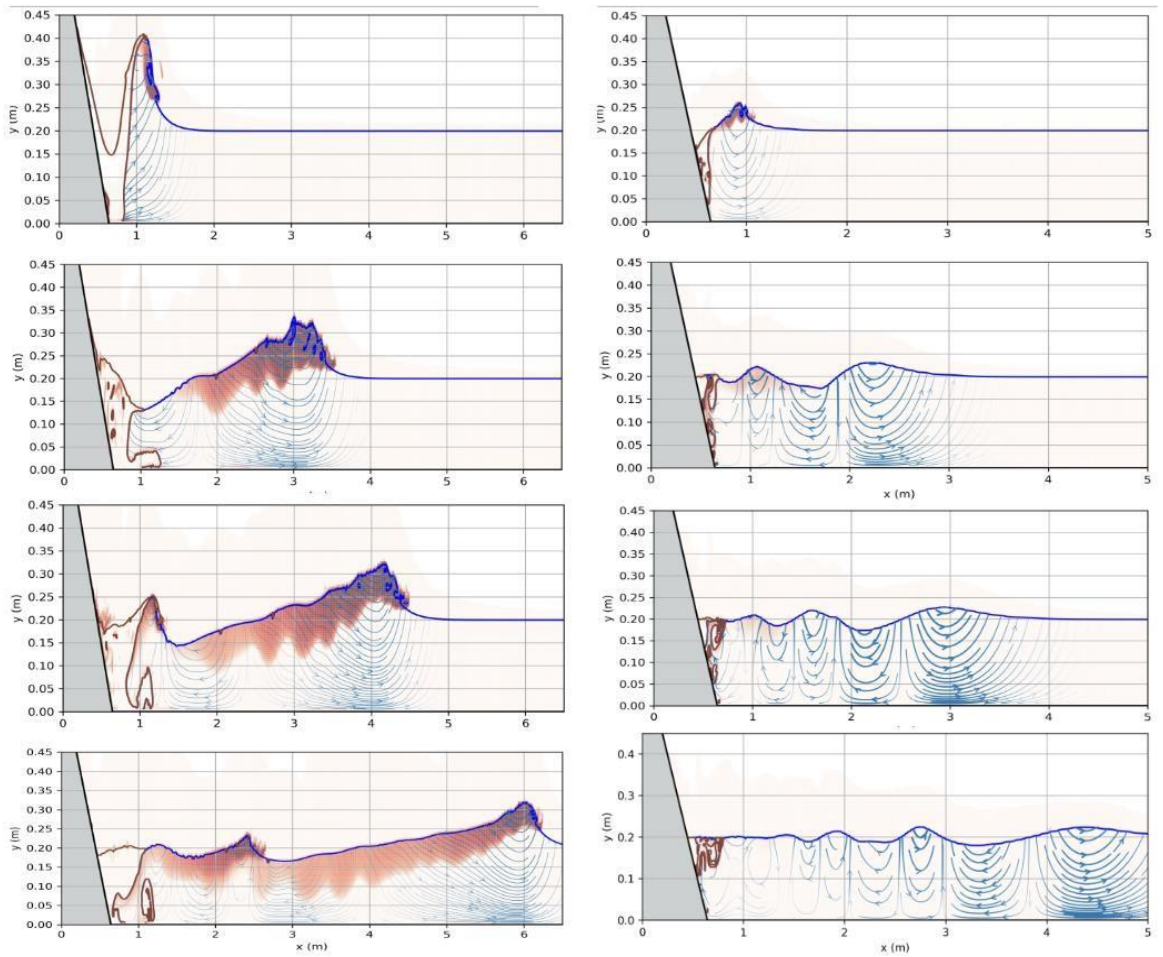



**Fig. 1** – Illustration of the generation process for two different initial volumes in the case of a water slide with no submergence. The panels show the snapshots of fluid interfaces, streamlines and turbulent dissipation rate ε (surface field, colorbar range 0. 1 J/(kg.s)), at t= 0.5s, 1.5s, 2s, 3s (from top to bottom) with left : $h_s=2h_0$, right: $h_s = 0.75h_0$ ($h_s$ slide initial height and $h_0$ water depth).

The detailed investigation of the simulations performed shows that the leading wave energy, at the end of the channel, is the result of a set of sequential processes. Generation determines the basic impulse wave characteristics and from there, the future evolution of the wave. Schematically, depending on its initial characteristics, the impulse wave will be either shaped by dispersion, by breaking or by a combination of the two. Finally, considering the global energetic process from the initial slide potential energy to the final leading wave energy, we show that the process efficiency has an optimum for an intermediate slide volume.

**References**

Bullard GK, Mulligan RP, Carreira A, Take WA (2019) Experimental analysis of tsunamis generated by the impact of landslides with high mobility, Coastal Engineering, 152, 103538.

Devolder B, Troch P, Rauwoens P (2018) Performance of a buoyancy-modified k-ω and k-ω SST turbulence model for simulating wave breaking under regular waves using OpenFOAM®, Coastal Engineering, 138, 49-65.

Rauter M, Hoße L, Mulligan RP, Take WA, Løvholt F (2021) Numerical simulation of impulse wave generation by idealized landslides with OpenFOAM, Coastal Engineering, 165, 103815.

# A new dimension in satellite altimetry: Insight into the SWOT data for assessing the dynamics of hydrosystems

Lionel ZAWADZKI[1], Nicolas GASNIER[1], Roger FJØRTOFT[1], Claire POTTIER[1], Damien DESROCHES[1], Santiago PENA LUQUE[1], Nicolas PICOT[1], Thérèse BARROSO[1]

[1] CNES, Centre National d'Etudes Spatiales, Toulouse, France
lionel.zawadzki@cnes.fr

ABSTRACT

Satellite altimetry has been used since the early 90s to estimate water levels and their temporal variations, enabling multiple breakthroughs in oceanography and providing hydrologists with valuable data on large lakes and rivers. The Surface Water and Ocean Topography (SWOT) satellite [1], launched in December 2022, is a CNES-NASA joint project, with contributions from UKSA and CSA. SWOT represents a major step forward in space altimetry as it is based on interferometric SAR imagery. In comparison to conventional nadir altimetry, which only provides point data along the ground track, SWOT provides two-dimensional images with a spatial resolution of the order of tenths or hundreds of meters over two 60-km-wide swaths. This mission will significantly improve both offshore and coastal ocean observations, and enable global measurements of the water level and extent of rivers, lakes, wetlands and flooded areas, with two or more observations per 21-day repeat period. This two-dimensional and multi-temporal information make it possible to compute water storage changes of lakes and reservoirs, and to estimate river discharge [2]. It will thus provide the most comprehensive view ever of the dynamics of the Earth's freshwater bodies.

This paper shares highlights from the first year of SWOT data and describes the different available products for assessing the dynamics of hydrosystems.

## 1. SWOT products and distribution platforms

SWOT science products are public and cost-free to use.

Particular care has been taken with the support of the SWOT Science Team to build up a portfolio of relevant products for hydrology studies. It includes 12 different science products, spanning from single-look complex radar images (Level-1b) to a range of Level-2 products ready for analysis, depending on the targeted application, the necessary resolution and accuracy, and the ease of use.

The Level-2 products include in particular a pixel cloud product in NetCDF4 format at 20-m average pixel spacing, featuring water classification and height (w.r.t. the WGS84 ellipsoid), with associated uncertainties, quality flags and geophysical corrections. Easier-to-use raster products are also available in NetCDF4 format, at 100-m and 250-m regular latitude/longitude grids. The raster products contain water surface elevation (w.r.t. the EGM2008 geoid), water fraction, along with uncertainties and flags. Dedicated lake vector products in ESRI shapefile format provide vectorized lake and reservoir data, i.e. lake polygons with their associated average water surface elevation (w.r.t. EGM2008), water surface area, estimated storage change, as well as uncertainties and flags. Likewise, there are river vector products in ESRI shapefile format, providing water surface elevation (w.r.t. EGM2008), river width at 200-m-spaced nodes along river centerlines defined in a prior river database, as well river slope and derived river discharge along ~10-km river reaches, together with uncertainties and flags. Note that there are also cycle-average river and lake vector products.

As of January 2024, these products are available in a so-called "pre-validated" release in two different cost-free data distribution platforms describing the different products and their characteristics. One is specialized for in-cloud computing on the NASA EarthData cloud (https://podaac.jpl.nasa.gov/cloud-

datasets?search=swot). The other one is specialized for hydrology experts with a webGIS solution, hydroweb.next (https://hydroweb.next.theia-land.fr), offering visualization features and centralized access to many other hydrology products. Public release of the SWOT data is scheduled for March 2024.

## 2. Overview of SWOT capacities after a year in science orbit

The first six months of SWOT's life consisted of a calibration and validation phase with a 1-day revisit orbit. This period provided a unique opportunity to verify the satellite observations against in situ measurements deployed during dedicated campaigns on selected sites. These first results showed that SWOT data were better than expected in terms of signal-to-noise ratio and thereby random height noise. Cases with excellent performance were observed, such as the detection of rivers down to 20-m width, while the science requirement is 100 m), and lakes with absolute water surface elevation error within the science requirement (10 cm 1-sigma for lakes > 1 $km^2$). More difficult cases were of course also encountered. Global statistics on the performance of the SWOT HR data are being prepared for the Science Validation meeting in June 2024.

While the validation phase is still ongoing and the final performance assessments are not available yet, this extended abstract provides some first insights into the applications of SWOT for complex human-modified hydrosystems. Additional examples will be presented at the conference.

**Figure 1** shows two examples of the SWOT water height map from the pixel cloud product for two complex, human-engineered hydrosystems. In **Figure 1-A**, the Gezira irrigation scheme (Sudan) is shown. The water comes from the Sennar Dam (not in the image) through an irrigation channel and is distributed to a secondary network that is used for irrigation. We see that the water elevation is much higher in the irrigation channels than in the river downstream of the Dam, and the that water level decreases as the water flows through the channels. In **Figure 1-B**, the confluence between the Moselle and the Rhine rivers is shown. While the water elevation decreases continuously in the Rhine River, we see two discontinuities in the Moselle water elevation, corresponding to run-of-the-river power stations.

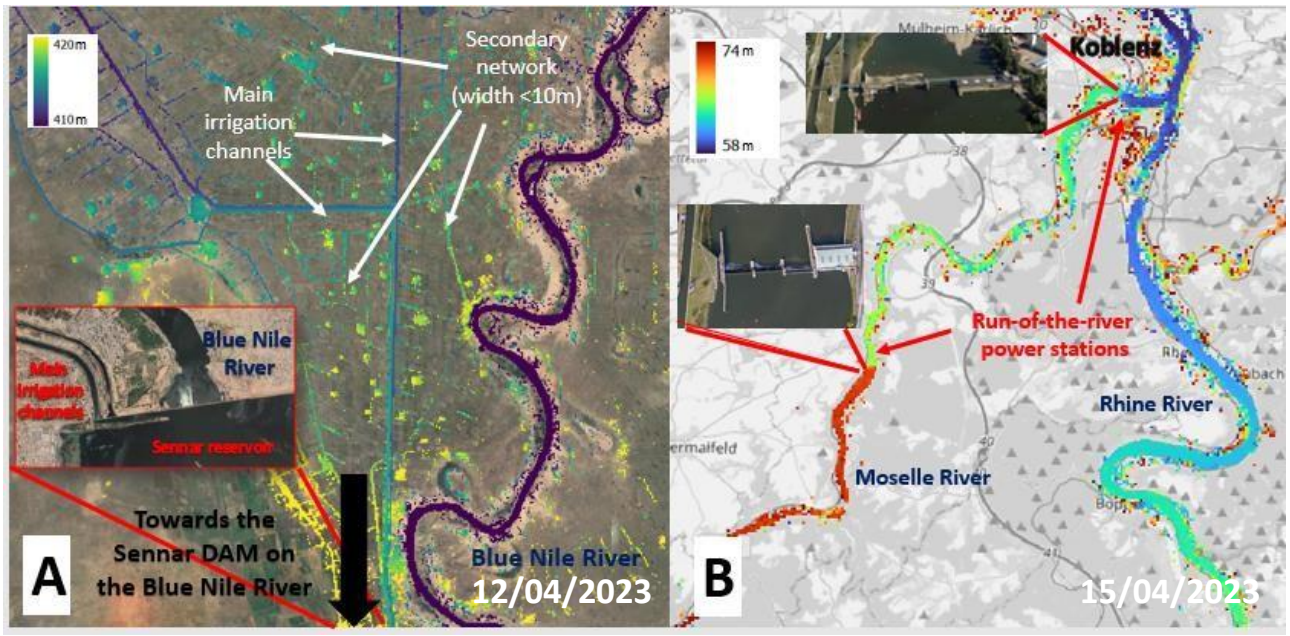



**Figure 1**. Example of SWOT water elevation maps based on pixel cloud products, (A) in the Gezira irrigation scheme, and (B) for the area around the Moselle-Rhine confluence.

**References**

[1] Biancamaria, S., Lettenmaier, D. P., & Pavelsky, T. M. (2016). The SWOT mission and its capabilities for land hydrology. Remote sensing and water resources, 117-147.

[2] Yoon, Y., Beighley, E., Lee, H., Pavelsky, T., & Allen, G. (2016). Estimating flood discharges in reservoir-regulated river basins by integrating synthetic SWOT satellite observations and hydrologic modeling. *Journal of Hydrologic Engineering*, *21*(4), 05015030.

rr

# Monitoring of coastal infrastructure – example of brine discharge system

Małgorzata ROBAKIEWICZ[1]

[1] Institute of Hydro-Engineering of Polish Academy of Sciences (IBW PAN), Gdańsk, Poland
marob@ibwpan.gda.pl

ABSTRACT

In the years 2010-2021 Polish Gas and Oil Company (PGNiG) constructed gas stores in salt deposits located in the north-eastern part of Poland. The discharge system was located 2300 meters from the western part of the Gulf of Gdańsk (South Baltic Sea). To discharge brine (saturation: 250 kg $m^{-3}$; flow rate: 300 $m^3$ $h^{-1}$) a system of 48 nozzles distributed in an area of 180x180 meters was proposed. Continuous monitoring of brine spreading confirmed compliance with the water permit, i.e. permissible excess salinity was below 0.5 PSU.

## 1. Introduction

Increasing demands for gas storage capacity encouraged Polish Gas and Oil Company (PGNiG) to build underground gas stores in salt deposits located in the north-eastern part of Poland, in the area bordering on the Gulf of Gdańsk (South Baltic Sea). The construction site was located about 4 km away from the Baltic Sea coast. The drilling of boreholes and diluting of salt rock was continued in the years 2011-2021, resulting in growth of gas storage capacity by $300*10^6$ $m^3$. During the construction time the monitoring program was carried out continuously.

## 2. Material and methods

The Gulf of Gdańsk is situated in the south-eastern part of the Baltic Sea in the area limited by the imaginary line between the Cape of Rozewie and the Cape of Taran (Fig. 1 - left). The Puck Bay is a shallow western sub-region of the Gulf of Gdańsk separated from the open sea by the Hel Peninsula. In the middle of the Hel Peninsula there is a shallow sandbank stretching from the Rewa Cape to Kuźnica, which divides the Puck Bay into two parts: the eastern part - the Outer Puck Bay (av. depth ~20.5 m), and the western part - the Puck Lagoon (av. depth ~3 m). Currents in the region are generated mainly by wind and the accompanying water level variations in time and space. In addition, circulation in the Puck Lagoon is influenced by water exchange with the eastern part of the lagoon (Nowacki 1993). In the Outer Puck Bay, salinity is closely related to the inflow of more saline water from the Gdańsk Basin through surface and bottom layers, additionally modified by fresh water from the Vistula river. Based on statistics it is known that the mean monthly salinity varies from 6.8 to 8.0 PSU in the Outer Puck Bay, and from 7.2 to 8.4 PSU in the Puck Lagoon.

Monitoring of brine mixing in the Puck Bay was carried out for the diffusing system distanced 2300 meters from the shore. The discharge installation consisted of 16 heads, each with 3 nozzles of 9 mm distributed every 120° of circumference. The installation was constructed to discharge brine with a saturation of 250 kg $m^{-3}$ at a rate of 300 $m^3$ $h^{-1}$, while permitted excess salinity had to be below 0.5 PSU and maximum salinity in the vicinity of installation not exceeding 9.2 PSU. The installation covered an area of 180x180 meters (Fig. 1 - right).

Two types of measurements were carried out by the operator of installation and IBW PAN: (a) characteristics of discharged brine – its quality and quantity; (b) environmental parameters - salinity and temperature variation in time and space (continuous and CTD in selected verticals), (c) occasionally recorded currents in selected locations and mixing in the vicinity of a single jet.

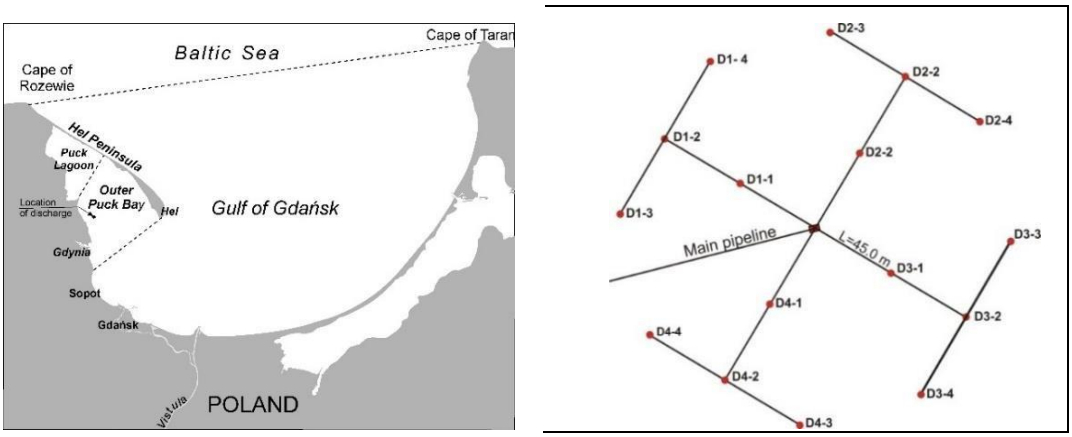



**Fig. 1.** General view on the Gulf of Gdańsk, including the location of the discharge site (left); a spatial view of the discharge system with 16 heads spaced every 45 m (D - location of a single head with 3 nozzles).

## 3. Results and conclusions

Monitoring of discharged brine continued during the construction period (2011-2021) allowed to document its operation. Continuous measurements confirmed correct work of discharge system; they have shown that requirements specified in the water permit were met.

Monitoring of environmental parameters enabled to draw the following conclusions:

- mixing of a single jet with natural environment was in a good agreement with results from the preliminary study;
- salinity variation in the center of discharge installation, controlled by the operator, did not exceed the permissible value 9.2 PSU;
- salinity distribution varied in time and space due to varying wind conditions, and inflows of fresh Vistula river water;
- monitoring program documented occasional presence of up-welling in the coastal region;
- occasional mutual influence of brine discharge and discharge from the neighboring Waste Water Treatment Plant Dębogórze has been found.

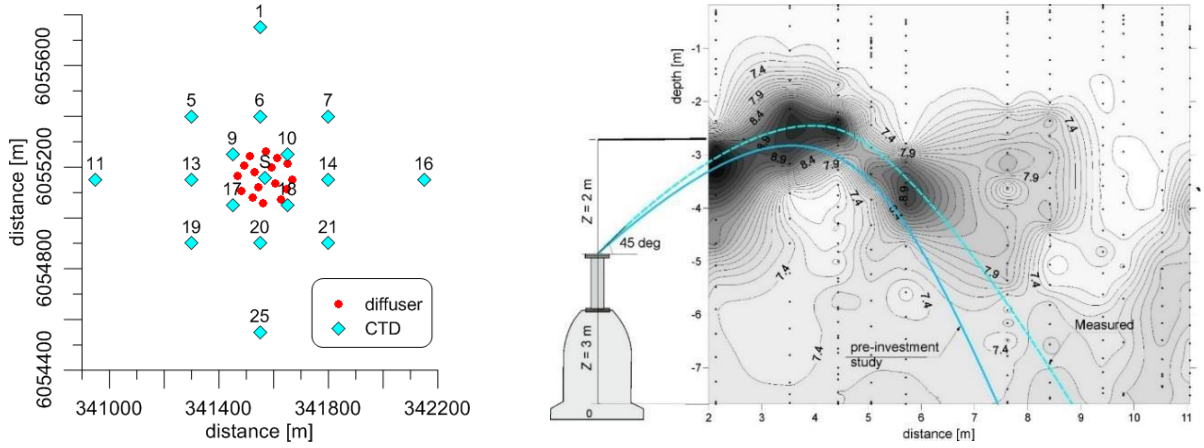



**Fig. 2.** Location of CTD measurements against location of diffusers (left); salinity distribution in vertical cross-section based on in-situ measurements in the vicinity of D1-1 diffuser (dots) and estimated theoretical shape based on laboratory experiments (right).

**Acknowledgements**

This paper is based on data from the research project carried out by IBW PAN and financially supported by GAS Storage Poland, a partner of PGNiG, the company responsible for the technical aspects of constructing the underground gas stores in Kosakowo.

**References**

Nowacki J (1993) Hydrophysics of the Puck Bay. In K. Korzeniewski (Ed), *Puck Bay* (79-111, 181-205, in Polish), Institute of Oceanography of Gdańsk University

# The coastal challenge of climate adaptation: discussion on systemic approaches

Bruno BARROCA[1], Maria Fabrizia CLEMENTE [2], Marion Eva Pauline PERNEY [1,2],

Charlotte HEINZLEF [3], Mattia Federico LEONE [2] , Isabelle THOMAS [4], Damien SERRE [3]

[1] Université Gustave Eiffel, Lab'Urba, France
bruno.barroca@univ-eiffel.fr
[2] Università degli Studi di Napoli Federico II, DiARC
mariafabrizia.clemente@unina.it
marion.perney@unina.it
mattia.leone@unina.it
[3] Université Paris Saclay, UVSQ, CEARC, France
charlotte.heinzlef@uvsq.fr
damien.serre@rescuesolutions.fr
[4] Université de Montréal, Canada
isabelle.thomas.1@umontreal.ca

ABSTRACT

The number of climate-related natural disasters, and especially floods, has more than doubled over the past decade, according to the United Nations Office for Disaster Reduction. Among these disasters, the risk of flooding appears to be the most "damaging". During the period 2000-2019, these disasters cost the lives of more than one million people and caused almost 3,000 billion dollars of economic losses (UNDRR, 2020). The Swiss Re insurance group, one of the world's leading risk insurers, estimates the cost of losses caused by flooding at 90 billion dollars by 2021, an increase of between 5 and 7% per year. This is confirmed by the extreme floods of recent years. For example, the floods that hit Germany and Belgium in July 2021 caused almost 230 deaths and more than €40 billion of damages (Bevere & Remondi, 2022).

At the same time, the increasing complexity of sociotechnical systems makes flood risk management difficult. Human concentration (37 per cent of the world's population lives within 100 km of the coast at a population density twice the global average (UNEP, 2017)), and urban population contribute to increase flood risk in such areas. The need to innovate in risk management approaches is explained by the awareness of the lack of consideration of vulnerable territories.

The aim of the presentation will be to provide a conceptual framework and to present practical applications concerning the development of dynamic tools and methods for assessing the relevance of territorial adaptation measures in urban coastal areas. The operational implementation of resilience in coastal areas could, first, be based on a functional analysis of technical systems and urban components. Then, this analysis will be carried out using a functional block diagram representing and modelling the urban systems. In terms of simulation, this functional approach can be deployed using two "tools" approaches, by means of spatial analyses based on GIS processes that can be generalized from open-source data, such as COPERNICUS data, and using more precise dynamic analyses with the development of a dynamic tool to simulate the effectiveness of technical measures and eventual disruptions under coastal flooding events. On the one hand, these tools integrate spatialized data, whether generic in the case of GIS analysis or specific to the area under study in the case of system dynamics. The solutions are presented in catalogues that provide the tool with the data collected and help resilience practitioners to identify potential measures.

These two tools' approaches will be illustrated using diverse case studies, selected because of their location in particularly vulnerable areas: coastal submersion is a serious issue in Canada, particularly on the Quebec coast, the Mediterranean basin, which is one of the areas most affected by climate change, and island areas (IPCC, 2023; MedECC, 2020).

The town of Maria in the Gaspé is suffering from this phenomenon, which is putting its residents at risk. A process of reflection aimed at transforming the area and strengthening the community's resilience demonstrates not only the need for advanced analysis tools, such as the Resiliaction Tool, but also for stakeholder involvement and the co-construction of scenarios.

Port cities play a strategic role in the transportation of goods and people, acting as catalysts for the development of urban and regional economies but are areas highly vulnerable to climate change impacts. Transformation of port infrastructures is essential to reduce physical impacts on facilities and logistics activities.

Mediterranean coastal cities, which are increasingly vulnerable to the growing impacts of climate change and to socio-cultural and political changes, need to implement adaptation solutions to deal with the increase in extreme and irregular climatic phenomena, such as coastal flooding. The evolution of Barcelona's stormwater drainage system shows a marked advance in response to urban pressure and the growing demand for water management, as well as the need to contrast the ecological and climatic impacts on the coastal zone during flood events (Saurí & Palau-Rof, 2017).

In the reports from the French Senate dealing with natural risks (Information Report No. 688, 2017-2018) conducted that French overseas territories (small islands mainly) are very concerned by floods, but this risk is poorly addressed by the national Government and local authorities. Several combined factors of overseas territories like geography, climate, land planning constraints and social structures are increasing the vulnerability to floods and risk issues in general at a higher level.

This presentation will provide an opportunity to discuss the frameworks and tools for meeting the above-mentioned needs in terms of science and technology. Since 2014, the actors have tried to address some of these topics, but separately at this stage and without enough support from national and local authorities. This session will help our international and pluridisciplinary team of researchers to structure and test some tools for enhancing resilience conditions like long term research and risk observatory design. Diverse coastal location examples will be presented, as Mediterranean and Pacific regions.

The results will be presented jointly and will be used to discuss the relevance of the systems and tools developed.

**References**


Bevere, L., & Remondi, F. (2022, mars 30). *Natural catastrophes 2021 : Flood gates are open - Swiss Re sigma | Swiss Re*. https://www.swissre.com/institute/research/sigma-research/sigma-2022-01.html

IPCC. (2023). *Weather and Climate Extreme Events in a Changing Climate. In Climate Change 2021 : The Physical Science Basis. Contribution of Working Group I to the Sixth Assessment Report of the Intergovernmental Panel on Climate Change* (1re éd.). Cambridge University Press. https://doi.org/10.1017/9781009157896

MedECC. (2020). *Climate and Environmental Change in the Mediterranean Basin – Current Situation and Risks for the Future. First Mediterranean Assessment Report* (Version 1). Zenodo. https://doi.org/10.5281/ZENODO.7224821

Saurí, D., & Palau-Rof, L. (2017). *Urban Drainage in Barcelona : From Hazard to Resource? 10*(2).

Senat Français (2018) *Risques naturels majeurs : urgence déclarée outre-mer. Rapport d'information n° 688 (2017-2018), tome* I, déposé le 24 juillet 2018

UNDRR. (2020, octobre 12). *The human cost of disasters : An overview of the last 20 years (2000-2019)*. http://www.undrr.org/publication/human-cost-disasters-overview-last-20-years-2000-2019

UNEP, U. N. (2017, août 18). *Coastal zone management*. UNEP - UN Environment Programme. http://www.unep.org/explore-topics/oceans-seas/what-we-do/working-regional-seas/coastal-zone-management

# Run-up and overtopping video analysis using Timestack methodology

Rute LEMOS[1], Miguel CARVALHO[2], Conceição FORTES[1], Umberto ANDRIOLO[3]

[1]National Laboratory for Civil Engineering, Portugal
rlemos@lnec.pt; jfortes@lnec.pt
[2]Nova School of Science and Technology, Portugal
mco.carvalho@campus.fct.unl.pt
[3]INESC Coimbra, Portugal
uandriolo@mat.uc.pt

ABSTRACT

This work evaluated a video camera-based technique for measuring wave run-up and identifying overtopping events in three-dimensional physical scale models of rubble-mound breakwaters. Run-up elevations inferred by the *Timestack* methodology were compared with the traditional measurements obtained by a resistive wave gauge. For both frontal and oblique incident waves, run-up statistical parameters returned by *Timestack* analysis agreed with the instrument measurements. Moreover, overtopping events were correctly identified. Overall, results indicated the feasibility of a non-intrusive video camera-based technique for hydraulic measurements in physical models.

## 1. Introduction

The determination of run-up and overtopping events in physical models is traditionally carried out using a resistive wave gauge placed along the slope of the structure. An alternative approach consists in the use of video cameras and image processing techniques, such as the *Timestack* methodology, proposed by Andriolo et al. (2016). At LNEC, promising results of wave run-up parameters were obtained on 2D physical models by using a common video camera and following the methodology *Timestack*, Lemos et al. (2023).

The objective of this work is to evaluate the performance of *Timestacks* in three-dimensional tests, in which the run-up that reaches the slope varies significantly along the structure, given the influence of the obliquity of the wave. With this new technique, based on videos obtained during tests on a physical model, it becomes possible to quantify, a posteriori, the run-up in any area of the breakwater, by defining the transect on the area of interest, as a virtual wave gauge. Another application of the technique is its use in identifying overtopping and determining the distance reached by the overtopping event.

## 2. Materials and methods

Tests were conducted in the wave tank of the Hydraulics and Environment Department of the Portuguese Laboratory for Civil Engineering (LNEC). The tank is 43 m long, 25 m wide and 1.5 m high. The model was built and operated at a 1:58.9 scale, according to Froud similarity law. Tests were conducted with both frontal and oblique wave incidence with an angle of attack of 70°. A video camera, with a frame rate of 25 frames/s, was positioned in front of the breakwater section. Tests were conducted with significant wave heights (Hs) of 6 and 8 m, associated with peak periods (Tp) of 16, 20 and 22 s and three different water levels: 0.0 m(CD); +1.8 m(CD) and +3.0 m(CD). These water levels correspond to low-water level (LWL), high-water level (HWL) and high-water level associated with sea level rising (HWLS), respectively.

The *TimeStack* methodology consists in the application of three MatLab algorithms for extracting the pixels array along a pre-defined image segment (transect). This extraction results in an image (the *TimeStack*), where is possible to identify, manually, the run-up crests, and to obtain a time series in pixel values which will then be converted into metric values, enabling to estimate the statistical parameters $Ru_{max}$, $Ru_{min}$, $Ru_{med}$ and $Ru_{2\%}$. To evaluate the application of *TimeStack* methodology, the run-up values obtained by video analysis were compared with those obtained in a resistive wave gauge placed along the slope of the breakwater. Figure 1

shows the three-dimensional model, as well as an example of a transect, located along the breakwater crest, to identify overtopping events and a transect defined to determine the run-up values. Figure 2 shows segments of two *TimeStack* images for identifying overtopping (left) and run-up events (right).



**Fig. 1.** Three-dimensional model and location of transects (red lines) to retrieve pixel array for Timestack production. Lines are chosen to identify overtopping (left) and run-up events (right).

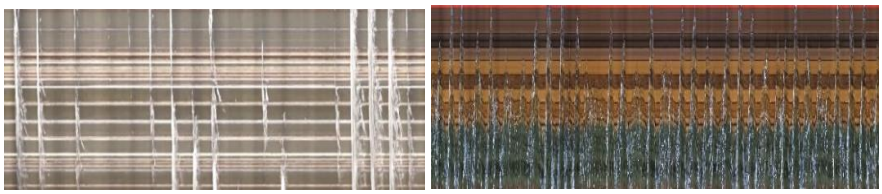


**Fig. 2.** *TimeStack* images for identifying overtopping (left) and run-up events (right).

## 3. Results and discussion

Table **1** summarizes the results obtained with both methodologies for tests conducted with a frontal wave direction (T1 and T2) and tests conducted with obliquity (T3 and T4).

**Table 1.** $Ru_{2\%}$ and $Ru_{max}$ obtained with the video analysis and with the wave gauge time series

| Test | Methodology | $Ru_{2\%}$ | $Ru_{max}$ |
|---|---|---|---|
| T1_S35E_Tp22_Hs8_HWL | Video | 8.45 | 8.74 |
| | Wave gauge | 8.01 | 8.09 |
| T2_S35E_Tp20_Hs6_HWLS | Video | 7.87 | 7.87 |
| | Wave gauge | 7.13 | 7.23 |
| T3_E20N_Tp16_Hs6_LWL | Video | 9.61 | 9.97 |
| | Wave gauge | 9.00 | 9.49 |
| T4_E20N_Tp16_Hs6_ HWL | Video | 8.71 | 8.81 |
| | Wave gauge | 7.79 | 8.94 |

The differences identified were, in part, due to the manual selection of the crests on the *Timestack* image, which can lead to a loss of run-up events. An automatic crest identification algorithm is currently being developed to improve the methodology. The definition of the slope geometry is also of an utmost importance, and, unlike in 2D models, the profile geometry in 3D models cannot be verified from the side. Thus, the design profile geometry should be confirmed by model surveying, as very small differences in the model can lead to important differences in prototype values. The analysis of the overtopping detection is undergoing.

## 4. Conclusions

The comparison of the results obtained with the video technique with the measurements of a wave gauge placed on the breakwater armour layer confirmed that the video technique is a viable alternative to measure the run-up on 3D physical models. It also allows the creation of "virtual wave gauges" (the transects), with the possibility of placing a practically unlimited number of transects enabling the run-up analysis in any part of the model. This asset is very useful in 3D scale model tests, where the run-up varies due to the wave obliquity.

**Acknowledgements**

This work was carried out within the scope of the projects: LIFE-GARACHICO (Project LIFE20 CCA/ES/001641) and C2IMPRESS (Horizon Europa, grant agreement N.º 101074004).

**References**

Andriolo, U., Poseiro, P., Reis, M.T., Bastos, A.P., Fortes, C.J.E.M.;, Garcia, T. (2016) "Investigating the use of a video-technique for wave run-up measurements on a breakwater in a laboratory flume". 4as Jornadas de Engenharia Hidrográfica. Lisbon, 21-23 de june. 478-480pp. ISBN 978-989-705-097-8.

Lemos, R.; Fonte, R., Fortes, C.J.E.M., Andriolo, U., Rito, R. (2023) Determination of wave run-up through the Timestack methodology and through a resistive wave gauge. A comparative analysis. Revista de Engenharia Térmica, 2023, 22.1: 25-31

# Where the Brazes and San Bernard Rivers Meet the Gulf of Mexico

Habib AHMARI[1], Nabila KHANDAKER[2], Trevor STULL[3]

[1] The University of Texas at Arlington, USA
habib.ahmari@uta.edu

[2,3] The University of Texas at Arlington
nabila.khandaker@uta.edu
trevor.stull@mavs.uta.edu

ABSTRACT

The sediment dynamics in the Texas coast, where the Brazos and San Bernard Rivers meet the Gulf of Mexico, (GoM) are complex. The configuration and location of the estuaries of both rivers have been shaped by the diversion of the Brazos River and the construction of the Gulf Intracoastal Waterway. These alterations have resulted in distinct patterns of sedimentation in the area, contributing to the closure of the San Bernard River mouth due to the rapid expansion of the Brazos delta. This has led to the frequent dredging of the San Bernard River mouth to maintain navigation, reduce the risk of flooding upstream, and preserve river connectivity to the Gulf. This paper presents the results of developing models that estimate suspended sediment concentrations using satellite images for the lower Brazos River and Brazos-San Bernard estuaries. This information provides baseline data for numerical models developed to better understand the sediment dynamics in the area.

## 1. Background and Study Area

The Brazos River watershed is the second-largest river basin in Texas by area, covering approximately 118,000 km$^2$ (Dunn and Raines, 2001). It also stands as the second-largest contributor of sediment to GoM following the Mississippi River (Milliman and Meade, 1983). In contrast, the San Bernard River has a smaller watershed of 2,330 km$^2$ (Texas Stream Team, 2020) and makes a limited sediment contribution to the Gulf. Figure 1 shows the Texas coast and the locations of the Brazos and San Bernard estuaries. On average, the Brazos River delivers an estimated $25\times10^6$ tonnes/yr of suspended sediment to GoM (Paine and Morton, 1989), while the San Bernard River contributes only 41,730 tonnes/yr (Yao et al., 2022).




**Fig. 1.** Texas Coast and Study Area

Wind-driven waves typically approach the southeastern shore of the Brazos River estuary, causing a pronounced asymmetrical alongshore transport of both Brazos River and coastal sediments along the shore to the San Bernard River mouth (Fig. 1). This natural coastal process, coupled with the excessive sediment

discharge into GoM and the diversion of the Brazos River by 10 km from its historical mouth, is regarded as the primary cause of the blockage at the mouth of the San Bernard River. The San Bernard navigation channel was dredged 20 times between 1943 and 2009, with a dredging frequency of 2.3 years (Thomas and Dunkin, 2012). Dredging has been conducted more frequently in recent years. The latest dredging started in the spring of 2022; however, the river mouth closed after a few months and has remained closed since then (Fig. 2). This closure is attributed to below-average rainfall within the San Bernard River watershed, leading to low flow volumes at the mouth of the river. It should be noted that the mouth of the San Bernard has also been naturally opened during major storms. Hurricane Harvey made landfall in Texas in August 2017, causing widespread and devastating flooding in various areas, including the San Bernard River mouth. The mouth opened into GoM during this event, even though the river transported 19,000 tonnes of sediment in one month, accounting for 50% of the annual average suspended sediment load (Yao et al., 2022). The river outlet was clogged again after a few years. Malito and Mohrig (2023) attributed the closure of the San Bernard River to coastal processes (alongshore transport and tidal flushing) rather than fluvial discharge.




**Fig. 2.** San Bernard River mouth after 2021-2022 dredging (left) and one year later (right).

## 2. Developing Suspended Sediment Concentration-Satellite Imagery Relationships

The complexity of sediment dynamics in the Brazos River and San Bernard River estuaries calls for a comprehensive study to meet the manifold challenges faced by the region. This research has focused on two interrelated aspects, namely assessing temporal changes in sediment regime in the study area and establishing predictive models that fully depict sedimentation processes over the Brazos and San Bernard estuaries. This paper presents the development of these models that estimate suspended sediment concentrations for the lower Brazos River and the Brazos and San Bernard estuaries using satellite imagery and publicly available suspended sediment data. In addition to a general discussion of the models' development, a case study will be presented for the time period before, during, and after Hurricane Harvey to evaluate the impact of this event on the sediment dynamics along the lower Brazos and San Bernard Rivers (Fig. 3).

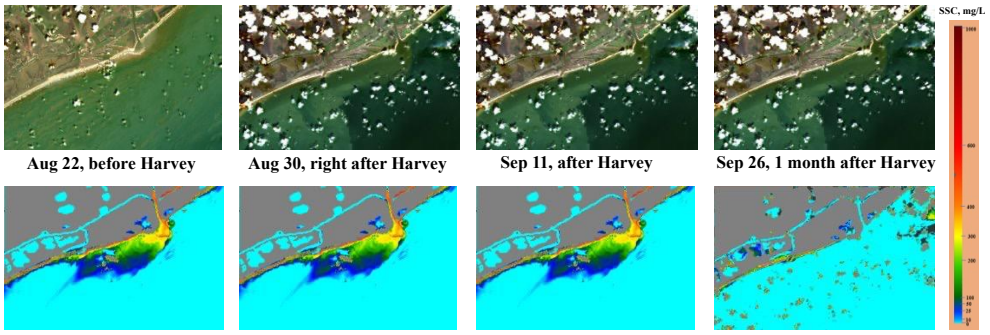



**Fig. 3.** Estimated suspended sediment concentrations (SSC) for Hurricane Harvey using relationships developed based on the satellite imagery.

The findings of this study will highlight the approach's benefits and limitations in understanding sediment dynamics in the study area. The results will provide the information necessary for devising a management and restoration plan to maintain the San Bernard River mouth open.

**References**

Dunn, DD, Raines, TH (2001) Indications and potential sources of change in sand transport in the Brazos River, Texas (No. 2001-4057). US Department of the Interior, US Geological Survey

Malito J, Mohrig D (2023) Intended vs unintended consequences of modifying coastal river channels. preprint. Preprints.

Milliman JD., Meade RH (1983) World-wide delivery of river sediment to the oceans. The Journal of Geology 9, 1–21

Paine JG, Morton RA (1989) Shoreline and vegetation-line movement, Texas Gulf Coast, 1974-1982

Texas Stream Team (2020) San Bernard Watershed Data Report. The Meadows Center for Water and the Envir, Texas State University

Thomas R, Dunkin L (2012) Erosion control and environment restoration plan development, Matagorda County, Texas; Phase 1: Preliminary investigation. ERDC/CHL TR-12-11, Coastal and Hydraulics Laboratory, U.S. Army Engineer Research and Development Center, 3909 Halls Ferry Road, Vicksburg, MS 39180-6199

Yao Q, Joshi S, Liu KB, Rodrigues E, Yin D (2022) A multi-decadal analysis of river discharge and suspended sediment load in three Texas coastal rivers in relation to hurricanes, seasonal rainfall, and ENSO. Frontiers in Earth Science, 10, 886614.

# CONNECT – Local coastal monitoring service for Portugal

Marta RODRIGUES[1], André B. FORTUNATO[2], Ricardo J. MARTINS[3], Gonçalo de JESUS[4], Alphonse NAHON[5], Ana C. BRITO[6], Anabela OLIVEIRA[7], José L. COSTA[8], Elsa ALVES[9], Zahra Mardani KORANI[10]

[1,2,3,4,5,7,9,10] Departamento de Hidráulica e Ambiente, Laboratório Nacional de Engenharia Civil, Portugal
{mfrodrigues, afortunato, rjmartins, gjesus, anahon, aoliveira, ealves, zmardani}@lnec.pt
[6,8] Faculdade de Ciências, Universidade de Lisboa; Centro de Ciências do Mar e do Ambiente (MARE), Portugal
{acbrito, jlcosta}@ciencias.ulisboa.pt

ABSTRACT

CONNECT provides a local, high-resolution, coastal monitoring service. It integrates model-based forecasts and observations to provide physical and biogeochemical data on Portuguese estuaries. The service is demonstrated in two use cases: the Tagus and the Mondego estuaries.

## 1. Introduction

Coastal areas provide multiple ecosystem services and are key for the blue economy. These systems harbor ecologically important habitats for fish, shellfish and birds, buffer nutrient and contaminant loads to the ocean and support diverse human activities. Growing human activities in coastal areas and climate change increase the hazards in these systems. Quantifying and anticipating how human-induced or climate drivers influence coastal systems became essential to support their sustainable management, and to meet the goals of the environmental directives and policies.

CONNECT offers a shelf-to-estuary, high-resolution, coastal monitoring service that integrates model-based forecasts and observations. It provides physical and biogeochemical data on Portuguese estuaries to the CMEMS – Copernicus Marine Service, enhancing the management, monitoring and forecasting of water quality and coastal inundation. This service integrates two operational coastal data infrastructures:

- the UBEST (http://ubest.lnec.pt/) coastal observatory (Rodrigues et al., 2021) focuses primarily on model forecasts partly forced by CMEMS regional models. Simulations are operated by the WIFF – Water Information and Forecasting Framework (Rogeiro et al., 2018) and the OPENCoastS service (Oliveira et al., 2020) and performed with the model SCHISM – Semi-implicit Cross-scale Hydroscience Integrated System Model (Zhang et al., 2016), in 2D barotropic (including waves) and 3D baroclinic modes. The 3D simulations include biogeochemistry variables.
- the CoastNet (https://coastnet.pt/) monitoring infrastructure (Castellanos et al. 2021; França et al. 2021) provides near real-time observations from in-situ sensors and remote sensing data mainly from CMEMS. In-situ measurements include pH, temperature, salinity, dissolved oxygen, chlorophyll-a and turbidity.

By combining complementary sources of information, the integrated service: 1) enhances confidence in both the model results and the observations by allowing automatic cross-comparison of data sources; 2) fosters the early detection of numerical and measurement anomalies (e.g., drifting time series due to biofouling); 3) strengthens the robustness by creating redundancy in the data access; 4) promotes the adoption of common formats and a seamless integration with CMEMS; 5) simplifies the extension to other coastal systems, given the adaptability and transferability of the underlying service.

The new integrated service will strengthen the support of the implementation of the Water Framework Directive (WFD), the Marine Strategy Framework Directive (MSFD), the Floods Directive (FD), and other EU policies, such as the Green Deal, by providing further and integrated historical and real-time information on physics and biogeochemistry.

## 2. The CONNECT service

CONNECT is a user-friendly service that seamlessly integrates and shares through a dedicated webGIS portal layers of physical and biogeochemical data (Fig. 1). These layers are aggregated at different spatial and temporal scales. The integrated service is globally accessible, comprehensive, flexible, and modular. It was designed to be easily customizable and transferable to other coastal systems. The service's main features are: i) shelf-to-river, high-resolution, circulation and water quality operational modeling with SCHISM operated by WIFF and OPENCoastS, downscaling CMEMS regional predictions to produce daily forecasts of local physical and biogeochemical variables; ii) real-time physical and biogeochemical data from in-situ observation networks, and EO-based data from CMEMS (CoastNet); iii) river flows at the models' upstream boundaries predicted using Artificial Intelligence; iv) automatic model-observations comparison, enhancing confidence in both; v) water level maxima and water quality indicators based on model forecasts and observations; vi) weekly reports of the modeled and observed variables that summarize both the physical behavior and the water quality status of the coastal systems; and vii) seamless integration with CMEMS regional models and EO data.

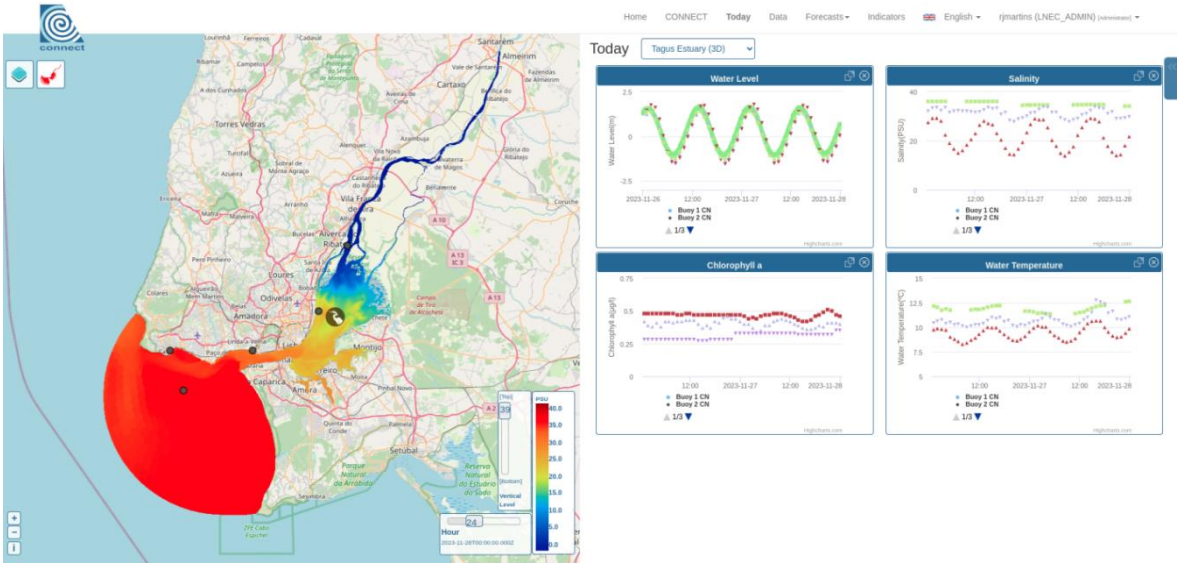



**Fig. 1.** CONNECT service: Today's dashboard - model forecasts and observations in the Tagus estuary.

## 3. Use cases

Two use cases demonstrate the added-value of the CONNECT service. First, model and observation data will support the assessment of the Tagus estuary's (Fig.1) ecological status in the context of the WFD, and quantify its contribution to the adjacent coastal area, supporting the MSFD. The service will also help to anticipate flooding events, thus contributing to the efficiency of the civil protection agents. Secondly, environmental conditions that can cause inundations or endanger ecosystems and economic activities (e.g., navigation) are predicted for the Mondego estuary. The service will equally provide physical-chemical data (e.g., salinity, temperature) to support the WFD and indicators for the protection of the ecosystems.

**Acknowledgements**

The CONNECT project is funded by the Copernicus Marine Service User Engagement Programme 2022-2028.

**References**

Castellanos P, Brito AC, Chainho P, Quintella B, da Costa L, França S, Cabral H, Costa JL (2021) CoastNet Dataset from Mondego, Tejo and Mira Estuaries: Multiparametric measurements during 2020, Frontiers in Marine Science, 8, 707089

França S, Fonseca VF, Tanner SE, Vasconcelos R, Reis-Santos P, Maia A, Ruano M, Cardoso I, Henriques S, Pais MP, Brandão P, Brito AC, Castellanos P, Chainho P, Quintella B, da Costa L, Costa MJ, Costa JL, Cabral HN (2021) Historical data in the CoastNet Geoportal: snapshot of estuarine fish communities in Portuguese estuaries, Frontiers in Marine Science, 8, 685294

Oliveira A, Fortunato AB, Rogeiro J, Teixeira J, Azevedo A, Lavaud L, Bertin A, Gomes J, David M, Pina J, Rodrigues M, Lopes P (2020), OPENCoastS: An open-access service for the automatic generation of coastal forecast systems, Environmental Modelling & Software, 124, 104585

Rodrigues M, Martins R, Rogeiro J, Fortunato AB, Oliveira A, Cravo A, Jacob J, Rosa A, Azevedo A, Freire P (2021) A web-based observatory for biogeochemical assessment in coastal regions, Journal of Environmental Informatics, 38(1), 1-15

Rogeiro J, Rodrigues M, Azevedo A, Oliveira A, Martins JP, David M, Pina J, Dias N, Gomes J (2018), Advances in Engineering Software, 117, 70-79

Zhang YI, Ye F, Stanev EV, Grashorn S (2016) Seamless cross-scale modeling with SCHISM, Ocean Modelling, 102, 64-81

# Sand waves and sediment recirculation along the main channel at the mouth of the Tagus estuary

Luís Ivens PORTELA[1]

[1] Laboratório Nacional de Engenharia Civil, Portugal
lportela@lnec.pt

ABSTRACT

Sand waves in the seaward part of the main channel of the Tagus estuary are examined. The study is based on high-resolution surveys conducted in 2019 and 2020. The average wavelength and height were found to be about 80 m and 2 m, respectively, and the asymmetry and evolution between surveys indicate that migration is mainly ebb-directed. The results suggest that sediment transported northwards by waves and flood currents over the main ebb-tidal delta shoal (Cachopo Sul) is partly mobilised by the ebb-dominant currents along the edge of the shoal and ultimately recirculated in a counterclockwise direction.

## 1. Introduction

Sand waves are bedforms with crests approximately transverse to the main flow direction, common on sandy bottoms in estuaries and shallow seas. Large sand waves (with wavelengths >50 m) have been described at the mouth of estuaries with strong tidal currents (Barnard *et al.*, 2013). They are of practical importance in the maintenance of safe access channels to ports. They also provide information on sediment transport pathways in ebb-tidal deltas that influence the equilibrium of adjacent shorelines. This paper investigates the dynamics of sand waves in the main channel of the Tagus estuary, where they have received little attention.

## 2. Methods

The study is based on Cosmo multibeam surveys of 2019 and 2020 (https://cosmo.apambiente.pt), available at a resolution of 0.3 m. The focus of the analysis is on the bedforms at the transition between the main sand body of the ebb-tidal delta platform (the Cachopo Sul shoal) and the main ebb channel, seaward of the point where the submerged spit (defined by the 4 m isobath) reaches its maximum progression over the channel (Fig. 1). Bedform parameters (wavelength, height and asymmetry) were estimated at selected transects, as were migration directions and rates between surveys.

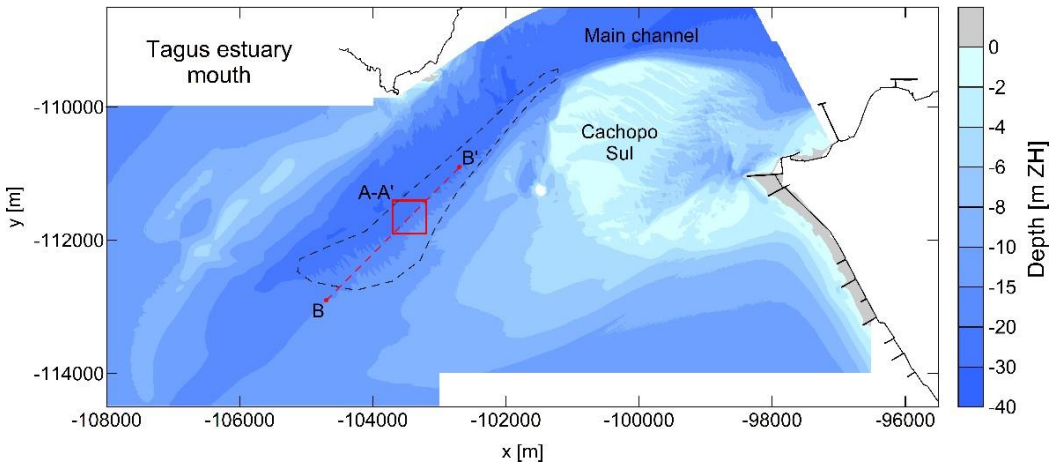



**Fig. 1.** Bathymetry of the mouth of the Tagus estuary in 2020 (data source: https://cosmo.apambiente.pt). Black dashed line shows sand wave region in the seaward (westward) part of the main channel. Box shows detail area in Fig. 2. Red dashed line shows cross-section B-B'.

## 3. Results

Sand waves in this part of the main channel cover an area of 2.5 km$^2$ in water depths of 10-30 m, and are confined to the side of the channel adjacent to the Cachopo Sul shoal. In section A-A', wavelengths and heights are on average 79 m and 2.2 m, respectively (Fig. 2a), consistent with those reported by Santos *et al.* (2018) for sand waves in a landward (eastward) area. Bedform asymmetry, an indicator of net sediment transport, is pronounced (ca. 30%) and always ebb-directed. The comparison of the 2019 and 2020 surveys shows that sand waves are active morphological features within the ebb-tidal delta (cf. detail area A-A' in Fig. 2b). At the seaward end of section B-B', migration is ebb-directed with maximum rates of ca. 60 m year$^{-1}$. However, over the entire section there is considerable variability in the apparent direction of migration, and the average migration rate is much lower (5 m year$^{-1}$ in section A-A'; Fig. 2c). A detailed analysis of migration rates is hindered by the large time interval between surveys.

## 4. Discussion

The results seem to support a model of sediment recirculation in the ebb-tidal delta of the Tagus estuary, where sediment transported northwards by waves and flood currents over the Cachopo Sul (which accumulates on its northern edge forming a steep slope with the main channel) is partly mobilised by the ebb-dominant currents of the channel. The sand wave field on the side of the channel adjacent to the shoal would be evidence of this net seaward-directed sediment transport. The sand waves eventually interfere with the dredged access channel in the outer bar. However, the widening of the sand wave field on the outer ebb-tidal delta also suggests sediment recirculation via the Cachopo Sul, thus completing the cycle.

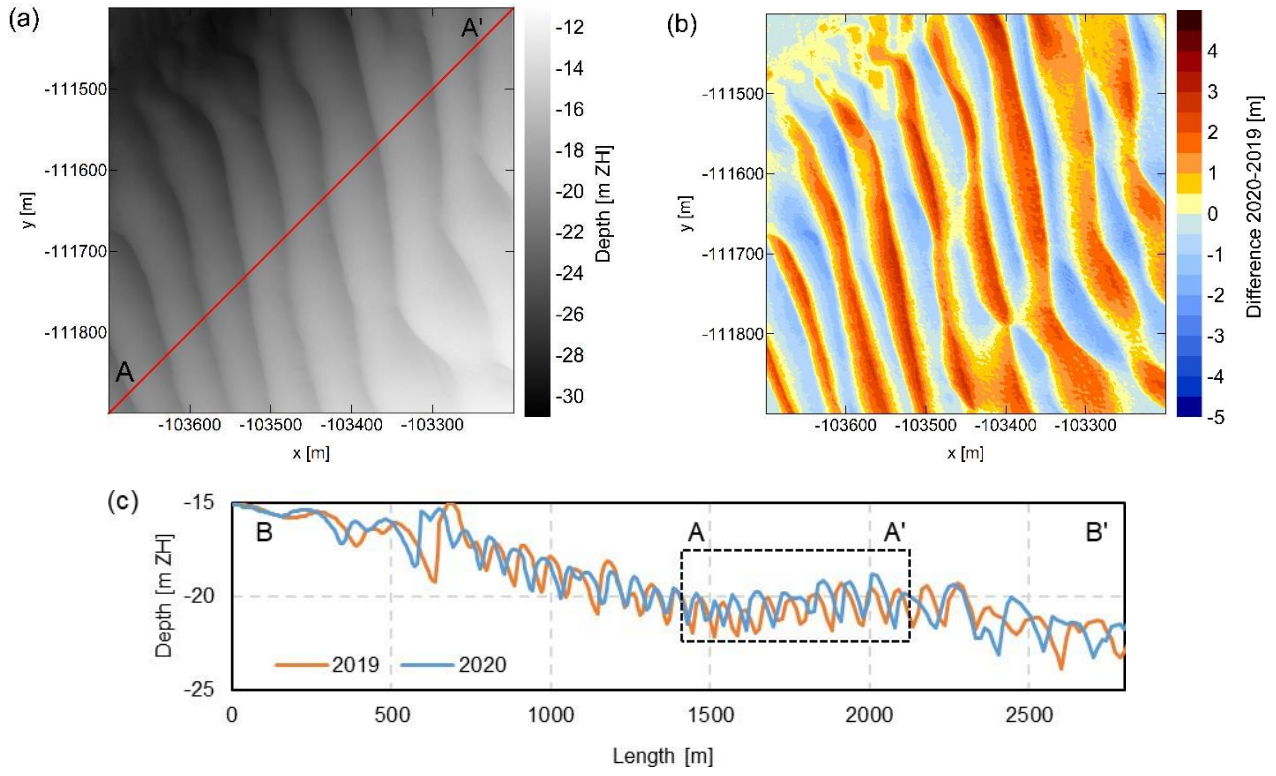



**Fig. 2.** (a) Detail A-A' of the 2019 bathymetric survey showing sand waves. (b) Difference between bathymetric surveys in 2019 and 2020. (c) Cross section B-B' in 2019 and 2020.


### Acknowledgements

Data obtained from the Portuguese Environment Agency's Coastal Monitoring Programme (COSMO), co-financed by the POSEUR Programme. Available at: https://cosmo.apambiente.pt.


### References


Barnard PL, Erikson LH, Elias EPL, Dartnell P (2013) Sediment transport patterns in the San Francisco Bay Coastal System from cross-validation of bedform asymmetry and modeled residual flux, Marine Geology, 345, 72-95

Santos R, Rodrigues A, Quartau R (2018) Acoustic remote characterization of seabed sediments using the Angular Range Analysis technique: The inlet channel of Tagus River estuary (Portugal), Marine Geology, 400, 60-75

# Improving Surfability Assessment along a Submerged Detached Breakwater at Praia da Vagueira, Portugal

Pedro TAVARES[1], Ana MENDONÇA[2], Conceição Juana FORTES[3], Pedro BICUDO[4]

[1,4] Instituto Superior Técnico, Physics Department, Lisbon, Portugal
pedro.f.tavares@tecnico.ulisboa.pt
bicudo@tecnico.ulisboa.pt

[2,3] Laboratório Nacional de Engenharia Civil, Hydraulics and Environmental Department, Lisbon, Portugal
amendonca@lnec.pt
jfortes@lnec.pt

ABSTRACT

A case study aiming to improve surfing conditions over a submerged detached breakwater, intended to be placed in front of Praia da Vagueira (Aveiro, Portugal), was concluded in April 2022. The final results are revisited and refined by incorporating an alternative wave breaking line detection method, using the resulting eddy viscosity parameter from the COULWAVE numerical model. Preliminary results demonstrate good agreement with experiments and indicate the potential for a more detailed analysis, but further investigation is required.

## 1. Introduction

The Portuguese Environment Agency, I.P., and the LNEC, UAveiro, and IST Consortium collaborated in carrying out the characterization and feasibility study of a multifunctional submerged detached breakwater (SDB) in front of Praia da Vagueira (Aveiro, Portugal), which concluded in April 2022. A physical and numerical modeling study was developed to assess the influence of the SDB on surfing conditions in the area for three cases: the current situation (without SDB); with the SDB parallel to the coastline (SDB 0º); and the SDB with a 45º angle relative to the coastline (SDB 45º).

Estimation of wave breaking-related parameters, such as the Iribarren number and peel angle, requires accurately capturing the wave breaking line. Regarding the numerical study by Sancho et al., 2022, the employed wave breaking line detection method enabled capturing only a breaking region and not necessarily pinpointing a specific breaking line along the structure.

In this paper, we present an alternative method to more accurately capture the wave breaking line by taking advantage of the implemented ad-hoc wave breaking model in COULWAVE (Lynett et al., 2008).

## 2. Previous Physical & Numerical Results

The reduced physical model utilized by Sancho et al., 2022 consisted of a sandy mobile bed replicating the conditions of the prototype from the -12 m (HZ) bathymetric contour to the upper beach. On the numerical front, the COULWAVE model was applied at prototype scale, and the results from the reduced physical model were appropriately scaled for meaningful comparison.

In the context of assessing surfability, all tests were conducted for regular waves with wave direction of 296ºN, following the initial conditions specified in Table 1.

**Table 1.** Tested wave conditions at prototype scale.

| $H_0$ (m) | $T_0$ (s) | Water Level (m (HZ)) |
|---|---|---|
| 1.5, 2 and 3 | 10 and 12 | +2.17 |

Overall, the study indicated that the SDB 45º configuration was more favorable for enhancing surfing conditions.

## 3. Wave Breaking Line & Surfability Parameters: COULWAVE

The COULWAVE model enables the numerical solution of a depth-integrated model consisting of a set of weakly dispersive Boussinesq-type equations, incorporating physically consistent viscosity and vorticity terms as derived in Kim et al., 2009. These equations are coupled to a wave breaking mechanism identical to the one presented in Kennedy et al., 2000. The breaking scheme is based on an eddy viscosity approach, where the eddy viscosity $\nu$ is a component of an ad-hoc dissipative term and expressed as,

$$\nu = Bh_t\eta \quad , \quad (1)$$

where $h_t = h + \eta$ represents the total water depth, and $B$ is a variable selected to ensure a smooth transition between breaking and non-breaking states.

Considering the SDB 45º configuration with $H_0$ = 2 m, $T_0$ = 12 s, and appropriate boundary conditions, the wave dynamics over the SDB were simulated for a computational domain of 2900 m in the longshore and 1670 m in the cross-shore directions, over 600 s total simulation time (Fig. 1). The available viscosity parameters were fixed to their default values, since an initial calibration attempt using physical model data showed no significant changes.

Using the output eddy viscosity quantity over space and time, the local maximum values were identified within a specified domain window for each time instant. These points were subsequently grouped into breaking lines by requiring them to be sufficiently close both in space and time. The results of this post-processing analysis are illustrated in Fig. 1. Comparison with physical model photographs shows good agreement with the detected breaking lines.

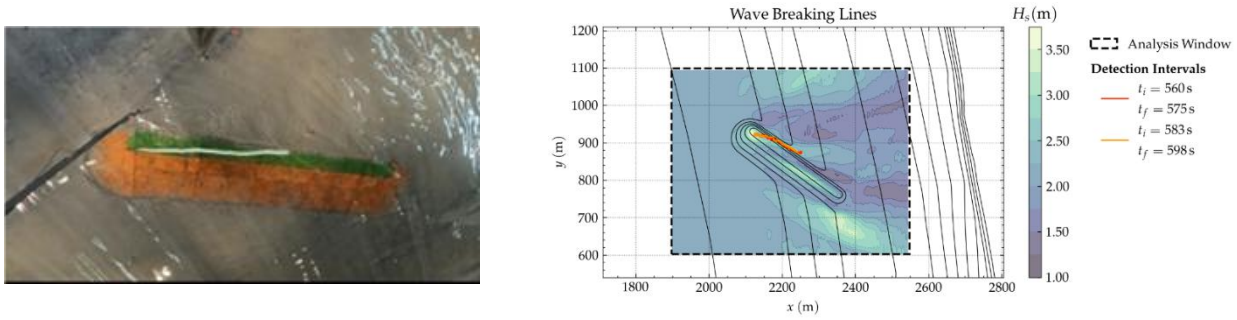



**Fig. 1.** Comparison between two examples of numerically detected wave breaking lines (right) and physical model photograph (left) for the SDB 45º configuration.

By interpolating the detected points, one can then determine the Iribarren number and peel angle over space, for each detected breaking line. For a more conclusive result, the results for each breaking line can be averaged, providing clearer results for the case study.

## 4. Conclusions

The present work showed an overall improvement in wave breaking line detection and holds the potential for a more consistent and detailed analysis of the surfability parameters along the SBD. However, it's important to note that, due to the nature of the numerical model in use, more detailed information on wave breaking along the structure, such as wave overturning patterns, cannot be directly simulated and can only be approached using fully 3D CFD models. Efforts to provide 3D analysis for the Praia da Vagueira case study are currently under consideration.

**Acknowledgements**

The results of the present study derive from the Program coordinated by Agência Portuguesa do Ambiente and co-financed by the Operational Program for Sustainability and Efficiency in the Use of Resources, POSEUR-02-1809-FC-000039. The authors thank the support of CeFEMA, funded by FCT under contract UIDB/04540/2020.

**References**

Kennedy, A., Chen, Q., Kirby, J. and Dalrymple, R. (2000) 'Boussinesq Modeling of Wave Transformation, Breaking, and Runup. I: 1D', Journal of Waterway, Port, Coastal, and Ocean Engineering, 126(1).

Kim, D.-H., Lynett, P. J. and Socolofsky, S. A. (2009) 'A depth-integrated model for weakly dispersive, turbulent, and rotational fluid flows', Ocean Modelling, 27(3–4), pp. 198–214.

Lynett, P. J., Liu, P., Sitanggang, K. and Kim, D.-H. (2008) 'COULWAVE Code Manual: Cornell University Long and Intermediate Wave Modeling Package'. Available at: https://isec.nacse.org/models/coulwave_description.php.

Sancho, F., Freire, P., Neves, M., Oliveira, F., Mendonça, A., Fortes, C., Roebeling, P., Baptista, P., Brito, F. and Coelho, C. (2022) Characterization and feasibility study of a multifunctional detached breakwater in front of Vagueira Beach (Final Report). Lisbon.

# Investigation of Seasonal Variation of Microplastics and Micropollutants in Inland Terrestrial Waters

Neval BAYCAN[1], Nefise ALYÜRÜK[1], Nursena KARA[1], Cumana ALPERGÜN[1], Füsun PELİT[2], İlknur ERBAŞ[2], Yiğithan KAZANCI[3], Orhan GÜNDÜZ[3]

[1] Dokuz Eylül University, Department of Environmental Engineering, Izmir, Türkiye, neval.baycan@deu.edu.tr

[2]Ege University, Department of Chemistry, İzmir, Türkiye, fusun.pelit@ege.edu.tr

[3]Izmir Institute of Technology, Department of Environmental Engineering, Izmir, Türkiye, orhan.gunduz@iyte.edu.tr

ABSTRACT

In recent years, studies on the effects of microplastics in environmental matrices have gained momentum due to the negative effects of these substances on both aquatic organisms and human beings. While extensive research has scrutinized the prevalence of microplastic pollution in oceans and seas, their impact on terrestrial waters still remains largely unexplored. Comprehending the intricate journey and transport of microplastics within river ecosystems is an enigmatic puzzle yet to be fully deciphered. Their movement within river systems is a complex interplay influenced by factors such as flow dynamics, sedimentation, and seasonal fluctuations. Understanding these mechanisms stands as a critical step in assessing the accumulation and dispersion of microplastics within river ecosystems.

In this study, water and sediment samples were collected from 20 and 5 different monitoring stations (Figure 1), respectively, along the Nif and Gediz rivers and the amounts of microplastics in water and sediment columns were investigated in four different seasons. The Gediz River is a 385 km long major river in western Anatolia, Türkiye, which has a total drainage area of about 17,000 square kilometers. The Nif Stream is a discharge dominated tributary of Gediz River and does not have natural flow in the channel during summer and fall seasons. Water and sediment samples collected during winter, spring, summer and fall seasons underwent rigorous laboratory analyses to identify potential seasonal variations. Utilizing a three-dimensional stereomicroscope (Leica S Apo), the prepared samples were closely examined to characterize the shape, color, and size of microplastics. Additionally, Fourier transform infrared (ATR-FT-IR) spectroscopy (Perkin Elmer Frontier) was employed to determine the types of plastic materials present in samples.

In addition, polyaromatic hydrocarbon (PAH) residues and Bisfenol A (BPA) were measured in water samples to determine the relationship between microplastics and micro-pollutants. The PAH species studied were naphthalene, acenaphthylene, acenaphthene, fluorene, phenanthrene, anthracene, fluoranthene, pyrene, benzo(a)anthracene and chrysene, Benzo(b)fluoranthene, Benzo(k)fluoranthene, Perylene, Benzo(a)pyrene, Benzo(e)pyrene, Indeno(1,2,3- cd)pyrene, Dibenz(a,h)anthracene and Benzo(g,h,i)perylene. Liquid-liquid extraction (LLE) method has been developed for the analysis of organic micropollutants in aqueous matrices in order to perform more sensitive analyses by miniaturizing the volume of the solvent and to increase the precipitation. The most important advantages of the method are the use of organic solvents at the micro litre level in the LLME process and the absence of the need for long evaporation processes. The aim of this study was to develop a new microextraction technique that will enable sensitive and selective analysis of polyaromatic hydrocarbon (PAH) residues. For this purpose, the project aimed to use the dispersive liquid liquid microextraction (DLLME) technique, which is frequently used as a green extraction technique today, by integrating it with the GC-MS system. Deep Eutectic Solvents (DES) were used to analyses for BPA. DES are new type of environmentally friendly solvent and used as an extraction solvent in a liquid-liquid microextraction (LLME) method for BPA analysis.

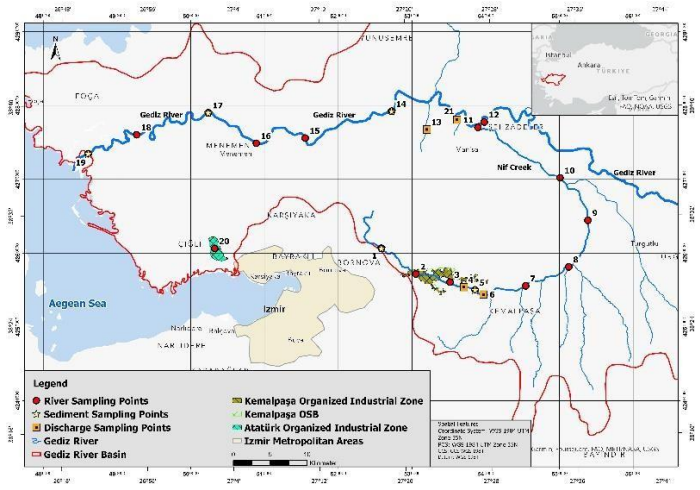



Figure 1. Sampling Points

The total amounts of microplastics were given in Table 1. The study's outcomes revealed a notably higher total count of microplastics during winter compared to the summer and fall season. This decline in microplastic prevalence during summer and autumn were attributed to fluctuating seasonal discharges, varying weather conditions, and the impact of local facilities contributing to microplastic pollution in the area. Furthermore, the results unveiled a progressive increase in microplastic contamination within a terrestrial aquatic system primarily influenced by effluents, intensifying along the flow path of the river. In particular, significant local peaks were observed within the industrial zone hosting multiple plastic processing facilities.

Table 1. Total amounts of microplastics in different seasons

| Stations | Winter (n/L) | Spring (n/L) | Summer (n/L) | Autumn (n/L) |
|---|---|---|---|---|
| 1 | 413 | 180 | 0 | 78 |
| 2 | 428 | 182 | 59 | 36 |
| 3 | 409 | 127 | 52 | 14 |
| 4 | 426 | 334 | 134 | 58 |
| 5 | 642 | 117 | 88 | 31 |
| 6 | 574 | 92 | 57 | 23 |
| 7 | 532 | 138 | 54 | 32 |
| 8 | 396 | 114 | 46 | 29 |
| 9 | 2853 | 172 | 46 | 8 |
| 10 | 474 | 207 | 56 | 22 |
| 11 | 3917 | 451 | 54 | 19 |
| 12 | 1235 | 180 | 48 | 16 |
| 13 | 1051 | 372 | 122 | 10 |
| 14 | 2553 | 132 | 53 | 113 |
| 15 | 790 | 61 | 34 | 60 |
| 16 | 910 | 79 | 154 | 33 |
| 17 | 446 | 127 | 56 | 30 |
| 18 | 798 | 60 | 34 | 46 |
| 19 | 325 | 126 | 43 | 14 |
| 21 | 2994 | 206 | 279 | 47 |

The study's findings revealed that the predominant colors of microplastics were transparent and yellow. The prevalence of transparent microplastics in the samples could be attributed to the physicochemical attributes of the MP polymer and the impacts of environmental degradation, such as erosion and exposure to UV radiation. Surface water samples commonly exhibited fibers and particles, with films and foams being comparatively less frequent. Research indicated a significantly higher presence of small-sized microplastic particles (< 0.1 – 5mm) in the Gediz and Nif rivers compared to European rivers, possibly due to the inefficacy of current wastewater treatment plants in eliminating very small microplastics. The analysis identified PP, PE, PS, and PET as the most common types of microplastics, respectively. Although the results of micropollutants varied according to the sampling points, it was determined that there was a correlation between micropollutants and microplastic counts.

**Acknowledgements:** This study was supported by Scientific and Technological Research Council of Turkey (TÜBİTAK) with project number of 121Y460.

# Occurrence of Microplastic in the Thai Aquatic Environment

Sudarshan KURWADKAR[1], Grace NATALIA[2], Suwanna BOONTANON[2], Somchai PATHOMSIRI[2]

[1] Department of Civil and Environmental Engineering, California State University, Fullerton, USA

skurwadkar@fullerton.edu

[2] Department of Civil and Environmental Engineering, Faculty of Engineering, Mahidol University, Thailand
mgracenat@gmail.com
suwanna.boo@mahidol.ac.th
Somchai.Pat@mahidol.ac.th

ABSTRACT

Microplastics are ubiquitous, as evidenced by their frequent detection in various environmental matrices, including lakes, rivers, marine, estuarine, and freshwater environments. Numerous studies have highlighted the occurrence, size, type, form, and chemical composition of microplastics. However, most of this research originated from developed countries with dedicated resources. Conversely, there's a noticeable gap in the literature concerning the occurrence of microplastics in the aquatic environments of developing countries, particularly within South Asian regions like Thailand. This study aims to fill that gap by documenting the occurrence and concentration of microplastics in both water and sediment within Thailand's coastal zones. In this study, we comprehensively reviewed microplastics' occurrence, distribution, and detection in major water bodies of Thailand's urban and rural environments. A comprehensive evaluation of existing studies suggests widespread microplastic contamination in surface waters and sediments of the Gulf of Thailand, Chao Phraya River Estuary, Bandon Bay, Songkhla Lagoon, Tapi-Phumduang River System, and Nonthaburi, and Rayong. Careful analysis of the existing data suggests that surface water, sediments, and wastewater have varying amounts of microplastics with the highest average concentrations ranging from 48 ±8 x$10^3$ pcs/L, >200,000 pcs/kg, and 76-192 pcs/L, respectively. The abundance of microplastics in the Thai aquatic environment is attributed to widespread improper plastic disposal, inadequate or poor recycling practices, untreated sewage discharge, and improper plastic disposal by the transient coastal communities, adversely impacting Thai water resources. The widespread occurrence of microplastics in aquatic environments adversely affects aquatic marine life due to their bioaccumulative potential, thus serving as a primary pathway to the food web. Ingestion of microplastic-laden seafood may adversely affect human health. This comprehensive study is vital in understanding the extent of microplastic pollution in Thailand and may drive improvements in waste management and environmental protection strategies.

## 1. Introduction

Microplastic pollution of water bodies in Thailand is mainly due to inadequate waste management practices, including improper disposal of plastics, insufficient recycling efforts, and the release of untreated sewage, particularly from transient coastal populations. Microplastics are persistent, and their continued occurrence in aquatic resources will adversely impact marine life and eventually impact human health due to their bioaccumulative potential in aquatic species.

## 2. Methodology

Extensive data on the type and size of the microplastics in water and sediment samples was collected from across the coastal areas of Thailand. The objective is to understand the magnitude and abundance of microplastic pollution in the Thai aquatic environment at sites with data tabulated and analyzed. These sites represent coastal areas frequented by seasonal tourists, and the likelihood of microplastic pollution is high due to the use of disposable plastic. These sites also include the areas that include sewage treatment plant outfalls and river discharges, specifically from the major rivers such as Chumphon, Tapi, Pumduang, and Pakphanang.

The sampling sites were selected based on the ocean surface circulation critical for the distribution and accumulation of microplastics. Various data was collected from the selected sites, including surface water, wastewater, drinking tap water, and sediments. The data was carefully tabulated based on the types of plastics and their respective size ranges observed in water and sediment samples. The data for sediment samples was recorded as the number of pieces per kilogram of sediments, while the microplastic concentration was recorded in pieces per liter of the water sample.

## 3. Results

Results show that surface water, sediments, and wastewater in Thailand have varying amounts of microplastics, with the highest mean concentrations ranging from 48 ± 8 x$10^3$ pcs/L, >2 x$10^5$ pcs/kg, and 76-192 pcs/L, respectively (Figures 1&2).

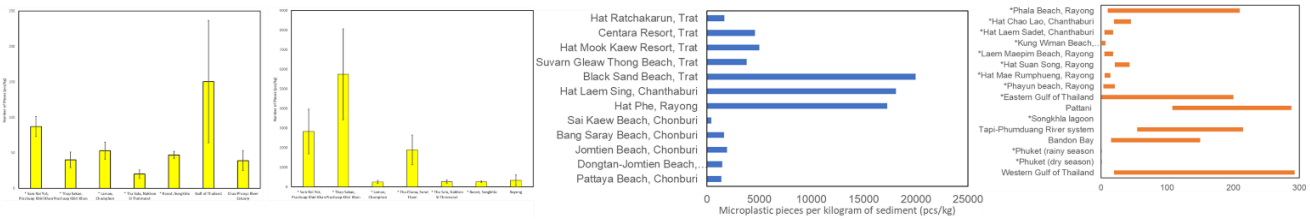



**Fig. 1.** Microplastic abundance (low and high) (left) and number of microplastic pieces at various sites (center) and the ranges of microplastics detected in sediment samples in different sites across coastal areas of Thailand. (*Concentration is multiple of thousands pieces/kg of sediments)

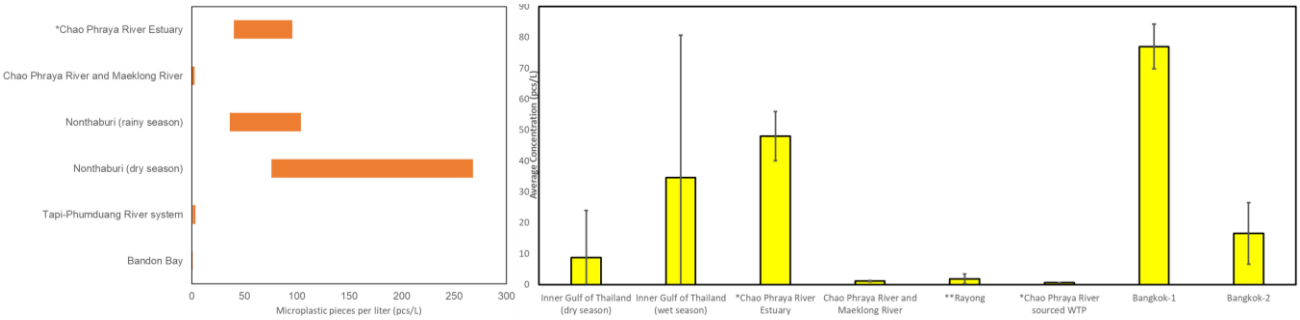



**Fig. 2.** Range (left) and abundance (right) of microplastic pieces detected (pcs/L) across various sites in Thailand (*Concentration are multiples 1000; ** multiples of 100,000)

## 4. Conclusion

Analysis of the compiled data shows widespread occurrence of microplastics of varying sizes and types throughout the Thai coastal areas. Most plastics are not biodegradable due to their chemical resilience; they grow brittle over time and disintegrate into tiny pieces. In addition to natural weathering, physical forces, such as the long-term effect of waves, further break down plastics into varying shapes and sizes. In Thai coastal areas, tiny plastic fragments of varying sizes ranging from 0.05 to 5 mm were abundantly detected in water and sediments. Specifically, the coastal areas frequented by seasonal tourists coupled with industrial complexes and illicit dumping of plastics of various forms have significantly impacted the Thai coastal regions. The continued occurrence of microplastics in the aquatic environment will adversely affect the aquatic food web since marine biotas often confuse microplastics with food, leading to their bioaccumulation. Ingestion of significant amounts of varying sizes and types of microplastic may adversely impact aquatic life due to their bio-accumulative potential, thus serving as a primary pathway to the food web. Ingestion of microplastic-laden seafood may adversely affect human health. This study has shown the extent, type, and size of microplastic pollution in Thai aquatic resources for the first time, justifying the need to protect and preserve Thailand's water resources.

**Acknowledgments**

Professor Sudarshan Kurwadkar was supported through the Short-term Visiting Scholarship Program (Fiscal year 2023) sponsored and managed by the Mahidol University, Salaya Campus, Thailand.

**References**

Bissen, R., Chawchai, S. (2020). Microplastics on beaches along the eastern Gulf of Thailand – A preliminary study, Marine Pollution Bulletin, 157,111345, https://doi.org/10.1016/j.marpolbul.2020.111345

Thepwilai, S., Wangritthikraikul, K., Chawchai, S., Bissen, R. (2021). Testing the factors controlling the numbers of microplastics on beaches along the western Gulf of Thailand, Marine Pollution Bulletin, 168, 112467, https://doi.org/10.1016/j.marpolbul.2021.112467.

# Optimization tool for the design of climate change robust Flood Control Areas in tidal zones

Danitza SALAZAR[1], Patrick WILLEMS[1]

[1] KU Leuven, Belgium
danitza.salazar@kuleuven.be
patrick.willems@kuleuven.be

## ABSTRACT

The Flemish government, through "De Vlaamse Waterweg" (DVW), an independent governmental agency for the management of navigable rivers and channels, has invested since 1976 in the design and implementation of the Sigmaplan. The Sigmaplan is a water management plan for the Schelde river and its tidal tributaries that focuses on the integrated improvement of its flood safety, nature, recreation and economic functions (Dauwe, 2017). The main flood safety measures are the construction of high and strong dikes and about 40 Flood Control Areas (FCAs, Fig. 1). Many of the planned FCAs are already built, while the remaining ones will be constructed or optimized by 2030. In view of the ongoing climate change (sea level rise and changes in inflow conditions), DVW is investigating the climate change robustness of the Sigmaplan and whether additional actions would be required. So, an analysis is made on how the already planned measures (dike levels, FCAs, depoldering areas, wetlands) react to updated climate change scenarios (horizons 2050 and 2100) and which strategies could make the designs more robust under any future climate change scenario (Willems et al., 2023).

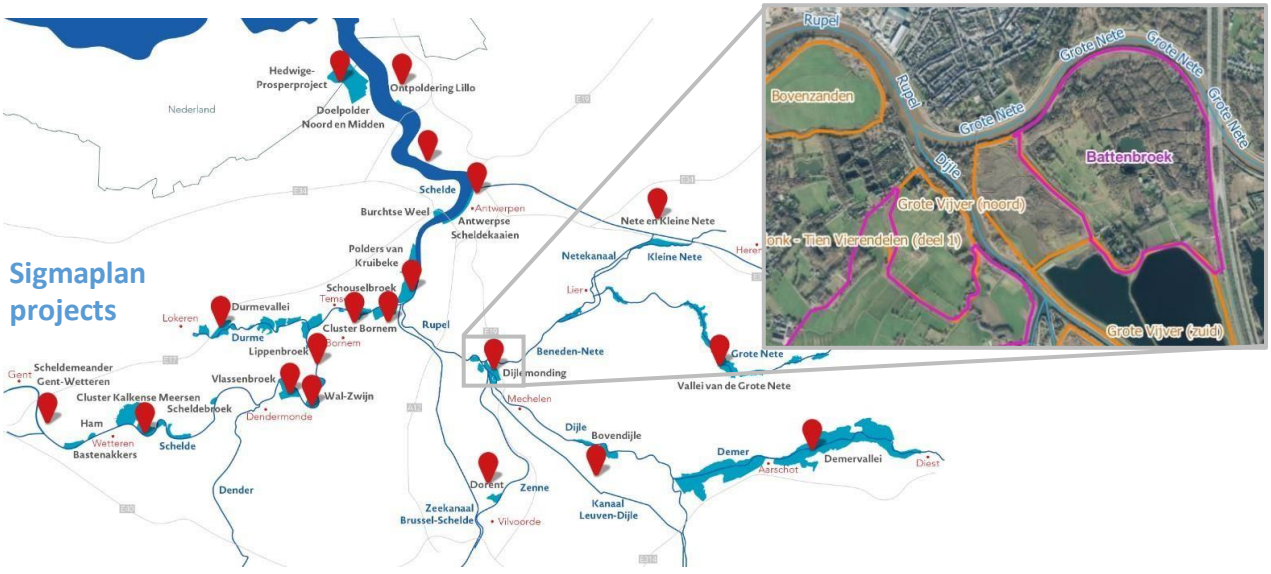



**Fig. 1.** Sigmaplan projects (source: https://www.sigmaplan.be/en/projects/, Nov 2023). Study area: FCA Battenbroek (right pink polygon).

One of the challenges here is to revise and optimize the FCAs in view of the increasing maximum water levels due to the sea level rise and the increasing upstream inland peak runoff flows. Optimizing the design of a FCA (see the scheme of the FCA dikes, inlets and outlets in Fig. 2) is a time consuming and very iterative process. Therefore, a tool is designed; it enhances the optimization of the FCA inlet and outlet for any given return period and (historical or future) storm event. This tool considers the tidal nature of the water level variation. As a study case, a conceptual model is built for the new FCA Battenbroek (Fig. 1), located along the Grote Nete river (Benedenete), which is one of the tidal tributaries of the Scheldt. This FCA is located just upstream where the Benedennete and the Dijle rivers join into the Rupel river.

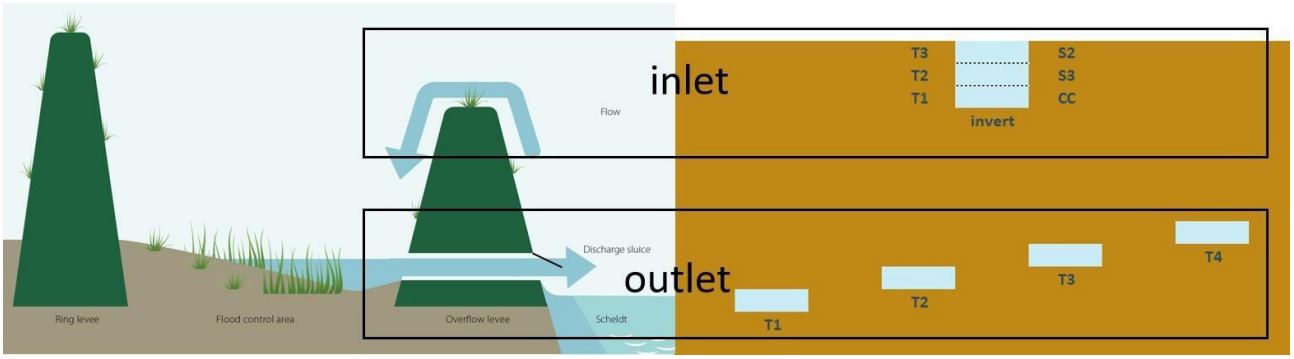



**Fig. 2.** Inlet/outlet schematization at the overflow banks towards a Flood Control Area.

The inputs of the tool are: 1) The geometry of the FCA; 2) Timeseries of water levels along the river, for all target events; 3) A set of optional invert levels; 4) The FCA maximum ring dike crest level or storage capacity and freebord. The tool has been built in Python 3.9.

In this study, storm events are considered for return periods of 1, 2, 5, 10, 50, 100, 500, 1000, 2500, 4000 and 10000 years. Based on a detailed full hydrodynamic model of the tidal river network, implemented in MIKE11 (validated for the high water event of January 2018), time series of river water level are obtained as input for the tool. With each of these events, a continuous logarithmic surface of optimal solutions for the FCA invert and width is obtained (Fig. 3, left); It is verified, using the MIKE11 model, that these solutions lead to the same maximum reduction of water level in the river (Fig. 3, right). It is concluded that existing FCAs are less effective in reducing water levels in the river under (more extreme) future climate scenarios (or higher target return periods). The root cause is that the FCAs fill up too rapidly for the future storm and they have no capacity left when the peak of the storm arrives. However, by either rising the inlet's invert, or by narrowing its width or both, the maximum reduction of the river water levels can again be achieved under future climate scenarios.

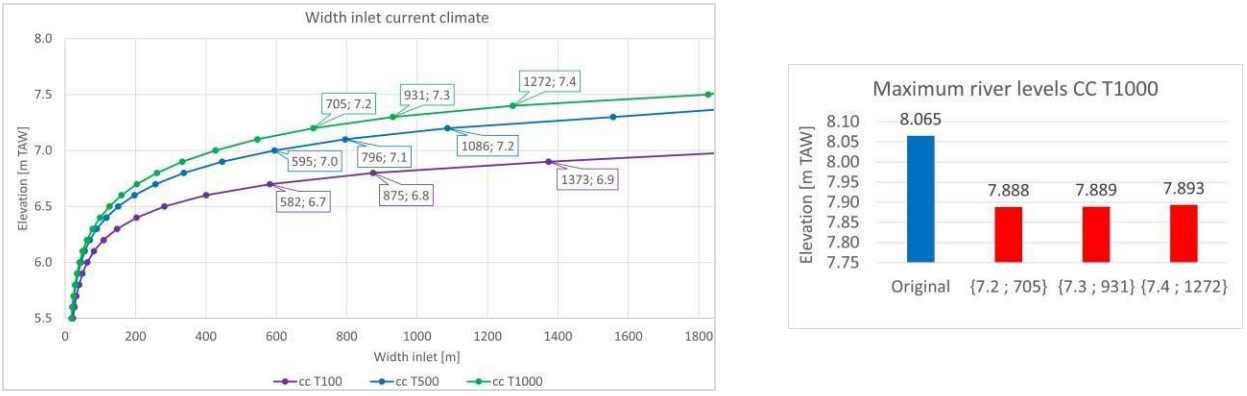



**Fig. 3.** Left: Selected combinations for the validation in the current climate CC T1000 (green upper line). Right: Maximum water level in the river for CC T1000 for the original cases, {invert [m TAW] ; width [m]} (source: Lebrun et Vandeweyer, 2023)

## Conclusions

The results of this tool can speed up the optimization of FCAs, considering the uncertain future climate conditions. This is especially useful in cases where a large number of FCAs need to be optimized. In this Sigmaplan case, there are around 40 FCAs whose design influence the design of their neighbor FCAs. Visualizing the whole range of optimal solutions for different climate scenarios can enhance the selection of more climate change robust (no regret) measures. The tool also includes the optimization of the outlets, is tested in more FCAs, and adapted to complex FCAs with interconnected areas. As a future research idea, the developed principles will be used in the design of adaptable inlets together with flood forecasting systems.

### Acknowledgements

The authors wish to thank De Vlaamse Waterweg nv and Flanders Hydraulics Research for their support, data and valuable remarks.

### References

Dauwe W (2017). The Sigma Plan. How do you want to live along the river Scheldt? De Vlaamse Waterweg nv,; Agency for Nature and Forest (ANB). https://www.sigmaplan.be/uploads/2017/08/170817-sigmabrochure-2017-en-lr.pdf

Lebrun L, Vandeweyer B, Salazar D, Willems P (2023) Optimization of a Flood Control Area in a tidal environment towards a climate change robust Sigmaplan. Master thesis, KU Leuven, Belgium.

Willems P, Salazar D, Mendoza S, Moustakas S, De Meester J, Zhu B, Schwarz C (2023) Evaluatie van de klimaatrobuustheid van het Geactualiseerde Sigmaplan en het Vlaamse Schelde-estuariumgebied. Study report for De Vlaamse Waterweg.

# Energy Transition in APS Ports

Eduardo BANDEIRA[1], Eduardo MOUTINHO[2], João ARAÚJO[3]

[1,3]APS - Port Authority of Sines and Algarve S.A., Portugal
eduardo.bandeira@apsinesalgarve.pt

[2,3]APS - Port Authority of Sines and Algarve S.A., Portugal
eduardo.moutinho@apsinesalgarve.pt, eduardo.moutinho@pianc.pt
joao.araujo@apsinesalgarve.pt

ABSTRACT

Following the EU external energy policy strategy the Portuguese ports are committed with the EU's plan for a green transition – the EU Fit for 55 shipping package and the REPowerEU.

This paper will focus on the strategy of APS – Port Authority of Sines and Algarve SA, regarding energy transition.

APS has the main port in Portugal located in Sines and two others business units, the commercial port of Faro and the commercial port of Portimão, with cruise ship activity. APS aims to have its ports 100% carbon emissions free by 2045, ahead of green deal 2050 goals, and striving for energy self-sufficiency.

APS has its objective the administration of the ports of Sines, Faro and Portimão, which is assigned direct port jurisdiction in the maritime, fluvial-maritime and land areas, aiming at their economic exploration, conservation and development, covering the exercise of the powers and prerogatives of the port authority that are or will be entrusted to it.

The Port of Sines is located at the crossroads of the main international maritime routes, north-south and east-west. This is the main port on the Ibero-Atlantic façade, whose geophysical characteristics have contributed to its consolidation as a strategic asset, as the country's main energy supply gateway and as a reference in the global containerized cargo market. The commercial ports of Faro and Portimão are located on the south coast of Portugal.

APS in its strategic plan aims to have its ports 100% carbon emission free by 2045. To achieve this goal, several measures are being taken in order to have a green and just energy transition.

## 1. Renewable Energy Production, Energy Storage and Renewable Energy Community

For APS the energy transition is imperative. Clean energy planning involves diversifying its origin. APS is considering the integration of various renewable sources, such as photovoltaic, wind and wave energy.

The port of Sines will have an estimated renewable power of 6.3 MW installed in the middle of 2024. APS is studying the possibility of installing a wind farm in the Port of Sines, enhancing renewable energy production on the port. Also, a wave energy converter will be tested at 1:10 scale.

With renewable energy production in the port of Sines, different storage solutions are being analyzed and studied according to the available technologies, their capacity, autonomy and investment planning. The use of storage technology will allow to plan and define when consuming the produced energy, thus minimizing surpluses. The constitution of a Renewable Energy Community will value the overproduction and will allow to share the benefits of port renewable production beyond the physical boundaries of the port, benefiting the adhering customers of the surrounding REC community.

## 2. Energy Needs and Installation of OPS Systems

In the port of Sines the energy needs in 2023 for consumption were 27 GWh/year and by 2030 should quadruple with expansion of the container terminal and the installation of Onshore Power Supply (OPS) systems.

It's estimated that four OPS systems will be installed in the container terminal at the port of Sines and one OPS system in the cruise terminal at the port of Portimão. With these installations it is expected that OPS systems will be responsible for 40% of the energy needs by 2030.

For 2030, port of Sines has the target of 70% renewable energy production installed with energy needs estimated of 68 GWh/year. The renewable energy production will be estimated of 27 MW split by 12 MW of wind power, 1 MW wave energy (pilot) and 14 MW photovoltaic.

The ambition for 2045 is target of 100% of renewable sources, with an estimated consumption energy needs of 130 GWh/year. The renewable energy production will be estimated of 48,5 MW split by 24 MW of wind power, 1 MW wave energy (pilot) and 17,5 MW photovoltaic.

### 3. Investments on the Electrical Grid, Mobility and Innovation Products & Services

A new 60/30kV substation will be operational in 2024, connected to the national high voltage grid. With the new high voltage substation, APS will have more power available from the grid and a higher stability on the port's grid. Also, APS is currently renewing the existing electrical grid installation focusing on the implementation of a centralized communication system in all the electric grid.

APS has been investing in electric mobility with 13 full electrical vehicles on their fleet and 9 charging stations situated on the administrative buildings and houses.

APS is currently on R&D projects such as the NEXUS Agenda that will induce relevant impacts in green transition objectives, such as the development of an energy management system that will provide data on real time energy consuming and production, while providing electric energy analytics, monitoring, storage, and management. OPS solutions are being studied on this agenda, a wave energy converter will be implemented, and a UAV monitoring photovoltaic solution will be tested on the new PV installations. Also, an environmental digital platform will be taken, and finally full electric vessels will be developed such as a new electric pilot boat, a multi-task boat and the retrofitting of a port boat from fuel to electric. These boats will need charger systems to supply them and a smaller OPS will be installed on APS service port.

Cooperating with the terminals operators, alternative fuels in the shipping industry are being analyzed, on the handling of alternative fuels such as ammonia, methanol and biofuels.

A new cryogenic liquefied gases terminal is being developed in order to supply natural gas to ships (bunkering) and other ports (transhipment).

### Conclusions

APS strategies are based on the development of specific action plans with short, medium and long-term development, which will be defined within the scope of the roadmap and with a high impact on emissions, with a high degree of innovation and taking advantage of synergies with the digital transformation. The measures will seek to harness the port's own natural resources to produce renewable energy, promote the electrification of piers and port terminals, means of transport and port equipment and the use of alternative fuels, involving the port authority and all the stakeholders during the process, paying particular attention to their economic and technical viability.

The periodic review and updating of the proposed roadmap, based on regulation updates and in the assessment of the progress made in achieving the established objectives, the degree of implementation of the proposed actions and measures, as well as the quantification of their impact, will be essential for its permanent adaptation to market evolution and technological development, particularly in the areas of installation of OPS, alternative fuels and renewable energies.

Finally, the green energy transition will require the effort, commitment and determination of all the entities involved: port authority, concessionaires, port community, stakeholders, local & governmental institutions and society in general, with global targets having been set to move towards carbon neutrality by 2045.

# Adapting coastal and port defence structures to facilitate the energy transition

Tomás CALHEIROS-CABRAL[1,2], Seyed Shahabedin KHALOOEI-TAFTI[1,2], Victor RAMOS[1,2], Gianmaria GIANNINI[1,2], Paulo ROSA-SANTOS[1,2], Francisco TAVEIRA-PINTO[1,2]

[1] Department of Civil Engineering, Faculty of Engineering of the University of Porto, Rua Dr. Roberto Frias, s/n, 4200-465, Porto, Portugal;

[2] Interdisciplinary Centre of Marine and Environmental Research (CIIMAR), Leixões Cruise Terminal, Av. General Norton de Matos s/n, 4450-208, Matosinhos, Portugal;

up201304327@up.pt; jvrc@fe.up.pt; shahab.khalooei@fe.up.pt; gianmaria@fe.up.pt; pjrsantos@fe.up.pt; fpinto@fe.up.pt

ABSTRACT

With the escalating energy demand in ports necessitated for both port operations and ship energy supply, it is imperative to identify solutions that can adequately meet this demand. This study explores the integration of a Wave Energy Converter into a port breakwater through physical modelling. The investigation assesses the impact of this integration on the stability and functionality of the breakwater, as well as the energy generated. A real-world port serves as the case study. The findings indicate that the device could significantly contribute to the port's energy needs despite potential impacts on the breakwater's stability. Moreover, the device could aid ports in adapting to sea level rise induced by climate change by reducing overtopping volumes.

## 1. Introduction

Ports are compelled to adapt to the dynamic maritime transportation needs of people and goods. Currently, they are grappling with the challenges of the energy transition and are under increasing pressure to shift towards a low-carbon and more sustainable energy model (Ramos *et al.*, 2022). However, transitioning from traditional equipment powered by combustion engines to electrical ones while ensuring adequate power supply is not straightforward, especially when time is a critical factor. Furthermore, as ports increasingly adopt the Industry 4.0 framework, including automation, AI, Digital Twins, IoT, Cloud Computing, Blockchain, Cybersecurity and 5G networks, to evolve into Smart Ports (Clemente *et al.*, 2023), and as ships become more reliant on shore electricity, the energy demand in ports is escalating quickly. Adding to this, Directive 2014/94/EU mandates European ports to establish facilities for Shore-to-Ship Power (SSP) by 2025 (European Union, 2014). Under these circumstances, it becomes almost imperative for ports to transition from mere energy consumers to energy producers. In this regard, ports could play a pivotal role in facilitating the energy transition's success. Within this context, Wave Energy Converters (WEC) could play a crucial role in the energy mix of ports. Furthermore, the integration of WECs into harbour breakwaters can yield several benefits, such as cost-sharing of structures, ease of grid connection, generation of currents in the interior harbour field, simplified maintenance, and enhanced performance of the protection structures due to efficient wave energy absorption (Calheiros-Cabral *et al.*, 2022).

### *1.1. Hybrid-WEC (h-WEC)*

The hybrid-WEC is a unique WEC that combines two operational principles, the OverTopping Device (OTD) and the Oscillating Water Column, and has previously been studied by Calheiros-Cabral *et al.* (2020a) and (2020b). It was designed to be integrated into rubble-mound breakwaters, with the extension of the North breakwater of the Port of Leixões, Porto, Portugal, serving as a case study. The OTD component comprises four reservoirs with crest heights at 0.75, 2.00, 3.25 and 5.00 m (MSL), while the OWC features a 27.4 m long horizontal chamber that transitions to an 18.1 m long vertical chamber. Figure 1a provides a schematic of the device elucidating both operational principles, and Figure 1b presents a photograph of the device tested at a

scale of 1:40 at the Hydraulics Laboratory of the Civil Engineering Department of the Faculty of Engineering of the University of Porto, Portugal. Figure 1c depicts a cross-section of the three tested geometries, which vary solely on the entrance of the OWC. The device was integrated into a 1.6 m wide section of the breakwater that consists of two layers of Antifer cubes with a height of H=0.052m and mean density of $\gamma$=2014 kg/m$^3$. The core is composed of stones ranging from 2-20 mm, the first filter from 14-20 mm and the second filter 30-35 mm. The toe berm is constructed from blocks with a density of $\gamma$=2600 kg/m$^3$, and two rows of blocks adjacent to the walls are made from blocks with a density of $\gamma$=3000 kg/m$^3$.

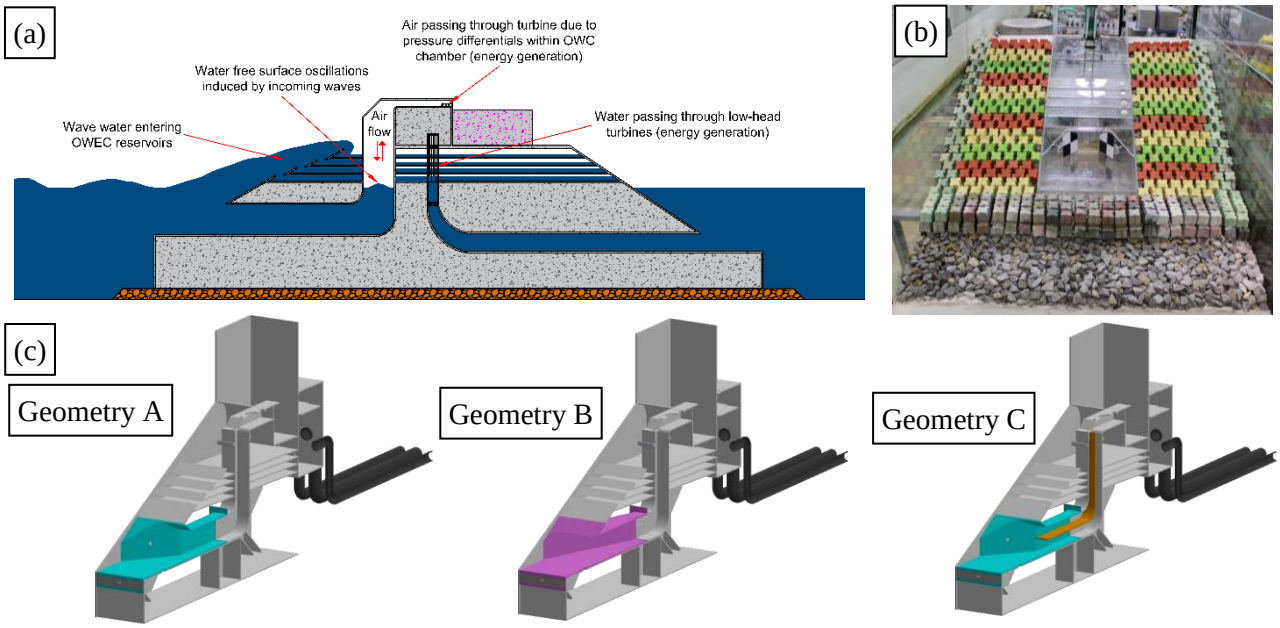



**Fig. 1.** (a) h-WEC cross-section and working principles, (b) photo of the tested physical model, (c) cross-section of the tested geometries.

Experiments were conducted with and without the integration of the h-WEC into the breakwater. Preliminary findings indicate that Geometry C has a superior performance overall, with an estimated energy production of 607 MWh/year for a module width of 20 m. This differential performance is attributed to increased OWC's performance owing to the dual-chamber configuration, as the OTD component yielded approximately equivalent energy across all geometries. The broader working range of the OWC, due to different chamber lengths and, consequently, different resonant periods, was a critical factor in the increased performance. Tests under survival conditions assess the impact of the device on the breakwater's stability (movement of armour layer units) and functionality (overtopping rates). Moreover, the occurrence of scour is also compared.

**Acknowledgements**

This research was partially funded by the Ports Towards Energy Self-Sufficiency (PORTOS) project co-financed by the Interreg Atlantic Area Programme through the European Regional Development Fund, grant number EAPA-784/2018, and by the OCEANERA-NET Second Joint Call 2019 project WEC4PORTS—a hybrid Wave Energy Converter for PORTS (proposal ID 5111), with the references HBC.2019.2443, under the frame of Agentschap Innoveren en Ondernemen (VLAIO), and OCEANERA/0004/2019, under the frame of FCT – Fundação para a Ciência e a Tecnologia. T. Calheiros-Cabral has been supported by the PhD scholarship grant 2021.07687.BD from FCT.

**References**

Calheiros-Cabral, T., Clemente, D., Rosa-Santos, P., Taveira-Pinto, F., Morais, T., Belga, F. & Cestaro, H. 2020a. Performance Assessment of a Hybrid Wave Energy Converter Integrated into a Harbor Breakwater. *Energies*, 13**,** p. 236. ISSN: 1996-1073. doi: https://doi.org/10.3390/en13010236.

Calheiros-Cabral, T., Clemente, D., Rosa-Santos, P., Taveira-Pinto, F., Ramos, V., Morais, T. & Cestaro, H. 2020b. Evaluation of the annual electricity production of a hybrid breakwater-integrated wave energy converter. *Energy*, 213**,** p. 118845. ISSN: 0360-5442. doi: https://doi.org/10.1016/j.energy.2020.118845.

Calheiros-Cabral, T., Majidi, A. G., Ramos, V., Giannini, G., Rosa-Santos, P. & Taveira-Pinto, F. 2022. Development and Assessment of a Hybrid Breakwater-Integrated Wave Energy Converter. *International Marine Energy Journal*, 5**,** pp. 281-291. doi: 10.36688/imej.5.281-291.

Clemente, D., Cabral, T., Rosa-Santos, P. & Taveira-Pinto, F. 2023. Blue Seaports: The Smart, Sustainable and Electrified Ports of the Future. *Smart Cities*, 6**,** pp. 1560-1588. ISSN: 2624-6511.

European Union 2014. DIRECTIVE 2014/94/EU.

Ramos, V., Giannini, G., Calheiros-Cabral, T., Rosa-Santos, P. & Taveira-Pinto, F. 2022. An Integrated Approach to Assessing the Wave Potential for the Energy Supply of Ports: A Case Study. *Journal of Marine Science and Engineering*, 10. doi: 10.3390/jmse10121989.

# Paving the way for greener mobility in small-medium ports

Maria Manuel CRUZ[1], Ricardo BARATA[2], Sebastião BARBOSA[3], Joaquim MACEDO[4], Margarida C. COELHO[5]

[1] APA - Administração do Porto de Aveiro, S.A., Portugal
mariamanuel.cruz@portodeaveiro.pt

[2,3] University of Aveiro, Department for Mechanical Engineering, Portugal
ricardo.barata@ua.pt
sebastiao.barbosa@ua.pt

[4] University of Aveiro, Department of Civil Engineering / Centre for risks and sustainability in construction (DECivil/RISCO), Portugal
jmacedo@ua.pt

[5] University of Aveiro, Department of Environment and Planning and Centre for Mechanical Technology and Automation and LASI – Intelligent Systems Associate Laboratory, Portugal
margarida.coelho@ua.pt

ABSTRACT

Ports have a key role to play in the energy transition process, as they are important hubs in logistics chains and support 90% of the world's maritime freight traffic.

As the high level of greenhouse gas emissions associated with transport, such as maritime, road, and rail, is a major concern, a study was carried out to quantify the greenhouse gas (GHG) emissions associated with the different modes of transport to/from the Port of Aveiro and the Port of Figueira da Foz. To pave the way towards a greener mobility it was propose a Port Mobility Decarbonisation Plan to these small and medium-size ports, based on alternative strategies, namely the use of alternative fuels, electrification and intermodality.

Another aim was to raise awareness of the consequences of the logistical and operational processes that take place in or near the port. For this purpose, a web calculator for greenhouse gas emissions has been set up for use by citizens, port workers, logistic companies, and shipowners.

These features were developed as part of the project "A-AAGORA - Blueprint for Atlantic-Artic Agora on cross-sectoral cooperation for restoration of marine and coastal ecosystems and increase climate resilience through transformative innovation", funded by Horizon Europe.

## 1. Introduction

Ports are multimodal nodes and the activities related to logistics are responsible for most of the GHG emissions associated with ports, such as cargo handling and transport activities. Therefore, one of the objectives of this paper is to study the impact on GHG emissions of a set of strategies to be implemented in a mobility decarbonisation plan for a small and medium-sized port areas (Barata *et al.*, 2024). The second objective is to develop a web calculator of greenhouse gas (GHG) emissions related to the different modes of transport to/from/within the ports (Sebastião *et al.*, 2024), which could be used by all port community, citizens, and schools in the neighbouring area. The study area will focus on the Ports of Aveiro (medium-sized port) and Figueira da Foz (small port), in the Centre region of Portugal.

## 2. Use cases

The Port of Aveiro and the Port of Figueira da Foz have several terminals to dry and liquid bulk, containers, general cargo, and intermodal logistic zones. With 5.8 and 2.2 million of tonnes handled in 2022, they were called by 1053 and 536 vessels, respectively.

### *2.1. GHG emissions quantification and a plan to decarbonise mobility*

The case study focuses on the quantification of GHG emissions, in 1990 and 2022, resulting from port mobility activities in terms of ships/vessels, rail locomotives, heavy-duty vehicles and passenger cars, as well as the movement of non-road cargo handling equipment movements, by using the EMEP/EEA methodology, authored by the European Environment Agency (EEA, 2019) to their calculation.

Alternative scenarios with different strategies, namely alternative fuels (hydrogen, methanol and biofuels), electrification, and intermodality were considered and applied depending on the transport mode and the likelihood of its implementation in the coming years. Based on the alternative scenarios studied, a path of possible measures to be implemented was established and the reduction of GHG emissions was predicted with the implementation of a Mobility Decarbonisation Plan (Figure 1).

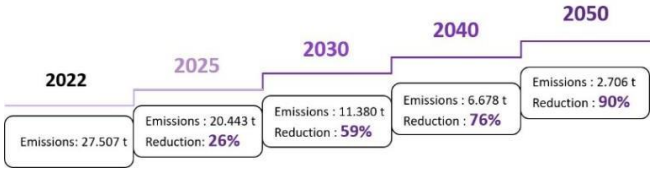



**Fig. 1.** GHG Emissions reduction with the implementation of a mobility decarbonisation plan (Barata *et al*., 2024)

### *2.2. A GHG emissions web calculator*

Aware of the need to develop specific energy transition and decarbonisation targets, following the EMEP/EEA emissions calculation method, and to create a calculator that accurately represents the $CO_2$ emissions of mobility to/from/within the Port of Aveiro and the Port of Figueira da Foz, an architecture was developed that divides the analysis of transport according to complexity (Figure 2). The first level is designed to assess a vehicle, piece of equipment, or vessel individually, and to be used easily by citizens or port workers. The second level calculates the emissions of a fleet and allows transport companies and entities to use it. The third level is the most comprehensive and aims to simulate a complete logistics chain to be used by logistics companies and port authorities. (Sebastião *et al.*, 2024)

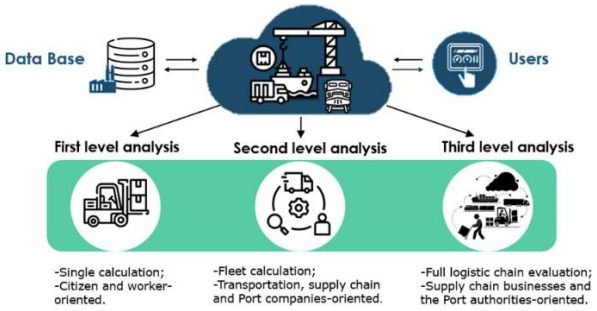



**Fig. 2.** Schematics of the calculator's architecture (Sebastião *et al*, 2024)

## 3. Conclusions

In the context of the general concern to decarbonise the economy, these projects and studies are very important in promoting the energy transition process in port communities, clarifying the path and raising the awareness of whole port communities to engage in this process and make environmentally responsible transport choices.

**Acknowledgements**

A-AAGORA Atlantic-Artic Mission Project (funding from the EU Horizon Europe research and Innovation Programme under Grant Agreement 101093956); UIDB/00481/2020; UIDP/00481/2020 and UIDB/ECI/04450/2020 - FCT; and CENTRO-01-0145-FEDER-022083 - Centro Portugal Regional Operational Program (Centro2020), under the PORTUGAL 2020 Partnership Agreement, through the European Regional Development Fund.

**References**

R. Barata, J. Macedo, M.M. Cruz and M.C. Coelho (2024) Improving Transport Performance and Decarbonisation Potential in Small-Medium Ports, Presented at Transport Research Arena 2024, Dublin, 16th of April 2024.
S. Barbosa, M. M. Cruz (2024) Green Mobility for Small-Medium Ports: a GHG Emissions Web Calculator, Presented at Transport Research Arena 2024, Dublin, 16th of April 2024.
EEA: EMEP/EEA air pollutant emission inventory guidebook. European Environment Agency. EEA Report No 13/2019. https://www.eea.europa.eu/publications/emep-eea-guidebook-2019, last accessed 2023/10/08.

# Decarbonization and Innovation in the Port of Lisbon

Isabel MOURA RAMOS[1], Susana PARREIRA[2], Paula Cristina SENGO[3],
[1,2,3] APL – Administração do Porto de Lisboa, S.A, Portugal,
[1]imouraramos@portodelisboa.pt; [2]sparreira@portodelisboa.pt; [3]psengo@portodelisboa.pt

ABSTRACT

Nowadays, ports are facing huge challenges to adapt to an ever-changing landscape in the supply chains deriving from disruptive trends such as e-commerce or circular economy. The port function has been changing from infrastructures for loading and unloading cargo and passengers, to complex business platforms that take the advantage of maritime or inland waterway access. At the same time environmental, social and governance (ESG) requirements are becoming more and more stringent and must be incorporated into the ports business strategy.

Sustainability must be addressed as part of any business and ports are no exception. As the international and European initiatives under way to mitigate and adapt to climate change, such as IMO's Greenhouse Gas Strategy to reduce emissions from ships and the Fit for 55 legislative train emerging from the European Geen Deal, are urging both, ports and shipping industry, to take action to achieve ambitious goals. At current time, energy and digital transition are among the prime issues to deal with. For that purpose, the Port of Lisbon is building a roadmap for energy and digital transition, that aggregates projects and investments in these areas.

In the Port of Lisbon, we believe that partnerships and innovative collaborations are crucial for the overall success of our strategy to tackle those issues. This abstract will highlight two major projects: the Onshore Power Supply and the Tagus Innov.

## 1. The energy transition in the Port of Lisbon

The port of Lisbon aims to be green, smart, and resilient and for that it must be sustainable. In 2022, the port authority has committed with the Ten Principles of the United Nations Global Compact and as a result is working on the reduction of CO2 emissions and the improvement of air quality in operational areas.

A roadmap for the energy and digital transition is being prepared. It will wrap up, in a portfolio, several investment projects to be developed until 2030 and will deliver new opportunities for partnerships.

Most of the main investment and R&D projects that are already ongoing or in the pipeline address the reduction of emissions. They include renewable energy production, Onshore Power Supply, inland waterway navigation and intelligent monitoring. Besides these projects the port is building on many other actions, some of them in partnership with the port stakeholders, such as electrification of the port operations, smart mobility, and resilience to climate change.

## 2. The Onshore Power Supply project

The main objective of this project is to minimize the impact of port activities, by improving air quality and reducing noise in the city of Lisbon through the reduction of emissions from ships moored in the terminals of the eastern area of the port. Electricity will be delivered to the cruise terminal and cargo terminals enabling ships to switch off their auxiliary engines while at quay.

To do that, a high voltage connection (60KV) to the national grid must be built. This infrastructure connecting the cutting station of Alto de São João to Santa Apolónia will be around 4km long and will cross densely populated urban areas, posing several challenges to avoid traffic disturbances and other impacts on the community. Within the port area, located in the cruise terminal parking plot, an electric substation will be built.

Also, a new medium voltage ring grid including two switching stations will be installed. This infrastructure and equipment will enable the delivery of electricity near to the terminals and the transformation of medium to low voltage power, adequate to service in the cargo terminals.

The terminal operators will be responsible for selecting and installing the “last mile” infrastructure and the equipment to connect to the ships.

In the future the port will face the challenge of supplying ships with renewable power.

## 3. The Tagus Innov

With the Tagus Innov initiative the Port of Lisbon Authority aims to create a living laboratory for the experimentation and scaling up of new technologies, products and services that will help ports assume more quickly their natural role as an integrator to a decarbonized, digital, and circular economy.

The Tagus Innov initiative is integrated into a wider strategy of the Lisbon Port Authority that focuses on 4 main pillars: Environment, Innovation, Economy, and Territory.

This project is organized in 3 strategic verticals - SMART&GREEN, MOBILITY, PORT-CITY - and is based on an Open Innovation Methodology, where the community of stakeholders select the main areas of action, prioritize challenges, and look for solutions to pilot and scale up (open innovation, via start-ups; new ventures, via corporate joint ventures; or internal developments).

Two pilot projects are currently ongoing: one with the startup” Windcredible” to test urban turbines and other with the technology company “Wavecom” to test digital solutions to optimize marina operations. Another project for testing autonomous electrical barges is being prepared with port stakeholders.




Fig.1: Tagus Innov. Pilot tests ongoing and in preparation.

This living lab also includes partnerships with other players to exchange knowledge and experiences. At this point, the port of Lisbon has established MoU’s with Port of Barcelona in innovation areas and with MOBI.E and Lisbon Municipality for electric mobility in port areas.



# Theme C

## Urban water

# A Novel IoT-based NBS with High Efficiency in Urban Runoff Quality and Quantity Management

Behrouz PIROUZ[1], Stefania Anna PALERMO[2], Michele TURCO[3], Hana JAVADI NEJAD[4], Patrizia PIRO[5]

[1,2,3,4,5] Department of Civil Engineering, University of Calabria, 87036 Rende, Italy
behrouz.pirouz@unical.it; stefania.palermo@unical.it; michele.turco@unical.it; hana.javadi@unical.it; patrizia.piro@unical.it

ABSTRACT

The advantages of nature-based solutions (NBS) are plenty, but conventional systems confront some limits. Therefore, developing new systems with higher efficiency and fewer limits seems necessary. In this regard, in this study, an innovative multifunctional NBS system has been proposed, combined with specific filters made from ceramic and soil, and is IoT-based, resulting in more effective flood control management. In addition, the system is multifunctional as one system can be applied for self-irrigated street-side planting, flood management, and runoff treatment.

## 1. Introduction

The main advantages of NBSs include stormwater management (Senes et al., 2021), improving runoff quality (Demirezen and Kazezyılmaz-Alhan, 2022), and moderating roof temperate (Pirouz et al., 2021). However, there are some limits in conventional NBS. For example, the irrigation in dry periods, the high weight of green roofs (Ascione et al., 2013), negative environmental impacts using materials such as polystyrene or high-density polyethylene (HDPE) as membrane, storage layer, and insulation (Bianchini and Hewage, 2012) and no control on runoff management capacity of the NBSs such as wetland, green roofs, etc.

## 2. Material and methods

In this study, to improve the conventional NBS systems, an in-depth literature analysis was first done, the main issues of the conventional NBS systems were investigated, and then the design elements and materials that could be improved were determined. In the next step, an innovative multifunctional NBS, combined with specific ceramic/clay/soil filters, IoT-based and usable for landscape and flood management purposes, besides runoff treatment, has been developed. Moreover, some laboratory tests have been done, and the system's performance has been examined using different rainfall intensities and different infiltration rates of the filters.

## 3. Results and Discussion

The schematic view of the proposed system is shown in Fig. 1. As can be seen in the figure, the new system contains two separate containers connected with specific ceramic/clay filters. The upper one is for soil media, and the bottom is for treated water storage due to filters. In addition, linking the system to IoT and smartly controlling the inlets and outlets in Fig 1 would result in better flood management and the potential to empty the storage before severe rainfall. Moreover, if the predictions show a dry period, the storage tank can remain with harvested rainfall, acting as a sub-surface irrigation system due to the capillary of the filters. In this way, before a severe rainfall based on IoT data, the container will be empty by the bottom outlet (No.1). However, during precipitation, the direct infiltration from the soil surface or runoff from the inlet (No. 3) will pass through the soil and filters, and fill the tanker, meaning the water retention capacity would be the combination of soil and filters. The extra water after the container is filled could be drained off using the upper outlet (No. 2). Nevertheless, this outlet can also be used as an inlet in the case of severe flood and if the infiltration rate of soil and filters are insufficient.

The main applications of the new proposed system are as follows:

- Multipurpose street-side planting for both landscape and urban runoff, as shown in Fig. 2-a;
- Drainage and self-irrigation of sports grounds as shown in Fig. 2-b;
- The system can be used in green roofs and urban drainage water treatment.

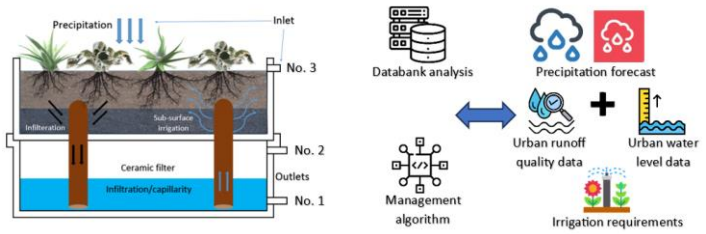
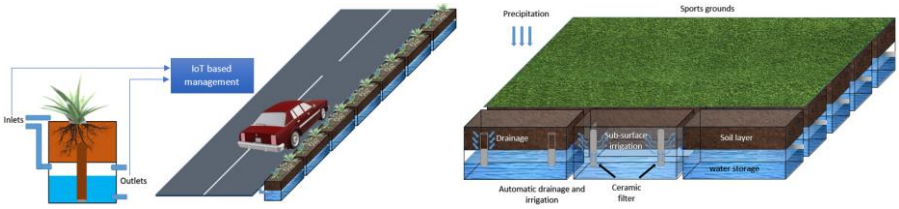



**Fig. 1**. The schematic view of the novel IoT-based multipurpose and self-irrigated NBS

The main comparisons between the proposed system and conventional NBS are presented in Table 1.

**Table 1. The main advantages of the proposed IoT-based NBS**

| Items | Comparisons with conventional NBS | Explanation |
|---|---|---|
| Flood management | Higher capacity | The filter's infiltration rate and element can be optimized according to rainfall. |
| | | Possibility of linking to IoT and making the storage empty before a severe flood. |
| Runoff treatment | Higher impacts | Higher water treatment impact due to the existence of specific changeable filters. |
| Water requirement for irrigation | Less than conventional systems | A sub-surface irrigation system that is more efficient than other irrigation |
| Environmental impact | Less than conventional systems | The system is without polystyrene or HDPE materials, which conventional systems use as membranes, storage layers, and insulation; |
| | | It is possible to make the entire system from clay or ceramic, similar to clay pots. |
| Others | More natural | Drainage and sub-surface self-irrigation are similar to a confined aquifer. |
| | Multipurpose | The novel system contains separate water storages that can be used for other urban water requirements such as firefighting. |




**(a)** **(b)**

**Fig. 2.** a). multipurpose street-side planting for both landscape and flood management; b). drainage and self-irrigation of lands

The results show the advantages of the proposed innovative multifunctional NBS. Moreover, the new system mechanism is more natural and similar to a confined aquifer (natural drainage and sub-surface self-irrigation). In the system, no polystyrene or HDPE materials are used, meaning less environmental impact, and could simultaneously improve the runoff control and treatment. The possible disadvantages of the proposed system could be the weight that might be high for green roofs and the initial cost due to the new design elements. In conclusion, the new system would allow flood control and management, decreasing the risk in the urban environment and improving urban life quality. The self-irrigation system and the benefits of a sub-surface irrigation system that is more efficient than other irrigation systems allow a return on investment in a short time.

**Acknowledgments**

This work was co-funded by the Next Generation EU - Italian NRRP, Mission 4, Component 2, Investment 1.5, call for the creation and strengthening of 'Innovation Ecosystems', building 'Territorial R&D Leaders' (Directorial Decree n. 2021/3277) - project Tech4You - Technologies for climate change adaptation and quality of life improvement, n. ECS0000009. This work reflects only the authors' views and opinions, neither the Ministry for University and Research nor the European Commission can be considered responsible for them.

**References**

Ascione, F., Bianco, N., de' Rossi, F., Turni, G., Vanoli, G.P., 2013. Green roofs in European climates. Are effective solutions for the energy savings in air-conditioning? Appl. Energy 104, 845–859. https://doi.org/10.1016/j.apenergy.2012.11.068

Bianchini, F., Hewage, K., 2012. How "green" are the green roofs? Lifecycle analysis of green roof materials. Build. Environ. 48, 57–65. https://doi.org/10.1016/j.buildenv.2011.08.019

Demirezen, K.İ., Kazezyılmaz-Alhan, C.M., 2022. Evaluation of the Hydrological Performance of Infiltration Trench with Rainfall-Watershed-Infiltration Trench Experimental Setup. J. Hydrol. Eng. 27. https://doi.org/10.1061/(asce)he.1943-5584.0002161

Pirouz, B., Palermo, S.A., Turco, M., 2021. Improving the efficiency of green roofs using atmospheric water harvesting systems (An innovative design). Water (Switzerland) 13. https://doi.org/10.3390/w13040546

Senes, G., Ferrario, P.S., Cirone, G., Fumagalli, N., Frattini, P., Sacchi, G., Valè, G., 2021. Nature-based solutions for storm water management—creation of a green infrastructure suitability map as a tool for land-use planning at the municipal level in the province of Monza-Brianza (Italy). Sustain. 13. https://doi.org/10.3390/su13116124.

# A Physics-Based Approach for Including Sewer Network Effects in Pluvial Flood Modelling in the Absence of Drainage Network Information

Carlos MONTALVO[1], Julian REYES-SILVA[2], Esteban SAÑUDO[3], Luis CEA[4], Jerónimo PUERTAS[5]

[1,3,4,5] Water and Environmental Engineering Group, Center for Technological Innovation in Construction and Civil Engineering (CITEEC), Universidade da Coruña, 15071, A Coruña, Spain.
carlos.montalvo@udc.es
e.sanudo@udc.es
luis.cea@udc.es
jeronimo.puertas@udc.es

[2] Department of Hydrosciences, Institute for Urban Water Management, TU Dresden, 01069, Dresden, Germany.
julian_david.reyes_silva@tu-dresden.de

ABSTRACT

Urban pluvial floods occur due to intense and/or prolonged precipitation, leading to sewer network overload and resulting in physical, economic, and even human losses. To address this hazard, effective methods are needed to estimate the scale and impact of pluvial flood events and to develop mitigation strategies (Reyes-Silva et al., 2023). In this context, 2D-1D dual drainage models have become one of the most useful tools for these purposes (Fraga et al., 2017; Martins et al., 2018; Sañudo et al., 2020).

However, these models require detailed information about the sewer network, which may not always be readily accessible (Reyes-Silva et al., 2022; Xing et al., 2022; Li et al., 2023). Consequently, in cases of limited data availability, simplified approaches have been devised to account for the drainage capacity of the sewer network within 2D models. These approaches, such as the rainfall reduction method or the infiltration rate method, lack a robust and realistic physical basis, as they assume a constant and spatially uniform drainage capacity over the urban area, neglecting all the complexity of hydraulic processes in sewer networks.

In this work we present a physics-based approach for assessing urban pluvial floods, aiming to overcome the frequent issue of limited information on the sewer system. Our method involves the use of available open-access information within a virtual sewer network generation tool (Reyes-Silva et al., 2022). This approach enables the implementation of 2D-1D dual drainage models, as the recently developed Iber-SWMM model (Sañudo et al., 2020), which is the one used in this work.

The results obtained using a virtual sewer network in Iber-SWMM were compared to those derived from a 2D-1D model using data from the actual sewer network in a coastal town located in NW Spain. This comparison revealed that the proposed approach can reasonably represent the sewer network's drainage capacity during pluvial floods, especially compared to other simplified methods, when the geometry of the real network is unknown. Consequently, it enables the identification of areas susceptible to pluvial flooding.

The results from a registered high-intensity precipitation event indicate that the extent of the maximum inundation maps simulated in Iber-SWMM using a virtual sewer network is comparable to the results obtained with the real network. Furthermore, these results are significantly superior to results achieved when the sewer network drainage effect is not considered or is represented using simplified methods as the rainfall reduction methods (Fig. 1).

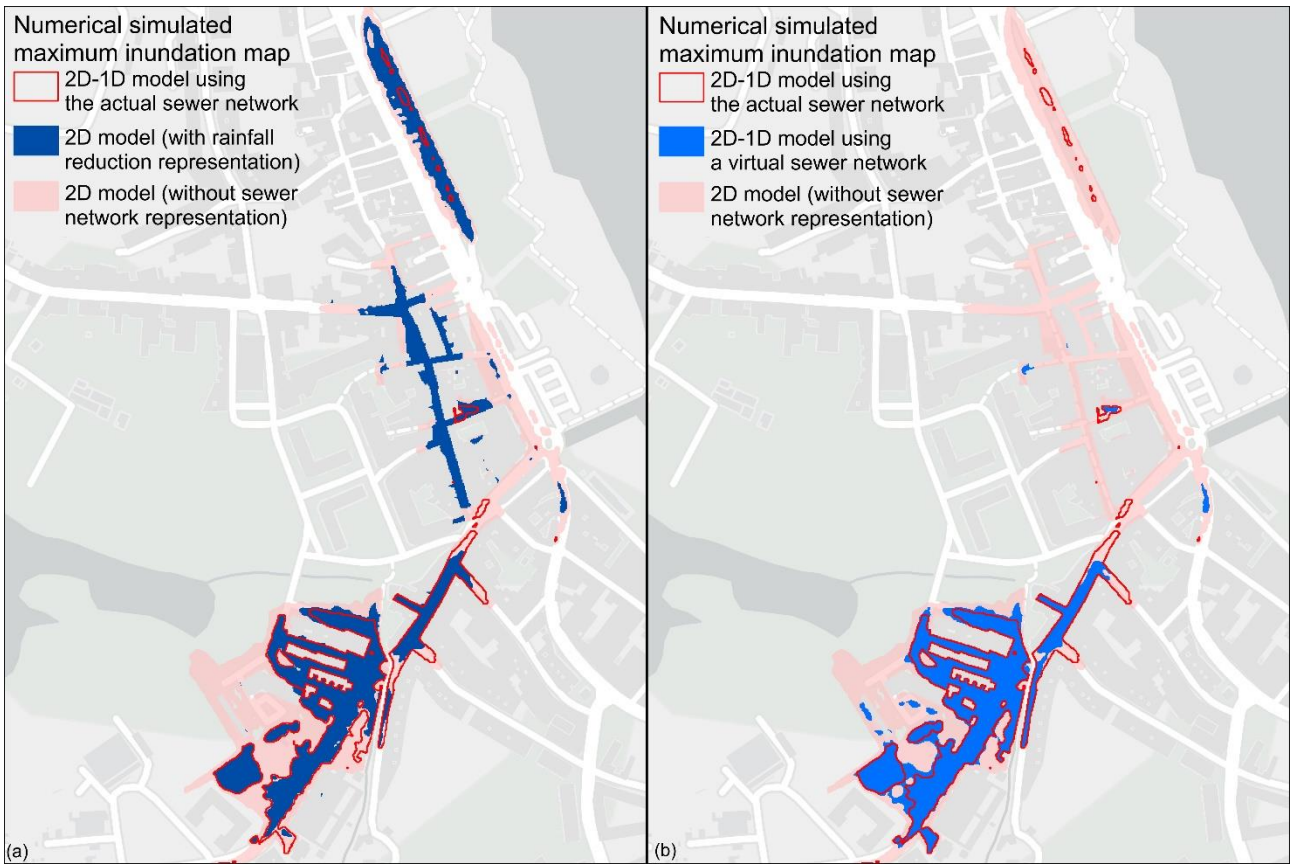



**Fig. 1.** Extent comparasion of the maximum inundation maps simulated with four different models, during a registered high-intensity precipitation event.

**Acknowledgements**

This project was received financial support from the Spanish Ministry of Science and Innovation (MCIN/AEI/10.13039/501100011033) within he project "SATURNO: Early warning against pluvial flooding in urban areas" (PID2020-118368RB-I00).

**References**

Fraga I, Cea L, Puertas J (2017) Validation of a 1D-2D dual drainage model under unsteady part-full and surcharged sewer conditions. Urban Water Journal, 14(1).
Li D, Hou J, Shen R, Li B, Tong Y, Wang T (2023) Approximation method for the sewer drainage effect for urban flood modeling in areas without drainage-pipe data, Frontiers in Environmental Science, 11.
Martins R, Leandro J, Djordjević S (2018) Influence of sewer network models on urban flood damage assessment based on coupled 1D/2D models. Journal of Flood Risk Management, 11.
Reyes-Silva J, Novoa D, Helm B, Krebs P (2023) An Evaluation Framework for Urban Pluvial Flooding Based on Open-Access Data. Water, 15(1).
Sañudo E, Cea L, Puertas J (2020) Modelling Pluvial Flooding in Urban Areas Coupling the Models Iber and SWMM. Water, 12(9).
Xing Y, Shao D, Liang Q, Chen H, Ma X, Ullah I (2022) Investigation of the drainage loss effects with a street view based drainage calculation method in hydrodynamic modelling of pluvial floods in urbanized area. Journal of Hydrology, 605.

# A numerical ecohydrological model for simulating the hydrological response of multi-layer green roofs to climate forcing

Dario PUMO[1], Matteo IPPOLITO[1], Francesco ALONGI[1], Marcella CANNAROZZO[1], Calogero MATTINA[1], Leonardo Valerio NOTO[1]

[1] Dipartimento di Ingegneria, Università degli Studi di Palermo, Italy
dario.pumo@unipa.it

ABSTRACT

The Mediterranean basin is a possible hot-spot for climate change (Noto et al., 2023a & 2023b), in which phenomena of extreme rainfall, water scarcity and heat waves are increasingly frequent and intense, and their impact on urban settlements is further exacerbated by anthropogenic activities and the growing loss of natural soils. Green roofs (GRs) are multi-purposes, sustainable and low-cost climate-adaptive measures, which in urban areas can effectively counteract the urban heat island phenomenon. Multilayer green roofs (MGR) are GRs characterized by a high-capacity water storage layer, which favors the rainwater lamination effect, mitigating possible stress on urban drainage systems during extreme storms. Moreover, the intercepted rainwater can be reused by the same vegetation of the system and/or as gray water for residential uses. The present work proposes a new model to simulate the hydrological response of MGRs to climate forcings. The model is implemented based on an experimental site in Palermo (Italy), using data collected over a monitoring period of more than 3 years. Model reproduction of the observed runoff generated by the system is very promising and demonstrates the suitability of the model as a valid tool for cost-benefit analyses and the evaluation of different ecosystem services offered by such urban green infrastructures.

## 1. Materials and Methods

### *1.1. Case Study: The Polder Roof of Palermo (Italy)*

As part of the project *Polder Roof field lab*, supported by the European Climate-KIC programme, four MGR prototypes, developed by the Metropolder company, called Polder Roofs, have been installed in four Italian cities (Cristiano et al., 2022). The Polder Roof is an innovative GR system whose structure is composed by multiple layers, including a vegetation-soil layer (named Green Layer, GL) and a buffer layer (named Blue Layer, BL) where the water can be stored. The buffer is made of a modular interlocking polypropylene void former, including support units and capillary cones, that connects the GL with the BL. Water storage and releases from the system can be regulated by a smart weir controlled remotely. The case study here considered is the Polder Roof of Palermo (Fig.1a), with drainage area of 32.1 $m^2$, GL with two thickness (10 and 20 cm), soil consisting of a mixture of volcanic materials covered by a combination of sedum, shrub and herbaceous species. The system is highly monitored by a set of integrated and external sensors (Cristiano et al.,2022; Pumo et al., 2023a and 2023b). Some of the variables monitored from Dec. 2020 and considered in this work are: rainfall, irrigation water volumes, and outflow generated by the system. An hourly series of crop reference evapotranspiration for the entire reference period was also derived through the FAO59-PM equation, using local atmospheric variables acquired from the ERA5-Land reanalysis dataset.

### *1.2. The Eco Polder Roof Model*

The *Eco Polder Roof Model*, is a lumped ecohydrological model based on the numerical solution of two water balance equations, the former referring to the GL and the latter to the BL. After settings some contour conditions describing the system configuration (i.e., drainage area, mean soil depth, depth of the BL, length of the weir) the model is forced by hourly time series of rainfall (P), irrigation ($I_{rr}$) and reference evapotranspiration (PET), as well as, the time series of the weir's heights (for the case study set constant and

equal to 70 cm corresponding to the maximum closure). Whereas the model returns hourly time series of: canopy interception, actual evapotranspiration and direct evaporation from the BL, leakage and capillary rise fluxes, relative soil moisture in the GL (s), water levels within the BL (h) and the outflow from the system (R). The model is rather parsimonious, and it is characterized by a total of 12 parameters, which are vegetation and soil parameters (i.e., threshold for canopy interception, porosity, four relative soil moisture points characterizing the water retention curve, two parameters of the hydraulic conductivity curve), the weir slope coefficient, two parameters related to the evaporation simulation, and a parameter for the adopted internal exfiltration model. In this study, the model was applied to the case study of Palermo over the full monitoring period of about three years (2020-2023). Parameters optimization around literature values was performed using genetic algorithms, and considering a Global Index as objective function, derived comparing simulated and observed runoff over a calibration period of two years as a function of the Root Mean Squared Error (RMSE) in hourly runoff, the Percent Absolute Error (PAE) in the cumulated runoff volume over the entire period and the PAE in the hourly runoff occurrence. Finally the model was validated over the remaing 1 year period.

## 2. Results

The model was applied to the case study considering both parameters from literature and after optimization via genetic algorithms, comparing the simulated and observed hydrological response of the system. Water fluxes computed with the two parameter sets are rather close with each other, despite the model with optimized parameters provides a more accurate reproduction of the outflow, with an almost exact estimation of the full period cumulated runoff volume. Figure 1b shows the daily time profiles of water input ($P+I_{rr}$), s, h, and, in the bottom panel, simulated and observed runoff over the full period. An analysis on the most significant rainy subperiods (with duration spanning from 2 to 31 days, and rainfall spanning from 17 to193 mm) shows that the simulated Stormwater Retention Rates (SRRs) is on average equal to 0.69 (vs. 0.71 computed using observed data). Thus, the model provided an almost exact assessment of the cumulative runoff volume over the entire reference period and a very accurate evaluation of the SRRs at the event scale, also allowing to evaluate the amount of water retained by the system and potentially available for other purposes, which are the most important information to evaluate the hydrological benefit of a MGR.

(a)



(b)

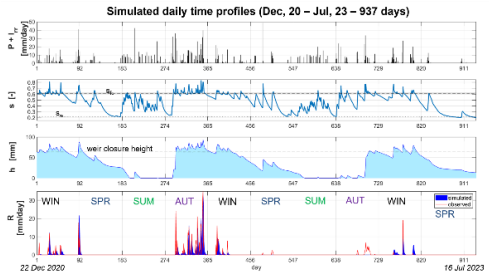



**Fig. 1.** Polder Roof of Palermo (a). Daily time profiles simulated by the model using optimized parameters (b).

## 3. Discussion and Conclusions

The application of the proposed *Eco Polder Roof Model*, demonstrated its potential for evaluating in a comprehensive manner the advantages of MGRs also showing a satisfying reliability in a range of time scales, form the event scale, useful for the assessment of the flood mitigation function, to the long term, useful for the assessment of the drought mitigation function. Input of the model are commonly available and the considered system configuration can be easily modified; for this reason, the model can be easily transferred to other cases, characterized by different drainage areas, depth of layers and soil-vegetation properties, as well as different climate conditions. The proposed model could be a useful tool for evaluating the potential of MGRs at different spatio-temporal scales and under different climate, also taking into account the effect of climate changes.

### References


Cristiano, E., Annis, A., Apollonio, C., Pumo, D., et al. (2022). Multilayer blue-green roofs as nature-based solutions for water and thermal insulation management. Hydrology Research 53 (9): 1129–1149. DOI: 10.2166/nh.2022.201

Noto, L.V., Cipolla, G., Francipane, A., Pumo D. (2023a). Climate Change in the Mediterranean Basin (Part I): Induced Alterations on Climate Forcings and Hydrological Processes. Water Resources Management, 37(6-7), 2287–2305

Noto, L.V., Cipolla, G., Pumo D., Francipane, A., (2023b). Climate change in the Mediterranean Basin (Part II): a review of challenges and uncertainties in climate change modeling and impact analyses. Water Resources Management, 37(6-7), 2307–2323

Pumo D., Francipane A., Alongi F., Noto L.V., (2023a). The potential of multilayer green roofs for stormwater management in urban area under semi-arid Mediterranean climate conditions. JEMA, 326, 116643, DOI: 10.1016/j.jenvman.2022.116643

Pumo D., Alongi F., Cannarozzo M., Noto L.V., (2023b). Climate adaptive urban measures in Mediterranean areas: Thermal effectiveness of an advanced multilayer green roof installed in Palermo (Italy). Building and Environment, 243, 110731, DOI: 10.1016/j.buildenv.2023.110731

# A comprehensive resilience assessment system for water distribution networks

Joana CARNEIRO[1], Dália LOUREIRO[2], Marta CABRAL[3], Dídia COVAS[4]

[1,3,4] CERIS, Instituto Superior Técnico, Universidade de Lisboa, Av. Rovisco Pais 1, 1049-001, Lisbon, Portugal
joana.carneiro@tecnico.ulisboa.pt
marta.f.cabral@tecnico.ulisboa.pt
didia.covas@tecnico.ulisboa.pt

[2] Urban Water Unit, National Civil Engineering Laboratory, Av. Brasil 101, 1700-066 Lisbon, Portugal
dloureiro@lnec.pt

ABSTRACT

The present work aims to present a resilience assessment system for water distribution networks (WDN) capable of adequately evaluating resilience characteristics, such as robustness, flexibility, reliability, redundancy and autonomy, at a tactical level. The resilience assessment system (RAS) covers both the infrastructure and the service dimensions of water distribution systems and is composed of seven resilience objectives. Each objective attends to different criteria and is assessed through different metrics. The proposed metrics allow two analyses: a global analysis, based on historical data, that provides prioritisation information at system level; and a comprehensive and sectorial analysis, based on more detailed data, that may require the hydraulic simulation of the network behaviour. Obtained results allow to identify critical resilience aspects of the WDN and to propose improvement measures to increase resilience.

## 1. Introduction

Water distribution networks are crucial infrastructures aiming to continually and efficiently deliver good quality water with sufficient pressure to the consumers. However, these systems face different types of unexpected events that may have a negative effect on the provided service. Water utilities must ensure their systems are resilient to cope with and overcome these events. In urban systems, resilience is defined as "the ability of a system to anticipate, prepare, respond to and absorb shocks, positively adapt and transform in the face of stresses and challenges" (adapted from ISO/TR 22370:2020). As per its definition, resilience is a broad and complex subject, involving different characteristics, such as robustness, flexibility, reliability, redundancy, autonomy, among others.

With the increasing awareness of the need to improve systems resilience given the climate changes, resilience assessment has been the scope of different studies. At a strategic level, resilience is a major component to be considered, particularly with the increase in events associated with climate change. The European Project RESCCUE (Resilience to cope with climate change in urban areas) is a strategic resilience assessment system, that evaluates a city's resilience in different services (e.g., water, energy, mobility) and dimensions (e.g., organizational, spatial, functional and physical), regarding different resilience characteristics, such as redundancy, robustness, reliability, preparedness, responsiveness (Cardoso et al., 2020). However, when assessing resilience at a tactical level, the literature has been focusing on a single resilience characteristic, either it be reliability, robustness or redundancy. The most commonly used metrics are the so called hydraulic reliability metrics, measuring the hydraulic capacity of the system to ensure the water supply (i.e., the service) under uncertain demand conditions (Todini, 2000; Carneiro et al., 2023).

The present work aims to develop a resilience assessment system, at a tactical level, able to assess different resilience characteristics, such as robustness, flexibility, reliability, redundancy and autonomy.

## 2. Resilience assessment system

The proposed resilience assessment system (RAS) is composed of a set of objectives (O1-O7), which attend to different criteria that are assessed through different metrics. It covers two main dimensions of water distribution systems: infrastructure and service. The main objectives and criteria are synthesised in Table 1.

**Table 1.** Objectives and respective criteria of the resilience assessment system

| Dimension | Objective | Criteria |
|---|---|---|
| Infrastructure | O1 Ensure the knowledge of critical assets and their protection | C1.1 Knowledge and protection of critical assets |
| | O2 Ensure infrastructure assets robustness | C2.1 Infrastructure integrity |
| | | C2.2 Infrastructural sustainability |
| | | C2.3 Water and energy efficiency |
| | O3 Ensure an autonomous and flexible water infrastructure | C3.1 Ensure the knowledge about the dependency on other services |
| | | C3.2 Promote infrastructure assets autonomy |
| | | C3.3 Promote infrastructure assets redundancy |
| | O4 Promote infrastructure assets preparedness for recovery and build back in challenging events | C4.1 Infrastructure restoration in the last challenging event |
| Service | O5 Ensure a reliable service (adequate pressure, quantity and quality of water at consumption nodes) | C5.1 Adequacy of water supply interruptions |
| | | C5.2 Adequacy of the delivered water quantity |
| | | C5.3 Adequacy of delivered water quality |
| | | C5.4 Adequacy of pressure requirements |
| | O6 Ensure a flexible service | C6.1 System water flexibility to supply water for potable uses |
| | | C6.2 System energy flexibility for increase water demand |
| | O7 Promote service preparedness for recovery and build back in challenging events | C7.1 Number and duration of failures in the last challenging event |

The metrics will be presented and detailed further on. Nonetheless, the metrics allow a primarily global analysis, based on historical data, providing prioritisation information at system level, and a detailed and sectorial analysis, based on more comprehensive data and requiring the numerical model of the system. In accordance with the event, a more appropriate set of metrics can be chosen from the RAS metrics, simplifying and focusing the assessment on the identified problem. Obtained results from the RAS allow to identify critical resilience aspects of the system and to further propose improvement measures to increase resilience. The RAS can also be applied to compare improvement measures, being a helpful tool in decision-making.

## 3. Conclusions

A tactical level resilience assessment system to help water utilities in the management of drinking water systems, particularly in envisioning a more resilient system, is presented herein. The proposed RAS is capable of assessing different resilience characteristics and is composed of seven major objectives that allow to evaluate the infrastructure robustness, autonomy, flexibility and preparedness, and the service reliability, flexibility and preparedness. The suggested metrics can be used for: a global analysis, based on historical data and providing prioritisation information; and for a detailed and sectorial analysis, based on more detailed data and in the numerical model of the system, identifying critical resilience aspects and components of the system. An application of the RAS to a case study will be presented along with the main conclusions.

**Acknowledgements**

The authors acknowledge Fundação para a Ciência e a Tecnologia (FCT) for funding Civil Engineering Research and Innovation for Sustainability (CERIS) through the project UIDB/04625/2020 and for funding the doctoral scholarship PD/BD/150694/2020.

**References**

Cardoso, M.A., Brito, R.S., Pereira, C., David, L., Almeida, M.C. (2020) Resilience Assessment Framework RAF. Description and implementation. Deliverable 6.4 RESCCUE - RESilience to cope with Climate Change in Urban arEas - a multisectorial approach focusing on water.

Carneiro J., Loureiro, D., & Covas, D. (2023). Exploratory Analysis of Surrogate Metrics to Assess the Resilience of Water Distribution Networks, Water Resources Research, 59(8), e2022WR034289 https://doi.org/10.1029/2022WR034289

International Organization for Standardization. (2020). ISO/TR 22370:2020: Security and resilience - Urban resilience - Framework and principles. Geneve, CH.

Todini, E. (2000). Looped water distribution networks design using a resilience index based heuristic approach. Urban Water, 2(2), 115–122. https://doi.org/10.1016/S1462-0758(00)00049-2

# The effect of selected SuDS on the tailwater urban drainage system: preliminary results

Erica ORSI[1], Gaetano CRISPINO [1], Michele IERVOLINO[1], Corrado GISONNI[1]

[1]Department of Engineering, Università degli studi della Campania Luigi Vanvitelli, Aversa, 81031, Italy
erica.orsi@unicampania.it
gaetano.crispino@unicampania.it
michele.iervolino@unicampania.it
corrado.gisonni@unicampania.it

ABSTRACT

Climate change and growing urbanization represent two of the main challenges facing the world. The climate change leads to an intensification of extreme rainfall events, and the urbanization changes natural or agricultural land uses to residential, commercial, and industrial areas with an increase in impervious surfaces. Sustainable Drainage Systems (SuDSs) offer a sustainable approach for managing stormwater in urban areas by mimicking natural hydrological processes and reducing the negative impacts of urbanization. Some common SuDS techniques include permeable pavements, green roofs and bioretention systems.

This paper examines the role of green roofs and permeable pavements installations in an urban catchment case-study as a strategic and sustainable response to mitigate the increasing urbanization. Green roofs and permeable pavements efficiency is assessed by varying the Effective Impervious Area (EIA) reduction. The reduction of choking occurrence in the sewer pipes and structures downstream from the SuDS-retrofitted lot is evaluated. To this end, numerical simulations are carried out by using the software Storm Water Management Model (SWMM) and different retrofitted scenarios are supposed. Preliminary results confirm the positive impact of the analyzed SuDS in reducing the effect of the growing urbanization on the occurrence of the pressurization phenomena into the drainage system.

## 1. Introduction

Over the past decades, the world has observed a rapid urbanization with the increase of the built environment. The growing urbanization influences the natural water cycle: the impermeable surfaces augment and, consequently, there is an increase of the surface runoff and a reduction in infiltration (Anon, 2016; Rademacher, 2019). Climate change further aggravates these problems by increasing both frequency and intensity of the extreme weather events (Liu et al., 2019; IPCC, 2022).

Urbanization increases the amount and velocity of surface runoff, as rainwater is unable to infiltrate into the ground and, consequently, it flows over impermeable surfaces. Furthermore, traditional drainage systems are often designed based on historical rainfall patterns and land uses. As urbanization progresses, these systems may become overwhelmed by the increased runoff, localized urban flooding, and infrastructure damage.

The need for innovative solutions to mitigate the impact of heavy rainfall and reduce urban flooding has become increasingly urgent. In this context, the installation of green roofs and permeable pavements in urban sites emerges as a remarkable and pragmatic strategy to mitigate the issue of the stormwater runoff. Green roofs and permeable pavements, indeed, intercept, detain and retain rainwater by contributing positively to the peak stormwater flows and volumes management and to the achievement of the hydraulic and hydrologic invariance. In this regard, the technical literature provides several research studies (Palla and Gnecco, 2015; Piro et al., 2018; Palermo et al., 2020). Conversely, few papers focus on the effect of SuDS techniques on the operative conditions of the sewer structures downstream of them.

This paper examines the role of green roofs and permeable pavements installation in an urban catchment as a solution to reduce the hydraulic overload on the tailwater drainage system due to the increasing urbanization. To this end, several numerical simulations were conducted using the freeware software SWMM. A real case-study consisting of an urban catchment (Capua, located in southern Italy), where the impervious surface has recently increased due to the construction of a terraced house lot, was considered. Different percentages of occupation of green roofs and permeable pavements were supposed along with various rainwater characteristics. The main results were used to provide preliminary practical guidelines for hydraulic engineers and practitioners facing a very common problem: the containment of runoff discharges generated in an urbanized area served by an existing drainage system.

## 2. Results

Several simulation results prove that the increase in EIA reduction, which corresponds to an augmentation of the surface covered by SuDS measures, improves the hydrologic and hydraulic efficiency of green roofs and permeable pavements in terms of peak flow and volumes reduction (Orsi et al., 2024). This feature also involves the reduction in the frequency of the occurrence of pressurization phenomena in the drainage system because the expected maximum flow discharge under intense rain events exceeds the conveyance capacity of the sewer collectors more rarely (Fig. 1a). Moreover, the presence of the SuDS upstream of the drainage system entails the tangible result of limiting the dimensions of sewer manholes in terms of curvature radius $R/D$ and a relative straight extension $L/D$ (Fig.1b).

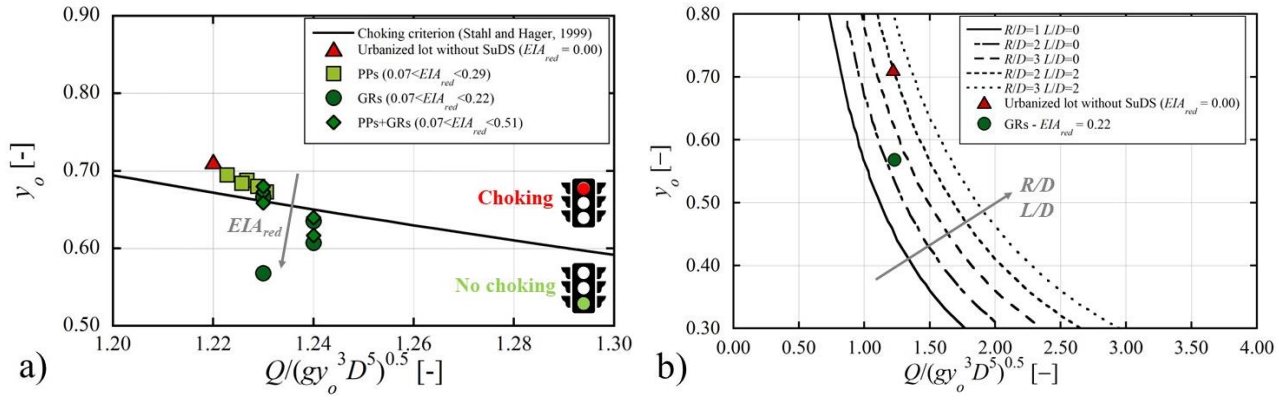



**Fig. 1.** Choking chart for: a) straight sewer pipe and b) bend manhole downstream of the urban catchment under a rainfall event with a return period of 20 years and a rainfall duration of 8 min ($Q$ = flow discharge, $D$ = pipe diameter, $y_o$ = upstream filling ratio).

## 3. Conclusions

This study aims to quantify the positive effect of SuDS installations at an urban catchment scale in improving the hydraulic behaviour of the different components belonging to the the tailwater sewer system. The SWMM-based simulation results confirm the hydraulic suitability of green roofs and permeable pavements in reducing the peak flow discharges and volumes without achieving the hydraulic and hydrologic invariance. However, the implementation of the selected SuDS provides a beneficial effect of the hydraulic performance of the tailwater drainage system, by reducing the frequency occurrence of the pressurization phenomena in the sewer collectors and by minimizing the dimensions of the sewer manholes without compromising their expected hydraulic conveyance.

**References**


Anon (2016) Rise of the City, Science 352 (6288): 906–907

IPCC 2022. Climate Change 2022: Impacts, Adaptation and Vulnerability. Contribution of Working Group II to the Sixth Assessment Report of the Intergovernmental Panel on Climate Change [Pörtner HO et al. (EdS.)]. Cambridge University Press. Cambridge University Press, Cambridge, UK and New York, NY, USA, 3056 pp.

Liu M, Vecchi GA, Smith JA, Knutson TR (2019) Causes of Large Projected Increases in Hurricane Precipitation Rates with Global Warming, Npj Climate and Atmospheric Science 2 (1): 38

Orsi E, Crispino G, Iervolino M, Gisonni C (2024) Are SuDS efficient measures for achieving the hydraulic and hydrologic invariance?, Journal of Irrigation and Drainage Engineering, under revision

Palermo SA, Talarico V, Turco M (2020) On the lid systems effectiveness for urban stormwater management: case study in southern Italy. IOP Conference Series: Earth and Environmental Science: 410, 012012

Palla A, Gnecco I (2015) Hydrologic modeling of Low Impact Development systems at the urban catchment scale, Journal of hydrology 528, 361–368

Piro P, Carbone M, De Simone M, Maiolo M, Bevilacqua P, Arcuri N (2018) Energy and hydraulic performance of a vegetated roof in sub-mediterranean climate, Sustainability ,10(10) :3473

Rademacher A (2019) Why Cities?, Science 364 (6437): 245

# Nature-based Solutions in urban watersheds – The SEE-URBAN-WATER project

Jochen HACK[1]

[1]Leibniz University Hannover, Institute of Environmental Planning, Germany
hack@umwelt.uni-hannover.de

ABSTRACT

Throughout a 5-year research project, the team of SEE-URBAN-WATER investigated the promotion and implementation of Nature-based Solutions (NbS) in urban watersheds. By taking the greater metropolitan area of San José, Costa Rica, and a highly urbanized watershed within the area as a case study, the research activities focused on three interrelated domains: (1) Spatial integration and governance, (2) Co-design and prototyping in a Real-World Lab, and (3) Modelling and multifunctional scenario analysis. The multidisciplinary methodological interlinkage of the three domains enabled for a holistic analysis of difficulties and opportunities for an effective promotion and implementation of multifunctional NbS in urban settings. It considers a multi-spatial scales (from building level to a larger metropolitan area) approach and multi-level actor involvement in the promotion, design, implementation, and upscaling process.

The Real-World-Lab (2) plays a central role in providing a physical space and a socio-economic context representative for functional preferences of NbS for different stakeholders, identification of suitable placement sites, and the testing of NbS prototypes resulting from a transdisciplinary co-design process. Results from this domain are preferred functions, designs, and the effective placement potential (suitable sites and legal complexity) for NbS at the building and street level – neighborhood scale. The experimental testing of NbS prototypes provided important insights through detailed reflections on the co-design, construction, operation, and maintenance. In combination with measurements the prototyping enabled an assessment of performance and supported the calibration and validation of hydrological models (3). In the modelling and multifunctional scenario analysis domain (3), the realistic NbS placement potential and hydrological performance to reduce flooding at different spatial scales (neighborhood – (sub)watershed) was evaluated in great detail based on the insights from the Real-World Lab using different implementation strategies. Besides hydrological, also social and ecological functions of different NbS as well as economic trade-offs were assessed applying different scenarios. The results from the Real-World Lab (2) and the modelling (3) supported the analysis in the spatial integration and governance domain. In this domain, NbS upscaling strategies were analyzed in political terms, considering the legal and socio-political readiness, as well as from a spatial integration perspective in form of a sustainable development of multifunctional green infrastructure.

Supported by the results of the three principle research domains, Guiasverdes.org – an interactive webpage providing guidelines for NbS promotion and implementation based on the project's experience and contributions from other successful examples from the region – was developed during a two-year stakeholder process. Furthermore, the watershed containing the Real-World lab and equipped with sensors for hydro-climatic monitoring is further developed into an experimental watershed to investigate the future implementation and performance of NbS in a highly urbanized watershed.

This contribution provides a summary of findings of this comprehensive work.

**References**


Hack, J., Peréz Rubí, M., Beissler, M., Ortega Sandoval, A., Bonilla Brenes, R., 2023. Implementing Nature-based Solutions and Green Infrastructure for Cities, Citizens and Rivers - The SEE-URBAN-WATER Project. Leibniz University Hannover, Hannover, Germany. https://doi.org/10.15488/15438

Hack, J., Perez Rubi, M., Beissler, M., Chapa, J.F., Neumann, V., Schiffmann, C., 2023. Guías Verdes: Infraestructura Verde para la ciudad, sus ciudadanos y sus ríos. SEE-URBAN-WATER Research Group, Hannover. https://doi.org/10.15488/14474

Hack, J., Ojeda-Revah, L., Pérez Rubí, M., Pradilla, G., Borbor-Cordova, M., Burgueño, G., Eleuterio, A.A., Rivera, D., Vásquez, A., 2024. Avances de infraestructura verde urbana para la gestión de agua en América Latina. Cuad. Geogr. Rev. Colomb. Geogr. 33. https://doi.org/10.15446/rcdg.v33n1.101947

Lopes Monteiro, C., Bonilla Brenes, J.R., Serrano-Pacheco, A., Hack, J., 2023. Multi-criteria site selection and hydraulic modeling of green flood retention measures in a highly urbanized basin in Costa Rica. Urban For. Urban Green. 85, 127957. https://doi.org/10.1016/j.ufug.2023.127957

Bonilla Brenes, R., Morales, M., Oreamuno, R., Hack, J., 2023. Variation in the hydrological response within the Quebrada Seca watershed in Costa Rica resulting from an increase of urban land cover. Urban Water J. 20, 575–591. https://doi.org/10.1080/1573062X.2023.2204877

Arthur, N., Hack, J., 2022. A multiple scale, function, and type approach to determine and improve Green Infrastructure of urban watersheds. Urban For. Urban Green. 68, 127459. https://doi.org/10.1016/j.ufug.2022.127459

Schröter, B., Hack, J., Hüesker, F., Kuhlicke, C., Albert, C., 2022. Beyond Demonstrators—tackling fundamental problems in amplifying nature-based solutions for the post-COVID-19 world. npj Urban Sustain. 2, 4. https://doi.org/10.1038/s42949-022-00047-z

Hack, J., Schröter, B., 2022. Nature-Based Solutions for River Restoration in Metropolitan Areas, in: Bears, R. (Ed.), The Palgrave Encyclopedia of Urban and Regional Futures. Springer International Publishing, Cham, pp. 1104–1113. https://doi.org/10.1007/978-3-030-87745-3_166

Aparicio Uribe, C.H., Bonilla Brenes, R., Hack, J., 2022. Potential of retrofitted urban green infrastructure to reduce runoff - A model implementation with site-specific constraints at neighborhood scale. Urban For. Urban Green. 69, 127499. https://doi.org/10.1016/j.ufug.2022.127499

Neumann, V.A., Hack, J., 2022. Revealing and assessing the costs and benefits of nature-based solutions within a real-world laboratory in Costa Rica. Environ. Impact Assess. Rev. 93. https://doi.org/10.1016/j.eiar.2022.106737

Pérez Rubi, M., Hack, J., 2021. Co-design of experimental nature-based solutions for decentralized dry-weather runoff treatment retrofitted in a densely urbanized area in Central America. Ambio 50, 1498–1513. https://doi.org/10.1007/s13280-020-01457-y

Chen, V., Bonilla Brenes, J.R., Chapa, F., Hack, J., 2021. Development and modelling of realistic retrofitted Nature-based Solution scenarios to reduce flood occurrence at the catchment scale. Ambio 50, 1462–1476. https://doi.org/10.1007/s13280-020-01493-8

Wiegels, R., Chapa, F., Hack, J., 2021. High resolution modeling of the impact of urbanization and green infrastructure on the water and energy balance. Urban Clim. 39, 100961. https://doi.org/10.1016/j.uclim.2021.100961


**Acknowledgements**


The SEE-URBAN-WATER project has been funded by the Bundesministerium für Bildung und Forschung [01UU1704].

# Tackling microplastic pollution with Nature-Based Solutions from urban runoff and wastewater

Darío CALZADILLA CABRERA[1*], Carmen HERNÁNDEZ-CRESPO[1], Ignacio ANDRÉS-DOMÉNECH[1]
[1] Instituto Universitario de Investigación en Ingeniería del Agua y Medio Ambiente (IIAMA), Universitat Politècnica de València (UPV), Camino de Vera SN, 46022 Valencia, Spain.
dcalcab@posgrado.upv.es

ABSTRACT

## 1. Introduction.

The substantial population growth in cities has resulted in an increase in both wastewaters directed towards urban WWTPs and impermeable surfaces, leading to increased runoff during rainy episodes. This has led to the discharge of many pollutants, affecting and degrading surface waters.

Furthermore, millions of tons of plastic are produced annually, and this has also been increasing each year (Plastic Europe, 2021). As a consequence, a wide range of plastic debris are accumulating in the biosphere (terrestrial and marine), which can be fragmented into smaller pieces, known as microplastics (MPs). These tiny plastic particles, measuring less than 5 mm, can transport other pollutants, such as heavy metals (Sarkar et al., 2021) or persistent organic pollutants, among others. Their presence in organisms has been linked to reduced growth, reproductive issues, intestinal damage, and even death. Moreover, MPs contribute to the overall degradation of water quality, disrupt ecosystems, and have long-lasting environmental consequences, making them a significant environmental concern worldwide (Lu et al., 2016; Wang et al., 2019).

The primary objective of this project is to assess the retention of MPs from both wastewater and stormwater generated in urban environments through the use of various Nature-Based Solutions (NBS), such as Treatment Wetlands (TW) and Sustainable Urban Drainage Systems (SUDS), with a particular focus on Vegetated Swales (VS). Two TW and two VS located in the province of Valencia (Spain) are evaluated within this work.

## 2. Methodology and results.

With respect to the TW, they have exhibited commendable efficiency in intercepting MPs. In this instance, two treatment plants were examined, one employing TW for both secondary and tertiary treatment, and another utilizing an aerated biological reactor with floating helophytes situated upon a buoyant structure as secondary treatment, along with TW for tertiary treatment (Fig. 1). Water samples were collected at the inlet and outlet of both WWTPs, as well as at intermediate points (inlet and outlet of TWs), in order to accurately quantify the efficiencies. Additionally, samples were taken from the sludge of the secondary treatments of both plants, and root samples were also collected to study their potential retention effect.

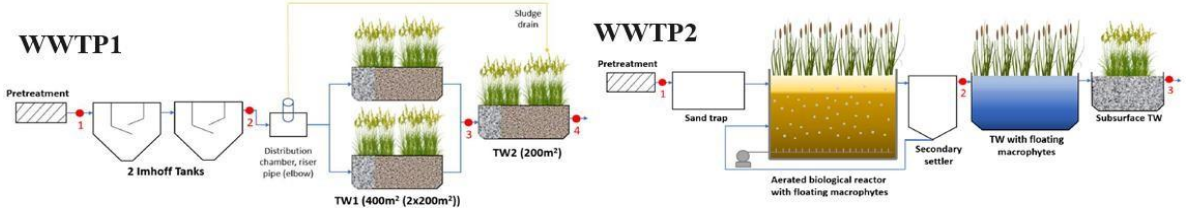



**Fig. 1.** Scheme of both WWTPs studied, with the red points where samples were taken.

Two VS are currently under study. These systems are mature, having been in place for over ten years. One of them receives runoff from sports facilities and shared green areas, while the other collects water from both roadways and pedestrian zones. Figure 2 displays both zones and the adjacent areas that contribute runoff to them during rainfall events. In this case, the evaluation encompasses both the water at their inlet and outlet points, as well as soil samples taken at three zones (initial, intermediate, and final sections) within each of them. Given that these systems are open and more accessible to the public, an assessment of their content in macroplastics (MAPs) and mesoplastics (MEPs) (ranging from 5 to 25 mm) was also conducted.

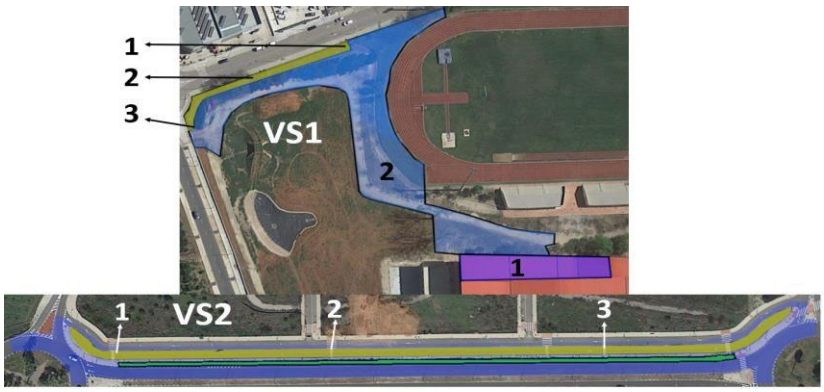



**Fig. 2.** Both VS studied (yellow zones) with the contributing areas (blue zones) and the sample points numbered.

Regarding the methodology employed, the steps outlined in previous studies have been adhered to (Cabrera et al., 2023). Additionally, it is pertinent to continue with the same techniques that have been utilized in various studies.

The following are results from the studies conducted thus far. Firstly, the average retention efficiencies in water samples are presented for both WWTPs employing TW, as well as the concentrations obtained in sediment samples and within the vegetation roots inside of the TWs themselves (Fig. 3). Furthermore, the average results of MPs in water samples obtained in two sampled rainfall events in the VS are displayed, along with the results of MAPs and MEPs obtained in soil (Table 1).

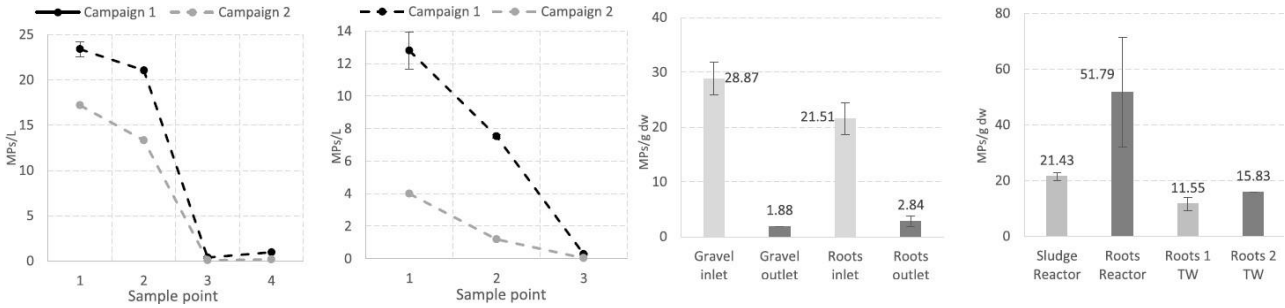



**Fig. 3.** MPs concentration in the different points in both WWTPs (WWTP1 right and WWTP2 left). Concentrations measured in both WWTPs in sludge and roots samples.

**Table 1.** MAPs and MEPs concentrations in soil samples of both VS. Additionally, concentration of MPs and classification for water samples taken during two rainfall events in VS1.

| Soil Sample | MAPs Total | MAP/m2 | MEPs/kg dw | Water Sample | | Fibers | Particles | Films | MPs/L |
|---|---|---|---|---|---|---|---|---|---|
| VS1.1 | 27 | 4.5 | 8.5 | Inlet | 425 µm | 17.5 | 5.5 | 0.5 | 1.8 |
| VS1.2 | 27 | 4.5 | 200.8 | | 75 µm | 20 | 5.5 | 1 | 2.1 |
| VS1.3 | 65 | 5.2 | 20.4 | | 40 µm | 12 | 4 | 0.5 | 1.3 |
| VS2.1 | 20 | 6.7 | 11.8 | Outlet | 425 µm | 6.5 | 0.5 | 0 | 1 |
| VS2.2 | 116 | 38.7 | 22.2 | | 75 µm | 10 | 1 | 1 | 1.7 |
| VS2.3 | 10 | 3.3 | 343.2 | | 40 µm | 6 | 0 | 0.5 | 0.9 |

In conclusion, the study suggests that both TWs and VS hold significant potential for retaining MPs. The initial findings underscore the importance of this issue, as the presence of MPs in both SUDS infrastructures built over a decade ago and in wastewater is notable.

**Acknowledgements**

This research is being developed within the framework of the SUDSLong-VLC project (PID2021-122946OB-C32), which is funded by MCIN/AEI/10.13039/501100011033 and by "ERDF A way of making Europe". Darío Calzadilla acknowledges the funding of the predoctoral contract for the training of doctoral students (Ref. 46707) within the Subprogram-2 (PAID-1-22) of the Universitat Politècnica de València.

**References**

Cabrera, D. C., Wang, Q., Martín, M., Rajadel, N. O., Rousseau, D. P., & Hernández-Crespo, C., 2023. Microplastics occurrence and fate in full-scale treatment wetlands. Water Research, 240, 120106.

Lu, Y., Zhang, Y., Deng, Y., Jiang, W., Zhao, Y., Geng, J., Ding, L., Ren, H., 2016. Uptake and accumulation of polystyrene microplastics in zebrafish (Danio rerio) and toxic effects in liver. Environ. Sci. Technol. 50, 4054.

PlasticsEurope, 2021. Plastics - the Facts 2021. Retrieved from. https://plasticseurope.org/knowledge-hub/plastics-the-facts-2021/.

Sarkar, D.J., Sarkar, S.D., Das, B.K., Sahoo, B.K., Das, A., Nag, S.K., Manna, R.K., Behera, B.K., Samanta, S., 2021. Occurrence, fate and removal of microplastics as heavy metal vector in natural wastewater treatment wetland system. Water Res. 192, 116853.

Wang, W., Ge, J., Yu, X., 2019. Bioavailability and toxicity of microplastics to fish species: a review. Ecotoxicol. Environ. Saf. (November), 109913.

8th IAHR EUROPE CONGRESS
LISBON - PORTUGAL
4-7 JUNE 2024

# Long-term laboratory analysis of the impact of sediment characteristics on the clogging process of permeable asphalt and its hydrological and water quality response.

Eduardo GARCÍA-HABA [1], Juan NAVES [2], Carmen HERNÁNDEZ-CRESPO [3], Angélica GOYA-HEREDIA [4], Joaquín SUÁREZ [5], Jose ANTA [6], Ignacio ANDRÉS-DOMÉNECH [7]

[1,3,7] Instituto Universitario de Investigación de Ingeniería del Agua y del Medio Ambiente (IIAMA), Universitat Politècnica de València, Camí de Vera s/n, 46022, Spain
edgarha@upv.es; carhercr@upv.es; igando@upv.es

[2,4,5,6] Universidade da Coruña, Water and Environmental Engineering Research Team (GEAMA), Center for Technological Innovation in Construction and Civil Engineering (CITEEC), Campus de Elviña, 15071, Spain
juan.naves@udc.es; angelica.goya@udc.es; joaquin.suarez@udc.es; jose.anta@udc.es

ABSTRACT

The clogging process and sediment properties have direct influence on hydrological behaviour and pollutant removal of permeable pavements (PP). Laboratory experiments simulated and analyzed the response of permeable asphalt under different sediment loading conditions. Permeability and efficiency in water quality treatment in effluents were measured. Sediment surface loads of more than 1 kg/m$^2$ caused significant reductions in permeability. Sediment with higher content of organic matter reduce infiltration ratios and increase runoff flows and volumes. Permeability recovery after vacuum cleaning varied between 8% and 100% of original permeability. The efficiency of the slab for pollutant retention was 96% for COD, 76% for TN, 79% for TP, and 98% for TSS.

## 1. Introduction

Technical challenges such as clogging and water quality are key concerns when implementing permeable pavements, and therefore need further research (García-Haba et al. 2022). The clogging process directly impacts the hydrological behavior and pollutant removal efficiency of permeable pavements. In order to improve the knowledge about the hydraulic performance and water quality of filtrated water and runoff, continuous porous asphalt slabs were tested at laboratory. The experiment was replicated at Universidade da Coruña (UDC) and Universitat Politècnica de València (UPV), simulating the same synthetic rainfall pattern and different clogging conditions. The tests carried out at UDC focus on the analysis of the influence of particle size on the clogging of the porous asphalt, while the experiments at UPV aim to evaluate its behaviour in terms of pollutant reduction for different degrees of clogging.

## 2. Materials and methods

Standardized Spanish PA-16 porous asphalt slabs were installed in rainfall simulators constructed at UDC and UPV according to Naves et al. (2020) and Fernández-Gonzalvo et al. (2021) respectively. A total of six road sediment classes, from UDC and UPV campus and the residentIal area of Benimaclet in Valencia (BEN), with different content in organic matter and diverse particle size distribution were tested. Permeability of the PP, and water quality variables in the PP effluents, such as chemical oxygen demand (COD), total suspended solids (TSS), ammonium, nitrites, nitrates, total nitrogen (TN), phosphates and total phosphorus (TP), were monitored during a progressive sediment accumulation on the pavement surface. A variable head permeameter was used to measure the permeability of the porous asphalt for different grades of clogging during the tests following the Spanish standard NLT-327/00 (CEDEX, 2000). Restoration of initial permeability was studied by vacuuming retained sediments.

## 3. Results and discussion

For every sediment class, permeability was exponentially reduced as sediment load increased on the slab surface (Fig. 1). Fine sediment UDC-1 was that least clogged the slabs, and allowed to restore almost 100% of initial permeability, whereas UDC-3 was the most unfavorable. Additionally, the effect of organic matter content in UDC-4 increased permeability loss.

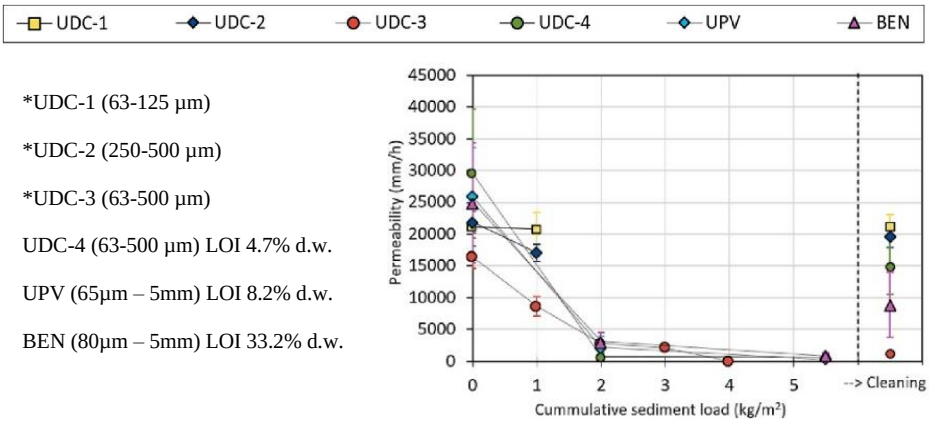



**Fig. 1.** Reduction of permeability observed for different sediment loading steps over the porous asphalt for each sediment class tested (García-Haba et al. 2023). * No content in organic matter,

All the water quality variables increased as the cumulative sediment load increased. After 1 kg/m$^2$ of cumulative sediment load, COD, TSS, phosphates and TP, showed higher concentrations than the limits for treated wastewater (Council Directive, 1991). Based on a mass balance, pollutant retention of the PP was 96% for COD, 76% for TN, 79% for TP, and 98% for TSS.

## 4. Conclusions

Fine sediments cause lower permeability loss compared to sediments with wider diameter ranges in porous asphalts, suggesting the need for standardized methods considering this variability. Porous asphalt exhibits high infiltration efficiency and sediment/pollutant retention capacity, suggesting its installation in urban areas as sustainable urban drainage solutions.


#### Acknowledgements

This research is developed within the framework of the Spanish “Plan Estatal de Investigación Científica y Técnica y de Innovación 2017–2020”, project HOFIDRAIN (Holistic characterization of filtering sections for smart and sustainable management of urban drainage systems at city scale), through the sub-projects ENGODRAIN (grant number RTI2018-094217-B-C31) and POREDRAIN (grant number RTI2018-094217-B-C33) funded by MCIN/AEI/10.13039/501100011033 and by “ERDF A way of making Europe”. Eduardo García-Haba appreciates the pre-doctoral contracts funding received for doctors training (Ref. PRE2019-089409) funded by MCIN/AEI/10.13039/501100011033 and by “ESF Investing in your future”.


#### References


CEDEX (2000). Normas NLT I.- Ensayos de Carreteras. Centro de Estudios y Experimentación de Obras Públicas. Ministerio de Transportes, Movilidad y Agenda Urbana. Gobierno de España. ISBN: 84-7790-361-1

Council Directive (1991). Council directive 91/271/EEC of 21 May 1991 concerning urban waste-water treatment. http://data.europa.eu/eli/dir/1991/271/oj.

Fernández-Gonzalvo, M, Hernández-Crespo, C., Martín, M., Andrés-Doménech, I. (2021). Comparison of permeable pavements effluent under Atlantic and Mediterranean rainfall regimes: a mid-term laboratory experience, Build. Environ. 206 (2021), 108332, https://doi.org/10.1016/J.BUILDENV.2021.108332.

García-Haba, E., Naves, J., Hernández-Crespo, C., Goya-Heredia, A., Suárez, J., Anta, J., & Andrés-Doménech, I. (2023). Influence of sediment characteristics on long-term hydrology and wáter quality behaviour during the clogging process of a permeable asphalt. Journal of Water Process Engineering, 53, 103658. https://doi.org/10.1016/J.JWPE.2023.103658

García-Haba, E., Rodríguez-Hernández, J., Andrés-Doménech, I., Hernández-Crespo, C., Anta, J., Martín, M. (2022). Design of permeable pavements in Spain: current situation and future needs. Ingeniería del agua, 26(4), 279-296. https://doi.org/10.4995/Ia.2022.18290

Naves, J., Anta, J., Suárez, J., Puertas, J. (2020). Development and calibration of a new dripper-based rainfall simulator for large-scale sediment wash-off studies, Water 12 (1) 152, https://doi.org/10.3390/w12010152.

# Decentralized management of urban wastewater through the implantation of artificial wetlands for the renaturalization of the Carraixet ravine

Enric GIL-MARTÍNEZ[1], Carmen HERNANDEZ-CRESPO[2], Mª Eugenia RODRIGO SANTAMALIA[3], Luís LIDON CEREZUELA[4] , Enrique Javier ASENSI DASI[5] , Miguel MARTÍN MONERRIS[6], Vicent BENEDITO DURÁ[7]

[1] Instituto Universitario de Ingeniería del Agua y Medioambiente (IIAMA) – Universitat Politècnica de València (UPV), Camino de Vera SN, 46022 Valencia, Spain

[2] Instituto Agroforestal Mediterraneo – Universitat Politècnica de València (UPV), Camino de Vera SN, 46022 Valencia, Spain

engiim@doctor.upv.es

ABSTRACT

The Carraixet ravine faces anthropogenic pressure and habitat loss, exacerbated by climate change. While serving as a vital ecosystem and an ecological corridor, it confronts challenges based on the impacts of centralized wastewater management systems. To address this situation, we propose a watershed-level study to identify the most problematic areas and the causes of degradation, enabling us to propose solutions tailored to each need.

## 1. Introduction

The Carraixet ravine, originating in Gátova (Valencia) and flowing into the Mediterranean Sea, faces anthropogenic pressure and lacks natural habitat along 75% of its length. Climate change exacerbates this, necessitating ecological restoration via corridors (Harris et al., 2006). The ravine is a unique aquatic ecosystem, serving as a refuge, food source, and breeding ground for diverse species. These ecosystems rely on wastewater treatment plants, which face challenges like non-compliance with standards and periodic overflows. Addressing these involves adapting wastewater management to climate change, ensuring compliance, and adopting decentralized, nature-based solutions to enhance effluent quality and mitigate sewer overflow impacts.

## 2. Methodology

Given the extensive scope of this project, spanning the entire basin and the existence of urban areas characterized by complex infrastructure and significant wastewater management systems, it is imperative to employ a structured methodology.

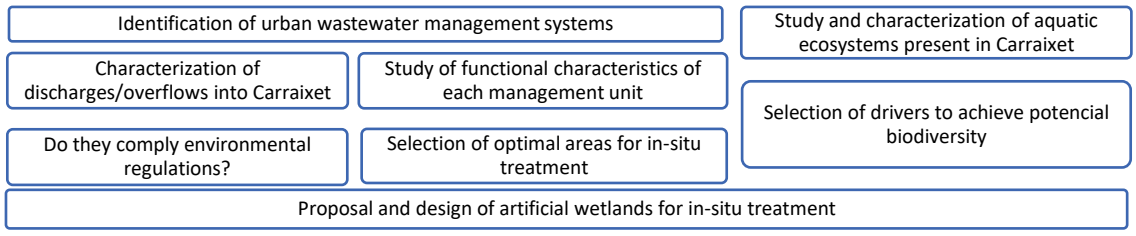



**Fig.1**. Proposed methodology for the analysis of the environmental situation of the Carraixet ravine and the proposal for improving current treated discharges and implementing decentralized in-situ treatment systems through artificial wetlands.

This framework (Fig. 1) examines the Carraixet ravine basin from three interconnected perspectives: urban wastewater management systems, discharge and overflow points over the ravine, and the aquatic ecosystems within the Carraixet.

## 3. Results and Conclusions

In the Carraixet basin, there are 12 wastewater treatment systems (Fig.2.Left), most of them serving less than 2,000 equivalent inhabitants. The systems of Bétera and the treatment plant located at the end of the ravine are the most significant, serving 16,000 and 160,000 equivalent inhabitants (ae) respectively. In this section, we focus on the results obtained for the Bétera system.

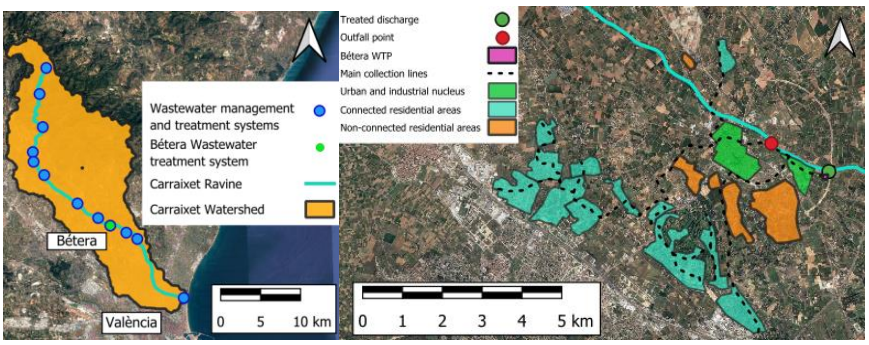



**Fig.2.** (Left) WTP's present in the Carraixet basin. (Right) Urban and functional layout of the wastewater management system of Bétera.

Wastewater in Bétera is managed centrally, with a treatment plant receiving an average flow of 6,700 $m^3$/day and serving a population of 14,264 (ae). The treated effluent shows good plant performance, but high phosphorus and total nitrogen levels due to the lack of tertiary treatment. The sewer network has one overflow point, sampled after several rainfall events, with peaks of 2,100 mg O2/L of COD during rainfall episodes as low as 5 mm. Numerous high and medium-density residential areas are connected to the sewer network, while various low-density areas are not connected and use septic tanks.

Table 1. Average concentrations for the period 2017-2022 of the effluent treated at the Bétera wastewater treatment plant

| SS(mg/L) | COD($mgO_2$/L) | $BOD_5$($mgO_2$/L) | TN(mg N/L) | TP (mg P/L) |
|---|---|---|---|---|
| 7,44±4,93 | 30,87±13,17 | 8,69±4,29 | 42,9092±10,39 | 5,31±3,06 |

The criteria for identifying suitable areas for disconnection from the existing network and proposing in-situ treatment will be based on management costs per equivalent inhabitant. Several studies indicate that pumping is one of the most significant costs (García-López et al., 2021; Sancho et al., 2011) and highlight that centralized models and the systematic expansion of existing networks result in diseconomies of scale (Eggimann et al., 2015). For residential areas without a treatment system, the direct design and implementation of wastewater treatment through artificial wetlands are proposed. The potential use of treated effluent will depend on the adopted solutions. Generally, treated areas within 2 kilometers of the ravine will allocate treated waters for moistening and revegetation.

The biodiversity study of ponds generated downstream from the treated discharge from Bétera shows that the macroinvertebrate community has not developed as fully as in other ponds in the same ravine receiving waters with lower nutrient and organic matter concentrations. This indicates the need for refining ponds at the Bétera plant to reduce concentrations and naturalize the water before discharge.With this decentralized management proposal, a triple objective beneficial for promoting biodiversity in the Carraixet ravine is achieved: reducing overflow events after rainfall, acquiring an ecologically reusable resource, and improving and renaturalizing the quality of the treated discharge.

**Acknowledgements**

The GARBIOFICAR project is funded by the European Union-Next Generation EU (TED2021-130907B-I00). Competitive research projects, Recovery, Transformation, and Resilience Plan, State Research Agency

**References**

Eggimann, S., Truffer, B., & Maurer, M. (2015). To connect or not to connect? Modelling the optimal degree of centralisation for wastewater infrastructures. *Water Research*, *84*, 218–231.

García-López, M., Melgarejo, J., & Montano, B. (2021). The Financing of Wastewater Treatment and the Balance of Payments for Water Services: Evidence from Municipalities in the Region of Valencia. *Sustainability*, *13*, 5874. Retrieved from https://api.semanticscholar.org/CorpusID:236356921

Harris, J. A., Hobbs, R. J., Higgs, E., & Aronson, J. (2006). Ecological restoration and global climate change. *Restoration Ecology*. Wiley Online Library.

Sancho, F. H., Senante, M. M., & Garrido, R. S. (2011). Eficiencia energética, una medida para reducir los costes de operación en las estaciones depuradoras de aguas residuales. *Tecnología Del Agua*, *31*(326), 46–54.

# Nature-based drainage systems: analysis of ecosystem services in the Manzanares River (Madrid, Spain)

María DÍAZ-REDONDO[1], Francisco M. CORTÉS SÁNCHEZ[1], Manuel GARCÍA[1]

[1] Centre for Studies and Experimentation on Public Works (CEDEX). Alfonso XII, 3, 28014 Madrid, Spain.
maria.diaz@cedex.es

Francisco.M.Cortes@cedex.es

manuel.colomer@cedex.es (for author 3)

ABSTRACT

The project “Recovery of the fluvial ecosystem Manzanares-Gavia-Bulera. Green and blue infrastructure Metropolitan Forest of Madrid”, funded under the NextGenerationEU's Recovery, Transformation and Resilience Plan (PRTR), focuses on the recovery of river ecosystems through a nature-based proposal for the adaptation of drainage systems’ outlets. This study presents the research hypothesis and methodology, as well as the Monitoring plan with the selection of indicators to evaluate the potential of the proposed solution to improve ecosystem services, and the pre-project results. Proposed indicators of the Monitoring Plan aim at evaluating the following key aspects: i) eco-hydrogeomorphological quality, ii) river-floodplain connectivity, iii) adaptation to global change, and iv) socio-economic connection.

## 1. Introduction

In the Manzanares River downstream from Madrid city, sanitation, railway and road infrastructures have confined artificially the riverbed, impairing the river’s ecological functions. More particularly, storm drains and sanitary sewers, built of concrete and sometimes reinforced with breakwaters, cause considerable environmental damage by interrupting the ecological corridor linked to the river, both in terms of the gallery forest and the valuable and delicate river banks.

The proposal for the recovery of river ecosystems consists of removing the current concrete outlets, setting them backwards and creating transition "buffer" areas with soil and vegetation, guaranteeing sufficient width to recover the environmental continuity of the banks and the gallery forest. At the same time, this solution will increase the river space and its capacity to reduce flood damage.

As this proposal implies a potential nature-based solution, its conception, design, execution, operation and monitoring must be supported by the characterization and assessment of ecosystem services. Therefore, this study aims to evaluate the potential of the proposed nature-based solution to improve ecosystem services. The objectives of the study include: i) the research hypothesis and methodology, ii) the selection of indicators of ecosystem services for the Monitoring Plan and pre-project results.

## 2. Research hypothesis and methodology

The hypothesis for this study is that the improvement of hydraulic, hydrological, geomorphological, ecological, cultural and landscape functions, allows for the recovery or enhancement of the ecosystem services of the riverine environment.

The methodology includes the following steps: 1) collection of available information and selection of indicators of ecosystem services, 2) evaluation of the available information and the possibilities of maintaining the monitoring of the indicators throughout the project, 3) implementation of the Monitoring Plan (pre-project, construction and post-project phases), 4) data collection according to the frequencies established in the Plan, 5) registration of the data in a georeferenced database, 6) preparation of reports.

## 3. Monitoring Plan: selection of indicators of ecosystem services and pre-project results

The main objectives of the Monitoring Plan are the collection and calculation of sufficient, relevant, and reliable indicators, and the comparative analysis between the initial situation (pre-project phase), the construction phase and that which would result from the execution of the proposed solution (post-project phase). Henceforth, the selection of the ecosystem services' indicators and their evaluation methods was based on relevant bibliography and the authors' own developed methods (Table 1), with the aim of reflecting the objectives of the proposal in relation to the following aspects: i) eco-hydrogeomorphological quality, ii) river-floodplain connectivity, iii) adaptation to global change, and iv) socio-economic connection.

**Table 1.** Selection of indicators of ecosystem services. NDVI: Normalized Difference Vegetation Index; ind.: individuals.

| Aspect to be evaluated | Indicator | Method of evaluation | Units | Reference |
|---|---|---|---|---|
| Eco-hydrogeomorphological quality | Mean width of the active channel | Field work, digitization on ortophotography | m | MITECO (2019) |
| | Sedimentary activity (fluvial bars and islands) | | Ratio (dimensionless) | Díaz-Redondo et al. (2022) |
| | Abundance, richness and biomass of ichtiofauna | Field sampling | nº ind., nº ind./$m^2$, gr/$m^2$, % | Seber & Le cren (1967) |
| | Abundance and richness of flying insects | | | Authors' own method[1] (to be published) |
| | Abundance and richness of pollinators | | | |
| | Abundance and richness of entomofauna | | | |
| River-floodplain connectivity | Longitudinal ecological connectivity | Field work, digitization on ortophotography | m | MITECO (2019) |
| | Permeable surfaces | | $m^2$, % | |
| | Mean width of the gallery forest | | m | |
| Adaptation to global change | Healthy vegetation cover | Remote sensing (NDVI) | $m^2$, % | Díaz-Redondo et al. (2022) |
| | Shading of the active channel | | | MITECO (2019) |
| | Trail shading | | | Authors' own method[2] (to be published) |
| Socio-economic connection | Agricultural land cover | Digitization on ortophotography | $m^2$, % | Adapted from Keele et al. (2019) |
| | Amenity land cover | | | |
| | Vegetated surfaces | | | |

[1] Method based on field sampling with a collector box on a vehicle and on metrics calculation in the laboratory. [2] Method based on orthophotography digitization and selection of trail shading and raster image reclassification (NDVI > 0.6) on the selected areas.

Currently, results from the pre-project phase can be summarized as: low eco-hydrogeomorphological quality (i.e., very narrow active channel, no unvegetated islands and predominancy of exotic fish species); low lateral river-floodplain connectivity (i.e., reduced width of the gallery forest), but high longitudinal connectivity (i.e., no transversal barriers); reduced adaptation to global change (i.e., low healthy vegetation cover and low shading of the active channel); and low socio-economic connection (i.e., low agricultural and amenity land cover). These results constitute the baseline for the subsequent comparative analysis with the results of the construction and post-project phases, which will inform on the success of the proposed solution.

**Acknowledgements**

This study is developed within the project "Recovery of the fluvial ecosystem Manzanares-Gavia-Bulera. Green and blue infrastructure. Metropolitan Forest of Madrid", with the finantial support of the Biodiversity Foundation (Ministry for Ecological Transition and the Demographic Challenge), under the NextGenerationEU's Recovery, Transformation and Resilience Plan (PRTR).

**References**

Díaz-Redondo M, Marchamalo M, Morcillo F, King JJ (2022). Naturalising a heavily modified urban river: Initial habitat evolution in the Manzanares River (Madrid, Spain). River Research and Applications, 38, 727–737

Keele V, Gilvear D, Large A, Tree A, Boon P (2019). A new method for assessing river ecosystem services and its application to rivers in Scotland with and without nature conservation designations. River Research and Applications, 35, 1338–1358

MITECO 2019. Protocolo de caracterización hidromorfológica de masas de agua de la categoría ríos. Ministerio para la Transición Ecológica y Reto Demográfico, anteriormente Ministerio para la Transición Ecológica.

Seber GAF, Le Cren ED (1967). Estimating Population Parameters from Catches Large Relative to the Population. Journal of Animal Ecology, 36, 631–643

# Experimental Investigations of Thin Layer Surface Runoff on Natural Grassland

Tim JAKOBS, Peter OBERLE, Mário J. FRANCA

Institute for Water and River Basin Management (IWG), Karlsruhe Institute of Technology (KIT), Germany
tim.jakobs@kit.edu

ABSTRACT

## 1. Introduction

In the global risks report by WEF (2021), the risk of "extreme weather events" has been rated with the highest probability of occurrence for the fifth time in a row. In addition to fires, heat waves and windstorms, heavy rainfall and flash floods regularly appear and cause severe flooding with considerable damage to property and human life. To address the risk, heavy rain hazard maps based on 2D hydraulic models are created in Baden-Württemberg (Germany). In contrast to river hydraulics methods, the simulation of heavy rain surface runoff contains significantly greater uncertainties which ultimately affect the risk assessment and emergency response. The main challenges are defining geometrical boundaries, choosing appropriate spatial resolutions and the adequate quantification of the flow resistance. In addition, the impact of dynamic processes in terms of morphology and vegetation must also be considered. In previous studies, the determination of roughness parameters for thin layer surface flow was primarily based on field tests or laboratory experiments. In field tests with rain simulators, hydrological parameters (e.g. infiltration, erosion) have been investigated in general neglecting the detailed measurement of small-scale hydraulic processes (Engman, 1986). In laboratory experiments, precise measurements have taken place, but the model setup was mostly based on synthetic materials (e.g. artificial grass, asphalt), lacking relevant effects of heterogenous flow processes (Ruiz Rodriguez and Trost, 2017). In this context, it must be noted that small-scale geometric irregularities on natural surfaces and the effects on runoff concentrations as well as retention effects have a major influence on unsteady flow characteristics and have not been sufficiently researched to date (Kerlin et al., 2022).

## 2. Experimental Setup on Natural Grassland

As shown above, there is a significant research gap at this point. To address this matter, a novel experimental setup (Fig. 1, left) was designed with the aim to enable outdoor measurements on natural surfaces under controlled conditions comparable to those in hydraulic engineering laboratories. The adaptable setup can be used to examine natural plots with a maximum width of 3 meters and a flexible length. In the actual study case, the first investigated plot contains natural grassland with a slope of 14 % and the dimension is 3 x 6 meters. To protect the plot from the weather, it was also covered by a freestanding roof. The discharge on the plot is induced by a pump which drains the water from storage tanks with an effective volume of approx. 6.700 liters. The flow is controlled by two valves and is in the range of 0 – 34 $ls^{-1}$. These components are connected with pressure tubes and will finally end in an inlet basin. Here great importance was attached to a turbulence-free and homogenous inlet flow onto the plot area. At the end of the examined surface the water is collected in a channel and flows back to the storage tanks to complete the circular system. During the experimental tests, discharge measurements are carried out upstream and downstream of the plot to monitor the discharge and thus observe also the varying infiltration rates. In addition, volume changes in the inlet tanks are recorded using water level probes. A camera is installed above the survey area. Hydraulic processes (transforming grass, forming of flow paths, step pools, etc.) can be documented here. Installed ArUco markers, which were previously measured with a terrestrial laser scanner (TLS), can later be used for automated registration of the image material. In selected experiments, fluorescent dye tracer (Fluorescein, Sulforhodamine B and Acid Amino G) is used, which are made visible with the help of 2 UV lights. The tracer is added directly at the inlet area using a pipe with drillholes of 1,7 mm and an air valve for evenly dosing. The injection is carried out

during the first flush and the later steady state. Alternatively, warm water can be used as a tracer using a thermal camera. Information about the heterogeneous flow velocity distribution can be derived from the tracer movement with the help of a developed algorithm.

## 3. Experiments and Evaluation

On the above-mentioned test area, until now 5 different vegetation conditions were sampled in order to determine the relevant parameters for the heavy rain simulation on the basis of in total 280 individual experiments. For each vegetation condition, the surface was photographed and measured with high resolution scans with a TLS. From this data, vegetation density and height distribution can be derived for each experiment series. First, the plot is irrigated with a very low flow rate for 20 - 30 minutes until the soil is completely saturated and the infiltration rate is constant. Afterwards the measurement procedure will begin. For 9 different discharges in the range of q: 0 – 10 $ls^{-1}m^{-1}$ measuring sets are carried out under stable conditions. For each of these, 3 experiments lasting 5 minutes each are carried out to minimize measurement errors. After each series of measurements, the surface is recorded again with the TLS to record possible erosive changes. When carrying out the experiments, the discharge spectrum initially ranges from low to high discharge. The same base points are then sampled again in the reverse order (high discharge to low discharge). This is intended to investigate possible differences in the flow resistance behavior during floods.

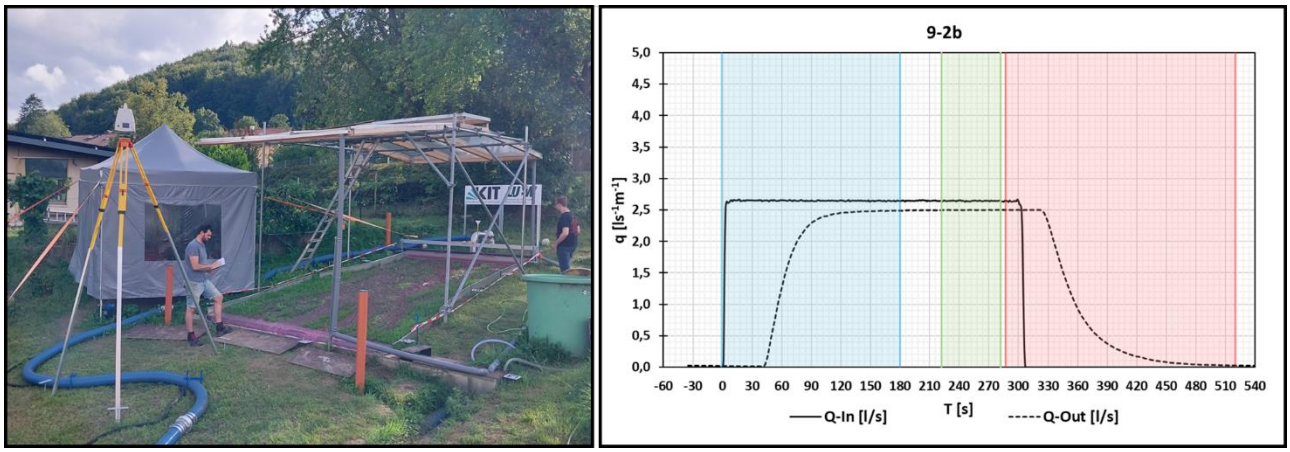



**Fig. 1.** Experimental setup (left) and illustrative result (right)

This results in a total of 56 individual measurements for a series of experiments regarding one vegetation condition. One of these individual measurements is shown illustratively in Fig. 1 (right). The inflow to the area and the outflow from the area are shown over the duration of the experiment. The constant infiltration rate is clearly visible. By looking into the three characteristic parts of the hydrograph (blue, green, red), hydraulic boundary conditions, the cavity volume and the active water volume (steady state) on the surveyed area can be calculated from the experiment. On this basis, relevant hydraulic parameters (e.g. friction factors) can be determined for the examined spectrum.

## 4. Outlook

Experiments on this plot will be completed this year. Next year, further tests will be continued for additional plots with different slopes. The TLS data will also be used for a 3D CFD model to gain further insights on the hydraulic processes. Finally, the findings should be used to improve 2D CFD to simulate flash floods due to heavy precipitation events.

**Acknowledgements**

This study was made on behalf and in collaboration with the LUBW (Institute for Environmental Protection from the State of Baden-Württemberg, Germany).

**References**

Engman, E.T. (1986): Roughness Coefficients for Routing Surface Runoff. Journal of Irrigation and Drainage Engineering. Vol. 112 (1): 39-53.

Kerlin, T., Oberle, P., Kron, A., Franca M.J. (2022): Parameterization of Flow Resistance for Hydrodynamic Numerical Simulation of Sheetflow. Ortega-Sánchez (Hg.) 2022 – Proceedings of the 39th IAHR. S. 7009–7018. 10.3850/IAHR-39WC252171192022882.

Ruiz Rodriguez E., Trost, L. (2017): Umgang mit Starkniederschlägen in Hessen. Auszug aus dem 3. Zwischenbericht. KLIMPRAX Starkregen Arbeitspaket 2. Hochschule RheinMain. Wiesbaden.

World Economic Forum WEF (2021): The Global Risks Report 2021. 16th Edition. Insight report. ISBN: 978-2-940631-24-7.

# An Assessment of the Potential for Wastewater Heat Recovery in the Zambian Food Processing Industry

Madhu K. MURALI[1,a] & Aonghus MCNABOLA[1,b]

[1] Department of Civil, Structural and Environmental Engineering, Trinity College Dublin, Ireland
[a] muralim@tcd.ie
[b] amcnabol@tcd.ie

ABSTRACT

Coal is widely used for heating water in Zambian food processing and manufacturing. In certain industries, Wastewater Heat Recovery (WWHR) may be an option to reduce carbon emissions and coal use associated with water heating. Feasibility assessments at several food processing plants showed that there was significant embedded heat in dairy processing and boiler blowdown wastewater discharges. Additional longer-term monitoring showed a consistent thermal resource in boiler blowdown wastewater discharges with mean temperatures between 40-50°C. The estimated energy savings across a number of discharge locations ranged from an equivalent reduction in coal use of 16 to 200 tonnes per year, around 24.2 to 294 tonnes of $CO_2$ equivalent ($tCO_2e$).

## 1. Background

With an increasing focus on reducing global anthropogenic carbon emissions, work is now underway on quantifying and reducing the emissions across Southern Africa (Phiri *et al.*, 2021). In Zambia, industries have long relied on coal for their energy needs due to its local availability through the Maamba Coal Mine (Kabombwe, 2023). An average of 175,000 tonnes of coal was used annually by Zambian industry between 1996 and 2002 (ZamStats, 2008). Zambian agriculture and food processing have been required to increase production in the last few years to keep pace with the growing population of the country and Zambia has significant potential to further expand agricultural output (Phiri *et al.*, 2020). Hence, reducing coal use in the Zambian food processing and manufacturing sectors will be important in reducing or maintaining the country's overall carbon emissions.

Previous work in Europe has found that the wastewater produced in meat processing facilities has significant levels of embedded heat and that there is a potential to recover this waste heat and use WWHR to recycle it (Spriet, 2021). Expanding this analysis to Zambian meat and dairy processing could be the first step in identifying opportunities for similar WWHR opportunities in Zambia, within the food manufacturing industry and more widely, leading to reduced coal usage and carbon emissions. Hence, this paper aims to offer an initial assessment of the potential for WWHR in the Zambian food processing sector.

## 2. Methods

Partnerships were developed with several Zambian food processors and detailed feasibility assessments were undertaken at several of their production facilities between April and November 2023, with the purpose of identifying processes where significant hot water utilization occurs resulting in the generation of hot wastewater discharges with WWHR potential. Further, the boiler and other hot water generation systems on-site were also identified to determine if the integration of WWHR savings was feasible in the future. Once this initial assessment was complete and some hot wastewater generating processes were identified, on-site temperature measurements were taken to assess the temperature of the hot wastewater. Following this, temperature sensors were placed in selected wastewater drains to record wastewater temperature over two weeks to expand on the initial on-site monitoring and one sensor was placed in a clean water input tank to estimate the temperature difference between the cold freshwater and warm wastewater.

## 3. Results & Discussion

A pork, stockfeed, beef, chicken, and dairy processing centre were assessed with the beef, chicken, and dairy processing occurring within one large production complex. The beef, chicken, pork, and stockfeed processing centres did not show a large potential for WWHR based on their hot water usage. This was primarily due to the use of 'cold' water (~23ºC) in the cleaning process. The dairy processing centre showed a significant potential based mainly on the frequent use of two 3-stage cleaning in place processes when the production line changes products, and for the milk receiving tanks, respectively (Figure 1b). Further, the use of a blowdown process in the coal boilers on two of the sites to periodically clean the boiler also resulted in the generation and discharge of significant volumes of near boiling wastewater (Figure 1a). Hence, temperature sensors were installed in the boiler blowdown drains of both these sites. A third sensor was placed in the combined wastewater from both the chicken and dairy processing centres.




**Fig. 1.** Two of the hot water processes identified on-site: (a) A steam boiler blowdown stream and (b) a Cleaning In Place control panel showing the high temperatures of the acid and caustic wash cycles.

The recorded temperature sensor data from the four sites (Table 1) showed that there is a significant consistent thermal resource for WWHR in the boiler blowdown drains that were measured with an average temperature above 40°C. There was significant variability in this temperature, especially for Blowdown Drain 1, but both of these temperatures still exceed the measured freshwater temperatures significantly. The chicken and dairy combined wastewater seemed less promising as a heat resource with only a slightly higher temperature than the freshwater. Any potential high temperature wastewater from the dairy processing centre may be suppressed by cooler wastewater from the chicken processing. Based on these results and the proximity of the boiler blowdown drains to the heating systems on-site, a WWHR system using a heat exchanger could likely be implemented relatively easily in these locations to reduce heating demand in the boiler and reduce coal use.

**Table 1.** Summary of monitored temperatures at the four selected food processing locations.

| Monitored Location | Average Weekday Temperature | Min.& Max. Measured Temperature Range | Estimated Energy Savings Potential |
|---|---|---|---|
| Boiler Blowdown Drain 1 | 49.6±10°C | 31.5-64.4°C | 16 tonnes/yr coal reduction (24.2 $tCO_2e$/yr) |
| Boiler Blowdown Drain 2 | 40.6±4.9°C | 19.1-58.5°C | 200 tonnes/yr coal reduction (294 $tCO_2e$/yr) |
| Chicken and Dairy Combined | 25.6±2.4°C | 20.2-41.1°C | Negligible |
| Input Freshwater Tank | 23.8±0.57°C | 22.6-25°C | N/A |

**Acknowledgements**

This project has emanated from research conducted with the financial support of Science Foundation Ireland (SFI) and the Department of Foreign Affairs (DFA) under the SDG Challenge Grant Number 22/FIP/SDG/10682.

**References**

Kabombwe, S. (2023) *A history of Maamba coal mine and its socio-economic impact on Zambia, 1968-2010.* Thesis. The University of Zambia. Available at: http://dspace.unza.zm/handle/123456789/8051 (Accessed: 27 September 2023).
Phiri, J. *et al.* (2020) 'Agriculture as a Determinant of Zambian Economic Sustainability', *Sustainability*, 12(11), p. 4559. Available at: https://doi.org/10.3390/su12114559.
Phiri, J. *et al.* (2021) 'Impact of Agriculture and Energy on CO2 Emissions in Zambia', *Energies*, 14(24), p. 8339
Spriet, J. (2021) *Wastewater as a thermal resource: Exploitation strategies, design methodologies & prototype development*. PhD Thesis. Trinity College Dublin.
The Zambia Statistical Agency (2008) *ENVIRONMENT STATISTICS IN ZAMBIA: Energy Statistics*. Available at: https://www.zamstats.gov.zm/download/5622/?tmstv=1695830511&v=5632 (Accessed: 20 September 2023).

# Optimal pump scheduling within a water distribution network by means of a global optimization solver

Oreste FECAROTTA[1], Armando CARRAVETTA[1], Renato MONTILLO[1], Maria Cristina MORANI[1]

[1] Department of Civil, Architectural and Environmental Engineering (DICEA) of University of Naples, "Federico II", Napoli, Italia.
oreste.fecarotta@unina.it
arcarrav@unina.it
renato.montillo@unina.it
mariacristina.morani@unina.it

ABSTRACT

Pump scheduling is among the most efficient strategies to increase the energy efficiency of water systems. The search for the best operation of pumping systems can be crucial to address the containment of energy consumptions, as well as the operational costs related to water supply and distribution.

This study proposes an optimization procedure for minimizing the energy requirements of three pumps working in parallel within a water network, relying on a mixed-integer nonlinear programming and the use of a global optimization solver. The procedure is applied to a literature synthetic network and the results are discussed and compared with previous research achievements on the same case study network.

## 1. The pump scheduling problem in water systems

The efficient management of water resources is a critical concern in the field of hydraulic engineering.. Pump scheduling, as a component of water distribution systems, has gained substantial attention due to its potential for reducing operational costs (Giacomello et al., 2013).

Pump scheduling aims to determine the optimal operation of pumps within a hydraulic system. Challenge lies in balancing the often conflicting goals of maintaining system stability, meeting varying demand patterns, and utilizing available resources efficiently. However, it was not until the advent of computational tools and advancements in control theory that pump scheduling gained prominence.

### *1.1. State of the art*

The optimal pump scheduling has received much attention in recent years and many researchers developed models and algorithms to determine the best pump operation aimed at optimizing different objective functions, with the aim of i) reducing the amount of requested energy, ii) reducing the water leakage, iii) control the network pressure, etc.

Different approaches have been investigated, such as linear and nonprogramming (Ormsbee & Reddy, 1995; Price & Ostfeld, 2014), and meta heuristic programmming, (Cimorelli et al., 2020; Savić et al., 2011).

### *1.2. Aim of the study*

This study presents a complete mathematical model which can be coupled with a global optimization programming method. The advantage of the global search lies in the possibility for the user to evaluate the quality of any solution found, which is not possible when heuristic approaches are used to perform the optimization. The study is focused on the optimization of pumps operations within the synthetic water distribution network of a literature synthetic network, i.e. Any town modified (Cimorelli et al., 2020; Rao & Salomons, 2007), presented in Fig. 1.

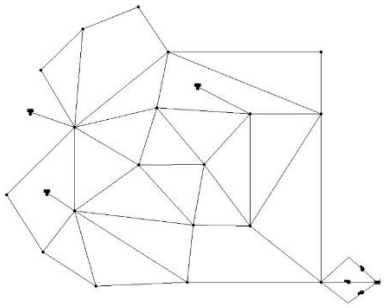


**Fig. 1.** Layout of Any town modified network (Cimorelli et al., 2020).

The network consists of 44 branches and 23 nodes, and three pumps are located in parallel to collect the water from the source and deliver it towards three tanks placed at the opposite side of the network.

The objective function proposed for the optimization problem is the minimization of the total cost spent for pumping ($C_p$):

$$C_p = \sum_{t=1}^{T} P(t)\, \Delta t\, I_0(t)\, \theta(t) \quad (1)$$

where $P(t)$ is the total power absorbed by the pumping system at the time step $t$, $\Delta t$ is the duration of the time step and $\theta(t)$ is the energy tariff assumed according to the study proposed by (Cimorelli et al., 2020). With reference to $I_0(t)$, it is a binary variable assuming value as 1 if the pumping system is active at the time step $t$, 0 otherwise. The mathematical model is then completed by the constraints, which involves hydraulic equations (i.e. continuity and momentum equations) to solve the network and further linear and nonlinear constraints (pump characteristic curves, minimum pressure at nodes, minimum and maximum level in the tanks and dependent variables definitions). As a result, due to the presence of both integer and continuous variables, the mathematical problem is mixed-integer nonlinear programming (MINLP) (Belotti et al., 2013).

### *1.3. Results*

The proposed mathematical model has been coupled to a literature global search method, such as SCIP 8.0.0 (Bestuzheva et al., 2021) to investigate the potentiality of a global algorithm in this kind of problems. The results highlight the capabilities of this global approach, as well as its drawbacks and limitations, which are mainly related to the strong nonlinearity of the problem and the consequent computational effort. In fact, the total cost is 3,361 USD per day versus 3,635 USD obtained by Cimorelli et al. (2020), while the software did not conclude the calculation, but was stopped after one day, reaching a 29% gap from the best so-far bound.

**Acknowledgements**

This work has been supported by the project "ACDC-P : Acoustic Characterization for Diagnostics of Cavitation in Pumps" funded by the MIUR Progetti di Ricerca di Rilevante Interesse Nazionale (PRIN) Bando 2022 - grant 20227AMAYL.

**References**

Belotti, P., Kirches, C., Leyffer, S., Linderoth, J., Luedtke, J., & Mahajan, A. (2013). *Mixed-integer nonlinear optimization. Acta Numerica*, 22, 1–131. https://doi.org/10.1017/S0962492913000032

Bestuzheva, K., Besançon, M., Chen, W.-K., Chmiela, A., Donkiewicz, T., van Doornmalen, J., Eifler, L., Gaul, O., Gamrath, G., Gleixner, A., Gottwald, L., Graczyk, C., Halbig, K., Hoen, A., Hojny, C., van der Hulst, R., Koch, T., Lübbecke, M., Maher, S. J., … Witzig, J. (2021). The SCIP Optimization Suite 8.0. http://www.optimization-online.org/DB_HTML/2021/12/8728.html

Cimorelli, L., D'Aniello, A., & Cozzolino, L. (2020). Boosting Genetic Algorithm Performance in Pump Scheduling Problems with a Novel Decision-Variable Representation. *Journal of Water Resources Planning and Management*. https://doi.org/10.1061/(asce)wr.1943-5452.0001198

Giacomello, C., Kapelan, Z., & Nicolini, M. (2013). Fast Hybrid Optimization Method for Effective Pump Scheduling. *Journal of Water Resources Planning and Management*. https://doi.org/10.1061/(asce)wr.1943-5452.0000239

Ormsbee, L. E., & Reddy, S. L. (1995). Nonlinear Heuristic for Pump Operations. *Journal of Water Resources Planning and Management*. https://doi.org/10.1061/(asce)0733-9496(1995)121:4(302)

Price, E., & Ostfeld, A. (2014). Discrete Pump Scheduling and Leakage Control Using Linear Programming for Optimal Operation of Water Distribution Systems. *Journal of Hydraulic Engineering*. https://doi.org/10.1061/(asce)hy.1943-7900.0000864

Rao, Z., & Salomons, E. (2007). Development of a real-time, near-optimal control process for water-distribution networks. *Journal of Hydroinformatics*. https://doi.org/10.2166/hydro.2006.015

Savić, D. A., Bicik, J., & Morley, M. S. (2011). A DSS generator for multiobjective optimisation of spreadsheet-based models. *Environmental Modelling and Software*. https://doi.org/10.1016/j.envsoft.2010.11.004

# Results of a methodology for the measurement of the CSO$^{i}$ polutograph in a continental Mediterranean climate region. The Madrid case study

Antonio LASTRA[1], Alejandro PINILLA[2], Jaime BOTELLO[3], Mónica ORTEGA[4], Celia ORTEGA[5], Laura RUIZ[6]

[1] Head of the Development innovation area. Canal de Isabel II. Madrid. SPAIN
alastra@canal.madrid
[2,3,4,5,6] Development innovation area. Canal de Isabel II. Madrid SPAIN
apinilla@canal.madrid [2] jbotello@canal.madrid [3] mortega@canal.madrid [4]
cortega@canal.madrid [5] l.ruiz@canal.madrid [6]

ABSTRACT

In a combined system, the release of water during an extreme rainfall event causes an impact in the receiving water body. Most of these discharges occur due to overflows necessary for network relief purposes, consisting of runoff polluted water without adequate treatment for its discharge. Moreover, as they are intermittent discharges and difficult to quantify due to their type of regime, so the magnitude of this impact in terms of pollutants is not so easy to measure.

The new regulatory context in Spain (Ministerio de transición ecológica y reto demográfico 2003) and the draft of the imminent European directive of wastewater treatment (Directorate-General for Environment 2023) requires the measurement of pollutant concentration discharged in those events. In this project, Canal de Isabel II (the public company that carries out the management of the whole urban cycle in the Madrid region, with more than 15.000 km of sewer network and more than 1200 points of CSO) has developed a methodology for quantifying the usual physicochemical parameters (COD, BOD, SS, TS, Ammonium, etc.) as pollution indicators and also a technique to calculate these parameters based on the turbidity measurement.

## Introduction and methodology

The most important aspects for the characterization of the pressures on a CSO are the demography, but also the city planning and the sanitary policies (SUAREZ, 2005). Taking this into account, the first step in this project was the classification of the different catchment in terms of population density, local climate, soil types, anthropic land use …

After this classification, several representative CSO points were selected and monitored. The update Madrid Region legislation (Decree 170/1998) indicates that CSO points located in collectors or discharge mains (collectors that pass through several municipalities) are the priority and are the first to be selected. Other decision-making guidelines for selection are established by the recently approved legislation in Spain for *Regulation of the Hydraulic Public Domain* (Ministerio de transición ecológica y reto demográfico, 2023), where one of the examples would be to prioritize CSO points that discharge into streams rather than meadows, as well as the different types of basins to be selected.

The campaigns were designed to range from dry to wet weather conditions to obtain hydrographs and polutographs. Each point has its own sampling protocol, but in all of them, a level and flow meter were installed to analyse the discharged flow and to trigger the taking of samples operative during the rainfall event. Those samples were obtained pumping into a portable sampler every 5 minutes (Fig 1 and 2). After the event, the samples were driven to the laboratory to obtain the pollutant values.

Due to the strong urban characteristics of the catchment, it was also necessary to obtain the pollutograph in a dry period. In this case an hourly sample was taken in every point both in a working day and in the weekend.

## Results and Conclusions

The population density as well as its activities and street cleaning policies are found to be key aspects to estimate the pollutants transported in a combined sewer system every time an extreme rainfall event occurs.

Based on this, it has been proven that in the Madrid region it is observed that the pollutants concentration peak is higher during some rainfall events than for dry periods. This applies to the densest sewer catchment of the region. This situation was previously demonstrated for Madrid city (LASTRA 2018) but now it is possible to see similar behaviour in smaller cities.

The first flush events occur almost in every one of the catchments, but the duration depends on the type of catchment. An interesting result is that this first flush duration does not depend on the length of the catchment but of the anthropic use of it.

It is possible to calculate the usual pollutants' parameters based on the turbidity measurement but the ratio between the different pollutants is different depending on the catchment (Fig 3).

In the extended paper we will present the full results of this study.



**Fig. 1 .** An instrumented CSO point



**Fig. 2 .** An instrumented manhole

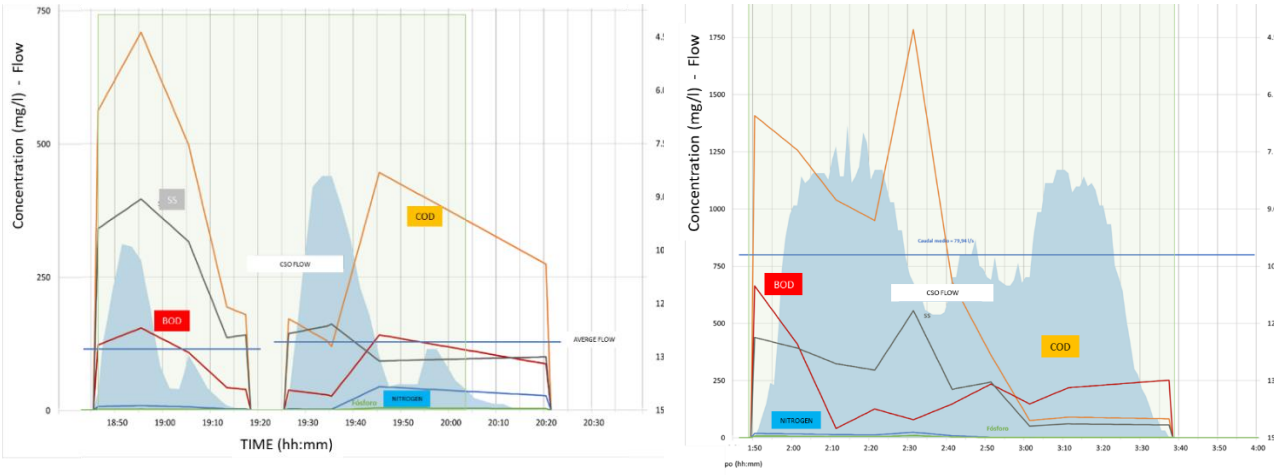



**Fig. 3 .** Some results of the pollutants released to the river in two different CSO points

### References


Decreto 170/1998, de 1 de octubre, sobre gestión de las infraestructuras de saneamiento de aguas residuales de la comunidad de Madrid. (1198) *Comunidad de Madrid*. [https://gestiona.comunidad.madrid/rlma_web/html/web/FichaNormativa.icm?ID=237]

Directorate-General for Environment (2023) *Proposal for a revised Urban Wastewater Treatment Directive*. European Commission [https://environment.ec.europa.eu/publications/proposal-revised-urban-wastewater-treatment-directive_en]

Lastra A. et al (2018) *Development of a Smart System for the Operation of a Complex Sanitation System*. UDM 2018, Palermo

Ministerio de transición ecológica y reto demográfico (2023) *Reglamento del Dominio Público Hidráulico* (Regulation of the Hydraulic Public Domain). Madrid, Spain. [https://www.boe.es/buscar/act.php?id=BOE-A-2023-18806#df-3]

Suárez J. and Puertas J. (2005) *Determination of COD, BOD, and suspended solids loads during combined sewer overflow (CSO) events in some combined catchments in Spain*, Ecological Engineering,Volume 24, Issue 3.


[i] CSO: Combined Sewer Overflow

# The factors affecting the domestic water consumption in Portugal: an econometric approach

António XAVIER[1], Carla ANTUNES[2], Maria de Belém COSTA FREITAS[3]

[1] CEFAGE (Center For Advanced Studies in Management and Economics) - University of Évora, Portugal
amxav@sapo.pt

[2,3] University of Algarve - Sciences and Technology Faculty and MED – Mediterranean Institute for Agriculture Environment and Development
cmantunes@ualg.pt, mbfreitas@ualg.pt

ABSTRACT

Water is a value resource, which needs to be managed carefully. In Portugal this is a relevant issue, namely due to the climate restrictions and evolution over the last years. In order to manage water use, the main determinants of consumption should be studied, and a model is relevant to explain those factors. To achieve this objective an ordinary least squares (OLS) regression model and a geographically weighted regression (GWR) are proposed. The models were implemented in the 278 municipalities of continental Portugal, considering the average situation of the last decade. The results showed promising results, identifying the main explaining factors for water consumption in the municipalities.

## 1. Introduction

Water is a scarce resource in Portugal, mainly at the south. The climate conditions lead us to think what are the main determinants of its consumption in order to valorize this resource in a sustainable way. To identify the main determinant factors conditioning water consumption, several studies have been already carried out; however, no model was yet developed for Portugal. To overcome this gap and ascertain the influence of different variables on domestic water consumption, an ordinary least squares (OLS) regression model and a geographically weighted regression (GWR) are proposed.

## 2. Methodological approach

Firstly, an expert analysis was conducted in order to select the main factors affecting domestic water consumption in Portugal. According to several research hypotheses, the following linear multiple regression model expressing the relationship between the explanatory variables and water use sustainability is presented as follows:

$$Y = \beta_0 + \beta_1(X_1) + \beta_2(X_2) + \beta_3(X_3) + \beta_4(X_4) + \beta_5(X_5) + \beta_6(X_6) + \beta_7(X_7) + \varepsilon \quad (1)$$

where, $Y$ is the domestic water consumption;: $X_1$ –number of hotel stays for measuring the level of tourism activity; $X_2$– urban areas; $X_3$ – purchasing power for measuring the income level; $X_4$ – area of irrigated green spaces; $X_5$ – percentage of population with 14 years old or less for assessing the young age population groups; $X_6$ – number of inhabitants with superior education; and $X_7$ – size of the household.

The above global regression models assume that the relationship between the response and explanatory variables is stationary (i.e., constant) across a study area which means that these relationships do not vary over space (Fotheringham et al., 1998; Mansour et al., 2021). To relax this assumption and allow the parameters to vary spatially, GWR assumes that non-stationary relationships exist between the response variable and the explanatory variable(s). Therefore, the model estimates a local parameter for each location separately (Charlton et al., 2009; Mansour et al., 2021). The GWR model is calculated as follows (Mansour et al., 2021):

$$Y_i = \beta_{0i} + \sum_{n=1}^{k} \beta_{ni}(u_i, v_i)x_{ni} + \varepsilon_i \quad (2)$$

where $Y_i$ is the domestic water consumption at municipality i, ($u_i$, $v_i$) represent the coordinates of the centroid of municipality i, $\beta_{0i}$, $\beta_{ni}$ indicates the local estimated intercept and effect of variable n for municipality $i$, respectively, $x_{ni}$ refers to the values of the i*th* explanatory variables while $\varepsilon_i$ denotes a random error term.

## 3.Results

For the OLS model, the $R^2$ and adjusted $R^2$ values of 0.435 and 0.420 indicate that about 42% of the domestic water consumption is explained by the independent variables. The Akaike's Information Criterion was 2519.267. The results of the ANOVA statistics of regression show that the F statistic is 29.689 with 277 degrees of freedom and the whole regression is significant at the 0.01 level (p-value = 0.000 < 0.01). Therefore, the null hypothesis is rejected, and all b regression coefficients are different from zero. The regression coefficients and the results of hypothesis testing are presented in Table 1.

Among others, these results show that the number of overnight stays by tourists has a significant and positive effect on domestic water consumption at the 0.01 significance level with a t-statistic of 9,050 and p=0.000 (p < 0.01). The standardized regression coefficient is 0.607, meaning that an increase of 100% in the explanatory variable results in an increase of 60.7% in the outcome variable. The statistical tests show that the effect of the Purchasing power is significant and that the Green urban spaces have a significant and positive effect on domestic water consumption. The number of population with superior education has a negative effect on domestic water consumption. These results have relevant policy implications: firstly in municipalities with a considerable number of tourists and green spaces measure must be taken to adequate the consumptions according to these findings. Also, a critical issue must be the promotion of the sustainable water use literacy among the citizens.

**Table 1.** Regression coefficients

| Model | Non-standardized coefficients | | Standardized coefficients | T | Sig. |
|---|---|---|---|---|---|
| | B | Std. Error | Beta | | |
| (Constant) | 35,525 | 8,292 | | 4,284 | 0,000 |
| POP014 | -1,049 | 0,677 | -0,090 | -1,549 | 0,123 |
| AURB | 0,000 | 0,000 | 0,002 | 0,051 | 0,960 |
| ESP VERD | 0,205 | 0,049 | 0,203 | 4,206 | 0,000 |
| AREA200m | -0,004 | 0,001 | -0,248 | -3,228 | 0,001 |
| PCOMP | 0,499 | 0,107 | 0,358 | 4,667 | 0,000 |
| DOR | 0,000 | 0,000 | 0,607 | 9,050 | 0,000 |
| PENSUP | -,001 | 0,000 | -0,299 | -2,930 | 0,004 |

ADH- Water consumption (dependent variable); PCOMP - purchasing power; POP014 -Population age; AURB - Urban areas; ESP_VERD- Green urban spaces; DOR -Touristic population; PENSUP - number of inhabitants with superior education; AREA200m -size of the household

The model residuals Moran's provide evidence of spatial autocorrelation among residuals (0.229 for p<0.001), which implies the necessity of consideration of the spatial context of the data. This implies that a GWR will improve the results. The results of the GWR show that the Akaike's Information Criterion was 2403.650 and the $R^2$ and the adjusted $R^2$ were respectively 0,7 and 0,646 showing clear improvements in this approach over the OLS. The sum of the squared residuals in the model is 62552,5. For the residuals, the Moran's I is 0.0448 with a p value of 0.09, which leads us a substantial reduction of spatial autocorrelation. The local coefficients of the GWR will provided information of the influence of the factors in the spatial context and will be determinant for policy implementation.

## 4. Concluding remarks

This article tried to understand the joint influence of a set of urban, sociodemographic, and socioeconomic factors on domestic water consumption in continental Portugal. Therefore, these findings have a set of practical implications, namely for water management in urban areas. Considering the future reduction of available water resources because of climate change, measures to address water scarcity are needed, but the budgetary constraints of public administrations make it difficult to maintain supply-oriented water policies, based on engineering solutions and the construction of large water infrastructures. Considering results 2 lines of work are pointed out: 1) The creation of a typology of municipalities with common features regarding water consumption; 2) Testing nonlinear regression techniques for predicting domestic water consumption.

**References**

Fotheringham, A. S., Charlton, M. E., & Brunsdon, C. (1998). Geographically weighted regression: A natural evolution of the expansion method for spatial data analysis. Environment and planning A, 30(11), 1905–1927.

Mansour, S., Al Kindi, A., Al-Said, A., Al-Said, A., & Atkinson, P. (2021). Sociodemographic determinants of COVID-19 incidence rates in Oman: Geospatial modelling using multiscale geographically weighted regression (MGWR). Sustainable cities and society, 65, 102627.

Charlton, M., Fotheringham, S., & Brunsdon, C. (2009). Geographically weighted regression. White paper. National Centre for Geocomputation. National University of Ireland Maynooth.

# Stormwater Attenuation & Enhanced Infiltration System to Mitigate Flood & Drought Conditions: Part I – Urban Environment

Stephen D. THOMAS[1], George R. FRENCH[1], James WATSON[1], Joseph A. O'MEARA[2], Matthew P. DALE[2], Bruno CASAL[3]
stephen.thomas@ogi.co.uk

[1] OGI Groundwater Specialists, Durham, UK
[2] Groundwater Dynamics Ltd, Leamington Spa, UK
[3] Sondagens Casal Lda, Sintra, Portugal

ABSTRACT

This paper describes a stormwater attenuation & enhanced infiltration system, specifically designed for an Urban Environment, comprising the construction of attenuation trenches, perforated pipes with gravel surround, integrated with large numbers of drilled vertical infiltrators installed through the base of the trenches.

Combining the pressure head of the collected stormwater in the attenuation trenches, with the negative suction pressure within the unsaturated vadose zone, provides the differential pressure to force the water into the ground via these infiltrators. Furthermore, by installing vertical infiltrators, higher permeable ground strata are often encountered, particularly in anisotropic ground conditions where the horizontal permeability is much greater than the vertical permeability.

Stormwater Attenuation & Enhanced Infiltration Systems (SAEIS) have been used regularly in the UK for many years, both to mitigate flooding, and to provide recharge to groundwater resources. With groundwater resources similarly in decline in Portugal, together with more frequent flooding conditions occurring during intense rainfall, such collection and enhanced infiltration systems would also be most beneficial to the hydrogeology and weather conditions of Portugal.

Mathematical modelling is presented which simulates the water flow through the infiltrator system and into the unsaturated soil strata. Combining the storage capacity of the attenuation trenches with a large number of infiltrators, produces a highly efficient attenuation and infiltration system that not only mitigates the impact of flooding but has no requirement for ongoing energy consumption.

With stormwater collected, filtered, attenuated, and then infiltrated into the vadose zone, collected stormwater will eventually find its way down to the water table, and so mitigate drought conditions by supplementing the aquifer water resources.

Stormwater attenuation & enhanced infiltration systems (SAEIS) exemplify true low-carbon sustainability, and contribute to the United Nations Department of Economic and Social Affairs for Sustainable Development - Goal 6: *Ensure availability and sustainable management of water and sanitation for all*.
Beneath the attenuation trenches are a series of vertical infiltrators (Figures 2 & 3) which are specially designed plastic pipes which aid the infiltration of water into the soil. Prior to installing the attenuation trench, each infiltrator is installed by placing it inside a 90mm diameter drilled borehole. The top of each infiltrator is set normally 300mm below the base of the trench (Figure 3). The length of infiltrator normally varies between 3m and 12m, depending on the geology and volumes of water that need to be infiltrated, together with the ambient water table level.

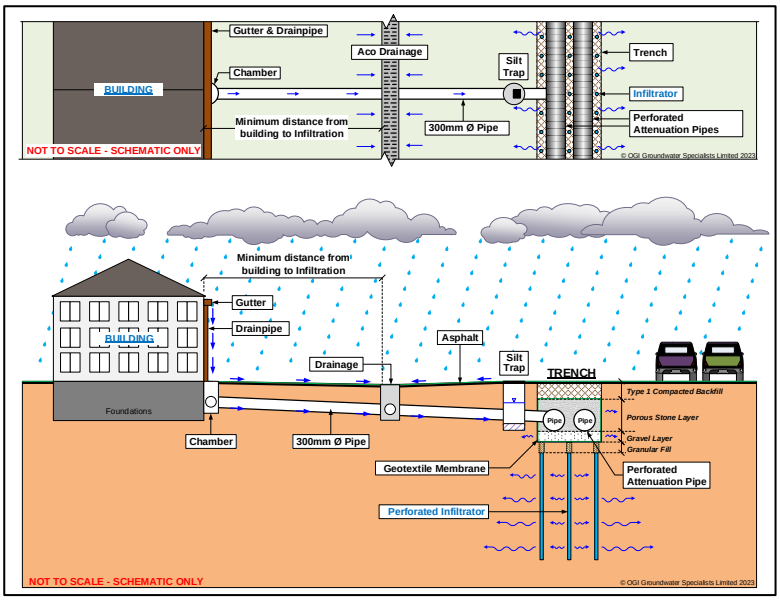



**Fig. 1.** Schematic of a Typical Attenuation and Enhanced Infiltration System.

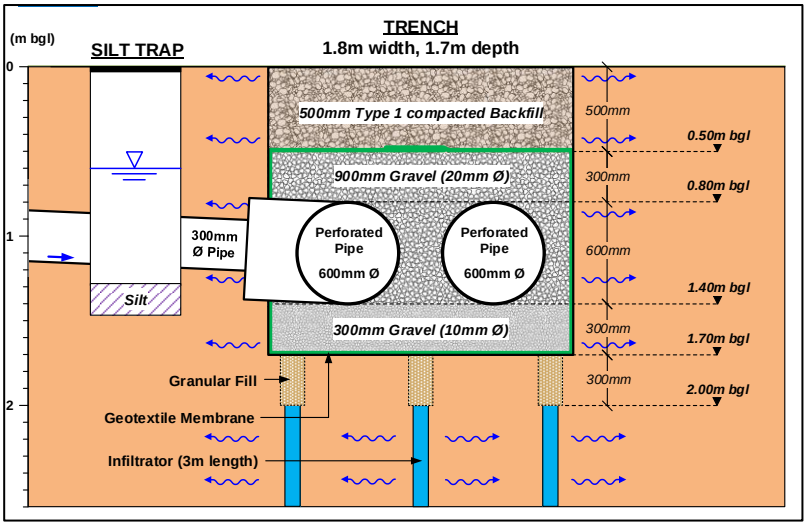



**Fig. 2.** Schematic of the Attenuation and Enhanced Infiltration system in section



**Fig. 3.** Construction of perforated pipes within attenuation trenches.

# From source to receptor: An integrated approach to analyse sediments and particle bound pollutants from urban wet weather discharges

Karen L. ROJAS-GÓMEZ [1,2], Jakob BENISCH[1], Björn HELM[1], Dietrich BORCHARDT[2], Peter KREBS[1]

[1] Technische Universität Dresden, Institute of Urban Water Management, Germany
karen.rojas@tu-dresden.de
jakob.benisch@tu-dresden.de
bjoern.helm@tu-dresden.de
peter.krebs@tu-dresden.de

[2] Helmholtz-Centre for Environmental Research, Department of Aquatic Ecosystem Analysis, Germany
dietrich.borchardt@ufz.de

ABSTRACT

## 1. Introduction

In urban areas, impervious surfaces accumulate contaminants and particulate matter. Fine particles carry particle bound pollutants like heavy metals and are highly mobile in the urban water system (Charlesworth & Lees, 1999). These fine particles are emitted from combined and separate sewer networks during storm events affecting the condition of the urban stream. Therefore, the concentration of fine suspended solids with a particle size smaller than 63 µm was introduced as a reference parameter for urban drainage impact assessment in Germany. In order to improve sediment management and the quality of the receiving water bodies, it is necessary to assess sediment sources, pathways and storage in urbanised catchments (Taylor & Owens, 2009). This study aimed at characterising the impacts of urban wet weather discharges (UWWDs) along a downstream urbanisation gradient in a small stream in Dresden, Germany. The export of fine sediments and the concentration of heavy metals in both suspended sediments and stream bed, was evaluated along the urban gradient. Including a comprehensive analysis of different sewersheds.

## 2. Methods

### *2.1. Study area and sampling campaign*

Our study area is a small catchment (Lockwitzbach, 84 km$^2$) located in Dresden, Germany. It has a main stream length of 29 km with a land use dominated by non-irrigated arable land (40%), pastures (21%) and urban areas (14%). The urbanised area is clustered towards downstream. In this study we focused on the last 7 km within the city of Dresden, where 9 combined sewer overflows (CSOs) and 19 storm water outlets are located. The urban catchment was subdivided into 9 sewersheds considering the characteristics of the urban drainage network.

Between March 2021 and August 2023, sediment samples were collected along the stream bed in 7 points, before and after heavy rainfall events. A total of 162 sediment samples were characterised considering 15 elements concentration (i.e., Al, As, B, Ba, Cd, Co, Cr, Cu, Fe, Li, Pb, Ni, P, Sr and Zn) of the fine sediment (<63µm) and coarse (63-630 µm) fraction, total solids and organic solids. Additionally, suspended sediment samples were taken upstream and downstream the urban area. In those two sampling points, high-resolution discharge and turbidity data were continuously monitored. The outlet of two sewer systems was monitored within the study period. Both outlets are equipped with online sensors for turbidity and flow rate as well as automatic sampling during rainfall events. Samples taken during rainfall events at the outlets of the two sewer systems were analysed for element concentration, fine fraction (<63 µm) and coarse fractions (>63 µm) of total and organic solids. Logarithmic transformed turbidity and suspended solids concentrations were related by linear regression. The regression equation was transferred to the high-resolution sensor readings for peak

concentration, mean event concentration and event load determination. This allowed to understand the dynamic transport mechanisms of fine sediments and relevant elements attached to particles in the urban stream, considering complex runoff and discharge processes.

## 3. Results and discussion

### *3.1. Export of fine particles and metals from sewer systems*

At the stormwater outlet, fine particles contributed 83.3 ± 1.1% of the total suspended sediments during storm events. Fine organic particles made up 32.1 ±1% and fine inorganic particles accounted for 67.9 ± 1%. In contrast, the fraction of coarse particles (>63 µm) was mostly composed by organics (67.4 ± 1.9%). Among the heavy metals, Zn and Cu concentration showed the stronger correlation with fine suspended solids ($R^2$= 0.98 and 0.97 respectively). Fine sediments and heavy metal export were calculated for each sewershed and areas with high loads were distinguished.

### *3.2. Impact of stormwater discharges on river bed and on surface water quality*

The urban discharges increased the element concentration in the fine sediment fraction along the first 6 km of the stream. This suggests an accumulation of contaminants towards the urban gradient. An increased concentration of contaminants associated to traffic/ vehicle emissions (e.g. Zinc in Fig. 1) shows the impact of stormwater discharges on the stream bed. The increased concentration of those contaminants after the urban discharges (i.e. see points 5.66 and 5.72 km in Fig. 1) are explained due to the intrusion of fine sediments. Those fine sediments and heavy metals are transported through runoff from the impervious urban surfaces and discharged into the river via CSOs (Schertzinger et al., 2018) or stormwater discharges.

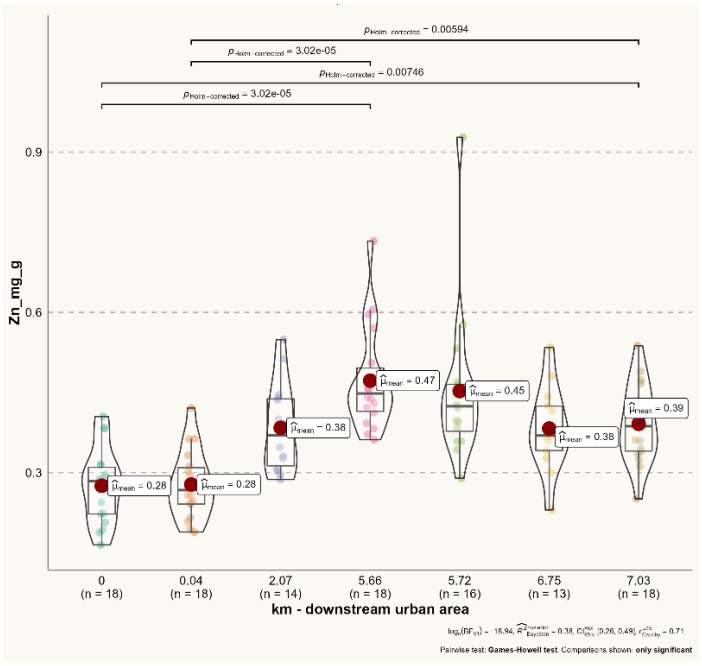



**Fig. 1.** Variation of Zinc concentration in the fine fraction (<63µm) of the sediment samples collected from the river bed along the urban stream. Only significant comparisons are shown using the Games-Howell pairwise test

## 4. Conclusions

Fine and inorganic sediments are prevalent in suspended solids emitted from urban wet weather discharges (i.e. stormwater outlets and CSOs). These sediments carry heavy metals that are likewise found in the stream bed of the receiving water body or in suspension. Our findings can help prioritising and locating possible strategies to improve river water and sediment quality.

**References**

Charlesworth, S. M., & Lees, J. A. (1999). Particulate-associated heavy metals in the urban environment: Their transport from source to deposit, Coventry, UK. Chemosphere, 39(5), 833–848. https://doi.org/10.1016/S0045-6535(99)00017-X

Schertzinger, G., Ruchter, N., Sures, B., (2018). Metal accumulation in sediments and amphipods downstream of combined sewer overflows. Sci. Total Environ. 616–617, 1199–1207.

Taylor, K. G., & Owens, P. N. (2009). Sediments in urban river basins: A review of sediment-contaminant dynamics in an environmental system conditioned by human activities. Journal of Soils and Sediments, 9(4), 281–303. https://doi.org/10.1007/s11368-009-0103-z

# Unlocking the Potential of Digital Twins in Water and Wastewater Systems: A Holistic Approach

Vincent MORAN[1], Mohsen BESHARAT[1], James BARTRAM[1], Helena M. RAMOS[2]

[1] school of Civil Engineering, University of Leeds, United Kingdom
cn19vm@leeds.ac.uk
m.besharat@leeds.ac.uk
j.k.bartram@leeds.ac.uk

[2] Department of Civil Engineering and Architecture, Instituto Superior Técnico, University of Lisbon, Portugal

helena.ramos@tecnico.ulisboa.pt

ABSTRACT

Digital Twins (DTs) are an innovative concept with vast potential for automating and optimising processes in the water and wastewater sectors. DTs enhance existing digitalisation and modelling methods by enabling seamless bidirectional data exchange between digital and physical assets. This capability offers greater adaptability and responsiveness than traditional modelling and simulation. This work presents a study on DT, focusing on monitoring transient flows in urban infrastructure, which includes a technical analysis of a water network in Madeira Island, Portugal. This investigation highlights the critical issue of underestimating transient conditions, leading to water loss and significant health and security risks. The study also explores DT's capacity to incorporate non-technical asset data including data related to management, decision-making, and other non-technical factors, enhancing understanding and management of complex systems. The final aim of presenting these findings and discussions is to achieve a holistic approach in smart systems.

## 1. Digital Twins Within the Water and Wastewater Industries

Technological systems like DTs are adopted across industries to enhance efficiency, gain commercial advantages, and align with environmental sustainability goals, often tied to the UN Sustainable Development Goals (SDGs). Academic and industrial interest in DT adoption is driven by Industry 4.0 technologies, including big data, analytics, cybersecurity, IoT, simulation, AR/VR, additive manufacturing, advanced robotics/AI, cloud computing, and system integration (Arup, 2019; Neto et al, 2020; Perno et al, 2022). In the water industry, digitalisation focuses on improving hydraulic and hydrological modelling, utilising remote sensor networks and machine learning for monitoring and prediction. While DTs aren't fully implemented, existing integration paves the way. Research into water distribution DTs enhances hydraulic modelling, SCADA platforms, and GIS for network management. Historically, data accuracy challenged water sector digitalisation, but improved data integration and modelling suggest feasible DT integration (Tomic et al, 2022). Key water sector DT benefits include operator training, emergency prediction, improved network planning, resource optimisation, and fault detection. Applications like leak detection, water quality monitoring, energy optimisation, and asset management will directly benefit from DT. Successful adoption requires accurate digital modelling, strong physical-digital connections, analytics, and system control (Conejos Fuertes et al, 2020; Rasheed et al, 2020).

To build on initial findings, expert interviews were conducted within the water and wastewater sectors to assess the current state of integrating technologies for DTs in water sector operations. Several barriers to DT integration emerged, including aging infrastructure, data limitations, real-time modelling challenges, and a prevalent short-term focus among clients and funders. Transient flow, a complex aspect that requires additional design time, was often underemphasised in industry operations, with systems primarily relying on steady hydraulic modelling. To evaluate the significance of capturing transient behaviour in intelligent pressure management systems, an analysis was conducted using a real water distribution system network in Madeira

Island, Portugal. Current industry practice, represented by steady hydraulic analysis in EPANET, was used to determine maximum pressures after gate valve closures under steady flow assumptions. This was contrasted with transient analysis of critical pipes using the Method of Characteristics (MoC) in MATLAB. Comparative results revealed that transient pressure increases after rapid valve closure were up to 13 times higher than those predicted under steady flow assumptions. Calculations based on these findings indicated that peak transient pressures exceeded allowable maximum levels, while peak steady pressures did not. The failure of steady hydraulic modelling to capture these rupture scenarios underscores the substantial risk associated with using automated or optimised pressure management systems without adequate monitoring of transient pressures. In this context, it can be concluded that for water distribution systems to manage pressure effectively and safely, they must adequately account for transient behaviour within their modelling capabilities. These findings provide a foundation for further research into methods for monitoring and controlling of adverse condition like what studied here.

## 2. Holistic Approach to Digital Twins: Incorporating Non-Technical Contexts

The potential for industry 4.0 technology such as DTs to streamline and optimise water sector operations is significant. Technical issues such as the availability of computational power and ensuring appropriate data transfer rates for real-time modelling are relevant when upscaling DTs to asset levels, however, the impact of non-technical factors related to DT integration within existing processes cannot be understated (Erkoyuncu et al., 2020). In particular, the focus on the impressive technological capabilities of DT systems has the potential to foster the pre-emptive assumption that this will directly drive DT adoption rates within the sector. To more appropriately consider the issues related to improving DT integration rates within the water and wastewater industries it is useful to consider similar technological trends within other sectors.

It can be noted that there is a significant overlap between DT systems and wider BIM processes. Within the broader built environment sector, BIM adoption has been heralded as appropriately addressing issues related to low productivity, inefficiency, and disconnection between stakeholders, whilst also encouraging increased digital fluency (Dixit et al., 2017). DT systems can largely be considered a direct extension of many of the capabilities associated with BIM processes which generally focus upon improved data-sharing, utilising 3D-4D modelling to streamline data visualisation, and creating shared digital platforms between stakeholders (Ullah et al., 2019). Facilitating software for BIM was first developed in the early 1980s, with most industry standard programs being developed in the early 2000s (Smith, 2014). However, despite near unanimous agreement on the benefits of BIM processes within the built environment, global BIM adoption rates remain low. Surveys have suggested that significant regions of the world are exhibiting extremely low uptake levels, whilst the degree of technological development for a country is not the primary predictor of adoption rates. Research has suggested that in most countries demonstrating impressive BIM integration levels, this can primarily be attributed to a collaborative effort between industry and government to encourage (and regarding specific aspects: mandate) integration of BIM within existing processes (Smith, 2014). Extending these trends towards DT adoption; it is likely that the rate at which any industry embraces DTs will depend on holistic variables beyond the scope of technological development and technical expertise.

**References**


Arup (2019) Digital Twin: Towards a Meaningful Framework, Arup, https://www.arup.com/perspectives/publications/research/section/digital-twin-towards-a-meaningful-framework.

Conejos Fuertes P, Martínez Alzamora F, Hervás Carot M, Alonso Compos JC (2020) Building and exploiting a digital twin for the management of drinking water distribution networks, Urban Water Journal, 17(8), pp.704-713.

Dixit S., Mandal SN., Sawhney A., Singh S (2017) Relationship between skill development and productivity in construction sector: a literature review, International Journal of Civil Engineering and Technology, 8(8), pp.649-665.

Erkoyuncu JA, del Amo IF, Ariansyah D., Bulka D., Roy R (2020) A design framework for adaptive digital twins, CIRP Annals, 69(1), pp.145-148.

Neto AA, Deschamps F, da Silva ER, Lima EP (2020) Digital twins in manufacturing: an assessment of drivers, enablers and barriers to implementation, Procedia Cirp, 93, pp.210-215.

Perno M, Hvam L, Haug A (2022) Implementation of digital twins in the process industry: a systematic literature review of enablers and barriers, Computers in Industry, 134, p.103558.

Rasheed A, San O, Kvamsdal T (2020) Digital twin: values, challenges and enablers from a modelling perspective, Ieee Access, 8, pp.21980-22012.

Smith P (2014) BIM Implementation – global strategies. Procedia Engineering, 85, pp.482-492.

Tomic S, Karmous-Edwards G, Kamoijala S (2022) Digital twins: case studies in water distribution management, Journal-American Water Works Association, 114(8), pp.44-56.

Ullah K., Lill I., Witt E (2019), An overview of BIM adoption in the construction industry: benefits and barriers In 10th Nordic Conference on Construction Economics and Organization, Emerald Publishing Ltd, pp.297-303.

8th IAHR EUROPE CONGRESS
LISBON - PORTUGAL
4-7 JUNE 2024

# Critical future demand scenarios for the robust design of water distribution networks

R. MAGINI[1], M.C. CUNHA[2], J. MARQUES[3], E. RIDOLFI[4]

[1,4] Sapienza, University of Rome, DICEA, Rome, Italy.
roberto.magini@uniroma1.it
elena.ridolfi@uniroma1.it

[2,3] University of Coimbra, CEMMPRE, Department of Civil Engineering, Coimbra, Portugal.
mccunha@dec.uc.pt
jmarques@dec.uc.pt

ABSTRACT

Water distribution networks (WDNs) are among the urban infrastructure systems that have the greatest impact on the quality of life and economy of our cities. These systems should be designed to function properly in the present, but also in the unpredictable future. In this regard, the demand for water represents the most uncertain factor due to the random behavior of users and the unknowns about the prospects for urban and socioeconomic development. We find ourselves in what might be termed the 'scenario uncertainty' context, which cannot be described using only information from available data, but requires hypothesizing plausible future scenarios, i.e. particular representations of how reality could behave. Therefore, the objective of this work is to create meaningful future demand scenarios using an entropy-based approach to identify the WDN nodes where changes in water demand will most influence the correct hydraulic operation of the network ('critical nodes'). This approach allows designing WDNs that can be more robust to future changes. Moreover, knowing the most sensitive areas of the WDN could also be a means of directing future urban development plans.

## 1. Entropy and uncertainty

According to information theory, entropy is a measure of the uncertainty associated with the occurrence of a specific event (Papoulis, 1991). The marginal entropy of a random variable (RV) X, with pdf $f_X(x)$, can be expressed as:

$$H(X) = -\int f_X(x) \ln[f_X(x)]dx \quad (1)$$

Similarly, if we consider a variable Y depending on N random variables **X**, i.e., $Y = \phi(\mathbf{X})$, where $\mathbf{X} = (X_1, X_2, \ldots X_N)$, the entropy of Y can be written as:

$$H(Y) = -\int f_Y(y) \ln[f_Y(Y)]dy \quad (2)$$

that represents the unconditional entropy, i.e., a measure of the uncertainty derived from all the N random variables, X. Mutual Information (MI), or Trans-information, quantifies the amount of common information provided by two or more random variables (Cover and Thomas 1991). Given the RVs X and Y, the MI can be interpreted as the reduction of the uncertainty of Y due to knowledge of $X_i$ and can be expressed as follows:

$$I(Y, X_i) = H(Y) - H(Y|X_i) \quad (3)$$

where $H(Y|X_i)$ is the entropy of Y conditioned by $X_i$.

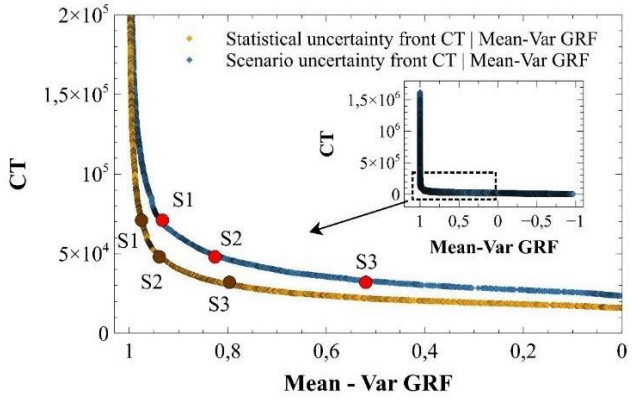
These concepts make it possible to identify the WDN nodes (critical nodes) where changes in water demand will most influence the correct hydraulic operation of the network. This is an important issue for describing uncertainty, which cannot be described only in statistical terms and exploiting information from available data.

Therefore, this approach is very useful to create meaningful future demand scenarios for representing 'scenario uncertainty' as defined by Walker et al., 2003.

## 2. Methods and Results

The proposed approach is applied to the Fossolo network studied by Bragalli et al. (2012) to define critical nodes. The computation of the Mutual Information of Δh (Y variable) conditioned by the water demand in the *ith* node (Xi variable) allows a list to be drawn up from the most critical nodes to the less critical nodes. This list shows that some of nodes located in the corners of the left and south border of the network are the most critical.

A multiobjective optimization model has therefore been developed, with two objectives: minimization of cost CT and maximization of mean-variance of the generalized resilience index GRF (see Cunha *et al.*, 2023 for further details). It integrates the information about critical nodes and manages scenario uncertainty (based on the entropy findings and worked out using the methods explained in Magini *et al.*, 2019) to find robust solutions (solutions that work well under future uncertain conditions, as defined by Mulvey et al., 1995). The multiobjective algorithm MOSA-GR (Cunha and Marques, 2020) has been applied to this end. The results depicted in the following figure show that solutions determined using scenario uncertainty analysis display a more robust beahavior (with regard to total pressure deficits, PD, and undelivared demand, UD) than that obtained by solutions with a similar cost but that just consider statistical uncertainty. In fact, if each solution is loaded with 18 scenarios (9 obtained under scenario uncertainty approach and 9 obtained just using statistical uncertainty) it can be seen that the scenario uncertainty approach performs better in that it presents lower pressure deficits (PDs) and and lower undelivered demand (UD).




| | CT (€) | Sum PD (m) | Sum UD (l/s) |
|---|---|---|---|
| S1 Scenario Uncertainty | 70022 | 0 | 0 |
| S1 Statistical Uncertainty | 70092 | 86 | 7 |
| S2 Scenario Uncertainty | 50124 | 19 | 0.2 |
| S2 Statistical Uncertainty | 50121 | 195 | 17.2 |
| S3 Scenario Uncertainty | 30017 | 757 | 9.4 |
| S3 Statistical Uncertainty | 30045 | 785 | 78.9 |

The entropy-based approach makes an important contribution to defining more robust solutions to tackle future uncertainty.

**References**


Bragalli, C, D'Ambrosio C, Lee J, Lodi A, Toth P (2012) On the optimal design of water distribution networks: A practical MINLP approach [Dataset]. Optimization and Engineering, 13, 219–246. https://doi.org/10.1007/s11081-011-9141-7

Cover TM, Thomas JA (2005) Elements of information theory (PDF). John Wiley & Sons, Ltd. pp. 13–55. ISBN 9780471748823

Cunha, M., Marques, J. (2020) A New Multiobjective Simulated Annealing Algorithm—MOSA-GR: Application to the Optimal Design of Water Distribution Networks. Water Resources. Research, 56(3).

Cunha, M. C., Magini, R., Marques, J. (2023) Multi-objective optimization models for the design of water distribution networks by exploring scenario-based approaches. Water Resources Research, 59, e2023WR034867. https://doi. org/10.1029/2023WR034867

Magini, R., Boniforti, M. A., Guercio, R. (2019) Generating scenarios of cross-correlated demands for modelling water distribution networks. Water, 11(3), 493. https://doi.org/10.3390/w11030493

Mulvey, J.M., Vanderbei, R.J, Zenios, S. (1995) Robust Optimization of Large-Scale Systems. Operational Research, 43(2), 264-281.

Papoulis A (1991) Probability, Random Variables and Stochastic Processes, 3rd Edn., McGraw-Hill, New York

Walker WE, Harremoes P, Rotmans J, van der Sluijs JP, van Asselt MBA, Janssen P,Krayer von Krauss MP (2003) Defining uncertainty: A conceptual basis for uncertainty management in model-based decision support. Integrated Assessment, 4(1), 5–17. https://doi. org/10.1076/iaij.4.1.5.16466

# Runoff coefficient of green roofs in Trondheim, Norway

Vitor SOUSA[1], José Pedro MATOS[2], Inês MEIRELES[3], Chiara BERTOLIN[4]

[1,2] CERI, IST – Universidade de Lisboa, Portugal
vitor.sousa@tecnico.ulisboa.pt
jose.matos@tecnico.ulisboa.pt

[3] RISCO, University of Aveiro, Portugal
imeireles@ua.pt

[4] NTNU, Norway
chiara.bertoloin@ntnu.no

ABSTRACT

Nature-based solutions are being increasingly adopted to improve urban spaces. Within these, green roofs are one of the most used because of their multiple benefits at both the building (e.g., sound and thermal performance; real estate valuation) and city (e.g., rainwater retention and detention; noise reduction; air quality improvement; heat island effect minimization) scales. The present communication assesses the hydrologic performance, namely in terms of runoff coefficient, of a pilot installation in Trondheim, Norway.

## 1. Introduction

Green roofs rainwater retention (and detention) has been and continues to be studied by researchers throughout the globe (e.g., see Zhen et al. 2021 literature review). However, rainwater retention results are either presented in some form of descriptive statistics (e.g., average and standard deviation; box-plots) or used to build models that are complex to implement and calibrate (in many cases, not even possible to replicate because neither the data or calibration parameters are disclosed). However, for many practical applications, such as simulating rainwater systems performance associated with green roofs, it would be useful to use other than a constant runoff coefficient, but it is not viable to build and calibrate complex models.

Under the scope of the KLIMA 2050 project (https://www.klima2050.no/hovringen-bluegreengray-roofs), a pilot installation was assembled at Høvringen wastewater treatment plant, consisting of three test areas with a total surface of 8x11 m equipped to measure the amount of water passing through the roof drain from each of the test areas. A meteorological station was also installed in the case study location and different roof covering solutions were tested, including a traditional flat roof, a blue roof (with expanded clay) and a green roof. Herein, only the data from the green roof is reported and the detailed description of the experimental setup can be found in Hamouz (2020).

## 2. Methods and results

The data reported herein covers the period between June 2018 and September 2021, totaling 996 days with monitored data. A precipitation event was defined as a period of consecutive days of precipitation with an antecedent dry period of at least 1 day, resulting in 127 events recorded in the time frame analyzed. Within these events, 43 did not generate runoff from the green roof, of which 31 occurred during periods of temperatures higher than 0°C. Regarding the events that generated runoff, 36 resulted in runoff coefficients higher than 1, which is explained by snowmelt and forced rainfall experiments taking place at the installation (experiments using irrigation to simulate rainfall). So, a total of 37 precipitation events produced runoff without being affected by snowmelt and/or forced rainfall experiments.

The data reported in Fig. 2 indicate that the hydrologic performance of the green roofs is not linear. To start with, a minimum amount of rainfall it is necessary to generate runoff. Analyzing the rainfall events that did not produce runoff, it is noticeable an increasing trend of the rainfall with the mean air temperature since the

previous rainfall event (Fig. 2 left). It is worthy to mention that the precipitation for the events without runoff has values lower than 1 mm. Since this assessment does not reflect necessarily the minimum rainfall to generate runoff, it was also evaluated the amount of rainfall accumulated before the start of the runoff (Fig. 2 right), confirming the trend observed in the events that did not produce runoff.

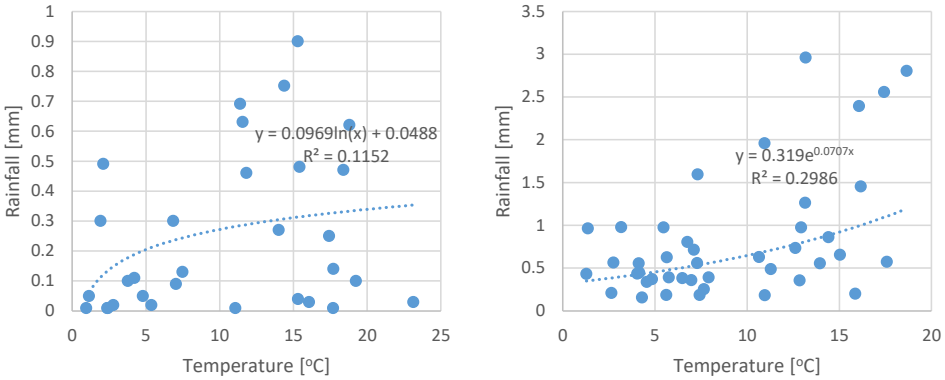



**Fig. 1.** Relation between the mean air temperature in the period preceding the event and the precipitation for the events without runoff (left) and the precipitation before runoff starts for the events with runoff (right)

Analyzing both graphs in Fig. 1, it is possible to conclude that minimum rainfall to generate runoff is bellow 1-1.5 mm for the majority of the events. For simplification, assuming a minimum value of 1.2 mm as the threshold for runoff generation to separate the rainfall events generating runoff, a clear pattern between rainfall and runoff for smaller events than such threshold cannot be detected (Fig. 3 left), contrarily to the larger events (Fig. 2 right).

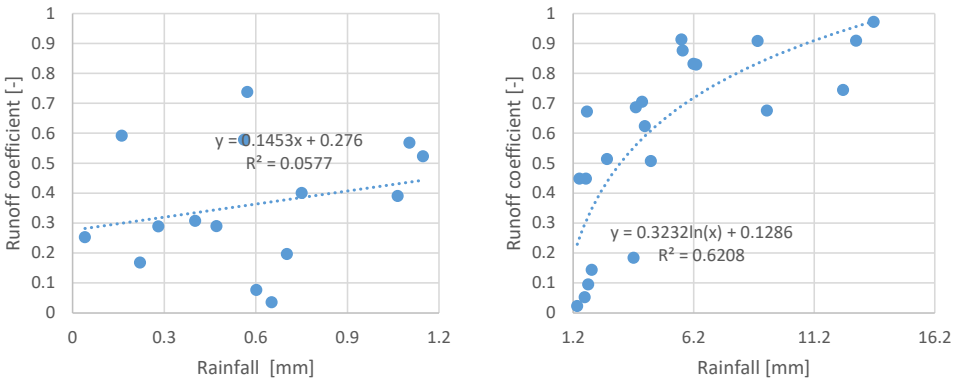



**Fig. 2.** Relation between the total rainfall of the event and the runoff coefficient for events under 1.2 mm (left) and above 1.2 mm (right)

## 3. Conclusions

The results confirm that there is a threshold bellow which there is no runoff, but lower than 2 mm frequently reported in the literature (e.g., Stovin et al. 2015). It also evidenced, as expected, that this threshold increases with the mean air temperature in the preceding dry period. Most importantly, there seems to be a good relation between the total rainfall amount of an event and the runoff coefficient above 1.2 mm. The model presented in Fig. 3 right can provide a dynamic estimate of the rainwater retention in green roofs that is more accurate than a constant value and easier to use than building physical models impossible to calibrate without experimental data.

**Acknowledgements**

This work was developed in the scope of the EEA grants project GREENER. VS, JPM and IM acknowledge the support of Fundação para a Ciência e a Tecnologia (FCT) through the funding of the research units CERIS (UIDB/04625/2020) and RISCO.

**References**

Hamouz V (2020) Retention and detention-based roofs for stormwater management in urban environments in cold climates. PhD. Thesis, Norwegian University of Science and Technology Faculty of Engineering Department of Civil and Environmental Engineering, Trondheim, Norway.

Stovin V, Poe S, De-Ville S, Berretta C (2015) The influence of substrate and vegetation configuration on green roof hydrological performance, Ecological Engineering, 85, 159–172. https://doi.org/10.1016/j.ecoleng.2015.09.076

Zheng X, Zou Y, Lounsbury AW, Wang C, Wang R (2021) Green roofs for stormwater runoff retention: a global quantitative synthesis of the performance, Resources Conservation and Recycling, 170, 105577 https://doi.org/10.1016/j. resconrec.2021.105577.

# Methodology for modelling rainwater harvesting with snow – Application to Trondheim, Norway

Vasco PASSANHA[1], Cristina Matos SILVA[2], Camillo BOSCO[3], Vitor SOUSA[2], Edvard SIVERTSEN[3]

[1] IST – Universidade de Lisboa, Portugal
vm.mpassanha@gmail.com

[2,4] CERIS, IST – Universidade de Lisboa, Portugal
cristina.matos.silva@tecnico.ulisboa.pt
vitor.sousa@tecnico.ulisboa.pt

[3,5] SINTEF Community, Norway
Camillo.Bosco@sintef.no
Edvard.Sivertsen@sintef.no

ABSTRACT

Rainwater harvesting is actively promoted in many regions of the world for various reasons. In drier regions, it is used as an alternative water source for non-potable uses. In wetter and/or more urbanized regions the contribution for reducing the amount of rainwater entering the stormwater networks is equally, if not more, relevant. The literature focuses mostly on modelling rainwater harvesting systems without snow, however precipitation in the form of snow will store water in the roofs, creating a discontinuity between precipitation and runoff that will impact the assessment of the rainwater harvesting systems performance. The present communication presents a methodology and the results of its application to a case study in Trondheim, Norway.

## 1. Introduction

In many regions of the world, precipitation occurs in the form of rain and snow depending on the season. This adds a new layer of complexity to the design of rainwater harvesting systems, since: i) the relation between the amount of water and snow depth is non-linear; and ii) the snow melt rate is dynamic. It is typical to consider a snow ratio of 10:1 (10 mm of snow entail 1 mm of water), but it varies significantly depending on the degree of packing of the snow. The snow melt rate is a function of the energy exchange with the surrounding environment (e.g., air, soil, roof), which depends on factors such as the air temperature, solar radiation, wind speed, relative humidity, rainfall amount and underlying surface temperature and conductivity.

Simplified methods have been developed and are frequently used since physical snowmelt models are computationally demanding and require data that is seldom available (Zhou et al. 2021). These simpler models can be grouped into empirical and hybrid. The empirical models are simple statistical relations between the amount of snow and the corresponding runoff generated. The hybrid models are based on combining variables known to influence the snowmelt rate (e.g., air temperature, wind speed, rainfall) with the snowmelt rate using recorded data to statistically find the underlying relation. These simplified methos entail the assumption of average constant snow ratio.

However, the simplified methods were developed for river flow and flood risk analysis, so they are based on data from large river basins and focused on the significant and fast snowmelt at the end of the cold season. As such, their applicability to slow and partial snowmelt during the warmer days of the cold season may be limited. However, rainwater harvesting systems simulation deal with small areas and the snowmelt during the warmer days of the cold season may be relevant for the performance assessment. Herein, a novel approach is proposed and applied to a case study in Trondheim where the average annual precipitation is 920 mm, 30% to 40% of which is snow. Snowfall events happen in their majority between December to March, registering its highest average values of 9 cm/day in February and lowest in December (1cm/day) (Failla, 2016).

## 2. Methods and results

The proposed method (Fig. 1), designated as naïve, requires data on the water content and snow depth. The method is based on the assumption that snowmelt only occurs when there is a decrease in the snow depth. So, a precipitation event during days with negative air temperature without affecting the snow depth increase the snow ratio.

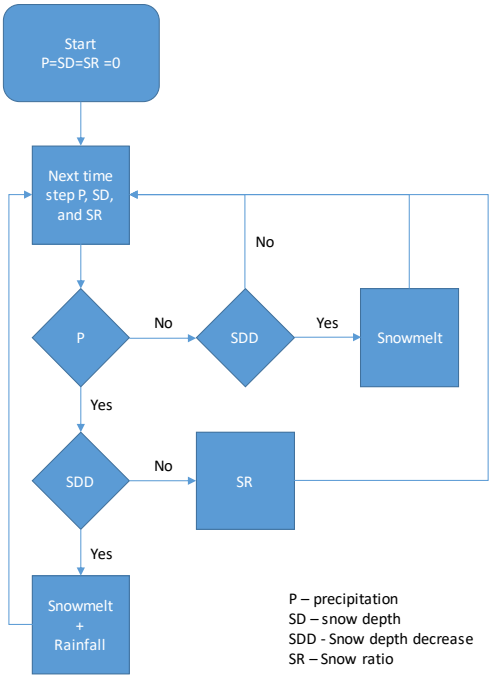



**Fig. 1.** Proposed methodology.

The method was applied to simulate a rainwater harvesting system to be installed in the ZEB Laboratory using the typical mass balance method. The non-potable water savings (Fig. 2) are identical using the proposed method and the degree-day method calibrated, but slightly higher than the estimates with the non-calibrated degree-day method using a degree-day coefficient of 2.74 mm/degree-day C, as recommend (USDA 2004).

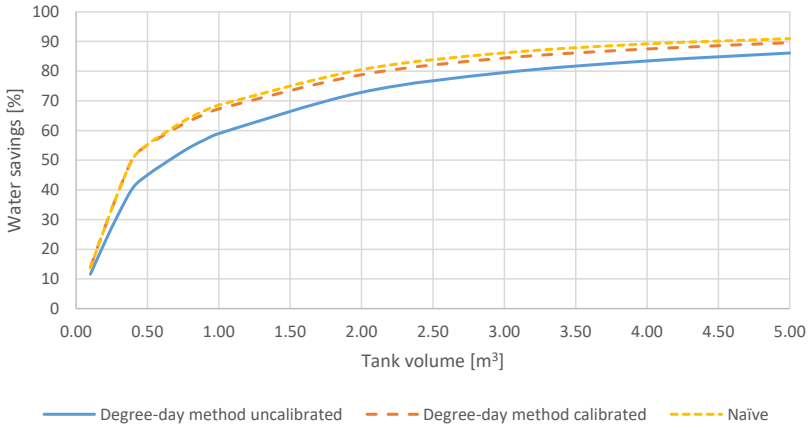



**Fig. 2.** Non-potable water savings

**Acknowledgements**

This work was developed in the scope of the EEA grants project EVIDENCE. CMS and VS acknowledge the support from CERIS Research Centre, Instituto Superior Técnico, Universidade de Lisboa. The study was also part of the Klima 2050 Project (grant no. 237859/030) which was financed by the Research Council of Norway and the project partners.

**References**

Zhou G, Cui M, Wan J, Zhang S (2021) A Review on Snowmelt Models: Progress and Prospect, Sustainability, 13(20), 11485. https://doi.org/10.3390/su132011485

Failla MC (2016) Snow and Ice on Photovoltaic Devices: Analysis of a Challenge and Proposals for Solutions [Master´s Dissertation]. Norwegian University of Science and Technology.

USDA (2004) NRCS National Engineering Handbook: PART 630 HYDROLOGY – Chapter 11: Snowmelt. United States Department of Agriculture, National Resources Conservation Service.

# Modelling the operation of wastewater pumping stations for wet-weather conditions

Luís Mesquita DAVID[1], António MARTINS[2]; Alexandre ATAÍDE[3]; Osvaldo SILVA[4]; Anabela OLIVEIRA[5]

[1,5] Laboratório Nacional de Engenharia Civil, Portugal
ldavid@lnec.pt
aoliveira@lnec.pt
[2,3,4] Águas do Algarve S.A., Portugal
antonio.m.martins@adp.pt
e.almeida@adp.pt
osvaldo.silva@adp.pt

ABSTRACT

## 1. Introduction

An intelligent real-time decision support system was developed in the SINERGEA project, aiming at the management of flooding and bathing water contamination events, and the efficient use of energy (David et al, 2022). This system was demonstrated at the city of Albufeira, Portugal, and its coastal neighbourhood.

Coastal wastewater systems often require multiple pumping stations (PS) along the coast, each with its own combined or sanitary sewer overflow (CSO or SSO). For wet-weather, increased inflows to pumping stations and wastewater treatment plants (WWTP) can lead to both significant increases in energy consumption and the discharge of contaminated water into the receiving bodies when WWTP capacity is exceeded. These flow increases occur not only in the combined sewer systems, but also in separate wastewater systems, due to water infiltration into the sewers, the rainfall-derived infiltration and inflow (RDII) component, and illicit connections between stormwater and sewage systems. Controlling rainfall-derived inflows into wastewater systems is a difficult challenge that has received increasing attention (Nasrin et al., 2017).

In most pumping stations, the pumped flow rates are monitored using electromagnetic sensors installed in the pumping pipes. These measurements tend to present much lower errors than measurements of free surface flow inside sewers. However, there are few pumping stations where the flows discharged to the receiving bodies are monitored, generally limited to a few cases of large facilities or particularly critical discharge sites.

Therefore, to model both the energy consumed in pumping stations and the CSO and SSO discharges, it is necessary to model the stormwater inflows to the pumping stations. This paper describes the methodology used for this purpose.

## 2. Modelling of stormwater inflows to pumping stations

To model stormwater inflows to pumping stations, simplified aggregate models calibrated with the flow rates measured in the pumping pipes were used. The objective was to calibrate these models using the well-known SWMM model. However, to obtain a first order of magnitude of the parameters, a time-area curve model and an automatic calibration procedure were initially used to calibrate the following three parameters: impervious area of the contributing catchment, the catchment's concentration time and the maximum flow rate that can be conveyed to the PS (without being discharged). The maximum flow rate that can be conveyed to the PS may not correspond exactly to the maximum capacity of the pumps operating simultaneously, as an upstream weir can limit the influent flow rate.

Based on the previous results, the parameters of the SWMM model were calibrated, which in the SINERGEA project is also used to model energy consumption. In this new calibration, the catchment concentration time is

replaced by the catchment slope and/or width and the difference in modelling methods may lead to the need for some readjustment of the catchment area.

## 3. Demonstration case results

The SINERGEA system was demonstrated on the city of Albufeira, Portugal, and its coastal neighbourhood, where the separate stormwater network, the sanitary interceptor sewer system, and coastal bathing waters were modelled in detail (David et al, 2022). The sanitary interceptor sewer system serves several coastal urban-tourist developments and has ten pumping stations, two submarine outfalls and a WWTP.

Existing monitoring data made it possible to calibrate flow rates in six of the ten pumping stations. The models were calibrated for a succession of rainfall events from late December 2021 and were verified for events occurring in March and November 2022. Figure 1 shows the results of calibration and a validation event for a PS. The upper graphs show the evolution of rainfall height and the red and green lines in the lower graphs compare the accumulated values of measured pumped flows and modelled pumped flows. It also shows the modelled values for the base flow (blue dotted line), the flow upstream of the SSO structure (brown dashed line), and the SSO discharge (black line).

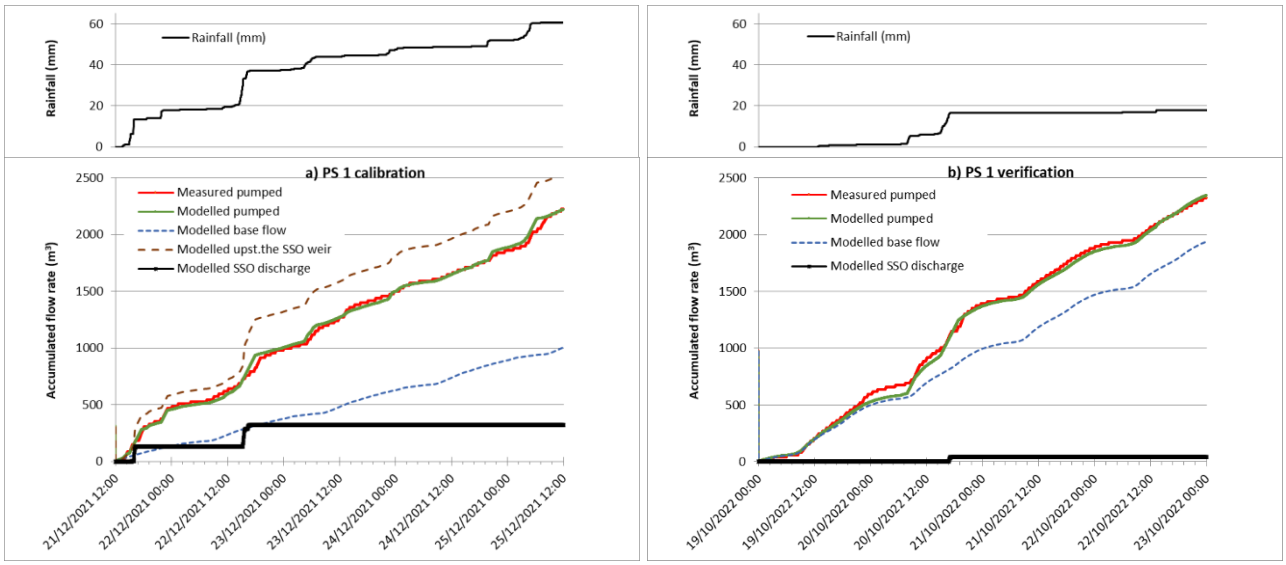



**Fig. 1.** Calibration (a) and verification (b) of the flow rates pumped at a pumping station and estimation of the SSO discharges.

## 4. Conclusions

The methodology presented herein was shown to be robust for estimating the flow rates pumped during rainy periods, allowing us to model energy consumption and better understand the functioning of the system, particularly with regard to undue flows. The uncertainty in estimating SSO discharges is greater, but it may represent a first approach to prioritize measures and to respond to the significant increase in monitoring requirements for wet-weather discharges required in the current proposed Revision of the Urban Wastewater Treatment Directive (EU, 2022)

The Algarve region where Albufeira is located records little rainfall and the demonstration case coincided with a period of severe drought. However, the small rainfall events that served to calibrate and validate the model are those that offer more management possibilities in the pursuit of two opposing objectives: the promotion of energy efficiency and the reduction of discharges to protect bathing waters.

**Acknowledgements**

This work was co-funded by the European Regional Development Fund (FEDER), under programs POR Lisboa2020 and CrescAlgarve2020, through Project SINERGEA (ANI 33595).

**References**

David et al. (2022). SINERGEA - Real-time forecasting system for managing floods, bathing water quality and wastewater energy consumption. 7th IAHR Europe Congress.

EU (2022). Proposal for a revised Urban Wastewater Treatment Directive, https://environment.ec.europa.eu/system/files/2022-10/Proposal%20for%20a%20Directive%20concerning%20urban%20wastewater%20treatment%20%28recast%29.pdf

Nasrin T, Sharma AK, Muttil N. Impact of Short Duration Intense Rainfall Events on Sanitary Sewer Network Performance. Water. 2017; 9(3):225. https://doi.org/10.3390/w9030225

# Implementation of a Real-Time Decision Model for the Reduction of Pollutant Loads Discharge in Combined Sewer Overflows. Study Case: Madrid

Antonio LASTRA[1], Alejandro CARRASCO[2], Mónica ORTEGA[3], Jaime BOTELLO[4], David SUNYER[5], Ángel VILLANUEVA[6]

[1] Head of the Development Innovation Area. Canal de Isabel II. Madrid SPAIN.
alastra@canal.madrid

[2,3,4] Development Innovation Area. Canal de Isabel II. Madrid. SPAIN.
acarrasco@canal.madrid [2] mortega@canal.madrid [3] jbotello@canal.madrid [4]

[5,6] Area of Resilience and Climate Change. Aquatec S.L. Barcelona. SPAIN.
david.sunyer@aquatec.es [5] angel.villanueva@veolia.com [6]

ABSTRACT

Canal de Isabel II, the company responsible for the management of the urban water cycle in the Community of Madrid, is taking the role of associated beneficiary in the European Project LIFE RUBIES. Within this collaboration, a real-time wastewater quality control decision taking model is being deployed and tested for the operation of part of its sanitation facilities (two stormwater tanks with an overall capacity of 600.000 $m^3$, two Waste Water Treatment Plants and the corresponding sewage network). Concerns about environmental health of water bodies have spotlighted the harmful effect in surface waters caused by combined sewer overflows (CSO) during rain episodes. Canal de Isabel II, being sensitive to this issue, has keen interest in evaluating the efficiency of this alternative management criteria, based on a sewage quality perspective.

## 1. Introduction

The Madrid basin has an area of more than 600 $km^2$ and a population of 6 million inhabitants. The mostly combined sewage network has about 16,000 km of sewers. Around 90% of this catchment area discharges into two main interceptors which run parallel to the Manzanares River on both riverbanks, taking the name of the Manzanares System. Despite de existence of several Storm Water Tanks with an overall storage capacity of 1.2 $hm^3$ and the possibility of inteconnecting both riverbanks during wet weather periods, the urban drainage system capacity is often exceeded, producing several CSO discharges into the Manzanares river.

It is expected that sewage discharge pollution and urban flooding will be more frequent due to climate change effects. At the same time, public awareness about the need to preserve the environment is arising. Thus, legislation is becoming more restrictive in what concerns to the need to improve the receiving bodies ecological status. EU is now revising the Urban Wastewater Treatment Directive and Spain has recently approved new legislation as a step forward for the transposition of the referred European Directive of Wastewater Treatment.

In consonance with previous regulation, the design of urban drainage infrastructure in the Manzanares System is based on the dilution concept. The system is designed to overflow occasionally if the capacity is exceeded, when the relation between sewage and rainfall water flow is below 1:17. However, this criterion neglects the fact that, in an urban basin, runoff drags an important quantity of pollutants that increases the pollutograph peaks in comparison with dry weather periods (Puertas et al, 2018). This scenario is specially challenging for Canal de Isabel II operation technicians, who are compelled to demonstrate that their performance during rain episodes is sufficiently safe in what regards to the receiving bodies ecological status. Under this scope, Canal has undertaken the role as Beneficiary in the European LIFE Program, LIFE RUBIES project (https://webgate.ec.europa.eu/life/publicWebsite/project/details/5685). The final stretch of the Manzanares System will be the pilot site for the implementation of a Real-time Control (RTC) solution which will enable to develop an integrated management protocol for the coordination of the operation of all facilities involved.

## 2. Methodology

The project outreach can be divided into four main issues: characterization of pollution fluxes in sewerages, continuous monitoring of the receiving water body quality, implementation of a short-term rainfall prediction model based on radar data and deployment of the real-time model for decision-making.

### *2.1. Sewage characterization*

Turbidity sensors are being installed in the sewage network for continuous monitoring of wastewater flow and urban runoff concentrations of pollutants, based on the existing positive correlations between turbidity and non-soluble contaminants. This data will be an input for the decision model. Besides, Canal de Isabel II has accomplished in previous studies thorough knowledge about pollutants evolution both in DWF and WWF.

### *2.2. River quality monitoring*

Control points have been defined upstream and downstream the stretch of the Manzanares River located within the pilot area. By means of continuous monitoring of classical parameters (organic matter, DO, temperature, EC, ammonium, nitrates, pH, turbidity/SS) it will be possible to characterize the effects of CSO discharges as well as the beneficial outcomes derived from a quality orientated management of the sewer system.

### *2.3. Rainfall prediction*

Long- and short-term rainfall forecasts will be a key input variable for the model simulator to assess about the best system operation and configuration. In this sense, Canal de Isabel owns a real time monitoring system of rainfall radar data from which short-term precipitation patterns are obtained for a time prediction of 4 hours. Both radar data and predictions will be enhanced so as to provide nowcasting information (10 minutes lapse).

### *2.4. Real time control model*

The model relies on a software implementation (AQUADVANCED® URBAN DRAINAGE (AQDV), developed by Suez Group) which provides real time monitoring and control of the sewerage network sensors and actuators in connection with Canal de Isabel II Central SCADA. Furthermore, a Model Predictive Control (MPC) solution will be integrated in AQDV. This model is linked to an optimizer program that searches for best solution, i.e. the operation procedure of the drainage network and associated infrastructure for which the negative effect of an eventual CSO in receiving water bodies is minimized. Therefore, the criterion is to reduce the pollutant load discharged rather than to minimize the total volume of CSO (Congcong et al. 2021). The model operates in real-time so simulations are run in a very short time lapse. To be able to provide all simulations required in the time scope, hydraulic and quality equations are linearized.

## 3. Results and Conclusion

Under the scope of the European LIFE RUBIES project, Canal de Isabel II is testing the performance of a Model Predictive Control tool for the operation of part of its drainage network and sanitary system. Its main objective is to minimize the effect on water receiving bodies caused by CSO discharges. Prior to the implementation of this tool, CSO Sewage pollutants' parameters have been identified both for WWF and DWF (Lastra et al. 2018). Results evidence that, in comparison with dry weather conditions, rainfall event pollutogram peaks reach up higher concentrations, due to resuspension which takes place in sewers plus the pollution which is mobilised from the surface catchment areas. In water stored in tanks, it is evidenced that pollutant concentrations are lower than that of the water circulating through the sewers, consequence of the settling effect of tanks. Removal rates are around 80% for contaminants associated with the non-soluble fraction (solids, BOD, COD) and around 50-60% for dissolved contaminants (nutrients, for example).

Implementation strategy of the real time control model, as well as monitoring of the river and sewerage system is ongoing. By the date of the conference, the authors pursue to present preliminary results that will allow evaluating the efficiency of this decision-making tool.

**References**

Puertas Agudo, J., Suárez López, J., & Anta Álvarez, J. (n.d.). *Gestión de las Aguas Pluviales. Implicaciones en el diseño de los sistemas de saneamiento y drenaje urbano*. España: CEDEX. ISBN:978-84-7790-475-5

Congcong S., Romero L., Joseph-Duran B., Meseguer J., Guasch Palma R., Martinez-Puentes M., Puig V. and G. Cembrano (2022) *Control-oriented quality modelling approach of sewer networks*. Journal of Environment Management, 294, 113031. ISSN 0301-4797. (DOI: https://doi.org/10.1016/j.jenvman.2021.113031)

Lastra, A., Suárez, J., Puertas, J., Falcó, X., Ortega, M., & Pinilla, A. (2018) *Development of a Smart System for the Operation of a Complex Sanitation System*. UDM 2018, Palermo.

# Water grid: Is electrical energy recovery possible? From the Water Supply Network? From the Water Distribution Network?

François NUC[1], Patrick HENDRICK[2]

[1] Université Libre de Bruxelles, Brussels, Belgium
francois.nuc@ulb.be

ABSTRACT

In the FlexWatter project, a research funded by the FPS Economy of Belgium (Federal level) and undertaken by some EERA Joint Program HydroPower active members, the research question is: "Could drinkable water network be a solution for electricity flexibility for the TSO or the DSO? To answer this question, several Belgian universities and the water DSO for the Brussels-Capital Region (BCR), called Vivaqua, gather their efforts to set up a case study based on the BCR water supply & water distribution networks (WSDN).
With recorded data from 2019 till 2022 (during about 4 complete years) in terms of water flow, water pressure, electricity consumption and climate data, a first picture has been drawn to better understand the topology of the BCR WSDN, based on the schematic depicted in Figure 1.

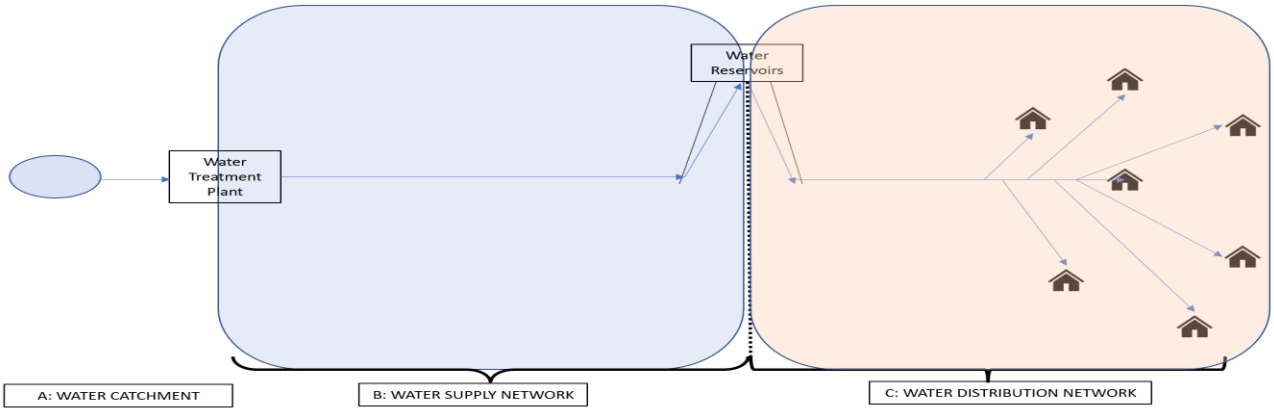



**Fig. 1:** Schematic of Water Supply & Water Distribution Networks

Numerous research projects have been done on WSDN to highlight the strategies used by water management companies such as: (i) multiple objectives optimization problems[1], (ii) pressure management (PMA)[2], (iii) district meters areas (DMA)[3] or (iv) energy recovery[4]. Those studies focused either on water supply network (WSN) or on water distribution network (WDN). In this FlexWatter study, a global overview for electrical energy recovery from the BCR water grid has been done including WSN & WDN, as shown in Figure 2. Based on this know-how, we ask the question, could energy recovery be carried out in the same way for WSN & WDN?

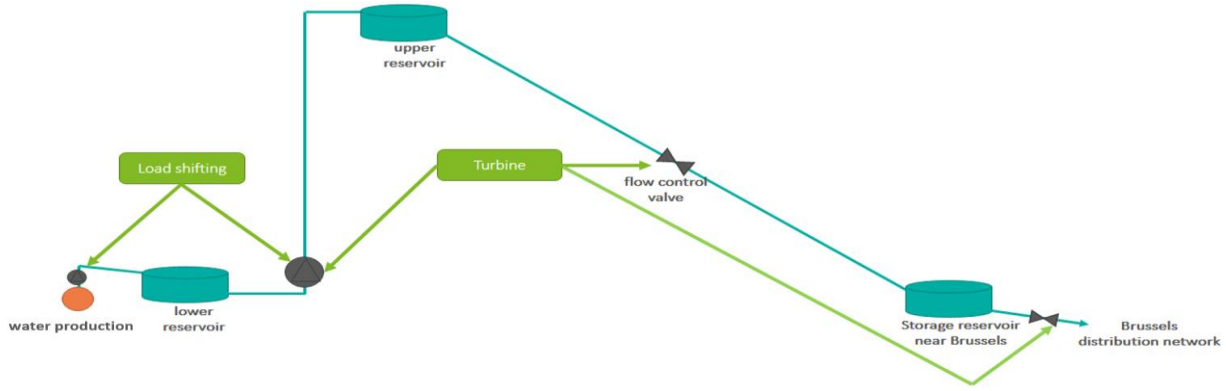



**Fig. 2**: Schematic of energy recovery possibilities on Brussels (BCR) WSDN

To carry out its mission, Vivaqua has meshed its water network with 4 main supply lines starting at respectively 42km, 55km, 65km and 91km away from Brussels. Although called a flat country, Belgium's topography induces that the 4 supply lines lay at different heights. So, in terms of water, those 4 lines are set at different

pressure levels. The WSDN includes numerous sub-stations with valves, reservoirs, and pumps. Some of the valves in the network have no other function that to reduce inlet pressure to a set value at the outlet. In other words, a differential pressure exists and could be available for another usage.
Among the many questions related to WSDN, the one we ask first is: *"Is this excess in pressure (Δ P) valuable as electrical energy recovery?*

$$\boldsymbol{P_{elec} = (P_{up} - P_{down}) * Q\rho g\mu} \quad \textbf{(1)}$$

where $\boldsymbol{P_{elec}}$ [kW] stands for electrical power, $\boldsymbol{P_{up}P_{down}}$ [m] of water column stand for water pressure (or head) upstream and downstream, $\boldsymbol{Q}$ [$m^3s^{-1}$] stands for water flow, $\boldsymbol{\rho}$ [kg/$m^3$] stands for water density, **g** stands for gravity field intensity and $\boldsymbol{\mu}$ stands for electrical efficiency.
We have therefore selected 4 substations of the WSDN where energy recovery could be studied: 2 of the stations belong to the WSN, and the 2 other stations belong to the WDN. The electricity power curves clearly show that the 2 networks behave in a quite different manner, as shown in Figures 3 & 4.

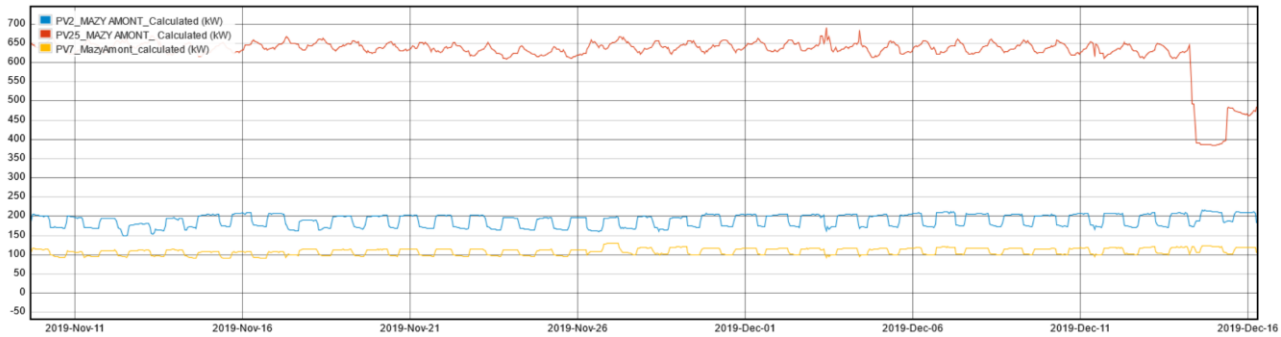



**Fig. 3**: Energy recovery from 1 station of the Water Supply Network

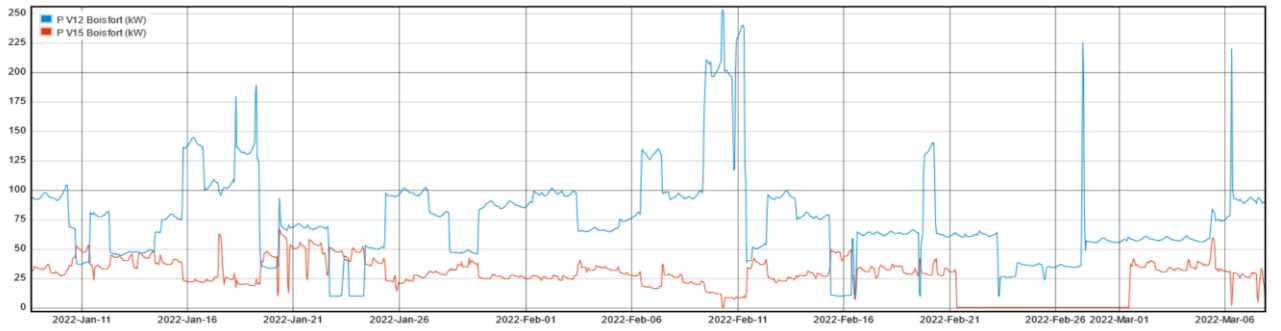



**Fig. 4:** Energy recovery from 1 station of the Water Distribution Network

On the WSN, the power curves are quite regular and stable. It would be quite simple to select machines (turbines and/or pumps) that would develop maximum power for the given conditions. On the WDN, the power curves are totally irregular. This makes it more difficult to select the right machines to develop maximum power for the given conditions.
The questions asked and discussed are then:
- Why is there such a difference in behavior between the 2 water networks, i.e. WSN and WDN?
- Which technologies should be used to enable energy recovery at WSN and / or at WDN level?
This will be analyzed and explained in the final paper.

**References**

(1) Ruiz-Vanoye, J.Barrera-Cámara, R. Díaz-Parra, O. Fuentes-Penna, A. Pérez Ortega, J. Bernabe Loranca, B. Canepa Saenz, A. Santiago-Pérez, J. del C. Surveying the Optimization Problems of Water Distribution Networks. Pol. J. Environ. Stud. 2018, 27 (4), 1425–1432. https://doi.org/10.15244/pjoes/76502.
(2) Monsef, H.; Naghashzadegan, M.; Farmani, R.; Jamali, A. Pressure Management in WaterDistribution Systems in Order to Reduce Energy Consumption and Background Leakage. J. Water Supply Res. Technol. - Aqua 2018, 67 (4), 397–403. https://doi.org/10.2166/aqua.2018.002
(3) Kowalska, B.; Suchorab, P.; Kowalski, D. Division of District Metered Areas (DMAs) in a Part of Water Supply Network Using WaterGEMS (Bentley) Software: A Case Study. Appl. Water Sci. 2022, 12 (7), 166. https://doi.org/10.1007/s13201-022-01688-2
(4) Hamlehdar, M.; Yousefi, H.; Noorollahi, Y.; Mohammadi, M. Energy Recovery from Water Distribution Networks Using Micro Hydropower: A Case Study in Iran. *Energy* **2022**, *252*, 124024. https://doi.org/10.1016/j.energy.2022.124024.

# Design and experimental validation of a Phononic crystal-based solution for improved noise and vibration behavior of ram pumps

Saber NASRAOUI[1], David FERRAS[1], Capucine DUPONT [1]

[1]IHE Delft Institute for Water Education, Delft, the Netherlands,

s.nasraoui@un-ihe.org , d.ferras@un-ihe.org, c.dupont@un-ihe.org

ABSTRACT

Hydraulic ram pumps are an environmentally friendly water pumping devices with no fuel and no electricity consumption. They operate on the principle of water hammer, and they have several important advantages and applications. However, their effectiveness is largely affected by noise and vibration of the drive pipe. This paper explores the concept of Phononic Crystals (PCs) in ram pumps, presenting a novel approach to enhancing their performance and extending their lifespan. PCs are artificially engineered materials that show distinct Bragg band gap characteristics, wherein waves and vibrations of particular frequencies cannot pass through. Along these lines, the drive pipe is designed to have a band gap in the vicinity of a dominant vibration modes, enabling vibration control strategies. In order to properly characterize the vibrational behavior of the drive pipe an experimental implementation of a hydraulic ram was conducted. Subsequently, a periodic drive pipe in the form of alternating materials of pipes is engineered. Using the Bloch-Floquet approach, the frequency range of the stopband zone created by the phononic drive pipe solution is predicted.

## 1. Experimental implementation of a ram pump

An in-house made ram pump with a diameter of 40 mm has been implemented in the IHE Delft laboratory. The experimental setup comprises a supply tank with a height of 3.3 m, a 40 mm diameter drive pipe with a length of 13.1 m, and a delivery pipe raised to a height of 6.5 m (see Fig.1).

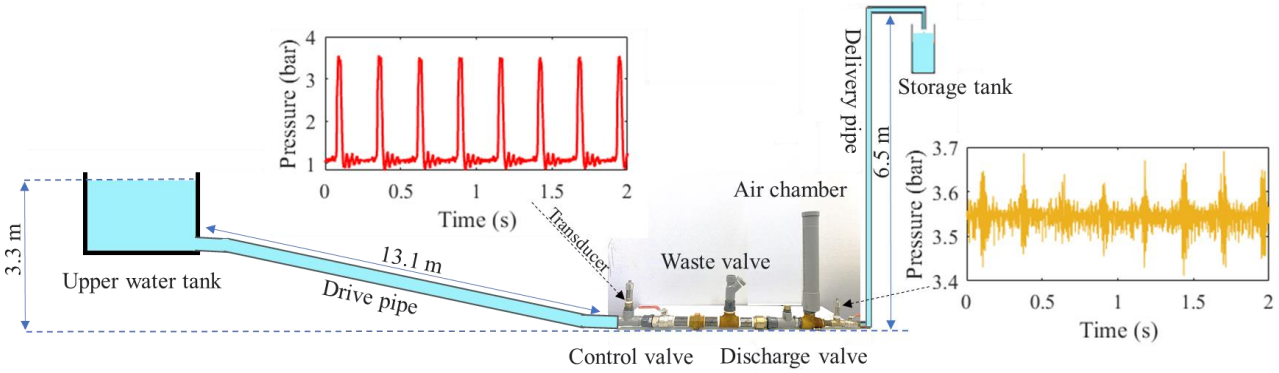



**Fig. 1.** Ram pump test rig configuration used to evaluate performance, efficiency, and to assess vibrational modes.

Multiple experimental tests have been conducted, systematically altering the delivery flow and measuring the corresponding delivery pressure and for each trial. The data collected from these experiments are used to plot characteristic curves for the ram pump. Fig.2 illustrates the characteristic curve, delivery pressure, and efficiency across a range of delivery flows, from the maximum, i.e. when the valve at the ram's outlet is fully open, to the minimum, i.e. when the valve is fully closed, respectively at q = 0.042 l/s and q = 0 L/s, respectively. When the pressure reaches 2.54 bar, the delivery flow rate and efficiency drop to zero, becoming the operational limit beyond which, the pump cannot deliver water. In contrast, as the delivery flow rate increases, efficiency rises, reaching its peak at 65.2% of the maximum delivery flow.

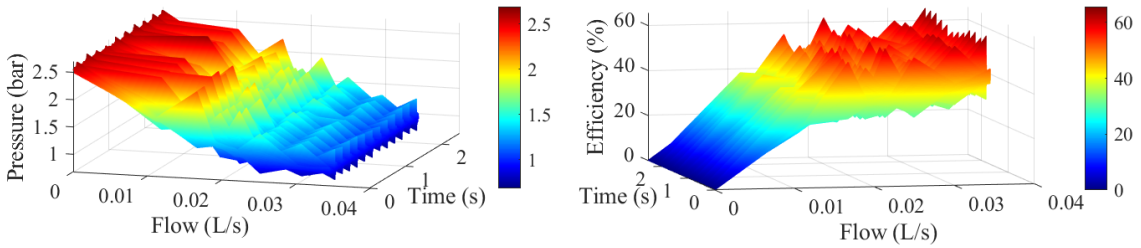



**Fig. 2.** 3D plots of the experimental pump characteristic and efficiency curves.

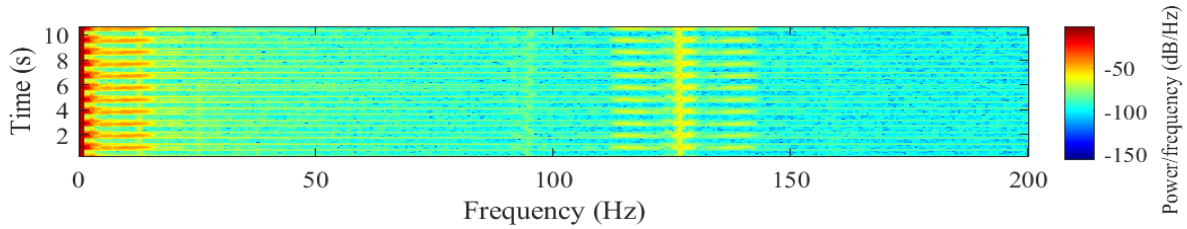



**Fig. 3.** Spectrogram of the pressure signal in the drive pipe.

During the experimental tests, it's worth noting that reports of vibrations and shaking in the drive pipe were observed. These vibrations lead to energy loss, consequently affecting the efficiency of the ram pump (Galantino et al., 2016). To distinguish between the operating frequency, which is related to the cyclic pumping action, and the vibration frequency, we plotted a spectrogram of the pressure in the drive pipe (see Fig. 3). As shown in Fig. 3, in addition to the pump's operating modes (below 30 Hz, corresponding to the maximum frequency generated by water hammer caused by the waste valve closure), there is a noticeable peak in the range of 110 to 140 Hz. This frequency range is related to the pips structure vibration modes and is therefore the design focus for a phononic crystal-based drive pipe.

## 2. Phononic crystal-based drive pipe

In this section our aim is to engineer a drive pipe that possesses a band gap, effectively blocking the passage of vibrations within the frequencies range 110 to 140 Hz. To this end, we delve into the concept of a periodic drive design, where the pipe walls are constructed using alternating materials denoted as A (with a length $l_a$) and B (with a length of $l_b$), see Fig.4.

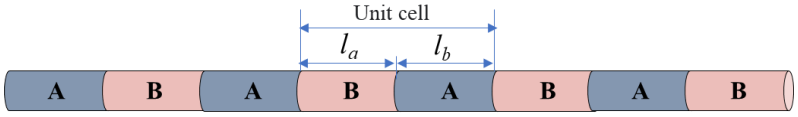



**Fig. 4.** A sketch of the water-filled periodic drive pipe structure.

The Bloch-Floquet theory (Collet et al.,2011) is employed to establish a dispersion relation representing wave motion in the considered pipe. The derived dispersion relation is then evaluated, and the results indicate that the desired band gap can be achieved for a 40 mm diameter pipe structure with cooper as the material of pipe A and PVC as the material of pipe B (see Fig. 5).

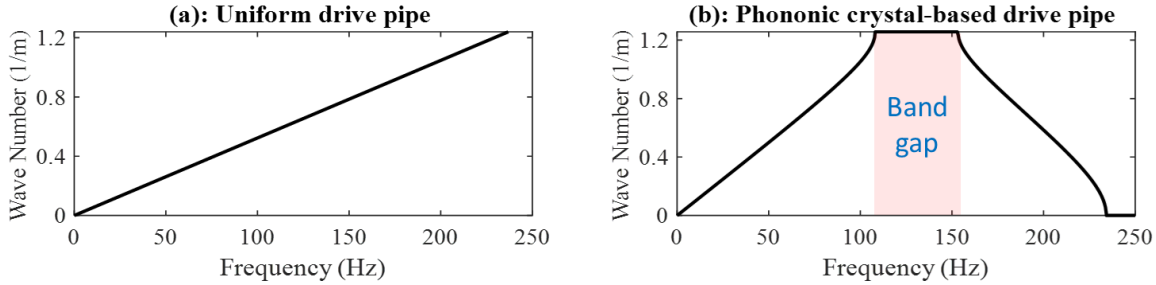



**Fig. 5.** Dispersion curve for the case of drive pipe without (a) and with (b) periodic structure (cooper/PVC) where $l_a$ =1m and $l_b$=1.5 m.

**References**

Galantino, C., Paternain Martinez, J., and Oiwa, L. (2016). Ram Pump, Fall 2016,pp 9.

M. Collet, M. Ouisse, M. Ruzzene and M. Ichchou (2011), Floquet–Bloch decomposition for the computation of dispersion of two-dimensional periodic, damped mechanical systems, International Journal of Solids and Structures 48, 2837–2848.

# Green Roofs Hydrological Performance and Contribution to Urban Rainwater Management

Ana Mafalda MENDES[1], Cristina M. MONTEIRO[2], Cristina SANTOS[1,3]

[1]FEUP- Faculdade de Engenharia da Universidade do Porto, Porto, Portugal, Rua Dr. Roberto Frias s/n, 4200-465 Porto, Portugal
amafaldacmendes@gmail.com

[2]Universidade Católica Portuguesa, CBQF – Centro de Biotecnologia e Química Fina – Laboratório Associado, Escola Superior de Biotecnologia, Rua Diogo Botelho 1327, 4169-005 Porto, Portugal
cmonteiro@ucp.pt

[3]CIIMAR – Centro Interdisciplinar de Investigação Marinha e Ambiental, Terminal de Cruzeiros de Leixões, Av. General Norton de Matos s/n, 4450-208 Matosinhos, Portugal
csantos@fe.up.pt

ABSTRACT

Urbanization and climate change leads to water management challenges in urban areas due to the increased frequency and intensity of extreme precipitation events. Green Roofs (GR) can retain and detain runoff, reducing it. The present study examined an extensive pilot GR system's hydrological performance, which achieved a mean peak attenuation of 90.8%, a peak delay of up to 14 min and a runoff delay between 3.70-6.21 min, showing that GR enhances urban stormwater management, contributing to cities resilience in a climate change scenario.

## 1. Framework

Highly developed and densely populated urban areas, are facing serious environmental problems due to the lack of natural permeable areas that are replaced by impermeable construction facilities. This leads to the increase of rainwater management difficulties, particularly during extreme precipitation events, resulting in urban flooding. GRhave gained popularity for reintroducing vegetation to cities and managing rainfall. However, one of the main GR challenges is the excessive building load that substrate layer can cause. To mitigate this, lightweight expanded clay aggregates (Leca®) are used to reduce weight and improve water retention of the multilayer GR system due to their characteristics. In this study, an extensive GR pilot system developed by Leca, S.A. and Nutrofertil, was implemented at the FEUP hydraulic laboratory to assess its hydrological efficiency. Various precipitation simulation events were conducted to evaluate the impact of the system on the runoff coefficient and hydrological parameters (retention, detention, peak delay).

## 2. Methods

### *2.1 Kit LECA® Nutrofertil Green Roof D*

An extensive GR pilot system named LECA® Nutrofertil GR-D kit, have been implemented in a wood box of 1m$^2$. The multilayer system has been implemented according the specifications of the supplier Leca Portugal, S.A. (Fig 1) with the following layers (from bottom to top): (1) impermeabilization layer of PVC; (2) protection layer (Ecofelt PES-SB300); (3) drainage layer (Leca® D – particle size range of 10-20 mm) (4) Filter layer (Ecofelt PES-SB150) and (5) vegetation support layer (substrate Nutreasy composed by organic compounds, peat and pine bark with a ratio of 4:15, and expanded clay Leca® Hydro).



(a) ……..(b) (c) (d)

***Fig 1**. Multilayer extensive pilot GR system implementation (wooden structure (a) PVS Aqualiner (b), protection and drainage layers (c) and filter and substrate layers (d)).*

### *2.2. Simulation conditions and Assessed Parameters*

Simulation precipitation conditions were determined in accordance with Portuguese legislation (Table 1). Before each test, the system was saturated until a constant runoff was achieved (FLL guidelines). The tests were performed using sprinklers and the water flow at the entrance of the GR system was controlled and monitored using the MV110 ISOMAG converter with a display for magnetic flow meters (reading accuracy ± 0.4%). The water runoff was collected in a tank and measured every 5 min for 2.5 h. GR's hydrological performance was assessed after multiple precipitation simulation events, at different time intervals, through evaluation of runoff coefficient, retention capacity and detention capacity parameters.

**Table 1:** Simulation Conditions.

| Return Period (years) | t (minutes) | Intensity (mm/h) | Flow (L/min) |
|---|---|---|---|
| 5 | 5 | 104.9 | 1.75 |
| | 10 | 71.1 | 1.18 |
| | 15 | 56.6 | 0.94 |
| 10 | 5 | 120.1 | 2.00 |
| | 10 | 82.1 | 1.37 |
| | 15 | 65.7 | 1.10 |

## 3. Results

Table 2 displays the results of the hydrological performance of the GR for each condition tested.

**Table 2:** Hidrologycal performance according to each Return period considered.

| Return Period (years) | t (minutes) | Total amount of rainfall (mm) | Runoff Coefficient | Retention (%) | Runoff Delay (min) | Peak Attenuation (%) | Peak Delay (min) |
|---|---|---|---|---|---|---|---|
| 5 | 5 | 8.74 | 0.819 | 18.1 | 4.03 | 86.4 | 12.0 |
| | 10 | 11.9 | 0.886 | 11.4 | 3.80 | 95.7 | 14.0 |
| | 15 | 14.2 | 0.619 | 38.1 | 4.33 | 87.8 | 11.0 |
| 10 | 5 | 10.0 | 0.899 | 10.1 | 3.70 | 92.4 | 12.0 |
| | 10 | 13.7 | 0.867 | 13.3 | 3.78 | 94.3 | 14.0 |
| | 15 | 16.4 | 0.602 | 39.8 | 6.21 | 88.2 | 11.0 |

## 4. Conclusion

Runoff coefficient varied between 0.6 and 0.9 - which may be related to the antecedent soil moisture and the previous saturation process made prior simulations tests. It was also determined that both the runoff coefficient and the retention performance depend more on the intensity than the total amount of rainfall. The GR system achieved an average peak attenuation of 90.8%, with a peak delay of up to 14 min and a runoff delay between 3.70-6.21 min. Based on the present results we can conclude that using a GR system with Leca® positively affects the downstream drainage system design process, with a design flow reduction by around 91%. Hence, GR systems installation may lead to smaller pipes and lower installation costs for the downstream drainage systems (assuming legislation allows it), besides contributing to reduce other costs related to the thermal comfort of the building, since it acts as protection and isolation of the building itself.

**References**

[1] e.V., FLL - Landscape Development and Landscaping Research Society. (2018). Green Roof Guidelines- Guidelines for the planning, construction and maintenance of green roofs. Bonn.

[2] Decreto Lei nº 23/95 de 23 de Agosto. Diário da República nº 194 - I Série B. Ministério das Obras Públicas, Transportes e Comunicações. Lisboa.

# Analysis of Water-Energy Consumption and Carbon Emissions in Urban Water Sectors using Sankey Diagrams and GIS Mapping

Kyoung Won MIN[1], Gyumin LEE[2], Hyunjung KIM[3], Doosun KANG[4]

[1,2,3,4] Department of Civil Engineering, College of Engineering, Kyung Hee University, Yongin, Republic of Korea
min0706@khu.ac.kr (for author 1)
greenbeing@khu.ac.kr (for author 2)
aquarine@khu.ac.kr (for author 3)
doosunkang@khu.ac.kr (for author 4)

ABSTRACT

This study proposes ways to increase energy efficiency and reduce carbon emissions in urban water sectors (i.e., water and wastewater treatment, water intake and distribution, etc). First, starting with the establishment of a database including water-energy consumption and carbon emissions according to urban water cycle, the status of the target city was identified. To accurately estimate the energy consumption and carbon emissions in water sectors, a calculation model for water-energy consumption and carbon emissions is proposed. In consideration of population and social changes, a future water-energy consumption scenario is established and applied to the model to suggest ways to increase energy efficiency. In addition, visualization services using Sankey diagrams and GIS mapping, which would provide clear understanding of water-energy consumption and carbon emissions in target city, are provided. Finally, the proposed methodology facilitates a comprehensive review and evaluation of water-energy consumption and carbon emissions in the target city, suggesting improvements for sustainable urban water management.

## 1. Introduction

Water and energy are essential resources to human life and are closely related to each other. The urban water sector includes various processes such as intake, water treatment, pumping and distribution, wastewater treatment, and significant amount of energies are used in these processes. It is estimated that about 7% of the energy used on the planet is used in the water resources system (James et al., 2002), and energy efficiency is essential to cope with climate change. Internationally, in parallel with greenhouse gas reduction efforts, the establishment of a water-related greenhouse gas inventory through an entire process evaluation is being implemented, and specific reduction plans are being established (Park et al., 2011). In this study, a tool for analyzing water-energy consumption and carbon emissions and a method to increase energy efficiency and reduce carbon emissions by applying scenarios to the target city were proposed.

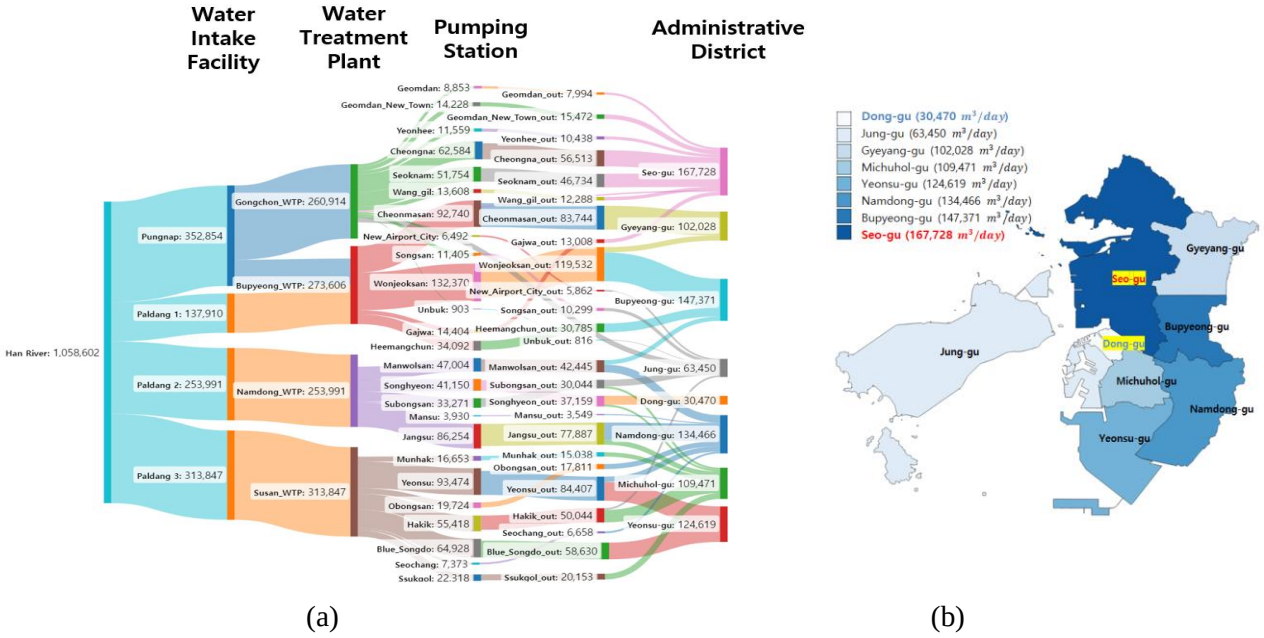
## 2. Methodology

This study begins with the collection and analysis of data related to water-energy consumption, and carbon emissions in the target city. Water-energy-carbon nexus in urban water sector is identified and computational models are developed. The scenario analysis involves constructing and simulating various scenarios related to population movements and social changes, water reuse, pump efficiency improvement, and increasing energy self-sufficiency in water treatment plants and sewage treatment plants. It aims to propose measures for reducing water and energy consumption as well as carbon emissions, such as implementing water-saving facilities, expanding water reuse, and increasing the use of solar energy. Visualization services are provided using Sankey diagrams and GIS mapping for simulation results and status data for target city. By analyzing

the fluidity between each element and identifying the energy and carbon emission efficiency of each administrative district by visualizing the spatial-temporal distribution, it is possible to identify areas that require special attention to water-energy use and carbon emission management. Finally, water-energy consumption and carbon emissions by administrative district are reviewed and improvement measures are proposed.

## 3. Application and Results

The proposed methodology was applied to Incheon Metropolitan City (IMC) in South Korea and Figure 1 illustrates the preliminary simulation results. Figure 1(a) is the Sankey diagram visualizing the movement of water from source to individual administrative district, and Figure 1(b) is the result of visualizing the water consumption by eight districts using GIS mapping. The darker the blue color, the higher the amount of water used.




(a) (b)

**Fig. 1.** Visualization of water consumption in IMC, South Korea using (a) Sankey diagram, and (b) GIS map

## 4. Conclusions

The water-energy consumption and carbon emissions in urban water sectors are estimated and visualized. By applying various future scenarios, the W-E-C nexus in urban water cycle will be analyzed and potential measures to reduce energy consumption and carbon emissions in the target area will be proposed for sustainable water management.


#### Acknowledgements

This work was supported by the Korea Institute of Energy Technology Evaluation and Planning(KETEP) and the Ministry of Trade, Industry & Energy(MOTIE) of the Republic of Korea (20224000000260).


#### References


James, K., Godlove, C. E., & Campbel, S. L. (2002). Watergy: Taking Advantage of Untapped Energy and Water Efficiency Opportunities in Municipal Water Systems, *Alliance to Save Energy*, Washington, DC.

Pabi, S., Amarnath, A., Goldstein, R., & Reekie. L. (2013). Electric Use and Management inn the Municipal Water Supply Wastewater Industries: Final Report, *Electric Power Research Institute, and Water Research Foundation*.

Park, S., Kim, J., & Kim, J. (2011). International Trends in Carbon Footprints in the Water Resources Sector. *Water and Future: Journal of the Korean Water Resources Association*, *44*(4), 36-44.

# Digitalization for modelling: the importance of data for improving sustainability in water distribution systems.

Christian CUELLAR[1], Modesto PÉREZ-SÁNCHEZ[2], P. Amparo LÓPEZ-JIMÉNEZ[3], Francisco-Javier SÁNCHEZ-ROMERO[4], Helena M. RAMOS[5]

[1,2,3]Hydraulic and Environmental Engineering Department, Universitat Politècnica de València, Valencia
ccuetri1@posgrado.upv.es; mopesan1@upv.es; palopez@upv.es

[4]Rural and Agrifood Engineering Department, Universitat Politècnica de València, Valencia
fcosanro@agf.upv.es

[5]Civil Engineering, Architecture and Environment Department, CERIS, Instituto Superior Técnico, Universidade de Lisboa, Lisboa, 1049-001, Portugal;
helena.ramos@tecnico.ulisboa.pt

ABSTRACT

Improving sustainability in water systems is important in all terms. In this sense, digitalization in the field of water distribution systems involves many aspects; the modeling of the systems, the implementation of tools that allow the interaction of the models with data in real time, and communication with the decision-making elements. To achieve this, Internet of Things (IoT) technologies, data analysis, cloud computing, augmented intelligence and blockchain, give us new capabilities to analyze, automate, correct in real time, predict, and manage networks. When these systems are well developed, there will be great advantages in the water distribution networks that will improve their sustainability conditions, such as extending the useful life of aging assets, reducing leaks, attacks (and other anomalies in the network distribution), improve water quality, service levels and supply reliability. When this is achieved and the networks are monitored sufficiently, through the methodology proposed here, digitalization will improve the sustainability of the networks from the monitoring of their main indicators, based on the UN SDGs.

## 1. Introduction

The operation analysis of any water system requires an evaluation of the different performance indicators, and it implies the measurement of all intervenient variables (Pokhrel et al., 2023). It could be a challenge in medium and small water systems when water managers do not have enough investment supports and economic resources to develop them (Ali et al., 2023). In general, modelling will help managers in the digitalization process. The mathematical model of a water distribution network consists of a set of lines and nodes represented by mathematical equations, which, once solved, provide the values of pressure and flow in the network (Makhmudov et al., 2022). The mathematical model aims to estimate the behaviour of the real distribution system, by calculating, for the elements that belong to the model, the hydraulic parameters that characterise them, improving the sustainability (Ramos et al., 2020). Nevertheless, mathematical models lead to sustainability when some sustainable indicators are integrated with them. In this sense, data are required for the proposal of sustainable indicators and comparison between several systems. Nowadays, data are more available than ever, but digitalization is not only data acquisition. Here we present a methodology to model a water distribution system and implement data at each step, to improve sustainability indicators and compare them with others in terms of categorizing the level of sustainability achieved by the entire system.

## 2. Results and discussions

The present methodology proposes the actions involved in several steps for preparing a digital tween of a water distribution system and use it for monitoring sustainable performance indicators across data inputs. These are enumerated in the follow steps: ***Step 1.*** Data collection: Various elements of the distribution system must be

collected, such as tanks, pumps, valves and injected flows, etc.; ***Step 2.*** An estimation of demand and consumption patterns should be made; ***Step 3.*** Construction of the mathematical model of the network using some simulation software ***Step 4***. Calibration of the mathematical model of the network. For calibration of models, a methodology is proposed to be used in terms of flow rates observed at the inlets, according to Pérez-Sánchez et al., 2017; ***Step 5.*** Analysis of the behavior of the network using the mathematical model, previously calibrated; ***Step 6.*** Application of sustainable indicators based on the research described in García et al. 2023; ***Step 7.*** Comparison with general standards defining if the system is good or bad in terms of these indicators; ***Step 8.*** Definition of actions to improve the sustainability network, ensuring the correct operation of the system in terms of the defined indicators, monitoring them in real time.

## 3. Results and discussions

The present methodology is being proposed to digitalize real systems and monitor them in terms of these indicators, at the moment in a small network in Campus Scale. Some systems are being modeled according to recorded data, which were developed in terms of pressure and flows. Several consumption pattern must be established as a function of the supplied area or known consumptions. In this case, a model of a particular network in the UPV water distribution network used as a lab is being used. As an example, a deep calibration process in this network has been performed. When comparing the results obtained with the thresholds for calibration proposal developed in (Pérez-Sánchez et al., 2017), all indicators are classified as "very good", indicating a satisfactory fit in the calibration of the model in terms of PBIAS, Root Relative Square Error (RRSE) and Nash-Sutcliffe (E) indexes.

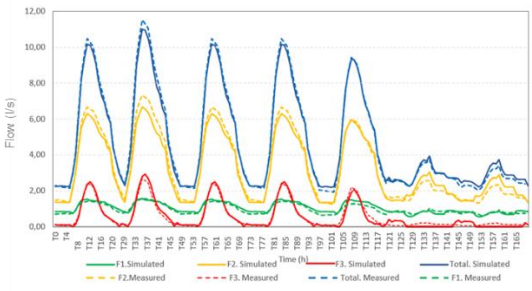



**Fig. 1.** Example of flow calibrated model in several pipes by using the methodology in Pérez-Sánchez et al., 2017

## 4. Conclusions

The present document presents a methodology for implementing many data collected in water distributions systems to make them more sustainable and to monitor the improvement in terms of sustainability by comparison with other similar systems. When calibrated models are developed, data must be used to implement Sustainability indicators that can be monitored in real time in order to improve the behavior of the systems. This process will lead to digitalization being the basis of more sustainable systems.

**Acknowledgements**

The authors would like to acknowledge grant PID2020–114781RA-I00 funded by MCIN/AEI/ 10.13039/501100011033

**References**

Ali, S.S.; Kaur, R.; Khan, S. Evaluating sustainability initiatives in warehouse for measuring sustainability performance: an emerging economy perspective. Ann. Oper. Res. 2023, 324, 461–500, doi:10.1007/s10479-021-04454-w.

García C.; López-Jiménez, P.A., Sánchez-Romero, F.J., Perez-Sanchez, M, 2023. Assessing water urban systems to the compliance of SDGs through sustainability indicators. Implementation in the valencian community. Sustainable Cities and Society, https://doi.org/10.1016/j.scs.2023.104704.

Makhmudov, I., Jumamuratov, D., Seytov, A., Sadiev, U., Jovliev, U., Shonazarov, J., & Muminov, O. (2022). Mathematical Models Of Typical Elements Of Water Management Systems. Journal of Positive School Psychology, 6871-6877.

Pérez-Sánchez, M.; Sánchez-Romero, F.; Ramos, HM.; López Jiménez, PA. (2017). Calibrating a flow model in an irrigation network: Case study in Alicante, Spain. Spanish Journal of Agricultural Research (Online). 15(1):1-13. doi:10.5424/sjar/2017151-10144

Pokhrel, S.R.; Chipi-Shrestha, G.; Hewage, K.; Sadiq, R. Key performance indicators for small and medium-sized urban water systems in a semi-arid region: a case study of Okanagan Valley, Canada. Urban Water J. 2023, 20, 435–449, doi:10.1080/1573062X.2023.2179927.

Ramos, H., McNabola, A., López-Jiménez, P., & Pérez-Sánchez, M. (2020). Smart Water Management towards Future Water Sustainable Networks. Water., 12(1). https://doi.org/10.3390/w12010058

# Nature-based solutions for urban flooding adaptation in unplanned settlement in Mozambique

Susanna OTTAVIANI[1], Livia SERRAO[1], Alessandra MARZADRI[1], Alfredo Manhota ANTONIO[2], Amerigo de Stela Vladimir MSOPELA[2], Harold Juvenal CHATE[2], Wilson Alberto Manguita PAULINO[3], Edilson PAULINO[3], Guido ZOLEZZI[1]

[1] University of Trento, Department of Civil, Environmental and Mechanical Engineering, Italy
susanna.ottaviani@unitn.it, livia.serrao@unitn.it, alessandra.marzadri@unitn.it, guido.zolezzi@unitn.it

[2] Zambeze University of Trento, Faculty of Science and Technology, Mozambique
alfredo.antonio@uzambeze.ac.mz, americo.msopela@uzambeze.ac.mz, hjuvchate@uzambeze.onmicrosoft.com

[3] Consorzio Associazioni con il Mozambico, Mozambique
wilson.paulino@consorciocam.org, edilson.paulino@consorciocam.org

ABSTRACT

The unplanned neighbourhood of Macuti, in Mozambique, experiences extended and prolonged flooding for half of the year during the wet season. Although cyclones and extreme weather events often hit the city, the lack of basic infrastructure and, above all, of a widespread drainage system makes the settlement particularly vulnerable to even minor events. In addition, the flat area is altimetrically prone to rainwater accumulation and the clay soil hinders infiltration. These peculiarities delineate an interesting case study that has been the focus of an international cooperation project, designed with a potentially replicable methodology in other similar cases worldwide. The project methodology integrates social surveys, hydraulic and hydrologic modelling, a participatory process among the key stakeholders and spatial multicriteria analysis. This has allowed to choose an optimal and agreed pilot solution for urban drainage in the specific unplanned neighbourhood, which also fits the principles set by a neighbourhood-scale urban plan proposed within the same project. The chosen solution can be viewed as an experimental pilot able to meet both the hydraulic and social needs of a space claimed by the community in the framework of a fast-growing environment.

## 1. Introduction

Beira, the second city of Mozambique, lies on the Pungwe River alluvial plain overlooking the Mozambique Channel in the centre of the Country. Since the end of the civil war, the city has experienced a significant increase in population that has not been matched by equally prompt urban planning. This is particularly true for Macuti, a coastal neighbourhood of 17 thousand inhabitants (2017). Its spontaneous growth has left no room for the expansion of the pre-existing basic infrastructures and services, such as streets, aqueducts and sewage. As a result, the dichotomy between the colonial settlement, built by the Portuguese, and the later enlargement is remarkable [1].

Furthermore, the vulnerability of this neighbourhood is exacerbated by extreme weather. Cyclones hit the city periodically with severe consequences, one among all the 2019 Tropical Cyclone Idai, whose wind gusts at 280 kph [2] damaged 49% of Macuti's households [3]. The rainfall pattern is also changing with an overall delay in the commencement of the rainy season [4] and a significant increase in Beira's precipitation intensity [5]. Hence, more frequent flash flooding and greater peak runoffs are expected. The effects on Macuti are impactful for various reasons: i) the clay soil on which the district is built strongly limits rapid infiltration and ii) the drainage directions channel water towards the interior of the neighbourhood, which is not reached by an efficient drainage network of free-surface canals surrounding the upper part of it.

The EuropeAid co-funded project MUDAR (Mozambique Integrated Urban Development by Actions and Relationships) aims to design a pilot intervention in Macuti to reduce the implications of floods in a vulnerable

context, introducing inclusive and sustainable actions. For this reason, the present research on Nature-based Solutions (NBS) for urban flooding adaptation has been conducted.

## 2. Methods

In a data-scarce context such as the study area, an integrated and multidisciplinary methodology became necessary to assess Macuti's needs and constraints. Such integrated methodology includes tools from social sciences, spatial multicriteria analysis, hydrological and hydraulic measurements and modelling.

Firstly, in the data collection, quantitative and qualitative information was gathered from nearly a thousand interviews and questionnaires to the population and stakeholders. Their spatialisation provided a key integration to the remotely sensed information, subsequently validated in situ, and to that provided by local authorities. Secondly, the spatial multicriteria analysis determined the areas prone to pluvial flooding through the identification of a Pluvial Flood Index (PFI) [6]and the most suitable spots for NBS implementation. Simultaneously, a 20-year daily rainfall heights dataset validated the Intensity Distribution Frequency (IDF) curves modelled in a WRF reanalysis [5], making the application of a hydrological rainfall-runoff model more accurate. Thirdly, EPA SWMM software helped to quantify the contribution, in terms of surface runoff, of possible Low Impact Development (LID) solutions draining into the aforementioned network.

## 3. Result and discussion

The limited environmental data available on Macuti, as in numerous other contexts worldwide, does not allow for a fine rainfall-runoff and hydraulic model. Therefore, the implementation of more traditional water infrastructure is expected to expose these solutions to a higher risk of failure. On the other hand, the level of detail achieved in this research was considered largely sufficient to propose the conversion of areas - that were already natural water storage sites - into dry ponds, safely connected to the existing channel network.

The spatial analysis and the participatory process built with the population and stakeholders made it possible to identify the site where dry ponds should have been implemented first. The simplicity of this intervention makes it replicable in the other locations defined as vulnerable.

More in detail, for the pilot action foreseen by the project, the targeted area has an extension of 0.19 ha and is situated in the middle of the neighbourhood, tightly surrounded by buildings whose expansion would have occupied it. The dry pond serves 3.1 ha of watershed on which an average rainfall of 1500 mm per year is estimated, with a precipitation height of 245.31 mm for a return period of 10 years. This blue infrastructure aims to prevent the inhabitants from evacuating every rainy season because the water level has been reported to reach up to 1.2 m height damaging facilities, contaminating wells, and overflowing latrines and septic tanks resulting in outbreaks of diarrheal diseases. The expected benefits of this technology are to convey the flow towards the existing drainage network, with an estimated reduction of the runoff peak by 9% in the subbasin in which it is embedded, increasing the contact time between the greened soil and the liquid matrix.

## 4. Conclusions

The proposed integrated methodology has proven to be a fruitful resource to tailor the most suitable solution to a context characterised by uncertainty. In fact, unlike simple drainage, creating a green space that can also be used in the dry season brings numerous benefits. On a neighbourhood scale, subtracting this space from uncontrolled edification and using it for community service is a valid response to the lack of green areas raised by the population. This pilot case represents an opportunity to explore how Nature-based Solutions can be a valid support to grey infrastructures for urban flooding adaptation, addressing the challenges of fast-growing unplanned settlements in sub-Saharan Africa.

**References**

[1] Newitt M (2017), A Short History of Mozambique, Oxford University Press, 254 pp.
[2] Mühr B, Daniell J, Schaefer A, Johannes B, Barta T, Neuweiler A, Mohr S, Kunz M (2019) Tropical Cyclone 18S IDAI, CEDIM Forensic Disaster Analysis Group
[3] UNOSAT-REACH (2019) Mozambique - Beira City - Macuti - Neighbourhood Damage Assessment of 26 March 2019. URL: https://m.reliefweb.int/report/3056948
[4] National Disasters Management Institute (INGC) (2009) Synthesis report. INGC climate change report: study on the impact of climate change on disaster risk in Mozambique.
[5] Muradás P, Puig M, Ruiz Ó, Solé JM (2021) Mainstreaming Climate Adaptation in Mozambican Urban Water, Sanitation, and Drainage Sector, African Handbook of Climate Change Adaptation. Springer, Cham. DOI: 10.1007/978-3-030-45106-6_132
[6] Pacetti T, Cioli S, Castelli G, Bresci E, Pampaloni M, Pileggi T, Caporali E (2022) Planning Nature Based Solutions against urban pluvial flooding in heritage cities: A spatial multi criteria approach for the city of Florence (Italy), Journal of Hydrology: Regional Studies, 41, DOI:10.1016/j.ejrh.2022.101081.

# Urban drainage control plan. Modelling the integrated drainage network. A case study in Caneças/Ramada/Odivelas, Portugal

Carlos RAPOSO[1], Susana FREITAS[1], Helder RODRIGUES[1], Leonor CAETANO[1], Rita PIRES[2], Conceição DAVID[2], Filipe TEIXEIRA[3]

[1] TPF Consultores de Engenharia e Arquitetura S.A., Department of Water and Environment, Portugal
carlos.raposo@tpf.pt

[2] Águas do Tejo Atlântico, S.A., Portugal
rita.pires@adp.pt

[3] SIMAR Loures|Odivelas, Portugal
fjteixeira@simar-louresodivelas.pt

ABSTRACT

Urban areas face growing challenges in managing and controlling drainage systems, especially in the context of climate change and urbanization. The aim of the present work was to develop a rainfall-runoff model to understand the drainage system's response to known precipitation events, enabling the design of effective flow control solutions. A combined hydrological and hydraulic modelling approach is applied to support that the designed overflow structures will be properly located and activated during heavy precipitation events.

## 1. Introduction

The sewer system in the area of Caneças/Ramada/Odivelas serves a total drainage area of 6,9 km$^2$. The study site could be described as an urban catchment in the south areas and with semi-urban areas in the north. The 6,5 km long Interceptor is the main sanitary sewer system in the area, however, both storm water and wastewater is being collected. As this infrastructure is not designed to handle the collective stormwater and wastewater during the stormy periods, combined sewer overflows (CSOs) occur. Moreover, on-going climate variability and climate changes may cause intensified precipitation events in some areas which may also lead to frequent CSOs (Tavakol-Davani et al., 2016a, Tavakol-Davani et al., 2016b, Dirckx et al., 2017). Though, CSOs sometimes prevent flooding in important places but it can bring significant environmental risk if they are not properly controlled (Jalliffier-Verne et al., 2016, Madoux-Humery et al., 2016). The scope of this project is modelling the integrated drainage network to support the design of flow control infrastructures, that will function to minimize both pollution load to receiving water and overall treatment and energy cost in sewer system simultaneously.

## 2. Materials and Methods

The riverbed topography of the main watercourse of the basin was surveyed to define its morphology. A total of 27 cross-sections were surveyed and flow depth was measured along 11 cross-sections. In the drainage system, a total of 20 flow meters were installed (with the resolution of 5 min) in selected pipes. Sub-daily precipitation data (i.e., 2 min interval) was abstracted from one rain gage station. The conducted study utilizes the Hydrologic Engineering Center-Hydrologic Modelling System (HEC-HMS) and Hydrologic Engineering Center-River Analysis System (HEC-RAS) as the modelling tool to develop runoff and water surface elevation evaluation model for known precipitation. Two periods were selected as input for the hydrological and hydraulic models, one with a two-year return period and one with a return period ranging from 5 to 10 years. The rainfall event with a return period of 2 years was used to calibrate the HEC-HMS model by varying the percent of impervious area and the lag time. To account for the loss, runoff estimation, and flow routing, Soil Conservation Service Curve Number and Soil Conservation Service Unit Hydrograph were selected. The

simulated runoff from HEC-HMS was then used in the calibrated and validated HEC-RAS model to generate the water surface elevation. For the simulation of the generated runoff through the HEC-RAS hydraulic model, an 1D unsteady flow analysis was performed. For the determination of roughness coefficients, appropriate Manning n value ranges were established per land use category based on the literature. The hydraulic variables, the inflow hydrograph, lateral inflow hydrograph, and the normal depth were used as boundary conditions in the hydraulic models. The calibration was conducted by changing the manning's n to get the simulated depth of flow same as the depth measured at the gaging stations. The capacity analysis of the existing and the modified drainage network for the study area was carried out using software SWMM (Storm Water Management Model). The catchment area was divided into sub-basins. The HEC-RAS water surface level results were considered as input in the outfall structures defined in the SWMM model. The model structure is shown in Fig. 1 showing the coupling of the model components used in the study.

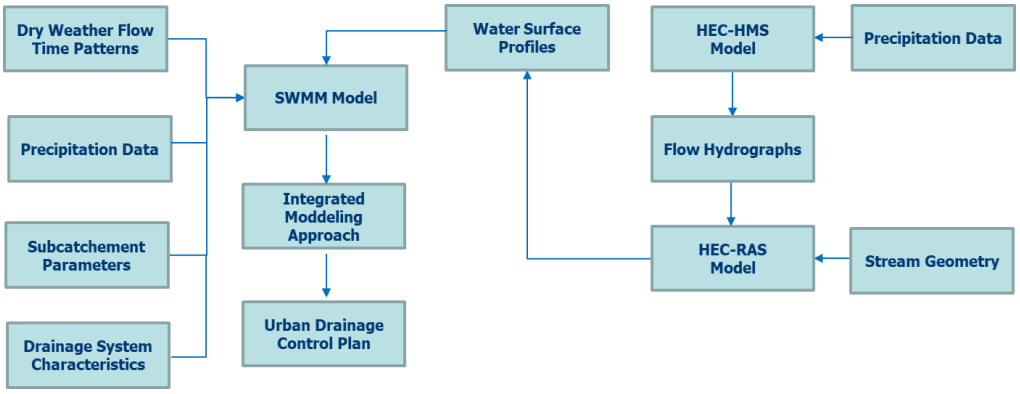



**Fig. 1.** Integrated modelling structure for designing flow control solutions incorporating HEC-HMS, HEC-RAS and SWMM.

## 3. Results and Conclusion

The results of the hydraulic simulations of the existing drainage system show that for dry weather there is no volume discharged at outfalls or manholes. For a 2 years return period event, with a rainfall intensity between 24 and 54 mm/h, there is one outfall activated, discharging 1900 $m^3$ (4% of the total intersected volume), 37 flooded manholes (11% of the total manholes), and 38000 $m^3$ were collected in the system for treatment. In comparison, for an event with a return period between 5- 10 years, with a rainfall intensity of 120 mm/h, 19500 $m^3$ (6% of the total intersected volume) is discharged through an outfall, there is an increase of the flooded manholes up to 20%, 212000 $m^3$ were collected for treatment, and external inflow occurs (31400 $m^3$), revealing the influence of the main watercourse and the downstream drainage system in the studied infrastructure. When considering the solutions designed for the drainage system in the hydraulic simulations, results show that for a 2 years return period there are no flooded manholes and for a 5- 10 years return period the number decreased 45% compared to the existing system. Regarding the controlled CSOs, defined according to an acceptable dilution rate, the volume increased to 13200 $m^3$, 27% of the total volume intersected in the system, and up to 32% for 2 and 5-10 years return period, respectively. The hydraulic simulations in the SWMM model considering the designed solutions indicate that external inflow no longer occurs and that there is a reduction up to 22% of the total volume collected for treatment, without compromising the receiving water quality.

**Acknowledgements**

This work was developed under the scope of the project "Hydraulic study of the Caneças/Ramada/Odivelas Interceptor and Flow control Detail Design", funded by the Portuguese public company Águas do Tejo Atlântico (AdTA). The authors would like to thank the members of the AdTA team and SIMAR Loures e Odivelas team, for their assistance throughout the entire project development process. Thanks are also due to the Odivelas City Council for providing information concerning the watercourse.

**References**

Brokamp, C., Beck, A., Muglia, L., Ryan, P. (2017). Combined sewer overflow events and childhood emergency department visits: a case-crossover study. Sci. Total Environ. 607–608, 1180–1187.
Dirckx, G., Korving, H., Bessembinder, J., Weemaes, M. (2017). How climate proof is real-time control with regard to combined sewer overflows? Urban Water J. 15, 544–551.
Jalliffier-Verne, I., Heniche, M., Madoux-Humery, A., Galarneau, M., Servais, P., Prévost, M., Dorner, S. (2016). Cumulative effects of fecal contamination from combined sewer overflows: management for source water protection. J. Environ. Manage. 174, 62–70.
Madoux-Humery, A., Dorner, S., Sauvé, S., Aboulfadl, K., Galarneau, M., Servais, P., Prévost, M. (2016). The effects of combined sewer overflow events on riverine sources of drinking water. Water Res. 92, 218–227.
Tavakol-Davani, H., Burian, S., Devkota, J., Apul, D. (2016[a]). Performance and cost-based comparison of green and gray infrastructure to control combined sewer overflows. J. Sustain. Water Built Environ. 2 (2) pp. 04015009–1 - 04015009–12.
Tavakol-Davani, H., Goharian, E., Hansen, C., Tavakol-Davani, H., Apul, D., Burian, S. (2016b). How does climate change affect combined sewer overflow in a system benefiting from rainwater harvesting systems? Sustain. Cities Soc. 27, 430–438.

# Modelling and Analyses of Micro Hybrid Pumped Hydropower Storage

João PINA[1], Modesto PÉREZ-SÁNCHEZ[2], P. Amparo LÓPEZ-JIMÉNEZ[3], Helena M. RAMOS[4]

[1,4] Civil Engineering, Architecture and Enviroment Department, CERIS, Instituto Superior Técnico, Universidade de Lisboa, Lisboa, 1049-001, Portugal;
joao.g.pina@tecnico.ulisboa.pt; helena.ramos@tecnico.ulisboa.pt

[2,3]Hydraulic and Environmental Engineering Department, Universitat Politècnica de València, Valencia
mopesan1@upv.es; palopez@upv.es

**ABSTRACT**

This research attempts to address the gap between the conceptual potential of hybrid energy systems and their practical implementation. The main objective is to develop a multi-variable model in Python to allow a new complete and comprehensive techno-economic analysis into the performance of hybrid power systems in a micro scale. The objective is to evaluate the influence of critical parameters, installed wind and solar power, energy storage capacity through pumping, reservoir storage volume and installed turbine and pump power, on the performance of the whole systems efficiency, flexibility and reliability. By changing main parameters in the developed model, it will be possible to recognize the performance, efficiency, feasibility, and economic costs of the system, and ultimately provide practical knowledge for optimizing and designing hybrid renewable energy solutions to meet different energy needs. This research covers the simulation, optimization and data analyses of hybrid energy solutions, combining wind, solar and hydropower energy sources with the energy storage technologies Pump Hydropower Storage (PHS).

## 1. Introduction

Pumped Storage Hydropower (PSH): This plant stores water at different elevations in a lower and an upper reservoir. During periods of high electricity demand, water is released from the upper into the lower reservoir through a reversible pump-turbine to generate electricity. This process is reversed during periods of low demand, when water is pumped back into the upper reservoir. PSH plants can be open- or closed-loop systems. Open-loop systems use a natural water source as their lower reservoir, while closed-loop systems do not.

A significant progress that has been made in the panorama of hydropower, with conventional hydropower growing by more than 75% in 2023, reaching an installed capacity of over 1 421 GW globally (IEA, Renewables, 2023). PSH capacity, on the other hand, grew by over 50% in the same period, reaching 130 GW in 2021.

Nowadays, the National Integrated Energy and Climate Plan (PNEC 2030- Plano Nacional Integrado Energia e Clima 2021-2030) overrides the previous plans (PNAER and PNAEE) but remains oriented towards Portugal's long-term goals for carbon neutrality, in coordination with the Roadmap to Carbon Neutrality 2050 (RNC 2050- Roteiro para a Neutralidade Carbónica 2050), signed in 2016 as part of the Paris Agreement.

## 2. Methodology

The use of a programming language such as Python, offers versatility, interactivity and complex systems handling with rigor and precision, that is fundamental to assess the performance of the system and its individual components under various conditions, the application and development of this code is not just a technical aspect, but a means to providing insights into the complex dynamics of hybrid renewable energy systems and their economic viability.
A conceptual hybrid energy system combining wind, solar, with a pumped hydro storage system is represented in Figure 1. The components of the system are, a photovoltaic (PV) system, a wind turbine, an energy storage system (pumped-hydro storage), a control station and an end-user (energy demand). This type of system can be used in isolation from the grid (i.e., a standalone system) or in a grid connection.

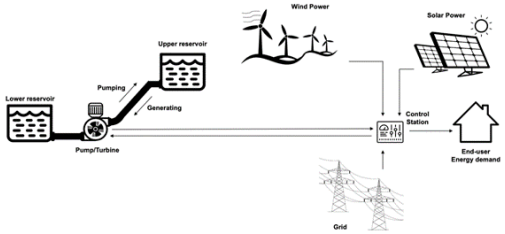



***Fig. 1-*** Conceptual Hybrid hydro-wind-solar with pumped storage system.

## 3. Results and discussions

Considering one of the objectives of this research is to evaluate the influence of critical parameters of hybrid system and to find optimal hybrid solutions of the whole system at different scales, by changing, wind-solar installed capacities, maximum upper reservoir volume and turbine/pump capacity, stated in Table 3, and fixing other parameters such as peak consumption, net head, pumping and turbine efficiency, turbine generation coefficient, ct,, and water pumping coefficient cp.

At the micro-scale, simulations varying wind, solar, and hydro installed power as well as the volume of the upper reservoir, were conducted. The key parameters for these simulations were as follows: Installed power of renewables: (0,01; 0,05; 0,1) MW; Volume of the upper reservoir: (1500; 7500;15 000) $m^3$; Peak consumption: 0,05 MW; Net head: 20 m; Turbine type: Pump as turbine; Turbine efficiency: 0,5; Pumping efficiency: 0,7 PAT installed power 0,01 MW, cases 1-27 (Figure 2).

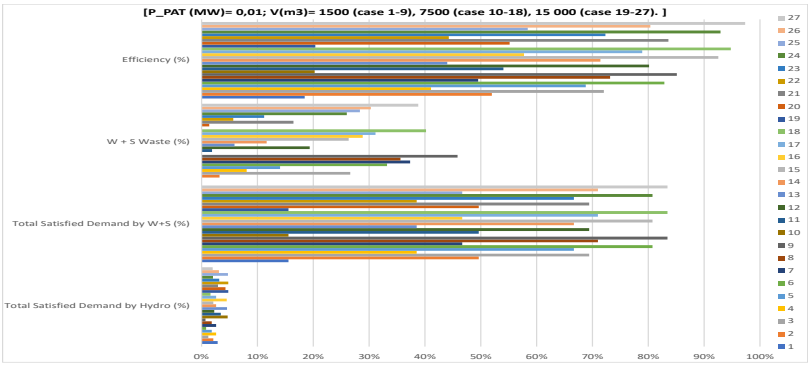



***Fig. 2.*** - Results: PAT 0,01 MW.

## 4. Conclusions

Micro-scale results showed that combining wind and solar power with pumped hydro storage is a viable solution for increasing energy supply and reducing waste. These systems hold potential for contributing to a more sustainable and reliable energy future, but they require careful design and optimization to achieve their full potential. The results highlight the importance of scalability, efficiency considerations, and economic viability in the deployment of these systems.

**Acknowledgements**

The authors would like to acknowledge FCT, through CERIS, project UIDB/04625/2020 and the project HY4RES (Hybrid solutions for Renewable Energy Systems) EAPA_0001/2022 from INTERREG ATLANTIC AREA PROGRAMME and CERIS, the Hydraulic Laboratory, for experiments on PATs.

**References**

Simão, M.; Ramos, H.M. Hybrid Pumped Hydro Storage Energy Solutions towards Wind and PV Integration: Improvement on Flexibility, Reliability and Energy Costs. Water 2020, 12, 2457. https://doi.org/10.3390/w12092457

Guruprasad, P.S.M.; Quaranta, E.; Coronado-Hernández, O.E.; Ramos, H.M. Hydropower Advantages over Batteries in Energy Storage of Off-Grid Systems: A Case Study. Energies 2023, 16, 6309. https://doi.org/10.3390/en16176309 .

Rasheduzzaman, M., et al. (2019). Review of Energy Storage Technologies Integrated with Wind Energy Systems. Applied Energy, 242, 498-516.

IEA - Renewables 2023 Abstract Analysis and forecasts to 2028, Revised version, Jan 2024 Information notice found at: www.iea.org/corrections. https://www.iea.org/reports/renewables-2023 .

Chen, Z., Miao, L., Yang, J., Song, J., & Fang, X. (2019). Efficiency of pumped hydro storage power station: A comprehensive review. Applied Energy, 233-234, 1225-1235.

Ramos, H., McNabola, A., López-Jiménez, P., & Pérez-Sánchez, M. (2020). Smart Water Management towards Future Water Sustainable Networks. Water., 12(1). https://doi.org/10.3390/w12010058

# A methodology for assessing water efficiency of office buildings – application to a full-scale case study

Paula VIEIRA[1], Ana POÇAS[1], Patrícia DIAS[2], Rita PESTANA[2]

[1] *Laboratório Nacional de Engenharia Civil, Av. do Brasil 101,1700-066 Lisboa, pvieira@lnec.pt, apocas@lnec.pt*

[2] *ADENE - Agência para a Energia, Av. 5 de Outubro 208, 2º, 1050-065 Lisboa, patricia.dias@adene.pt, rita.pestana@adene.pt*

ABSTRACT

## 1. Introduction

It is expected that, in Europe, by 2030, and in the context of climate change, water stress and scarcity will affect around half of the river basins (EC, 2012). The buildings sector is among the top priorities in terms of efficient use of resources in the EU. Water saving potentials of 30-50 % may be estimated for buildings (EC, 2017). Office buildings in particular present a significant potential as they are, by nature, large water consumers. In these buildings, the main water uses are similar to residential ones but with higher frequencies (uses/fixture.day) due to the higher number of users, and the technology can be more complex (e.g., hot water recirculation networks). The benefits of implementing water saving measures in office buildings include reduced operational costs (lower consumption of water and energy) and reduced risks associated with water scarcity (higher resilience of buildings).

In response to the above-mentioned challenges, ADENE – Portuguese Agency for Energy developed the AQUA+® methodology and tools (www.aquamais.pt) for auditing and classifying the water efficiency of different types of buildings, namely, residential (in 2020) and hotels (in 2022). The methodology is currently being expanded to office buildings and provides a classification of the building water efficiency and a set of improvement measures for greater resilience in terms of water and energy use (water-energy nexus). Unlike previous approaches that targeted building sustainability with a few water related indicators (e.g., certification schemes like LEED or BREEAM) or that addressed only water fixtures (e.g., labelling schemes like WELS), this methodology focusses on the building water efficiency in an holistic and extensively detailed way, assessing a large number of parameters (66) comprising not only aspects related with water fixtures but also several other building characteristics that could lead to water savings. Another innovative feature is that the methodology specifically provides an objective classification of the building's overall water efficiency, acting as a comparative framework for office buildings. The development of AQUA+® Offices included testing and optimization in real case studies. This article presents results from one of those cases.

## 2. Methodology for auditing and classifying water efficiency of office buildings

The AQUA+® methodology evaluates the water performance of the infrastructural aspects of office buildings, excluding consumer behavior. It covers indoor and outdoor water uses. The combined efficiency in the use of energy associated with water (e.g., hot water) is also considered. Performance is assessed in seven main areas of evaluation (which are divided into topics): water sources and supply network (e.g., alternative water sources); outdoor uses (e.g., irrigation, soil use); efficiency of fixtures in bathrooms and kitchens; car wash; hot water (production system, distribution network); actions for water use efficiency (e.g., awareness campaigns, manual of best practices, certifications). Performance evaluation in each topic is carried out based on assessment parameters. The weighted sum of the scores for each parameter allows to obtain a classification (0 % to 100 %) of the building efficiency, scaled in seven classes: from F (less efficient) to A+ (most efficient).

## 3. Application of the methodology and results

The methodology was applied to an office building located at LNEC campus (22 ha, Lisbon), with a permanent staff of 90 people. The building, from 1972 has an outdoor irrigated area (565 $m^2$) and is supplied through

LNEC's campus network by the public water system.

Water efficiency audits were carried out in 2023-24. In the first part of an audit, measurements of flow rate/volume of fixtures were made. For taps and showers, flow rate was measured by filling a container of known volume (2, 6 or 10 L) and by measuring the filling time with a stopwatch. Three measurements were made for each fixture. Volume of WC cisterns was determined based on their dimensions. A total of 49 fixtures were audited. Figure 1 shows the performance assessment of each fixture by comparison against benchmark values (3 or 4 efficiency ranges). These results reveal a high variability of flow rates, ranging from 4.2 to 35.6 L/min for bathroom taps (all lavatory taps), from 4.1 to 14.0 L/min for kitchen taps and from 8.4 to 48.1 L/min for showers. Unequal flow rates were found for similar fixtures located in the same bathroom, thus emphasizing the importance of defining a good sampling approach when it not feasible to audit all fixtures. Most of the bathroom taps (72 %), showers (67 %) and WC (100 %) fell in the lowest efficient range. In some cases, values were greater than five times the maximum efficiency level. Of all fixtures, only one kitchen tap fell in the most efficient range.

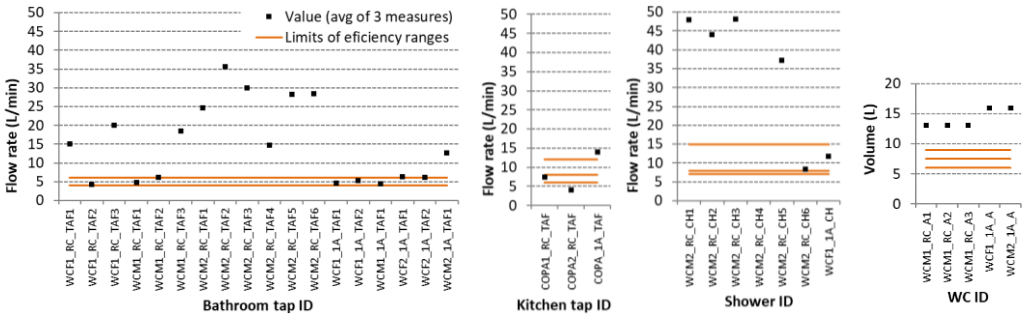



**Fig. 1.** Flow rate and volume of audited fixtures

The second part of the audit consisted of assessing the building performance in the seven main areas of evaluation. Figure 2 (left) shows the performance achieved for each subarea (the 100 % value would be reached if all available water efficiency measures were implemented in the building). Efficiency of kitchen and bathroom taps and urinals were the best performing subareas, achieving 58 %, 45 % and 43 %, respectively. Hot water distribution network and water sources were the subareas with lower performance (0 % and 9 %, respectively). All areas exhibit a large improvement potential.

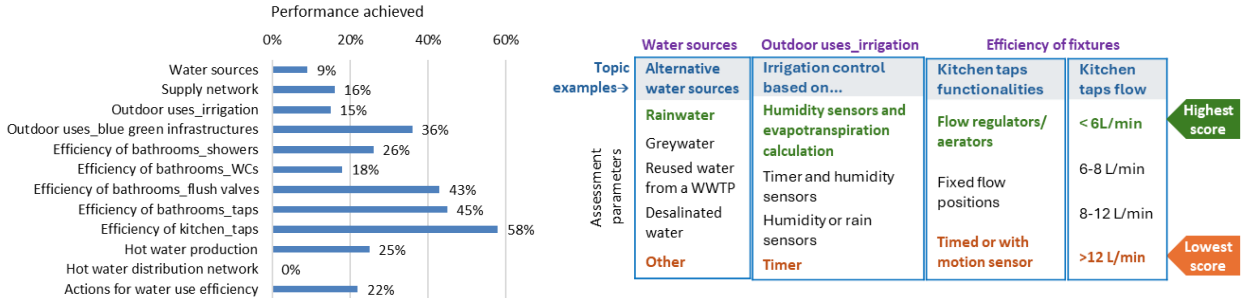



**Fig. 2.** Performance in each evaluation subarea (left) and examples of topics and assessment parameters (right)

Measures for improving the building current water efficiency level (class D) were identified and prioritized according to water savings, implementation costs and payback periods. Such measures targeted the building low performing areas and included the replacement of non-efficient water use fixtures in all bathrooms (quick win measures), the installation of an exclusive flowmeter for indoor/outdoor consumption breakdown, water leakage control, hot water pipe insulation, use of smart irrigation systems and awareness campaigns for employees. By implementing all quick win measures, the building will reach class B. With all the proposed measures, it will reach class A.

## 4. Final remarks

The application of the AQUA+® methodology to LNEC case study provided an overall water efficiency classification of the building and allowed the identification of opportunities to increase water savings highlighting priority building areas targeted for retrofitting. It also identified measures to increase the current efficiency and established a baseline for tracking progress from efficiency upgrades.

**References**

EC (2012). Report on the review of the European Water Scarcity and Droughts Policy. European Commission.
EC (2017). Study on cost and benefits of working towards environmental macro objectives in the building sector. European Commission.

# Tróia WWTP Expansion and Retrofit to Produce Reuse for Water

Carlos RAPOSO[1], João GUIMARÃES[2]

[1] Director of Hydraulic and Environmental Service, TPF – Consultores de Engenharia e Arquitetura, S.A
carlos.rapos@tpf.pt

[2] Head of Asset Services - Project Management & Architecture, Sonae Sierra, S.A
jpguimaraes@sonaesierra.com

ABSTRACT

## 1. Introduction

Troia touristic development have two distinct water supply networks, each serving a specific purpose. One network provides water for human consumption, while the other is designed to irrigate the green spaces within the area. In both networks, the water source is from underground boreholes.

The Troia WWTP treats effluents generated in the Troia touristic development area in the municipality of Grândola. Currently, the treated wastewater is discharged into the natural environment.

With the new development of the Troia Peninsula and a commitment to sustainable water resource management, there is a recognized need to implement a Water for Reuse (WfR) system for irrigating green spaces within the resort.

Decree-Law No. 119 of August 21, 2019, establishes the legal framework for WfR production in Portugal. Considering the use of WfR for irrigating of green spaces with public free access, it was determined that the WfR produced in Troia WWTP should meet the requirements for water quality Class A Standard, with the following maximum limit values to be achieved: $BOD_5 \leq 10$ mg/L O2; TSS ≤ 10 mg/L; E. coli ≤ 10 CFU/100 mL.

Through the expansion and retrofit of the WWTP, there is the possibility to connect reused water into the irrigation network, resulting in a substantial reduction in the consumption of groundwater within the irrigation system. This sustainable approach not only optimizes water resources but also aligns with environmentally conscious practices by minimizing reliance on underground sources for irrigation purposes. The illustration presented in figure 1.0 below presents a general layout of the irrigation water network, which is prepared to receive treated water for irrigation.



**Fig. 1.0** General layout of Troia irrigation network (1)

## 2. Existing Treatment System

The Troia WWTP receives wastewater from the entire Troia tourist resort. The existing treatment infrastructure, designed in the 1970s with a capacity for 6,500 inhabitants, commenced operation in 1980. The treatment process involves a preliminary treatment (screening), succeeded by secondary treatment using activated sludge with extended aeration. Subsequently, sludge treatment involves dehydration in drying beds. Since 1982, additional infiltration/maturation ponds have been constructed to mitigate the impact of the

discharge of treated wastewater on the environment. The quality objectives stipulated in the current WWTP discharge license are as follows: COD ≤ 125 mg/l; $BOD_5$≤ 25 mg/L O2; TSS≤ 35 mg/L;

Wastewater production at the WWTP fluctuates throughout the year, with a notable increase during the summer months due to the peak tourist influx. This variability in production proves advantageous for reuse in irrigation, aligning with the period of heightened demand for water in maintaining green spaces. The months with the highest production of treated wastewater correspond to those with the greatest need for irrigation water, optimizing resource utilization, as evident from the analysis of the graph presented in figure 2.0.

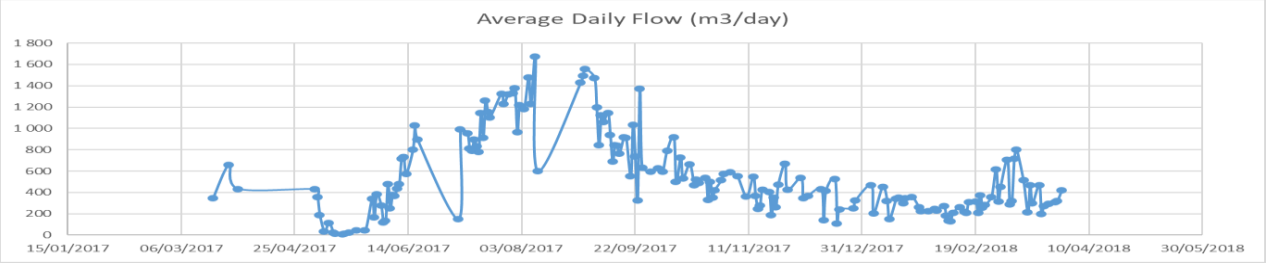



**Fig. 2.0** Troia WWTP average daily flow from March 2023 to April 2018 (1)

## 3. New Treatment System

The Troia WWTP will have to be expanded to treat the effluents from 16,500 equivalent inhabitants in the project horizon and produce Water for Reuse (WfR) that complies with the Quality Class A standards outlined in Decree-Law No. 119 of August 21, 2019.

After the evaluation of various technologies for the expansion of the WWTP, the chosen solution is the Membrane Bioreactor (MBR) for several key reasons: The MBR system facilitates the removal of bacteria through a physical barrier, eliminating the need for additional disinfection reagents; The inclusion of a physical barrier serves as an additional safeguard, reducing the risk of microbiological contamination in the Water for Reuse (WfR); The MBR solution enables the production of effluent with virtually zero Total Suspended Solids (TSS) concentration and Biochemical Oxygen Demand (BOD5) lower than 10 mg/l, ensuring water quality suitable for various applications; Implementing the MBR solution allowed for the utilization of the existing volume in aeration tanks, minimizing the required space for plant capacity extension. This approach enables the expansion of the plant's capacity within the current footprint, thereby reducing the impact on the landscape.

Figure 3.0 shows an extract of the overall layout illustrating the expansion and retrofit of Troia WWTP.

The treatment system employed for the expansion and retrofit of Troia WWTP consists of the following main steps: Liquid phase treatment: Intake with a 6 mm screening and equalization tank; Preliminary Treatment, with grit removal, degreasing and 1 mm screening; Biological Treatment in MBR; Addition of residual chlorine; WfR reservoir and pumping station; Infiltration ponds for excess unreused treated wastewater. Sludge Treatment: Sludge thickening; Sludge dehydration with centrifuge; Drying beds (reserve)

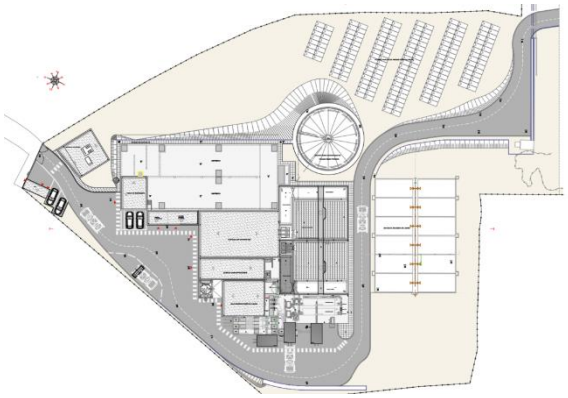


**Fig. 3.0** Troia WWTP Expansion and Retrofit General Layout (3)

**Acknowledgements**

This work was developed under the scope of the "Technical assistance during procurement, construction and commissioning phase of the design and build contract for extension and retrofitting of Troia WWTP. The authors would like to thank the members of TroiaResort – Investimentos Turísticos, S.A.

**References:**

(1) Troia General Infrastructure Design, 2006; (2) Troia WWTP operation data, 2017 and 2018; (3) Troia WWTP Rehabilitation Detailed Design, 2022.
Takashi Asano; Franklin Burton; Harold Leverenz; Water Reuse: Issues, Technologies, and Applications, 1st Edition; Metcalf & Eddy, Inc. an AECOM Company; 2007
Judd Simon; The MBR Book: Principles and Applications of Membrane Bioreactors for Water and Wastewater Treatment 1st Edition;2006

# Energy balances as tools for assessing carbon neutrality in urban water systems

Catarina JORGE[1], Maria do Céu ALMEIDA[2], Dália LOUREIRO[3], Maria Adriana CARDOSO[4], Dídia COVAS[5]

[1,2,3,4] Laboratório Nacional de Engenharia Civil, Av. do Brasil 101, 1700-066, Lisbon, Portugal
cnjorge@lnec.pt
mcalmeida@lnec.pt
dloureiro@lnec.pt
macardoso@lnec.pt

[5] CERIS, Instituto Superior Técnico, Universidade de Lisboa, Av. Rovisco Pais, 1049-001, Lisbon, Portugal
didia.covas@tecnico.ulisboa.pt

ABSTRACT

Urban water systems are essential infrastructures for urban sustainability. According to the International Energy Agency (IEA), the water sector uses 4% of the energy worldwide. The energy cost for wastewater and water supply systems is 30%-40% (IEA, 2019) of the energy global spending. These authors expect the energy consumption in the water sector to double by 2040. Influencing factors for this rise are the increasing use of desalination and higher coverage in wastewater treatment (IEA, 2016). The water supply and wastewater sectors are energy intensive and have a substantial energy footprint. Water utilities typically manage the services in these sectors, including the water supply and wastewater systems. Emissions from these utilities' activities are significant for greenhouse gas (GHG). Water losses and undesirable flows to sewers directly influence the performance and costs of water supply and wastewater systems. with significant effects on process efficiency, total energy consumption, and cost (Jorge *et al.*, 2022a).

A hydraulic energy balance comprises calculating the energy inputs and outputs in a system. These include energy use, dissipation, recovery, or generation (ISO 50002:2014, ISO, 2014). Several authors suggested the development of energy balances for urban water systems; research studies to assess energy use efficiency in water supply systems include, among other, Cabrera *et al.* (2010), Lenzi *et al.* (2013), Walski (2016), and Mamade *et al.* (2017). In the wastewater sector, existing studies focus on the integrated management of the urban water cycle (Loureiro *et al.*, 2020; Jorge *et al.*, 2022b); treatment processes (Nowak *et al.*, 2015; Silva *et al.*, 2016); the improvement of individual assets' efficiency, like pumps (Hou *et al.*, 2015; Zhang *et al.*, 2016) and reducing energy costs (Hashemi *et al.*, 2014; Menke *et al.*, 2015).

A systemic analysis of a water system simplifies the pursuit of opportunities to increase performance; unlike energy audits, energy balances do not focus solely on energy-consuming components. The detail required depends on the data available and the objectives of the analysis. Required information includes the system layout, equipment characteristics, data on energy supplied or produced, energy consumption by each subsystem or component, and estimation of dissipated energy. Calculation of the amount of energy consumed or dissipated during the transport is necessary. By itself, an energy balance will not affect energy consumption, but it highlights systems' inefficiencies and areas that need improvement.

Hydraulic energy balances for water supply and wastewater systems have diverse approaches depending on whether free surface or pressure flows predominate. In water supply systems, the basis for energy balances is pressure flows, while in wastewater systems, free surface flows predominate. Other important issues are data availability and calculation constraints; inventory data and measurement information gaps are more extensive in wastewater systems, among other specific issues associated with these systems. When presenting the

research work, differences between these approaches are discussed, and the feasibility to developing a common approach applicable to both types of systems.

Furthermore, operation and maintenance of water supply and wastewater systems requires several tasks involving the use of electric, gas, and fuel energy. If the aim is to achieve carbon neutrality in the water sector, a broader approach incorporating other types of energy including those used in operation and maintenance operations and the deploying of renewable energy resources (for instance solar photovoltaic generation, generation of electricity from small hydropower, generation of electricity from biogas) is required (Jorge *et al.*, 2022a). But emissions herein are not only associated with energy consumption or production; wastewater also contributes to global emissions with emissions of nitrous oxide and methane emissions (Ganigué *et al.*, 2014).

Different sources of energy, renewable or non-renewable, are used for the operation and maintenance of water systems, but the assessment of carbon neutrality status requires a systematic approach, including evaluation of all uses. A broader approach must be adopted to fulfil the aim of achieving carbon neutrality and consider the issue of emissions in these types of analyses. A discussion regarding the feasibility of comprehensive balances for managing hydraulic and non-hydraulic energy components and emissions, common for both water supply and wastewater systems, is included in the final presentation.

**References**


Cabrera, E., Pardo, M.A., Cobacho, R., Cabrera, E. Jr. (2010). Energy audit of water networks. *Journal of Water Resources Planning and Management*, 136, pp. 669–677.

Ganigué, R., Yuan, Z. (2014). Impact of oxygen injection on CH4 and N2O emissions from rising main sewers. Journal of Environmental Management, 144, 279-285, doi: 10.1016/j.jenvman.2014.04.023.

Hashemi, S.S., Tabesh, M., Ataeekia, B. (2014). Ant-colony optimization of pumping schedule to minimize the energy cost using variable-speed pumps in water distribution networks. *Urban Water J.*, 11 (5), 335–347.

Hou, S., Li, D., Xi, Y. and Cen, L. (2015). *Energy-saving optimization of urban drainage system based on pump performance.* In 27th Chinese Control and Decision Conference (2015 CCDC) (pp. 308-313).

IEA. (2016). *Water Energy Nexus - Excerpt from the World Energy Outlook 2016*. International Energy Agency. https://doi.org/10.1021/es903811p.

IEA. (2019). International energy agency - *world energy outlook*. p. 2019.

ISO. (2014a). *ISO 50002:2014(E): Energy audits - Requirements with guidance for use.* Geneve, CH.

Jorge, C., Almeida, M.C., Covas, D. (2022b). A novel energy balance tailored for wastewater systems. *Urban Water Journal*, 1-12. doi: 10.1080/1573062X.2022.2035409.

Jorge, C., Almeida, M.C., Brito, R. S., Covas, D. (2022a). Water, Energy, and Emissions Nexus: Effect of Inflows in Urban Drainage Systems. Water, 14(6), 868.

Lenzi, C., Bragalli, C., Bolognesi, A., Artina, S. (2013). From energy balance to energy efficiency indicators including water losses. *Wat. Sci. and Tech.: Water Supply*, 13(4), 889-895. doi:10.2166/ws.2013.103.

Loureiro, D., Silva, C., Cardoso, M.A., Mamade, A., Alegre, H., Rosa, M.J. (2020). The Development of a Framework for Assessing the Energy Efficiency in Urban Water Systems and Its Demonstration in the Portuguese Water Sector. *Water*, 12, 134; doi:10.3390/w12010134.

Mamade, A., Loureiro, D., Alegre, H., Covas, D. (2017). A comprehensive and well tested energy balance for water supply systems. *Urban Water Journal*, 14, pp. 853–861.

Menke, R., Abraham, E., Parpas, P., Stoianov, I. (2015). Approximation of system components for pump scheduling optimisation. *Procedia Engineering*, 119, 1059-1068.

Nowak, D., Krieg, H., Bortz, M., Geil, C., Knapp, A., Roclawski, H., Böhle, M. (2018). Decision support for the design and operation of variable speed pumps in water supply systems. *Water*, 10, 734.

Silva, C., Quadros, S., Ramalho, P., Alegre, H., Rosa, M.J. (2016). Translating removal efficiencies into operational performance indices of wastewater treatment plants. *Water Res.*, 57, pp. 202–214.

Walski, T. (2016). *Energy Balance for a Water Distribution System.* In Proceedings of the World Environmental and Water Resources Congress 2016, West Palm Beach, FL, USA, 22–26 May.

Zhang, Z., Kusiak, A., Zeng, Y. and Wei, X. (2016). Modelling and optimization of a wastewater pumping system with data-mining methods. *Applied energy*, 164, 303-311.

# Impact of Seawater inflows into Drainage Network on Water for Reuse Treatment – Case study of the Alvor Irrigation System

Carlos RAPOSO1, Paulo OLIVEIRA[2]

[1]Director of Hydraulics and Environment Service, TPF – Consultores de Engenharia e Arquitetura, S.A.
carlos.raposo@tpf.pt

[1] Deputy Director of Hydraulics and Environment Service, TPF – Consultores de Engenharia e Arquitetura, S.A.
paulo.oliveira@tpf.pt

RESUMO

TPF is currently executing a contract for the Alvor Hydro-Agricultural Scheme Modernization Project.

In the Terms of Reference (ToR) of this contract, in a diagnostic context, it is stated that if "*there is or will be in the short term a large increase in the demand for water for the irrigation of agricultural land within the area of AH Alvor or in land adjacent to it, the current availability of water will not be sufficient to meet such an increase* " as well as that, "*... the reduction in inflows that has occurred in the last decade raises doubt on whether the current extension of the perimeter is appropriate, since the limitations of water availability have not allowed the full use of irrigation in a sustained manner.*"

These ToR establish the need to identify water sources to reinforce water availability for irrigation and, among other possibilities, consider the Water for Reuse (WfR) produced at the Companheira WWTP, characterize the potential users (e.g. golf courses) and outline a technical solution to allow the use and deliver the WfR.

The studies and projects referred to in this contract are part of a National strategy, as illustrated in the Introduction of the "Guide for the Reuse of Water for Non-Potable Uses" (APA, 2019), where it is stated that "*In Portugal, water reuse should be seen as an opportunity not only to enable the expansion of some projects strongly dependent on water availability, but also to minimize the effects of droughts and shortages, as well as to improve the state of the environment, .... In addition, when compared to other alternative sources of water supply, such as desalination or water transfer, water reuse often requires lower investment and energy costs, and can in some situations also contribute to reducing emissions...*".

More specifically, it is expected to comply with the provisions of the Investment Line of the Algarve Regional Water Efficiency Plan (RE-CCT-C9-i1), under the scope of the Recovery and Resilience Program (PRR). This investment is part of the "Bases of the Algarve Regional Water Efficiency Plan (PREH)", in which several ministerial areas (Environment and Climate Action, Agriculture and Tourism) and the main stakeholders directly interested in the implementation of the solutions and the verification of their results were involved, with the coordination of APA - Portuguese Environment Agency, I.P. and DGADR - Directorate General for Agriculture and Rural Development.

The Portimão wastewater sanitation system is jointly managed by the Municipality of Portimão (Low system) and the company Águas do Algarve (High system), which is responsible for the operation and maintenance of the Companheira WWTP, including monitoring the volume and compliance with the quality parameters of the treated effluent defined in the respective license.

Considering the Legal Regime for the production and use of WfR (RJApR), Decree-Law No. 119/2019, August 21th, the monitoring data of the Companheira WWTP and the salinity reference values for irrigation established in the Decree-Law No. 236/1998, of August 1st (Conductivity Maximum Recommended Value[1] of 1000 uS/cm), a critical constraint was identified for the use of ApR in irrigation: the conductivity of the treated water of the Companheira WWTP is frequently above 2700 uS/cm, which is above the VMR[1] and close to the threshold of less sensitive crops (3000 uS/cm, crops severe restriction).

[1] Portuguese acronym: VMR

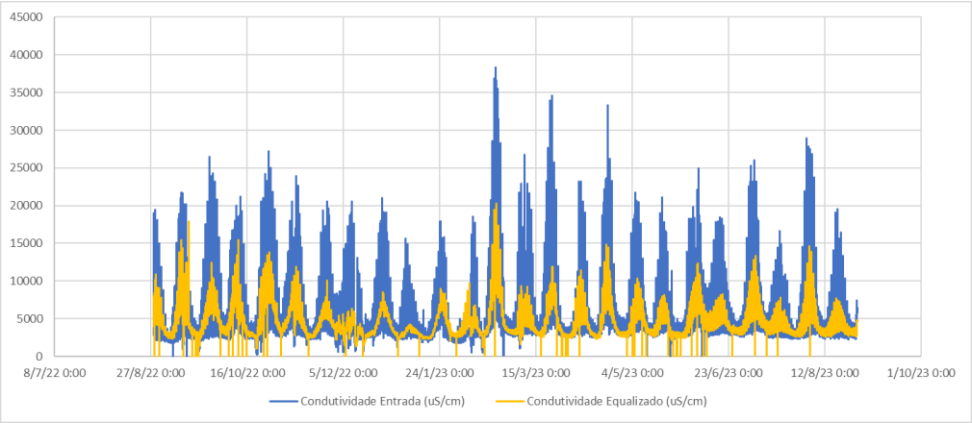



**Figure 1 –Conductivity of treated Water of the Companheira WWTP**

It was concluded that the high salinity of the treated water is due to the inflow of brackish water to the WWTP transported by the sewerage network.

Two options were considered to solve the problem: **(1)** improve the domestic wastewater drainage system of Portimão to minimize the entry of sea salt water, particularly accentuated during high tide periods or, **(2)** fine-tuning treatment for ApR production.

The **first option** suggested a joint work between the *Empresa Municipal de Águas e Resíduos de Portimão,* the *Águas do Algarve* and the APA, with close monitoring of DGADR and of the golf sector in order to perceive the possibilities of developing remediation measures (Inclusion of tidal gates in the collectors of lower areas of the city and strategic sectorization of the network, among others) in order to minimizing the undue seawater inflows in the wastewater collector system, which may have a very significant impact on the feasibility of reusing the WfR of the Companheira WWTP in irrigation.

Within the **second option** reverse osmosis (RO) and reverse electrodialysis (ED) solutions were analyzed. For both technologies is not expected to have acceptable economic sustainability for use by irrigation. On the other hand, the implementation of this type of technology always implies the rejection of a concentrate, so that the volume of water produced WfR will always be lower than the total volume of effluent from the WWTP. Considering current experience of these solutions it was assumed 40% of concentrate production.

Table 1 summarizes the comparison of both options.

**Table 1 – Summary of Options 1 and 2**

| Criteria | Option (1) | Option (2) |
|---|---|---|
| Distributed WfR flow (m3/day) | 20 600 | 12 360 |
| Investment cost, not accounting for the improvement of the collectors (€) | **5 883 861** | **21 816 956** |
| Operation and maintenance cost (€/year) | **473 102** | **1 169 148** |
| Investment + Opertion Costs (40 years at 4%) (€) | **15 247 869** | **44 957 644** |

Any of them can be **complemented** by mixing the WfR with natural water resources at the final distribution points, using real time monitoring of conductivity and storage situation at those reservoirs to fine tune the operation of the WWTP and of the pumping station feeding the distribution system.

This is possible because the golf courses have medium to high capacity reservoirs and because the water distributed by the irrigation system (Bravura dam) has a conductivity around 300 uS/cm (monitored).

Together with the first option, mixing will allow the WWTP to accept water with higher conductivity and so to reduce the complexity and standards of the rehabilitation of the existing network and, as well, the related investment cost. Together with the second option, will allow a higher treatment threshold for conductivity of the WfR and, so, to low down the desalination investment and the operation costs.

References:

APA, 2019. Agência Portuguesa do Ambiente, I.P. Guia para a Reutilização de Água para Usos Não Potáveis. Outubro de 2019 (versão 1.0)

Decree-Law No. 119/2019, August 21th

Decree-Law No. 236/1998, of August 1st

# Time Frequency Analysis of Anomalies in Water Distribution Networks Using Pressure Wave Signals

Marta CABRAL[1], José Pedro MATOS[2], Ana PAUSEIRO[3], Dídia COVAS[4]

[1,2,3,4] CERIS, Instituto Superior Técnico, Universidade de Lisboa, Lisbon, Portugal
marta.f.cabral@tecnico.ulisboa.pt
jose.matos@tecnico.ulisboa.pt
anamariapauseiro@tecnico.ulisboa.pt
didia.covas@tecnico.ulisboa.pt

ABSTRACT

The current paper aims at analysing the effect of different types, sizes and locations of anomalies in water distribution networks using transient pressure wave signals. Three time-frequency analyses are carried out to study the transient pressure features for each anomaly, including Fast Fourier Transform, Short-Time Fourier Transform and Continuous Wavelet Transform. Numerical and experimental data are used, considering different initial flow rates and initial sizes and locations of water leaks, entrapped air, and pipe blockages. Similar results for entrapped air are obtained for the three time-frequency analyses reinforcing that the presence of this anomaly leads to frequency components in the pressure wave signal and that, as the air pocket size increases, the main frequency tends to decrease as well as its amplitude. Obtained results from the frequency analyses can be integrated into classification/regression models to detect anomalies in water distribution networks and infer information about their properties (e.g., size and location).

## 1. Introduction

Water distribution networks inevitably undergo a degradation process, leading to the occurrence of anomalies, such as water leaks, pipe blockage, entrapped air and water contamination (Naderi and Pishvaee, 2017). Numerous utilities are challenged by the urgent need to replace their most degraded assets to meet existing and future requirements. This aspect is more significant in developed countries, where infrastructures were built decades ago and, often, little investment has been made in their renovation (Carriço et al., 2021). Several studies have been carried out to detect anomalous events in water distribution networks using flow time series (e.g., Loureiro et al., 2016). The current paper focuses on the analysis and discussion of the effect of anomalies in transient pressure wave signals using three methods of time frequency analysis: Fast Fourier transform (FFT), Short-Time Fourier transform (STFT) and Continuous Wavelet Transform (CWT). This study analyses the transient pressure features in simple pipe setups considering different types, sizes, and locations of anomalies.

## 2. Time Frequency Analysis

An existing hydraulic transient solver developed by Covas (2003) for pressurized water pipe networks is used to numerically generate pressure-head data. Three different anomalies are simulated, such as water leaks, air pockets and pipe blockages, representing potential issues that affect water distribution networks. Numerical data are complemented with experimental tests carried out in a copper pipe rig assembled at the Laboratory of Hydraulics, Water Resources and Environment of Instituto Superior Técnico, in Lisbon. The aforementioned three time frequency analysis methods (FFT, STFT, and CWT) are employed to study the dynamic effects of the anomalies in pressurized transient flows. Additionally, these analyses are useful to understand the effect of the initial flow rates and the initial anomaly sizes and locations in transient pressure features, such as the maximum and minimum pressure variations, the wave damping, and the wave phase shift.

Figure 1 presents the results obtained with FFT for a test case with a flow rate of 300 l/h and different air pocket sizes. FFT allows the transformation of a time-domain pressure wave signal into its frequency-domain representation, revealing its constituent frequency components. The first peak observed for an air pocket height of 1 mm (AP1) presents a frequency value close to the natural frequency of the system, i.e., 20.8 Hz. As the air pocket size increases, this main frequency tends to decrease as well as its amplitude.

Figure 2 depicts the comparison results of FFT, STFT and CWT for the same flow rate of 300 l/h and an initial air pocket size of 10 mm. STFT results present the frequency composition of the signal over time; whereas the CWT results show the time-frequency signal distribution, highlighting the presence of frequency peaks throughout the duration of the signal. Compatible results are obtained for the three methods, reinforcing the credibility of the observed frequency peaks and suggesting that entrapped air has a consistent and identifiable impact on the transient pressure wave signals.

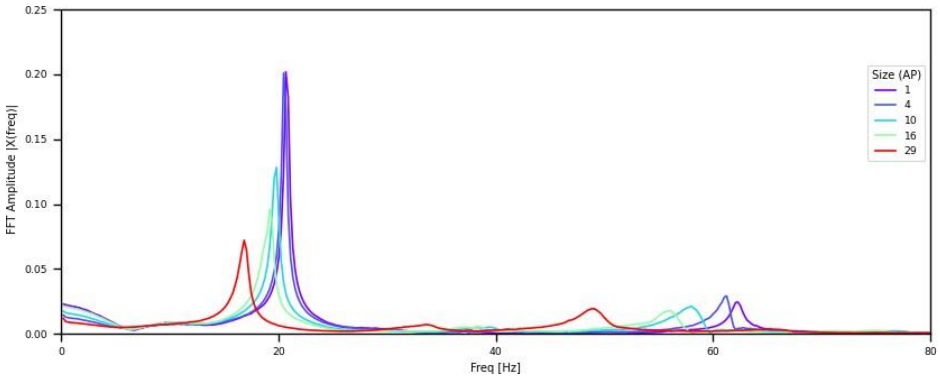



**Fig. 1.** FFT results for a flow rate of 300 l/h and different air pocket sizes.

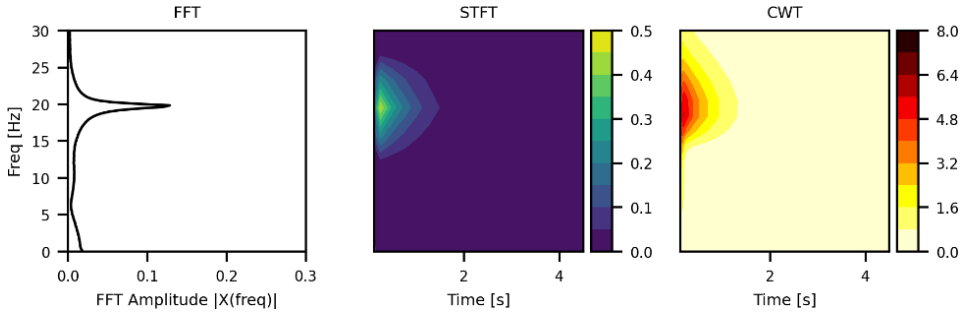



**Fig. 2.** FFT, STFT and CWT for a flow rate of 300 l/h and an initial air pocket size of 10 mm.

## 3. Conclusions

The time frequency analysis on pressure wave signals allows the quantification of their frequency components, which is a step forward in understanding the underlying phenomena and an essential step toward the identification and characterization of anomalies. Time frequency analysis will be applied to the anomalies of water leaks, entrapped air and pipe blockages and transient pressure features will be identified and characterized depending on the type of anomaly, size and location. Future works include the incorporation of frequency analysis results into classification models for identifying these anomalies in pressurized transient flows and classifying their size and location.

**Acknowledgements**

The authors would like to thank to the *Fundação para a Ciência e a Tecnologia* (FCT) through funding UIDB/04625/2020 from the research unit CERIS – Civil Engineering Research and Innovation for Sustainability, from Instituto Superior Técnico. The author Ana Pauseiro is grateful for the grant support by project number 1018P.01427.1.01.

**References**

Carriço, N., Covas, D., Almeida, M. C. (2021). *Multi-criteria decision analysis in urban water asset management*. Urban Water Journal, 18(7):558–569, DOI: 10.1080/1573062X.2021.1913613.

Covas, D. (2003). *Inverse Transient Analysis for Leak Detection and Calibration of Water Pipe Systems Modelling Special Dynamic Effects*. PhD Thesis, Imperial College.

Loureiro, D., Amado, C., Martins, A., Vitorino, D., Mamade, A., Coelho, S. T. (2016). *Water distribution systems flow monitoring and anomalous event detection: A practical approach*, Urban Water Journal, 13:3, 242-252, DOI: 10.1080/1573062X.2014.988733.

Naderi, M. J., Pishvaee M. S. (2017). *Robust bi-objective macroscopic municipal water supply network redesign and rehabilitation*. Water Resources Management, 31:2689–2711, DOI: 10.1007/s11269-017-1655-0.

# Advanced Image Processing Techniques to Analyse the Air Volume Variation in Pressurized Transient Flows

Marta CABRAL[1], João Paulo FERREIRA[2], Bernardo QUADRADO[3], Dídia COVAS[4]

[1,3,4] CERIS, Instituto Superior Técnico, Universidade de Lisboa, Lisbon, Portugal

[2] Department of Water Management, Faculty of Civil Engineering and Geosciences, Delft, Netherlands
marta.f.cabral@tecnico.ulisboa.pt
j.p.ferreira@tudelft.nl
bernardo.quadrado@tecnico.ulisboa.pt
didia.covas@tecnico.ulisboa.pt

ABSTRACT

The current paper aims at analysing the volume variation of air pockets in pressurized transient flows using video recordings and advanced image processing techniques. An experimental facility is used to collect pressure-head data and high-speed video recordings of air pockets during hydraulic transient events. In-house software is developed for image processing, including Gaussian filtering and Image sharpening. This study compares the experimental air pocket volume variation with the theoretical value obtained by the ideal gas law equation, assuming a constant temperature under different initial conditions.

## 1. Introduction

The existence of air is inevitable in any water pipe system. Air can enter into pressurised pipes through water intakes and remain in these systems due to malfunctioning of air valves (Ramezani et al., 2016). However, air can cause several types of problems in water supply and distribution, namely, increased local head losses that reduce the transport capacity and extremely high transient pressures that can compromise the system's safety and lead to pipe rupture (Lauchlan et al., 2005). The effect of air pockets on the pressure variation under a transient event was firstly investigated by Covas et al. (2006) and, later, by Ferreira et al. (2021). The current paper uses advanced image processing techniques to analyse the air volume variation in pressurized transient flows. This study estimates experimental air volume variation and compares it with the theoretical value obtained through the ideal gas law equation.

## 2. Experimental facility

Experimental tests collected in previous studies (Ferreira et al., 2021) carried out in an experimental pipe rig assembled at the Laboratory of Hydraulics, Water Resources and Environment of Instituto Superior Técnico, in Lisbon, are used herein. The rig consists of a copper pipe with a 15 m length, an inner diameter of 20 mm and a wall thickness of 1 mm. At the upstream part of the pipe, a centrifugal pump supplies the system with a rated flow rate of 3.6 $m^3$/h and a maximum head of 44 m from a tank with a capacity of 0.1 $m^3$. Immediately downstream of the pump, a 60 l hydropneumatic vessel is installed to simulate a constant level reservoir and to stabilize the pressure coming from the pump. At the downstream end of the system, a pneumatic actuated valve is installed to generate transient events. A manual quarter-turn ball valve is located after the pneumatic actuated valve to control the initial flow rate. The air pocket is simulated experimentally by injecting air into an acrylic cylinder with a drilled hole inside, installed at 7.83 m from the pneumatic valve. The hole has an inner diameter of 5 mm and a total length of 51 mm. The height of the air pocket during the initial steady state is used to identify each air pocket size (i.e., AP10 has 10 mm of initial height).

The data acquisition system is composed of one computer, an oscilloscope, two strain-gauge flush-mounted pressure transducers, an electromagnetic flow meter and a high-speed camera. The first pressure transducer (PT1) is located at the upstream side of the pneumatic valve (distanced +/- 0.22 m) and the second pressure

transducer (PT2) is located just below the air pocket. The Allied Vision Bonito CL-400B 200 fps high-speed camera allows a frame rate of 193 fps for a 2320 × 1726 pixels resolution, higher frame rates can be achieved with lower resolutions. The data acquisition is synchronized by a trigger system that sends a signal to start both the video recording and the pressure data acquisition. Both pressure data and image recordings were acquired with a 1000 Hz frequency.

## 3. Image processing

The image processing is carried out using in-house software developed in MATLAB. Fig. 1 presents the several steps applied in the image processing for a flow rate of 100 l/h and an initial air pocket size of 2.5 mm. Firstly, the original image (Fig. 1a) is transformed into a negative one by subtracting the water-filled cylinder (Fig. 1b) and two different filters are applied (Fig. 1c), the Gaussian filtering and the Image sharpening. The Gaussian filtering assesses the colour of each pixel by comparing it to the adjacent ones, and by changing the colour of the pixel to better match its neighbours through the adjustment of the sigma value or the standard deviation of the function. This filter allows to blur or unblur the negative image. The Image sharpening uses an unsharp masking technique, that first blurs the image, creating a mask that when combined with the initial image creates a sharper result. Finally, the filtered image is binarized to identify what is or is not air (Fig. 1d).

Fig. 1(e) presents transient pressure-head values collected at transducers PT1 for a flow rate of 100 l/h and an initial air pocket height of 2.5 mm, as well as the experimental air pocket volume variation obtained through image recording and processing. A fast effective valve closure generates the transient event, in which a pressure wave propagates back and forward in the pipe system, with successively positive (overpressures) and negative (underpressures) amplitude of pressure that decays over time. The air pockets in the pipe system will expand and compress respectively with the underpressures (that releases energy) and overpressures (that absorb energy).

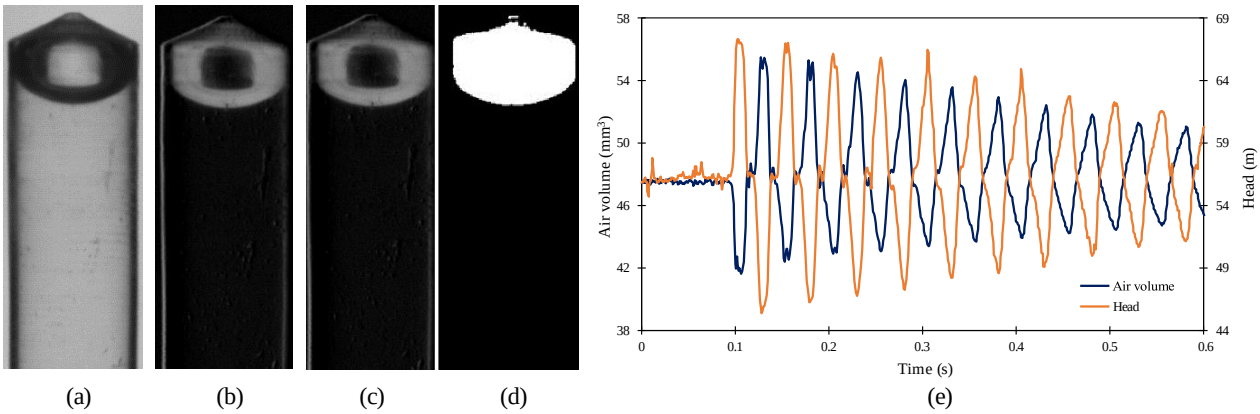



**Fig. 1.** Image processing and results for a flow rate of 100 l/h and an initial air pocket size of 2.5 mm: (a) original image; (b) negative image; (c) filtered image; (d) binarized image; (e) air volume and head variation.

## 4. Conclusions

This study allows to estimate the experimental air volume variation using advanced image processing techniques and to compare it with the theoretical value obtained through the ideal gas law. This analysis will be applied for different initial flow rates (i.e., between 100 and 300 l/h) and for different air pocket sizes (i.e., between 2.5 and 10 mm). Experimental tests include two types of behaviour: one associated with lower transients, characterized by an air pocket volume variation with a clear air-water interface; and another one associated with more severe transients in which air mixes with water.

**Acknowledgements**

The authors would like to thank to the *Fundação para a Ciência e a Tecnologia* (FCT) through funding UIDB/04625/2020 from the research unit CERIS – Civil Engineering Research and Innovation for Sustainability, from Instituto Superior Técnico.

**References**

Covas, D., Ramos, H., Lopes, N., Almeida, A. B. (2006). *Water Pipe System Diagnosis by Transient Pressure Signals*, in Water Distribution Systems Analysis Symposium 2006. Cincinnati, Ohio.

Ferreira, J. P., Buttarazzi, N., Ferras, D., Covas, D. (2021). *Effect of an Entrapped Air Pocket on Hydraulic Transients in Pressurized Pipes*. Journal of Hydraulic Research, 59(6), 1018–1030, DOI: 10.1080/00221686.2020.1862323.

Lauchlan, C. S., Escarameia, M., May, R. W. P., Burrows, R., Gahan, C. (2005). *Air in Pipelines: A Literature Review*. Report SR 649, HR Wallingford.

Ramezani, L., Karney, B., Malekpour, A. (2016). *Encouraging Effective Air Management in Water Pipelines: A Critical Review*. Journal of Water Resources Planning and Management, 142(12): 04016055. DOI: 10.1061/(ASCE)WR.1943-5452.0000695.

8th IAHR EUROPE CONGRESS
LISBON - PORTUGAL
4-7 JUNE 2024

# Hydraulic transients in water supply systems with hydropower plants

Dídia I. C. COVAS[1*], João P. FERREIRA[2], João N. DELGADO[3], Marta CABRAL[4], António B. ALMEIDA[5]

[1,3,4,5] CERIS, Instituto Superior Técnico, Universidade de Lisboa, Lisbon, Portugal

[2] Department of Water Management, Faculty of Civil Engineering and Geosciences, Delft, Netherlands
[1]didia.covas@tecnico.ulisboa.pt

ABSTRACT

The current paper aims at presenting the hydraulic transients analysis and the proposed surge protection devices, designed for three micro-hydropower plants to be installed in existing water supply systems in Portugal. Surge protection is designed for the most severe operating scenario, the full load rejection of the turbine with a wicket gate closure. Different surge protection solutions have been analysed. The three solutions have a bypass pipe to the turbines coupled with other surge protection devices – a downstream surge tank or a set of pressure relief valves – to ensure double surge protection to the water supply whose main purpose is to transport water to downstream municipalities.

## 1. Introduction

Water supply and wastewater systems are essential infrastructures to provide access to safe drinking water and the sustainable management of sanitation, while preserving the health and well-being of the population. Still, the water and wastewater sectors account for a 3.5% share of all the electricity use in the European Union in 2018 and, in Portugal, water supply infrastructures are responsible for a 60% share of the water sector consumption [1]. Experience has shown that these systems have a high potential for energy recovery at sites with already installed flow or pressure control valves, typically at the upstream end of storage tanks, at delivery points or at the inlet of pressure management areas [2-4]. Several technologies are available for energy recovery [5]. The installation of hydropower plants has several benefits to the water utilities, not only allowing electricity generation and the inherent economic benefit, but also the reduction of the normal operating pressures, and the reduction of burst frequency and water losses. EPAL has done a survey to identify the sites with the highest potential for energy recovery. The produced electricity is primarily used for self-consumption within the utility or used by other utilities from the AdP group. These projects contribute to reduce the carbon footprint and to reach carbon neutrality in the AdP group. This paper reports the hydraulic transient analysis conducted in three systems with new hydropower plants to be installed in the EPAL systems.

## 2. Case studies description

The hydropower plants presented herein are located in the Castelo do Bode bulk water supply system. The first is the Asseiceira hydropower plant located 600 m downstream of Asseiceira water treatment works, the second is located 500 m upstream Várzea das Chaminés storage tank and the third is located immediately upstream of the Amadora tank. All trunk mains have over 30 km and are composed of two parallel lines with a large diameter (DN1000-1800), made of reinforced concrete and/or steel. The design of the hydropower systems was carried out based on the transported flow rate time series and the available heads at those locations. The rated characteristics of the turbines were specified to maximize the recovered energy. The main characteristics of the pipe systems, hydropower plant and surge protection are summarized in Table 1.

**Table 1 – Summary of main characteristics of the systems**

| Case | Solution | Discharge range [rated] ($m^3/s$) | Head range [rated] (m) | Installed power (kW) | Annual energy (GWh) | Surge protection (this analysis was carried out for 110% rated discharge) |
|---|---|---|---|---|---|---|
| Asseiceira | One Kaplan | 4 – 6 [6.5] | 15 - 30 [25] | 1500 | 10 | Bypass pipe with a needle valve DN1600 ($Q_{max}$=6.5 $m^3/s$) + Downstream surge tank (500 $m^3$) |
| Várzea das Chaminés | One Francis | 3 - 5 [5.5] | 20 - 45 [32] | 1500 | 12 | Bypass pipe with a needle valve DN1200 ($Q_{max}$=4.50 $m^3/s$) + Surge relief valves 6×DN700 ($Q_{max}$=4.50 $m^3/s$; $H_{open}$=85 m) |
| Amadora | One/two | 0 - 1.5 | 5 - 33 | 110×2 | 0.62 | Bypass pipe with a needle valve DN600 ($Q_{max}$=1 $m^3/s$) or Surge |
| | Francis | [0.5×2] | [25] | | | relief valves ($Q_{max}$=1 $m^3/s$; $H_{open}$=41 m) |

## 3. Hydraulic transient analysis

The surge protection devices were designed for the emergency operation of the hydropower plants, corresponding to the full load rejection of the generator due to an electrical power grid failure, while the turbines are operating at the maximum discharge. Design criteria were: (i) maximum pressures not exceeding 15% of the static pressure; (ii) sub-atmospheric pressures not occurring and (iii) the turbine overspeed not exceeding 2.2 times the rated speed.

The surge protection of the Asseiceira system consists of the construction of a turbine bypass pipe with a flow control valve and a 500 $m^3$ tailrace surge tank immediately after the turbine and the bypass. This tank allows higher operational flexibility to the system. Results have demonstrated that, with this surge protection, extreme pressure variations in the downstream pipeline are negligible (Fig. 1): minimum pressures correspond to the initial hydraulic grade line and maximum overpressures are lower than 5 m from the energy grade line from steady state flow. This is because the surge tank installed immediately after the turbine protects the downstream pipe, attenuating the transient pressures generated by the turbine, the wicket gate and the bypass valve. The water level in the surge tank variation corresponds to a maximum volume variation of 70 $m^3$.

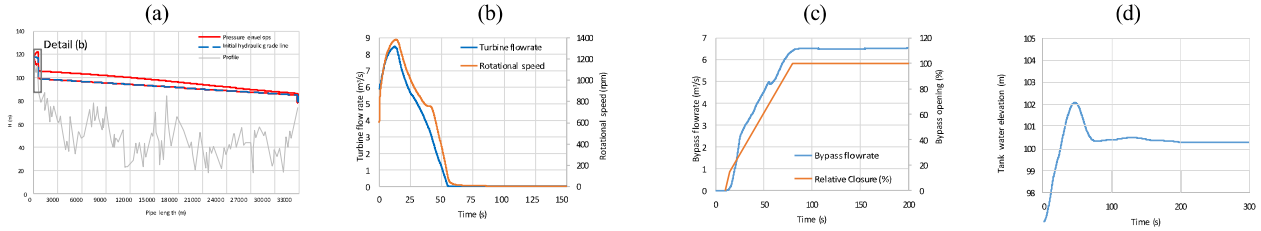



**Fig. 1** – Asseiceira system. Simulation results for the load rejection with wicket gate closure in 55 s and bypass opening in 55 s: (a) piezometric-head envelopes; (b) turbine flowrate and rotational speed; (c) bypass discharge and valve opening; (d) surge tank water level.

The Várzea das Chaminés System has a bypass pipe with a flow control valve and a set of pressure relief valves. Surge protection is mostly ensured by the safety bypass, as the total volume discharged by the surge relief valves is 6 $m^3$, with a maximum discharge of 0.9 $m^3/s$. Amadora system is protected either by a bypass with a safety valve or by a set of surge relief valves. Given the low-pressure surges occurring in the system, it is not needed the installation of two devices. Pressure envelopes for these two systems are presented in Fig.2.

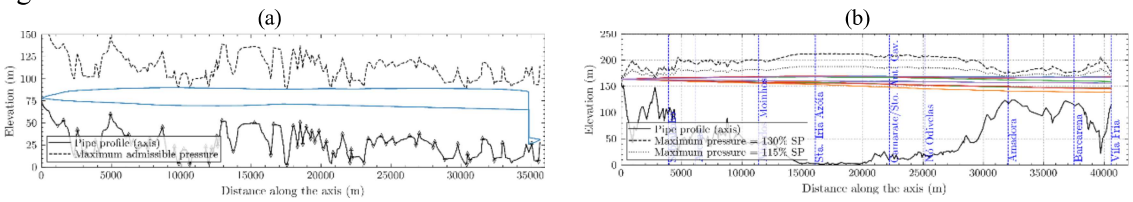



**Fig. 2** – Piezometric-head envelopes for: (a) Várzea das Chaminés System; and (b) Amadora system.

## 4. Conclusions

This paper presents three case studies of surge protection necessary to be installed after the construction of hydropower plants in existing water supply systems. Hydraulic transient analyses were carried out for the most severe situation that can occur in hydropower plants – the turbine total load rejection of the electric grid for the maximum discharge. The first system (Asseiceira), under construction, has two surge protection devices – a bypass pipe with a safety valve and a tailrace pressure tank – to ensure double protection. The second (Várzea das Chaminés) was also protected with two surge protection devices: a bypass and a set of surge relief valves. In the third, only one surge protection device is necessary given the small transients generated.

**Acknowledgements**

The authors would like to thank to the *Fundação para a Ciência e a Tecnologia* (FCT) through funding UIDB/04625/2020 from the research unit CERIS – Civil Engineering Research and Innovation for Sustainability, from Instituto Superior Técnico.

**References**

[1] ERSAR and ADENE (2018). *The efficient use of energy in the water and wastewater services, Technical guide n. 24, ISBN 978-972-98996-5-2 (in Portuguese).*

[2] McNabola, A., P. Coughlan, L. Corcoran, C. Power, A.P. Williams, I. Harris, J. Gallagher, and D. Styles (2014). *Energy recovery in the water industry using micro-hydropower: an opportunity to improve sustainability.* Water Policy. **16 (1): 168–183.**

[3] MR, N.V. and P.B. JA. (2014). *Energy and hydraulic efficiency in conventional water supply systems.* Renewable and Sustainable Energy Reviews. **30:701–14**.

[4] Delgado, J., J.P. Ferreira, D.I.C. Covas, and F. Avellan (2019). *Variable speed operation of centrifugal pumps running as turbines. Experimental investigation.* Renewable Energy. **142**: p. 437-450.

[5] Breeze, P. (2018). *Hydropower. Elsevier, London, U.K*

# Hydraulic Analyses of a Sustainable Urban Drainage System for Highly Urbanized Areas

James LI[1], Darko JoksimOVIC[2], Celia FAN[3], Patelle FONG[4], Boji CHEN[5], and Bianca DICKEL[6]

[1,2,3,4] Department of Civil Engineering, Toronto Metropolitan University, Canada
jyli@torontomu.ca; darkoj@torontomu.ca; celia_fan@hotmail.com; patelle.fong@torontomu.ca
[5] Department of Civil Engineering, University of Hong Kong, Hong Kong, China
bojichen@connect.hku.hk
University of Siegen, Germany
bianca.dickel@student.uni-siegen.de

ABSTRACT

A full-scale (46m x 2.3m x 1.7m) sewer model was used to study the hydrologic/hydraulic performance, and sediment accumulation of an innovative Sustainable Urban Drainage System (SUDS) for highly urbanized areas. The SUDS, termed Toronto Exfiltration System (TES), was developed in the City of Toronto to capture urban runoff along the pore space of the granular sewer trench between connecting manholes and allow exfiltration to the underlying soil. The objectives of the TES experiments were to determine (1) the hydraulic grade lines (HGL) along the TES; (2) the inflow and outflow rates through the TES; and (3) the sediment accumulation rate, under various inflow conditions. It was found that (1) the unsteady HGLs during the filling of TES storage showed a high inlet loss and a gentle system head loss; (2) an average 30% attenuation of the inflow peak rates; and (3) sediment accumulation inside the two PVC perforated pipes was about 40% of the inflow sediments. The data collected will be used to calibrate a hydrologic/hydraulic model for the simulation of TES performance under different hydrologic design conditions.

## 1. Toronto Exfiltration System (TES)

Urbanization causes high peak runoff rates and volume and shorter time to peak runoff rates, resulting in surface flooding, channel erosion, and associated water pollution problems (Bradford and Denich 2007; Egodawatta *et al*. 2012). The Toronto Exfiltration System (TES) was designed to exploit the pore space within the sewer trench for runoff retention and attenuation. Figure 1 shows a schematic of the 2.5 km of TES in Toronto. Two perforated pipes (downstream ends plugged) were installed below the storm sewer between connecting manholes within the sewer trench. An orthogonal concrete cut-off wall was installed at the downstream manhole (Manhole 3) to promote exfiltration between connecting manholes (Manhole 2 and 3). Runoff enters the perforated pipes (manhole 2), fills the porous space of the trench, and exfiltrates to the underlying soil. To promote the use of TES under other hydrologic design conditions, we need to collect hydrologic and hydraulic data to calibrate a design hydrologic/hydraulic model.

Sponsored by the Collaborative Urban Drainage Research Labs Communities, a full-scale sewer model (46m x 2.3m x 1.7m) sewer model was constructed and tested at the Integrated Civil and Infrastructure Research Centre of the University of Sheffield in the United Kingdom. The objectives of the TES experiments were to determine (1) the hydraulic grade lines (HGL) along the TES; (2) the inflow and outflow rates through the TES; and (3) the sediment accumulation rate, under various inflow conditions.

## 2. Methods

The full-scale hydraulic model was designed for a small drainage area, as shown in Fig. 2. The total length was 46 m with a 300 mm concrete storm sewer, seven 1.2 m standard concrete manholes, and two 200 mm PVC perforated pipes with end plugged. The left and right sections represent sandy and clay underlying soil.

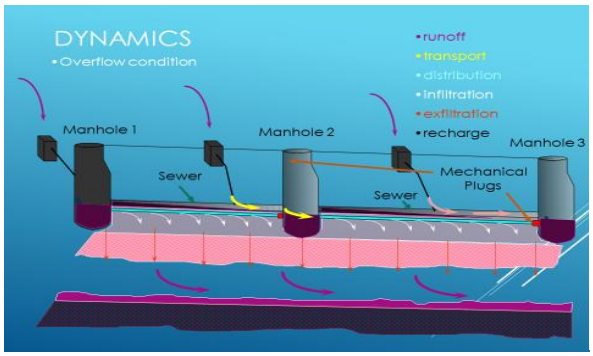



**Fig. 1.** Schematic of the TES.

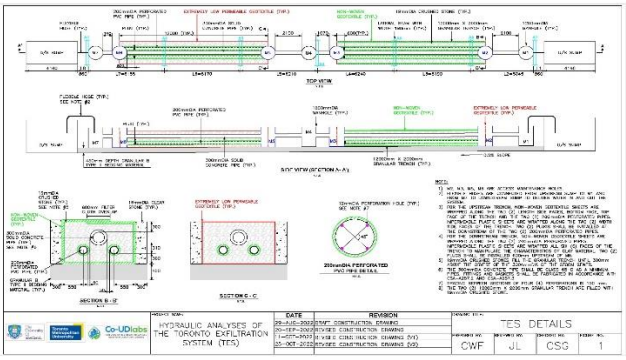



**Fig. 2.** Full-scale Hydraulic Model of the TES.

Three flow testing groups were devised: (1) three steady-state inflows (3 to15 L/s); (2) two unsteady inflow hydrographs (5-year, 10-year, 50-year 1-hr design storm); and (3) one 4-hr unsteady inflow hydrograph for sediment experiments. A computerized inflow header tank was used to simulate all experimental flows. For the sediment experiments, silica flour ($d_{50}$ 39 microns, $d_{90}$ 105 microns, $d_{10}$ 6 microns) was used to simulate typical runoff sediments in urban areas. Each flow experiment was repeated three times.

Eighteen wave probes were used (at 100 Hz) to measure the hydraulic grade lines at the upstream manhole, along the two PVC perforated pipes, at the four corners of the sewer trench, the downstream manhole, and the terminal downstream manhole (M7). Inflow was measured at 10 Hz by a calibrated Siemens flowmeter, while the outflow was measured at 100 Hz using the wave probe and a calibrated weir at M7. Instantaneous velocities were measured at the inlets of the two PVC pipes using an ADV velocity meter.

## 3. Results

The experimental results of the clay section are reported here. Three general observations are listed below.

1. Runoff at the upstream manhole entered the inlets of the two PVC pipes, filled the two 200 mm PVC pipe volume and the 30% porosity space of the trench, and eventually overflowed to the 300 mm upper storm sewer. The unsteady hydraulic grade lines along the inlets of the PVC perforated pipes to the plugged ends showed a relatively high inlet loss and a gentle system head loss.
2. Steady or unsteady inflow rates were attenuated by the system storage (which was about 3 $m^3$ over the left 10 m section) until it overflowed to the upper storm sewer. In general, the peak inflow rates were attenuated to lower outflow rates by an average of 30%.
3. An average 4-hour design runoff event of a typical urban drainage area in Toronto was used to estimate the runoff sediment trapped within the two 200 mm PVC perforated pipe. Test results indicate the trapping efficiency was about 40%.

## 4. Conclusions

Preliminary results of the clay section indicate that (1) the performance of TES can be improved by reducing the inlet head loss of the two 200 mm PVC perforated pipes (e.g., smooth and beveled inlets); (2) the peak runoff controlled under frequent storm events (e.g., 5-year) is encouraging for only a 10 m sewer section; and (3) the sediment accumulation rate can be used to estimate the maintenance frequency of the two PVC perforated pipes.

**Acknowledgments**

The research team would like to acknowledge the research support by Prof. Simon Tait and Fabio Muraro, PhD Candidate (University of Sheffield, UK). Additionally, the planning support by Prof. J. Leandro (University of Siegen, Germany), Dr. May Chui (University of Hong Kong), Dr. S. Gholamreza-Kashi (GHD Canada Ltd.), William Trenouth (AECOM Canada Inc.), and Dr. S. Chan (Binnies Hong Kong Ltd.) are appreciated.

**References**

Bradford, A.; Denich, C. (2007) Rainwater management to mitigate the effects of development on the urban hydrologic cycle. Journal of Green Building, 2(1), 37-52.
Egodawatta, P.; Miguntanna, N.S.; Goonetilleke, A. (2012) Impact of roof surface runoff on urban water quality, Water Science & Technology, 66(7), 1527-1533, DOI: 10.2166/wst.2012.348.
Li, J.; Joksimovic, D.; Tran, J. (2015) A Right-of-Way Stormwater Low Impact Development Practice. J. of Water Management Modeling, DOI: 10.14796/JWMM.C390.

# Water Neutral Garden Calculator

Tse-Hui TEH[1], Adrian BUTLER[2], Javid YOUSAF[3], Svea RAUTENBERG[3], Carl WATSON[3]

[1] University College London, United Kingdom
t.teh@ucl.ac.uk

[2] Imperial College London, United Kingdom
a.butler@imperial.ac.uk

[3] British Geological Survey, United Kingdom
jyou@bgs.ac.uk

ABSTRACT

The expansion of private paved surfaces is one of the causes of flash flooding in urban areas in London. This problem is not unique to London. It can be seen in any private vehicle dominated city in the world. Vehicles need smooth surfaces to drive, then they need paved surfaces to park. People want to park them in locations convenient to loading and unloading the vehicle, therefore they pave a driveway to their front or rear door, a carport, or a garage. While this is all logical, it leads to a reduction of water permeable land surfaces and an expansion of impermeable surfaces. These impermeable surfaces drain water rapidly into sewer systems. Sewers that become overwhelmed, either flooding roadways or flow into urban waterways which can also flood.

The three main difficulties of this problem are that it is both distributed, private and unknown. Each landholder is only responsible for a relatively tiny portion of the problem. On its own, no single private driveway is responsible for flooding, but collectively the impact is immense. Each landholder is also free to pave whatever land they own without care or governmental oversight of its collective impact. Finally, no landholder knows that their paved driveway is a problem. The water drains away from their site and the flooding occurs elsewhere: on another street, in another neighbourhood, in a watercourse far away.

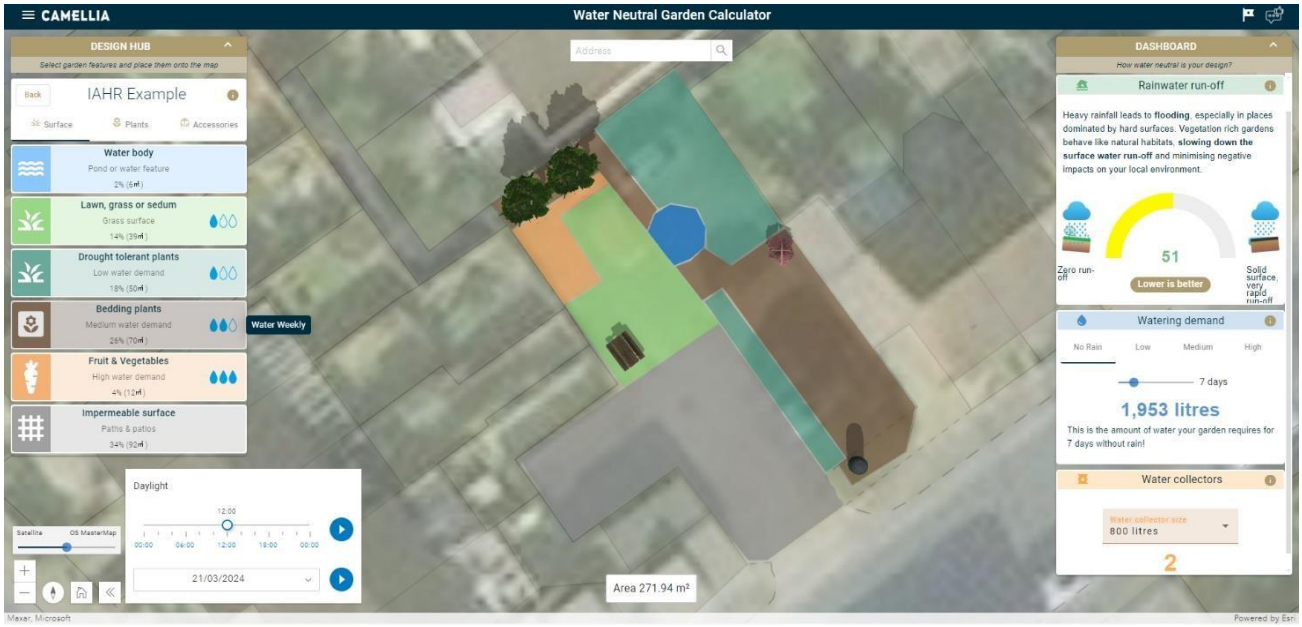
Is it possible to get people to care and change their paved areas back to garden? The Water Neutral Garden Calculator gives information to enable people to see their effects on flooding, and water use for gardening, to facilitate thinking about this change.

The calculator was initially developed for a specific housing estate in the borough of Southwark, London, to redesign a concrete paved area to become blue-green infrastructure aka a community garden. The calculator was successfully used by the community to codesign a garden that alleviated flooding. From this experience it was decided by the research team to put effort to change the calculator from a bespoke system into one that could be used widely.

The Water Neutral Garden Calculator (https://mapapps.bgs.ac.uk/water-neutral-garden-calculator/) can now be used all over the United Kingdom (UK) and any geographic area with similar precipitation to the UK. It allows you to find your property, described both as an ordnance survey map and a satellite map giving you both your property boundary and what is existing on the ground which helps with understanding the scale which you are drawing. After finding your property you can draw a garden on it with varying planting types: high, medium and low water needs; as well as paved surfaces and water bodies. The website then gives you estimates of how much water you would attenuate to prevent flooding with this garden, and how much water you need to store in order to keep your plants alive both in litres and standard sized water butts for 7-20days without rain. There are also three-dimensional components of plants, trees, garden furniture and buildings for you to decorate the surfaces, think about sunlight and shade in the garden, have fun, and make it look like your garden, or the garden of your dreams (Figure 1).

The estimate of both water needs for plants and water attenuation are based on the surfaces that have been drawn. If you draw a paved surface, your flood score will show that 100% of the water will runoff that surface and no water is necessary for plants. If you draw a surface of planting, your flood score will show approximately 30% of the water will runoff that surface, and some litres of water will be necessary to keep the plants alive. The litres of water to keep the plants alive will depend on whether low, medium or high water need planting (Ayling etal 2021) was selected and the area of planting drawn. It was assumed that if the area was lawn, no watering was necessary, therefore it achieved the highest amount of rainwater attenuation and only 10% of water would runoff the surface.

The water requirement for the planted areas is associated with the number of days without rain, which can be set from 7-20days. This is because most plants need watering every one or two weeks, so 7 days with no rain would be the minimum water storage required to keep the garden alive without resorting to a piped water supply. Our statistical analysis of 10,059days (28.5years) of weather records at Heathrow Airport, showed that 17days without rain is likely to happen once a year in London.




The original bespoke garden water calculator was used to successfully bid for a community greening project administered by the metropolitan authority. The current calculator is in the process of being modified so that it can be used by local authorities to incentivise private residents with a small amount of funding to connect their roof runoff to water collectors, install green roofs, and replace paving with plants.

The Water Neutral Garden Calculator is a web-based modelling tool which is free for all users. Its aim is to be an educational tool to open the conversation about how private actions impact flooding and water ecologies. It shows how gardens can prevent flooding, how paving contributes to flooding, and how much water different types of planting requires to stay alive. All of these calculations are broad estimates but give enough information for the effects to be seen and acted upon. By making this information free and fun to use, it is hoped that more people, policy makers, landscapers, gardeners and funders can increase their impact to prevent flooding and create gardens that make use of available rainfall. Thereby creating more ecologically sensitive places to live.

**Acknowledgements**
Natural Environment Research Council (NERC) United Kingdom, funded project, “CAMELLIA: Community Water Management for a Liveable London”, NE/S003495/1.
Professor Sarah Bell for her inputs into the original garden water calculator. Dr Charlotte Johnson for her inputs into the original garden water calculator and her contributions to the initiation of the water neutral garden calculator.

**References**

Ayling SM, Phillips N, Bunney S. Allotments in the Future: Building Resilience to Climate Change through Improved Site Design and Efficient Water Practices. Water. 2021; 13(11):1457. https://doi.org/10.3390/w13111457
British Geological Survey, Imperial College London, University College London (31/1/2023) Water Neutral Garden Calculator. https://mapapps.bgs.ac.uk/water-neutral-garden-calculator/ (accessed 30 October 2023)

# Little catchments on the rooftop - effects of irrigation on water, matter and heat fluxes in green roofs

Björn HELM[1], Laura Elisa HERR[1], Richard WALTHER[2], Valeri GOLDBERG[3], Peggy FREUDENBERG[4]

[1] TU Dresden, Chair of Urban Water Management | bjoern.helm@tu-dresden.de, laura_elisa.herr@tu-dresden.de

[2] TU Dresden, Chair of Landscape Engineering | richard.walther@tu-dresden.de

[3]TU Dresden, Chair of Meteorology | valeri.goldberg@tu-dresden.de

[4]TU Dresden, Chair of Building Services and Climate Responsive Architecture | peggy.freudenberg@tu-dresden.de

ABSTRACT

This contribution concludes some findings of experimental research at the green roof research facility Dresden. The facility provides a monitoring system for coupled water, heat and matter fluxes in irrigated green roofs. Experimental results from 2020 to 2022 demonstrate that irrigation improves evaporation potential, substrate and surface cooling as well as plant vitality in green roofs. In contrast, stormwater retention is reduced.

## 1. Introduction

An increasing number of people experience the adverse effects of heat waves in urban areas.Global warming and ongoing urbanization reinforce one another and contribute to the urban heat island phenomenon. Factors such as greater heat retention, reduced reflection of solar radiation, and a lack of evaporative cooling potential compared to natural areas, alter the energy balance and result in higher temperatures within urban zones. Plant covered, pervious surfaces provide conditions with more natural energy and water balances, as concluded by (Antoszewski et al., 2020). Green roofs have been promoted and extensively researched as a suitable solution for existing and newly built roof areas. Irrigation of green roofs decreases sensitive heat emission and surface temperatures (Coutts et al., 2013) and supports plant diversity and may even become a necessity in summer in order to keep the vegetation vital (MacIvor et al., 2013) and ensure evaporative cooling in draught conditions (Suter 2018). Despite the potentials, previous research predominantly focused on non-irrigated extensive green roofs. Only 5% of the studies reviewed by (Van Mechelen et al., 2015) involve irrigation demands and consequences. (Oberndorfer et al., 2007) demand focused research on water quality dynamics in green roofs and specifically potentials and challenges related to greywater reuse.

## 2. Material and Methods

### *2.1. Research facility*

The research facility is located on the rooftop of a basement level building, which houses common rooms and service amenities of the botanical garden employees. The total roof area is 210 m² of which 75 m² are designated for 21 experimental parcels. The green roof is configured as semi-intensive with 26 plant species adapted to different light exposure and water requirements. Grey water from showers and washing amenities is collected, stored and treated in a constructed wetland. A real-time controlled irrigation system conveys the treated water to the experimental parcels distributes it with dripper hoses. The parcels are all placed at the edge of the roof and grouped in sections of varying exposure to shade and contain different plant compositions.

### *2.2. Data collection, study design and data evaluation*

The measurement configuration enables a high-resolution monitoring of environmental climate, building climate as well as water, matter and energy fluxes in the green roof layers. Helm et al. (2019) give a detailed overview on the sensor selection and configuration. The evaluation includes the calendar years 2020 - 2022

with May to October as irrigation periods. Three levels of irrigation intensity (0.6, 1.2 and 2.4 mm/d) are compared to non-irrigated conditions. In addition to the sensor based, continuous evaluation of water and energy balances, plant conditions are rated every two weeks. The water balance of each parcel is obtained from measured inflow, outflow and change in substrate water storage with evaporation as remainder. Mean monthly evaporation rates are compared and related to plant rating and climate conditions. A daily water balance simulation validated the measurement based balances. Substrate and surface temperatures are set in relation to water balance components and plant ratings.

## 3. Results

### *3.1. Water balance and runoff*

Maximum irrigation enables an increase of 1.1 mm/d evaporation during the irrigation period. This corresponds to 58% more than non-irrigated conditions and 83% of potential evaporation. Even minimum irrigation increases the evaporation by 28%. At the same time, drought stress (water content lower than 50% of field capacity in the substrate layer) is reduced by irrigation. Non-irrigated parcels experience on average 110 days of drought stress per year, of which 102 days occur during the irrigation period. The second number is reduced to 83 and 18 days by minimum and maximum irrigation respectively. 43 storm events with a total height of more than 5 mm and a maximum intensity of more than 2 mm/h provide a reference for stormwater retention. During non-irrigation periods (November to April), green roofs reduced the runoff volume by 17% and peak discharge by 43%. Non-irrigated roofs achieved 64% volume reduction and 58% peak reduction, whereas maximum irrigated roofs performed with 38% volume reduction and 52% peak reduction.

### *3.2. Plant vitality*

All plant vitality parameters, including overall appearance, coverage rate, flower quantity, leaf size and plant volume perform best under a maximum irrigation regime. Despite this, improvements in vitality are not linearly related to irrigation volume. Plants with intermediate irrigation exhibit vitality parameters almost as good as those with maximum irrigation. Moreover, higher precipitation volumes during the irrigation season 2021 led to reduced differences in plant vitality. By contrast, an extended drought and heat period in summer 2022 caused dehydration and die back, even of drought tolerant non-irrigated plant species.

### *3.3. Thermal response*

Irrigation lowers temperatures in green roof substrate through two primary mechanisms: increased water content elevates specific heat capacity, leading to more effective diurnal temperature moderation. While non-irrigated substrates with succulent plant cover exhibited up to 18.1 K/d temperature fluctuation in the substrate, those receiving maximum irrigation exhibit fluctuations as low as 6.3 K/d. At the same time, mean and maximum surface temperatures are lower for irrigated green roofs. Surface temperature reduction is on average 1.6 K for minimum irrigation and 2.4 K for maximum irrigation. Although evaporative cooling accounts for part of this reduction, the reflection and insulation properties of healthier plant cover contribute significantly.

## 4. Conclusions

Irrigation provides various benefits for the performance of green roofs. The green roof research facility delivers experimental data as a basis for process identification, effect size evaluation and performance optimization of irrigation with pretreated greywater. Different performance aspects benefit in different ways from irrigation. Evaporation increase and drought reduction are strongly linked to irrigation volume. For surface temperature reduction and plant vitality, intermediate irrigation amounts appear sufficient. In contrast, stormwater retention capacity is reduced by irrigation. The prioritization of various potential benefits enables an informed approach to climate resilient urban planning.

**References**


Antoszewski P, Świerk D, Krzyżaniak M. (2020) Statistical Review of Quality Parameters of Blue-Green Infrastructure Elements Important in Mitigating the Effect of the Urban Heat Island. https://doi.org/10.3390/ijerph17197093

Coutts AM, Daly E, Beringer J, Tapper NJ (2013) Assessing practical measures to reduce urban heat: Green and cool roofs. https://doi.org/10.1016/j.buildenv.2013.08.021

Helm B, Weber S, Meyer S, Petzoldt H (2019) The green roof research facility Dresden – a high resolution monitoring system for coupled water, heat and matter fluxes in green roofs. Novatech 2019, Jul 2019, Lyon, France.

MacIvor, J. Scott, Liat Margolis, Curtis L. Puncher, and Benjamin J. Carver Matthews (2013) Decoupling Factors Affecting Plant Diversity and Cover on Extensive Green Roofs. https://doi.org/10.1016/j.jenvman.2013.09.014.

Oberndorfer E, Lundholm J, Bass B, Coffman RR, Doshi H, Dunnett N, Gaffin S, Köhler M, Liu KKY, Rowe B (2007) Green Roofs as Urban Ecosystems: Ecological Structures, Functions, and Services. https://doi.org/10.1641/B571005

Van Mechelen C, Dutoit T, Hermy M (2015) Adapting green roof irrigation practices for a sustainable future: A review. https://doi.org/10.1016/j.scs.2015.07.007

# The use of hydrants for anomaly detection in the water distribution networks. Preliminary laboratory tests.

Filomena MAIETTA[1], Silvia MENICONI[2], Caterina CAPPONI[2], Gaetano CRISPINO[1], Corrado GISONNI[1], Bruno BRUNONE[2]

[1] Department of Engineering, University of Campania "Luigi Vanvitelli", Italy
filomena.maietta@unicampania.it, gaetano.crispino@unicampania.it, corrado.gisonni@unicampania.it
[2] Department of Civil and Environmental Engineering, University of Perugia, Italy
silvia.meniconi@unipg.it, caterina.capponi@unipg.it, bruno.brunone@unipg.it

ABSTRACT

In recent times, maintaining the integrity of Water Distribution Networks (WDNs) has become paramount due to the complexity of these systems and their aging components. The detection of anomalies, such as water leakages and blockages (e.g., Colombo et al., 2009; Ghazali et al., 2011) is essential to this maintenance. Transient Test-Based Techniques (TTBTs) have emerged as powerful tools in diagnosing these anomalies by monitoring pressure wave patterns (e.g., Meniconi et al. 2021). The main objective of this research is to probe into the methodologies for generating these pressure waves, with a specific focus on hydrants – often the primary access point to WDNs. Hydrants, often linked to the network via branches of variable lengths and reduced diameters, have been previously suggested as potential pressure wave generators. Numerous studies in the literature propose the use of hydrants, in whose downstream end section a control valve is installed with the aim to generate the pressure wave to be analyzed (Taghvaei et al. 2010; Shucksmith et al. 2012; Haghighi et al. 2012; Ghazali et al., 2011; Waqar, et al., 2021). This paper undertakes an in-depth study of the impact of branch lengths on the transient quality produced, which subsequently influences the accuracy of system diagnostics.

## 1. Laboratory tests and results

The experimental set-up (Fig. 1) at the Water Engineering Laboratory (WEL) of the University of Perugia, Italy is a pipe network with two loops simulating a District Metered Area (DMA). All the pipes are high-density polyethylene (HDPE) pipes and they are supplied by a pressurized tank, connected to the network by a 42.3 m long DN110 pipe ($D$= 93.3 mm and $e$ = 8.1 mm). The first loop has four 100 m long DN75 pipes ($D$ = 63.8 mm, and $e$ = 5.6 mm), whereas the second one has four main pipes one of which in common with the first loop and the other three ones with length of 100 m and diameter DN50 ($D$ = 42.6 mm, and $e$ = 3.7 mm). The supplied steady-state discharge is measured at section 2 by means of an electromagnetic flow meter. Pressure is monitored at nodes 7 and 7u, with absolute (A) and relative (G) piezoresistive transducers. Moreover, during tests, the pressure is sampled at a frequency of 2048 Hz by a National Instrument cDAQ-9188 data acquisition system. In order to simulate the hydrant, a DN25 branch ($D$ = 20 mm, and $e$ = 3 mm) has been installed at sections 7. At the downstream end of such a branch, a solenoid valve (indicated as VM) is installed to generate controlled, repeatable, and sharp transients (Table 1). In test #2 the branch length is $L_{hy}$ = 15.26 m, comparable to the fire hydrants described by Waqar (2021). Two benchmark tests were also considered. Test #1 allows verifying the effectiveness of a wave generated by a valve placed directly in the network; in fact, $L_{hy}$ is equal to 0 and VM is installed at node 7. Test #3 allows identifying the arrival of the wave generated by the maneuver and the wave reflected by the singularities of the network: in fact $L_{hy}$ = 101.08 m. The pressure wave speeds have been evaluated by measuring the travel time of the pressure wave generated by the maneuver: specifically, the value of the branch pressure wave speed is $a_{hy}$ = 455.91 m/s. In all the carried out tests, the network is intact and free of anomalies (no leakages and blockages were modelled in the

experimental set-up) in order to avoid that the generated pressure wave could be reflected or transmitted by anomalies, and the flow rate is $Q_0$ = 0.12 L/s.

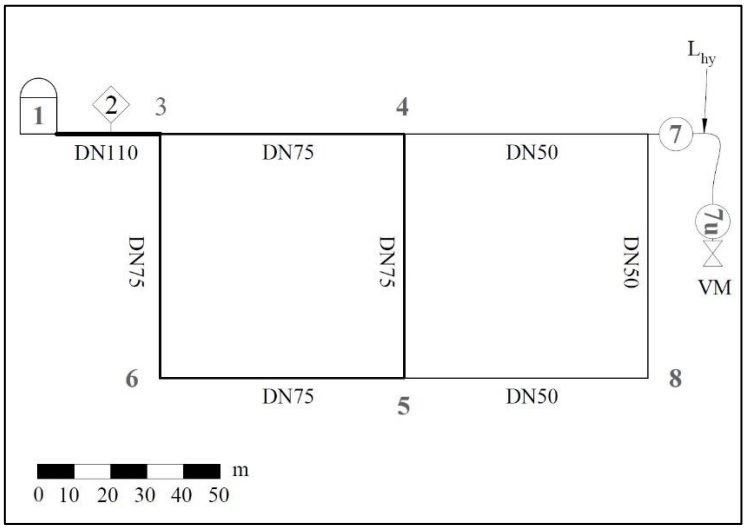



**Fig. 1.** The network at the Water Engineering Laboratory (WEL) of the University of Perugia, Italy: layout.

**Table 1.** Tests carried out at the Water Engineering Laboratory of the University of Perugia

| test (#) | $L_{hy}$(m) | VM location |
|---|---|---|
| 1 | 0.00 | 7 |
| 2 | 15.26 | 7u |
| 3 | 101.08 | 7u |

In both tests #2 and #3, the pressure wave generated by the maneuver at section 7u was identical, with a value closely matching the Allievi-Joukowsky overpressure benchmark. During test #2, such a pressure wave interacts multiple times with node 7. During the first phases of the transient, this repetitive interaction results in a more rapid and pronounced decrease in oscillations when compared to test #3, where the pressure wave at node 7 has a singular interaction with the valve. In contrast, test #1 exhibits a significantly smaller pressure wave. This can be attributed to the direct location of VM at the junction 7. This location makes the pressure signal's interpretation straightforward, since it eliminates the complexities and potential overlaps that might arise from hydrant branch lengths and their interactions with network junctions. Nonetheless, additional experimental evaluations and on-field verifications remain essential.

**References**

Colombo, A. F., Lee, P., & Karney, B. W. (2009). A selective literature review of transient-based leak detection methods. Journal of hydro-environment research, 2(4), 212-227.

Ghazali, M., Staszewski, W., Shucksmith, J., Boxall, J., & Beck, S. (2011). Instantaneous phase and frequency for the detection of leaks and features in a pipeline system. Structural Health Monitoring, 10 (4), 351-360.

Haghighi, A., Covas, D., & Ramos, H. (2012). Direct backward transient analysis for leak detection in pressurized pipelines: from theory to real application. Journal of Water Supply: Research and Technology|AQUA, 61 (3), 189-200.

Meniconi, S., Capponi, C., Frisinghelli, M. & Brunone, B. (2021). Leak detection in a real transmission main through transient tests: deeds and misdeeds. Water Resources Research, 57(3), e2020WR027838.

Shucksmith, J. D., Boxall, J. B., Staszewski, W. J., Seth, A., & Beck, S. B. (2012). Onsite leak location in a pipe network by cepstrum analysis of pressure transients. Journal American Water Works Association, 104 (8), E457-E465.

Taghvaei, M., Beck, S., & Boxall, J. (2010). Leak detection in pipes using induced water hammer pulses and cepstrum analysis. Int. Journal of COMADEM, 13 (1), 19.

Waqar, M., Louati, M., Wang, X., & Ghidaoui, M. S. (2021). Model-Free Matched Field Processing for Condition Assessment of Pressurized Pipes. Journal of Water Resources Planning and Management, 147(10), 04021066.

# Assessing the Impact of Urbanisation on Combined Sewer Networks: A Case Study in Thessaloniki, Greece

Antigoni ZAFEIRAKOU[1], Panagiota GALIATSATOU[2], Anastasia KATSOULEA[1], Argyro GATZIOURA[1], Iraklis NIKOLETOS[1], Maria KAPOUNIARI[1]

[1] Division of Hydraulics & Environmental Engineering, A.U.Th., Greece

[2] EYATH S.A., Greece

irakniko@civil.auth.gr

ABSTRACT

Urban intensification is a key factor affecting the response of combined sewer systems, especially during storm events. In this regard, the impact of several population density scenarios on combined sewer networks has been evaluated. The application of the proposed framework is demonstrated for a case study catchment in Thessaloniki, Greece. Hydraulic performance of the examined sewer network has been assessed using InfoWorks ICM model. The results indicate that mitigation strategies as the upgrade of the sewer system and the application of Low Impact Development techniques are considered crucial for the management of combined sewer overflows.

## 1. Introduction

The sewer networks are under significant stress due to ageing infrastructures, climate change and rapid urbanisation (Elga et. al. 2015; Gogien et. al. 2023; Kvitsjoen et. al, 2021; McGrane 2014; Nasrin et. al. 2017). As a result of the aforementioned factors, urban flooding occurs more frequently due to the exceedance of the sewer capacity (Iliadis et. al, 2023). This study examines how density population growth affect urban sanitation networks. Consequently, accurate prediction of the optimal population density is considered essential to assess the sewer systems' optimal capacity, or whether mitigation measures are required to support the flows from the proposed urban developments (Bellos and Tsakiris, 2016; Kilsdonk et. al., 2022; Zafirakou 2017)

## 2. Study Area

The metropolitan area of Thessaloniki, with over one million residents, and a combined sewer system, is our case study. The population density is very high, especially in the city's center, estimated at 20 capita per hectare. The location of the study area as well as the layout of Thessaloniki examined network are shown in Fig.1.



**Fig. 1.** Combined Network Drainage area plan of Thessaloniki's City Centre.

## 3. Combined Capacity and Overflow Analysis

The InfoWorks ICM model is selected to assist in the evaluation and assessment of the drainage collection system. Three scenarios were considered for the analysis, covering existing conditions (low population density), proposed conditions including all the active development applications and potential land uses (mid to high population density) and ultimate conditions including all the projected development application (high population density). All these scenarios were performed on the existing combined network. For calibration and verification of the model, two historical rainfall events are selected. In order to get a good fit between the modelled results and the observed data, the parameters of RTK unit hydrograph, direct runoff surface, roughness and depression storage have been adjusted. Upon completion of the calibration procedure, the modelled hydrograph's shape is closely resemble the shape of the observed hydrograph for the duration of the event, for a 5-year return period storm event. Table 1 summarizes the peak flow, peak velocity, number of surcharging segments and the minimum available freeboard in the entire network under the existing, proposed and projected conditions.

**Table 1.** Summary Results

| Analysis Scenario Breakdown | Peak Flow (l/s) | Peak Velocity (m/s) | Surcharging Segments | Minimum Freeboard (m) |
|---|---|---|---|---|
| Scenario 1: Existing Conditions | 1,241.4 | 2.7 | 26 | 1.22 |
| Scenario 2: Proposed Conditions | 1,318.2 | 2.9 | 31 | 1.12 |
| Scenario 3: Ultimate Conditions | 1,599.1 | 3.2 | 40 | 0.88 |

## 4. Concluding Remarks

In this paper, the impact of urbanization on combined sewer networks has been studied. The modelling results show that under ultimate development conditions the combined sewer system is experiencing surcharging at 40 segments and the minimum available freeboard attained is below 1m. To ensure that the existing infrastructure will be able to support the population growth mitigation measures are required or the equivalent population density should be less than 10 capita per hectare. Implementation of Low Impact Development methods and the possibility of downspout disconnection as mitigation measures will be addressed in the future.

**Acknowledgements**

The authors wish to thank EYATh S.A. for providing the necessary data used in this paper.

**References**

Bellos V. and Tsakiris G. (2016) A hybrid method for flood simulation in small catchments combining hydrodynamic and hydrological techniques, Journal of Hydrology, 540, 331-339

Elga S., Jan, B. and Okke B. (2015) Hydrological modelling of urbanized catchments: A review and future directions, Journal of Hydrology, 529, 62-81

Iliadis C, Galiatsatou P, Glenis V, Prinos P., Kilsby C. (2023) Urban Flood Modelling under Extreme Rainfall Conditions for Building-Level Flood Exposure Analysis, Hydrology, 10, 172

Gogien F., Dechesne M., Martinerie R. and Lipeme Kouyi G. (2023) Assessing the impact of climate change on Combined Sewer Overflows based on small time step future rainfall timeseries and long-term continuous sewer network modelling, Water Research, 230, 119504

Kilsdonk RAH, Bomers A, Wijnberg KM. (2022) Predicting Urban Flooding Due to Extreme Precipitation Using a Long Short-Term Memory Neural Network, Hydrology, 9, 105

Kvitsjoen J., Paus KH., Bjerkholt, JT., Fergus T. and Lindholm O. (2021) Intensifying rehabilitation of combined sewer systems using trenchless technology in combination with low impact development and green infrastructure, Water Science & Technology, 83

McGrane S.J. (2014) Impacts of urbanisation on hydrological and water quality dynamics, and urban water management: a review, Hydrological Sciences Journal, 61 (13)

Nasrin T., Sharma AK, Muttil N. (2017) Impact of Short Duration Intense Rainfall Events on Sanitary Sewer Network Performance, Water, 9, 225

Zafirakou A. (2017) Sustainable Urban Water Management, City Networks, Springer Optimization and Its Applications, Vol. 128

# A comparison between the potential for storm water control of blue roofs: results of field experiments

Aurora GULLOTTA[1], Alberto CAMPISANO[2]

[1,2] Department of Civil Engineering and Architecture, University of Catania, Italy
aurora.gullotta@unict.it (for author 1)
alberto.campisano@unict.it (for author 2)

ABSTRACT

The present work discusses the results of a one-year long field experimental campaign aimed at monitoring three different full-scale pilot installations of blue roof (BR) systems for the control of stormwater runoff in urban areas. The three pilots are installed in the roof terrace of a building in the campus of the University of Catania (Italy) and are based on the use of tray modules, artificial turf and marble pebbles. Highest performances are shown by the modular BR, with mean 53% runoff reduction and mean 67% flow peak attenuation. BR with turf revealed mean 31% runoff reduction and mean 51% flow peak attenuation while the one with pebbles showed the lowest retention and detention efficiencies (24%).

## 1. Introduction

Application of Sustainable Urban Drainage Systems (SUDs) in urban areas includes many kinds of solutions aimed at reducing runoff from building rooftops. Studies have shown that Blue Roofs (BRs) provide large potential for runoff control since they increase on-site detention and retention of roof catchments (Andenæs et al., 2018; Martin and Kaye, 2020; Richter and Dickhaut, 2023). Furthermore, they enable easy retrofit of existing terraces, more so than traditional green roofs whose significant extra loading may not be compatible with the underlying structure.

In order to investigate the hydrological performances of BR systems in the Mediterranean climate, three full-scale pilots were installed on the rooftop terrace of a building of the campus of the University of Catania, in southern Italy. The first pilot is a tray-based modular BR (Campisano et al., 2021). The second pilot is a BR based on the use of artificial turf. Finally, the last pilot is a BR based on the use of marble pebbles. The work summarized the results of one-year long monitoring campaign aimed at comparing the performances of the three BRs.

## 2. Methods

The BR pilots are installed in the rooftop terrace of one building of the Catania University Campus. The area is characterized by a Mediterranean climate with dry summers and wet autumn/winter seasons. The area of installation concerns four separate roof catchments (Fig. 1). The roof catchment equipped with the tray-based modular system (TR) is placed in the south-east corner of the rooftop, side to the catchment in the north-east corner (REF) used as reference for the experiments. The BRs based on the use of artificial turf (AT) and marble pebbles (MP) are placed in the south-west and north-west corners of the rooftop, respectively. Each roof catchment has a separate roof drainage system (including separate downspout outlets) and has a mean surface slope of 1.6%. Catchments TR and REF have a surface area of 26.31 $m^2$ (rectangular 5.72 m x 4.60 m), while catchments AT and MP are about twice (rectangular 5.72 m x 9.00 m) close to 51.48 $m^2$ each.

The terrace is equipped with a meteorological station that allows for continuous measurement of precipitation. Barrels are placed at the field level at base of the building to store runoff collected by the downspouts of the four catchments, respectively. Based on the different surface areas of the catchments, TR and REF are equipped with barrels of 1 $m^3$ each while AT and MP are equipped with 2 $m^3$ barrels each. A

piezo-resistive silicon probe was installed in each barrel and used for indirect estimation of the outflow from the four catchments through differential water level measurements (i.e., of the collected water volume).

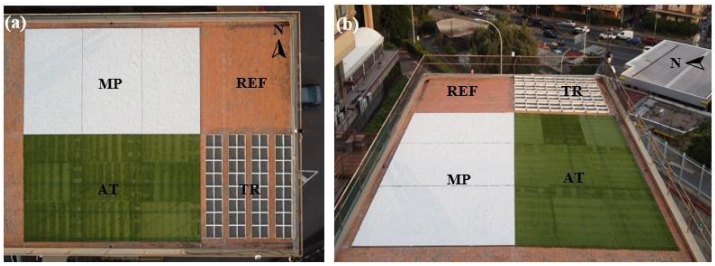



**Fig. 1.** Blue roof installations: (a) view from above, (b) view from west direction.

A 15 rainfall events were recorded in the period October 2021 - November 2022 and considered for the analysis. The events generated a total precipitation of 156.1 mm, with rainfall P of the single events ranging between 4.8 mm and 24.2 mm and mean value of 10.4 mm. Events were characterized by values of the peak rainfall intensity in the range 6.3–50.8 mm/h and mean value of 22.2 mm/h. Antecedent Dry Weather Period (ADWP) varies between 1 and 44 days (the latter value during summer) with average value of 8.1 days.

## 3. Results

The experiments show that, although designed for detention, the BRs may also perform in terms of rainfall retention. Fig. 2 shows, as an example, the curve of the accumulated precipitation *P* for the event of August 28th, 2022, as well as the hydrological response of the four catchments in terms of accumulated runoff *h*.

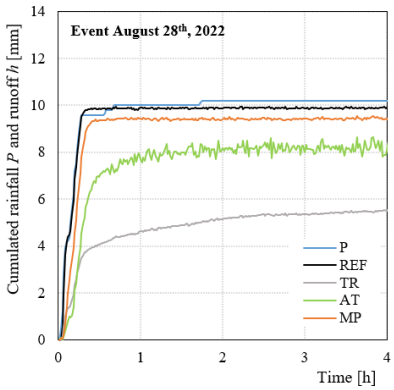



**Fig. 2.** Accumulated precipitation P and runoff from REF, TR, AT and MP for the event of August 28th, 2022.

The TR catchment provides average retention and detention efficiencies (for all the analyzed events) of 53% and 67%, respectively. These results are in agreement to those found in Campisano et al., (2021). The catchment equipped with AT shows average retention and detention efficiencies of 31% and 51%, respectively. The BR equipped with MP provides average retention and detention efficiencies of 24%. Globally, the conducted experiments revealed that the tray-based modular BR performs better than the other pilots. However, AT and MP have the advantage of being cheaper and improving usability of the rooftop. The obtained results open perspectives for the development of modelling approaches for BR systems in roof cover terraces. The use of such models might give a contribution to the identification of appropriate at source BR-based storm water control strategies in urban contexts.

**Acknowledgements**

This work has been [partially] funded by the University of Catania within the projects 'Piano della Ricerca Dipartimentale' 2016–2018 and 2020-2022, as well as by the Italian Ministry for Research within the national project 'PRIN 2020 – URCA!'.

**References**

Andenæs, E., Kvande, T., Muthanna, T.M., and Lohne, J. (2018). Performance of Blue-Green Roofs in Cold Climates: A Scoping Review. Buildings, 8, 55.

Campisano, A., Modica, C., and Gullotta, A. (2021). Long-term Experiments for the Evaluation of the Potential for Storm Water Control of Modular Blue Roofs in Mediterranean Climate. Urban Water Journal 18 (1): 33–42.

Martin, W.D., and Kaye, N.B. (2020). A simple method for sizing modular green–blue roof systems for design storm peak discharge reduction. SN Appl. Sci., 2, 8.

Richter, M., and Dickhaut, W. (2023). Long-Term Performance of Blue-Green Roof Systems—Results of a Building-Scale Monitoring Study in Hamburg, Germany. Water 15(15):2806.

# Advancing Combined Sewer Network Management: The Smart Infiltration/Inflow Management System (SiiMS)

Míriam TIMIRAOS[1,2], Jesús F. ÁGUILA[1], Óscar BRANDÓN[1], Juan Luis SOBREIRA[1], Lucía GARABATO[1], Carlos BARROS[1], Alejandro MARTÍNEZ[1], Saul DÍAZ[1], Xela GARCÍA[1], Gonzalo BLÁZQUEZ[1], Andrea Camila FORERO[3], Nicolás MORALES[3]

[1] Instituto Tecnológico de Galicia, Spain.
mtimiraos@itg.es

[2] University of A Coruña, Spain.

[3]Aqualia, Innovation and Technology department, Spain.

ABSTRACT

Urban wastewater infrastructures are facing increasing challenges due to variations in precipitation patterns induced by climate change, impacting the frequency and intensity of extreme hydrological events. This work presents the Smart Infiltration/Inflow Management System (SiiMS), a digitization tool whose main objective is to locate and quantify inflow and infiltrations (I/I) in combined sewer networks (CSNs). By processing real-time sensor data and integrating AI-based, numerical, and hybrid models, the SiiMS addresses the growing concern about the impact of climate change on wastewater systems. Early results achieved by the implementation of the SiiMS in two real European pilots highlight the promising usefulness in both detection and quantification of I/I and prediction of overflows in CSNs.

## Introduction

Urban wastewater infrastructures are being increasingly affected by changes in precipitation patterns and the increase in the frequency and magnitude of extreme hydrological events resulting from climate change (DG Environment, 2021). Recent studies highlight an increase in annual precipitation in northern and northwestern Europe of up to 70 mm per decade (Field, 2014), while climate models predict an increase in heavy daily precipitations during winters by up to 35% throughout the 21st century (EC, 2019).

The impact of changes in rainfall regime is particularly relevant in urban areas with CSNs transporting sewage and urban runoff to wastewater treatment plants (WWTPs), typically designed without considering climate change. Undersized infrastructures are not able to handle the more rapid stormwater inflow and increased flows, leading to overflows and, consequently, the discharge of wastewater without sufficient treatment (UWWTD, 2021). These capacity issues are exacerbated by groundwater infiltrations in aging CSNs through cracks or fissures (Ohlin et al., 2021). According to Su et al. (2020), the rate of groundwater infiltrations has increased by 10% over the past five years, leading to a 25% increase in overflows in coastal urban areas.

## Methodology

Reducing groundwater infiltration and stormwater inflow in CSN is one of the major challenges in the field of wastewater due to aging infrastructures and climate change. The SiiMS is presented here as a solution whose main objective is to locate and quantify I/I in CSNs. Comprising a data collector, calculation engine, and visualization interface, SiiMS not only assesses I/I but also facilitates smart asset management and climate change impact analysis on CSNs (Fig.1). Being implemented and validated in real Demo Sites in Spain and Denmark, SiiMS utilizes real-time data from sensors strategically placed along sewer networks (rain gauges, flow meters, level meters, water quality probes, etc.), with measurements typically taken every 5 to 15 minutes.

SiiMS incorporates a robust calculation engine for real-time management of data from sensors and additional sources, applying various types of models (AI-based, hydraulic, and hybrid) to locate and quantify I/I, as well as predict stormwater overflows (SWOs) and assess water quality. By analyzing data series in detail and comparing dry and wet periods, SiiMS identifies and quantifies flow components (such as base sanitary flow,

infiltration, inflow, and tides) at specific points in CSNs. These calculations are expanded network-wide through hydraulic modeling, calibrated with measured data and refined applying artificial intelligence. AI-based models, including Temporal Fusion Transformer (TFT) among others, are also employed for overflow predictions. TFT stands out for its ability to capture temporal dependencies in the data measured by sensors, enabling accurate forecasting of overflow events. For both calibrating hydraulic models and training AI-based models, SiiMS requires input data series covering at least one hydrological year to assess temporal patterns resulting from climatic variability. These considerations aim to ensure a more accurate representation of CSN operation, with the goal of enhancing the management of sewerage systems in real-time

## First results and next steps

Preliminary results from the implementation of SiiMS in real Demo Sites show its promising usefulness both in the detection and quantification of I/I and in overflow prediction. Analysis of measured data at control points in CSNs highlights the strong dependence of seasonality in the operation of sewage infrastructures. Wastewater flows may be doubled and overflows increase by up to an order of magnitude during wetter months compared to dry seasons. Initial hydraulic simulations (Fig. 1a) suggest that rainfall-derived inflow and infiltrations may be as much as 80% of the wastewater flowing through CSNs during wet seasons. Investigations on groundwater infiltrations in the sewer networks under study highlight their special significance, which may cause contributions of up to 30% of total flows. In addition, specific points were identified as susceptible to saltwater intrusion in coastal areas, causing significant increases in electrical conductivities. AI-based models integrated in SiiMS also yield good initial results in terms of overflow predictions. The current TFT model can accurately predict overflows that will occur within 24 hours by analyzing historical data from the previous week (Fig 1b), allowing for proactive and effective management of wastewater treatment system operations.

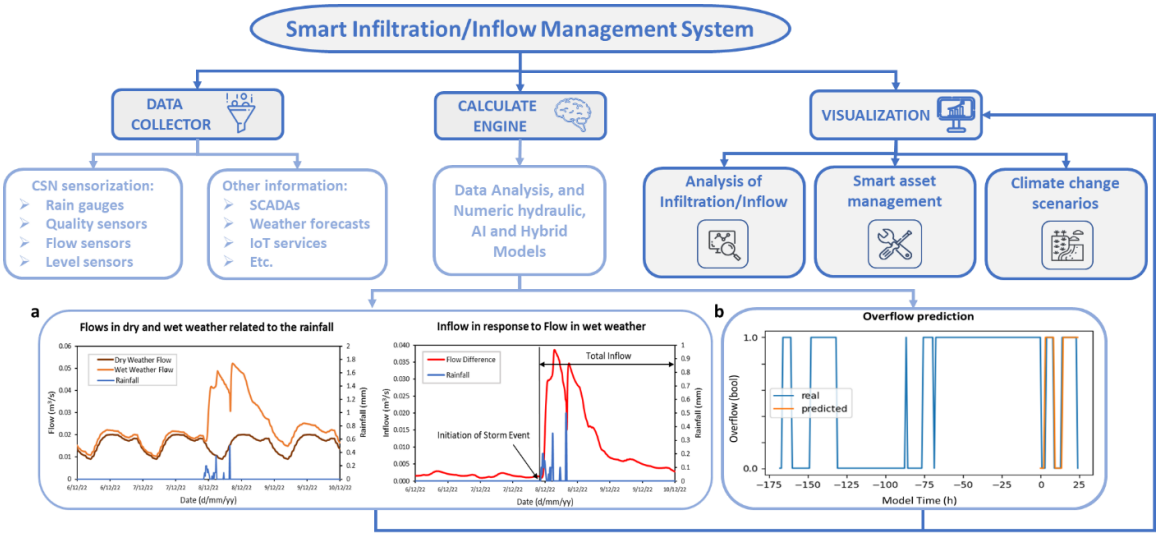



**Fig. 1**. Diagram of the SiiMS showing its main components, and initial results from hydraulic models for I/I quantification (a) and AI-based models for overflow predictions (b).

Next steps in SiiMS improvements involve further refinement and validation of the models presented in this research work for application in the two real pilots. This approach will strengthen the current system's robustness and applicability, allowing a more effective implementation in real scenarios.


### Acknowledgments

This research work resulted from the project LIFE RESEAU, funded by the LIFE program of the European Union under Grant Agreement No. LIFE20 CCA/ES/001706. Míriam Timiraos's research was supported by "Xunta de Galicia" (Regional Government of Galicia) through grants to industrial Ph.D., under the "Doutoramento Industrial 2022" grant with reference: 04/IN606D/2022/2692965.


### References


Field C.B (2014) Climate Change 2014 Impacts, adaptation, and Vulnerability, Cambridge University Press eBooks.

Directorate-General for Environment (2021) Implementation of the Water Framework Directive and the Floods Directive.

European Commission (2019) Report from the Commission to the European Parliament and the Council: implementation of the Water Framework Directive and the Floods Directive.

UWWTD (2021) Urban wastewater treatment for 21st-century challenges.

Su X, Liu T, Beheshti M, Prigiobbe V (2020) Relationship between infiltration, sewer rehabilitation, and groundwater flooding in coastal urban areas, Environ Sci Pollut Res Int, 27, 14288-14298.

Ohlin Saletti, A. (2021) Infiltration and inflow to wastewater sewer systems: literature review on risk management, Gothenburg: Chalmers University of Technology.

# Flood assessment and risk mitigation in Quelimane, Mozambique

Inês AFONSO[1], Paloma FURLAN[2], Pedro MANSO[2], Pedro VICENTE[3], Jorge MATOS[1,4]

[1] Instituto Superior Técnico (IST), Universidade de Lisboa, Lisbon, Portugal;
ines.filipa.f@tecnico.ulisboa.pt
jorge.matos@tecnico.ulisboa.pt

[2] MHYD Group, Lisbon, Portugal;
paloma.furlan@mhyd.group
Pedro.Manso@mhyd.group

[3] Nova School of Business and Economics, Universidade Nova de Lisboa, Portugal;
email: pedro.vicente@novasbe.pt

[4] CERIS, Instituto Superior Técnico (IST), Universidade de Lisboa, Lisbon, Portugal

ABSTRACT

Quelimane is a coastal city in Mozambique exposed to cyclones, flooding, erosion and fast urbanization due to rural migration. The city lies in the province of Zambezia, Mozambique, close to the River *Dos Bons Sinais* and approximately 20 kilometers inland from the Indian Ocean. The influx of people from rural areas resulted in informal settlements, increased deforestation of mangroves and unplanned use of land in parts of the municipality that were or became vulnerable to flooding and storm surges. This study aims at providing a holistic understanding of the complex interplay between environmental factors, territorial features, urban and land use planning. The main outcome of the project is to showcase the potential positive impacts that scaling up local low-cost solutions may have in improving resilience to climate changes in a fast-changing social context.

## 1. Introduction

Floods can have significant impacts in cities, due to increased population density and the influence of changes in land use, such as urbanization and deforestation (Chang and Franczyk, 2008). In March 2023, Cyclone Freddy brought intense rainfall (surpassing 200 mm/24h), specifically in Zambezia over 22000 people took refuge in temporary accommodation centers, leading to 10 deaths and 14 injuries (Office for the Coordination of Humanitarian Affairs, 14 March, 2023).

Quelimane, the capital of the province of Zambezia, is a coastal city in Mozambique located on the north bank of the River *Dos Bons Sinais*. The city and surrounding areas are vulnerable to the impacts of climate change and seasonal flooding, especially in the rainy season, from October to February. As result of the Mozambique Civil War of 1977–1992 and current migration driven by socio-economic factors, the lack of formal management has resulted in increased mangrove deforestation and informal settlements in areas prone to flooding and erosion. This study aims at identifying and categorizing flood risk zones within the urbanized area and assess and propose structural measures to mitigate negative impacts of floods.

## 2. Methods

The methodology involves a holistic, innovative approach to flood risk management, utilizing satellite imagery and georeferenced data to identify critically vulnerable areas. Distinct from conventional strategies, this approach synergizes technical infrastructure assessments with an extensive examination of socio-economic

factors. Fieldwork involved gathering data, such as drainage system characteristics and qualitative assessments, and engaging with the community to understand their expectations and past experiences. A set of risk mitigation strategies will be formulated, and the measures will be subject to a multi-criteria analysis, in which cost-benefit, social impact, community acceptance, sustainability, origin of materials, and carbon footprint will be assessed. Subsequently, a set of selected alternatives will be designed and proposed to the local community and regional government for implementation in the following months. A later stage of this work will assess the effectiveness of the measures implemented from a perspective of risk mitigation.

## 3. Results and discussion

The outcomes foreseen in this study are to identify and categorize flood risk within the urban of Quelimane and outskirts, through an *ex-post* analysis of recent river flood and cyclone events. Regarding to Cyclone Freddy, a survey yielded 1949 georeferenced data points on indoor water depth, provided by NOVAFRICA Center for Business and Economic Development (Fig. 1). At the time of this event, Quelimane city had already established a drainage system, designed according to the guidelines in the article 106 of Decree nº. 30/2003. In general, the drainage system is characterized by concrete channels with rectangular cross-sections. In certain areas, it encompasses concrete channels with triangular cross-sections and trapezoidal channels made of cyclopean concrete. Additionally, the system's design discharge is based on a return period of five years.

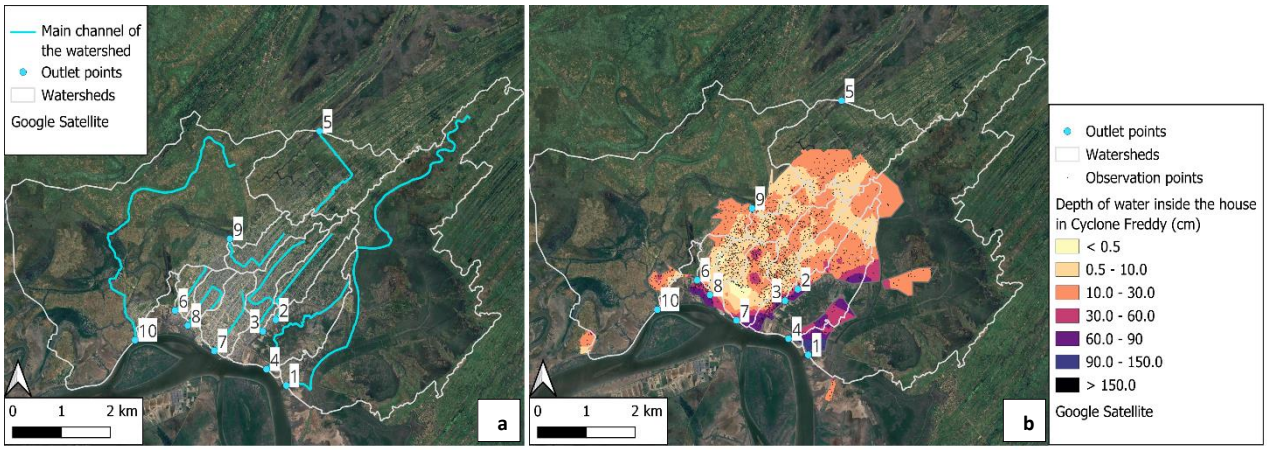



**Fig. 1.** a) Watersheds division according to topography and city drainage system. b) Results of interpolation with ordinary kriging for water depth inside the house in Cyclone Freddy ($R^2$=0.85), event corresponding to an approximate return period of 50 years.

Based on fieldwork, it was possible to verify that since 2013 the city has had a stormwater drainage system, but in general its operation has great potential for improvement given the lack of maintenance of the system and the accumulation of solid waste inside the channels. The envisaged measures include estimating a percentage increase in the capacity or dimensions of existing channels to accommodate increased flow rates, alongside the reinforcement of embankments, evaluating additional drainage solutions, such as new channels. Maintenance of these infrastructures are also part of the structural interventions. Nature-based solutions, including mangrove restoration and green infrastructure development will also be assessed.

**Acknowledgements**

This work was funded by MYHD water and energy solutions SARL and Nova School of Business and Economics - International Growth Centre - Research Grant (UK) Project "Urbanization meets the environment: how can communities manage migration and protect against floods in a coastal Mozambican city?". We wish to acknowledge the support and collaboration of the NOVAFRICA Center for Business and Economic Development and the research team that made possible the field mission and data gathering as well as the enriching discussions.

**References**

Chang, H., & Franczyk, J. (2008). Climate Change, Land-Use Change, and Floods: Toward an Integrated Assessment. *Geography Compass*, 2(5), 1549-1579. [DOI: 10.1111/j.1749-8198.2008.00136.x]

Office for the Coordination of Humanitarian Affairs Southern Africa. (2023). Tropical Cyclone Freddy: Flash Update No. 7, 14 March 2023.

Decree No. 30/2003. Approves the Regulation of Public Water Supply and Wastewater Drainage Systems and repeals Orders No. 10367, from April 14, 1943, and No. 11338, from May 8, 1946.

# Improved Mixed Flow Model for Large-Scale Multi-Shaft Pipeline

Yanqing LU[1], Ling ZHOU[1], Rui-lin FENG[1], Zijian XUE[1], Yinying HU[1], Qian-qun CHEN[1]

[1] Hohai University, China
yanqinglu@hhu.edu.cn
zlhhu@163.com
rl.feng@hhu.edu.cn
hhuxzj@163.com
yinyinghu_hhu@hhu.edu.cn
qianxun.chen@hhu.edu.cn

ABSTRACT

In large-scale stormwater drainage systems and water diversion projects, rapid flow transitions frequently occur due to heavy rainfall or large upstream inflow. This flow regime is characterized by long distance air pockets being compressed by the forward water flow at first, and in succession with irregular intermittent flow regime transitions. On account of the multiple vertical shaft arrangements, these pipeline systems also have multi-shaft air release problems. These complex flows pose a huge threat to the safe operation of pipeline systems, which is a strong motivation for the development of mixed flow models.

In the current research, due to the large aspect ratio of actual pipeline systems, a great number of grid units need to be set up, and long-distance water filling operations require a long simulation time, which makes the 2D and 3D simulation methods that require huge computing resources unsuitable for such problems. As for 1D simulation methods, there are widely used Two-Component Pressure Approach (TPA) with entrapped air pockets considered and gas model improvements to commercial software such as Storm Water Management Model (SWMM). However, these 1D methods lack consideration for the size effect of large long distance air pockets between prototype and model, and the mutual influence between vertical shafts.

Therefore, this work aims to address the gaps with an improved mixed flow model established. The model innovatively combines TPA for water part simulation and discrete Euler method for gas part. Further emphasis is placed on demonstrating applicability in large air pockets, and analysis of the size effect and multi-shaft problem. The numerical solution is the Godunov-type finite volume method, combined with Random Choice Method (RCM) for numerical stability improvement.

It has been found that the proposed model can accurately simulate complex mixed flows in large-scale multi-shaft systems with high computational efficiency. In the conversion of air parameters between prototype size and model size, the one-parameter Lie group of point-scaling transformations is also required for the air pocket compression in mixed flows, apart from the traditional Froude scaling laws (FSLs). In addition, the ventilation between multi-shafts has different staged mutual influence, in close relation to inflow discharge and pipeline configuration.

# Comparative Analysis of Urban Rainwater Harvesting Potentials: Case Studies of Tijuana, Mexico, Lisbon, Portugal, and Trondheim, Norway

Laura OCARANZA[1], Cristina MATOS SILVA[2]

Instituto Superior Técnico, Portugal
[1]lauraocaranza@tecnico.ulisboa.pt
[2]cmsilva@civil.ist.utl.pt

ABSTRACT

This research project aims to simulate and compare the urban rainwater harvesting potentials across three cities: (i) Tijuana, Mexico (ii) Lisbon, Portugal, and (iii) Trondheim, Norway, each representative of a distinct climate type. The study evaluates the RWH potential at both building and urban scales, considering the unique weather conditions and consumption patterns of each city. The overarching objectives are to determine and compare the rainwater harvesting potential of buildings and assess the non-potable water savings.

## 1. Objectives

The research outlines specific objectives. Firstly, it aims to assess the viability of rainwater harvesting within individual buildings, evaluating the rainwater harvesting (RWH) potential in structures across the three cities while considering their unique weather patterns and catchment areas. Moving to the urban scale, the second objective involves evaluating the potential for rainwater harvesting and subsequent non-potable water savings, including an analysis of how different building typologies within each city impact overall water consumption levels. Through these objectives, this research seeks to contribute a comprehensive analysis that advances the understanding of urban RWH systems and offers practical insights for sustainable water management practices in diverse urban environments.

## 2. Methodology

The research follows a comprehensive methodology, see Fig.1., adapted from (Silva et al., 2015) for

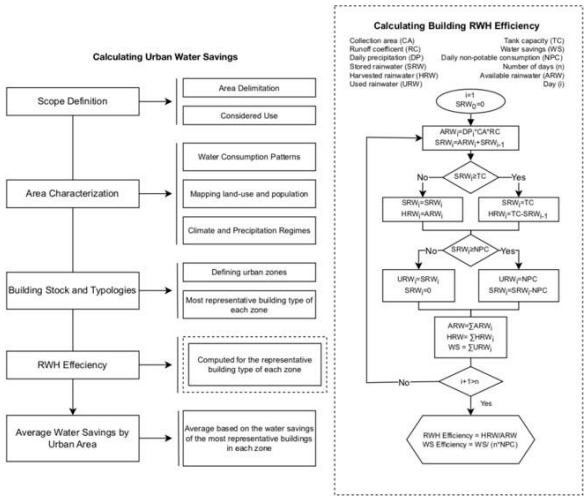



**Fig.1.** Urban and building scale methodology adapted from (Lúcio et al., 2019) and (Silva et al., 2015) respectively.

building-scale RWH potentials and non-potable water savings. For the urban-scale analysis, the methodology presented by (Lúcio et al., 2019) is applied, with adjustments to account for the multi-national city

comparison and diverse weather factors. Data collection involves gathering information including, but not limited to, precipitation, building typologies, inhabitants, water consumption and type of water usage.

## 3. Significance

The inclusion of the 3 cities in this comparative study aims to enhance comprehension of urban RWH systems and how diverse climate and building typologies offer distinctive challenges and opportunities for their implementation and efficiency.

### *3.1. Diverse Weather Types*

The viability of RWH systems is entirely dependent on precipitation and weather, which vary significantly among the selected cities. In terms of climate, Lisbon, with a warm summer classification (CSa), following (Beck et al., 2018), experiences an average maximum temperature of 22°C and a minimum of 14°C. Tijuana, characterized by an arid climate (BSk), has slightly higher temperatures, with an average maximum of 24.75°C and a minimum of 12.3°C. Trondheim (DFc) stands out as the coldest city among the three, with a maximum average temperature of 10°C and a minimum average of 2.5°C. Precipitation also varies significantly among the cities. In Lisbon, there are periodic yet forceful rains, with a yearly average of 750mm. There is little to no precipitation in the summer months, providing insights into how RWH systems can cope with sudden influxes of precipitation and reduce runoff in urban areas. Similarly, Tijuana experiences precipitation peaks in the colder months, with a yearly average of 257mm per year. Dry summers and low precipitation rates allow for the assessment of the methodology's effectiveness in regions with limited water resources. Quite differently, Trondheim's snowy climate introduces an additional factor, emphasizing the need to adapt RWH systems to account for snowmelt. The city receives an average of 866mm of precipitation per year, dispersed throughout the year, peaking in September, with an additional 100mm of snowfall in the winter.

### *3.2. Building Typologies and Catchment Areas*

In terms of building stock, the building typology varies significantly among the three cities. Tijuana predominantly consists of single-family homes accounting for 70% of residences, with a smaller percentage of apartment complexes at 9%. Trondheim exhibits a more diverse residential stock, with 48% of buildings being single-family homes, 22% rowhouses, and 8% complexes. In Lisbon, the building typology leans towards a higher concentration of apartment complexes, representing 61% of residences, followed by 30% single-family homes. These typologies influence the total number of inhabitants per building, consequently affecting the overall non-potable water consumption and water savings. Additionally, the availability of collected rainwater is dependent on the total catchment area by urban zone, another variable directly influenced by building typology.

In conclusion, this research study goes beyond rainwater harvesting by providing a comprehensive analysis of urban rainwater harvesting system that accounts for the diversity in climate, building typologies and urban planning. The findings are expected to help inform future sustainable water management practices beyond borders.

**Acknowledgements**

This work was developed in the scope of the EEA grants project EVIDENCE. CMS also acknowledges the support from CERIS Research Centre, Instituto Superior Técnico, Universidade de Lisboa.

**References**

Beck HE, Zimmerman NE, McVicar TR, Vergopolan N, Berg A, Wood EF (2018) Present and future Köppen-Geiger climate classification maps at 1-km resolution, Scientific Data, 5

Lúcio C, Silva CM, Sousa V (2020) A Scale-Adaptive Method for Urban Rainwater Harvesting Simulation, Environmental Science and Pollution Research, 27, 4557–4570

Silva CM, Sousa V, Carvalho NV (2015) Evaluation of Rainwater Harvesting in Portugal: Application to Single-Family Residences, Resources, Conservation and Recycling, 94, 21–34

# Challenges and Opportunities to Manage Wastewater and Rainwater in Lisbon

Maria do Céu ALMEIDA[1], Miguel FERNANDES[2], Fernando FERNANDES[3]

[1] Laboratório Nacional de Engenharia Civil, Av. do Brasil 101, 1700-066, Lisbon, Portugal
mcalmeida@lnec.pt

[2,3] Câmara Municipal de Lisboa, Departamento de Saneamento, Rua Dom António Luís de Sousa, Lotes B1 a B8, 1070-326, Lisbon, Portugal
dmmc.ds@cm-lisboa.pt

ABSTRACT

Urban water systems are essential for public health, quality of life, and urban sustainability. Despite the progress in the last decades in managing wastewater and rainwater in urban areas, challenges persist and are exacerbated by climate changes. Existing urbanisation and infrastructure systems are valuable assets and ultimately are barriers to urban sustainability transition, including the type of drainage systems and their condition. New paradigms should act as drivers for change, incorporating these into new solutions while providing multiple benefits not limited to drainage.

Lisbon wastewater and rainwater systems have a long history, developed using the combined system paradigm, similar to those in other European cities of the same period. Systems built in the mid-eighteenth century, after the 1755 Lisbon earthquake, still function today. The transition to separate systems set as a requirement by new regulations in 1995 applied only to new developments. The efforts to improve the level of service by wastewater treatment plants in response to the Urban Wastewater Treatment Directive (91/271/EEC) led to a significant reduction of emissions of organic matter, nutrients and pathogens to surface waters, implied changes in the sewer systems leading to better performance during dry weather conditions. However, combined sewer overflows occur even for frequent rain intensities, and monitoring to provide an actual picture of polluted discharges is insufficient.

Monitoring to support performance assessment of services and city sustainability is challenging. It requires accounting for spatial and time variations and accurate data and information. Compliance with the annual quality of service national assessment, promoted by the Water and Waste Services National Regulator (ERSAR), created conditions to collect essential data at the utilities.

The Lisbon Municipal Master Plan objectives embrace the city transition by implementing green infrastructure and nature-based and water-sensitive solutions to meet city objectives while reducing flooding, emission of pollution to surface waters (e.g., by combined sewer overflows), air pollution and heat-island effect (CML, 2020). New challenges from the revised UWWT directive to come (Halleux, 2023) or the EU action plan-Towards Zero Pollution for Air, Water and Soil (European Commission, 2021) are only achievable if the cities with combined sewer systems promote substantial changes. The drainage master plan (Plano Geral de Drenagem de Lisboa, PGDL, 2016-2030) already incorporates a set of actions to face some recurrent problems of flooding in Lisbon, primarily adopting the construction of large infrastructures including two large tunnels with a total length of 6 km.

Management of wastewater and rainwater systems develops by recognising the strategic issues requiring detailed planning. Among these, the sanitation department strategic plan setting the main strategies to pursue in Lisbon is a basis together with other tactical plans, e.g., the infrastructure asset management plan, providing a systematic approach to the operational plans in a city where a valuable infrastructure needs to be rehabilitated

and adapted, given the long service life of most components, and paradigm transitions. It is critical to separate wastewater based on its quality, i.e. the flows from different origins, to effectively tackle the various issues mentioned above. Within this context, control of the flows originating from each source and ensuring its adequate management allows the promotion of circularity, reduction of pollution and increase of efficiency.

Implementing local solutions to foster the separation of wastewater and stormwater and resourcing to nature-based and water-sensitive solutions contributes to urban sustainability in many dimensions. The cross-departmental work based on close collaboration to create solutions addressing multiple objectives is an opportunity that Lisbon municipality is pursuing, involving municipal services covering areas of urban water management, environment, energy, climate change, and urban requalification. In parallel, an ongoing ambitious assessment of the large sewers' structural condition to detect situations requiring urgent rehabilitation promotes circularity while improving performance. Extending the service life of system components reduces the need for new construction and the risk of failures leading to high consequences. Adopting nature-based and water-sensitive solutions is a challenge and an opportunity to alter the old drainage paradigm, rehabilitate and convert the existing combined sewer network, and foster the local management of rainwater (starting in upstream catchments) to reduce inflows to an overload system. A new paradigm can have multiple benefits, such as improving citizens' quality of life while increasing city resilience to climate change and better compliance with European directives and city commitments.

The presentation summarises the current situation in Lisbon, local challenges, and ongoing work.

**References**

CML (2020). Plano Director Municipal de Lisboa. <https://www.lisboa.pt/cidade/urbanismo/planeamento-urbano/plano-diretor-municipal/pdm-em-vigor, 2023-12-29>.
European Commission (2021). Pathway to a Healthy Planet for All. EU Action Plan: 'Towards Zero Pollution for Air, Water and Soil', COM (2021) 400.
Halleux, V. (2023). Revision of the Urban Wastewater Treatment Directive - Q2 2022. Legislative train 12.2023.1 A European Green Deal. <https://www.europarl.europa.eu/legislative-train/carriage/revision-of-the-urban-wastewater-treatment-directive-(refit)/report?sid=7601, 2023-12-29>.
CML (2015). Plano Geral de Drenagem de Lisboa 2016-2030. <https://planodrenagem.lisboa.pt, 2023-12-29>

# Lisbon Urban Water Cycle Observatory

Rui MENDES[1], Rui DINIS[2], Eduardo SILVA[3]

[1,2,3] Lisboa E-Nova – Agência de Energia e Ambiente de Lisboa, Portugal
ruimendes@lisboaenova.org
ruidinisisboaenova.org
eduardosilva@lisboaenova.org

ABSTRACT

Lisboa E-Nova developed the Lisbon Urban Water Cycle Observatory to systematize, collect and facilitate access to water data of the City of Lisbon, which is part of the 'Lisbon Observatories' and 'E-Nova Utilidados' Platforms, both with developments driven by the European project B-WaterSmart - Accelerating intelligent water management in coastal regions in Europe.

The Lisbon Urban Water Cycle Observatory (hereinafter “Observatory”) is a data visualization instrument to monitor and communicate water data, support planning and decision making.

The main objective of the Observatory is to act in the information to citizens, demand management, efficient use of water, promotion of alternative sources and raising awareness in society. In parallel, it supports, and it’s integrated within the scope Lisbon city policies.

Following the motto "know to reduce", the ‘Lisbon Observatories’ covers the dimensions of water and wastewater, in parallel with other environmental dimensions of the city, such energy consumption, urban waste, GHG emissions and mobility.

This Observatory includes two complementary tools:

- The ‘Lisbon Observatories’, a public access tool, with open data information of the water and wastewater city dimensions (top-down approach).
- The ‘E-Nova Utilidados’, a private access tool, for individual entities to integrate and analyse, via a set of analytics, the water consumption data of their facilities (bottom-up approach).

The ‘Lisbon Observatories’ privileges the use of infographics with creative data to build awareness, engage and empower citizens.

It provides information on the city's water matrix, on an annual basis, regarding main water flows, such as the total water consumption, consumption disaggregation by type of water source (potable, reclaimed water, groundwater and spring water), water consumption by type of use (residential, non-residential, green spaces, urban hygiene, etc) and by type of user (residential, commerce and industry, institutional, central government, municipal local authorities, etc), information on per capita indicators, spatialization of water consumption per local administrative area (parish), amount of treated wastewater and reclaimed water production.

This accessible, comprehensive, and clear data allows citizens and city stakeholders to be informed, to know their impact and feel motivated to participate and act towards increasing efficiency, assessing the impact of implemented policies, monitoring the benefits of behaviour changes and, consequently, continue the path towards the sustainable transition. The tool is updated annually in cooperation with the water supply and wastewater treatment entities of the city of Lisbon.

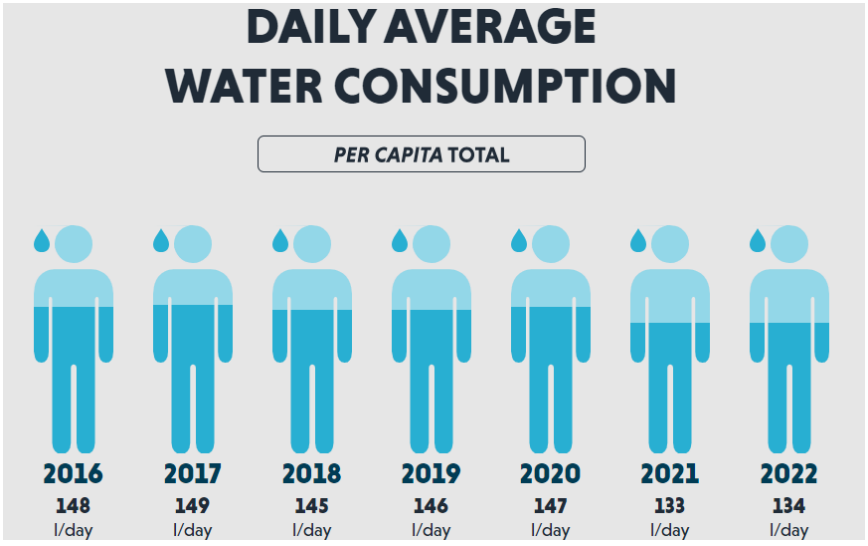



***Fig. 1.*** *Caption of the Lisbon Observatories Water dimension with information of the per capita indicator of residential water consumption*

The 'E-Nova Utilidados' is a web application integrating water consumption of user's facilities, with several characteristics and also a set of data analytics to the data for a deeper understanding of use of water.

This tool has a bottom-up approach, since it is aimed at single entities to monitoring and analyse their water consumption. It allows visualization of water consumption per facility and its evolution, aggregation in categories per type of use, water source, associated costs, indicators, identify water efficiency opportunities and monitor their impact after implementation.

The tool also allows to perform individual analysis per facility, which can be more detailed depending on the frequency of available data per water meter, integrating monthly, daily or quarter-hour data. Users can generate automatic reports based on all the data analytics presented for each facility and also set up the analysis of customised alerts for specific consumption levels for each facility.

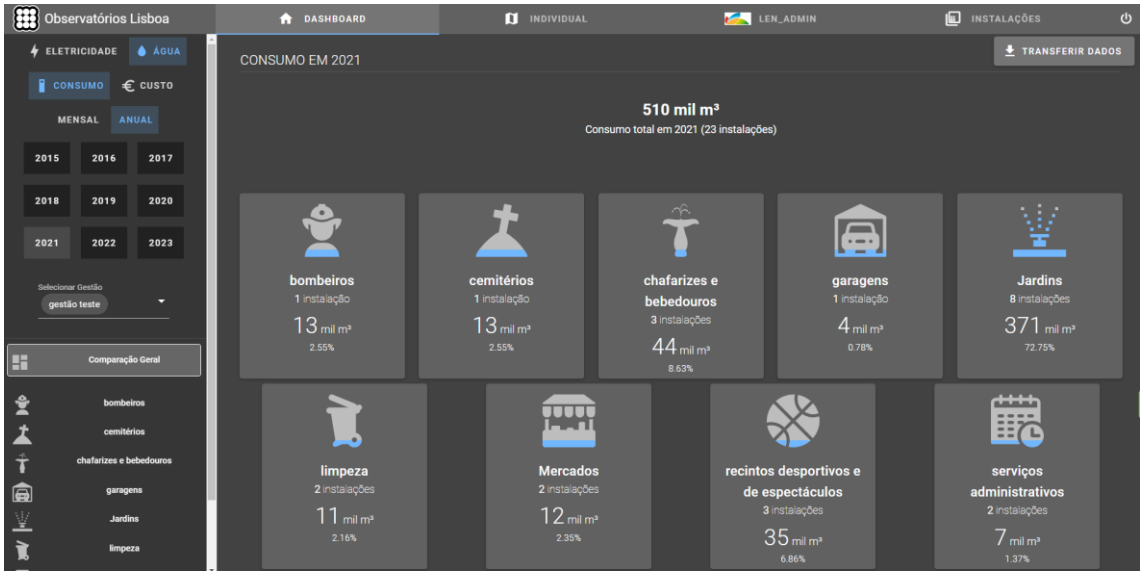



***Fig. 2.*** *Caption of the 'E-Nova Utilidados' showing the dashboard of a single user with the disaggregation of consumption of 2021 per type of use (fireman, cemeteries, fountains, gardens, markets, administrative services, etc), as well the number of water meters per type of use.*

- 'Lisbon Observatories':

https://observatorios-lisboa.pt/en/info_agua.html - Water dimension

https://observatorios-lisboa.pt/en/info_aguasresiduais.html - Wastewater dimension

- 'E-Nova Utilidados' – https://privado.observatorios-lisboa.pt/login

**References**

EPAL - Empresa Portuguesa das Água Livres, SA.

AdTA – Águas do Tejo Atlântico, SA.

# Reinventing Urban Water Management: The Lisbon Drainage Master Plan (LDMP)

José SILVA FERREIRA[1], Gonçalo DINIZ VIEIRA[2], Tiago ANDRADE GOMES[3]

[1,2,3] Municipality of Lisbon, Portugal
jose.silva.ferreira@cm-lisboa.pt
goncalo.diniz.vieira@cm-lisboa.pt
tiago.andrade.gomes@cm-lisboa.pt

ABSTRACT

Lisbon has been suffering from intense and more frequent flood events in the past years. These events not only negatively affect the tourism industry, but more importantly, cause long-lasting detrimental effects to the city population and its property and heritage.

The Lisbon Drainage Master Plan (LDMP) is intended to minimize the recurring and increasing flooding problem while increasing infrastructure resilience in specific vulnerable areas of the City of Lisbon, including parts of the historical city center. The tunnel's project is part of the Lisbon's Drainage Master Plan 2016-2030 strategy, which includes recommendations regarding a number of structural interventions in the city. It will deliver substantial environmental quality improvements, notably increased resilience against damages from high-intensity floods. It is the largest investment ever made by the Lisbon City Council, 150M€ for tunnels and globally 250M€ for the whole LDMP 2016-2030 project.

The main project is already ongoing (works started in September 2022, and will end in 2025), integrated into actions focused on flow diversion with the construction of two tunnels (5,5m internal diameter; 5km + 1 km long) and other infrastructures (retention/infiltration basins and three shafts with vortex that will link superficial pipes to main tunnel) in order to reduce the frequency and magnitude of floods in the city and minimize potential damages. This ambitious project faces unique challenges due to the complexity of the urban environment. The tunnel boring machine (TBM), a critical component of the project, is now actively engaged in tunnel excavation, being a significant phase in the project's progression.

While the tunnel boring machine (TBM) is actively excavating the tunnel, several construction sites across the city continues to operate, contributing to the overall progress of the project. For instance, the excavation work at the tunnel entry point (TMSA) has been completed and it now serves as the main hub for supporting the tunnel excavation process, including the extraction of excavated material. Additionally, works is ongoing at the tunnel exit areas, particularly for constructing the discharge channels to the Tagus River and connecting vortex wells for surface flow tunnel discharge in city areas periodically prone to flooding.

The drainage **tunnel construction includes an internal water recycling distribution system**, aiming not only to mitigate flood risks but also to **promote circular economy through water reuse in the city**. Recycled water from the Alcântara Water Factories (Wastewater Treatment Plant) will be distributed throughout the city center for various activities, such as irrigation of green spaces, street cleaning, and potentially firefighting, thereby saving potable water and reducing costs for citizens.

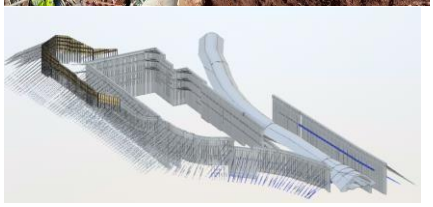
It is important to notice that the Lisbon Drainage Master Plan (LDMP) is an innovative and comprehensive strategy designed to tackle the challenges posed by climate change, particularly the intensification of pluviometric events leading to frequent and severe floods in Lisbon. The **use of innovated technologies and processes, in particular the Building Information Modeling (BIM),** integrates all relevant project information, facilitating communication among various entities and enhancing the construction process's quality and efficiency. BIM also allows for anticipating and resolving construction issues and preparing for infrastructure maintenance and exploitation, thus adding long-term value to these assets. The **Lisbon Municipality was the first public entity that prepared the tender in order to promote the use of BIM** (mandatory for the design phase, as well as the construction and future life-cycle of the infrastructures).

This strategic plan aligns with the themes of climate change, circular economy, and innovation. Its guiding principle is to develop an integrated flood control solution for Lisbon and provide the city with structural drainage infrastructures prepared for the challenges of the 21st century, while promoting water reuse and efficient underground use.

In conclusion, the LDMP exemplifies how innovation and technology can address climate change challenges and promote city sustainability and resilience. By constructing efficient drainage infrastructures and promoting water reuse, the plan contributes to transforming Lisbon into a more resilient and sustainable city.

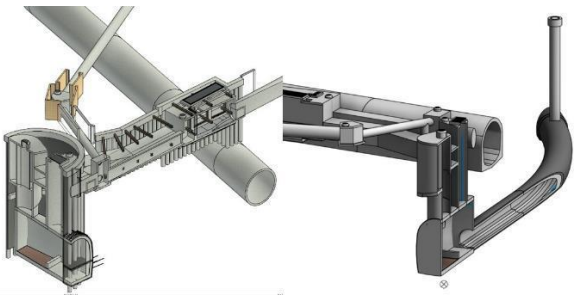










## References

(2015) Matos, J. S., Monteiro, A., Guerreiro, A., Ferreira, F., Braunschweig, F., Simões, J., . . . Fernandes, Z.. Plano Geral de Drenagem de Lisboa 2016-2030. Lisboa.
(2018). "Utilização de água reciclada na cidade de Lisboa" . Lisboa: O Caminho da Inovação 18 AdTA.
(Maio 2019). Águas do Tejo Atlântico - Plano Estratégico de Reutilização de água da Cidade de Lisboa. Lisboa.
IPMA. (1983). IPMA. Obtido de www.ipma.pt: https://www.ipma.pt/pt/oclima/series.longas/
(Julho de 2019) Matos, J. S., Monteiro, A., Santos, A., Ferreira, F., Guimarães, J., Leboeuf, Y., . . . Gama, C.. OBRAS DE DESVIO, INTERCEÇÃO E DE DESCARGA DOS TÚNEIS DE MONSANTO - STA. APOLÓNIA E DE CHELAS-BEATO.
(2023).Mota-Engil / Pie Batignolles. Projeto de Estaleiro.
(2002). Parque das Nações vai usar água reutilizada para rega. Lisboa.
(2019). Plano de reutilização de água permite poupar 3 milhões de m3 de água potável. Lisboa.
(Outubro de 2021) Vieira, G. D., & Ferreira, J. S.. PLANO GERAL DE DRENAGEM: OBRA INVISÍVEL QUE PROTEGE A CIDADE.

# Numerical modelling and experimental verification in time domain of hydraulic rams

David FERRAS[1], Saber NASRAOUI[1], Capucine DUPONT [1]

[1]IHE Delft Institute for Water Education, Delft, the Netherlands,
d.ferras@un-ihe.org, s.nasraoui@un-ihe.org , c.dupont@un-ihe.org

ABSTRACT

A hydraulic ram is a type of pump device that makes use of the potential energy of a water source to elevate a portion of that water mass to a higher elevation without the need of any external energy input. The potential energy is first converted to kinetic energy through a drive pipe. Then the pumping effect is generated by means of a fast valve closure, producing a pressure surge that is used to divert part of the flow to a higher elevation. Hydraulic rams were first proposed and designed at the end of the 18th century by John Whitehurst and Joseph Montgolfier. However, only during the 20th century the scientific explanations, both experimental and numerical, of the underlaying hydraulic ram mechanisms were provided with the support of water hammer theory. The present paper aims at contributing to the mathematical description of hydraulic rams by providing a new hydraulic model in time domain and a new experimental data set for model calibration and verification.

## 1. Introduction

A hydraulic ram (or ram pump) is composed of an upper reservoir, a long conduit (drive pipe), a lower reservoir, an elevated storage tank, and the pump body with the hydraulic elements to induce oscillatory (transient) flow in the drive pipe and to divert the flow towards the storage tank. An air chamber transforms the strong oscillatory flows to continuous flow. For a critical flow velocity, the waste (or impulse) valve closes, generating a water hammer wave that propagates throughout the drive pipe. During this propagation the delivery valve opens, diverting part of the flow and pressure towards the air chamber, which is connected with the upper tank through the delivery pipe. Even though hydraulic rams were first introduced by Joseph Montgolfier in 1797 (Cabanes, 1936), its mathematical description requires water hammer theory, which was developed especially during the second half of the 20th century (Streeter and Wylie 1967; Chaudhry, 2014). A number of scientific contributions have been provided towards the mathematical description of the ram pump system (Tacke 1988; Verspuy and Tijsseling 1993; Glover 1994). However, none developed a model fully describing the check valve mechanisms conceived by Joseph Montgolfier and that made hydraulic rams autonomous pumping systems. The present paper introduces a mathematical model especially describing this mechanism, which is then verified by experimental evidence.

## 2. Methodology, experimental facility and numerical model

A laboratory pipe rig was assembled at IHE Delft laboratory to test an in-house made hydraulic ram. As shown in figure 1-left, the facility consists of a water tank (water source) at 2.12 m elevation, a drive pipe 12.12 m long made of PVC material, with a diameter DN = 40 mm, and an experimental wave celerity of a = 242 m/s. The hydraulic ram body is placed at the downstream end of the drive pipe and is composed of a piston check valve for the delivery flow and a tilting disk check valve for the waste flow. Two pressure transducers (Wika P-30) were used inside the ram body and at the delivery side to measure respective transient pressures. A float flowmeter was assembled next to the waste valve to record steady flow rates. The tests were carried out for a maximum waste flow of 0.4 l/s and the delivery flow was regulated with a spherical valve covering the whole system spectrum of delivery flows, spanning from 0.086 l/s to 0 l/s.

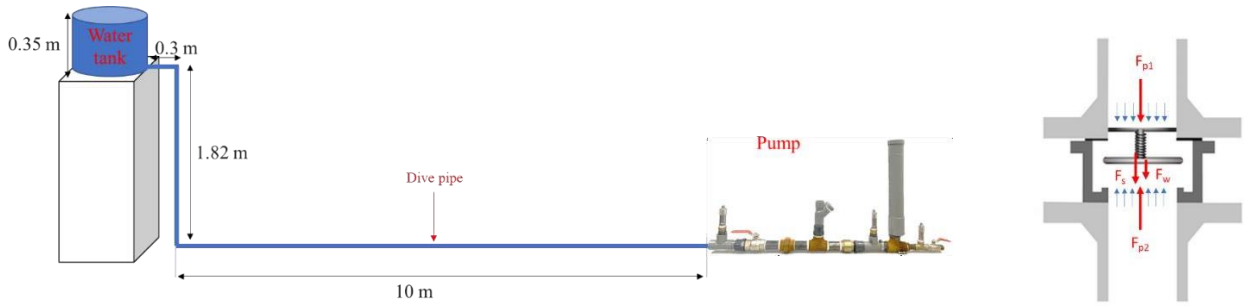



Figure 1 Schematic of the hydraulic ram pump system (left); Balance of forces at check valve (right).

The implemented numerical scheme is based on the method of characteristics (MoC) and special boundary conditions have been conceived for the modelling of the check valves located at the ram body. As indicated in figure 2-right, balance of forces and the second law of Newton are considered in each check valve to calculate the piston or disk positions and therefore the valve opening. Based on the valve opening, respective delivery and waste flows are computed at every time-step.

## 3. Results and discussion

The model was calibrated by adjusting the check valve spring stiffness, and friction and minor head losses coefficients at the drive pipe and ram body. Figure 2 shows the model verification for measured pressures at the ram body and delivery pipe. The numerical output with regard to the steady pressure at the delivery, the transient pressures at the ram body, and the operation period, match with accuracy the respective measurements, suggesting a successful experimental verification of the model.

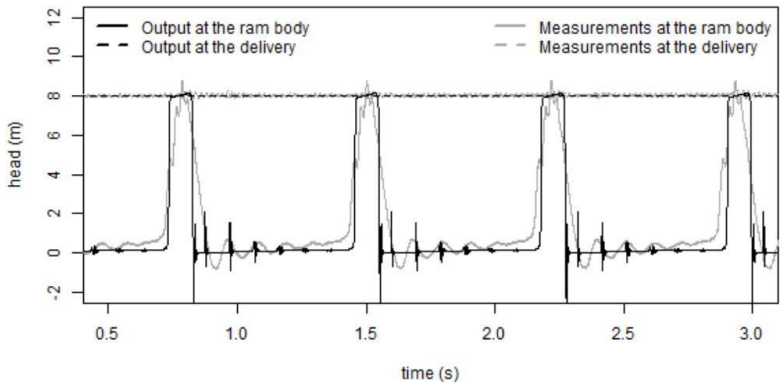



Figure 2 Numerical output and model verification.

## 4. Conclusions

The model provides a complete description of hydraulic ram operation with a full breakdown of its elements, including the dynamic behavior of the delivery and waste valves, enabling the analysis of the ram operation phases, with accurate descriptions of the flow acceleration and recoil periods. The proposed model is a good basis for a modal analysis considering different hydraulic ram configurations, which would provide a deeper understanding of the dynamic interaction between the different elements of the hydraulic ram.

**References**

Cabanes, Charles. "Joseph de Montgolfier et le Bélier Hydraulique." Transactions of the Newcomen Society 17.1 (1936): 85-90.
Streeter, V. L. and Wylie, E. B., 1967, Hydraulic Transients, McGraw-Hill, New York.
Chaudhry MH (2014) Applied hydraulic transients, 3rd edn Springer, New York, United States of America DOI https://doi.org/10.1007/978-1-4614-8538-4
Tacke, J. H. P. M. (1988) Hydraulic rams; a comparative investigation. Communications on hydraulic and geotechnical engineering, No. 1988-01.
Verspuy C, Tijsseling AS (1993) Hydraulic ram analysis. Journal of Hydraulic Research 31: 267-278 DOI https://doi.org/10.1080/00221689309498849
Glover, Peter Benedict Myers. Computer simulation and analysis methods in the development of the hydraulic ram pump. Diss. University of Warwick, 1994.

# Protecting Beira City (Mozambique) from frequent floods

Pedro SERRA[1], Geert PRINSEN[2], Victória D'OREY[3], Jenny PRONKER[4]

[1] TPF, Portugal, pedro.serra@tpf.pt
[2] DELTARES, Netherlands, geert.prinsen@deltares.nl
[3]TPF, Portugal, victoria.dorey@tpf.pt
[3] CDR-International, Netherlands, j.pronker@cdr-international.nl

ABSTRACT

Beira is the provincial capital of Sofala, Mozambique, located approximately 1200 km to the north of Maputo and third largest city of Mozambique by population. Its port is of strategic importance, being the gateway for cargo transport from and towards the land-locked countries, Zimbabwe, Zambia and Malawi, the so-called Beira Corridor. Because of this the population of Beira is expanding very rapidly, thus placing great pressure on urban development, which is rapidly expanding into floodable areas of Central and Eastern Beira, as well as new neighbourhoods towards river Maria estuary.

The coastal city of Beira has in the last few years suffered severe cyclones and tropical storms. This, associated to the morphological conditions of the city, with low-lying flatlands, has made the city prone to extensive flooding and has led to the necessity of improving the City's storm water drainage system and coastal protection. On the other hand, the city recently expanded to low-lying territory, where floods are frequent and severe and produce extensive damages, as could be seen recently during Idai (2019) and Eloise (2021) cyclones.

The main goal of the study was the rehabilitation of the storm water drainage system in Beira, to optimize the City's safety against flooding under the impacts of ongoing urban expansion and climate changes. The aim of this study was to improve the storm water drainage infrastructure and provide a resilient system for the central and the eastern areas of Beira, with an overall intervention area of approximately 20 sq. km.

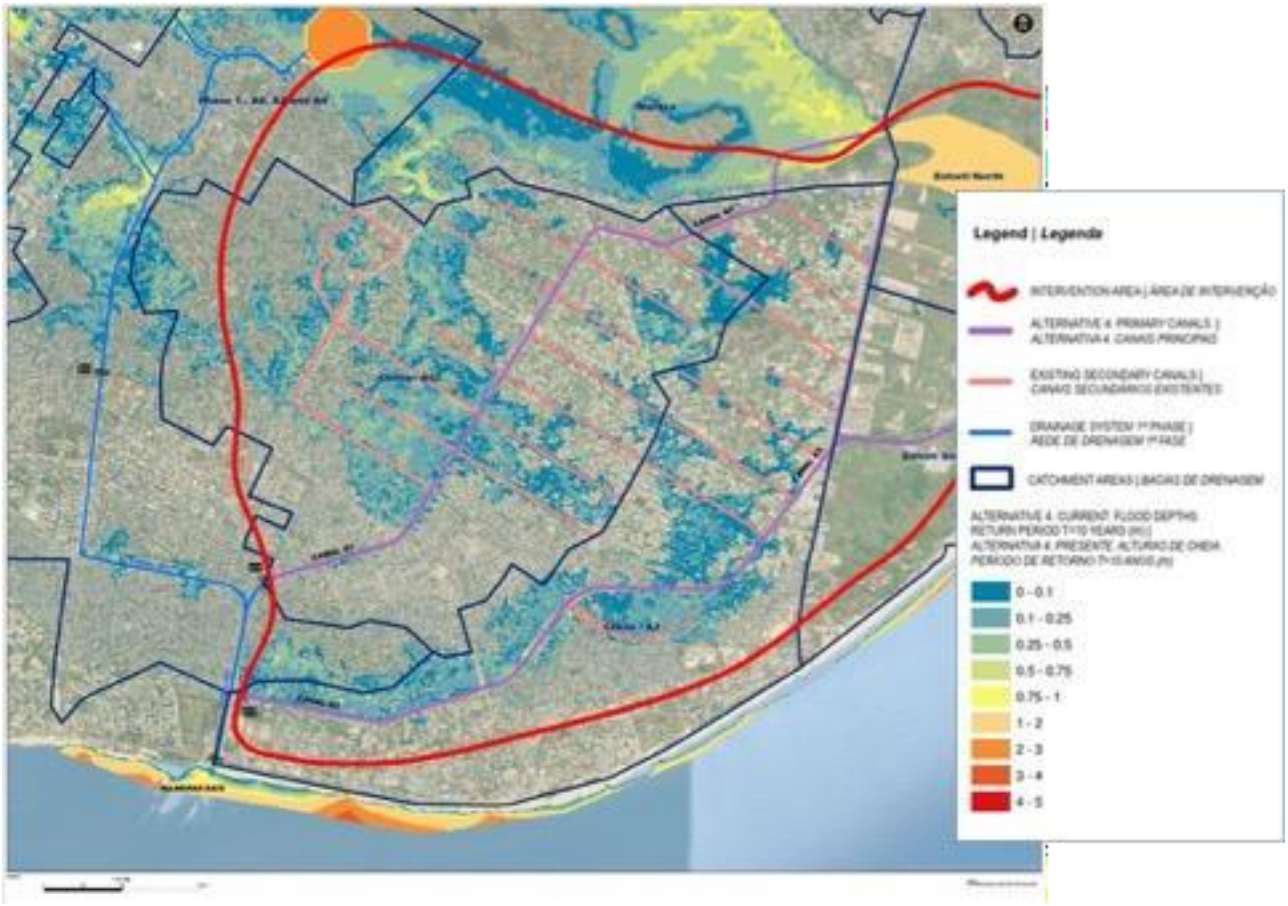
The project included the rehabilitation of the main canals, which receive the network of secondary canals that already exist in the territory. The flow along these canals shall be inverted and redirected northwards, to a retention basin to be built. This proved to be not an easy task, as the terrain is low-lying and very flat, being a rice field in the colonial era, and has been densely occupied in the last decades. The outlet structure shall be located upstream from a dyke which is to be built as part of an also on-going coastal protection project.

The study included a flood hazard and risk assessment, which performs a data analysis of rainfall and tidal boundary condition for cyclone and non-cyclone conditions, the setup and validation of the hydrological and hydraulic model, and model results. This model uses results of the flood hazard model in combination with data on assets and damage functions to estimate damages and risks. The flood hazard and risks have been discussed for the present situation and the future situation without measures.

With hydrological and hydraulic models, using design storms and tidal conditions with various return periods, the flood hazard was determined. The flood hazard indicates the possible flood depths and flood extent, for design events with a defined return period (up to T=100 years). The flood hazard modelling results in flood hazard maps, in which the extent and magnitude of the flood is indicated for various return periods. The maps are typically showing maximum flood depths and flood durations.

To translate flood hazard to flood risks, the definition of Kron (Kron, 2005) as used in the Sendai framework was adopted. Thus, risks are defined as the product of hazard, exposure and vulnerability. Important drivers for increased flood risk are climate change, which increases the hazard, and socio-economic development (including population growth, urbanisation) which increases peak runoff and thus the hazard, but also increases economic asset values, exposure and vulnerability. The exposure to flooding of people and assets

(like buildings, critical infrastructure) and the monetary values of these assets were estimated. In the present study, the focus was on pluvial flooding caused by severe precipitation and insufficient capacity to drain the water to sea via the existing outlet structures. The tidal boundary conditions play an important role in limiting drainage capacity. All these had to be considered in the design of the network of drainage channels.




Solution selected for the drainage of the project area

Four alternative solutions were evaluated for this project, following the methodology described above, with varying canal dimensions, type (trapezoidal or rectangular retaining walls) and varying routes. The alternatives were compared for the present and future situation, during non-cyclone events.

Results were then compared by analysing the hydraulic effectiveness, damage reductions and the economical cost-effectiveness of each solution, where calculated damages (resulting from flood extents and duration), as well as resulting benefits were compared. This determined the solution to be carried forward to design and construction (not yet started).

**References**

Kron, W. (2005). Flood Risk = Hazard. Values. Vulnerability. Water lnternational, 30(1), 58-68. http://doi.org/10 1080/02508060508691 837

Deltares (2021), Beira Coastal Protection Preparation study: flood hazard modelling. Deltares report (April 2021).

TPF et al. (2022b): Rehabilitation of the Storm Water Drainage System in the City of Beira Phase 2, Stage 1 Feasibility Study, Flood Hazard and Risk Assessment Report. TPF, CDR, Deltares, Wissing, 2022.

# Inclusion of natural areas in a holistic resilience assessment framework

Rita BRITO[1], Maria Adriana CARDOSO[2], Athanasios SFETSOS[3], Alex de la CRUZ, Beniamino RUSSO

[1,2] LNEC – Portuguese National Laboratory for Civil Engineering
rsbrito@lnec.pt
macardoso@lnec.pt
[3] INRASTES, NCSR Demokritos
ts@ipta.demokritos.gr
4 AQUATEC, Proyectos para el Sector del Agua S.A.U.
alex.cruz@aquatec.es
UPC, Universitat Politècnica de Catalunya
beniamino.russo@upc.edu

ABSTRACT

A holistic resilience assessment identifies opportunities and priorities for enhancing urban resilience, namely when considering interacting services and infrastructure. Several studies highlighted the mitigation of climate change impacts due to natural areas either preserving and/or enhancing those already existing or implementing novel man-made nature-based solutions within urban environments. A resilience assessment framework adding the natural areas to other services has several benefits. This paper presents the ICARIA project and the methodology to expand the ICARIA Resilience Assessment Framework, focusing on the approach and scope to include natural assets as a service provided by the cities or regions to their citizens, workers, and tourists.

## 1. Introduction

Urban resilience describes the ability of human settlements to withstand, recover quickly and adapt from any plausible hazards, both for acute shocks and slower changes in circumstances (UN-Habitat, 2018; UNDRR, 2017a and b; ARUP, 2105). Resilience to disruptive events comprises reducing risks and damage from disasters, and the capacities to withstand and to rapidly bounce back to a stable state. A resilience assessment is imperative to identify the opportunities and priorities for enhancing urban resilience. A resilience assessment framework and webtool are being upgraded and broadened within ICARIA (Improving ClimAte Resilience of crItical Assets, https://www.icaria-project.eu/), within the Mission "Adaptation to climate change", Horizon Europe. The overall aim of the Mission is to support European regions to become climate resilient. ICARIA aims to achieve a better understanding of climate change (CC) related impacts and adaptation measures on critical assets. The results of modelling tools, along with data on governance, socio-economic aspects, spatial planning, and service management, contribute to a holistic infrastructure resilience assessment, for selected hazards and scenarios, and with the possibility to focus on critical infrastructure.

Resilience assessment considers coexistence of different assets and services' functions in time and space. Their performance is interlinked, in everyday life, and even more while enduring disruptive events (Brugmann, 2012). The ICARIA Resilience Assessment Framework (RAF) builds on existing frameworks and app (from the RESCCUE project, the RAF (Cardoso et al., 2020) and the RAF App (Lopes et al., 2019), and from the EU-CIRCLE, the RAT tool (Katopodis et al., 2018). It was developed to enlarge the city-wide assessment to address a regional scope, complementary assets (beyond those already covered), namely natural areas, and to diagnose additional hazards beyond those already covered (flooding, storm surge, heat waves, drought, and windstorms), namely forest fires.

## 2. Methods

The inclusion of natural areas in the RAF comprised the steps represented in Fig.1.

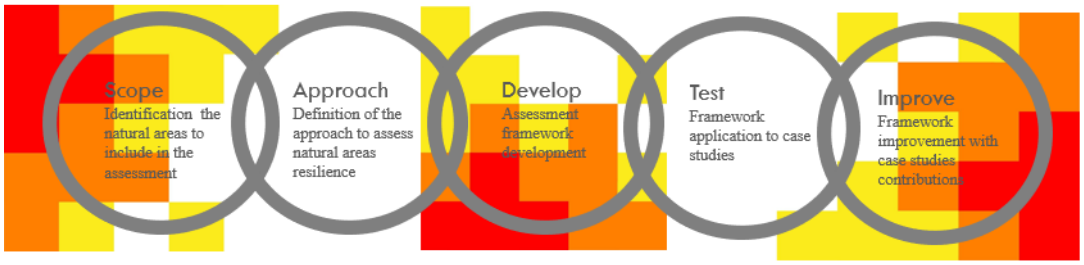



**Fig. 1.** Methodology to include natural areas in a resilience assessment.

### *2.1 Scope*

Natural areas, both native and constructed grey-blue-green infrastructure, comprise large reserves, forests, rivers, urban streams, urban parks, and urban nature-based solutions (NBS) such as infiltration basins, green roofs and walls, vegetated swales, infiltration trenches, or porous pavements. NBS are man-made solutions "inspired and supported by nature, which are cost-effective, simultaneously provide environmental, social and economic benefits and help build resilience" (EC, 2021). Protected areas and forests are mostly native or have long existed. Urban parks, ponds, lakes, tree lines or vegetated squares were frequently designed and implemented to address a specific problem (environmental or urbanistic) but still provide several other co-benefits. For a holistic point of view, it is advantageous to include both NBS and other existing natural areas in the same resilience assessment, to account for all the integrated co-benefits. Moreover, integrating all natural areas in a framework comprising other urban services enables including the existing interdependencies.

### *2.2 Approach*

Several studies highlighted the mitigation of CC impacts due to natural areas, either focused on the urban heat island mitigation and stormwater management as potential benefits (Almaaitah et al., 2021), or with more holistic approach, detailing the multiple ecosystem services, socio-economic challenges (Beceiro et al., 2020; Sarabi et al., 2019; Cardinali et al., 2023), or embracing ther contexts, such as earthquakes, fires, or hurricanes (EC, 2021). The UN-Habitat resilience dimensions are a comprehensive approach providing both an overview of the city as a whole and of each service in specific, by considering the following resilience dimensions: organisational and spatial (for the whole city); functional and physical (for each service). This structure was used in RESCCUE for the urban services (water services, solid waste management, energy provision, and mobility (Cardoso et al, 2020). Natural areas may be considered as a complementary and region-wide service provided by local authorities, in line with the UN-Habitat and RESCCUE approaches. This way forward has the advantage of disaggregating the contribution of diverse service and assets aspects to the overall resilience.

## 3. Results

The RAF has a hierarchical tree structure of dimensions, objectives, criteria and metrics. Some of the ICARIA RAF were adapted from existing frameworks (e.g. UNDRR, RESCCUE and EU-CIRCLE projects), and other metrics were newly developed. Table 1 summarizes the RAF functional dimension, its objectives, and criteria for natural areas. This preliminary version of the framework will be applied to case studies for feedback.

**Table 1.** Overview of RAF functional dimension for natural areas

| OBJECTIVE | CRITERION |
|---|---|
| SERVICE PLANNING AND RISK MANAGEMENT | Strategic planning |
| | Resilience engagement |
| | Risk management |
| | Reliable service |
| | Flexible service |
| AUTONOMOUS SERVICE | Natural areas' importance |
| | Inter-dependency with other services considering CC |
| SERVICE PREPAREDNESS | Preparedness for disaster response |
| | Preparedness for CC |
| | Preparedness for recovery and build back |

**Acknowledgments**
The ICARIA project (Improving Climate Resilience of Critical Assets) is funded by the European Commission through the Horizon Europe Programme, grant number 101093806. https://www.icaria-project.eu/.

**References**
ARUP (2015). City Resilience Framework. 100 Resilient Cities; The Rockefeller Foundation, ARUP: New York, USA.
Lopes, P.; Martins, R.; Oliveira, A.; Cardoso, M.A.; Brito, R.S.; Pereira, C. (2019). Resilience Assessment Framework Tool-RAF APP Description and Implementation; Lisboa.

# Climate Change Impacts on Lisbon Floods and the Potential Benefits of Nature-Based Solutions for Adaptation

Luís DIAS[1,2], Francesco FERRARA[3], Miguel RODRIGUES[2], João MOURATO[3], Maria João TELHADO[1], Catarina FREITAS[1].

[1] Lisbon Municipality, Portugal
luis.filipe.dias@cm-lisboa.pt
joao.telhado@cm-lisboa.pt
catarina.freitas@cm-lisboa.pt
[2] CE3C - Center for Ecology, Evolution and Environmental Changes & CHANGE - Global Change and Sustainability Institute, Faculdade de Ciências of the Universidade de Lisboa
luisdias@ciencias.ulisboa.pt
miguelsilvarodrigues@ ciencias.ulisboa.pt
[3] Instituto de Ciências Sociais of the Universidade de Lisboa
francescoferrario19@gmail.com
joao.mourato@ics.ulisboa.pt

ABSTRACT

Climate change, a critical issue of the 21st century, has already led to an increase in extreme weather events worldwide. These events pose a significant risk to urban areas, particularly those located in climate change hotspots. The city of Lisbon is highly susceptible to these changes, with flash floods being a significant concern. This study assesses the flood risk in downtown Lisbon under various climate change scenarios and examines the potential of nature-based solutions to adapt the city to these impacts.

## 1. Methods

In the analysis of precipitation data, the maximum annual daily precipitation between 1961 and 2000 from the Lisbon Geofísico meteorological station (IGIDL) was used, and recurrence intervals were calculated based on extreme value distributions. The precipitation associated with each return period was the basis for the estimation of rainfall hyetographs that were derived from IDF curves designed for the same meteorological station. Given the typical biases in climate change model data, a correction process was implemented using the cell values nearest to the IGIDL station. The bias correction method proposed by Willems Vrac, 2011 was applied to address systematic errors in the selected models, based on historical precipitation series from the IGIDL meteorological station.

Subsequently, return periods and rainfall hyetographs for the climatic normal 2061-2090 were calculated for each model, and an ensemble was created based on the median of the results from the 9 members. Hydrological modelling based on rainfall hyetographs was conducted for the entire watershed, encompassing Downtown Lisbon, the focal area of the risk evaluation. The SWMM was employed for drainage network modelling, using information from the 2007 General Drainage Plan of Lisbon and the drainage infrastructure available. This was coupled with the MOHID Land model, responsible for the surface runoff. Applying depth–damage curves to different assets enabled the creation of probability-damage curves to calculate the actual risk, translated into average annual damage.

To diminish flood risk, adaptation measures are needed, particularly when considering the impacts of climate change. In this context, NbS emerged as cost-effective and win-win adaptation measures. With a focus on this type of measures, a meta-analysis was conducted to understand the most effective solutions available for reducing runoff during heavy precipitation events. To accomplish this, structured research was carried out by

applying a search query in the online database Web of Science. The database query is based on the PICO/PECO framework and the main geographical target of the review is European cities. The development of the search query underwent stages of adjustments until the final version, which was executed in March 2023. The meta-analysis follows the PRISMA methodology, being selected, in total, and between 2005 and 2023, 922 papers. After the screening process, 29 papers were selected, based on the availability of information needed for the meta-analysis. These papers contain 90 useful NbS observations.

## 2. Results

Flood risk was estimated considering 7 recurrence intervals for the observed climate and the RCP8.5 climate change scenario, accounting for the structure and main occupations of the buildings. This resulted in considerable increases in average annual damage in all cases when comparing the results of the current situation with the future. Non-industrial fixed assets located on the ground floor and stocks are of relevance, with average annual damages increasing by 5.79% and 3% per year, respectively. Additionally, the total number of buildings exposed to floods increases from the current 344 affected to 378 by the end of the century.

One of the potential measures to minimize flood risk involves NbS. To assess the effectiveness of these measures in reducing flood impacts, both generally and specifically in downtown Lisbon, a meta-analysis was conducted. This analysis encompasses various NbS categorized and quantified for their effects on urban resilience as measured in peer-reviewed studies. Besides the overall impact of NbS, the analysis considers how different NbS contribute to the goal of increasing urban resiliency. The analysis covers bioretention cells, green roofs, parks and urban forests, and single trees. When considering the effect of the different NbS, the one reducing runoff the most is bioretention cells (about 77% reduction). Green roofs and Parks are also quite effective, impacting runoff reduction of about 60% and 57%, respectively. However small the impact (about 14% reduction), single trees positively increase urban resilience regarding runoff reduction. All the results are statistically significant, except for the one describing the impact of single trees. However, the direction of the effect is nonetheless relevant. Trees have a positive impact on runoff reduction in urban areas and this evidence confirms the literature on the topic indicating that the interception of rainfall by tree canopies and the increased water absorption in the soil have a positive effect on reducing the overall urban runoff. The case of green roofs is interesting as these NbS can be either intensive or extensive. Almost all the cases included in this analysis were extensive green roofs (leading to a 60% runoff reduction); per contra, the one case that presented the impact of an intensive green roof showed a very high reduction of 84% of the overall excess water. Also in this case, the split does not provide an indication that has statistical significance, but it indicates an unexplored potential when it comes to intensive green roofs.

**References**


Action Modulers. (2013). Urban Floods - Final report on numerical modeling of urban floods in 4 Portuguese cities.

Beck, H. E., Zimmermann, N. E., McVicar, T. R., Vergopolan, N., Berg, A., & Wood, E. F. (2018). Present and future Köppen-Geiger climate classification maps at 1-km resolution. Scientific Data, 5(1), 180214. https://doi.org/10.1038/sdata.2018.214

Brandão, C., Rodrigues, R., & da Costa, J. P. (2001). Análise de fenómenos extremos precipitações intensidades em Portugal continental.

Dias, L. F., Aparício, B. A., Nunes, J. P., Morais, I., Fonseca, A. L., Pastor, A. V., & Santos, F. D. (2020). Integrating a hydrological model into regional water policies: Co-creation of climate change dynamic adaptive policy pathways for water resources in southern Portugal. Environmental Science & Policy, 114, 519–532. https://doi.org/10.1016/j.envsci.2020.09.020

Dias, L. F., Mendes, M. C., Neves, R., & Santos, F. D. (2016). *As alterações climáticas, as inundações e a cidade. Contributos para o estudo da resiliência urbana em situações de chuvas torrenciais* [Tese de Doutoramento]. Universidade de Lisboa. Faculdade de Arquitetura.

Moel, H. de, Huizinga, J., & Szewczyk, W. (2017). *Global flood depth-damage functions: Methodology and the database with guidelines*.

Sowińska-Świerkosz, B., & García, J. (2022). What are Nature-based solutions (NBS)? Setting core ideas for concept clarification. *Nature-Based Solutions*, *2*, 100009. https://doi.org/10.1016/j.nbsj.2022.100009

van der Laan, E., Nunes, J. P., Dias, L. F., Carvalho, S., & Mendonça dos Santos, F. (2023). Assessing the climate change adaptability of sustainable land management practices regarding water availability and quality: A case study in the Sorraia catchment, Portugal. *Science of The Total Environment*, *897*, 165438. https://doi.org/10.1016/j.scitotenv.2023.165438

Willems, P., & Vrac, M. (2011). Statistical precipitation downscaling for small-scale hydrological impact investigations of climate change. *Journal of Hydrology*, *402*(3–4), 193–205. https://doi.org/10.1016/j.jhydrol.2011.02.030

# AgIR Project Action no. 3 - Characterization of Wastewater Affluent to Wastewater Treatment Plants from Hospital Units in the Municipality of Lisbon

Dora SILVA[1], Liliana BÉRTOLO[1], Eugenia CARDOSO[1], Diogo BENTO[1], Catarina PECURTO[1], Pedro TEIXEIRA[2]

[1] Águas do Tejo Atlântico, S.A.
geral.adta@adp.pt

[2] Câmara Municipal de Lisboa
pedro.teixeira@cm-lisboa.pt

ABSTRACT

Wastewater sanitation activities contribute to people's quality of life and public health, promoting more environmentally friendly and sustainable cities. Characterization of wastewater that flows into Wastewater Treatment Plants (WWTPs) enables processes to be managed with improved efficiency in terms of treatment, contributing to environmentally safe treated wastewater, either for final disposal or reuse. In this context, the AgIR - Action Plan for Management of Industrial Wastewater in Greater Lisbon and West, emerged and was approved by Portuguese Government on the 31.st December 2021 with funding of 4.4 million Euros from the Portuguese Environmental Fund, to be implemented between 2022 and 2026. The Action Plan includes the following Action Lines:

- Action no. 1 "Technical support for municipalities and the respective municipal management entities";
- Action no. 2 "Technical support for industries, in coordination with municipalities and the respective municipal management entities";
- Action no. 3 "Characterization of wastewater flowing to Wastewater treatment plants from hospital units in the Municipality of Lisbon in order to help respond to possible outbreaks of disease in the population, improve the response of WWTP treatment processes, with a view to reducing pathogenic environmental risks and emerging pollutants present";
- Action no. 4 "Training for technicians of the management entities of municipal services and industries in the field of industrial effluents";

Action No. 3 of the AgIR "Characterization of wastewater affluent to Wastewater treatment plants from hospital units in the Municipality of Lisbon", aims to promote the reduction of environmental risks arising from the presence of pathogenic microorganisms and emerging pollutants and to improve the quality of life and the environment in the city of Lisbon, and has the following main objectives: 1) To deepen and broaden the objectives of the previous study on the characterization of hospital wastewater flowing into municipal sanitation networks (CML's responsibility) and multi-municipal systems (AdTA's responsibility) carried out in 2013/2014 in various hospital units in Lisbon - Report: "Proposed Recommendation for the microbiological characterization of hospital wastewater - the case study: Lisbon"; 2) Updating the licensing processes for discharging hospital wastewater with the Lisbon Municipality; 3) Contribute not only to establishing the conditions for discharging wastewater into the municipal drainage system, but also contribute with more information to the epidemiological surveillance systems that are being studied, to help improve the response to possible disease outbreaks in the population; 4) Promote the optimization of treatment processes in wastewater treatment plants (WWTP) and hospital units.

This study includes microbiological tests (bacteria, virus and fungi relevant in a hospital environment), genetic tests (antibiotic resistance genes), emerging pollutants (pharmaceuticals) and ecotoxicity tests. Given the scope of the study, a partnership was organized between various entities (AdTA - Águas do Tejo

Atlântico, CML – Câmara Municipal de Lisboa, IST - Instituto Superior Técnico, INSA - Instituto Nacional de Saúde Doutor Ricardo Jorge, EPAL - Empresa Portuguesa de Águas Livres, DGS - Direção-Geral da Saúde and ARSLVT - Administração Regional de Saúde de Lisboa e Vale do Tejo).

The project includes three sampling campaigns in 2023 and two campaigns in 2024, distributed between the dry and wet seasons. Each campaign includes sampling at all the 13 participating hospital units, the points at the entrance and exit of the WWTP. The activities to be carried out within the scope of this project include the characterization of the affluent and treated wastewater from the drainage basins of the Beirolas, Chelas and Alcântara WWTP, as well as wastewater from hospital units.

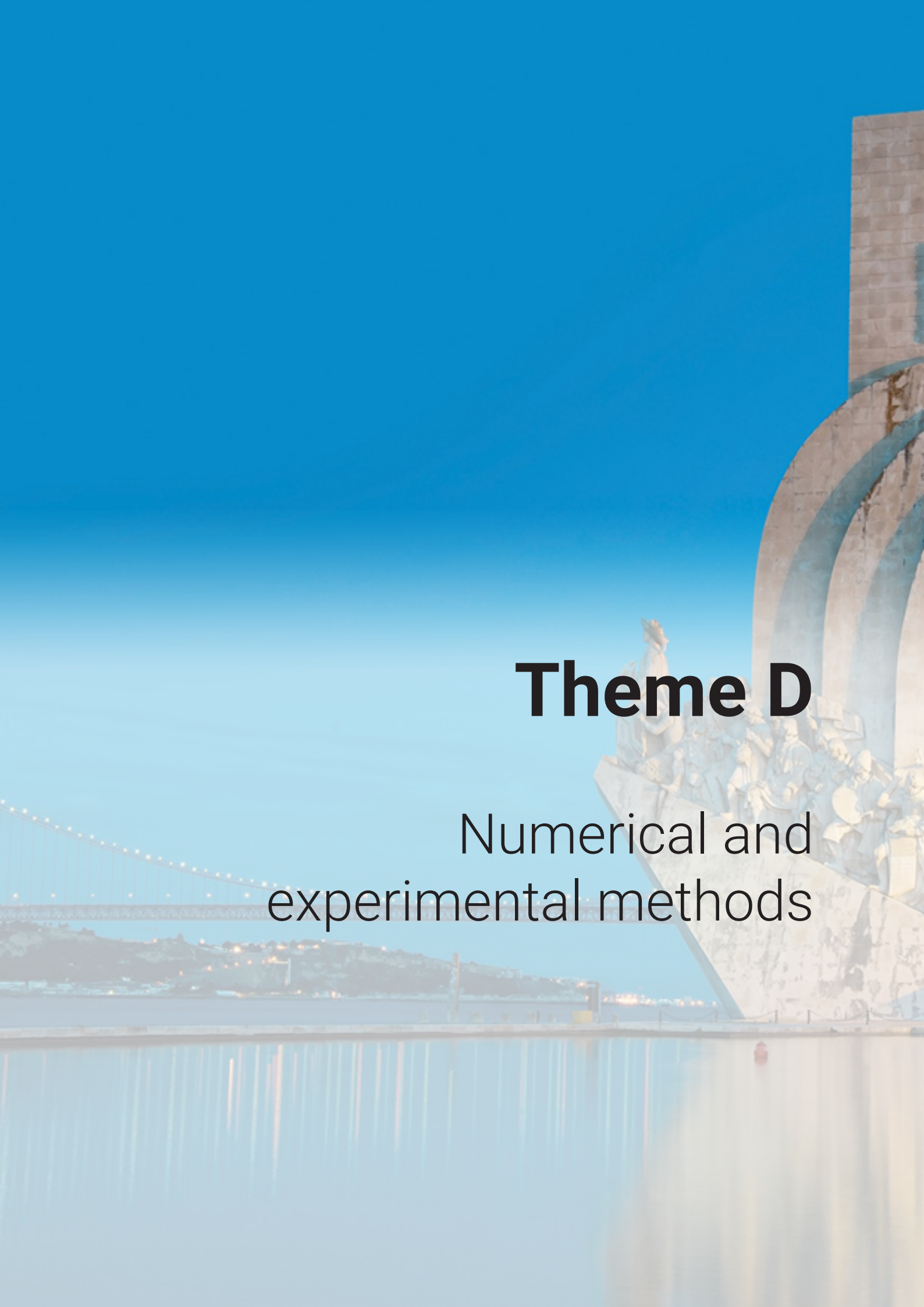
The results obtained in the various campaigns are analyzed and interpreted, concluding on the influence of hospital discharges on the characteristics of domestic effluents and the respective impact on the treatment processes of WWTP.

**Acknowledgements**

Fundo Ambiental, Direção Geral da Saúde, Administração Regional da Saúde de Lisboa e Vale do Tejo, Águas do Tejo Atlântico, Câmara Municipal de Lisboa, Instituto Ricardo Jorge, Instituto Superior Técnico, Empresa Portuguesa das Águas Livres (EPAL), all participating Hospital Units.

**References**

Council of Ministers Resolution no. 204/2021, of December 31st.



# Theme D

## Numerical and experimental methods

# Microplastic particles in cohesive sediment mixtures as an additional factor influencing erosion

Stefan HAUN[1], Maria PONCE[2], Naung Naung HTUN [3], Silke WIEPRECHT[4]

[1,2,3,4] Institute for Modelling Hydraulic and Environmental Systems, University of Stuttgart, Germany
stefan.haun@iws.uni-stuttgart.de
maria.ponce-guzman@iws.uni-stuttgart.de
n.naunghtun20@gmail.com
wieprecht@iws.uni-stuttgart.de

ABSTRACT

Due to the wide range of parameters that affect the erosion behavior of cohesive sediments, knowledge of ongoing processes and the interactions between them is still very limited. Adding to cohesive sediment mixtures microplastic particles (MPs) will change the structure of the sediment matrix and subsequently the erosion behavior. In the present study, the influence of MP inclusions on the erosion behavior of artificially produced cohesive sediment mixtures was studied by using data from erosion tests. The artificially produced sediment samples differ in the amount of clay, the type of clay mineral, and the water content. The physical properties of the added MPs, like the polymer type, and the number of particles were varied to investigate changes in erosion behavior in detail. The findings of this study show that the impact of MPs on sediment erosion is strongly dependent on the composition of the sediment itself (especially the amount and type of clay and the water content), but also on the characteristics of the MPs. For cases with a low clay content and only kaolinite as a clay mineral, the highest critical bed shear stresses were measured when microplastic pellets were present in the sediment mixture. For all other samples, the presence of MPs is causing a stochastic erosion behavior, which results in a reduced bed strength and an increasing erosion volume.

## 1. Introduction

Synthetically produced plastics have become indispensable for modern society due to their universal and diverse applicability. At the same time, the pollution of our freshwater ecosystems by plastics is a growing problem and results in negative impacts on aquatic ecology. Research on MPs and their impact on the ecosystems is currently conducted mainly for the water phase of rivers. However, MPs are also bonded to fine sediments due to cohesive and adhesive forces. If the flow behavior of rivers is disturbed due to anthropogenic influences, such as the construction of dams, these particles may sink and accumulate as a result of decreasing flow velocities and turbulences. Reservoirs are therefore sink for sediments, pollutants, and MPs.

Accumulations of MP may significantly alter the properties of sediment depositions, and may as a result change their erosion potential. However, the influence of MPs on the erosion behavior of sediment accumulations is not known so far. Within this study, a systematic analysis of the erosion behavior of artificially produced sediment mixtures, with a different amount of clay and water, and spiked with MPs was performed. The artificially produced sediment mixtures enable the reproducibility of the samples.

## 2. Methods

In the first step, sediment mixtures with different clay mineralogy (15 % of kaolinite as well as 2-15 % of kaolinite - bentonite mixture), water content (18% to 25%), and fine sand ($d_{50}$ of 0.29 mm) were produced. To ensure the reproducibility of the samples bulk density (based on the gamma-ray attenuation method) and grain size distribution measurements (based on laser diffraction) were performed in several axes and layers after six days of consolidation (Htun, 2023).

In the second step, different polymers, and quantities of MPs were added to the sediment mixtures to investigate the dependency of MPs on sediment erosion. The quantity of MPs varied from 1,000/kg dry mass

to 3,000/kg dry mass. The polymers used in this study were linear low-density polyethylene granulates (PE) with a size of 3-5 mm and a density of 0.92 g/cm$^3$ and PLA (polylactic acid) pellets with a mean diameter of 2.5 to 4 mm and a density between 1.21 and 1.43 g/cm$^3$, resulting in a total of twelve investigated samples.

The erosion behavior of the artificial sediment mixtures was investigated in the third step by using the SETEG (Strömungskanal zur Ermittlung der tiefenabhängigen Erosionsstabilität von Gewässersedimenten) erosion flume (Beckers et al., 2020). During the experiment the critical bed shear stress was therefore increased stepwise (Tab. 1), and the erosion evolution was recorded with high spatial and temporal resolution by using the pixel-based topographic detection method PHOTOSED (Noack et al., 2018). The determination of the critical shear stress for erosion was defined when the erosion depth reached 1 mm (McNeil et al., 1996).

## 3. Results

From the experiments can be seen that the effect of MPs on erosion was strongly dependent on the composition of the sediment mixture, and here mainly on the amount of clay. The sediment mixtures with the lowest clay content (< 5 %) and those with only kaolinite as a clay mineral demonstrated the highest resistance to erosion when microplastics were present in the sediment mixture. This finding is supported by the study of Ingraffia et al. (2021) where microplastics added to soil samples increased the overall stability as the inclusion of MPs enhanced the network structure of the sediment sample. In sediment mixtures with a clay content of 5 % and above, gamma-ray attenuation measurements showed a clear decrease in the bulk density for the samples containing MPs in comparison to those without MPs. The erosion tests showed for these samples a lower erosion resistance and hence, a lower erosion threshold. In addition, an increase in eroded volume could be observed for all samples. Fig. 1 shows the measured eroded volume for the test case with 20 % water and 5 % clay content (kaolinite), for the sample without MPs (circles), and for samples containing PE 1,000/kg (crosses), PLA 1,000/kg (squares), and PLA 3,000/kg (triangles). From the measurements can be seen that the erosion starts earlier for all samples containing MPs. The sample with PE 1,000/kg shows the smallest eroded volume during the experiments. Samples spiked with PLA show a clear increase in eroded volume especially when the number of particles changes from 1,000/kg to 3,000/kg. From the high-resolution measurements temporal and spatial variability of erosion is visible, where the highest erosion rates occurred mainly around the MPs, making the influence of MPs on sediment stability evident.

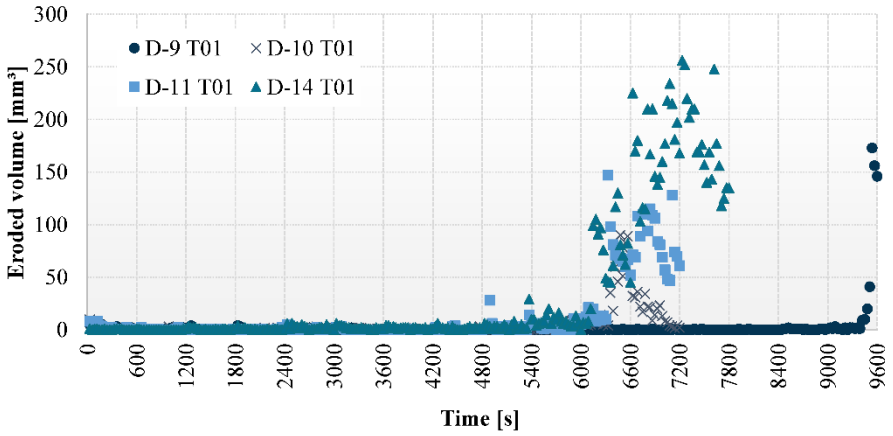



**Fig. 1.** Comparison of measured eroded volume between the sediment samples with the same amount of water 20% and clay 5% without MPs (D-9), with 1,000 PE particles (D-10), with 1,000 PLA particles (D-11), and with 3,000 PLA particles (D-14)

| Time [s] | $\tau$ [Pa] |
|---|---|
| 600 | 0,04 |
| 1200 | 0,10 |
| 1800 | 0,18 |
| 2400 | 0,27 |
| 3000 | 0,38 |
| 3600 | 0,51 |
| 4200 | 0,65 |
| 4800 | 0,81 |
| 5400 | 0,99 |
| 6000 | 1,18 |
| 6600 | 1,39 |
| 7200 | 1,61 |
| 7800 | 1,85 |
| 8400 | 2,11 |
| 9000 | 2,38 |
| 9600 | 2,66 |

**Tab. 1.** Sequence of bed shear stresses used in the experiments

**Acknowledgments**

The first and last authors are indebted to the Baden-Württemberg Stiftung for the financial support of the Elite program for Postdocs.

**References**

Beckers F, Inskeep C, Haun S, Schmid G, Wieprecht S, Noack M (2020) High spatio-temporal resolution measurements of cohesive sediment erosion. Earth Surface Processes and Landforms 45(11): 2432-2449.

Htun, Naung Naung (2023) Effects of Microplastic Particles on Swelling Clay-Sand Mixtures with High Liquid Limit Sediment Erosion. Naung Naung Htun, Master's thesis, University of Stuttgart.

Ingraffia R, Amato G, Bagarello V, Carollo FG, Giambalvo D, Iovino M, Lehmann A, Rillig MC, Frenda AS (2021) Polyester Microplastic Fibers affect Soil Physical Properties and Erosion as a Function of Soil Type. SOIL 8, 421–435.

McNeil J, Taylor C, Lick W (1996) Measurements of erosion of undisturbed bottom sediments with depth. J. Hydraul. Eng., 122(6), 316–324.

Noack M, Schmid G, Beckers F, Haun S, Wieprecht S (2018) PHOTOSED - PHOTOgrammetric Sediment Erosion Detection. Geosciences 8: 243.

8th IAHR EUROPE CONGRESS
LISBON - PORTUGAL
4-7 JUNE 2024

# Horizontal wave paddle for wave-current interaction experiments

Gerald MULLER[1]

[1] University of Southampton, UK
g.muller@soton.ac.uk

ABSTRACT

The interaction of waves and currents is of great interest in many areas of coastal engineering, in sediment transport and scouring at offshore foundations as well as e.g. pollution dispersal. Because of the non-linearities involved, experiments are here of importance. The experimental facilities are however mostly expensive purpose-built installations. Most employ vertical wave paddles which interfere with the current and therefore generate additional problems. At Southampton University a simple horizontal wave paddle was developed which has a minimal flow resistance and which can be retrofitted into existing current flumes. A wave absorption plate which also has a very low flow resistance was also developed. Tests showed that the wave paddle generated very regular waves and that the wave absorber plates were very effective. The system is currently being developed further for implementation in a new experimental installation at Southampton.

## 1. Introduction

The interaction of waves and currents is an important aspect in coastal engineering. The effect of the interaction is that the waves become shorter and steeper when they run against, and longer and shallower when they run with the current. Wave-current interaction is of specific importance for offshore foundations of wind turbines, where scouring is an important design issue. Although there has been a significant amount of theoretical and numerical work done on wave-current interaction, experiments are still difficult, see e.g., Markus et al. (2015). This is linked to the complexity of a combined generation of waves and currents plus the necessity for wave absorption. Existing wave-current flumes are mostly expensive purpose-built installations. There is therefore a need for a simple yet effective retrofit solution to generate and absorb waves in an existing current flume.

## 2. Horizontal wave paddle

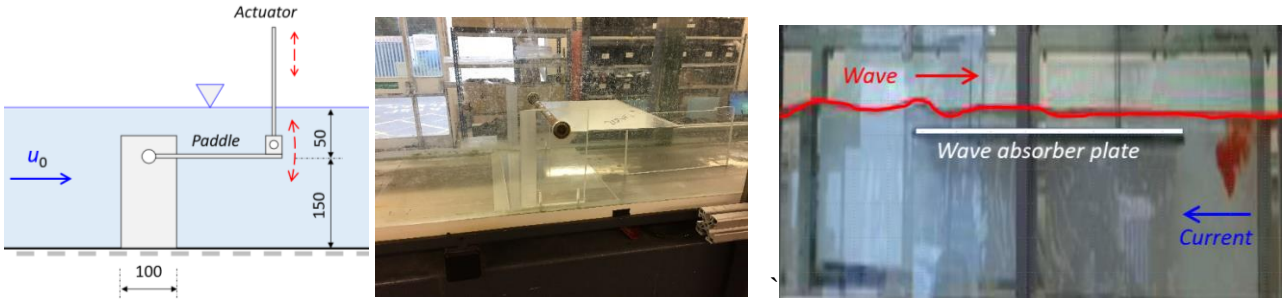
### *2.1. Problem definition*

In existing wave-current flumes, mostly vertical wave paddles are used to generate waves. These paddles at least partially block the cross section for the current. This means that secondary currents and turbulence are induced. In addition, the contact between waves and currents can produce problem such as a deformation or a partial reflection of the wave. The wave then has to be absorbed, since undesirable reflections can occur at the flume boundaries. A wave paddle in a current should therefore have a minimum of flow resistance / cross sectional area, and the wave absorption system should also cause a minimum interference with the flow.

### *2.2. The wave paddle and wave absorber*

The solution developed at Southampton University is a horizontal hinged plate located approximately 50 mm below the water surface, Costaras (2017). The paddle consisted of a 3 mm thick aluminum plate of 300 mm length and 280 mm width, Fig. 1a and 1b. The tip of the plate was moved up- and down by 25 mm using an electric motor situated above the water surface. This generated two wave sets, one traveling up- and one downstream of the wave paddle. The experiments were conducted in a 12 m long hydraulic flume. During the experiments, several different wave absorbers were assessed. The chosen absorber consisted of a thin horizontal plate made of 3 mm aluminum and located appr. 0.8 $H$ below the water surface. The width was 298 mm, the length was around 1m, or 1.5 $L$. Two plates were installed at either end of the flume. At the upstream end, the plate was horizontal whilst on the downstream end it was slightly inclined. The observations showed that the wave when running onto the plate starts to break and literally disappears before reaching the end of

the plate. The plates only cover 1.5% of the total cross-sectional area, so that their flow resistance is minimal. Fig. 1c shows the upstream absorber plate with the water surface drawn in red. The wave is completely dissipated before even reaching the end of the plate, no reflections were measured or observed.

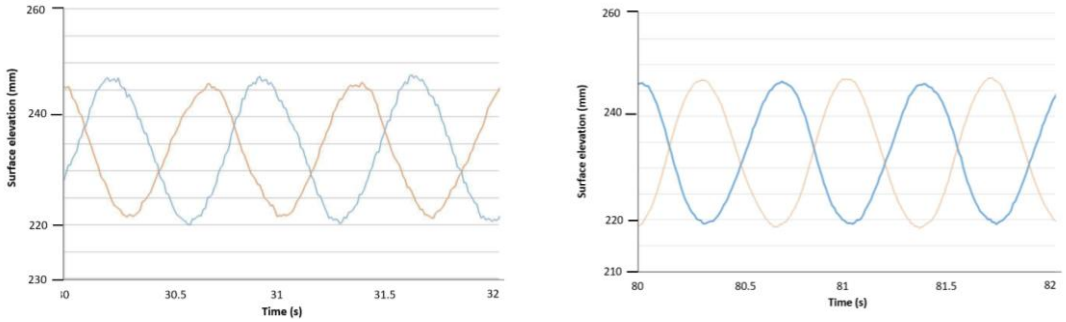



(a) (b) (c)

**Fig. 1.** The horizontal wave paddle, (a) side elevation, (b) Picture of the completed paddle. (c) Wave absorber (distorted length scale)

## 3. Experiments and results

A series of initial experiments was conducted in the 12 m long, 300 mm wide and 400 mm deep flume. The wave paddle was located in the mid-section of the flume. Two sets of two wave probes were located in between the wave paddle and the wave absorbers. These probes were used to measure the wave height and to determine the wave speed. In addition, the comparison of the wave surface profiles would show if a reflective wave was present. The wave period was 0.69 seconds. With a water depth of 0.234 m, the wave velocity can be determined as 1.04 m/s, and the group velocity as $c_g$ = 0.59 m/s. The flow velocity was 0.07 m/s = 0.12 $c_g$. As expected, the upstream waves are higher. Fig. 2a shows the downstream, and Fig. 2b the upstream wave heights of $H$ = 25 mm and 29 mm respectively, giving a ratio of 29 / 25 = 1.16. This compared reasonably well with the theoretical ratio of 1.14. The regular sinusoidal surface profile indicates the effectiveness of the wave paddle. The surface profiles of both wave probes in each set are nearly identical, indicating that there is no reflected wave present. This can be regarded as a measure for the efficiency of the wave absorber plates.




(a) (b)

**Fig. 2.** Experimental results - wave surface profiles (a) downstream, $H$ = 25 mm, (b) upstream, $H$ = 29 mm

Further tests with a flow velocity of 0.15 m/s corresponding to 0.254 $c_g$, led to similar results.

## 4. Discussion and conclusions

At Southampton University, a simple system for the generation and absorption of waves in a current was developed. The system has a minimum of flow resistance and can be retrofitted into existing flumes. The experimental results showed very good wave surface profiles, demonstrating the quality of the wave generation, The wave absorption plates also have a minimal flow resistance and work very effectively. Currently, a further development programme is underway to optimize the wave paddle geometry and to determine the performance parameters of the system. This is part of a new hydraulic research facility in Southampton which comprises a 30 m long, 1.8 m wide, 0.8 m deep, bi- directional two-way tilting flume with wave-current generation. This facility is currently under construction and is expected to define the state-of-the art of such installations.

**References**

Costaras, M. (2017) Wave – current interaction. Individual project Report. University of Southampton (72 pp).
Markus, D., Jakobsen, M. M., Bletzinger, K. U., & Frigaard, P. B. (2015). Damping of unwanted turbulence in wave–current experiments. Coastal Engineering, 96, 38-48.

# Hybrid physically based and machine learning model for streamflow prediction

Sergio Ricardo LÓPEZ-CHACÓN[1], Fernando SALAZAR[1,2], Ernest BLADÉ[2]

[1] International Centre for Numerical Methods in Engineering (CIMNE), 08034 Barcelona, Spain; slopez@cimne.upc.edu, fsalazar@cimne.upc.edu

[2] Flumen Institute, Universitat Politècnica de Catalunya (UPC BarcelonaTech)—International Centre for Numerical Methods in Engineering (CIMNE), 08034 Barcelona, Spain; ernest.blade@upc.edu

ABSTRACT

Fully representing the complexity of the rainfall-runoff processes occurring in a catchment for a variety of precipitation events is a challenging task for the physically based hydrological models: the calibration procedure is usually difficult and it might not accurately capture the streamflow response of the catchment for unseen scenarios. In order to achieve a model with enhanced capabilities, this study proposes a methodology to create a hybrid model combining a surrogate model based on the physical model Iber and a machine learning model to compensate for the possible residuals. Since the proposed methodology is designed to be used in early warning system applications, the evaluation is mainly focused on the high streamflow values. The results show that the hybrid model provides higher accuracy than the physically based model and closer approximations to the peak values than a single machine learning model. This results in an increased utility for the intended application. Moreover, it might represent an alternative to the calibration procedure for physically based models.

## 1. Introduction

Accurate prediction of streamflow is essential in early warning systems (EWS). In that regard, recent studies have shown that models that rely on machine learning (ML) algorithms can achieve higher accuracy than physically based (PB) models (Kratzert et al., 2019). However, ML models require long time series of streamflow data, often unavailable. Consequently, their accuracy decreases considerably for poorly represented values and extrapolation scenarios (Duan et al., 2020). The scarce data usually corresponds to high streamflow values, which are the most relevant for EWS applications. Under these circumstances, the PB models have the potential to support the ML models by adding valuable information for a closer prediction of the most important data.

To combine the benefits of both approaches and overcome their limitations, we propose a methodology to generate hybrid models for short-term (three hours ahead) flood prediction.

## 2. Methodology

The predictions of the hybrid model f($M_{HYB}$) result from the combination of those from a physically based model (f($M_{PB}$)) and from an ML-based model fitted to the residuals of the former (f($M_{ML,res}$)), as follows:

$$Y = f(M_{PB}) + res \quad (1)$$

$$res \approx f(M_{ML,res}) \quad (2)$$

$$Y \approx f(M_{HYB}) = f(M_{PB}) + f(M_{ML,res}) \quad (3)$$

where Y stands for the observed streamflow values and *res* are the residuals of the $M_{PB}$.

The hybrid model aims at being useful in EWS applications. Consequently, in order to deliver a quick simulation that is completely focused on the streamflow for the prediction time, this study employs an ML-

based surrogate model ($M_{ML,sur}$), instead of the $M_{PB}$ directly, which may be computationally costly (Huang et al., 2021). The $M_{PB}$ was calibrated using high events available in the training set.

Therefore, the overall process includes: a) create a $M_{PB}$ based on Iber (Bladé et al., 2014) and on the physical features of the catchment; b) fit an ML-based surrogate ($M_{ML,sur}$) taking as inputs the accumulated precipitation at several previous time steps; c) compute the residuals of the surrogate; d) fit an ML model to estimate the residuals ($M_{ML,res}$) considering the same inputs as for $M_{ML,sur}$ and adding past streamflow data; e) generate the hybrid model, $M_{HYB,}$ and compute its predictions.

This work employs the Random Forest (RF) (Breiman, 2001) algorithm both for the surrogate and for the residual estimation. To evaluate the performance of the hybrid model, the accuracy of its streamflow predictions are compared to the surrogate ($M_{ML,sur}$) and to a single RF model ($M_{ML}$) trained with the same variables as the residuals model, as described in López-Chacón et al. (2023).

The study area adopted in this research is the upper Fluvià catchment with outlet point in Olot (Spain). There is one meteorological station and one streamflow gauge within the area (11 years of hourly data). We took 75% of the data for model fitting and the more recent 25% of the data for testing, which contains the highest flows records in the catchment (the Gloria Storm).

## 3. Results and discussion

The $M_{ML,sur}$ is able to reproduce the Iber simulated streamflow values with a Nash-Sutcliffe Efficiency (NSE) of 0.94 for the Gloria storm hydrograph. For the testing set, the RMSE for streamflow values larger than 75 [m³ s$^{-1}$] ($RMSE_{Q\geq 75}$) is 30.66 [m³ s$^{-1}$] for $M_{ML,sur}$, 26.62 [m³ s$^{-1}$] for the $M_{ML}$, and 19,75 [m³ s$^{-1}$] for $M_{HYB}$. This represents an improvement of 36% and 27% with respect to $M_{ML,sur}$ and to $M_{ML}$, respectively.

Figure 1 depicts the Gloria storm hydrograph for the observed values and models used for comparison. The $M_{ML}$ underestimates the streamflow peaks, while the $M_{ML,sur}$ shows a considerable overestimation of them and does not capture the first maximum of the hydrograph. The $M_{HYB}$ is able to both capture the first part of the hydrograph and achieve close approximations to the peak values. The $M_{ML}$ is not able to adequately reach high values due to the scarcity of them in the training set. However, this is not a limitation for $M_{HYB}$, which, supported by the physically based model, is able to predict streamflow peaks with higher accuracy. At the same time, the contribution of $M_{ML,res}$ in the hybrid model is significant, which represents a possible alternative to the calibration process. From the EWS application perspective, $M_{HYB}$ is more suitable due to its higher accuracy overall and especially for high values.

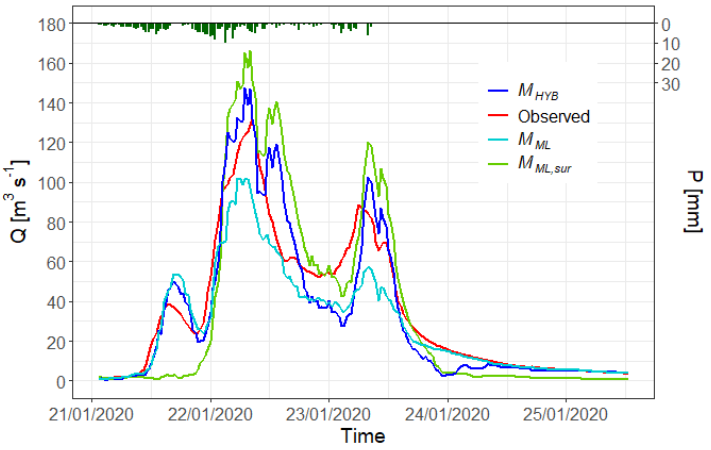



**Fig. 1.** The Gloria storm hyetograph (half-hourly, green) and hydrograph with the observed, surrogate, single RF, and hybrid models.

**References**


Bladé E, Cea L, Corestein G, Escolano E, Puertas J, Vázquez-Cendón E, Dolz J, Coll A (2014) Iber: Herramienta de Simulación Numérica Del Flujo en Ríos, Revista Internacional de Métodos Numéricos para Cálculo y Diseño en Ingeniería, 30, 1-10.

Breiman L (2001) Random Forest, Machine Learning, 45, 5-32.

Duan S, Ullrich P, Shu L (2020) Using Convolutional Neural Networks for Streamflow Projection in California, Frontiers in Water, 2, 28.

Huang X, Li Y, Tian Z, Ye Q, Ke Q, Fan D, Mao G, Chen A, Liu J (2021) Evaluation of Short-term Streamflow Prediction Methods in Urban River Basins, Physics and Chemistry of the Earth, 123, 103027.

Kratzert F, Klotz D, Shalev G, Klambauer G, Hochreiter S, Nearing G (2019) Benchmarking a Catchment-Aware Long Short-TermMemory Network (LSTM) for Large-Scale Hydrological Modeling, Hydrology and Earth System Sciences Discussions, 1–32.

López-Chacón SR, Salazar F, Bladé E (2023) Combining Synthetic and Observed Data to Enhance Machine Learning Model Performance for Streamflow Prediction, Water, 15, 2020.

# Parameters of flow over a Coanda screen by Particle Image Velocimetry (PIV) measurements

Katherine GUACHAMÍN-PALADINES[a1], Juan T. GARCÍA[a2], José M. CARRILLO[a3], Luis G. CASTILLO[a4]

[a] Hidr@m Group, Civil Engineering and Mining School, Universidad Politécnica de Cartagena, Spain
[a1]katherine.gpaladines@edu.upct.es, [a2]juan.gbermejo@upct.es, [a3]jose.carrillo@upct.es, [a4]luis.castillo@upct.es

ABSTRACT

The Particle Image Velocimetry (PIV) technique was applied on Coanda screens with an inclination of 45 degrees. This campaign aimed at analysing the velocity field in a longitudinal plane of the flow on three different screen configurations, with 1.6 mm width of the wedge wires, 1.5 mm slot between each two wires and different tilt wire angles (3, 5 and 7°). The experiments were carried out in a 0.5 m wide flume with a flow rate of 102.22 [l $s^{-1}$ $m^{-1}$] and a high-speed camera IX Camera I- Speed 720 was used to define the velocity field. The results obtained represent additional information of interest for the characterization of the flow on screens with Coanda effect, and thus be able to improve the design of these screening systems.

## 1. Introduction

A main concern stated in the European Union (EU) urban wastewater treatment directive (91/271/EEC) is to improve the stormwater quality coming from urban runoff in paved areas. Among the processes used to remove pollutants in stormwater, screening is a suitable technique, in where Coanda effect screens offer remarkable advantages from the point of view of their low clogging capacity and their high degree of solids separation, reaching sizes of separation up to 0.3 mm. Rotary drum fine screens are nowadays more frequently used for this purpose, although these systems need mobile parts and electrical supply. Static screening Coanda based may result in an optimal design, in comparison with other systems that need further assistance and maintenance. Hence, more experimental studies are needed for a better understanding of the behavior and optimization of these systems to help their spread in sewer networks.

To broaden the knowledge of this type of screening systems, in this work several flow parameters were studied on three Coanda screens using Particle Image Velocimetry (PIV) measurements. The characterization of the velocity field in a longitudinal plane of a flow by means of the PIV technique allows the determination of the instantaneous velocity values in the vertical and longitudinal directions, which also allows to obtain various statistics such as velocity fluctuation, curvature of streamlines or vorticity in the vertical plane, among other variables of interest (Raffel et al., 1998; Adrian and Westerweel, 2011). Therefore, being able to know the velocity field along the screen, as flow rates are derived and solids are longitudinally dragged is immensely helpful in understanding the occlusion phenomena of these type of screens, as well as to avoid them, by selecting optimal design conditions.

## 2. Materials and Methods

### *2.1. Physical model*

For the tests, an experimental installation of the Hydraulic Laboratory of the Universidad Politécnica de Cartagena (UPCT) has been used. The device consists in an inlet flume of 5.00 m long and 0.50 m wide. The hydraulic device also has a discharge flume for the non-collected water and the flume to collect the derived water located underneath the rack. The incoming flowrate was measured by an electromagnetic flowmeter Endress Häuser Promag 53W of 125 mm, with an accuracy of 0.5%. In this study, the screens with inclination of 45º were located downstream of an acceleration plate ogee type profile. The screens were made of stainless steel (AISI 304), wedge wire screen 0.48 m width (wire) by 0.50 m length (backing bars). The main characteristics of the screen bars are detailed in Fig. 1.a and Table 1.

### *2.2. The PIV campaign*

For this work, a high-speed camera IX Camera I-Speed 720 has been used, with a sensor resolution of 2048x1536 pixels and images have been taken with a frequency of 2000 images per second (fps). The camera works with various lenses with focal ranges ranging from 18 to 200mm. The placement distance of the camera from the measurement plane ranges from 0.4 to 1.5 m away. With this configuration the pixel size in the measuring region is 0.04 x 0.04 mm. The laser used is a Terra PIV Nd:YLF with a duration of 30 μs. The clear water flow was seeded with polyamide particles of 20 microns, whose density is close to that of water. The images taken were analyzed using the PIVlab analysis software (Thielicke and Sonntag, 2021), with window sizes starting at 128x128 pixels, ending at 32x32 pixels when considering three passes. The design of the experiment is shown in Figure 1.b.

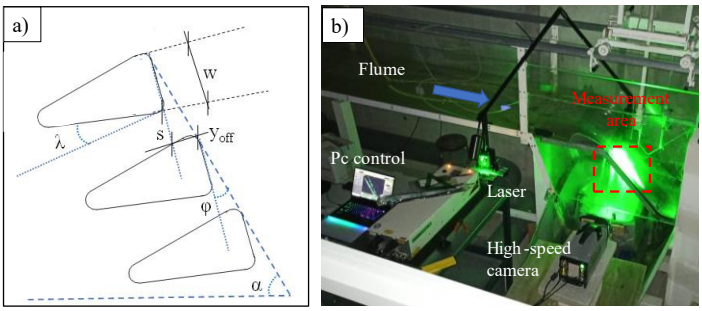



**Fig. 1.** a) Variables that define the configuration of the screen and its cross bars called wedge wires; b) Desing of the experiment

**Table 1**. Screen dimensions and layout.

| # Screen | *L/W* [m] | *w* [mm] | *s* [mm] | *φ* [°] | $y_{off}$ [mm] | *m* [%] | Number of wires |
|---|---|---|---|---|---|---|---|
| 1 | 0.50/0.48 | 1.6 | 1.5 | 3 | 0.16 | 0.48 | 161 |
| 2 | 0.50/0.48 | 1.6 | 1.5 | 5 | 0.27 | 0.48 | |
| 3 | 0.50/0.48 | 1.6 | 1.5 | 7 | 0.38 | 0.48 | |

where $L$ is the length of the screen in the flow direction, $W$ the rack width, $w$ the width of the wedge wires, $s$ the slot between each two wires, $\varphi$ the tilt angle, $y_{off}$ the wire offset (the length of the projection of the tilted upstream wire profile in the next wire), and $m$ the void ratio (ratio between the void area and the total area).

## 3. Results

Figure 2.a shows the velocity field through the analysis software, while Figure 2.b shows the longitudinal and vertical velocity components of a 32x32 pixel analysis window without any type of filtering or data completion.

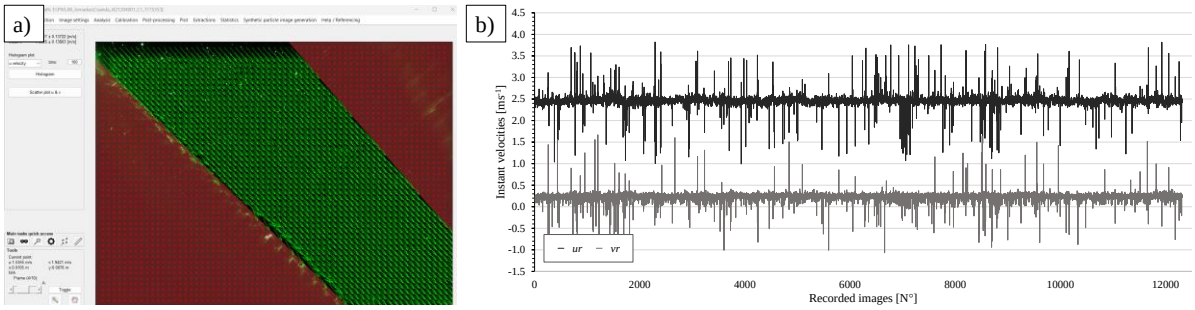



**Fig. 2.** a) PIVlab analysis software; b) instant velocities in 32x32 pixels window.

In view of the results, it can be concluded that the images taken allow us to characterize the velocity field, as well as other parameters such as inclination and curvature of the streamlines (allowing to determinate the discharge coefficient per unit length), statistics of turbulence, fluctuations of velocity, vorticity, among others.

**Acknowledgements**

The publication is part of the TED2021-132098B-C21 project, financed by MCIN/AEI/10.13039/501100011033 and by the European Union "NextGenerationEU"/PRTR.

**References**

Adrian, R. & Westerweel, J. (2011) Particle image velocimetry (No. 30). Cambridge university press. ISBN: 978-0-521-44008-0
DOCE (1991) Directiva 91/271/CEE, de 21 de mayo de 1991, sobre el tratamiento de las aguas residuales urbanas, Bruselas.
Raffel, M., Willert, C. E., & Kompenhans, J. (1998) Particle image velocimetry: a practical guide (Vol. 2, p. 218). Berlin: Springer.
Thielicke, William, and René Sonntag (2021) Particle Image Velocimetry for MATLAB: Accuracy and Enhanced Algorithms in PIVlab. Journal of Open Research Software, vol. 9, Ubiquity Press, Ltd. doi:10.5334/jors.334.

# From hindcast to forecast with distributional neural networks in water demand forecasting

Gregor JOHNEN[1], André NIEMANN[1], Alexander HUTWALKER[2], Christoph DONNER[3]

[1] Institute of Hydraulic Engineering and Water Resources Management, University of Duisburg-Essen, Germany
Gregor.Johnen@uni-due.de
Andre.Niemann@uni-due.de

[2] Harzwasserwerke GmbH, Hildesheim, Germany
Alexander.Hutwalker@harzwasserwerke.de

[3] Berliner Wasserbetriebe, Berlin, Germany
Christoph.Donner@bwb.de

## ABSTRACT

In recent years, the water supply-demand balance has become increasingly concerning to supply companies. Their goal is to control and manage resources efficiently. Visible demand patterns, resulting from the long-term effects of climate change, include demand peaks lasting multiple hours during the day or several days during prolonged dry periods, and numerous heat days throughout summer. Being able to make risk-based decisions, such as whether to fill up storage capacities or not, prior to events requires dependable short-term probabilistic forecasts.

While deep learning has become the accepted norm for water demand forecasting (Xenochristou et al., 2021; Zanfei et al., 2022), the majority of research and development has been conducted using hindcast models and point forecastin (Ghalehkhondabi et al., 2017). The main obstacle in utilising deep learning models for prediction, such as water demand, rests in the fact that the meteorological input data is sourced from varied distributions in hindcast and forecast.

The study introduces two innovative probabilistic deep learning structures founded on long short-term memory (LSTM) networks to forecast hourly water demand up to 10 days in the future. Both models process various temporal sequences of data, such as hindcast and forecast as inputs with varying sequence length (see Figure 1).

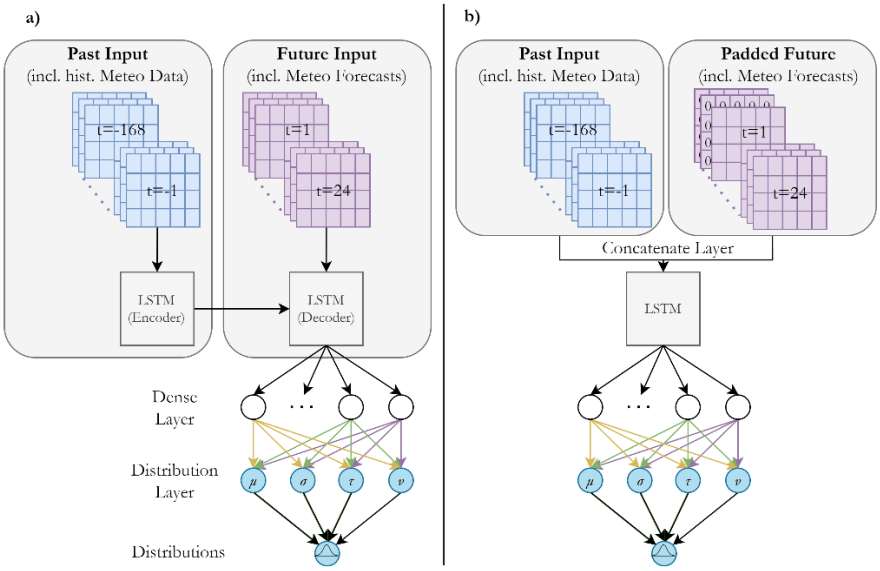



**Fig. 1.** Visualization of both distributive neural network approaches using (a) a traditional encoder-decoder approach and (b) Zero-Padding to extend the shorter future sequence and model both inputs within a single LSTM.

The models encode long-term historical data on water demand and features, including meteorological information, while simultaneously incorporating short-term data on calendar and weather features using statistically optimised point forecasts (DWD MOSMIX). Additionally, we propose a new approach whereby all networks are distributional neural networks, based on a deep neural network incorporating a probability layer. This implies that the network outputs are parameters of either the normal or Johnson's SU distribution (see Figure 1). As a result, the model generates inherently distributional multi-step-ahead forecasts of variable length by utilising future information.

The approach was validated in several case studies using demand data from a German water supply company. The proposed deep neural networks for distributional analysis were compared to other state-of-the-art models, such as a feedforward deep neural network, a Lasso-estimated high-dimensional time series model, and a conventional AR(p) model. The results obtained suggest that the proposed approach of employing weather forecasts for short-term water demand prediction has potential, particularly for lead times exceeding 24 hours and when the distribution's bias is not too severe. Moreover, since probabilistic forecasting is integral to risk management, the results have crucial implications for managing drinking water distributions in the water supply sector.

**References**

Ghalehkhondabi, I., Ardjmand, E., Young, W. A., & Weckman, G. R. (2017). Water demand forecasting: Review of soft computing methods. Environmental Monitoring and Assessment, 189(7), 313. https://doi.org/10.1007/s10661-017-6030-3

Xenochristou, M., Hutton, C., Hofman, J., & Kapelan, Z. (2021). Short-Term Forecasting of Household Water Demand in the UK Using an Interpretable Machine Learning Approach. Journal of Water Resources Planning and Management, 147(4), 04021004. https://doi.org/10.1061/(ASCE)WR.1943-5452.0001325

Zanfei, A., Brentan, B. M., Menapace, A., & Righetti, M. (2022). A short-term water demand forecasting model using multivariate long short-term memory with meteorological data. Journal of Hydroinformatics, 24(5), 1053–1065. https://doi.org/10.2166/hydro.2022.055

# Local analysis of the gas exchange in a step-and-pool configuration via numerical simulation

Paolo PERUZZO[1], Nicola DURIGHETTO[1], Gianluca BOTTER[1]

[1] Department of Civil, Environmental and Architectural Engineering, University of Padua, Italy
paolo.peruzzo@dicea.unipd.it
nicola.durighetto@dicea.unipd.it
gianluca.botter@dicea.unipd.it

ABSTRACT

## 1. Introduction

Despite their small surface area, mountain streams are a significant source of greenhouse gases by efficient exchange processes at the water-air interface. The physical mechanisms responsible for the gas emission are modulated by the microtopography that characterizes the stream bed, whose steps and pools are peculiar examples (Botter et al., 2022). While it is well established that the gas transfer in correspondence with riverbed drops is promoted by the concurrence of high turbulence and bubble entrainment, a deep knowledge of the physical processes driving the outgassing dynamics in local steps still lacking. This study aims to bridge this knowledge gap by reproducing numerically the hydrodynamics of an idealized step-and-pool configuration.

## 2. Methods

The hydrodynamics of a step-and-pool configuration of a 0.3 m width rectangular section was simulated by the software Flow-3D Hydro 2022R1, and consisted in a broad-crested weir and a tapered positive step of height 25 and 9 cm, respectively, placed at a distance of 1 m. The limited pool has then a depth, $z_0$, of about 10 cm and is fed by a small cascade of almost 15 cm. The grid had nearly 7.5 million structured orthogonal cells. We solved the Reynolds-Averaged Navier-Stokes equations coupled with the re-normalization group $e_k$-$\varepsilon$ scheme, $e_k$ and $\varepsilon$ being respectively the turbulent kinetic energy per unit of mass and the turbulent kinetic energy dissipation rate. Further, Flow-3D included the bubble entrainment due to the water flow according to the standard Advection-Diffusion Equation of a scalar of concentration $C$. Here, the air bubbles were assumed as spheres with a radius, $r$, of 0.5 mm. The model estimated both all the relevant hydrodynamic quantities and the entrained air concentration and escaping bubbles flux across the free surface, $q_B$. We set steady inflow of 2.0 l/s upstream of the weir, free outflow downstream of the step, and no-slip condition on both the bottom and channel sides. Initially, fluid was at rest, and the transient was less than 20 seconds before achieving the stationary solution. The results were preliminary assessed with data collected in a similar in-flume experiment.

## 3. Theory

The exchange of volumetric gas, $F$, through the water-air interface is described by the Henry's law as

$$F = k\left(C_w - \frac{C_a}{K_H}\right), \quad (1)$$

with $k$ the gas transfer velocity, $C_w$ and $C_a$ the gas concentration in water and atmosphere, respectively, and $K_H$ the Henry constant of the specific gas. In the present problem, $k$ is due to the sum of the contributions induced by the turbulence, $k_T$, and the bubble mediated process, $k_B$, i.e., $k=k_T+k_B$. The eddies generated by the turbulence continuously exposed different portion of the water to the atmosphere, increasing $k_T$ according to

$$k_T = \alpha_T Sc^{-0.5}(\nu\varepsilon)^{0.25}, \quad (2)$$

where $\alpha_T$=0.2-0.4 is a coefficient, $\nu \approx 1\ 10^{-6}$ m$^2$/s is the kinematic viscosity of water, and $Sc=\nu/D$ is the Schmidt number, which expresses the link between kinematic and molecular diffusivity, $D$. Here, $k_T$ was calculated

using the computed value of $\varepsilon$ near the free surface and assuming $\alpha_T$=0.4 and the standard value of $Sc$= 600. The bubble-mediated process accounts the gas exchange between water and bubbles as long as they last in the water column. The exchange velocity, $k_B$, is proportional to the bubble flux according to

$$k_B = q_B\left(1 - e^{-T_B/T_g}\right)/\beta, \tag{3}$$

with $\beta$ the Ostwald coefficient. $T_B \approx z_0/u_B$ ($u_B$ the bubble rising velocity) is the bubble life time and $T_g(D, r, u_B)$ is the time scale of the gas transfer process (see Klaus et al., 2022). In this case, $k_B$ was estimated for the $CO_2$.

## 4. Results and Discussion

In the pool, the cascade dissipates its energy through the local production and the subsequent dissipation of turbulent kinetic energy. The turbulence depletes indicatively 20% of the flow energy near the surface within a length that does not exceed a few centimeters near the cascade with consequent peak values of $k_T$ of about 100 m/d (Fig. 1a). In addition, the falling jet is responsible for the entrapment of the air in the pool. The air bubbles extend for almost 30 cm downstream of the jet, but most of the air escaped in the first 10 cm, where $k_B$ achieves a local maximum of about 500 m/d in small spots of 10 dm$^2$ (Fig. 1b). We compared the two mechanisms of gas evasion by the transverse-averaged values of the mass transfer rate $\bar{k}_T$ and $\bar{k}_B$ (Fig. 1c). The transfer velocity driven by the bubble-mediated process is almost one order of magnitude larger than that controlled by the turbulence in the central portion of the entrained air region. Accordingly, the outgassing in this region can be equivalent to the amount caused exclusively by the turbulence along some meters of the reach, which may be longer than the average two-next-steps distance in the headwaters.

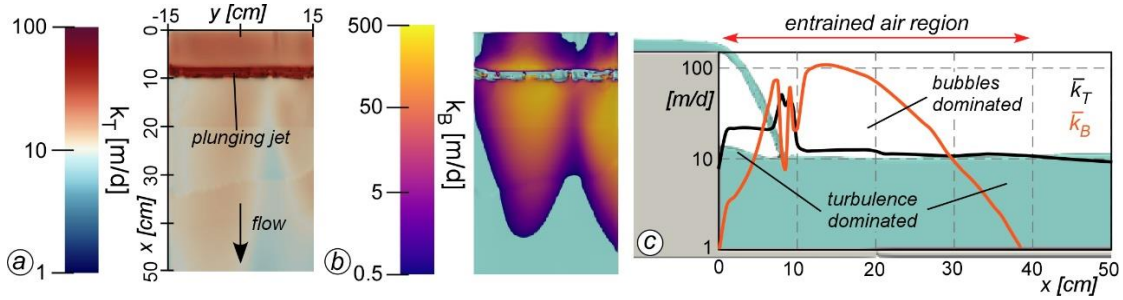



**Fig. 1.** Gas evasion in the pool. a) Field of $k_T$. b) Field of $k_B$. c) Transverse-averaged values of $k_T$ and $k_B$. Adapted from Peruzzo et al. (2023).

Although direct transposition of the results to real-world scenarios requires caution, our simulation suggests that most of the observed gas evasion in mountain streams is likely bubble-mediated. The results raises two concerns about the correct procedure to quantify $k$ in the stream. First, in this circumstance, $k$ should be standardized not only in terms of $Sc$ but also of $\beta$ (and $D$), in particular, if tracer gases with different solubilities are used. Second, to correctly define an upscaling law between $k$ and $\varepsilon$, as found in the literature (see, Ulseth et al., 2019), one needs to include the spatial frequency of steps and the relative contribution of the bubbles.

## 5. Conclusions

The present numerical analysis investigates the spatial patterns of energy dissipation and gas exchange, as well as the characteristic length scales of turbulence-induced and bubble-mediated gas transport in a step-and-pool configuration. According to the results, the gas evasion in the pool may be a very local process, taking place in a few dm$^2$ close to the plunging jet. Accordingly, aggregating $k$ across heterogeneous reaches might be inherently biased (Botter et al., 2021), and $k$ should be used with caution. In these cases, the mass transfer rate could be highly site-specific, and its extrapolation could be possible only through a detailed analysis of the evasion produced by the constitutive geomorphic elements of the reach. The outcomes may have significant implications in biology and environmental sciences that rely on correctly modeling gas cycles, such as $CO_2$.

### References


Botter, G., Carozzani, A., Peruzzo, P., & Durighetto, N. (2022). Steps dominate gas evasion from a mountain headwater stream. Nature Communications, 13(1), 7803

Botter, G., Peruzzo, P., & Durighetto, N. (2021). Heterogeneity matters: aggregation bias of gas transfer velocity versus energy dissipation rate relations in streams. Geophysical Research Letters, 48(17), e2021GL094272.

Klaus, M., Labasque, T., Botter, G., Durighetto, N., & Schelker, J. (2022). Unraveling the Contribution of Turbulence and Bubbles to Air-Water Gas Exchange in Running Waters. Journal of Geophysical Research: Biogeosciences, 127(3), e2021JG006520.

Peruzzo, P., Cappozzo, M., Durighetto, N., & Botter, G. (2023). Local processes with global impact: unraveling the dynamics of gas evasion in a step-and-pool configuration. Biogeosciences, 20, 3261–3271, https://doi.org/10.5194/bg-20-3261-2023.

Ulseth, A. J., Hall Jr, R. O., Boix Canadell, M., Madinger, H. L., Niayifar, A., & Battin, T. J. (2019). Distinct air–water gas exchange regimes in low-and high-energy streams. Nature Geoscience, 12(4), 259-263.

# Non-hydrostatic Galerkin Model with Linear/Quadratic Weighted Average Pressure

Lucas CALVO[1], Diana DE PADOVA[2], Michele MOSSA[3], Gisselle GUERRA[4]

[1,4] Universidad Tecnológica de Panamá, Panamá
lucas.calvo@utp.ac.pa
gisselle.guerra@utp.ac.pa
[2,3] Polytechnic University of Bari, Italy
diana.depadova@poliba.it
michele.mossa@poliba.it

ABSTRACT

In this work, a new two-dimensional depth-integrated non-hydrostatic model for the simulation of wave propagation using a linear/quadratic weighted average vertical non-hydrostatic pressure profile is developed. The use of the new model in an experiment consisting of regular waves propagating over a submerged bar in a channel proved its applicability.

## 1. Description of the Model

The new model is a modification of a previous one (Calvo, 2021) constructed using a combination of discontinuous and continuous Galerkin methods, where the depth-integrated non-hydrostatic equations are separated into hydrostatic and non-hydrostatic parts. The hydrostatic part corresponds to the shallow water equations and is solved with a discontinuous Galerkin finite element method for the simulation of discontinuous flows, wave breaking and runup. The non-hydrostatic part resulted in a Poisson-type equation, where the non-hydrostatic pressure was resolved by a continuous Galerkin finite element method for the modeling of wave propagation and transformation. The model is given by:

$$\frac{\partial HU}{\partial t}+\frac{\partial HUU}{\partial x}+\frac{\partial HUV}{\partial y}=-gH\frac{\partial \xi}{\partial x}-\frac{gn^2U\sqrt{U^2+V^2}}{H^{\frac{1}{3}}}-\frac{1}{\rho}\left(\frac{\partial Hq}{\partial x}-\left\{2q\Theta+(1-\Theta)\left(\frac{3}{2}q+\frac{1}{4}\rho H\phi\right)\right\}\frac{\partial h}{\partial x}\right) \quad (1)$$

$$\frac{\partial HV}{\partial t}+\frac{\partial HUV}{\partial x}+\frac{\partial HVV}{\partial y}=-gH\frac{\partial \xi}{\partial y}-\frac{gn^2V\sqrt{U^2+V^2}}{H^{\frac{1}{3}}}-\frac{1}{\rho}\left(\frac{\partial Hq}{\partial y}-\left\{2q\Theta+(1-\Theta)\left(\frac{3}{2}q+\frac{1}{4}\rho H\phi\right)\right\}\frac{\partial h}{\partial y}\right) \quad (2)$$

$$\frac{\partial H}{\partial t}+\frac{\partial UH}{\partial x}+\frac{\partial VH}{\partial y}=0 \quad (3)$$

$$\frac{\partial W}{\partial t}+U\frac{\partial W}{\partial x}+V\frac{\partial W}{\partial y}=\frac{1}{\rho H}\left\{2q\Theta+(1-\Theta)\left(\frac{3}{2}q+\frac{1}{4}\rho H\phi\right)\right\} \quad (4)$$

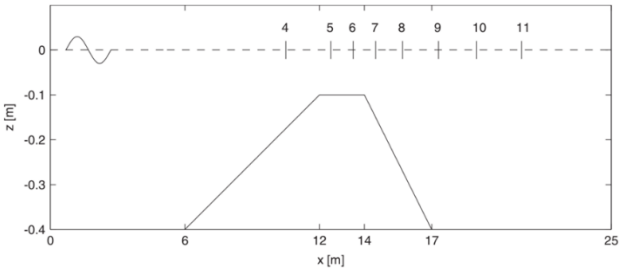
$$\phi=-\nabla h\cdot\left(\frac{\partial \boldsymbol{u}}{\partial t}+(\boldsymbol{u}\cdot\nabla)\boldsymbol{u}\right)-\boldsymbol{u}\cdot\nabla(\nabla h)\cdot\boldsymbol{u} \quad (5)$$

where $U, V$ and $W$ are the depth-averaged velocity components in the $x$, $y$ and z directions; $\boldsymbol{u}=\{U,V,W\}$; $\rho$ is the water density; $n$ is Manning's roughness coefficient; $g$ is the gravitational acceleration; and $q$ is the depth-averaged non-hydrostatic pressure. The flow depth is $H=\xi+h$, where $\xi$ is the surface elevation measured from the still water level and $h$ is the water depth measured from the still water level. The value of $\Theta$ determines the non-hydrostatic pressure profile (linear, quadratic or weighted average linear/quadratic). Choosing $\Theta = 1$, we will have a linear non-hydrostatic pressure profile, while taking $\Theta = 0$, we will have a

quadratic non-hydrostatic pressure profile. Any value $0 < \Theta < 1$ will give a weighted average linear/quadratic non-hydrostatic pressure profile.

## 2. Model Validation

The validation of the model was carried out using an experiment of regular waves propagating over a submerged bar in a channel (Beji and Battjes, 1993), schematized in Fig. 1. In the numerical simulations (Fig 2.), incident sine waves with amplitude of 1.0 cm and period of 2.02 sec are generated on the left side boundary based on the linear wave theory.




| Gauge | G4 | G5 | G6 | G7 | G8 | G9 | G10 | G11 |
|---|---|---|---|---|---|---|---|---|
| x [m] | 10.5 | 12.5 | 13.5 | 14.5 | 15.7 | 17.3 | 19.0 | 21.0 |

Fig. 1. Periodic waves over a submerged bar. Setup of the Beji & Battjes experiment.

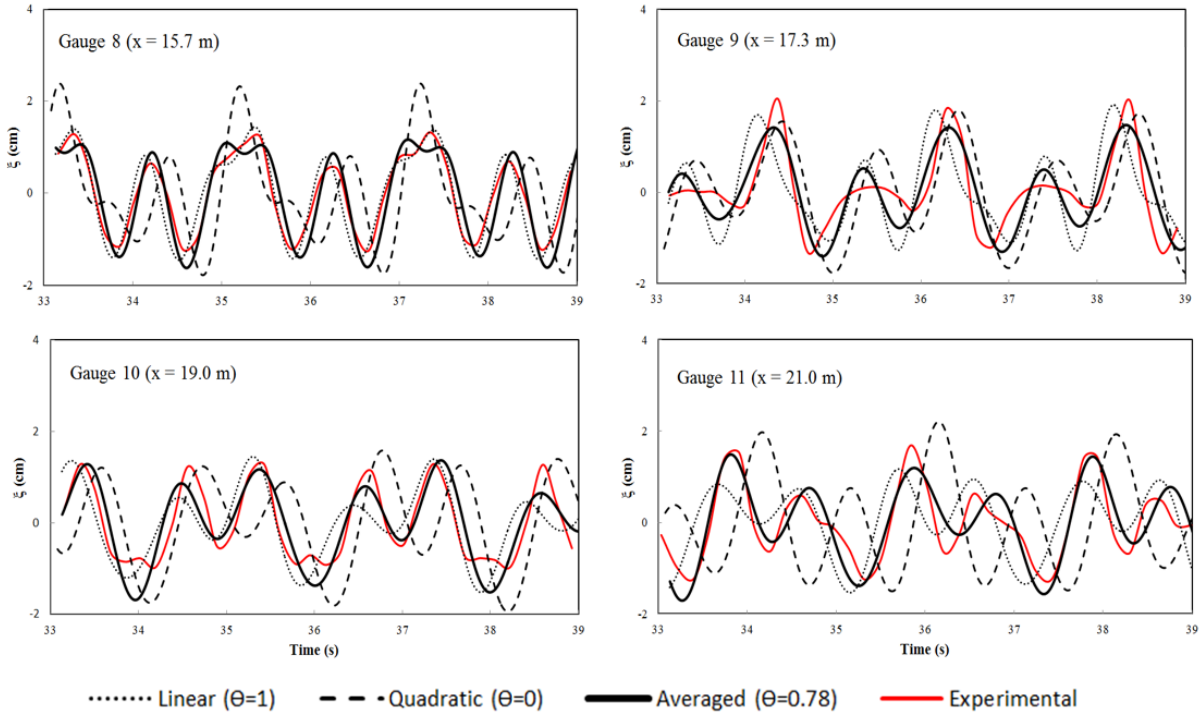



Fig. 2. Comparison of simulated and measured surface elevations. Linear pressure profile ($\Theta = 1$, dotted), quadratic pressure profile ($\Theta = 0$, dashed), weighted averaged pressure profile ($\Theta = 0.78$, solid black), experimental data from Beji and Battjes (solid red).

The results show that the dispersion properties of the linear and quadratic profiles differ noticeably. The outcomes can be improved by the use of a weighted average linear/quadratic non-hydrostatic pressure profile ($\Theta = 78$), as seen clearly in Gauges 9 to 11.

## 3. Conclusions

A new two-dimensional depth-integrated non-hydrostatic model for the simulation of wave propagation using a weighted average linear/quadratic non-hydrostatic pressure profile has been developed. The utilization of a weighted average linear/quadratic non-hydrostatic profile improved the performance of the previous model.

**References**

Calvo, L., De Padova, D., Mossa, M., Rosman, P. (2021). Non-hydrostatic discontinuous/continuous Galerkin model for wave propagation, breaking and runup. Computation. 9, 47.

Beji, S., Battjes, J. A. (1993). Experimental investigation of wave propagation over a bar. Coastal Eng. 19, 1, 151–162.

# Investigation of Inclined Negatively Buoyant Jets with RANS and LES Numerical Simulations

Marta ALVIR[1], Ivana LUČIN[2], Ante SIKIRICA[4], Lado KRANJČEVIĆ[3]

[1,2,3] University of Rijeka, Faculty of Engineering, Croatia
marta.alvir@riteh.hr
ilucin@riteh.hr
lado.kranjcevic@riteh.hr

[4] Center for Advanced Computing and Modelling, University of Rijeka, Croatia
ante.sikirica@uniri.hr

ABSTRACT

The process of discharging effluent with higher density in marine areas with lower density can be extremely harmful to the environment due to the deposition of hypersaline and chemical wastes on the seabed. This process causes the formation of negative buoyant jets, which occur during industrial wastewater discharge, such as brine from desalination plants. In order to determine the environmental impact and to select the appropriate geometry and flow conditions, it is crucial to know their behavior for different flow conditions and outfall geometries. Numerical simulations are helpful for detailed investigations of complex mixing behavior for buoyant jets and are cheaper than experimental investigations. Therefore, in this work, the results of RANS and LES numerical simulations of negatively inclined buoyant jets are compared with experimental results from the literature. Compared results include velocities field, concentration, calculation times, and negatively inclined buoyant jet trajectories.

## 1. Introduction

Wastewater from treatment plants, power plants, industrial plants, and desalination plants are usually discharged with coastal outflows and represent significant environmental and public health concerns. Negatively buoyant jets occur when the density of the effluent is greater than the density of the recipient, mostly sea. Therefore, the jet rises to a certain height due to the initial momentum flux caused by the jet velocity. After reaching the maximum height, the buoyant forces become more dominant, and the jet returns to the bottom, spreading further through sea currents (Roberts et al., 1997). Hence, negative buoyant jets are often angeled depending on flow conditions. They manifest when discharging brine from desalination plants or cooling water from liquefied natural gas (LNG) plants. Nowadays, desalination is increasing due to water scarcity and green hydrogen production. In desalination, seawater produces drinking water by removing suspended matter and dissolved minerals, mainly salt, so the effluent with high salt concentration and other chemicals is discharged back into the coastal marine area. Therefore, the mentioned problem is becoming increasingly important.

## 2. Numerical Simulation

Several approaches can be used to analyze the mixing of negatively buoyant jets. Although most previous analyses were done by experiments, numerical simulations in OpenFOAM are increasingly used nowadays, enabling a more economical and straightforward approach. For turbulence modeling on buoyant jets, most previous research uses LES (Large Eddy Simulation) or RANS (Reynolds Averaged Navier Stokes) models, which will be used in the present study. The numerical model is validated based on research by Zhang et al. (2016) on a nozzle inclined at 45°. The Smagorinsky model was used for the LES simulation, while RANS simulations were done with the realizable $k$-$\varepsilon$ turbulent model (Kheirkhah Gildeh et al., 2015). Calculations

were performed using a twoLiquidMixingFoam solver in OpenFOAM. The model was calculated for 120 seconds, while the results were averaged between 50 and 120 seconds. Calculations were performed at the supercomputer Bura from the Center for Advanced Computing and Modeling, University of Rijeka.

## 3. Results

Fig. 1 represents a comparison of RANS and LES simulation results with experimental and LES simulation values from Zhang et al. (2016). The trajectories were analyzed based on the maximum values of the concentration $\alpha$ for different cross-sections. The RMSE value between RANS simulation and experimental results is 0.0028, while $R^2$ is 0.98. RMSE between LES simulations and experimental results is 0.0117, and $R^2$ is 0.75. It can be observed that with the LES simulation performed in this research, slightly worse results are obtained compared to the experimental values in the other part of the graph, where buoyant forces have a more significant influence. However, in the initial part, where buoyancy forces dominate, the LES simulation has a higher accuracy. Therefore, it can be concluded that the LES simulation better describes the initial part of negatively buoyant jets, but the RANS simulation performed better in the second part with negative buoyant forces.

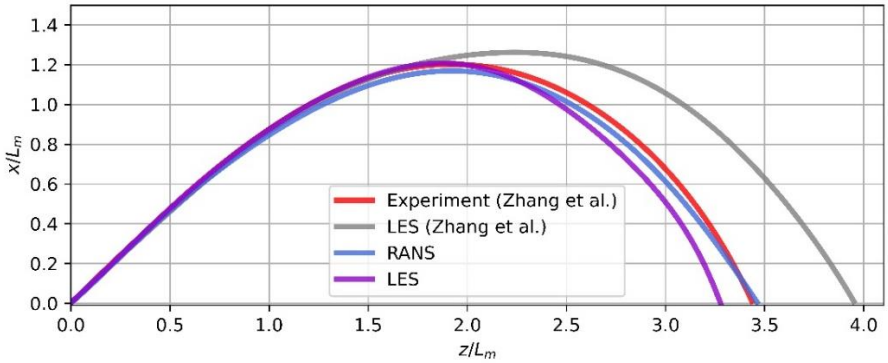



**Fig. 1.** Comparison of the trajectories of the experimental results and LES model from Zhang et al. (2016) with numerical results from RANS and LES simulations

Fig. 2 shows the time-averaged contours of concentration $\alpha$ for RANS and LES simulation. It can be noticed that the jet rises in the initial part due to the high velocity and then falls to the bottom due to the influence of gravity. Because of this, a layer with an increased concentration remains at the bottom, which is particularly dominant in the RANS simulation. In the second part, in the LES simulation, the turbulent behavior of the jet and the eddying that occurs is more pronounced than in the RANS simulation.

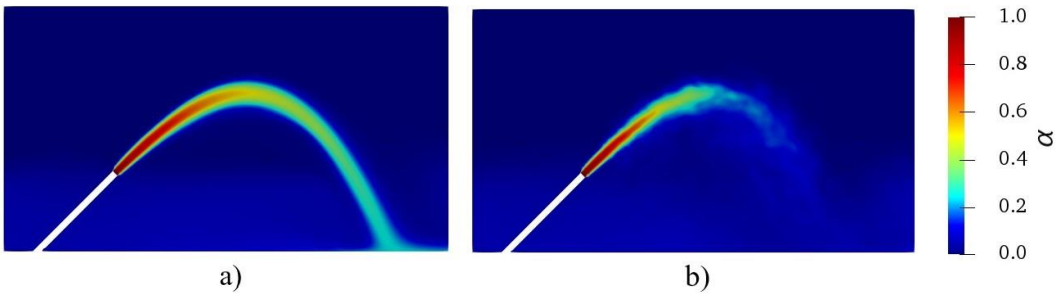



**Fig. 2.** Contours of time-averaged concentration $\alpha$ on the central cross section for a) RANS and b) LES simulation

**References**

Kheirkhah Gildeh, H, Mohammadian, A, Nistor, I, Qiblawey, H (2015) Numerical modeling of 30∘ and 45∘ inclined dense, turbulent jets in stationary ambient, Environmental Fluid Mechanics, 15, 537-562
Roberts, PJ, Ferrier, A, Daviero, G (1997) Mixing in inclined dense jets, Journal of Hydraulic Engineering, 123(8), 693-699.
Zhang, S, Jiang, B, Law, AWK, Zhao, B (2016) Large eddy simulations of 45 inclined dense jets, Environmental Fluid Mechanics, 16, 101-121.

# Machine Learning Approach to Modelling Compound Coastal-Fluvial Flooding

Agnieszka Indiana OLBERT, Sogol MORADIAN

College of Science and Engineering, University of Galway, Galway, Ireland.
Indiana.olbert@universityofgalway.ie
Sogol.moradian@universityofgalway.ie

ABSTRACT

Accurate flood modelling plays a pivotal role in averting flood-related damages. In different studies, the existing guidelines for assessing compound flood risks arising from the interplay between coastal and fluvial factors often fall short in considering their intricate interactions. This omission can lead to an underestimation of the flood risk. This paper introduces a comprehensive approach to compound coastal-fluvial flood mapping, even in scenarios with restricted hydraulic and hydrological data. This approach leverages the power of seven distinct Machine Learning (ML) models. The core of this study revolves around the examination of ocean-fluvial floods, taking into account upstream hydrographs in the fluvial section and downstream ocean water level timeseries in coastal areas as pivotal boundary conditions. These ML algorithms were applied to a specific study area in the southwestern part of Ireland, with a focus on generating high-resolution flood maps. The study particularly zoomed in on a significant historical compound ocean-fluvial flood event that occurred on November 19-20, 2009. The results obtained in this study substantiate the reliability of ML models in estimating the extent of compound flood inundation. To gauge model performance, a set of skill scores were calculated. This research underscores the ability of ML models to generate coastal-fluvial flood inundation.

## 1. Introduction

Within coastal floodplains, the confluence of heightened river flows and elevated coastal water levels often conspires to trigger extensive flooding, as highlighted by Olbert et al. (2023). These dynamic factors are essential in defining flood characteristics, imparting distinctive features to the propagation of floodwaves and the scale of impacted regions. In cases where a flood event is incited by the influence of just one of these factors, the accuracy of flood likelihood prediction hinges largely on the richness of available data and the statistical techniques employed for assessing extreme events. However, the complexity escalates considerably when flooding arises from the confluence of multiple processes, a commonplace occurrence in coastal regions where a diverse array of variables such as astronomical tides, surges, wind waves, and high river discharges can merge in tandem, as noted by Olbert et al. (2017). In such scenarios, it no longer suffices to consider the individual probabilities of each contributing driver in isolation (Olbert et al., 2023). Instead, there is a compelling need to account for the collective probability of these multifaceted drivers synchronously culminating in a flood event. In light of this challenge, this paper unveils a pioneering methodology for assessing compound flooding, applying the capabilities of ML methods.

## 2. Methodology

This paper employs a sophisticated approach to model compound flooding, drawing from two distinct sets of inputs to capture the intricate interplay between water levels in both the fluvial and coastal domains. Simultaneously, it leverages a single set of target data, which comprehensively encapsulates water depth changes incurred during the flood event. This balanced data setup facilitates the utilization of a diverse array of ML techniques, including Gaussian Process Regression (GPR), Support Vector Regression (SVR), Decision Tree (DT), Support Vector Machine (SVM), Linear Regression (LR), Radial Basis Function (RBF), and Artificial Neural Network (ANN). The selection of the optimal ML method is conducted with utmost rigor, underpinned by an exhaustive evaluation of each method's performance across a spectrum of diverse statistical metrics together with a cross-validation 10-Fold method. This meticulous analysis ensures that the chosen approach demonstrates superior predictive capabilities. Beyond its academic significance, the framework

developed in this study holds considerable practical utility. It serves as a powerful tool for predicting compound flooding events, offering valuable insights into the potential extent and severity of such events. This predictive capability is invaluable in disaster preparedness and risk mitigation efforts, enabling timely and informed decision-making to safeguard coastal communities and valuable assets. As such, the contributions of this research extend beyond the confines of academia, offering benefits for coastal regions susceptible to the dynamics of compound flooding. More explanations about the method can be found in Moradian et al. (2024).

## 3. Results

To demonstrate the effectiveness of the seven ML methods employed in this project, a random pixel was selected. Then, all ML methods were implemented for this pixel, and the best method was chosen using a multi-criteria decision-making technique based on various statistical metrics (i.e., Bias, Corr, MAE, ME, RMSD, RMSE, and StD) and the 10-Fold cross validation method for the flood event in November 2009. A similar methodology has been explained in Moradian et al. (2023; 2024). In order to showcase the efficacy of the ML techniques utilized in this project, a random pixel located at coordinates A(i,j)=(454,798) was selected. Subsequently, all of these ML methods were applied to this specific pixel, and the selection of the optimal method was conducted, grounded in a comprehensive evaluation of various statistical metrics. These metrics encompassed critical measures, with a focus on analyzing their performance in the context of the November 2009 flood event (see Figure 1). The results clearly highlight that, based on the specified criteria, the RBF model outperformed all other models in terms of accuracy. Using the RBF model, Figure 2 shows the performance of the ML models comparing to the available observed flood maps from the Office of Public Works (OPW). This methodology was applied to model two flood events with return period of 20 and 1000 years, as discussed in Moradian et al. (2024).

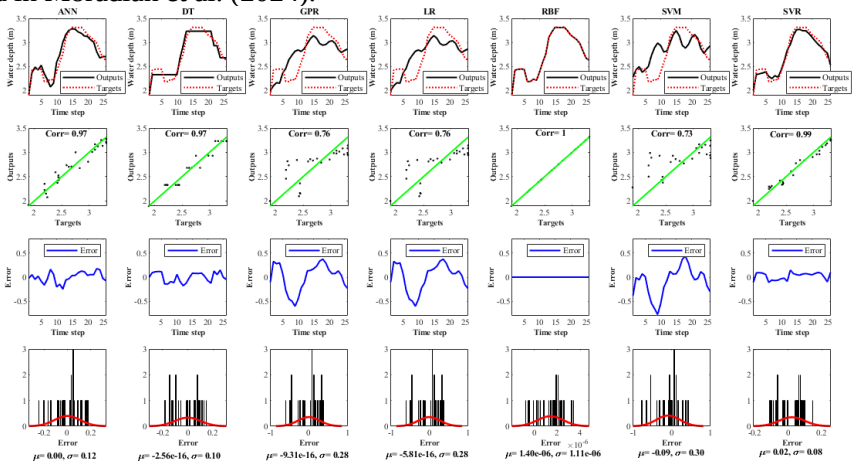



**Fig. 1.** The performance results of the ML model at a randomly chosen location (Moradian et al., 2024).

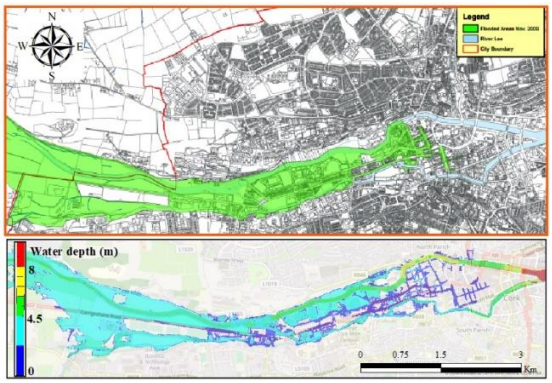



**Fig. 2.** Comparing the post-event mapping by OPW (above) with the modelled extents (below) for the 2009 flood (Moradian et al., 2024).

**References**


Moradian S., AghaKouchak A., Gharbia S., Broderick C., Olbert A.I. (2024) Forecasting of Compound Ocean-Fluvial Floods Using Machine Learning. Journal of Environmental Management. Volume 364, 121295. https://doi.org/10.1016/j.jenvman.2024.121295.

Moradian S., Olbert A.I., Gharbia S., Iglesias G. (2023) Copula-based projections of wind power: Ireland as a case study. Renewable and Sustainable Energy Reviews. 175, 113147. https://doi.org/10.1016/j.rser.2023.113147.

Olbert AI, Comer J, Nash S, Hartnett M (2017) High-resolution multi-scale modelling of coastal flooding due to tides, storm surges and river inflows. A Cork City Example, Coastal Engineering, 121, 278-296

Olbert A.I., Moradian S., Nash S., Comer J., Kazmierczak B., Falconer R., Hartnett M. (2023) Combined statistical and hydrodynamic modelling of compound flooding in coastal areas- Methodology and application. Journal of Hydrology. https://doi.org/10.1016/j.jhydrol.2023.129383.

# Influence of different numerical setups on scour pattern at the initial scour stage next to bridge pier protected with riprap

Antonija HARASTI[1], Gordon GILJA[2], Nikola ADŽAGA[3], Mark ŽIC[4]

[1,2,3] University of Zagreb, Faculty of Civil Engineering, Croatia
antonija.harasti@grad.unizg.hr (for author 1)
gordon.gilja@grad.unizg.hr (for author 2)
nikola.adzaga@grad.unizg.hr (for author 3)
[4] Division of Materials Physics Ruder Boskovic Institute, Croatia
Mark.Zic@irb.hr (for author 4)

ABSTRACT

This paper presents the ability of Flow3D software to simulate scour around a bridge pier that is protected against scour with riprap. Unlike single piers where scouring typically occurs upstream, the presence of riprap around the piers induces a scour process downstream. The objective of this study is to investigate how various numerical setups influence the initial scour stage downstream of such a specific structure.

## 1. Methodology

Flow-3D is a software that solves Navier-Stokes equations using the finite volume method. The Sediment transport model is determined by selecting bed-load sediment transport formula, which mainly depends on the Shields number. The numerical model is established in a rectangular 5 m long and 0.8 m wide flume. The erodible channel bed is composed of uniform material with a mean sediment size of 0.1 mm. Riprap is placed around a cylindrical pier with a width of 3.5 cm, extending up to 8 cm above the flat bed and forming a slope of 1:1.5. In the numerical model, the riprap is designed as a solid obstruction with a surface roughness of 0.1 m, which cannot be carried away by the flow current. The simulations maintain a constant discharge of 37 l/s at the inlet and a water depth of 17 cm at the outlet. To validate the numerical model, results of physical experiments in clear water are used (Gilja et al., 2022). After reaching equilibrium scour depth, the numerical model aligns well with the experimental results.

## 2. Results and discussion

This paper presents 8 simulation runs and their influence on scour pattern next to riprap protection. Scour patterns have been analyzed at the initial scour stage since it plays an important role in shaping the final scour pattern. Numerical setups that have been varied are: 3 bedload transport equations, 2 turbulence models, 2 sediment sizes, 2 critical Shields numbers, 2 roughness heights, and 2 angles of sediment repose (Table 1).

**Table 1.** Arrangement of 8 different numerical setups with corresponding flow velocity and time of incipient motion evolution around pier protected with riprap sloping structure

| Run | Bedload transport equation | Turbulence model | Sediment size [mm] | Critical Shields number | Roughness height | Angle of repose | Scour depth at initial scour stage [cm] |
|---|---|---|---|---|---|---|---|
| A | Nielsen | RNG | 0.2 | 0.050 | 0.0005 | 32 | 0.8 |
| B | Van Rijn | RNG | 0.2 | 0.050 | 0.0005 | 32 | 0.3 |
| C | Meyer-Peter Müller | RNG | 0.2 | 0.050 | 0.0005 | 32 | 0.4 |
| D | Meyer-Peter Müller | LES | 0.2 | 0.050 | 0.0005 | 32 | 1.1 |
| E | Meyer-Peter Müller | LES | 0.1 | 0.050 | 0.0005 | 32 | 0.8 |
| F | Meyer-Peter Müller | LES | 0.2 | 0.027 | 0.0005 | 32 | 1.0 |
| G | Meyer-Peter Müller | LES | 0.2 | 0.027 | 0.002 | 32 | 2.0 |
| H | Meyer-Peter Müller | LES | 0.2 | 0.027 | 0.002 | 15 | 1.6 |

The analysis of flow structure revealed a common feature for all simulation runs around the pier protected with riprap. The slope of the riprap directs the flow current upward, resulting in the absence of a downward flow that typically causes a horseshoe vortex. Instead of scouring in front of the pier, a recirculating vortex leads to the deposition of material upstream of the pier. The acceleration of two flow currents over the riprap generates two elongated scour holes downstream of the riprap (Petersen et al., 2015). After 10 minutes of computational time scour has developed to its initial stage (Figure 1). Different numerical setups result in variations in the predicted scour patterns. After reaching the equilibrium scour depth, the same scour patterns occur, only to a more pronounced extent.

The results indicate that different bedload transport equations (A, B and C) affect slower or faster development stage of scour. The Nielsen equation produced the largest scour depth, followed by the Meyer-Peter Müller and Van Rijn equations. The difference between RNG (C) and LES (D) turbulence models showed that LES model generates a more realistic scour pattern due to its improved ability to capture unsteady flow phenomena and larger turbulent structures, unlike the Reynolds averaging process of the RNG model. The LES model generates deeper and shorter scour holes and influences the sediment movement start earlier. Changes in sediment size had no effect on scour pattern; however, smaller particles (run E) were carried away earlier due to lower velocities, as expected. The variation in the critical Shields number ($\theta_{cr}$), indicator of threshold of sediment motion, can be observed from run D ($\theta_{cr}$=0.050) to F ($\theta_{cr}$=0.027). A higher critical Shields number implies that the flow must reach a higher intensity before sediment transport begins, as was observed in run D. Decreasing $\theta_{cr}$ can contribute long-term riverbed instability, as evident in run F where scour pattern is more elongated and follows main flow current direction. Roughness refers to the height of irregularities on the bed surface. A higher roughness leads to flow separations and vortices, resulting in non-uniform bed shear stress distribution and larger scour dimensions. Increasing roughness from 0.0005 (F) to 0.002 (G) resulted in a narrower and deeper scour hole with a more pronounced local scour pattern. The last numerical change concerns the repose angle of sediment, which has no effect on the initial sediment movement since the initial channel bed was flat. Run H differs from run G in decreased angle of repose, from 32 to 15, resulting in a wider and shallower scour hole with a more gradual shape.

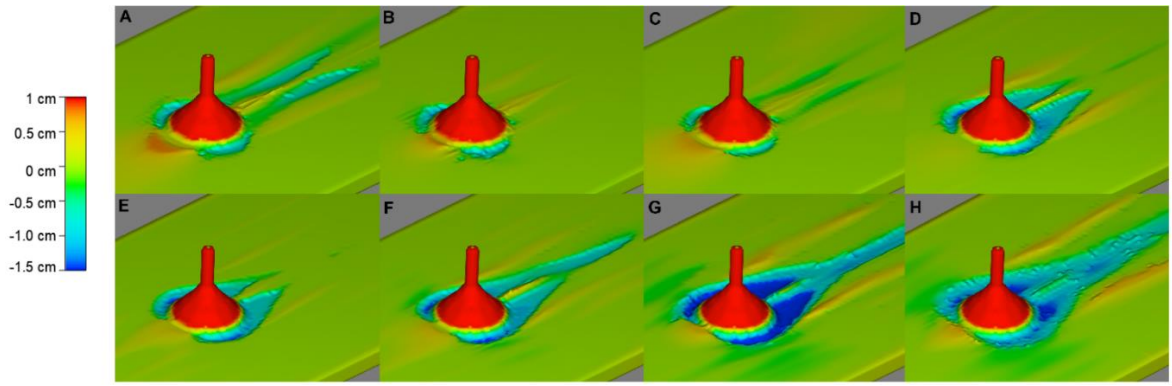



**Fig. 2.** Scour patterns around riprap protection at the initial stage for different numerical setups A – H as explained in Table 1.

This study demonstrates that different numerical setups affect scour pattern next to riprap in the initial scour stage. Results indicate that surface roughness has a significant impact on scour depth in the initial stage followed by bedload transport equation and turbulence model, while critical Shields number and repose angle have more impact on the shape of the scour hole. Comparing the scour patterns with the physical model reveals that the numerical model has difficulties in accurately reproducing identical real-world bed formations. The flow around riprap creates a complex vortex structure with many small eddies that cannot be captured numerically due to the simplifications in calculating governing mathematical equations.

**Acknowledgements**

This work has been supported in part by Croatian Science Foundation under the project R3PEAT (UIP-2019-04-4046).

**References**

Gilja G, Fliszar R, Harasti A, Valyrakis M (2022) Calibration and Verification of Operation Parameters for an Array of Vectrino Profilers Configured for Turbulent Flow Field Measurement around Bridge Piers—Part I., Fluids, 7, 315, https://doi.org/10.3390/fluids7100315

Petersen TU, Sumer BM, Fredsøe J, Raaijmakers TC, Schouten JJ (2015) Edge scour at scour protections around piles in the marine environment — Laboratory and field investigation, Coastal Engineering, 106, 42-72, https://doi.org/10.1016/j.coastaleng.2015.08.007

# Modelling the velocity coefficient $\alpha$ for the optimization of discharge estimation by non-contact techniques

Francesco ALONGI[1], Carmelo NASELLO[1], Calogero MATTINA[1], Dario PUMO[1], Leonardo Valerio NOTO[1]

[1] Engineering Department, University of Palermo, Italy
francesco.alongi01@unipa.it

ABSTRACT

In recent decades, river monitoring field has experienced a strong impulse thanks to the widespread use of non-intrusive discharge measurement methods. Radar- and image-based techniques can face and address typical issues arising from the adoption of traditional measurement approaches; for instance, they are suitable also in dangerous situations, such as floods, since they do not require direct contact between instruments, personnel, and water flow. Simplicity in the use of instruments and availability of free open-source processing software, make non-conventional discharge measurements reliable, easy, and fast, compared to traditional approaches. Radar instruments are based on Doppler effect for the evaluation of the velocity of floating matter over the liquid surface, by calculating the delay between emitted and reflected signals. Image-based techniques exploit cheap and easy-to-use recording devices and floating tracer for tracking river surface motion, statistically reconstructed by frame-by-frame cross-correlation analysis. Both radar- and image-based techniques use the velocity-area method for river discharge assessment. The bathymetry along a transect must be known, and the depth-averaged velocity is usually obtained by adopting simplifying assumption on the vertical velocity distribution. A velocity coefficient $\alpha$ is then introduced as the ratio between the depth-averaged and surface velocities, approximately equal to 0.85. Field experiments demonstrate how the velocity coefficient can differ significantly from theoretical value due to geometric and hydraulic factors (e.g., depth, distance from banks, roughness, turbulence). The present work aims to explore the influence of some of the aforementioned factors on the $\alpha$ coefficient over a wide range of real cases, evaluating the error arising from the use of the standard value for $\alpha$ in estimating discharge via non-contact techniques and proposing a new method for a more accurate estimation of $\alpha$.

## 1. Materials and Methods

The analyses were conducted on a large dataset of discharge measurements collected during an extensive measurement campaign (2020-2023) in several rivers in Sicily (Italy). Discharge was acquired by an ADCP moved from banks or bridge along specific transects. Data acquisition was performed by discretizing water columns with 5- or 10-cm cells depending on the maximum water depth along transect.

For the purposes of the analyses, sections were divided into 40-cm wide sectors, vertically binned into cells of constant height (10 cm). ADCP data were then aggregated in cell-ensemble subsets of velocity along each sector. A preliminary outlier removal was performed for all the cell-ensembles, averaging the remaining values, and obtaining the final velocities of the cell center. The cell ensemble-averaged velocity was retained only when the cell ensemble size exceeded 20 data, otherwise it was discarded from the analysis. Once ensemble-averaged velocities were computed for the cells of a sector, the corresponding vertical velocity profile was derived by fitting a power law, using a weighted interpolation method, with weights assigned based on the coefficient of variation $CV$ at each cell-ensemble. Power law curve was used only for interpolating missing velocity values in sector cells, and for extrapolating the corresponding surface velocity value. Power law interpolation/extrapolation along a vertical was performed if more than 5 ensemble-averaged velocities were available, or if at least 3 ensemble-averaged velocities were available, and they represent more than the 50% of the total number of cells for the sector. Sectors not matching such criterion were discarded from the analysis. Considering a null velocity at riverbed (i.e., no-slip condition), the final vertical velocity profiles were calculated at sectors considering both retained cell ensemble-averaged velocities from ADCP where

available and data reconstructed via power law in cells with missing velocity, including the extrapolated surface velocity. It was thus possible to compute the depth-averaged velocities at each sector and derive the corresponding velocity coefficient $\alpha$.

Velocity coefficients analysis allowed for studying possible underlying relationships with factors that may affect $\alpha$ and that are routinely computed for discharge measurements via non-contact methods. Roughness represents one of the main factors influencing velocities in a river, and it usually increases approaching the banks or for shallow river depths. In such conditions, local velocity coefficient can assume values far from standard theoretical value of 0.85. The present work thus proposes a method for estimating an $\alpha$ value variable along the various sectors in a transect, depending on the distance from the banks ($d$) and the depth ($h$).

The proposed method is based on a Multi-Layer Perceptron (MLP) Artificial Neural Network (ANN) which allows for removing a-priori assumptions about the analytical form of the relationships between $\alpha$, $d$ and $h$. The ANN was trained using the "Levenberg-Marquardt" error backpropagation algorithm, considering as "response" variable the $\alpha$ values obtained from all the velocity profile reconstructed in the real cases, while four variables were used as "input": the minimum distance of the sector vertical from the banks, $d$, the sector vertical depth, $h$, the ratio between the maximum and the average section depth, $H_{max}/H_{avg}$ , and the ratio between the section width and the maximum section depth, $W/H_{max}$. A unique dataset containing almost 2000 input-output samples was considered, using 70% of data for the ANN training, 15% for validation, and 15% for testing purposes. Different ANN topologies were explored, considering a Hidden Layer (HL), and progressively varying the number of nodes from 5 to 100. The final network is characterized by 15 nodes (Fig. 1a). The simulated velocity coefficient values provided by the ANN showed a very high matching degree with the $\alpha$ reconstructed from the real case studies, with a coefficient of determination $R^2$ equal to 0.81 (Fig. 1b).

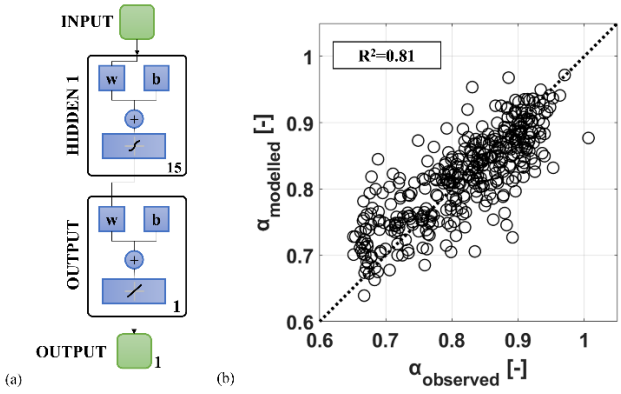



**Fig. 1.** (a)ANN model: Input Layer with 4 nodes ($h$, $d$, $H_{max}/H_{avg}$, $W/H_{max}$), a HL with 15 nodes, and an Output Layer with a single node. (b)Regression plot between observed and modelled α velocity coefficients over the entire dataset. Dashed line shows the perfect matching.

## 2. Preliminary results

The implications in using a coefficient $\alpha$ variable along the transect and simulated by the ANN rather than constant and equal to the literature value (=0.85), were evaluated in terms of error in the discharge estimation over all the case studies, considering benchmark discharges collected by ADCP. Velocity coefficient estimation with the proposed model improves the estimation of discharge in more than 80% of the case studies, producing a Mean Percentage Error (MPE) lower than 0.15%. Considering a constant value of $\alpha$, the MPE was almost two orders of measure higher. The proposed work is framed within the need for a simple and practical tool for better estimating river discharge using non-contact methods, such as radar- or image-based techniques. The generated ANN can be easily applied, since it is based on variables easily obtainable during a field measurement campaign and, however, essential to derive discharge from surface velocity based methods.

**References**


Alongi, F., Pumo, D., Nasello, C., Nizza, S., Ciraolo, G., & Noto, L. V. (2023). An automatic ANN-based procedure for detecting optimal image sequences supporting LS-PIV applications for rivers monitoring. Journal of Hydrology, 626, 130233.

Patel, P., Kar, R., & Sarkar, A. (2021, December). Estimation of Velocity Index for Flow Calculation in Open Channels Using Geometric and Hydraulic Characteristics. In International Conference on Hydraulics, Water Resources and Coastal Engineering (pp. 223-232). Singapore: Springer Nature Singapore.

Pumo, D., Alongi, F., Ciraolo, G., & Noto, L. V. (2021). Optical methods for river monitoring: A simulation-based approach to explore optimal experimental setup for LSPIV. Water, 13(3), 247.

Welber, M., Le Coz, J., Laronne, J. B., Zolezzi, G., Zamler, D., Dramais, G., ... & Salvaro, M. (2016). Field assessment of noncontact stream gauging using portable surface velocity radars (SVR). Water Resources Research, 52(2), 1108-1126.

# A comparative analysis of flow velocities at the outlet structure of Alqueva II pumped storage power plant

Adriano OLIVEIRA[1], Irene FERNANDES[2], Maria TERESA VISEU[3], Marco ZORN[4], Stefan RIEDELBAUCH[5]

[1,2] Hydraulics Department, Dam Engineering Division, EDP Produção, Porto, Portugal
[3] Water Resources and Hydraulic Structures Division, LNEC, Lisbon, Portugaladriano.oliveira@edp.com, irene.fernandes@edp.com, tviseu@lnec.pt
[4,5] Institute of Fluid Mechanics and Hydraulic Machinery, University of Stuttgart, Stuttgart, Germany
marco.zorn@ihs.uni-stuttgart.de, stefan.riedelbauch@ihs.uni-stuttgart.de

## ABSTRACT

The Alqueva dam has created one of the largest artificial lakes in Europe on the Guadiana River in southern Portugal. The Alqueva II Pump Storage Power Plant (PSPP) began operating in 2012 and is equipped with two reversible pump-turbines (PT1 and PT2), each one with a nominal turbine flow of 200 $m^3s^{-1}$. The outlet structure diverges symmetrically across two draft tubes and four tailrace channels per power unit, all of them equipped with trash racks (14x4.25 $m^2$ cross section each) at the tailwater reservoir connection (see fig.1).

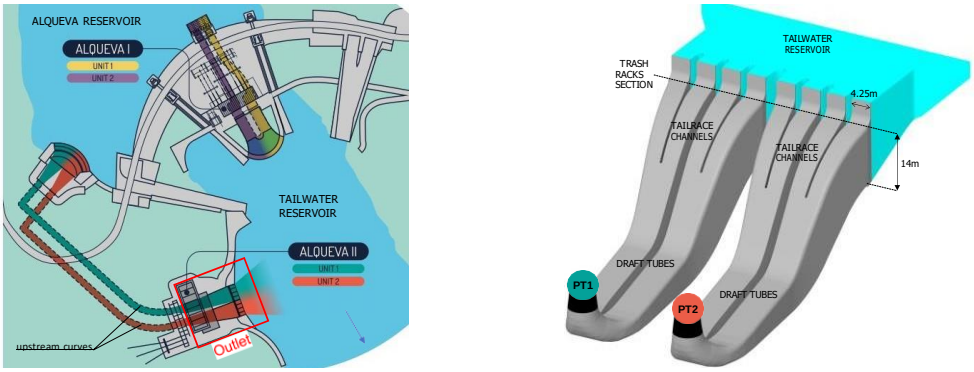



**Fig. 1.** Alqueva dam (GE Renewable Energy, 2022) and Alqueva II PSPP outlet structure 3D model.

In the project design, the overall dimensions of the outlet structure and trash racks were defined based on the flow rate, to allow maximum performance and operational efficiency. Design validation was conducted using a scale physical model where several analyses were performed focusing on the flow velocities along the outlet structure (LNEC, 2008). More recently, in the scope of the XFLEX Hydro project[1], both computational fluid dynamics (CFD) simulations and prototype tests were performed in collaboration with the University of Stuttgart, further complementing our overall knowledge regarding the prior results (M. Zorn et al., 2023).

This abstract presents a comparative analysis of flow behaviour and mean velocities obtained at the trash racks section of the outlet structure through physical and numerical models, as well as within prototype tests, considering different inlet conditions in turbine mode, as well as distinct tailwater reservoir levels.

The physical model investigated water flows, only by gravity effect, between an upper and a lower tank, through two tubes replicating the entire hydraulic circuit, without considering the effect of the pump-turbine runner rotation expected in the prototype. This study was performed according to Froude similarity, based in a 1:65,8 scaled model, considered suitable and leading to negligible scale effects in what concerns flow velocities analysis. A traditional propeller current meter (OTT model C2) was used for measuring the velocity field at the trash racks section area. Boundary conditions were established guarantying flow discharges by electromagnetic flow meters (upstream) and water levels by floodgates (downstream).

[1] Project funded by the European Union's Horizon 2020 research and innovation program (https://www.xflexhydro.com/).

The numerical model simulated the outlet structure and tailwater reservoir. It considered inlet flow velocities, in turbine mode, with either a theoretical homogeneous distribution, or a more realistic distribution estimated from a CFD simulation. Tailwater reservoir levels were imposed as an outlet condition. A minimum of 1M cells, above which flow results were independent, was generated and a maximum size of 0.2 m at the trash racks were considered. The time step was 0.1 s and the numerical solution became stable after approx. 200 s. The results are unsensitive to friction effects since the flow velocities and walls roughness have low values.

Both physical and numerical models applied full load turbine modes, simultaneously, for PT1 and PT2 and tailwater reservoir varying between normal 84.8 m and minimum 79.0 m water levels.

The main results for the average velocities at the trash racks section considering full load turbine mode and a normal water level (84.8) are presented in fig.2.

As shown in fig.2a and 2b, CFD simulation results are similar to the physical tests, although with a less symmetrical distribution, mainly because of the secondary flow phenomena induced by the plan curves considered upstream of the PSPP (see fig.1). Both graphics display higher velocity concentrations near the bottom ($\approx$ 1,6 $ms^{-1}$), which can be justified by the secondary flow phenomena induced by the elbow of draft tubes, and a non-uniform flow field on each trash rack spam due to the influence of the tailrace channels piers.

On the other hand, the velocity field obtained for the realistic velocity inlet shows a greater asymmetry and concentration in one of the trash racks spams (see fig.2c), with maximum velocities about two times greater, when compared with the other two graphics. This behaviour is explained by the clockwise runner's rotation effect and the influence of the draft tubes' central pier, which guides the flow primarily along one side of the tailrace channels.

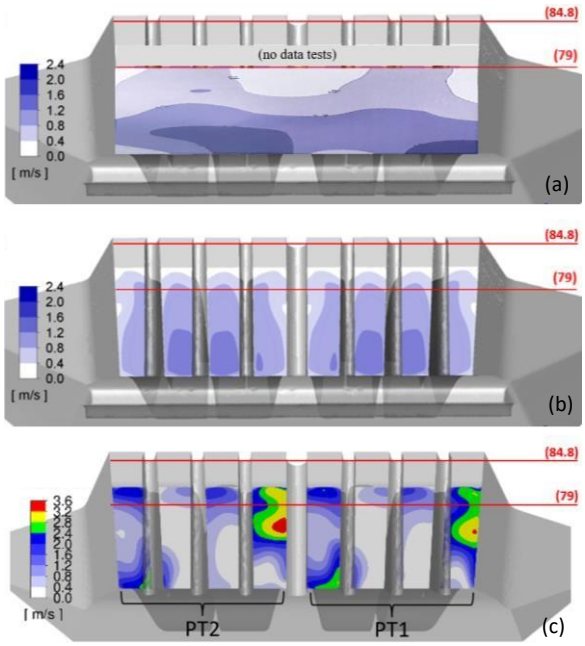



**Fig. 2**. Average velocities at the trash racks section for full load turbine mode: physical tests (a); CFD simulations for homogeneous velocity inlet (b) and for realistic velocity inlet (c).

Those last results were expected to be observed during prototype tests, even for single-machine operation, since pump-turbine runner rotation prevails under secondary flow phenomena existing upstream the PSPP. The most relevant aspects previously mentioned are also valid, regardless the tailwater reservoir level.

Regarding the site tests (see fig.3), it was considered that the flow behaviour was, generally and qualitatively, in accordance with the CFD simulation results obtained for realistic velocity inlet, since the higher flow velocities concentration were observed at the same trash rack spams.

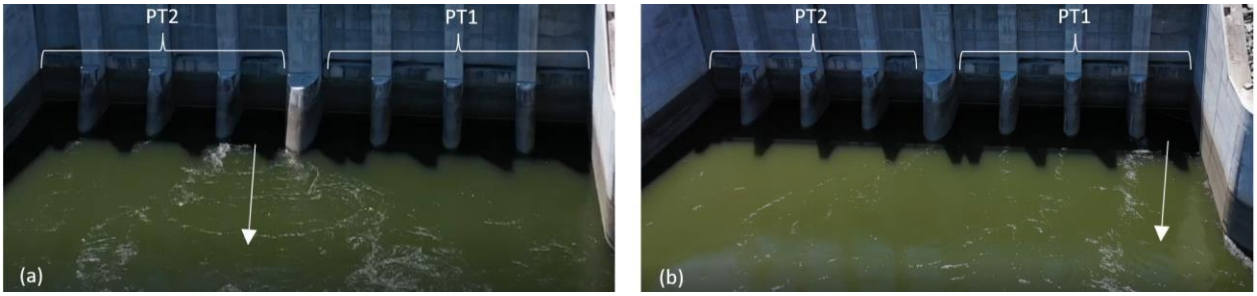



**Fig. 3**. Flow velocity concentration observed during site tests for full load turbine mode: (a) only PT2 operated; (b) only PT1 operated.

Finally, we can conclude that CFD simulations provided high confidence results, signifying an important complement to physical models, especially when employed to predict more realistic operational conditions, such as the influence of the machine runner rotation, in turbine mode, on the flow behaviour along an outlet structure like Alqueva II PSPP.

**References**

GE Renewable Energy (2022) D7.1 – Alqueva demonstration system use case, XFLEX Hydro report
LNEC (2008) Estudo Hidráulico em Modelo Reduzido do Reforço de Potência do Aproveitamento de Alqueva, Estudos de 1ª Fase
M Zorn, J Ada, L Auch, E Micciche, S Riedelbauch, C Gouveia, A Oliveira (2023) Investigation of the tailwater flow during hydraulic short circuit operation in the Alqueva II pumped storage power plant, IAHRWG2023

8th IAHR EUROPE CONGRESS
LISBON - PORTUGAL
4-7 JUNE 2024

# Parameterization of Roughness Distribution on Floodplains in 2D Shallow-Water Simulations

Jean-Paul TRAVERT[1,2], Cédric GOEURY[1,2], Vito BACCHI[1], Fabrice ZAOUI[1], Sébastien BOYAVAL[2,3]

[1] National Laboratory for Hydraulics and Environment, EDF R&D, Chatou, France
jean-paul.travert@edf.fr

[2] LHSV, Ecole des Ponts, EDF R&D, Chatou, France
[3] MATHERIALS, Inria, Paris, France

ABSTRACT

Modelling geophysical dynamics as floods leads to constructing large systems of Partial Differential Equations (PDEs) models with uncertain parameters. In the Shallow-Water Equations (SWE), one of the uncertain input parameters is the roughness (often assumed time-independent for flood modelling, but which varies in space). Our objective is to find the best parameter structure (assigning a single coefficient to different subdomains) depending on the water depths observations. With the growing number of observations on floodplains, like satellite images e.g., one can consider data assimilation techniques to improve the numerical value of the roughness parameter. First, we resort to sensitivity analysis for reducing the dimensionality of the roughness parameter to identify, i.e. for reducing the number of subdomains with uniform roughness here.

## 1 Introduction

Floods are often modelled using the solution of the Two-Dimensional (2D) SWE. In these equations, the roughness term represents a source term in the momentum equations. It represents the water flow resistance caused by underlying surfaces, leading to energy losses and changes in water depths and velocities. The roughness term mainly depends on the nature of the soil (Chow, 1959), so it should be spatialized on the domain. A usual practice in engineering studies is to use only one roughness zone for the floodplain (Horritt and Bates, 2002) because of a lack of information on it. This approach may not characterize the complex heterogeneities of different land uses. Another approach is to divide the domain into subdomains of homogeneous land use and assign them roughness values based on experts' opinions (tables, experimentations, physical laws, etc.) (Chow, 1959; Barnes 1967). With satellite images, it may be possible to calibrate these subdomains with distributed observations on the floodplains.

We aim to identify the minimal number of zones in the floodplains that can be calibrated to represent floods depending on the density of spatial and temporal observations. Other goals of having fewer zones are to limit the computational cost for future calibration and improve data assimilation efficiency for estimating the parameters based on uncertain satellite observations such as flood extent and water depths. We aim to quantify the input's (roughness) influence on output (water depths) variability with sensitivity analysis techniques.

## 2 Methods and materials

The prior structure of the roughness parameters is based on physical considerations. The floodplains are separated into subdomains of homogeneous soil properties based on the Corine Land Cover (CLC) dataset. This dataset represents a map of Europe's land cover at a resolution of 25 m. Then, for each subdomain, experts' opinions give a range of possible values following a uniform distribution between a minimum and maximum value for each land use.

Different sensitivity analysis techniques such as Sobol decomposition and Delta Moment-Independent Measure are tested (Pianosi et al., 2016). 2000 parameter samples are generated from the prior distributions. The simulations are performed with TELEMAC-2D (www.opentelemac.org) computation code. Water depths

are retrieved at 290 locations across the domain. The methodology is applied on the Garonne River in France, with the observation nodes represented in Fig. 1.

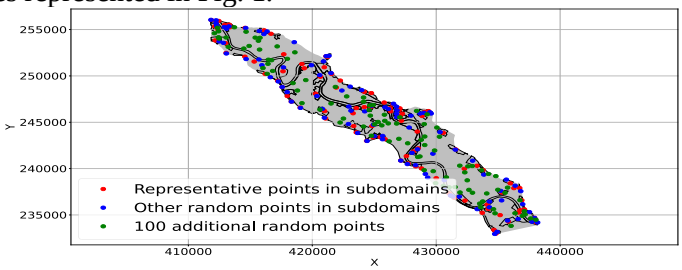



Fig. 1. Locations of the water depths observations across the simulation domain.

Different scenarios are considered for the prior guess on the structure of the roughness parameters. For instance, the channel roughness structure can be considered unknown or defined (without uncertainty). In our test case, it corresponds to 92 and 95 uncertain subdomains, respectively.

## 3 Results

During the flood propagation, the sensitivity of the water depths to the roughness subdomains changes. The sensitivity analysis has been computed for every observation node at different times. We present here only a global overview for the 290 points simultaneously from Fig. 1. In Fig. 2, we see the influential subdomains with a first-order Sobol (S1) higher than 0.1 for at least one of the water depths at two observation times.

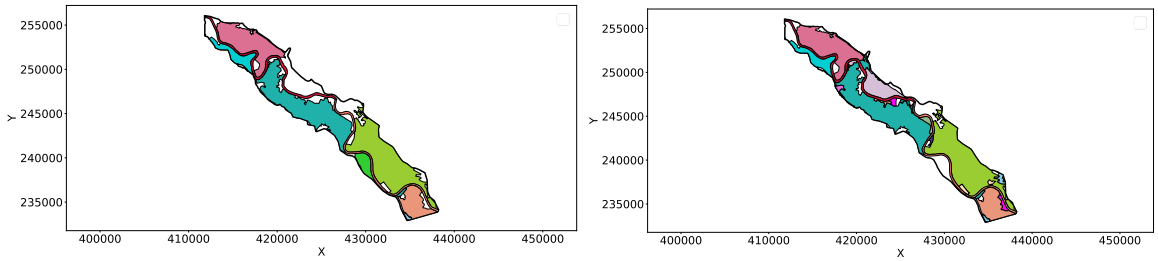



**Fig. 2.** Subdomains (in different colours to distinguish them) with S1>0.1 for at least one of the water depths at T = 210 hours (left) and T= 285 hours (right) of simulation.

From the sensitivity analysis, the number of subdomains can be at least divided by 2 for the 290 selected observation nodes because some subdomains never influence (Sobol below a given threshold) any water depth for all the observation times. The quantification of the reduction for different numbers of temporal and spatial observations was carried out but is not presented here. The insensitive subdomains can then be aggregated with their neighbors based on dependencies between the zones such as the second-order Sobol index.

From all the simulations, we also compare the simulated and observed flood extent with an example in Fig. 3.

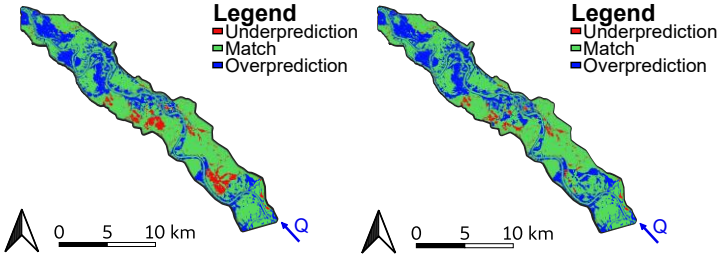



**Fig. 3.** Example of comparison of the flood extent from an observation (reference) with simulations for two roughness parametrizations.

For some sets of uncertain parameters, the flood extent shows a better correlation with the satellite flood extent (considered perfect). The flood seems better represented upstream of the domain with the second parameter sample. Different indices (Critical Success Index, hit rate, etc.) are computed to find the best set of parameters.

**Acknowledgements**
The authors acknowledge the French National Association of Research and Technology (ANRT) [CIFRE #2022/0972] for funding.

**References**

Barnes H.H (1967) Roughness characteristics of natural channels, US Government Printing Office, Number 1849.
Chow V (1959) Open Channel Hydraulics, McGraw-Hill.
Horritt M, Bates P (2002) Evaluation of 1D and 2D numerical models for predicting river flood inundation, Journal of hydrology, 268-1-4), 87-99.
Pianosi F, Beven K, Freer J, Hall J. W, Rougier J, Stephenson D. B, Wagener T (2016) Sensitivity analysis of environmental models: A systematic review with practical workflow. Environmental Modelling & Software, 79, 214-232.

# A Comparative Analysis of Deep Learning Techniques for River Flow Forecasting in Northwest Spain

Juan F. FARFÁN-DURÁN[1], Luis CEA[1]

[1] Universidade da Coruña, Water and Environmental Engineering Group, Center for Technological Innovation in Construction and Civil Engineering (CITEEC), Elviña, 15071 A Coruña, Spain
j.farfan@udc.es

ABSTRACT

Streamflow forecasting is crucial for water resources management, with its complexities stemming from various factors including weather patterns and basin characteristics. This study evaluates the efficiency of Deep Learning (DL) techniques, such as LSTM, GRU, CNN, and their hybrid combinations, in predicting hourly streamflow in two basins (Groba and Anllons) located in Northwest Spain, using as input the observed rainfall and discharge previous time steps. Our results indicate a context-dependent performance, with the GRU model excelling in 1 – 3-hour predictions for Groba, while all models perform comparably in Anllons. Interestingly, added complexity in hybrid models did not guarantee superior accuracy. The results highlight the challenge of doing 12-hour predictions in basins with short concentration times and underscores the significance of including the hydrological characteristics of the basin in the forecast.

## 1. Introduction and Objectives

Streamflow forecasting is pivotal for effective water resources management, from hydroelectric power generation to flood risk management. Predicting streamflow is complex due to the non-linear nature of the streamflow time series, which are influenced by factors like spatial weather patterns, basin characteristics, and human activities (Han et al., 2019). Traditional hydrological models, both physically-based and data-driven, have been employed to simulate watershed responses to precipitation (Huo et al., 2016). However, the emergence of Deep Learning (DL) techniques, such as Long Short-Term Memory (LSTM) networks, Gated Recurrent Units (GRU), and Convolutional Neural Networks (CNN), offer a promising alternative. These DL models can capture patterns in extensive historical datasets, relying on numerical input-output relationships, making them potent tools for streamflow forecasting (Han et al., 2019; Van et al., 2020).

In this study, various DL models, including LSTM, GRU, CNN, and hybrid models like CNN-LSTM, CNN-GRU, and CNN-RNN, were evaluated for predicting hourly streamflow in two distinct basins, Groba, with an area of 17 km², and Anllóns, with an area of 433 km², are located in Galicia, Northwest Spain, using only the observed rainfall and discharge from previous time steps as input. The performance of these models was assessed across different lead times of 1, 3, 6, and 12 hours. The performance of the models is evaluated by means of three goodness-of-fit metrics: the Nash-Sutcliffe Efficiency (NSE) coefficient, and two of its modifications, NSE for high flows and NSE for low flows (Farfán & Cea, 2022; Nash & Sutcliffe, 1970).

## 2. Preliminary Results

The results underscore the context-dependent nature of the model performance, influenced by the unique hydrological complexities of each basin. For instance, while the GRU model excels in short-term predictions for the Groba basin, all models exhibit comparable performance in the Anllons basin. Interestingly, hybrid models, which combine architectures like CNN-LSTM, CNN-GRU, and CNN-RNN, did not significantly outshine simpler LSTM and GRU models, suggesting that added complexity does not necessarily guarantee enhanced predictive accuracy.

As expected, the prediction accuracy declines with extended lead times, a loss of accuracy that is quantified by our results and that can be related to the characteristics of the basin. This loss of performance is especially evident in the Groba river and can be attributed to the short times of concentration, which renders past data irrelevant for 12-hour predictions. In contrast, the Anllons basin, with its larger area and milder slope, maintains more consistent prediction accuracy across time horizons. The findings of the study emphasize the importance of considering hydrological characteristics, such as basin area and slope, which influence the temporal dependencies between rainfall and runoff data.

Despite the advancements in DL models, there remain challenges in achieving accurate 12-hour forecasts, crucial for flood early warning systems. This is especially pertinent in regions like Galicia, characterized by varied rainfall patterns. Future research will be focused on the integration of satellite data, such as soil moisture and rainfall information, as well as weather forecasts, in order to enhance model accuracy. Additionally, the development of hybrid models, combining DL techniques with physical hydrological models, might offer a more adaptive approach to changing hydrological conditions.

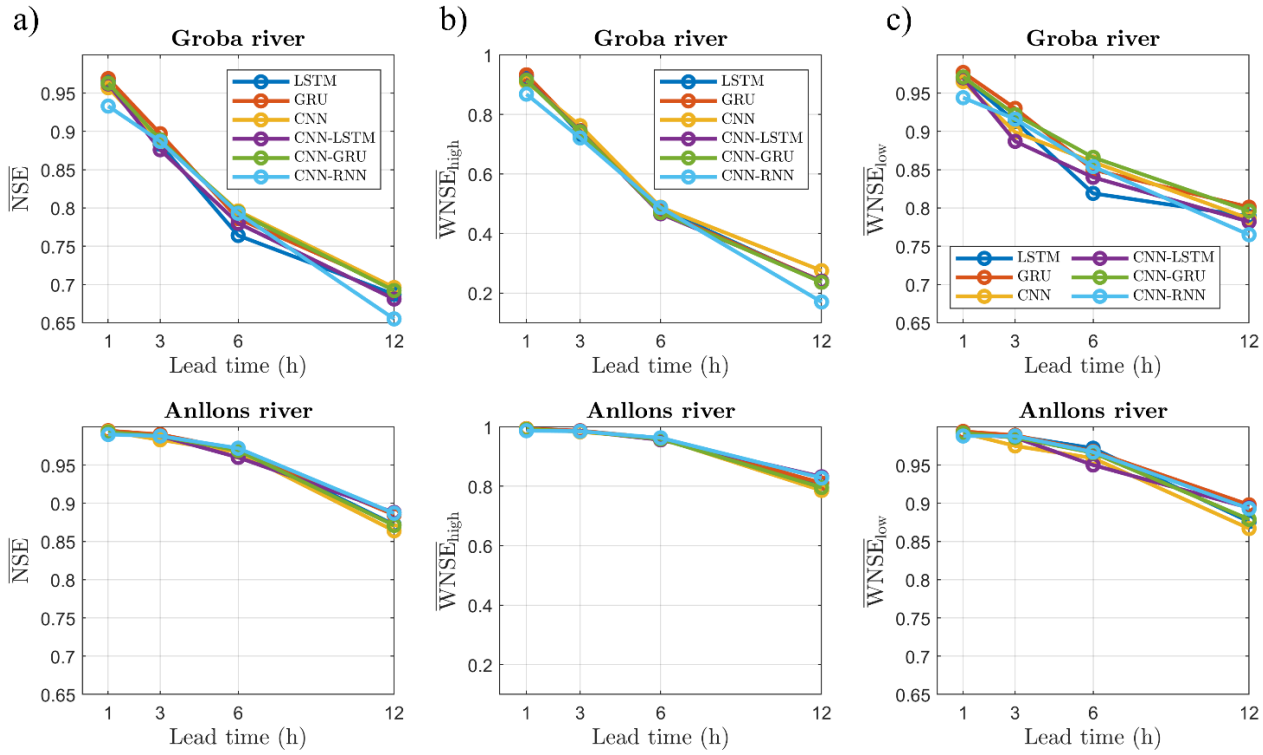



**Fig. 1.** Deterioration of Goodness-of-Fit Values in the Groba and Anllons Rivers: An evident decline in fit quality as lead time increases.

**Acknowledgements**

The main author of this work (J. Farfán) was financed by the Galician government (Xunta de Galicia) as part of its pre-doctoral fellowship program (Axudas de apoio á etapa predoutoral 2019) Register No. ED481A-2019/014.

This work was received financial support from the Spanish Ministry of Science and Innovation (MCIN/AEI/10.13039/501100011033) within he project "SATURNO: Early warning against pluvial flooding in urban areas" (PID2020-118368RB-I00).

The meteorological data was obtained from the agency MeteoGalicia at https://www.meteogalicia.gal/.

The discharge data has been provided by the regional water administration Augas de Galicia at https://augasdegalicia.xunta.gal/.

**References**

Farfán, J. F., & Cea, L. (2022). Improving the predictive skills of hydrological models using a combinatorial optimization algorithm and artificial neural networks. *Modeling Earth Systems and Environment*, 1–16.

Han, Z., Zhao, J., Leung, H., Ma, K. F., & Wang, W. (2019). A review of deep learning models for time series prediction. *IEEE Sensors Journal*, *21*(6), 7833–7848.

Huo, J., Liu, L., & Zhang, Y. (2016). Comparative research of optimization algorithms for parameters calibration of watershed hydrological model. *Journal of Computational Methods in Sciences and Engineering*, *16*(3), 653–669.

Nash, J. E., & Sutcliffe, J. V. (1970). River flow forecasting through conceptual models part I—A discussion of principles. *Journal of Hydrology*, *10*(3), 282–290.

Van, S. P., Le, H. M., Thanh, D. V., Dang, T. D., Loc, H. H., & Anh, D. T. (2020). Deep learning convolutional neural network in rainfall--runoff modelling. *Journal of Hydroinformatics*, *22*(3), 541–561.

# Why computational fluid dynamics is mandatory in physical modelling of large hydraulic structures: a six-step methodology of integration

Lourenço SASSETTI MENDES[1], António MURALHA[1], José F. MELO[1], Teresa VISEU[1]

[1] Laboratório Nacional de Engenharia Civil, Portugal
lmendes@lnec.pt
amuralha@lnec.pt
tviseu@lnec.pt
jfmelo@lnec.pt

ABSTRACT

A six-step methodology is proposed to integrate physical modelling with computational fluid dynamics for the evaluation of flow in large hydraulic structures, with practical examples of two case studies. Significant efficiency gains are obtained, demonstrating that integrating CFD analysis is mandatory.

## 1. Introduction

Physical modelling is essential to validate the design of complex hydraulic structures, such as intakes, spillways, stilling basins, and plunge pools, due to the flow complexity, regardless of the scale effects and experimental limitations, and significant construction and operation costs.

Over the past two decades, the application of computational fluid dynamics (CFD) modelling to hydraulic structures has gained prominence among researchers and practising engineers due to technological advances. CFD allows for the evaluation of multiple designs with time and cost savings, and delivers flow data in all domain cells, in contrast to experimental measurements. The main challenges in CFD of hydraulic structures are: geometry complexity and large dimensions, extended range of time and length scales, high-velocity flows, turbulence, aeration, and erosion. CFD requires complex models, efficient meshes that are difficult to build, fluid mechanics and numerical methods' knowledge, and access to high-performance computers. Furthermore, calibration and validation against experimental and prototype flow data is essential. Therefore, CFD is not yet common practice in hydraulic structures engineering and is a lively topic for research.

The Water Resources and Hydraulic Structures group at Portugal's National Civil Engineering Laboratory (LNEC) has been developing a methodology that incorporates both physical modelling and computational fluid dynamics, referred to as integrated modelling (Fig. 1).

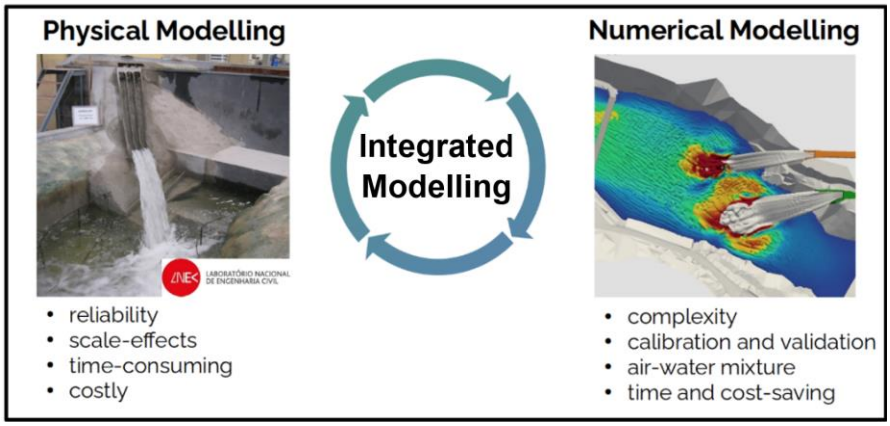



**Fig. 1.** Integrated modelling of large hydraulic structures.

## 2. Activities

A six-step methodology for integrating physical modelling with CFD is proposed, consisting of:

1. Preliminary CFD, aiming at:
    a. having a general understanding of the flow characteristics, and identifying potential design issues. The structures' geometry may be improved before physical modelling is performed,
    b. providing important information for the conception, construction, and observation of the physical model,
    c. suggesting a more efficient placement of measurement sensors and anticipating zones of the physical model that require more attention.
2. Preliminary physical modelling, aiming at:
    a. analysing the initial structure's design,
    b. collecting data to calibrate and validate the CFD model.
3. CFD model validation and calibration with physical model data
4. CFD tests of progressively enhanced designs
5. Physical modelling of the selected design with thoroughly analysis
6. CFD high-resolution replication of the physical model's selected design, aiming at providing a more in-depth understanding of the flow patterns and phenomena involved.

This methodology is substantiated by two case studies: the investigation of an erosion issue in the dissipation basin of the double ski-jump spillways at Fierza Dam (Melo et al., 2019), and the development of a fish passage in the tailwater channel of an existing large dam.

Furthermore, the performance evaluations conducted on the Two-Phase Volume-of-Fluid (TPVoF) and the Complete Two-Phase Euler (CTPE) models provided significant insights into the model's potential and limitations (Muralha et al., 2020; Mendes, 2021; Mendes et al., 2021). The TPVoF model is the most suitable in the absence of air-entrainment and air-water mixture (as the differences between the TPVoF and the physical model are not as expressive) and when facing time and computational effort constraints. The CTPE simulates highly aerated flows, overcoming the limitations of the TPVoF model. Despite requiring a higher level of expertise, the CTPE shows an efficient cost-benefit performance.

## 3. Conclusions

An integrated approach using physical and CFD models mitigates shortcomings of both techniques, potentiating each other. The proposed six-step methodology resulted in significant efficiency enhancements. Hence, integrating CFD in physical modelling is nowadays mandatory.

Nonetheless, certain intricate phenomena, such as the rock scouring or severe damaging of concrete aprons associated to high power flows are still strongly relying on physical model validation.

**Acknowledgements**

This research was funded by Fundação para a Ciência e Tecnologia (FCT), Portugal, grant numbers SFRh/BD/99815/2014 and PD/BD/135593/2018, and Laboratório Nacional de Engenharia Civil (LNEC). The authors thank all those involved in the organization of the 8th IAHR Europe Congress and to all the contributors that will enrich this event.

**References**

Melo JF, Kacurri E, Mendes LS, Topore A (2019) Modelling of Fierza Dam spillway operation and downstream effects on river bed and slopes, Dam Engineering, vol. 29, no. 2

Mendes LS (2021) Computational Fluid Dynamics of Aerated Flows in Spillways Chutes, PhD thesis, Universidad de Cantabria, http://hdl.handle.net/10902/23909

Mendes LS, Lara JL, Viseu MT (2021) Do the Volume-of-Fluid and the Two-Phase Euler Compete for Modeling a Spillway Aerator? 13, 21, https://www.mdpi.com/2073-4441/13/21/3092

Muralha A, Melo JF, Ramos HM (2020) Assessment of CFD Solvers and Turbulent Models for Water Free Jets in Spillways, Fluids, 5, 3, https://www.mdpi.com/2311-5521/5/3/104

# Hydraulic Performance for innovative erosion protection systems

Diogo FREITAS[1], Laura MOLANO[2], Diego GARCÍA[3], Ginna TORRES[4]

[1,2,3,4] A. Bianchini Ingeniero, S.A. (Maccaferri), Spain
d.freitas@maccaferri.com
l.molano@maccaferri.com
dg.gordo@maccaferri.com
g.torres@maccaferri.com

ABSTRACT

Rivers are constantly changing their behavior and morphology, which may result in alterations to the river channel course and the development of the flood plain due to erosion processes and sediment transport. Preventing soil loss and maintaining riverbank integrity under the flow effect requires implementing an erosion control system. The forces balance for bank stability depends on geometry, the properties of bank materials, and the hydraulics of flow in the channel. This study analyses the design of mattresses as an erosion control system. The design was improved by optimizing the connection between the base, panel, and lid, including cell fit through diaphragm spacing. Significant improvements can be attributed to the introduction of vertical connections, enabling fast installation, especially on steep slopes. The new mattress features greater allowable shear stresses with a lower thickness, implying the reduction of stone fill volume. A better erosion control system will be of great importance for river engineering regarding soil and water management and even environmental protection.

## 1. Introduction

Alluvial meandering rivers represent a dynamic system that flows undercut the outside banks because of mass failure processes and soil loss (Bertalan et al., 2018). Moreover, lateral bank erosion is responsible for the extensive destruction of arable lands and sometimes threatens human environments. Different mitigation measures have been developed to ensure the stability of the cross section such as riprap and mattresses. The riprap is a traditional protection that is limited to dumped medium-sized blocks, while mattresses are units manufactured from double-twisted hexagonal woven steel wire mesh that is filled up with stones. Comparing both mitigation measures, mattresses with vertical connections require a much lower thickness of revetment compared to riprap for the same shear stress, allowing for thickness savings up to 73% (see Fig. 1).

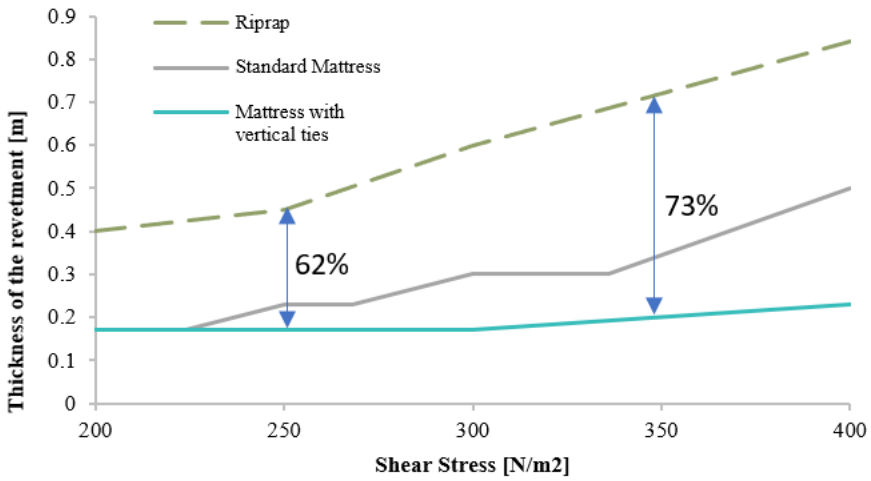



**Fig. 1.** Thickness required about the flow (expressed in shear stress units) for two erosion control systems (Pietro et al., 2021).

## 2. New mattresses improvements

In general, mattresses are manufactured with a 6x8 steel wire mesh type, made with a wire diameter of 2.2 mm nominal steel wire, coated with a high abrasion resistance polymer with a nominal thickness of 0.5 mm, resulting in a 3.2 mm outer diameter. Each mattress unit is divided into uniform cells by internal diaphragms at 1m spacing in a longitudinal direction. An innovative system with vertical bracing elements was added to the design to firmly connect the lid to the base of the unit as illustrated in Fig.2. The stability of erosion control systems using mattresses depends on the effect of the stone motion inside the mattress, in relationship to its thickness and stone size, under variable hydraulic flow regimes. According to research, the lining protective function is guaranteed when minimal or no movement of individual stones occurs inside the mattress compartment (Pietro et al., 2021). Thus, its performance against erosion was tested by quantifying the limit condition when erosion underneath starts developing and assessing the effect of the stone motion inside the compartments. Experimental results have shown that diaphragm spacing does not significantly affect the water flow dissipation, meanwhile, the changes in uniformity of the rock grading have predominantly impacted the energy dissipation. Outcomes reported of maximum stress allowable values are higher for mattresses filled with uniformly graded rock (Cu=1.0) than the test using Cu=1.5 which is the value conventionally in the design practice. There is also a notable improvement in the allowable shear stress with the newest mattress designs, especially the mattress with vertical connections (see Fig. 2).

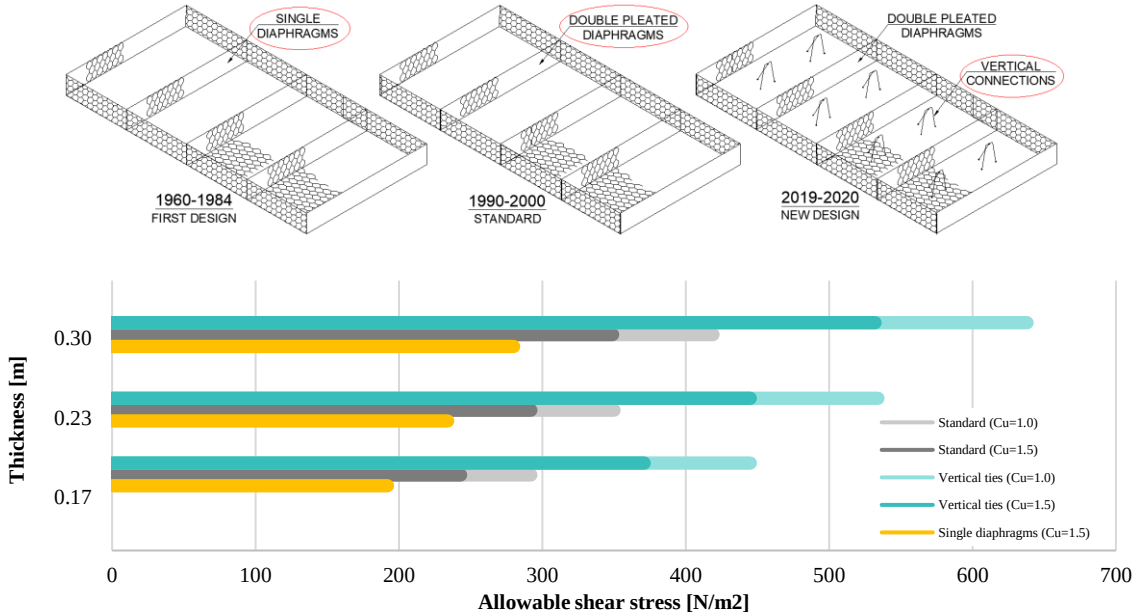



**Fig. 2.** Allowable shear stress for different mattresses and rock uniformity (Pietro et al., 2021).

The new mattress improvement is awarded to the vertical connections which maximizes the structural performance over the conventional mattresses. These vertical bracing components are connected in a special U-shape characterized by higher stiffness allowing the capability to distribute the forces over a larger surface. Further advantages of this new design are the reduction of installation time and the decrease in filling material required because of small thicknesses. This saving can be up to 60-80% lower. Regarding material reduction, a lesser environmental impact is expected due to a very low CO2 emission and expected riverbed revegetation compared to riprap in high-flow regimes.

In essence, the redesign started as an initiative to boost the use of sustainable products in the field of water resources management, generating added value for clients and suppliers without affecting performance. Therefore, all the features described above confirm the optimization of the concept of standard mattresses to the new erosion protection system.

**References**

Bertalan, L., Novák, T. J., Németh, Z., Rodrigo-Comino, J., Kertész, Á., & Szabó, S. (2018). Issues of meander development: Land degradation or ecological value? The example of the Sajó River, Hungary. Water, 10(11), 1613.
Pietro, P. D., Lelli, M., & Rahman, A. (2021). Hydraulic Tests and Interpretation of Test Data for Reno Mattresses in Open Channel Flow. In IOP Conference Series: Earth and Environmental Science, 930, 012025.

# Hydraulic resistance of near-natural floodplain vegetation: A dataset for validating numerical models using a laboratory scale model

Frederik FOLKE[1], Jochen ABERLE[2]

[1] Federal Waterways Engineering and Research Institute, Karlsruhe, Germany
frederik.folke@baw.de

[2] Leichtweiß-Institute for Hydraulic Engineering and Water Resources, Technische Universität Braunschweig
jochen.aberle@tu-braunschweig.de

ABSTRACT

For the validation of vegetation approaches against data of near-natural floodplain vegetation, a laboratory scale model was setup. In contrast to existing investigations, special focus was set on the transferability of the hydraulic conditions to natural rivers with large floodplains. To model flexible vegetation, special silicone elements were developed. The vegetation was scaled using the hydrodynamic density for rigid vegetation and the leaf area index for flexible vegetation. The collected data offer the possibility to validate vegetation approaches for natural conditions and thus strengthening their applicability in practice.

## 1. Introduction

Natural river banks and floodplains are characterized by species-rich vegetation, which provides an important habitat for flora and fauna. However, vegetation can also have a significant influence on the flow field and lead to an increase in water levels during flood events. Tools to model the interaction between flow and vegetation in hydrodynamic numerical models are therefore essential for the design and implementation of near-natural solutions. In recent decades, a variety of vegetation approaches have been developed to estimate the roughness of emerged and submerged vegetation. Almost all approaches are based on laboratory flume studies using artificial vegetation elements. However, there are significant differences between them –the effect of the flexibility of natural vegetation is often neglected and there are unanimous opinions about the shape of the velocity profile in the free upper layer in the case of submerged vegetation. In addition, the vegetation approaches are usually not or only validated for natural conditions. Unfortunately, no comprehensive field data for natural conditions of emerged and submerged floodplain vegetation is available). This limits the application of vegetation approached in practice. The collection of appropriate field data is complicated due to several reasons. In particular, the selection of a suitable site and the difficulty of planning the field measurements due to the dependence on hydrologically infrequent events pose a major challenge. In addition, it is difficult to quantify individual components of the overall hydraulic resistance (e.g. bed forms, log jams) during flood events. Furthermore, measurements during high water conditions are generally only possible to a limited extent for safety reasons. Therefore, a scaled laboratory model was set up with the aim of providing a comprehensive dataset for validation of vegetation approaches for near-natural conditions.

## 2. Laboratory scale model

The laboratory model was setup in a 32 m long and 5 m wide non-tiltable flume at the Federal Waterways Engineering and Research Institute (BAW). The laboratory model was setup with a scale of 1:60. The compound channel consisted of a 3 m wide floodplain, a 1 m wide embankment and a 1 m wide main channel (see Fig. 1a). This corresponds to a 180 m wide floodplain, a 60 m wide embankment and a 60 m wide main channel in nature scale. In longitudinal direction a slope 0.5‰ was chosen, according to the natural conditions at the Upper Rhine close to Karlsruhe.

The scale model intentionally omitted the incorporation of control structures, bends, and surface roughness, so as not to be influenced by three-dimensional effects in the flow. In order to ensure hydraulic conditions in the

laboratory model that are as close to nature as possible, a high bed roughness had to be selected for the model, which was achieved through the use of metal gratings. Additionally, the metal gratings provide an efficient means for the installation and removal of various vegetation elements.

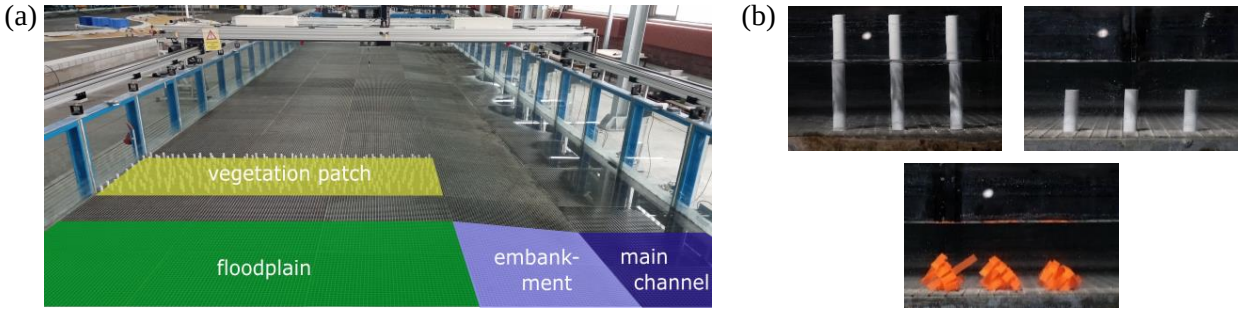



**Fig. 1.** Laboratory scale model (a), artificial rigid and flexible vegetation elements (b)

In the scale model, different vegetation elements were installed, whereby the selection and dimensioning of the elements aimed at transferability to near-natural conditions. The vegetation elements were arranged in patches on the floodplain, which differ in position and extent. In total three different elements were applied – both rigid and flexible (see Fig. 1b). The artificial elements were not scaled to represent individual vegetation elements (e.g. individual tree trunks), but rather corresponding homogeneous vegetation stands. Rigid vegetation was modelled using rigid cylinder elements with a diameter of 0.02 m. The diameter was chosen to ensure fully turbulent conditions. In the experiments, elements with heights of 0.18 m and 0.06 m were used in the installed state, whereby the higher elements were emerged in all experiments and the smaller ones were emerged and submerged depending on the discharge. In order to represent a vegetation density similar to nature, the installation density of the cylinders in the model was scaled using the hydrodynamic vegetation density $mD$ (e.g. Baptist et al., 2007), which is defined as the frontal projected area per volume. To model flexible vegetation in a scaled model, special silicone elements were developed. The silicone elements were designed in such a way that they exhibit behavior as similar as possible to natural floodplain vegetation with correspondingly higher flow attack. According to natural vegetation, the elements deform in terms of flow with increasing velocity, resulting in a reduction of the resistance force. The vegetation density was scaled using the leaf area index.

## 3. Results

A total of 45 experiments were conducted by varying vegetation elements, patch configurations, vegetation densities and using three discharges. For reference, all three discharge conditions were also investigated without vegetation elements. In addition to water levels, extensive velocity profiles were measured. Fig. 2 shows an exemplary comparison between measured and simulated flow depths. In the current case, the vegetation approach of Baptist et al. (2007) was used to model the roughness effect of rigid vegetation. Overall, the 2D-model is in good agreement with the measured values.

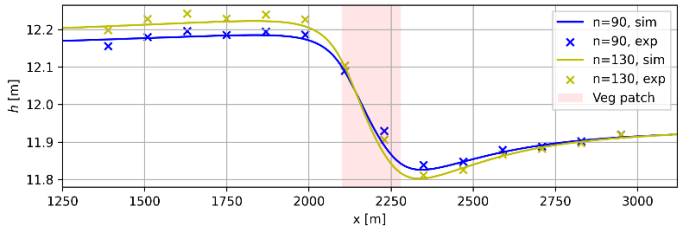



**Fig. 2.** Flow depths (nature scale) in main channel for two vegetation densities (exp: scale model, sim: 2D-model using vegetation approach)

## 4. Conclusion

Through innovative methods, both rigid and flexible vegetation could be replicated in a scaled model. This allowed for the first-time collection of an extensive dataset for validating vegetation approaches under natural conditions. This marks another successful step towards accurately representing the roughness effect of vegetation.

**References**

Baptist, M. J., Babovic, V., Rodríguez Uthurburu, J., Keijzer, M., Uittenbogaard, R. E., Mynett, A. und Verwey, A. (2007). On inducing equations for vegetation resistance. In: Journal of Hydraulic Research 45.4, p. 435–450.

Mewis, P. (2021). Estimation of Vegetation-Induced Flow Resistance for Hydraulic Computations Using Airborne Laser Scanning Data. In: Water 13 (13), 1864.

# Surface flow velocity estimations in low-luminosity environments using quinine-based tracer techniques

Soheil ZEHSAZ[1,2], João L. M. P. DE LIMA[1,2], M. Isabel P. DE LIMA[1,2], Jorge M. G. P. ISIDORO[2,3] and Ricardo MARTINS[4]

[1]University of Coimbra, Faculty of Sciences and Technology, Department of Civil Engineering, Rua Luís Reis Santos, Pólo II-Universidade de Coimbra, 3030-788 Coimbra, Portugal

[2]University of Coimbra, MARE–Marine and Environmental Sciences Centre/ARNET-Aquatic Research Network, Coimbra, Portugal
s.zehsaz@dec.uc.pt, plima@dec.uc.pt, iplima@uc.pt, jisidoro@ualg.pt

[3]University of Algarve, Institute of Engineering, Department of Civil Engineering, 8005-139 Faro, Portugal

[4]University of Aveiro, Department of Civil Engineering, RISCO–Research Centre for Risks and Sustainability in Construction, 3810-193 Aveiro, Portugal
ricardo.d.martins@ua.pt

ABSTRACT

This study explores the applicability of a novel fluorescent-based quinine tracer for estimating surface velocities of sheet flows and open channel flows under different ambient light conditions (day, twilight, night). The fluorescence of quinine is revealed under ultraviolet-A light. A quinine liquid solution was tested over several types of soil surfaces for estimating sheet flow velocities, both in the laboratory and in the field. Additionally, field experiments were conducted in open-channel flows to test the application of quinine tracers in both liquid and solid (ice cubes) states, and an Unmanned Aerial System (UAS) was used to record images of the behaviour of the tracers. The results revealed that quinine can be used as a fluorescent tracer to estimate sheet flows and open-channel surface flow velocities under low luminosity conditions. The main advantage of the quinine tracer lies in its high visibility under low luminosity conditions, which can be detected by optical sensors, while remaining environmentally non-toxic. These findings highlight the potential of quinine-based tracing techniques for surface flow velocity estimation in diverse and challenging scenarios, offering valuable insights for hydrological research and applications.

## 1. Introduction

Accurate measurement of surface water flow velocities and discharges is crucial for both engineering applications and environmental monitoring. Flow measurement plays a significant role in various hydraulic and hydrologic studies, including the transport of pollutants and erosion dynamics. However, these measurements face challenges, particularly in conditions such as steep slopes, shallow flows, heavy suspended sediment loads and low luminosity (e.g., at night, twilight, shielded environments or close conduits).

In this study, a novel quinine-based fluorescent tracer was used to estimate surface flow velocities. Laboratory and field experiments were carried out to test the performance of the tracer. The main objectives of this study were to: i) evaluate the quinine's applicability as a tracer for estimating sheet flow and open channel flow velocities; ii) assess its visibility compared to colour dye and thermal tracers and determine the best conditions for its use in terms of surface morphology and ambient luminosity; iii) compare the results between quinine tracers in liquid and solid states; iv) test the use of UAS to track the quinine tracer, under low luminosity conditions.

## 2. Materials and Methods

The materials used for the laboratory set of experiments included a rectangular soil flume, a constant head tank water supply system, various soil surfaces, quinine, colour dye and thermal tracers, a tubular ultraviolet-A

lamp, and optical and infrared sensors. The quinine tracer consisted of a quinine solution of 80 mg/L with a pH of 3.7. In the field experiments, the quinine solution was used in a liquid state for estimating sheet flow velocities on vegetated and paved surfaces, while in open-channel flow it was utilized in both liquid and solid (ice cubes) states. A UAS was used during the field experiments for tracking the quinine tracer.

The flow velocities were estimated from video snapshots, for all tracers. The surface velocity $V_s$ was estimated by assessing the travel distance of the tracers' plume leading edge over time $\Delta t$, within the measuring frame (de Lima et al. 2021; Zehsaz et al. 2022; Zehsaz et al. 2023). When using solid tracers, the travel distance of each ice cube or particle over time $\Delta t$ was calculated separately. The surface flow velocity $Vs$ was then considered as the average of the velocities estimated for a group of ice cubes.

## 3. Results

Snapshot images from both laboratory and field experiments, conducted on various types of soil surfaces, are presented in Fig. 1. The visibility of fluorescent quinine, dye, and thermal tracers can be compared. For detecting either the dye or quinine tracers, favourable light conditions were set. The detection of the thermal tracer was independent of any light conditions. Figure 2 shows images from an open channel flow, when using the quinine tracer in liquid and solid states.

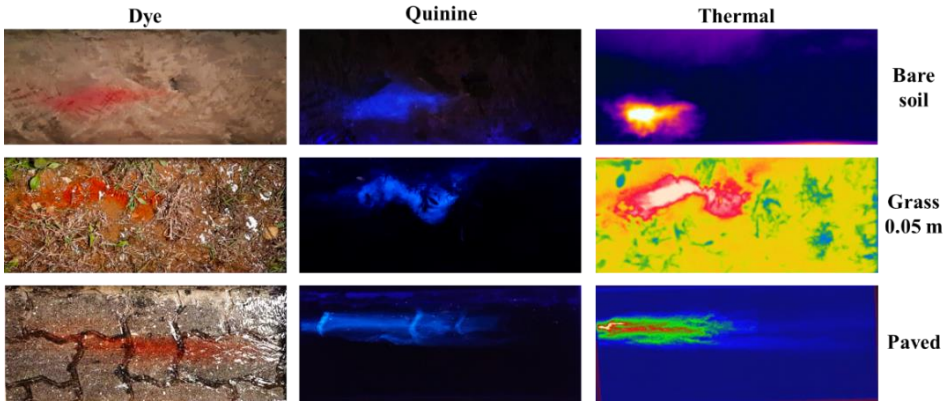



**Fig. 1.** Comparison between images of the dye tracer, the quinine tracer exposed to ultraviolet-A light, and the thermal tracer added to sheet flow over different surfaces. The flow direction is from left to right. Each image covers a length of 0.55 m.

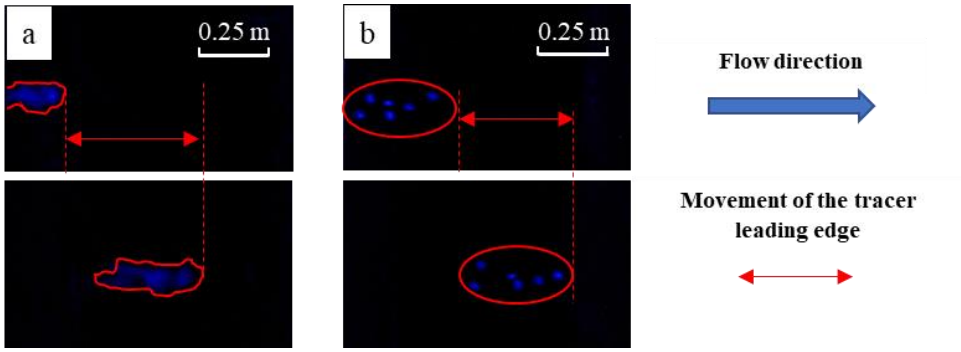



**Fig. 2.** Visualisation of the displacement of the tracer during a time interval Δt = 1 s (paired images), for different types of application of the quinine solution tracer in an open channel: (a) liquid tracer, (b) solid tracer. The horizontal and vertical scales in all images are the same.

## 4. Conclusion

Quinine-based tracers, when exposed to ultraviolet-A light, can assist in estimating sheet flow and open channel flow velocities under low luminosity conditions. In contrast to the thermal tracing method, which requires a costly infrared sensor, the quinine-based technique has the advantage of needing a more affordable optical sensor, while providing high visibility and ensuring environmental safety due to its low quinine concentration requirement.

**References**

de Lima JLMP, Zehsaz S, de Lima MIP, Isidoro JM, Jorge RG, Martins RG (2021) Using quinine as a fluorescent tracer to estimate overland flow velocities on bare soil: proof of concept under controlled laboratory conditions. Agronomy 11 (7), 1444. https://doi.org/10.3390/agronomy11071444.

Zehsaz S, de Lima JLMP, de Lima MIP, Isidoro JM, Martins R (2022) Estimating sheet flow velocities using quinine as a fluorescent tracer: bare, mulched, vegetated and paved surfaces. Agronomy 12 (11), 2687. https://doi.org/10.3390/agronomy12112687.

Zehsaz S, de Lima JLMP, Isidoro JM, de Lima MIP, Martins R (2023) Fluorescent quinine-based tracking techniques for measurement of open-channel surface flow velocities under low luminosity conditions using a UAS. Hydrology Research. https://doi.org/10.2166/nh.2023.011

# Visualisation and simulation of solute transport in water distribution networks

Zhangjie PENG[1], Stefania PIAZZA[2], Fred SONNENWALD[1] , Jesus Leonardo CORREDOR GARCIA[1], Gabriele FRENI[2], Ian GUYMER[1]

[1] Department of Civil and Structural Engineering, University of Sheffield, Sheffield, United Kingdom
zhangjie.peng@sheffield.ac.uk

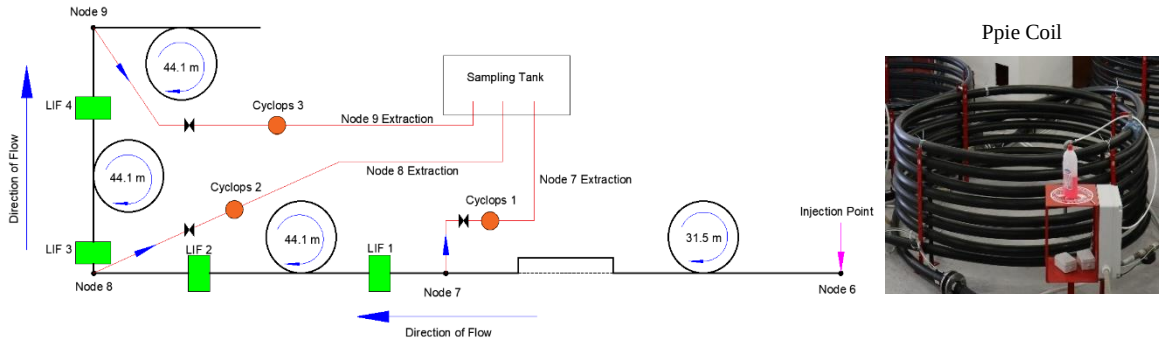
[2] School of Engineering and Architecture, University of Enna 'Kore', Cittadella Universitaria, 94100 Enna, Italy

## ABSTRACT

Modelling water quality in drinking water systems is complex. Previous work has relied on simple 1D plug flow (advection-only) assumptions to predict water quality changes in these systems, which have been shown to be insufficient to predict water quality (Piazza et al. 2022). The addition of dispersion (mixing) into models has improved predictions (Piazza et al. 2022). However, at laminar flow conditions where the pollutant is not cross-sectionally uniformly distributed for very long time periods, a 2D approach was suggested. To date, the 2D modelling approach has not been fully explored nor validated with 2D experimental data. This study aims to fill this gap by utilising four 2D in-pipe Laser Induced Fluorescence (LIF) concentration measurement systems to collect data in controlled complex network experiments at the University Kore of Enna. In this study, 2D cross-sectional pollutant distributions were recorded under various laminar and turbulent flow conditions within common full-scale pipe architectures to enable model validation. In this study pollutant transport in the network has been modelled using 1D advection, 1D and 2D diffusion-dispersion, and Computational Fluid Dynamics (CFD) models.

## 1. Experimental Set-up and modelling approach

Fig. 1 illustrates the pipe network configuration and instrumentation. Water in the pipe was extracted from three nodes, and the extraction rate was controlled to achieve the design flow regime in the 50 mm diameter main pipe between two nodes. Tests were conducted at various laminar and turbulent flow conditions with reducing flow rate from upstream to downstream. Injection of tracer was made at Node 6 before a pipe coil, where the flow was turbulent to ensure initial cross-sectional mixing. LIF 1 and 2, LIF 3 and 4 were installed before and after pipe coils, respectively, to investigate the impact of velocity separation on mixing. Detailed descriptions of the 2D LIF system can be found in Peng et al. (2022). Cyclops fluorometers were installed on the extraction pipes for point measurement of the extracted mean concentration from nodes, and the measurements were recorded for 1.5 to 6 hours to ensure that the tracer passed all the measurement locations.




Ppie Coil



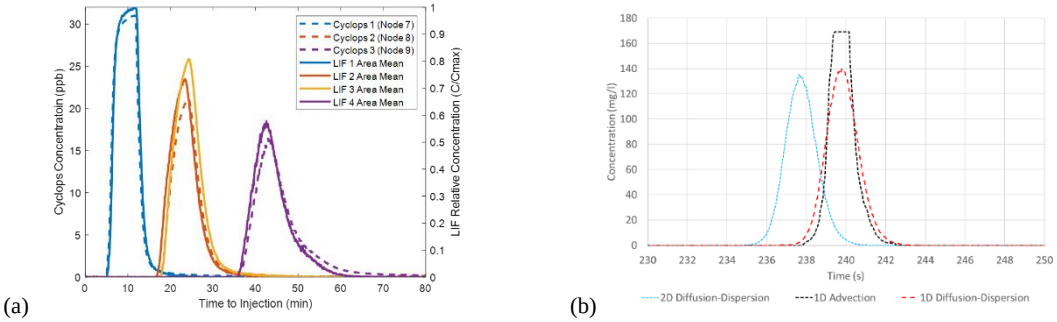
Fig.1. Experimental instrumentation and test section.

Four modelling approaches were used to simulate the solute concentration in the network. The first three approaches, 1D Adection, 1D Diffusion Dispersion and 2D Diffusion Dispersion, were implemented in EPANET-MATLAB-Toolkit (Piazza et al. 2022). The fourth approach was implemented in ANSYS Fluent

CFD, where the velocity was initially modelled and then concentration was simulated using the discrete phase particle tracking model.

## 2. Preliminary Results

Fig. 2(a) shows the Cyclops measurements and the derived area mean tracer concentration from LIF in a test where the Reynolds number was reduced from 3500 (nodes 7 to 8) to 2300 (nodes 8 to 9). Fig.2(b) illustrates that the modelled downstream tracer concentration profiles can exhibit significant differences depending on which model was employed. The 1D advection model only represents the advection process and shows limited spread on the concentration profile whereas the diffusion-dispersion models considering longitudinal or radial mixing show more spread. Fig. 3 shows the tracer cross-sectional concentration distribution at selected times during the test. The tracer was uniformly distributed at LIF1 (Camera 1) and was less uniformly distributed after the pipe coil at LIF2 (Camera 2). After a 90° elbow, the tracer became well-mixed at LIF3 (Camera 3) and then exhibited a non-uniform concentration distribution at transitional flow at LIF4 (Camera 4). Fig. 4 presents the CFD modelling results for the cross-sectional velocity and concentration distribution at different loops in the pipe coil (Fig. 1). The bottom loop is where the water enters the coil, and the top loop is where it leaves the coil. The CFD results demonstrated a clear velocity separation/internal secondary flow after several loops in the pipe coil, and the secondary flow is more evident when the water leaves the coil from the top loop. The influence of this velocity separation is reflected in the tracer concentration, with an accumulation observed on one side of the pipe. This phenomenon is clearly observed in the LIF measurements at LIF2 (Fig. 3), where a region along the Y-axis shows no tracer. These observations suggest that the diffusion-dispersion models are better than the advection only model in describing area mean concentrations, whereas to describe detailed cross-sectional concentration distributions 3D CFD simulations are required.




(a) (b)

Fig. 2. Measured concentration profiles for a Turbulent to Laminar flow test (a) and the comparison of different modelling approaches (b).

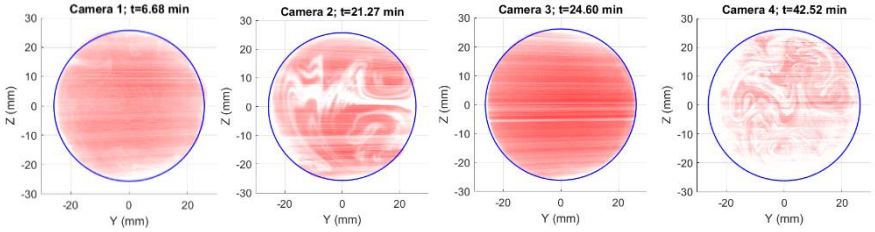



Fig. 3. Cross-sectional concentration distribution for the selected time in a Turbulent to Laminar flow test.

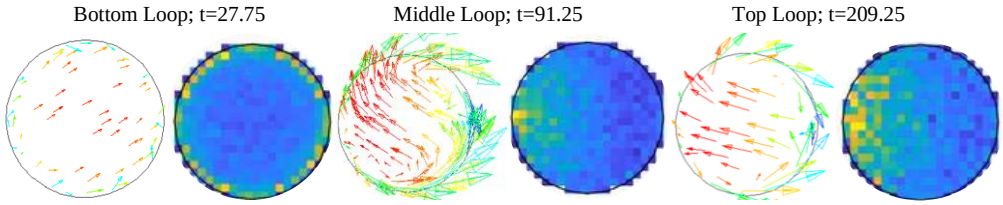



Fig. 4. Modelled cross-sectional velocity (vectors) and concentration distribution (colour map) at different heights in the pipe coil.

**Acknowledgements**

The authors would thank Joseph Milner, who provided technical support. This work is funded by the EPSRC Grant No. EP/P012027/1.

**References**

Piazza, S., Sambito, M., and Freni, G. (2022). "A Novel EPANET Integration for the Diffusive–Dispersive Transport of Contaminants." *Water 2022, Vol. 14, Page 2707*, Multidisciplinary Digital Publishing Institute, 14(17), 2707.

Peng, Z. Ho, Luan, and Guymer, I. (2022). " Disaggregation Phenomena in Mixing Processes During LaminarTurbulent Acceleration in Pipe Flows. " Proceedings of the 7th IAHR Europe Congress, Athens, Greece, 7-9 August 2022.

# Free surface velocity measurement in highly-transient viscoplastic flows: combining NIR surface detection and PIV techniques

Sergio MARTÍNEZ-ARANDA[1], Ignacio GARCÍA-PALACÍN[2], Pilar GARCÍA-NAVARRO[3]

[1,2,3] Fluid Dynamic Technologies-I3A, University of Zaragoza, Spain
sermar@unizar.es (S. Martínez-Aranda)
ignacio@unizar.es (I. García-Palacín)
pigar@unizar.es (P. García-Navarro)

ABSTRACT

Hydro-morphodynamical gravity-driven flows involve the mobilization of large fluidized masses composed of water, sediments, wood and multiple solid materials. These non-Newtonian flows are highly transient and unpredictable processes with a huge destructive potential for facilities and humans. The understanding of these complex flows requires both to improve numerical models and to collect more reliable laboratory and field data. This proof-of-concept work shows a novel non-intrusive technique to measure both the free surface position and velocity field in highly transient viscoplastic flows. The proposed technique deploys near-infrared (NIR) detection to reconstruct the 3D free surface within each time-window and to correct the synchronized time-resolved PIV measurement of the free surface velocity field. This technique was tested for the impact of a viscoplastic dambreak shock-wave on a rigid flat obstacle. The results provide an excellent characterization of the complex flow field and help to get insight into the mechanical response of the obstacle.

## 1. Validation of viscoplastic surface flow models

Flash sediment-laden floods, wetted soil avalanches, muddy slurries, debris flows, levees and dam failures and intense runoff erosion in bare soils after wildfires are examples of hydro-morphological surface processes which can damage infrastructures, agroforestry production, environmental systems and even human lives. Furthermore, climate change increases the frequency, intensity and severity of these hazards. Massive hydro-morphodynamical surface flows show a highly transient non-Newtonian behaviour and exert huge impact forces on buildings and infrastructures (Figure 1).



**Fig. 1.** Structures affected by shock-wave impacts in surface flows: (left) collapsed railway bridge by mine tailings dam failure in Brumadinho, Brazil, 2019 and (right) demolished buildings by mud flow in Shenzhen, China, 2015.

To design effective risk management plans, numerical viscoplastic models for gravity-driven flows play a key role, since they allow to test multiple hypothesis on the dynamical response of these Earth surface processes (Martínez-Aranda & García-Navarro, 2022). The proper validation of these computational models requires reliable field and laboratory data for highly transient cases, such as shock-wave impacts on civil structures. However, measuring such transient flows in laboratory is a challenging task due to the 3D behavior of the flow and the complex nature of the instantaneous forces exerted on the structures. Moreover, simultaneously acquired data on the free surface position and the fluid velocity are needed to achieve a complete characterization of the non-Newtonian flow dynamics.

## 2. 2.5D surface-PIV technique for highly transient flows

A novel non-intrusive laboratory technique is proposed to acquire both the free surface position and velocity field simultaneously in highly transient viscoplastic flows. The experiment consisted of a dambreak shock-wave of a shear-thinning fluid (0,18% w/w Carbopol 940 solution in water) which moved over a $16°$ slope and impacted on a rigid obstacle. The Carbopol solution was tinted using Titanium dioxide ($TiO_2$, white colour) and PVC particles (grey colour, approx. 3 mm diameter) were added. The fluid was placed in an upstream reservoir and released by opening a pneumatic gate.

The dambreak-wave movement was captured using a costumer-grade RGB-D device (Kinect v1, Microsoft, 2010), controlled by an *ad-hoc* recorder code (C++, OpenKinect project) with $30\ Hz$ adquisiton rate. The depth-image provided by the Kinect near-infrared (NIR) sensor was reassembled to reconstruct a 3D point-cloud of the instantaneous flow free surface (Navas-Contreras et al., 2021). Then the free surface elevation over the inclined plane was interpolated into an orthogonal grid, allowing to characterize the evolution of the 2D flow depth around the rigid obstacle during the impact of the shock-wave (Figure 2).




**Fig. 2.** Measured 3D free surface with the Kinect sensor: flow depth at (left) $t = 0{,}658\ s$ and (right) $t = 1{,}175\ s$.

The near-field upstream the rigid obstacle was recorded simultaneously using a CMOS computer-vision camera (Triton 016S, Lucid, 2019) with 70 frames per second. Both the Kinect device and the CMOS camera were synchronized with the gate opening. The images were processed using a time-resolving PIV algorithm (LabPIV, Matlab, 2021), obtaining the cross-correlated pixel-displacements within an interrogation grid. Then, the displacements were corrected using the 3D free surface position provided by the Kinect sensor for each interrogation window. Therefore, the 2.5D surface-PIV allowed to reconstruct both the free surface vertical celerity ($\omega$) and the horizontal free surface velocity ($u, v$) at the near-region of the rigid obstacle (Figure 3).

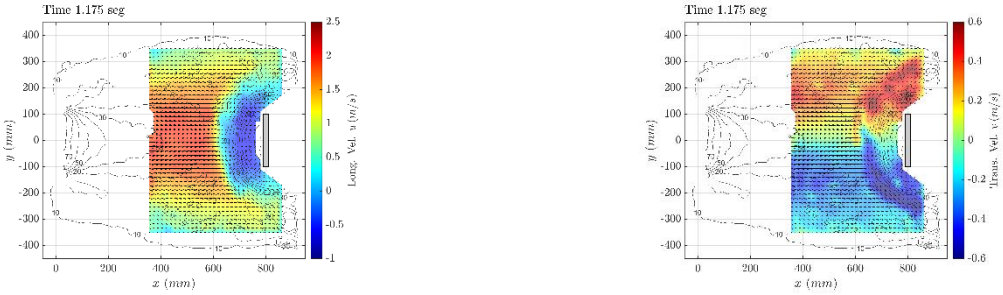



**Fig. 3.** Measured surface velocity using 2.5D surface-PIV technique: (left) x-velocity $u$ and (right) y-velocity $v$ at $t = 1{,}175\ s$.

To concluding, this novel non-intrusive technique combines affordable RGB-D sensors and surface-PIV measurements to reconstruct both the transient 3D free surface and the instantaneous 2.5D velocity in non-Newtonian flows. The technique is able to provide enough temporal-spatial resolution and accuracy to characterize properly the impact of complex shock-waves on rigid structures. The obtained data provide essential information on the forces exerted by the flow on the structure and can be used to validate computational models for viscoplastic surface flows.

**Acknowledgements**

This work was supported by grant PID2022-137334NB-I00 funded by MCIN/AEI/10.13039/501100011033 and by "ERDF A way of making Europe".

**References**

Martínez-Aranda S, García-Navarro P (2022) Efficient Simulation Tools (EST) sediment-laden for shallow flows. Chapter in *Modeling of sediment transport*, Intechopen Limited, London.

Navas-Montilla A, Martínez-Aranda S, Lozano A, García-Palacín I, García-Navarro P (2021). 2D experiments and numerical simulation of the oscillatory shallow flow in an open channel lateral cavity, Advances in Water Resources, 148, 103836.

# Effect of Submergence Ratio on Flow Characteristics of Rigid Vegetation Array

Emre HASPOLAT, Mete KOKEN

[1,2] Civil Engineering Department, Middle East Technical University, Turkey
haspolat@metu.edu.tr
mkoken@metu.edu.tr

ABSTRACT

The present study aims to investigate the influence of the submergence ratio on the flow characteristics inside the rigid vegetation array using Detached Eddy Simulation (DES). Three cases having different submergence ratios were tested under a constant stem Reynolds number and vegetation density. The numerical results demonstrate that the mean streamwise velocity in the stem layer increases as the submergence ratio increases. Moreover, increasing the submergence ratio amplifies the turbulent kinetic energy (TKE) downstream region of each vegetation stem. Therefore, the overall TKE values along the array increase as the submergence ratio increases. A shear layer height also grows more rapidly for a vegetation array with a higher submergence ratio. Although greater wake length is developed in an array with a larger submergence ratio, the wake width remains unaffected by the submergence ratio variation. Finally, a detailed flow visualization reveals that there is not any horseshoe vortex development at the base of any vegetation stem for the given flow condition and vegetation density.

## 1. Introduction

The canopy flow has been one of the main interests of hydraulic engineers in the last decades. The aquatic canopies can decrease the bed shear stress by applying an additional drag to flow, which affects sediment transport and deposition capacity of the river. Therefore, the vegetation can considerably affect and change the river morphology. Moreover, the vegetation significantly modifies the hydrodynamics of rivers (Ghisalberti & Nepf, 2009) by altering the velocity distribution, mean velocity and turbulence intensity. The flow characteristics can be utilized to clarify the hydrodynamics and morphological processes in the rivers. At this point, the present study was carried out to investigate the effect of the submergence ratio on the flow characteristics of rigid vegetation arrays by using the DES model in the numerical analyses. The numerical model was validated based on several comparisons where DES results are in good agreement with experimental measurements and data from well-resolved Large Eddy Simulation (LES) (Koken & Constantinescu, 2021).

## 2. Dimensional and Physical Features of the Numerical Models

In the numerical models, the vegetation stems are imitated by rigid cylinders and distributed in a staggered pattern. The vegetation arrays having different submergence ratios (i.e., a ratio of the vegetation length to the flow depth, $SR=h_v/H$) were numerically modeled with a constant stem Reynolds number ($Re_d=6157$) and vegetation density ($\lambda=0.03924$). The submergence ratio of numerical models and the grid point numbers of each computational domain are presented in Table 1.

**Table 1.** Submergence ratios and grid points of each numerical cases

| Case | Submergence ratio (SR) | Grid Points (in x, y and z directions) |
|---|---|---|
| SR25 | 0.25 | 2688x320x30 |
| SR50 | 0.50 | 2688x320x30 |
| SR75 | 0.75 | 2688x320x32 |

The diameter of the vegetation stem and the length of the channel are 0.153H and 74H, respectively. The other geometrical properties of the computational domain are demonstrated in Fig.1.

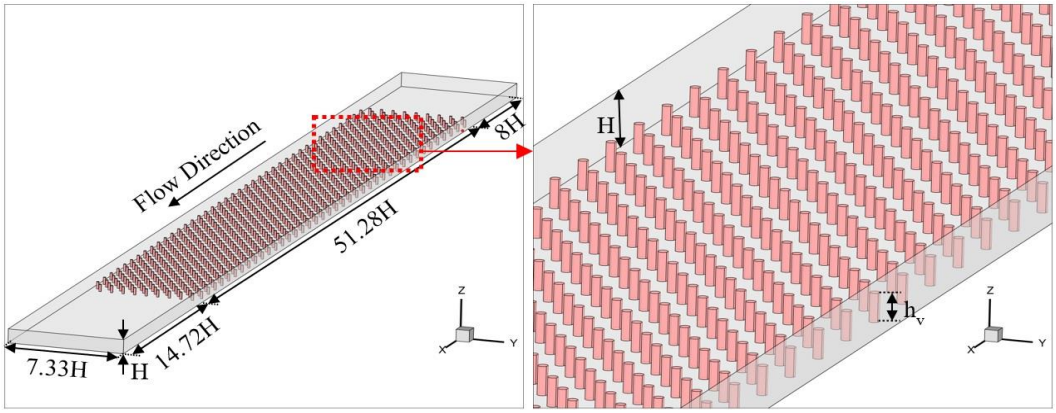



**Fig. 1.** Dimensional properties of the channel and the vegetation array

## 3. Results of the Numerical Simulations

Figures 2a and 2b demonstrate the variation of cross-sectionally averaged streamwise velocities in the stem layer ($\overline{u_s}/U$) and in the surface layer ($\overline{u_{sl}}/U$) and the variation of cross-sectionally averaged TKE in the stem layer ($\bar{k}/U^2$) along the streamwise direction, respectively.

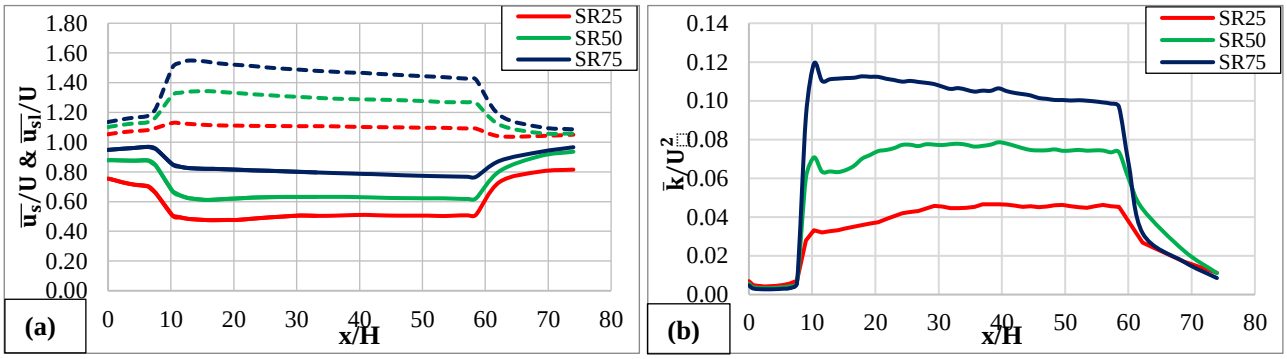



**Fig. 2. a)** Variation of cross-sectionally averaged mean streamwise velocity inside the stem layer (i.e., solid lines) and in the surface layer (i.e., dashed lines) **b)** Variation of the cross-sectionally averaged TKE in the stem layer

Figure 2a reveals that mean streamwise velocity in the stem layer increases with an increase in the submergence ratio. Since a certain amount of flow in the stem layer moves into the surface layer along the initial adjustment region, the mean streamwise velocities decrease and then reach a constant value for SR25 and SR50 cases. However, the streamwise velocity monotonically decreases up to the end of the vegetation array in SR75 case. On the other hand, Fig. 2b shows that the higher submergence ratio results in a larger TKE formation in the vegetation array. Although the averaged TKE values nearly reach a constant level for SR25 and SR50 cases, there is a continuous reduction in the TKE amount along the vegetation array for SR75 case.

Furthermore, the width-averaged TKE profiles (not given here) indicate that a growth rate of shear layer height increases with an increase in the submergence ratio. For instance, the shear layers of SR50 and SR75 cases coincide with the free surface at the distance x/H≈17.5 and x/H≈11, respectively. Moreover, the depth-averaged vertical vorticity profiles (not given here) demonstrate that while the wake lengths slightly increase with increasing submergence ratio, the wake widths are not changed by variation in the submergence ratio. Finally, a Q-criterion was used to detect whether the horseshoe vortices are developed around the vegetation stems. The horseshoe vortices locally increase the bed shear stresses and are responsible for the sediment entrainment in loose beds (Koken & Constantinescu, 2021). However, it was observed from the numerical simulations that the horseshoe vortices are not formed for the given flow condition and vegetation density. Consequently, the present study indicates the effect of the submergence ratio on the flow characteristics inside the rigid vegetation array for a given stem Reynolds number and vegetation characteristics.

**Acknowledgements**

The numerical models were performed at TUBITAK ULAKBIM, High Performance and Grid Computing Center in the present study.

**References**

Ghisalberti M, & Nepf H (2009) Shallow flows over a permeable medium: The hydrodynamics of submerged aquatic canopies, Transport in Porous Media, 78(2), 309–326

Koken M, & Constantinescu G (2021) Flow structure inside and around a rectangular array of rigid emerged cylinders located at the sidewall of an open channel, Journal of Fluid Mechanics, 910, A2

8th IAHR EUROPE CONGRESS
LISBON - PORTUGAL
4-7 JUNE 2024

# Design of a Low-head Shaft Driven Contra-Rotating Reversible Pump Turbine for Pumped Hydro Storage Application

Melvin JOSEPH[1], Mehrdad ZANGENEH[2], Ruben Ansorena RUIZ[3], Nils GOSEBERG[4]

[1,2] Advanced Design Technology Ltd., 30 Millbank, Westminster, London, SW1P 4DU, United Kingdom
m.joseph@adtechnology.com
mzangeneh@adtechnology.com

[3,4] Leichtweiß-Institute for Hydraulic Engineering and Water Resources, Division of Hydromechanics, Coastal and Ocean Engineering, Technische Universität Braunschweig, Beethovenstraße 51a, 38106 Braunschweig, Germany
r.ansorena-ruiz@tu-braunschweig.de
n.goseberg@tu-braunschweig.de

[4] Coastal Research Center, Coastal Research Center, Joint Research Facility of Leibniz Universität Hannover and Technische Universität Braunschweig, Hannover, Germany
goseberg@fzk.uni-hannover.de

ABSTRACT

Widespread adoption of renewable energy sources such as solar and wind power to reduce greenhouse gas emissions calls for supplementary green technologies for stabilizing a grid because of their intermittent nature. Pumped hydro storage (PHS) systems are a proven and reliable technology that can be used for this purpose. Traditionally hydro power systems require high head and so the potential installation sites are limited. A low head PHS system is very desirable for flat geographies where high head reservoirs are not possible. ALPHEUS project funded by the European Union's Horizon 2020 program aims at developing a low head seawater PHS system for augmenting grid stability. To meet the requirements, a shaft driven contra-rotating reversible pump turbine is designed using inverse 3D blade design approach. Computational fluid dynamic analysis is performed in both pump and turbine modes of operation to assess the performance across a range of conditions. An optimization is carried out in the model scale using a Design of Experiments approach to maximize the performance. A laboratory model test will be carried out for the optimized design to validate the performance.

## 1. Introduction

Energy storage systems are an effective balancing measure for the integration of higher proportion of intermittent renewable energy sources into the power supply. Pumped hydro storage is a natural choice as it is a mature and cheaper technology with good life span. Within the context of the ongoing transformation of our energy systems from fossil fuels to renewables, more energy storage options ideally with decreasing LCOE remain one of the most challenging technological aspects in energy and power engineering (Ruiz et al., 2022). Conventional hydroelectric technology is developed for a high head and are suited for mountainous regions. This work presents, for the first time, a coordinated effort to develop a low to ultra-low head (2-20 [m]) reversible pump turbine (RPT) technology for low lying areas with flat geographies, with a target round trip efficiency of 70-80%. Due to long operational lifetime, levelized costs of storage (LCOS) of this solution is expected to be competitive (40–140€/MWh) (Ruiz et al., 2022). Due to high specific speeds, reversible Francis turbines are not ideal for this application; Axial Kaplan and propeller-based devices are not optimized as reversible pump-turbines (Ruiz et al., 2022). Based on preliminary assessments, a Shaft-Driven variable-speed Contra-Rotating propeller RPT technology (SDCRRPT) could meet the complex set of requirements.

## 2. Methodology for Design, Analysis and Optimization

The rotors for the SDCRRPT are designed based on 3D inverse design method (Zangeneh, 1991) using Advance Design Technology's (ADT) TURBOdesign Suite software. It computes the blade shape for a given

blade pressure distribution along streamwise direction for different span locations. The design of the RPT is carried out in the pump mode, then the performance is assessed in both pump and turbine modes using CFD analysis. A 3D steady Reynolds-Averaged Navier-Stokes CFD method is used to estimate the performances in both modes of operation using ANSYS CFX software. A single blade passage computational domain with rotational periodicity and mixing plane interface between 2 rotor domains is used. Initial design is created at a design flow rate of 130[$m^3s^{-1}$] flow rate, rotor 1 speed of 50[rev $min^{-1}$], rotor 2 to rotor 1 speed ratio of 0.9; it delivered a head 8.3[m] at 11.5[MW] power with 92% efficiency. In turbine mode, target power of 10[MW] is achieved at 7.8[m] head, 143[$m^3s^{-1}$] flow rate with >91% efficiency. The prototype design is scaled down to model scale based on the lab test specifications. A multi-objective optimization is carried out in the model scale to maximize the performance of the stage at 3 operating points in each mode. The optimization process is based on a Design of Experiments (DoE) and Response Surface surrogate model approach (Bonaiuti et al, 2009) with optimization carried out using NSGA-II (Non-dominated Sorting Genetic Algorithm II) algorithm (Deb et al, 2002). A large number of parameters covering a wide range of geometry variation are chosen. Initially a sensitivity DoE study is done with 2X designs (X = number of input parameters) to identify most influential design parameters. Then a full DoE matrix consisting of ~10X designs is created for an optimization. Maximization of power in turbine mode and minimization of power in pump mode are the optimization objectives with head constrained in the required range. Dassault Systèmes Isight software is used for generating the surrogate model for sensitivity analysis and optimization; optimized designs are analyzed using CFD.

## 3. Results

The average stage efficiency across 3 operating points is improved by ~2.6% points in pump mode for the best performing candidate. As a result of the power minimization objective, power is reduced considerably for the optimized design at lower flow rates compared to the baseline, consequently the head is also reduced; At the same time optimized designs are meeting the minimum head requirement of 7 [m] at the 120% flow rate. In turbine mode, the average stage efficiency is improved by ~ 1.1% points for the best candidate. The power maximization objective has resulted in higher power for the optimized designs primarily owing to the increased flow rates. A comparison of optimized design with baseline efficiency and geometry is shown in Fig. 1; optimized design has a lower hub to tip ratio compared to the baseline.

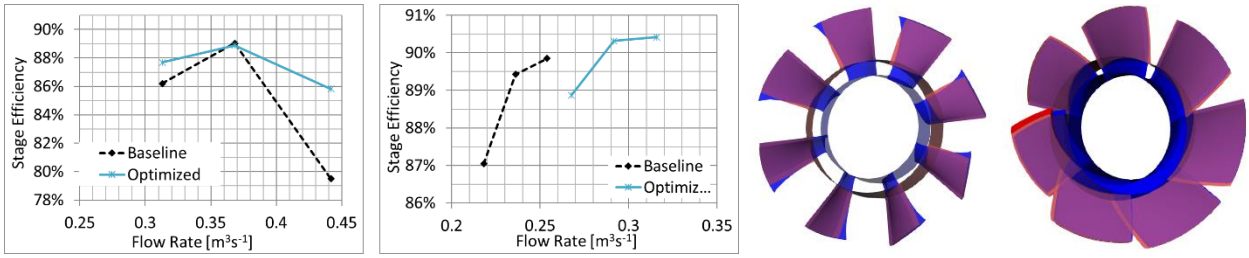



**Fig. 1.** Stage efficiency vs flow rates in pump (left plot) and turbine mode (right plot); Comparison of optimized (blue colour) and baseline rotor geometries (rotor1 – left and rotor2 – right.)

## 4. Conclusions

The initial SDCRRPT design is delivering good efficiency based on CFD analysis predictions; tests are being carried out at TU Braunschweig and results will be published in the future. A design and operation optimization of the whole system implementing operation simulation models could minimize investment costs; combining this with revenue models could maximize revenue making it a very competent technology (Prasati et al, 2024).

**Acknowledgements**

This work is part of ALPHEUS project funded by the European Union's Horizon 2020 research and innovation program under grant agreement No. 883553.

**References**

Bonaiuti D, Zangeneh M (2009) On the Coupling of Inverse Design and Optimization Techniques for the Multiobjective, Multipoint Design of Turbomachinery Blades, Journal of Turbomachinery, vol. 131, no. 2

Deb K, Pratap A, Agarwal S and Meyarivan T (2002) A fast and elitist multiobjective genetic algorithm: NSGA-II, IEEE Transactions on Evolutionary Computation, vol. 6

Ruiz R A, De Vilder L H, Prasasti E B, Aouad M, De Luca A, Geisseler B, ... & Goseberg N (2022) Low-head pumped hydro storage: A review on civil structure designs, legal and environmental aspects to make its realization feasible in seawater. Renewable and Sustainable Energy Reviews, 160, 112281

Zangeneh M (1991) A compressible three-dimensional design method for radial and mixed flow turbomachinery blades, International Journal for Numerical Methods in Fluids

E.B. Prasasti, M. Aouad, M. Joseph, M. Zangeneh, K. Terheiden, Optimization of pumped hydro energy storage design and operation for offshore low-head application and grid stabilization, Renewable and Sustainable Energy Reviews, Volume 191, 2024, 114122

# Quadrant analysis of flow structures downstream of a bridge pier protected with riprap

Gordon GILJA[1], Robert FLISZAR[2], Antonija HARASTI[3], Manousos VALYRAKIS[4]

[1,2,3] University of Zagreb, Faculty of Civil Engineering, Croatia
gordon.gilja@grad.unizg.hr
[4] Department of Civil Engineering, Aristotle University of Thessaloniki, Thessaloniki, Greece

ABSTRACT

Traditional river training structures are built using riprap that can be undermined and must be undergo through costly maintenance to preserve its function. Especially for bridge piers protected with riprap, its failure can contribute to bridge collapse. The objective of the current project is to investigate the temporal development of scour around bridge pier protected with a riprap sloping structure. In this preliminary investigation, the results from a flume experiment of the scour around the riprap protection of a model bridge pier are presented. Results for the first six hours of the scour development are shown to assess the flow contributing to the scour hole development. To that goal, bed morphology and flow conditions were collected in 1-hour intervals, and distribution of quadrant events along the flume centerline was investigated.

## 1. Introduction

Reliable scour estimation is required for optimal bridge design and efficient maintenance during its lifetime. Once the pier has been protected with riprap, scour risk is significantly reduced, while as a result the flow pattern in the vicinity of bridge is altered and can potentially induce scour in the riverbed away from the pier, affecting adjacent structures. Studies conducted next to submerged structures that have similar effect on the flow field, such as groynes which are overtopping structures that significantly obstruct the flow. Common findings are that high bed shear stress values are observed around the groyne tip (Koken and Gogus, 2015), increasing the size of the groyne the flow structure upstream changes from the vertical to the dominantly horizontal circulation (Safarzadeh et al., 2016). In the zone downstream of the pier sweeps are the most dominant bursting events (Ikani et al., 2023), showing significant differences before and after scour hole development (Lee and Hong, 2019). This research is focused on the pier protected with riprap formed into a sloping structure, which significantly affects the flow field. The objective of this research is to determine baseline conditions for subsequent experiments: scour extent, scour pattern, and flow field. Based on these results, velocimetry measurement matrix for subsequent research will be established.

## 2. Experimental setup

Experiments were conducted in the hydraulic flume set up for scour simulations. The recirculating hydraulic flume is 18 m long, 0.9 m wide, and 0.9 m deep with rectangular cross-section, and glass sidewalls (Fig 1a). Experiments were run with single flow rate in total duration of six hours to obtain the scour development in the rapid development phase, until a clearly defined scour hole is formed. Bed morphology and flow conditions were collected in 1-hour intervals. Bed morphology was measured using the optical 3D scanner, and flow field data were collected using the acoustic Doppler velocimetry profiler Vectrino ADVP (Gilja et al., 2023). Flow velocity was measured across the entire flow depth at 5 locations along the pier axis: one point upstream at the distance of 9 cm, and 4 points downstream at 9 cm, 12 cm, 18 cm and 24 cm. The analysis of turbulent events in the bed vicinity was done using the quadrant analysis that was applied in similar experiments where different turbulent events were found to be associated with different location within the scour hole: ejections have been found over the area of the scour hole with negative bed slope and sweeps over the area with positive bed slope (Termini and Sammartano, 2012).

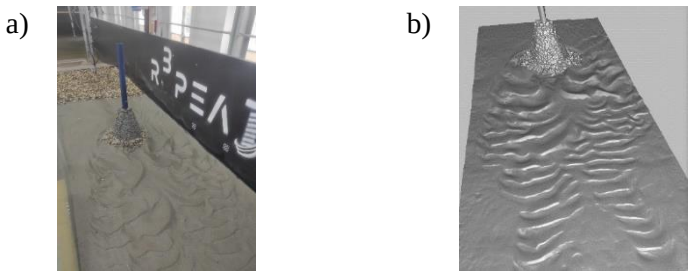



**Fig. 1.** Photo of the experimental setup in the flume (a); corresponding bed surface scan (b).

## 3. Results and discussion

Flow structures downstream of the pier generate scour at the sides of the riprap (Fig 1), while further downstream, the bed is fully developed into bedforms, which evolve over time in term modifying flow structures intensity. Change in flow structures was analyzed through quadrant analysis – distribution of events in each quadrant with emphasis on shear stress producing events - ejections (Q2 events) and sweeps (Q4 events). Pier axis was selected to evaluate the influence of the sloping structure as a design feature that controls the flow structures. The results show that for the initial timestep and flat bed (t0) events are evenly distributed across all 4 quadrants for the 3 points closest to the pier, while at the point furthest downstream (24 cm) most common events are ejections. At the point closest to the pier (9 cm), after initial scour development phase, ejections are the most common events, contributing ~50%, followed by and sweeps (~30%), while Q1 and Q3 events are significantly less present (<10%). Moving further downstream, decreasing trend is observed for ejections, and increasing for all other events. At the point 18 cm all events are evenly distributed over the entire flow duration, while at the downstream point 24 cm, sweeps are the most common events. When the temporal development of scour is observed, the initial constant scour development is present until t4, after which bedforms start developing, in turn influencing flow structure.

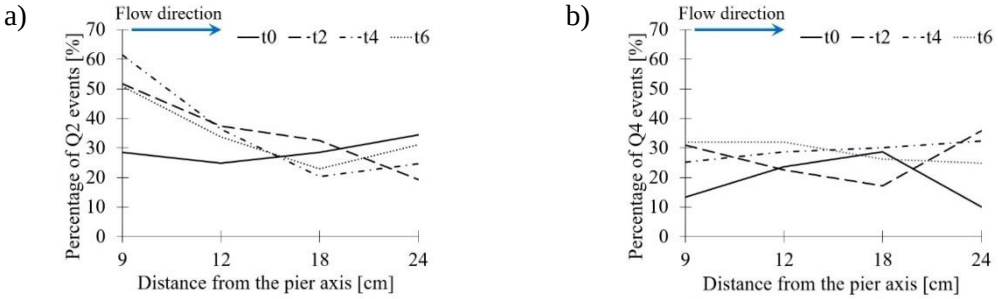



**Fig. 2.** Distribution of ejections (a) and sweeps (b) along the measurement points for even timesteps (t0, t2, t4, and t6).

## 4. Conclusion

This study shows preliminary results of flow structures downstream of the bridge pier protected with riprap. The results show that change in distribution of turbulent events over time corresponds to the scour hole development and consequent evolution of bed features downstream, indicating that quadrant analysis can be used in subsequent research. The measured scour hole extent and identified quadrant events will be used as a base to adjust experimental matrix of flow measurements.

**Acknowledgements**

This work has been supported in part by Croatian Science Foundation under the project R3PEAT (UIP-2019-04-4046).

**References**

Gilja G, Fliszar R, Harasti A, Valyrakis M (2022) Calibration and Verification of Operation Parameters for an Array of Vectrino Profilers Configured for Turbulent Flow Field Measurement around Bridge Piers—Part I, Fluids, 8(7), 199

Ikani N, Pu, JH, Taha T, Hanmaiahgarib PR, Penna N (2023) Bursting phenomenon created by bridge piers group in open channel flow. Environmental Fluid Mechanics, 23, 125–140

Koken, M, Gogus M (2015) Effect of spur dike length on the horseshoe vortex system and the bed shear stress distribution, Journal of Hydraulic Research, 53(2), 196-206

Lee SO, Hong SH (2019) Turbulence Characteristics before and after Scour Upstream of a Scaled-Down Bridge Pier Model, Water 11(9), 1900

Safarzadeh A, Salehi Neyshabouri SAA, Zarrati AR (2016) Experimental Investigation on 3D Turbulent Flow around Straight and T-Shaped Groynes in a Flat Bed Channel, Journal of Hydraulic Engineering, 142(8), 04016021

Termini D, Sammartano V (2012) Morphodynamic processes downstream of man-made structural interventions: Experimental investigation of the role of turbulent flow structures in the prediction of scour downstream of a rigid bed, Physics and Chemistry of the Earth-Parts A/B/C, 49, 18-31

# Sensitivity Analysis of the SWAT Distributed Hydrological Model to the Curve Number (CN2) Parameter

Kaline GOMES1, Jonathan Mota SILVA2, Sandra Isay SAAD[3].

[1]Federal University of Rio Grande do Norte, Brazil
kmuriel2001@gmail.com

[two]Federal University of Rio Grande do Norte, Brazil
jonathan.mota@ufrn.br

[3]Federal University of Campina Grande, Brazil
sandraisaad@gmail.com

ABSTRACT

This work presents a sensitivity analysis of the Soil and Water Assessment Tool (SWAT) hydrological model to the Curve Number (CN2) parameter on the surface runoff in the Maxaranguape River Basin, located in the Northeast of Brazil (NEB). The CN2 is based on soil hydrological class, landuse and land cover (LULC) and Antecedent Moisture Condition (AMC). This parameter was varied by -30%, -10%, +10% and +30 of your initial prescription. These variations in CN2 caused considerable changes in surface runoff ranging from -79% to 107%, which shows the attention that must be given when prescribing this parameter in SWAT.

## 1. Introduction

Pressure on water supply at local and national levels in several countries has been caused mainly by population growth and changes in land use and land cover. Changes in land use affect the hydrological processes, altering albedo, and the evapotranspiration and water interception by vegetation, which results in changes in surface runoff and underground water flows.

A simple and widespread method for determining the approximate volume of surface runoff of a rain event is the Curve Number method. The method was developed by SCS (Soil Conservation Service – 1957), is widely used in several countries, and uses as input only rainfall and CN, based on the hydrological soil class, LULC and Antecedent Moisture Condition (AMC). The AMC is divided into three groups, according to the amount of rain that occurred in the five days prior to the day of analysis. AMC 1 is the dry soil condition (represented by CN1); AMC 2 is the average moisture condition (represented by CN2) and AMC 3 is the saturated soil condition (represented by CN3). The Model used in this paper is the Soil and Water Assessment Tool Model, which uses CN2 in the hydrological component. The SWAT has been used in studies around the world, with the aim of understanding hydrological processes (Abbaspour, et. al., 2015) and how changes in the LULC impact water resources (Li et. al., 2024), these changes are capable of altering the CN and runoff values in a basin.

The study area was chosen because it is considered a water reserve for the public water supply in the capital of Rio Grande do Norte (RN), and because there are intense processes of change in LULC. It is necessary to analyze how the variation in CN2 is impacts on the flow of the basin. Therefore, the objective of the paper is to test the sensitivity of the hydrological model SWAT, to the CN2 parameter on the flow in the Maxaranguape River Basin, like area of study.

## 2. Methodology

The study area is the Maxaranguape River Hydrographic Basin, located in the NEB and the location is illustrated in Figure 1. The Baisin has a climate that varies between rainy tropical and dry summer, with average annual precipitation of around 1,300 mm at the mouth. Semiarid with an annual average of 900 mm at the head of the basin in the extreme west and has a drainage area of 990km².

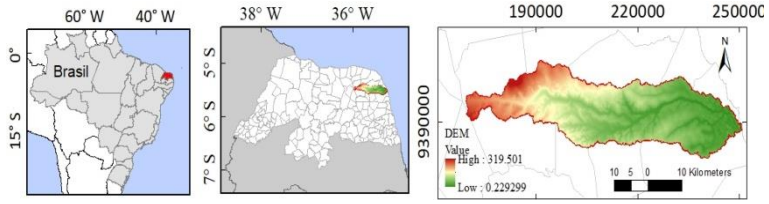



**Fig. 1.** Location of **the** Hydrographic Basin

SWAT is a mathematical model that uses physical and conceptual equations to simulate the hydrological cycle. The Model was running with daily, monthly or annual outputs, being capable of simulating long periods, to estimate the effects of variations in the physical characteristics of the basin, predicting the hydrology in each Hydrological Response Unit (HRU). The area was discretized containing 15 sub-basins and 104 HRU (Fig.2), generated with the Digital Elevation Model (DEM), from the NASA Shuttle Radar Topography Mission Global (SRTM) with a spatial resolution of 30m, LULC, from MapBiomas and Solos, from Radam. Brazil, which were grouped into four classes of hydrological soils, considering the potential for generating surface runoff: Low (Latosol), Medium (Argisol), High (Neosols, Vertisols, Cambisols and Gleisols) and floodplain soils (alluvial and hydromorphic soils). The climatic data used to force the model are as described: Rain, Temperature, Solar Radiation, Relative Humidity and Wind. To make up for the lack of climate data, it was used the database by Xavier *et. al.* (2022), with a georeferenced grid of 0.1ºx0.1º and daily values. In the sensitivity analysis, SWAT was integrated into the period from 01 Jan 1997 to 31 Dec 2019 (3 Initial years for the warm up) and was running 5 times. The first simulation was called initial and the remaining 04 simulations, according to the change in the CN2 parameter, for all Land Use and Land Cover, for the following variation: -30%, -10%, +10% and + 30 in relation to the CN2 of the initial simulation.

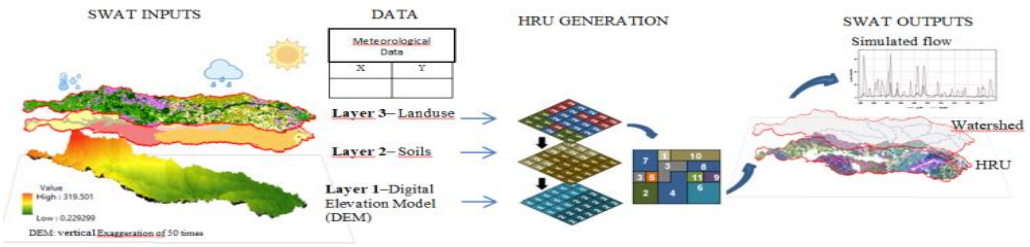



**Fig. 2.** Illustration of how SWAT works integrated with ArcGis

## 3. Results and conclusions

The average annual surface runoff (SURQ) in the initial simulation (without changing CN2) was 334 m³/s. For simulations with an increase in CN2 by 10% (502 m³/s) and 30% (690 m³/s), there was an increase in relation to the initial SURQ of 50% and 107%, respectively. For the simulations in which CN2 decreased -10% (214 m³/s) and -30% (69 m³/s), the average annual surface runoff corresponded to a decrease of 36% and 79%, respectively. We noticed that CN2 has a significant control on the surface runoff pattern and that modifications to this parameter generated percentage changes much higher than the percentages prescribed in the tests. As expected, an increase in CN2 increases surface runoff, just as a reduction in it reduces surface runoff. The effects of this change alter the water balance, mainly modifying evapotranspiration, which is greater the lower the surface runoff. Given the sensitivity of CN2 in SWAT with respect to surface runoff, we conclude that this parameter must be prescribed with considerable attention.

**References**

ABBASPOUR, K.C.; S., ROUHOLAHNEJAD; VAGHEFI, S; SRINIVASAN, R.; YANG, H.; KLØVE, B. A continental-scale hydrology and water quality model for Europe: Calibration and uncertainty of a high-resolution large-scale SWAT model. Journal of Hydrology. 2015. DOI:https://doi.org/10.1016/j.jhydrol.2015.03.027

LI, Wuhua; CHENG, Xiangju; Zhu, Dantong. Towards the hydrological effects of land use change in karst area, a case study in Lijiang River Basin, China.Journal of Hydrology. 2024. DOI:https://doi.org/10.1016/j.jhydrol.2024.130629

XAVIER, Alexandre C.; KING, Carey W.; SCANLON, Bridget R. New improved Brazilian daily weather gridded data (1961–2020). International Journal of Climatology, 2022. DOI: 10.1002/joc.7731.

# Insights from Energy Dissipation Basin downstream of free-falling jets through Numerical Simulations

Alicia ROS-BERNAL[1], José M. CARRILLO[2], Juan T. GARCÍA[3], Luis G. CASTILLO[4]

[1,2,3,4] Civil Engineering and Mining Engineering School, Universidad Politécnica de Cartagena, Cartagena, Spain.
alicia.ros@upct.es
jose.carrillo@upct.es
juan.gbermejo@upct.es
luis.castillo@upct.es

ABSTRACT

## 1. Introduction

The current understanding of energy dissipation basins located at the base of rectangular free-falling jets is significantly limited. The hydraulic jumps generated in these structures play a crucial role in energy dissipation, driven by the creation of large-scale turbulence structures. These structures are associated with notable hydrodynamic pressure fluctuations acting on the bottom and sidewalls of the energy dissipation basin.

The behavior of vortices is influenced by the presence of trapped air pockets. Recognizing the effect of trapped air is essential due to the disparities in apparent density between aerated jets and clear water jets. Aerated jets, owing to their lower density, possess reduced momentum, contributing to the generation of lower pressures at the bottom of the energy dissipation basin. However, the existence of air bubbles diminishes shear stresses in the basin, enabling aerated jets to flow at higher velocities (Duarte et al., 2015). Consequently, both effects must be considered during the design phase of hydraulic structures aimed at dissipating the energy stored in the reservoir, thereby ensuring the safety of the structure during its operational lifespan.

## 2. Materials and Methods

Experimental data was measured at an experimental device situated in the Hydraulic Laboratory of the Universidad Politécnica de Cartagena (Spain). The infrastructure includes an inlet channel measuring 4.00 m in length and 1.00 m in width, ending in a sharp-crested rectangular weir with a crest length of 0.85 m and a height of 0.325 m. The elevation of the spillway crest is located at a vertical distance of 2.20 m from the bottom of the energy dissipation basin. The basin itself features dimensions of 1.05 m in width, 3.00 m in length, and 1.60 m in height (Fig. 1). Additional information of the experiments can be found in Carrillo et al. (2020).

For numerical simulations, the computational package FLOW-3D® was selected. The core of the numerical approach in FLOW-3D® is based on the finite difference and finite volume methods. A structured mesh of rectangular cells is used to define the computational domain, with a mesh size of 0.01 m. The inlet boundary condition was determined by considering the width of the incident jet at a point located 0.20 m above the water cushion with a discharge flow of 0.072 $m^3/s$. The width of the rectangular jet was computed using the formulation proposed by Castillo et al. (2015), and experimentally validated by Carrillo et al (2021). A hydrostatic pressure type condition was specified in the outlet, considering the fluid elevation at 0.34 m. The turbulence model that exhibited the best performance was the k-epsilon ($k$-$\varepsilon$) model, and different values of turbulent mixing length were applied to analyse its influence. Additionally, the air entrainment model was selected, considering the entrainment rate coefficient equals to 0.5 and the surface tension coefficient was set at 0.073 $kg/s^2$. The bulking and buoyancy options were also activated in order to consider a variable density model and the interaction between the liquid and the gaseous phases, respectively. In this sense, it was necessary to activate the drift model to describe the relative flow of two intermixed fluid components, one continuous and the other dispersed, with different densities. Finally, we have considered the second-order

density evolution model. All simulations have been carried out using the "Volume of Fluid" (VOF) method proposed by Hirt and Nichols (1981) for modelling the free surface.



**Fig. 1.** Experimental device for the study of free-falling jets.

## 3. Results

Figure 2 illustrates the simulated results in a longitudinal section of the submerged hydraulic jump, showcasing the stagnation point and recirculation zones. Figure 3 displays the variation of velocity and void fraction with the length scale parameter, *Tlen*, of the turbulence model $\kappa$-$\varepsilon$ in FLOW-3D®. Despite the substantial aeration, the program yields a reasonable representation of the phenomenon. Additionally, it is observed that the velocity profiles exhibit a lower sensitivity to variations in the *Tlen* parameter compared to the void fraction profiles.

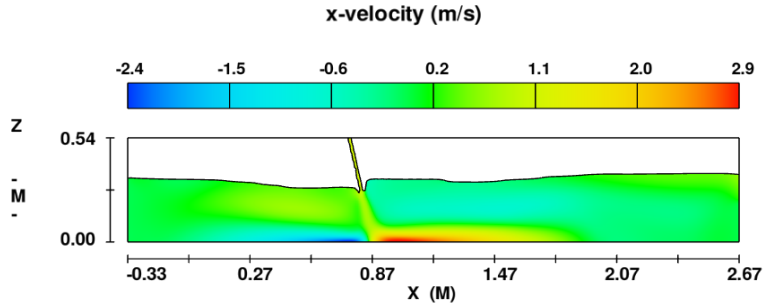



**Fig. 2.** Instantaneous variation of horizontal velocity in submerged hydraulic jump generated with a discharge $q$ = 0.085 m$^3$/s/m, water cushion $Y$ = 0.34 m and *Tlen* = 0.020 m. Stagnation point located at X = 0.86 m.

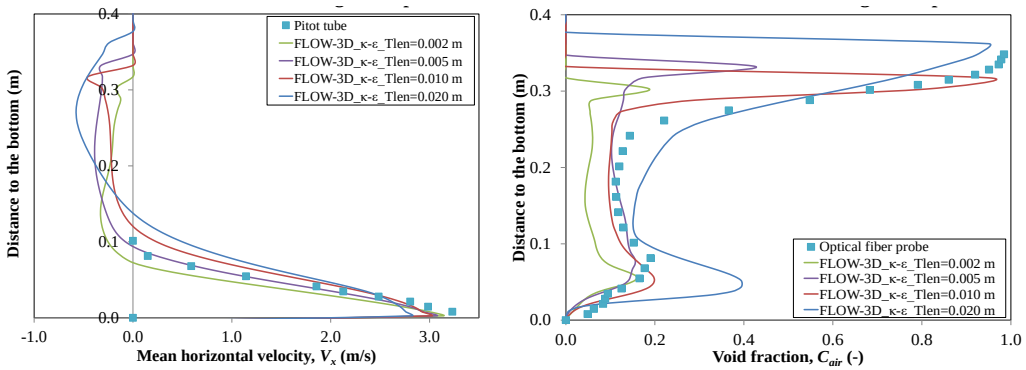



**Fig. 3.** Variation of horizontal velocity and void fraction with the *Tlen* parameter in a cross-sectional section located at $X$ = 0.96 m (0.10 m from the stagnation point) ($q$ = 0.085 m$^3$/s/m, $Y$ = 0.34 m).


### Acknowledgements

The first author expresses her gratitude for the financial aid received from "Fundación Séneca, Agencia de Ciencia y Tecnología de la Región de Murcia" for the training of research staff, grant number 21592/FPI/21. The authors also thank the support given through the Project with Grant PID2022-142037OB-I00 funded by MCIN/AEI/ 10.13039/501100011033 and by "ERDF A way of making Europe".


### References


Carrillo JM, Ortega PR, Castillo LG, García JT (2021) Air-water properties in rectangular free-falling jets, Water, 13(11), 1593.
Carrillo JM, Castillo LG, Marco F, García JT (2020) Experimental and numerical analysis of two-phase flows in plunge pools, Journal of Hydraulic Engineering, ASCE, 146 (6).
Castillo LG, Carrillo JM, Blázquez A (2015) Plunge pool mean dynamic pressures: a temporal analysis in nappe flow case, Journal of Hydraulic Research, 53(1), 101–118.
Duarte RJM, Schleiss AJ, Pinheiro A (2015) Optical fibre probe measurements of bubble flow in hydraulic jumps, Environmental Fluid Mechanics, 15, 673-693.

# Numerical Simulations of Head Losses at Fish-Friendly Fine Screens

Cumhur OZBEY[1], Serhat KUCUKALI[2]

[1,2] Hacettepe University, Civil Engineering Department, Hydraulics Division, Turkey
kucukali78@gmail.com

ABSTRACT

High head losses at fine screens built for fish protection at hydropower plants lead to energy and revenue loss. We addressed this operational problem by investigating the hydrodynamics characteristics of a streamlined Oppermann bar profile. Accordingly, two types of physical barriers used at the water intakes of hydropower plants, the Oppermann and the rectangular fine screen, each having the same bar spacing of 10 mm, were numerically compared by the head losses. The flow through both screens was simulated in FLOW-3D under identical initial and boundary conditions, and the up-and downstream water surface profiles were analyzed to evaluate the head losses. Simulations were performed under three different turbulence models, namely the standard k-ε, k-ω, and the Large Eddy Simulation (LES). The numerical results revealed that the head loss generated by the Oppermann fine screen was 21.5% less than the rectangular fine screen. This head loss difference was attributed to the fact that the recirculation zone area is reduced by almost 90% behind the Oppermann profile due to the streamlined bar shape. Among the tested turbulence models, different from the existing studies, it was numerically shown that the triangular shape of the recirculation zone was only captured by the LES model for very fine mesh indicating the importance of mesh resolution.

## 1. Introduction

The fish-friendly Oppermann fine screen is a physical barrier having hydrodynamically designed vertical bars to reduce the head losses by enhancing the hydraulic conditions around the screen and they are implemented in various hydropower plants (Kucukali et al., 2018). The leading advantages of these screens comprise optimal fish protection due to narrow bar spacing and rounded leading edge coupled with smooth bar surface, hydraulically optimized shape, increased hydropower output, low weight, and highly efficient cleaning and manufacturing processes. The so-called Oppermann fine screen is numerically compared to a rectangular fine screen, with the same bar spacing of 10 mm, and the simulations were performed in FLOW-3D. The water surface profiles at the up-and downstream of both screens are analyzed to determine the head losses. Accordingly, the head loss generated by a screen can be expressed by applying energy conservation within a horizontal system where the frictional losses are neglected, as given in Eq. (1):

$$\Delta H = d_1 + \frac{V_1^2}{2g} - d_2 - \frac{V_2^2}{2g} \quad (1)$$

where $\Delta H$ – screen head loss [m], $d_1$ – upstream flow depth [m], $d_2$ – downstream flow depth [m], $V_1$ – approach flow velocity [m s$^{-1}$], $V_2$ – downstream flow velocity [m s$^{-1}$], and $g$ – gravitational acceleration [m s$^{-2}$]. Accordingly, the head loss coefficient is calculated from Eq. (2):

$$\zeta = \Delta H / (V_1^2 / 2g) \quad (2)$$

where $\zeta$ – screen head loss coefficient [-]. The measured head loss coefficients for the bar spacing of 10 mm were obtained as 0.54 and 1.27 for the Oppermann and the rectangular profiles, respectively (Hassinger, 2009).

## 2. Results and Discussion

Numerical results have revealed that the head loss generated by the streamlined bar profile of the Oppermann fine screen is on average 21.5% less than the rectangular profile. In Fig. 1, the water surface profiles (WSP) that were numerically obtained for the rectangular and Oppermann fine screens both having a bar spacing of 10 mm are compared. It can be observed that given the same upstream flow depth, the rectangular fine screen

causes a larger dip at the downstream region compared to the Oppermann fine screen. The numerical head loss coefficients for the Oppermann and rectangular fine screens were found as 0.49 and 1.21, respectively, which are consistent with the experimental findings of Hassinger (2009).

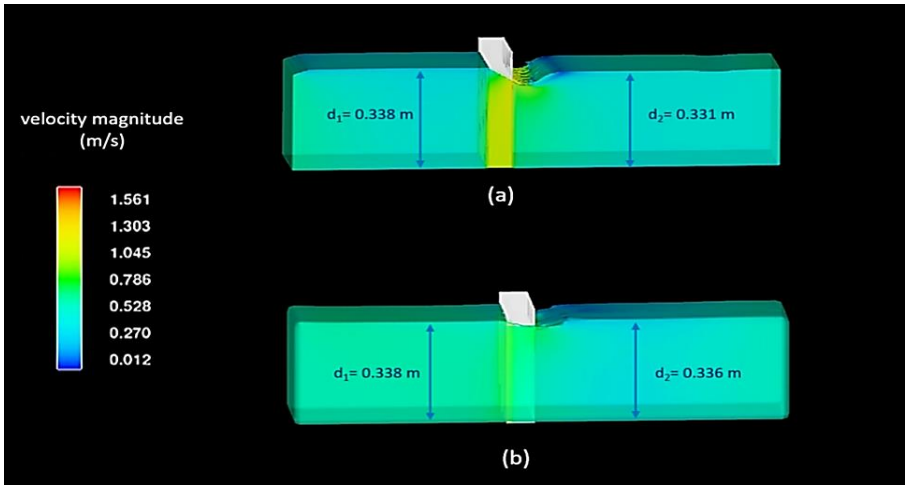



**Fig. 1.** Water surface profiles for: (a) rectangular and (b) Oppermann fine screen. Simulations were performed under the same initial and boundary conditions. For both screens, the bar spacing is 10 mm, and the approach flow velocity, $V_1$ = 0.3 m/s. The head loss coefficients for the Oppermann and the rectangular fine screens are found as 0.49 and 1.21, respectively. Turbulence model = LES.

To explain the above-mentioned difference in the head losses and the WSPs, in Fig. 2, the recirculation zones formed at the immediate wake region of the rectangular and the Oppermann bar profiles are illustrated as a numerical model comparison considering three different turbulence models. The results revealed that the area of the recirculation zone was reduced by almost 90% in the Oppermann profile due to the rounded leading edge creating a streamlined bar shape. The reduction in the recirculation zone area explains the fact that the Oppermann profile generates noticeably lower head loss values than the rectangular profile with sharp edges. Moreover, the LES turbulence model was shown to capture the triangular shape of the recirculation zone (Fig. 2c) whereas such a triangular wake formation was not revealed in the standard k-ε, and k-ω models (Fig. 2).

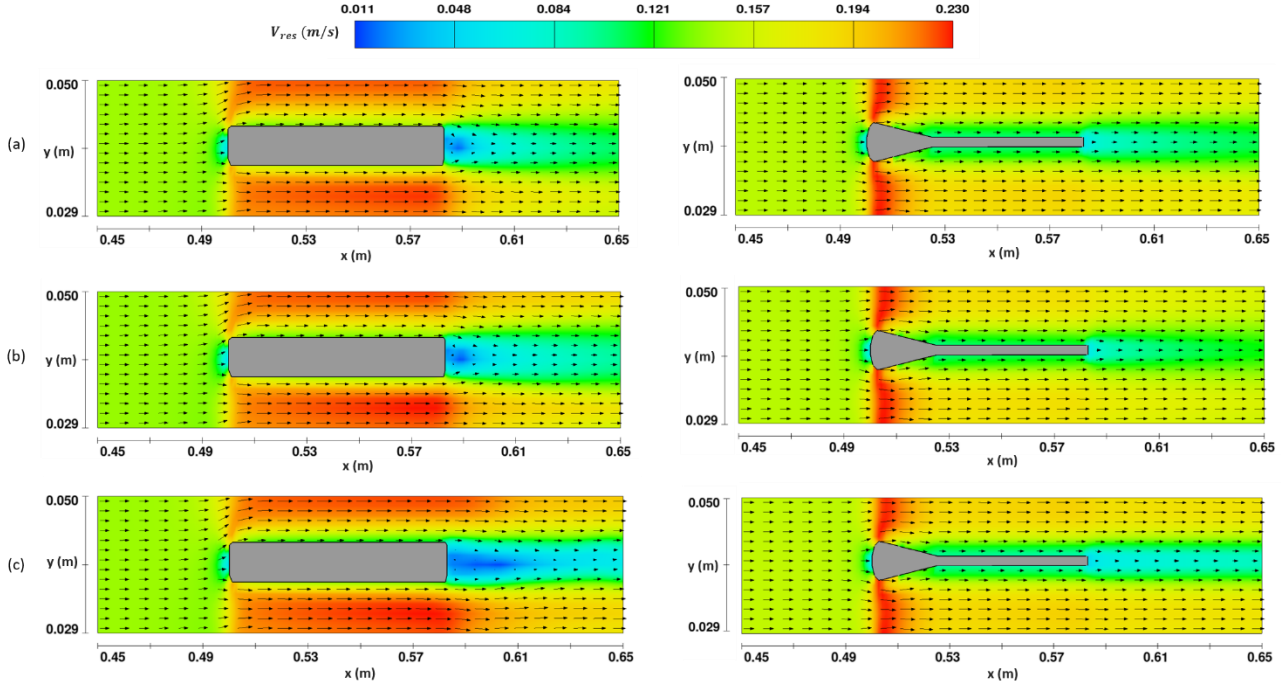



**Fig. 2.** Recirculation zones downstream of the rectangular profile (left) and the Oppermann profile (right) on the horizontal x-y plane: (a) the standard k-ε, (b) k-ω, and (c) the LES model. Simulations were performed under the same initial and boundary conditions. The thickness of the leading edge and the total bar length of both profiles are 0.006 m and 0.083 m, respectively. Approach flow velocity, $V_1$ = 0.15 m/s, and upstream flow depth, $d_1$ = 0.20 m, mesh resolution = 0.0015 m.

**References**

Hassinger, R (2009) Neuartiger Fisch schonender Rechen für Wasserkraftanlagen, Universität Kassel.
Kucukali S, Hassinger R, Turan A (2018) A Two-dimensional Numerical and Experimental Study on Fish-Friendly Hydrodynamic Fine Screens, Proceedings of 5th IAHR Europe Congress, Trento, Italy.

# Machine learning-based hydropower turbine designs

Ante SIKIRICA[1], Marta ALVIR[2], Zoran ČARIJA[3], Lado KRANJČEVIĆ[4]

[1] Center for Advanced Computing and Modelling, University of Rijeka, Croatia
ante.sikirica@uniri.hr

[2,3,4] Faculty of Engineering, University of Rijeka, Croatia
malvir@riteh.hr, zoran.carija@riteh.hr, lado.kranjcevic@riteh.hr

ABSTRACT

The optimal design of hydropower turbines is of great importance as it affects performance, energy production and environmental sustainability. The traditional approach to design often involves complex simulations, which can be time-consuming and resource-intensive. This is suitable for new construction sites, but for existing turbines that are to be revitalised, this investment is often difficult to justify. In addition, revitalisation efforts are usually focused on a specific part of the turbine. In this context, machine learning techniques offer a promising way to simplify the design process. Our research focuses on the application of machine learning in conjunction with optimisation techniques to improve the design of the draft tube and other parts of turbines that need to be revitalised. We propose an optimisation workflow that leverages deep neural network surrogates, which can be complemented by in situ measurements.

## 1. Introduction

The growing interest in renewable energy, particularly hydropower, and efforts to revitalise current turbines require efficient design optimisation workflows. We hereinafter propose a workflow that uses deep neural networks (DNN) as surrogates. Surrogate-based optimisation of turbine draft tubes is a cost-effective solution. The underlying methodology can be extended to different segments and contexts as well as to multiple operating points.

The majority of papers dealing with draft tube design optimisation have coupled computational fluid dynamics (CFD) simulations with optimisation frameworks (Abbas and Kumar, 2017, Tiwari et al., 2020). Recently, the design of experiments technique, the response surface method and single-objective and multi-objective optimisation algorithms have been used in unified optimisation workflows (Demirel et al., 2017, Orso et al., 2020). Several studies (Marjavaara et al., 2007, McNabb et al., 2014) considered radial basis neural networks as an alternative to simplify the process. The proposed surrogates were subsequently coupled with various optimisation algorithms to generate optimal designs. Neural network surrogates were shown to have excellent accuracy (Shojaeefard et al., 2014).

## 2. Workflow

The proposed systematic workflow is based on data obtained using CFD. The code, however, is designed so that in-situ measurements and other data can be easily included as well. Latin hypercube sampling is used to generate a diverse set of initial design candidates that mimic real data. The design space is large, allowing for a comprehensive assessment. CFD simulations are performed using the open-source toolbox OpenFOAM in a standardised and automated manner. The flow at the inlet of the draft tube is assumed to be constant and corresponds to the average flow for this section at the investigated Rijeka hydroelectric power plant (Fig. 1.). However, the implementation allows the use of precomputed velocity profiles. The pressure recovery factor (Cp) and the drag coefficient (Cd) are considered and monitored in the assessment process.

The collected numerical data were used to train DNN surrogate models. Rudimentary DNNs were implemented using TensorFlow v2.10.0. Network parameters were fine-tuned using the hyperparameter optimisation framework Optuna v3.1.0. The datasets considered were preprocessed using the unsupervised local outlier

factor algorithm. The optimal DNNs were the networks with the highest mean coefficient of determination ($R^2$).

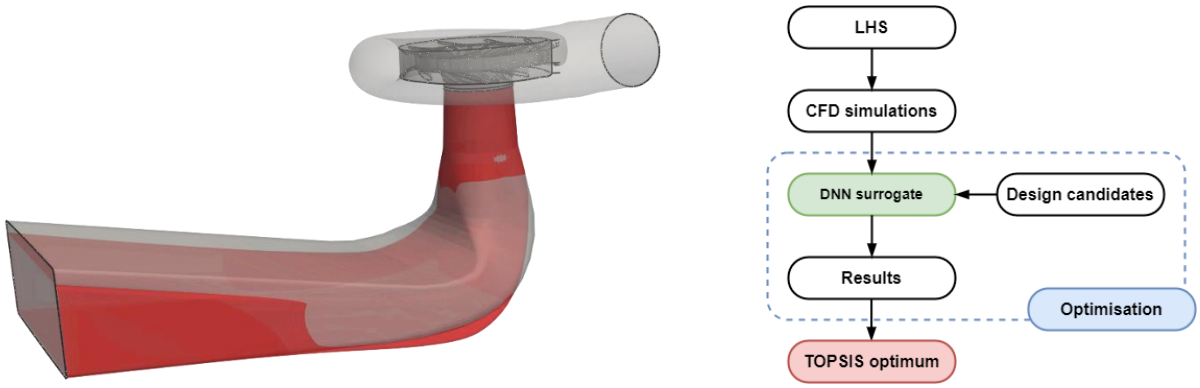



**Fig. 1.** The original design of the turbine is shown in grey (right). The optimal design of the draft tube achieved with the proposed workflow is shown in red. The proposed DNN-based workflow (left).

Tuned DNNs were subsequently coupled with the multi-objective optimisation algorithm MOEA/D in order to generate the optimal draft tube design. The optimum was determined using the multi-criteria decision analysis method TOPSIS on the Pareto-optimal solutions. Different design scenarios representing construction constraints were assessed. Improvements of up to 1.5% and 17% for the pressure recovery factor and drag coefficient were observed, respectively. Additionally, the disparity between the predictions generated by the DNN and the validated numerical results for the obtained optimal solutions is less than 0.5% for the pressure recovery factor and 3% for the drag coefficient. A comparison between the original design of the draft tube design and the proposed optima for different evaluation scenarios is given in Fig. 2.

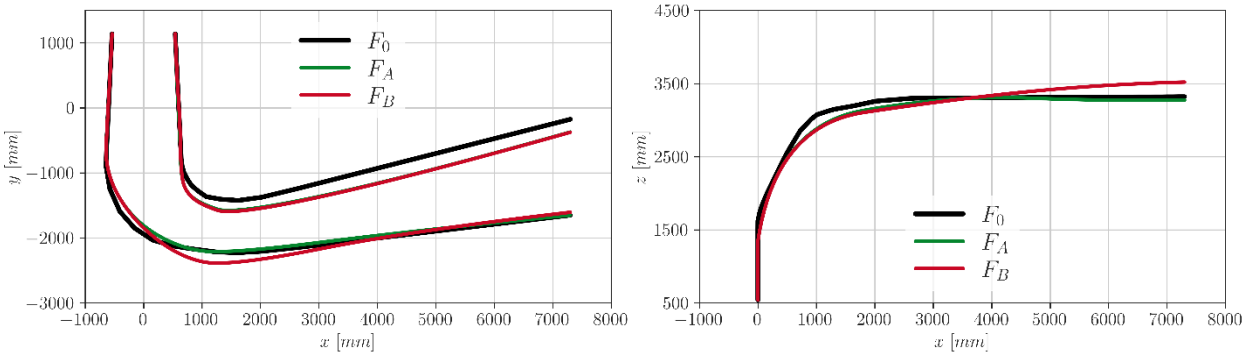



**Fig. 2.** Sectional comparison between the reference draft tube design $F_0$ and the proposed optima for different test scenarios. In scenario $F_A$, the new draft tube is limited to the extents of the original design. In scenario $F_B$, a flexible design is encouraged (all sections can change).

## 3. Conclusion.

The application of machine learning techniques presents a compelling opportunity to revolutionise the hydropower industry by significantly reducing design times and improving efficiency. This is particularly important in revitalisation scenarios. However, there are important questions that still need to be addressed in order to ensure that the methodology is truly viable. The machine learning models need to be robust, accurate and applicable to a wide range of designs and operating conditions. Validation and testing under different scenarios are therefore essential to build confidence in the predictive capabilities of these models.

**References**

Abbas A, Kumar A (2017) Development of draft tube in hydro-turbine: review, International Journal of Ambient Energy, 38, 323-330
Demirel G, Acar E, Celebioglu K, Aradag S (2017) CFD-driven surrogate-based multi-objective shape optimization of an elbow type draft tube, International Journal of Hydrogen Energy, 42, 17601-17610
Marjavaara BD, Lundström TS, Goel T, Mack Y, Shyy W (2007) Hydraulic turbine diffuser shape optimization by multiple surrogate model approximations of Pareto fronts, Journal of Fluids Engineering, 129, 1228-1240
McNabb J, Devals C, Kyriacou SA, Murry N, Mullins BF (2014) CFD based draft tube hydraulic design optimization, IOP Conference Series: Earth and Environmental Science, 22, 12-23
Orso R, Benini E, Minozzo M, Bergamin R, Magrini A (2020) Two-objective optimization of a Kaplan turbine draft tube using a Response Surface Methodology, Energies, 13, 1-13
Shojaeefard MH, Mirzaei A, Babaei A (2014) Shape optimization of draft tubes for Agnew microhydro turbines, Energy conversion and management, 79, 681-689
Tiwari G, Kumar J, Prasad V, Patel VK (2020) Utility of CFD in the design and performance analysis of hydraulic turbines - A review, Energy Reports, 6, 2410-2429

8th IAHR EUROPE CONGRESS
LISBON - PORTUGAL
4-7 JUNE 2024

# Generalizing hydraulic-based graph neural networks to irregular meshes and time-varying boundary conditions

Roberto BENTIVOGLIO[1,*], Elvin ISUFI[1], Sebastiaan Nicolas JONKMAN[1], Riccardo TAORMINA[1]

[1] Delft University of Technology, Netherlands
r.bentivoglio@tudelft.nl

ABSTRACT

Numerical methods for flood modelling are accurate but computationally expensive. Surrogate models based on deep learning emerged as alternative solutions to speed up flood mapping while keeping accurate results. In particular, hydraulic-based graph neural networks seem a promising way ahead as they showed transferability to domains where they were not trained on. However, they have been so far corroborated only for regular meshes and they also require initial conditions from the numerical solver. In this paper, we aim to overcome these two issues and propose an extension of hydraulic-based graph neural networks to time-varying boundary conditions. This is achieved by using ghost cells, which enforce the solution at the domain's boundary. We validate the proposed method on a dataset of irregular meshes, over varying topographies and input hydrograph discharges. The results show that the model can replicate the overall dynamics of the flood evolution over unseen meshes, topographies, and boundary conditions, without any input from the numerical model, opening up possibilities for simulating also realistic case studies.

## 1. Introduction

Precise flood models are invaluable for evaluating risks, issuing early warnings, and improving preparedness against flood events. Two-dimensional (2D) hydrodynamic models determine the evolution of floods over space and time by solving the Shallow Water Equations (SWE). To address the intensive computational demands required to solve the SWE, we can resort to several strategies, such as using simplified physical models and high-performance clusters. More recently, data-driven models based on deep learning emerged a promising alternative with better potential to integrate data (Bentivoglio *et al.*, 2022).

In particular, (Bentivoglio *et al.*, 2023) proposed a hydraulic-based graph neural network (SWE-GNN) that predicts the spatio-temporal flood evolution over unseen topographies, thanks to the model's connection to finite volume approaches. However, it was validated only for regular meshes and it requires the first time step given by the numerical solver. In this work, we extend the original SWE-GNN on non-squared domains, discretized by irregular meshes, and on time-varying boundary conditions. Moreover, we also remove the model's necessity to use the numerical model for the initial conditions, by accounting for boundary conditions via ghost cells.

## 2. Methods

The shallow water equations graph neural network (SWE-GNN) model of (Bentivoglio *et al.*, 2023) takes as input static and dynamic features that represent the topography of the domain and the hydraulic variables at time t, respectively. It then predicts autoregressively the hydraulic variables at time t+1 as

$$\widehat{U}^{(t+1)} = U^t + \Phi(X_s, U^{(t-p:t)}, \mathcal{E}) \quad (1)$$

where the output $\widehat{U}^{(t+1)}$ corresponds to the predicted hydraulic variables at time t+1, $U^t$ are the hydraulic variables (water depth [m] and unit discharge [$m^2\ s^{-1}$]) at time t, $\Phi(\cdot)$ is the GNN model that determines the evolution of the hydraulic variables for a fixed time step, $X_s$ are the static node features, $U^{(t-p:t)}$ are the dynamic node features, i.e., the hydraulic variables for time steps t – p to t, and $\mathcal{E}$ are the edge features that describe the geometry of the mesh. For more information, the reader is reminded to (Bentivoglio *et al.*, 2023).

To account for time-varying boundary conditions, we extend the model by adding ghost cells to the input domain. These are computational cells located outside the boundary of the domain that provide information on the behavior of the domain's processes at the boundary interface. In our experiments, we explicitly define a ghost cell only in correspondence of where the boundary conditions are applied, disregarding wall ghost cells, that is boundary cells with reflective property.

## 3. Experiments and Results

We created a dataset of randomly generated polygons, over which we define an irregular mesh, created using the MeshKernel software (Deltares, 2023). For each mesh, we use a randomly generated digital elevation model (DEM) as in (Bentivoglio *et al.*, 2023). We select a random border edge for the boundary conditions, and we apply an inflow discharge hydrograph, whose shape is generated based on Weibull-like probability density functions with different shape parameters (Bhunya, 2011). The dataset is composed in total of 30 simulations, 20 of which are used for training, 5 for validation, and 5 for testing. Each simulation has an output temporal resolution of one hour and a total simulation time of 48 hours.

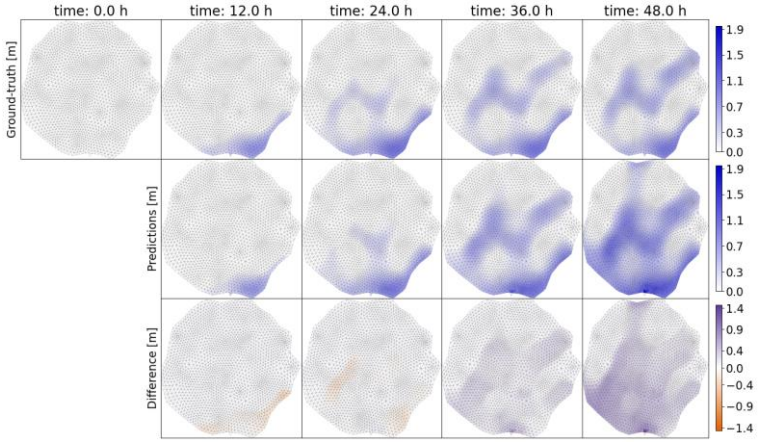



**Fig. 1.** Model's predictions for water depth over time for a test sample, comparing the ground-truth output of the numerical simulation (top row) with the predictions (middle row). The difference (bottom row) is evaluated as the predicted value minus the ground-truth one; thus, positive values correspond to model over-predictions while negative values correspond to under-predictions.

Figure 1 reports the spatio-temporal evolution of water depth for one of the testing samples. Despite the limited amount of training samples and the amount of variability in simulated conditions, the model understands the correct behavior of the flow patterns. The mean average errors in time for water depth and unit discharge for the test dataset are, respectively, 0.06 m and 0.0098 $m^2 s^{-1}$, while the critical success index (CSI) for the water depth threshold of 0.05m is 0.71, indicating overall accurate performance. Moreover, the model has mean speedups of up to 60 times faster than the underlying numerical model. Most errors in the testing dataset are associated to rapid changes in hydraulic loads, close to the boundary location. The simulations tend to also overpredict the flood map in correspondence of the falling limb of the input hydrograph. Those errors could be addressed by increasing the model complexity, for example via multi-scale methods, and by accounting for physical terms in the loss during training.

## 4. Conclusions

We extended the SWE-GNN model (Bentivoglio *et al.*, 2023) by generalizing also to non-squared domains, irregular meshes, time-varying boundary conditions. Preliminary results show that the model can accurately replicate the overall dynamics of the flood evolution over unseen meshes, topographies, and boundary conditions, with no dependance from any numerical solver. This opens up new possibilities to model probabilistically flood uncertainties in realistic case studies, which future works should investigate.

**Acknowledgements**

This work is supported by the TU Delft AI Initiative program.

**References**

Bentivoglio, R. *et al.* (2022) 'Deep learning methods for flood mapping: a review of existing applications and future research directions', *Hydrology and Earth System Sciences*, 26(16), pp. 4345–4378. doi: 10.5194/hess-26-4345-2022.
Bentivoglio, R. *et al.* (2023) 'Rapid Spatio-Temporal Flood Modelling via Hydraulics-Based Graph Neural Networks', *Hydrology and Earth System Sciences*, 2023, pp. 1–24.
Bhunya, P. K. (2011) 'Synthetic Unit Hydrograph Methods: A Critical Review', *The Open Hydrology Journal*, 5(1), pp. 1–8. doi: 10.2174/1874378101105010001.
Deltares (2023) 'MeshKernel', *GitHub repository*. GitHub.

# Experimental Investigation of Flow Turbulent Structures Along Pier Spacing in Open Channel

Nima IKANI[1], Jaan H. PU[2], Kavian COOKE[3]

[1] PhD Student, Department of Engineering and Digital Technologies, University of Bradford, UK
n.ikani@bradford.ac.uk
[2,3] Associate Professor, Faculty of Engineering and Digital Technologies, University of Bradford, UK
j.h.pu1@bradford.ac.uk
k.cooke1@bradford.ac.uk

ABSTRACT

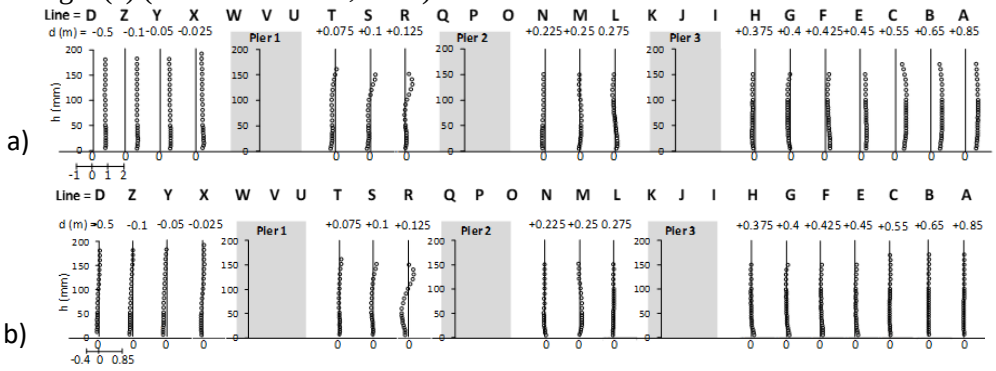
The aim of this investigation was to determine the complex effect of three square-bridge piers on turbulence structures and vortices behavior which is still a research gap in understanding the complex flow dynamics. Its novelty is to enhance understanding of how complex bridge piers contribute to the development of turbulence. The experiment has been conducted in smooth bed within a clear-water open channel flow by utilizing Acoustic Doppler Velocimeters (ADV), in order to determine variations in the flow's turbulent structural dynamics along longitudinal, transverse, and vertical axes. Flow patterns after piers have been examined, where average velocities and Reynolds shear stresses (RSS) were studied along with bursting analysis.

## 1. Experimental setup

Experiments were conducted in a 12m long, 0.5m high, and 0.45m wide rectangular open channel flume. The flume featured glass sidewalls, with a bed slope of 0.0033. Water was recirculated at a discharge of 0.072 m³/s, achieving a uniform flow depth of 0.21m before piers were implemented. In the middle of the open channel, three square piers of 0.05*0.05 m were placed 0.1 meters apart.

## 2. Velocity profiles

The reverse flow pattern was conspicuous after the bridge piers, with the most prominent reversal velocity found in the wake of the first pier (Fig. 1(a)). Consequently, the turbulent structures immediately downstream of the initial pier displayed an enhanced tendency to form swirling patterns and the generation of substantial vortices (Ikani et al., 2024). Furthermore, in the restricted areas between piers where the flow is heavily obstructed, transverse fluctuations significantly affect mixing and vortex formation, as shown by the Fig. 1(b). This phenomenon was facilitated by the presence of a significant downward velocity component after the first pier shown in Fig. 1(c) (Keshavarzi et al., 2018).



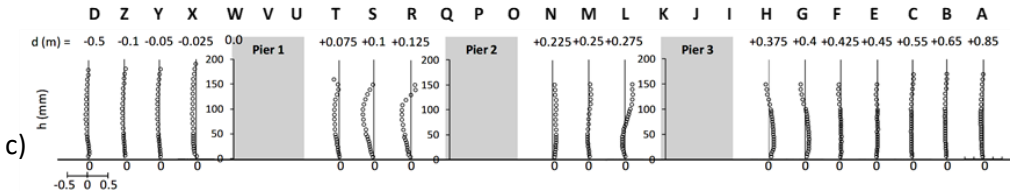



**Fig. 1.** (a) Streamwise, (b) Transverse, and (C) Vertical time-average velocity profile alonge the piers.

## 3. Reynolds shear stress (RSS)

From Fig. 2, there is a significant change in RSS, $-\overline{u'w'}$ after each pier, value from positive to negative, indicating a transfer in flow momentum across flow dimensions. The $v'$ and $w'$ variations from negative to positive can be attributed to the presence boundary layer separations, which influence to the distribution and behaviour of the RSS (Ikani et al., 2024).

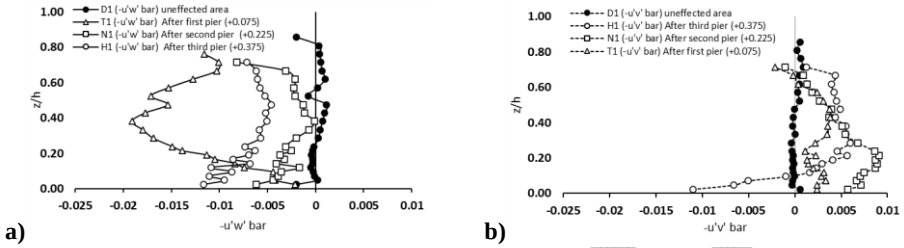



**Fig. 2.** Reynolds shear stress data profiles (a) ($-\overline{u'w'}$), (b) ($-\overline{u'v'}$).

## 4. Quadrant distribution analysis

Fig 3. shows the contributions of each bursting event (u′ and w′) to the generation of Reynolds shear stress were examined in details. Using the quadrant analytical approach, it was possible to identify significant events and characterize the trubulent structures near the bridge piers (Cellino and Lemmin, 2004). While there is a greater proportion of ejections and inward interactions near the surface, outward interactions and sweep events seem to have a greater impact near the bedwall. This observation is confirmed by the research conducted by Hanmaiahgari et al. (2017). Furthermore, it the vicinity of first and second piers (T and N locations), the mixing of fast and slow flow took place, which is a phenomenon described in depth by Ikani et al. (2023).

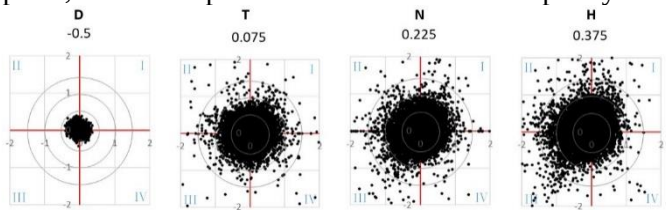



**Fig. 3.** Quadrant distribution across u′ and w′ in z/h=0.05.

## 5. Conclusion

Reverse flow, turbulence, and vortex formation were found to be influenced by piers, especially behind the first pier. As a result of turbulence, there was a change in flow direction near the bed after each pier, indicating the importance of low-speed flow areas between piers in the formation of vortices. Furthermore, based on the quadrant analysis, there was a significant reversal of flow direction, indicating that inward and outward interactions dominated near the bed, strongly influencing the distribution of turbulence. In particular, the turbulence at T locations was more significant due to the higher RSS within the near bed-wall which this variation in RSS over the depth is mainly due to the dispersion and formation of vortices.

**References**

Cellino, M. & Lemmin, U. 2004. Influence of coherent flow structures on the dynamics of suspended sediment transport in open-channel flow. *Journal of Hydraulic Engineering,* 130**,** 1077-1088.

Hanmaiahgari, P. R., Roussinova, V. & Balachandar, R. 2017. Turbulence characteristics of flow in an open channel with temporally varying mobile bedforms. *Journal of Hydrology and Hydromechanics,* 65**,** 35.

Ikani, N., Pu, J. H., Taha, T., Hanmaiahgarib, P. R. & Penna, N. 2023. Bursting phenomenon created by bridge piers group in open channel flow. *Environmental Fluid Mechanics***,** 1-16.

Ikani, N., Pu, J. H., Zang, S., Al-Qadami, E. H. H. & Razi, A. 2024. Detailed turbulent structures investigation around piers group induced flow. *Experimental Thermal and Fluid Science,* 152**,** 111112.

Keshavarzi, A., Shrestha, C. K., Zahedani, M. R., Ball, J. & Khabbaz, H. Experimental study of flow structure around two in-line bridge piers. Proceedings of the institution of civil engineers-water management, 2018. Thomas Telford Ltd, 311-327.

# Analysis of flow velocity profile for immobile bed condition next to bridge pier protected with riprap

Gordon GILJA[1], Luka OPAČAK[2], Antonija HARASTI[3], Manousos VALYRAKIS[4]

[1,2,3] University of Zagreb, Faculty of Civil Engineering, Croatia
gordon.gilja@grad.unizg.hr
[4] Department of Civil Engineering, Aristotle University of Thessaloniki, Thessaloniki, Greece

ABSTRACT

Bridge piers protected with riprap sloping structure exhibit significantly different flow environment and scour pattern in comparison to unprotected piers. The objective of this study is to investigate the flow velocity profiles flows ranging from clear-water scour up to incipient conditions used for bridge scour experiments at piers protected with a riprap sloping structure, targeting to determine flow conditions that induce scour but not full bed development. The results from a series of flume experiments are presented, investigating flow velocity profiles obtained from acoustic velocimeter profiler under five different flow rates. Results show that while differences in flow velocity profile, Reynolds stress and bed development across flow rates exist, they are not significantly correlated.

## 1. Introduction

Experiments involving scouring around structures, such as bridge piers, are often conducted using hydraulic flume under clear-water conditions to decouple from other sediment transport mechanisms. While clear water conditions can be sustained in the approach section, downstream of the structure flow acceleration and enhancement of the secondary currents induces formation of the ridges and bed development. To investigate maximum erosion under clear water scour, flow rate should be increased up to the incipient motion conditions which represent threshold of sediment entrainment. The hydrodynamic environment associated with incipient motion can be estimated from direct velocity measurements, using selected relevant metric, such as critical velocity or critical shear stress. The focus of this research is the hydrodynamic environment around bridge pier protected with riprap sloping structure, where the majority of scour is expected to develop downstream of the structure under the flow accelerated along the riprap boundary. The objective of this research is to determine flow characteristics at the representative vertical profile for range of flows ranging from clear-water scour up to incipient conditions, to be later used in experimental investigations of scour pattern.

## 2. Experimental setup

Experiments were conducted in the recirculating hydraulic flume set up for scour simulations – bridge pier was constructed on top of the false riverbed filled up with coarse sand. Experiments were run with five flow rates (Q1 – Q5), with velocimetry data acquisition in duration of 12 minutes after the hydrodynamic conditions stabilized in the working section. Flow field data were collected using the acoustic Doppler velocimetry profiler Vectrino ADVP (Gilja et al., 2023). Flow velocity was measured in a single location aligned with the flume centerline, using 1 mm cell size over the 1 cm depth, resulting in the velocity profile containing the total of 10 measurement points. The measurement location and distance from the bed correspond to the position and size of the instrumented particle that will be used in subsequent experiments of incipient motion (Alhusban and Valyrakis, 2022). Velocity measurement profile is selected to span the size of the instrumented particle to extract impulses entraining the particle into movement (AlObaidi and Valyrakis M, 2023). The distribution of Reynolds stress u'w' and streamwise flow velocity u under different flow rates below and above the incipient motion threshold were calculated and compared with bed development.

## 3. Results and discussion

In a uniform flow over the flat bed surface, the incipient motion is generally related to the critical flow velocity or shear stress that can be straightforwardly extracted from measurements. For more detailed analysis of entrainment events, high frequency ADV instantaneous velocity data can be used to extract turbulent events and individual particle motion (Diplas et al., 2008). ADVP data were used to extract the bed evolution data together with velocimetry, with bed level updated every second, while velocimetry data rate was 100 Hz. Bed evolution shows that for the lowest flow rate bed was immobile, followed by intermittent particle movement under Q2 and Q3, after which general erosion occurred under Q4, and under Q5 bed has fully developed with visible bedform movement (Fig 1).

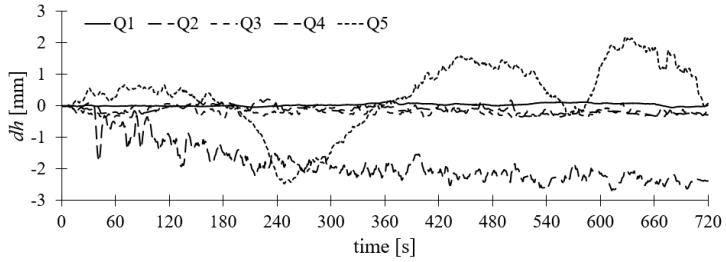



**Fig. 1.** Bed evolution over time for different flow rates, measured at a location of the ADVP velocity profile.

When streamwise velocity u and instantaneous Reynolds stress u'w' are compared with the bed change for two distinct flows (Q2 and Q5), it can be noted that there is no significant difference in velocity and Reynolds stress pattern that can be associated with the bed level change (Fig 2a). For Q1 flow that corresponds to immobile bed condition, both u and u'w' show relatively uniform distribution over the sampling time and bed difference (calculated as bed elevation change between two sampling times) is within the margin of error (<1mm). When the same data is analyzed for the largest flow rate Q5, there is visible, and opposite trend in u and u'w' values: velocity increases over time, while Reynolds shear decreases (Fig 2b). This trend can be associated with change in flow velocity profile induced by lowering of the bed. Several timesteps that show with largest bed deposition correspond with peaks in the u'w' values, resulting primarily from high w' component. However, if all pairs of u'w' and bed elevation change are plotted against each other, there is no significant correlation between them.

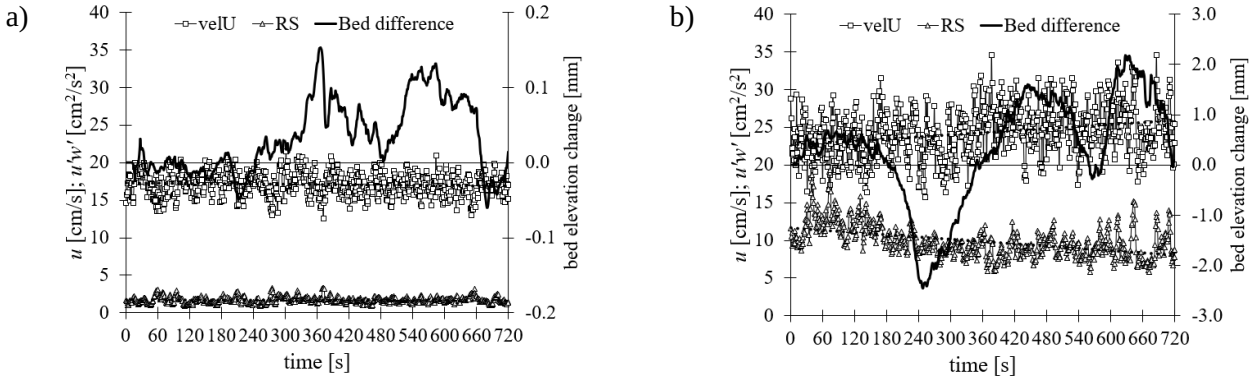



**Fig. 2.** Change of streamwise flow velocity, Reynolds stress and bed elevation for two distinct flow rates: Q1 (a) and Q5 (b).

## 4. Conclusion

This study shows that incipient motion analysis needed for scour investigations is too complex to be extracted from the ADVP data. Correlation of instantaneous events comparing the bed elevation change and flow is not significant. Continuation of this research, introducing the instrumented particle data paired with the ADVP, will aim to overcome the gaps in velocimetry data and explore the influence of the impulse on bed change.

**Acknowledgements**

This work has been supported in part by Croatian Science Foundation under the project R3PEAT (UIP-2019-04-4046).

**References**

Alhusban Z, Valyrakis M (2022) Assessing sediment transport dynamics from energy perspective by using the instrumented particle, International Journal of Sediment Research, 37(6), 833-846

AlObaidi K, Valyrakis M. (2023) Coherent Flow Structures Linked to the Impulse Criterion for Incipient Motion of Coarse Sediment. Applied Sciences, 13(19), 10656

Diplas P, Dancey CL, Celik AO, Valyrakis M, Greer K, Akar T, (2008) The Role of Impulse on the Initiation of Particle Movement Under Turbulent Flow Conditions, Science, 322(5902), 717-720

# Machine Learning Methodologies for Leakage Flow in a Masonry Dam (Santa Fe's dam)

Enric BONET[1], María Teresa YUBERO[2], Lluís SANMIQUEL[3], Marc BASCOMPTA[4]

[1] Universitat Politécnica de Catalunya
enrique.bonet@upc.edu

[2,3,4] Universitat Politécnica de Catalunya
maria.teresa.yubero@upc.edu
lluis.sanmiquel@upc.edu
marc.bascompta@upc.edu

ABSTRACT

Historically, one of the most common causes of dam failure has been overtopping, primarily in earthfill dam , accounting for approximately 34% in the United States, according to the Association of State Dam Safety Officials. There have been other contributing factors to dam failures throughout history, with a significant issue in masonry dams being water infiltration through the dam body, leading to erosion of the mortar that binds the rocks forming the dam body. As a result, quantifying the flow rate from these leakages is an important parameter to consider and measure in the operation of such dams. In this article, a tool is developed using Artificial Intelligence methodologies, specifically artificial neural networks, for predicting water leakages in a masonry dam. The tool learns from historical data collected from the Santa Fe del Montseny Dam (Barcelona) over the past 10 years (although not all dataset is completed), taking into account factors such as temperature, precipitation, reservoir levels, water levels in observation wells within the dam, as well as water leakage measurements.

The leakage flow prediction tool is developed in a MATLAB environment. The methodology used is an artificial neural network and different model options such as hold-out and k-folds were provided. In this study, different layer sizes, different number of neurons, different k folds values are considered to minimize the leakage prediction error.

The results indicate that the tool can predict infiltration flow with an accuracy close to 90%, making it a valuable tool for decision-making in the operation of this type of dam. In that sense, the leakage flow prediction is a useful tool for dam management as well as monitoring the dam's behavior.

## 1. Area of study

The dataset was built from measurement data at the Santa Fe del Montseny dam, located in the Montseny massif in the province of Barcelona (Spain), as shown in Fig. 1. The Santa Fe del Montseny dam is a double arch-gravity dam and masonry structure whose construction was completed in 1933. The main arch of the dam has a radius of 260 m, and the secondary one measures 126.40 m, with a crest length of 245.22 m and a maximum height between foundation and crest of 24 m.

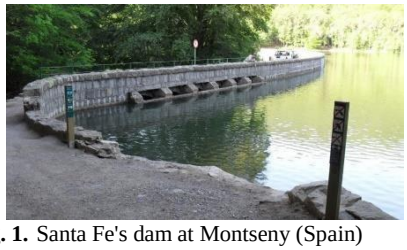


**Fig. 1.** Santa Fe's dam at Montseny (Spain)

## 2. Measurement, data preprocessing and data selection

The dataset employed for training the ANN (artificial neural network) includes climatic as well as wells and reservoirs data. The objective parameters required for the ANN, such as leakage flow rates (left and right sides), were also measured from the dam, since the leakage areas were divided between the central part to the right abutment and the central part to the left abutment. Setting up distinct areas enabled the operators to quickly identify which area of the dam presents higher leakage values and requires mitigation actions.

Temperature and precipitation measurements were obtained from historical data stored from the PuigSesolles meteorological station, located just 2 km from the dam. The measured data from water levels in wells, reservoirs, and leakage flow rates in each area of the dam were stored daily and provided by PICCSA, the company responsible for operating the dam. In this regard, a dataset spanning 10 years was analyzed, although the series were not continuous because measurements were not taken every day by the operating company.

The measured data was processed to detect anomalous values, as well as, correlations between variables or other statistical parameters, which helped to conduct a more thorough analysis. The boxplot function of MATLAB was used to represent a complete dataset. Fig. 2 displays the data of minimum, maximum, and mean temperature, precipitation and well water levels. In each box, the central mark indicates the median, and the lower and upper edges of the box indicate the first quartile and third quartile, respectively, with outliers represented by the symbol "+".

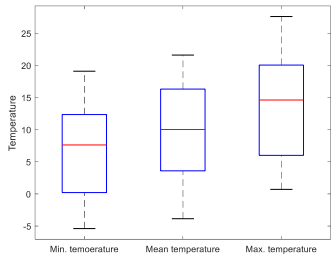



**Fig. 2a.** Boxplot temperature data

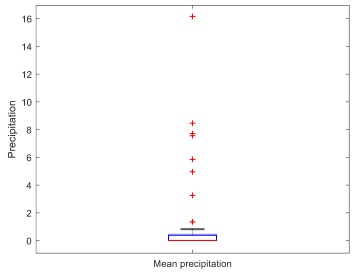



**Fig. 2b.** Boxplot precipitation data

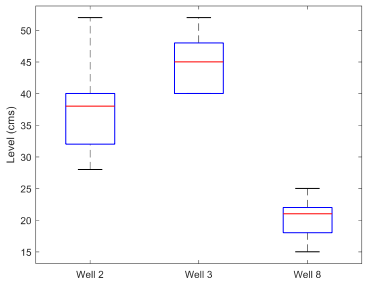



**Fig. 2c.** Boxplot Wells water level data

## 3. Methodology

In the present study, an artificial neural network is used as a forecasting model to predict leaks in dams based on independent variables such as temperature, precipitation, and levels. Given that data related to the dam is often limited, and neural networks are known to perform well even with insufficient data, this was a compelling reason to use neural networks in the present study. Artificial Neural networks have other important advantages, such as the ability to perform parallel processing, distributed memory, and fault tolerance. However, all methods also have disadvantages. The artificial neural network behaves more like a black box compared to other machine learning methods.

Taking into account both advantages and disadvantages, the artificial neural network (ANN) was selected as the prediction method. The ReLu activation function was applied after analyzing the results with other activation functions, such as Sigmoid or Hyperbolic Tangent. On the other hand, it was verified that the optimal number of layers for the neural network was two layers, as it did not worsen the results compared to three layers. Instead, the greatest improvement in algorithm accuracy was identified with the application of the Hold-out or K-Fold model, as indicated by the results.

## 4. References

Association of State Dam Safety Officials. (2024). Dam Failures and Incidents. https://damsafety.org/dam-failures.
Qiu, J., Zheng, D., Zhu, K., Seepage Monitoring Models Study of Earth-Rock Dams Influenced by Rainstorms, Mathematical Problems in Engineering, 2016, https://doi.org/10.1155/2016/1656738
Department of Environment (UK), Impact of Climate Change on Dams and Reservoirs, FD2628, May 2013.
Song, C.R., Yosef, T., Seepage Monitoring of an Embankment Dam Based on Hydro-Thermal (H-T) Coupled Analysis, Journal of Engineering Materials and Technology, Transactions of the ASME 139(2), February 2017.
Cuong, B.Q., Thai, N.C., Yihong, Z., Chunju, Z., Estimating Seepage in Embankment Damns based on Temperature Measurement: A Review Paper, International Journal of Engineering Research & Technology (IJERT), Vol. 6 Issue 01, January-2017.
Befetta, H., Quadja, A., Hocini, N., Enhancement of the study of water leaks in the Algerian dam of Foum El Gherza, Arabian Journal of Geosciences, volume 10, Article number: 482, 2017.
Anthony, M., Neural Network Learning: Theoretical Foundations, Cambridge University Press, 2009.

# Innovative Image-based techniques for Scour Monitoring and Measurement around Offshore Foundations

Ana Margarida BENTO[1,2], Tiago FAZERES-FERRADOSA[1,2], João CHAMBEL[1,2], Filipe MIRANDA[1], Tomás CABRAL[1,2], Paulo, ROSA-SANTOS[1,2], Francisco TAVEIRA-PINTO[1,2],

[1]Hydraulics, Water Resources, and Environmental Division, Department of Civil Engineering, Faculty of Engineering of the University of Porto, 4200-465 Porto, Portugal

[2]CIIMAR – Interdisciplinary Centre of Marine and Environmental Research, Marine Energy and Hydraulic Structures group, 4450-208 Matosinhos, Portugal

anabento@fe.up.pt; tferradosa@fe.up.pt; up201304674@fe.up.pt; up201706240@fe.up.pt; up201304327@edu.fe.up.pt; pjrsantos@fe.up.pt; fpinto@fe.up.pt

ABSTRACT

Scour phenomena have been recognized over decades as a serious threat to the stability of foundations in both the fluvial and the maritime environments. Due to the intervention of various complex mechanisms, mainly of hydraulic nature, the scouring process remains a challenging engineering problem. Thus, the management of its severity and damage is crucial to ensure the serviceability and operability of infrastructures. The harsh environmental conditions at offshore foundations, as well as the associated high costs, dictate the purpose of studying better methods to characterize the scour effects of two different types of foundation. Physical modelling tests were performed at the Hydraulics Laboratory of the Faculty of Engineering of the University of Porto (FEUP) for a monopile foundation and a Gravity-Based Foundation (GBF), at a scale of 1:50. To address such challenges, innovative technologies, based on advanced image-based approaches, were investigated and employed for comprehensive scour hole and deposition zones measurements at their vicinities, by means of a 3D laser scanner (FARO Focus$^S$ 70) and the close-range photogrammetric technique. The photogrammetry application allowed a more reliable and accurate characterization of the topographic representation of the scour hole and inherent features for the studied cases. By highlighting these key issues, and by describing good practice in managing the challenges of dealing with the adverse and complex offshore environment, as well as the implicit experimental uncertainties, the present research explains how an efficient, flexible and responsive approach can help reduce risks and deliver appropriate and resilient approaches for studying the scour phenomena around offshore foundations with complex geometries.

## 1. Introduction

The integration of high-resolution topographic data from mobile bed flume studies has significantly improved our understanding of river and marine morphodynamics. Structured from Motion (SfM) models have been extensively used in flume and geomorphic-based investigations, particularly in the study of local scour, and have provided invaluable insights into various phenomena. For example, close-range photogrammetry effectively reconstructs scour holes around bridge foundations in controlled experimental settings (Ramos et al., 2015; Bento et al., 2018). In addition, innovative approaches such as continuous scour monitoring have enabled the generation of accurate 2D bed profiles, as seen in the study of an oblong foundation by Bento et al. (2022). Furthermore, 3D laser scanners (FARO Focus$^S$ 70) have demonstrated commendable performance in reconstructing 3D surface maps (Bento et al., 2018). However, while these image-based techniques provide satisfactory accuracy and high-resolution 3D models, validating the accuracy of the 3D laser scanner for characterizing scour patterns remains challenging. Successive differencing of topographic datasets has provided critical insights into phenomena such as the formation and migration of alternating bars, meanders,

and bed patterns. In this context, our study focused on the three-dimensional characterization of scour effects around a 1:50 scale model of offshore foundations, based on a North Sea prototype.

## 2. Experimental facilities and methodologies

The physical modelling activities were carried out at the Hydraulics Laboratory of the Faculty of Engineering of the University of Porto (FEUP), in a 29 m long and 1 m wide wave-current flume. The flume is equipped with an HR Wallingford piston wavemaker. A passive wave absorption system was installed at the downstream end of the flume to mitigate reflection effects (Miranda et al., 2023).

The aim of the experiments was to characterize the resulting bathymetry using close-range photogrammetry and the 3D laser scanner, two different image-based methods. Both strategies required the prior emptying of the flume and the placement of ground control points at specific locations on the model with known dimensions for their intended use.

## 3. Results and discussions

The study produced 3D bed morphology models, surface contour plots and scour profiles, which are essential for analysing scour depths of offshore foundations (see Figure 1). Advanced survey and sensor technologies such as 3D point clouds and Digital Elevation Models (DEMs) were used. These technologies were used to produce three-dimensional bed morphology maps at the beginning and end of each 1000 wave cycle.

Close-range photogrammetry proved to be a cost-effective alternative to traditional topographic surveying methods, providing higher resolution data sets in less time. In addition, the 3D laser scanner, although more expensive, demonstrated comparable accuracy to close-range photogrammetry and also contributed to the improved investigation of offshore foundation scour patterns. The 3D bed morphology models derived from both techniques provided consistent and comprehensive measurements.

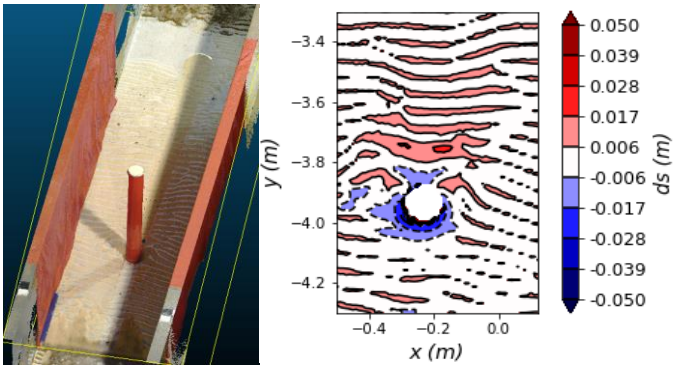



**Figure 1.** Experimental wave-induced scour around an offshore foundation: 3D bed morphology model (left panel) and surface contour plot (right panel). The variable ds is the scour depth.

## 4. Conclusions

This paper presents scour experiments carried out around 1:50 scale offshore foundations in a 1 m wide flume at the Hydraulic Laboratory of the Faculty of Engineering of the University of Porto (FEUP), under combined wave and current conditions. The study validates the accuracy of the 3D laser scanner in analyzing scour patterns and offers a reliable alternative to close-range photogrammetry, albeit at a higher cost.

**Acknowledgements**

This work was financially supported by the project PTDC-ECI-EGC-5177-2020, POSEIDON - DAMAGE PREDICTION AND DESIGN OF SCOUR PROTECTIONS IN COMPLEX FOUNDATIONS FOR MARINE RENEWABLE ENERGY, funded by national funds through FCT – Portuguese Foundation for Science and Technology. The experimental work was conducted in the Hydraulics laboratory of the Faculty of Engineering of the University of Porto (FEUP).

**References**

Bento, A., Couto, L., Pêgo, J. P., & Viseu, T. (2018, September). Advanced characterization techniques of the scour hole around a bridge pier model. In E3S Web of Conferences. https://doi.org/10.1051/e3sconf/20184005066.

Bento, A. M., Couto, L., Viseu, T., & Pêgo, J. P. (2022). Image-based techniques for the advanced characterization of scour around bridge piers in laboratory. Journal of Hydraulic Engineering, 148(6), 06022004.

Miranda, F., Bento, A. M., Chambel, J., Sarmento, M. F., Rosa-Santos, P., Taveira-Pinto, F., & Fazeres Ferradosa, T. (2023). A novel and simple passive absorption system for wave-current flumes. Alexandria Engineering Journal, 71, 463-477. https://doi.org/https://doi.org/10.1016/j.aej.2023.03.067

Ramos, P. X., Bento, A. M., Maia, R., & Pêgo, J. P. (2016). Characterization of the scour cavity evolution around a complex bridge pier. Journal of Applied Water Engineering and Research, 4(2), 128-137.

# Experimental prediction of 1-dimensional riverbed deformation using machine learning along the Mogami river, Japan

Tao YAMAMOTO[1], So KAZAMA[1]

[1] Department of Civil and Environmental Engineering, Graduate School of Engineering, Tohoku University, Japan
yamamoto.tao.t8@dc.tohoku.ac.jp

ABSTRACT

In order to maintain the river environment, there is a need to predict the change of riverbed morphology. Physically based computational models are widely used for prediction. Yet, the more precise model has heavier computational cost, therefore we tried to develop a model that can predict long-term riverbed deformation with low computational load by applying machine learning. In this work, as a first step, we began developing a model to predict the 1D riverbed deformation based on measured bed deformations. We built a simple artificial neural network, where the riverbed elevation change was used as objective variable, and the spectrum of river discharge and riverbed slope as explanatory variables. The prediction accuracy was 0.47 m in RMSE and this is within the range of measured riverbed deformation. However, the coefficient of determination was low and it was not sufficient to predict the trend of riverbed deformation. We have developed an early-stage model for predicting riverbed deformation from measured data, and future challenges have been identified.

## 1. Introduction

In river channel management, it is important for river administrators to grasp and predict the river morphology change. Especially, the riverbed deformation is critical issue to maintain river channels and hydraulic structures. To predict these change of river conditions, physical-based computational models have been developed to calculate the change in riverbed elevation for a long time. Most models solve the continuity and the Navier-Stokes equations, along with the sediment mass balance equation. It takes heavy computation cost to compute the fluid flow and sediment transport for long distance and period.

Recently, machine learning techniques have been used to clear similar hydrology problems. Some studies that try to predict riverbed changes also exist. Rahman and Chakrabarty (2020) predicted the 1D riverbed elevation change for the 8 km reach of the Nittany River. Discharge, sediment gradation, and dam gate opening height were input to the Artificial Neural Networks, and the change of the riverbed was obtained. Hoang et. al, (2018) estimated the local scour depth around complex piers with the support vector regression. However, there are no studies that predict riverbed deformation using actual river topography data at the channel scale and machine learning. As a first step in developing a model that can predict riverbed deformation over a long period of time and over large reaches, we attempted to build a one-dimensional riverbed deformation prediction model using a machine learning and consider the future work to proceed this methodology.

## 2. Materials and methods

### *2.1. Machine learning model description*

A simple artificial neural network (ANN) was constructed as a machine learning algorithm. This ANN has 4 layers; the input layer consists of the neurons of which number of explain variables, the two intermediate layers consist of 25 and 10 neurons, respectively, and the output layer consists of one neuron. ReLU was used as the activation function, and the data was standardized with the mean set to 0 and the variance set to 1. The learning method is backpropagation with mean squared error (MSE) as the loss function. The parameters (weights) were optimized using stochastic gradient descent (SGD). Since there was not a large amount of training data, batch size is set to 10 and the five-fold cross-validation were conducted. The neural network was tested by randomly allocating 20% of the total data.

### *2.2. Datasets*

The target river channel is the mainstream of the Mogami River, which runs through Yamagata prefecture, northeast part of Japan. The target span covers a section from the 89.1 km upstream to 206.2 km. The regular bathymetry surveys were conducted in each cross section approximately every 5 to 10 years at 200 m intervals. In this study, riverbed elevation at each cross section was defined as the average elevation across the lower channel.

The daily average river discharge dataset was obtained from the Water Information System provided by MLIT (2023). Inakudashi, the discharge observation station is located 105.7 km from the river mouth.

For each cross-section, the combinations of the two survey results were created. The daily discharge data for these periods were then obtained and transformed by Fast Fourier Transform. Finally, 1,216 combinations of the objective variable and the explanatory variables were prepared. The objective variable is the change of riverbed elevation. The explanatory variables are amplitudes and frequencies of the discharge spectrum and bed slopes. The amplitudes correspond to 10%tile, 20%tile, 30%tile, 40%tile, 50%tile, 60%tile, 70%tile, 80%tile, 90%tile and 100%tile value. The frequencies corresponding to ones at the amplitudes.

## 3. Results and discussion

Figure 1 shows the comparison between the observed riverbed elevation change and the predicted riverbed elevation change. The proportional line shows the best fit line. The RMSE value was 0.47(m) and $R^2$ score was -0.99. The many plots in Fig.1 are located around 0 m. It shows that many portion of the cross sections has not experienced significant riverbed changes. Due to the lack of data on large changes, the ANN model is considered to be unable to predict such extreme changes.

In this study, the magnitude and frequency of river discharge in any given period were considered to have a significant effect on sediment transport, and the relevant variables were used as explanatory variables. However, because the study was based on a single point of observation, it did not reflect the differences in river discharge upstream and downstream. It is considered that the observed flow at a single point could not adequately represent the flow information of each cross-section because the riverbed fluctuation was predicted for a long section of river. Therefore, we need more variables specific to each section. For instance, the shape of river cross section and the material of riverbed are desirable.

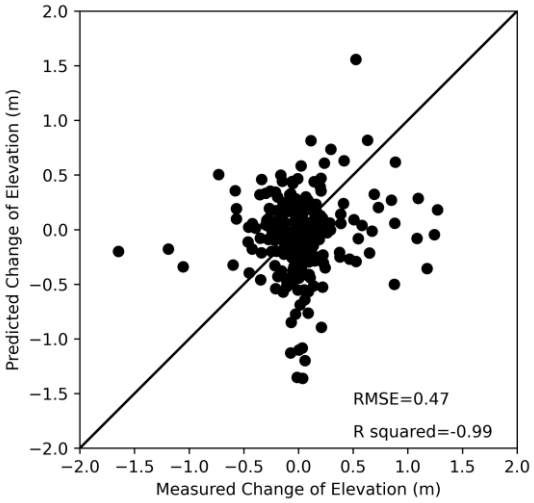



**Fig. 1.** The comparison between the prediction and observation of the riverbed change

**Acknowledgements**

This work was supported by JSPS KAKENHI Grant Number 23KJ0183. The authors are grateful to Yamagata River and National Highway Office under the Tohoku Regional Development Bureau of MLIT for providing the river bathymetry data.

**References**

Hoang, ND., Liao, KW. & Tran, XL. (2018) Estimation of scour depth at bridges with complex pier foundations using support vector regression integrated with feature selection, Journal of Civil Structural Health Monitoring, 8, 431–442

Ministry of Land, Infrastructure, Transport and Tourism (2023) Water Information System, http://www1.river.go.jp/ (Accessed at 14th July 2023)

Rahman, S. A., & Chakrabarty, D. (2020) Sediment transport modelling in an alluvial river with artificial neural network, Journal of Hydrology, 588, 125056

8th IAHR EUROPE CONGRESS
LISBON - PORTUGAL
4-7 JUNE 2024

# Dam break in power-law cross-section channels with different upstream/downstream widths

Alessandro VALIANI[1], Valerio CALEFFI[1]

[1]Department of Engineering, University of Ferrara, Italy
alessandro.valiani@unife.it
valerio.caleffi@unife.it

ABSTRACT

The dam break problem is studied in a channel characterised by a power-law cross-section, with different widths upstream and downstream of the dam. This research is the extension of a previous study by Valiani and Caleffi (2019), designed for rectangular cross-sections, to different and more complex geometries. A 1D a-SWE (one dimensional *augmented* Shallow Water Equation) system is developed, which has been shown to capture the full range of possible solutions.

To address abrupt changes in the section, the classic SWE system is augmented with a third equation consisting of the time-invariance of the width scale. The idea of the augmented system was introduced by LeFloch and Thanh (2011) for the unit-width SWE, using the bed elevation as an additional variable, and by Valiani and Caleffi (2019) for rectangular narrowing/widening cross-sections, using the channel width as an additional variable.

The numerical model is a Finite Volume Method, second-order accurate in space and time, using a path conservative scheme to evaluate the numerical flux at the cell interfaces. A nonlinear path is adopted, which is shown to be optimal for capturing both the sharp contact wave at the dam and the moving shock(s) downstream of the dam.

The comparison of the numerical results with the analytical results for different solution patterns of the solution supports the confidence in the reliability of the model.

## 1. Mathematical Model

We consider a channel with a power-law cross section, characterised by the following geometry:

$$b = b_0 \left(\frac{Y}{Y_0}\right)^m \; ; \; A = \frac{b_0 Y_0}{1+m}\left(\frac{Y}{Y_0}\right)^{1+m} \; ; \; I = \frac{b_0 Y_0^2}{(1+m)(2+m)}\left(\frac{Y}{Y_0}\right)^{2+m} \tag{1}$$

where $b_0$ is the width scale, $Y_0$ is the depth scale, $m$ is the shape coefficient, $b$ is the current width, $Y$ is the current depth, $A$ is the wetted area, $I$ is the static moment of the cross section (Valiani and Caleffi, 2009).

A discontinuous width scale is considered, specifically $b_{0L}$ upstream of the dam and $b_{0R}$ downstream. Both cases of contraction and expansion cases are analysed. $Y_L$ and $Y_R$ ($<Y_L$) are the initial upstream and downstream depths. The water is initially at rest everywhere. The 1D a-SWE system governing the problem is:

$$\begin{gathered} \frac{\partial A}{\partial t} + \frac{\partial Q}{\partial x} = 0 \\ \frac{\partial Q}{\partial t} + \left[\left(g\frac{A}{b}\right) - \left(\frac{Q^2}{A^2}\right)\right]\frac{\partial A}{\partial x} + \left(2\frac{Q}{A}\right)\frac{\partial Q}{\partial x} - \left(g\frac{A}{b}\right)\Lambda\frac{\partial K}{\partial x} = 0 \\ \frac{\partial K}{\partial t} = 0 \end{gathered} \tag{2}$$

where ($x$, $t$) are space and time, respectively; $Q$ is the discharge, $g$ is the acceleration due to gravity, $K$ is the additional geometrical variable ($b_0$ in this specific case), and $\Lambda$ is a geometrical variable ($A/b_0$ in this specific case), whose definition ($\eta$ is the water surface elevation) is:

$$\Lambda \frac{\partial K}{\partial x} = \left(\frac{\partial A}{\partial x}\right)_{\eta=const} \tag{3}$$

Such a term is crucial when geometric discontinuities occur but vanishes in smooth cases.

## 2. Numerical Model

Numerical integration is performed using a second-order accurate Finite Volume Method, with a DOT (Dumbser and Toro, 2011) Riemann solver to compute the flux at the cell boundaries, where the solution is discontinuous (Toro, 2009). A path-conservative scheme (Dal Maso et al., 1995; Castro et al., 2008) is employed; the linear path introduced by *Parés* (2006) is modified here as proposed in *Valiani & Caleffi* (2019), introducing an original nonlinear path that can be adopted for cross-sections of arbitrary shape.

Referring to cell $i$, its boundaries are $x_{i-1/2}$ and $x_{i+1/2}$. At this last boundary, each state variable $W$ has two different values, $W^-_{i+1/2}, W^+_{i+1/2}$, on the left and right respectively. We assume a linear path in the variables $H$, $Q$, $K$, where $H$ is the total head of the flow:

$$\begin{aligned} \Psi_H\left(H^-_{i+1/2}, H^+_{i+1/2}; s\right) &= H^-_{i+1/2} + \left(H^+_{i+1/2} - H^-_{i+1/2}\right) s \\ \Psi_Q\left(Q^-_{i+1/2}, Q^+_{i+1/2}; s\right) &= Q^-_{i+1/2} + \left(Q^+_{i+1/2} - Q^-_{i+1/2}\right) s \qquad 0 \le s \le 1 \\ \Psi_K\left(K^-_{i+1/2}, K^+_{i+1/2}; s\right) &= K^-_{i+1/2} + \left(K^+_{i+1/2} - K^-_{i+1/2}\right) s \end{aligned} \tag{4}$$

and a nonlinear path for the cross-sectional area, $\Psi_A\left(A^-_{i+1/2}, A^+_{i+1/2}; s\right)$, which must be derived from:

$$H(s) = \eta(s) + \frac{[Q(s)]^2}{2g[A(s)]^2}, \quad 0 \le s \le 1 \tag{5}$$

## 3. Results

Depending on the ratios $b_{0R}/b_{0L}$ and $Y_R/Y_L$, 6 different solution patterns are possible (2 for contractions and 4 for expansions). There is a contact wave occurs at the dam position, and one (or more) shocks downstream of the dam. The augmented system approach is crucial to capture the correct solution when the resonant case (two eigenvalues are both zero) occurs at the dam position. The proposed numerical method gives excellent results for the whole range of cases considered. Examples are shown in Fig. 1.

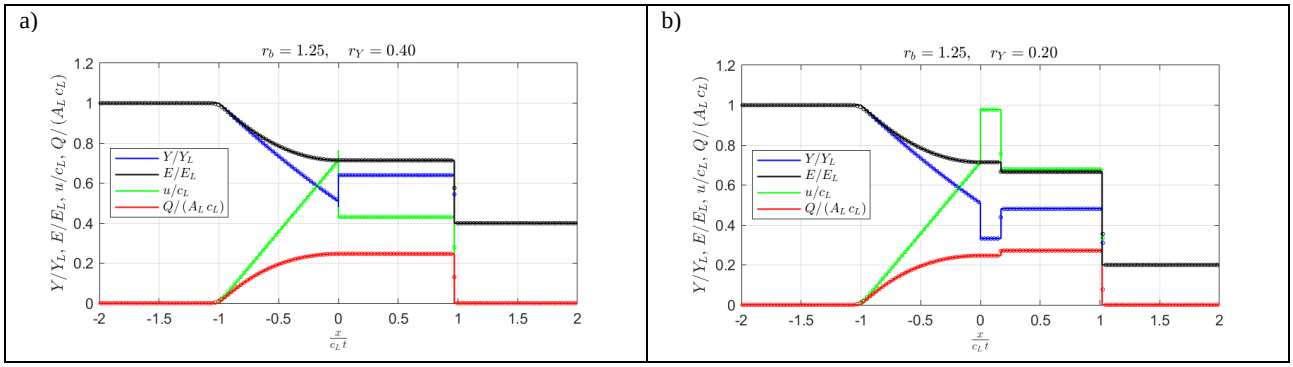



**Fig. 1.** Dam break in power-law cross-sections for a sudden expansion, $b_{0R}/b_{0L} = 1.25$, for different initial depth ratios: a) $Y_R/Y_L = 0.40$; b) $Y_R/Y_L = 0.20$. Lines/dots are analytical/numerical solutions. $c$ is the relative celerity of small waves, $E$ is the specific energy (=$H$ for horizontal flat bed), $u$ is the mean velocity; the subscript $L$ is the initial reference value upstream of the dam.

### References


Castro MJ , LeFloch PG , Muñoz Ruiz ML , Parés C (2008) Why many theories of shock waves are necessary: convergence error in formally path-consistent schemes. Journal of Computational Physics 227 (17), 8107-8129.

Dal Maso GD, LeFloch P, Murat F (1995) Definition and weak stability of nonconservative products. J. de Mathématiques Pures et Appliquées 74, 483-548.

Dumbser M, Toro EF (2011) A simple extension of the Osher Riemann solver to non-conservative hyperbolic systems, Journal of Scientific Computing 48 (1–3), 70-88.

LeFloch PG, Thanh, MD (2011) A Godunov-type method for the shallow water equations with discontinuous topography in the resonant regime, Journal of Computational Physics 230 (20), 7631-7660.

Pares C. (2006) Numerical methods for nonconservative hyperbolic systems: A theoretical framework, SIAM Journal on Numerical Analysis 44 (1), 300-321.

Toro EF (2009) Riemann Solvers and Numerical Methods for Fluid Dynamics, Springer-Verlag, 724 pp.

Valiani A, Caleffi V (2009) Depth–energy and depth–force relationships in open channel flows. II: Analytical findings for power-law cross-sections, Advances in Water Resources 32, 213-224.

Valiani A, Caleffi V (2019) Dam break in rectangular channels with different upstream-downstream widths, Advances in Water Resources 132, 103389.

# Sediment Scaling Effects in Physical Modelling on Depositional and Erosional Patterns

Siedersleben JAKOB[1], Schuster MARCO[1], Achleitner STEFAN[1], Aufleger MARKUS[1]

[1] University of Innsbruck, Austria

jakob.siedersleben@uibk.ac.at

ABSTRACT

Physical modelling of bed load transport is a challenging task due to a number of factors. A key issue is the correct sediment scaling without oversimplifying the essential sediment behavior of the prototype scale. Due to laboratory space and funding restrictions, correct sediment scaling is often not possible and the Shields diagram may reveal, that some proportions of bed load are not transported in the rough transport regime. In addition, limiting the minimum particle diameter is a common way to avoid cohesive effects and transport bodies in physical model experiments. This work evaluates the effects of modifying the particle size distribution (PSD) using the numerical model Telemac2d coupled with the sediment transport model Gaia. The numerical simulations refer to physical experiments which were carried out on a 1:25 scale model to investigate sediment management at the Reutte weir facility on the alpine Lech River in Austria. The results of the numerical simulations show that changing the particle size distribution has an effect on erosion and deposition magnitude, timescales and transport rates. However, the deposition and erosion patterns are still reproduced within an acceptable accuracy.

## 1. Introduction

### *1.1. Study site*

The hydropower facility in Reutte, Austria on the Lech River is the first major transversal structure in this alpine river. As a result, the stream transports large amounts of sediment, demanding for challenging sediment management of the facility. Fig. 1 (a) shows the essential features of the facility and the physical and numerical model boundaries. The facility is comprised of the Höfen run-off-river hydropower plant (HPP) on the orographic left side and the Ehenbichl diversion HPP on the orographic right side. The annual mean discharge is at 44.1 m³/s, the HPP Höfen is designed for an operational discharge of 15 m³/s and the HPP Ehenbichl is designed for an operational discharge of 28 m³/s.

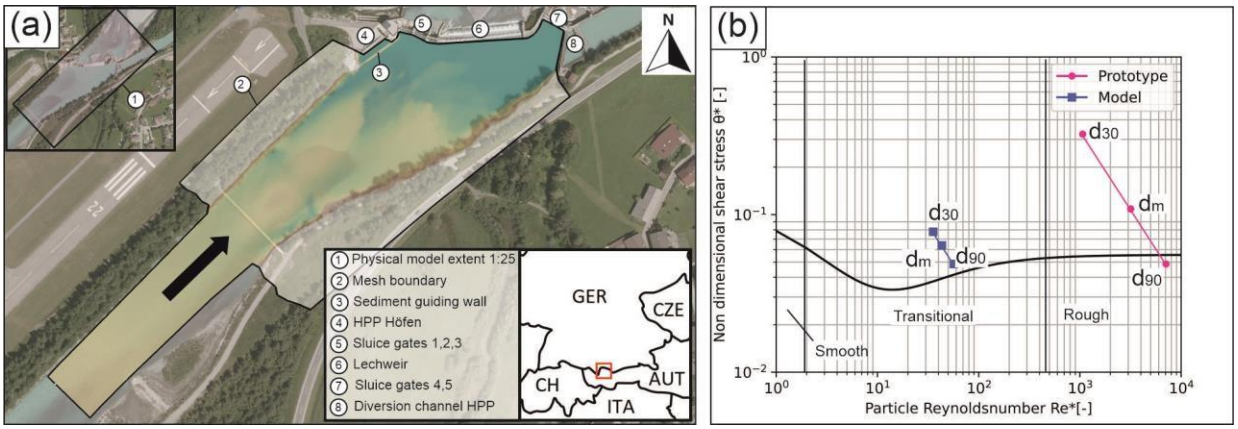



**Fig. 1.** Overview of the study site including the physical and numerical model boundaries (a) and the theoretical sediment behaviour for Q = 150 m³/s at a representative cross section close to the facility (b).

### *1.2. Physical model tests and sediment scaling*

Physical model tests were carried out to asses erosion and deposition patterns for flushing, aggradation and flooding events at the hydropower facility in Reutte. Additionally, a sediment guiding structure, a novel approach for a flushing channel design and the effect of increasing the diversion discharge on the environmental flow reach were tested (Siedersleben et al., 2022, 2023). In order to avoid cohesive effects and the formation of transport bodies, the minimum particle size diameter was limited to 0.5 mm. Therefore, the resulting model $d_m$ in prototype scale is 30 mm instead of 18 mm. Consequently, the fines are not represented by the physical model and the material is generally too coarse. Fig. 1 (b) shows the theoretical prototype and model particle size behavior according to the Shields diagram for the investigated discharge of 150 m³/s.

## 2. Results and Discussion

Fig. 2 shows the cumulative bed evolution of the numerical simulation conducted with the prototype particle size distribution (PSD) (a) and the model PSD (b). The discharge of 150 m³/s corresponds to the maximum discharge at which the HPP Höfen is still in operation. The numerical model tests were run for 12.5 h in prototype scale. Since the sediment scaling results in sediment transport in the transitional regime as indicated by Fig. 1 (b), the threshold for the initiation of motion ($\theta_{crit}$) was adjusted according to an analytical solution of the Shields curve of Guo (2020). Therefore, $\theta_{crit}$ values range from 0.034 to 0.047.

The prototype simulation shows erosion at the upstream end of the model with depths of up to 0.5 m. Further downstream, in the vicinity of the facility, sediment is deposited with maximum depositional heights of over 1 m. In contrast, the magnitude of the erosion and deposition of the model simulation is reduced. The erosion depth at the model inflow reaches a maximum depth of 0.3 m and the deposition close to the facility reaches up to 0.5 m. The difference in the cumulative bed evolution can be explained by the effect of not considering the fines on the transport rate: the average transport rate of the numerical model considering the prototype PSD reduces from 0.39 kg/ms to 0.19 kg/ms within the simulation time with an average of 0.28 kg/ms. The transport rate of the numerical model considering the model PSD is significantly lower as it reduces from 0.11 kg/ms to 0.06 kg/ms within the simulation time with an average of 0.08 kg/ms. The development of the reduction can be approximated linearly for both cases.

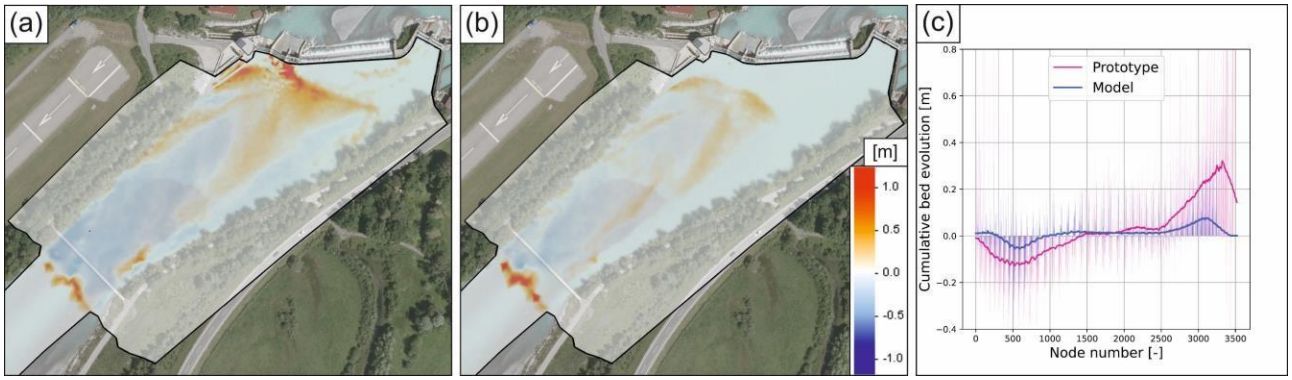



**Fig. 2.** Cumulative bed evolution of the numerical simulations with a discharge of 150 m³/s considering the prototype PSD (a) and the model PSD (b). Cumulative bed evolution for each node of the simulation considering the prototype PSD and the model PSD (c).

Fig. 2 (c) shows the cumulative bed evolution for all nodes of the computational mesh. Negative values correspond to erosion and positive values to deposition. Since the lines representing the prototype and model simulations are both negative or both positive for 82% of the nodes, it can be concluded that the model simulation, while strongly underestimating the magnitude, still manages to predict erosion and deposition according to the prototype simulation. However, the deposition near sluice gates 2 and 3 and the Höfen HPP is depicted poorly.

Further analysis could still highlight the impact on sorting processes and provide recommendations on how to adjust the simulation time of the physical model test to reduce the impact of underestimated transport rates.

**References**

Guo J. (2020) Empirical Model for Shields Diagram and Its Applications, Journal of Hydraulic of Hydraulic Engineering, 146
Siedersleben J, Jocham S, Aufleger M, Achleitner S. (2023) Morphodynamic Impact of Increasing Diversion Discharge in an Alpine River, Proceedings of the 40th IAHR World Congress, Vienna.
Siedersleben J, Schuster M, Aufleger M, Achleitner S. (2022) Solution for a Sluicing Channel with high and coarse Sediment Intake in an alpine River, Proceedings of the 39th IAHR World Congress, 1202–1207. Granada.

# Dike failure experiments. Influence of inflow conditions and soil composition

Ricardo JÓNATAS[1], Silvia AMARAL[1], Rui ALEIXO[2], Marta PALINHOS[1], Teresa VISEU[1], Rui FERREIRA[3]

[1] LNEC, Laboratório Nacional de Engenharia Civil, Portugal
rjonatas@lnec.pt; samaral@lnec.pt; tviseu@lnec.pt; A46366@alunos.isel.pt
[2] Institute of Hydroengineering, Polish Academy of Sciences, Poland
rui.aleixo@ibwpan.gda.pl
[3] IST/ CERIS – Instituto Superior Técnico/ Civil Engineering Research and Innovation for Sustainability, Portugal
ruimferreira@tecnico.ulisboa.pt

ABSTRACT

It is of paramount importance to shed light on dike failure studies because although these fail frequently and cause severe impacts in protected and urbanized areas, they are still at an early stage of research. This was the motivation for the experimental research on failure of fluvial dikes currently being developed at the Portuguese National Laboratory for Civil Engineering. A medium-scale facility entirely designed for the purpose was used to perform the experiments presented in this study. A set of three experiments is presented in which the soil composition and the inflow conditions were varied. Conclusions regarding the impact of the inflow conditions and soil composition on the dike's failure processes are drawn.

## 1. Experiments framework

Although dikes fail more frequently than dams there are far more failure studies on the latter that in the former. In Portugal, an example of such catastrophic events, is the failure of the Mondego River dikes system, on December 22 of 2019, causing a severe floodplain and inundations in Coimbra city area. Considering that dike failures can also induce devastating scenarios in protected and urbanized areas, if no flood risk management tools or prevention practices are implemented it is of paramount importance to shed light on dike failure studies and also to improve the current ability to numerically simulate dike breaching processes (Amaral, et al., 2020).

The dike failure experiments were conducted in a facility located at LNEC, specifically developed for this purpose to test dikes up to 0.5m height and 2.0m long (Figure 1).

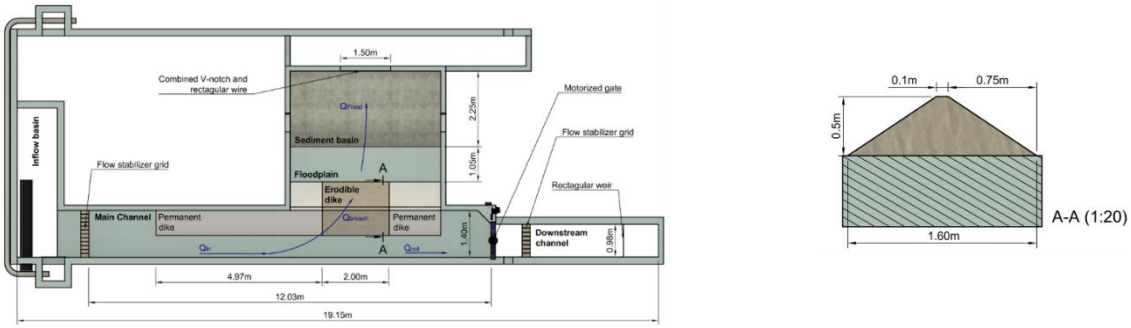



Figure 1. Dike breach facility. Left – Plain view; Right – cross-section at the dike site.

Experiments analysis was based on breach morphologic evolution and breach effluent hydrographs. The instrumentation layout included: i) *2 HD cameras* and *2 Azure Kinect sensor* (depth cameras) to characterize the breach morphology through imaging techniques and 3D reconstruction; ii) 1 *Go Pro high-speed camera* operating at an acquisition rate of 240fps combined with an *automatic particle dispenser* to estimate the surface velocity maps in the breach vicinity through the application of a PTV algorithm; iii) several *acoustic level probes* to measure the water levels inside the main channel and sediment's basin; iv) an *electromagnetic flow meter* to determine the inflow.

The breach effluent hydrograph was estimated in two ways: i) data processing of the water levels inside the sediment's basin, i.e. above the crest of a v-notch weir, considering the respective rating curve (non-local estimation); ii) through the multiplication of the flow velocity (surface velocity maps) by the area of the breach (flow transition area, i.e. defined as the vertical space between the free water surface and the dike wet bank, where the vertical component of the surface flow velocity can no longer be disregarded).

Three dike failure experiments are presented (S1T1; S1T2 and S2T1), all of them with 0.5m high, 2.0m long, a crest width of 0.10m and with upstream and downstream slopes of 1V:1.5H. Two silty-sands soils differing on the granulometric mixtures (S1; S2) and two inflow conditions were used in the experiments ((1); (2)). Samples collected during construction ensured dikes were constructed under the *stand. Proctor test* conditions. The soils, inflow conditions and geotechnical characteristics of the three experiments are resumed in Table 1.

Table 1. Dikes experiments geotechnical characteristics

| Failure Test | Soil | IC | $w_{op}$ (%) | $\gamma_d^{max}$ (kN/m$^3$) | $w_{exp}$ (%) | $\gamma_d^{exp}$ (kN/m$^3$) | CD (%) |
|---|---|---|---|---|---|---|---|
| S1T1 | $d_{50}^{S1}$=0.6mm 10% fines | variable | 9.2 | 18.6 | 7.3 | 17.7 | 95.4 |
| S1T2 | | constant 80 l/s | 9.2 | 18.6 | 10.4 | 18.6 | 99.8 |
| S2T1 | $d_{50}^{S2}$=0.2mm 20%fines | | 14.4 | 16.6 | 13.4 | 15.6 | 94.2 |

IC – Inflow conditions; $w_{op}$ – Optimum water content; $\gamma_d^{max}$ – maximum dry density; $w_{exp}$ – experiment water content; $\gamma_d^{exp}$ – experiment dry density; CD – Experiment compaction degree;

## 2. Experimental results

The observation of the morphologic evolution of the breach (Figure 2, right) shows that for the same breach effluent flow (FB-Flow≈30 l/s), the breach is much wider and shallow in both experiments S1T2 and S2T1(≈0.4m), while in experiment S1T1 the breach is narrower but deeper (≈0.16m). In the latter experiment (S1T1) it was also observed that the variability of the main channel inflow led to the detachment of large masses of soil from the dike body, while in the former (S1T2 and S2T1) the dike erosion was found to be mainly of hydraulic nature, i.e., a progressive erosion with no sudden widening of the breach. These sudden detachments, lead the breaching process to take place much faster, meaning the peak discharge of the breach effluent flow to be achieved considerably sooner as it is demonstrated by Figure 2, left.

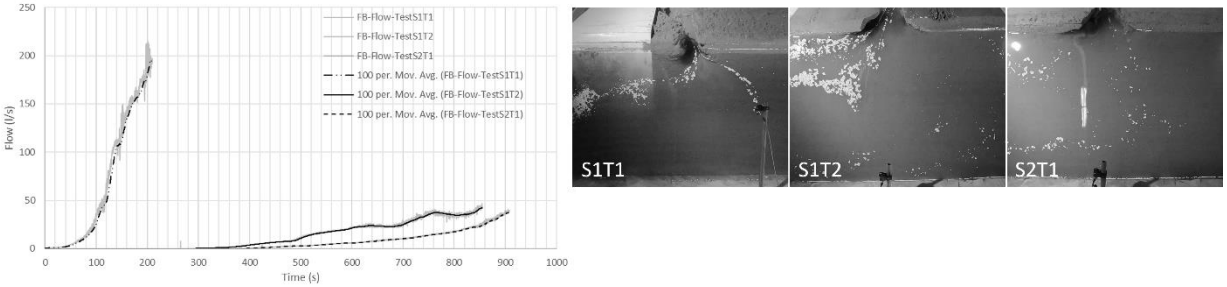



Figure 2. Left – Breach effluent hydrographs; Right – Breach morphologic evolution in each experiment for the same flow (30 l/s).

## 3. Conclusions

This study allowed to evaluate the impact on the breach morphologic evolution of the soil composition and inflow conditions. It was found that maintaining the inflow conditions, through a constant water level, is essential for tests reproducibility, since sudden variations in the water levels upstream the dike can lead to erosion phenomena on the dike body that do not occur at a prototype scale. Also, contrary to expectations, the variation in the granulometric mixture of the soil, within the range of silty sands, did not have any impact on the dike breaching behavior, neither in terms of peak flows nor in the morphologic evolution of the breach. As no effective model is actually available for these processes simulation, all new experimental data contributes to a better understanding of the phenomenon as a whole, and hence, to calibrate computational models, which is also one of the future aims of this work.

**Acknowledgements**

Financial support of the Portuguese Foundation for Science and Technology through the PhD scholarship 2021.07337.BD and the FCT project DikesFPro with reference: PTDC/ECI- EGC/7739/2020.

**References**

Amaral, S., Caldeira, L., Viseu, T. & Ferreira, R., 2020. Designing experiments to study dam breach hydaulic phenomena. Journal of Hydraulic Engineering, 146(4).

# A New Regulation System for PRS Turbines

Calogero PICONE[1], Marco SINAGRA[1], Tullio TUCCIARELLI[1]

[1] Department of Engineering, University of Palermo, 90128 Palermo, Italy
tullio.tucciarelli@unipa.it

ABSTRACT

The variability of the flow rate in mini-hydro plants is one of the major sources of energy dissipation and efficiency reduction. A new Regulation System for Power Recovery System (PRS) turbines, able to maintain good efficiencies working within a large range of flow rates, is proposed. This is accomplished by changing the present flap regulation system with a new device component moving in linear direction in order to reduce the normal cross flow section of the nozzle. The energy dissipation due to the change of the section is minimized with a smooth shape of the new component. The expansion of the flow rate inside the runner is controlled with the use of the baffles dividing the total width of the runner in several parts.

## 1. Cross-flow type turbines regulation systems review

PRS (Sinagra et al, 2021) is a Cross-flow type turbine which combines both the functions of Pressure Regulation Valves (PRV) and of mini-turbines for hydropower production. PRS has shown in numerical simulations (Sinagra et al, 2021), in several laboratory (Sinagra et al, 2019) and real field applications (Sinagra et al, 2023) to achieve hydraulic efficiencies up to 80%, especially in the case of medium and low head jumps.

In order to provide hydraulic regulation, PRS has a mobile part that can be controlled by an actuator. The original Banki turbine (also named Ossberger) has a specially shaped regulating system which has the property to regulate the velocity field inside the nozzle outlet according to the occurring flow rate. The PRS turbine is equipped with patented pressurized diffuser (Tucciarelli et al, 2021), and in case of positive outlet pressure the Ossberger regulation mechanism is no more efficient. A possible alternative device is a cylindric curve arc (marked 3 in Fig. 1) which partially closes the nozzle outlet surface in order to keep constant the inlet velocity in spite of the flow rate changes. This flap maintains good efficiencies, at least for a total inlet reduction smaller than 25%. For larger reductions, an efficiency drop larger than 30% occurs. Another major inconvenient of the above flap is that the noise generated by the turbine increases along with the flap closure. Because hydraulic regulation nodes, along aqueducts, are usually placed close to residence areas, the noise increment turns out to have a significant environmental impact.

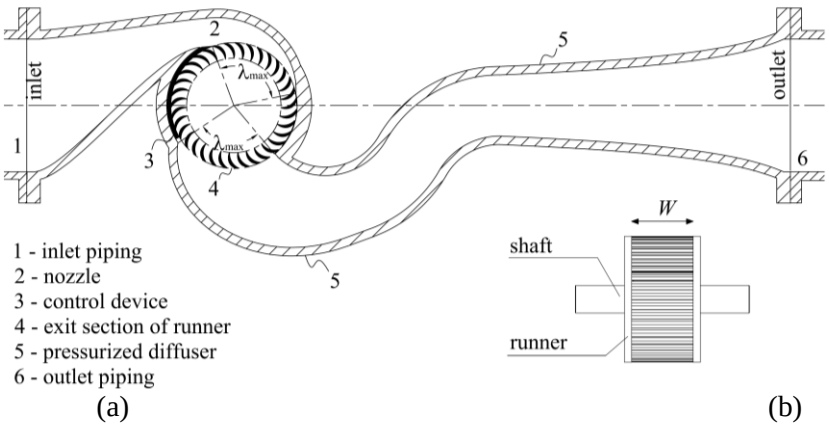



**Fig. 1.** PRS turbine: (a) Section view of the turbine in a symmetry plan; (b) Side view of the runner.

## 2. New PRS Regulation System

In order to improve the PRS performance a new regulation device is proposed. The device leaves unchanged the extension of the nozzle outlet arc, measured along a plane normal to the turbine axis, but regulates the width of the nozzle through a strut with rectangular section moving in the same turbine axis direction. This solution allows the flow to converge into a smaller cross-section which varies continuously with the variation of the flow rate (Fig. 2).

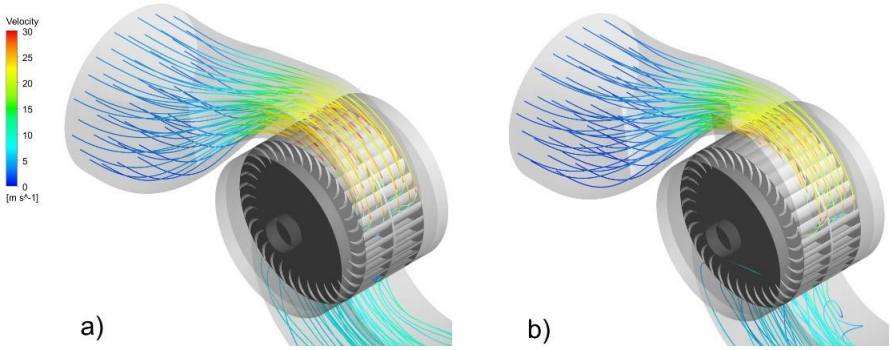



**Fig. 2.** PRS turbine with new regulation system: a) 100% opening; b) 65% opening.

The reduction of the width of the water flow inside the nozzle leaves of course unchanged the width of the runner. If the width of the blades is designed for a given flow rate, the reduction of the width of the nozzle section leads to an expansion of the water flow inside the runner. To avoid this expansion a proper number of baffles is designed, in order to limit the maximum expansion of the flow rate to the distance between two consecutive baffles.

## 3. Preliminary numerical results

The efficiency of the new device is computed solving the associated CFD problem using ANSYS CFX software (Sinagra et al, 2021, Picone et al, 2021), for a given study case and according to different strut regulations. The same code has previously proven to provide results very close to the experimental ones in several applications of PRS type turbines (Sinagra et al, 2019). In Table 1 the 3D Hydraulic efficiency, computed for 4 positions of the regulation system (100%, 75%, 50%, 25%), are shown. The results show the same maximum efficiency, equal to 73.5%, for both cases of 100% and 50% opening. For the case of 75%, we observed a reduction of efficiency lower than 2%. Instead, the 3D hydraulic efficiency, computed for case of 25% opening, is equal to 62%. The value of flow rate varied in the range 4.85 – 16.40 L/. Results seem to highlight a non-linear relationship between the reduction of the inlet section and the flow rate regulation for small relative wall distance.

**Table 1.** Summary of the numerical results to characterize new Regulation System

| Opening [%] | Head drop [m] | Flow rate [L/s] | Efficiency [%] |
|---|---|---|---|
| 100 | 16 | 16.4 | 73.5 |
| 75 | 16 | 13.0 | 72.8 |
| 50 | 16 | 9.0 | 73.5 |
| 25 | 16 | 4.9 | 62.0 |

The new Regulation System will soon be tested in our experimental facility for micro-turbine analysis.

**Acknowledgements**

This work was supported by the project “SWAMM - Azione 1.1.1 POC 2014-2020 Completamento graduatoria Azione 1.1.5 P.O. FESR SICILIA 2014 – 2020 Cod. Prog 08CT00CT270264 CUP G77H18001660006”.

**References**

Picone C, Sinagra M, Aricò C, Tucciarelli T (2021). Numerical analysis of a new cross-flow type hydraulic turbine for high head and low flow rate. Eng. Appl. Comput. Fluid Mech 15:1491–1507. https://doi.org/10.1080/19942060.2021.1974559

Sinagra M, Aricò C, Tucciarelli T, Amato P, Fiorino M (2019) Coupled electric and hydraulic control of a PRS turbine in a real transport water network. Water 11:1194. https://doi.org/10.3390/w11061194

Sinagra, M., Creaco, E., Morreale, G. (2023). Energy Recovery Optimization by Means of a Turbine in a Pressure Regulation Node of a Real Water Network Through a Data-Driven Digital Twin. Water Resour Manage 37:4733–4749

Sinagra M, Picone C, Aricò C, Pantano A, Tucciarelli T, Hannachi M, Driss Z (2021). Impeller Optimization in Crossflow Hydraulic Turbines, Water 13, 313. https://doi.org/10.3390/w13030313

Tucciarelli T, Sinagra M, Morreale G, Amato P, Picone (2021). Diffuser for in-line hydraulic turbine, Italian Patent n. 102021000001214 submitted 22nd January 2021.

# Cross Border Cascading Hazard Scenarios in Sava River Basin – Results of the CROSScade Project

Gašper RAK[1], Matjaž ČETINA[1], Mirko KOSIČ[2], Jure ŽIŽMOND[3], Andrej ANŽLIN[2], Gorazd NOVAK[1]

[1] Faculty of Civil and Geodetic Engineering, University of Ljubljana, Slovenia
gasper.rak@fgg.uni-lj.si; gorazd.novak@fgg.uni-lj.si; matjaz.cetina@fgg.uni-lj.si

[2] Slovenian National Building and Civil Engineering Institute (ZAG), Slovenia
mirko.kosic@zag.si; andrej.anzlin@zag.si

[3] SPEKTRAL Engineering d.o.o, Slovenia
jure.zizmond@spektral.si

ABSTRACT

CROSScade (Cross-border cascading risk management for critical infrastructure in the Sava River Basin) project addressed the risks caused by earthquakes, floods, and their possible cascading sequence of events along the Sava River within the border region between Slovenia and Croatia. This paper discusses the developed scenarios focusing on flood and seismic scenarios, which are used in the following stages of the project to assess the critical infrastructure in the studied area.

## 1. Introduction

The recent extreme events, i.e. the earthquakes in Croatia in 2020 and the floods in Slovenia in 2023, exposed seismic and flood vulnerability of the neighbouring countries Slovenia and Croatia. To investigate cross-border and cascading consequences of such events, representative scenarios were studied using both, hydraulic and seismic simulations. The hydraulic simulations were used to examine the consequences of malfunction or breaching of HPP Brežice due to severe earthquakes, while seismic simulation provided input for vulnerability analysis of other critical assets (bridges, levees, roads etc.) that are crucial for emergency response.

## 2. Hydraulic simulations

Five most relevant HPP Brežice malfunctioning and breaching scenarios were first selected based on the results of previous studies. The hydraulic modelling was performed in two stages: i) for the model of the reach between HPP Brežice and the Slovenia–Croatia border, and ii) for the reach between the Slovenia - Croatia border and Zagreb.

The five scenarios were first analysed using the MIKE FLOOD software that combined a one-dimensional (1D) and a two-dimensional (2D) approach. The 1D approach was used for the main channel and the accumulation between the embankments, while 2D was used for the flow over inundations. The 1D and 2D parts were dynamically coupled, allowing the 1D+2D model to function as a unit. Input for the numerical model was generated from LIDAR data, featuring a typical cell size of 20 x 20 m. The model underwent calibration, validation, and testing based on field measurements and results obtained from the physical model. The main features of the model are shown in the left part of Fig. 1.

The results of this model were in the second stage used as input for a HEC-RAS 6.3.1 dynamically coupled 1D+2D model covering reach between the Slovenia - Croatia border and Zagreb. To capture details of topography that significantly influence the water flow, the computational mesh was locally refined with dimensions of 10 x 10 m to 20 x 20 m. The model was calibrated based on rating curves of gauge stations Podsused and Zagreb. An example of the flooded area for one of the examined scenarios (Scenario 5 - breaching of the Brežice HPP embankment) is shown in the right part of Fig 1.

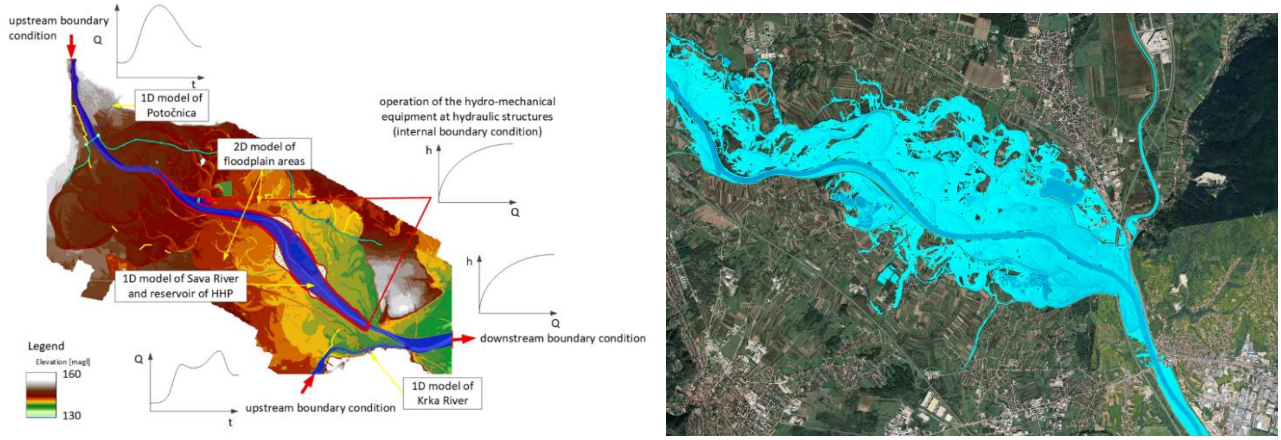



**Fig. 1.** Hydraulic model of the Brežice – state border reach (left), flooded areas of the state border – Zagreb reach for scenarios 5 – breaching of the Brežice HPP embankment (right).

## 3. Seismic simulations

Two representative seismic scenarios were selected for examination of cross-border impacts in the case study area. Scenario 1 represents the historic Brežice 1917 earthquake with an estimated magnitude of $M_w$ = 5.7, while Scenario 2 represents the 1880 Great Zagreb earthquake with an estimated magnitude of $M_w$ = 6.0.

The two seismic scenarios were quantified based on numerical simulations to provide the spatial distribution of peak ground acceleration (PGA), used to analyse the seismic vulnerability of critical infrastructure in the area. For each scenario, a set of 500 simulations was performed to provide appropriate consideration of inter- and intra-event variability. For this purpose, the case study area was divided into a raster of cells with dimensions 0.5 km x 0.5 km. The simulations were based on a regionally-adaptable ground motion model developed with the European research project ESHM20 (Danciu et al. 2021). An example of the mean PGA fields obtained for the two scenarios is shown in Fig. 2.

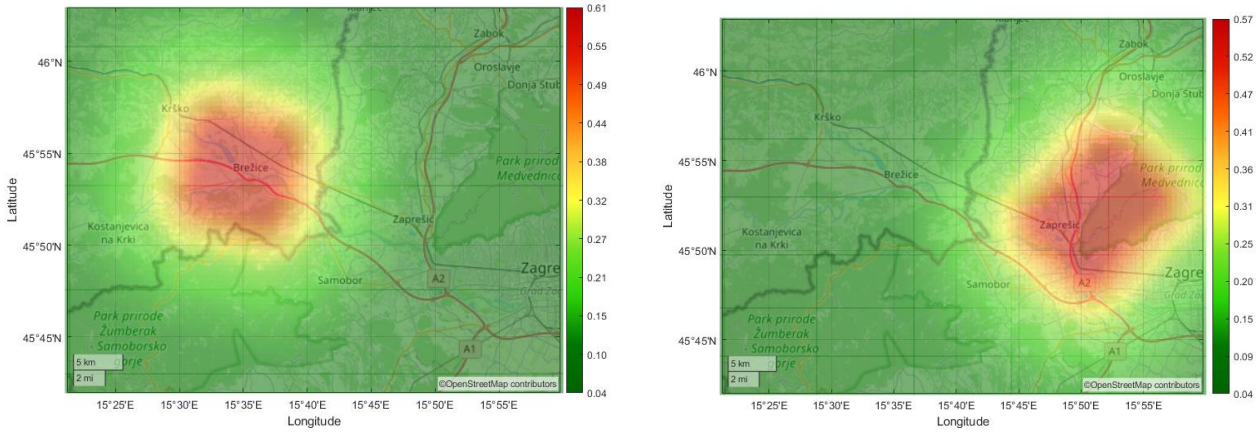



**Fig. 2.** Mean PGA fields for the seismic scenario in Slovenia (left) and Croatia (right).

## 4. Conclusions

The presented hydraulic models allowed adequate determination of the time series of water depths and flow velocities acting on bridge piers and levees, as well as the expected flood extent. The seismic simulations provided the input for the vulnerability analysis of the bridges and levees in the case study area. The results of both simulations have been used as state-of-the-art input for various detailed studies performed within the following tasks of the CROSScade project. More information can be found on the project's webpage.

**Acknowledgements**

Project CROSScade (Cross-border cascading risk management for critical infrastructure in the Sava river Basin) is co-funded by European Union, Grant Agreement Number 101048395.

**References**

Project CROSScade, Deliverable D3.2, Cross–border cascading hazard events and scenarios, https://crosscade.eu/documents/
L. Danciu et al. The 2020 update of the European Seismic Hazard Model ESHM20: Model Overview. EFEHR Technical Report 001, v1.0.0, pp. 1–121, 2021.

# Statistically sound approach to compare oil patterns and assess the accuracy of the forensic findings

Ana Catarina ROCHA[1,2], Carla PALMA[1], Ricardo J.N. BETTENCOURT DA SILVA[2]

[1] Hydrographic Institute, Rua das Trinas 49, Lisbon, Portugal
catarina.rocha@hidrografico.pt

carla.palma@hidrografico.pt

[2] Centre for Structural Chemistry, Faculty of Science of the University of Lisbon, Lisbon, Portugal
rjsilva@ciencias.ulisboa.pt

ABSTRACT

## 1. Introduction

Oil spills in marine environments are common and represent a significant environmental concern. Chemical analyses of spill samples (Sp) and suspected sources (SS), collected in the spill and potential sources, are used in court to assign legal liability. These analyses rely on characterizing the chemical composition of oil samples (oil fingerprints), using a set of ratios between abundances of oil-discriminating compounds, known as diagnostic ratios (DR), and comparing the fingerprints using statistical approaches. The Nordtest guideline (Faksness et al., 2002) and the standard EN 15522-2 (European Committee for Standardization, 2023) are two analytical methodologies that have been employed for the comparison of DR observed in two samples using distinct DR comparison conditions and approaches, *i.e.*, *t*-Student test (S-t) and a single criterion (SC) applied to the comparison of all DR of the fingerprint, respectively. These approaches assume assumptions or approximations, such as the normality of the DR probability distributions, that can lead to a higher probability of inaccurate findings. However, it is known that the ratio of independent or correlated random variables, such as oil component abundances, can deviate significantly from normality (Bettencourt da Silva, 2016). Therefore, it is necessary to develop new methods for interpreting results that are based on suitable statistical approaches and assumptions in order to guarantee the quality of the identifications. Moreover, the weight of the chemical analysis presented as evidence (E), often expressed as a likelihood ratio (LR), must be demonstrated in court. The LR is a ratio of conditional probabilities that assesses the evidence's contribution to the prosecution and defense hypotheses, namely, that the perpetrator of the oil pollution is the defendant and the perpetrator of the oil pollution is someone other than the defendant, and its determination is challenging and requires databases or statistical models (Thompson et al., 2012).

This work introduces a novel approach to accurately model DR probability distributions, using simulation by Monte Carlo Method (MCM), providing statistically sound criteria for DR comparison. The developed set of computational tools compare samples' fingerprint, and estimate the probabilities of true (TD) and false (FD) declaration of oil fingerprints equivalence used to determine LR. This allowed compare the performance and the quality of the identifications obtained by the new approach with the S-t and SC approaches.

## 2. Methodology

Four computational tools were developed in MS-Excel spreadsheets: one tool to simulate different output variables ($DR_{Sp}$, $DR_{SS}$ or DR means, and $\left(\overline{DR}_{Sp} - \overline{DR}_{SS}\right)$), and three tools to estimate the FD by MCM, S-t and SC approaches using the simulated data (Fig. 1). Rocha et al. (2022) describe the MCM simulation procedure and the estimation of DR comparison criteria in detail.

To show the applicability of the proposed computational tools and assess the performance of the MCM, S-t and SC approaches, Sp and SS from a Round Robin Test were used. All samples were prepared and analysed by Gas Chromatography-Mass Spectrometry according to EN 15522-2. Two DR comparison scenarios were

tested: Nordtest, which compared DR means from triplicate analysis, $A/(A+B)$ ratio format and S-t approach, and EN 15522-2 which compared DR means from duplicate analysis, $A/B$ ratio format and SC approach.

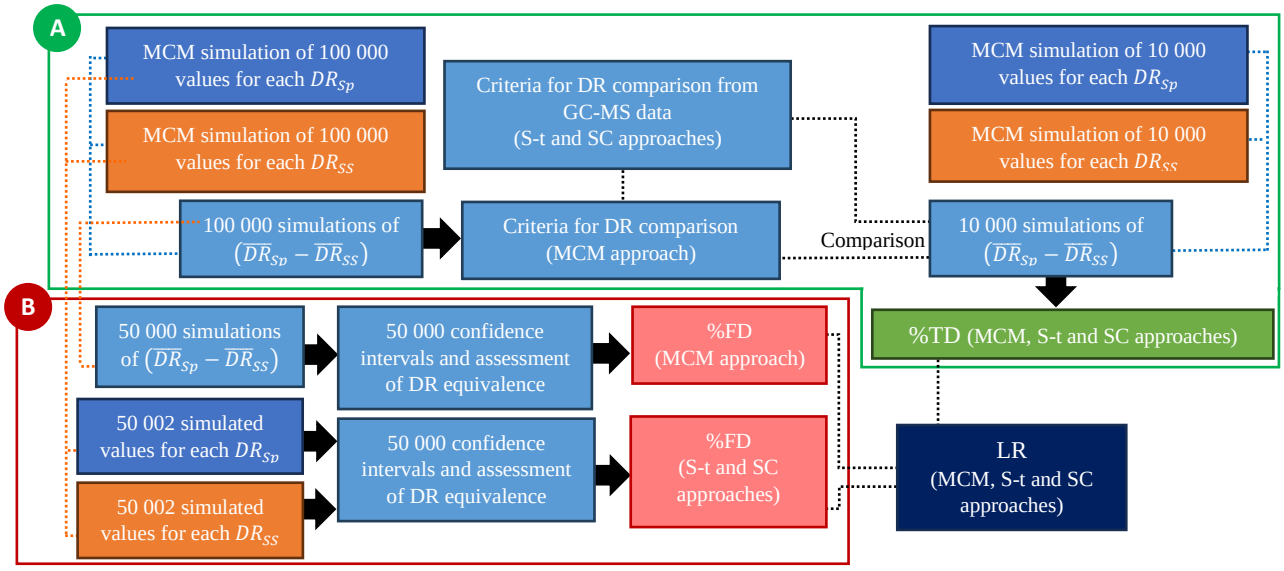



**Fig. 1.** Assessing of spill (Sp) and suspected sources (SS) compositional equivalence and determining true (TD) and false (FD) declarations of samples' compositional equivalence used for likelihood ratio (LR) calculation: A – Simulation of DR for Sp and SS and simulation of TD where Sp is a spill from SS; B – Simulation of FD where Sp is not a spill from SS.

## 3. Results

The MCM, S-t, and SC approaches were used to perform compositional equivalence/difference declarations and assess the evidence's strength using LR. The S-t approach demonstrated to create stricter DR comparison criteria, comparing to MCM approach, resulting in decreased TD and decreased or increased FD rates depending of the number of DR compared (*e.g.*, 95.3% and 2.42% by MCM, and 83.4% and 3.31% by S-t, respectively). The SC approach produces criteria that are both broader and narrower than those provided by the MCM approach, but they vary less along to 50,000 performed simulations (dependent only on the DR means of Sp and SS) than those defined by the MCM, which depend on the degrees of freedom and the DR dispersion for both samples. Thus, it is more unlikely that the produced SC criteria identify equivalent DR, which reduces TD and FD (*e.g.*, 95.4% and 4.19% by MCM, and 64.5% and 0% by SC, respectively). Thus, the potential of the S-t approach to identify the spill source and to discriminate a pair of SS, stated by the LR, was found to be lower than that of the MCM approach, owing to the S-t's propensity to estimate lower TD and greater FD, particularly when a small number of DR is compared. An analysis using the SC approach appears to discriminate better SS than the MCM approach. Despite estimating zero FD, the SC approach estimates lower TD, allowing for SS discrimination but identifying the spill source with lower reliability.

## 4. Conclusions

The computational tools developed achieved the proposed objectives, allowing evaluating the performance of the MCM, S-t and SC approaches in identifying a spill source. The developed MCM approach demonstrated performance advantages over the other approaches, such as notably greater TD rates. As a result, when this approach is used to compare oil fingerprints, the strength of the evidence provided is assured to be increased.

**Acknowledgements**

The authors are thankful for the volunteer organisation of Round Robins Tests on the identification of oil spills by the Oil Spill Identification Network of Experts within Bonn Agreement (Bonn-OSINet).

**References**

Bettencourt da Silva, R.J.N., (2016) Evaluation of trace analyte identification in complex matrices by low-resolution gas chromatography – mass spectrometry through signal simulation, Talanta, 150, 553–567.
European Committee for Standardization (2023) Oil Spill Identification - Petroleum and Petroleum Products - Part 2: Analytical Method and Interpretation of Results Based on GC-FID and GC-low Resolution-MS Analyses; EN 15522-2:2023 E. European Committee for Standardization, Management Center, Brussels, Belgium.
Faksness, L.-G., Weiss, H.M., Daling, P.S. (2002) Revision of the Nordtest methodology for oil spill identification; STF66 A01028. SINTEF Applied Chemistry: Trondheim, Norway.
Rocha, A.C., Palma, C., Bettencourt da Silva, R.J.N. (2022) Optimisation of the uncertainty of oil spill identification from replicate comparative analyses: Comparison of standardised and novel identification methods, Chemosphere, 308, 136201.
Thompson, W.C., Grady, R.H., Lai, Eric, Stern, H.S. (2018) Perceived strength of forensic scientists' reporting statements about source conclusions Law, Probability and Risk, 17,133-155.

# Planning and development of burst event field tests in a real water distribution network

Bruno FERREIRA[1], João CAETANO[2], Soraia ALMEIDA[3], Nelson CARRIÇO[4], Dídia COVAS[5]

[1,4] Escola Superior de Tecnologia do Barreiro, Instituto Politécnico de Setúbal, Rua Américo da Silva Marinho, s/n, 2839-001, Barreiro, Portugal
bruno.s.ferreira@estbarreiro.ips.pt
nelson.carrico@estbarreiro.ips.pt

[2,5] CERIS, Instituto Superior Técnico, Universidade de Lisboa, Av. Rovisco Pais 1, 1049-001, Lisboa, Portugal
joao.caetano@estbarreiro.ips.pt
didia.covas@tecnico.ulisboa.pt

[3] Inframoura, Rua das Amoreiras, 8125-497, Quarteira, Portugal
soraiaalmeida@inframoura.pt

ABSTRACT

The current study describes the planning and implementation of a procedure for collecting pressure and flow rate data during the occurrence of simulated pipe burst events. A real water distribution network (WDN) was selected, and pipe burst events were simulated by opening an existing hydrant whilst monitoring the flow rate at the inlet of the system and pressure at five specific locations. The collected data will be used to assess the effectiveness of developed pipe burst detection and location techniques.

## 1. Purpose

Recent developments in online hydraulic modelling allow the use of techniques based on steady-state or extended-period hydraulic simulations to locate burst events in near-real time. Distinct approaches have been developed which can be based on solving the inverse problem, calculating the network sensitivities, focusing on error-domain model falsification, or using a classifier (Hu et al. 2021; Wan et al. 2022). Most techniques are tested by artificially generating pressure and flow rate data on pipe burst events using a hydraulic simulation model (i.e., using artificial data) and are rarely validated using real data collected during the occurrence of pipe burst events.

## 2. Materials and Methods

The WDN is in a touristic area in Portugal's southernmost region with high-demand seasonality. The WDN has a total length of 16 km of pipes with 309 service connections. The supplied area is mainly composed of villas with large irrigated gardens and some hotels. The network is supplied by one storage tank connected to a pumping station. An electromagnetic flowmeter is installed downstream of the pumping station with an acquisition time step of 5 minutes. Consumption is measured at all households on an hourly basis using 1133 smart meters. Most users have two smart meters, one for household consumption and another for irrigation.

Figure 1 depicts a spatial representation of the WDN in terms of closed valves, pipe diameters, pressure sensors, and simulated pipe burst events. The network operation scheme was changed to increase the head losses during the tests (and, consequently, during a pipe burst event) by closing six isolation valves. This was done because the burst tests were carried out during the winter season and the pipe diameters are oversized for the actual water consumption. A week of water consumption was analyzed to ensure that the new operation scheme did not jeopardize the minimum pressure requirements during peak hours. Five pressure sensors were installed at specific locations. The number and location of such sensors were obtained using the method described by Ferreira et al. (2021, 2022). The acquisition time step for pressure data was set as 1 minute.

The pipe burst events were simulated by opening a fire hydrant at four specific locations. A hose was connected to the hydrant so that the discharged water filled urban hygiene equipment (such as sweepers), which was later used for street washing and garden irrigation.

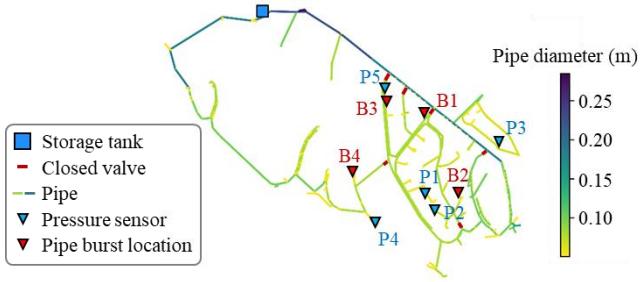



**Fig. 1.** Spatial representation of the WDN in terms of closed valves, pipe diameters, pressure sensors, and simulated pipe burst events.

## 3. Results and Discussion

The network sectioning was carried out on February 3rd, 2023, and the burst simulations were carried out on February 7th. The data between the February 3 and 7 will be used in the future to calibrate the hydraulic simulation model in terms of pipe roughness, nodal elevation, and pumping settings.

The fire hydrants had a total diameter of 1.5'' (38.1 mm) and with full opening, it was possible to produce burst flow rates between 2 and 3 L/s (depending on the location and respective pressure). This increase in flow rate originated considerable pipe head loss and, consequentially, a distinct signature across the five pressure sensors is observed. Figure 2a depicts the inlet flow rate data, whilst Figure 2b depicts the pressure in each of the five pressure sensors. The beginning and end of each pipe burst event is depicted as blue vertical lines.

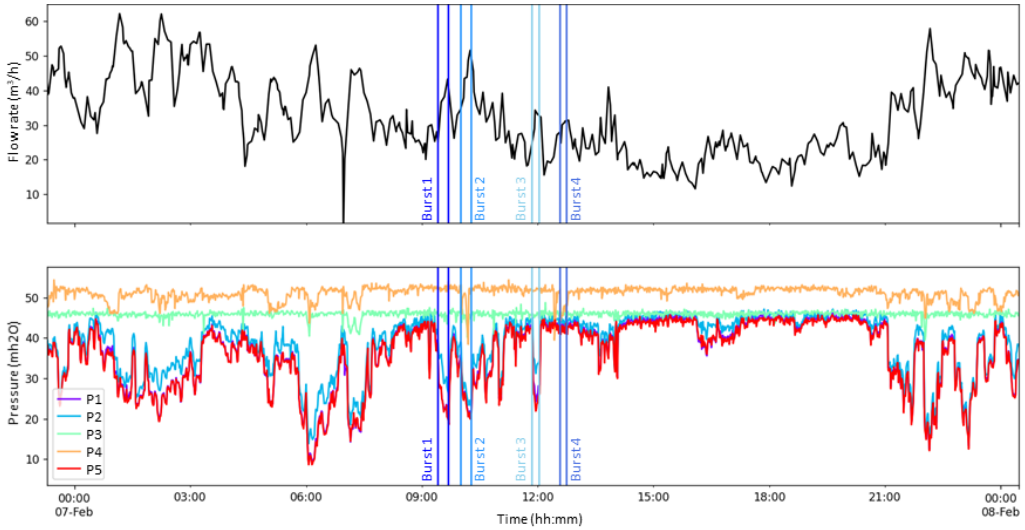



**Fig. 2.** (a) inlet flow rate; (b) pressure data in each of the five pressure sensors.

## 4. Final remarks

The burst tests were successfully carried out since collected pressure and flow rate data during the four events contain a clear signature of the burst event. Data were collected with the highest sampling rate allowed by the available equipment, that is, 1 minute for pressure sensors, 5 minutes for inlet electromagnetic flowmeter, and 1 hour for household consumption. Still, this sampling rate does not provide true instantaneous results since household consumption is associated with a period of 1 hour. The next steps will focus on testing the developed burst detection and location techniques using the collected data.

### References


Ferreira, B., A. Antunes, N. Carriço, and D. Covas. 2022. "Multi-objective optimization of pressure sensor location for burst detection and network calibration." Comput. Chem. Eng., 162: 107826. Elsevier Ltd. https://doi.org/10.1016/j.compchemeng.2022.107826.

Ferreira, B., N. Carriço, and D. Covas. 2021. "Optimal Number of Pressure Sensors for Real-Time Monitoring of Distribution Networks by Using the Hypervolume Indicator." Water, 13 (16): 2235. https://doi.org/10.3390/w13162235.

Hu, Z., B. Chen, W. Chen, D. Tan, and D. Shen. 2021. "Review of model-based and data-driven approaches for leak detection and location in water distribution systems." Water Supply, 21 (7): 3282–3306. https://doi.org/10.2166/ws.2021.101.

Wan, X., P. K. Kuhanestani, R. Farmani, and E. Keedwell. 2022. "Literature Review of Data Analytics for Leak Detection in Water Distribution Networks: A Focus on Pressure and Flow Smart Sensors." J. Water Resour. Plan. Manag., 148 (10). https://doi.org/10.1061/(asce)wr.1943-5452.0001597.

# AI-Anomaly Project: Condition Assessment of Urban Water Assets through the Detection of Cracks based on Artificial Intelligence Methods

Marta CABRAL[1], José Pedro MATOS[2], Ana SILVA[3], Jónatas VALENÇA[4], Isel GRAU[5,6], Bruno SANTOS[7], Tiago CORREIA[8]

[1,2,3,4,7,8] CERIS, Instituto Superior Técnico, Universidade de Lisboa, Lisbon, Portugal
[5] Information Systems Group, Eindhoven University of Technology, The Netherlands
[6] Eindhoven Artificial Intelligence Systems Institute, Eindhoven University of Technology, The Netherlands
marta.f.cabral@tecnico.ulisboa.pt
jose.matos@tecnico.ulisboa.pt
ana.ferreira.silva@tecnico.ulisboa.pt
jonatas.valenca@tecnico.ulisboa.pt
i.d.c.grau.garcia@tue.nl
oliveirasantos@tecnico.ulisboa.pt
tiago.pinto.correia@tecnico.ulisboa.pt

ABSTRACT

The current paper aims at presenting the project AI-Anomaly which contributes to innovate, extend and automate the existing condition assessment approach of urban water assets by identifying and classifying anomalies in inspectable components. A dataset of photographic recordings collected from in situ inspections of water storage tanks and pumping stations is used and processed, including drawing and labeling of cracks, image binarisation and division into patches with a specific resolution. An existing convolutional neural network pre-trained with images of concrete surfaces with and without cracking is applied to these urban water assets. Different explicability artificial intelligence methods are applied to ensure the transparency of the used artificial intelligence methods and the identification of bias in the results.

## 1. Introduction

Urban water assets are continuously deteriorating and more investments are necessary to maintain adequate levels of service despite investment budgets are often limited. In the context of the urban water rehabilitation process, the asset condition assessment plays a key role in the investment planning and the establishment of operation & maintenance (O&M) programmes, being the basis and the first step towards the development of infrastructure asset management plans (Banjevic, 2009). The current paper aims to present the "AI-Anomaly Project: Condition Assessment of Urban Water Assets through the Detection and Classification of Anomalies based on Artificial Intelligence Methods" developed by a multidisciplinary team, including specialists in computer science and civil engineering, such as hydraulics, hydrology, construction and structures.

## 2. AI-Anomaly Project

The AI-Anomaly Project aims at innovating, extending and automating the existing condition assessment approach of vertical water assets developed by Cabral et al. (2022), by identifying and classifying anomalies in inspectable components. Vertical assets are assets that are not buried and whose condition is likely to be directly assessed by visual inspection (e.g., water storage tanks, pumping stations and treatment plants). The project is divided into five tasks: (i) Review and improve the current condition assessment approach of vertical water assets, considering the procedures used in other areas of civil engineering, namely construction and structures; (ii) Improve the inspection process and organize the inspection data; (iii) Apply and compare Artificial intelligence (AI) methods to identify and classify anomalies of inspectable components; (iv) Apply and compare explainable AI methods; and (v) Scientific dissemination of the project.

In situ inspections of vertical urban water assets are carried out, including a complete photographic record of identified anomalies in different inspected components, as well as the technical characterization of the assets and the identification of operation and maintenance practices. A dataset of photographic recordings collected from low-resolution cameras is obtained not taking into consideration the camera positions and environment conditions to represent real-world situations. Figure 1 depicts the steps of image processing that include drawing and labeling of cracks (Fig. 1b) and image binarisation (Fig. 1c). Additionally, drawn and binary images are divided into patches with a 224 px × 224 px resolution, leading to more than 4000 images.

An existing convolutional neural network (CNN) developed by Santos et al. (2022) and pre-trained with images of concrete surfaces in buildings with and without cracking will be applied to processed images of urban water assets and results will be discussed. Additionally, different explicability artificial intelligence methods will be applied to guarantee the transparency of the methods and highlight possible biases in the results.



(a) (b) (c)

**Fig. 1.** Image processing: (a) original image; (b) image with drawn cracks; and (c) binarized image.

## 3. Conclusions

The implementation of AI methods allows for the automatic detection of anomalies, such as cracks, in urban water assets, which significantly reduces the resources needed for condition assessment. Furthermore, the use of explainable AI enhances the results for users, making the models more transparent and less similar to a “black box”. The present work is currently under development. More detailed results and conclusions will be provided further on.

**Acknowledgements**

The authors would like to thank to the *Fundação para a Ciência e a Tecnologia* (FCT) through funding UIDB/04625/2020 from the research unit CERIS – Civil Engineering Research and Innovation for Sustainability, from Instituto Superior Técnico. B.O. Santos also acknowledges the support of FCT through the Ph.D. Grant SFRH/BD/144924/2019.

**References**

Banjevic, D. (2009) Remaining useful life in theory and practice, Metrika, 69(2-3), 337-349.
Cabral, M., Loureiro, D., Flores-Colen, I., Covas, D. (2022). A Distress-Based Condition Assessment Approach of Urban Water Assets Using Novel Deterioration Indices. Water Resources Management, 36, 1075–109, DOI: 10.1007/s11269-022-03074-8.
Santos, B. O., Valença, J., Costeira, J. P., Júlio, E. (2022). Domain Adversarial Training for Classification of Cracking in Images of Concrete Surfaces. AI in Civil Engineering, 1:8. DOI: 10.1007/s43503-022-00008-6.

# Large Eddy Simulation in a Lateral Cavity Physical Model

Rita F. CARVALHO[1], Steven RESTREPO[2], Rui M.L FERREIRA[3]

[1] Dep. Civil Engineering, University of Coimbra, MARE- Marine and Environmental Research Centre, ARNET - Aquatic Research Network,
ritalmfc@dec.uc.pt
[2,3] CERIS – Instituto Superior Técnico, Universidade de Lisboa,
steven.arv2@gmail.com
ruimferreira@tecnico.ulisboa.pt

ABSTRACT

This work assesses the prediction of the flow in a lateral cavity, which is a semi-enclosed volume attached to a main channel, using Large Eddy simulation (LES). Velocity field obtained by PIV on a physical model was compared with LES results, which captured the main eddies. The main structures of the flow and the exchange mechanisms across the interface between main channel and lateral cavity were predicted.

## 1. Introduction

A lateral cavity adjacent to a main channel create stagnant zones, where the flow velocity decreases, inducing the accumulation of sediments, nutrirents, contaminants, or garbage as micro-plastics. On the other hand, contaminants released in the lateral cavity are easily sprayed to the main channel. Therefore, it is important to understand the flow patterns, velocity fields in the cavity**,** which can be influenced by various factors, including its geometrical aspect ratio, as well as the evolution of the turbulent structures responsible for the mixing processes occuring between main channel and lateral cavity. The shear layer tipical contains unsteady turbulent structures which are responsible for the entrainment of substances from or to the lateral cavity. LES is an ideal numerical model for the study of these large scale structures. For the tested conditions in this work, ratio between lateral cavity Width and Lenght (W/L) was 0.5, two contra-rotating recirculation cells are expected to be aligned longitudinally, along the channel axis with the most upstream of smaller horizontal extension and located further from the interface (Mignot et al, 2019).

## 2. Methodology

### *2.1. Physical model*

A physical model was constructed in the laboratory to reproduce a flow at the main channel, 0.39 wide and 10 m long, interacting with a lateral cavity with 0.193 m length and 0.096 m width (W/L=0.5) as can be seen in Figure 1a). A uniform flow with a discharge of 5.6 l/s is 0.072 m depth and has a velocity of 0.2 m/s, which lead to a Froude number of 0.23 and a Reynolds number of 1.6 x $10^4$, based on the free stream at the main channel. A PIV, constituted by a FlowSense USB 2M-165 camera at 1920 x 1200 px, a wave Solo PIV 120 dual laser-head system, and an imaging synchronizer from Dantec Dynamics system, was used to characterize velocity fields. With a camera placed in the flume side and a mirror under the channel, several horizontal plans of photos were aquired and treated with specific software from Dantec to obtain the velocity field.

### *2.2. Numerical model*

LES decomposes the primitive flow variables into resolved scale components that are solved explicitly, and subgrid scales components that are solved algebraically. Thus, particular attention has to be paid to the grid resolution and subgrid-scale models to close filtered equations. In this work, a fixed free-surface was considered with three dimensional spatial filtering of the Navier–Stokes equations (LES) – Eqs (1).

$$\nabla \cdot \rho\bar{\mathrm{v}} = 0; \quad \frac{\partial \rho\bar{\mathrm{v}}}{\partial t} + \nabla \cdot (\rho\bar{\mathrm{v}}\bar{\mathrm{v}}) = -\nabla\bar{\mathrm{p}} - g \cdot x\nabla\rho + \nabla \cdot \left((\nu + \nu_{SGS})\left(\nabla\bar{\mathrm{v}} + (\nabla\bar{\mathrm{v}})^T\right)\right) + F \qquad (1)$$

where $t$ – time [s], $\rho$ – density [kg m$^{-3}$], $x$ = (x, y, z) – coordinate [m], $\bar{v}$ = ($\bar{v}_x$, $\bar{v}_y$, $\bar{v}_z$) – time-filtered velocity vector [m s$^{-1}$], $\bar{p}$ – filtered pressure [N m$^{-2}$], $F$ – general source term, $\nu$ – kinematic viscosity [m$^2$ s$^{-1}$], $\upsilon_{SGS}$ – subgrid kinematic viscosity. The fluid, with a kinematic viscosity of 1.15 x 10$^{-6}$ m$^2$/s, was considered incompressible. Three distinct meshes are used with grid spacing of Δ=L/64, Δ=L/100 and Δ=L/200, leading to meshes with cells of 1 to 3 mm. Three subgrid scale models are considered: the standard Smagorinsky model with cube root ($\upsilon_{SGS} = (C_s\bar{\Delta})^2|\bar{S}|$, where $C_s$ – Smagorinsky coefficient, $\bar{\Delta}$ – is the cut-off length which is set to the cube root of the cell volume and the stress tensor $\overline{S_{ij}} = 0.5\left(\partial\bar{u}_i/\partial x_j + \partial\bar{u}_j/\partial x_i\right)$); the Van Driest model, which includes a damping function, which improve the near wall behavior, defining a damping coefficient, yielding an eddy viscosity that is zero at the walls, as it should be, and in regions in the viscous near wall region is $\bar{\Delta} = \min\left(\left(1 - e^{-y^+/A^+}\right)\kappa y/C_s, \Delta_g\right)$, where $\Delta_g$ is a geometric-based delta function such as the cube root delta; the dynamic Smagorinsky model, which is known to correct the deficiencies of the standard model through the dynamic computation of the model constant ($C_s{}^2 = \frac{0.5\langle L_{ij}M_{ij}\rangle}{\langle M_{ij}{}^2\rangle}$, where $L_{ij} = 2C_s{}^2M_{ij} + \delta_{ij}L_{kk}/3$ , $M_{ij} = \hat{\Delta}^2\widehat{|S|S_{ij}}$ , $\delta_{ij}$ – Kronecker delta, symbols with a hat denotes a test filtered quantity and $\langle\ldots\rangle$ denotes local face-averaging approach to compute the dynamic Smagorinsky coefficient). The LES reported here are performed using OpenFOAM® v2206.

## 3. Results

Unsteady simulations were performed starting from an uniform flow in the main channel, considering a uniform streamwise velocity as inflow boundary and a zero gradient at the outflow boundary. The model ran for 60 s (around 40 times relation between channel length, L, and average velocity,U) to attain a stabilized flow and then it ran until 200L/U and in this second period was averaged. Figure 1 illustrates the physical model and the PIV plans of measures in three different vertical coordinates, the streamlines of mean velocities obtained from PIV, as well as a selection of the results obtained using the different LES simulations performed with different grids and subgrid scale models.

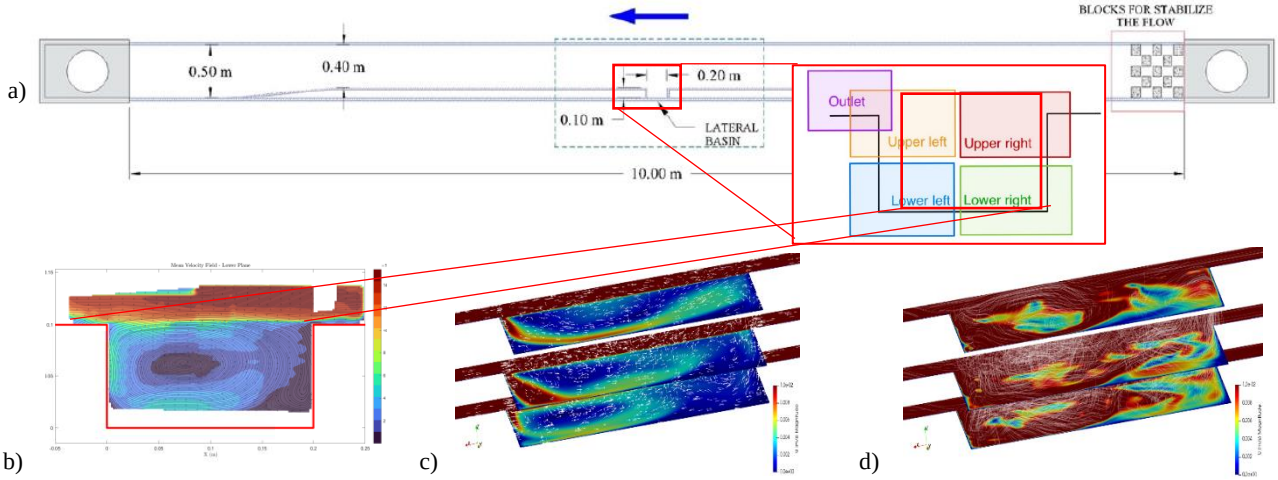



**Fig. 1**.a) Physical model scheme with the indication of PIV measurements; b) streamlines of mean velocity computed from PIV system, c) streamlines of mean velocity from LES simulations (VD mesh of 2 mm); d) instantaneous field (k, mesh of 2mm, t =250 s)

## 4. Conclusion

A CFD study employing LES to model the flow in a lateral cavity was done within OpenFOAM®, using three meshes and three sub-grid models. The use of LES allows the visualization of 3D large scale structures starting from the cavity edges and propagating downstream. The standard Smagorinsky model offers poor prediction on the coarsest grid. Performing finer grid is advantageous for producing good predictions.

**Acknowledgements**

This study had the support of national funds through Fundação para a Ciência e Tecnologia, I. P (FCT), under the projects UIDB/04292/2020, UIDP/04292/2020, granted to MARE, and LAP/0069/2020, granted to the Associate Laboratory ARNET. Grant for doctoral studies by the Convocatoria 906 of 2021 sponsored by the Ministry of Science, Technology and Innovation of Colombia (CTeI).

**References**

Mignot et.al. 2019 Environmental Fluid Mechanics (2019) 19:231–253 https://doi.org/10.1007/s10652-018-9620-x

# Numerical simulation of a plunging jet. Performance comparison between volume-of fluid and two-phase Euler solvers

António MURALHA[1], José F. MELO[1], Helena M. RAMOS[2]

[1] Hydraulics and Environment Department, Laboratório Nacional de Engenharia Civil (LNEC)
amuralha@lnec.pt, jfmelo@lnec.pt

[2] Civil Engineering, Architecture and Georesources Department - CERIS, Instituto Superior Técnico, Universidade de Lisboa,
hramos.ist@gmail.com

ABSTRACT

Complex high-velocity water flow analyses have been mainly experimentally conducted. Numerical simulations of complex flows are increasingly becoming possible, although thorough validations and calibrations are still required. In recent studies at LNEC, experimental data of dynamic pressures experimentally obtained were used to validate results from numerical simulations of a high-velocity water jet plunging into a pool. Two different OpenFOAM solvers were used: interFoam, more commonly used in free surface flows; and twoPhaseEulerFoam. An assessment was conducted to verify which of these solvers better performs in simulating the jet diffusion and energy dissipation in the plunge pool. Mean pressure, velocity and the air concentration results evidenced that, using experimental results as a reference, the twoPhaseEulerFoam, an Euler-Euler type solver, performs better than interFoam, a VOF solver. This study allowed to conclude that twoPhaseEulerFoam is an adequate option for simulating high-velocity diffusing water jets when the aim is the assessment of mean dynamic pressures on the plunge pool floor.

## 1. Introduction

Characterizing the flow inside a plunge pool is a key aspect when assessing the pressure field at the bottom of these structures, which are very relevant in the context of dam spillways safety. Simulating in experimental facilities jets with prototype velocity magnitudes is quite challenging and encompasses many feasibility limitations. Alternatively, or complementarily, numerical simulations may constitute useful means for simulating free-falling and plunging jets. For this study, numerical simulations were performed along with experimental tests. The pressures at the floor of a plunge pool produced by the diffusion and deflection of a vertical circular jet with a mean impinging velocity of 7.4 m/s into 0.8 m deep a pool were experimentally measured. Corresponding flow parameters were numerically obtained using two different solvers: interFoam, a Volume of Fraction (VOF) solver, and twoPhaseEulerFoam, an Euler-Euler solver.

## 2. Experimental Facility

An experimental facility built at LNEC with a 4.00 m long by 2.35 m wide pool was built to receive vertical water jets with impinging velocities up to 18.0 m/s. This facility was used in the present study to measure pressures in many locations of its flat horizontal floor for a jet with an impinging velocity of 7.4 m/s and a pool depth of 0.8 m.

## 3. Numerical Modeling

Two different OpenFOAM solvers, involving quite distinct formulations, were used to perform the numerical simulations: interFoam, a VOF solver; and twoPhaseEulerFoam, an Euler-Euler solver. InterFoam uses the VOF method to track the water surface and is a single-phase Euler model able to solve the Navier-Stokes equations for two incompressible, isothermal, immiscible fluids with no mixture. Two-phase Euler-Euler, a more complex and computationally demanding solver, can be used for applications with two compressible and inter-penetration phases, with the possibility of heat transfer between phases.

A numerical domain was set up to simulate the flow conditions inside the experimental facility. The domain covers the exact dimensions of the plunge pool of the experimental facility. The boundary conditions were defined as close as possible to those occurring in the experimental set-up. Four increasingly locally refined meshes with cubic cells were iteratively used until mesh independent results were achieved.

## 4. Results

### *4.1. Mean pressure at the plunge pool floor*

The mean pressure obtained using the solver twoPhaseEulerFoam is independent of the mesh for a mesh with more than 24 cells in the cross-section of the jet. Conversely, the values obtained using the solver interFoam results showed that mesh independence was not achieved during the mesh refinement process, as the dynamic pressure coefficient kept growing with the mesh refinement. Comparing the values produced by the numerical simulations with the ones measured in the experimental facility, Jamet *et al.* (2022) for the same conditions at the exact location, it is possible to conclude that the dynamic pressure coefficient derived from the solver twoPhaseEulerFoam matches quite well the experimental data for meshes with more than 24 cells in the jet cross-section. In contrast, the results obtained using the VOF solver, interFoam, tend to underestimate the pressures at the stagnation point.

### *4.2. Velocity field in the plunge pool*

The mean velocity and the air concentration along the shear stress region of the diffusing jet progressing through the plunge pool were also analysed. The numerical results can be directly compared with the published experimental results of Duarte (2014). Mesh independence is found in the results obtained by the solver twoPhaseEulerFoam, as the behaviour verified for the pressure. However, the results for the solver interFoam reveal mesh dependence. Comparing the results obtained in the numerical simulations with those provided by Duarte (2014), one finds that the solver twoPhaseEulerFoam produces higher velocities in the jet central line. However, no significant differences were found between the mesh with 24 cells in the jet diameter and the finer mesh with 36 cells, so mesh independence could be reached using this solver. Contrarily, the interFoam solver produces a velocity field closer to the experimental data, but mesh independence has not been achieved in the range of mesh refinements.

### *4.3. Air concentration in the plunge pool*

The air concentration near the impact point was analysed by comparing values obtained by the numerical simulation with Duarte's (2014) experimentally obtained values. The air concentration near the jet central line reveals that the twoPhaseEulerFoam solver is not very sensitive to mesh refinement, and the results obtained present some coherence with the measurements performed by Duarte (2014), as opposed to the results produced by the interFoam solver, that show a considerable mesh dependency, thus evidencing the limitations of the VOF model for this type of phenomenon. The result obtained by this solver for the finer of the considered meshes reveals an air concentration close to the experimental data, but no mesh independence was found.

## 5. Conclusion

The solver twoPhaseEulerFoam has proven a better capability in reproducing the pressures at the jet stagnation point and air concentrations inside the plunge pool. For the velocity field, interFoam solver analyses were inconclusive as although the results are close to those measured by Duarte (2014), the obtained core jet penetration is too short compared to previous studies. Conversely, twoPhaseEulerFoam produces a velocity field with higher velocities than interFoam and closer to the above referred author. Regarding mesh dependency, with twoPhaseEulerFoam, mesh independence was reached as opposed to interFoam. Since the computation costs are in the same range of values for both solvers, and twoPhaseEulerFoam is less mesh sensitive, allowing coarser meshes leading to similar results and a significant reduction in the computation cost, one concludes that this solver is the better suited to simulate high-velocity jets diffusion in plunge pools.

**Acknowledgements**

This research was funded by Fundação para a Ciência e Tecnologia (FCT), Portugal, grant number PD/BD/135593/2018. Infraestrutura Nacional de Computação Distríbuida (INCD) funded by FCT and FEDER (European Regional Development Fund) under the project CPCA/A2/7192/2020, Portugal, computational resources.

**References**

Jamet G., Muralha A., Melo J. F., Manso P. A., and De Cesare, G. (2022) Plunging Circular Jets: Experimental Characterization of Dynamic Pressures Near the Stagnation Zone, Water (Switzerland), vol. 14, n. 173.
Duarte R., (2014) Influence of Air Entrainment on Rock Scour Development and Block Stability in Plunge Pools, PhD Thesis, EPFL.

# Experimental Investigation of Microplastics Entrainment in Grid-Generated Turbulence: Effect of Size and Shape

Arefeh SHAMSKHANY[1], Shooka KARIMPOUR[2]

[1,2] Department of Civil Engineering, Lassonde School of Engineering, York University, Canada
shams019@yorku.ca

ABSTRACT

The surge in global plastic production has led to more plastic debris ending up in the aquatic environment. Plastic pollution has detrimental effects on aquatic ecosystems. To mitigate this pollution, it's essential to understand the behaviour and distribution of microplastics (MPs) in water. Various factors, like physical properties of MPs and transport mechanisms such as turbulent-induced mixing, affect the movement of MPs in water. This study presents experimental investigations into the behaviour of MPs of various sizes and shapes in grid-generated turbulent flow. Three distinct particle shapes - spheres, fibre-like elongated cylinders, and film-like flattened cylinders - are examined at different equivalent diameters. Multiple experiments have been conducted in a recirculating flume with varying flow rates to study the mixing and distribution of MPs affected by both the physical characteristics of the particle and hydrodynamics of the ambient flow. It is anticipated that smaller non-spherical shapes exhibit increased drag effects. As a result, smaller fibres and films deviate more from their gravity driven behaviour, leading to longer entrainment periods with the ambient flow, and ultimately, they are transported to areas farther from their source. This research provides valuable insights into the complex interaction between the physical characteristics of MPs and the ambient turbulent flow in aquatic environments, contributing to our understanding of MP distribution in water bodies.

## 1. Introduction

Over the last decade, plastic waste in aquatic environments has surged due to its durability and cost-effectiveness. Plastic waste enters water bodies via rivers, wastewater treatment plants, and stormwater runoff. Aquatic microplastics (MPs), sized between 10 μm and 5 mm, grow exponentially due to weathering, with variations in density, size, and shape affecting their distribution (Shamskhany et al., 2021). Gravity and buoyancy significantly affect the vertical transport of MPs (Song et al., 2014). Additionally, particle size plays a key role in determining transport and mixing behavior, governed by the drag force (Shamskhany & Karimpour, 2022). Shape is a crucial particle characteristic that affects drag. MPs exhibit a wide range of shapes, from regular spheres to irregular fragments. Recent studies have examined the abundance and distribution of various MP shapes in aquatic environments (Chubarenko et al., 2016). Notably, fibers are frequently detected in deep water and sediment layers. Despite the limited understanding of how non-spherical shapes impact drag force, recent experiments and numerical investigations are working towards enhancing our knowledge in this area (Khatmullina & Isachenko, 2017). This study presents an experimental investigation into the response of MP particles of varying shapes to turbulent flow.

## 2. Methodology

This study involves experiments with three different particle shapes: spheres, elongated cylinders resembling fibers, and flattened cylinders resembling films, all produced with a 3D printer. These three particle shapes are examined so far in three different equivalent diameters of $d_{eq}$ =5mm, 3mm, and 1mm. We introduce 30 particles of identical size and shape into grid-generated turbulent structures in a flume using injection pipe, varying flowrates between $Q$ =5.56e-3 $m^3/s$ and 2.22e-2 $m^3/s$. Subsequently, these particles are captured using a net positioned at specific stations downstream of the flume. A camera records the total number of particles accumulating behind the net over time, enabling the calculation of the accumulation rate in each

case. The experimental setup is depicted in Fig. 1. By comparing the accumulation rates of these MPs in different scenarios, we gain insights into the combined effects of particle size and shape on their entrainment.

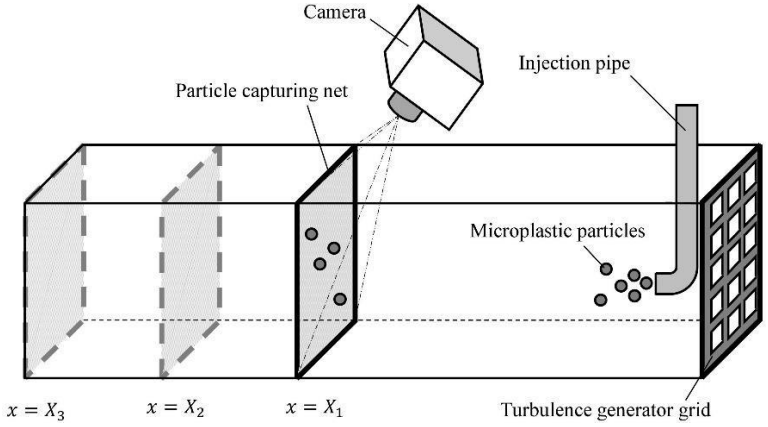



**Fig. 1.** Experimental setup sketch

## 3. Results and Discussion

The present study encompasses a broad spectrum of particle Reynolds numbers within the transitional regimes, specifically 25 < $Re_p$< 1000. This range was achieved by manipulating both the size and shape of the particles under investigation. The terminal particle Reynolds number, as observed in a quiescent flow, serves as an important indicator of the variations in particle behaviors. In this study, we use the Putnam (1961) and the Haider and Levenspiel (1988) equations to calculate the drag coefficient of spherical and non-spherical particles, respectively. Fig. 2 illustrates the relationship between the drag coefficient, $C_D$, and particle Reynolds number, $Re_p$, for each of the distinct particle shapes examined in this study. The discrete data points in Fig. 2 demonstrate the unique drag coefficients and Reynolds numbers associated with each case study.

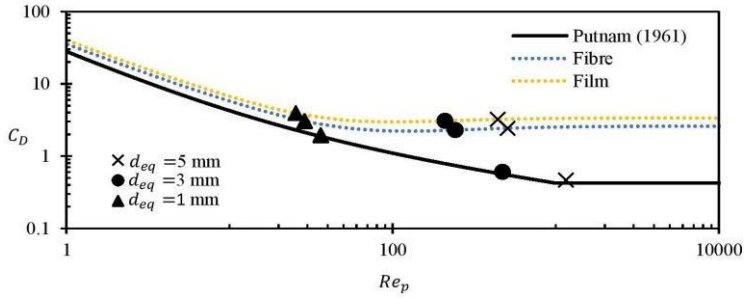



**Fig. 2.** Drag coefficient as a function of particle Reynolds number; comparison of present case studies calculated based on the equations of Putnam (1961) for spherical shape and Haider & Levenspiel (1988) for non-spherical ones.

Spheres, fibers, and films exhibit varying surface area-to-volume ratios, with spheres having the lowest, fibers intermediate, and films the highest. A smaller equivalent diameter, $d_{eq}$, and a higher surface area-to-volume ratio, lead to lower particle Reynolds numbers, $Re_p$, and increased drag coefficients, $C_D$. Consequently, the effect of drag becomes more dominant for small non-spherical shapes. It is anticipated that our results will comply with a faster arrival of small non-spherical particles at the capturing net. These particles, due to their larger drag (compared to spherical or larger particles), remain entrained in the flow and are therefore carried more quickly to farther regions from their injection source. Further analysis of the rate of accumulation of different particles will be presented at the congress.

**References**

Chubarenko I, Bagaev A, Zobkov M, & Esiukova E (2016) On some physical and dynamical properties of microplastic particles in marine environment, Marine pollution bulletin, 108(1-2), 105-112.

Haider A & Levenspiel O, (1989) Drag coefficient and terminal velocity of spherical and nonspherical particles, Powder technology, 58(1), 63-70.

Khatmullina L & Isachenko I (2017) Settling velocity of microplastic particles of regular shapes, Marine pollution bulletin, 114(2), 871-880.

Putnam A, (1961) Integratable form of droplet drag coefficient, Ars Journal, 31(10), 1467-1468.

Shamskhany A, Li Z, Patel P, Karimpour S (2021) Evidence of microplastic size impact on mobility and transport in the marine environment: a review and synthesis of recent research, Front, Mar. Sci., p. 1869, 2021.

Song YK, Hong SH, Jang M, Kang JH, Kwon OY, Han GM, Shim WJ (2014) Large accumulation of micro-sized synthetic polymer particles in the sea surface microlayer. Environmental science & technology, 48(16), pp.9014-9021.

# Power Performance Assessment of SC-Darrieus Vertical Axis Water Turbine Using CFD Simulation

Derya KARAKAYA[1] and Şebnem ELÇİ[1]

[1] Department of Civil Engineering, Izmir Institute of Technology, Izmir, Turkey
deryakarakaya@iyte.edu.tr
sebnemelci@iyte.edu.tr

ABSTRACT

Hydrokinetic energy is often considered a more environmentally sustainable and flexible approach to harnessing power from natural water sources, particularly in areas where traditional hydropower may not be feasible. A vertical-axis hydrokinetic turbine is engineered to capture the kinetic energy in flowing water, such as rivers or tidal currents. In this study, the SC-Darrieus (straight blade) vertical axis water turbine is numerically modeled in 3D with the ANSYS Fluent program. The turbine has a height of 20 cm and a width of 15 cm. The turbine has three blades, and NACA S-1046 symmetrical blade profile is used. The turbine design and computational domain area were drawn in the Autodesk Inventor program. The dynamic mesh method accurately represents the simulation of turbine motion with water flow in areas with moving boundaries. The Semi-Implicit Method for Pressure-Linked Equations (SIMPLE) was implemented with a shear stress transfer (SST) k-ω turbulence model. The effects of time-variable flow and constant flow models on simulation results were compared. The coefficient of power ($C_P$) and coefficient of torque ($C_T$)-tip speed ratio (TSR) graphs are obtained according to these two different flow conditions. To determine the effect of unsteadiness in the flow, the pressure distribution, velocity distribution and turbulent kinetic energy distribution of the water flow around the rotor were examined by comparing the results for two flow conditions: under a given hydrograph (unsteady flow) versus under constant flow velocity (steady flow).

## 1. Introduction

A vertical axis hydrokinetic turbine is a type of renewable energy technology designed to harness the power of flowing water, such as rivers or tidal currents, to generate electricity. Vertical axis turbines have their rotor axis perpendicular to the direction of the fluid flow, which allows them to capture energy from water currents or airflows coming from any direction. These turbines are often more compact and can be installed in a variety of water environments, making them suitable for locations with variable flow patterns. When the literature is examined (Mejia et al., 2018; Kumar and Sarkar, 2022), Darrieus type water turbine, one of the frequently used vertical axis turbines, offers an innovative approach to producing clean energy from water flows. To fully understand their operational capabilities and limitations, it is essential to evaluate their performance under different flow conditions, including unsteady flow scenarios, which are often encountered in natural water bodies.

## 2. Methodology

CFD simulations are performed to acquire a more profound understanding of the fluid dynamics surrounding the turbine. These simulations use the Navier-Stokes equations to predict fluid behavior, enabling an in-depth analysis of the forces and moments acting on the turbine. Preceding practical applications in simulating turbine performance, the SST k-ω turbulence model was chosen. This model is highly regarded for its efficient representation of the boundary layer and free stream regions. The accurate representation of flow characteristics in the near-wall and far-wall areas is achieved using the SST k-ω model (Kumar and Sarkar, 2022). Simulations were made by writing user-defined function (UDF) and velocity equations (which vary depending on time) in the Fluent program for unsteady flow conditions (having mean velocities of 1, 2 and 3 m/s) and for steady flows with the constant flow velocities of 1, 2 and 3 m/s. The dynamic mesh model can describe flows with changing domain geometry due to boundary motion (Ansys, 2018). This model

allows modeling according to changes in angular velocity at each time step and simulates flow around the turbine at different flow velocities. This simulation assumes the vertical axis water turbine rotates within the water flow, affecting the surrounding meshing. The moment force-based Dynamic Mesh 6DOF approach replicates turbine rotation in this simulation.

## 3. Results and conclusion

According to the results, maximum power coefficient ($C_P$) and maximum torque coefficient ($C_T$) graphs were obtained, as shown in Figure 1. The $C_P$ for velocities of 1, 2 and 3 m/s increased by 6.25%, 13.83% and 21.84%, respectively, when operating under a given hydrograph (having the mean velocities of 1, 2 and 3 m/s) in unsteady flow conditions. While the $C_T$ value decreased by 6.61% for v=1 m/s, it increased by 12.84% for v=2 m/s and 5.48% for v=3 m/s.

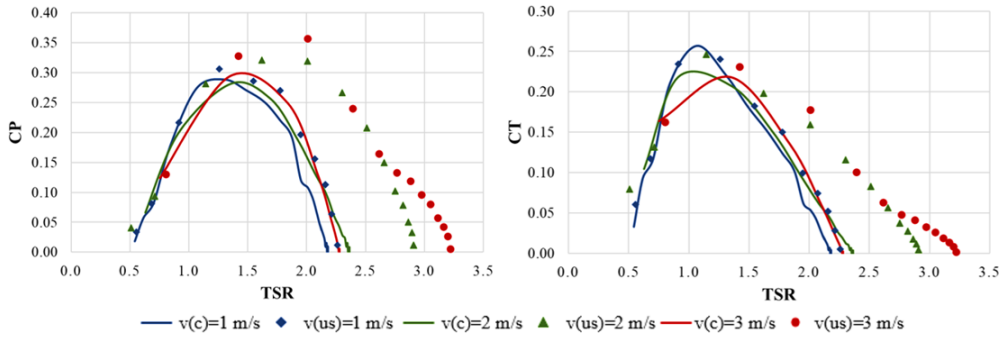



**Fig.1.** Comparison of turbine $C_P$ and $C_T$ values for three different velocity values. In the graphs 'us' in v(us) represents unsteady flow, 'c' in v(c) represents constant flow velocity in steady flow conditions.

Based on the analysis findings, Figure 2 presents pressure, velocity, and turbulence kinetic energy contours for steady flow condition having a constant flow velocity of 2 m/s and for the provided hydrograph having an mean velocity of 2 m/s (unsteady flow). While the high-pressure values occurring in the upstream part of the turbine increased due to the acceleration movement, the low-pressure values appearing in the downstream region of the turbine also increased. Similarly, the velocity values affecting the leading edge turbine blades increased with this acceleration movement, and the turbulence kinetic energy occurring in the tailing edge of the turbine blades has grown.

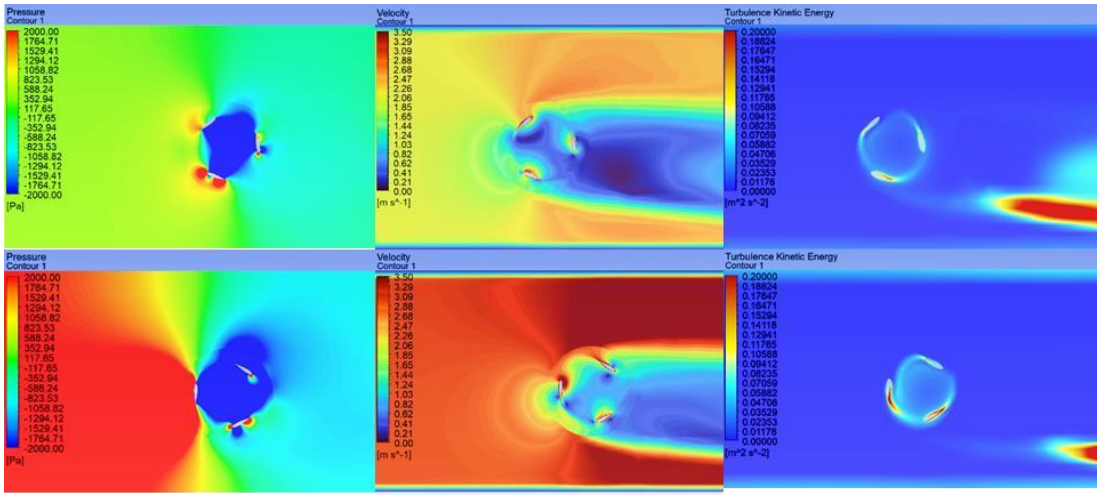



**Fig.2.** Comparison of the top views of pressure, velocity and turbulence kinetic energy distribution from the model domain for constant velocity of 2 m/s (steady flow) (top) and for unsteady flow provided by a hydrograph having mean velocity of 2 m/s (bottom).

The turbine exhibits a significantly higher power output in accelerated flows due to the increased kinetic energy. This research contributes to a more comprehensive understanding of the turbine's capabilities, offering valuable insights into its effective use in diverse aquatic environments for sustainable energy generation.

**References**

Ansys, I. (2018). ANSYS fluent tutorial guide R18.

Kumar, R., and Sarkar, S. (2022). "Effect of design parameters on the performance of helical Darrieus hydrokinetic turbines", *Renewable and Sustainable Energy Reviews*, 162, 112431.

Mejia, O. D. L., Quiñones, J. J., and Laín, S. 2018. RANS and hybrid RANS-LES simulations of an H-type Darrieus vertical axis water turbine. Energies, 11(9), 2348.

# Photogrammetry for Flow Measurement at the Air-Water Interface of Flow Past a Semi-Circular Cylinder

Hang TRIEU[1], Per BERGSTRÖM[2], J. Gunnar I. HELLSTRÖM[3], Mikael SJÖDAHL[4]

[1,2,3,4] Division of Fluid and Experimental Mechanics, Luleå University of Technology, 97754 Luleå, Sweden
hang.trieu@ltu.se; per.bergstrom@ltu.se; gunnar.hellstrom@ltu.se; Mikael.Sjodahl@ltu.se

ABSTRACT

This paper presents the estimation of the flow field at the interface of water flow past a semi-circular cylinder, obtained using a multiple-camera system. The surface water flow behind the cylinder is observed by a four-camera system. The field of view of the water surface is divided into a grid of sub-regions, each represented by its center point. These surface points are tracked in an image sequence, and their 3D coordinates are determined using the calibrated camera network. The results show that the proposed method effectively measures the surface velocity field of periodic vortex shedding at the air-water interface. Furthermore, the utilization of the multiple-camera system allows for the assessment of water surface deformation of the flow behind the cylinder in different velocity conditions.

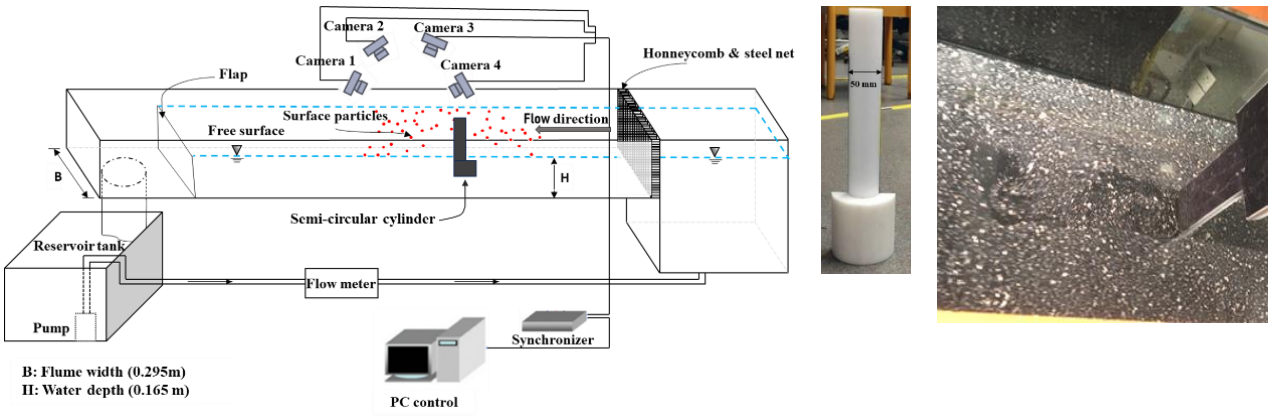
## 1. Introduction

Vortex shedding occurs due to the flow separation around the structures when the fluid flows past a bluff body. The vortices are generated and shed alternately from one side to the other side. Vortex shedding is widely studied due to the variety of applications in the industry. While the flow around a cylinder piercing an air-water interface is crucial in applications like offshore structures and surface vessels, it hasn't received as much attention as its single-phase equivalent. Suh et al. (2011) studied how the air-water interface impacts vortex shedding from a vertical cylinder. Their findings show that the vortical structures at the interface differ significantly from those in the deep flow. Akilli and Rockwell (2002) observed a significant distortion of the free surface caused by a horizontal vortex resulting from the upward ejection of fluid through the center of a Karman vortex. Measurement of the flows around these structures is therefore important in various applications. This study aims to investigate photogrammetry's applicability in measuring the 3D flow field of a vortex shedding behind a semi-circular cylinder in an open channel flow.

## 2. Experiment and Method

The measurement was conducted in a laboratory flume flow employing the four-synchronized camera system. Fig. 1(a) illustrates the experimental setup. The semi-circular cylinder has a diameter of 50 mm and is located at the center of the flume, see Fig. 1(b) and Fig. 1(c). The dimensions of the flume are 7.5 × 0.295 × 0.310 meters in length, width, and height respectively. To ensure a consistent inflow, a steel net and honeycomb are situated at the channel's inlet. The flow was seeded by wheat flour to create random patterns on the surface of the water flow, see Fig. 1(c). The experiment was conducted across various inlet velocities, capturing datasets in the form of image sequences from all cameras. A checkerboard pattern was used for the calibration of the multiple-camera system. The checkerboard pattern was 40 cm × 38 cm and was placed in arbitrary 50 positions and orientations in the measurement volume. The intrinsic and extrinsic camera parameters were estimated from the detected calibration pattern (Trieu et al. 2021).

The method involves computing the flow surface within a 3D coordinate system utilizing all cameras in the imaging setup. Initially, the identification of corresponding points across all cameras is performed. Subsequently, the positions of grid surface points in the initial image of the sequence are utilized for cross-correlation to estimate the movement of surface patterns in the image sequences. The surface points are tracked across all camera sequences, and their spatial coordinates are calculated by triangulation in the geometry of the camera network. Consequently, the velocity field and surface elevation of the flow are reconstructed in the 3D coordinate system.




(a) (b) (c)

**Fig. 1.** Experimental arrangement, (a) Camera setup and water circulation in the flume, (b) Semi-circular cylinder d = 50 mm, (c) Surface seeding of water flow past the semi-circular cylinder.

## 3. Results and Conclusions

The photogrammetric approach has been investigated for measurement at the air-water interface of the vortex shedding behind a semi-circular cylinder. Fig.2 shows an example of an instantaneous surface velocity field obtained by photogrammetry. The vortical structures and their spatial location are obviously visible in the flow field. The flow in this measurement exhibits a Reynolds number of 2400. According to the relationship between Strouhal Number and Reynolds number established by Lienhard (1966) and Achenbach and Heinecke (1981) the flow has a Strouhal number of 0.22. In this measurement the Strouhal number is calculated using the equation (1):

$$St = \frac{fD}{U} \tag{1}$$

where f is frequency estimated from the measurement, D is diameter of the cylinder and U is inlet velocity. The Strouhal number estimated from the measurement in this flow is 0.20, indicating good agreement with previous studies. The observed vortical structures and the deformation of flow surface behind the bluff body at various inlet velocities provide discussions on the interaction between vortices at the interface.

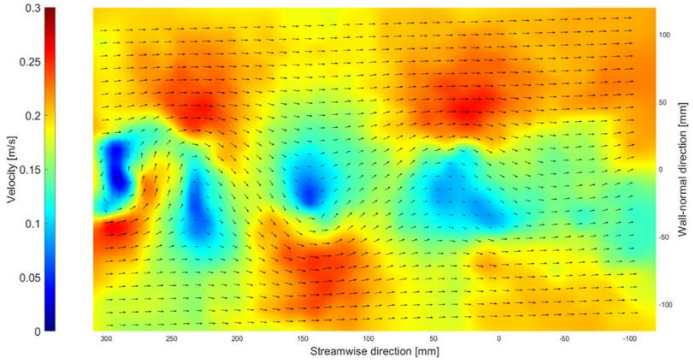



**Fig. 2.** Instantaneous surface velocity field

**Acknowledgments**

The research presented has been carried out as a part of "Swedish Hydropower Centre / SVC". SVC has been established by the Swedish Energy Agency, Energiforsk and Svenska Kraftnät together with Luleå University of Technology, Chalmers University of Technology, The Royal Institute of Technology and Uppsala University.

**References**

Achenbach, E., and Heinecke, E. (1981). "On vortex shedding from smooth and rough cylinders in the range of Reynolds numbers 6× 103 to 5× 106." *Journal of fluid mechanics*, 109, 239-251.
Akilli, H., and Rockwell, D. (2002). "Vortex formation from a cylinder in shallow water." *Physics of Fluids*, 14(9), 2957-2967.
Lienhard, J. H. (1966). *Synopsis of lift, drag, and vortex frequency data for rigid circular cylinders*, Technical Extension Service, Washington State University Pullman, WA.
Suh, J., Yang, J., and Stern, F. (2011). "The effect of air–water interface on the vortex shedding from a vertical circular cylinder." *Journal of Fluids and Structures*, 27(1), 1-22.
Trieu, H., Bergström, P., Sjödahl, M., Hellström, J. G. I., Andreasson, P., and Lycksam, H. (2021). "Photogrammetry for Free Surface Flow Velocity Measurement: From Laboratory to Field Measurements." *Water*, 13(12), 1675.

# 3D simulation of landslide generated waves with OpenFOAM

Aurélie LOUIS-NAPOLEON[1], Philippe HEINRICH[1], Stéphane ABADIE[2]

[1] CEA, DAM, DIF, 91297 Arpajon Cedex, France
email: aurelie.louis-napoleon@cea.fr

[2] Université de Pau et des Pays de l'Adour, E2S UPPA, SIAME, Anglet, France

## ABSTRACT

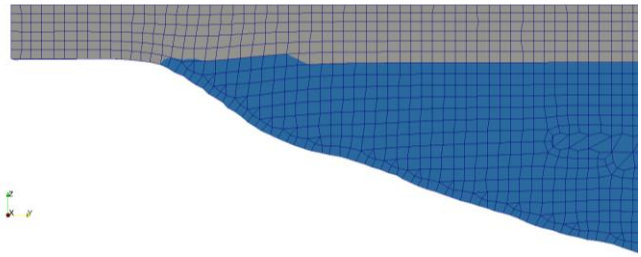


Fig. 1 Snapshot of the initial mesh and water surface. Water is in blue and air in grey. Mesh is non horizontal, and as the water follows the mesh, water surface is not flat.

Many tsunamis, consecutive or not to strong earthquakes, are generated or accentuated by the triggering of sub-aerial or submarine land collapses. This is the case of several historical tsunamis (Nice, 1564, 1979; Ligure Sea, 1887; Polynesia 1979; Papua, 1998; Java, 2012; Greenland, 2017; Anak Krakatau, 2018) that have impacted several kilometers of near or distant coasts. In this context, the scientific community faces the challenge of accurately simulating potential gravity tsunamis to estimate the inundation heights at the coast.

Navier-Stokes simulation of multiphase flow (e.g., Abadie et al., 2021 and 2020) would be one of the most advanced alternative to tackle this challenge (compared for instance to the often used shallow water model). Among the different platforms which proposes this type of models, OpenFOAM is maybe one of the most promising, owing to the large community of developers involved. For landslide tsunamis, it was previously validated on experimental subaerial and submarine tsunamis problems in both 2-D and 3-D (Romano et al., 2023, Paris et al., 2021, Rauter et al., 2022). Regarding 3D real cases, only very few attempts are reported in the literature (e.g., Rauter et al., 2022). Beyond the computational load which is significant, the difficulty has also to do with the construction of the case and the strategy adopted. To that respect, several bottlenecks can be listed :

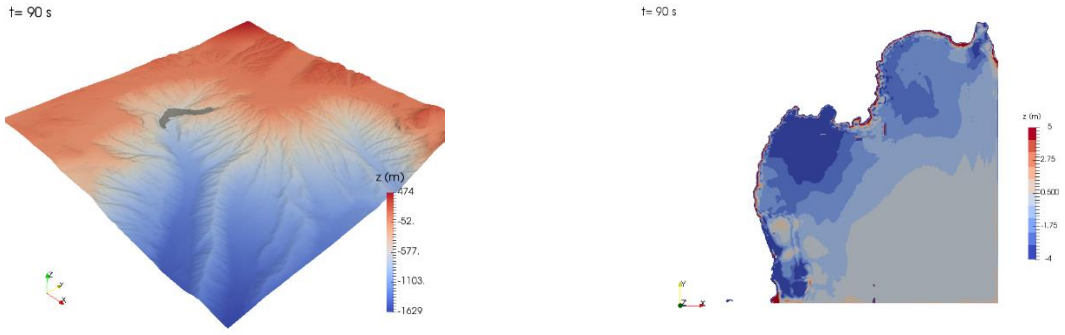
- First, the mesh has to respect strong constraints. It has to account for a complex bathymetry/topography which may cross the water surface. It should be as horizontal as possible at the ocean surface, to allow for an accurate initiation of the water volume fraction. And finally, the mesh construction should allow refinements where complex processes are expected (i.e., around the free surface, along the slide path),

- The second difficulty lies with the water and slide volume fraction definition. The water volume fraction definition is strongly related to the mesh definition around the free surface. In case, the mesh is not horizontal in this area (see Fig. 1), partial volume fraction may have to be employed, or other strategies considered, to prevent the apparition of spurious waves generated by a non-flat ocean surface. As for the slide material initiation, a portion of the sea bottom of the soil should be replaced with the slide material. Depending on the case considered, this operation may not be straightforward. Here, a simple repeatable procedure should be defined and automatized,

- The third difficulty, and the deepest in terms of scientific content, is related to the choice of the slide rheological law. For a real case study (past or potential), the slide material may be more or less known. Nevertheless, the accurate representation of the complex behavior of the slide material during the event (slide, dynamics, dislocation, erosion, multiple interactions with water etc., among which penetration within the grains) is far from being currently achievable. Here, there is an obvious gap between the available rheological laws, even the most advanced ones (i.e., Si et al., 2018; Yu and Lee, 2019; Lee and Huang, 2021, Rauter et al., 2022), and the complexity of the real processes to be described. As the cost of computation is also a critical question for 3D cases, only the most important processes have to be accurately described if possible. Nevertheless, the work of identifying which processes are really critical during the critical stages of the wave generation is not often performed,

- The last point has to do with the scale of the computation in general and more specifically the distance between the assets and the wave source. A complete 3D Navier-Stokes simulation is not practically feasible in 3D if the propagation distance is much more than a few wave lengths. In that case, which may be the most common, a procedure for transferring the results from the 3D OpenFOAM simulations into a depth integrated 2D "tsunami" code as initial or boundary condition has to be employed (e.g., Abadie et al., 2012 and 2020). The way this transfer is achieved is worth discussing as well as the necessary filters to apply in order to allow a smooth transition between a 3D solution to a 2D depth averaged flow.

The four previous questions are being currently tackled by our team. During the conference, we will propose a few repeatable solutions and procedures aiming at solving those issues. Finally, our procedures will be illustrated on the Nice tsunami example (see Fig. 2).




a) Bathymetry of the Nice coast and slide (in grey) position at t=90s

b) Free surface elevation at t=90s

Fig. 2 3D preliminary numerical modeling of the 1979 tsunami in Nice. This tsunami is induced by a submarine slide. Waves of up to 3.5 m were observed during the event (Labbé et al., 2012). The modeling needs to be improved with a more refined mesh, a flat initial water surface, and tests on the slide rheology.

**Acknowledgements**

We thank the French Alternative Energies and Atomic Energy Commission (C.E.A) which supported this work Some numerical simulations were performed using HPC resources from the super computing center TGCC.

**References**

Abadie, S. M., Harris, J. C., Grilli, S. T., & Fabre, R. (2012). Numerical modeling of tsunami waves generated by the flank collapse of the Cumbre Vieja Volcano (La Palma, Canary Islands): Tsunami source and near field effects. *Journal of Geophysical Research: Oceans*, *117*(C5).

Abadie, S., Paris, A., Ata, R., Le Roy, S., Arnaud, G., Poupardin, A., ... & Krien, Y. (2020). La Palma landslide tsunami: calibrated wave source and assessment of impact on French territories. *Natural Hazards and Earth System Sciences*, *20*(11), 3019-3038.

Labbé, M.**,** C. Donnadieu**,** C. Daubord**,** and H. Hébert **(**2012**),** Refined numerical modeling of the 1979 tsunami in Nice (French Riviera): Comparison with coastal data**,** *Journal of Geophyical. Research*, 117, F01008.

Lee, Cheng-Hsien, and Zhenhua Huang. "Multi-phase flow simulation of impulsive waves generated by a sub-aerial granular landslide on an erodible slope." *Landslides* 18.3 (2021): 881-895.

Paris, Alexandre, Philippe Heinrich, and Stéphane Abadie. "Landslide tsunamis: Comparison between depth-averaged and Navier–Stokes models." *Coastal Engineering* 170 (2021): 104022.

Rauter, Matthias, et al. "Granular porous landslide tsunami modelling–the 2014 Lake Askja flank collapse." *Nature communications* 13.1 (2022): 678.

Romano A, L. J. (2023). Numerical modelling of tsunamis generated by granular landslides in. *Coastal Engineering*, 378-3839.Si, P., Shi, H. & Yu, X. A general numerical model for surface waves generated by granular material intruding into a water body. *Coastal Engineering* 142, 42–51 (2018).

Yu, Ming-Lan, and Cheng-Hsien Lee. "Multi-phase-flow modeling of underwater landslides on aninclined plane and consequently generated waves." *Advances in Water Resources* 133 (2019): 103421.

# Numerical Simulation of Flow Patterns Around Triple Square Pier: Vortices Formation

Nima IKANI[1], Jaan H. PU[2]

[1] PhD Student, Department of Engineering and Digital Technologies, University of Bradford, UK
n.ikani@bradford.ac.uk

[2] Associate Professor, Faculty of Engineering and Digital Technologies, University of Bradford, UK
j.h.pu1@bradford.ac.uk

ABSTRACT

In this study, the flow characteristics around a complex group-pier in open channel flow were investigated numerically using a second-order characteristic. The principal aim was to analyse the three-dimensional flow velocity and vortices behaviour around a configuration of three-square bridge piers arranged in tandem in clear water in smooth bed to unerestand how this complex model can be similar to the real-nature flow behavior. The simulation utilized the k-ε method, implemented through Ansys Fluent 21 software, to model the free surfaces. The obtained results were subsequently analysed to determine the vortices' distribution around the piers, based on the velocity distribution at the two different depths (z/h=0.15, and 0.62). The accuracy of the proposed CFD model has been validated through the experimental analysis using Acoustic Doppler Velocimeter (ADV) measurements, demonstrating the model's ability to reproduce key aspects of velocity distribution across undisturbed and recovery regions (Pu et al., 2014). As part of the validation process, simulation results were compared with data derived from laboratory experiments, including flow channel dynamics and pier configurations. Furthermore, the study examined the impact of the piers on flow characteristics by analysing flow patterns and extracting relevant distributions and can provide effective strategies for controlling scouring and minimizing destructive vortex effects

## 1. Model definition

As illustrated in Fig. 1(a), the VOF using the k-e turbulence model was employed to analyse a two-phase domain in which water is flowing in a channel with an upper region occupied by air (Amina and Tanaka, 2022). Three square piers were characterized by dimensions of $0.05\ m \times 0.05\ m$ and positioned at 2d (d= 0.05 m) from each other, precisely located in the middle (centre) of the channel width, as showed in Fig. 1(b).

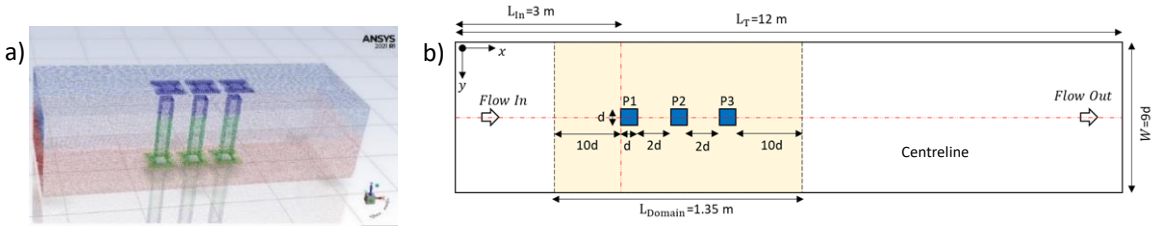



**Fig. 1.** a) Domain area in VOF model in ANSYS FLUENT software 2021, b) Modeled schematic plan for the located piers (domain area)

## 2. Flow features in vertical planes xz

As can be seen in Fig. 2, the contour plots of u velocity reveal that the flow velocity decreases as it approaches the first pier, followed by an acceleration around the second pier. In the wake of the piers, flow separation occurs, resulting in the formation of a reverse flow region. A change in velocity past the initial pier suggests the formation of vortex patterns, which significantly affect the flow's movement. The intensity of these vortical formations decreases steadily as one moves from upstream to downstream. The downward flow is also more pronounced than the upward flow following the first pier (Salaheldin et al., 2004, Lade et al., 2019; Ikani et al., 2024).

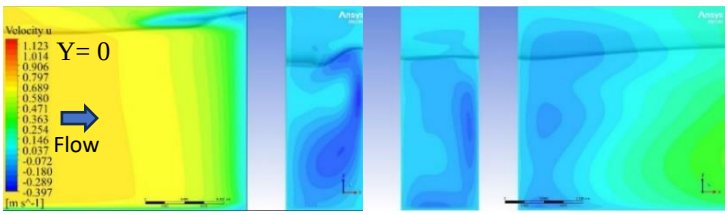



**Fig. 2.** Numerical simulation contour plots of u velocity flow in vertical planes xz ( y=0 in centreline from y axis).

## 3. Flow features in horizontal planes

The velocity vectors around piers are given in Fig. 3 which shows the simulated flow at z/h=0.15, and 0.62 m. There is clearly circulation and reverse flow near the piers, which contributes to wake vortices near the wall bed. By successfully reproducing the phenomenon of reversal velocity and reasonable magnitude, the CFD model demonstrates its capability to capture key flow characteristics in complex flow scenarios. While the results of the CFD model confirm the well-known separation zone behind piers, they emphasize its prominence near the bedwall (Ikani et al., 2023). Furthermore, the model includes lateral flow shifts at these depths after encountering piers, proving our model to be accurate by validating these phenomena against experimental data.

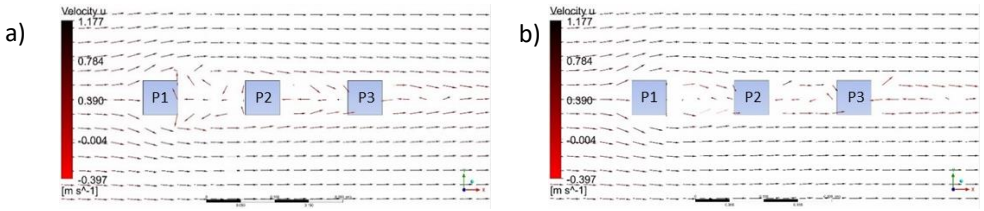



**Fig. 3.** Velocity U distribution in numerical model in XY plane a) z/h=0.15 and, b) 0.62 m.

## 4. Model validation

Both the experimental and proposed computational data demonstrated that flow velocity decreased when approaching the upstream side of the first pier. The CFD model was validated to capture the flow dynamics of the complex pier groups satisfactorily. However, the simulated velocity profile near free-surface (i.e. between Blocks 1 and 2) over-estimated the measured data due to vortex impact. This indicates the limitation of the utilised k-ε model, even though its computation efficient is high.

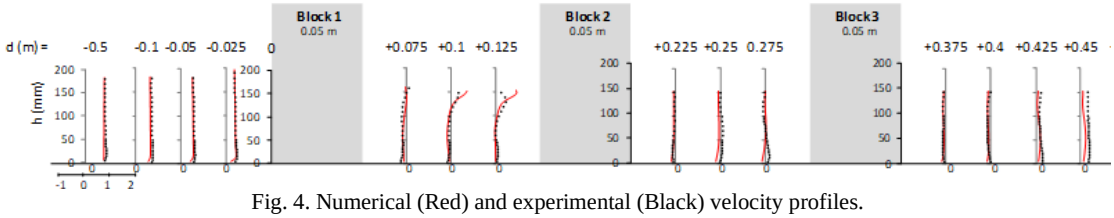



Fig. 4. Numerical (Red) and experimental (Black) velocity profiles.

## 5. Conclusion

Despite some limitations in representing turbulence, the simulations exhibited an acceptable degree of accuracy in capturing the complex dynamics in piers-induced flow. It was demonstrated that the proposed model was capable to simulate flow turbulence efficiently, demonstrating its suitability for real-world applications. Key findings include the identification of a distinct separation zone mostly behind the initial pier, extended downstream and influenced by a downward flow mechanism driven by a negative pressure gradient near the piers' face. Furthermore, these results provide a basis for future research to investigate the adaptability into real-world scenarios, i.e. for enhancing flood and sediment transport management.

**References**

Amina & Tanaka, N. 2022. Numerical Investigation of 3D Flow Properties around Finite Emergent Vegetation by Using the Two-Phase Volume of Fluid (VOF) Modeling Technique. Fluids, 7, 175.

Ikani, N., Pu, J. H., Taha, T., Hanmaiahgarib, P. R. & Penna, N. 2023. Bursting phenomenon created by bridge piers group in open channel flow. Environmental Fluid Mechanics, 1-16.

Ikani, N., Pu, J. H., Zang, S., Al-Qadami, E. H. H. & Razi, A. 2024. Detailed turbulent structures investigation around piers group induced flow. Experimental Thermal and Fluid Science, 152, 111112.

Lade, A. D., Deshpande, V., Kumar, B. & Oliveto, G. 2019. On the morphodynamic alterations around bridge piers under the influence of instream mining. Water, 11, 1676.

Pu, J. H., Shao, S. & Huang, Y. 2014. Numerical and experimental turbulence studies on shallow open channel flows. Journal of Hydro-Environment Research, 8, 9-19.

Salaheldin, T. M., Imran, J. & Chaudhry, M. H. 2004. Numerical modeling of three-dimensional flow field around circular piers. Journal of Hydraulic Engineering, 130, 91-100.

# Application of machine learning techniques for the generation of optimal layouts in branched water networks

Roberto DEL TESO[1], Elena GÓMEZ[2], Álvaro MONTAÑA[3], Elvira ESTRUCH-JUAN[4]
[1, 2, 3, 4] Department of Hydraulic Engineering and Environment.
Universitat Politècnica de València. Valencia (Spain)
[1]rodete@ita.upv.es
[2]elgosel@ita.upv.es
[3]almonol1@posgrado.upv.es
[4]maesjua1@ita.upv.es

## ABSTRACT

The analysis of solutions for designing water distribution networks must encompass various aspects. One aspect to consider is the energy required to supply the system, aiming to achieve efficient and sustainable systems. It is crucial to define a layout that is energetically favorable, adapting to the morphology of the area and user requirements. Another key aspect is the implementation cost of the network. This work proposes a methodology to identify a set of layouts deemed energetically favorable, requiring less head energy, exhibiting lower energy excesses at nodes, and incurring lower total costs, including energy costs during operation.

The proposed methodology employs clustering, specifically utilizing K-means and hierarchical clustering algorithms. These algorithms are valuable for identifying patterns or structures without the need for labels or external information, enabling the grouping of data based on similarities.

By leveraging graph theory, potential routes for pipe installation are determined. This involves considering both the available paths on which the network can be laid out and the base topology generated based on the initial sectors (clusters). This base topology corresponds to an undirected graph, serving as the foundation for generating all possible layouts for the water distribution network.

## 1. Methodology for the generation and selection of layouts.

The proposed methodology is divided into five phases, each with a set of input and output data, as depicted in Figure 1:

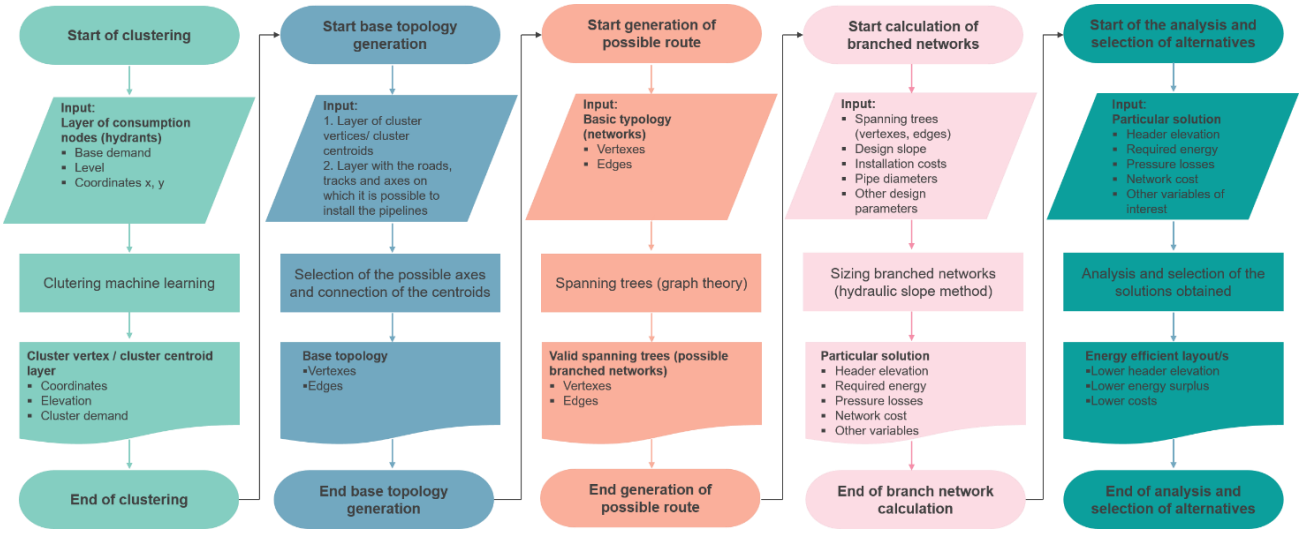



**Fig. 1.** Methodology for the generation of optimal layouts in branched water networks

*1.1. Clustering.*

Clustering is performed on the network by grouping nodes based on their location and demand. Techniques such as K-Means or hierarchical clustering, commonly employed for the generation of district management areas (DMA) (Rong et al., 2022), are used for this purpose. These techniques help to identify closely interconnected node groups in the network and delineate geographical areas with similar hydraulic characteristics. Once the clusters are defined, centroids representing each node aggregation are obtained, and they are assigned the characteristics that define the cluster. This information will be used to determine the connection point of the cluster with the main network.

*1.2. Generation of the base topology.*

The spatial distribution of clusters defined in the previous step delineates the deployment space for the network. In this second stage, a base graph is defined from which potential layouts can be generated. The process to define the base graph begins with the overlay of layers containing the centroids defining the clusters and the layer indicating possible paths for pipe construction. The routes must stay on passable roads and avoid private land. The generation of the base graph is completed by defining edges and vertices.

*1.3. Generation of potential layouts.*

The generation of all possible layout configurations is achieved through the application of graph theory, considering the equivalence between elements in a network model, such as nodes and pipes, and the concepts of vertices and edges in a graph. Layout alternatives are derived from combinations of the edges constituting the base graph obtained in the previous step. This involves applying Depth-First Search (DFS) algorithms.

*1.4. Calculation and sizing of potential layouts.*

The calculation and sizing of each potential layout obtained in the previous step are carried out using Epanet (Toolkit) version 2.2. A crucial aspect to consider in both cases is the definition of the inlet node of the network, as this point determines the energetically most convenient solutions. Therefore, for each evaluated network alternative, the inlet node is modified, generating as many possibilities as there are nodes in the network.

The calculation of water distribution networks is performed using the hydraulic gradient design method. Sizing is conducted considering a range of slopes (between 1 and 10 m/km), as lower slopes imply solutions that require less head energy but tend to be costlier in terms of construction, leading to larger diameters.

Ultimately, the calculation of the water distribution networks provides the three variables that form the criteria for evaluating layouts: the energy required at the inlet, the lowest excess energy values at nodes, and the lowest network cost, including operational costs (Vasconcelos et al., 2022). However, at this stage, operational costs are associated with the minimum values of required energy and, since the temporal variation of flows is not considered, the hourly energy cost does not fluctuate and remains constant over time.

*1.5. Analysis and selection of alternatives.*

Once all possible branched networks are calculated and sized, the results are analyzed to identify those requiring the least energy. From the filtered solutions with the lowest energy requirements, networks with the least excess energy are identified and compared with those having the lowest total cost. The layouts that prove to be more energetically convenient are then selected. Solutions depend on project conditions such as existing elevation differences (del Teso et al., 2019), flow distribution in the layout, and the size of the network.

## 2. Conclusions.

The proposed analysis to determine the most energy efficient layouts is suitable for studying solutions for new networks, defining the mains infrastructure, and investigating improvements in energy efficiency in operational networks. Variables such as the inlet node and how flow is distributed through the network influence the selection of layouts that are more energy-efficient. However, the significance of each of these variables will depend on the topology of the area.

**References**

Rong K, Fu M, Huang Y, Zhang M, Zheng L, Zheng J, Scholz M, Yaseen ZM (2022) Graph attention neural network for water network partitioning, Applied Water Science, 13(1), 3. https://doi.org/10.1007/s13201-022-01791-4

Vasconcelos JG, Cabrera E, Gomez E, del Teso R (2022) Optimal energy gradient for pumping systems supplying variable flow demands, Journal of Water Resources Planning and Management, 148(11). https://doi.org/10.1061/(ASCE)WR.1943-5452.0001600

del Teso R, Gomez E, Estruch-Juan E, Cabrera E (2019) Topographic energy management in water distribution systems. Water Resources Management, 33(12), 4385-4400. https://doi.org/10.1007/s11269-019-02375-9

# Modified Discharge Rating Curve Applicable under Strong Backwater Effects due to Nearby Reservoirs

Rui MARINHEIRO[1], José Pedro MATOS[1,2], Jorge MATOS[1,2], Vítor Faria e SOUSA[1,2], Inês MEIRELES[3] and Manuel MAHUNGUANA[4]

[1] Instituto Superior Técnico, University of Lisbon (IST/UL), Portugal.
ruismarinheiro@tecnico.ulisboa.pt
[2] Civil Engineering Research and Innovation for Sustainability (CERIS), IST/UL, Portugal.
jose.matos@tecnico.ulisboa.pt; jorge.matos@tecnico.ulisboa.pt; and vitor.sousa@tecnico.ulisboa.pt

[3] Research Center for Risks and Sustainability in Construction (RISCO), University of Aveiro, Portugal
imeireles@ua.pt

[4] Hidroeléctrica de Cahora Bassa, Mozambique
manuel.mahunguana@hcb.co.mz

ABSTRACT

River discharge estimation using discharge rating curves is a widely used technique due to its performance and practicality. Discharge rating curves are most appropriate when measurement sections are ideal (straight river reaches, free from backwater effects, and stable in time), and calibration includes measurements taken from low to high discharges. Unfortunately, it is not always possible to measure at such locations. A telling example is the hydrometric station of Zumbo, which is located between the Cahora Bassa reservoir and the border of Mozambique, Zambia, and Zimbabwe, being affected by the backwater curve of the former. This work introduces and explores a conceptual modification to the classical discharge rating curve that, with the addition of 1 calibration parameter, achieves more accurate results than existing formulations that add 2 or more.

## 1. The modified discharge rating curve

The classical discharge rating curve (DRC) is defined according to eq. (1):

$$Q = a \cdot (h - h_0)^b \tag{1}$$

where:

$Q$ is the discharge [m$^3$/s];
$h$ is the water level [m];
$h_0$ is the minimum water level [m];
$a$ is a calibration parameter [m$^{(3-b)}$/s]; and
$b$ is a calibration parameter [-].

When variable backwater effects are present, for example due to flow controls or waterbodies downstream, the classical DRC is not applicable. To extend its use to such situations, several methods have been proposed. Examples are the USGS/WMO discharge rating with variable slope caused by variable backwater (WMO, 2010) and formulations derived from the work of Petersen-Øverleir and Reitan (2009). Despite its substantial improvement over the classical DRC, USGS/WMO (2010) entails a complex calibration procedure and evidences some deviations when applied under strong backwater effects due to a fixed water level downstream. The formulations derived from Petersen-Øverleir and Reitan (2009) display similar issues.

To simplify application and improve performance, a geometrically inspired modification of the classical DRC explores the asymptotic behavior of the discharge rating curves for different downstream water levels in the log-space (see Fig. 1, left plot). In normal space (see Fig. 1, center and right plots), it translates into a smooth transition between fixed water level and the curve of a classical DRC.

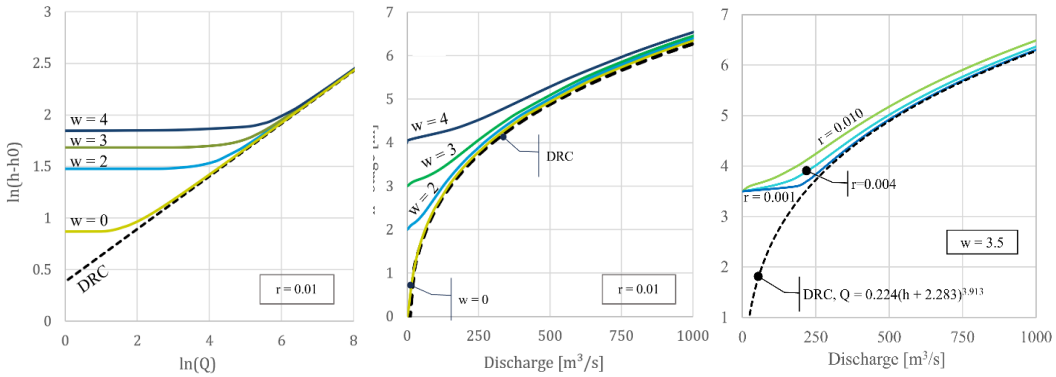



**Fig. 1.** Illustration of the behaviour of the modified discharge rating curve.

The mathematical formulation of the proposed method is depicted in eq. (2):

$$Q = a \cdot (h - h_0)^b \cdot \exp\left[\frac{-r \cdot b}{\ln(h-h_0) - ln(w-h_0)}\right] \quad (2)$$

including the new parameters:

$w$ – the known water level of the water body downstream [m]; and

$r$ – a calibration parameter that controls the curvature of the transition [-].

In addition to the calibration of the traditional parameters $a$, $b$, and $h_0$, that control the relation between the water level and the discharge when backwater effects are negligeable, the calibration parameter $r$ controls the transition between the downstream water level and the level predicted by the classical DRC.

## 2. Validation

The method performs as expected when compared with numerical backwater calculations. When applied to historical data collected at the Zumbo hydrometric station, eq. (2) can reproduce remarkably well the relationship between measured water level-discharge pairs, including when the backwater effect resulting from high reservoir levels is significant (Fig. 2).

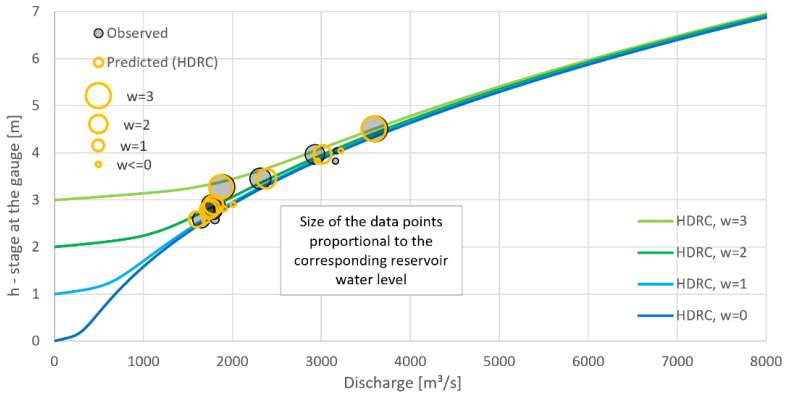



**Fig. 2.** Adjustment of the modified discharge rating curve to historical data collected at the Zumbo hydrometric station (2012-2015). In this case $a$=16.378, $b$=2.701, $h_0$=-3.077, and $r$=0.00691.

## 3. Conclusion

This work introduces a geometrically inspired modification to the discharge rating curve eq. (2), that is particularly useful when backwater effects strongly influence measured stages but may have broader applicability. The equation, whose derivation and potential will be explored, was developed following a new approach and is valuable due to its simplicity and accurate results when compared with other alternatives.

**Acknowledgements**

We thank Hidroeléctrica de Cahora Bassa for providing the data and proposing the challenge of finding a discharge rating curve formulation suitable to estimate inflows to the Cahora Bassa reservoir. We also thank the support of CERIS and RISCO.

**References**

Petersen-Øverleir, A.; Reitan, T. Bayesian analysis of stage-fall-discharge models for gauging stations affected by variable backwater. Hydrological Processes 2009, 23, 3057–3074. https://doi.org/10.1002/hyp.7417.

World Meteorological Organization (WMO). Manual on Stream Gauging, Volume II, Computation of Discharge. WMO- 408 No. 1044, 2010.

# Numerical Modelling of the Canales Dam Middle Outlet

María CASTEJÓN ZAPATA[1], David LÓPEZ GÓMEZ[2]

[1,2] Centre for Public Works Studies and Experimentation (CEDEX), Madrid, Spain
maria.castejon@cedex.es; david.lopez@cedex.es

ABSTRACT

The Canales dam is an embankment dam with impervious clay core built in 1988 and located in the south of Spain. The objective of this structure is to ensure the water supply to Granada, which is an important city within the Andalucia region located downstream of the dam. Due to the ground settlements, Canales Dam was built in two different phases. In the first phase, a middle outlet at an elevation of 900 m.a.s.l was required to drain the income flow, acting as the interim spillway, and hence ensuring the safety of the constructed dam. In the second phase, the dam crest reached the 966.76 m.a.s.l and hence a spillway adjacent to the dam at 958.42 m.a.s.l was built. Therefore, the middle outlet was no longer required at that time.

Nowadays, the Guadalquivir Water Administration regulates water flows only with the bottom outlet. However, due to the increase of flash flood events and the snow melting of the Sierra Nevada Mountain Range, Guadalquivir Water Administration would like to utilize the middle outlet as a second structure to regulate water flows in order to ensure the safety of the Granada city.

The mentioned outlet has not been opened since the construction of the Canales Dam phase 2. It has four Bureau gates at the upstream mouth of the tunnel, that has not been operated since that time. Therefore, the hydraulic behaviour of the middle outlet once the gates are open and the water level of the reservoir is at a normal operation level is unknown. Studies to assess the safety of the tunnel if the gates get opened are required.

The objective of this paper is to show the analysis carried out with numerical methods to analyse the main problems with the existing middle outlet design and to study the different solutions in order to solve those problems. The next phase of the project will be focused on the physical methods to check the hydraulic behaviour of the proposed solution.

The middle outlet has been designed with a complex geometry. It has four Bureau gates at the upstream mouth of the outlet. Downstream of that point, the middle outlet is comprised of a tunnel that keeps a 45º slope for 90 meters, after which it keeps a steady slope of 0.6% until the outfall of the outlet. Furthermore, there are two elbows across the top view of the tunnel, one of which is located very close to the suddenly change of slope. The middle outlet has a diameter of 5 m and a maximum discharge of 223 $m^3/s$ if the gates are fully open and the water level is at 958 m.a.s.l, which is the maximum operating level. Consequently, the entrance velocity is 33 m/s, which can be considered very high.

In order to fully understand the hydraulic performance of the middle outlet, a 3D numerical model was developed utilizing SPHERIMENTAL (SPH), which is a three-dimensional numerical model based on the "Smoothed Particle Hydrodynamics" method and developed by CEDEX (López et al, 2010). With the SPHERIMENRAL tool and its simulation capacities, it is possible to reduce the project timescale due to the program versatility and the computational efficiency. Moreover, in comparison to the budget associated in the modifications needed till achieve the optimal solution in the physical model, numerical models save a significant cost. Some of the data that has been introduced in the numerical model of the middle outlet is the geometry of the outlet, previously described, and the roughness of the tunnel, which is built with rough concrete. A calibration study was carried out to assess that roughness. The 3D numerical model requires a roughness coefficient, called Crough, that is also affected by the flows. A 2D model, that uses the manning coefficient was also built to compare water levels between both models. After the analysis, a Crough of 0.004

was applied to the model, which was equivalent to a manning coefficient of 0.018. This manning coefficient is a common value for rough concrete. Other data introduced in the SPH 3D model was the particle size. Regarding the length of the middle outlet, a 20 cm particle size was stablished. Finally, the simulations were done with two different flows. The first simulation utilised a flow of 223 $m^3/s$, which is the inflow if the Bureau gates are fully opened. In the second simulation, a flow of 160 $m^3/s$ is applied, which is the minimum flow required to increase dam safety.

After the study of the numerical model for both flow simulations, several areas of the tunnel show flow behaviours that can be improved, such as the area in where the slope changes drastically. In that area, the flow reaches the bottom and walls of the tunnel with very high velocities and turbulences, which can lead to tensions and erosions. In the first elbow, which is located after the change in slope, the flow does a swirl along the tunnel walls (Figure 1). In the second elbow, which is located downstream, almost near the downstream outfall, flow slows down and gets pressurized. In this last spot, the tunnel gets pressurized intermittently, which can cause problems in the outlet structure because of a lack of a constant air supply.

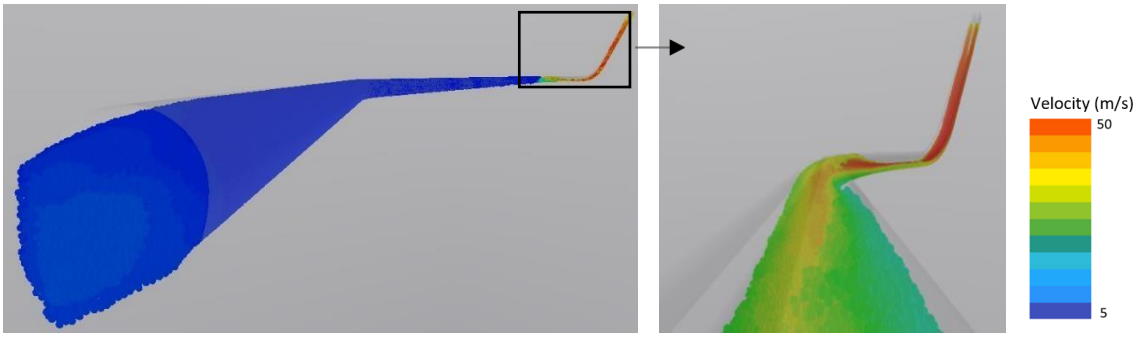



**Fig. 1.** Hydraulic performance of the outlet (left) and the hydraulic performance of the outlet mouth (right) in the numerical model for the 223 $m^3/s$ simulation.

The hydraulic capacity of the middle outlet is enough to drain the flows required to regulate water levels in the dam, and hence improve dam safety. However, velocities along the upstream extend of the outlet are excessive. The aim of the proposed solution is to reduce those velocities and therefore avoid the erosion and instabilities. An extensive study of alternatives is being carried out with numerical models based on the SPH method. At present, the solution being studied includes two gates at the downstream outfall of the tunnel and the removal of the four gates at the upstream outlet mouth. In this option the tunnel gets under pressure and the velocities are considerably reduced by restricting the flow downstream. A second solution is also studied, that includes the insertion of two pressurized pipes within the tunnel.

The next phase of the project will be the verification of the proposed solution throughout the development of a physical model. The previous experience with SPHERIMENTAL models shows that the results are accurate, however specific values of parameters will be more representative in a physical model than in the numerical model. Physical models in the CEDEX laboratory are constructed with concrete and bricks and the high precision pieces with white concrete. The physical model will be developed with the same principles as the physical model developed for the morning glory spillway at Nagore dam due to the similarities in their hydraulic behaviour (López et al, 2016).

As main conclusion, numerical models have allowed to easily study a wide range of simulations and hence understand the hydraulic behaviour of the current middle outlet and the proposed solutions. The next phase of the project will be focused on developing the physical model to ensure that the results of the numerical models are correct.

**References**

López, D., Marivela, R., Garrote L. 2010. “Smooth Particle Hydrodynamics Model Applied To Hydraulic Structures: A Hydraulic Jump Test Case”. Journal of Hydraulic Research. Vol 48. , Extra Issue. pp. 142-158. ISSN: 0022-1686.

López, D., Díaz, R., Rebollo, J.J., Ramos, T., Andrés, F.R., Berga, M.I. 2016. “Application of the SPH method in hydraulic structures studies. Hydrodynamic analysis of the Nagore dam morning glory spillway (Navarra, Spain)”. RIBAGUA. Issue 3., Num 1. pp 1-7.

# Assessing the Impacts of Simplified Methodology and Shuttle Radar Topography Mission in Inundation Map

Sérgio Ricardo Toledo SALGADO[1], Elsa Maria da Silva CARVALHO[1], Maria Teresa VISEU[3], Othon Fialho de OLIVEIRA[4]

[1] Faculty of Engineering, University of Porto, Portugal
up202001034@fe.up.pt

elsac@fe.up.pt

[3]Research Assistant at the National Laboratory of Civil Engineering (LNEC), Portugal

tviseu@lnec.pt

[4] Federal University of Pernambuco, Brazil
email: othonfialho@yahoo.com.br

ABSTRACT

This study emphasizes the importance of inundation maps in dam safety, highlighting how methodologies and Digital Elevation Model (DEM) significantly impact flood prone area definition. The study targeted Brazil's Copiti dam, employing a simplified methodology and HEC-RAS models for dam-break simulations and utilizing SRTM and high-precision PE3D LIDAR data from Pernambuco state.

## 1. Introduction

Inundation maps are essential for dam safety. In areas with limited data, such as Brazil, finding alternatives to their definition is crucial. One solution is to apply the simplified method from Portugal's National Laboratory of Civil Engineering (LNEC), which utilizes Shuttle Radar Topography Mission (SRTM) data (Melo et al., 2015; Petry et al., 2018).

The SRTM is a global DEM with a resolution of 30 meters and an average accuracy of less than 9 meters (Farr et al., 2007). However, relying solely on SRTM and simplified methods can misrepresent dam failure risks due to the common low resolution and vertical errors in global DEMs, leading to potential flood extent overestimations (Hawker et al., 2018). Using more advanced model and accurate DEM, such as Light Detection and Ranging (LIDAR), with an accuracy of between 0.5 and 1 meter, reduces these inaccuracies, offering more reliable flood mapping (Bhuyian & Kalyanapu, 2018; McClean et al., 2020).

The study targeted Brazil's Copiti dam in Custódia-PE, employing LNEC Simplified Methodology and HEC-RAS model (USACE, 2023), in both steady and unsteady conditions, and utilizing SRTM and PE3D LIDAR data from Pernambuco state. The goal was to assess the impact of models and DEM accuracy on inundation mapping, a key aspect of effective dam safety management.

## 2. Results and discussion

The study conducted four simulations combining flood map methods, flow conditions and DEM models, in which the same characteristics were adopted, such as breach flow, river course and cross-sections. The latter were defined along a 8.4 kilometer river stretch, accounting 20 cross-sections, nearly 420 meters apart. In the steady flow HEC-RAS model simulation, flows calculated for the upstream boundary by the simplified methodology were used. The unsteady flow HEC-RAS model simulation incorporated an inflow hydrograph into the input data, simplified through a triangular hydrograph. The study applied the water static water level criterion (Viseu, 2006) to assess the population at risk, using population density data from census tracts provided by the Brazilian Institute of Geography and Statistics (IBGE, 2011). Table 1 presents the simulation conditions and results.

**Table 1.** Simulation conditions and results

| Sim. | Methodology | DEM | Flood Area ($km^2$) | Population at risk based on flood depth range. | | | |
|---|---|---|---|---|---|---|---|
| | | | | **d ≤ 1 m** | **1m < d ≤ 3m** | **3m < d ≤ 6m** | **d > 6m** |
| 1 | Simplified method | SRTM | 3,79 | 109 | 121 | 54 | 0 |
| 2 | HEC-RAS – steady flow | SRTM | 3,31 | 86 | 100 | 51 | 0 |
| 3 | HEC-RAS – unsteady flow (1D) | SRTM | 3,04 | 84 | 98 | 40 | 0 |
| 4 | HEC-RAS – unsteady flow (1D) | PE3D | 2,72 | 47 | 106 | 46 | 2 |

Simulation 1 resulted in the largest flood area and affected population. Simulation 2 had a slightly smaller flood area and affected population. Simulation 3 reduced both flood area and affected population further. Simulation 4, with the smallest flood area and least affected population, uniquely showed people affected at depths over 6 meters.

Figure 1, illustrating part of the inundation map, emphasizes the DEM's impact on flood depths, with shaded areas marking census tracts and highlighting variations in population impact across simulations. This demonstrates how methodology and DEM choice crucially influence flood risk mapping.

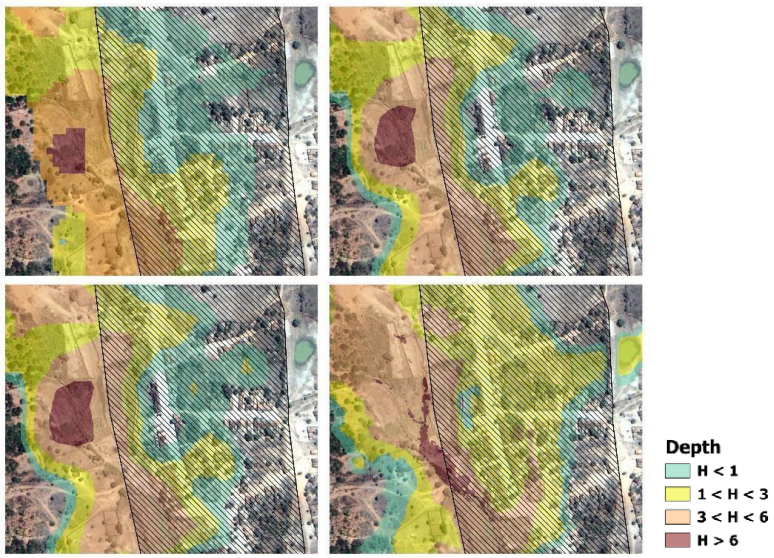



**Fig. 1. Inundation and depth maps**

**Acknowledgments**

The authors acknowledge the support of the Faculty of Engineering of the University of Porto and the Brazilian National Water and Sanitation Agency (ANA). Additionally, they acknowledge the Foundation for Science and Technology (FCT) for providing a research grant to the first author [2023. 02769.BD].

**References**

Bhuyian, Md. N.M., and A. Kalyanapu (2018). "Accounting digital elevation uncertainty for flood consequence assessment." Journal of Flood Risk Management 11 (S2): S1051-S1062. https://doi.org/https://doi.org/10.1111/jfr3.12293.

Farr, Tom G., Paul A. Rosen, Edward Caro, Robert Crippen, Riley Duren, Scott Hensley, Michael Kobrick, Mimi Paller, Ernesto Rodriguez, Ladislav Roth, David Seal, Scott Shaffer, Joanne Shimada, Jeffrey Umland, Marian Werner, Michael Oskin, Douglas Burbank, and Douglas Alsdorf. (2007). "The Shuttle Radar Topography Mission." Reviews of Geophysics 45 (2). doi: https://doi.org/10.1029/2005RG000183.

Hawker, Laurence, Paul Bates, Jeffrey N., & Jonathan Rougier (2018). "Perspectives on Digital Elevation Model (DEM) Simulation for Flood Modeling in the Absence of a High-Accuracy Open Access Global DEM." Frontiers in Earth Science 6. https://doi.org/10.3389/feart.2018.00233.

IBGE (2011). Base de informações do Censo Demográfico 2010: Resultados do Universo por setor censitário. Rio de Janeiro: Instituto Brasileiro de Geografia e Estatística.

McClean, Fergus, Richard Dawson, and Chris Kilsby (2020). "Implications of Using Global Digital Elevation Models for Flood Risk Analysis in Cities." Water Resources Research 56 (10): e2020WR028241. Doi: https://doi.org/10.1029/2020WR028241.

Melo J, Araújo L, Oliveira M, Martin T, Pinto M and Freitas P. (2015). "Hazard potential classification of dams using a simplified methodology." 2nd International Dam World Conference, Lisboa, Portugal.

Petry A, Bonfim M, Laus F, and Anderaos A. (2018). "Classification of dams by their hazard potential: the experience of the Brazilian national water agency." Third International Dam World Conference, Foz do Iguaçu, Brazil.

USACE (2023). HEC-RAS River Analysis System User's Manual. March-2023.: United States Army Corps of Engineers

Viseu, Maria Teresa (2006). "Segurança dos vales a jusante de barragens – metodologias de apoio à gestão dos riscos." Doutoramento, Instituto Superior Técnico, Universidade Técnica de Lisboa.

# Physical Model Tests on Slope Deformation at Mining Pit Lakes due to Wave Impact

Torsten HEYER[1], Jürgen STAMM[1], Paul RAABE[2], Dieter DAHMEN[2]

[1] TUD Dresden University of Technology, Institute of Hydraulic Engineering and Technical Hydromechanics, Germany
torsten.heyer@tu-dresden.de; juergen.stamm@tu-dresden.de

[2] RWE Power AG, Main Department Geomechanics, Germany
paul.raabe@rwe.com; dieter.dahmen@rwe.com

ABSTRACT

The planned decommissioning and recultivation of former opencast lignite mines often leads to the creation of artificial lakes with a wide range of potential uses (e. g. tourism, water management). The slopes of these mining pit lakes must permanently withstand the impact of wind-induced waves both during the filling phase and after reaching the target water level. In this context, physical model tests were conducted in which morphological changes at steep slopes due to wave impact were investigated for different soil materials and scenarios. It could be shown that the final morphology of wave-impacted slopes varies significantly, primarily depending on the cohesive properties of the soil type. Based on these findings, the most suitable material to be used as cover layer for pit lake slopes can be determined.

## 1. Introduction

With the aim of contributing to a climate neutral European continent by 2050, lignite mining in Germany and other countries is being phased out. The controlled flooding of the open-cast pits that remain after the end of mining activities is often the most economical and environmentally friendly method of recultivating these landscapes. In this way, the largest artificial lake district in Europe is currently being created in the Lusatia region in Eastern Germany. From a soil- and hydromechanics perspective, ensuring the stability of the pit lake slopes is of particular importance both during and after completion of the lake filling. It is to be expected that wind-induced waves will lead to a significant reshaping of the pit lake slopes, especially at intermediate water levels during the filling phase, with slope inclinations of 1 : 2,5. For this reason, it is necessary to design the pit lake slopes both in terms of shape and cover material in a suitable manner in order to generate predictable and stable shore conditions. While scientific studies on the prediction of the deformation of sandy embankments focus mainly on gently sloping coastal areas (e. g. Aagaard & Huges, 2017), Wagner (1996) also investigated the deformation behaviour of steep opencast mine embankments. However, the analytical formulae for the prediction of equilibrium profiles derived from his physical model tests are limited to sandy, non-cohesive material only.

## 2. Physical Model Tests

On this background, physical model tests (test setup, see Fig. 2) were carried out in the hydraulic engineering laboratory of the Dresden University of Technology, in which the wave-induced deformation behaviour was investigated for seven different soil materials (cohesive and non-cohesive). As shown in Fig. 1, a typical slope geometry of a mining pit lake is characterised by a stepped form (several berms with individual slopes inclined at 1:2.5 in between) and a large total height. Due to these conditions and to limits related to scaling effects, the physical modelling of the entire lake slope was not possible. To overcome this problem, each soil material was tested in three different scenarios that represent specific conditions during the filling phase of the pit lake:

- water level just above lower terrace → "Scenario 1",
- water level at mid-height of berm → "Scenario 2",
- water level just below upper terrace → "Scenario 3".

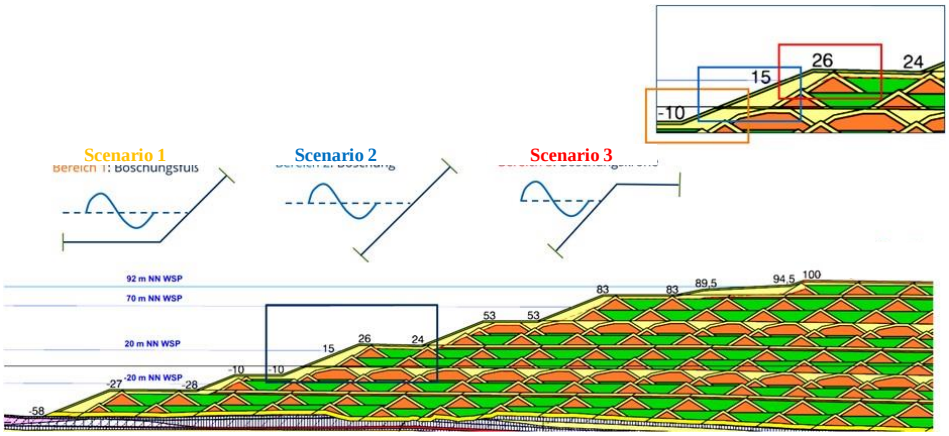



**Fig. 1.** Typical geometry and composition of slopes at mining pit lakes and scenarios 1-3 for different water level conditions (source: RWE)

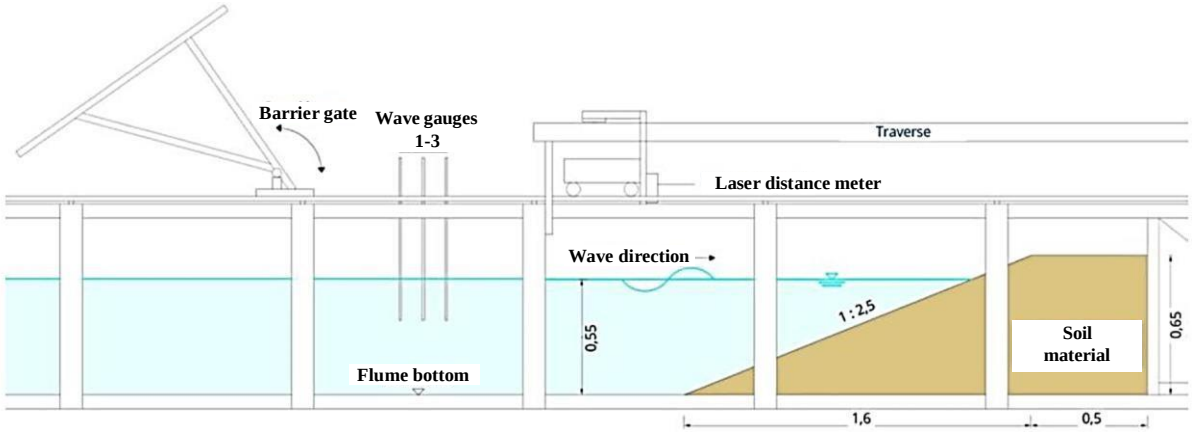



**Fig. 2.** Setup of physical model test

## 3. Results and Conclusions

With the aim of investigating the material-dependent characteristics of slope deformation for identical wave impact, the final slope profiles for all materials (A0-A6) were overlaid and parameterised for all three scenarios. Additionally, the profile evolution over time (duration of wave impact) was analysed (see Fig. 3).

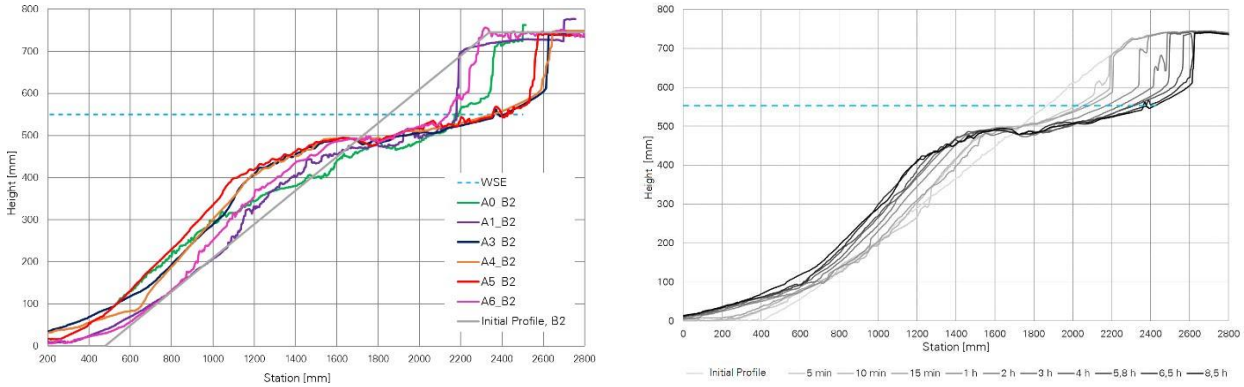



**Fig. 3.** Final profiles of slope for different materials (left) and slope geometry development over time for material "A3" (right) in setup 2

The results of the model tests showed that cohesive materials with higher erosion resistance exhibit less reef development, which leads to spontaneous and blocky failure in the cliff area above the water level. For such conditions, an equilibrium slope profile will not be reached. In contrast, slopes made of non-cohesive materials have lower erosion resistance and are characterised by a pronounced reef formation that will lead to a stable slope geometry in the long run. With regard to practical implementation, a slightly cohesive material was therefore recommended as a surface layer that, besides an increased erosion resistance, develops a long-term predictable and stable profile of the lake shore.

**References**

Aagaard T & Hughes MG (2017) Equilibrium shoreface profiles: A sediment transport approach, Marine Geology, Vol. 390, 2017, p. 321-330, ISSN 0025-3227, https://doi.org/10.1016/j.margeo.2016.12.013.

Wagner H (1996): Böschungsumbildung durch Wellen (Embankment Reshaping due to Waves) (in German) In: Technische Universität Dresden, Dresdner Wasserbauliche Mitteilungen 9. Institut für Wasserbau und technische Hydromechanik. p. 155-161

# Optimization of supervised learning chain models for monthly flow prediction

Jadran BERBIĆ[1], Eva OCVIRK[2]

[1] Technical High School Šibenik, Croatia
jberbic@hotmail.com

[2] Faculty of Civil Engineering, University of Zagreb, Croatia
ocvirk@grad.hr

ABSTRACT

The objective of the work is to improve modeling procedure of mean monthly flows for the purpose of long-term prediction. After the treatment and choice of independent variables, genetic algorithm has been applied to select optimal model hyperparameters of supervised learning models - artificial neural network (ANN), support vector machine (SVM), histogram gradient boosting regressor (HGBR) and elastic net (EN). Models were applied in chain modeling procedure in a manner of providing mean monthly flow at Vinalić (river Cetina, Croatia) for six (6) months per every sample of dataset.

## 1. Introduction

The work is the continuation of previous researches where accuracies of ANN and SVM were exhaustively examined in dependence of dataset length, followed by optimization of hyperparameters and input variables choice by genetic algorithm (GA) and simulated annealing (Berbić et al., 2017, 2022). Monthly mean, maximum and accumulated precipitation ('Pr') and mean, minimum and maximum temperature ('T') at near-by stations were chosen as inputs (meteorological station Knin, precipation gauge Vinalić, climatological station Sinj - labels 'K', 'V' and 'S'). After exclusion of missing values from data (1951-2015, DHMZ, 2017), totally 675 samples were left for modeling. Additonal variables were created by fast Fourier transform to reach out periodicities of flows, similarly as proposed at TensorFlow time series forecasting tutorial (Abadi et al., 2015). For training, calibration and verification dataset is split in ratios 40, 15 and 45 %, resulting in slightly less then 40 years for training and calibration (similarly as 40 years dataset length in previous researches). Based on cross-correlations plotted on training part (Figure 1), seasonal periodicites were turndown. The mean monthly flow 'Qavm' (hydrological station Vinalić, river Cetina, overall mean is 28,4 m3/s) was also turndown, in order to use exclusively exogenous variables as inputs. After the normalization of data, 18 successive steps of 16 chosen variables (totally 288) were used to feed models.

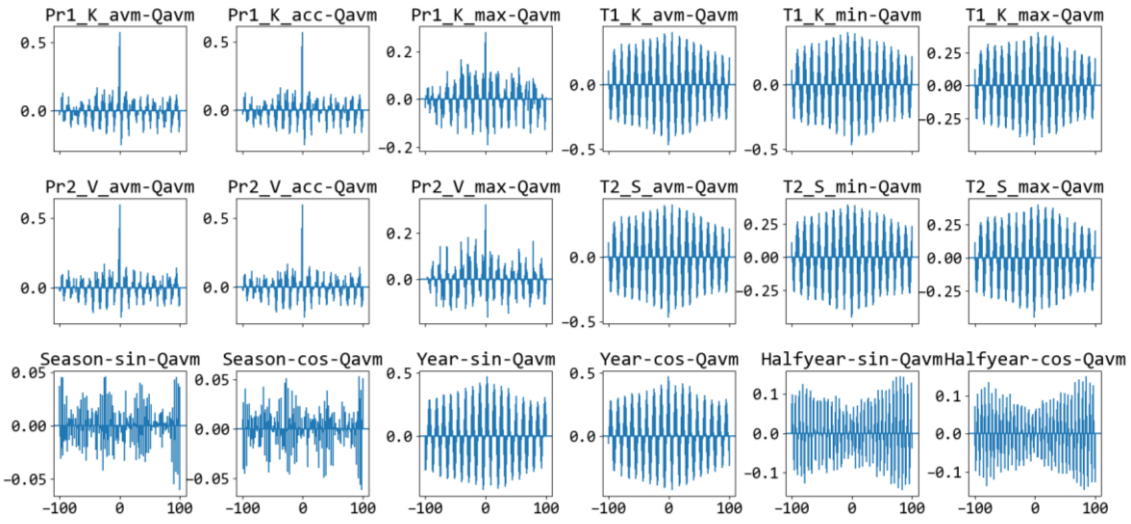



**Fig. 1.** Correlations of potential input variables with mean monthly flow, with lag value of 100

## 2. Results of optimization by genetic algorithm

For choice of model hyperparameters, previously developed GA (Berbić et al., 2022) used to maximize coefficient of determination ($R^2$), was adopted for chain modeling procedure and to minimize root mean square error on normalized data (RMSE*). 30 generations were set for ANN and HGBR (due to high durations), and 100 for SVM and EN. Generation counted 120 individuals with crossover probability of 95 %. For every individual, error measures are calculated as average on all six outputs (mean monthly flows) on calibration part. The procedure is developed in Python, by using scikit-learn library (Van Rossum and Drake, 2009, Pedregosa et al., 2011). Achieved fitness and performance is shown in Table 1, while evolution through generations is shown on Figure 2.

**Table 1.** Results of model's hyperparameters optimization and model performance on all parts of dataset

| Model | Objective function | Fitness [/] | Duration [min] | Training $R^2$[/] | RMSE [$m^3$/s] | Calibration $R^2$[/] | RMSE [$m^3$/s] | Verification $R^2$[/] | RMSE [$m^3$/s] |
|---|---|---|---|---|---|---|---|---|---|
| ANN | RMSE* | 0.1385 | 680.3 | 0.856 | 3.621 | 0.567 | 7.087 | 0.708 | 4.632 |
| SVM | RMSE* | 0.1440 | 13.1 | 0.985 | 1.168 | 0.574 | 7.034 | 0.685 | 4.811 |
| SVM | $R^2$ | 0.565 | 4.3 | 0.910 | 2.878 | 0.570 | 7.066 | 0.674 | 4.891 |
| HGBR | RMSE* | 0.1847 | 395.2 | 0.996 | 0.575 | 0.561 | 7.136 | 0.572 | 5.606 |
| EN | RMSE* | 0.1347 | 12.1 | 0.739 | 4.907 | 0.629 | 6.570 | 0.678 | 4.862 |
| EN | $R^2$ | 0.623 | 28.7 | 0.742 | 4.877 | 0.629 | 6.565 | 0.680 | 4.848 |

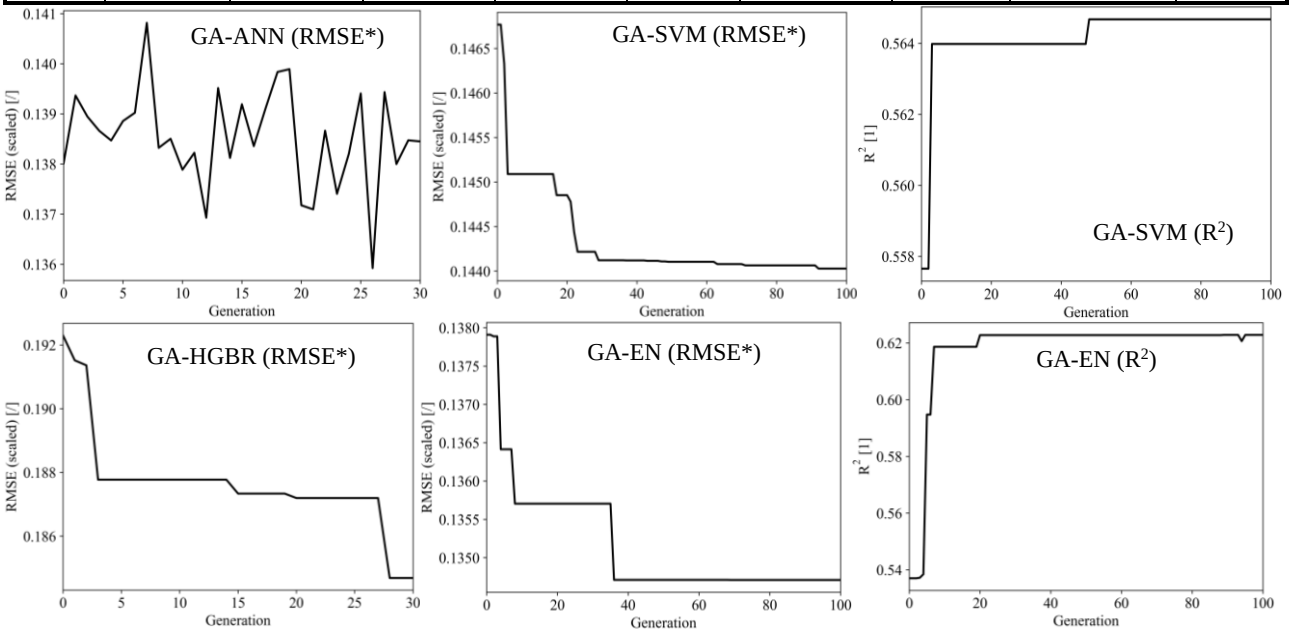



**Fig. 2.** Optimization of model's hyperparameters by GA, objective function through generations

## 3. Conclusion

Usage of new objective function (RMSE*) did not result in any substantial improvement of accuracies. However, as usage of $R^2$, it enabled efficient choice of model hyperparameters, especially for EN and SVM, with low durations of search for optimal hyperparameters. In further research obtained models will be combined into ensemble model to improve accuracy of flow prediction. Hence, developed procedures will be used for choice of ensemble base models, according to the criteria of procedure duration and model accuracy.

**References**


Berbić J, Ocvirk, E, Gilja G. (2018) Comparison of Supervised Learning Methods for Prediction of Monthly Average Flow, Građevinar 70(8), 643-656

Berbić J, Ocvirk E, Gilja G (2022) Optimization of supervised learning models for modeling of mean monthly flows, Neural Comput & Applic 34, 17877–17904

DHMZ - Croatian Hydrological and Meteorological Service (2017) Hydrological Database, HIS 2000

DHMZ - Croatian Hydrological and Meteorological Service (2017) Relational Meteorological Database

Abadi M, Agarwal A, Barham P, Brevdo E, Chen Z., Citro C., ... & Zheng X. (2015) TensorFlow: Large-scale machine learning on heterogeneous distributed systems, arXiv preprint arXiv:1603.04467

Van Rossum G and Drake FL (2009) Python 3 Reference Manual, Scotts Valley, CA: CreateSpace.

Pedregosa F, Varoquaux G, Gramfort A, Michel V, Thirion B, Grisel O, Blondel M, Prettenhofer PP, Weiss R, Duborg V, Vanderplas J, Passos A, Cournapeau D, Brucher M, Perrot M, Duchesnay É (2011) Scikit-learn: Machine Learning in Python, Journal of machine learning research 12(85), 2825-2830

# On the Performance Assessment of Hydro-Morphodynamic Models: Fuzzy Logic versus Subjective Correlation

Sebastian SCHWINDT[1], Paul Jacques GRIGULL[1], Beatriz NEGREIROS[1], Stefan HAUN[1]

[1] Institute for Modelling Hydraulic and Environmental Systems (IWS), University of Stuttgart, Germany
sebastian.schwindt@iws.uni-stuttgart.de
paul.grigull@gmx.de
beatriz.negreiros@iws.uni-stuttgart.de
stefan.haun@iws.uni-stuttgart.de

ABSTRACT

Numerical modeling of hydro-morphodynamic processes, encompassing fluvial sediment erosion, transport, and deposition, involves mathematical simplifications translated into adjustable parameters for each case study. This calibration process aims to achieve accurate simulations of measured quantities. Before utilizing a numerical model to predict hydrodynamic or morphodynamic changes in rivers or lakes, additional model validation is required. Validating model quality entails statistically quantifying the accuracy of modeled outputs compared to measured data. A satisfactory validation of a morphodynamic model, focusing on sediment transport, relies on correctly reproducing landscape patterns within model boundary conditions. However, a direct pixel-by-pixel quantification of measured topographic changes may indicate poor model quality despite achieving correct landscape patterns. Thus, the challenge arises of objectively distinguishing morphodynamic models capable of predicting morphological patterns from entirely nonsense models. To address this challenge, a recently developed fuzzy logic approach incorporates blur to pardon some degree of inaccuracy for a fuzzy-statistical assessment of morphodynamic model goodness. In this study, we investigated the performance of fuzzy-logic-based model quality assessment and human perception. Through an online survey, amateurs, somewhat experienced individuals, and experts were asked to subjectively rate correlation levels in six pairs of maps. Expert opinions exhibited increasing agreement with calculated fuzzy correlations, contrary to biases observed in other disciplines. Also, in the survey, experts confirmed the significance of fuzzy-logic metrics for hydro-morphodynamic model validation, enabling precise assessments while considering the inherent impreciseness of these models.

## 1. Introduction

Forecasts of fluid and sediment dynamics of river systems can be implemented with hydro-morphodynamic models, where state-of-the-art modeling builds on at least two-dimensional (2d) numerical simulations or physical experiments. In the process of model calibration and validation, the agreement between simulations and experiments can be verified by comparing spatially explicit maps of simulated and precisely measured events in the past, referred to as *hindcasts*. Direct statistical model verification uses pixel-by-pixel comparisons for calculating, for example, some error or correlation coefficient. However, quantifying topographic change pixel-by-pixel may reflect poor model quality, even when accurate fluvial landscape patterns were simulated. A pixel-by-pixel comparison may yield globally low correlation coefficients, as not all pixels in the simulation precisely match the pixels in the hindcasts because of considerable model simplifications. In this case, pixel-by-pixel statistics are not meaningful, but an objective differentiation between morphodynamic models that can at least correctly predict morphological patterns and models that are complete nonsense was still required. To address this issue, Negreiros et al. (2021) proposed two ways of fuzzy map comparison. Notably, a fuzzy numerical map comparison to account for spatial offset of modeled quantities (e.g., topographic change), and a fuzzy kappa map comparison to reduce model penalization because of quantitative inaccuracy. In this study, we asked how well the calculated fuzzy correlation statistics relate to human opinion.

## 2. Methods

Topographic maps comparing modeled and measured bed elevations of a shallow reservoir in lab experiments (Kantoush et al., 2008) and resulting from a numerical model of a gravel-cobble-bed river (Beckers et al., 2018) served to calculate fuzzy correlation coefficients with the methods proposed by Negreiros et al. (2021). The same topographic maps were shown to self-identified "amateurs", "somewhat experienced individuals", and "experts" in a broad online survey to get feedback on their subjectively perceived correlation between pairs of maps (Figure 1). The map representations were varied regarding color (vs. gray scale), resolution, and presented for the two case studies. Also, quasi-randomized images (Figure 1b) were shown with intended correlations of zero and one. In total, 6 pairs of maps were displayed in the survey (full list in Table 1).

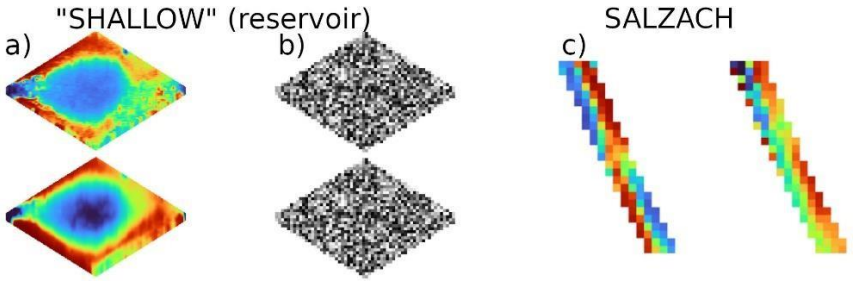



Figure 1: Excerpt of the survey using topography data from a shallow reservoir (lab), and the Salzach River at the Austro-German border.

## 3. Results and Discussion

155 responses were collected between November 24, 2021, and December 9, 2021. All participants estimated the correlation between the identical randomized maps of the shallow reservoir (first two rows in Table 1) being close to one, similar as the fuzzy correlation coefficients. The random maps falsely suggesting high correlation less intrigued the group of somewhat experienced individuals only. All other comparisons should have ideally yielded "some degree" of correlations, but neither zero nor one. While the fuzzy map comparisons were not affected by color or gray-scale representations, human eyes wrongly assigned lower correlation to gray-scale imagery. Finally, the group of experts attested the fuzzy correlation coefficients high relevance for representing their opinion.

**Table 1.** Correlation coefficients approximated with the fuzzy map comparison technique and estimated by self-identified "amateurs", "somewhat experienced individuals", and "experts".

| Map pair | Fuzzy correlation | Amateurs | Somewhat experienced | Experts |
|---|---|---|---|---|
| Shallow reservoir two random, colorized | 1.000 | 0.898 | 0.862 | 0.897 |
| Shallow reservoir two random, gray scale | 0.747 | 0.422 | 0.333 | 0.366 |
| Shallow reservoir physically modeled vs. measured, colorized | 0.907 | 0.668 | 0.691 | 0.731 |
| Shallow reservoir physically modeled vs. measured, gray scale | 0.907 | 0.711 | 0.691 | 0.724 |
| Salzach numerically modeled vs. measured, colorized | 0.418 | 0.453 | 0.433 | 0.421 |
| Salzach numerically modeled vs. measured, gray scale | 0.418 | 0.350 | 0.348 | 0.379 |

## 4. Conclusions

The evaluation of 155 survey responses and subsequent comparison with fuzzy methods showed promising outcomes. The utilization of fuzzy methods demonstrated considerable potential in effectively capturing the subjective perception of correlation, thus, objectively refining expert opinion for the validation of hydro-morphodynamic models. Additionally, the findings highlight that human visual perception and its associated perceived correlation exhibit a color dependency.

**Acknowledgements**

This research was partially funded by the Deutsche Forschungsgemeinschaft (DFG, German Research Foundation) in the framework of the China-NSFC-DFG 2020 program (GEPRIS GZ SCHW 2027/2-1, AOBJ: 673857). Thank you to all survey participants.

**References**

Negreiros B, Schwindt S, Haun S, Wieprecht S (2021) Fuzzy Map Comparisons Enable Objective Hydro-Morphodynamic Model Validation. Earth Surface Processes and Landforms 47 (3), 793–806.
Kantoush SA., Bollaert E, Schleiss AJ (2008) Experimental and numerical modelling of sedimentation in a rectangular shallow basin. International Journal of Sediment Research 23, 212–232.
Beckers F, Noack M., Wieprecht S (2018) Uncertainty analysis of a 2D sediment transport model: an example of the Lower River Salzach. Journal of Soils and Sediments 18, 3133–3144.

# Wake characteristics of flow past circular cylinder with and without helical strakes in open channels

Abhinav THAKURTA[1], Ram BALACHANDAR[2]

[1] Department of Mechanical, Automotive and Materials Engineering, University of Windsor, Windsor, Canada
thakurta@uwindsor.ca

[2] Department of Civil and Environmental Engineering, University of Windsor, Windsor, Canada
rambala@uwindsor.ca

ABSTRACT

Helical strakes have been suggested for use as a passive method of control to prevent the occurrence of vortex shedding from circular wall mounted cylinders. The present study experimentally investigates the complex wake flow patterns behind a wall-mounted helical straked cylinder using particle image velocimetry (PIV) in a shallow flow. The paper compares the mean velocities, Reynolds stresses and wake structures of a plain cylinder with that of helical straked cylinders. The strakes' configuration consists of three-start helical strakes with pitch ($p$) equal to $10d$ and a height ($h$) of $0.2d$, where $d$ is the diameter of the plain cylinder. The preliminary results show that the presence of helical strakes drastically changes the wake characteristics, which can influence not only the drag but also alter the flow structures. This can have important implications in reducing scour behind bridge piers. Further details will be discussed in the final paper.

## 1. Introduction

The fluid flow surrounding a circular cylinder exhibits intricate phenomena such as vortex shedding and flow separation occurring behind the cylinder. As a result, various passive control methods have been investigated to mitigate the occurrence of vortex shedding (Zdravkovich, 1981). Utilization of helical strakes has been suggested because the flow separation around a circular cylinder remains unaffected by the Reynolds number, owing to the fixed separation points along the edges of these strakes and hence becomes an important flow characteristic as it disrupts vortex coherence.

The tip of the strakes predominantly governs the flow separation over a significant portion of the cylinder's span and leads to three-dimensional flow characteristics in the wake. Additionally, the helical strakes restrict the interaction between the two shear layers originating from opposite sides of the cylinder. The flow visualization provided by Constantinides (2006) shows a notable vertical movement due to the channeled flow of fluid. Furthermore, the results reveal an abrupt pressure change on the surface compared to the plain cylinder.

While researchers have undertaken investigations into comprehending how the geometry of helical strakes influences vortex shedding (Korkischko et al., 2007; Baarholm, 2005; Quen et al., 2018), the impact of the strakes on the turbulent flow features in the wake of a wall-mounted circular cylinder in a shallow open channel needs to be explored. Also, there is a need for a more comprehensive understanding of the flow physics in the presence of these strakes. The available literature lacks a detailed investigation on the vertical plane whose study can lead to better insights into the wake structure due to the vertical motion in the presence of strakes. Acquiring a detailed understanding of flow physics is crucial for unravelling the coherent structures and comprehending how they can potentially impact the flow around circular cylinders in various applications.

## 2. Experimental Setup

The experimental setup comprises a recirculating water channel having a rectangular cross-section with dimensions of 16 m in length, 1.2 m in width, and 0.8 m in height. The depth of water in the flume is 85 mm.

The pump bulk velocity is 0.29 m/s, resulting in a Reynolds number based on the cylinder diameter, $d$ of $Re_d$ = 7000. A schematic representation of the flow field is shown in Fig. 1. Two cylindrical bluff bodies were manufactured: one with strakes having a three-start configuration (number of strakes is equal to 3), a pitch ($p$) equal to 10$d$ and a height ($h$) of 0.2$d$ and the other one without strakes (plain cylinder). The diameter($d$) of the bluff body is 25.5 mm with a total height, $H$ of 85 mm which is equal to one-third of the pitch since the circular section repeats itself every one-third of the pitch length.

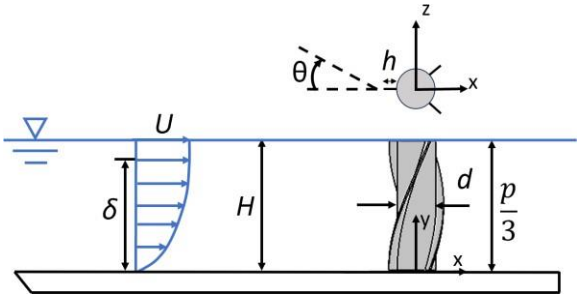
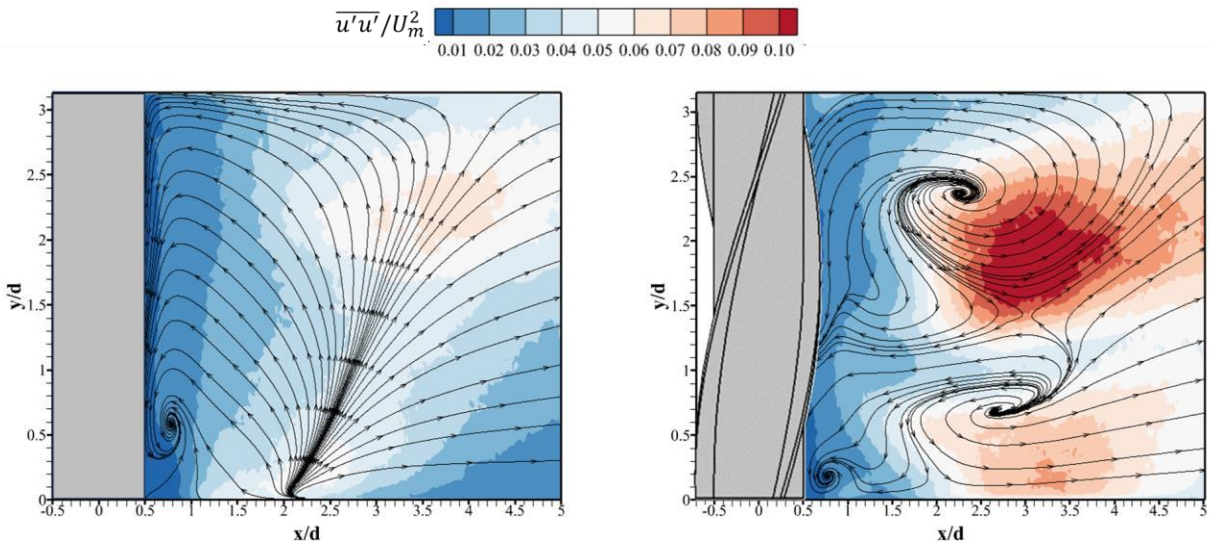



**Fig. 1.** Schematic of the field of view

## 3. Preliminary Results

The presence of helical strakes induces modifications in the flow characteristics of the wake. For instance, Fig. 2 presents a comparison based on Reynolds normal stress in the wake region. The contours on the mid-vertical plane have been depicted in Figs. 2(a) and 2(b) along with the mean streamtraces. It is evident from Fig. 2(a) that there is a significant upward flow from the bed up toward the free surface in the case of a plain cylinder, which is absent in the case of the helical straked cylinder. While a single vortex structure can be observed in the wake of the plain cylinder, helical strakes give rise to multiple vortices in the wake of a cylinder with strakes. The strakes also induce a vertical motion of the fluid near the cylinder due to the channel formed by the strakes. Reynolds normal stress is larger for the helical straked cylinder near the bed and the mid-region, as compared to the plain cylinder. These larger values may be because of the shear layers originating across the strakes. Additional details and analysis will be provided in the final paper.




(a) Plain cylinder (b) Helical straked cylinder

**Fig. 2.** Comparison between the circular cylinders with and without helical strakes based on Reynolds normal stress.

**References**


Baarholm R, Lie H (2005) Systematic parametric investigation of the efficiency of helical strakes, In: Proceedings of the Deep Offshore Technology, Vitoria, Brazil

Constantinides Y, Oakley OH Jr (2006) Numerical prediction of bare and straked cylinder VIV, International Conference on Offshore Mechanics and Arctic Engineering. Hamburg, Germany, OMAE 2006-92334

Korkischko I, Meneghini JR, Gioria RS, Jabardo PJ, Casaprima E, Franciss R (2007) An Experimental Investigation of the Flow Around Strakes, In: Proceedings of the 26th International Conference on Offshore Mechanics and Arctic Engineering, San Diego, California, USA, OMAE 2007-29057

Quen LK, Abu A, Kato N, Muhamad P, Tan LK, Kang HS (2018) Performance of two- and three-start helical strakes in suppressing the vortex-induced vibration of a low mass ratio flexible cylinder, Ocean Engineering 166, 253-261

Zdravkovich MM (1981) Review and classification of various aerodynamic and hydrodynamic means for suppressing vortex shedding, J Wind Energy & Industrial Aerodynamics 7,145–18

# Granular cooling of uni-sized particles during jamming process

Solange V. MENDES[1], Rui ALEIXO[2], Michele LARCHER[3], Sílvia AMARAL[4], Rui M.L. FERREIRA[5]

[1,5] CERIS, Instituto Superior Técnico, Universidade de Lisboa, Portugal
solange.mendes@tecnico.ulisboa.pt
ruimferreira@tecnico.ulisboa.pt
[2] Institute of Hydro-Engineering of Polish Academy of Sciences
rui.aleixo@ibwpan.gda.pl
[3]Faculty of Engineering, Free University of Bozen-Bolzano, Italy
Michele.Larcher@unibz.it
[4]LNEC, National Laboratory of Civil Engineering
samaral@lnec.pt

ABSTRACT

This research aims to experimentally characterize a granular flow during jamming process induced by a sudden constriction. An ensemble of 31 equal experiments in a 1.5 m long chute sloping at 19 degrees was conducted. The outlet area of the chute was obstructed by a wall with two vertical gaps, twice the diameter of the granular material used. It was observed that a clogging event triggers a generalized jamming process. The granular system is highly dissipative due to collisions and enduring contacts among the particles, resulting in a general cooling process. Fields of the ensemble mean granular velocity and granular temperature were calculated. The most relevant remarks on these results are presented.

## 1. Introduction

The study of granular materials motion in fluids of low density and viscosity, as dry granular flows, provides insights on granular processes namely stony debris flows. Slit dams or open check dams control debris flows in steep streams (Takahashi, 2007). Some studies have shown that mechanical clogging, the fully ceasing of the granular flow, may occur for grainsizes smaller than those of design conditions (Frey & Tannou, 2000) decreasing the efficiency of check dams. In this sense, it is of major importance to evaluate the behaviour of the granular flow after a clogging event.

## 2. Experimental set-up and instrumentation

The dry granular experiments were conducted in an acrylic chute with a 1.5 m length and 0.08 m width tilted at 19 degrees in the facilities of Free University of Bozen-Bolzano (Fig.1). Downstream of the chute, a vertical barrier with a double gap, replicating slit dam conditions, was positioned. The width of each gap was twice the size of the uni-sized polystyrene particles used ($d$=1.8mm) with a volume of 3 liters. The facility was composed by a sediment reservoir with an acrylic gate. The instrumentation included two high-speed (HS) cameras and one spotlight. One camera was located upstream – C1, at the reservoir gate location, and another was placed downstream at the slit site - C2.

The recorded images from both cameras presented a maximum 4096x744 pixel resolution with a target frame rate of 300 fps and an exposure time of 200 µs. The experimental protocol consisted in the sudden release of the particles and recording its development along the chute. The image recording was stopped once all granular motion came to a complete stop in front of the slit.

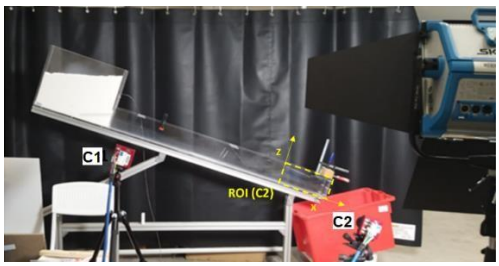



**Fig. 1.** Laboratory chute. Instrumentation: two high-speed cameras: C1 and C2. Representation of the region of interest (ROI) analysed in the images from the C2.

## 3. Experimental results

Through visual analysis of the images captured by the HS cameras, for the ensemble performed, the instant when the particles first formed a stable arch-like structure at the slit, as described by To & Lai, 2002 was identified as the clogging instant – *ts* (time=0) The C1 images were only used for this purpose. The images of C2 required pre-processing to improve the signal-to-noise ratio for the later application of a velocimetry algorithm.

The results presented were analysed in a region of interest (ROI) specifically defined to capture the chute from its bottom to a height of about 39*d*. The ensemble-averaged along-chute velocity (*u*) and granular temperature (*T*) were calculated, revealing that three phases of granular matter, gas-like, liquid-like and solid-like are presented in this flow. Before *ts* the granular flow shows a gas-like behaviour (Fig.3a) after the release of the flow through the upstream floodgate, where in terms of particle motion, it is quite a chaotic flow, until it faces the downstream obstruction. Then, in a limited space, there is a strong cooling of the system (z=3 at VP1 – Fig.2) featuring zero granular temperature. The system becomes intermittent and eventually transits to a liquid-like state (Fig.3b and Fig.3c ). The liquid-solid phase transition occurs as a wave front that progresses upstream. At this stage, the jamming process is triggered (Fig.3d) and the wavefront progresses faster once the system has cooled down as particles become aggregated to the jamming region at a higher rate.

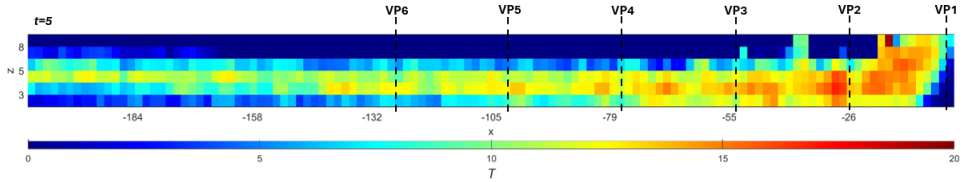



**Fig.2.** Spatial distribution of the granular temperature (*T*) represented in non-dimensional form and location of six vertical profiles (VP).

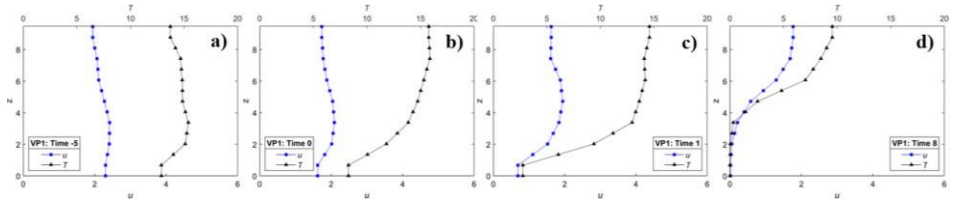



**Fig.3.** Non dimensional along-chute velocity (u) and temperature (*T*) variation for VP1.

## 4. Conclusions

This research aims to experimentally characterize the cooling process of a granular flow during jamming induced by a sudden constriction. First, we identified the clogging instant, identified by the formation of arch-like structures, that eventually triggered jamming as a cooling wavefront that progresses upstream. The phase transitions observed in the granular flow show that there is never a triple point in the system. In other words, before jamming process the system always previously transits from gas-like to liquid like.

**Acknowledgements**

PhD student Solange Mendes thanks the financial support of the Portuguese Foundation for Science and Technology through the scholarship PD/BD/150693/2020. This research was also supported through the project with reference: DikesFPro PTDC/ECI-EGC/7739/2020.

**References**

Frey, P., & Tannou, S. (2000). Experimental study on bed load control in torrents by open slit dams. In *Building Partnerships* (pp. 1–10).
Takahashi, T. (2007). Debris Flow: Mechanics, Prediction and Countermeasures.



# Theme E

## Climate change and risk mitigation

# Exploring the Escalating Occurrence of Heatwaves in Portugal: Insights from a Validated ERA5-Land Dataset from 1980 to 2021

Luis Angel ESPINOSA[1], Maria Manuela PORTELA[2]

[1] Associação do Instituto Superior Técnico para a Investigação e Desenvolvimento (IST-ID), Civil Engineering Research and Innovation for Sustainability (CERIS), Av. António José de Almeida, No. 12, 1000-043; Lisbon, Portugal
luis.espinosa@tecnico.ulisboa.pt

[2] Instituto Superior Técnico (IST), University of Lisbon (ULisboa), CERIS; Lisbon, Portugal
maria.manuela.portela@tecnico.ulisboa.pt

## ABSTRACT

Heatwaves pose a significant concern within the context of climate change, exerting impacts on various sectors including human health, agriculture, and ecosystems. A comprehensive understanding of the spatiotemporal patterns of heatwaves is crucial for the development of effective adaptation strategies. This extended abstract presents the findings of a study that investigates the spatiotemporal patterns of heatwaves in Portugal from 1980 to 2021, utilising a validated ERA5-Land dataset. The objective of this research is to enhance the understanding of heatwave occurrence and intensity in the region while examining their potential trends in terms of heatwave days per year.

## 1. Materials and Methods

Aiming at addressing heatwaves in Portugal, the temperature data from the ERA5-Land dataset were collected at representative climatic locations (nine grid-points in Figure 1) and subjected to validation against ground-based records from the Portuguese Institute for Sea and Atmosphere (IPMA), ensuring reliability and accuracy. By comparing the ERA5-Land temperature data with IPMA observations, the quality and suitability of the dataset for analysing spatiotemporal heatwave patterns in Portugal can be confidently assessed.

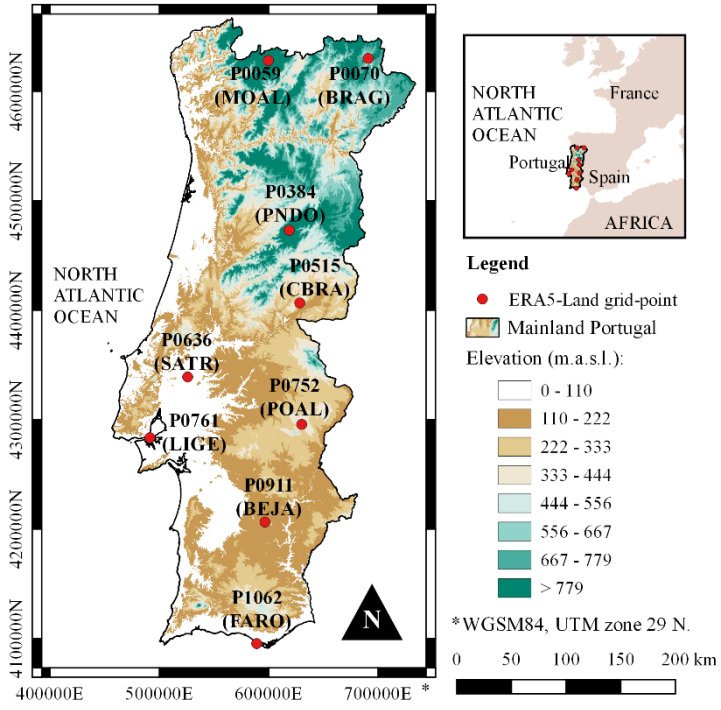



**Fig. 1.** Location of the analysed ERA5-Land grid-points and their nearest IPMA ground-based meteorological stations between brackets.

The analysis focused on examining maximum daily temperatures, which is a key indicator of heatwave events. Heatwaves were identified using the Heatwave Magnitude Index (HWMI) proposed by Russo *et al*. (2014), which defines heatwaves as three consecutive days with maximum daily temperatures exceeding the 90th percentile of daily maxima, centred on a 31-day window. Hence, for a given day $d$, the threshold series $A_d$ of the dataset is given by Eq. (1):

$$A_d = \bigcup_{y=1980}^{2021} \bigcup_{i=d-15}^{d+15} T_{y,i}, \tag{1}$$

where ∪ denotes the union of sets and $T_{y,i}$ is daily temperature of the day $i$ in the year $y$. The kernel technique was applied to analyse the spatial distribution of heatwaves across Portugal.

## 2. Results

The comparison between Tmax values from ERA5-Land and the IPMA Tmax records revealed a commendable level of agreement. The analysis of the data exhibited strong consistency and reliability, indicating a good match between the two datasets. This agreement underscores the accuracy and quality of the ERA5-Land dataset in capturing and representing the maximum temperature (Tmax) in Portugal. The validation process provides confidence in the ERA5-Land dataset, making it a valuable resource for studying spatiotemporal heatwave characteristics and their impacts in the region.

### *2.1. Escalating Heatwave Occurrence*

The spatiotemporal analysis of heatwave patterns was performed at a regional scale, encompassing diverse areas within Portugal, to capture the inherent variability. The dataset unveiled a distinct upsurge in both the frequency and intensity of heatwaves throughout the study period, as depicted by the red lines, λ(*t*), in Fig. 2. Portugal experienced a noteworthy escalation in the occurrence of heatwave events, with a particularly prominent upward trend observed in recent decades. Furthermore, the duration of heatwaves displayed a progressive increase, indicating prolonged periods of extreme heat (Barriopedro *et al*., 2020). These findings strongly suggest that climate change has played a substantial role in shaping the evolving characteristics of heatwaves. Subsequent investigations should delve into the relationship between heatwaves and local climatic factors, such as humidity and wind patterns. Such an examination may shed light on the potential influence of specific atmospheric conditions in certain regions of Portugal, contributing to the facilitation of more intense and enduring heatwaves. An enhanced understanding of these localised patterns would provide invaluable insights for the development of targeted adaptation strategies and effective risk management measures.

In conclusion, this study highlights the increasing frequency of heatwaves in Portugal based on an analysis of a validated ERA5-Land dataset. The findings underscore the importance of addressing the spatiotemporal patterns of heatwaves in the region and their potential implications for climate change adaptation.

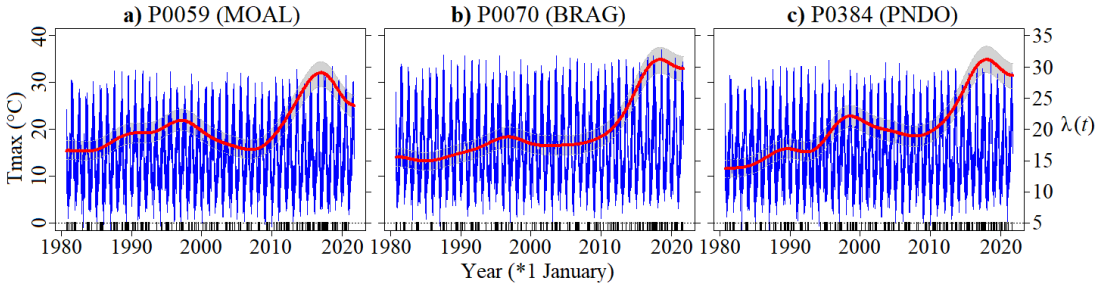



**Fig. 2.** Time-dependent occurrence rates of Tmax heatwave days (1980–2021) at three ERA5-Land grid-points from Fig. 1. Left y-axis: ERA5-Land daily Tmax values in dark blue. Right y-axis: The number of heatwave days per year, λ(*t*), in red — confidence band represented by the grey area around λ(*t*). Vertical ticks: The dates of occurrence of heatwave days.

**Acknowledgements**

This research was supported by the Foundation for Science and Technology (FCT) through funding UIDB/04625/2020 from the research unit CERIS and by the European Union's Horizon 2020 research and innovation programme SCORE under grant agreement No 101003534.

**References**

Barriopedro, D., Sousa, P. M., Trigo, R. M., García-Herrera, R., & Ramos, A. M. (2020). The exceptional Iberian heatwave of summer 2018. Bulletin of the American Meteorological Society, 101(1), S29-S34.

Russo, S., Dosio, A., Graversen, R. G., Sillmann, J., Carrao, H., Dunbar, M. B., & Vogt, J. V. (2014). Magnitude of extreme heat waves in present climate and their projection in a warming world. Journal of Geophysical Research: Atmospheres, 119(22), 12-500.

# Characterization of Extreme Warm Events in the Lisbon Region (Portugal) Based on ERA5-Land Data

Laryssa FREITAS[1], Maria Manuela PORTELA[1,2], Luis Angel ESPINOSA[2,3], José MATOS[1,2]

[1] Instituto Superior Técnico, University of Lisbon (IST/UL), Portugal. [2] Civil Engineering Research and Innovation for Sustainability (CERIS), Portugal. [3] Associação do Instituto Superior Técnico para a Investigação e Desenvolvimento (IST-ID), CERIS, Portugal

laryssa.freitas@tecnico.ulisboa.pt; maria.manuela.portela@tecnico.ulisboa.pt; luis.espinosa@tecnico.ulisboa.pt; jose.matos@tecnico.ulisboa.pt

ABSTRACT

Compared with heavy precipitation and droughts, the hot extremes (including heatwaves) have more consensus in the scientific community about the increase in its occurrence. Its effects include health problems, worse air pollution and limited functioning of key infrastructure, such as transportation, sanitation, and energy systems. The goal of the study is to investigate heatwaves (HW) over a highly populated region of mainland Portugal using ERA5-Land reanalysis data for a series of 41 years.

## 1. Materials

Climate reanalysis combines past observations with the current weather model to create a complete and consistent data set of past weather around the globe. ERA5-Land is a component of ERA5, the fifth-generation reanalysis dataset produced by the European Centre for Medium-Range Weather Forecasts (ECMWF), with 50 variables over land with hourly values. It has been validated for Portugal by Almeida & Coelho (2023).

The study area comprises 21 ERA5-Land grid-points (grid cell with ca. 8.7 x 11.1 km²) covering a region of Lisbon and its surroundings (area slightly above 2000 km²) - Figure 1. The reference period adopted in the study spanned from 1 October 1980 to 30 September 2021 (41 hydrological years).

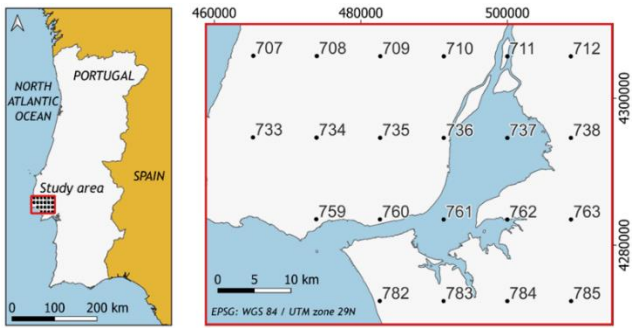



**Fig. 1.** Study area, general location and 21 ERA5-Land grid-points.

## 2. Methods

Based on the methodology proposed by Russo (2014), the HW were identified using the Heat Wave Magnitude Index (HWMI) for both daily maximum (Tmax) or minimum (Tmin) temperatures. The HWMI defines a heatwave as a period of at least 3 consecutive days in which the temperature is above the daily threshold for the reference period. The daily threshold is given by the 90th percentile of daily maximum temperature centered on a 31-day window, comprehending the day and the 15 days before and after it. Apart from the absolute values of the computed variables, a trend analysis of the annual number of HW days (HWD), i.e., the number of days belonging to a HW was performed via the Mann-Kendall and Sen's Slope estimator tests.

## 3. Results and discussion

The spatial pattern of the temperature in the study region is very smooth due to its small area, location near the sea and flat topography - Figure 2. During heatwaves, the annual average of daily maximum temperature increased up to 34% in the areas with higher annual average temperatures - Figure 2 d).

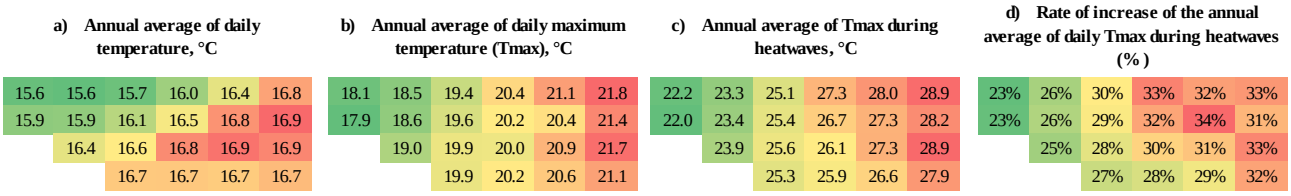



**Fig. 2.** Characteristic temperatures of the grid-points shown in Figure 1. Continuous color temperature scale adopted.

The trend analysis showed that the annual number of HWD is consistently increasing over the study period, being more pronounced regarding Tmax than Tmin. However, except for Tmax in two points located north of Lisbon, the trends are not statistically significant. This result might be associated with the substantial decadal and interannual variability identified in the globally averaged surface temperature. Therefore, the longer and further back in time that period is, the more pronounced the trends are and may become statistically significant.

The spatial pattern over the study area of the trends of annual HWD is very smooth regardless of whether they refer to Tmax or Tmin. Specifically, for Tmax - Figure 3 a) - the average increase of annual HWD varies from ca.1 to 4 days per decade, this last result being statistically significant. Regarding Tmin - Figure 3 b) -, the average increase in annual HWD ranges only from less than 1 to almost 3 days by decade, the highest values occurring south of Lisbon.

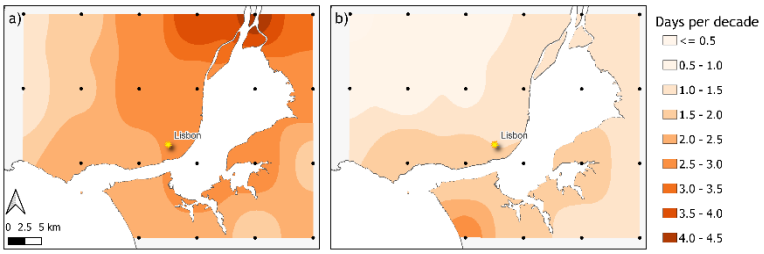



**Fig. 3.** Spatial pattern over the study area of the trends of annual HWD in days per decade for a) Tmax and b) Tmin.

The temporal pattern of the annual number of HWD showed a sinusoidal behavior with an increase towards the more recent years, reinforcing the issue related to decadal variability of the trends. Furthermore, the most in-land grid points (712, 738, 763 and 785) present a more pronounced trend - Figure 4 b) - than the most coastal ones (707 and 733) - Figure 4 a). The trends of Tmax and Tmin in the coastal grid-points have a more similar pattern than in the most in-land grid points, in which the Tmax trend is much more pronounced.

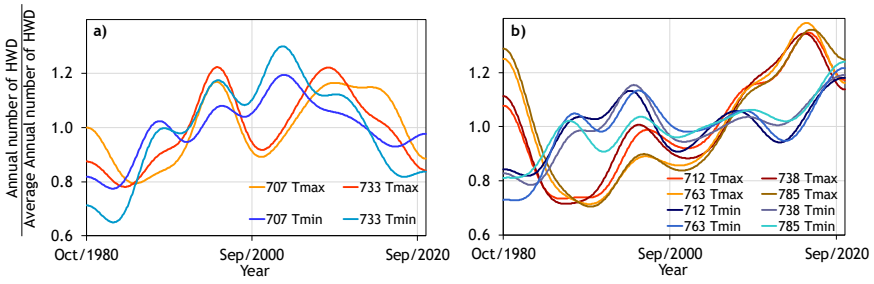



**Fig. 4.** Temporal pattern of the annual number of HWD divided by the average annual number of HWD in the period of analysis for the a) most western or coastal and b) most eastern or in-land points.

**Acknowledgements**

This research is part of the framework of the EU H2020 research and innovation programme SCORE, under grant agreement No. 101003534.

**References**

Russo, S., Dosio, A., Graversen, R. G., Sillmann, J., Carrao, H., Dunbar, M. B., Singleton, A., Montagna, P., Barbola, P., and Vogt, J. V. (2014), Magnitude of extreme heat waves in present climate and their projection in a warming world, J. Geophys. Res. Atmos., 119, 12,500– 12,512, doi:10.1002/2014JD022098

Almeida, M., & Coelho, P. (2023). A first assessment of ERA5 and ERA5-Land reanalysis air temperature in Portugal. International Journal of Climatology, 43(14), 6643–6663. https://doi.org/10.1002/joc.8225

# Understanding the evolving landscape of droughts in a changing climate: exploring global responses of different drought types

Parisa HOSSEINZADEHTALAEI[1], Piet TERMONIA[1,2] and Hossein TABARI[2,3]

[1] Department of Physics and Astronomy, Ghent University, Ghent, Belgium.

[2] Department of Meteorological and Climate Research, Royal Meteorological Institute of Belgium, Uccle, Belgium.

[3] Faculty of Applied Engineering, University of Antwerp, Antwerp, Belgium.

parisa.hosseinzadehtalaei@ugent.be

piet.termonia@ugent.be

hossein.tabari@uantwerpen.be

ABSTRACT

Climate change has significantly altered the natural patterns of droughts, resulting in increased frequency, longer durations, and heightened severity in certain global regions. However, the effects of climate change on precipitation, runoff, and soil moisture can vary, resulting in diverse responses among different types of droughts to climate change. Therefore, understanding the effects of climate change on each drought type becomes crucial in developing effective adaptation and mitigation strategies that are tailored to the specific characteristics and vulnerabilities of each type. These strategies are essential for addressing the challenges posed by the escalating frequency and severity of drought events and safeguarding communities, ecosystems, and water resources. This study explores the evolving landscape of droughts, encompassing meteorological, hydrological, and agricultural drought types on a global scale, under the influence of accelerating climate change. We examine and compare the impacts of climate change on these distinct drought categories globally using CMIP6 GCMs. Our results reveal distinct patterns in the responses of the three drought types to climate change across all Shared Socioeconomic Pathways (SSPs). The spatial distribution and magnitude of increasing signals in all five drought characteristics, including median intensity, peak intensity, median duration, longest duration, and frequency, exhibit an ascending order from meteorological to hydrological and then agricultural droughts. We observed that this same order holds for projections uncertainty and the significance of climate change signals. This finding has important implications for accurately assessing drought risks and tailoring effective mitigation and adaptation strategies in different regions. The study highlights that an all-in-one approach may not be applicable for drought analysis for different sectors under climate change due to the diverse and complex nature of drought impacts and responses across various types.

## 1. Introduction

Drought, as a major natural hazard, has garnered increasing attention due to its increasing prevalence and devastating impacts in recent decades. Climate change, driven by anthropogenic factors, has significantly altered the patterns of droughts, leading to more frequent, prolonged, and severe events in various regions across the globe. The escalating frequency and severity of drought events pose significant challenges to water resources management, agriculture, and ecosystem stability (Cook et al., 2018), necessitating the development of effective adaptation and mitigation strategies. Understanding the evolving landscape of droughts under climate change impacts becomes crucial for formulating tailored approaches to safeguard communities, ecosystems, and water resources from the detrimental effects of drought.

Drought manifests in three primary physical types - meteorological, hydrological, and agricultural - each characterized by specific aspects of the hydroclimate processes. Meteorological drought initiates with a lack of precipitation and can propagate into soil moisture deficits, leading to agricultural drought. The transition

from meteorological to agricultural and hydrological drought involves additional processes that affect the surface water balance, potentially creating variations in their responses to climate change (Berg and Sheffield, 2018). The complexity and variability of these responses across different regions and time scales necessitate a comprehensive understanding of the response of different drought types in a changing climate.

The objective of this study is to explore and compare the impacts of climate change on the three distinct drought types - meteorological, hydrological, and agricultural - at a global scale. We aim to investigate the spatial distribution and magnitude of climate change signals for five key drought characteristics: median intensity, peak intensity, median duration, longest duration, and frequency. Additionally, we will assess the projection uncertainties associated with each drought type and examine the significance of climate change signals.

## 2. Data and methods

The study utilized data from eighteen CMIP6 GCMs, including precipitation, runoff, and soil moisture, to characterize different drought types over two time scales (3 and 12 months). Three standardized indices, namely Standardized Precipitation Index (SPI), Standardized Runoff Index (SRI), and Standardized Soil Moisture Index (SSI), were employed for this purpose. Drought characteristics were determined using the run theory. To assess sources of uncertainty, the study quantified the uncertainty in projected changes for different drought characteristics at each model grid using a variance decomposition method, separating it into GCM and SSP uncertainties. The signal-to-noise ratio was calculated to ascertain the significance of the changes.

## 3. Results

The findings reveal a clear progression of climate change impact on droughts, moving from meteorological to hydrological to agricultural droughts. Agricultural droughts, in particular, exhibit, on average, twice as much increase in spatial extent and magnitude compared to meteorological droughts (Fig. 1A). Moreover, similar to climate change signals, the total uncertainty also escalates from meteorological to hydrological to agricultural droughts (Fig. 1B). This enlarging pattern is consistently observed for both GCM and SSP uncertainties (Fig. 1B). However, despite this growing uncertainty, this order remains valid for the spatial extent of significant signal-to-noise ratios for all drought characteristics except frequency (not shown).

Given the observed differences in this study regarding the responses of different drought types to climate change, it is essential to exercise caution when using drought indicators for various drought categories. To ensure effective management and accurate assessment of drought impacts, it is crucial to consider the specific characteristics and responses of each drought category to climate change.

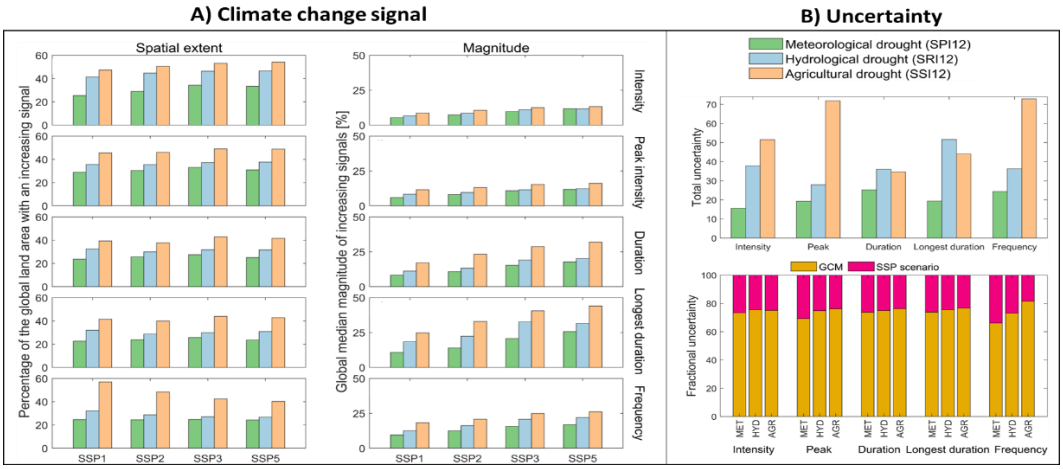



**Fig. 1.** Comparison of A) spatial extent and magnitude of the increasing signals in different characteristics of three drought types, and B) uncertainties for changes in different drought types. Changes were calculated between 1971–2000 and 2071–2100 at the 12-month scale. SSP1, SSP2, SSP3, and SSP5 denote Shared Socioeconomic Pathways (SSPs) SSP1-2.6, SSP2-4.5, SSP3-7.0, and SSP5-8.5, respectively.

**Acknowledgments**

The authors express their gratitude to the Research Foundation – Flanders (FWO) for funding this research (grant No.: 1255423N).

**References**

Berg A, Sheffield J (2018) Climate change and drought: the soil moisture perspective, Current Climate Change Reports, 4(2), 180-191.
Cook B I, Mankin, J S, Anchukaitis K J (2018) Climate change and drought: From past to future, Current Climate Change Reports, 4, 164-179.
Tabari H, Willems P (2023) Sustainable development substantially reduces the risk of future drought impacts, Communications Earth & Environment 4, 180 https://doi.org/10.1038/s43247-023-00840-3.

# The role of governance structure in shaping global risks of compound hot-dry events

Hossein TABARI[1,2]

[1] Faculty of Applied Engineering, University of Antwerp, Antwerp, Belgium, email: hossein.tabari@uantwerpen.be

[2] Department of Meteorological and Climate Research, Royal Meteorological Institute of Belgium, Uccle, Belgium, hossein.tabari@meteo.be

ABSTRACT

As the world experiences rapid socioeconomic developments and the effects of climate change intensify, the risks posed by compound hot-dry events to water resources are becoming a growing concern. These events have the potential to exacerbate damages caused by drought events and significantly impact water systems, as well as both natural and human systems. This study aims to assess the global risk of future compound hot-dry events by focusing on the pivotal role of governance structure in shaping these risks. Leveraging simulations from 18 CMIP6 GCMs for four Shared Socioeconomic Pathways (SSPs), the analysis reveals a substantial increase in the probability of compound hot-dry events, affecting vast areas across the globe. Most importantly, the findings underscore the critical link between governance structures and the risks associated with compound events. Countries with weaker governance face disproportionately higher risks of compound hot-dry events compared to those with robust governance practices. The study further highlights a significant escalation in projected population and cropland exposure to future compound hot-dry events. Vulnerable communities in regions with weak governance are particularly at risk, facing potential consequences of food insecurity, water scarcity, and social instability. This underscores the urgent need for effective governance, proactive measures, and robust policies to enhance resilience and adaptive capacity with respect to water resources.

## 1. Introduction

In the face of rapid climate change and socioeconomic transformations, the world is witnessing an escalating frequency and intensity of extreme events (Tabari et al., 2020; WMO, 2021). Among these, the emergence of compound hot-dry events stands as a pressing concern, as they bring simultaneous heatwaves and droughts that have profound and far-reaching impacts on water resources, ecosystems, and human livelihoods (Ribeiro et al., 2020). As we confront unprecedented environmental changes, the role of governance structures in effectively managing these risks becomes a paramount consideration (Cash et al., 2006).

Governance, encompassing the complex interplay of political, institutional, and societal systems, holds a pivotal role in shaping societies' adaptive capacity and resilience against the impacts of compound hot-dry events. Effective governance serves as a key enabler, facilitating the implementation of policies, interventions, and sustainable development strategies aimed at mitigating the consequences of climate change (Andrijevic et al., 2020). It becomes the bedrock upon which adaptive measures are built, ensuring that communities and nations can respond effectively to these challenges (Galaz et al., 2017).

Despite the qualitative recognition of governance's significance, our understanding of its future pathways and quantification remains limited. The absence of systematic assessments hinders our ability to comprehensively comprehend the profound impacts of governance on global risks associated with compound hot-dry events. Therefore, a robust understanding of governance dynamics and their influence on climate change adaptation and mitigation efforts becomes imperative.

This research aims to illuminate the extent to which governance structures across countries can either amplify or alleviate the risks posed by compound hot-dry events. The study focuses on assessing the global risk of future compound hot-dry events by examining the pivotal role of governance structure in shaping these risks using simulations from CMIP6 GCMs as well as exposure and vulnerability projections for different SSPs.

## 2. Data and methods

In this study, risk is assessed as a function of hazard, exposure, and vulnerability/coping-capacity. The occurrence probability of compound hot-dry events is assessed at the global scale using climate simulations from 18 CMIP6 GCMs for four SSPs. A bivariate copula is employed to assess the dependence between hot and dry events at each grid cell, and three copula functions that capture different types of dependence are considered. The standardized compound hot-dry event index is obtained by transforming the remapped joint probability derived from copula functions. Population and cropland exposure, as well as a governance indicator (Andrijevic et al., 2020), are incorporated to quantify the risk of compound hot-dry events.

## 3. Results and discussion

The assessment of the risk of compound hot-dry events is conducted at the country level by aggregating model grid-level exposure and hazard and integrating them with the country-level governance indicator. The analysis reveals that the risk is projected to increase in 72-112 countries, with a fourfold increase in 11-55 countries, depending on the SSP scenarios considered. A noteworthy observation is that countries with weak governance exhibit a more pronounced increasing trend in risk compared to those with good governance, except for SSP1. In particular, the risk multiplication factors for SSP2, SSP3, and SSP5 increase from 0.6, 0.7, and 1.3 in countries with good governance to 1.2, 1.6, and 2.2, respectively, in countries with weak governance (Fig. 1).

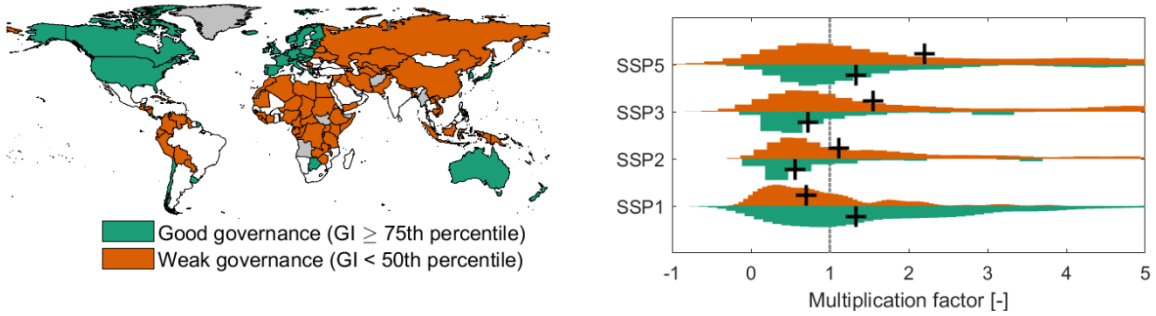



**Fig. 1.** A comparison of risk factors for compound hot–dry events between countries with good and weak governance. The countries with medium governance (50th–74th percentile), which are not used in this study, are shown in white color.

This study emphasizes the crucial role of governance in shaping global risks associated with compound hot-dry events, underscoring the urgency to bolster coping capacities in vulnerable countries and mitigate risks for society. Addressing these challenges requires strategic improvements in governance efficiency and coping capacities, which can be achieved through targeted educational and economic development initiatives. Furthermore, addressing the global risks of compound events calls for effective international cooperation. Countries with greater capacities and resources have the opportunity to extend support to those with weaker governance structures through technology transfer, financial aid, and capacity-building initiatives. Collaborative efforts can facilitate the exchange of best practices and knowledge related to climate adaptation, disaster risk reduction, and sustainable development, empowering societies worldwide to cultivate resilience and adapt to compound hot-dry events amidst the rapid changes in climate and socioeconomic landscapes.

SSP1, the sustainable development scenario, stands out as an exception where the risk of compound hot-dry events is not significantly influenced by the governance indicator. This highlights the potential of sustainable development policies in building adaptive capacity and resilience to climate-related challenges. Sustainable development practices emphasize inclusive economic growth, improved education, reduced inequality, and increased environmental protection. By implementing such policies with strong governance structures, societies can enhance their ability to cope with the consequences of extreme weather events. It is important to note that the results are based on a specific governance indicator used to compare governance across global countries and do not directly assess the governance structure within individual countries.

**References**

Andrijevic M, Crespo Cuaresma J, Muttarak R, Schleussner C F (2020) Governance in socioeconomic pathways and its role for future adaptive capacity, Nature Sustainability, 3(1), 35-41.

Cash D W, et al (2006) Scale and cross-scale dynamics: governance and information in a multilevel world, Ecology and Society, 11(2).

Galaz V, Tallberg J, Boin A, Ituarte-Lima C, Hey E, Olsson P, Westley F (2017) Global governance dimensions of globally networked risks: The state of the art in social science research, Risk, Hazards & Crisis in Public Policy, 8(1), 4-27.

Ribeiro A F S, Russo A, Gouveia C M, Páscoa P, Zscheischler J (2020) Risk of crop failure due to compound dry and hot extremes estimated with nested copulas, Biogeosciences, 17(19), 4815-4830.

Tabari H, Madani K, Willems P (2020) The contribution of anthropogenic influence to more anomalous extreme precipitation in Europe, Environmental Research Letters, 15(10), 104077.

WMO (2021) Atlas of Mortality and Economic Losses from Weather, Climate and Water Extremes (1970–2019), WMO-No. 1267.

# Water availability analysis along navigable waterways in Flanders using conceptual modelling and time series analysis

Laurens BREUGELMANS[1], Daan BERTELS[2], Patrick WILLEMS[3]

[1,2,3] KU Leuven, Department of Civil Engineering, Hydraulics and Geotechnics Section, Belgium
laurens.breugelmans@kuleuven.be
daan.bertels@kuleuven.be
patrick.willems@kuleuven.be

## ABSTRACT

Water availability is an important aspect to take into account when continuing economic development along navigable waterways, even more so in the light of the increasing frequency of extreme drought periods, such as the recent drought in Western-Europe. Predicting the impact of new infrastructure on waterways is crucial when preparing for extreme circumstances regarding water availability. This is especially true in complex systems with a high water demand, pre-existing water quality problems and high economic value. Water management of such complex systems requires numerical simulation models that allow to account for both water quantity and quality aspects. An extensive study on the impact of new infrastructure typically requires the simulation of a large number of scenarios, with varying boundary conditions, such that decision makers can rely on infrastructure design to prove effective in a wide range of possible circumstances. Performing such an extensive scenario analysis calls for a flexible and easy adjustable model with low calculation times, even for simulating very long time series. Conceptual models can provide an efficient approach for modelling large multi-user water systems. Based on a division of the waterways system in a number of interconnected reservoirs, they are capable of simulating water flows between the waterway reaches and are easily adjustable to the required scenarios (Bertels et al. , 2022). In this study, such approach based on conceptual models was tested for the network of navigable waterways in Flanders and used to investigate water allocation under extreme conditions.

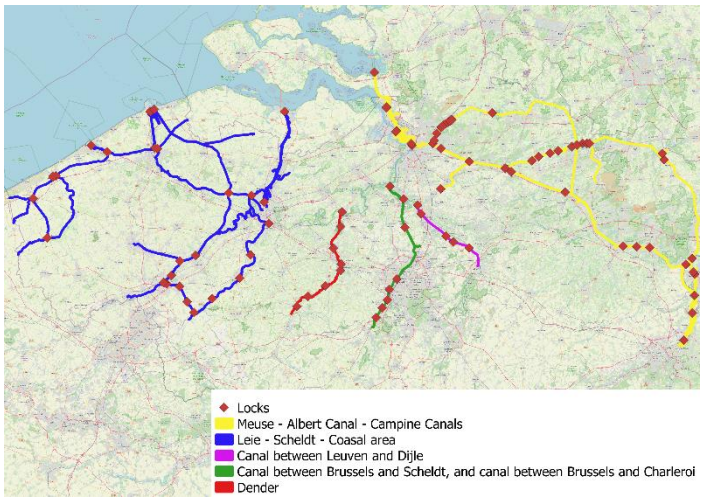



**Fig. 1**. network of navigable waterways in Flanders modelled in this study (Breugelmans et al., 2024)

The navigable waterways in Flanders (Fig. 1) are managed by De Vlaamse Waterweg (DVW), an agency of the Flemish government. Many of these waterways are characterized by a high water demand for shipping, industry, agriculture and drinking water production.

The waterways are modelled as a series of interconnected reservoirs for which in every timestep the water balance is calculated, taking into account the different water abstractions and discharges, the water volumes through the locks depending on the shipping traffic, the influence of the downstream tidal rivers and coast. For each reservoir, additional water flows due to level regulation and water management were taken into account based on general water management regulations provided by DVW. The main drawback of this approach is that hydraulic effects along the waterway reaches are simulated less accurately due to the assumption of a constant water level in each reservoir. However, when investigating water availability, one is not interested in the small scale water flow variations but where the water is allocated (Breugelmans et al., 2024).

Figure 2 shows the comparison between simulated and measured discharges (weekly averaged) at the measuring points in Kanne (Albert Canal), Machelen (Leie), Evergem (canal between Ghent and Terneuzen) and Dendermonde (Dender) (Breugelmans et al., 2024).

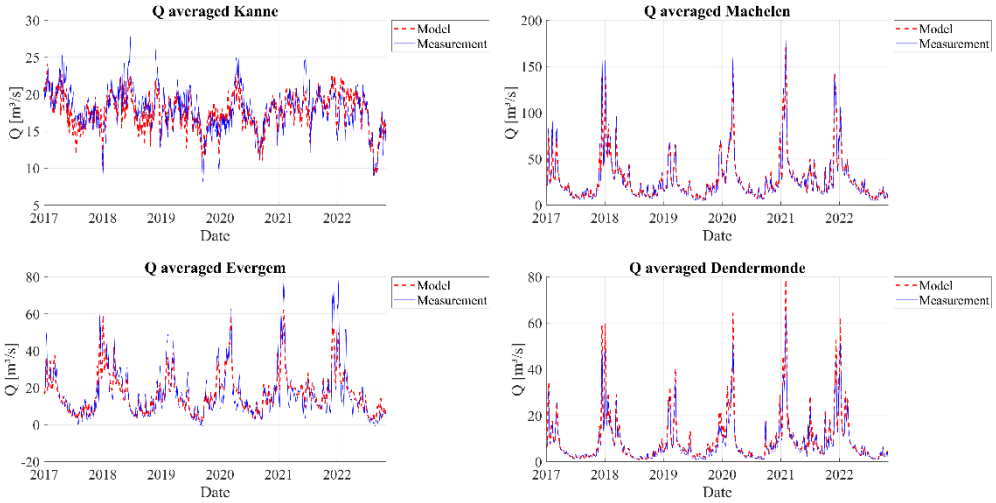



**Fig. 2**. comparison between the simulated and measured discharge at multiple locations (Breugelmans et al., 2024)

Climate change impacts were studied as well as the impact of the construction of new locks and related changes in shipping traffic, higher water demand due to industrial expansion, etc. Results demonstrate that the frequency and intensity of water scarcity conditions in the region will strongly increase in the future, which makes it necessary to implement extra measures to provide water to all users. The impact and effectiveness of different types of measures such as pumps at the sluices to compensate for the shipping volumes, smart real-time regulations of the waterway levels and pumping discharges, shipping and draft limitations, new basins, etc. were also simulated. A stunning example of the increased water scarcity is the case of the canal between Ghent and Terneuzen. At least 13m³/s (2 month average) of fresh water from Leie and Schelde is needed to overcome salt intrusion. According to climate impact analysis, by 2100, there will be a period of water shortage occurring almost every year (Breugelmans et al., 2023).

**Acknowledgements**

The authors wish to thank De Vlaamse Waterweg for their data and support.

**References**

Bertels, D., Willems, P. (2022), Climate change impact on salinization of drinking water inlets along the Campine Canals, Belgium, Journal of Hydrology: Regional Studies, 42, 101129, ISSN 2214-5818, https://doi.org/10.1016/j.ejrh.2022.101129.
Breugelmans L., Bertels D., Willems P. (2023). Water- en zoutbalans voor het kanaal Gent-Terneuzen opbouw en scenario-analyse. KU Leuven Hydraulics and Geotechnics voor North Sea Port
Breugelmans L., Bertels D., Willems P. (2024). Ondersteuningsopdracht Waterbeschikbaarheid op de Vlaamse waterwegen, Deelrapport 1: Opbouw en validatie van het waterbalansmodel. KU Leuven Hydraulics and Geotechnics voor De Vlaamse Waterweg

# Analysis of historical drought in Lisbon region, in the west of Portugal, using Reconnaissance Drought Index, RDI

Hany ABD-ELHAMID[1,2], Martina ZELENAKOVA[1], Maria Manuela PORTELA[3], Luis Angel ESPINOSA[3], Issa OSKOUI[3], Jacek BARANCZUK[4] and Katarzyna BARANCZUK[4]

[1] Technical University of Kosice, 040 01 Košice, Slovakia, hany.abdelhamid@tuke.sk , martina.zelenakova@tuke.sk
[2] Faculty of Engineering, Zagazig University, Zagazig, 44519, Egypt, hany_farhat2003@yahoo.com
[3] Instituto Superior Técnico (IST), CERIS, Lisbon, Portugal
maria.manuela.portela@tecnico.ulisboa.pt , luis.espinosa@tecnico.ulisboa.pt , issa.oskoui@tecnico.ulisboa.pt
[4] University of Gdansk, Poland, jacek.baranczuk@ug.edu.pl , katarzyna.baranczuk@ug.edu.pl

ABSTRACT

Drought is a natural hazard that is expected to become more frequent under changing weather conditions, requiring new water resources management policies. Drought analysis can be done using different indices such as the Reconnaissance Drought Index (RDI). This study aims to assess the historical droughts in Lisbon region (Portugal) by applying the RDI to long time series (157 years, from Oct/1864 to Sep/2021) of monthly rainfall and temperature data from a meteorological station located in the region. The results show that extreme droughts are recurrent events and that drought with the highest severity took place in 2005.

## 1. Introduction

Drought frequency and severity have been worsening because of climate change, cross affecting the society. One of the indices developed to characterize the droughts is the Reconnaissance Drought Index, RDI, which uses monthly precipitation and temperature to compute evapotranspiration. Similarly to other indices, different three types of droughts can be considered according to the time scale adopted to compute RDI (Zeleňáková et al., 2022): meteorological, agricultural, and hydrological drought for 3 (RDI-3), 6 (RDI-6), and 12 (RDI-12) months, respectively. Extreme dry conditions are reached when RDI<-2. Like many Southern European countries, Portugal is facing more frequent and more intense droughts. This study aims to analyze the historical droughts in Lisbon region by applying the RDI to very long precipitation and temperature monthly records.

## 2. Materials and methods

Portugal, located in the southwest of Europe, is characterized by a Mediterranean climate. The current study area is Lisbon region in the west of Portugal – Figure 1. Lisbon is the capital and largest city in Portugal, with an estimated population of 550,000 and an area of 100 km$^2$. The monthly precipitation and temperature data utilized to compute RDI was acquired at Lisboa-Geofísico climatological station (latitude 38 42 59.4º N and longitude 9 08 56.7º W) and relates to a period of 157 hydrological years, spanning from Oct/1864 to Sep/2021.




**Fig. 1.** Location map of the study area and Lisboa-Geofísico climatological station (adapted from Espinosa et al., 2022).

Drought indices, like RDI, are important tools for monitoring extreme dry conditions. RDI was computed at a monthly scale based on the Drought Indices Calculator (DrinC) applied to precipitation and, via temperature, potential evapotranspiration. DrinC is a simple, user-friendly tool and has a full graphical user interface (GUI) (Tigkas et al. 2015). The time scales considered were 3, 6 and 12 months to analyze different types of droughts, namely, meteorological, agricultural, and hydrological.

## 3. Results

Figure 2 shows the RDI values ate the different time scales; RDI-3, RDI-6, and RDI-12. Some of the drought characteristics are summarized in Table 1.

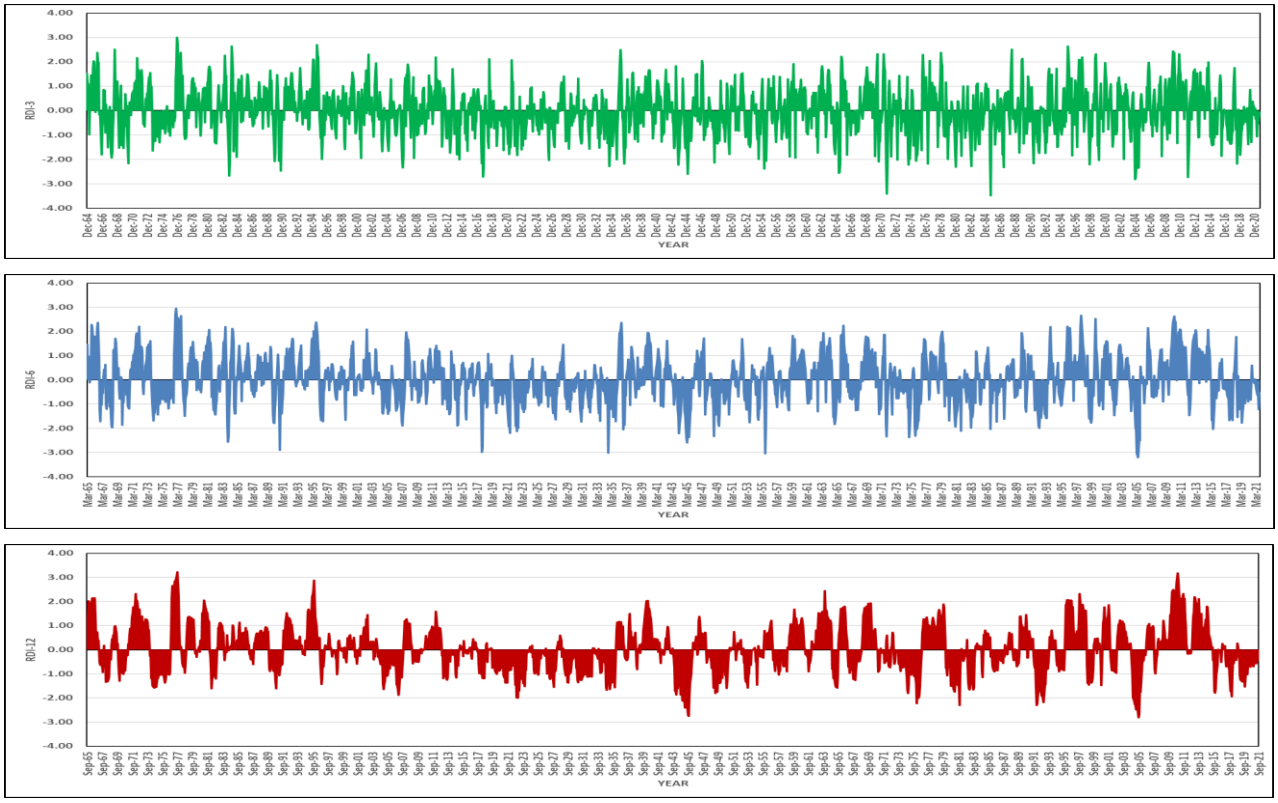



**Fig. 2.** RDI-3, 6 and 12 at Lisbon region for the period 1864-2021 (from top to bottom).

In what concerns the meteorological drought (RDI-3), the results show that 39 events extreme events took place with a total duration of 51 months. The longest extreme meteorological drought event (5 months) was recorded in 2005. Regarding the agricultural drought (RDI-6), 18 extreme events were recorded with a total duration of 27.61 months. The longest extreme agricultural drought event (7 months) was also recorded in 2005. Finally, according to the RDI-12, 9 extreme hydrological drought events occurred, with a total duration of 25 months. The longest extreme hydrological drought event (9 months) was once more recorded in 2005.

**Table 1.** Drought identification using RDI at Lisbon region for the period (1864-2021)

| Index | Number of events | Duration (month) | Severity | Average inter-arrival time (month) | Average return time (year) | Years |
|---|---|---|---|---|---|---|
| RDI-3 | 39 | 51.00 | -117.58 | 45.28 | 3.77 | 1870, 1883, 1890, 1896, 1907, 1914, 1917, 1926, 1934, 1935, 1944, 1945, 1948, 1954, 1955, 1965, 1970, 1971, 1973, 1974, 1975, 1977, 1980, 1981, 1983, 1985, 1987, 1991, 1998, 2000, 2003, 2005, 2012, 2018 |
| RDI-6 | 18 | 27.61 | -76.79 | 87.06 | 7.25 | 1883, 1890, 1917, 1921, 1922, 1943, 1936, 1944, 1945, 1948, 1955, 1971, 1974, 1975, 1981, 1985, 2005, 2015 |
| RDI-12 | 9 | 25.00 | -58.65 | 142.11 | 11.84 | 1923, 1944, 1945, 1976, 1981, 1992, 1993, 2005 |

## 4. Conclusion

The results showed that extreme drought events (RDI<-2) took place often, having the more intense drought occurred in the year 2005, regardless the time scale. The average return time is estimated to be 3.77, 7.25, 11.84 years for meteorological, agricultural, and hydrological droughts, respectively.

**Acknowledgements**

This work was supported by the Slovak Research and Development Agency under the Contract no. APVV-20-0281.

**References**

Espinosa, L.A., Portela, M.M.; Matos, J.P., Gharbia, S. (2022) Climate change trends in a European Coastal Metropolitan Area: rainfall, temperature, and extreme events (1864-2021). Atmosphere, 13(12):1995, https://doi.org/10.3390/atmos13121995.

Tigkas, D., Vangelis, H., Tsakiris, G. (2015) DrinC: a software for drought analysis based on drought indices. Earth Science Informatics, 8(3), 697-709.

Zeleňáková, M., Soľáková, T., Purcz, P. and Abd-Elhamid, H.F. (2022) Analysis of drought in the eastern part of Slovakia using standardized precipitation index. International conference on water resources management and sustainability: solutions for arid regions, (22-24 March 2022), Dubai, UAE.

8th IAHR EUROPE CONGRESS
LISBON - PORTUGAL
4-7 JUNE 2024

# Addressing class imbalance problems in data-driven rainfall-runoff modelling

Federico VILASECA[1], Christian CHRETIES[1], Alberto CASTRO[2,3] and Angela GORGOGLIONE[1]

[1] Institute of Fluid Mechanics and Environmental Engineering (IMFIA), Universidad de la República, Uruguay
[2] Institute of Computer Science (INCO), Universidad de la República, Uruguay
[3] Institute of Electrical Engineering (IIE), Universidad de la República, Uruguay
fvilaseca@fing.edu.uy; chreties@fing.edu.uy; acastro@fing.edu.uy; agorgoglione@fing.edu.uy

ABSTRACT

This paper proposes a methodology based on data augmentation to improve the performance of data-driven rainfall-runoff models on high flows. Problems in the representation of such range of discharges by data-driven models were presented in previous research, which the authors of this work attribute to class imbalance of discharge data, where high flows are underrepresented. This ends up biasing the learning process towards the representation of low flows. The proposed methodology was tested for two incremental watersheds of the Santa Lucía Chico basin in Uruguay, showing an increase in performance of 17 % for Nash-Sutcliffe efficiency and 38 % for peak-flow Nash-Sutcliffe efficiency. Results demonstrate that class imbalance is a relevant issue affecting the performance of data-driven rainfall-runoff models and that the proposed methodology allows to tackle said issue and improve model performance for high flows.

## 1. Introduction

Data-driven rainfall-runoff models serve as valuable tools in hydrological studies, offering insights into the complex relationships between rainfall patterns and runoff dynamics. However, recent investigations have highlighted their limited representation of flood peaks in daily step implementations (Barbosa-Reis et al., 2021; Chen et al. 2023; Rezaie-Balf et al., 2019, Vilaseca et al., 2023). We theorize that these limitations can often be attributed to class-imbalance issues present in both input and output time series. Typical hydrographs encountered in alluvial rivers show prevailing low and mid-flow conditions, occasionally punctuated by rapid streamflow increase generating flood events. Classifying flow events based on their magnitude places floods in the minority category, starkly contrasting with the abundant base flows. Consequently, this class imbalance distorts the learning process of algorithms during the training phase, impairing the model's ability to accurately predict and capture high-flow events. To address this issue, in this work, we present a methodology to balance the weight of high flows, with respect to base flows, during the training stage of data-driven rainfall-runoff models. By ameliorating the class imbalance, we aim to enhance the model's capacity to effectively predict and characterize flood events, contributing to the refinement of hydrological simulations and bolstering our understanding of the intricate interplay between precipitation and runoff dynamics.

## 2. Materials and methods

### *2.1. Study area and data*

The study area is the Santa Lucía Chico basin, located in the south-central region of Uruguay. The entire watershed (2478 km$^2$) with closure at Paso Severino (PS) dam and an incremental watershed (1748 km$^2$) with closure at the city of Florida (FL) were considered to test the methodology. Available data included daily time series of river discharge, accumulated rainfall and air temperature, covering the period 1989-2016. These data were used to build two input datasets (A and B) for the data-driven models (Table 1). Further details about the study basin together with data description and analysis can be found in Vilaseca et al. (2023).

### *2.2. Workflow description*

A series of 88 experiments were conducted per watershed, each of which consisted of the training and evaluation of a Random Forest model. For each, the input dataset was built out of the two possible variable combinations (Table 1), and randomly split into training and testing subsets with a 75/25 ratio. Then, a data augmentation workflow was applied to the training set to increase the weight of the high-flow data. Each experiment was carried out considering different: (1) input dataset, (2) method for classification of events, (3) data augmentation algorithm, (4) increase ratio of the amount of high flow (minority class) events.

**Table 1**. Input datasets for the models. MAP = mean areal precipitation, $MAP_{accum}$ = 7-day accumulated MAP, Tmax = max. temperature, Tmin = minimum temperature, Q = discharge, $Q_{t-I}$ = Q of the $i^{th}$ previous day

| Dataset | Input variables | Output variable |
|---|---|---|
| Dataset A | MAP, $MAP_{accum}$, Tmax, Tmin | Q |
| Dataset B | MAP, $MAP_{accum}$, Tmax, Tmin, $Q_{t-1}$, $Q_{t-2}$ | Q |

Events were classified with two possible alternatives: peaks-over-threshold (POT) or k-means. The POT classification consisted of identifying local maximums in the discharge series over a fixed threshold of 500 $m^3/s$. This led to a binary event classification where flood peaks represented the minority class. The alternative was using the k-means clustering algorithm for unsupervised classification of the events. In this case, values of k = 2, 3, 4, or 5 were considered. Possible data augmentation algorithms included random sampling with replacement from the known high flow (minority class) events or generation of new synthetic minority class events using four variants of the SMOTE (Chawla et al., 2002) algorithm: SMOTE, Borderline SMOTE (Han et al., 2005), SVM SMOTE (Nguyen et al., 2009) or ADASYN (He et al., 2008). Each augmentation algorithm was set to increase the amount of minority class events in a ratio of $IR = N^*/N$, being N the number of events of such class prior to the data augmentation and $N^*$ said number after the augmentation. IR was set to take values between IR = 1.5, 2.5, 5.

During the training process for each model, a selection of the Random Forest hyperparameters was optimized using four-fold cross-validation and the genetic algorithm Optuna (Akiba et al., 2019), following the same pipeline described in Vilaseca et al. (2023). The objective function for optimization was Nash-Sutcliffe efficiency (NSE), and models were evaluated for percent bias (PBIAS), ratio of mean squared error to standard deviation (RSR), NSE calculated for peaks (pkNSE), and NSE calculated for log-transformed flows (logNSE).

## 3. Results and discussion

The results of the best experiment compared to the baseline model (without data augmentation in the training set) for each watershed and each of the two input datasets are shown in Table 2.

**Table 2**. Results of the best experiments compared to baseline models for each watershed and dataset.

| Watershed | Input dataset | Experiment | k (k-means) | Sampling method | IR | NSE | PBIAS | RSR | logNSE | pkNSE |
|---|---|---|---|---|---|---|---|---|---|---|
| PS | Dataset A | Baseline | - | None | - | 0.34 | 0.17 | 1.32 | -0.06 | 0.22 |
| PS | Dataset A | Best | 4 | SMOTE | 2.5 | 0.46 | -17.6 | 0.94 | -0.07 | 0.41 |
| PS | Dataset B | Baseline | - | None | - | 0.62 | 3.01 | 0.81 | 0.76 | 0.54 |
| PS | Dataset B | Best | 4 | SMOTE | 1.5 | 0.76 | -2.41 | 0.6 | 0.66 | 0.71 |
| FL | Dataset A | Baseline | - | None | - | 0.38 | 4.69 | 1.42 | 0.25 | 0.29 |
| FL | Dataset A | Best | 4 | SMOTE | 2.5 | 0.39 | -11.99 | 1.12 | 0.18 | 0.34 |
| FL | Dataset B | Baseline | - | None | - | 0.64 | -3.87 | 0.73 | 0.85 | 0.58 |
| FL | Dataset B | Best | 3 | SVM SMOTE | 1.5 | 0.71 | -10.77 | 0.64 | 0.85 | 0.66 |

Results show an improvement in the estimation of the flow peaks after applying the proposed data augmentation methodology. This is indicated by the increase in NSE and pkNSE indicators. It should also be noted that performance decreases for low flows, as evidenced by the comparison of logNSE indicators. In most cases, the best results are obtained for the SMOTE algorithm, with the k-means algorithm set for k = 4 clusters.

## 4. Conclusions

Results allow to conclude that the posed hypothesis is accurate, and that class imbalance is a relevant issue for data-driven rainfall-runoff modeling. The proposed method allows improving the representation of high flows based on known data augmentation techniques, while slightly lowering the performance for low flows, which shows a balancing of the learning process. On average, performance increased by 17% for NSE and 38% for pkNSE and decreased by 14% for logNSE.

**Acknowledgments**

This work was made possible thanks to a Ph.D. scholarship granted to F.V. by the Academic Postgraduate Commission (CAP), Universidad de la República, Uruguay.

**References**

Akiba T, Sano S, Yanase T, Ohta T, Koyama M (2019) Optuna: a next-generation hyperparameter optimization framework, KDD' 19: Proceedings of the 25th ACM SIGKDD International Conference on Knowledge Discovery & Data Mining, 2623-2631.

Barbosa G, da Silva DD, Fernandes EI, Moreira MC, Vieira G, de Souza M, Rocha SA (2021) Effect of environmental covariable selection in the hydrological modeling using machine learning models to predict daily streamflow, Journal of Environmental Management, 290, 112625.

Chawla NV, Bowyer KW, Hall LO, Kegelmeyer WP (2002) SMOTE: Synthetic Minority Over-sampling Technique, Journal of Artificial Intelligence Research, 16, 321-357.

Chen Z, Lin H, Shen G (2023) TreeLSTM: A spatiotemporal machine learning model for rainfall-runoff estimation, Journal of Hydrology: Regional Studies, 48, 101474.

Han H, Wang W, Mao B (2005) Borderline-SMOTE: A new over-sampling method in imbalanced data sets learning, ICIC 2005: Proceedings of the International Conference on Intelligent Computing, 878-887.

He H, Bai Y, Garcia BE, Li S (2008) ADASYN: Adaptive Synthetic Sampling Approach for Imbalanced Learning, Proceedings of the International Joint Conference on Neural Networks (IJCNN 2008), 1322-1328.

Nguyen H, Cooper EW, Kamei K (2009) Borderline over-sampling for imbalanced data classification, Proceedings of the Fifth International Workshop on Computational Intelligence and Applications, 24-29.

Rezaie-Balf M, Nowbandegani SF, Samadi SZ, Fallag H, Alaghmand S (2019) An ensemble decomposition-based artificial intelligence approach for daily streamflow prediction, Water, 11, 709.

Vilaseca F, Chreties C, Castro A, Gorgoglione A (2023) Assessing influential rainfall-runoff variables to simulate daily streamflow using Random Forests, Hydrological Sciences Journal, DOI: 10.1080/02626667.2023.2232356.

# Evaluation of the effects of climate change on flood, case study: Cork, Ireland

Sogol MORADIAN, Agnieszka Indiana OLBERT

College of Science and Engineering, University of Galway, Galway, Ireland.
Sogol.moradian@universityofgalway.ie
Indiana.olbert@universityofgalway.ie

ABSTRACT

This paper focused on conducting a comprehensive analysis of urban coastal-fluvial flooding, employing advanced high-resolution modelling techniques. To exemplify this approach, the study chose Cork City, Ireland, as its primary case study area, given its recurrent susceptibility to both fluvial (river-related) and coastal flooding events. The core methodology employed in this study revolved around the utilization of a statistical-hydrodynamical model. This model was instrumental in simulating the intricate interplay of various factors contributing to flood inundation, including their spatial distribution and temporal progression. These factors encompassed a wide range of future stressors that are increasingly relevant in the context of changing climate patterns. The study took into account several critical elements in its simulations, including extreme river discharges, anticipated sea level rise, surge residuals, and astronomical tides. These projections are crucial for understanding and mitigating the potential consequences of climate change on coastal communities and urban infrastructure. Furthermore, the high-resolution modelling approach allows for a detailed examination of the dynamics of flooding events, providing a foundation for informed decision-making and the development of effective adaptation strategies.

## 1. Introduction

In coastal floodplains, extensive flooding can occur due to a combination of high river flows and elevated coastal water levels (Olbert et al., 2023). These factors are pivotal in shaping the characteristics of floods, leading to distinct variations in how floodwaves spread and the extent of the affected areas. When a flood event is triggered by just one of these factors, the accuracy of predicting the likelihood of a flood largely relies on the availability of data and the statistical techniques employed for extreme event assessment. The situation becomes more intricate when flooding results from a combination of processes, as is the case in coastal areas where various variables like astronomical tides, surges, wind waves, and high river discharges can all act concurrently (Olbert et al., 2017). In such scenarios, it's not enough to consider the probabilities of each individual driver alone (Olbert et al., 2023). Instead, we must also account for the joint probability of these multiple drivers occurring simultaneously. This paper introduces a methodology for evaluating the probability and severity of urban compound flooding, offering a valuable tool for gaining insights into the factors influencing flood occurrences, including the evolving influence of climate change. Furthermore, it enables the estimation of the cumulative impact when multiple sources of flooding, often exacerbated by climate change-related factors, converge.

## 2. Methodology

The process for assessing flood likelihood and intensity involves several steps, primarily encompassing two fundamental components: (1) a statistical examination of the joint likelihood of their simultaneous occurrence, and (2) hydraulic modelling that simulates the spread of flooding due to factors such as astronomical tides, storm surges, and river discharges. Joint probabilities are calculated to estimate the likelihood of events of two different variables occurring simultaneously, such as fluvial and coastal drivers (Yazdandoost et al., 2020; Moradian et al., 2023; Olbert et al., 2023). In this regard, 26 different Copula functions under 17 statistical distribution functions were used as explained in Moradian et al. (2023; 2024). Regarding to the hydraulic modelling, a high resolution nested coastal model (MSN_Flood) of Cork Harbour was applied. The nested model consists of a sequence of four nested domains that progressively enhance the horizontal resolution of

the model. This refinement begins at 90 meters in the broadest domain, which encompasses Cork Harbour, and culminates in a finer resolution of 2 meters within the most detailed domain, covering Cork City. A detailed technical description of the model, its configuration, and the validation outcomes can be found in the works of Olbert et al. (2017), and Comer et al. (2017). This study used water level simulations from Coastal Dataset for the Evaluation of Climate Impact (CoDEC) dataset as well as stream flow data from different the Phase 6 of the Climate Model Intercomparison Project (CMIP6) from MPI-ESM1-2-LR. The flood maps were produced for different return period (RP) of 50, 100 and 500 years for the city.

## 3. Results

This part presents the final flood inundation maps for the study area. We prepared these maps to illustrate the potential flood scenarios for RPs of 50, 100, and 500 years, utilizing the climate model of MPI-ESM1-2-LR. As an illustrative example, the flood map corresponding to a 500-year RP represents an exceptionally rare event, with a mere 0.2% (1/500) likelihood of occurrence in any given year. The flood maps, prepared with a precision of two meters, provide an accurate depiction of the flood zoning in Cork. Analysis of the provided data reveals that the upstream regions along the river are significantly affected by fluvial flooding. Conversely, the city center is susceptible to inundation, particularly during higher return periods. It is evident that the scope and severity of flooding escalate notably during greater RPs, underscoring the importance of comprehensive flood risk management strategies for the area. The results help guide long-term planning and infrastructure development in areas where the risk of flooding is particularly low but not entirely absent. In general, these maps provide crucial information to help governments, communities, and individuals make informed decisions about land use, infrastructure development, and emergency preparedness. In conclusion, flood maps under different RPs are invaluable tools for assessing and mitigating flood risks in various communities. They help policymakers, planners, and individuals make informed decisions to protect lives and property while considering the probability and severity of flood events. These maps are dynamic and require periodic updates to remain relevant in the face of evolving climate and environmental factors.




**Fig. 1.** Spatial evolution of joint coastal-fluvial flood through Cork City for 50-year return period.




**Fig. 2.** Spatial evolution of joint coastal-fluvial flood through Cork City for 100-year return period.




**Fig. 3.** Spatial evolution of joint coastal-fluvial flood through Cork City for 500-year return period.

**References**


Comer J, Olbert AI, Nash S, Hartnett M (2017) Development of high-resolution multi-scale modelling system for simulation of coastal-fluvial urban flooding, Natural Hazards and Earth System Sciences, 17, 205-224.

Moradian S., Gharbia S., Iglesias G., Olbert A.I. (2024) A Copula Post-Processing Method for Wind Power Projections Under Climate Change. Energy Conversion and Management: X. Volume 23, 100660. https://doi.org/10.1016/j.ecmx.2024.100660.

Moradian S., Olbert A.I., Gharbia S., Iglesias G. (2023) Copula-based projections of wind power: Ireland as a case study. Renewable and Sustainable Energy Reviews. 175, 113147. https://doi.org/10.1016/j.rser.2023.113147.

Olbert AI, Comer J, Nash S, Hartnett M (2017) High-resolution multi-scale modelling of coastal flooding due to tides, storm surges and river inflows. A Cork City Example, Coastal Engineering, 121, 278-296.

Olbert A.I., Moradian S., Nash S., et al. (2023) Combined statistical and hydrodynamic modelling of compound flooding in coastal areas- Methodology and application. J. of Hydrology. https://doi.org/10.1016/j.jhydrol.2023.129383.

Yazdandoost, F., Moradian, S., Zakipour, et al. (2020) Improving the precipitation forecasts of the North-American Multi Model Ensemble (NMME) over Sistan Basin. Journal of Hydrology. 590, 125263. https://doi.org/10.1016/j.jhydrol.2020.125263.

# Exploring the effectiveness of Nature-Based Solutions through the Assessment Framework Tool implemented within the H2020 PHUSICOS project

Francesco PUGLIESE[1], Giuseppe ASCIONE[2], Maurizio GIUGNI[3]

[1,2,3] Department of Civil, Architectural and Environmental Engineering, University of Naples Federico II, Italy
francesco.pugliese2@unina.it
giuseppe.ascione2@unina.it
maurizio.giugni@unina.it

ABSTRACT

Nowadays Nature-Based Solutions (NBS) are widely regarded as a viable approach to deal with natural hazards in urban, rural and mountainous areas. Despite the increasing interest, the proper assessment of NBS effectiveness relies on the comprehensive evaluation of the technical outcomes and the environmental and socio-economic co-benefits. Within the H2020 PHUSICOS project (Grant Agreement nr. 776681), an Assessment Framework Tool (AFT) was structured, based on the selection, estimation, multi-level weighting and then aggregation of a set of Key Performance Indicators (KPI), depending on the site features, the data availability and the stakeholders' expectations. In this work, the main outcomes of the PHUSICOS AFT application to an Italian case study are discussed.

## 1. The H2020 PHUSICOS Assessment Framework Tool (AFT)

### *1.1. The H2020 PHUSICOS Project*

PHUSICOS, meaning in Greek 'According to nature', is a 5-year H2020 project (05/2018 to 04/2023) involving 15 organizations from 7 countries (Norway, Germany, Austria, Italy, France, Spain and Switzerland) among universities, research centers, consulting and territorial administrations. The main scope of the project was to assess the NBS effectiveness against hydro-meteorological hazards in mountainous and rural areas, with different field applications across Europe (Italy, Norway and Pyrenees).

### *1.2. The PHUSICOS Assessment Framework Tool (AFT)*

Within the PHUSICOS project, a comprehensive hierarchic Assessment Framework Tool (AFT) was proposed, including a set of KPI (about 100 in the current version), grouped into sub-criterion, criterion and ambit levels, respectively to be estimated at both the current scenario (baseline) and different design ones (i.e. NBS, hybrid or grey). Five ambits were detected, grouping all the indicators belonging to the technical, environmental and socio-economic categories, as shown in the simplified matrix of Table 1.

**Table 1.** Simplified structured matrix composing the PHUSICOS AFT

| Ambit | Criterion | Sub-Criterion | KPI | Unit |
|---|---|---|---|---|
| Risk Reduction | Hazard | Flooding Risk Resilience | Peak Discharge | $m^3/s$ |
| | … | … | … | … |
| Technical and Feasibility Aspects | Technical Feasibility | Cost-Benefit Analysis of the Intervention | Initial and Maintenance costs | mln € |
| Environment and Ecosystems | Water | Effects on water quality | Fluvial Functionality Index (FFI) | - |
| | … | … | … | … |
| Society | Quality of Life | Leisure and Connections Increasing | New pedestrian, cycling paths | m |
| | … | … | … | … |
| Local Economy | Revitalization of Marginal Areas | Promotion of local socio-economic development of marginal areas | New activities in the tourism sector | nr |
| | … | … | … | … |

The number and the selection of KPI depend on the specificity of a) case study site; b) data availability and c) stage of analysis (Caroppi et al., 2023). At ex-ante stage, both a limited number of KPI, for a swift assessment, and a more detailed investigation, including more KPI, can be accounted for. At ex-post stage, after the measure implementation, a wide set of KPI is useful to assess the effectiveness of the implemented solution, depending on the accuracy of the monitoring activities and the available budget for data collection and processing. Once selected and estimated are the KPI, the normalization, the multi-level weighting and the aggregation steps allow for the estimation of the overall score of the *i*-th scenario $S_i$ as follows:

$$S_i = \sum_{a=1}^{p} \frac{\sum_{j=1}^{NA_a} KPI_{j,i} \cdot w_{KPI,j} \cdot w_{C,j} \cdot w_{A,j}}{NA_a} \quad (1)$$

where $p$ is the number of ambits, $NA_a$ is the number of KPI belonging to the $a$-th ambit, whereas $w_{KPI,j}$, $w_{C,j}$ and $w_{A,j}$ are the weight of the $j$-th KPI, the criterion and the ambit of the $j$-th KPI, respectively.
The numerousness of the selected KPI at each level relies on multi-level weighting using the typical procedures from the literature, such as the Likert scale (Pugliese et al., 2022), eventually fostering the stakeholders' involvement, through the Living Lab approach, to compare the outcomes from individuals owing different expertise and expectations.

### *1.3. The PHUSICOS Assessment Framework Tool application to Quindici (IT) case study*

In this work, the AFT was tested on the Quindici (IT) case study at the ex-ante stage, given the relevant hydro-geological hazards occurring in the area in the last decades, specifically, consisting of intense flood and landslide events. Starting from the current baseline, two design scenarios were developed, namely: a) a NBS consisting of afforestation practices using native trees for about 56 ha; b) a hybrid one, coupling the afforestation with both riverbank reprofiling and the installation of a reinforced concrete tank of 30000 $m^3$ useful to deal with flooding.

Three different stakeholders' categories were simulated to weigh the AFT parameters. Results showed that the NBS scenario, despite achieving a lower score for risk reduction KPI, is more prone to enhance the socio-economic benefits in the area. Depending on the stakeholders' category, significant discrepancies were specifically observed between technical and co-benefits ambits, thus remarking the relevance of weighting procedure. Notably, at the ambit level, the higher overall score of the NBS scenario was mainly due to the significantly greater relevance given to the social KPI by both neutral and political stakeholders, with specific reference to both the landscape and heritage and quality of life categories of the criterion level. Conversely, the technical stakeholder category entailed major relevance to the risk reduction KPI, thus making the two design scenarios widely comparable. As expected, for this category, the greater score was achieved by the hazard indicators, thus justifying the different overall outcomes against the other two stakeholders' categories.

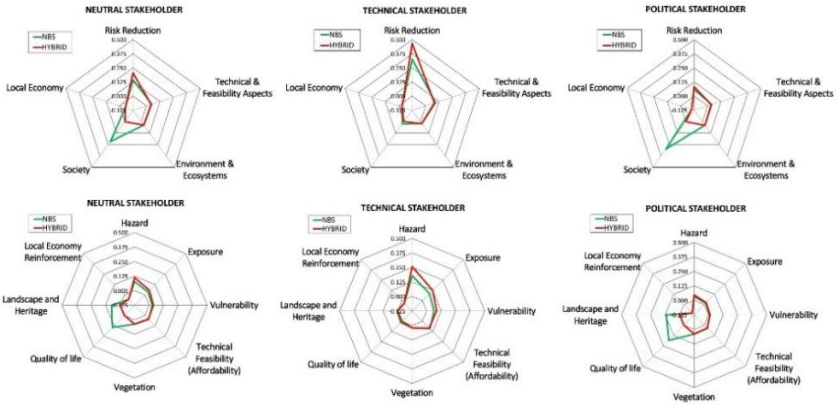



**Fig. 1.** Comparison of scores of NBS and hybrid scenarios at ambit and criterion level for Quindici (IT) case study.

**Acknowledgements**

This research was funded by the H2020 Innovation Action 'PHUSICOS – According to Nature' (Grant Agreement No. 776681).

**References**

Caroppi G, Pugliese F, Gerundo G, De Paola F, Stanganelli M, Urciuoli G, Nadim F, Oen A, Andrés P, Giugni M (2023) A comprehensive framework tool for performance assessment of NBS for hydro-meteorological risk management, Journal of Environmental Planning and Management.
Pugliese F, Caroppi G, Zingraff-Hamed A, Lupp G, Gerundo C (2022) Assessment of NBSs effectiveness for flood risk management: The Isar River case study, AQUA – Water Infrastructure, Ecosystems & Society, 71(1), 42-61.

# Effective Flood Emergency Response: Rapid Deployment Solutions

Diogo FREITAS[1] , Laura MOLANO[2], Diego GARCÍA[3], Ginna TORRES[4]

[1,2,3,4] A. Bianchini Ingeniero, S.A. (Maccaferri), Spain
[1]d.freitas@maccaferri.com
[2]l.molano@maccaferri.com
[3]dg.gordo@maccaferri.com
[4]g.torres@maccaferri.com

ABSTRACT

Climate variability is a major component that increases flood risk due to more frequent heavy precipitation and sea level rise. Population growth and rapid urbanization of cities further raise the potential for flood damage. To respond effectively to such events, emergency management strategies have been developed, including flood forecasting for hazard alerts and risk-mitigating solutions. Any response to flood emergencies must be rapidly deployed and effective to reduce potential damages. This paper aims to display the use of a damage control system that is faster and more cost-effective compared to traditional sandbags. The system consists of a multicellular structure made of hexagonal double-twisted wire mesh internally lined with a geotextile sleeve. Considering its successful global applications, this system constitutes an effective and versatile solution for flood protection and emergency works.

## 1. Background

Climate change has affected the frequency and scale of natural disasters. In recent years, floods, storms, droughts, wildfires, and extreme temperatures have become more frequent and the occurrence of a disaster affects people and economies. The Emergency Database (EM-DAT) recorded 387 natural hazards and disasters worldwide in 2022 (CRED, 2023). The events in 2022 caused the loss of around 30 thousand lives and an economic loss of about US$ 223 billion (CRED, 2023). Over the last five years, climate-related disasters have had a very high recurrence rate and floods were the most frequent type of disaster, as illustrated in Fig. 1.

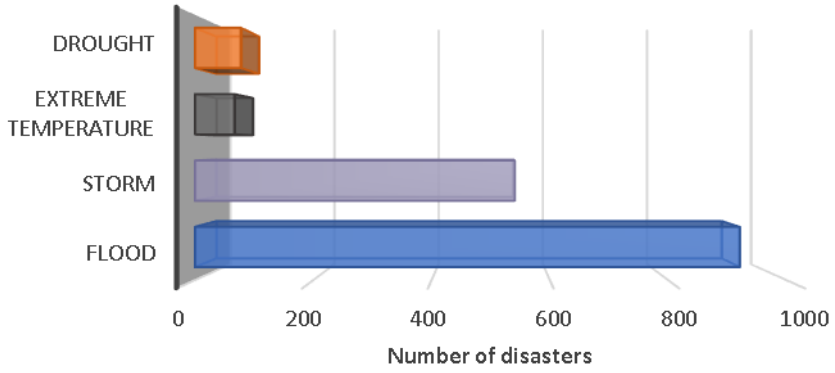



**Fig. 1.** Occurrence of climate-related disasters between 2018 and 2022 as recorded by EM-DAT (CRED, 2023).

In 2015, UNISDR adopted the Sendai Framework for Disaster Risk Reduction 2015-2030, where one of the priorities for action is to enhance emergency management for effective response and to “Build Back Better” (UNDRR, 2015). Thus, international institutions have developed strategies to obtain baseline indicators for understanding the factors driving up an emergency's likelihood.

### *1.1. Emergency management*

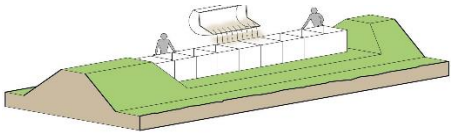
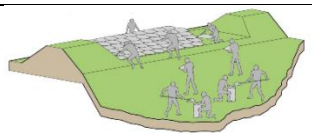
A successful strategy for disaster management is the combined methodology of monitoring and mapping to forecast a potential risk. Current technology, such as satellite remote sensing, provides timely and accurate geospatial information for risk reduction and rapid response coordination. The EFAS, which is part of the Copernicus EMS, provides the forecasted floods in Europe up to 10 days in advance (Dottori et al., 2017).

## 2. Flood protection

The emergency flood works require versatility to allow easy deployment, therefore protecting assets from rising flood water on time. The system is supplied in folded units that can be easily connected to rapidly build large barriers without requiring skilled labor. The system showcased is a multicellular structure made of hexagonal double-twisted wire mesh internally lined with a geotextile sleeve. The geotextile lining enables the system to be filled with locally available materials such as sand or general fill.

The great advantage of this multicellular system is the quick and easy assembly compared with traditional sandbags. Below, a comparison of the construction rate of a straight-line barrier with the two solutions is shown in Table 1, where the sandbag requires more intensive labor. It was noted that the seepage rate is registered for a water depth of 0.9 m is higher for sandbags and for most cases has damage to repair.

**Table 1.** Comparison between multicellular structure and sandbags

| System type | Construction rate [lm/h] | Seepage [$m^3$/h/m] | Severity of damage |
|---|---|---|---|
|  | 1.70 | 0.1 | Reusable |
|  | 0.13 | 0.4 | Repair needed for each event |

### *2.1. Successful application*

A successful case in September of 2023 is shown in Fig. 2, where Hurricane Isabel triggered the rise in water levels of the Potomac River, threatening buildings in the C&O National Park. Due to the value and heritage of the buildings, flood emergency response plans were developed. Once the water levels went back to normal the units were folded up and efficiently stored for another emergency. The system can serve also as a permanent proactive solution to protect land developments placed in floodplains. When used as a permanent solution after an emergency, the structure can be covered and revegetated in harmony with the environment.




**Fig. 2.** Flood protection system during the Hurricane Isabel.

**References**

CRED (2023). Disasters in numbers 2022. Centre for Research on the Epidemiology of Disasters (CRED).
Dottori, F., Kalas, M., Salamon, P., Bianchi, A., Alfieri, L., & Feyen, L. (2017). An operational procedure for rapid flood risk assessment in Europe. Natural Hazards and Earth System Sciences, 17(7), 1111-1126.
UNDRR (2015). Sendai Framework for Disaster Risk Reduction 2015-2030. United Nations.

# Enhancing flood exposure analysis of cultural heritage

Claudia DE LUCIA[1], Serena FRANCESCHINI[2], Carlo FRANCINI[3], Fabio CASTELLI[1], Chiara ARRIGHI[1]

[1] Department of Civil and Environmental Engineering, Università degli Studi di Firenze, Italy
claudia.delucia@unifi.it
chiara.arrighi@unifi.it
fabio.castelli@unifi.it

[2]Northern Apennines River Basin District Authority, Italy
s.franceschini@appenninosettentrionale.it

[3]World Heritage and UNESCO relationship Office of the Municipality of Florence, Italy
carlo.francini@comune.fi.it

ABSTRACT

## 1. Introduction

In the last decades, flooding has been the costliest hazard in Europe and the presence of cultural heritage assets (hereinafter CH) increases enormously the vulnerability to floods in an urban area. Moreover, the evaluation of CH exposure is challenging, due to its intangible value, but also to the peculiar characteristics of the assets; in fact, frequently CH are rich in artworks and decorative elements that increase their susceptibility. At the same time, CH is crucial for post-disaster resilience, especially for art cities, whose economy is mainly based on tourism (Arrighi et al., 2022). The UNESCO-Resilience project aims to define a framework to analyse the flood risk for CH in art cities through an enhanced exposure characterization, to support the stakeholders to prioritize the adaptation interventions and to improve CH resilience.

## 2. Materials and methods

### *2.1. Hazard and impact assessment*

The flood hazard is defined adopting an HEC-RAS 1D/2D hydraulic model. The terrain data, underlying the floodplain, has 1 m resolution and specific Manning's coefficient associated to the land use type; buildings are considered as waterproof blocks. The channel and the flood prone area are connected by a set of lateral structures and the outflow from the riverbanks is determined using the weir equation (Arrighi et al., 2022). Four scenarios with annual exceedance probabilities of 1/30, 1/100, 1/200, 1/500 are simulated. Moreover, scenarios with upstream structural interventions, such as detention basins, are also considered. The model outcomes are the flood inundation map, the water depth data and the velocity data.

To assess the flood impact to CH, exposure and vulnerability information such as the presence and mode of use of basement and the presence and typology of artworks are collected on site through surveys, specifically designed. Finally, the existence of the flood emergency plan and insurance against flood allow to comprehend the capacity of CH sites to respond to a disastrous event (Bonazza et al, 2021).

Knowing the flood water depth along the perimeter of the CH sites and the elevation of the water entry points, it is possible to calculate the actual water depth into the buildings. Also, an exposure parameter E is defined by Eq. (1).

$$E = B + B_A + D + GF_A + A_W \quad (1)$$

Where B stands for the presence of basement, $B_A$ for artworks in the basement, D for decoration on walls or floor at the exposed levels, $GF_A$ for artworks on the exposed ground floor, $A_W$ for artworks below the calculated actual water depth. Each addendum could be equal to 0, when it is absent, or to 1 when it is present. Based on the parameter E, the CH sites are classified. Finally, the CH sites' social value is evaluated with a participatory approach through a paired comparison survey administered to a panel of people.

*2.2 Case study*

The framework has been applied to the historical centre of Florence, listed as UNESCO Heritage since 1982. Since 1177, Florence has been hit by flood 56 times: the 4$^{th}$ of November 1966 the last exceptional event occurred, causing 38 deaths and many damages and destruction of precious works of art (Galloway, 2020).

## 3. Results

The hydraulic model result reveals that, simulating 1/200 and 1/500 exceedance probability scenarios, the Florence UNESCO site is flooded. By increasing the upstream reservoir volume, the flooded area decreases about 68%, with 1/200 exceedance probability scenario.

As concerns the 1/200 exceedance probability scenario, without mitigation measures, 106 CH sites within the UNESCO perimeter are flooded, including 17 CH declared of Outstanding Universal Value. Considering the elevation of the potential water entry points, in 79% of surveyed CH sites the actual water depth decreases, but only for 7 CH sites it becomes 0.

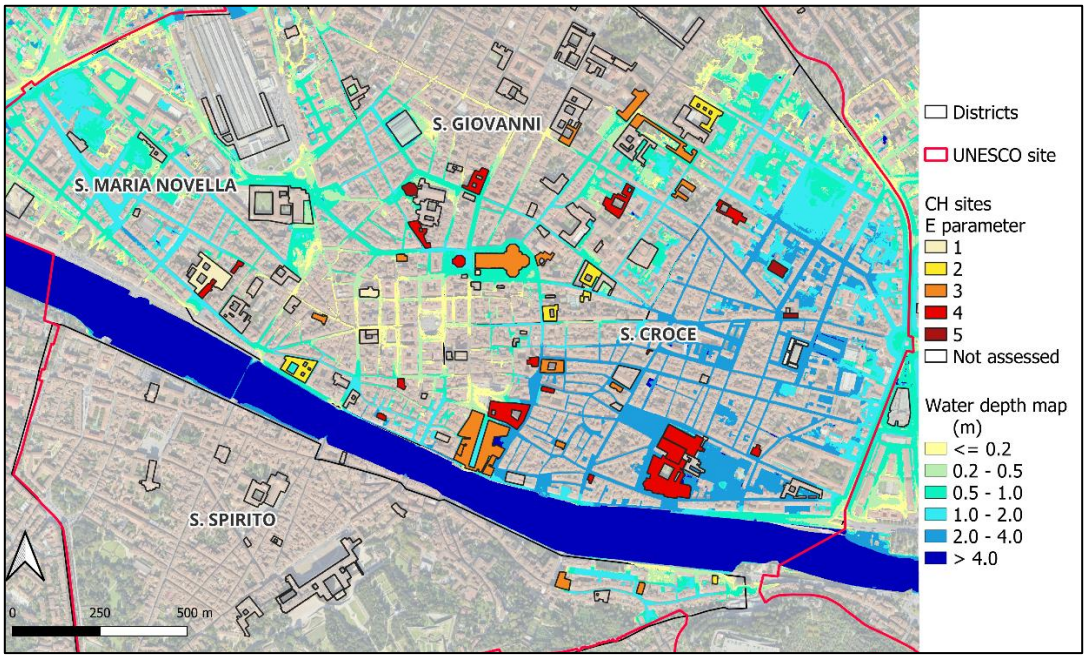



**Fig. 1.** Flood inundation map in the UNESCO site for 1/200 exceedance probability, without mitigation measures. Classification of CH sites, based on "E" parameter.

Fig. 1. illustrates the distribution and the classification of CH sites, based on E parameter: the CH sites most exposed are mainly in the Santa Croce district. About 87% of CH sites surveyed have the basement and 34% have artworks in the basement. Moreover, about 83% have artworks on the flooded ground floor. Finally, only 36% of the assessed CH sites have a flood emergency plan to safeguard the artworks.

**References**

Arrighi, C., Carraresi, A., & Castelli, F. (2022). Resilience of art cities to flood risk: A quantitative model based on depth-idleness correlation. Journal of Flood Risk Management, 15(2), e12794.

Bonazza, A., Sardella, A., Kaiser, A., Cacciotti, R., De Nuntiis, P., Hanus, C., Maxwell, I., Drdácký, T., Drdácký, M., Safeguarding cultural heritage from climate change related hydrometeorological hazards in Central Europe. International Journal of Disaster Risk Reduction, Volume 63, 2021, 102455, ISSN 2212-4209

Galloway, G. E., Seminara, G., Blöschl, G., García, M. H., Montanari, A., & Solari, L. (2020). Reducing the flood risk of art cities: The case of Florence. Journal of Hydraulic Engineering, 146(5), 1–7.

# Identification of compound flooding hotspots along the Andalusian coastline (Spain)

Juan Del-Rosal-SALIDO[1], Marcus Silva de SANTANA[1], María BERMÚDEZ[1], Miguel Ortega-SÁNCHEZ[1]

[1]Andalusian Institute for Earth System Research – University of Granada. CEAMA Building, Av. del Mediterráneo, s/n, 18006, Granada, Spain.

jrsalido@ugr.es, marcussanta@ugr.es, mariabernudez@ugr.es, miguelos@ugr.es

ABSTRACT

Coastal regions face escalating social, environmental and economic challenges due to floods. Flood impacts can be magnified by the combined effects and interaction of maritime, atmospheric, and fluvial drivers, a phenomenon which is typically known as compound flooding. Holistic flood assessments that account for compound flooding, while comprehensive, are resource intensive and often of limited use in decision-making. To address this critical gap, our study develops a streamlined probabilistic approach to decipher compound flood patterns along the Andalusian coastline, Spain. By means of the "extreme values simultaneity" and "extreme values correlation" methods, we identify flooding hotspots where further local analysis is needed. Preliminary results from the Guadiaro river mouth reveal significant insights, emphasizing the usefulness of these techniques in guiding resource allocation for flood analysis.

## 1. Introduction

Globally, floods are the most common natural hazard and have major economic, social, and ecological impacts on communities (CRED & UNISDR, 2015). However, many of these catastrophic floods have a compound dimension, where the interaction of multivariate and multiscale drivers (e.g., river discharge, storm surge or precipitation) exacerbates their effects. During recent years different works have been done regarding compound flooding at global (Vousdoukas et al. 2017), regional (Camus et al. 2021) and local scale (Del-Rosal-Salido, 2020). Nevertheless, previous studies assessing compound flooding at local scale have three major drawbacks: they are complex, expensive and highly computational demanding (Del-Rosal-Salido, 2021), and thus tend to be of limited use for local governments and administrations. Therefore, the objective of this work is to characterize the Andalusian coastline in Southern Spain in terms of their compound flooding drivers, identifying hotspots and combinations of drivers that are more likely to contribute to compound flooding throughout a straightforward probabilistic approach. This characterization constitutes an easy-to-use, low-cost, and computationally efficient decision-making method that can inform administrators and stakeholders about the nature of the dependence between the forcing drivers along the coastline. It will allow coastal administration to decide if a local compound flooding analysis is required (with its implications of cost, time and difficulty) or a simpler approach can be applied in local scale to optimize public resources.

## 2. Methodology

The two selected approaches for this work meet the following criteria: they are easy to implement, computationally cost-free, while maintaining a probabilistic focus. To this end, the dependence and correlation between the different variables is analyzed to identify the concurrence of these events in time and space using two different probabilistic approaches. The final result will be a zonation of the Andalusian coastline based on the statistical dependence between the simultaneous extreme events of the forcing drivers to identify areas where local-scale compound flood modelling must be performed. The method can be easily extended to any coastline around the globe where data is available. The first method, named "extreme values simultaneity", allows for quantifying the probability of experiencing a compound flooding event from various agents through conditional probability (Eq:1).

$$P(\eta_{surge} > s \mid Q_{river} > q);\ P(\eta_{surge} > s \mid W_{Hs} > w);\ P(W_{Hs} > w \mid Q_{river} > q) \quad (1)$$

where *s*, *q* and *w* are the 99th percentile threshold values (leading to 2-3 extreme events per year) that delimitate extreme regime of storm surge ($\eta_{surge}$), significant wave height ($W_{Hs}$) and river discharge ($Q_{river}$). The second approach "extreme values correlation" follows the methodology proposed for JRC 2016 to calculate the correlation between extremes of primary variables as an estimation of the joint probability of occurring simultaneously through the assessment of the statistical dependence ($\chi$) in (Eq:2).

$$T_{x,y} = \sqrt{\frac{T_x \cdot T_y}{\chi^2}} \quad (2)$$

Where ($T_{x,y}$) is the joint return period, ($T_x$) the return period of the variable X (fluvial driver as $Q_{river}$), and ($T_y$) the return period of the variable Y (maritime driver, as ($\eta_{surge}$) and ($W_{Hs}$).

## 3. Preliminary Results

Results for the Guadiaro river mouth area in Sotogrande (Cadiz, southern Spain) are presented using the extreme value simultaneity approach. The analysis uses 25-year historical period of river discharge data measured at 20 km to the river mouth. Hourly surge data from the Coastal Dataset for the Evaluation of Climate Impact (CoDEC) have also been used for the same period of time. Surge model was forced with meteorological fields from the ERA5 climate reanalysis to capture steady and extreme sea levels for the period 1979 to 2017. Significant wave heights were also used in the analysis from SIMAR database. Storm cycles were extracted from the normalized historical series using a POT analysis. Finally, the probability of an extreme surge event conditioned on the occurrence of an extreme river discharge event is obtained. Results with wave height will be shown during the congress. For this location and drivers, a conditioned probability of 0.32 is obtained. The implications of this value can then be analyzed based on the data obtained using the second approach (correlating extreme values). The analysis will be extended along the Andalusian coastline to discuss the use of these simple approaches before tackling a composite flooding problem in coastal areas.

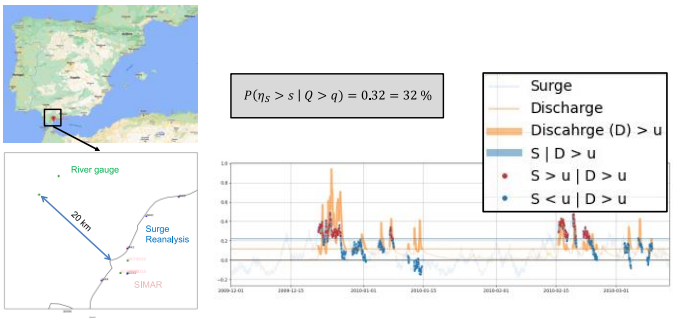



**Fig. 1.** Probability of having a river discharge extreme event simultaneously with an extreme event of storm surge for the Guadiaro river mouth (southern Spain)

**Acknowledgements**

This research was supported by Grant PLEC2022-009362 (MCIN/AEI/10.13039/501100011033 and European Union NextGenerationEU/PRTR), Grant RED2022-134880-T (MCIN/AEI/10.13039/501100011033) and Grant PID2021-125895O (MCIN/AEI/ 10.13039/501100011033 and ERDF "A way of making Europe").

**References**

Camus, P., Haigh, I.D., Nasr, A.A., Wahl, T., Darby, S.E. and Nicholls, R.J. (2021) Regional analysis of multivariate compound coastal flooding potential around Europe and environs: sensitivity analysis and spatial patterns. Natural Hazards Earth Systems. Science Discussion., 21, 2021–2040.

CRED, & UNISDR. (2015). The human cost of weather related disasters 1995–2015, 30 pp.

Del-Rosal-Salido, J., Folgueras, P., Ortega-Sánchez, M., and Losada, M. A. (2019). "Beyond flood probability assessment: An integrated approach for characterizing extreme water levels along transitional environments". In: Coastal Engineering 152, p. 103512.

Del-Rosal-Salido, J., Folgueras, P., Bermúdez, M., Ortega-Sánchez, M., and Losada, M. A. (2021). "Flood management challenges in transitional environments: Assessing the effects of sea-level rise on compound flooding in the 21st century". In: Coastal Engineering 167, p. 103872.

JRC Technical Report European Commission. (2016). Joint Probabilities of Storm Surge, Significant Wave Height and River Discharge components of coastal flooding events. 84 pp.

Vousdoukas, M. I., Mentaschi, L., Voukouvalas, E., Verlaan, M., & Feyen L. (2017). Extreme sea levels on the rise along Europe's coasts. Earth's Future, 5, 304–323.

# Temporal Compounding of Hydrological Extremes Across the Upper Jhelum Basin in a Changing Climate

Rubina ANSARI[1], Ana CASANUEVA[2,3], Giovanna GROSSI[1]
[1]Department of Civil, Environmental, Architectural Engineering and Mathematics, University of Brescia (Italy)
r.ansari@unibs.it, giovanna.grossi@unibs.it
[2]Dept. Matemática Aplicada y Ciencias de la Computación (MACC), Universidad de Cantabria, Santander (Spain)
[3]Grupo de Meteorología y Computación (Unidad Asociada al CSIC por el IFCA), Santander (Spain)
ana.casanueva@unican.es

ABSTRACT

The temporal compounding of two contrasting extremes of the hydrological spectrum (droughts and floods) reflects a volatile hydrological cycle, thereby rendering water and emergency management more difficult due to the need to balance the long-term storage of water and short-term flood control. The present study aims to investigate the temporal compounding of extreme wet and dry events in the Upper Jhelum Basin (UJB) in the context of climate change, utilizing simulations from three modeling initiatives (CMIP6, CORDEX, and CORDEX-CORE) under low, medium, and high emission scenarios for two time segments, i.e., near future (2040-2059) and far future (2080-2099). Meteorological wet and dry conditions, as drivers of hydrologic floods and droughts, are characterized by using a multivariate drought index (namely the Standardized Precipitation Evapotranspiration Index, SPEI). The temporal compounding of wet and dry events, their statistical interdependency and significance are investigated using event coincidence analysis (ECA). Results show that the probability of dry to wet (D-to-W) compound events (CEs) is much higher and statistically significant than the wet to dry (W-to-D) CEs under both retrospective and prospective climate contexts. Specifically, the southwest part of the basin under monsoon dominated precipitation pattern is found to be the hotspot for D-to-W CEs, which was not found to be hotspot historically neither for dry nor for wet extreme events.

## 1. Introduction

Climate change is projected to intensify the global hydrological cycle, leading to more frequent and severe floods and droughts. As a result, more severe droughts, intense precipitation events, and frequent anomalous dry and wet spells are expected to become the new normal for many ecosystems. These extreme events can further exacerbate their impacts when occur concurrently or consecutively, even if the individual contributing event is not extreme. These extreme events have put a strain on society's ability to predict and adapt effectively to these extreme phenomena. To reduce risks and improve water management policies, it is essential to understand how these extreme events compounded over time in a changing environment. This will help to characterize their impacts on water-related sectors, develop efficient reservoir operation rules, and enhance agricultural planning.

## 2. Data

The present study employs climate model simulations from 2 Global Climate Models (GCMs) of the CMIP6, (Eyring et al., 2015), 17 Regional Climate Models (RCM) simulations of the CORDEX, (Giorgi et al., 2009) and 9 RCM simulations of the CORDEX-CORE, (Teichmann et al., 2021) under low, medium and high emission scenarios. Climate model simulations are bias corrected by Multivariate Bias Correction with N-dimensional probability density function transform-MBCn (Cannon, 2018) using W5E5 (Cucchi et al., 2020) as reference dataset.

## 3. Methods

Meteorological wet and dry conditions, as drivers of hydrologic floods and droughts, are characterized by using a SPEI (Vicente-Serrano et al., 2010) as SPEI≤+1and SPEI≤−1, respectively. SPEI is calculated using a 30-day accumulation period of climatic water balance (precipitation minus potential evapotranspiration) at daily time step with potential evapotranspiration estimated using the Hargreaves-Samani method (Hargreaves

and Samani, 1985) based on daily maximum and minimum temperature. The CEs, which is defined as a successive transition from one powerful state to another, includes D-to-W and W-to-D events in the adjacent month. The statistical interdependency of wet and dry extreme events and their statistical significance are investigated using ECA (Donges et al., 2016) which characterized the lagged and time-varying responses between two events.

## 4. Results and Discussion

The spatial distribution of probability of CEs (only D-to-W) and their statistical significance for the historical and projected future climate is shown in Fig. 1. Results show that the observed probabilities of D-to-W and W-to-D CEs are found to be high, at up to 60% (statistically significant at 5% level) and 30%, respectively. The probability of D-to-W CEs is projected to increase from 60% to 80% for specific grid boxes and model simulations, while the probability of W-to-D CEs is expected to remain relatively unchanged under warming conditions (not shown here). The observed probability of D-to-W CEs is statistically significant over 23.33% of the domain, located in the southwest of the basin under monsoon-dominated region. It is interesting to note that this region is not found to be a hotspot neither for dry nor for wet events (Ansari et al., 2023). The northeast part of the basin with high mountains of western Himalayas (under westerlies precipitation pattern) is found to be least effected by CEs despite of its higher susceptibility towards wet and dry extreme events (Ansari et al., 2023). The physical mechanism behind D-to-W CEs is often attributed to the disrupted energy budget and can be understood in the context of global warming. The increased temperature leads to higher evapotranspiration rates which promote atmospheric instability and convective development, and results in increased drought and flood risk (He and Sheffield, 2020). Furthermore, such CEs may also be driven by large-scale thermodynamics, circulation shifts, and land-sea atmospheric feedbacks (Deng et al., 2020).

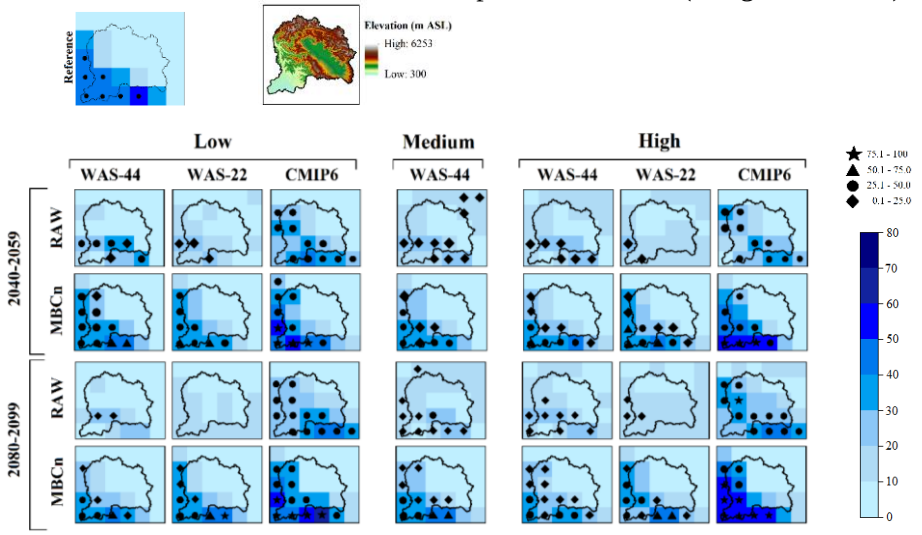



**Fig. 1** Probability of temporal compound dry-to-wet events (%), in the historical reference dataset (1986-2005, first row, left), digital elevation model in meters above sea level (first row, right) and future projected probabilities under low (RCP2.6/SSP126), medium (RCP4.5/SSP545), high (RCP8.5/SSP585) emission scenarios for the multi-model ensemble mean raw ensembles (second row) and bias-corrected ensembles under near future (2040-2059) and far future (2080-2099). In the projections, the different shapes denote the percentage of ensemble members with statistically significant probability at the 5% level.

### References


Ansari R, Casanueva A, Liaqat MU, Grossi G (2023) Evaluation of bias correction methods for a multivariate drought index: case study of the Upper Jhelum Basin. Geoscientific Model Development 16:2055-2076.

Cannon AJ (2018) Multivariate quantile mapping bias correction: an N-dimensional probability density function transform for climate model simulations of multiple variables. Climate dynamics 50:31-49.

Cucchi M, Weedon GP, Amici A, Bellouin N, Lange S, Müller Schmied H, Hersbach H, Buontempo C (2020) WFDE5: bias-adjusted ERA5 reanalysis data for impact studies. Earth System Science Data 12:2097-2120.

Deng K, Jiang X, Hu C, Chen D (2020) More frequent summer heat waves in southwestern China linked to the recent declining of Arctic sea ice. Environmental Research Letters 15:074011.

Donges JF, Schleussner C-F, Siegmund JF, Donner RV (2016) Event coincidence analysis for quantifying statistical interrelationships between event time series: On the role of flood events as triggers of epidemic outbreaks. The European Physical Journal Special Topics 225:471-487.

Eyring V, Bony S, Meehl G, Senior C, Stevens B, Stouffer R, Taylor K (2015) Overview of the Coupled Model Intercomparison Project Phase 6 (CMIP6) experimental design and organization. Geoscientific Model Development Discussions 8

Giorgi F, Jones C, Asrar GR (2009) Addressing climate information needs at the regional level: the CORDEX framework. World Meteorological Organization (WMO) Bulletin 58:175.

Hargreaves GH, Samani ZA (1985) Reference crop evapotranspiration from temperature. Applied engineering in agriculture 1:96-99.

He X, Sheffield J (2020) Lagged compound occurrence of droughts and pluvials globally over the past seven decades. Geophysical Research Letters 47:e2020GL087924.

Teichmann C, Jacob D, Remedio AR, Remke T, Buntemeyer L, Hoffmann P, Kriegsmann A, Lierhammer L, Bülow K, Weber T (2021) Assessing mean climate change signals in the global CORDEX-CORE ensemble. Climate Dynamics 57:1269-1292

Vicente-Serrano SM, Beguería S, López-Moreno JI (2010) A multiscalar drought index sensitive to global warming: the standardized precipitation evapotranspiration index. Journal of climate 23:1696-1718.

# River monitoring in extreme low flow using Sentinel-2 and Landsat 9 imagery: the Lower Tagus River (Portugal)

Romeu GERARDO[1,2,3], Isabel PEDROSO DE LIMA[1,4], João PEDROSO DE LIMA[1,4]

[1] University of Coimbra, Faculty of Sciences and Technology, Department of Civil Engineering, Rua Luís Reis Santos, 3030-788 Coimbra, Portugal
romeu.jorge@uc.pt; iplima@uc.pt; plima@dec.uc.pt
[2] CERIS, University of Coimbra, Rua Pedro Hispano, 3030-289 Coimbra, Portugal
[3] Itecons—Institute of Research and Technological Development in Construction, Energy, Environment and Sustainability, Rua Pedro Hispano, 3030-289 Coimbra, Portugal
[4] University of Coimbra, MARE—Marine and Environmental Sciences Centre/ARNET–Aquatic Research Network, Rua Sílvio Lima, 3030-790 Coimbra, Portugal

ABSTRACT

River monitoring is crucial for various reasons, including environmental protection, flood prevention, water resources management, and scientific research. The unique challenges posed by low-flow conditions to conventional in-situ monitoring require innovative alternative approaches. Presently, remote sensing technologies offer state-of-the-art tools for rapid and cost-effective water body mapping based on multispectral indices. The primary objective of this study was to compare the capabilities of utilizing imagery from the Sentinel-2 and the newly launched Landsat 9 satellites to achieve this objective. Data were collected for a segment of the Tagus River in Portugal during a period of exceptionally low river discharge in July 2022. Results indicated that the datasets and mapping from both satellites were consistent, thus allowing for their complementary use.

## 1. Introduction

Mapping riverbed sandbars and water surfaces is essential for describing and monitoring the morphological, hydraulic, and biological characteristics of alluvial rivers. This understanding helps in comprehending fluvial processes, reducing navigation hazards, and gaining insights into erosion and deposition responses to natural and human influences on the river. One of the challenges hindering the development of models in these fields is the lack of data. Low-flow conditions in rivers, whether resulting from river management or hydrological dry periods, make sandbars more visible. Conventional approaches for monitoring river sandbars during such conditions rely on historical photographs, ground-based surveys, and sporadic aerial datasets (e.g., Rinaldi, 2003; Dufour et al., 2015). Nowadays, remote sensing (RS) data with short revisiting times are readily available and are expected to serve as valuable tools for investigating the geomorphic processes that shape channel bars (e.g., Wang et al., 2015; Gerardo and de Lima, 2023).

The aim of this study was to explore the mapping of surface water and sandbars in rivers using data from the Sentinel-2 (S2) and the newly launched Landsat 9 (L9) satellites to better understand the utility of data from both sources for this purpose. The study focused on the Lower Tagus River in Portugal and provides the first evaluation of L9's data for calculating water and sandbar surfaces in fluvial systems.

## 2. Materials and Methods

This study focused on a specific segment of the main course of the Tagus River, located in Portugal (Figure 1). This river segment had a length of approximately 11 km and covered an area of ≈4.12 km$^2$; the central point coordinates were: 39°19′36″N; 8°31′44″W. The surrounding area of this river segment is characterized by irrigated agriculture. In 2022, severe drought conditions affected several regions of Europe due to a persistent negative precipitation anomaly. This situation significantly impacted river discharges across Europe, including Portugal and Spain. In the Tagus River, sandbars that are rarely exposed were directly observable (Figure 1).

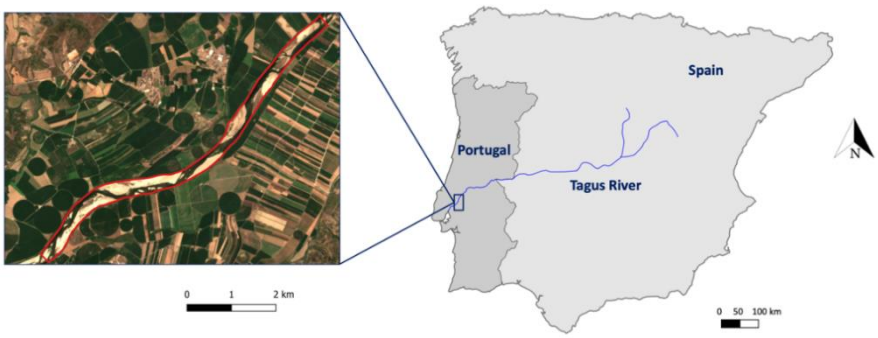



**Fig. 1.** Identification of the river segment investigated in this study (left) and its location in the Tagus River (right). The view of the river segment, which captured a condition of very low river discharge that occurred in the summer of 2022, reveals the extensive presence of sandbars along the riverbed.

The S2 satellite imagery (orthoimages in UTM/WGS84 projection) was recorded on 8 July 2022, and the L9 satellite imagery (L9 Collection 2 Surface Reflectance) was obtained on 7 July 2022. The daily average river discharge was 24.9 $m^3/s$ on 7 July and 24.8 $m^3/s$ on 8 July. The multispectral wavelength bands' data spatial resolutions were available at 10 m and 20 m for S2, and 30 m for L9.

Five multispectral satellite-based indices were used: the Normalized Difference Water Index (NDWI), the Modified Normalized Difference Water Index (MNDWI), the Augmented Normalized Difference Water Index (ANDWI), and two variants of the Automated Water Extraction Index (AWEIsh and AWEInsh). These indices have been developed for surface water extraction from satellite imagery. Their calculation is based on algebraic expressions and combinations of multispectral band reflectance data. The wavelength bands involved are the Blue, Green, Red, Near Infrared (NIR), Short Wave Infrared 1 (SWIR1), and Short Wave Infrared 2 (SWIR2) bands. The methodology included the comparison of the water and sandbar areas in the river segment, and the investigation of the correlations and relationships between the S2 and L9 data. Various class-separation approaches based on decision values were explored, including the Otsu method, the Jeffries–Matusita (J–M) distance method and the application of manual criteria.

## 3. Results

Maps of the water indices calculated using the S2 and L9 satellite data were analyzed and compared. The water and non-water (sandbars) surfaces were extracted for each case. To better understand the relationship between the S2 and L9 data, correlations between the satellite-based indices were explored. The linear relationship between paired pixel-scale index values and the correlation coefficients were determined. A cross-comparison of the S2 and L9 indices for the examined area revealed that there was generally good agreement between the S2 and L9 datasets. AWEInsh had the highest correlation coefficient (0.95), whereas NDWI had the lowest (0.83). MNDWI was the normalized index for which the S2 and L9 data agreed most closely, while NDWI showed the greatest disparity in the categorization criteria used. The results obtained for a given index also showed that water/sandbar mapping can be affected more by inadequate decisions in image classification than by differences in the response signal in the different spectral water indices.

## 4. Conclusions

RS satellite-based approaches offer efficient means to inspect riverbed conditions, map the presence of water and sandbars, and quantify their areas. The water body mapping achieved with the S2 and L9 datasets proved to be consistent in this study. This opens up opportunities for combining relevant data from the S2 and L9 satellites regarding water and non-water (sandbar) surface features. Consequently, this increases the frequency of available RS imagery due to the offset orbits of the S2 and L9 satellites, which could have practical implications for river management and environmental protection. Future work on the use of these RS products could involve a broader evaluation of S2 and L9 data and an in-depth comparison of classification criteria.

**References**

Dufour S, Rinaldi M, Piégay H, Michalon (2015) A How do river dynamics and human influences affect the landscape pattern of fluvial corridors? Lessons from the Magra River, Central–Northern Italy, Landscape and Urban Planning, 134, 107–118.

Gerardo R, de Lima, IP (2023) Comparing the capability of Sentinel-2 and Landsat 9 imagery for mapping water and sandbars in the river bed of the Lower Tagus River (Portugal), Remote Sensing, 15, 7, 1927.

Rinaldi M (2003) Recent channel adjustments in alluvial rivers of Tuscany, Central Italy, Earth Surface Processes and Landforms, 28, 587–608.

Wang B, Xu Y (2018) Dynamics of 30 large channel bars in the lower Mississippi River in response to river engineering from 1985 to 2015, Geomorphology, 300, 31–44.

# SIMPCCe: A Software Tool for the Analysis of Reservoir Inflows under Climate Change Scenarios

Salvador NAVAS[1], Manuel DEL JESUS[2]

[1] Institute of Environmental Hydraulics, University of Cantabria, Spain
salvador.navas@unican.es

[2] Institute of Environmental Hydraulics, University of Cantabria, Spain
manuel.deljesus@unican.es

ABSTRACT

Because of climate change and global warming, precipitation and temperature regimes are expected change in many areas of the planet. This, in turn, could have major impacts on hydrology and water resource availability, resulting in alterations to surface runoff and aquifer recharge. The alteration of hydrological dynamics can reduce the minimum contributions that the reservoirs receive during periods of lower rainfall, which could have a serious impact on the operation of these reservoirs and the demands they may meet. For this reason, it is necessary to carry out climate change impact studies, to determine the possible evolution of the availability of water resources and to propose adaptive routes to mitigate the effects of climate change on reservoirs. The latest regional climate change studies carried out in Spain highlight the convenience of making all the information produced from these studies easy to use, which is why we have developed the SIMPCCe software tool (Navas and del Jesus, 2023) to complement the "Methodological guide for the estimation of minimum contributions to reservoirs in the context of climate change" (Navas et al., 2022). This tool allows preliminary analyses of inflows under climate change scenarios at any point of the Spanish water network to make robust assessments of the risks of climate change in the minimum inflows to reservoirs and the implications they could have for management. Thus, the tool that has been developed focuses on providing initial and quick assessments to evaluate if the adaptation to climate change in this sector can be achieved through improving the monitoring, operation and maintenance regime that already exists. The tool has been developed to enable reservoir managers to carry out simple assessments, enable the development of adaptation pathways and assist in decision making. Moreover, the tool is open source and can be adapted to be used in any other region of the planet.

## 1. The SIMPCCe Software Tool

SIMPCCe is a software tool developed in Python that complements the guide of minimum inflows to reservoirs (Navas et al., 2022). With this application, from a given location on the river network, it is possible to make climate change forecasts of reservoir inflows. The analysis starts by downloading information from official sources to build and train a regression model based on neural networks to reproduce the series of inflows at a point in the river network from monthly-scale climate data (precipitation and temperature). Once the neural network has been trained and through climate change data, it is possible to obtain forecasts of future inflows. The software tool can also work with real inflow observations where they are available, and tests have been carried out to ensure that both functioning ways provide equivalently good estimations.

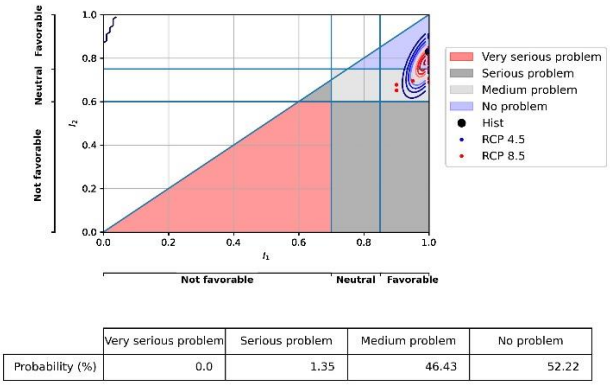
The model assumes that reservoir inflows can be treated as a stochastic variable whose statistical distribution can be obtained. Therefore, it may not be able -in its current incarnation- to capture complex interactions among different reservoirs.

The software tool automatically downloads the required information from public sources when observations are not readily available. Moreover, the tool automatically delineates the watershed over which climate change analysis need to be performed.

The tool uses the climate projections for each one of the available GCMs -ideally all the ones used to develop IPCC's assessment reports- to update the input drivers to the machine learning-based hydrological emulator and runs this emulator to update the historical time series and generate their equivalent under the specific climate change scenario. Thus, there will be a time series per model and per scenario. The tool analyzes all these time series to evaluate the effects of climate change in the inflows to the reservoir and provide a statistical description of these changes.

In locations where river discharge time series are not available, a neural network is automatically calibrated to reproduce observed river discharge statistics. Public databases of atmospheric variables are used as predictors. These atmospheric variables are then bias corrected to include climate change effects and generate the reservoir inflow projections.

We will show how to use the tool for decision making under climate change scenarios, using multi-model ensembles to analyze the uncertainties in the generated projections as shown in figure 1. The left-hand side of the figure shows the regions generated by the interaction of two water availability indices, defining areas ranging from operation without disturbances to serious problems. The dots represent the projected values obtained from climate change analysis and the ellipses are the multivariate distribution of climate projections values.




| | Very serious problem | Serious problem | Medium problem | No problem |
|---|---|---|---|---|
| Probability (%) | 0.0 | 1.35 | 46.43 | 52.22 |

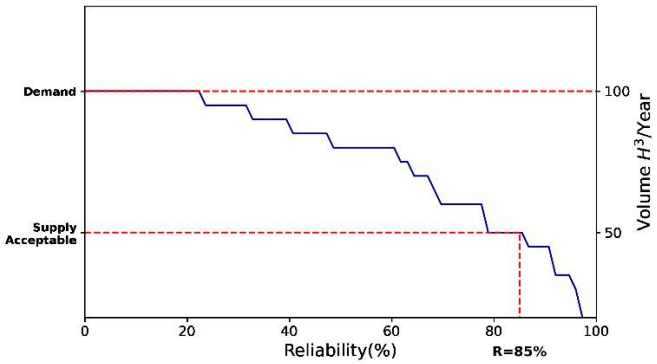



**Figure 1** | Example of a decision-making analysis based on tool results.

The tool allows the user to generate many potential futures deriving from the available climate models, thus allowing to evaluate the probabilities of different scenarios. Indeed, the right-hand side figure shows water demand and availability based on the generated climate projections.

These simple results provide information to managers and decision makers so that they can evaluate an initial assessment of the risk that they are exposed to and, from there, decide if additional finer studies need to be done, or if adaptation measures are going to be required.

The ease of use of the tool and it being open-source, will allow an easy adoption by technicians and an easy extension by others researchers. Indeed, as next steps, we envision to improve the tool to deal with watersheds anywhere in Europe, work for which we will require collaborators in each one of the countries to be covered.

**Acknowledgements**

The authors would like to thank the Fundación Canal de Isabel II for the facilities provided for the dissemination of the contents of the "Methodological guide for the estimation of minimum contributions to reservoirs in the context of climate change", owned by the foundation and also developed by the authors.

**References**

Navas, S., del Jesus, M., & Gómez, D. V. (2022). Guía metodológica para la estimación de aportaciones mínimas a embalses en el contexto de cambio climático. Fundación Canal.
https://www.fundacioncanal.com/docs/guia_embalses_cbio_climatico_FundCanal_2022.pdf (accessed 29/09/23)
Navas, S. & del Jesus, M. (2023). SIMPCCe: Simulador de Pronósticos de Cambio Climático en Embalses. URL
https://github.com/IHCantabria/SIMPCCe (accessed 29/09/23)

# Multivariate Models for Flood Prediction: A Glimpse into the Future

Diego URREA Méndez[1], Dina GOMEZ RAVE[1], Salvador NAVAS[1], Manuel DEL JESUS[1]

[1] IHCantabria - Instituto de Hidráulica Ambiental de la Universidad de Cantabria, Santander, Spain
dum834@alumnos.unican.es
dinavanesa.gomez@unican.es
Salvador.navas@unican.es
manuel.deljesus@unican.es

ABSTRACT

The integration of multivariate analysis into the study of compound hydrological events reveals its potential to better understand the complexity of extreme events and generate likely scenarios. Our methodology, divided into two parts, focuses on comparing different multivariate models that capture all the uncertainty and implementing machine learning techniques that enable the simulation of floods considering multivariate scenarios. The analysis underscores the importance of carefully selecting the appropriate multivariate model, as Gaussian models underestimated extreme events, while extreme vine copula models provided more accurate results. This approach contributes to the understanding and effective management of compound hydrological events, benefiting critical infrastructure planning and flood prediction, and opening new perspectives in climate risk management.

## 1. Introduction

As we delve further into the analysis of compound hydrological events, it has become evident that the integration of multivariate analyses, which consider the interaction among a greater number of variables, can optimally capture, and characterize uncertainty compared to conventional analyses. Multivariate approaches, especially when the study variables are correlated, not only provide a deeper understanding of extreme event complexity but also enable the generation of a wide range of probable scenarios. Studies such as those by Salvadori et al. (2011) and Tosunoglu et al. (2020) have demonstrated the applicability of multivariate models in the study of compound events.

In multivariate analysis of the frequency of compound extreme events, it is essential to consider the dependency structure in the tails of the variables of interest. If the selected copula fails to accurately capture this extreme dependence, the estimation of extreme values can be significantly affected by uncertainty (Hangshing et al., 2018). Therefore, it is crucial to conduct a comprehensive evaluation of the copula model fit to the data, including tail dependency (Serinaldi et al., 2015). This process guides us in selecting the most suitable copula family to model these extreme compound events.

Modeling compound events using multivariate approaches can provide a more precise measure of the return period, benefiting critical infrastructure design, flood prediction, risk management, and more. However, performing simulations considering many multivariate scenarios requires substantial computational resources. In recent years, hybrid downscaling techniques (as demonstrated in previous works such as Camus et al., 2011; Lin et al., 2016; Navas et al., 2017) have been developed to mitigate this challenge by reducing computational time. These techniques rely on machine learning methods that simplify conventional computationally expensive models. Despite advancements in hybrid downscaling, further research and development are still needed in this area.

## 2. Methodology

We propose a two-part methodology: (I) This phase focuses on the comparison of various multivariate models that capture all the uncertainty. It involves researching different models and copula structures. The main objective here is to assess the goodness of fit and tail dependence of these copula models. Additionally, it integrates synthetic data generation with the selection of representative events through the analysis of design storms. This strategy has the potential to further simplify the number of scenarios that need to be modeled using hybrid downscaling techniques. The inclusion and selection of representative events enable the study of the joint behavior of multiple variables, even surpassing the common dimensionality limitations in many studies. A concrete example would be evaluating the behavior of events measured at multiple rain gauges within a watershed to adequately capture spatial structure.

(II) In this second stage, we create a more robust methodology that includes the study, evaluation, and implementation of multiple statistical and machine learning techniques. The focus is on using the results obtained in the first stage to develop flood models. These models allow us to compare multivariate models in terms of their performance in flood prediction and other related impacts.

## 3. Results

The results of this research offer valuable insights into the significance of selecting different approaches in the hydrological analysis of precipitation-linked design events. Our findings indicate that using a multivariate approach leads to significantly more accurate precipitation estimations compared to the univariate approach. The analysis underscores the importance of carefully choosing the appropriate multivariate model, as Gaussian models underestimated extreme events, while extreme vine copula models provided more precise results.

The underestimation by Gaussian models also manifested in flood predictions. We observed that floods generated by extreme vine copula models exceeded the predictions of Gaussian copula models significantly. This discovery suggests that tail-dependent vine copula structures outperform Gaussian structures in modeling extreme events. This development has a positive impact on the field of engineering, reducing uncertainty in engineering design processes and providing a more precise approximation of climate-related impacts. Additionally, the proposed methods have the potential to offer crucial climatic information applicable to planning, infrastructure design, adaptation proposals, and managerial decision-making, ultimately leading to more effective territorial management.

**References**


Camus, p., Mendez, f. J. and Medina, r, 2011. A hybrid efficient method to downscale wave climate to coastal areas', coastal engineering, 58(9), pp. 851–862. Doi: 10.1016/j.coastaleng.2011.05.007.

Lin, g.-f., chang, m.-j. And wu, j.-t., 2016. A hybrid statistical downscaling method based on the classification of rainfall patterns', water resources management 2016 31:1, 31(1), pp. 377–401. Doi: 10.1007/s11269-016-1532-2.

Gräler, B., Berg, M. J. van den, Vandenberghe, S., Petroselli, A., Grimaldi, S., De Baets, B. & Verhoest, N. E. C., 2013. Multivariate return periods in hydrology: a critical and practical review focusing on synthetic design hydrograph estimation. Hydrol. Earth Syst. Sci., 17(4), 1281–1296.

Hangshing, L. and Dabral, P.P. (2018) 'Multivariate Frequency Analysis of Meteorological Drought Using Copula', *Water Resources Management*, 32(5), pp. 1741–1758. Available at: https://doi.org/10.1007/s11269-018-1901-0.

Navas, S., & del Jesus, M. (2017). Análisis del riesgo de inundación mediante técnicas estadísticas avanzadas. V Jornadas de Ingeniería Del Agua, 24-26.

Salvadori, G., De Michele, C. & Durante, F., 2011. On the return period and design in a multivariate framework. Hydrol. Earth Syst. Sci., 15(11), 3293–3305.

Serinaldi, F., Bárdossy, A. and Kilsby, C.G. (2015) 'Upper tail dependence in rainfall extremes: would we know it if we saw it?', Stochastic Environmental Research and Risk Assessment, 29(4), pp. 1211–1233. Available at: https://doi.org/10.1007/s00477-014-0946-8.

Tosunoglu, F., Gürbüz, F. & İspirli, M. N., 2020. Multivariate modeling of flood characteristics using Vine copulas. Environ Earth Sci, 79(19), 459.

# Save OceanVille: a risk game enhancing communication among public decision-makers

Marta MERINO[1], Thorsten PIONTKOWITZ[1], Kaija Jumppanen ANDRESEN[1]

[1] The Danish Coastal Authority, Denmark
mam@kyst.dk

ABSTRACT

The number of coastal urban areas impacted by flooding is increasing year after year as floods become more frequent and more intense due to climate change. As floods become more frequent and intense, the negative impacts of flood events on local communities and the economic consequences of these events are expected to increase as well. At the same time, these floods are raising awareness in the public and leading to calls for coastal flood risk management that balances urban development, economic growth, climate change adaptation and nature conservation. In order to understand the different wishes for flood protection, land use etc., an ongoing dialogue between municipalities, policy makers, stakeholders and citizens is required. This dialogue is further challenged by the complexity and uncertainty of trying to predict future climate changes and their negative impacts in detail. Municipalities are expected to initiate a productive dialogue and facilitate additional understanding between different interests in order to plan and implement the best possible development of their areas. For this, open and illustrative communication is key.

The aim of this board game is to improve collaboration between public decision-makers involved in the development and flood risk management of coastal urban areas by creating mutual understanding of the different perspectives and the importance of present and future consequences of risk mitigation. In our project, the game has been played with municipal employees, local politicians, and a mix of both.

## 1. Methodology

The board game is a cooperative role-playing game where participants are divided into groups that represent the city council of the fictional coastal city OceanVille through different roles. All the groups play in the same virtual reality of OceanVille city and have identical starting conditions such as economy and city establishment. Having an equal start across city councils is key in order to later comprehend how the correlation between the different future outcomes is affected by their earlier decisions.

Each city council has the task to make a city plan through various initiatives for the next three decades within a determined time cap and budget. These initiatives are equally available for all and are either oriented towards city development, coastal protection or storm warning. They also have different prices, maintenance costs, effect on the flood risk and nature impact according to each available location in the city. After settling the city plan, a random flood event occurs in OceanVille, which requires a calculation of the new economic situation in proportion to the flood risk. Once again, the city councils have to make a new assessment and a new city plan for the next two decades but this time, starting in different situations based on the latest budgets and damages. The new initiatives are presented right before a random flood event takes place again, which requires yet another budget adjustment and a new flood risk assessment.



**Fig. 1.** Gaming board of OceanVille city where the players can identify the different areas, building locations and vulnerabilities.

## 2. Results and conclusions

The project highlights the significance of participant engagement in facilitating meaningful discussions about flood risk management. Active involvement of participants is crucial for fostering in-depth and productive conversations during decision-making processes. The feedback provided by participants indicate an overall highly positive experience, marked by the creation of an environment of open dialogue and fresh perspectives.

Regarding interactions between the different city councils, we could see that participants exhibited strong reactions to the actions and decisions made by the others. This underscores the interdependence of the groups in the decision-making process, indicating that the outcome of one decision could significantly affect others.

The risk assessment within the game exhibited a broad spectrum, ranging from highly technical aspects to considerations aligned with citizen interests, climate change scenarios or nature protection. This diversity highlights the multi-dimensional nature of risk evaluation in urban planning scenarios.

Participants demonstrated an understanding of the dilemma in the delicate balance required between risk mitigation strategies and city development goals. Furthermore, they acknowledged the importance of flexibility in adapting to potential extreme events that can disrupt city planning and the need to consider all factors comprehensively, as today's decisions serve as the foundation for tomorrow's reality.

Overall, the findings suggest that encouraging active engagement, fostering discussions, and considering a holistic approach to decision-making are essential elements in achieving effective urban development planning that balances risk mitigation with sustainable city growth.

# River-basin restoration hydraulic complexities in some Estonian rivers

Janek LAANEARU[1]

[1] Tallinn University of Technology, Ehitajate tee 5, 19086 Tallinn, Estonia
janek.laanearu@taltech.ee

ABSTRACT

At present, many existing dams in Estonia are mostly recreational purposes, and most of them have been now largely decayed or lost their original functionality. The man-made structures in the river basins are changing the hydrographs of natural streams and therefore directly affect the local ecosystem and its biota. The condition of these structures on estuarine rivers and their use, can adversely affect coastal areas and aquatic life, e.g., due to the fish migration. Many Estonian rivers end their streams at the Baltic Sea and thus affect the coastal processes (Laanearu et al, 2007) and are also important in transport, energy and agricultural use. The study focuses on the environmental engineering projects hydraulic performances of some dams in Estonia. There are more than 1,000 dams (Estonian GIS data of dams on the territory of Estonia) at the Estonian rivers.

## 1. Introduction

Estonian catchment area is located on the eastern coast of the Baltic Sea and includes many dams and abandoned infrastructure in the river basins. Unlike some European countries with abundant water resources and a need for hydroelectric power generation or flood control, Estonia's geography and natural features have limited the development of major dams within its Eastern border. However, there have been few notable dams and water management projects in Estonia (see Jokinen et al, 2021). The major rivers in Estonian are rather short, having a small catchment area, are relatively water-poor, and the river system is rather dense. Therefore, many dams have been built over time in order to get expansion or a large, deeper water body at the river basins.

The Sindi Dam removal project was a notable environmental restoration effort in Estonia. Located on the river Pärnu at the town of Sindi, the Sindi-dam was firstly constructed in 1834 as the bridge for the labors of the local wool industry, and thus reconstructed in the 1950s for the hydroelectric power generation, and finally reconstructed in the 1975s as the technological water source for the local industry. However, over the years, concerns about its environmental impact and the degradation of the river's ecosystem ended with its removal.

The Nehatu-dam reconstruction project is one successful dam retrofitting example. The rebuilding project for this dam, which was originally constructed in the 1980s for generation of cooling water for the Iru-power-station on the river Pirita (see Laanearu et al, 2017) was made in 2013. The dam is needed until today for the water supplies for the Estonian power grid and rebuilding it made it safer and allowed mitigate some environmental impacts, e.g., fish migration, and increase usage of the water paths for recreational purposes.

In summary, while Estonia may not be known for large dams like those in the Scandinavian countries, it has implemented various water management and protection projects to effectively address its specific geographical and environmental challenges. These initiatives contribute to the sustainable development and conservation of Estonia's natural resources while ensuring the safety and well-being of its inhabitants.

## 2. Materials and methodology

In the present study, two different projects are described. The general data from these projects are summarized in Table 1. The first of these was a project in river Pärnu. With the aim to allow upstream and downstream migrations of fish, the dam-removal method was used. The second study was a project in river Pirita, where the downstream part was filled with stones. In addition, new spawning grounds were established. These projects were a long-term campaign targeted to a great part of the river catchment. These projects demonstrated a success in terms of restoring the abundance and diversity of sea fishes, and also had positive effects locally.

**Table 1.** River-basin restoration projects

| No | River | Project year | Activity | Purpose | Outcome |
|---|---|---|---|---|---|
| 1 | Pärnu | 2019 | Removal | Hydro-energy | Watter supply and fish passage |
| 2 | Pirita | 2013 | Restoration | Water supply | Watter sports and fish passage |

### *2.1. River Pärnu: Sind-dam/rapids*

The Sindi-dam was located at the river Pärnu, around 14 km upstream from the river estuary (see Laanearu et al, 2011). The dam was built in the 19th century as the part of local wool industry campaign. The 151 m wide and 4.5 m high ogee-shaped weir was built in 1975 to help provide the water for the local wool industry. In the lower reaches of the river Pärnu, the long-term average annual flow rate of 50 $m^3/s$ and the estimated maximum flow rate of 800 $m^3/s$. The regular river stream has confined to narrow channel of the wider basin.

### *2.2. River Pirita: Nehatu-dam*

The Nehatu-dam is located at the river Pirita, around 12 km upstream from the river estuary. The dam was built in the 20th century for the water intake of the Iru-power-station. The river Pirita is a part of the Tallinn drinking water system, and therefore the changes of water level have impacts. In the lower reaches of the river Pirita, the long-term average annual flow rate of 6 $m^3/s$ and the estimated maximum flow rate of 160 $m^3/s$.

The trapezoidal-shape dam, with a concrete surface and filled with stones inside, is built directly on the bottom of a limestone riverbed. On the slope of the lower bjeff, there are openings for the release of excess pressure that extend into the interior of the dam. The Nehatu-dam is a broad-crested weir with the following dimensions: the length of the threshold part is 8 m, the width of the concrete part of the threshold is 14.7 m - 15.8 m. In addition to the main overflow, the fish passage was included. The dam installation height is 2.1 m.

The purpose of the dam reconstruction was to eliminate the dangerous vortex at the lee side of overflow. For this purpose, the stones of a suitable size behind the dam were used. In 2012, the rapid pass was built in the lee side of the dam, which was supposed to eliminate the dangerous vortex structure and also improved the ecological condition of the river, e.g., allowing recover the fish migration conditions.

## 3. Concluding remarks

Any river restoration projects often require collaboration among various stakeholders, including government agencies, environmental organizations, local communities, engineering enterprises, and private landowners. These projects have strong impact due to scales and multi-year endeavors. Therefore, these projects require careful planning, monitoring, and adaptive management to ensure they achieve their economical, ecological and societal goals. However, also some unforeseen conditions due to climate changes need more careful consideration in future to mitigate any adverse impacts resulting from the river-restoration projects. For instance, the drought conditions may temporally be harmful for the local ecological conditions, since the water level in the Estonian rivers is strongly dependent from rains. Therefore, some measures should be used to increases the amount of water flowing in a river by storing it. Also, due to the riverbed geometry changes, the hydraulic modelling has been become a challenging taking use the momentum and specific-energy curves.

**Acknowledgements**

This research has received funding from the Estonian Research Council, under grant PRG1487, and the Tallinn University of Technology, under grants SSGF21002 and SS19046. The author acknowledges the assistance and input of the Water and Environmental Engineering Research Group of Tallinn University of Technology.

**References**

Laanearu J, Koppel T, Soomere, T, Davies P (2007). Joint influence of river stream, water level and wind waves on the height of sand bar in a river mouth, Nordic Hydrology, 38(3), 287-302.

Estonian GIS data of dams on the territory of Estonia. Source: Ministry of the Environment and the Land Board. Environmental register public service, Paisud. incl. as a file, shape data from the public service register of the Environmental Register and a map from the map server of the Land Board. http://register.keskkonnainfo.ee/ and http://geoportaal.maaamet.ee/, April 17, 2013.

Jokinen H, Kesler M, Abersons K, Bajinskis J, Drigins E, Roge E, Nika N, Kalinowski M, Kuczyński T, Piotrowicz J, Häggström H (2021). RETROUT Restoration Demonstration Case Reports. Interreg Baltic Sea Region, EU, 119 pp.

Laanearu J, Borodinecs A, Rimeika M, Palm B (2017). A review on potential use of low-temperature water in the urban environment as a thermal-energy source, IOP Conference Series: Materials Science and Engineering, 251, Article number 012054. 3.rd International Conference on Innovative Materials, Structures and Technologies, IMST 2017 Riga. 27 September 2017 through 29 September 2017. Code 131651.

Laanearu J, Vassiljev A, Davies P (2011). Hydraulic modelling of stratified bi-directional flow in a river mouth, Proceedings of the Institution of Civil Engineers: Engineering and Computational Mechanics, 164(4), 207-216.

# Simulation of the Brague flood of October 2015 in Southeast of France

Florian CORDIER[1], Thibaut DAVAREND[2], Emmanuel AH-WOANE[2], Zied AMAMA[1,3], Arkadii SOCHINSKII[2], Samer MAJDALANI[4], Roger MOUSSA[5] and Olivier DELESTRE[2,3]

[1] EDF R&D National Laboratory for Hydraulics and Environment
Corresponding author florian.cordier@edf.fr

[2] Université Côte d'Azur Polytech Nice-Sophia
[3] Laboratoire d'Hydraulique Saint-Venant
[4] HydroSciences Montpellier, Univ Montpellier, Centre national de la recherche scientifique, Institut de recherche pour le développement
[5] Laboratoire d'Etude des Interactions entre Sol-Agrosystème-Hydrosystème, Univ Montpellier, Institut national de recherche pour l'agriculture, l'alimentation et l'environnement, Institut de recherche pour le développement, Montpellier SupAgro

ABSTRACT

The Brague watershed (Alpes-Maritimes) is recurrently subjected to flash floods known as "cévenoles", which result in flooding and damage. In October 2015, the municipalities of Biot and Antibes were particularly severely affected. The hydrometric station of the Brague river was damaged during the flood and did not provide a complete record. This flood event was previously studied using hydrological approaches or 2D hydraulic modeling tools with adaptive mesh refinement. Here, we propose to model and simulate this event in the downstream area of the Brague, based on a 2D approach on an unstructured mesh using the TELEMAC modeling software.

## 1. The Brague study case

The study site is located within the Brague watershed, including its main four tributaries, the floodplain including the urban areas (Fig. 1a). The area is surrounded by the city of Biot until the sea at Antibes, covering a surface of approximately 9 km². The Brague river has experienced 3 major floods in the last decade, respectively in 2011, 2015 and 2019. The study domain is delimited with the water level marks resulting from the 2015 historical flood (Préfecture des Alpes Maritimes, 2019). Previous numerical modelling work has been conducted using 1D and 2D shallow-water models implemented in HEC-RAS, including model calibration based on the 2015 flooding event.

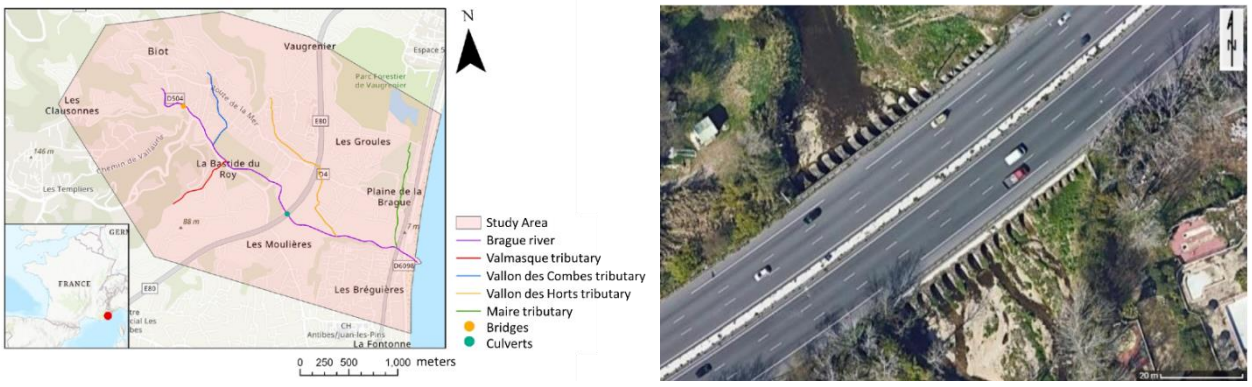



**Fig. 1.** (a) study site location in France, with main tributaries and hydraulic structures, (b) satellite photography of A8 highway's culverts.

Available data for the current study includes DTMs from (IGN, 2018) with spatial resolution of 1 m, modified manually to account for the elevation of emerged buildings, flow under bridges and the bathymetry of small tributaries. Hydrological data, including water stages and flow hydrographs, were recorded during the flood

events mentioned hereabove, or reconstructed manually. Several bridges and culverts are also present in the study area and are supposed to impact -at least moderately- the flood dynamics (Fig. 1b).

## 2. Numerical model set-up

The model is built with the open-source numerical code Telemac-2D (http://www.opentelemac.org/), which computes the solution of the 2D shallow water equations. Finite elements are used on an unstructured mesh composed of 102,437 triangles. The mesh is defined to follow longitudinally the main channels directions, assuming a minimal number of cross-channel nodes equal to 3. In the floodplain, the mesh size is approximately uniform and around 15 m. The time-step is set equal to 1 s, which ensures model stability. The Manning friction law is used to compute the bottom friction, where a coefficient equal to 0.035 $m^{-1/3}/s$ is uniformly set. This coefficient corresponds to a clean, straight main channel without deep pools (Chow, 1959). This coefficient was previously set for the main channels of HEC-RAS model and generalized for the whole study domain for TELEMAC, giving acceptable results in terms of flood extent (Fig. 2b). Obviously, the model could be improved in the future considering a spatialized Manning friction law or another friction law. Turbulence is modeled using a constant eddy viscosity of $10^{-4}$ $m^2/s$. Upstream boundaries are set as flowrates for the river and tributaries, and a downstream free surface of 0 m A.S.L is set on the sea. A scenario assuming steady flows is first simulated to generate realistic initial conditions, before launching a second scenario using unsteady upstream hydrographs to simulate the 2015 flood. The first scenario lasts for 72 h for a computational time of 1h15 using a single CPU.

## 3. Preliminary results and ongoing work

First preliminary results (Fig. 2a) show that the flooding inundation map extent matches quite satisfactorily the observations and results from the HEC-RAS model, despite the number assumptions addressed below.

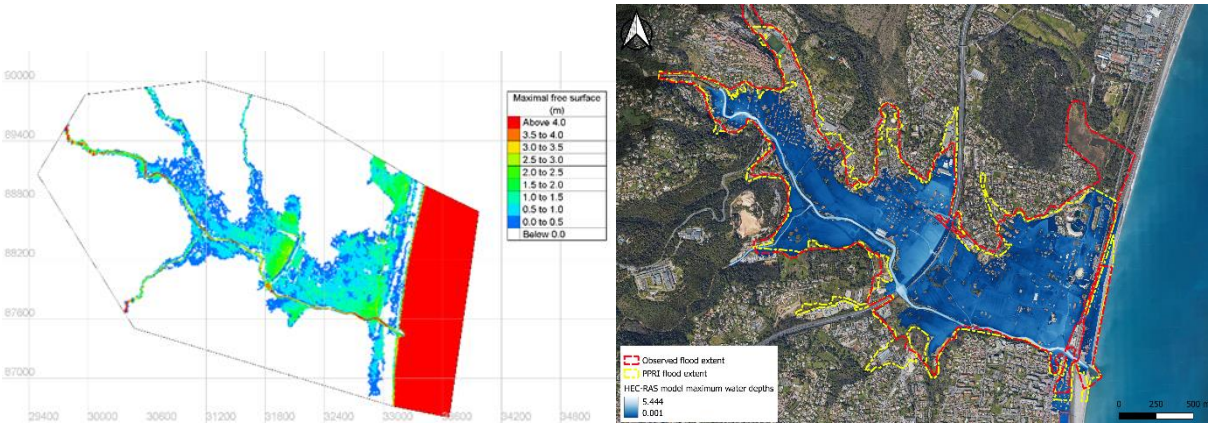



**Fig. 2.** Flooding inundation maps with (a) maximal free surfaces and (b) maximal water depths obtained from the HEC-RAS 2015 flood model.

Indeed, the present simulation does not account for the presence of hydraulic structures (bridges and culverts) nor buildings located in the floodplain. Future work will account for the presence of such structures, plus comprehensive comparisons based on sensitivity analyses on physical and numerical parameters. Further comparisons will be also carried out with the numerical results obtained with HEC-RAS.

**References**

Préfecture des Alpes Maritimes (2019), Carte des phénomènes naturels Brague et Affluents, 16/12/2019, https://www.alpes-maritimes.gouv.fr/content/download/35946/275635/file/04.%20Carte%20Ph%C3%A9nom%C3%A8nes%20Naturels_Brague%20et%20Affluents.pdf, last checked on September 2023 30th

IGN (2018), RGE ALTI® Version 2.0 Descriptif de contenu, https://geoservices.ign.fr/sites/default/files/2021-07/DC_RGEALTI_2-0.pdf, last checked on September 2023 30th

Chow, V. T. (1959) Open Channel Hydraulics, McGraw-Hill Book Company, ISBN 07-020776-9

# Drought Characterization for the Ciénaga Grande de Santa Marta (Colombia)

Andrés Felipe CORTÉS[1], Allen BATEMAN[2], Vicente MEDINA[3]

[1] Universitat Politecnica de Catalunya, Spain
andres.felipe.cortes@estudiantat.upc.edu

[2,3] Universitat Politecnica de Catalunya
allen.bateman@upc.edu
vicente.de.medina@upc.edu

ABSTRACT

The Ciénaga Grande de Santa Marta is a wetland located in the northern part of Colombia inside of the Magdalena River basin. The ecosystem experiences recurrent drought events due to hydrometeorological conditions and water management practices, particularly reservoir operations related to hydropower production. The main objective of the research was the characterization of the drought events in order to understand the conditions and dynamics of the system. This process was conducted evaluating different traditional drought indices, among which the Palmer Index and the SPI, diverse sources of remote sensing and two modified drought indices that considered the infiltration of water from the Magdalena River to the Ciénaga. The results showed that the modified Palmer Drought Severity Index and water salinity were the most effective parameters for characterizing the droughts, as they could be used simultaneously for the forecasting and the evaluation of the intensity of the events.

## 1. Introduction

The Ciénaga Grande de Santa Marta (CGSM) is the largest coastal lagoon system in Colombia and is part of a larger and complex ecoregion known as the socio-ecological system of the CGSM (Vilardy Quiroga et al., 2011). It is an area of big economic and ecological relevance for the country as its mangroves and wetlands host a wide diversity of fauna (fishes, reptiles, mammals, and birds) and flora, but also provides an important source of economic benefits due to its food production potential (because of agriculture and fishery) (Aguilera, 2011).

Droughts in the area are a recurrent phenomenon in the ecoregion due to the influence of the Inter Tropical Convergence Zone (ITCZ) and more specifically with El Niño Southern Oscillation (ENSO) but also due to the climatic characteristics of the area, which are represented by the constant imbalance between precipitation and evapotranspiration. The characterization of these events currently is being done using only one drought index, the Standardized Precipitation Index (SPI). Nevertheless, under the natural arid conditions, and the water dynamics of the system, the use of the SPI index may not be sufficient or adequate to assess droughts.

## 2. Methods

For the drought characterization different indices and methodologies were tested considering the available information in the study area. Regarding traditional drought indices, two main alternatives were selected: the SPI, which as was mentioned is the main tool used nowadays in the country for drought assessment, and the Palmer Drought Severity Index (PDSI). Regarding remote sensing, two main parameters were considered, the surface water area, which was evaluated using the Global Surface Water dataset (Peckel et al., 2016) and made available as part of the Joint Research Centre of the European. The second was the Normalized Difference Vegetation Index (NDVI), used as a proxy for analyzing the health of the vegetation. In addition, the salinity and the discharges of the Magdalena River were also considered for the drought analysis. The salinity has been proved to be related to the ENSO, and therefore to the droughts in the swamp, nevertheless its information is limited and scares. For the analysis of the effect of the discharges of the Magdalena River into the water dynamics of the Ciénaga (through infiltration), a modification for the SPI and the PDSI was proposed. Using

the discharge and the levels of the river, and the levels of the swamp, the infiltration due to the hydraulic gradient was calculated in a monthly time series. This new input of water later was added to the precipitation obtaining a new available water quantity, than was used as the main input for the SPI – now called SWI (Standardized Water-input Index) - and for the mPDSI (Modified Palmer Drought Severity Index).

## 3. Results

For all the selected parameters, monthly time series were built in order to evaluate their capacity to identify the occurrence of drought events and their main characteristics (intensity and duration), using as reference the ONI (Oceanic Niño Index) and the recorded previous drought events. For the drought identification, the best results were found using the salinity and the modified Palmer index, with which was possible to identify more events than with the original index. Regarding the duration and intensity of the events, interesting results were found for the salinity, as the duration of the droughts (but also of the wet periods) could be clearly identified by the changes in the normal values of salinity, and the intensity of these events presented a high correlation with the salinity peaks. For the drought indices it was found that the mPDSI and the SWI outperformed the traditional indices, as the proposed indices generated more stable results, allowing a clearer identification of dry and wet periods, and the changes between them. Regarding the comparison between the SPI (and the SWI) and the PDSI (and the mPDSI) it is relevant to mention that the Palmer index presented more effective results in both the identification and the analysis of the events, as was expected. Finally, the results obtained for the remote sensing parameters were not satisfactory, but their use for the water management and the development of a multivariate drought index for the area is recommended. The results obtained for the salinity and the modified index are presented in Fig. 1.

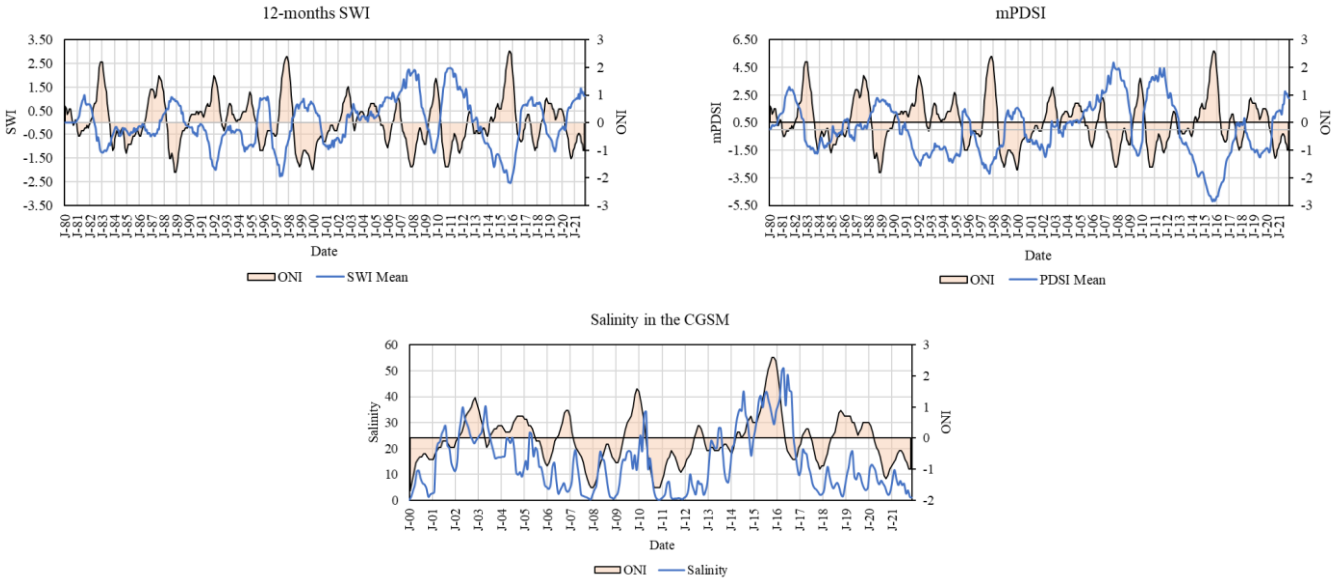



**Fig. 1.** Comparison of the main results for the 12-months SWI, mPDSI and the salinity with the ONI (Oceanic Niño Index) for the drought characterization

## 4. Conclusions

Through the research it was identified that the salinity and the mPDSI were the most effective methodologies for the assessment of droughts in the CGSM. These indices could be used simultaneously for the assessment of the severity and duration of the events and for the identification of the occurrence of the events and their forecasting, allowing a more efficient management of the hazard in the swamp. In addition, the consideration of the infiltration of water from the river to the Ciénaga (that can also change direction) and the proposal of modified drought indices resulted in more effective results and more importantly in a more realistic representation of the actual water dynamics of the system.

### References


Aguilera, M. (2011). Habitantes del agua: El complejo lagunar de la Ciénaga Grande de Santa Marta, Banco de la República, 49 pp.

McKee, T. B., et al., (1993). The Relationship of Drought Frequency and Duration to Time Scales, 8th Conference on Applied Climatology, Anaheim.

Palmer, W. C. (1965). Meteorological Drought. Washington, D.C.: U.S, Department of Commerce, 65 pp.

Pekel, J.F., et al., (2016). High-resolution mapping of global surface water and its long-term changes, Nature 540, 418-422.

Vilardy Quiroga, S. P., et al. (2011). Repensando la Ciénaga Nuevas Miradas y Estrategias para la Sostenibilidad en la Ciénaga Grande de Santa Marta

# Regional assessment of climate change impacts. The case of the Ceira river basin, Portugal.

Miguel COSTA[1,2], Juliana MENDES[1,2], Rodrigo MAIA[1,2]

[1] FEUP – Faculty of Engineering of the University of Porto, Porto, Portugal
[2] Interdisciplinary Centre of Marine and Environmental Research (CIIMAR), University of Porto, Matosinhos, Portugal
mapcosta@fe.up.pt
juliana@fe.up.pt
rmaia@fe.up.pt

ABSTRACT

## 1. Introduction

The Intergovernmental Panel on Climate Change (IPCC) states that climate change impacts are already greater than expected at lower temperatures than anticipated before. Therefore, to better prepare, adapt and mitigate climate change impacts, the assessment of those expected impacts at more refined scales, namely the regional level (IPCC, 2022), becomes crucial. In this context, the main purpose of the present work is to assess the regional climate change impacts of the Ceira river basin, in center Portugal. This assessment will be performed in terms of variation of the meteorological variables, as also in their repercussion in the basin's streamflow and in the occurrence of extreme drought events. To do this, a methodology adapted to Portuguese river basins was applied (Ramos et al., 2014). The work was developed under the scope of the Rio Ceira project (EEA Grants, 2022).

## 2. Methodology

To assess the regional climate change impacts on the Ceira river basin 5 climate change scenarios (CCS) were defined based on the expected mean annual future changes of precipitation (Pr) and temperature (T). The mean annual future changes were defined for three future periods (2011-2040, 2041-2070 and 2071-2100) based on the historical period 1971-2000 and considering two Representative Concentration Pathways (RCP), RCP4.5 and RCP8.5. For this work, daily Pr and T climate change projections of 13 regional climate models (RCM) from the EURO-CORDEX project were used - given their good ability to reconstruct the current Portuguese climate (Lima et al., 2023) – originating 26 climate change projections for each future period (RCP4.5 and RCP8.5 projections considered together). For the historical period, Pr and T daily data were collected from Iberia01 dataset. Once collected the data, the daily climate change projections of Pr and T were bias corrected using the Quantile Mapping technique (Gudmundsson et al., 2012) and aggregated into mean annual values.

With the expected future changes, 5 CCS were defined, in which 4 of the 5 CCS (CCS 1, 2, 4 and 5) were defined to represent the range/spread of the projections. To this, the 25$^{th}$ and 75$^{th}$ percentile of Pr and T mean annual changes were considered. The CCS 3, defined based on the median value of the mean annual changes (50$^{th}$ percentile), represented the central tendency of the projected changes. For each future period, the 5 CCS were obtained considering the frame limit intersection points to those 3 percentiles of Pr and T (Fig 1). Each CCS data was defined by the average of the 3 nearest climate change projections, determined based on the Euclidean distance.

Based on the meteorological CCS data for each future period, the corresponding CCS flows (Q) were obtained through hydrological modelling. For this, the HEC-HMS software was used in a continuous simulation mode and with a daily time-step, considering as input variables the daily Pr and evapotranspiration (ETP) data - defined based on the Hargreaves method. The daily runoff obtained has then aggregated to annual values and the expected mean annual changes were calculated.

For the drought evaluation two indices were computed, the Standardized Precipitation Index (SPI) and the Standardized Precipitation Evapotranspiration Index (SPEI). Both indices were defined based on the Pr and ETP monthly data accumulated at 12 months.

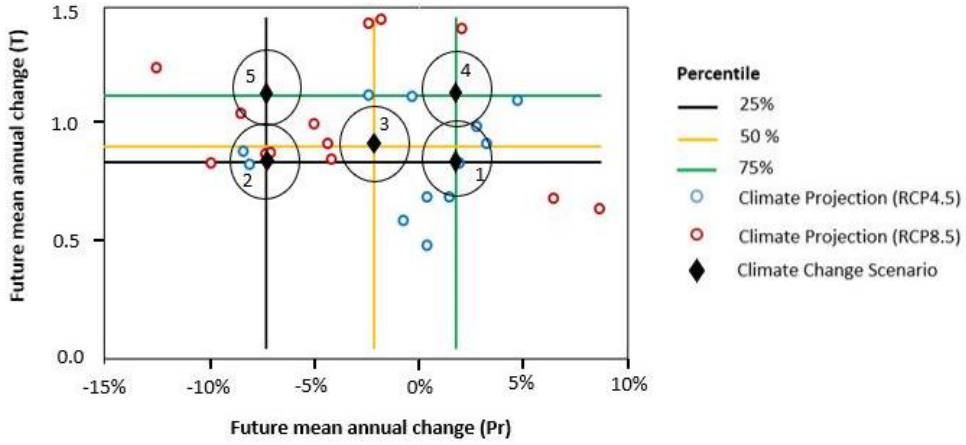



**Fig. 1.** Climate change scenarios obtained for the period 2011-2040.

## 3. Results and discussion

Table 1 presents the range of the mean annual meteorological and hydrological future changes for each period.

**Table 1.** Hydrometeorological climate change scenarios

| CCS | Percentile | | Definition | 2011-2040 | | | 2041-2070 | | | 2071-2100 | | |
|---|---|---|---|---|---|---|---|---|---|---|---|---|
| | Pr | T | | Pr (%) | T (°C) | Q (%) | Pr (%) | T (°C) | Q (%) | Pr (%) | T (°C) | Q (%) |
| 1 | 75% | 25% | Warmer and drier / wetter | 1.8% | 0.8 | 2.5% | -2.7% | 1.5 | -1.7% | -5.4% | 1.9 | -2.7% |
| 2 | 25% | 25% | Warmer and more drier | -7.3% | 0.8 | -5.9% | -15.1% | 1.5 | -7.7% | -20.4% | 1.9 | -19.7% |
| 3 | 50% | 50% | Central Tendency | -2.1% | 0.9 | -2.2% | -7.2% | 1.8 | -5.7% | -13.2% | 2.9 | -12.4% |
| 4 | 75% | 75% | Hotter and drier | 1.8% | 1.1 | 3.2% | -2.7% | 2.1 | -2.6% | -5.4% | 3.6 | -12.9% |
| 5 | 25% | 75% | Hotter and more drier | -7.3% | 1.1 | -6.6% | -15.1% | 2.1 | -8.1% | -20.4% | 3.6 | -21.1% |

Whichever CCS is considered, an increase of T is expected. In 2011-2040 all the 5 CCS predict a similar increase (nearly 1°C); nevertheless, by the end of the century it is expected a more widespread increase for all CCS, that could result in an alarming 4°C increase under the pessimist warmer scenarios (CCS 4 and CCS 5). Regarding the Pr and Q, in the near future (2011-2040) it is expected an increase under CCS 1 and CCS 4. Nevertheless, through the remaining periods, all CSS show a decrease in Pr and Q, that could, under the more pessimistic scenario (CCS 5) reach an alarming 20% decrease by the end of the century.

Concerning the drought events, SPI and SPEI for all 5 CCS show that, in general, there will be more drought events in future and with greater duration. The results also point that evapotranspiration will be an aggravating factor for the frequency and intensity of drought events, since SPEI projects more drought events and with greater intensity than SPI. Regarding the occurrence of extreme drought events (SPI and SPEI < -2.0) under the more optimistic scenario (CCS1) SPI and SPEI project an increase of 4 and 7 months during 2071-2100. On the other hand, if the more pessimistic scenario occurs, there can be more 36 months (SPI) or 42 months (SPEI) of extreme drought by the end of the century.

**Acknowledgements**

EEA Grants Portugal 2014-2021 (through the Pre-defined Project 3 “Management of the Ceira river basin adapted to a changing climate”, of the Environment Programme).

**References**

Lima D, et al. (2023) A multi-variable constrained ensemble of regional climate projections under multi-scenarios for Portugal – Part I: An overview of impacts on means and extremes, Climate Services, 30. https://doi.org/10.1016/j.cliser.2023.100351.
EEA Grants (2022) PDP#3 – Gestão da Bacia Hidrográfica do Rio Ceira face às Alterações Climáticas. https://ceira.apambiente.pt/.
Gudmundsson L et al. (2012) Technical Note: Downscaling RCM precipitation to the station scale using statistical transformations - a comparison of method, Hydrology and Earth System Sciences, 16, 3383-3390, https://doi.org/10.5194/hess-16-3383-2012.
IPCC (2022) Climate Change 2022: Impacts, Adaptation, and Vulnerability, Contribution of Working Group II to the Sixth Assessment Report of the Intergovernmental Panel on Climate Change, H.-O. Pörtner et al. (eds.). Cambridge University Press. Cambridge University Press, Cambridge, UK and New York, NY, USA, 3056 pp. https://doi.org/10.1017/9781009325844.
Ramos V et al. (2014) Methodology for the Development of Climate Change Scenarios and Climate Inputs to Run Impacts Models. Application to the Guadiana River Basin, 3rd IAHR Europe Congress, Porto, Portugal.

8th IAHR EUROPE CONGRESS
LISBON - PORTUGAL
4-7 JUNE 2024

# Assessing Drought Conditions Using Precipitation Values Completed with K-Nearest Neighbors (KNN)

Sefa Nur YESILYURT[1], Eyyup YILDIZ[2], Gulay ONUSLUEL GUL[1], Huseyin Yildirim DALKILIC[2]

[1]Dokuz Eylul University, İzmir, Turkey
[2]Erzican Binal Yildirim University, Erzincan, Turkey
sefanur.yesilyurt@deu.edu.tr, eyyup.yildiz@erzincan.edu.tr
gulay.onusluel@deu.edu.tr, hydalkilic@erzincan.edu.tr

ABSTRACT

Data availability is vital for hydrology and water resources engineering studies. The measurement of hydrological variables is subject to systematic and random errors. Therefore, hydrologists often deal with the problem of missing data. Due to the pivotal role of precipitation data as a fundamental input in hydrological research, ensuring the availability of thorough and precise precipitation datasets takes on utmost importance. To this end, this paper proposes to integrate the KNN (K-Nearest Neighbors Classification) algorithm with the K-Means algorithm. This innovative approach effectively augments precipitation data for the Konya Closed Basin using a method that has not been explored so far in this geographical context. The model firstly clusters stations based on location, altitude, annual mean, maximum and minimum temperature values using the K-Means method. It then applies the KNN method for the clustered data sets and completes the missing data. The resulting model shows a performance reaching a maximum value of 0.775. The findings of this study not only confirmed the utility of the proposed model in imputing missing data, but also demonstrated its potential as a viable alternative to traditional imputation methods in hydrological research. The comprehensive data obtained through this innovative model was used to assess drought status of the basin using the Standard Precipitation Index (SPI) based on severity, duration and magnitude of droughts. For the 1-month SPI, the most severe drought occurred in the period 1988-1998; for the 3-month SPI in the period 2010-2019; for the 6-month and 12-month SPI in the period 1966-1976.

## 1. Introduction

Data availability is crucial for the correct implementation of hydrological studies. However, measurements of hydrological variables are prone to systematic and random errors. Hydrologists, meteorologists and environmental scientists are therefore often faced with the problem of missing data. Several methods have been proposed in the literature, such as traditional weighting, Thiessen polygons and interpolation techniques (ASCE, 1996). However, most of these methods require a predefined functional form for the relationships. In contrast, the KNN method stands out for its ability to efficiently supplement missing data with only initial values (Sahoo and Ghose, 2022). Therefore, this study addresses the problem of missing precipitation data in the Konya Closed Basin, a drought-sensitive region, by introducing an application for the case study that combines clustering with the KNN algorithm. It is very important to consider that precipitation stations have similar characteristics before filling in the missing data. Because using different station data together can significantly affect the modeling results as the minimum and maximum values in the data may change. In order to use similar stations together, the K-means method, one of the most commonly used data clustering methods, was used before applying the KNN method (Xu et al., 2022; Komuscu et al., 2022). This method, which integrates KNN with K-Means clustering, is the first example of such a use in this Konya Closed Basin. This method aims to categorize stations into groups based on location, elevation and annual mean, min and max temperature values. Model performance was determined by randomly removing data from the full time series at specific rates. After obtaining complete data, it was aimed to evaluate the drought conditions of the basin in the 1966-2019 period by determining the severity, duration and magnitude of drought.

SPI was chosen because it is an index that has been proven accurate by many studies in the literature and can only be calculated with precipitation data (Onusluel Gül et al., 2022; Şen et al., 2012).

## 2. Study extent, data and Methodology

Within the scope of the study, monthly precipitation records from the Konya Closed Basin, located geospatially between 36°53'-39°29' north latitude and 31°07'-35°03' east longitude within Turkey, were utilized. It is noteworthy that the Konya Closed Basin is notably distinguished as Turkey's largest closed basin. This region is characterized by a semi-arid climate. The meteorological station datasets have been obtained from the General Directorate of Meteorology of Turkey. Missing values in the dataset were addressed and then completed using the KNN method employing the Python programming language. In addition, the calculation of the SPI was performed in the R Studio.

The K-Means clustering technique is a data classification method that entails user-defined or preprocessing-derived selection of the number of clusters (k). In this way, it enables the creation of a meaningful group that is compatible with the data. Within the scope of the study, the K-means method was applied by considering the latitude, longitude, altitude, average annual precipitation, average temperature, maximum and minimum temperature values of monthly precipitation data. The KNN algorithm can be used in problems such as assignment of missing data, regression analysis and data classification. The method aims to find the closest value for the assignment and minimize the distance. The method considers the closest values for the data in each cluster created with K-Means and estimates a value for the missing one (Sahoo and Ghose, 2022). The success of the methods was evaluated by RMSE, $R^2$ and NSE. These metrics are statistical measures frequently used to evaluate model performance (Sahoo and Ghose,2022). SPI, quantifies the deviation of precipitation from the average over a specified time period and is the most widely used method globally for monitoring drought conditions, allowing assessment over 1, 3, 6, and 12-month periods. After calculating the SPI index, drought conditions can be analyzed by calculating the severity, magnitude and duration of drought. (McKee et al, 1993).

## 4. Result and conclusions

In this study, monthly precipitation data of Konya Closed Basin, the largest closed basin in Turkey, were classified using the K-Means method. The minimum and maximum values in the data were prevented from negatively affecting the model performance, and dissimilar stations were prevented from limiting the algorithm's forecasting ability. In the second stage, the missing values in each cluster were completed with the KNN algorithm. The outputs were evaluated using RMSE, $R^2$ and NSE and the model results showed that the KNN algorithm provided adequate performance (Table 1). These results show that the algorithm has a good prediction ability and can be used for studies on similar features.

**Table 1.** KNN Model Results

| | Number of Station in Cluster | NSE | RMSE | $R^2$ |
|---|---|---|---|---|
| **Cluster 1** | 10 | 0.7750 | 11.8501 | 0.7751 |
| **Cluster 2** | 3 | 0.7132 | 34.1456 | 0.7132 |
| **Cluster 3** | 2 | 0.6395 | 17.2715 | 0.6396 |

Past drought conditions of the basin were analyzed using the new datasets. When the most severe droughts are analyzed, it is seen that the most severe drought for 1-month SPI occurred in the period 1988-1998; for 3-month SPI in the period 2010-2019; for 6-month and 12-month SPI in the period 1966-1976. When the severity, magnitude and duration of drought are evaluated for the whole basin, it is seen that the 1966-1976 period is the driest period.

**Acknowledgements**

The authors would like to thank the Turkish Directorate General of Meteorology **(MGM)** for providing daily precipitation data.

**References**

ASCE (1996) Hydrology Handbook, American Society of Civil Engineers, NewYork.

Komuscu AU, Turgu E, DeLiberty T (2022) Dynamics of precipitation regions of Turkey: A clustering approach by K-means methodology in respect of climate variability, Journal of Water and Climate Change, 13,10, 3578-3606.

McKee TB, Nolan J, Kleist J (1993) The relationship of drought frequency and duration to time scales. Prepr Eighth Conf Appl Climatol Amer Meteor, Soc.

Onusluel Gul G, Gul A, Najar M (2022) Historical evidence of climate change impact on drought outlook in river basins: analysis of annual maximum drought severities through daily SPI definitions, Natural Hazards, 1-16.

Sahoo A, Ghose DK (2022) Imputation of missing precipitation data using KNN, SOM, RF, and FNN, Soft Computing, 26,12, 5919.

Sen B, Topcu S, Türkes M, Warner J (2012) Projecting climate change, drought conditions and crop productivity in Turkey, Clim Res.

Xu, W., Tang, M., & Li, Y. (2022). A new method for assessment of regional drought risk: information diffusion and interval mapping adjustment based on k-means cluster points. Journal of Water and Climate Change, 13(12), 4302-4316.

# Investigating the impact of time interval between rainstorms and wave storms to characterize compound events in the NW Mediterranean

Maria AGUILERA-VIDAL[1], Maria I. ORTEGO[2], Marc SANUY[1], José A. JIMÉNEZ[1]

[1] Laboratori d'Enginyeria Marítima, Universitat Politècnica de Catalunya, Barcelona·Tech. Barcelona, Spain. maria.aguilera.vidal@upc.edu; marc.sanuy@upc.edu; jose.jimenez@upc.edu

[2] Departament d'Enginyeria Civil i Ambiental, Universitat Politècnica de Catalunya, Barcelona·Tech. Barcelona, Spain. ma.isabel.ortego@upc.edu

ABSTRACT

The NW Mediterranean coastal zone is frequently subject to the impact of rainstorms, leading to flash floods, as well as wave storms, resulting in coastal erosion and flooding. The associated damages from these events have exhibited an increasing trend in recent decades (e.g. Llasat et al. 2014; Jiménez et al. 2012). Moreover, a recent study in this area has revealed that the joint occurrence of rainstorms and wave storms is relatively common, albeit with a high spatial variability (Sanuy et al. 2021). These compound events pose a significant challenge for risk management services, as they have the potential to exacerbate the impacts of individual (contributing) events and distribute damages across the territory, thereby straining such services. From a risk management perspective, it is crucial to comprehensively characterize the occurrence of such compound events, complementing the traditional approach of studying individual events. In this context, the main aim of this work is to characterize compound events in the Catalan coast (NW Mediterranean) by adapting its definition to the specific conditions of the area and approaching it from a risk-management perspective.

Among the different types of compound events (Zscheischler et al. 2020), our focus lies on multivariate compound events, where two or more hazards coincide simultaneously at the same location. The first aspect influencing the definition of the event is the interpretation of "same location"( Bevacqua et al. 2019). However, we adopt the methodology introduced by Sanuy et al (2021), wherein the study area is divided into catchment basins along the coastal zone. The hazard at the "land point" is characterized by the peak daily rainfall (P24h) recorded at any location within the basin during the rainstorm. This approach is adopted because of the dominance of heavy rainfall episodes in relatively small catchments to control the terrestrial component of the event. For the corresponding marine hazard, wave storms recorded at a point along the coastal fringe of the basin are selected.

The second aspect we need to consider is the concept of "simultaneity". This factor determines the selection of a time window, $\tau$, between the occurrences of both contributing events to define their co-occurrence and thus identify a multivariate compound event (Fig. 1). This time window not only indicates that both storms have been triggered by the same meteorological conditions but also establishes the timeframe within which risk management services must address damages caused by both rainstorms and wave storms. The choice of $\tau$ is a critical step, as it directly influences the frequency of compound events in a specific area, shaping their characteristics and interdependency between variables. This consideration is particularly valuable in addressing risk management questions, such as assessing the likelihood of concurrent rainstorms and wave storms within a specific timeframe of **X** days. Here, **X**, represents the duration required to efficiently allocate resources for mitigating damages induced by these events.

In this study, we investigate the impact of different time windows on characterizing compound events along the Catalan coast (NW Mediterranean). The analysis span a 63-year period and utilizes daily rainfall from a set of meteorological stations across the region, along with hindcast and reanalysis wave data along the coast. To conduct the analysis, we first identify extreme rainfall and wave events using the POT method. Then, we determine their co-occurrence and thus the presence of compound extreme events across a range of time

windows. These time windows, varying from 0 (simultaneous) to 7 days, are chosen based on the typical duration required by risk management services to address damages from severe storm events comprehensively. For each time window, we characterize the regime of extreme rainfall-storm waves compound events. This involves assessing the statistical dependence between contributing drivers using the Kendall correlation coefficient and analyzing their joint probability of occurrence through copula analysis. Finally, we investigate the development of synoptic meteorologic conditions triggering identified major compound events across the selected time windows, aiming to identify potential variations in their stability throughout the event.

Figure 1 illustrates the obtained results for the northernmost basin along the Catalan coast, where the influence of the time window on identified events is clearly seen. First, it is evident that the occurrence of events is directly impacted by the time window, as the number of events increasing progressively from the lowest count (163) for strictly co-occurring ($\tau = 0$) to approximately constant levels (190) for $\tau > 4$ days. Furthermore, the dependency analysis revealed statistically significantly dependence between the events, with the Survival Gumbel consistently emerging as the best fitting copula regardless of the time window. Despite this, the Kendall correlation coefficient exhibited relatively modest values, with no significant variation observed across the tested $\tau$-values.

When extending the analysis to cover the Catalan coast (along about 500 km), notable variations in the characteristics and occurrence of compound events became apparent. While these events stem from large-scale synoptic weather patterns, the observed variability underscores the necessity of local characterization. Thus, while the case illustrated here pertains to relatively frequent compound extreme events (>2 events/year), there are areas marked by infrequent events (<1 event/year) that are also uncorrelated. In conclusion, the judicious selection of appropriate thresholds to define the occurrence of these events, coupled with the implementation of suitable joint analysis methods, will empower coastal risk managers to more effectively anticipate the need for DRR measures for addressing both meteorological and marine hazards-induced damages simultaneously.

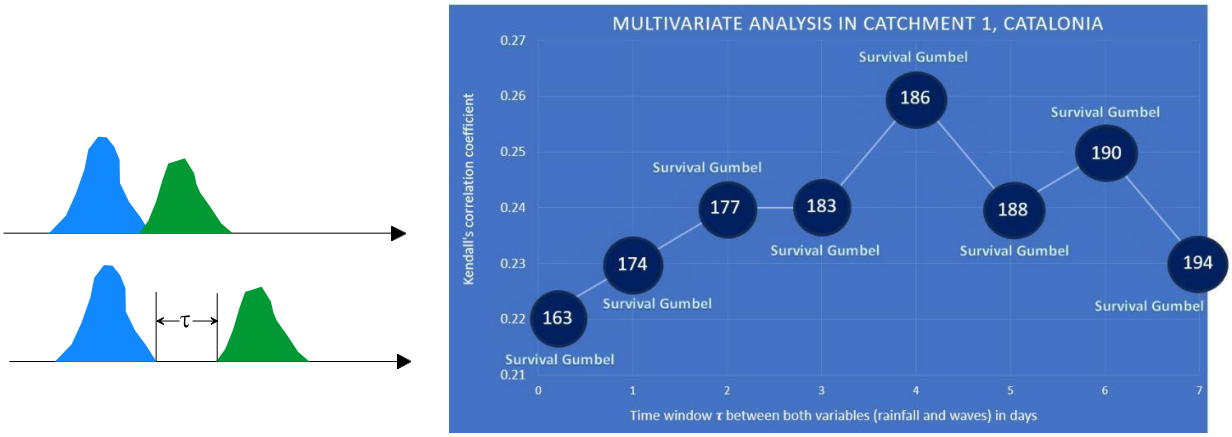



Fig. 1. Left: time window between components of compound events (Upper left, $\tau = 0$, lower left $\tau > 0$). Right: Kendall correlation coefficient between rainfall and waves in the northernmost basin in Catalonia for time windows $\tau$ from 0 to 7 days. The filled circles indicate strong evidence against the null hypothesis Ho: Kendall correlation coefficient = 0. The numbers inside the circles denote the number of events identified for each time window, and the name of the best fitting copula among 36 tested copulas (plus the independence copula) is also indicated.

**Acknowledgements**

This work has been done within the C3RiskMed and CONBACO research projects (PID2020 – 113638RB-C21, PID2021-125380OB-I00) funded by the Spanish Ministry of Science and Research (AEI/10. 13039/501100011033) and by ERDF A way of making Europe.

**References**

Bevacqua E, Maraun D, Vousdoukas MI, Voukouvalas E, Vrac M, Mentaschi L, Widmann M (2019). Higher probability of compound flooding from precipitation and storm surge in Europe under anthropogenic climate change, Science Advances, 5(9), eaaw5531.

Jiménez JA, Sancho-García A, Bosom E, Valdemoro HI, Guillén J (2012). Storm-induced damages along the Catalan coast (NW Mediterranean) during the period 1958-2008, Geomorphology, 143, 24-33.

Llasat MC, Marcos R, Llasat-Botija M, Gilabert J, Turco M, Quintana-Seguí P (2014). Flash flood evolution in North-Western Mediterranean, Atmospheric Research, 149, 230-243.

Sanuy M, Rigo T, Jiménez JA, Llasat MC (2021). Classifying compound coastal storm and heavy rainfall events in the north-western Spanish Mediterranean, Hydrology and Earth System Sciences, 25(6), 3759-3781.

Wu W, Westra S, Leonard M (2021). Estimating the probability of compound floods in estuarine regions, Hydrology and Earth System Sciences, 25(5), 2821-2841.

Zscheischler J, Martius O, Westra S, Bevacqua E, et al., Vignotto E (2020). A typology of compound weather and climate events, Nature Reviews Earth & Environment, 1(7), 333-347.

# Urban Wastewater Infrastructure Adaptation Strategies: Methods and Implementation Towards Climate Change Resilience

Paulo A. DIOGO[1], António C. RODRIGUES[2], António P. MANO[3], Pedro A. MIRANDA[4], Susana SANTOS[5], Paulo INOCÊNCIO[6], Ana S. SANTOS[7,] , Nuno, BROCO[8], Joana P COELHO[9]

[1,2] MARE - Marine and Environmental Sciences Centre, ARNET - Aquatic Research Network Associate Laboratory, NOVA School of Science and Technology, NOVA University Lisbon, Caparica, Portugal
pad@fct.unl.pt; acr@fct.unl.pt

[3] NOVA School of Science and Technology, NOVA University Lisbon, Caparica, Portugal
apmcm@fct.unl.pt

[4] Faculty of Sciences, University of Lisbon (FCUL), Portugal
pmmiranda@fc.ul.pt

[5,6,7] Águas do Tejo Atlântico (AdTA), Portugal
s.santos@adp.pt; p.inocencio@adp.pt; assantos@adp.pt

[8,9] Águas de Portugal (AdP), Portugal
n.broco@adp.pt; j.coelho@adp.pt

ABSTRACT

Climate change poses multiple risks to the operation of drainage and wastewater treatment plants, mostly related to extreme events such as floods, droughts, and heat waves. Also, reduced water availability threatens receiving waterbodies assimilation capacity, both in terms of quantity and quality. In face of these risks, infrastructural and operational challenges which require adequate planning and implementation and Águas do Tejo Atlântico (AdTA), company responsible for wastewater drainage, treatment, and discharge in the region of Lisbon, Portugal, serving ca. 2,4 million people, is carrying out the development of a Climate Change (CC) Adaptation Plan. With this purpose, historical events data and climate projections obtained from EURO-CORDEX for scenarios RCP 4.5 and RCP 8.5 are the basis for climate vulnerability and risk assessment. Heat waves (HW) and water availability have been assessed and will be used to establish CC adaptation strategies. According to the obtained results, HW episodes are likely to increase, and thus potentially inducing changes in urban water uses and thus in wastewater flows, changes in water treatment processes and may also increase electrical power failure risks. Furthermore, according to precipitation runoff modelling results, water availability is very likely to be reduced in receiving water bodies, resulting in enhanced water quality degradation risks, reduced assimilation capacity and thus increase of discharge limitations and technical concerns. The Adaption Plan under development is expected to be concluded in March 2024.

## 1. Introduction

As a company part of the Águas de Portugal Group (AdP), AdTA is responsible for the drainage, treatment, and discharge of waste urban wastewater in the most populated area of Portugal, including the metropolitan area of Lisbon and additional 20 municipalities located northwest from Lisbon, in a coastal region. AdTA is therefore responsible for the operation of the main urban wastewater treatment plants (WWTP) serving a total population of ca. 2,4 million inhabitants. Following the goals of the Strategic Plan for Adaptation to Climate Change of AdP Group namely the definition of adaptation strategies to reduce vulnerabilities to climate change and increase resilience associated with AdTA activities, the AdTA Climate Change Adaptation Plan is under development. With this purpose, historical climatological data, climate change scenarios from EURO-CORDEX, modelling tools, vulnerability assessment and risk analysis are the basis for the development of adaptation strategies aimed to tackle infrastructural and operational risks, related to climate induced impacts such as flooding, heat waves (HW), reduced receiving waterbodies assimilation capacity (quantity and quality)

and sea level rise (flooding and discharge limitations). Climate risk assessment was also based on relevant characteristics of each infrastructure, such as altitude and distance to sea shoreline, wastewater treatment and drainages systems capacity and discharge location. Extreme events - storms, droughts as well as water scarcity situations are also considered.

The first step for planning adaptation was the collection of registered events potentially related to climatological events and previously mentioned vulnerabilities. These include mainly flooding of infrastructures, operational limitations due to HW related power failures, storm events leading to untreated wastewater discharges and reduced receiving water bodies assimilation capacity. Up to this point multiple methods have already been implemented and early results are under analysis as the basis and essential part for the identification of vulnerabilities and risks. The presented work integration in the CC Adaptation Plan for AdTA will be the basis for planning and delineation of adequate adaptation strategies and required interventions, enabling more efficient asset management. In this work results regarding water availability and HW episodes are presented.

## 2. Methods

Implemented methods include analysis of relevant climate related registered events, historical climate data and future climate projections. The latter include 11 regional climate models are considered to characterize projections for RCP 4.5 and 8.5, for a period until the year 2100. Model performance evaluation is based on comparing modelled and observed data for the historical reference period 1970-2005. Climate data analysis includes daily precipitation and temperature. Future fluvial and flash floods risk will be assessed based on comparison of historical events data and observed daily precipitation and future scenarios for daily precipitation.

HW associated risks were analysed based on the World Meteorological Organization (WMO) definition considering 5 consecutive days of temperature 5ºC above maximum daily reference temperature (IFRC, 2016). Precipitation-runoff modelling for monthly time scale was performed using a modified version of the Thornthwaite-Mather model (Thornthwaite and Mather, 1957). This model has been previously calibrated for Portugal (Gonçalves *et al*, 2018) and is able to produce monthly surface flow time series based on precipitation, evapotranspiration (according to Hargreaves and Samani, 1985) and the 3 calibrated parameters. All these results are part of the Adaptation Plan and will be used to support de development of adaptation strategies.

## 3. Results and Conclusions

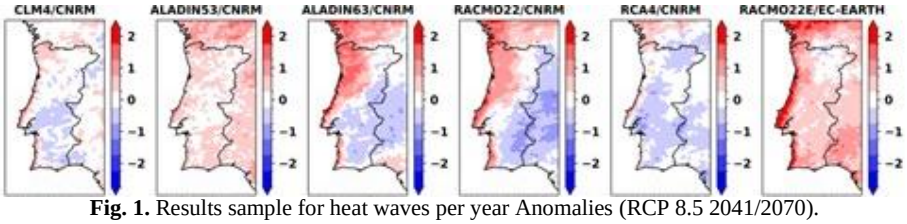


**Fig. 1.** Results sample for heat waves per year Anomalies (RCP 8.5 2041/2070).

Climate change projections denote tendencies regarding precipitation patterns change, as well as increased risks of heat wave episodes (Fig 1), although relevant variations are found among different models results. Precipitation-runoff modeling demonstrates relevant surface water availability reductions, suggesting risks associated with lower receiving waterbodies assimilation capacity leading to wastewater discharge limitations, increased treatment needs and operational challenges that require adequate planning. These results demonstrate a clear tendency for precipitation reduction, reduced surface water availability, increase of heat wave episodes and potential risks associated with sea level rise at least related to some of the infrastructures located very near the coastline.

**Acknowledgements**

The authors acknowledge Águas do Tejo Atlântico (AdTA), for the initiative, development, and financial support of this work. This work was funded by Fundação para a Ciência e a Tecnologia (FCT, Portugal), through the strategic projects UIDB/04292/2020 (https://doi.org/10.54499/UIDB/04292/2020) and UIDP/04292/2020 (https://doi.org/10.54499/UIDP/04292/2020) granted to MARE - Marine and Environmental Sciences Centre, and the project LA/P/0069/2020 (https://doi.org/10.54499/LA/P/0069/2020) granted to the Associate Laboratory ARNET - Aquatic Research Network.

**References**

Gonçalves, A.R., Cunha, S. & Diogo, P.A. (2018). Aplicação do Modelo de Thornthwaite e Mather na Avaliação das Disponibilidades Hídricas em Portugal Continental. APRH, 14.º Congresso da Água. Évora, March de 2018 (in Portuguese).
IFRC (2016) Small and simple actions to address climate change. Geneva. International Federation of Red Cross and Red Crescent Societies.
Hargreaves, G.H. and Samani, Z.A. (1985) Reference Crop Evapotranspiration from Temperature. App. Eng. in Agriculture, 1, 96-99.
Thornthwaite, C.W. & Mather, J,R. (1957). Instructions and Tables for Computing Potential Evapotranspiration and the Water Balance. Publ. in Climatology, vol.10, no.3, p. 185-311.

# Hydropower Production impacts from Climate Change future scenarios at the Cabril Dam, Portugal

Paulo A. DIOGO[1], António C. RODRIGUES[1], Gonçalo A. DUARTE[2]

[1] MARE - Marine and Environmental Sciences Centre, ARNET - Aquatic Research Network Associate Laboratory, NOVA School of Science and Technology, NOVA University Lisbon, Caparica, Portugal
pad@fct.unl.pt
acr@fct.unl.pt

[2] NOVA School of Science and Technology, NOVA University Lisbon, Caparica, Portugal
gm.duart@gmail.com

ABSTRACT

Hydropower is essential for sustainable development based on renewable energies. It is renewable energy that can be stored and used only when it is needed. However, it depends directly on variables that are affected by climate change, so that the availability of the water resource can be compromised, affecting the entire energy sector and its production. Presented work targets the evaluation of the installed capacity, annual energy production under climate change scenarios and how much can dam operation minimize the impacts related to potential precipitation/ runoff reductions. For this purpose, the operation of the Cabril dam, located along the Zêzere river, in central Portugal, was simulated under climate change scenarios. Precipitation modelling was performed using an adaptation of the Thornthwaite and Mather precipitation-runoff model.

According to the obtained results a monthly average reduction of hydropower production of 3% and 18% for future scenarios, respectively for scenarios RCP 4.5 and RCP 8.5. It was also possible to conclude that for this case study and according to the methodology used, the variation between the affluent runoff between periods is not directly proportional to the variation of the turbined flow as the latter decreases less than the affluent flow, demonstrating the importance of adequate dam operation strategies.

## 1. Introduction

The continuous and growing use of renewable energy sources is a fundamental strategy to meet the world's energy needs and limit the rise of climate change. Renewables in electricity generation rise from 28% in 2021 to about 50% by 2030 and 80% by 2050 (WEO, 2022). Hydropower is an important renewable energy source and the main electricity source within renewable energies in Portugal. Reservoirs enable energy storing and flexibility of operation and adaptability to energy demands. But climate and meteorological conditions have a significant impact on how to operate such systems. Thus, managing hydropower reservoirs is most relevant for water resources management and climate change impacts must be adequately addressed. For this purpose, the use of coupled simulation models is determinant to support system operations in face of changing hydrological conditions.

The Cabril dam was considered as a representative case study. This dam is in the central region of Portugal, in the Zêzere river, (Fig 1) an important affluent of the Tagus River. The Cabril dam presents a total installed capacity of 108 MW, using two turbine groups and with a total head of 121 meters and an average annual productivity of 289 GWh.

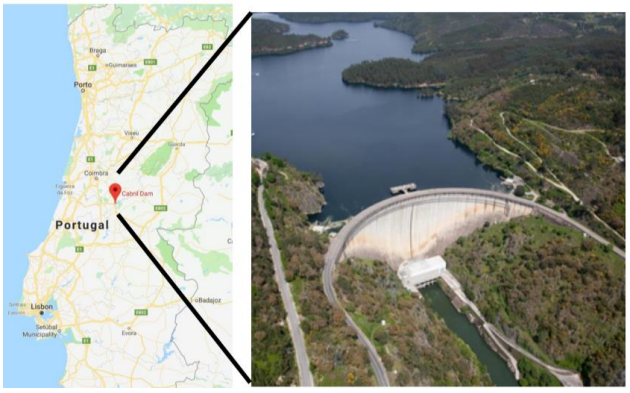



Fig. 1. Cabril Dam location in Portugal (without scale).

The presented research aims to better understand how dam operation may influence adaptation and help maintain energy production efficiency in face of relevant hydrological changes. Climate change scenarios from the Cordex project for RCP 4.5 and RCP 8.5 were used to compare dam energy production under historical, present and future hydrological scenarios.

## 2. Methods

Precipitation from RCP 4.5 and RCP 8.5 ensemble of models scenarios obtained from the Climate Portal developed by Instituto Português do Mar e Atmosfera (IPMA) and the Faculty of Sciences of the University of Lisbon (FCUL) in 2015 (http://portaldoclima.pt/en/) were used to model reservoir inflows, on an average monthly basis, using a Thornthwaite-Matter approach (Thornthwaite & Mather, 1957) calibrated for the Portuguese territory by Gonçalves *et al* (2018). Dam operation under future hydrological scenarios was defined according to present rule curves of the reservoir and energy production estimated based on head and flow simulations. Climate change Impacts were accessed by comparing results for a reference period and future climate scenarios.

## 3. Results and Conclusions

Results under scenario RCP 4.5, comparing inflows for the periods 2010 – 2040 and 2041-2070 denotes an annual average reservoir inflow reduction of 8% while turbined flow are reduced by 4%. Likewise, comparing 2010-2040 and 2071-2100 average reservoir inflow reduction is also 8% and turbine flow reduction limited to 3%. The same comparison for scenario RCP 8.5 results in 10% and 25% reservoir inflow reductions but 5% and 18% turbined flow reduction. These results emphasise that reservoir rule curves can be effectively used as a climate change adaptation strategy.

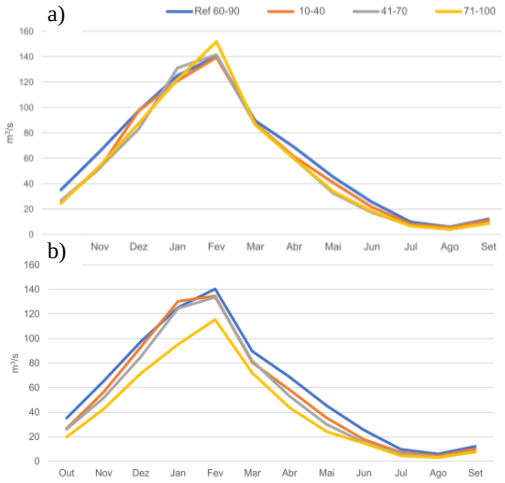



Fig. 2. Simulated inflows into Cabril reservoir, for scenarios RCP 4.5 (a) and RCP 8.5 (b).

The study demonstrated that precipitation changes induced inflow changes of the same magnitude, but reservoir management enabled lower reductions in energy production. Thus, hydrological changes could be potentially offset by changes in future system operations in response to changing hydrologic conditions, for which sophisticated coupled simulation models could adequately support decision making regarding dam operation.

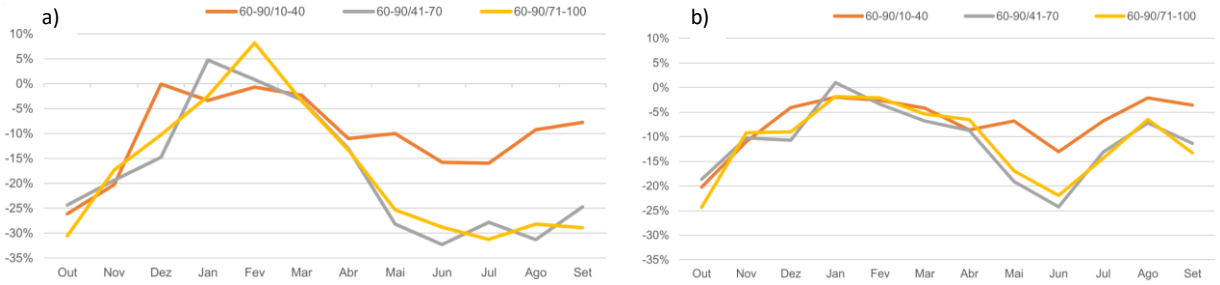



Fig. 3. Variations to the reference scenario of average reservoir inflows and average turbined flows, scenarios RCP 4.5 (a) and RCP 8.5

Further analysis is required to understand and define suitable rule curves to insure adaptation in the hydropower sector. Operation simulations can be an effective tool to improve rule curves and achieve improved water resources management strategies.

**Acknowledgements**

This work was funded by Águas do Tejo Atlântico and by Fundação para a Ciência e a Tecnologia (FCT, Portugal), through the strategic projects UIDB/04292/2020 (https://doi.org/10.54499/UIDB/04292/2020) and UIDP/04292/2020 (https://doi.org/10.54499/UIDP/04292/2020) granted to MARE - Marine and Environmental Sciences Centre, and the project LA/P/0069/2020 (https://doi.org/10.54499/LA/P/0069/2020) granted to the Associate Laboratory ARNET - Aquatic Research Network.

**References**

Gonçalves, A.R., Cunha, S. & Diogo, P.A. (2018). Aplicação do Modelo de Thornthwaite e Mather na Avaliação das Disponibilidades Hídricas em Portugal Continental. APRH, 14.º Congresso da Água. Évora, March (in Portuguese).

Thornthwaite, C.W. & Mather, J,R. (1957). Instructions and Tables for Computing Potential Evapotranspiration and the Water Balance. Publ. in Climatology, vol.10, no.3, p. 185-311.

WEO (World Energy Outlook), (2022). World Energy Outlook 2022. International Energy Agency. Available at https://www.iea.org/reports/world-energy-outlook-2022.

# A methodology for climate-proofing inland navigation infrastructure projects: the Seine-Schelde project

Carmen LOPEZ-FABARA[1], Nivedha ELANGO[1], Renaat DE SUTTER[1, 2], Annick DE WINTER[2], Frank SERPENTIER[2], Jeroen VAN WAEYENBERGE[2], Peter RATINCKX [2]

[1] Haedes bv, Belgium
carmen.lopez@haedes.eu
nivedha.elango@haedes.eu
renaat.desutter@haedes.eu

[2] De Vlaamse Waterweg

ABSTRACT

The effects and impacts of climate change are increasingly evident in Flanders. The persisting drought experienced during the summer of 2020 or the flood events in the summer of 2021, resulted in significant damage to both populated areas and biodiversity (KU Leuven, 2022). As part of the Flemish adaptive plan, the Department of Mobility of Belgium has initiated efforts to promote climate-adaptive and climate-neutral buildings and transportation infrastructure. Seine-Schelde Flanders is a large-scale inland shipping project that aims to make inland shipping a fully-fledged alternative to road freight transport, which results in less traffic, safety, and a cleaner environment, decreasing $CO_2$ emissions. In addition to promoting inland shipping, the project encompasses riverbank redevelopment, encourages recreational activities both on and along the water, and contributes to urban renewal. Considering the scale of the project and to achieve the aforementioned goals, a strategic approach is necessary, for integrating climate-proofing considerations into every stage of the project. This approach ensures the development and design of projects with minimal carbon footprints and the mitigation of risks from the project's inception. To this end, our primary aim was to formulate a strategy and practical guidelines enabling project management to effectively assess and incorporate climate resilience measures into the project and its components from the project design.

## 1. Climate proofing

Climate proofing refers to the systematic integration of climate change adaptation and mitigation measures into infrastructure projects that align with the objectives of the Paris Agreement. This process is structured around two key pillars: mitigation, aimed at achieving climate neutrality, and adaptation, focused on enhancing climate resilience (European Commission, 2014, 2021).

Each analysis pillar comprises two distinct phases. The initial phase involves a screening process with the dual purpose of assessing the magnitude of potential climate-related risks and evaluating alignment with the climate commitments of the European Union (European Commission, 2021). The outcome of this screening phase determines whether a more comprehensive second phase of detailed assessment is warranted. To facilitate this process, a climate-proofing tool in the form of an Excel Workbook has been developed for analysing both pillars within the screening stage of inland navigation projects. The methodology for each pillar encompasses:

- Calculation of the $CO_2$ footprint for the lifecycle of the project;
- Performing a vulnerability analysis of the components of each project to the changing climate.

### *1.1 Climate Mitigation*

The carbon footprint calculation was carried out in this project considering the uncertainty that the project might exceed the thresholds (20,000 tonnes of $CO_2$/year for absolute and relative emissions) (EIB, 2020). To

calculate the $CO_2$ footprint, the tool determines total carbon ($CO_2$) emissions for three types of infrastructure or activities: i) grey infrastructure, ii) blue-green infrastructure, and iii) dredging activities. The tool determines the $CO_2$ emitted during the project cycle, i.e., site set-up, construction and maintenance, and close-off. This carbon footprint tool aims to quickly and easily obtain a whole-life $CO_2$ value with minimal starting information.

The total emission value is based on the embodied carbon in the material used in the construction, the number of machines used on site and the hours of usage, the mode of transport, and the distance travelled for sourcing the materials and the elements. In the grey infrastructure, the carbon emissions of different structures such as Bridges, Quay walls, Jetty, Roadways, Buildings, and Discharge/Outlet pipes were calculated. In the case of blue-green infrastructure, the tool estimates the $CO_2$ emissions as well as the carbon pool of interventions made in the river banks using the natural and semi-natural landscape elements. The methodology used to estimate the carbon pool is the verified carbon standard by calculating the above-ground biomass, below-ground biomass, and litter. Finally, the carbon emissions during dredging processes are also estimated within the tool. The calculation considers the type of dredging, sediment handling, maintenance dredging, and monitoring. The results are presented as $tCO_2$-equivalent for the type of infrastructure within the project.

### *1.2 Climate Adaptation*

The vulnerability analysis is prepared to identify the relevant climate hazards for the specific project type at the planned site. The analysis combines two aspects namely, sensitivity and exposure. They are ranked from low to high and used as input for vulnerability analysis. The sensitivity analysis is carried out per component of the project irrespective of the site location, grouped as properties (Infrastructure, physical systems), process (operational aspects), inputs, outputs, and interrelationships. Guiding questions and explanations are provided to ensure more objectivity during the evaluation. The exposure analysis is focused on the site and whether the project location shall be influenced by defined climate hazards in the current and future climate.
In the context of the assessment of the project's climate resilience, it should be assessed whether the project increases the vulnerability of neighbouring economic and social areas, for example in the case of a dike that may increase vulnerability to flooding in the vicinity. An additional evaluation should therefore be carried out to assess the impact of the project on the reinforcement of a hazard, either at the project site or within the broad network to which it belongs. This step should be understood as broadly as possible to identify the plausible consequences of the second-order project. This should be considered a "double-check". The evaluation is based on three categories: increase, neutral, and decrease.

## 2. Conclusion

Practical guidelines and a dedicated tool have been developed to assess both climate adaptation and mitigation aspects within inland navigation projects. This tool contributes to identifying vulnerable elements that require further investigation and possible measures to ensure resilience to specific climate hazards. It also facilitates the identification of carbon emission sources and raises awareness among project management teams, enabling them to explore alternative solutions for effectively reducing carbon emissions. The user-friendly nature and the simplicity of the tool help in adopting it for any project to achieve a climate-proofed infrastructure and development. Notably, this assessment encompasses the entire life cycle of the project, yielding insights into total $CO_2$ emissions, carbon pools, and the project's vulnerability to both current and future climate scenarios. These insights empower stakeholders to take informed measures to enhance project sustainability in response to climate challenges.

**References**

EIB, (2020). EIB Project Carbon Footprint Methodologies. Methodologies for the Assessment of Project GHG Emissions and Emission Variations. Version 11.1, July 2020. European Investment Bank.
European Commission. (2014). Non-paper Guidelines for Project Managers: Making Vulnerable Investments Climate Resilient.
European Commission. (2021). Commission Notice: Technical guidance on the climate proofing of infrastructure in the period 2021-2027.
KU Leuven. (2022). Climate change in Flanders and Belgium. https://bwk.kuleuven.be/hydr/CCI/cci-hydr-fl
VERRA. (2021). Methodology for tidal wetland and seagrass restoration, verified carbon standard, version2.0 September 2021.

# Prevalence and physical properties of Urban Flood Drifters (UFDs) in extreme floods

Arnau BAYÓN [1], Daniel VALERO [2], Mário J. FRANCA [2]

[1] Department of Hydraulic Engineering and Environment, Universitat Politècnica de València (Spain)

arbabar@upv.es

[2] Institute for Water and River Basin Management, Karlsruhe Institute of Technology (Germany)
daniel.valero@kit.edu
mario.franca@kit.edu

ABSTRACT

Floods result in substantial economic, environmental, and human life losses. Climate change is further exacerbating these devastating effects. Hydrological and hydraulic models are pivotal in identifying and safeguarding flood-affected areas, serving as the cornerstone of flood management practices. Flood risk management rarely accounts for the presence of large-scale debris and the potential increase in hazards caused by the mobilization of these that eventual clog drainage infrastructure and damage by impact. This is partly due to our limited knowledge about the prevalence of these and their transport mechanics by running water. Herein, we present an analysis of the prevalence of these so-called Urban Flood Drifters (UFDs) in floods by a survey made in media and we discuss the main physical properties of these which are relevant to their stability and further transport.

## 1. Urban Flood Drifters (UFDs)

Flood risk assessment through modeling often overlooks the fact that floods carry Urban Flood Drifters (UFDs), loose objects capable of obstructing drainage infrastructure such as culverts or tunnels. This obstruction leads to stagnation and increased water depths due to backwater propagation. Furthermore, when transported by the flow, UFDs may damage lives and infrastructures by impact (Jalayer *et al.*, 2018; Zhang *et al.*, 2018). Recent flood disasters have underscored the importance of identifying and incorporating UFD transport in flood hazard quantification. These drifters typically include various vehicle types (bikes, motorbikes, e-scooters, cars, vans, recreational vehicles, buses, trucks...), urban furniture (trash bins, containers, construction materials...), and even household items (fluid tanks, garden sheds...).

## 2. Prevalence

Our objective was to confirm or refute the hypothesis regarding the significant role of UFDs in exacerbating urban floods, seeking to ascertain whether their presence is sporadic and, if not, quantify it. For this purpose, we conducted a comprehensive global analysis of photographic material sourced from social media, covering 25 major floods from the year 2000 onwards (for full analysis cf. Bayon *et al.*, 2023). This analysis aimed to characterize and quantify the occurrence of various debris types in urban flooding. Our findings corroborate the substantial presence of diverse debris in post-flood scenarios. We discuss their primary characteristics and prevalence, including the frequency of appearance of each UFD type and their geographic distribution patterns.

## 3. Physical properties

Following the identification, we proceeded to characterize and parameterize the identified debris based on several variables relevant to flood hazard assessment, including weight, dimensions, and other physical properties, aiming to evaluate their potential to destabilize and obstruct hydraulic structures.

To identify the most relevant physical properties of a UFD, we defined three limit states of stability: flotation, sliding, and toppling, contingent on the mechanical properties of UFDs and flow characteristics (depth and velocity). Formulation of the stability equations raise which variables are most important.

### *3.1. Flotation*

Flotation occurs when the buoyant force surpasses the weight, resulting in an upward force that enables the object to float, rise, and be transported by the flow.

### *3.2. Sliding*

Sliding occurs when the drag force overcomes the friction between the UFD and the surface it is on, causing the object to move.

### *3.3. Toppling*

Toppling occurs when the combination of the drag and buoyancy moments surpasses the combination of the friction and weight moments. This leads to the UFD losing balance and potentially tipping over or rotating. This leads to the UFD losing balance and potentially tipping over or rotating.

## 4. Conclusions

This study emphasizes the significant role of Urban Flood Drifters in exacerbating urban floods by obstructing drainage infrastructure. The mechanical properties that determine the destabilization and movement of UFDs dictate their susceptibility to three distinct destabilization mechanisms: flotation, sliding, and toppling. While some research has explored the impact of specific UFDs, such as cars (Smith et al., 2019) and, more recently, trash bins (Martínez-Gomariz et al., 2020), a notable gap in investigations pertains to numerous UFDs that profoundly influence urban floods. This underscores the urgent need for a comprehensive examination covering a broader spectrum of UFDs, with a specific focus on understanding their destabilization and movement dynamics. These comprehensive insights are critical for developing effective strategies to mitigate flood impacts and enhance urban resilience in the face of escalating flood risks.

**Acknowledgements**

The authors acknowledge the contribution of Temir Vinokhodov in the press and social media review and Tiago L. Franca in cataloging UFDs. This research was partially supported by the Erasmus+ STA program (EU), the UPV2030 Strategic Plan's Academic Career Support Program for Professors (PACAP-2022), the UPV Program to Support Research & Development (PAID-06-22), the Program for Emerging Research Groups of the Government of Valencia, Spain (CIGE/2022/7) and the Program for Collaboration of Researchers and Industry of the Government of Valencia, Spain (CIAEST/2021/56).

**References**

Bayón, A., Valero, D., Franca, M.J. (2023). Urban Flood Drifters (UFDs): identification, classification and characterisation. Preprint: https://arxiv.org/abs/2304.01780.

Jalayer, F., Aronica, G. T., Recupero, A., Carozza, S., and Manfredi, G. (2018). Debris flow damage incurred to buildings: an in situ back analysis, Journal of Flood Risk Management, 11.

Martínez-Gomariz, E., Russo, B., Gómez, M., and Plumed, A. (2020). An approach to the modelling of stability of waste containers during urban flooding, Journal of Flood Risk Management, 13.

Smith, G. P., Modra, B. D., and Felder, S. (2019). Full-scale testing of stability curves for vehicles in flood waters, Journal of Flood Risk Management, 12.

Zhang, S., Zhang, L., Li, X., and Xu, Q. (2018). Physical vulnerability models for assessing building damage by debris flows, Engineering Geology, 247.

# A multipurpose alpine lake - Modelling supplies and withdrawals in view of climate change

Evanice RUEGG[1], Giovanni DE CESARE[2], Alexandre GILLIOZ[3]

[1,2] EPFL, PL-LCH, CH-1015 Lausanne, Switzerland
evanice.ruegg@epfl.ch
giovanni.decesare@epfl.ch

[3] ALTIS, Place de Curala 5, 1934 Bagnes, Switzerland
alexandre.gillioz@altis.swiss

## 1. Introduction

Lac de Louvie is a high alpine artificial reservoir located at an altitude of 2214 masl that stores 450'000 $m^3$ of water to meet the drinking water, irrigation and snowmaking needs of the Val de Bagnes municipality, located in Valais, Switzerland (Fig 1). Its watershed, with a surface area of about 8 $km^2$, extends up to 3320 masl with no glacier cover. At the end of summer 2022, the lake level began to fall alarmingly, threatening the winter reserves. The need arose to better understand the behaviour of the Lac de Louvie watershed, to be able to forecast lake inflows and to predict climate change consequences on the watershed's hydrology and water usage.

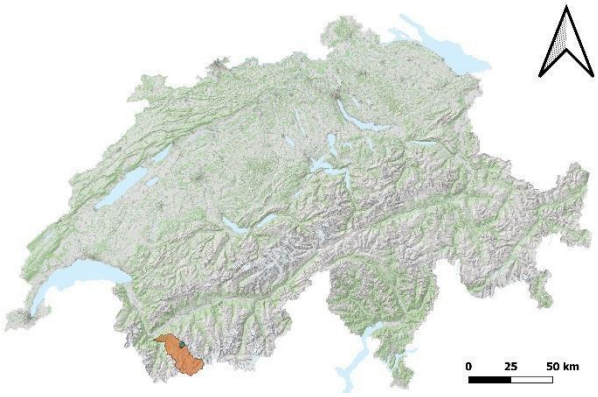



**Fig.1.** Map of Switzerland showing the boundaries of Val de Bagnes municipality (orange) and of Lac de Louvie (blue dot)

## 2. Methodology

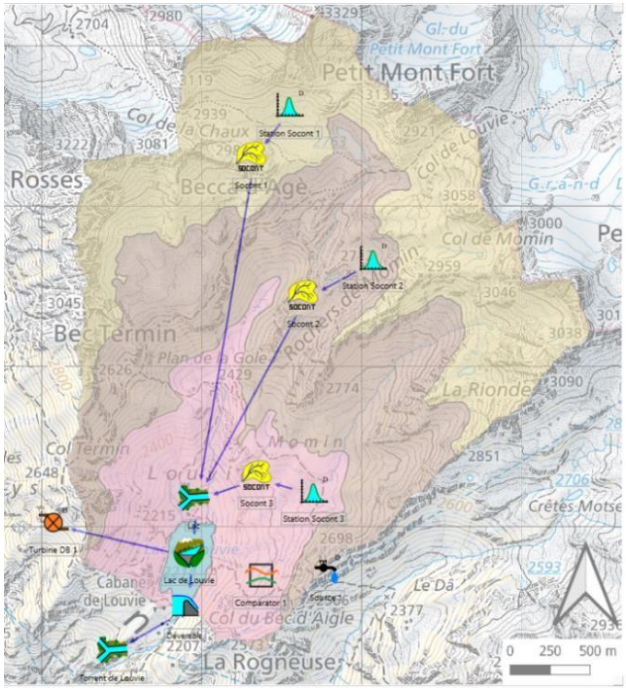



**Fig.2.** Georeferenced representation of the model with three elevation bands on RS MINERVE. The model consists of a virtual meteorological station and a SOCONT rainfall-runoff model per band, a junction, a reservoir, a spillway, a withdrawal to the water network and a comparator of the water level measured and simulated by the model.

In order to determine the accuracy required to simulate the Louvie watershed, several hydrological rainfall-runoff model approaches are considered: a global model that considers the watershed as a single entity, a model that divides the surface into elevation bands, and a model that divides the watershed into several sub-basins. The models are based on the RS MINERVE software (Garcia Hernández et al., 2007). The hydrological model used is SOCONT, a model based on four reservoirs: two for precipitation and snowmelt, one for infiltration and one for runoff. (Schaefli et al., 2005). The data used are precipitation and temperatures from four nearby automated stations in the MeteoSwiss network. In addition, measurements of water levels and water withdrawals for the municipal water supply are used.

The consequences of climate change are then assessed using the most appropriate model from the first part. The climate data used come from the CH2108 climate scenarios downscaled to hourly time steps for meteorological stations (Michel et al., 2021). For this study, the 31 climate simulations of the dataset based on the RCP 8.5 scenario are considered. The station selected from the data set is Arolla Les Fontanesses. An estimation of the future evolution of water consumption is based on Gonin et al. (2021). This study

was commissioned by ALTIS, the local water company. Three time periods are considered: short, medium and long term, corresponding to 2020-2030, 2050-2060 and 2080-2090 respectively.Results

The most appropriate approach to modelling the Louvie catchment is to divide it into elevation bands. Figure 2 shows the model constructed using the three elevation bands selected for the remainder of the study.

Climate change will alter the annual dynamics of Lac de Louvie. By 2090, snowmelt and lake filling will occur a month earlier, and in some years the maximum lake level will not be reached. Despite no significant reduction in the annual inflow to the lake and a 25% reduction in the volume of water released by the dam by 2080, water shortages are expected to occur every year between 2080 and 2090, with an average duration of 58 days per year. Figure 3 shows the lake volume and its seasonal variations for the long-term period.

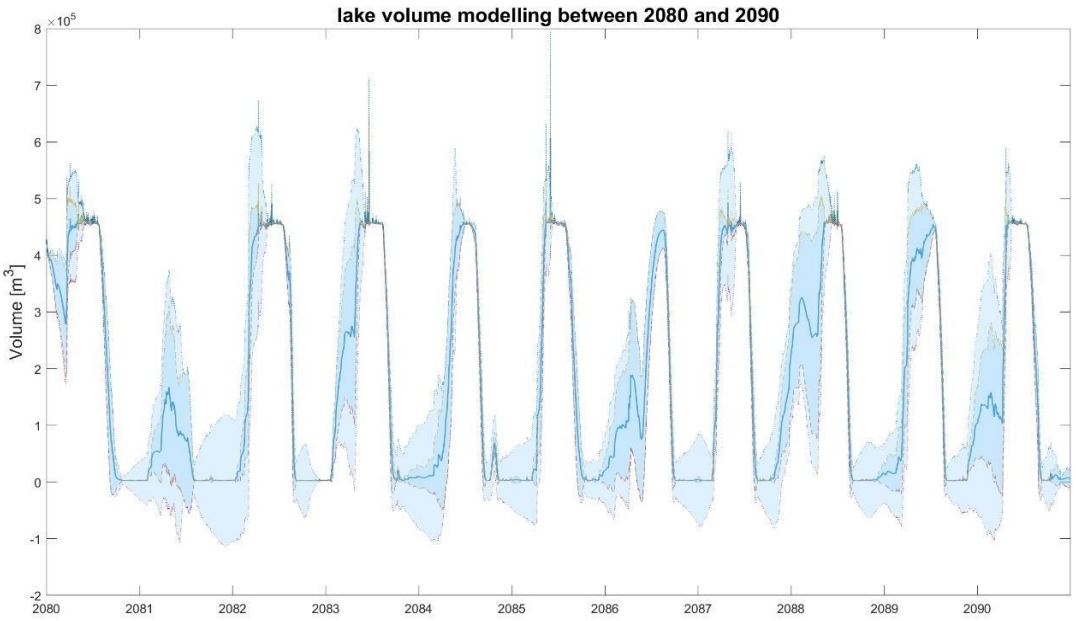



**Fig. 3.** Modelling the volume of Lac de Louvie using the mean of the 31 climate simulations and their two associated standard deviations (sd) for 2080-2090. Blue line for the mean, dashed line and dark blue area for the first sd, dotted line and light blue area for the second sd. The lake has a capacity of 450'000 m3. The negative values in this figure correspond to the calculed sd and should not be considered.

## 3. Discussion

The result of the comparison of the three modelling approaches was expected due to the large difference in altitude between the lowest and highest points (more than 1’000 m). Dividing the watershed into elevation bands allows better modelling of snow-related physical phenomena, which is the main driver of the system.

Although the annual volume of water entering Lac de Louvie is not significantly different between the three periods, water shortages are to be expected. Part of the explanation may be the change in the seasonal dynamics of Lac de Louvie. In addition, climate change will significantly increase the demand for water, especially for irrigation purposes and to meet the needs of a growing population. The evolution of future consumption has a major influence on the level of the lake. A more accurate assessment of future water demand would lead to a better understanding of the future withdrawals and could improve the results of this modelling.

## 4. Conclusion

Climate change will have a significant impact on the capacity of Lac de Louvie to meet the needs of the local community. Solutions such as diverting water from existing hydroelectric facilities in the region or raising the Louvie dam to increase storage volume could be implemented, in addition to measures to reduce water consumption for households and irrigation.

**References**

Garcia Hernández J, Jordan F, Dubois J, Boillat J-L, Schleiss A (2007) Routing System II: Modélisation d’écoulements dans des systèmes hydrauliques. Communication du Laboratoire des Constructions Hydrauliques, Ed A. Schleiss, EPFL, Lausanne, 32 (available also on CREALP, HydroCosmos SA, EPFL, UPV, Hydro10 (2012) Logiciel RS MINERVE.

Gonin T, Decaix J, Münch-Alligné C (2021) Smart Water, Retenues d’eau multi-usages : une nécessité pour l’irrigation future ?, HES-SO Valais, final report WP3 of SmartWater project.

Michel A, Sharma V, Lehning M, Huwald H (2021) Climate change scenarios at hourly time-step over Switzerland from an enhanced temporal downscaling approach, International journal of climatology, 41, 3503-3522.

Schaefli B, Hingray B, Niggli M, Musy A (2005) A conceptual glacio-hydrological model for high mountainous catchments, Hydrology and Earth System Sciences, 9, 95-109.

# Monitoring Surface Soil Moisture, Evapotranspiration, and Vegetation Greenness from Multi-Level Observations in the UAE Dryland Ecosystems

Youngwook KIM[1], Abdalla Saber Abdalla ABDELHAMID[1], Benazir MEERASHA[1], Young Ki KIM[1], Ashley KIM[2]

[1] United Arab Emirates University, UAE
youngwook.kim@uaeu.ac.ae

[2] Lehigh University, USA

ABSTRACT

Seasonal dynamics and inter-annual variation of vegetation productivity is closely linked with temperature variations in most of terrestrial biomes, but soil water moisture is an additional factor to determine eco-hydrological processes in the water-limited regions. Studies using in-situ observation and satellite remote sensing have been widely used to monitor temporal variations of terrestrial ecosystem productivity and associated biogeochemical processes, including carbon and water cycles. However, there are few studies on the changes of seasonal eco-hydrological dynamics and the resulting biogeochemical cycles, and associated hydroclimate impacts on dryland ecosystems, particularly sparsely vegetated areas. In this study, we used optical and microwave satellite remote sensing data records, to monitor spatial and temporal patterns of surface soil moisture (SFSM), root-zone soil moisture (RZSM), vegetation greenness and evapotranspiration (ET) associated with regional carbon and water cycles over a sparsely vegetated area of the United Arab Emirates (UAE). The multi-source satellite data records include the six-year (2016-2021) surface soil moisture, and optical- and microwave-based vegetation index (VI) and ET derived from MODIS, LANDSAT-8, and Sentinel-2. We also used Delta-T WET-2-K4 sensor to measure in-situ surface soil moisture at the sparsely vegetated site in Al Ain, UAE. The surface soil moisture measured represents the point-level water content in the surface soil (~5cm depth). The combined satellite remote sensing data provide the enhanced ability to monitor vegetation dynamics and biogeochemical cycles. The results will show a better understanding of how the seasonal responses of the vegetation productivity, ET, and carbon and water cycle feedback to hydro-climate change. Knowledge obtained from this study will provide important insights for future feedbacks and their consequences on biogeochemical dynamics in hyper-arid ecosystems .

## 1. Data and methods

As a proxy of vegetation productivity, we used the Normalized Difference Vegetation Index (NDVI) derived from Moderate Resolution Imaging Spectroradiometer (MODIS) Nadir BRDF-Adjusted Reflectance (Schaaf & Wang, 2015) and the Harmonized Landsat Sentinel-2 (HLS) reflectances (Masek et al., 2021). The daily surface and root-zone soil moisture provided by Soil Moisture Active Passive (SMAP) mission were used for representing water availability on the ecosystem processes (Reichle et al., 2017). Total surface precipitation and land surface temperature (LST) were obtained from the Goddard Earth Observing System, Version 5 (GEOS-5) Forward Processing (FP) system at the NASA Global Modeling and Assimilation Office (GMAO) (Reichle et al., 2015; Reichle and Liu, 2014). These remote sensing (RS) data were accessed through the NASA AppEEARS system (LP-DAAC – AppEEARS, 2023). The global daily satellite ET data estimated using a modified Penman-Monteith (mPM) approach was used to monitor seasonal pattern of three ET components, including soil evaporation, transpiration and evaporation of canopy-intercepted precipitation (Kim et al., 2023). The NDVI and ET data were used as indicators of ecosystem carbon and water-energy fluxes, respectively. In-situ surface soil moisture content was measured using the HH2 Moisture meter with a WET Sensor (DeltaT, Burwell, Cambridge, UK) from March to October 2023 over a study site in Ain Al Faydah desert area (24°03'20.6"N 55°41'48.8"E) of the UAE. Measurements were conducted by vertically inserting the sensor probe into the soil, recording data at the 6cm depth. The in-situ surface soil moisture was measured monthly to capture seasonal variations.

## 2. Results

Multiple readings were collected at the study site to augment precision and accuracy. Subsequently, the average value and standard deviation for the site was used to show the seasonal variations of the in-situ SM. The temporal patterns of the SM decrease from February to August 2023 and increase by October at Ain Al Faydah desert area (Fig. 1a). The 6-year satellite SFSM and RZSM shows the seasonal patterns of surface moisture condition, with generally higher SM at spring season (~March) and larger variability in RZSM (Fig. 1b). The higher SM during wet season is likely due to short-term rainfall and humid air condition. In-situ SM pattern shows a similar pattern to satellite observations. NDVI results show a distinct seasonal pattern of vegetation greenness observed from two independent satellite sensors for 2021 (Fig. 2a), with relatively higher values during winter period (December to February) due to more moisture availability. At the study site, soil evaporation is a major contribution to total ET (Fig. 2b, c), while transpiration does not contribute to the total ET (not shown). In December 2021, sudden precipitation rapidly increases evaporation of canopy-intercepted precipitation (Fig. 2b). Higher soil evaporation during summer increase soil water loss (Fig. 1b). However, the seasonal progression of ET is not closely linked to NDVI. It indicates that the soil evaporation tends to be depressed as a result of frequent cloudy, humid air and wet condition due to the rainfall events (Baalousha et al., 2022), and relatively lower LST (not shown) during the winter period. Further study will provide a better understanding of the complex interaction between vegetation productivity and ET components, between land and atmosphere, and associated carbon and water cycles over the hyper-arid regions.

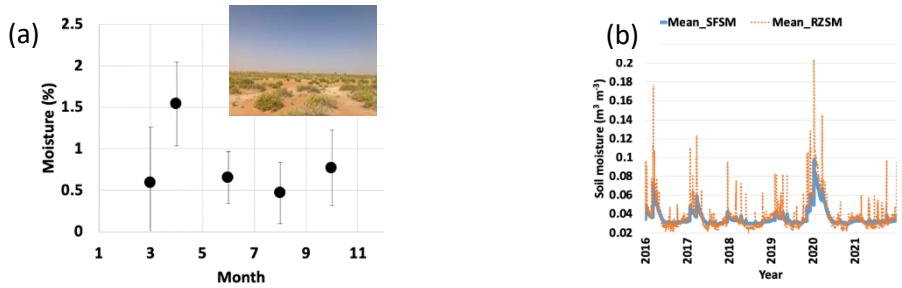



**Fig. 1.** Mean soil moisture (black dot) and standard deviation (error bars) measured from March to October 2023 (a) and 9-km SMAP daily surface soil moisture and root-zone soil moisture for the period 2016-2020 in Ain Al Faydah Desert Area. Inset map shows the landscape view taken from an iphone7 camera at the study area.

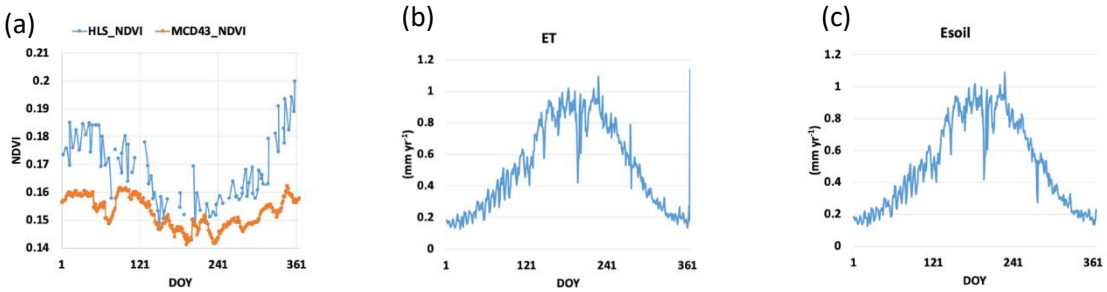



**Fig. 2.** The 500-m daily MOD43 reflectance derived NDVI and 30-m harmonized Landsat Sentinel (HLS) reflectance derived NDVI (a), and 9-km SMAP daily mPM total ET (b) and soil evaporation (c) for the 2021 in Ain Al Faydah Desert Area.


### Acknowledgements

This work was partially supported by ASPIRE 2020 & UPAR 2023 grants at the United Arab Emirate University.


### References


Baalousha H M, et al. (2022) https://doi.org/10.3390/w14182787
Kim Y et al. (2023) https://doi.org/10.1016/j.rse.2023.113803 (Data source: http://files.ntsg.umt.edu/data/ET_global_daily_mPM/)
LP DAAC - AppEEARS (2023) Application for Extracting and Exploring Analysis Ready Samples. Available online: https://lpdaac.usgs.gov/tools/appeears/
Masek J, et al. (2021) https://doi.org/10.5067/HLS/HLSL30.002
Reichle, et al. (2017) J. Hydrometeor., 18, 3217–3237
Reichle, R.H. et al. (2014) https://gmao.gsfc.na sa.gov/pubs/docs/Reichle734.pdf
Reichle, R., et al., 2015. Soil Moisture Active Passive (SMAP) Mission Level 4 Surface and Root Zone Soil Moisture (L4_SM) Product Specification Document. (Reichle789.pdf, 724 KB).
Schaaf C et al. (2015). https://doi.org/10.5067/MODIS/MCD43A4.006

8th IAHR EUROPE CONGRESS
LISBON - PORTUGAL
4-7 JUNE 2024

# Analysis on spatial return period of extreme rainfall in different regions

So KAZAMA[1], and Hajime YANAGISAWA[2]

[1] Department of Civil and Environmental Engineering, Tohoku University, Japan
so.kazama.d3@tohouk.ac.jp

[2] Penta-ocean Construction Co., Ltd, Japan
hajime.yanagisawa@mail.penta-ocean.co.jp

ABSTRACT

Spatial return period of extreme precipitation events is analyzed. Spatial return period is the recurrent period during which extreme precipitation occurs even once within a certain spatial area. For the precipitation data, we used d4PDF's large-scale ensemble data and divided Japan into five regions based on climate classification to consider the differences in spatial return periods in each region. The spatial return period with 100-year extreme precipitation is 3.82 years in Hokkaido and 2.34 years in the Pacific side of western Japan, showing regional differences. Additionally, as a result of comparing the spatial return periods of past experiments, 2℃ increase experiments, and 4℃ increase experiments, the rate of increase in the frequency of extreme precipitation is higher in northern Japan, and the frequency may especially increase approximately three times in the Hokkaido region.

## 1. Methodology

The target area is all of Japan. The precipitation data used is the database for policy decision-making for future climate change (d4PDF) (Mizuta, et al., 2017). We used a high-resolution regional atmospheric model with a horizontal resolution of 20 km that was downscaled for the Japanese region. There are model experiment outputs for 3000 years of past experiments (60 years x 50 members), 3240 years of 2℃ rise experiments (60 years x 54 members), and 5400 years of past experiments (60 years x 90 members). From a total of 13,560 cells that cover all of Japan, 1,038 cells (approximately 410,000 km$^2$) including land areas are selected as the target area. Furthermore, based on climate classification, the entire Japan was divided into five regions (Hokkaido, East Japan Pacific side, East Japan Japan Sea side, West Japan Pacific side, and West Japan Japan Sea side) so that the number of cells was as equal as possible. Daily precipitation is used for analysis.

Return period (RP) is used as an index to express the frequency. Extreme precipitation that occurs once every 100 years is called RP100-year extreme precipitation. Firstly, the probability precipitation amount for each cell is calculated and this is the standard for RP100-year extreme precipitation. A nonparametric method is used to calculate the probability precipitation amount. This analysis to obtain the spatial probability followed Yanagisawa et al.(2022).

The probability precipitation amount for RP100-year extreme precipitation is calculated for each cell, so the return period for RP100-year extreme precipitation to occur at a certain point is 100 years. However, when the target area is expanded, the frequency of RP100-year extreme precipitation spatially increases within the target area. This frequency is called the spatial return period. Here, the spatial return period is defined as "the period from when extreme precipitation occurs once until it occurs again within a target area consisting of multiple cells." The target area in this study is each region based on climate classification. Therefore, the spatial return period indicates the frequency at which RP100-year extreme precipitation occurs within each region. In addition, the frequency increase rate is calculated as an indicator of future changes in the spatial return period.

The frequency increase rate is the ratio of the spatial return period of future experiments (2℃ increase experiment, 4℃ increase experiment) to the spatial return period of past experiments.

## 2. Results and discussion

Table 1 shows the spatial return period (past experiment, 2℃ increase experiment, 4℃ increase experiment) and frequency increase rate of RP100-year extreme precipitation in five regions based on climate classification. From the results of past experiments, the region with the longest spatial return period (lowest frequency) is Hokkaido (3.82 years). On the other hand, the region with the shortest spatial return period (highest frequency) is the Pacific side of western Japan (2.34 years), where the frequency is 1.6 times higher than in Hokkaido. Regarding the difference in spatial return period between the Pacific Ocean side and the Japan Sea side, almost no difference can be seen in eastern Japan. On the other hand, a difference is seen in western Japan, with the frequency on the Pacific side being 1.27 times higher than on the Japan Sea side. Here, the total number of extreme precipitation occurrences in each cell is equal in each region. In other words, a short spatial return period (high frequency) suggests that extreme precipitation occurs frequently in a narrow range. Conversely, a long spatial return period (low frequency) suggests that extreme precipitation occurs over a wide range and rarely. This is thought to be due to the difference in precipitation type that causes extreme precipitation.

**Table 1.** Future change (the unit is year) and increase rate of frequency (in parentheses) of spatial return period in different climate area

| | Past experiment | 2℃ Increase | 4℃ Increase |
|---|---|---|---|
| Hokkaido | 3.82 | 2.08 (1.83) | 1.27 (3.00) |
| East: Pacific side | 2.74 | 1.74 (1.58) | 1.29 (2.12) |
| East: Japan Sea side | 2.67 | 1.78 (1.51) | 1.26 (2.21) |
| West: Pacific side | 2.34 | 1.67 (1.40) | 1.33 (1.75) |
| West: Japan Sea side | 2.99 | 2.07 (1.45) | 1.59 (1.88) |

The 2℃ increase experiment has a long spatial return period in Hokkaido and western Japan on the Japan Sea side (2.08 years, 2.07 years). Additionally, the spatial return period on the Pacific side of western Japan was the shortest (1.67 years). The rate of increase in the frequency of RP100-year extreme precipitation compared to past experiments is highest in Hokkaido, which is 1.83 times. The rate of increase in frequency tends to be lower in southern regions with lower latitudes, with the rate of increase in frequency on the Pacific side of western Japan being the lowest at 1.40 times. There are no areas where the frequency decreases.

The 4℃ increase experiment has a long spatial return period (1.59 years) on the Japan Sea side of western Japan. The spatial return period in other areas is almost the same (approximately 1.3 years). The rate of increase in the frequency of RP100-year extreme precipitation compared to the spatial return period of past experiments is highest in Hokkaido, 3.00 times. The frequency increase rate is lower in southern regions with lower latitudes, and the frequency increase rate on the Pacific side of western Japan is 1.75 times.

There are two ways to interpret the frequency increase. The first is that the amount of precipitation in future experiments has increased compared to past experiments, and the occurrence of extreme precipitation has also increased. Second, the spatial return period has become shorter due to changes in precipitation patterns and an increase in local extreme precipitation. It is predicted that the degree of influence of both will differ depending on the region. The future challenge is to elucidate the factors increasing the spatial return period.

**Acknowledgements**

This research was performed by the Environment Research and Technology Development Fund (JPMEERF20S11813) of the Environmental Restoration and Conservation Agency of Japan, and the Ministry of Education, Science, Sports and Culture, Grant-in Aid for Challenging Research (Exploratory), 2019-2021（19K21982, So Kazama）

**References**

Mizuta, R., et al. (2017) Over 5,000 years of ensemble future climate simulations by 60- km global and 20-km regional atmospheric models. Bulletin of the American Meteorological Society 98(7), 1383–1398.

Yanagisawa, H. and Kazama S., Touge, Y.(2022) Spatial frequency analysis of annual extreme daily precipitation across Japan, Journal of Hydrology: Regional Studies, 42, 101131, 2022. DOI: 10.1016/j.ejrh.2022.101131

# Assessing hydrological impacts of urbanization and climate change in Orunia basin, Gdańsk, Poland

Khansa GULSHAD[1], Michał SZYDŁOWSKI[1]

[1]Gdańsk University of Technology, Faculty of Civil and Environmental Engineering, Poland
khansa.gulshad@pg.edu.pl; mszyd@pg.edu.pl

ABSTRACT

Due to intensive land use land cover (LULC) development in Orunia basin in Gdańsk, Poland, Hydrologic Modeling System (HEC-HMS) was used to examine surface runoff for different time frames (1985-2022, 2050-2100) under three scenarios: isolated LULC effect, isolated climate change effect, and combined LULC and climate change effect.

## 1. Introduction

The rapid population growth globally leads to a significant LULC changes, affecting hydrologic and hydraulic processes and causing urban floods (Zope et al., 2016). Additionally, climate change alters rainfall patterns, atmospheric water content and soil moisture (Sinha et al., 2023). Therefore, understanding the combined impact of LULC changes and climate change on surface runoff in Gdańsk, Poland is essential for effective urban planning and flood management.

## 2. Methodology

### *2.1. Study area*

Gdańsk, the largest city in northern Poland, is situated on the southern coast of the Baltic Sea within the Gulf of Gdańsk. One of the catchments of Gdańsk, Oruński/Orunia basin (Fig. 1), has been chosen for detailed runoff analysis due to the observed extensive LULC changes that have occurred over the past 37 years. With an area of 16.55 km$^2$, the Orunia basin is in the rapidly developing Południe district of Gdańsk, offering potential for new construction projects. The rapid urban expansion observed in the last decade, characterized by the rapid emergence of new residential areas and the establishment of large commercial and service companies, has substantially exerted significant pressure on the region (Kolerski, and Kalinowska, 2019; Pietruszyński, and Cieśliński; 2019).

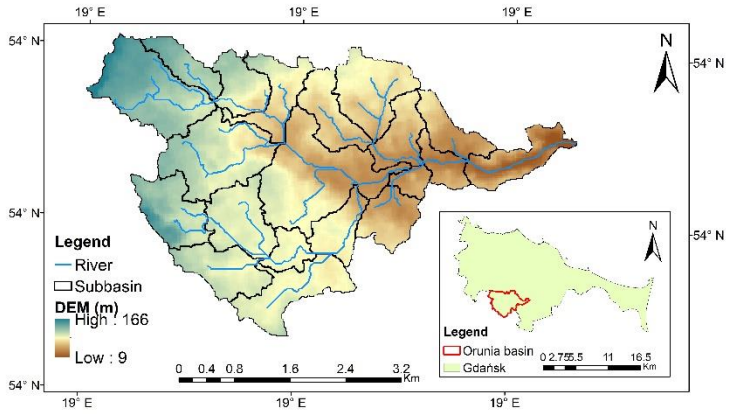



**Fig. 1.** Location map of Orunia basin in the southwest of Gdańsk, Poland (bottom right), Schematic map of hydrologic elements in the HEC-HMS model showing Orunia basin (top left)

*2.2. Methods*

This research utilized the cloud-based platform Google Earth Engine (GEE) to prepare historical LULC maps. To predict the future LULC of Orunia basin for the year 2050, 2100 the Land Change Model (LCM) within the TerrSet software system was employed.

HEC-HMS model with fixing changing approach (Mekonnen et al., 2018) was utilized to simulate the historical and future hydrological response of the basin over an analysis period from 1974 to 2100, divided into four periods: 1974–2000 (baseline), 2000-2005 (moderate development), 2005–2022 (human activities), and 2022–2100 (climate change). Biased corrected, downscaled climate data was sourced from CHASE-PL (Mezghani et al., 2016). Three scenarios were established. In isolated LULC effect, LULC maps for each year were utilized while retaining the baseline climate data. Under isolated climate change impact, climate data was altered for each year while keeping the baseline LULC constant. For combined effect of LULC and climate change, HEC-HMS model was executed for each land use map, along with their corresponding climate data.

## 3. Results

The analysis of LULC changes revealed a significant expansion of the built-up area, shift in forest and vegetation cover and a reduction in agricultural land from 1985 to 2005, 2022, 2050 and 2100 respectively. Figure 2 depicts the comparison between all considered scenarios. The isolated LULC impact indicates that the increase in runoff coefficient of 0.57, and 0.63 for 2050 and 2100 while isolated climate change impact has also significantly influenced the surface runoff with coefficient of 0.57, 0.59 and 0.58,0.66 for 2050, and 2100, based on Representative Concentration Pathway (RCP) 4.5, RCP 8.5.

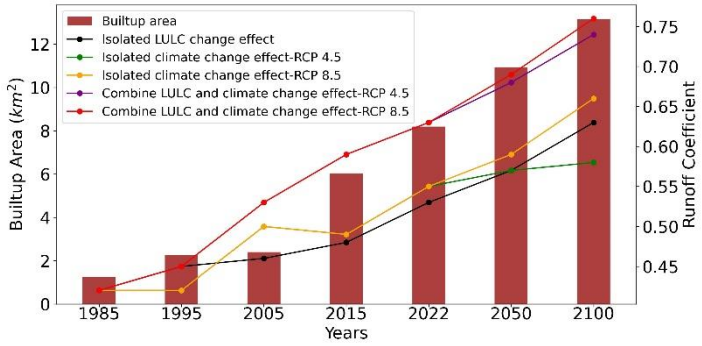



**Fig. 2.** Comparison between three simulations in HEC-HMS; i) combined LULC and climate change effect, ii) isolated LULC change effect, and iii) isolated climate change effect.

The combined effect of climate change (RCP 4.5 and 8.5) and LULC scenarios is significantly more severe. HEC-HMS simulations demonstrated a 49.41% increase in the runoff coefficient between the 1970s and the 2000s, attributed to the combined effect of LULC and climate change. It is expected to further increase by 61.08 %, 74.58%, and 62.33%, 78.26% in the RCP 4.5 and RCP 8.5 scenarios compared to the baseline period (1974-2000) for the years 2050 and 2100.

## 4. Conclusion

This study explores the long-term effects of urbanization and climate change on runoff in the Orunia basin, Gdańsk, Poland. Notably, the combined effects of LULC and climate change have a greater impact on Gdańsk's hydrology compared to their isolated effects. This study highlights the need to consider both historical and future LULC and climate changes while assessing the potential impact on hydrological processes in the study area.

**References**

Zope PE, Eldho TI, Jothiprakash V (2016) Impacts of land use–land cover change and urbanization on flooding: A case study of Oshiwara River Basin in Mumbai, India, Catena (Amst), 145, 142–154.
Sinha RK, Eldho TI, Subimal G (2023) Assessing the impacts of land use/land cover and climate change on surface runoff of a humid tropical river basin in Western Ghats, India, International Journal of River Basin Management, 21, 141–152.
Kolerski T, Kalinowska D (2019) Mathematical modeling of flood management system in the city of Gdańsk, Oruński Stream case study, Acta Scientiarum Polonorum Formatio Circumiectus, 18, 63–74.
Pietruszyński Ł, Cieśliński R (2019) The Impact of Hydrometeorological Events on the State of the Urban River Quality, Ecological Chemistry and Engineering, 26, 521–533.
Mekonnen DF, Duan Z, Rientjes T, Disse M (2018) Analysis of combined and isolated effects of land-use and land-cover changes and climate change on the upper Blue Nile River basin's streamflow, Hydrol Earth Syst Sci, 22, 6187–6207.
Mezghani A, Dobler A, Haugen JH (2016) CHASE-PL Climate Projections: 5-km Gridded Daily Precipitation & Temperature Dataset (CPLCP-GDPT5). Norwegian Meteorological Institute. Dataset. DOI: 10.4121/uuid:e940ec1a-71a0-449e-bbe3-29217f2ba31d

8th IAHR EUROPE CONGRESS
LISBON - PORTUGAL
4-7 JUNE 2024

# Impact of climate change on the supply-demand balance of Collective Irrigation Systems. Methodological approach

Antónia FERREIRA[1], João ROLIM[2], Cláudia BRANDÃO[3], Maria do Rosario CAMEIRA[4]

[1, 2, 4] LEAF - Linking Landscape, Environment, Agriculture and Food-Research Center, Associated Laboratory TERRA, Instituto Superior de Agronomia, Universidade de Lisboa, Tapada da Ajuda,1349-017 Lisbon, Portugal
aferreira@isa.ulisboa.pt
joaorolim@isa.ulisboa.pt
roscameira@isa.ulisboa.pt

[3] DGADR - Direção dos Serviços de Regadio da DGADR- Direção Geral da Agricultura e Desenvolvimento Rural, Ministério da Agricultura, Av. Afonso Costa, 3, 1949-002 Lisboa, Portugal
cbrandao@dgadr.pt

ABSTRACT

According to the IPCC, climate change (CC) threatens the sustainability of agriculture, particularly in vulnerable regions such as parts of southern Europe where water shortages and increasing aridity make it difficult to sustain agriculture (IPCC, 2014). Of particular concern are regions where crop cycles coincide with high climatic demands and reduced precipitation (Zhang *et al.*, 2019). Projections indicate a potential increase in irrigation demand due to increased crop water requirements, which serves as a basis for understanding the imminent pressures on water resources (Rolim *et al*., 2017). At the same time, water availability is expected to decline, due to the projected reduction in precipitation (Mourato, 2009). In this particular context, farmers rely on Collective Irrigation Systems (CIS) to store and equitably supply water to irrigate their fields (Cunha *et al*., 2019). The overall aim of this study is therefore to assess the potential consequences of this increasing demand combined with reduced water availability when using artificial reservoirs. Two key manifestations of this challenge are highlighted: first, the possibility that peak water demand exceeds the initial capacities of the CIS, leading to failures in water supply during periods of high demand (Daccache *et al*., 2010); second, there is a risk that cumulative seasonal water demand exceeds the capacity of reservoirs derived from direct precipitation and watershed inflows (Rocha *et al*., 2020; Esteves *et al*., 2023). A supply-demand balance is being developed and applied to assess of the dynamics of water resources management at a CIS level in the context of climate change. This study is being developed with data from the *Minutos* CIS in the southern of Portugal but can be also applied to other CIS in arid and semi-arid regions. In particular, the aim is to calculate water availability and demand under various climate change scenarios, with a particular focus on identifying potential failures in irrigation water supply. This approach will enable a more comprehensive understanding of how climate change affects water management in the CIS in these regions.

## 1. Methodological approach

The approach developed at the CIS level, based on a balance between irrigation water demand and water availability. Data from the *Minutos* Collective Irrigation System (MCIS) in the southern of Portugal, and the surrounding watershed are used. MCIS is located on the Almansor River, in Évora district. Established in 2003, it supplies water from the *Minutos* reservoir to 1532 hectares of agriculture. This CIS has a pressurized irrigation network that operates on demand serving 162 farmers. The watershed has an area of 95 $hm^2$, with an average annual precipitation of 712 mm and an average annual inflow of 215 mm. The storage capacity is 2.3 times the mean annual inflow and the specific demand is 63% of the mean annual inflow (DGADR, 2023). The predominant soil types in the irrigated area are Luvissols (74.1%), Fluvissols (16.7%), and Cambisols (8.6%), (DGADR, 2023). For the 2023 season, annual crops accounted for 54.3% of the irrigated area, including fodder, maize, and pastures, while permanent crops accounted for 18.2%, consisting of orchards, vineyards, and olive groves. Around 27.5% of the area was fallow. The main irrigation systems are sprinkler (79.8%) and drip irrigation (20.2%).

### *1.1 Irrigation demand*

The anomalies projected by the Copernicus Climate Change Service were used to perturb the historical precipitation and temperature (IPMA, 2023; SNIRH, 2023). The EURO-CORDEX project's regional climate models were considered for RCP4.5 and RCP8.5, as well as for the near and long term (C3S, 2023). To eliminate biases in the climate change data, the quantile mapping method was used. Remote sensing images, particularly from Sentinel-2, were used to define cultural patterns and obtain biophysical parameters of crops by processing images on the Google Earth Engine platform.Due to the lack of historical climate data on variables such as relative humidity, solar radiation, and wind speed, the Hargreaves-Samini equation ($ET_{0-HS}$) (Eq 1) was used to calculate evapotranspiration. The radiation adjustment coefficient ($K_{Rs}$) was adjusted for the region (Hargreaves and Samani, 1982; Allen et al., 1998). The ISAREG model was used to estimate irrigation requirements for both the current cropping pattern and climate change scenarios. The crop parameters were defined using agronomic concepts as the growing degree days and assuming that the crop pattern remains unchanged. Water balance to obtain irrigation requirements is computed for homogenous units of analysis by overlaying information on crops, soils, and on-farm irrigation systems.

### *1.2 Water availability*

The simulation of the monthly inflow series is obtained using the Temez Hydrological model, the calibrated parameters for the basin and the perturbed precipitation series (as referred above in 1.2). The water availability and irrigation demand results for the observed historical period and the climate change scenarios are used to calculate the balance per period using a reservoir exploitation simulation model. This will make it possible to identify the years and periods in which water supply is insufficient to meet demand with different probabilities.

## 2. Final remarks

It is important to emphasize that this study is still ongoing. With this study we want to anticipate and provide valuable insights into the challenges that climate change poses to agriculture in southern Europe's arid and semi-arid regions. These results will highlight the risks of water supply failures during periods of high-demand and the strain on reservoir capacities.

**Acknowledgements**

The authors acknowledge the support of FCT under the projects UIDB/04129/2020 of LEAF, Research Unit, LA/P/0092/2020 of Associate Laboratory TERRA and under the grant PRT/BD/154133/2022 and DL 57/2016/CP1382/CT0021. The authors would like to thank the COTR, DGADR and IPMA for providing data for the development of this work.

**References**

Allen, R. G., Pereira, L. S., Raes, D., & Smith, M. (1998). Crop evapotranspiration. Guidelines for computing crop water requirements. In *Irrigation and Drainage Paper No.56*. Rome: FAO.

Copernicus Climate Change Service. Retrieved May 15, 2023, from Climate Data Store, https://cds.climate.copernicus.eu/cdsapp#!/home

Calera Belmonte, A., Jochum, A. M., García, A. C., Rodríguez, A. M., & Fuster, P. L. (2005). Irrigation management from space: Towards user-friendly products. *Irrigation and Drainage Systems*, *19*(3–4), 337–353. https://doi.org/10.1007/s10795-005-5197-x

Cunha, H., Loureiro, D., Sousa, G., Covas, D., & Alegre, H. (2019). A comprehensive water balance methodology for collective irrigation systems. *Agricultural Water Management*, *223*(January), 105660. https://doi.org/10.1016/j.agwat.2019.05.044

Daccache, Andre; Lamaddalena, Nicola; Fratino, U. (2010a). Assessing Pressure Changes in an On-Demand Water Performance — Case Study in Italy. *Journal of Irrrigation and Drainage Engineering*, *136(4)*(April), 261–270.

DGADRa. Sistema De Informação De Regadio. Retrieved May 15, 2023, from Sistema de Informação do Regadio, Autoridade Nacional do Regadio, Direção Geral de Agricultura e Desenvolvimento Rural website: https://sir.dgadr.gov.pt/

Esteves, R., Calejo, M. J., Rolim, J., Teixeira, J. L., & Cameira, M. R. (2023). Framework for Assessing Collective Irrigation Systems Resilience to Climate Change—The Maiorga Case Study. *Agronomy*, *13*(3), 661. https://doi.org/10.3390/agronomy13030661

GEE. Platform Google Earth engine. Retrieved May 15, 2023, from https://code.earthengine.google.com/

IPCC. (2014). Climate Change 2014: Synthesis Report. Geneva, Switzerland: Contribution of Working Groups I, II, and III to the Fifth Assessment Report of the Intergovernmental Panel on Climate Change. In *II and III to the fifth assessment report of the intergovernmental panel on climate change* (Vol. 151). (Core Writing Team, R.K. Pachauri and L.A. Meyer (eds.)].

IPMA. Dados meteorológicos. Retrieved May 29, 2023 Instituto Português do Mar e da Atmosfera, website www.ipma.pt

Mourato, S. D. J. M. (2009). Modelação do impacte das alterações climáticas e do uso do solo nas bacias hidrográficas do Alentejo. Tese de Doutoramento. Universidade de Évora.

Rocha, J., Carvalho-Santos, C., Diogo, P., Beça, P., Keizer, J. J., & Nunes, J. P. (2020). Impacts of climate change on reservoir water availability, quality and irrigation needs in a water scarce Mediterranean region (southern Portugal). *Science of the Total Environment*, *736*. https://doi.org/10.1016/j.scitotenv.2020.139477

Rolim, J., Teixeira, J. L., Catalão, J., & Shahidian, S. (2017). The Impacts of Climate Change on Irrigated Agriculture in Southern Portugal. *Irrigation and Drainage*, *66*(1), 3–18. https://doi.org/10.1002/ird.1996

SNIRH. Redes De Monitorização. Retrieved May 15, 2023, from https://snirh.apambiente.pt/

Zhang, Y., Wang, Y., & Niu, H. (2019). Effects of temperature, precipitation and carbon dioxide concentrations on the requirements for crop irrigation water in China under future climate scenarios. *Science of the Total Environment*, *656*, 373–387.

# Assessment of blue water availability for agriculture in the Mediterranean

Luis GARROTE[1], Álvaro SORDO-WARD[1], Paola BIANUCCI[1]

[1] Universidad Politécnica de Madrid, Spain
l.garrote@upm.es

alvaro.sordo.ward@upm.es
paola.bianucci@upm.es

ABSTRACT

This communication focuses on assessing current and future water availability for Mediterranean basins under different policy and climate scenarios. Utilizing high-resolution water resources modeling techniques within a GIS framework, an ensemble of state-of-the-art climate models was employed to project runoff for the Mediterranean over various timeframes. The study compiled diverse datasets on meteorological variables, water resources, runoff, land cover, and population density to create a geospatial database covering river basins draining into the Mediterranean Sea. The database was used to generate high-resolution maps of potential water availability for irrigation using the Water Availability and Adaptation Policy Analysis (WAAPA) model, considering environmental and population needs. Results indicate shifts in hydrological regimes due to expected changes in precipitation patterns, affecting future water availability. This GIS-based approach offers valuable inputs for integrated water resources management and climate change adaptation planning, enabling informed decisions to ensure sustainable water resource utilization in the face of climate uncertainty.

## 1. Introduction

Water availability is a critical aspect of sustainable development and environmental planning, particularly in regions like the Mediterranean, characterized by diverse landscapes and variable climatic conditions. With the advent of climate change, understanding the potential impacts on water resources becomes essential for effective water management strategies. The research described in this communication aims to assess the current and future water availability for the Mediterranean basins under different policy and climate scenarios, utilizing high-resolution water resources modeling techniques integrated within a Geographic Information System (GIS) framework. We employed an ensemble of state-of-the-art climate models to obtain runoff projections for the Mediterranean for current, mid- and late-21st century periods. These climate data were then processed using the GIS-based water resources management model WAAPA to obtain potential water availability under a set of realistic hypotheses.

## 2. Data and methods

This communication presents the data compiled from diverse sources to characterize water availability and water use in the Mediterranean. The data were stored in a geospatial information system that drew information from available global datasets. The geographical scope of the analysis is the river basins draining directly into the Mediterranean Sea, excluding the Nile River. The basins were delimited using the detailed topographical model provided by the Hydrosheds dataset. Data on meteorological variables and water resources in the past and for future scenarios were obtained from the Inter-Sectoral Impact Model Intercomparison Project (ISIMIP3b output datasets). Other geospatial datasets on runoff, soil types, land cover, population density, irrigated areas or crops, were also compiled. These data were combined with national and regional datasets, like AQUSTAT, to obtain a detailed description of the spatial distribution of water resources and agricultural activities across the Mediterranean basin.

The geospatial database was used to produce high-resolution maps of potential water availability for irrigation along the river network of the analyzed domain using the Water Availability and Adaptation Policy Analysis (WAAPA) model. WAAPA can allocate water to environmental flows and several water uses with different

seasonality and reliability requirements, accounting for the regulation provided by reservoirs. The assessment acknowledged ecosystem and population needs and subtracted water allocation to environmental flows and urban water supply before computing water availability for irrigation. Data from reservoirs was obtained from a georeferenced dataset of reservoirs derived from ICOLD World Registry of Large Dams. Hydrological forcing for the WAAPA model was taken from the results of global hydrological models H08 and CWatM, compiled in ISIMIP scenarios. Hydrological models were forced with climate drivers for three historical scenarios (obsclim, picontrol and historical) and three future scenarios (ssp126, ssp370 and ssp585). Hydrological input was validated by comparison with the GRDC dataset and with results from the SIMPA model in Spanish basins. The validation results confirmed the good agreement between H08 and CWatM models and fair agreement between ISIMIP models and SIMPA. Results were better for H08 model than for CWatM model, and for mean annual flow than for seasonality. The conclusion of the validation was that no bias correction was required.

## 3. Results and conclusions

Potential water availability is defined as the maximum demand that could potentially be supplied at a given point in the river network using available reservoir storage for flow regulation, with realistic management that respects environmental flows, satisfying given reliability criteria. The WAAPA model was run for selected historical and future scenarios to provide a high-resolution description of water availability along the Mediterranean rivers. An example of the results in shown in Fig. 1.

The results indicate that expected changes in precipitation patterns will lead to shifts in hydrological regimes across the region that may have a significant impact on future water availability. The GIS-based approach allowed for the identification of areas vulnerable to changes in water availability, providing spatially explicit information along the main rivers of the Mediterranean basin for decision-makers and stakeholders. The high-resolution spatial outputs and detailed water availability estimates presented in this study serve as valuable inputs for integrated water resources management and climate change adaptation planning. By combining advanced GIS-based hydrological modeling and climate scenarios, this research offers a robust framework for assessing water resources under a changing climate, applicable to other regions facing similar challenges. Ultimately, our study provides vital insights for policymakers and stakeholders, enabling them to make informed decisions and devise adaptive measures to ensure the sustainable utilization of water resources in the face of uncertain future climatic conditions.

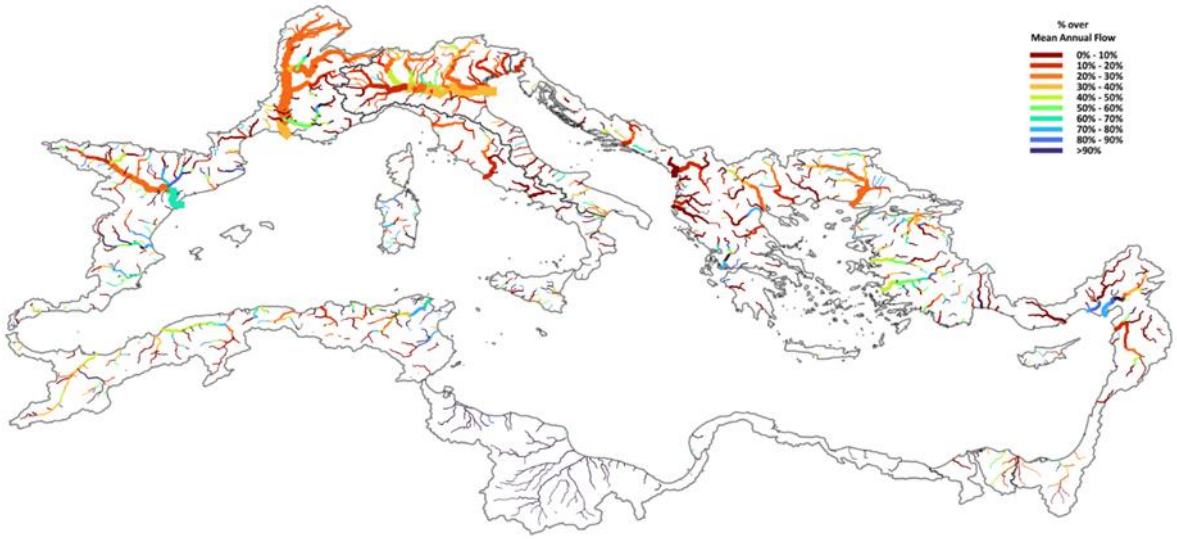



**Fig. 1.** Results of the WAAPA model for the obsclim scenario with CWatM model. Potential water availability expressed as percentage of mean annual flow.

**Acknowledgements**

The research was conducted within the EU-Prima AG-WaMED project. The authors wish to acknowledge financial support from the Spanish Ministry of Science and Innovation through the 2022 International Collaboration Projects Call.

# Fine Scale Rainfall Disaggregation in Greece using RBLRPM

Sofia SKROUFOUTA[1], Evangelos BALTAS[2]

National Technical University of Athens, Greece
sofiaskroufouta@chi.civil.ntua.gr

baltas@chi.civil.ntua.gr

ABSTRACT

The fine-scale disaggregation of rainfall is an essential tool for hydrological applications because of the strong stochasticity that underlies natural hydrological phenomena and the scarcity of available data. In two study areas in Greece, the Random Bartlett-Lewis Rectangular Pulse Model (RBLRPM) is applied for two distinct distributions of the impulse intensity (Gamma and Exponential). The corresponding daily time series will be divided into hourly ones, and the HYETOS-R package will be used to assess the behavior of the alternative distributions based on the required statistical quantities.

## 1. Introduction

Data at fine temporal scales are essential to the accuracy and dependability of many hydrological applications, including the design of drainage systems, reservoirs, and flood control projects. The scarcity of precipitation data on precise time scales, particularly in Greece, is a serious issue. Hydrological applications therefore require the use of stochastic rainfall models at various time scales. These models have the advantage of being able to accurately describe the precipitation process using a limited number of parameters. An important, also, advantage of the RBLRPM is that it manages to adequately capture both the structure of the selected historical statistical parameters, as well as the probability of drought for various time scales, for an exclusive set of parameter values for each month, ensuring the temporal independence of the model.

## 2. Material and Methods

The disaggregation algorithm implemented by the HYETOS-R package is based on the Koutsoyiannis and Onof (2001) algorithm. In order to accurately replicate the historical time series with a larger time scale, the model consists of a Bartlett-Lewis model and an exact correction procedure that modifies the shorter synthetic time series (Grygier, Stedinger, 1988). Applying the adjusting procedure, to optimally compute the statistical parameters, requires a substantial computational effort that is reduced by simulating the time series with shorter periods for rainy events as opposed to the full duration. The assumption that storms follow a Poisson distribution and that there is independence between clustered rain days are two of the highly realistic assumptions that the Bartlett-Lewis model is found to accept. The chosen model in this research is the RBLRPM, which is an improved version of the Bartlett-Lewis Rectangular Pulse Model (BLRPM) (Rodriguez-Iturbe et al., 1988), differing in the way it models the random variable of pulse duration.

An enhanced version of the evolutionary annealing-simplex algorithm (Efstratiadis, Koutsoyiannis, 2002) is used to estimate the unique set of parameters of the Barlett-Lewis model for the two study areas (Thessaloniki and Heraklion), since it is a probabilistic heuristic optimization method that combines the effectiveness of hill-climbing techniques in convex regions with the robustness of rough response surface annealing simulation. The primary characteristic of the algorithm, which is based on the Simplex method, is that none of the moves are completely deterministic, which increases the possible rough search field of the iterative process.

## 3. Results and Discussion

For Thessaloniki, the Gamma distribution appears to fit the best for the driest month (June), but the Exponential distribution appears to preserve better the historical statistical features of the time series for the wettest month (January). The structure of the autocorrelation coefficient is not satisfactorily preserved, even though the Gamma distributions' deviations are not great in the case of the dry probability. Maintaining the structure of the autocorrelation coefficient is a crucial requirement, but the deviations of the coefficients of variation and skewness are comparable to those of an Exponential distribution. For example, the structure of the skewness coefficient and the probability of dry conditions are fully preserved when creating a daily synthetic time series of January assuming an Exponential distribution. The variation coefficient, in particular, appears to be overestimated by the model by 18%, with a 45% deviation from the historical coefficient in the case of skewness (Fig. 1a). Whereas the coefficients of variation and skewness (37% and 38%) are underestimated and deviate more from the historical ones, the deviations of the synthetic statistical characteristics for June seem to be larger than those of the corresponding rainy month and already of the autocorrelation coefficient (Fig. 1b).

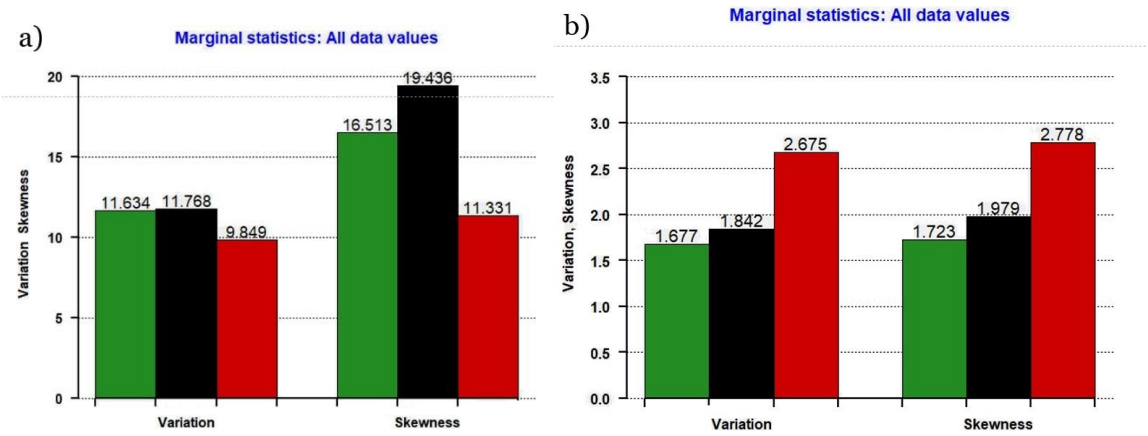



**Fig. 1.** Statistical Characteristics, considering that the intensity of the pulses follows the exponential distribution for: a) January and b) June (the diagrams for the volatility coefficient (left) and the asymmetry coefficient (right))

Conversely, the Gamma distribution is proved to be more appropriate for both months in the Heraklion region, since it maintains more satisfactorily the coefficients of variability and asymmetry, in addition to the structure of the autocorrelation coefficient at the time scales of 1, 6, 12 and 24 hours. Both distributions simulate dry probabilities equally well, fully preserving the structure of the skewness coefficient. For both the wettest and the driest month, the variation's deviation is less than 5% and the skewness is less than 15%. With the largest deviation occurring in the skewness and being only 7%, the model's performance in breaking down the daily synthetic time series into hourly is also very impressive, given that the structure of the statistical characteristics under study is fully preserved.

## 4. Conclusions

Based on this study, for the Greek region, the RBLRPM can preserve the essential statistical properties that control the daily structure of the precipitation and simulate precipitation to multiple aggregation scales using a single set of parameters, regardless of the historical time series' time scale. Specifically, it can preserve the coefficients of autocorrelation, variability, and asymmetry for the entire time series, as well as, for the rainy days individually, while maintaining the likelihood of rain, which is another crucial feature of the precipitation time series. Given that the independent intensities of the rectangular pulses follow a Gamma distribution, the results also demonstrate that most of the months of the study areas in Greece are better simulated. Nonetheless, the time series can also be divided using the Exponential distribution.

**References**

Koutsoyiannis D. and Onof, C., Rainfall disaggregation using adjusting procedures on Poisson cluster model, Journal of Hydrology, 246(1):109-122, 2001, DOI: 10.1016/S0022-1694(01)00363-8

Grygier J. C. and Stedinger J. R., Condensed disaggregation procedures and conservation corrections for stochastic hydrology, Water Resour. Res., 24( 10), 1574– 1584, 1988, doi:10.1029/WR024i010p01574

Rodríguez - Iturbe I., D. R. Cox, F.R.S. and V. Isham, A point process model for rainfall: further developments, Proc. R. Soc. Lond. A 417, 283 – 298, 1988

Efstratiadis, A. and Koutsoyiannis D., An evolutionary annealing-simplex algorithm for global optimisation of water resource systems, Proceedings of the Fifth International Conference on Hydroinformatics, Cardiff, UK, 1423-1428, International Water Association, 2002. (http://itia.ntua.gr/en/docinfo/524/)

# Coastal Adaptation Strategies for Infrastructures: A Global to Local Approach

Javier LARA[1], Alberto FERNANDEZ[2], David LUCIO[3], Maria Alvarez de EULATE[4], Inigo LOSADA[5]

IHCantabria - Instituto de Hidráulica Ambiental de la Universidad de Cantabria, Calle Isabel Torres 15, Santander 39011, Spain

[1]lopezjav@unican.es; [2]alberto.fernandezperez@unican.es; [3]david.lucio@unican.es; [4]maria.fuentes@unican.es; [5]losadai@unican.es

ABSTRACT

Ports, vital for coastal and maritime transport and key economic contributors to coastal regions, face increased criticality to climate change impacts due to their coastal location. This necessitates comprehensive impact assessment approaches to gauge the effects of climate change and rising sea levels on port infrastructure, considering the intricate interplay of climate drivers and the complex mix of structures, equipment, and socio-economic services within ports. Effective port adaptation planning is essential, involving the identification of measures and determining the optimal implementation time and location. This paper presents a robust tool tailored for port planners and decision-makers, enhancing the economic and technical resilience of ports at different scales in the face of climate change. The comprehensive methodology performs a top-down approach in order to first locate ports with the highest adaptation requirements, then conveying a coherent adaptation planning for those of them requiring urgent CC-adaptation portfolios.

## 1.1. Introduction

Climatic factors like rising sea levels, storm surges, waves, and intense winds are expected to impact coastal transportation. These extreme events, intensified by climate change, have the potential to inflict substantial damage on critical coastal infrastructure. Moreover, port services are particularly vulnerable to these climatic stressors compared to the physical assets themselves. Hence, it's imperative to integrate the effects of climate change-induced variability into adaptation assessment frameworks that assess the performance of port assets under the influence of various climatic factors. This inclusion is essential for developing comprehensive sets of measures aimed at mitigating the impacts of climate variability on port infrastructure.

## 1.2. Methodology

In this study, a multi-level risk-adaptation assessment framework is developed to evaluate and diminish CC-derived impacts of port infrastructure systems. At the initial level, we conduct a preliminary risk assessment for all ports, based on a CC-index variation analysis. For those with a moderate to high-risk level, we proceed to a perceived risk evaluation (2nd level), conducting a number of surveys to port stakeholders. Ports with a mild to high-perceived risk then undergo a high-resolution risk analysis (3rd level). Subsequently, we create comprehensive recommendations for developing portfolios of adaptation measures, which shall be general ones for tiers 1 and 2 in the risk assessment, and a high-resolution adaptation assessment for those ports with the highest projected impacts. All the proposed adaptation and recommendations are gathered under a coherent adaptation planning scheme.

Regarding the risk and adaptation assessment approaches, the methodology encompasses the characterization of the hazard, exposure and vulnerability of the evaluated infrastructures (IPCC, 2022). Generally, it evaluates a variety of elements (including coastal structures, port equipment, infrastructures and socio-economic activities) exposed to diverse climatic hazards (waves, storm surge, winds and sea level), through a multi-impact full-probabilistic assessment approach. Evaluation of impacts is based on the relation of those hazards and the exposed elements through vulnerability models (here called impact models). Climate change impacts

are projected, considering two different RCP scenarios and two different timeframes (short and long term) and analyzing its variation in terms of the compliance of technical requirements (Burcharth & Sørensen, 2006; ROM, 2009) and Baseline (historical) conditions. When required, the adaptation assessment of the measures conducts a re-evaluation of the risk and computes its reduction for each of the proposed measures, acting as needed to prevent major failures and disruptions in the assessed infrastructures. For each of the tiers, different granularity is applied to the assessment, which is depicted in *Fig, 1.*

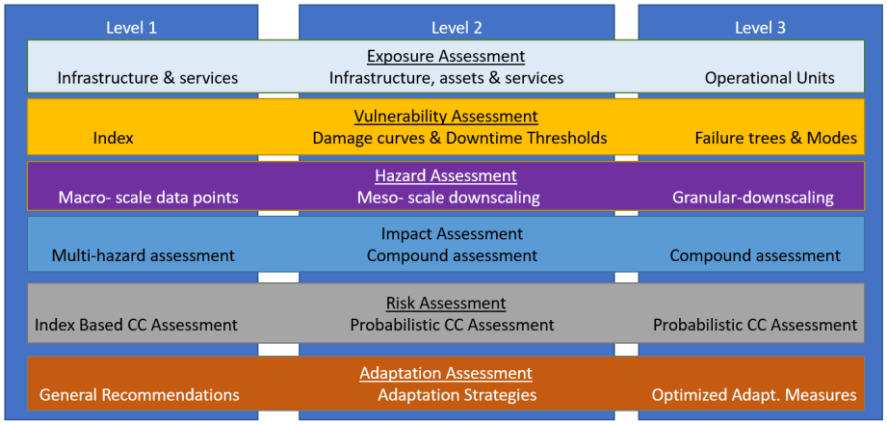



**Fig. 1.** Multi-tier risk-adaptation assessment methodology for port infrastructures.

## 1.3. Study case

This three-step methodology has been applied along the north Spanish coast, involving four regional governments and with the final output of adaptation plans for 126 ports. The outputs of the study includes, on the one hand, an homogenized CC-risk assessment for the set of infrastructures, with different grades of adaptation urgency and severity, This leads to the second output of the study, a global adaptation planning for infrastructures located at the Spanish north coastal façade, encompassing general adaptation measures for the ports with less urgency of adaptation, and precisely located (in space and time) optimized adaptation measures for those ones requiring imminent action.

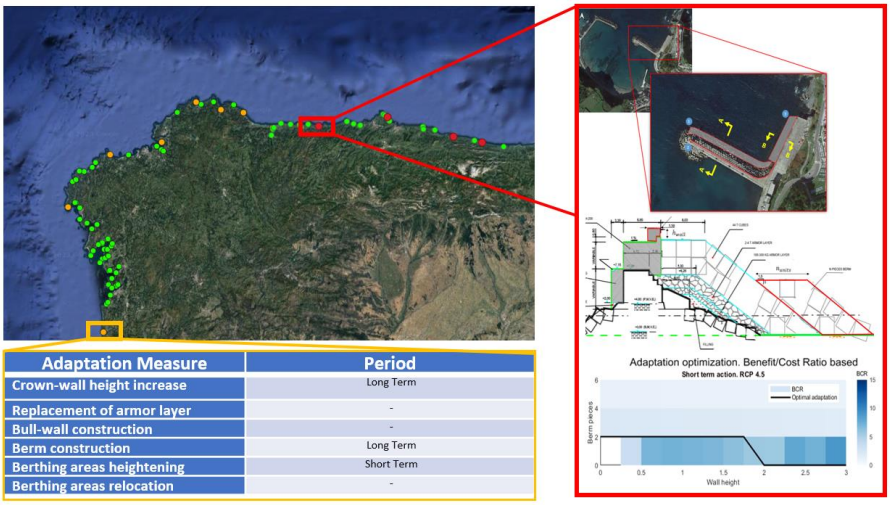



**Fig. 1.** Multi-level Adaptation planning for the study case. In orange, Level 2, mid-resolution Adaptation Strategies. In red, Level 3 high-resolution Adaptation Optimization

Altogether, a robust tool has been developed for planers and decision makers to prioritize actions based on risk assessment that account for CC and SLR affection on port infrastructure's at a macro to micro scale, ensuring economical and technical solidity to ports and resilience against climate change.

**References**


Burcharth, H. F., & Sørensen, J. D. (2006). *On Optimum Safety Levels of Breakwaters* (Vol. 2).
IPCC. (2022). *AR6 Impacts, Adaptation and Vulnerability. Technical Report*. 20–22.
ROM. (2009). *Recomendaciones del diseño y ejecución de obras de abrigo. ROM 1.0-09.*

# Mapping inundation of estuarine margins driven by ocean and fluvial forcings

André B. FORTUNATO[1], Paula FREIRE[1], Ana RILO[1], Teresa VISEU[1], Marta RODRIGUES[1]

[1] National Laboratory for Civil Engineering, Portugal
{afortunato, pfreire, arilo, tviseu, mfrodrigues}@lnec.pt

ABSTRACT

Inundation maps are required for spatial planning. This paper describes the generation of inundation maps for the margins of the upstream region of the Tagus estuary (Portugal). Maps are constructed separately for a major river flood and an extreme storm surge, and then combined. The impact of sea level rise is also assessed.

## 1. Introduction

Spatial planning for territories located on the margins of water bodies requires inundation maps for both present and future conditions. Estuarine margins are a peculiar case, as they can be inundated by either oceanic phenomena, namely spring tides combined with storm surges, or extreme river flows. The dominant cause of inundation varies spatially: river floods dominate in the upper estuary, while floods of oceanic origin are preponderant downstream. To generate inundation maps for a municipality at the upstream limit of the Tagus estuary, flood events of oceanic and river origin are simulated separately. The final flood maps are generated by combining information for floods of oceanic and river origins.

## 2. Methods

Inundation maps were generated with a 2DH implementation of the shallow water model SCHISM (Zhang et al., 2016), including its wind-wave module WWM. The model domain (Fig. 1a) extends from the ocean to 90 km upstream, including all the areas that can potentially be flooded in the Vila Franca de Xira municipality located in the upper estuary. The grid resolution varies between 10 m in some floodable areas to 2000 m at the ocean boundary. Because this resolution is insufficient to represent narrow dikes, a row of nodes is placed over the crest of the dykes. The model is forced by tides, surges, waves, atmospheric pressure, wind and river flow (Fortunato et al., 2017). Elevation root-mean square errors are of the order of 5-20 cm for a one-year period (Fig. 1b). The model was also validated for extreme events, including a river flood with a return period of 100 years and a major storm with large waves. Past inundation occurrences were used for the spatial validation of the model results.

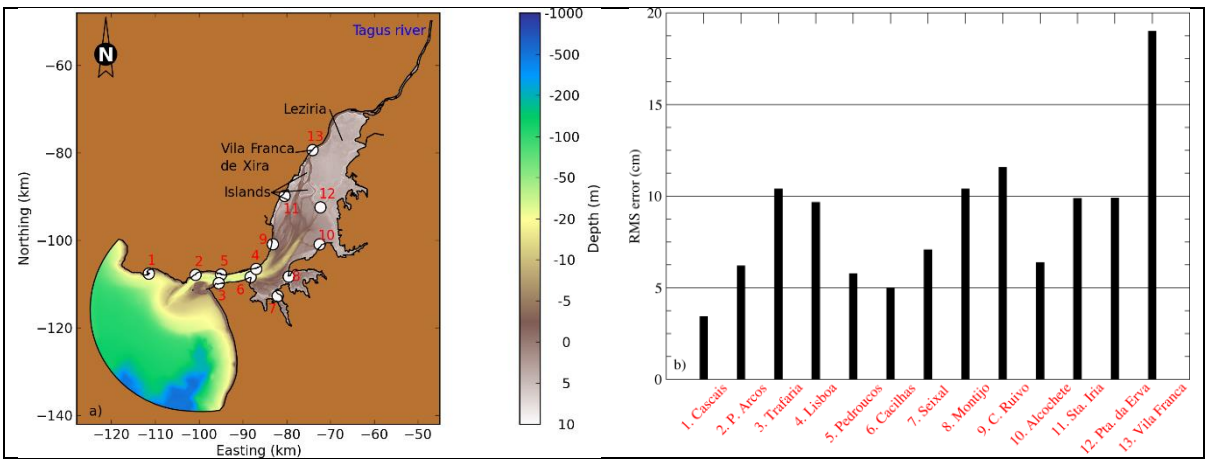



**Fig. 1.** Estuarine model: a) domain and bathymetry – the orange points indicate nodes located on the crest of the dykes; b) model validation

Inundation maps were generated for two events with return periods of the order of 100 years: the February 1941 cyclone, and the February 1979 river flood. Atmospheric conditions for the 1941 were provided by an application of the model WRF-ARW forced by the 20th Century Reanalysis (20CRv2). These conditions were also used to force the wave model WW3 in the North Atlantic to provide the wave boundary conditions for the estuarine model (Fortunato et al., 2017). Atmospheric pressure, offshore significant wave height (Hs) and river flow reached 952 hPa, 14 m and 4500 $m^3/s$, respectively. For the 1979 flood, the hydrograph at the river boundary was obtained by routing the hydrograph gauged at the Almourol staff, 40 km upstream. Observations from another staff gauge were available closer to that boundary, but the rating curve was only defined inside the main channel. For river flows above 2200 - 4000 $m^3/s$ (depending on the sediments accumulated in the riverbed), that rating curve is inadequate because the river spills onto the flood plain. Atmospheric pressure, Hs and river flow reached 998 hPa, 6 m and 15100 $m^3/s$, respectively.

## 3. Results and discussion

Inundation maps for the two extreme events described above were produced for the present mean sea level and assuming a 1.5 m sea level rise (Fig. 2). For each mean sea levels, the maps for the two events were combined by assuming the worst of the two scenarios at each location.

For the present mean sea level, the inundation of ocean origin includes the three islands, 15.5 $km^2$ in the left margin of the Tagus, and 4.1 $km^2$ in the right margin. For the river flood case, the Lezíria is partially flooded from upstream, and the three islands are also partially or totally flooded. In the right margin, the inundation is significantly smaller than for the storm surge case.

Considering an additional 1.5 m rise in mean sea level, the extent of the inundation increases drastically. The Lezíria and the three islands are totally inundated in the storm surge scenario. The extreme water levels increase from 2-3 m to about 4 m. This growth is due not only to the direct effect of the higher sea level, but also to an increase in the amplification of tidal amplitudes by resonance (Guerreiro et al., 2015). Flooding of ocean origin becomes more severe than the one of fluvial origin.

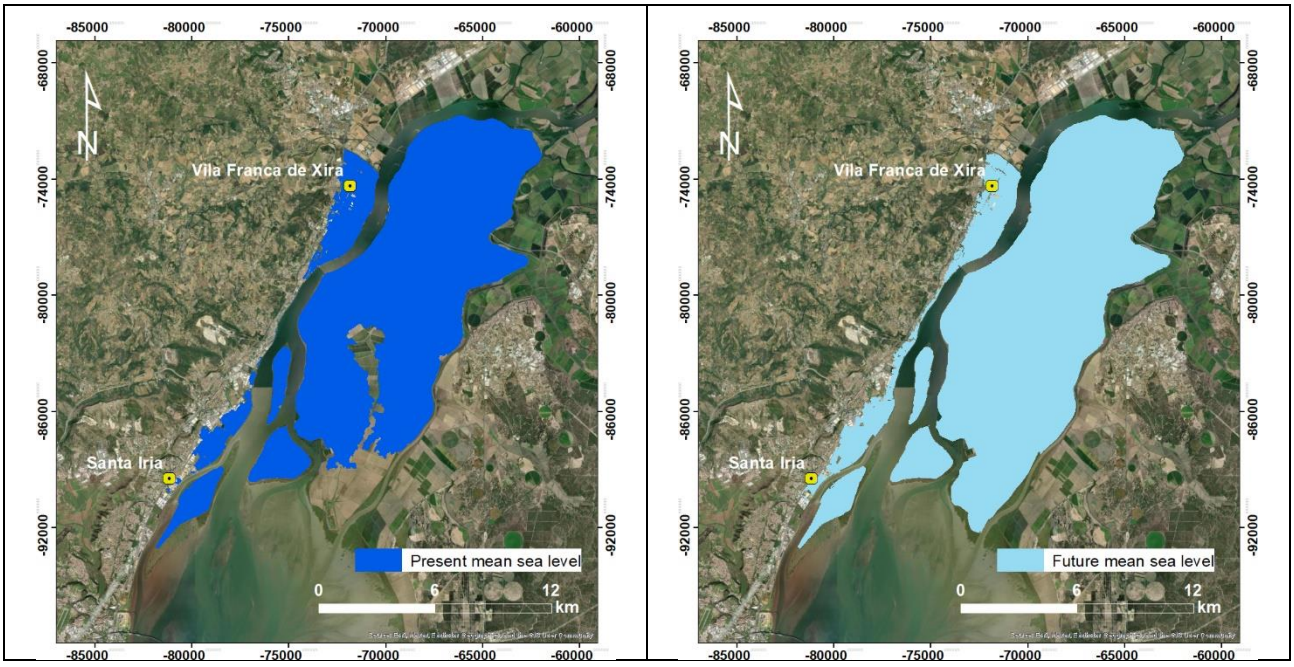



**Fig. 2.** Combined inundation of ocean and river origins in the upper Tagus estuary for the present and future mean sea levels

**Acknowledgements**

This study was funded by the Vila Franca de Xira Municipality.

**References**

Fortunato AB, Freire P, Bertin X, Rodrigues M, Ferreira J, Liberato ML (2017) A numerical study of the February 15, 1941 storm in the Tagus estuary, Continental Shelf Research 144, 50-64

Guerreiro M, Fortunato AB, Freire P, Rilo A, Taborda R, Freitas MC, Andrade C, Silva T, Rodrigues M, Bertin X, Azevedo A (2015) Evolution of the hydrodynamics of the Tagus estuary (Portugal) in the 21st century, Journal of Integrated Coastal Zone Management 15/1, 65-80

Zhang YJ, Ye F, Stanev EV, Grashorn S (2016) Seamless cross-scale modeling with SCHISM, Ocean Modelling 102, 64-81

# Flash flood risk assessment in data scarce regions vulnerable to climate change: Hydrological lessons learnt from Jordan

Clara HOHMANN[1], Christina MAUS[2], Hanna LEBERKE[3], Ahmad AWAD[4], Peter HOFFMANN[5], Dörte ZIEGLER[6]

[1,2,6] Koblenz University of Applied Sciences, Germany
hohmann@hs-koblenz.de, maus@hs-koblenz.de, ziegler@hs-koblenz.de

[3] Institute for Technical and Scientific Hydrology (itwh GmbH), Germany
h.leberke@itwh.de

[4] Institute for Social-Ecological Research (ISOE), Germany
ahmad.awad@isoe.de

[5] Potsdam Institute for Climate Impact Research (PIK), Germany
peter.hoffmann@pik-potsdam.de

## ABSTRACT

Jordan is one of the water-scarcest countries worldwide but is simultaneously vulnerable to extreme heavy rainfall events which can lead to severe flash floods. These hydroclimatic hazardous events might change in intensity and/or frequency due to climate change and/or land use land cover (LULC) changes that in turn could aggravate flash flood risks (IPCC, 2021). The BMBF-funded German-Jordanian research project “Capture and reTain heavy rainfall in Jordan” (CapTain Rain, www.captain-rain.de) studies flash flood risks and vulnerability with a transdisciplinary approach, interacting with local stakeholders. In this study, we want to analyze heavy rainfall events and flash flood hazards while highlighting necessary adaptations in data and water scarce regions such as Jordan compared to assessments conducted in Germany (DWA, 2016).

To understand the past and potential future scenarios including climate and LULC changes, we employed various hydrological and hydraulic models, including the Hydrological Modeling System of the Hydrologic Engineering Center within the U.S. Army Corps of Engineers (HEC-HMS), and the hydraulic model HE2D/FOG2D. A multi-model approach was adopted for enhanced analysis and uncertainty estimation, essential for effective hazard assessment in Jordan's data-scarce context. Even though runoff data for calibration is missing, a hydroclimatic overview about the effects of feasible changes is possible with the multi-model approach and flood marks for validation. The effects of changes in rainfall pattern and LULC can thus be compared.

Historical rainfall events were analyzed in our study region Amman, the capital of Jordan. Beside local station data we included hourly satellite rainfall estimates (GSMaP) as well as daily global and regional reanalyses (ERA5, UERRA) to provide longer time series and partly higher time resolution. As a result, we saw sometimes considerable discrepancies between the different products, not only within the intensity, but also with the timing of reported extreme rainfall events. At regional scale, these data products describe the spatial and seasonal occurrences of heavy rainfall patterns according to observations. For the future we can see a probable increase of rainfall amounts for short events with high annualities. Beside our baseline scenario with 5.5 h intense period of the February 2019 heavy rainfall event, we therefore also analyze three different rainfall scenarios: moderate (baseline + 20 % climate change effect), intense (27 h event, only station with highest rainfall intensity) and catastrophic (27 h event, 300 mm which is around the yearly rainfall amount).

Beside the climatic input, we analyzed the spatio-temporal dynamics of LULC changes. Past and present LULC conditions were generated using remote sensing imageries from Corona, SPOT1-5, Landsat 5-7, and Sentinel-2. Spatio-temporal drivers of LULC change were used to predict future LULC conditions using a MLP-Markov Chain model. This analysis demonstrated that built-up surfaces increased 10-fold from 1968 to

2021 from a mere 20 km² to 223 km². Simulated built-up areas in 2050 are expected to increase by around 70 % mainly at the expense of rangelands, see Fig.1.

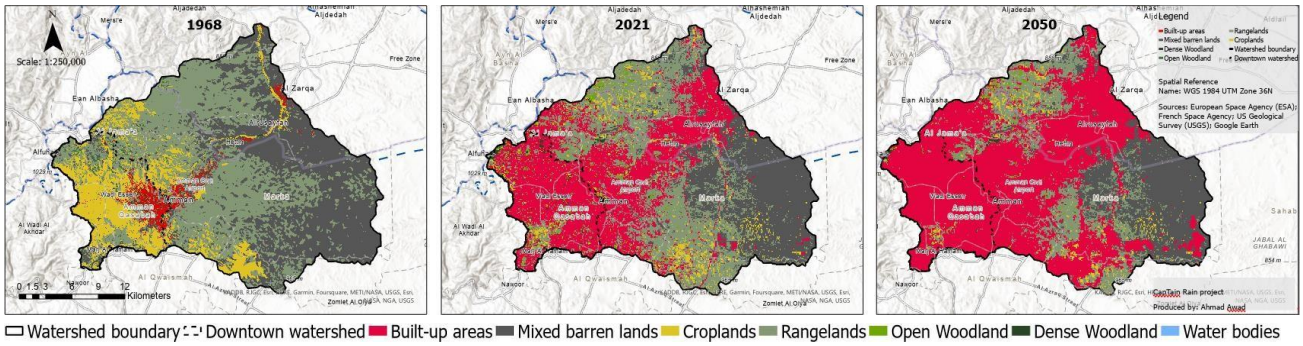



**Fig. 1.** Observed and predicted LULC changes for our study region Amman, Jordan from 1968 to 2050.

Figure 2 shows the results of the hydrological simulation runs with four different rainfall scenarios (see above), respectively with three different LULC datasets (Fig. 1), always shown as percentage change of peak runoff at the catchment outlet in comparison to the run with baseline rainfall and present LULC as input. The results show that the change in rainfall has a higher influence than the changes in LULC based on the analyzed scenarios. The more extreme rainfall events predicted for the future in combination with more urbanized areas strongly increase the modelled runoff. The catastrophic event, with drastic increase of peak runoff was included to identify further flood prone areas and possible precautionary measures.

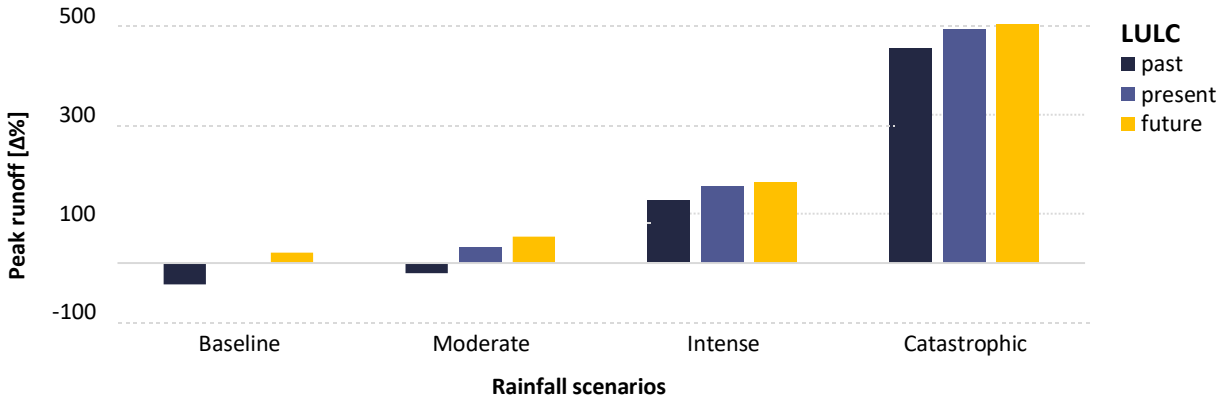



**Fig. 2.** With the hydrological model HEC-HMS simulated rainfall scenarios and respectively with the LULC datasets of the past – 1968, present – 2021, and future – 2050, calculated differences to run with baseline rainfall and present LULC in percent change of peak flow.

The data scarcity in Jordan is one of the most challenging aspects when assessing flash flood risks, but we could show how open source data sets can be combined with local knowledge to further create usable datasets, e.g. for precipitation, infrastructure, geoinformation, or LULC. The risk analysis methodology used in Germany can be transferred to Jordan, even though there are big discrepancies in data availability, resulting mainly in higher uncertainties in model results. Nevertheless, our findings strengthen the knowledge of the local stakeholders for future decisions and support the development of measures to reduce flash flood risks in Amman.

**Acknowledgements**

The project "CapTain Rain – Capture and ReTain Heavy Rainfalls in Jordan" is funded by the German Federal Ministry of Education and Research (BMBF) as part of the funding measure "CLIENT II – International Partnerships for Sustainable Innovation" in the context of the framework program "Research for Sustainable Development" (FONA). Project duration: 01.06.2021 – 31.07.2024.

**References**

DWA (2016) Risikomanagement in der kommunalen Überflutungsvorsorge für Entwässerungssysteme bei Starkregen, November 2016, German Association for Water, Wastewater and Waste, Hennef, Germany 55 pp.

HEC-HMS Hydrological Modeling System of the Hydrologic Engineering Center within the U.S. Army Corps of Engineers (HEC-HMS), www.hec.usace.army.mil/software/hec-hms/ (last excesses 12.10.2023)

HE2D/FOG2D Hydraulic Model by itwh https://itwh.de/en/software/desktop-software/urban-flash-floods/ (last excesses 12.10.2023)

IPCC (2021) Climate Change 2021: The Physical Science Basis, Contribution of Working Group I to the Sixth Assessment Report of the Intergovernmental Panel on Climate Change, Ed.: Masson-Delmotte, V., P. Zhai, A. Pirani, S.L. Connors, et al. Cambridge University Press, Cambridge, United Kingdom and New York, NY, USA, doi:10.1017/9781009157896.

# A mechanical-based calibration for a rapid vulnerability assessment of masonry buildings subject to floods

Francesco Salvatore LIGUORI[1], Giovanna CAPPARELLI[2] , Antonio MADEO[3], Pasquale VERSACE[4]

[1,2,3,4] Department of Computer Science, Modelling, Electronics and Systems Engineering, University of Calabria, Rende, Italy
francesco.liguori@unical.it email:
giovanna.capparelli@unical.itemail:
antonio.madeo81@unical.it email:
linoversace@unical.it

ABSTRACT

The frequency and the extension of high intensity flood events are expected to increase in the nearest future because of to the intensification of the hydrological cycle caused by the climate change (Tabari (2020)). Therefore, the development of risk assessment strategies, aimed at quantifying the flood risk of large areas is a research topic of great relevance. Masonry buildings represent a structural typology that could be highly vulnerable to the action of high intensity floods. In fact, the masonry walls generally lack of out-of-plane strength and, if subject to high intensity hydraulic forces (Marvi (2020)), can undergo severe damage or collapses that can compromise the overall stability of the structure.

In order to cope with this problem, in this work we propose a rapid tool for the risk assessment of masonry structures subject to floods (Capparelli et al.(2023)). The proposed strategy is based on the estimation of a risk class, through the calculation of a simplified damage level (DL) that is a function of two indices, namely a Hazard Index (HI) and a Vulnerability Index (VI). Both indices are linear combinations of scores and weights assigned to some indicators of the event, for HI, and of the intrinsic structural features (VI). One of the key aspects of the proposed approach resides in its calibration that is carried out by adopting the results of numerical simulations.

The numerical simulations, based on a Finite Element model of the masonry building, are first employed to detect the most significant parameters. Subsequently, a large population of buildings and events is generated using a Monte Carlo approach and analysed. Finally, the best fit between the DL estimated by the proposed method and that evaluated through the numerical simulations is found.

The accuracy of the proposed method is tested by comparing the obtained results with those provided by the accurate numerical simulations. Then, the method is applied to assess the vulnerability to three different floods of the buildings located near the river Esaro, in the municipality of Crotone, Italy. The application of the method has required input data easily obtained through outdoor site visits and by consulting available census database. The results can help to identify the most at-risk buildings, providing valuable guidance on necessary mitigation or retrofitting measures.

**References**

Capparelli G, Liguori F.S., Madeo A and Versace P. (2023) A rapid numerical-based vulnerability assessment method for masonry buildings subject to flood, International Journal of Disaster Risk Reduction 97, 104001.
Marvi M.T. (2020) A review of flood damage analysis for a building structure and contents, Natural Hazards 102 (3), 967-995
Tabari H. (2020) Climate change impact on flood and extreme precipitation increases with water availability, Scientific Reports 10 (1) 13768.

# On development of extreme rainfall intensity-duration-frequency relations for urban water infrastructure design in the climate change context

Van-Thanh-Van NGUYEN[1]

[1] Department of Civil Engineering, McGill University, Canada
van.tv.nguyen@mcgill.ca

ABSTRACT

Most countries in the world have significant investments in urban water infrastructures (e.g., storm drainage and flood management systems). Every day, people rely on these systems to protect lives, property, and natural water environment. These infrastructures have reduced the vulnerability of the cities, but at the same time could make them more vulnerable to climate extremes, due to the lack of consideration of what might occur when the design criteria are exceeded. Furthermore, recent assessment reports on climate change have indicated a worldwide increase in the frequency of extreme weather events because of global warming. Consequently, research on developing innovative approaches for limiting and adapting climate change impacts on urban water infrastructures is highly critical due to the substantial investments involved. However, it has been widely recognized that the main difficulty in dealing with climate change impacts for urban water infrastructure design is "how to estimate accurately the changes in the extreme rainfall processes at the urban basin scale projected by global/regional climate models because these models do not contain an adequate description of the governing physical processes at relevant high temporal and spatial resolutions as required by the impact and adaptation studies". This necessitates some form of downscaling of the climate model simulations from a coarse spatial resolution (20 – 250 km) down to much finer spatial grids, and even point values if changes in local extreme rainfall processes are to be assessed. In addition, the required time scales for assessing the climate change impacts on the urban hydrologic processes are usually less than one day. Therefore, the overall objective of this paper is to provide an overview of some recent advances and shortcomings in the downscaling of extreme rainfall processes in the climate change context from both theoretical and practical viewpoints. Another focus of this work is on the development of a technical guide to provide some guidance to water professionals in Canada on how to consider the climate change information in the design of urban water infrastructures (CSA, 2019).

More specifically, extreme rainfalls for short time scales (less than one day) are commonly used for estimating the "design storm" for the design of various urban infrastructures. This design storm is computed from the "intensity-duration-frequency" (IDF) relations, which provides extreme rainfall intensities for various durations and return periods at a given site of interest (CSA, 2019). In current engineering practice, the IDF relations are derived based on statistical frequency analyses of available annual maximum (AM) rainfall series for different durations. However, these AM rainfall records for sub-daily durations are often limited or unavailable at the location of interest while those for the daily scale are widely available. Hence, it is necessary to develop innovative methods for modeling extreme rainfall processes over a wide range of time scales such that information related to sub-daily extreme rainfalls could be inferred from the available daily extreme rainfalls in the context of a changing climate. In Canada, Environment and Climate Change Canada (ECC) provides short-duration extreme rainfall data for nine different rainfall durations (D = 5, 10, 15, 30, 60, 120, 360, 720, and 1440 minutes) and the IDF relations for approximately 650 stations across Canada with at least 10-year rainfall record. Traditionally, the extreme rainfalls for six different return periods (T = 2, 5, 10, 25, 50, and 100 years) were computed by fitting the two-parameter Gumbel distribution to the AM series for each rainfall duration independently using the method of moments (MOM). However, it has been widely known that this Gumbel/MOM-based traditional approach may not produce accurate and robust extreme rainfall estimates as compared to those given by, for instance, the Generalized Extreme Value (GEV)/L-Moment method (Nguyen et al. 2017). Consequently, there are several recently developed IDF products in Canada. The

key differences between these products are: (i) the different probability models that were selected for describing the distribution of extreme rainfalls; (ii) the different estimation methods that were used for estimating the probability model parameters; (iii) the different regression models that were chosen to represent the IDF curves; (iv) the different estimation methods that were used for estimating the regression model parameters; (v) the different spatial interpolation techniques that were used for transferring IDF information from gaged sites to the target ungaged location; and (vi) the different considerations of the scale-invariance property of the extreme rainfall processes for different rainfall durations. Hence, a detailed comparative study was carried out to assess the performance of the traditional and newly developed rainfall estimation methods to identify the best approach for use in practice for deriving the IDF relations in Canada. In general, the traditional methods were based on the relationships between the extreme rainfall quantiles with the rainfall durations while the new approaches were relied on the scale-invariance relationships between the statistical moments of extreme rainfalls and the rainfall durations. It has been demonstrated that the traditional methods were less accurate than the new scale-invariance approaches in the estimation of extreme design rainfalls (Nguyen and Nguyen, 2020). Hence, the proposed scaling GEV model can be used for updating at-site IDF relations as well as regional extreme rainfall maps for urban infrastructure design for Canada (Fig.1). In summary, it is expected that the development of improved at-site IDF relations and regional extreme rainfall maps as presented in this study could provide more cost-effective design of urban water infrastructures in Canada.

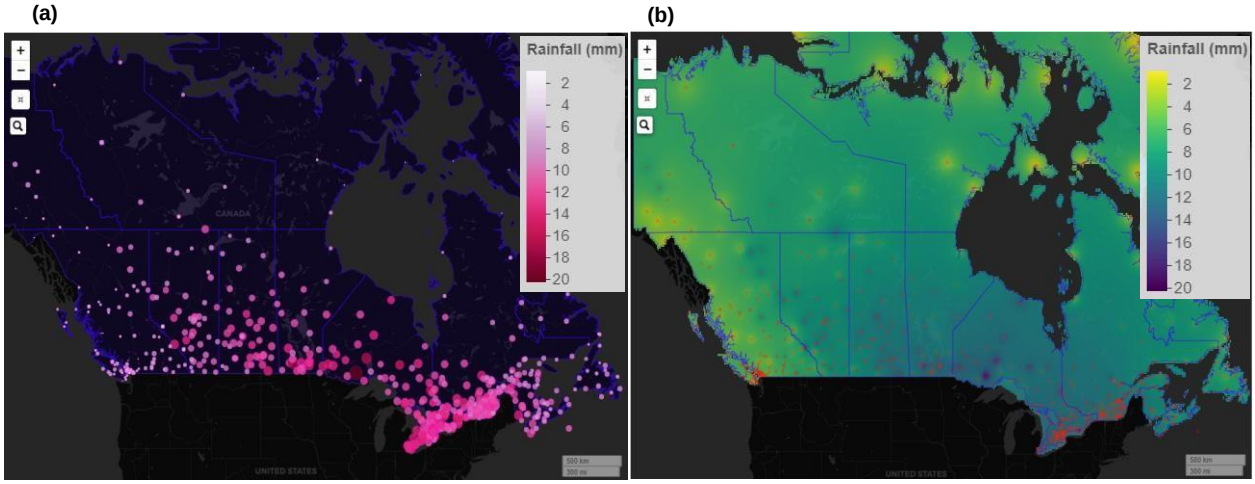



**Fig. 1.** An example of (a) point-scale and (b) grid-scale extreme design rainfalls of 5-minute duration and of 10-year return period. For (a), at-site rainfall depths are represented in the form of circle markers with continuous diameter and color scales (larger diameters and darker colors represent higher values). For (b), rainfall depths are plotted using continuous color scale (darker colors represent higher values) while locations of control points are represented with red dots.

**Acknowledgements**

The author would like to acknowledge the funding support provided by Natural Science and Engineering Research Council Canada (Discovery Grant) for this project.

**References**

CSA (Canadian Standards Association) (2019) Technical guide: Development, interpretation, and use of rainfall intensity-duration-frequency (IDF) information: Guideline for Canadian water resources practitioners. CSA PLUS 4013:19, 126 pages.
Nguyen T.-H., El Outayek S., Lim S.H., Nguyen V.-T.-V. (2017) A systematic approach to selecting the best probability models for annual maximum rainfalls – A case study using data in Ontario (Canada). Journal of Hydrology, 553: 49-58.
Nguyen T.-H., Nguyen V.-T.-V. (2020) Linking climate change to urban storm drainage system design: An innovative approach to modeling of extreme rainfall processes over different spatial and temporal scales. Journal of Hydro-environment Research, 29: 80-95.

# Anthropogenic disaster vulnerability in European rivers

Paweł M. ROWIŃSKI[1,5], Monika B. KALINOWSKA[2],
Tomasz OKRUSZKO[3], Piotr PARASIEWICZ[4], Vilmos JÓZSA[6]

[1,2] Institute of Geophysics, Polish Academy of Sciences, Poland
p.rowinski@igf.edu.pl
monika.kalinowska@igf.edu.pl

[3] Institute of Environmental Engineering, Warsaw University of Life Sciences, Poland
tomasz_okruszko@sggw.edu.pl

[4] National Institute for Fisheries Research, Poland
p.parasiewicz@infish.com.pl

[5] IAHR Europe Division Leadership Team
[6] Hungarian University of Agriculture and Life Sciences, Fisheries Research Centre Hungary
jozsavilmos57@gmail.com

ABSTRACT

In the presented study on anthropogenic disaster vulnerability in European rivers, the focus was on global environmental challenges of anthropogenic origin, which significantly impact human health, the state of the environment, and the economy. Special attention was given to European rivers. Example case studies were analysed: the first one concerned the 2022 Odra River catastrophe, resulting from a multitude of factors, including sewage discharges and low flows. The second was a description of the catastrophic 2000 Baia Mare cyanide spill, affecting multiple Central and Eastern European countries. The third case discussed the release of toxic sludge from the Ajka alumina plant in 2010. The study also highlighted issues related to river management and monitoring. The conclusions underscored the pivotal role of human factors in all the described disasters, emphasising the necessity of monitoring and the implementation of alarm systems in regions vulnerable to such threats.

## 1. Introduction

World faces various environmental disasters, and many of them have anthropogenic origins. Those disasters around the world have caused significant health, environmental, and economic damages. Such tragedies have also led to lengthy legal challenges and prompted new regulations. Many of them were related to aquatic environment. We cannot say in Europe that we are free from such risks. In this study, we concentrate on rivers and threats caused by humans, although in many cases, a combination of natural circumstances and mismanagement problems are the core of the problem.

## 2. Cases studies

### *2.1. The Odra River (2022)*

This review has been directly motivated by an unprecedented and the largest 21st-century environmental disaster in Poland in the summer of 2022. As a result, most likely of combination of natural and human factors, dozens of tons of fish and other organisms have died in the Odra River, the second longest Polish river on the border between Poland and Germany. Experts point to, among other things, sewage discharges and modified hydromorphology as likely causes of the disaster. Among the many factors that may have contributed is a prolonged, very low water level in regulated river bed that has increased the river's vulnerability to incoming pollution. The second factor is wastewater discharges containing nutrient compounds, especially nitrogen and phosphorus, which are essential for phytoplankton growth and greatly accelerate the process, and discharges of saline industrial or mine water, which may have been the direct

cause of the proliferation of so-called golden algae, which produce toxins that kill fish and other gill-breathing fauna. It is obviously not the only example revealing strong vulnerability of rivers due to anthropogenic threats.

### *2.2. The Baia Mare Cyanide Spill (2000)*

Definitely one of the most catastrophic disasters that ever happened in Europe was the one from 2000 when the Baia Mare gold mine in Romania spilt about 130 thousand cubic meters of cyanide into the Lupes, Somes, Tisza, and Danube Rivers. The spill decimated aquatic and plant life for dozens of miles, affecting local fishing industries and impeding access to drinking water for residents of Serbia, Hungary, Romania, and Bulgaria for several months. In April 2000, an estimated 1241 tonnes of fish were killed in the affected rivers. Interestingly, the river has recovered faster than expected. Bathing was possible soon after the pollution had subsided, and by 2002 the population of lower organisms (mussels, dragonflies, crabs, crustaceans) had recovered, and within 3-4 years 95% of the aquatic fauna had returned to the Szamos and Tisza. At the very beginning that catastrophe caused a huge debate, which resulted in the proposal of the European Parliament to ban cyanide use in mining across the EU, but the European Commission has never implemented the ban.

### *2.3. The Ajka Alumina Plant Disaster (2010)*

Another extreme example is from October 4, 2010 when the dam of the alumina factory reservoir near Ajka burst and one million cubic meters of toxic, corrosive red sludge flooded Kolontar, Devecser, Somlóvásárhely and the surrounding 40 square kilometers. Ten Kolontar residents died in the disaster and 123 people suffered severe burns from the highly alkaline, corrosive substance. Diluted by the protective measures, the pollution entered the Marcal, then the Rába and finally the Danube via the Torna stream. The Torna and the Marcal river practically wiped out the entire living world, not a single bacteria or even aquatic plants survived, while the Mosoni-Duna was protected by reducing the alkaline chemistry. The red sludge spillage also poisoned about a thousand hectares of land in the Ajka area.

## 3. Lessons Learned and Recommendations

In the analysed cases, the mix of natural reasons (extreme events of flood or drought) and human errors led to the catastrophes. The stress test for the significant potential polluters should be provided, additional operational monitoring introduced, and crisis management plan implemented in order to minimise the risk of significant human and environmental losses. Methods from the broad area of environmental hydraulics should be used for the assessment and improvement of river status (Rowiński et al., 2022). Very specific lesssons, e.g. from levee engineering were also learned, say Ajka Alumnia Plant Disaster taught us that the embankmenets should be designed in a way limiting the impact on the groundwater flow whereas the catastrophe in the Tisza River revealed the serious mistake in the construction of its levees - type and condition of soils in levee body and condition of levee areas (inter-levee and landside) play the most important role for levee safety. The Odra catastrophe triggered the continuous development of the 24-hour monitoring system not only in that river but also in other major Polish rivers. New guidelines in surface water testing methodology are elaborated and also procedures for monitoring the so-called golden algae are being implemented.

## 4. Conclusions

Multiple factors caused all the discussed catastrophes, but poor management was a driving force in every case. Each of the disasters mentioned above is due to direct or indirect human influence on the natural system, so it cannot be claimed that they had a natural cause. In each of the above cases, there were also monitoring problems; no alarm model was in operation in these locations. One can also find positive examples in Europe with the working Rhine Alarm Model and the development of similar tools for the Meuse and Danube rivers. Such models are able to calculate the development of the wave of pollutants after their accidental release and constitute an excellent tool in risk management practices.

**Acknowledgements**

MB Kalinowska and PM Rowiński were supported within statutory activities no. 3841/E-41/S/2023 of the Ministry of Science and Higher Education of Poland.

**References**

Rowiński PM, Okruszko T, Radecki-Pawlik A. (2022) Environmental hydraulics research for river health: recent advances and challenges, Ecohydrology & Hydrobiology, 22,2, 213-225 https://doi.org/10.1016/j.ecohyd.2021.12.003

# Numerical study to quantify the role of morphological parameters in the coastal flooding: Zarautz beach

Aritz ABALIA[1,2], Iñaki DE SANTIAGO[1], Roland GARNIER[1], Pedro LIRIA[1], Irati EPELDE[1], Asier NIETO[1], Denis MORICHON[2]

[1] AZTI Marine Research, Basque Research and Technology Alliance (BRTA), Spain
aabalia@azti.es; idsantiago@azti.es; rgarnier@azti.es; pliria@azti.es; iepelde@azti.es; anieto@azti.es
[2] Université de Pau et des Pays de L'Adour, UPPA, France; denis.morichon@univ-pau.fr

ABSTRACT

The interaction of hydrodynamic conditions and beach morphology may modify the coastal flooding and hence the hazard level for natural values and coastal facilities. So far, the knowledge on how the hydrodynamic and beach morphology interactions affect the coastal flooding is scarce. Here, the performance of a process-based hazard level forecasting modelling chain is assessed and then applied to different storm scenarios and morphological profile configurations in a highly urbanized beach (Zarautz, Basque coast). The aim of the present study is twofold; first, the validation of the modelling chain and its application to obtain a database of compound flooding scenarios; and second, the quantification of the influence of morphological parameters on the coastal flooding intensity under different storm scenarios through statistical approaches.

## 1. Introduction

The coastal flooding associated to storms represents a critical challenge with significant consequences for both natural environments and human societies. By comprehensively understanding the parameters that influence coastal flooding and their interaction, decision-makers can develop more effective strategies to mitigate and manage the consequences of coastal flooding. The difficulties associated with acquiring and maintaining flooding field data over large periods derive into the use of alternative approaches. For instance, de Santiago et al., 2024 shows that process-based numerical models could generate reliable flooding results as they consider the influence of climatic and morphologic parameters including the presence of coastal defenses.

The aim of the present study is to validate a modelling chain and implement it for different compound flooding ("compound" in the sense of compound influence of beach morphology and hydrodynamics) scenarios to obtain the associated hazard levels and quantify the influence of morphological parameters on the coastal flooding intensity under different storm scenarios through statistical approaches.

## 2. Study site and dataset

Zarautz beach is a 2 km long highly urbanized beach located on the Basque coast (northern Spain). This embayed beach is divided into two distinct sectors: i) a natural zone formed by sand dunes and ii) an urban zone backed by a vertical seawall that is used as a promenade (Fig. 1b). The latter will be the object of study.

Hydrodynamic data is based on hourly measurements from 2004 until 2023 of offshore directional wave spectrums available at the Bilbao-Vizcaya wave buoy, moored in 580 m water depth and water level (WL) from the Bilbao-Vizcaya tide gauge. Morphological data is obtained analysing the evolution of coastal videometry indicators along 13 years of data (Liria et al., 2021), such as the berm height (BH), dry beach width (DBW), the foreshore slope (tanB) and sandbars position (SP), and from measured topobathymetric data (3 Mar 2021) of the study site from the promenade until 30 m depth. Hazard level data is obtained by means of coastal videometry through the number of overtopping events detected at timestacks images (Gaztelumendi et al., 2016). The modelling chain is composed by 3 modules: (1) a spectral wave model (SWAN) to propagate offshore wave conditions up to 19 m depth off the study site, (2) a process-based phase-resolving model

(XBeach NH) to compute the mean overtopping discharge in a 1D profile at the promenade and (3) a hazard level estimation table based on the computed mean overtopping discharge (Garzon et al., 2023).

## 3. Methods

The modelling chain is validated by comparing the computed hazard levels (inputting the measured topobathymetric profile and offshore wave directional spectrums) against the observed hazard levels by the videometry station during 28 observed events between 23 Feb 2021 – 1 Apr 2021. The hazard levels are described as: Level 0 (green) represents no damage, Level 1 (yellow) no major damage expected, Level 2 (orange) severe damage to non-structural elements and Level 3 (red) structural damage.

Then a compound flooding database is generated by running the validated modelling chain for different storm scenarios and synthetic morphological profiles. Storm scenarios are identified offshore between 2004 and 2023 following the methodology proposed by Gaztelumendi et al., 2016. Since the modelling chain coastal hazard computation for each identified storm scenario offshore would be computationally expensive, these are clustered into bins, in a 3D rectangular grid, represented by Hs, Tp and WL values. Synthetic morphological profiles are generated through the combination of the previously described morphological parameters.

## 4. Preliminary results

The modelling chain validation is shown in Fig. 1a for the 28 observed storms. The validation shows accurate forecasting of hazard levels with a recall of 0.6, precision of 0.75, accuracy of 0.89 and f1 score of 0.66 for calibrated parameters. There is a single case where the computed hazard level underestimates by 2 the observations. It corresponds to the storm 25 (red rectangle in Fig. 1a), the unique storm that occurs when the subaerial zone of the morphological profile is eroded (Fig. 1b, the red rectangle shows a berm height decrease from storm 24 to 25). In this storm, because of not inputting the eroded "real" pre-storm profile into the modelling chain, it underestimates the observed hazard level, highlighting therefore the need of considering morphological changes to compute with accuracy the coastal flooding.

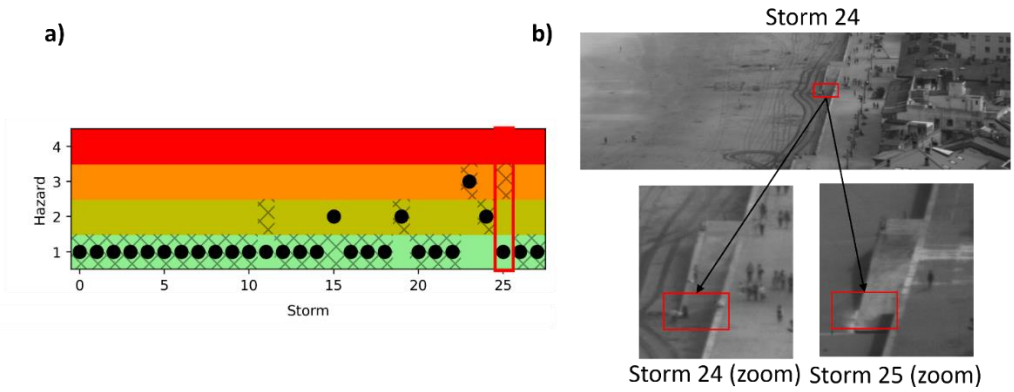



**Fig. 1.** Modelling chain validation with observed hazard levels at the observed 28 storms (23 Feb-1 Apr 2021). a) Hazard levels comparison. Black dots represent the hazard level computed through the modelling chain. Hatched lines represent the hazard level observed through coastal videometry. b) Snap images of the study area the moment before storms 24 and 25. Red rectangles represent the same position.

The validated modelling chain will be implemented to obtain the hazard level at 27 identified offshore storm scenarios with different Hs, Tp and WL combined with 3 synthetic profile configurations composed by different BH, DBW, tanB and SP. This will lead into a compound flooding database of 81 simulations. This database will then be assessed obtaining the significance of each morphological parameter into coastal flooding under different storm scenarios through a statistical approach.

**Acknowledgements**

This study has been supported by the KOSTARISK joint laboratory and the PLEC2022-009362 (MCIN/AEI/10.13039/501100011033 and European Union Next GenerationEU/PRTR), Urban Klima 2050 – LIFE 18 IPC 000001 project (funded by the European Union's LIFE program) and Regions4Climate (Horizon Europe, DOI: 10.3030/101093873) projects.

**References**

de Santiago I, Plomaritis TA, Avalos D, Garnier R, Abalia A, Epelde I, Liria P (2024). Comparison of wave overtopping estimation models for urban beaches. Towards an early warning system on the Basque coast. Science of The Total Environment, 912, 168783.
Garzon JL, Ferreira O, Reis MT, Ferreira A, Fortes CJEM, Zózimo AC (2023). Conceptual and quantitative categorization of wave-induced flooding impacts for pedestrians and assets in urban beaches. Scientific reports, 2023, vol. 13, no 1, p. 7251.
Gaztelumendi S, Egaña J, Liria P, González M, Aranda JA, Anitua P (2016). The new Euskalmet coastal–maritime warning system. Advances in Science and Research, vol. 13, p. 91-96.
Liria P, Epelde I, de Santiago I, Garnier R, Abalia A, Mader J (2021). KOSTASystem, a coastal videometry technology: development and applications. In 9th EuroGOOS International conference.

# Evaluation of combined fluvial, coastal and pluvial flooding using a data-driven enhanced physically-based model: A Case Study in NW Spain

Luis CEA[1], Carlos A. FIGUEROA[2], Juan F. FARFÁN-DURÁN[3], Jerónimo PUERTAS[4], Javier SOPELANA[5], Paula CAMUS[5], Jared ORTIZ-ANGULO[5], Fernando MÉNDEZ

[1,2,3,4] Water and Environmental Engineering Group, Center for Technological Innovation in Construction and Civil Engineering (CITEEC), Universidade da Coruña, 15071, A Coruña, Spain.
luis.cea@udc.es, carlos.fcastillo@udc.es, j.farfan@udc.es, jeronimo.puertas@udc.es
[5] Aquatica Ingeniería Civil S.L.36202, Vigo, Spain
jsopelana@aquaticaingenieria.com
[6,7,8] Geomatics and Ocean Engineering Group, Departamento de Ciencias y Técnicas del Agua y del Medio Ambiente, Universidad de Cantabria, Santander, Spain.
paula.camus@unican.es, jared.ortizangulo@unican.es, fernando.mendez@unican.es

ABSTRACT

Catastrophic floods often manifest a compound dimension, with the interaction of various climatic factors like astronomical tides, storm surges, waves, rainfall and river flow. While these elements may act independently, they are frequently interconnected sharing the same meteorological origin. Several efforts have been performed at regional, continental, or global scale to quantify the flooding potential using statistical approaches that quantify the dependence among drivers (Bevacqua et al., 2019; Ward et al., 2015; Couasnon et al., 2020; Camus et al., 2021). These approaches serve as an initial screening tool, providing insights that inform more detailed risk assessments. However, at the local level, a more intricate framework comes into play, involving the integration of diverse hydrologic, ocean and hydraulic numerical models. This integration follows a one-way nesting approach, where each model operates independently, utilizing specific data inputs that then feed into subsequent models. Despite the effectiveness of this linking model approach, its application has been largely limited to specific/historical events due to the substantial computational demands involved. Furthermore, the computational efforts required for probabilistic risk assessments, which rely on multi-year simulations, are notably time-consuming, adding an additional layer of complexity to the overall modeling process.

This study introduces a hybrid local approach for modelling compound flooding in the coastal town of Ponteceso, located inside the Anllon's estuary in a macrotidal coastal riverine area in the Northwest coast of Spain. Ponteceso was born and developed occupying part of a marsh of the estuary and protected from sea level by levees. Besides, part of the town locates below the high tide mean level and is surrounded by drying salt marshes, which adds complexity to the flooding processes. The town suffers compound flooding triggered by the interplay of Anllon's river discharge from a 392 km2 basin that flows through the southern part of the town and interacts with sea level due to astronomical and meteorological tides, and local rainfall-runoff originated from an 18 km² basin located to the north of the town.

The proposed approach combines a physically-based 2D inundation model with AI techniques that are used to generate synthetic time series of the forcing variables and a surrogate model of the 2D inundation model (Jhong et al., 2017; Bermúdez et al., 2019), in order to reduce substantially the computational burden for the inundation simulations. A similar hybrid approach has been previously employed in analogous studies (Sopelana et al., 2018), demonstrating its efficiency in modelling long-term water depth series when dealing with specific drivers (e.g., river discharge, astronomical tide, storm surge) in regions characterized by complex bathymetry. In this case study precipitation is introduced as a new flood driver to the method, enhancing the model's capacity to accurately estimate adequate inundation dynamics of the site (Fig.1).

The outcomes of our study enable a quantitative assessment of compound flooding on a local scale. The synthetic time series of flooding drivers and the hybrid methodology used for the estimation of the inundation extents makes possible the characterization of the risk without the necessity of relying on a limited number of return period events. The hydraulic inundation modeling, executed using the Iber software, utilized inputs and boundary conditions specific to each compound case, resulting in 2D maps of the water depth and velocity in the study area. While a substantial number of simulations were undertaken, the computational burden was not a limiting factor in terms of time, given the GPU implementation of Iber (García-Feal et al., 2018). The primary time investment lay in constructing the hydrodynamic model, which must run coherently with the case scenarios.

The results contribute to advancing our understanding of compound flooding in estuarine areas and rivers influenced by tidal dynamics, particularly with the inclusion of rainfall as a new driver. The continuous methodology, putting together 2D hydrodynamic modeling with surrogate models, has demonstrated notable consistency and robustness, especially in dealing with the intricacies of complex compound flooding of the pluvial-fluvial-coastal dimension. This approach stands out as a compelling alternative to prevailing methods, which often exhibit a tendency to overestimate inundation water depths and flood maps.

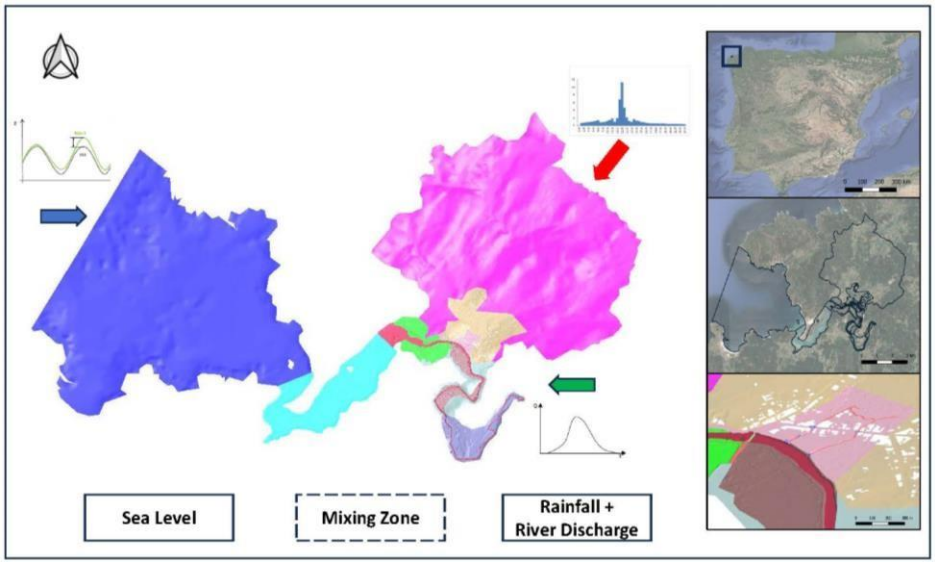



**Fig. 1**. Extent of the inundation model including the forcings considered, and location of the case study.

**Acknowledgements**

This study was received financial support from the Spanish Ministry of Science and Innovation (MCIN/AEI/10.13039/501100011033) and from the European Union-NextGenerationEU/PRTR, within the project "MyFlood: Multi-scale hybrid short term predictions and climate change projections system for compound flooding (MyFlood)" (PLEC2022-009362. C17. I3. BDNS 632932).

**References**

Ward, P. J., Couasnon, A., Eilander, D., Haigh, I. D., Hendry, A., Muis, S., Veldkamp, T. I. E., Winsemius, H. C. and Wahl, T. (2018). Dependence between high sea-level and high river discharge increases flood hazard in global deltas and estuaries, Environ. Res. Lett., 13(8), 084012

Bevacqua, E., Maraun, D., Vousdoukas, M.I., Voukouvalas, E., Vrac, M., Mentaschi, L., Widmann, M.: Higher probability of compound flooding from precipitation and storm surge in Europe under anthropogenic climate change. Science Advances, 5 (9), art. no. eaaw5531, 2019.

Couasnon, A., Eilander, D., Muis, S., Veldkamp, T.I.E., Haigh, I.D., Wahl, T., Winsemius, H.C., Ward, P.J.: Measuring compound flood potential from river discharge and storm surge extremes at the global scale. Natural Hazards and Earth System Sciences, 20 (2), pp. 489-504, 2020.

Camus, P., Haigh, I.D., Nasr, A.A., Wahl, T., Darby, S.E. and Nicholls, R.J. (2021) Regional analysis of multivariate compound coastal flooding potential around Europe and environs: sensitivity analysis and spatial patterns. Natural Hazards Earth Systems. Science Discussion., 21, 2021–2040. https://doi.org/10.5194/nhess-2021-50.

Jhong B-C, Wang J-H, Lin G-F (2017) An integrated two-stage support vector machine approach to forecast inundation maps during typhoons. J Hydrol 547:236–252. https://doi.org/10.1016/j.jhydrol.2017.01.057.

Bermúdez, M., Cea, L., & Sopelana, J. (2019). Quantifying the role of individual flood drivers and their correlations in flooding of coastal river reaches. Stochastic Environmental Research and Risk Assessment, 33(10), 1851–1861.

Sopelana, J., Cea, L., & Ruano, S. (2018). A continuous simulation approach for the estimation of extreme flood inundation in coastal river reaches affected by meso- and macrotides. Natural Hazards, 93(3), 1337–1358. https://doi.org/10.1007/s11069-018-3360-6

García Feal, Orlando & Cea, Luis & González-Cao, & Domínguez, J.M. & Gómez-Gesteira. (2020). IberWQ: A GPU Accelerated Tool for 2D Water Quality Modeling in Rivers and Estuaries. Water. 12. 413. 10.3390/w12020413.

8th IAHR EUROPE CONGRESS
LISBON - PORTUGAL
4-7 JUNE 2024

# Assessing compound flooding hazards in estuaries by integrating a climate emulator and a hybrid model

Jared ORTIZ-ANGULO[1], Paula CAMUS[2], Fernando MÉNDEZ[3], Sonia CASTANEDO[4], Mirian JIMÉNEZ[5], Laura CAGIGAL[6], Beatriz PÉREZ-DÍAZ[7]

[1,2,3,4,5,6,7] Universidad de Cantabria
jared.ortizangulo@unican.esemail:
paula.camus@unican.es email:
fernando.mendez@unican.esemail:
sonia.castanedo@unican.es email:
mirian.jimenez@unican.es email:
laura.cagigal@unican.es email:
beatriz.perez@unican.es

ABSTRACT

The statistical distribution of compound flooding extents at coastal river deltas is the result of the non-linear interaction and co-occurrence of combination of multiple oceanographic, hydrologic, geologic and meteorological forcings (e.g. astronomical tides, monthly mean sea level, large-scale storm surge, dynamic wave set-up, river discharge, surface runoff). To address this complex problem and to manage with models that are highly computationally expensive, we propose a hybrid statistical-dynamical framework approach that combines: (a) climate-based statistical downscaling techniques; (b) a new version of the climate-based emulator TESLA (Cagigal et al., 2020); and (c) a metamodel based on Delft3D simulations. The proposed framework has been tested at the Santoña Estuary, or estuary of the river Asón, located in the northern Spain.

## 1. Motivation

Many coastal settlements are located in estuaries where flooding can result from oceanographic sources (e.g. tides, storm surges and waves), but also from river discharge (fluvial) and direct surface runoff (pluvial). These drivers are typically causally linked through associated storms, and may therefore occur simultaneously or in close succession, exacerbating the impact of flooding. Historical observations of these multivariate drivers represent only a small fraction of the possible range of conditions capable of causing adverse flooding consequences. Therefore, a joint probability method is needed to generate many synthetic extreme multivariate events (tides, storm surge, precipitation and river discharge). On the other hand, a numerical model is required to simulate the interactions between river discharge and downstream sea level in estuaries. However, these models are typically too computationally expensive to dynamically simulate the new full parameter space of oceanographic and pluvial/fluvial conditions.

## 2. Methodological framework

In this study, a hybrid statistical-dynamical framework is proposed to efficiently predict spatially varying estuarine water levels and inundation areas for assessing compound flooding hazard, see Fig.1. A new version of the climate-based emulator TESLA (Cagigal et al., 2020) is used to generate new compound flooding events by identifying their relationship with a set of weather types representing different large-scale atmospheric pressure patterns. The use of weather types allows for analyzing the historical climate variability and provides insights into the spatial and temporal variability in the region.

This climate emulator is coupled to a metamodel, similarly to Anderson et al. (2021), based on Delft3D simulations, in this case, to emulate water levels and flood inundation under any combination of tidal, storm surge and river discharge conditions. This fast and efficient method to predict estuarine hydrodynamics is

based on selection, and interpolation techniques (Camus et al., 2011) reducing the computationally intensive cost of classical dynamical modeling.

## 3. Results

The application of the proposed methodological framework at the Santoña Estuary requires the parametrization of the problem. We have considered the following seven parameters: tidal range, storm surge, river discharge hydrograph: defined by the peak and base discharge, rising and falling limb, and the time lag between river discharge and storm surge.

The new version of the climate-based emulator TESLA, (1) produces synoptic weather patterns based on sea level pressure fields, sea level pressure gradients component and 500 hPa geopotential height, in the selected area (Daily Weather Types, left - Fig.1.) ; (2) defines the relationship between weather patterns and local predictands (i.e., precipitation) (Daily Weather Types, right - Fig.1.); (3) fits an autoregressive logistic regression model to drive weather type chronology, considering variability at season to interannual time scales based on large-scale predictors; and (4) generates synthetic time series of plausible conditions for the seven variables in which the problem is parameterized, using Gaussian copulas and Monte Carlo simulations (Tesla - Fig.1.).

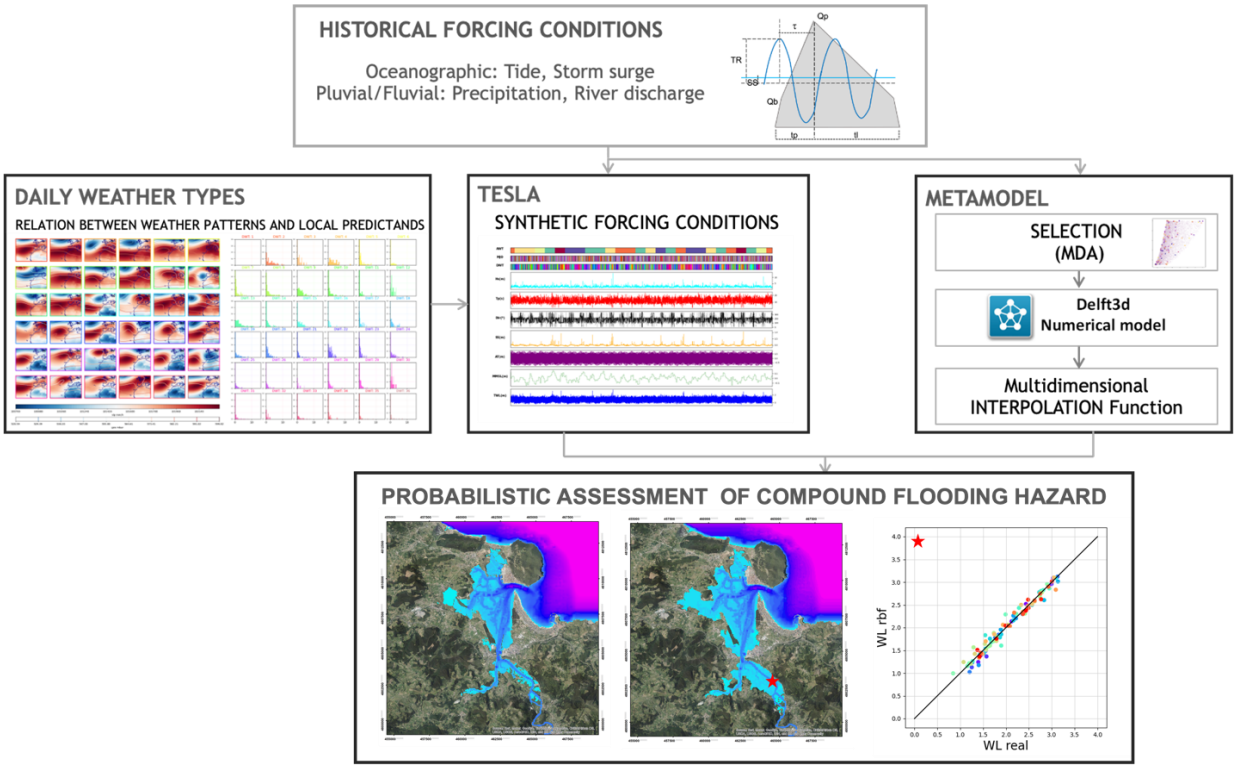



**Fig. 1.** Methodological framework for assessing compound flooding hazards in estuaries.

The first step of the metamodel consists of selecting a reduced number of cases to be simulated using Delft3D. Two flooding maps at the Santoña estuary corresponding to two simulated cases, both at neap tides, are shown in the lower panels of Fig.1. The differences between the two are in the magnitude of the river discharge and storm surge. The map on the left is generated by a discharge and surge of small intensity, while the map on the right is due to a combination of extreme values. The metamodel requires fitting a radial basic function based on the selected parameters for any considered output (e.g., water level or flooding area) obtained from the simulations. As an example, and preliminary result, the scatter plot shows the comparison between the water level obtained from 100 simulations at the marked location in the flooding map and the water level obtained using a metamodel fitted for this output.

**References**

Cagigal L, Rueda A, Anderson D, Ruggiero P, Merrifield MA, Montaño J, Coco G, Méndez FJ (2020) A multivariate, stochastic, climate-based wave emulator for shoreline change modelling, Ocean Modelling, Volume 154, 101695, ISSN 1463-5003
Anderson DL, Ruggiero P, Méndez FJ, Barnard PL, Erikson LH, O'Neill AC, Merrifield M, Rueda A, Cagigal L, Marra J (2021) Projecting climate dependent coastal flood risk with a hybrid statistical dynamical model, Earth's Future, 9, e2021EF002285
Camus P, Méndez FJ, Medina R (2011) A hybrid efficient method to downscale wave climate to coastal areas. Coastal Engineering, Fuel and Energy Abstracts. 58. 851-862.

# The Gloria storm January 2020, a state-of-the-art compound event

Montserrat LLASAT-BOTIJA[1,2], Maria Carmen LLASAT[1,2], Raül MARCOS-MATAMOROS[1], Maria AGUILERA VIDAL[3], Marc SANUY[3], Herminia I VALDEMORO, Salvador CASTÁN[1], José A. JIMENEZ[3]

[1]Department of Applied Physics, University of Barcelona, Barcelona, Spain
[2]Water Research Institute, University of Barcelona, Barcelona, Spain
mllasat@meteo.ub.edu, carmell@meteo.ub.edu, rmarcos@meteo.ub.edu, castan@agpericial.es
[3]Laboratori d'Enginyeria Marítima, Universitat Politècnica de Catalunya·BarcelonaTech, Barcelona, Spain
maria.aguilera.vidal@upc.edu, marc.sanuy@upc.edu, herminia.valdemoro@upc.edu, jose.jimenez@upc.edu

ABSTRACT

## 1. Introduction

Floods are the natural hazard with the greatest impact in the Mediterranean area. Since 1900, they have caused more than 85 billion euros in damages (MEDECC, 2021). Sometimes this hazard does not occur in isolation but together with other hazards such as sea storms, snowfalls or landslides. When these hazards affect different areas simultaneously, or when several of them occur in a common time interval, they are referred to as compound events. According to Zscheischler et al. (2020), four types of compound events can be distinguished: preconditioned, multivariate, temporally compounding and spatially compounding.

A paradigmatic case of compound events is Gloria storm. From January 19 to 25, 2020, it ravaged the Spanish Mediterranean coast, leaving a lasting impact due to its unprecedented magnitude and simultaneous array of hazards. This multi-compound event brought heavy rainfall, floods, high winds, sea storm, surge and even snow across the Mediterranean Spanish coast. From all of this, the storm Gloria stands as a prime illustration of complex compound events. Its multi-hazard nature, the cumulative and enhanced impacts, and the diverse requirements for disaster management -both during and after the event- underscore its significance as a state-of-the-art example. Thus, it exhibited characteristics of preconditioned, multivariate, temporally and spatially compound events, along with cascading effects.

## 2. Objectives

This analysis aims to present the characteristics of the event by examining specific situations in the affected area throughout the event. Our focus will be on tracing the entire source-pathway-consequence-management cycle with an emphasis on the identification and characterization of the various components that contributed to the observed impacts.

## 3. Study area and methodology

The study focuses on the peninsular Mediterranean coastal area of Spain (Fig. 1). To characterise the hazard, the spatio-temporal distribution of precipitation, wind and waves during the episode has been analysed, based on information provided by AEMET and the SIMAR model database. To assess the impacts, compensation data provided by the Spanish Reinsurance Consortium (CCS) has been used, as well as information obtained from other sources such as the 112 emergency service, the press and reports on the event.

## 4. Main results

***Record rainfall (over 400 mm) and wave height (over 7.5 m) were recorded during the event***. The study area experienced record-breaking cumulative precipitation, with approximately 50% of the stations recording more than 100 mm and 20% exceeding 200 mm. In particular, some places in Alicante and Girona experienced maximum precipitation values exceeding 500 mm each, despite being approximately 800 km apart from south to north. This distance between the locations underscores the large spatial scale of the event.

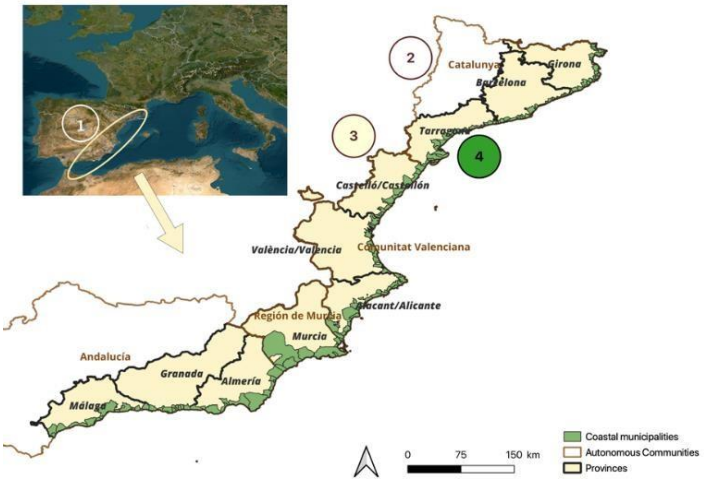



**Fig. 1.** Map of the study area showing (1) Spain, (2) Autonomous Communities, (3) Provinces, (4) Coastal municipalities.

**The economic cost for Spain as a whole exceeded 140 million Euros (zone 1, Fig. 1).** Significant damages resulted from the various hazards, with river overflow and storm waves emerging as the primary drivers causing infrastructure damage. Roughly 75% of the coastal municipalities along the Spanish Mediterranean coast experienced varying degrees of impact. Conversely, wind and rainfall played significant roles in causing harm to private properties and small urban infrastructures. To highlight the extent of these damages, the CCS paid approximately 150 million Euros in compensation for insured properties alone. This figure is indicative of the extensive impact, yet it does not encompass all losses. In addition, several breakwaters along the Catalan coast suffered structural damages, while a railway bridge over the Tordera River collapsed, disrupting train services. Tragically, the event left to 14 fatalities and 2 missing individuals.

**The hazards act simultaneously but in different places, distributing the impact throughout the territory due to their simultaneous occurrence in remote places. An increase in spatial extension means an increase in the risk and impacts, overwhelming the capacity of emergency response services.** In terms of risk management, various emergency plans for floods, wind and snowfall were activated within each affected community, alongside the European Copernicus Emergency Management Service. To illustrate the demand, Catalonia alone received more than 15,000 emergency calls through the 112 telephone number, resulting in more than 8,000 interventions by firefighters. The post-disaster recovery efforts were protracted, influenced by several factors including the onset of the Covid-19 pandemic (officially declared in Spain in March 2020), the extensive damages sustained, particularly in some infrastructures, and administrative inefficiencies. As an example, the repair of the Tordera bridge was completed by November 2020 (incurring a cost of approximately €10 M). Restoration works on damaged groins in Barcelona beaches and other affected breakwaters along the Catalan coast began in July 2020. Yet, by 2022, some damages in affected areas remained unrepaired.

**Five case studies have been selected to illustrate the different types of compound events:** a) preconditioned (previous erosion on beaches); multivariate compound events (river floods and sea floods); temporally compounding (consecutive floods in Murcia); spatially compounding (floods in Catalonia); cascading effects (bridge destruction in the Tordera River).

**Key elements have been identified to assess the impact**: the exposure and vulnerability of the infrastructures, the social and economic differences across the territory, the temporal evolution of the hazards and the synergies between them, and the emergency management.

**Acknowledgements**

This research has been done in the framework of the C3Riskmed research project. Grant PID2020-113638RB-C21, C22 funded by MCIN/AEI/ 10.13039/501100011033.

**References**

MedECC (2020) Climate and Environmental Change in the Mediterranean Basin – Current Situation and Risks for the Future. First Mediterranean Assessment Report [Cramer, W., Guiot, J., Marini, K. (eds.)] Union for the Mediterranean, Plan Bleu, UNEP/MAP, Marseille, France, 632pp, ISBN 978-2-9577416-0-1, doi: 10.5281/zenodo.4768833.

Zscheischler, J., Martius, O., Westra, S., Bevacqua, E., Raymond, C., Horton, R. M., van den Hurk, B., AghaKouchak, A., Jézéquel, A., Mahecha, M. D., Maraun, D., Ramos, A. M., Ridder, N. N., Thiery, W. and Vignotto, E.: A typology of compound weather and climate events, Nat. Rev. Earth Environ., 1(7), 333–347, doi:10.1038/s43017-020-0060-z, 2020.

# Stress test scenarios as a useful addition to a risk approach

Karin DE BRUIJN, Kymo SLAGER, Bart VAN DE HURK

[1] Deltares, Delft, The Netherlands.
karin.debruijn@deltares.nl
Kymo.slager@deltares.nl
Bart.vdHurk@deltares.nl

ABSTRACT

Flood-prone areas are home to societies who developed the areas, used them for agriculture, built cities and prospered. Over time, these societies have developed strategies to cope with flood hazards. Recently, however, floods seem to happen more frequently and cause more severe impacts. In recent years, floods caused by climate extremes and outliers have surprised the inhabitants of flood-prone areas, also in developed areas like western Europe. The strategies who protect them seem not adequate anymore. Whether this results from climate change, or a short memory of the citizens in the flood-prone areas, or due to land use changes is not completely clear and probably differs per case. However, it indicates that more attention for those outliers or extremes is needed (Merz, 2015).

An important trigger for more attention for outliers in the Netherlands was the 2021 flood event caused by severe long-duration rainfall in summer in the Netherlands, Belgium and the Netherlands. The event was caused by unusual large-scale weather pattern which created a lot of moisture flowing in from a very large area (Kreienkamp, 2021). In the Netherlands, the consequences in the affected area were severe, but luckily no fatalities occurred. In Belgium and Germany more than 200 people were killed and many houses and infrastructure networks were damaged (ENW, 2021). This event came as a surprise: this type of large-scale rainfall event was in the Netherlands not considered in any risk approach, nor was it included in the 10.000 years of generated weather series for the Meuse River, the main river in the area, or included in procedures for response or crisis management (Asselman, 2022; ENW, 2021). In fact, the high-water/flood risk season is the winter and usually summer is used for repairs, maintenance and the warning and emergency services are then not alert. Therefore, water authorities were not well-prepared and had to challenge their experts to cope as well as possible and reduce impacts and rescue inhabitants.

The event is also considered a wake-up call for other areas in the country (De Bruijn & Slager, 2022). Policy makers and other have started taking actions to improve the resilience of the Netherlands for such large-scale rainfall event by improving awareness, better preparation, land use adaptation, increasing the sponge behaviour of areas, adaptation of critical infrastructure and improving crisis management procedures (Min, I&W, 2022).

To cope with flood risks the Netherlands has adopted a risk approach in which all potential events should be considered and weighed according to their probability of exceedance. However, this risk approach had a very strong focus on selecting the economic optimal design standard for water systems. Beyond-design events, with smaller probabilities, received little attention. Measures not related to adapting the water system were often found inefficient and therefore, not selected. As a consequence, strategies for adaptation of land use, or flood impact mitigation in general and for enhancing recovery are rarely implemented. This makes the country less resilient to extreme events that go beyond design standards of water systems.

Understanding of what may happen if beyond-design events occur, the potential flood extent and resulting water depths and flood durations, the impacts on the functioning of critical infrastructure, on agriculture and on cities is lacking. In December 2022, the government published recommendations stating that because prevention of flooding may not always be possible, preparation and adaptation must be better taken care of.

The risk information available was found not sufficient for preparing and implementing flood preparation and adaptation measures. It was found too complex for non-experts. It often consists of aggregate numbers and maps resulting from technical analyses of many model runs with a lot of assumptions and has little meaning to the common practice of local and regional authorities and stakeholders. This hampers them to discuss the link to their procedures and makes it difficult to discuss the need for adaptation or preparation measures.

Therefore, another additional approach was adopted called "stress testing". In this approach only one or a few scenarios are analysed in depth and the probability is only provided as a very wide range ("beyond design but feasible"). The consequences both direct and indirect, are analysed and discussed with many different relevant stakeholders such as local governments, provinces, water authorities, emergency management organisations, spatial planners, critical infrastructure operators, and also shared with the public.

In this approach the scenarios or events are stepped through and paused at various moments in time starting by the first signs and warning, then during the actual rainfall or flooding itself, next at the process of getting the water out the flooded areas and finally during the recovery phase. Those scenarios are not forecasts, but they help to discuss what can and should be done, increase understanding of the responsibilities and roles of different organisations and also reveal the questions and information needs they have. Those scenarios or stresstests are "just" selections out of a set of all potential events considered in the risk approach, but by focusing on just them, they serve as a communication vehicle (De Bruijn & Maas, in prep.).

The stresstests cannot be used for cost-benefit analyses, or to evaluate the embankments or water systems. They are not replacing but adding to more common approaches. For beyond-design events (which are also included in risk approaches but with a small weight) measures are needed which reduce impacts and enhance recovery and for those type of measures typically other institutes and citizens are needed and not water authorities. For such measures a storyline which enhances understanding and communication is thereofore crucial (De Bruijn et al., 2017).

In this research a method has been developed to explore vulnerable areas and to do stresstests. The first stresstests have been carried out for the urban areas in South Holland and explorations were carried out for the urbanized area along the Amsterdam-Rhine canal area (which includes amongst others Amsterdam, Utrecht and Leiden, and Amsterdam Airport) (De Bruijn, 2022). The resulting flood and impact maps and discussions on actions resulted in significant increase in understanding of potential consequences and in follow-up actions to improve crisis management and recommendations for spatial planning and design recommendations for new critical infrastructure objects.

**References**


Asselman, N. en KJ van Heeringen (2022) Een watersysteemanalyse – wat leren we van het hoogwater van juli 2021? Inzichten in het functioneren van beeksystemen bij grote hoeveelheden neerslag en het effect van systeemmaatregelen. Deltares rapport 11207700-000-ZWS-0035

De Bruijn, K.M. & Slager, K. (2022a). *Wat als 'de waterbom' elders in Nederland was gevallen? Hackathon Deltares,* November 2021. Deltares rapport 11206890-010-GEO-0006. Deltares, Delft.

De Bruijn, K.M. (2022b). *Casestudie Zuid-Holland: 'Analyse grootschalige wateroverlast'.* 11208520-000-ZWS-0002, 2023. Deltares, Delft

ENW (2021). Hoogwater 2021. Feiten en duiding. Expertise Netwerk Waterveiligheid.

De Bruijn, Joost Buurman, Marjolein Mens, Ruben Dahm, Frans Klijn, Resilience in practice: *Five principles to enable societies to cope with extreme weather events*,Environmental Science & Policy http://dx.doi.org/10.1016/j.envsci.2017.02.001 21-30

Merz, B. et al. Charting unknown waters - On the role of surprise in flood risk assessment and management. Water Resour. Res. 51, 6399–6416 (2015).

De Bruijn, K.M. & Maas, B. (in prep.*). Methode voor bovenregionale stresstesten voor grootschalige neerslag. Ten behoeve van een landelijk uniform beeld*. Deltares, Delft.

Kreienkamp, F. et al. Rapid attribution of heavy rainfall events leading to the severe flooding in Western Europe during July 2021. World weather attribution, www.worldweatherattribution.org (2021)

Ministerie van Infrastructuur en waterstaat (2022). Eindadvies B*eleidstafel wateroverlast en hoogwater*. Voorkomen kan niet, voorbereiden wel. Allemaal aan de slag. 102 pp.

# Lessons learnt from recent flood disasters in Europe: Indicative cases

Ana Margarida BENTO[1,4], Florian CORDIER[2], Benjamin DEWALS[3], Kamal EL KADI ABDERREZZAK[2], Tiago FERRADOSA[1,4], Corrado GISONNI[5], P. Amparo LÓPEZ-JIMÉNEZ[6], Daniela MOLINARI[7], Elena PUMMER[8], Paweł M. ROWIŃSKI[9], Kai SCHRÖTER[10], Anastasios I. STAMOU[11]

[1] Hydraulics, Water Resources, and Environmental Division, Department of Civil Engineering, Faculty of Engineering of the University of Porto, 4200-465 Porto, Portugal, anabento@fe.up.pt
[2] EDF R&D National Laboratory of Hydraulics and Environment, Chatou, France, florian.cordier@edf.fr; kamal.el-kadi-abderrezzak@edf.fr
[3] Research Group of Hydraulics in Environmental and Civil Engineering (HECE), University of Liège, Belgium, b.dewals@uliege.be
[4] Interdisciplinary Centre of Marine and Environmental Research, 4450-208 Matosinhos, Portugal, tferradosa@fe.up.pt
[5] Chair of Hydraulic Engineering and Hydraulic Structures, Università della Campania 'Luigi Vanvitelli', Italy. corrado.gisonni@unicampania.it
[6] Universitat Politècnica de València. DIHMA. Camino de Vera s/n. Valencia. Spain, palopez@upv.es
[7] Politecnico di Milano, Department of Civil and Environmental Engineering, Italy, daniela.molinari@polimi.it
[8] Department of Civil and Environmental Engineering, Norwegian University of Science and Technology (NTNU), Norway, elena.pummer@ntnu.no
[9] Institute of Geophysics, Polish Academy of Sciences, Poland, p.rowinski@igf.edu.pl
[10] Technische Universität Braunschweig, Leichtweiss-Institute for Hydraulic Engineering and Water Resources (LWI), Division Hydrology and River Basin Management (HYDRIV), Germany, kai.schroeter@tu-braunschweig.de
[11] National Technical University of Athens, School of Civil Engineering, Department of Water Resources and Environmental Engineering, Laboratory of Applied Hydraulics, Greece, stamou@mail.ntua.gr

ABSTRACT

Europe suffers from flood disasters, which have increased in intensity and frequency in recent years and are likely to be exacerbated by the effects of increased urbanization, climate change and inadequate drainage infrastructure and storage areas. The question facing hydro-environmental researchers is: “What lessons have we learnt from recent flood disasters in Europe?”. The IAHR Leadership Team Europe is organizing the preparation of a detailed paper to answer this question. The present abstract provides a brief description of the main parts of this paper, together with an indicative list of flood disasters in the last ten years with their basic characteristics.

## 1. Recent catastrophic floods in Europe

Flood risk management in Europe has steadily improved, but catastrophic floods with high human losses and damages continue to occur. Relatively recent flood disasters, such as the floods of July 2021 in Western and Central Europe, have shown that European countries continue to experience catastrophic high magnitude floods with significant loss of life and damage, even in some countries with sophisticated risk mitigation measures.

Italy experienced 43 events between 2020 and 2023, causing 43 deaths and affecting 80,000 people. In particular, unrecorded major events in Marche (2022) and Emilia Romagna (2023) caused 26 additional deaths, over 35,000 evacuations and significant financial losses. Recent floods in Tuscany (November 2023) caused 8 deaths and affected 23,000 people, with estimated losses of €2 billion. Unprecedented floods in several European countries, including Belgium, Poland, Greece, Germany, Norway, Spain, France and Portugal, have highlighted the urgent need for improved flood-resilient urban planning and crisis management. In Belgium, the Meuse River Basin experienced record-breaking flows in July 2021, resulting in deaths, severe property damage and infrastructure disruption. Similar catastrophic floods occurred in Poland in 2010, causing significant economic losses and casualties. Greece faced more than 380 floods with 132 deaths between 2000 and 2020, with the deadliest event in Mandra in November 2017. Germany suffered extensive losses of over

€30 billion and 180 deaths in July 2021, highlighting deficiencies in communication and flood risk management. In Norway, heavy rainfall led to flooding and landslides, highlighting the need to adapt infrastructure to climate change. Spain, facing both floods and droughts, implemented flood risk assessment measures and identified more than 1,300 areas at risk. France, with a high annual cost of flood-related damage, experiences frequent flash floods in the south-east, resulting in significant economic losses and casualties. In northern France, heavy rainfall in November 2023 caused local rivers to overflow, causing €1.3 billion in damage and affecting 517,000 people. Portugal has a history of devastating floods, with the tragic "Ponte Entre-os-Rios" event in 2000/2001 and coastal flooding affecting 75% of the population. The case of Furadouro beach in Aveiro illustrates the persistent challenges of coastal flooding that Portugal has faced since 1857.

These collective experiences highlight the critical importance of comprehensive flood risk management and adaptation strategies in the face of increasing climate-related challenges. On the basis of the above brief descriptions, hydro-environmental researchers are faced with the question “What lessons have we learnt from the recent flood disasters in Europe?” The IAHR Leadership Team Europe is organizing the preparation of a detailed paper to answer this question. This paper will consist of the following four parts: (1) the formulation of a catalogue of the most important flood disasters that have occurred in different European countries, (2) the collection of detailed characteristics of these floods, (3) the processing and inter-comparison of these characteristics, and (4) the presentation of the answer to the question posed. Table 1 summarizes the main characteristics of recent floods in Europe, highlighting their severity over the last fifteen years. The records provide a valuable database for thorough cross-analysis, revealing common features and site-specific conditions that influence mitigation and prevention plans across regions. Despite centuries of exposure to extreme floods in Europe, a comprehensive literature benchmark is lacking. Our study aims to collect detailed data on meteorological, hydrological and hydrodynamic aspects, as well as existing flood management systems during disasters, such as early warning systems. The results will be presented in tables and figures, providing insights into lessons learned and addressing the research question.

Table 1. Main characteristics of indicative recent catastrophic floods in Europe.

| Country, Region | Period | Brief description |
|---|---|---|
| France, South-East, French Riviera | 2-3.10.2015 | Cause: rainfall = 110 mm in Cannes/Mandelieu in 1 h – 160 mm in the Brague in 3h, exceeds 100-year return period; Combination of factors: low-pressure system born in the Mediterranean Sea and precipitation lasted all day; 20 casualties; damage= €1 billion. The 2015 event becomes the reference flood for the catchment, the plan for Flood Risk Prevention is therefore revised for ten municipalities. |
| Greece, West Attica | 15.11.2017 | Cause: barometric low Eurydice & Cyclone Numa; rainfall = 150 mm in 7 hours; deaths = 24; damaged buildings: ≈ 1000. |
| Greece, Northern Greece, Halkidiki | 11.07.2019 | Cause: overnight storm in 20 mins; deaths = 7; wounded: 100. |
| Greece, Central Greece, Evia | 09.08.2020 | Cause: severe thunderstorms and heavy precipitation due to storm Thalia; rainfall=300 mm in 8 h; water depths = 1.5 m, deaths=8; homes destroyed = 2000, road network: extensive damages; cost of damage = millions. |
| France, South-Est, upstream catchments of Alpes-Maritimes | 02.10.2020 | Cause: powerful early-season extratropical cyclone; particularly devastating floods and resulting landslides, especially in three catchments (Roya, Vésubie and Tinée); rainfall of 500 mm in less than 24h; Damages: around 60 km of roads destroyed, 20 bridges collapsed, around 100 houses at Saint-Martin-Vésubie; deaths = 11, and 8 missing; damage= €1 billion. |
| Belgium, Eastern part, Meuse basin; | 14-15.07.2021 | Extreme riverine floods in tributaries of the Meuse River, following two days of rainfall with an accumulated volume of up to 300 mm. About €5 billion of flood losses. |
| Germany, Ahr and Erft Rivers | 14-15.07.2021 | Extreme flash floods and river floods in the tributaries and main channel of the rivers Ahr and Erft following two days of rainfall with an accumulated volume of more than 150 mm. Losses in excess of €30 billion and more than 180 fatalities. |
| Italy, Central Italy, Marche, and Umbria Region | 15.09.2022 | Cause: self-regenerating storm; rainfall = 400 mm in 6 hours with peaks of 90 mm in 1 hour; deaths: 12; damage to houses, economic activities, infrastructures. |
| Italy, North Italy, Emilia Romagna Region | 1-15. 05.2023 | Cause; cyclone; rainfall 250 mm in 48 hours; more than 24 rivers flooded, deaths 14; billions of damages to houses, economic activities, infrastructures, environmental goods. |
| Greece, Central Greece, Thessaly | 07.09.2023 | Cause: very heavy rainfall due to storm Daniel; deaths = 23; killed livestock: tens of thousands; area flooded: 8500 $km^2$ mostly prime farmland; crops: destroyed; swamped buildings: hundreds; main railway, roads, and bridges: savaged; cost of damage = billions. |
| Italy, Central Italy, Tuscany | 2-3.11.2023 | Cause: cyclone; rainfall 200 mm in 2 h; several rivers flooded, deaths: 8; 2 billion of damage to houses, economic activities, infrastructures, environmental goods. |

# Probabilistic study of flooding and erosion processes in coastal zones of Andalucía (Spain) for the XXI century

Marcus SANTANA[1], Pedro OTIÑAR[1], Manuel COBOS[1], Pedro MAGAÑA[1], Agustín MILLARES[1], David GUTIÉRREZ[2], Jorge MARTÍN[3], Pablo ARJONA[3], Andrea LIRA-LOARCA[4], Asunción BAQUERIZO[1]

[1] Andalusian Institute for Earth System Research (IISTA), University of Granada, Avda. del Mediterráneo s/n, 18006, Granada (Spain)
marcussanta@ugr.es
potinar@ugr.es
mcobosb@ugr.es
pmagana@ugr.es
mivalag@ugr.es
abaqueri@ugr.es

[2] SandS, Bajada San Juan, 73B, 39012, Santander (Spain)
david.gutierrez@sands.es
[3] Estudio 7 Soluciones Integrales, Calle Cuarteles, 27, 2ªPlanta, 29002, Málaga (Spain)
jorgemv@estudio7soluciones.es
pabloal@estudio7soluciones.es
[4] Andrea Lira-Loarca, Università degli Studi di Genova, Via Montallegro 1, 16145 Genova (Italy)
andrea.lira.loarca@unige.it

ABSTRACT

We propose a methodology for the study of erosion and flooding impacts in a climate change scenario that accounts for: (1) the stochastic character of climate and its variability at different time scales; (2) the joint effect on the coast of maritime and fluvial events; (3) the presence of infrastructures that interfere with the hydrodynamic and sedimentary processes, such as dams in the river course, harbors, breakwaters and promenades; (4) the availability of sediment, its 3D spatial layout, as well as its granulometry and degree of consolidation. The methodology has been implemented all along the almost 1000 km of the Andalusian coast. Results are characterized in terms of probability for different time horizons and, when applicable, for two touristic seasons.

## 1. Introduction

Littoral zones are valuable areas that are also capable to mitigate the consequences of hazardous natural events. Their occupation during the last decades has been done without taking into account that the concentration of population and economic activities considerably increases the risk of economic and environmental losses. In addition, according to the fifth assessment report of the Intergovernmental Panel of Experts on Climate Change (IPCC, 2023), the situation will worsen in a scenario of global change at 2100 horizon where sea level rise and variations in climate patterns will occur concurrently with an increase in the coastal population. The situation is critical in the coast of Andalucía (Spain) that host more than 60 % of its population in a variety of coastal morphologies (estuaries, spits, deltas,…) that are suffering severe human induced stresses. This will certainly bring up different management problems that will require innovative, informed-based solutions to mitigate/adapt to climate change impacts or even to rearrange existing developments.

## 2. ICCOAST project

In this context, the University of Granada (UGR) has developed a new methodology to study the spatial and temporal variability of coastal zone in a climate change scenario. The methodology is based on the work by Payo et al. (2008) and Baquerizo and Losada (2008). It has been implemented in the provinces of Huelva, Cádiz and Málaga by the Temporary Joint Venture Estudio 7-SandS and in Granada and Almería by UGR. It consists of the following steps.

▪ Characterization of the study site: Different morphological units of regional scale O(10 km) are distinguished along the coast and treated as control volumes, identifying sediments available within it, sources, sinks and exchange rates with adjacent regions. Each unit is further divided into sections of local scale O(10-100 m) sharing similar morphological characteristics and approximately the same climatic conditions.

▪ Analysis of climatic conditions: wave, wind, atmospheric pressure, and precipitation are considered, taking into account their variability at different time scales, random nature, and their interaction with morphology.

▪ Random generation of climatic series: Simulation techniques are employed to reproduce climate conditions and to simulate hydro-morphodynamic processes

▪ Stochastic characterization of the coastal zone: simulations are analyzed with statistical techniques capable of associating a probability of occurrence with different events related to erosion and flooding in the future.

Different time horizons ($t_H$) are considered in the study. Additionally, for some random variables, two seasonal periods corresponding to tourist seasons are distinguished.

## 3. Results

Figure 1 shows some of the probabilistic information related to the curves delimiting the envelope of the places that are reached by the sea water at different $t_H$ for the peak tourist season.

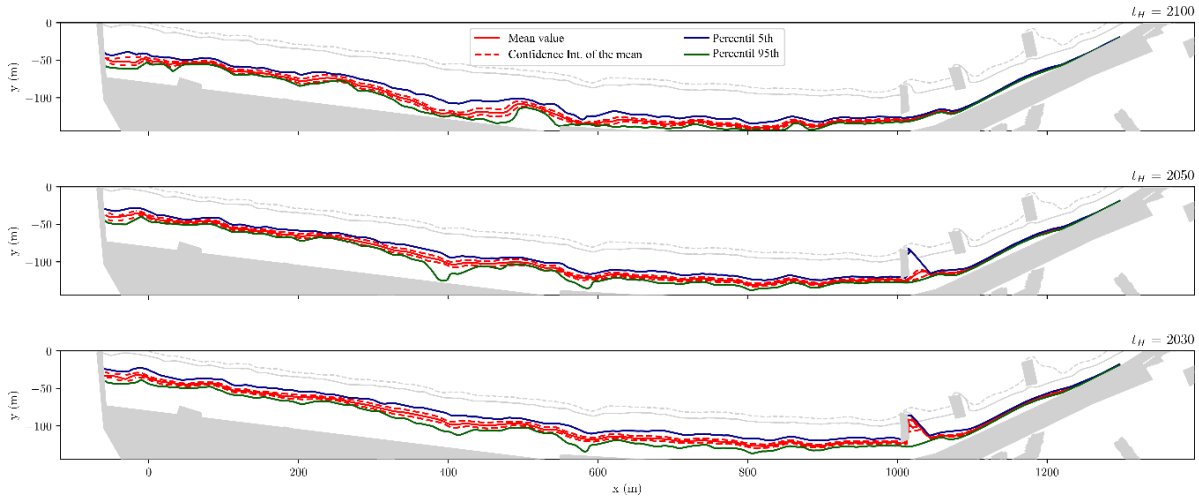



**Fig. 1.** Curves representing, for the envelope of the places that are reached by the sea water, the mean value and its 95 % confidence interval as well as the 5th and 95th percentiles.

In the conference, the work done will be illustrated by presenting the probabilistic characterization of different indicators and curves selected for the analysis of erosion and flooding at selected sites.

**Acknowledgements**

This work was carried out within the framework of a contract (Exped. Contr. 2018 66984) that was competitively bid by the Junta de Andalucía (with funds of the Fondo Europeo de Desarrollo Regional) and awarded to the University of Granada and the Temporary Joint Venture Estudio 7-SandS.

**References**

Baquerizo A, Losada MA (2008) Human interaction with large sale coastal morphological evolution. An assessment of the uncertainty. Coastal Engineering. Special Issue. Vol. 55, pp. 569-580.

IPCC (2023) Summary for Policymakers. In: Climate Change 2023: Synthesis Report. Contribution of Working Groups I, II and III to the Sixth Assessment Report of the Intergovernmental Panel on Climate Change [Core Writing Team, H. Lee and J. Romero (eds.)]. IPCC, Geneva, Switzerland, pp. 1-34.

Payo A, Baquerizo A, Losada MA (2008). Uncertainty assesment: application to the shoreline. Journal of Hydraulic Research. Vol. 46, Extra Issue 1, pp. 96–104.



# Theme F

## Governance and water resources management

# Comparative Analysis of River Management between France and China

Yixin CAO[1], Karl Matthias WANTZEN[1,2]

[1] UNESCO Chair River Culture – Fleuves et Patrimoine, CITERES - UMR 7324 CNRS, University of Tours, France
yixin.cao@etu.univ-tours.fr

[2] EUCOR Excellence Chair in Water and Sustainability, Institut Terre & Environnement de Strasbourg – ITES, University of Strasbourg, France; karl.wantzen@univ-tours.fr

ABSTRACT

In the Anthropocene epoch, rivers worldwide face unprecedented challenges. These not only threaten freshwater ecosystems but are also exacerbated by inconsistent river management across different regions. To achieve sustainable river management, it is imperative to adopt a holistic approach that takes into account the river's physical environment, the biodiversity of river-floodplain systems, and the human communities that rely on and interact with them. However, there's a disparity in knowledge and best practices, especially between Europe and China. In Europe, the European Union Water Framework Directive (EU WFD) set forth standards and objectives to achieve good conditions for all water bodies in EU member states. Meanwhile, China's river ecosystems have faced degradation due to the last four decades of rapid economic growth; and the river management scheme was highly fragmented. Our study offers a comparative assessment of river management strategies between France (as a European representative) and China. Our analysis delves deep into aspects such as legislative measures, water quality improvement and restoration efforts, dam removal, and overarching management structures. Specifically, we juxtapose France's watershed governance, refined since the 1960s, with China's top-down approach and the recent introduction of the River Chief System (RCS) in 2016.

## 1. River protection and restoration in France and China

### *1.1. Legal framework for protecting river environment*

Both France and China have established specific laws emphasizing pollution control and water resource protection, underscoring their dedication to preserving freshwaters (Tab. 1). In France, legislation related to comprehensive protections at the river basin level was established as early as the 1960s. With the introduction of the EU WFD in the 2000s, France adjusted its laws to align with these directives with the 2004 Environmental Act. Further reinforcing its commitment, the 2006 LEMA law emphasized preserving France's aquatic environment, mandating, for instance, the measures to facilitate migratory fish movement. On the other hand, China began addressing environmental issues in the 1970s. The Water Law, introduced in 1988 and revised in 2002, served as China's inaugural legislation for a consolidated administration of water resources. Realizing the importance of a watershed perspective, China introduced laws for the Yangtze and Yellow Rivers, often referred to as the nation's "mother" rivers, in 2020 and 2021, respectively. These two laws represent China's first legislation targeting river basin management (Cao & Vazhayil, 2023).

**Table 1.** The major laws concerning river management in France and China

| France | China |
|---|---|
| Law No. 64-1245 of December 16, 1964, relating to the management and distribution of water and the fight against its pollution | Law on Prevention and Control of Water Pollution: adopted in 1984; last amended in 2020 |
| Law No. 92-3 of January 3, 1992, on water | Water Law: adopted in 1988; last amended in 2016 |
| Law No. 2004-338 of April 21, 2004 transposing Directive 2000/60/EC of the European Parliament and of the Council of October 23, 2000 establishing a framework for Community action in the field of water | Environmental Protection Law: adopted in 1989; last amended in 2014 |
| Law No. 2006-1772 of 30 December 2006 on water and aquatic environments (LEMA) | Water and Soil Conservation Law: adopted in 1991; last amended in 2010 |
| | Yangtze River Protection Law: adopted in 2020, took effect in 2021 |
| | Yellow River Protection Law: adopted in 2022, took effect in 2023 |

### *1.2. River water quality and restoration*

During the 1970-80s, French rivers suffered extensive pollution from agriculture and industry. However, the late 1980s' phosphate ban on washing powders and improved wastewater treatments in the 2000s, following European directives, significantly reduced eutrophication in French rivers (Garnier et al., 2018). The 2006 LEMA law further bolstered France's efforts in safeguarding river biology and hydromorphology. Although most French rivers achieved good chemical quality, their ecological status remains compromised. Physical interventions, such as dams and weirs, have resulted in a high degree of fragmentation in French rivers (Belletti et al., 2020). To address this, France has recently initiated dam removals to restore rivers' longitudinal connectivity. The removal of two hydroelectric dams on the Sélune River in 2022 stands as an example. Meanwhile, China's river conservation began in earnest with the introduction of the Environmental Quality Standards for Surface Waters in 2002, grading water quality from I to Poor V. By 2013, it became evident that widespread water degradation posed a severe environmental threat, and dam constructions leading to notable species extinctions. However, 2012-2013 marked a turning point as China's focus transitioned from mere economic growth to sustainable development. The implementation of the River Chief System (RCS) has since instigated swift improvements in water pollution. By 2022, 90.2% of the water at 3,115 major river monitoring points was of quality class I-III (MEE, 2023). While efforts have been made, issues like cultural eutrophication and heavy metal pollution persist, with phosphorus and ammonia being the main culprits for poor water quality (Huang et al., 2021). Lastly, China's commitment to hydropower is a linchpin for its 'double carbon' targets — peaking carbon emissions by 2030 and achieving carbon neutrality by 2060. Hence, unlike France, China currently doesn't view dam removal as a viable strategy for improving river ecosystem health.

## 2. River management structure in France and China

Since the 1964 Water Act, France has developed a framework for integrated water resource management at the river basin level (Fig. 1, left). This management involves the establishment of the Water Agency and Basin Committees, emphasizing a hydrological basin approach. Local entities, often at the municipal level and referred to as "maîtres d'ouvrage," spearhead the execution of river management plans like SAGE & SDAGE. France's river management also involves both public and private stakeholders, various associations, and the general public. In contrast, China has adopted a top-down, sectoral river management approach with minimal public involvement (Fig.1, right). China's previous water governance model is riddled with ambiguity, inefficiencies, and limited inter-departmental cooperation. To address these issues, the River Chief System (RCS) was nationally instituted in 2016. The RCS, characterized by its "One river – one file" and "One river – one strategy", has shown its efficacy in curbing river pollution in China. Furthermore, it fosters public engagement, providing the opportunity for the public to be appointed as Civil RCs (Cao & Wantzen , 2023).

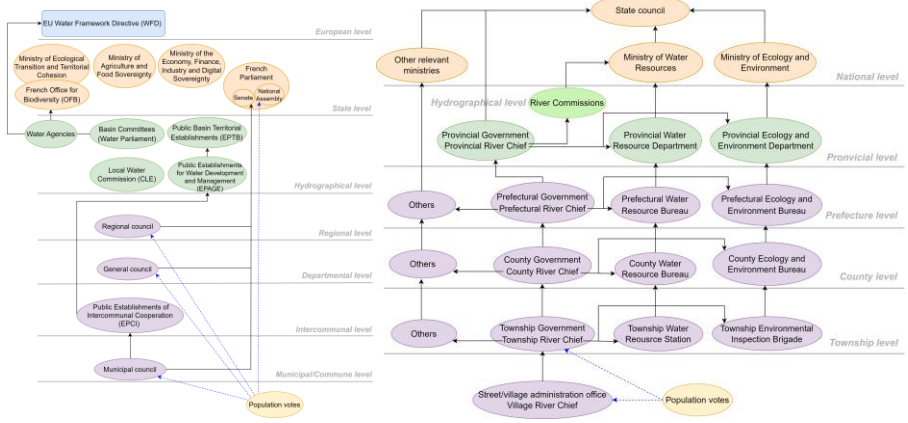



**Fig. 1.** River management structure in France (left) and China (right). The direction of the arrows indicates which department has authority/responsibility over another department. A blue arrow signifies a point where the population can vote for elected representatives.

**References**


Belletti B, Garcia de Leaniz C, Jones J, Bizzi S, Börger L, Segura G, Castelletti A, van de Bund W, Aarestrup K, Barry J, and others (2020) More than one million barriers fragment Europe's rivers, Nature, 588(7838), 436–441.

Cao Y, Vazhayil AM (2023) River culture in China and India, a comparative perspective on its origins, challenges and applications, In KM Wantzen (Ed.), River culture: life as a dance to the rhythm of the waters, UNESCO Publishing, pp. 281–311.

Cao Y, Wantzen KM (2023) China's new policies to improve environmental quality in rivers: the River Chief System, In KM Wantzen (Ed.), River cultures: Life as a dance to the rhythm of the waters, UNESCO Publishing, pp. 853-874.

Garnier J, Ramarson A, Billen G, Théry S, Thiéry D, Thieu V, Minaudo C, Moatar F (2018) Nutrient inputs and hydrology together determine biogeochemical status of the Loire River (France): Current situation and possible future scenarios, The Sci. of the Total Environ., 637-638, 609–624.

Huang J, Zhang Y, Bing H, Peng J, Dong F, Gao J, Arhonditsis GB (2021) Characterizing the river water quality in China: Recent progress and on-going challenges, Water Research, 201, 117309.

Ministry of Ecology and Environment (MEE) of People's Republic of China (2023) 2022 China ecological environment status bulletin. https://www.mee.gov.cn/hjzl/sthjzk/zghjzkgb/202305/P020230529570623593284.pdf.

# A stakeholder-adapted methodology to identify feasible regions for managed aquifer recharge in the Mijares and Palancia basins (Spain)

Syrine GHANNEM[1], Rafael J. BERGILLOS[1], Constantinos F. PANAGIOTOU[2], Javier PAREDES-ARQUIOLA[1], Abel SOLERA[1] and Joaquín ANDREU[1]

[1] Research Institute of Water and Environmental Engineering (IIAMA), Universitat Politècnica de València, Valencia, Spain
sghanne@upv.es, rbermec@upv.es, jparedea@upv.es, asolera@upv.es, ximoand@upv.es

[2] Department of Environment and Climate, ERATOSTHENES Centre of Excellence, Cyprus
constantinos.panagiotou@eratosthenes.org.cy

ABSTRACT

The ever-increasing demand for water resources, coupled with excessive groundwater extraction, has led to a significant decline in aquifer levels (López-Alvis et al., 2019). As a result, there is a pressing need for innovative solutions to replenish and restore these depleted aquifers. Managed Aquifer Recharge (MAR) has emerged as a promising technique to address these challenges and enhance water availability, contributing to sustainable water resource management (Dillon et al., 2019). In this context, GIS-based multi-criteria decision analysis has proven to be a valuable tool to identify suitable regions for MAR implementation (Sallwey et al., 2019). These suitability maps consist of physical factors relevant to the MAR objective, particularly hydrogeological characteristics, water availability, demand for groundwater-dependent services, and non-physical considerations such as economic viability, social acceptance, environmental impacts, and legal constraints. This work proposes a stakeholder-adapted methodology for creating feasibility maps for MAR via the integration of GIS tools and multi-criteria decision analysis.

The proposed methodology encompasses two approaches for weighting the relevance of factors with respect to the pre-defined MAR objective: Streamflow 1, a general expert-based baseline that explicitly incorporates non-physical information into the weighting process based on the opinion of MAR experts, and Streamflow 2, which relies on the stakeholders' engagement, for example via surveys. Three thematic layers based on physical factors were identified for analysis: the intrinsic suitability, water availability and water demand. Streamflow 1 aims on weighting physical criteria in terms of non-physical criteria based on their relevance to the pre-selected MAR objective. On the other hand, Streamflow 2 is based on the preselection of physical criteria through an extensive database of feasibility criteria (Panagiotou et al., 2022), which were weighted through a dedicated questionnaire targeting key stakeholders of the water sector. Comparing the importance of the physical criteria in terms of their relevance to the MAR objective, stakeholders are asked to weight those criteria for evaluating the feasibility of MAR.

The weighting coefficients from both Streamflow 1 and 2 are standardized within the range of 0 to 1, as well as the values of the physical criteria. By weight-averaging the previously computed weights from Streamflow 1 with the weights derived from stakeholders in Streamflow 2, the final weighting coefficients of the physical criteria are determined. It is important to note that Streamflow 1 calculated the weights at the category level, while Streamflow 2 computed them at the criteria level. To ensure consistency between the two approaches, the values obtained for one category in Streamflow 1 can be directly assigned to all associated criteria. Using the weighting coefficients from Streamflow 1 and 2, suitability indicators were calculated for each thematic layer to generate the suitability maps, Eq. (1), indicating potential MAR sites based on the selected criteria,

$$SI_i = \sum W_{p,j} \times SD_{j,} \quad (1)$$

where $SI_i$ – Suitability indicator for thematic layer i, $W_{p,j}$ – weighting coefficients for physical criteria j, $SD_j$ – standardized values for the physical criteria j, i – thematic layer, j – physical criteria.

The combination of these suitability indicators resulted in a comprehensive feasibility indicator, Eq. (2), providing valuable insights into MAR implementation potential at different locations within the study site:

$$FI = \begin{cases} 0; if\ SI_{IS} = 0\ or\ SI_{WA} = 0\ or\ SI_{WD} = 0, \\ \alpha.SI_{IS} + \beta.SI_{WA} + \gamma.SI_{WD}, \\ \alpha + \beta + \gamma = 1, \end{cases} \quad (2)$$

where $FI-$ feasibility indicator, $SI_{IS}$ – suitability indicator for intrinsic suitability, $SI_{WA}$ – suitability indicator for water availability, $SI_{WD}$ – suitability indicator for water demand, $\alpha, \beta$ and $\gamma -$ weighting coefficients to calculate the feasibility indicator.

The applicability of the proposed methodology was demonstrated in two study sites, located within the Júcar Water District in Spain: the Mijares river basin and the Palancia river basin. These regions face specific challenges, including intensive groundwater exploitation for irrigation and low reliability of water supply during droughts. Additionally, issues such as seawater intrusion, depletion of groundwater levels, and the reversal of river-aquifer relationship pose significant water management concerns. To ensure stakeholder involvement, a needs assessment workshop was conducted, where their valuable insights, concerns, and proposals were gathered (Fig. 1). An additional questionnaire was compiled and submitted to relevant stakeholders in order to weight the importance of the different criteria of intrinsic suitability, water availability, existence of water demand benefiting from recharge, as well as legal, social, environmental and economic aspects. As a result of the approach, feasibility maps for both the Mijares and Palancia river basins were generated (Fig. 2).

These maps are expected to serve as support to decision-makers in the identification of suitable locations for potential MAR projects, thus contributing to improving the water resource management and the successful implementation of MAR initiatives.



**Fig. 1.** Needs assessment workshop and meetings with stakeholders from the Júcar Water District in Spain

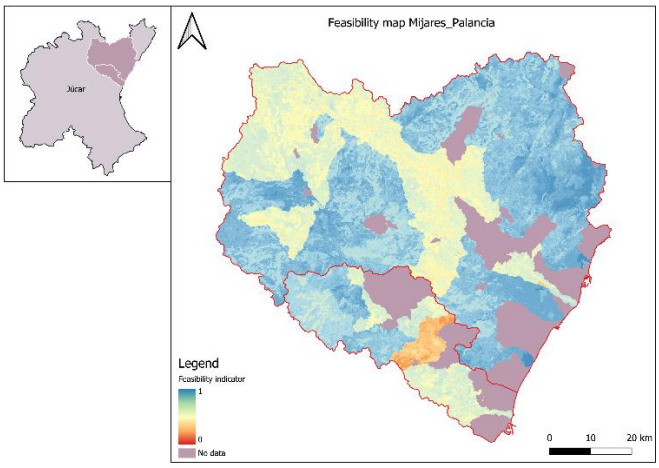



**Fig. 2.** Feasibility maps for the Mijares river basin and Palancia river basin

**Acknowledgements**

This work has been supported by the Spanish Ministry of Science and Innovation (MCIN) and Spanish Research Agency (AEI) through the research project AGREEMAR (PCI2022-133001), which is funded by European Union NextGeneration EU/PRTR. (MCIN/AEI/10.13039/501100011033). RB was partly funded by MCIN/AEI/10.13039/501100011033 through Juan de la Cierva-Incorporación program (IJC2019-038848-I).

**References**

Dillon, P., Stuyfzand, P., Grischek, T., Lluria, M., Pyne, R. D. G., Jain, R. C., ... & Sapiano, M. (2019). Sixty years of global progress in managed aquifer recharge. Hydrogeology journal, 27(1), 1-30.

López-Alvis, J., Carrera-Hernández, J. J., Levresse, G., & Nieto-Samaniego, Á. F. (2019). Assessment of groundwater depletion caused by excessive extraction through groundwater flow modeling: the Celaya aquifer in central Mexico. Environmental Earth Sciences, 78, 1-22.

Panagiotou, C.F., Chkirbene, A., Stefan, C., Martins, T.N., Leitão, T.E. 2022. AGREEMAR Deliverable D2.1: Matrix of feasibility criteria for managed aquifer recharge. Available online at https://www.agreemar.inowas.com/deliverables.

Sallwey, J., Bonilla Valverde, J. P., Vásquez López, F., Junghanns, R., & Stefan, C. (2019). Suitability maps for managed aquifer recharge: a review of multi-criteria decision analysis studies. Environmental Reviews, 27(2), 138-150.

# A Brazilian Approach to Monitoring Water Governance and its Governance System at Different Planning Levels

Maycon Breno Macena da SILVA[1], Márcia Maria Rios RIBEIRO[1]

[1] Federal University of Campina Grande, Department of Civil Engineering, Aprígio Veloso 882, Campina Grande, Paraíba, Brazil.
maycon.breno@estudante.ufcg.edu.br
marcia.ribeiro@ufcg.edu.br

ABSTRACT

Good water governance is increasingly essential in a world under chronic stress in the social and ecological dimensions of water systems. Water governance operates within the social dimension and aims to direct water systems toward a desirable scenario by regulating management at different levels (Pahl-Wostl, 2015). Water governance includes legal aspects and formal and informal norms important for resource management and decision-making arenas. The governance system comprises actors, institutions and their interactions responsible for developing water governance (Pahl-Wostl, 2015). Monitoring water governance is essential to increase knowledge and learning, to solve gaps and to improve the relationship within the governance system (Costa and Neto, 2023).

In Brazil, Federal Law 9,433 of 1997 established the National Water Resource Policy (PNRH), defining guidelines for participatory and decentralized water governance. Additionally, Law 9,433 created the National Water Resource Management System (SINGREH), which encompasses institutions responsible for implementing the PNRH at different planning levels (Ribeiro, 2017). The Brazilian water governance primarily considers three levels of planning: national, state (Brazil is a federation composed of 26 states and the federal district), and river basins. However, reservoirs play an essential role in the country, serving as vital source of water supply for a significant portion of the population and contributing to over half of the nation's electricity generation. Thus, although the reservoirs are already considered in the planning carried out at the three aforementioned levels, the planning that has been carried out at the reservoir level through negotiated water allocation processes and regulatory frameworks is also highlighted (Marques, 2022).

After the ratification of Federal Law 9,433, concerns arose about how to monitor the implementation of the PNRH and the performance of SINGREH, and consequently, how to monitor the water governance in Brazil. After years of discussion and meetings with various actors in water resources management, indicators for monitoring water governance in Brazil and the Water Governance Observatory (OGA Brazil) were proposed (Lima, 2022). The OGA Brazil aims to generate, systematize and disseminate good governance practices through self-assessment of the actors and institutions comprising SINGREH (Costa and Neto, 2023). The structure of OGA Brazil is illustrated in Figure 1a. Currently, OGA Brazil is composed by 62 institutions from the public sector, the private sector, NGOs, and 22 researchers (Lima, 2022). In 2019, OGA Brazil launched the Water Governance Monitoring Protocol (or OGA Brazil protocol) as a tool to assist monitoring. The protocol encompasses 55 indicators divided into five dimensions, summarized simply in Figure 1b. Each dimension is characterized by a varying number of indicators.

Seventeen river basin committees and a state management body are already signatories to OGA Brazil and their monitoring protocol. Therefore, the application of the protocol has been implemented at both the river basin and the state levels to this point. We analyzed water governance at the reservoir level, knowing the importance that reservoirs have for Brazil, and that, within the same river basin, there might exist reservoirs with varying complexities, issues, and planning requirements. Our goal was to present the OGA Brazil protocol to the international community and analyze whether this monitoring protocol, originally designed for the reality of Brazilian governance, can be extended to the different levels of planning within the country.

The Epitácio Pessoa Reservoir (EPR) was selected as the case study due to its significance within the State where it is located, its history of crises, and its complex institutional composition. Located in the semi-arid region of the State of Paraíba, within the Paraíba River Basin (BHRP), it stands as the second-largest reservoir in the State and the largest within the BHRP, holding a capacity of 466 hm³. In this region, rainfall is concentrated in only three to four months of the year. The rivers are intermittent, flowing during just these months. Then, such reservoirs function as inter-annual flow regularization structures. Groundwater is almost inexistent since the geology is crystalline rocks. Therefore, the reservoirs are necessary for water supply. The EPR provides water to approximately half a million people, over 400 irrigators and transfers water to another downstream strategic reservoir. Over the past two decades, the EPR has gone through two water crises. Management problems are considered the main cause of crises, as the droughts affecting the region were not considered. During the second crisis (between 2012 and 2017) the EPR reached a stored volume of water of 3% and the supply service almost collapsed. The EPR was built with federal funds, so it is under federal control, but the BHRP is completely inserted in the State of Paraíba, so it is under state control, as recommended by the Brazilian Federal Constitution. This aspect causes institutional complexity and demands more effort from SINGREH to properly execute the PNRH.




**Fig. 1.** a) OGA Brazil governance model (in the left); b) overview of the OGA Brazil Protocol (in the middle); and c) overview of the application of the OGA Brazil protocol in the case study (in the right), in green the number of indicators met, in yellow the number of partially met indicators and in red the number of indicators not met. Source: Based on Lima (2022) and Costa and Neto (2023).

Based on a documental analysis and institutional data, we judged whether each indicator was fulfilled (when the indicator's recommendations were fully adhered to), partially fulfilled (when only some of the indicator's recommendations were followed), or not fulfilled (when none of the indicator's recommendations were observed). The time scale of analysis was from 2012 to 2020, a period comprising the last water crisis and the beginning of a recovery from it. Figure 1c shows an overview of the governance situation within each dimension of the OGA Brazil protocol. The dimension concerning state capacities presented the best results, as it highlighted several sources of financial resources for water governance and several actors engaged in the improvement of the water system. The biggest gaps are associated with intergovernmental relations and the implementation of management instruments, which are a fundamental part of the PNRH. Consequently, it is up to the reservoir governance system to focus on improving these gaps, increasing coordination, cooperation, flexibility, and innovation of the entities that make up the system.

The results demonstrate two important aspects. First, it is necessary to pay attention to the indicators that need to be improved and what has been applied correctly, so that it continues in this way or becomes more efficient. In the last two years, there have been some improvements that may reflect in a better situation of the indicators in a future analysis: a regulatory framework was discussed and approved to guide participatory governance through negotiated water allocation meetings and there were improvements in the implementation of two of the PNRH management instruments (bulk water fee and water permits). Second, the OGA Brazil protocol proved to be suitable for monitoring governance at the reservoir level as well, showing that this tool can contribute in a multilevel way to water governance in Brazil.

**Acknowledgements**

The first author is grateful for the scholarship grant from CAPES Foundation (Finance Code 88881.934199/2024-01). The authors acknowledge the funding from the Paraíba State Research Foundation (FAPESQ), grant 016/2023.

**References**

Costa MM, Neto S (2023). Exploratory analysis of the water governance frameworks regarding the OECD principles in two river basins in Brazil and Portugal, Utilities Policy, 101556.
Lima AJR (2022). OGA Brasil: a novidade para o aperfeiçoamento da democracia e da gestão descentralizada e participativa das águas [OGA Brasil: the novelty for the improvement of democracy and decentralized and participatory water management], Diálogos Socioambientais, 5(15), 45-50.
Marques, GF (2022). Water allocation in Brazil: main strategies, learning and challenges, In Water resources allocation and agriculture: trasitioning from open to regulated access, London, 159-171.
Pahl-wostl C (2015). Water Governance in the Face of Global Change: From Understanding to Transformation, Heidelberg, 287 pp.
Ribeiro MMR (2017). A Few Comments on the Brazilian Water Resource Policy, New Water Policy & Practice Journal, 3, 22-32.

# Multi-level analysis of water governance through the robustness framework

Maycon Breno Macena da SILVA[1], Maria Eduarda Barbosa da VEIGA[2], Márcia Maria Rios RIBEIRO[3], Carlos de Oliveira GALVÃO[4]

[1,2,3,4] Federal University of Campina Grande, Department of Civil Engineering, Aprígio Veloso 882, Campina Grande, Paraíba, Brazil
maycon.breno@estudante.ufcg.edu.br
maria.veiga@estudante.ufcg.edu.br
marcia.ribeiro@ufcg.edu.br
carlos.galvao@ufcg.edu.br

## ABSTRACT

Water governance refers to the capacity to regulate the development, management, and service provision of water resources at different social tiers (Pahl-Wostl, 2015). According to the OECD (2015), the water sector is fragmented and requires a multi-level governance system. Each of these scales comprises various levels, which characterizes a multi-level governance. For instance, within the spatial scale, there are different levels of water systems, such as basins, aquifers, and reservoirs. This multi-level governance must effectively uphold environmental equilibrium and facilitate the successful execution of diverse services, such as water supply and urban water management.

The robustness of Social-Ecological Systems (SES) is a systemic characteristic that can indicate adequate water governance. Robustness refers to the system's performance when impacted by uncertainties or external factors (Anderies et al. 2004). Therefore, the system is more robust if it maintains good performance while experiencing disturbances. The Robustness of Social-Ecological Systems Framework (RSES-F) (Figure 1a) is a tool developed to systematize the interactions within an SES, and comprehends crucial aspects of governance, identifies weaknesses, and enables system enhancement for increased robustness (Anderies et al. 2019). The RSES-F divides an SES into four main components: resource users (RU), public infrastructure providers (PIP), public infrastructure (IP), and natural infrastructure (NI).

We applied the RSES-F, as an analytical tool, to understand aspects of socio-ecological robustness in water governance across various planning levels, diverse ways of using natural resources, and from the perspective of different sanitation services (reservoir management for water supply and urban drainage management to prevent flooding). A qualitative application of the RSES-F based on document analysis was carried out on two systems at different spatial levels in a Brazilian river basin: Epitácio Pessoa Reservoir and Ramadinha micro-basin. We analyzed the interactions between RU, PIP, IP, and NI in terms of whether they increase (indicated with a "+" in Figure 1) or decrease (a "-" in Figure 1) robustness. These interactions were categorized into possible quantitative transformations (red arrows in Figure 1), possible qualitative transformations (green arrows in Figure 1), and interactions that affect the ability of the system's components to change (blue arrows in Figure 1).

The Epitácio Pessoa Reservoir (EPR) is the largest reservoir in the Paraíba River Basin (PRB), with a total storage volume of 466 $hm^3$. The reservoir's drainage area is 13828 $km^2$. The EPR provides water to nearly half a million people and over 400 irrigators located along its banks. In the last 25 years, the EPR has experienced two major water crises as a result of management problems catalyzed by long periods of drought (characteristic of the Brazilian semi-arid region). Currently, the EPR receives water from another river basin through Brazil's largest water infrastructure for inter basin water transfer, the São Francisco River Integration Project (PISF), which is responsible for transferring water from the São Francisco River Basin to other basins in northeastern Brazil. Therefore, managing the EPR system has becomes even more complex. Given this inherent complexity

and the added institutional complexity, we intend to understand which aspects can favor or disfavor robustness in the water governance of this system.

At the local level, the sub-basin that we analysed was the Ramadinha Basin, a 129-hectare urban basin within the PRB. About 30% of it is composed of one of the municipality's Special Zones of Social Interest (ZEIS) – a restrictive zoning regulation – the ZEIS Invasão Ramadinha II. The basin was assisted by federal funds to improve its urban drainage system, mainly with elements of gray infrastructure, although drainage problems are still observed as flooding occurs. Municipalities serve as important stakeholders in the usage of water resources in river basins, but they also own urban drainage services and management. In which, the drainage systems' management is conducted by municipal departments and agencies, such as the Civil Defense. Civil Defense plays a crucial role in monitoring channels and flood-prone areas, as well as guiding residents in public actions to minimize the impact of flooding. Due to the complexity of dealing with the resources in the basin, the intention here is to use an appropriate framework to assess its operating structure and local governance capacity.

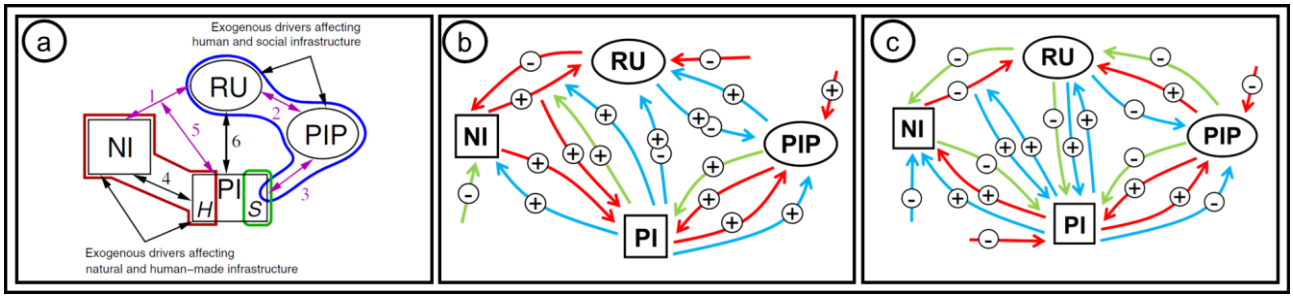



**Fig. 1.** a) The Robustness of SES Framework from Anderies et al. (2019) (in the left); b) Application of RSES-F in REP (in the middle); and c) Application of RSES-F in Ramadinha Basin (in the right). Source: Prepared by the authors.

Despite the spatial scales, both proved to be complex systems, due to the amount of interactions between the components, and with interactions that affect robustness. In both cases, exogenous factors negatively affect robustness and are linked to climatic factors: in the case of the EPR due to periods of water scarcity and in the Ramadinha Basin due to heavy rainfall. This is an interesting aspect, which shows that in the same river basin, water governance problems can be linked to the lack or abundance of rainfall, depending on the level of planning and the role water plays. In the case of the EPR, it can be seen that the relationship between PIP and PI increases robustness, because there are currently mechanisms in place to deal with the system's problems. One example is the regulation and monitoring of users in negotiated water allocation processes. In the Ramadinha Basin, the relationship between the PIPs and IPs can also decrease systemic robustness, mainly because of the PIPs' difficulty in maintaining structures. There is also a decrease in the interaction between the PIPs and URs due to the top-down approach to urban water management.

The RSES-F supported systematizing and understanding two complex water systems at different planning levels and scales, contributing to find gaps in water governance. We argue that appropriate governance strategies have to be designed with a thorough understanding of the issues and identification of the components that make up a system. The application of the method suffers a degree of subjectivity, but when applied collectively in decision-making arenas, this subjectivity can be interesting for the discussions that can be generated among the actors.

**Acknowledgements**

The first and second authors are grateful for the scholarship grant from CAPES Foundation. The authors acknowledge the funding from the Paraíba State Research Foundation (FAPESQ), grant 016/2023, and from the Brazilian Ministry of Science, Technology and Innovations's National Institutes of Science and Technology: Metropolis Observatory, Climate Change and Observatory of Water Security and Adaptive Management.

**References**

Anderies JM, Janssen MA, Ostrom E (2004). A framework to analyze the robustness of social-ecological systems from an institutional perspective. Ecology and society, 9(1).
Anderies JM, Barreteau O, Brady U (2019). Refining the robustness of social-ecological systems framework for comparative analysis of coastal system adaptation to global change. Regional Environmental Change, 19, 1891-1908.
Organisation for Economic Co-operation and Development (OECD) (2015). OECD Principles on water governance. OECD Water Governance Programme.
Pahl-Wostl, C (2015). Water Governance in the Face of Global Change: From Understanding to Transformation. Springer.

# A Modelling Framework and a Testbed Model for Demonstrating Novel Greenhouse Wastewater Treatment and Nutrient Recovery

Barry EVANS*[1], Mehdi KHOURY[1], Lydia Vamvakeridou-LYROUDIA[1,2], Otto CHEN[3], Navonil MUSTAFEE[3], Tavishi GULERIA[2], Joep van den BROEKE[2], Albert CHEN[1]

[1] Centre for Water Systems, University of Exeter, United Kingdom
*b.evans@exeter.ac.uk

[2] KWR Water Research, Netherlands

[3] Centre for Simulation, Analytics and Modelling, University of Exeter, United Kingdom

ABSTRACT

This paper presents the development of a modular testbed model framework, integrated into a web-based system to showcase water treatment technologies for a circular economy approach, within a Smart Water Industrial Symbiosis context, developed under the EU H2020 funded ULTIMATE project. Focusing on the greenhouse horticulture sector in the Netherlands, the paper presents the use of a modelling testbed approach integrated into a web-based interface to highlight the potential of electrodialysis water treatment in this sector for enhancing water and nutrient recovery for greenhouse crop cultivation while aiming to reduce energy consumption, system losses and wastewater discharge.

## Introduction

The horticultural sector of the Netherlands is a billion-euro industry that in 2022 accounted for approximately 2.7% of the country's GDP with greenhouse horticulture generating €9.2 billion in terms of export value (New Zealand Foreign Affairs and Trade, 2022). The high production rates from this sector results in high consumption of nutrients and plant protection products (PPPs) that can result in contamination of surface water, through leaching, discharge, or leakage (van der Salm et al., 2020). As such, there are various legislative mechanisms in place to control discharge from this sector with a target of nearly zero emissions for soilless greenhouse horticulture by 2027 (van der Salm et al., 2020).

With legislation and increasing pressures on resources due to climate change, and rising energy prices, there are increasing drives to adopt more circular economy-based approaches, where the three governing principles are to eliminate waste and pollution, recycle products and materials, and regenerate nature (Ellen Macarthur Foundation, 2010). Previous work outlined in Evans et al., (2023) showed the use of a modelling testbed for modelling aspects of the circular economy in the context of water. By integrating this model into a Serious Game (SG) the model aided in showcasing how to improve water and energy security within a town (Khoury et al., 2023). To promote effective communication and enhance comprehension of the advantages associated with water treatment technologies within the context of the circular economy, we developed a modelling testbed within the Smart Water Industrial Symbiosis (WSIS) framework, promoting wastewater reuse in various industrial settings (ULTIMATE project, 2020). The example testbed model demonstrated in this paper showcases the potential of electrodialysis and innovative electro-chemical membrane technology as an alternative, low-energy-cost method for treating greenhouse wastewater as compared to current state-of-art technologies such as reverse osmosis, facilitating water and nutrient recovery, integrated into an online web-based interface for users to visualise and explore.

## Model design

An abstract customisable greenhouse testbed model was developed to demonstrate water treatment technologies for greenhouse wastewater. The model can be connected to a wastewater treatment device to treat wastewater for reuse and examine the potential of nutrient recovery from this process. The testbed model is

designed in a modular fashion to allow for future updates and comprises three main aspects, i.e., supply (water and nutrients), demand (water, nutrients, and energy), and re-use (water, nutrients). The model itself is a demand-driven model, determined by the requirements of the selected crops being grown within the greenhouse and irrigation methods. Using a System Dynamics Model (SDM) such as that outlined in Evans et al., (2023), the cycle of water and nutrients within the system is tracked at a daily resolution, over a simulated 20-year period, with outputs relating to water, nutrient, and energy use fed back to the user along with the estimate quality values of reclaimed water, along with the quality and volume of discharged water.

For the treatment of greenhouse wastewater using electrodialysis, the user can specify the rate of wastewater they wish to recover and the quality requirements of the treated water. Utilising data from pilot studies, the corresponding energy requirements for meeting the selected criteria are derived along with estimates relating to the percentage of ions ($NO_3^-$, $NH_4^+$, $PO_4^{3-}$, $K^+$, $Ca^{2+}$, $Mg^{2+}$, $Na^+$, and $SO4^{2-}$) that are present in the reclaimed water and the discharged concentrate. This nutrient rich recovered treated water can then be utilised in the next irrigation cycle as part of the fertigation water mix thus reducing the demand for additional nutrients.

## Results and Discussion

Initial analysis of results of electrodialysis as a means of treating greenhouse wastewater has shown that the main benefit of such a system lies within its low energy consumption in comparison to alternative methods such as reverse osmosis, with nutrient recovery being an additional secondary benefit of this approach.

The use of a testbed modelling framework integrated into a web-based UI (Fig 1) helps highlight the benefits of such a system by facilitating exploration of different configurations and providing information and feedback to the user in a tangible and interactive way.

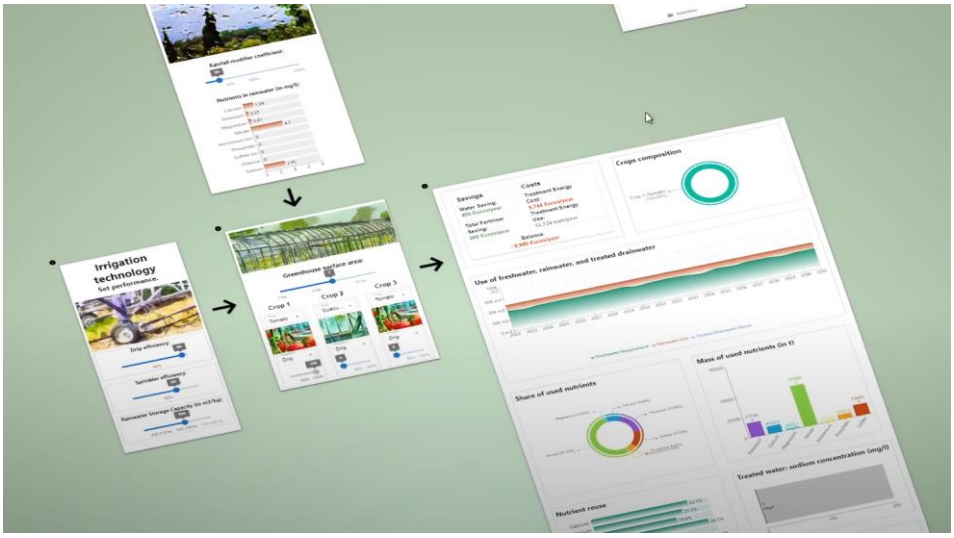



**Fig. 1.** Screenshot of the online user interface for the testbed model examining the use of electrodialysis for water and nutrient recover

**Acknowledgements**

The work presented in this paper was funded by the project ULTIMATE, a European Union Horizon 2020 project, under grant agreement No. 869318 as part of the circular economy call CE-SC5-04-2019.

**References**

Ellen Macarthur Foundation. (2010). *Circular economy introduction*. https://ellenmacarthurfoundation.org/topics/circular-economy-introduction /overview

Evans, B., Khoury, M., Vamvakeridou-Lyroudia, L., Chen, O., Mustafee, N., Chen, A. S., Djordjevic, S., & Savic, D. (2023). A modelling testbed to demonstrate the circular economy of water. *Journal of Cleaner Production*, *405*, 137018. https://doi.org/https://doi.org/10.1016/j.jclepro.2023.137018

Khoury, M., Evans, B., Chen, O., Chen, A. S., Vamvakeridou-Lyroudia, L., Savic, D. A., Djordjevic, S., Bouziotas, D., Makropoulos, C., & Mustafee, N. (2023). NEXTGEN: A serious game showcasing circular economy in the urban water cycle. *Journal of Cleaner Production*, *391*, 136000. https://doi.org/https://doi.org/10.1016/j.jclepro.2023.136000

New Zealand Foreign Affairs and Trade. (2022). *The Dutch Horticulture sector: an innovative sector facing an energy crisis and rising costs - September 2022*.

ULTIMATE project (2020). https://ultimatewater.eu/the-project/ (last visited 29/09/2023)

van der Salm, C., Voogt, W., Beerling, E., van Ruijven, J., & van Os, E. (2020). Minimising emissions to water bodies from NW European greenhouses; with focus on Dutch vegetable cultivation. *Agricultural Water Management*, *242*, 106398. https://doi.org/https://doi.org/10.1016/j.agwat.2020.106398

# Small reservoir siting 'from scratch': merging GIS-based and participatory approaches in a multi-criteria analysis

Chiara ARRIGHI[1], Matteo MASI[1], Francesco PIRAGINO[2], Fabio CASTELLI[1]

[1] Department of Civil and Environmental Engineering, University of Florence, Florence, Italy
chiara.arrighi@unifi.it

[2]Consorzio di Bonifica Medio Valdarno, Florence, Italy

ABSTRACT

## 1. Introduction

Adaptation measures are key to help communities to face natural hazards, including drought and water scarcity, in the face of climate change. As part of a research project involving the Department of Civil and Environmental Engineering at the University of Florence and the Consorzio di Bonifica 3 Medio Valdarno, we examine how the construction of small reservoirs in a rural area with multiple and competing water uses can help increase the resilience of the local water infrastructure. A reservoir is an engineering work that can occupy a portion of territory originally dedicated to other uses (e.g., agricultural areas, woodlands) or have an impact on territorial elements, for example on areas with protected landscape or existing infrastructures. On the other hand, a reservoir can offer several benefits both from a water resource perspective (availability of summer water reserve, flood mitigation, downstream groundwater recharge) and from a socio-ecological perspective (maintenance of ecological flows in the summer period, energy production, and recreational purpose). The construction of a new reservoir must consider these and many other criteria, often incommensurable, to qualify the sustainability of the planned measure. The aim of the work is to complement the GIS morphological analysis with a participatory approach to select and weight the siting characteristics in a Multi-Criteria Decision Making (MCDM) analysis for the identification of the most appropriate reservoir siting. The working hypothesis is that no prior siting study exist in the given area of interest, while in-depth site analysis prior to actual project implementation needs to be focused on a limited number of optimal sites.

## 2. Method and case study

The methodology is structured around three main phases: (i) the development and application of an algorithm which performs a geomorphological and geospatial analysis, (ii) the involvement of stakeholders, (iii) the MCDM approach for the best reservoir siting. The method is summarized in Fig. 1.

### *2.1. Geomorphological and spatial analysis*

One of the most common siting methods for dams and reservoirs is based on GIS analysis, which can include many different types of variables, such as topography, hydrology, and geology (Wang et al., 2021). In this work we developed an algorithm which, based on Digital Terrain Model, for each assigned dam height automatically finds all possible reservoirs and the optimal dam orientation.

### *2.2. Stakeholders' involvement*

A group of stakeholders with different expertise and interests has been involved since the beginning of the process, first to identify the criteria to be used in the analysis of the potential impacts of a new reservoir, second, to weight the criteria. The criteria refer to the (i) impacts of potentially submerged items within the reservoir surface, i.e., structures, infrastructures, population, economic activities, landscape, cultural heritage, environmentally protected areas, natural hazards; and to the (ii) benefits of the reservoir, i.e., resource storage, energy production, ecological support, flood hazard reduction. Weights are obtained through an online survey

built as a pair-wise comparison between criteria with a rating scale, to quantify the relative importance of each criterion. The questions asked to the participants are prioritized based on the Swiss tournament method, which maximizes the occurrence of all criteria among the respondents. Weights are assigned to the criteria with the AHP method (Saaty, 1990).

### *2.3. Reservoir site ranking*

GIS analysis is again applied to evaluate the attributes of each site according to the criteria selected by the stakeholders. A payoff matrix containing all siting alternatives and their representative attributes is built and the Simple Additive Weighting (SAW) technique is applied to rank the alternatives.

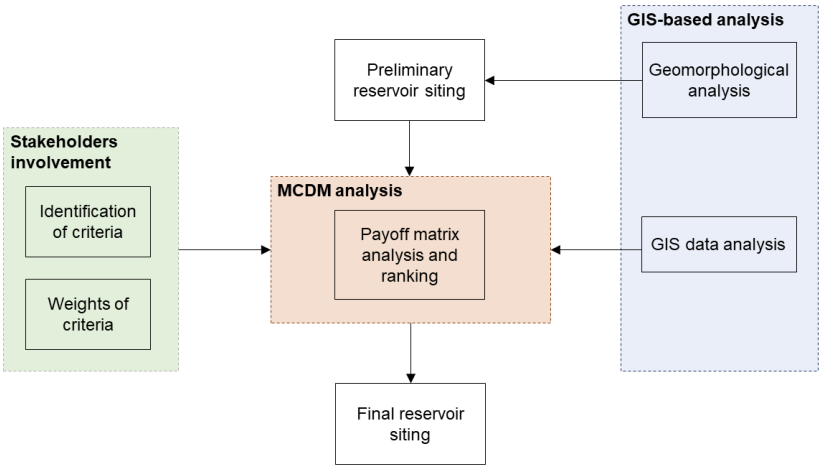



**Fig. 1.** Scheme of the methodology for the reservoir siting based on GIS analysis, stakeholders' involvement and MCDM analysis.

### *2.4. Study area*

The method is applied to the Pesa river catchment (surface area 330 $km^2$, mean annual precipitation ca. 800 mm) located in Chianti area of Tuscany (central Italy) to identify the sites of potential new small reservoirs with prescribed constraints (dam height lower than 12 m and volume lower than $10^6$ $m^3$). Climate change projections foresee a significant reduction of summer precipitation in the area (Spano et al., 2020) which are crucial for agricultural and civil water uses. The panel of stakeholders involved includes majors of the main municipalities, water utilities managers, hydraulic engineers, ecologists, academic researchers, and members of civil society for a total of 25 people.

## 3. Results

The geomorphological analysis identified and ranked approximately 180 potential reservoir sites. The answers to the paired-comparison survey were more than 2000 and the most important criteria were to minimize the impacts on (i) landslides, (ii) flood risk downstream, (iii) river ecology, (iv) resident population. Based on the SAW analysis and on new consultations with stakeholders, the 5 reservoirs which obtained the best scores have been identified for an in-depth feasibility study and preliminary engineering design.

**Acknowledgements**

Authors kindly acknowledge the panel of stakeholders which participated in the two phases of the identification and weighting of decision criteria for their fruitful contribution. This study was carried out within the RETURN Extended Partnership and received funding from the European Union Next-GenerationEU (National Recovery and Resilience Plan – NRRP, Mission 4, Component 2, Investment 1.3 – D.D. 1243 2/8/2022, PE0000005)

**References**

Saaty, T.L. (1990) How to make a decision: The Analytic hierarchy Process, Europran Journal of Operational Research, 48 9-26.
Spano D., Mereu V., Bacciu V., Marras S., Trabucco A., Adinolf M., Barbato G., Bosello F., Breil M., Chiriacò M. V., Coppini G., Essenfelder A., Galluccio G., Lovato T., Marzi S., Masina S., Mercogliano P., Mysiak J., Noce S., Pal J., Reder A., Rianna G., Rizzo A., Santini M., Sini E., Staccione A., Villani V., Zavatarelli M. (2020) Analisi del rischio. I cambiamenti climatici in Italia, available online at DOI: 10.25424/CMCC/ANALISI_DEL_RISCHIO, last access 2/5/2024.
Wang, Y., Tian, Y., Cao, Y. (2021) Dam siting: a review, Water, 13, 2028, https://doi.org/10.3390/w13152080.

# Monitoring the water distribution network and its management optimisation: the Calvagese della Riviera case study

Hossein AZIZI NADIAN [1], Filippo BRUNATI[2], Marco PELI [3], Roberto RANZI[4]

[1,2,3,4] Department of Civil, Environmental, Architectural Engineering and Mathematics, University of Brescia, Brescia, Italy
hossein.azizinadian@unibs.it

ABSTRACT

The leakage of water supply pipes and the increase of water consumers and demand have raised the importance of knowing the actual conditions of water supply network pipelines for optimizing their operation and management. In this study, after a detailed survey on the existing network in the Calvagese della Riviera municipality (province of Brescia, Italy), nine leakages were identified with acoustic methods. Different solutions for the water supply from wells, reservoirs, and pumping were investigated to identify the annual operation costs, considering also fluctuations in the cost of energy, in order to optimize the cost-benefit of the water distribution network (WDN) management.

## 1. Introduction

The efficiency of water supply networks is important in supplying water needed for drinking, agriculture, and industry (Fares et al., 2022). However, due to several reasons, such as aging and decay, these networks suffer from water losses, also called leakages (Pan et al., 2021). The amount of water leakage varies widely between countries, from 3% to about 60% depending on operation conditions (El-Zahab and Zayed, 2019). Therefore, various studies were conducted on leak detection, e.g Meniconi et al. (2017), Marsili et al. (2022), Vafaei Rad et al. (2022), and Brunone et al. (2022). In this paper, leakage detection and annual energy consumption management of Calvagese della Riviera's water network are investigated by conducting a series of field and numerical tests.

## 2. Material and Methods

This research case study is the water distribution network (WDN) of Calvagese della Riviera, a town of 3,645 inhabitants in the province of Brescia (Fig.1.a), located a few kilometers from Lake Garda. This water distribution network suffers from leakages. The Calvagese della Riviera municipality network extends for about 37 km, serving the main town of Calvagese and the hamlets of Carzago, Mocasina, and Terzago. The water network (Fig.1.b) is fed by two wells in the municipal area, Pozzo Sant'Antonio and Pozzo San Pietro (Fig.1.c), and by an inter-municipal pipeline that derives from the Levrini well field located in the neighboring municipality of Soiano del Lago. There are also two storage tanks, S.Pietro and Pineta.

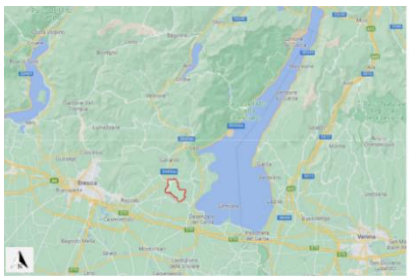


**Fig. 1.**a

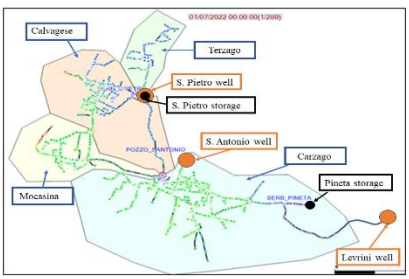



**Fig. 1.**b



**Fig. 1.**c

**Fig. 1.** (a) Map of Calvagese della Riviera (1:650,000); (b) Details of the water distribution network; (c) Exterior of the San Pietro facility.

To achieve the goals of this research, first, the water network map was created using a GPS with the Leica CS20 model, Leonardo's XE365 software, and QGIS 3.24. Then, hydraulic modeling of the water network was done using MIKE+ software. The network was divided into four separate areas to create a correct and accurate model. Noise loggers from Gutermann company, pre-listening rod, and bell geophone of Hydroskop DRX 100 were used for leak detection. Flow meter and pressure gauges were installed on each area's inlet and outlet pipes to have enough information and energy optimization calculations. Also, comparing the hydraulic simulation results with the data measured by remote control, the simulation model was found to have trends and transients that are quite similar and compatible with the measured ones.

## 3. Results

In the field investigations, nine large leaks were detected in the municipal area after opening the manhole covers. On the other hand, with the help of noise loggers, the frequency of each found acoustic intensity was extracted. Figure 2.a shows the existing peaks of a test, which represent the existence of leakage. Next, to better manage energy and economic considerations, the substitution of pumping from the S. Antonio well was investigated in comparison with the pumping of the Levrini wells, located in the municipality of Soiano del Lago. So that, the intercity pipeline from Soiano was excluded, and the outflow from the Levrini well was set zero in the model. The result of the energy efficiency indices (EEI) found that pumping from the S. Antonio well (0.72 kWh/m3) guarantees economic savings compared to pumping from the Levrini wells (0.93 kWh/m3), located in the municipality of Soiano del Lago. Figure 2.b represents the reservoir level changes of Pineta in this scenario. Finally, it was estimated that the actual annual energy consumption required a cost of about € 72,200. Instead, the proposed solution involves a cost of € 64,538, thus guaranteeing annual savings of € 7,662 in 2021 costs. So, In addition to leak detection, an estimate of the economic savings was also made.

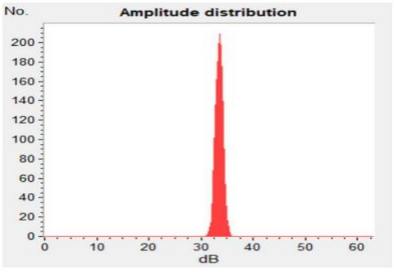



**Fig. 2.**a

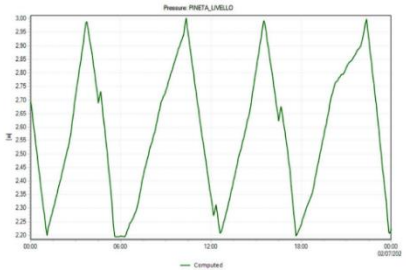


**Fig. 2.**b

**Fig. 2.** (a) Result of a noise logger; (b) Pineta reservoir level in the hypothesis of closure of the Soiano-Calvagese inter-municipal pipeline.

## 4. Conclusions

In this research, the water distribution network of Calvagese della Riviera was investigated for leak detection, energy optimization, and to better manage its water resources by field and numerical investigations. Leaks were found in various places, and the proposed way to reduce costs was successfully extracted. The results of this study show how detailed surveys combined with simulation tools can provide valuable support for optimizing WDN management and operations.

**Acknowledgements**

The authors highly appreciate the University of Brescia, Italy, for providing conditions for our study conducting this research and ISLE for its support.

**References**

Brunone B, Maietta F, Capponi C, Keramat A, Meniconi S (2022) A review of physical experiments for leak detection in water pipes through transient tests for addressing future research. Journal of Hydraulic Research, 60(6), 894-906.
El-Zahab S, Zayed T (2019) Leak detection in water distribution networks: an introductory overview. Smart Water, 4(1), 1-23.
Fares A, Tijani IA, Rui Z, Zayed T (2022) Leak detection in real water distribution networks based on acoustic emission and machine learning. Environmental Technology, 1-17.
Marsili V, Meniconi S, Alvisi S, Brunone B, Franchini M (2022) Stochastic approach for the analysis of demand induced transients in real water distribution systems. Journal of Water Resources Planning and Management, 148(1), 04021093.
Meniconi S, Brunone B, Frisinghelli M, Mazzetti E, Larentis M, Costisella C (2017) Safe transients for pipe survey in a real transmission main by means of a portable device: The case study of the Trento (I) supply system. Procedia Engineering, 186, 228-235.
Pan B, Duan HF, Meniconi S, Brunone B (2021) FRF-based transient wave analysis for the viscoelastic parameters identification and leak detection in water-filled plastic pipes. Mechanical Systems and Signal Processing, 146, 107056.
Vafaei Rad N, Rahmanshahi M, Shafai Bejestan M, Bahrami Yarahmadi M (2022) Leakage-induced transient pressure signal alteration in a viscoelastic pipeline. 3rd IAHR Young Professionals Congress.

# Integrated Hydraulic Modeling for water level control in the Moëres lowland, using Delft3D-FM coupled with real time control tool.

Mohamad ACHOUR[1], Eric MASSON[2], Briz PARENT[3], Olivier BLANPAIN[4]

[1,2,4] Lab. TVES UR 4477, Université de Lille, France
mohamad.achour@univ-lille.fr
eric.masson@univ-lille.fr
olivier.blanpain@univ-lille.fr

[1,3] IXSANE, Villeneuve d'Ascq, France, France
mohamad.achour@ixsane.com
briz.parent@ixsane.com

ABSTRACT

This study presents a spatially distributed hydraulic modeling approach of the Moëres lowland, using the integrated hydraulic model of Delft3D-FM. Located in the vicinity of Dunkirk, France. This 102 km² lowland, which spans across both France and Belgium, triggers unique challenges due to its location below sea level. Water levels regulation within its canals and ditches network is vital for both agriculture and flood risk mitigation. A balance must be reached between 1) maintain minimum freshwater levels to limit saltwater intrusion; 2) ensure adequate water supply for irrigation; 3) prevent fields flooding. To address these challenges, the Moëres lowland relies on a complex network of pumps and valves for water control (Fig 1).

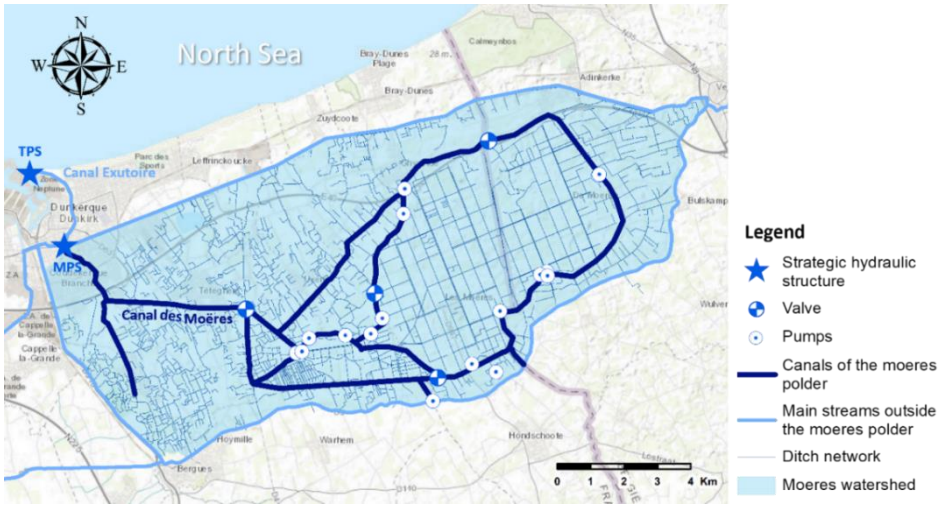



**Fig 1.** Map of the Moëres lowland. MPS: Moëres Pumping Station, TPS: Tixier Pumping Station.

The Moëres Pumping Station (MPS) is equipped with three pumps (two with a capacity of 4 $m^3/s$ each and one with a capacity of 2.5 $m^3/s$.) and three sluice gate. The MPS efficiently manages excess water from the Moëres by diverting it into the Canal Exutoire, ultimately discharging this excess water into the North Sea through the Tixier Pumping Station (TPS). During high tides, the TPS pump the Canal Exutoire waters, which sits below sea level, to the sea. During low tides, the TPS allows gravity water discharge at sea through gates.

## 1. Methodology

Multiple factors influence the water levels modeling within the Moëres lowland, therefore making it a complex task. These factors include groundwater flow, precipitations, pumps and valves operations, and tides. To tackle this complexity, we used the Delft3D-FM software. This software integrates three modules: D-

Rainfall_Runoff, D-Flow FM, and D-RTC. The D-Rainfall_Runoff module is dedicated to resolving diverse hydrological conceptual models. The D-Flow FM module is employed to solve 1D Saint-Venant equations, providing insights into canal flow dynamics. The D-RTC module is used to model hydraulic feedback mechanisms, incorporating pumps and valves control into the simulations (Fig 2).

We calibrate the model to adjust the hydraulic structures operations and the water levels at the MPS. This calibration covers three critical hydrological parameters: infiltration rate, surface and groundwater drainage reaction factor, and canals roughness . Boundary conditions include water level downstream of the MPS, mirroring the measured levels in the Canal Exutoire, four water levels points within the canals, and groundwater levels within each sub-catchment. We assume a correlation between groundwater levels and water levels in the lowland canals. We based interpolations on inter-sensor distances due to the lack of piezometric data.

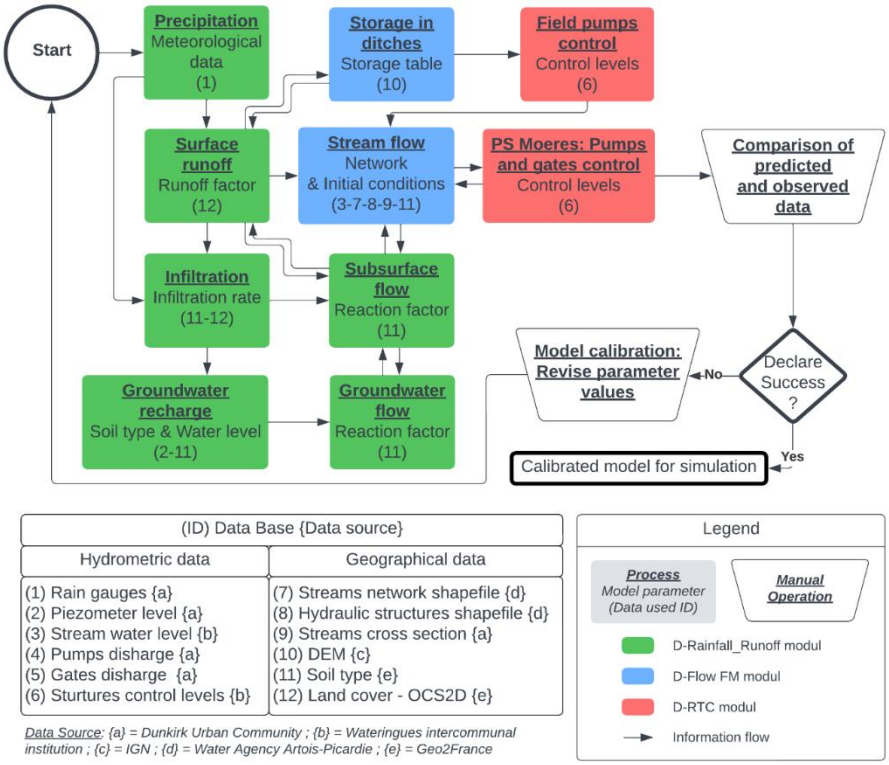



**Fig 2.** Conceptual diagram of model operation and model calibration.

Hydraulic structures are operated based on two seasonal modes, winter, and summer. The modeling process shows the need to adopt two different models to reflect these two functioning modes. Furthermore, each of these two models (winter and summer) are driven by the seasonal variations in groundwater levels within each sub-catchment. Therefore, each of the two models were further divided in two based on different groundwater levels. Each of these four models (two winter and two summer modes) were calibrated and validated using three rainfall events corresponding to the respective seasons, with return periods of one month, one year (for calibration), and ten years.

## 2. Results.

The study highlights the crucial impact of the initial groundwater levels within each sub-catchment and the response factor of groundwater drainage in the hydraulic model calibration which determines the dynamics of groundwater flow. Modelling several modes depending on seasonal conditions has proved successful in predicting pumps and valves activity and canal water levels, and the ability of the conceptual hydraulic model to predict lowland water level response without the use of spatially distributed 2D mechanistic models. This method can potentially lead to significant computational time decrease. This model demonstrates significant potential for implementing a new approach to managing hydraulic infrastructure that can address the challenges posed by climate change. The model can be extended to evaluate several modifications to the system, including the replenishment of the Moëres canals with water from canals in the vicinity of the Moëres region. The calibration technics employed for this model can be adapted to any lowland model, including systems of similar or lower level of complexity.

# Sensitivity of water stress indices to climate change in Tuscany (Italy)

Marco De SIMONE[1], Chiara ARRIGHI[1], Fabio CASTELLI[1]

[1] Department of Civil and Environmental Engineering, Università degli Studi di Firenze, Florence, Italy
marco.desimone@unifi.it

ABSTRACT

Water resources are fundamental to ecosystems, human survival, and socioeconomic development. In the face of climate change, understanding its impacts on water availability, quality, and management is imperative. This study focuses on Tuscany, Italy, employing advanced methodologies to assess the multifaceted relationship between climate change and water resources. The study integrates climate projections, hydrological modeling, and water management data to comprehensively evaluate the impacts of climate change on Tuscany's water resources. The foundation of this study rests upon the integration of cutting-edge methodologies and a deep appreciation for the complex interplay between climate, hydrology, and human activities. At its core, our research hinge balances on the application of the MOBIDIC (MOdello di Bilancio Idrologico DIstribuito e Continuo) hydrological model—a powerful tool capable of dissecting the intricate energy and water balances within the region's watersheds (Yang et al., 2014). In the face of a changing climate, this research extends its purview to consider the RCP8.5 scenario—a high-emission pathway that forecasts the altering climatic conditions of the future in Italy (Spano et al. 2020). By employing this scenario, we seek to elucidate how climate change might reshape Tuscany's hydroclimatic landscape, affecting water availability and ecosystem dynamics.

## 1. Materials and methods

MOBIDIC is a distributed, raster-based model designed to simulate the energy and water balances within a watershed. It divides the study area into discrete cells and simulates various components of the hydrological cycle, including precipitation, runoff, evapotranspiration, and groundwater storage. MOBIDIC's capacity to consider complex interactions between surface and subsurface flows, along with its ability to integrate hydrometeorological data, makes it well-suited for this comprehensive assessment.

The study relies on diverse sources of data to inform the modeling and analysis. Hydrometeorological data serve as critical inputs for MOBIDIC's simulations. These data include historical records of precipitation, maximum and minimum temperature, humidity, wind velocity, and solar radiation. These variables are essential for estimating key hydrological parameters and understanding the energy balance within the watershed. The study period spans from April 1, 2000, to September 30, 2020, with a daily time step, ensuring a robust dataset for analysis. A crucial aspect of this study is the consideration of human impacts on water resources. Data on water abstraction, including withdrawals for agriculture, industry, and municipal use, are integrated into the analysis. Additionally, information regarding water released from wastewater treatment plants (WWTPs) is included. These data provide insights into the human dimension of water management and are pivotal for assessing the sustainability of water use practices in Tuscany. MODIS data, sourced from Terra EOS AM-1 satellite (Running, 2017), enables the calibration of evapotranspiration flux within the model, contributing to more realistic estimates of water loss to the atmosphere. Meanwhile, Sentinel data from the Sentinel-1 C-SAR satellite assists in calibrating simulated soil moisture levels, vital for understanding groundwater dynamics. The study employs the RCP8.5 scenario downscaled using the Regional Climate Model COSMO-CLM in a specific configuration developed for Italy (Spano et al., 2020) to evaluate the potential impacts of climate change on Tuscany's water resources. This scenario represents a high-emission pathway, projecting changes in temperature, precipitation patterns, and other climate variables. The integration of this scenario allows for the assessment of how changing climate conditions may influence water availability and quality in the region.

The annual WEI+ is defined as the ratio between the annual water abstraction (the total volume of water extracted from surface water body) minus the annual volume of water released by WWTPs and the internal renewable water resource i.e., the average annual flow of rivers and groundwater generated from endogenous precipitation Eq. (1). A WEI+ exceeding 20% commonly denotes water stress. WEI is obtained if the release of water is neglected in Eq. (1).

$$WEI + \frac{Abstraction - Release}{RenewableWaterResource} \times 100 \quad (1)$$

Calculated on an annual and monthly basis, WEI+ offers a comprehensive assessment of water resource exploitation, considering both withdrawals and releases. It serves as a critical metric for understanding the balance between human water demands and the natural flow of rivers, providing vital insights into the resilience of ecosystems and the potential impacts of climate change. WEI+ is a powerful tool that guides responsible water management practices, highlighting areas where resource use may be reaching unsustainable levels and helping policymakers and stakeholders make informed decisions to ensure the long-term sustainability of water resources.

## 2. Results

The output shapefile resulting from this study encapsulates a wealth of hydrological information, serving as a comprehensive repository of essential data for understanding and managing water resources in Tuscany. Through its diverse fields, it provides insights into the hydrological hierarchy, basin characteristics, precipitation patterns, flow statistics, and water management dynamics across the region. The results reveal notable changes in the Tuscany River's flow patterns for the considered RCP8.5 climate change scenario (Fig. 1) for the months of August and November. In August, the simulated flow shows a significant decrease ranging from -50% to -20% in most segments of the river network. This reduction implies potential challenges for water availability during the summer season, warranting careful water resource management strategies. The simulated WEI+ increase during the summer months, particularly in the upper segments of the river network. On the other hand, in November, the simulation indicates a positive shift, with an increase of +1% to +5% in flow across most simulated, while the WEI+ index shows a modest decrease by a few percentage points. This change suggests a potential enhancement of water resources during the autumn months, which could benefit various sectors reliant on water supply.

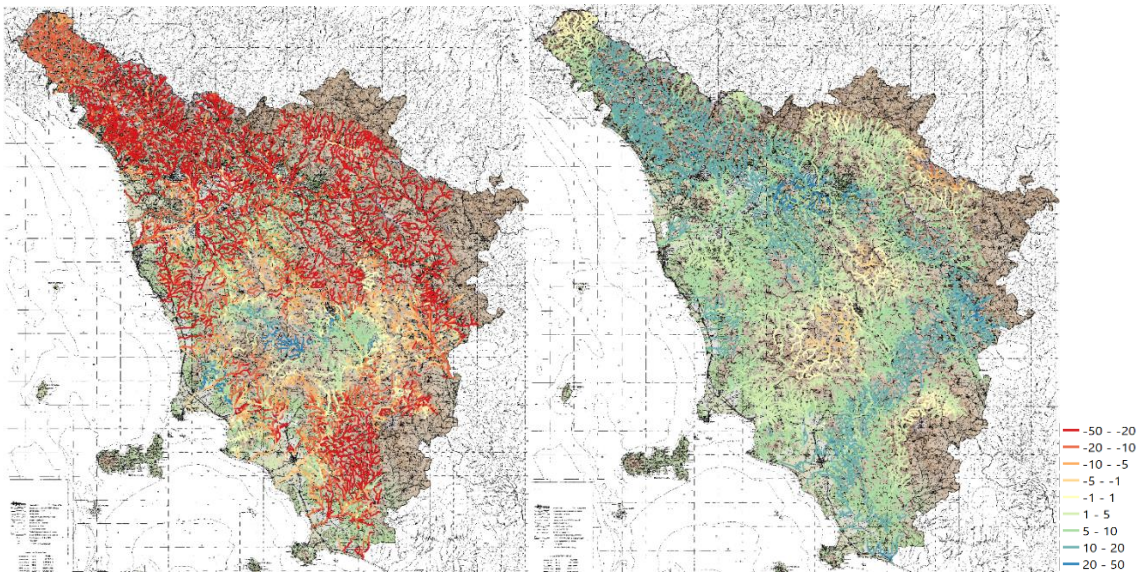



**Fig. 1.** % Change of August (left) and November (right) river flow in a RCP8.5 scenario over main Tuscany river basins.

**References**

Yang, J., Castelli, F., and Chen, Y.: Multiobjective sensitivity analysis and optimization of distributed hydrologic model MOBIDIC, Hydrol. Earth Syst. Sci., 18, 4101–4112, https://doi.org/10.5194/hess-18-4101-2014, 2014.

Spano D., Mereu V., Bacciu V., Marras S., Trabucco A., Adinolf M., Barbato G., Bosello F., Breil M., Chiriacò M. V., Coppini G., Essenfelder A., Galluccio G., Lovato T., Marzi S., Masina S., Mercogliano P., Mysiak J., Noce S., Pal J., Reder A., Rianna G., Rizzo A., Santini M., Sini E., Staccione A., Villani V., Zavatarelli M., 2020. "Analisi del rischio. I cambiamenti climatici in Italia". DOI: 10.25424/CMCC/ANALISI_DEL_RISCHIO

Running, S., Mu, Q., Zhao, M. (2017). MOD16A2 MODIS/Terra Net Evapotranspiration 8-Day L4 Global 500m SIN Grid V006 [Data set]. NASA EOSDIS Land Processes DAAC, https://doi.org/10.5067/MODIS/MOD16A2.00

# Does sampling frequency matter? Comparative analysis of physicochemical quality elements in the Manzanares River (Madrid, Spain)

Francisco M. CORTÉS SÁNCHEZ[1], María DÍAZ-REDONDO[1], Manuel GARCÍA[1]

[1] Centre for Studies and Experimentation on Public Works (CEDEX). Alfonso XII, 3, 28014 Madrid, Spain.
Francisco.M.Cortes@cedex.es

maria.diaz@cedex.es

manuel.colomer@cedex.es

ABSTRACT

The environmental monitoring of water quality is widely adopted in the European Union upon the entry into force of the Water Framework Directive (WFD). However, the sampling frequency of the monitoring programmes have barely change in some Member States since then, more than 20 years ago. In the Manzanares River, where there exist several sampling points from public institutions and where the project "Recovery of the fluvial ecosystem Manzanares-Gavia-Bulera. Green and blue infrastructure Metropolitan Forest of Madrid" is being developed, an opportunity has arisen to study the sampling frequency on physicochemical quality element indicators. From the analysis of the available data, the aim is to determine whether the sampling frequency could affect the assessment of the physicochemical status, and hence influence the classification of the ecological status. To do this, data will be used from the Tagus River Basin Authority and from the Madrid City Council.

## 1. Introduction

The Water Framework Directive (WFD) 2000/60/EC obliges Member States to develop different monitoring programmes (surveillance, operational and investigative) to monitor and assess the ecological status of water bodies. It also sets the minimum frequency of monitoring for the surveillance and operational programmes, defining a frequency of three months for sampling parameters indicative of physicochemical quality elements under the surveillance programme, and suggesting the same guideline for the operational programmes, which should be determined ultimately by Member States. In Spain, the Royal Decree 817/2015, of September 11, which establishes the criteria for monitoring and evaluating the state of surface waters and environmental quality standards regulates the design and implementation of the monitoring programmes for the assessment of the ecological status of water bodies, which includes the frequency of monitoring. In this regard, it establishes that physicochemical quality elements and specific contaminants will be controlled at least every three months, although monthly control is recommended.

In the Manzanares River, the project "Recovery of the fluvial ecosystem Manzanares-Gavia-Bulera. Green and blue infrastructure Metropolitan Forest of Madrid" for recovering the riverine vegetation corridor through the removal of the current concrete outlets and their setting backwards, further from the riverbank, is being carried out. Given that this is a work in the vicinity of the river, with possible impact on the river ecosystem, it is mandatory to carry out environmental monitoring that includes, among other indicators, physicochemical parameters of water quality. Sampling points from the Tagus River Basin Authority (TRBA) and the Madrid City Council will be analysed to evaluate whether the sampling frequency could influence the results obtained in the determination of the status given by the physicochemical quality elements.

## 2. Methods

The study site comprises the section of the Manzanares River downstream the dam number 10 until the municipal boundary of Madrid, La Gavia stream and La Bulera stream, being the Manzanares River part of the "Río Manzanares a su paso por Madrid (ES030MSPF0427021)" water body (Fig. 1).

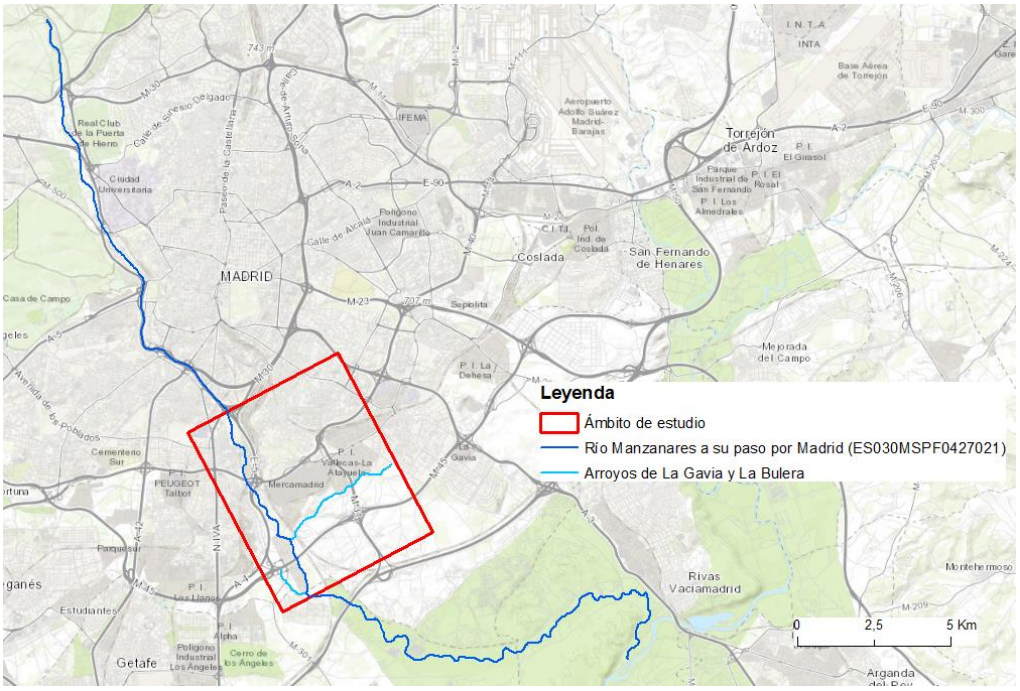



**Fig. 1.** Location of the study site within the "Río Manzanares a su paso por Madrid (ES030MSPF0427021)" water body.

Within the study area there exist two physicochemical sampling points from the TRBA and four sampling points from the Madrid City Council. Nonetheless, only two of them, coincident with the TRBA sampling points, will be used (Table 1). To determine whether the sampling frequency could affect the assessment of the physicochemical status, the assessment will be focused on the physicochemical quality elements and it will be carried out from a period of the last six years (period 2017 – 2023). According to the criteria established by the Spanish Ministry of Ecological Transition and Demographic Challenge (MITERD, 2021), the assessment unit is the hydrological year, so the evaluation will be made both individually and then in an aggregate way for the six-year period. The value per assessment unit and variable will be obtained using the medians of the annual observations. For the aggregate evaluation (multi-year) the median of the medians will be used.

**Table 1.** Information of the physicochemical control points in the "Río Manzanares a su paso por Madrid (ES030MSPF0427021)" water body for the years analysed (2017-2023).

| Sampling point | Name | Institution | **UTMX** | **UTMY** |
|---|---|---|---|---|
| TA55905002 | SAN FERMÍN - MANZANARES | TRBA | 441496 | 4470243 |
| TA55905003 | VILLAVERDE - MANZANARES | TRBA | 442123 | 4467982 |
| 9,3 | | Madrid Council | 441506 | 4470193 |
| ABCH | | Madrid Council | 442396 | 4467695 |

**Acknowledgements**

This study is developed within the project "Recovery of the fluvial ecosystem Manzanares-Gavia-Bulera. Green and blue infrastructure. Metropolitan Forest of Madrid", with the finantial support of the Biodiversity Foundation (Ministry for Ecological Transition and the Demographic Challenge), under the NextGenerationEU's Recovery, Transformation and Resilience Plan (PRTR).

**References**

European Commission (2000). Directive 2000/60/EC of the European Parliament and of the Council of 23 October 2000 Establishing a Framework for Community Action in the Field of Water Policy (Official Journal L 327, 22/12/2000).

Ministerio de Agricultura, Alimentación y Medio Ambiente (MAGRAMA) (2015). Real Decreto 817/2015, de 11 de septiembre, por el que se establecen los criterios de seguimiento y evaluación del estado de las aguas superficiales y las normas de calidad ambiental. BOE núm. 219, de 12 de septiembre de 2015, págs. 80582-80677. Permalink ELI: https://www.boe.es/eli/es/rd/2015/09/11/817.

Ministerio para la Transición Ecológica y Reto Demográfico (MITERD) (2021). Guía para la evaluación del estado de las aguas superficiales y subterráneas.

# Integrating hydrological modelling and System Dynamics tools for understanding Water-Ecosystems-Food Nexus: hints from the Tarquinia area (Italy)

Marwah YASEEN[1,2], Ivan PORTOGHESE[2], Vito IACOBELLIS[1], Silvia VANINO[3], Valentina BARATELLA[3], Stefano FABIANI[4], Mert Can GUNACTI[5], Ali GUL[5], Filiz BARBAROS[5], Raffaele GIORDANO[2], Alessandro PAGANO[2]

[1] Polytechnic University of Bari (PoliBa) - Department of Civil, Environmental, Land, Construction and Chemistry Engineering (DICATECh), Italy
marwah.yaseen@poliba.it

[2] Water Research Institute - National Research Council (IRSA-CNR), Italy

[3] Council for Agricultural Research and Economics (CREA), Centre of Agriculture and Environment, Italy

[4] Council for Agricultural Research and Economics (CREA), Centre of Policy and Bioeconomy, Italy

[5] Dokuz Eylul University, Faculty of Engineering, Department of Civil Engineering, Izmir, Turkey

marwah.yaseen@poliba.it

ABSTRACT

The present work proposes an operational approach to the concept of Water-Ecosystems-Food Nexus, based on the integration of Participatory System Dynamics Modeling techniques (PSDM) and hydrological modelling, specifically the Soil and Water Assessment Tool (SWAT). Specific reference is made to the Tarquinia Plain area (Central Italy), one of the pilot areas within the LENSES project (PRIMA Foundation, GA n. 2041), where irrigated agriculture plays a vital role for local communities, yet with increasing concerns for the impacts on the state of the environment and for the interplay with water resources availability (due to climate change impacts) and quality. In summary the proposed approach is based on the use of: i) Causal Loop Diagrams (CLD) for an improved conceptual understanding of system state and potential evolution, as well as for the identification of key challenges and leverage points; ii) hydrological modelling (SWAT) for getting a deeper understanding of the main implications of agricultural practices on the state of the area; iii) stock and flow models, for scenario analysis and policy design. The methodological approach is being replicated in several case studies in Europe and beyond.

## 1. Introduction and objectives

Access to clean water, energy, and food is vital for human well-being and environmental sustainability. In the face of various threats affecting the availability of natural resources, including the impacts of climate change, there is a growing need to understand the complex relationships among these resources. Resources security requires the adoption of 'Nexus' approaches, oriented to minimize conflicts between different sectors while promoting synergies, compared to a silo approach (Wu et al., 2021).

Reducing conflicts related to natural resources availability and use also requires a wider participation of stakeholders. Their engagement helps incorporating knowledge into model construction, tailoring the model to their specific needs, and ensuring accurate representation of the potential consequences of actions. Ultimately, this approach fosters ownership of the modelling results. In this regard, multiple System Dynamics Modelling (SDM) tools, such as Causal Loop Diagrams (CLDs) or stock and flow models, can help better co-define and understand the dynamic behavior of complex Nexus systems (Phan et al., 2021). The coupling of SDM tools with sectoral models (e.g., hydrological models), can help get a holistic perspective on the state of

natural resources in complex environmental systems, while also taking into account the relevance of 'soft' elements (such as socio-institutional actions).

The present work proposes an approach based on the use of SDM tools, coupled with a hydrological model (SWAT) to: i) identify the main Nexus challenges of an irrigated area; ii) understand in detail the implications of irrigation and agricultural practices on the state of the environment and on the local development; iii) suggest potential leverage points (and actions) to support the sustainability transition of the system. Reference is made to the Tarquinia plain area (Italy), one of the case studies of the LENSES project (PRIMA Foundation, GA n. 2041).

## 2. Methods

The proposed approach proposes the integration of three main tools, as summarized in the following:

1. CLDs have been used to support the conceptualization of the 'Nexus' in the area. Baseline analyses and participatory activities have been coupled in order to get a detailed – and consensual - understanding of the main interdependencies among sectors over the area. In particular, semi-structured interviews have been first performed, to get sectoral perspectives on the system, followed by workshops/focus groups oriented to dive deep into the cross-sectoral connections. Both 'structural' (based on the use of graph theory metrics) and 'descriptive' analyses (based on the analysis of loops) have been performed to identify the main challenges for the investigated system and to preliminarily identify potential leverage points.
2. Based on the key challenge identified in the previous step, i.e. the role of irrigated agriculture in the area and the implications for water resources availability and their state as well as for environmental conditions, the Soil and Water Assessment Tool (SWAT) hydrological model was used. Based on a wide set of available data (including measurements), the model has been calibrated and validated, and then used to assess various components of the hydrological system and to understand the evolution of some key variables related to water quality (such as nutrient load and erosion rate), quantity (runoff, evapotranspiration and infiltration), considering the influence of climate change scenarios.
3. A stock and flow model has been developed to support integrating the evidence from sectoral (including hydrological) models into a holistic picture, supporting the development of a tool to be used for identifying, screening and testing several actions using a Nexus perspective.

## 3. Results and way forward

The implementation of the methodological approach helped building a consensual view of the area (effectively visualized and shared through CLDs), driving stakeholders towards the identification of consensual Nexus challenges, that can be crucial to guarantee the sustainable development of the area in the next few decades. Some activities (like the participatory mapping) facilitated the dialogue among policy- and decision-makers, and the identification of suitable solutions. The coupling with hydrological modelling was particularly useful in providing deeper technical knowledge on the impacts of irrigation practices on the system under a multiplicity of scenarios, helping to understand also the implications of policies and actions (with a focus on Nature-based Solutions). The development of the stock and flow model (ongoing) will help understand all the implications (including potential side effects) of the selected actions on the system as a whole.

**Acknowledgements**

The research activities described in the present work have been performed within the the LENSES Project (PRIMA programme – Grant Agreement n. 2041, https://www.lenses-prima.eu/). The Authors would like to thank both project teams for many inspiring discussions. Moreover, a great thanks goes to the stakeholders who provided their knowledge and expertise, significantly contributing to this work.

**References**

Phan T D, Bertone E, Stewart R A (2021) Critical review of system dynamics modelling applications for water resources planning and management, Cleaner Environmental Systems, 2, 100031, https://doi.org/10.1016/j.cesys.2021.100031

Wu L, Elshorbagy A, Pande S, and Zhuo L (2021) Trade-offs and synergies in the water-energy-food nexus: The case of Saskatchewan, Canada, Resources, Conservation and Recycling, 164, 105192. https://doi.org/10.1016/j.resconrec.2020.105192

# A methodological approach for supporting socio-hydrological modelling of a complex Nexus system

Claudia PANCIERA[1], Alessandro PAGANO[2], Raffaele GIORDANO[2], Ivan PORTOGHESE[2], Mert Can GUNACTI[3], Sefa Nur YESILYURT[3], Mohamed NAJAR[4], Cem Polat CETINKAYA[3], Gulay ONUSLUEL GUL[3], Estrella LOPEZ[5], Manuel BEA[5]

[1] DICATECh, Politecnico di Bari, Bari, Italy; c.panciera@phd.poliba.it
[2,] Water Research Institute-National Research Council (IRSA-CNR), Bari, Italy; alessandro.pagano@cnr.it raffaele.giordano@cnr.it , ivan.portoghese@cnr.it ,
[3] Dokuz Eylul University, Faculty of Engineering, Department of Civil Engineering, Izmir, Turkey, mert.gunacti@deu.edu.tr , sefanur.yesilyurt@deu.edu.tr , cem.cetinkaya@deu.edu.tr , gulay.onusluel@deu.edu.tr
[4] GIS Department, Islamic University of Gaza, Gaza, Palestine; eng.mhmd.najar@gmail.com ,
[5,] Asociaciòn ECOADAPTA, Madrid, Spain, estrellalm@ecoadapta.org , manuelbm@ecoadapta.org

ABSTRACT

The Water-Ecosystems-Food Nexus is increasingly studied and adopted both in the research and in the policy fields, since there is evidence of the side effects of sectoral policies implemented without considering any cross-sectoral analysis (Sušnik et al., 2021). In a scenario of accelerated changes, both from a climatic and socio-economic point of view (demographic and economic expansion), natural resources such as water are constantly threatened by competing multiple sectors such as agriculture, tourism, industry and environment (Karamouz et al., 2021). The complexity of natural resources management becomes more critical in areas where natural reserves are jeopardized by human action, such as the Doñana National Park, a coastal area in SW Spain where the environmental and economic interests have varied over time with increasing contrasts among stakeholders. The LENSES project is operating in the Doñana area (as one of the case studies in the Mediterranean area), with the objective to propose a new approach based on Participatory System Dynamic Modelling (PSDM) to recognize the major challenges and the drivers for the system, ultimately suggesting potential actions/strategies, using a Nexus approach. Our work focuses on the assessment of the system under current and future conditions, integrating PSDM with other sectoral models (in particular, hydrological modeling and water resources allocation). This integrated model supports decision making processes in view of the implementation of Nexus approaches, to make the system resilient and more sustainable over time.

## 1. The case study

The Doñana region, which covers one of the most important wetlands in Europe, is an area between the Tinto River and Guadiamar River estuary and overlooks the Atlantic. It is historically considered a place of high naturalistic value as well as a notable biodiversity hub straddling two continents (Serrano, 2016). Nowadays it is under protection by important institutions such as the WWF, as it has undergone different anthropogenic pressures over time such as channel diversion, and the overexploitation of surface and underground water bodies due of the increased water demand for irrigation and tourism. The effects of this exploitation regime are tangible, and, without a clear and coherent action plan, the situation can only become worse.

## 2. Methodological approach and preliminary results

The value added of the modeling approach presented in this work is the direct involvement of stakeholders in SDM development and analysis. In this regard, a series of individual interviews and workshops have been organized throughout project duration to elicit stakeholder knowledge on the main challenges over the area,

ultimately feeding the Causal Loop Diagram (CLD). The CLD was used to get a holistic perspective on the system under investigation, helping to analyze in a structured way the conflicts between intensive water users (such as green-house farmers) and environmental organizations interested in the protection of marshland ecosystems. In particular, during the first workshop a participatory mapping exercise was performed, to represent the complexity of the main processes (including bio-physical, socio-economic and behavioral variables) characterizing the study area. Stakeholders helped identifying the main processes, the central variables and critical interdependencies, supporting the definition of a comprehensive system picture. The key challenges identified for the area were the exploitation of the groundwater resources reducing the environmental flow to the wetland, the need to undertake strategies for the restoration of the different natural ecosystems (marshland and temporary ponds) and for the protection of biodiversity over the whole area. The analysis of the CLD supported highlighting the central role of water security for the state of the area, and a water resource allocation software (WEAP) was therefore used to investigate water management options. The WEAP model included demand nodes, supply nodes and connections between them, and was focused on the description (in a quantitative form) of the environmental water demand within the water balance of the area. One of the most useful and innovative outputs obtained through the water allocation modeling is the *unmet water demand* of the Doñana marshland during dry and ordinary years based on the historical climate records. The preliminary results of these modelling activities have been presented in the second workshop with local stakeholders, with the aim of discussing into details the competitive water and land uses in the study area, focusing the discussion on potential solutions to guarantee a sustainable transition of the area (e.g., Nature-based Solutions, different water allocation criteria, etc.). This participatory process, encompassing challenges and objectives of various stakeholders, resulted in a consensual need for developing a robust quantitative tool for the evaluation of the marshland water balance, enabling to investigate the environmental water requirements of Doñana coastal plain under different management scenarios. In this direction, we envisage the integration of the water allocation model with the PSDM (specifically, building a stock and flow model), in order to perform a 'what-if' scenario analysis able to consider the role of multiple drivers (e.g., climate change) and the impact of the suggested strategies.

## 3. Overview of future activities

The creation of future scenarios and the co-evaluation of their feasibility and potential effectiveness using a stock and flow model is a future result that aims to close the whole process started with the participatory identification of problems and the modeling of the baseline scenario. The scenario analysis will be also coupled with the definition and calculation of relevant indicators aimed at transferring the results of the modeling activities to stakeholders, in order to facilitate the understanding of system functioning and to better inform decisions considering the role and needs of actors (de Vito et al., 2019). The results obtained can be used in a simple and effective way also in other areas, to allow policy- and decision-makers makers to make informed decisions based on the development of a holistic view of complex systems based on a Nexus approach.

**Acknowledgements**

The present work has been funded by the LENSES project (PRIMA Programme, GA n°2041). This paper and the content included do not represent the opinion of PRIMA Foundation, PRIMA foundation is not responsible for any use that might be made of its content.

**References**

Sušnik J, Masia S, Indriksone D, Bremere I, Vamvakeridou-Lydroudia L, (2021) System dynamics modelling to explore the impacts of policies on the water-energy-food-land-climate nexus in Latvia, Science of Total Environment, 775, 0048-9697.

Karamouz M, Barkhordari H, Ebrahimi E (2021) Dynamics of Water Allocation: tradeoffs between allocator's and farmers' benefit of irrigation practices, Journal of Irrigation and Drainage Engineering Online 147(6), DOI: 10.1061/(ASCE)IR.1943-4774.0001550.

Serrano L (2016) Balancing water uses at the Donana National Park, Spain, The Wetland Book, DOI 10.1007/978-94-007-6172-8_232-4.

de Vito R, Pagano A, Portoghese I, Giordano R, Vurro M, Fratino U (2019) Integrated approach for supporting sustainable water resources management of irrigation based on the WEFN framework, Water Resources Management, 33, 1281-1295, DOI 10.1007/s11269-019-2196-5.

# A web-based decision co-creation platform for the circular economy by representing wastewater treatment, the extraction of value-added compounds, biogas, water and nutrients

Mehdi Khoury*[1], Barry Evans[1], Tavishi Guleria[2], Joep Van Den Broeke[2], Lydia Vamvakeridou-Lyroudia[1,2], Otto Chen[1,3], Navonil Mustafee[3], Albert S. Chen[1]

[1] Centre for Water Systems, University of Exeter, United Kingdom
*m.khoury@exeter.ac.uk

[2] KWR Water Research Institute, Netherlands

[3] Centre for Simulation, Analytics and Modelling, University of Exeter Business School, United Kingdom

ABSTRACT

This paper presents a web-based decision co-creation platform designed to showcase water treatment technologies for a circular economy approach developed as part of the EU H2020-funded ULTIMATE project. This system will investigate three case studies focusing on water and nutrient recovery in greenhouses, pre-treatment of wastewater from olive mills before integration into communal wastewater systems, and value-added compound recovery from wastewater in a juice factory, respectively. In the subsequent development phase, the three cases will be merged into one abstract composite case; this would show all three aspects of the problem, connect greenhouses, juice factories, and olive mills, and develop examples of an industrial "metabolic network" of the circular economy. The paper describes the interactive visualization framework developed to allow users to explore these problems and offer corresponding solutions.

## Introduction

Ellen Macarthur Foundation (2010) suggested that the circular economy provides an opportunity for addressing challenges posed by climate change and the growing scarcity of resources. In this work, typical goals such as eliminating waste and pollution, looking for ways to recycle materials and products, and finding solutions to restore the natural environment and translating them into valid principles are applied to three case studies. The first study applies to the horticultural sector, the second to the management of olive mills, and the third to the juice industry. This works builds on some design principles and technologies initially developed in the NextGen web-based Serious Game (Khoury et al., 2023) themed around improving the circular economy of a virtual toy town via combinations of measures and tools. Additional features have been derived in this work to provide a more flexible framework with modular modelling and interface elements that can be combined to produce a web-based decision co-creation platform accessible from multiple devices.

## User Interface design

The system is designed to enable professionals from all three case studies to access the system through the Internet. Further, irrespective of the access device (e.g., personal computer, laptop, smartphone, tablet), the system enables seamless investigation of the solution space in a graphically friendly manner using novel visualization techniques. This maximizes the potential of the decision co-creation platform as a tool for exploring solutions and outcomes. The developed interactive framework needs to be lightweight, adaptive, and modular. These goals have been realized by choosing a software stack which includes recent and flexible web-programming tools, including JavaScript open-source visualization libraries such D3js, and component-based cross-platform development libraries based on React technology (such as Recharts). The web page reconfigures itself depending on the screen size to display either a zoomable dashboard that can be panned on, or a smartphone interface where all details are accessible from a small screen (Figure 1).

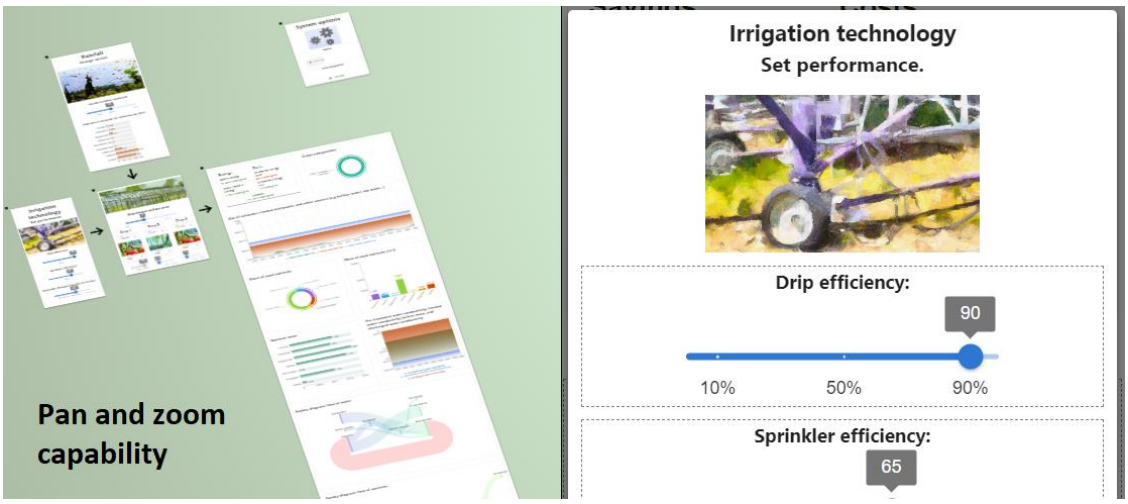



**Fig. 1**. *Left*: Screenshot of online user interface where the user can zoom and pan an extended dashboard to explore different solutions and outcomes. *Right*: Screenshot of the same adaptive online user interface when accessed from a smartphone.

The simulations of scenarios based on users' settings are computed and displayed by a system dynamic model running in the background on a Julia-based server. The computation is extremely fast (usually takes less than a second). In the greenhouse case, the browser-based interface allows users to set the irrigation technologies in use, the rainfall, and the greenhouse crops and surface area, and see the difference in how water, energy, and fertilizers are reused and how the quality and volume of discharged water are impacted. The olive mill interface is groups parameters into four sections: olive mills, wastewater transportation, wastewater treatment, scheduling of seasonal activity.

## Results and Discussion

The existing prototype covers two of the three case studies: the greenhouse and the olive mill case studies.

For the greenhouse case study, the interface allows decision-makers to understand better how using specific crops can lower the water, energy, and nutrient footprint. Furthermore, it shows the impact of efficient versus inefficient irrigation on savings when using novel electro-chemical membrane processes, such as electrodialysis (as opposed to current state-of-the-art reverse osmosis), to treat and recover nutrients and water from the greenhouses.

For the olive mills case study, the interface highlights how crucial the distance to the nearest advanced anaerobic wastewater treatment plant is to the price of waste transportation. It also emphasizes the role of seasonal scheduling on biogas production due to the sensitivity to weather-induced temperatures. Finally, the contribution of value-added compound recovery is shown to lead to potentially significant savings.

The final case study, which is a work in progress, will focus on juice factories and the reuse of value-added compounds in external industries (i.e. pharmaceutical and food industry). This particular circular economy business model of value extraction is still in its infancy but quite promising! Thus in our final case, we start the work of identifying how recovered products in the previous models could be linked via a "metabolic" network of industries.

After covering the greenhouse and the olive mill cases, we can confirm that making an abstract composite model of all three case studies is feasible, and the desirable outcome will provide compelling and interesting insights into the valorization of the circular economy of water.

**Acknowledgements**

The work outlined in this paper was funded by the European Union's Horizon 2020 research and innovation programme under grant agreement No. 869318 as part of the circular economy call CE-SC5-04-2019.

**References**

Ellen Macarthur Foundation. (2010). *Circular economy introduction*. https://ellenmacarthurfoundation.org/topics/circular-economy-introduction /overview

Khoury, M., Evans, B., Chen, O., Chen, A. S., Vamvakeridou-Lyroudia, L., Savic, D. A., Djordjevic, S., Bouziotas, D., Makropoulos, C., & Mustafee, N. (2023). NEXTGEN: A serious game showcasing circular economy in the urban water cycle. *Journal of Cleaner Production*, *391*, 136000. https://doi.org/https://doi.org/10.1016/j.jclepro.2023.136000

# Would short term online monitoring improve the WFD-sampling strategy? Subsampling of high frequency data from four watersheds in Saxony

Jakob BENISCH[1], Björn HELM[1], Peter KREBS[1]

[1] TU Dresden, Chair of Urban Water Management
Jakob.benisch@tu-dresden.de

## ABSTRACT

The European Union Water Framework Directive (European Commission, 2000) aims to achieve a good ecological and chemical status of all bodies of surface water by 2027 and has developed an integrated guidance on surface water chemical monitoring (e.g. WFD Guidance Document No. 7/19, Hanke et al. 2009; WFD-CIS 2003) which is transferred into national German law (Ordinance for the Protection of Surface Waters, OGewV, Bundesministeriumder Justiz und für Verbraucherschutz, 2016). For the majority of compounds, this act requires a monthly sampling frequency to assess the chemical water quality status of a surface water body.

To evaluate the representativeness of the sampling strategy under the OGewV, high-frequency online monitoring data is investigated under different sampling scenarios and compared with current, monthly grab sampling strategy. About 23 million data points were analyzed for this study, three chemical parameters (dissolved oxygen, nitrate-nitrogen, chloride concentration) and discharge data were selected from four catchment of different sizes ranging from 51 391 km² to 84 km² (Elbe, Vereinigte Mulde, Neiße and two stations at Lockwitzbach, see Figure 1).

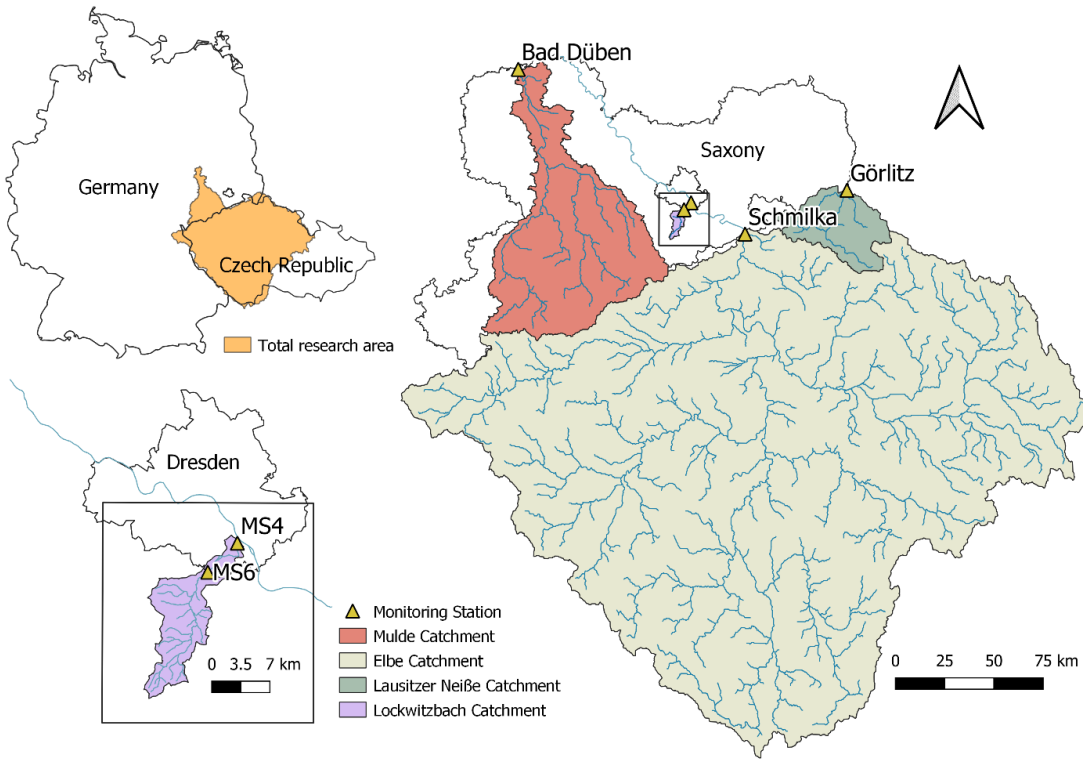



Fig. 1: Catchments of the investigated streams and location of the monitoring stations

In this contribution we want to (I) compare the results of conventional grab sampling with short-term online-monitoring (STOM), where online sensors are applied over a limited duration and return interval in the

investigated rivers, (II) to use discharge data as proxy for the event mobilized pollutants to investigate the different performance of STOM, the procedure is summarized in Figure 2.

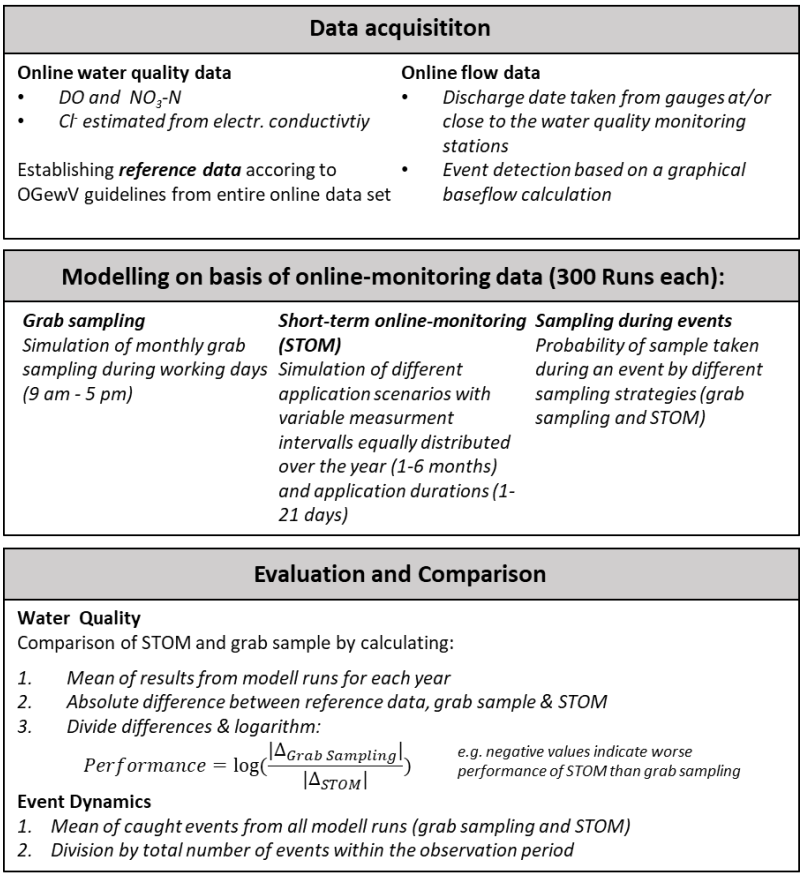



Fig. 2: Scheme for comparing different sampling approaches

Results show, that STOM outperforms grab sampling for parameters where minimum/maximum concentrations are required by law as the probability to catch a single extreme value is higher with STOM. Furthermore, parameters showing a pronounced diurnal pattern, like dissolved oxygen, are also captured considerably better. The performance of STOM did not provide improvements for parameters with small concentration variability, as Nitrogen-Nitrate and Chloride showed no substantial improvements by STOM monitoring. The analysis of discharge events as surrogate parameter for event-mobilized pollutants proved that the probability of capturing samples during events is significantly increased by STOM.

Literature

*Bundesministeriumder Justiz und für Verbraucherschutz (Ed.), 2016. Verordnung zum Schutz der Oberflächengewässer (Oberflächengewässerverordnung - OGewV).*

*European Commission, 2000. DIRECTIVE 2000/60/EC OF THE EUROPEAN PARLIAMENT AND OF THE COUNCIL of 23 October 2000 establishing a framework for Community action in the field of water policy'' or, in short, the EU Water Framework Directive.*

*Hanke, G., Lepom, P., Quevauviller, P., Allan, J., Batty, J., Bignert, A., Borga, K., Boutrup, S., Brown, B., Carere, M., 2009. Guidance Document No. 19 Guidance on Surface Water Chemical Monitoring under the Water Framework Directive.*

*WFD-CIS, 2003. Guidance Document No. 7. Monitoring under the Water Framework Directive Luxembourg. oi.org/10.1002/2017GL074889*

# Impact of beaver activity on water resources in the catchment and water quality

Stanisław ZABOROWSKI[1], Tomasz KAŁUŻA[2], Paweł STRZELIŃSKI[3], Mateusz HAMMERLING[4]

[1,2,3,4] Poznań University of Life Sciences
stanislaw.zaborowski@up.poznan.pl
tomasz.kaluza@up.poznan.pl
pawel.strzelinski@up.poznan.pl
mateusz.hammerling@up.poznan.pl

ABSTRACT

The European beaver (Castor fiber) is the second most highly impacted species after humans, and is able to affect vast areas with its activities (McKinstry et al., 2001). It is the largest rodent inhabiting Eurasia, and by the turn of the 19th and 20th centuries it was almost completely extinct throughout Europe. In the middle of the 20th century in Poland, the beaver population was estimated at about 130 individuals, while after the introduction (between 1949 and 1985) in 2015 the population was determined at about 100,000, and today it is estimated that it may already number more than 120,000 (Omelczuk and Kozieł, 2017). Like humans, beavers shape the environment to facilitate their movements, store food and secure entrances to their burrows or lodges by building dams and small channels. The resulting damming causes numerous changes both in and near the watercourse. The change in the level of the water level in the riverbed, and sometimes the emergence of water from the banks and the formation of a beaver pond, constitute water retention that can be easily estimated. Equally important is soil retention and the groundwater level system, as well as the range of impact of damming on nearby land (Westbrook et al., 2020). McKinstry et al., 2017 note the many feedbacks occurring in the environment as a result of beaver activity. Research in the UK has shown the contribution of beaver dams to mitigating the impact of storm rainfall on flood wave formation minimizing takeoffs and adverse effects (Puttock et al., 2020).

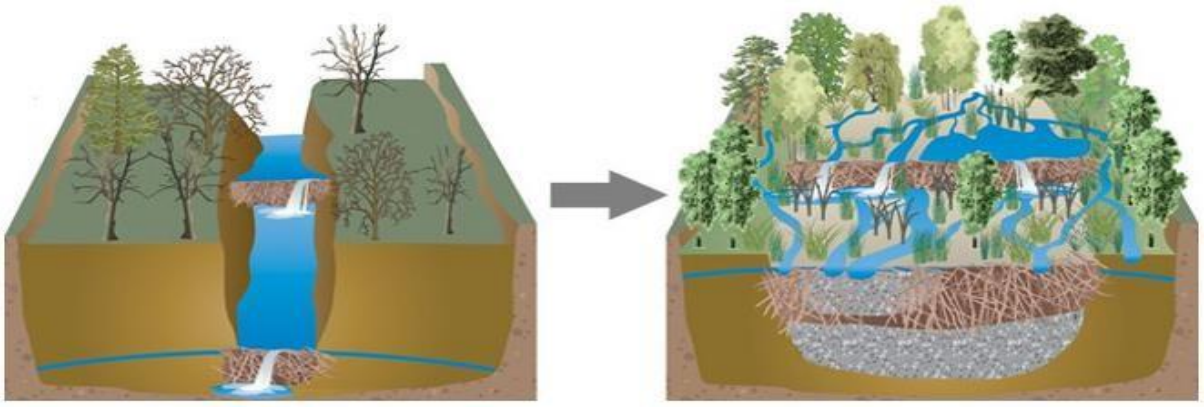


**Fig. 1.** Changes caused by beaver activity in the lowland river (Pollock et al., 2014).

## 1. Metodology

The paper presents the impact of beaver activity on the formation of water resources and water quality in the catchment area. In addition to channel retention gained from the construction of dams by beavers, water is still stored in the soil profile. The resources and quality of this water have not yet been estimated. Field studies were carried out on 10 objects (beaver dams), among which can be identified 5 dams in the forest environment and 5 dams in other areas. All beaver dams were located in Great Poland Province (Poland). Measurements included inventory of beaver dams (e.g., width, height and length), building material, riverbed and valley geometry, species composition of nearby flora, and water table system in the riverbed (above and below the

dam) and in 10 piezometers located in an area of about 1000 $m^2$. During the measurements, physicochemical parameters were checked and heavy metals were ordered to be determined in the bottom sediments upstream and downstream of the dams. The inventoried objects were characterized by a width of 3 – 10 m and a height of no more than 0.9 m.

## 2. Results

Based on the measurements, the amount of both riverbed and soil retention was estimated. For one structure with an impoundment height of 0.7 m, the amount of retained water was 4,200 $m^3$ in the riverbed and valley alone. The extent of the dam's impact reached 300 m upstream of the dam. The system of the water level in the ground significantly depended on the shape of the river valley and the soil parameters. With steep valley banks, a very small range of impact and thus elevation of the groundwater level curve was observed. On the other hand, for a watercourse with a flat valley, a noticeably greater impact of damming was observed for changes in the groundwater system and resources. At one site, an rise in the water level of up to 0.40 meters was observed in the range of installed piezometers. It is worth adding that it was often asymmetric due to the river course in the plan. On the basis of water quality studies, a significant improvement in water quality was determined downstream of the dam compared to samples taken upstream of the dam.

## 3. Conclusion

Beaver activity in the form of building their dams is extremely beneficial. The increase in natural retention of trough as well as soil in the catchment area is very important in times of water scarcity. The resources thus secured provide a valuable source for nearby animals and allow nearby plants to survive. Slowing of the flow in the resulting floodplains (beaver ponds) contributes to sedimentation of pollutants and improvement of the quality of retained water, and the water overflowing on the surface dam becomes oxygenated, improving its physicochemical properties. In addition, the hydromorphological changes occurring in the watercourse contribute to the creation of new habitats for flora and fauna. The impact of rising groundwater levels on the forest stands growing in river valleys is inconclusive. On the one hand, trees growing in the close vicinity of watercourses were often in worse condition or felled by beavers. However, within the river valleys, the increase in retention and raising of the groundwater level, positively affected the remaining tree stands (especially riparian forests). It is worth adding that many times there are several dams on the watercourse (cascade of structures), which multiplies the retention effect.

**Key words**

European beaver, beaver dams, water resources, water quality, hydraulic conditions, hydromorphology of lowland watercourses.

**Acknowledgements**

The research was co-founded by the National Science Centre of Poland within the PRELUDIUM project (No. 2021/41/N/ST10/02490): “Evaluation of a zoogenic factor in the modification of environmental, retention and hydromorphological conditions in small lowland watercourses based on the action of beavers (Castor fiber)” (2022–2025).

**References**

Macfarlane WW, Wheaton JM., Bouwes N, Jensen ML, Gilbert JT, Hough-Snee N, Shivik JA. (2017) Modeling the capacity of riverscapes to support beaver dams, Geomorphology, Volume 277, 15 January 2017, Pages 72-99

McKinstry, M. C., Caffrey, P., & Anderson, S. H. (2001). The importance of beaver to wetland habitats and waterfowl in Wyoming, Journal of the American Water Resources Association, 37(6), 1571–1577. https://doi.org/10.1111/j.1752-1688.2001.tb03660.x.

Omelczuk Ł, Kozieł M (2017) Wpływ działalności bobra europejskiego Castor fiber L. na zmiany stosunków wodnych na Polesiu Zachodnim, WPTPN, Badania Fizjograficzne, Seria A, Tom 68, 2017, s. 99-113

Pollock M, Beechie T, Wheaton J, Jordan C, Bouwes N, Weber N, Volk C (2014) Using Beaver Dams to Restore Incised Stream Ecosystems, BioScience, Volume 64, Issue 4, April 2014, pp. 279–290, doi.org/10.1093/biosci/

Puttock A, Graham HA, Ashe J, Luscombe DJ, Brazier RE (2020) Beaver dams attenuate flow: A multi-site study, Hydrological Processes. 2021; 35:e14017.

Westbrook CJ, Ronnquist A, Bedard-Haughn A (2020) Hydrological functioning of a beaver dam sequence and regional dam persistence during an extreme rainstorm, Hydrological Processes, 34(18), 3726–3737. http://dx.doi.org/10.1002/hyp.13828.

# Aggregating opinions of the stakeholders in a fuzzy environment

Thomas BAKAS[1], Dionissis LATINOPOULOS[1], Christopher PAPADOPOULOS[1], Ifigenia KAGALOU[1], Mike SPILIOTIS [1*]

[1] Civil Engineering/School of Engineering, Democritus University of Thrace, Xanthi, Greece
m.spiliotis@gmail.com

ABSTRACT

Bottom-up management in a catchment scale is deemed the efficient way to avoid conflicts among water users through the participation of stakeholders, strategy co-shaping, and solutions co-creation. The incorporation of the stakeholders' opinion in measures hierarchy introduces discussion and participation while guarantees the measures' acceptance of the local communities. From a mathematical point of view, provides an acceptable way to assess the weights and sometimes the evaluation of some criteria when dealing with decision support. To comply with this difficult task, two approaches are developed for the assessment of the criteria's weights. The first one is based on the principle of intuitionistic fuzzy sets (IFS) whilst the second is based on the measure of fuzzy similarity. The methodologies are applied in a real case study for the Laspias River watershed, which is characterized by intense agricultural and industrial activity and furthermore and severe water quality issues. Finally, a holistic multicriteria approach is applied which will incorporate the stakeholders' opinion. Propositions regarding the use of the proposed methods were made.

## 1. Introduction

Including stakeholders' opinion in measures hierarchy to respect the integrated nature of water management is usually an important but difficult task. The usefulness lies in the fact that is a tool for bottom-up management that eliminates conflicts and strengthens solutions viability through strategy co-shaping. This is broadly accepted at a global scale where EU (i.e. 2000/60/EC, WFD), UN (i.e SDGs) and OECD (3rd goal "Trust and engagement) have set goals for enhancing awareness and ownership of management uptake. Though, the opinion quantification and its incorporation in decision making can be achieved through mathematical ways that can deal with the inherent uncertainty of qualitative answers. Fuzzy sets, can offer the tool to assist management planning by incorporating such information in a quantifiable manner. Despite their widespread use in algorithm design, they are often characterized by a number of limitations, most of which are related to the requirement of a well-defined membership function. To surpass some obstacles of conventional Fuzzy sets, Intuitionistic Fuzzy Sets (IFS) can be applied to address the uncertainty due to the imperfect nature of information. Hence, the main scope of the proposed analysis is to compare two widely used methods for weights calculations, to ultimately support better decision making by quantifying all available stakeholder input and pinpoint discernible differences and benefits for a more tailored decision making.

## 2. Study area

The Laspias River watershed (EL12-07) occupies an area of 221.8 km$^2$. It is characterized by a cascade of pressures including WWTP, landfills, industrial parks, agricultural fields and farms resulting in poor/ bad water quality. It is a peri-urban basin located near the city of Xanthi, Thrace. The catchment of the Laspias is characterized by rather plains and natural areas with low vegetation while the intense agricultural activity operates without an integrated irrigation network that could cover water needs (Bakas et al., 2023).

## 3. Materials and Methods

The data for the analysis was gathered with the use of semi-structured interview formed in a set of pre-designed queries (non-exclusive). Campaigns were held in-situ where all scale of actors were interviewed, meaning stakeholders grouped in three clusters farmers, citizens and experts (practitioners and academia). The majority of answers were in qualitative form so as not to predefine or bias the results. Then the analysis took place.

In classical logic, an element X either belongs or does not belong to a set, represented by binary true or false values. In fuzzy logic, the membership of element X to a set is expressed in degrees, allowing for a gradual transition between absolute membership and non-membership. The first part of the methodology applied is based on the principle of IFS which are an extension of ordinary fuzzy sets. In intuitionistic fuzzy logic, the consideration extends beyond membership to include degrees of non-membership and hesitancy, providing a more nuanced representation of uncertainties and hesitations in reasoning processes. The IFS besides the positive information determined by the membership function (μ) in a set, also have the possibility of expressing negative information with the aid of the non-membership (ν) function. They provide also the possibility to describe and define mathematically the concept of hesitancy (π). The widely used Intuitionistic Fuzzy Weight Averaging Operator (IFWA) is then applied to aggregate sets. In brief two approached are investigated for criteria wights' assessment: a) intuitionistic fuzzy sets with IFWA operator (Xu, 2007); b) fuzzy trapezoidal numbers where the criteria weights are calculated based on the degree of similarity by taking account the stakeholders' opinions (scores) (Chen, 2010) with the ability to discriminate experts (if needed).

## 4. Results & Discussion

In case that the IFWA operator was used, this aggregator is near to the fuzzy union, if at least one stakeholder proposes that μ=1 (Bakas et al., 2023). In the case that the similarity measure is used then the weight is not so commensurate. Indeed, the standard deviation is larger in this case compared with the first methodology (Table 1). The use of similarities measures in the case of fuzzy intuitionistic sets are recently investigated and can be an object for further consideration. The ranking promotes as first criterion in both methods the economic one, while there is an agreement on half of the criteria, however, there is a variation concerning the rest.

**Table 1.** The weights based on IFWA and its defuzzification values.

| Criteria | μ (membership) | ν (negation) | π (hesistancy) | Defuzzified (normalized) IFWA | Defuzzified (normalized) trapezoidal similarity |
|---|---|---|---|---|---|
| Economic | 0.83 | 0.13 | 0.04 | 0.109 | 0.113 |
| Social | 0.73 | 0.18 | 0.10 | 0.101 | 0.105 |
| Environmental | 0.79 | 0.16 | 0.05 | 0.104 | 0.106 |
| Covering water needs | 0.77 | 0.16 | 0.07 | 0.104 | 0.102 |
| Climate change | 0.72 | 0.18 | 0.09 | 0.100 | 0.100 |
| Local acceptance and know-how due to measures | 0.72 | 0.20 | 0.08 | 0.098 | 0.098 |
| Part of the water body affected by measures | 0.69 | 0.21 | 0.10 | 0.096 | 0.097 |
| Water saving due to measures | 0.73 | 0.19 | 0.09 | 0.100 | 0.097 |
| Cooperation and coordination between water policy measures | 0.66 | 0.24 | 0.10 | 0.092 | 0.089 |
| Attracting new people to the countryside to live and work | 0.70 | 0.22 | 0.09 | 0.096 | 0.093 |
| Standard Deviation | | | | 0.005 | 0.007 |

This variation may be crucial for alternatives selection. It seems that the use of IFWA is promoted as the data gathering was single-staged and thus all the stakeholders' opinions are taken into account by "respecting the minority" (Perny, 1998). If more convergence were needed, the second method would be preferable, assuming a two-stage workshop was held. The hole procedure was in line with WFD consultation phase, supported SDGs related to WRM (3, 6, 11, 12, 13) and the 11th OECD (2015) principle "Promote stakeholder engagement for informed and outcome-oriented contributions to water policy design and implementation", even though the social-justice dimension is not fully outlined (Taylor et al., 2019). Further, the research emphasizes in robust incorporation of the uncertainty, correlated with quantification of more absurd ideas/opinions. Human reasoning is efficiently "translated" through Fuzzy operators.

**References**


Bakas, T., Papadopoulos, C., Latinopoulos, D., Kagalou, I., Akratos, C., Angelidis, P., ... & Spiliotis, M. (2023). Supporting Participatory Management Planning for Catchment Operationalization with Intuitionistic Fuzzy Sets—A Study in Laspias River, Thrace, Greece. Water, 15(16), 2928.

Chen, S. (2010). Aggregating fuzzy opinions in the group decision-making environment, Cybernetics and Systems, 29(4), 363-376.

OECD Principles on Water Governance Welcomed by Ministers at the OECD Ministerial Council Meeting on 4 June 2015, Directorate for Public Governance and Territorial Development, Organization for Economic Cooperation and Development, Paris (2015)

Perny, P. (1998). Multicriteria filtering methods based onconcordance and non-discordance principles. Annals of operations Research, 80(0), 137-165.

Taylor, K. S., Longboat, S., & Grafton, R. Q. (2019). Whose rules? A water justice critique of the OECD's 12 principles on water governance. Water, 11(4), 809.

Xu, Z. (2007). Intuitionistic fuzzy aggregation operators. IEEE Transactions on fuzzy systems, 15(6), 1179-1187.

# Water 2.0 | Going Local – The Territorial Approach/Portuguese Case – Grândola Municipality

Edília PENA, Paulo VARANDA

CertiAmb, Lda, Portugal

ABSTRACT

Even though water scarcity in Portugal, resulting from diverse and specific factors for each territory, is an acknowledged concern at almost all governance levels, resulting in relevant imbalances in the resource levels, where demand exceeds availability, the water security as a final state is far and needs to be scientifically addressed in its different dimensions.

When added to extreme phenomena, with causes of broader origin, such as cyclical droughts, for example, and the impact of climate change, this water imbalance has relevant impacts that are important to *anticipate*, through detailed planning in order to guarantee the stabilization of water masses, with regard to their nature and levels.

Without prejudice to macro reflections, proving to be of great importance, no less important is to state that the "*bottom up*", as an exercise of the desired permanent cycles of analysis-synthesis related with local-based territorial planning, must be taken as a priority, as a path to integrate, not only the specificities of each territory, but also to increase levels of systematization and anticipation (with faster risk mitigation of the consequences associated with the levels of scarcity and drought predicted for the next decade).

With emphasis on integrating the water resource and associated projects into the diverse planning instruments, it is (also) necessary to intervene in the effectiveness of models that impose their correct dynamics, resulting from the need to review or change them, as a way to integrate, in a timely manner, the evolution of economic, social and environmental conditions and, therefore, the respective impactful projects.

This process inevitably involves the analysis, evaluation and increase of technological innovation factors, changes in the socio-behavioral forum at the consumer level, community awareness and involvement, improving the performance of support infrastructures or leveraging resilient projects that incorporate emerging challenges. In this context, territorial planning instruments and the legal framework are fundamental tools, not only at a strategic and programming level, but also for normative regulation of interventions on a scale close to the territory, with sustainable practices that are intended to be encouraged, with design evolution of new public policies.

The aim of this article is to pave the way for this systematization, based on the study prepared by the authors on the use of the water resource, in the Portuguese municipality of Grândola[1], with exploration of the main resulting aspects, with the scope on the sustainability of water use and the integration with other resources, in their different applications and phases.

[1] The study is currently ongoing and will be publicly presented in January 2024.

8th IAHR EUROPE CONGRESS
LISBON - PORTUGAL
4-7 JUNE 2024

# The impact of human activities on the flood risk

Gašper RAK[1] and Mateja ŠKERJANEC[1]

[1] University of Ljubljana, Faculty of Civil and Geodetic Engineering, Slovenia
gasper.rak@fgg.uni-lj.si, mateja.skerjanec@fgg.uni-lj.si

ABSTRACT

The rising frequency of floods, coupled with increasing human encroachment on water corridors and floodplains, makes floods severe disasters. In 2007, the European Union enacted the Floods Directive, guiding member countries in legislation for identifying flood hazard and risk areas. Despite significant human impacts, current flood hazard mapping often neglects scenarios from extreme events. Stochastic land use changes, driven by economic and social interests, should be considered. Mitigation measures, like dams and levees, aimed at reducing flood risk can alter flow regimes and transfer risk. Levee construction changes floodplain retention capacity, influencing flood peak attenuation and propagation time. This article introduces the analysis of exceptional events in assessing flood hazards and risks through examples of man-made extreme flood events using detailed hydraulic models.

## 1. Introduction

To enhance flood risk management and spatial planning aimed at reducing vulnerability through preventive measures, the European Parliament and Council of the European Union enacted the Flood Directive in 2007. Slovenia established detailed regulations, including the Rules on flood hazard determination and land classification (Ministry of the Environment and Spatial Planning, 2007), and the Decree on conditions for activities in flood-threatened areas.

While climate change is a topic of discussion, the primary factor increasing risk is human intervention in vulnerable areas. Factors include intensive land use, economic development in flood-prone zones, reduced retention areas, minimal flood protection measures, and inadequate maintenance. Structural measures, like flood protection, have limited functionality, and their effectiveness diminishes in catastrophic events (Rak et al., 2018). Flood protection measures are designed based on the "design discharge," making protected areas attractive for intensive land use, potentially increasing damage potential during floods.

Flood risk analysis often overlooks extraordinary events such as breaches in flood protection, incorrect operation of hydro-mechanical equipment, and inadequate maintenance, leading to adverse anthropogenic effects (Šantl and Rak, 2010). Uncontrolled land use changes in retention areas alter runoff regimes, affecting the effectiveness of interventions and spatial planning. The paper provides two examples of anthropogenic impact on flood hazard: the uncontrolled land use during infrastructure lifespan altering runoff regimes and the sudden or progressive failure of flood protection embankments during extreme events.

## 2. Land use in riparian areas

Riparian areas and floodplains, especially in flatland regions, offer significant development potential. However, these areas, with their retention capacity, play a crucial role in forming the runoff regime, attenuating flood waves, prolonging propagation times, and thereby reducing flood risk downstream. Given the inherent conflicts of interest in spatial planning, building placement, and long-term land use, a judicious strategy for spatial development and intervention planning in riparian areas is needed (Rak, 2013; Rak et al., 2016).

Preserving the runoff regime in these influenced zones while avoiding adverse effects downstream is a challenging yet vital task. Achieving a static state in these areas is impractical due to the dynamic nature of spatial development. However, it is essential to analyze potential negative impacts resulting from spatial

changes. Legislation aligned with the Flood Directive places restrictions on interventions in flood-prone areas, aiming to balance diverse changes within the region.

## 3. Malfunction of flood protection measures

After completing structural flood protection measures (FPMs), consolidation occurs, dependent on factors like soil quality and terrain load-bearing capacity. Regular maintenance and stability checks are essential to uphold the flood protection function. Between interventions, critical sections may emerge in areas with higher settlements, increasing the risk of embankment overflow. FPM designs typically consider normal conditions, but extraordinary events like bridge clogging or sediment transport and depositions should be factored in. Properly constructed and maintained FPMs should withstand loads, yet instantaneous collapse or gradual breaching can occur. The spilling of water mass into floodplains increases during breaches, impacting areas initially considered to have acceptable flood risk. Overflow can also happen in extreme events, termed "force majeure," exceeding design discharge. Analyzing such scenarios helps formulate guidelines, restrictions, and requirements in spatial planning and coordinated actions during extraordinary events. Predicting erosion processes, breach timing, and assessing the destructed section's width and overflow onset are crucial aspects in preparing flooding scenarios. Fig. 1 presents flood dynamics in urban area after collapse of an FPM.

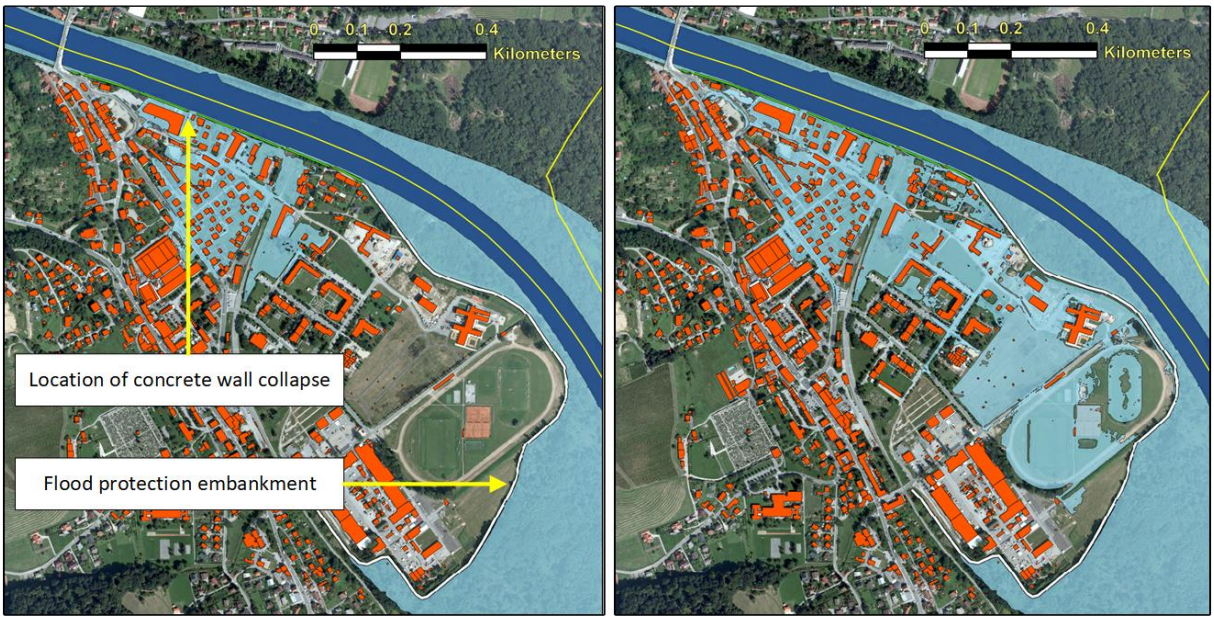



**Fig. 1.** Propagation of flooding 2 hours (left) and 4 hours (right) after the collapse of a part of the flood protection wall.

## 4. Conclusions

The paper highlights a few examples of anthropogenic activities impacting flood risk, emphasizing the importance of hydraulic research in predicting and analyzing adverse effects on runoff in river channels and riparian areas. Such analyses improve emergency plans and aid in formulating practical solutions and guidelines for spatial development planning. Establishing this expert basis enables the incorporation of concerns that could hinder protection and rescue efforts and helps prevent excessive risk. Land use planning must consider the experiences that demonstrate significant changes after interventions in riparian areas, affecting FPM objectives. The allure of reduced flood risk can lead to intensified use of riparian areas, increasing damage potential during floods. Monitoring land use from FPM completion to any changes or degradation is crucial to prevent harmful effects throughout their lifespan. A comprehensive plan for sustainable development should systematically manage flood-endangered areas, considering both temporal and spatial dynamics.

**References**

Ministry of the Environment and Spatial Planning, 2007. Rules on the methodology for determining the areas threatened by floods and associated erosion of inland and marine waters, and the method of classifying land in hazard classes, Official Gazette of RS, Nos. 60/07.

Rak G (2013) Hydraulic Analysis of Floodplain Land Use Effects on Flood Wave Propagation. Master's thesis, Ljubljana, University of Ljubljana, Faculty of Civil and Geodetic Engineering.

Rak G, Grobljar S, Steinman F (2018) Flood modelling in urban areas, Acta hydrotechnica, 31(54), 21-33.

Rak G, Kozelj D, Steinman F (2016) The impact of floodplain land use on flood wave propagation. Natural hazards 83; 1: 425–443.

Šantl S, Rak G (2010) Flood hazard and run-off regime analysis - approach with use of different types of hydraulic models, Gradbeni vestnik, Ljubljana, 147–156.

# SDGs-EYES: a novel European project to enhance, integrate and monitor water-related SDG indicators

Melissa LATELLA[1], Monia SANTINI[1], Marco MANCINI[1], Monica MIGUEL-LAGO[2], Stefano NATALI[3], Michele LAZZARINI[4], Roberta PADULANO[5] and all the SDGs-EYES team

[1] CMCC Foundation – Euro-Mediterranean Center on Climate Change (Italy)
melissa.latella@cmcc.it; monia.santini@cmcc.it; marco.mancini@cmcc.it

[2] The European Association of Remote Sensing Companies (EARSC) (Belgium)
monica.miguel-lago@earsc.org

[3] Sistema GmbH (Austria)
natali@sistema.at

[4] European Union Satellite Centre (SatCen) (Spain)
Michele.Lazzarini@satcen.europa.eu

[5,1] Università degli Studi di Napoli Federico II (Italy)
roberta.padulano@unina.it ; roberta.padulano@cmcc.it

ABSTRACT

Ensuring access to clean water and proper sanitation is vital for human well-being, supporting efforts to combat climate change, protect marine environments, and conserve terrestrial ecosystems. By addressing these interrelated goals, significant strides can be made toward a more sustainable and harmonious world. This issue is captured by the EU project "SDGs-EYES – A Copernicus driven service for monitoring UN SDG indicators", which is aimed at enhancing the modelling and monitoring of a selection of SDG indicators in an integrated perspective by leveraging Earth Observation data provided by Copernicus services. SDGs-EYES's pilot indicators are picked within SDG 13 (Climate Action), 14 (Life Below Water), and 15 (Life on Land), which are intrinsically connected to SDG 6 (Water Sanitation). This contribution focuses on describing the project's ambition, implementation and preliminary results.

## 1. The framework

The Sustainable Development Goals (SDGs) are a set of 17 global goals established by the United Nations in 2015 to address a wide range of social, economic, and environmental challenges, with the overall ambition to create a more sustainable and equitable world by 2030. SDGs are deeply interrelated: for instance, SDG 6 (Clean Water and Sanitation) is closely related to many SDGs such as SDG 13 (Climate Action), SDG 14 (Life below Water), and SDG 15 (Life on Land), as they all share a common thread of environmental sustainability.

## 2. The project

"SDGs-EYES: A Copernicus driven service for monitoring UN SDG indicators" (https://sdgs-eyes.eu/) is a major new European initiative aiming at boosting the European capacity for monitoring the UN SDGs. SDGs-EYES addresses current gaps in the UN SDGs monitoring by exploiting data and information from the European Copernicus Programme. In particular, the project aims to design, implement and deploy a Copernicus-based Service that enhances the usability of Earth Observation data offered by Copernicus services and associated Data and Information Access Services in order to build, access and visualise indicators for monitoring SDGs targets. The SDGs-EYES scientific approach is demonstrated with particular reference to SDGs 13, 14 and 15. These SDGs are mostly focused on the biosphere ensuring prosperity, development and co-benefits in the society and economy, but they are also relevant due to their nexus with additional SDGs,

targets and indicators related to socio-economic and (geo)political factors (e.g. human health, environmental crimes, water and food insecurity, poverty, conflicts, displacements, migrations). Five Pilots are used to demonstrate and validate the SDGs-EYES approach and results, which consist of application-oriented scientific products, technological solutions and user-tailored services. The overall ambition is to facilitate both understanding and uptake of indicators information by stakeholders (e.g. protection agencies, territorial planners, policymakers, investors) that can efficiently incorporate data and tools in their decision-making process, increasing their capability through a scientific and evidence-based rigorous approach, overcoming challenges in accessing and using EO for SGD indicators' monitoring and reporting.

## 3. The development and first results

Table 1 lists the seven SDG indicators selected for implementation and enhancement in the project. For each indicator, the spatial domain of the analysis and the first enhancements provided by the project are also shown, related to both scientifical and technical issues.

**Table 1.** SDG indicators and main features of the Project.

| Code – name | Pilot Area | Current gaps vs. main advances |
|---|---|---|
| **SDG 13 – Climate Action** | | |
| **EU 13_21** – Net GHG emissions for the LULUFC sector | Cosenza (IT) | Novel workflow enabling for automatic computation of the indicator. Replacement of current field-based data (burnt area, forest type and scorch height) with EO products, reducing time and cost of computation and improving comparability over time and across space. |
| **EU 13_30** – Mean near-surface temperature | Turin (IT) | Renewing the workflow to compute the indicator to include other meaningful physical variables in addition to near-surface temperature (e.g. wind, humidity, cloudiness, etc.) and accounting for exposure and vulnerability data. Using high-resolution, continuously-distributed climate datasets to improve the reference area and comparability among countries |
| **SDG 14 – Life below Water** | | |
| **EU 14_50** – Global mean surface seawater acidity | North Sea | Integrating EO data will widen the reference area and ensure comparability among countries (currently: only global estimates; SDGs-EYES: a value for each EU Member State). Computation of acidity is improved by considering hydrogen ion concentration to enhance the robustness of cross-domain comparisons, as recommended by the scientific community. |
| **EU 14_60** – Marine waters affected by eutrophication | North Sea | The integration of different Copernicus components will bridge the gap between current in-situ measurements and continuous monitoring. Moreover, it allows covering all EU seawaters (currently: gap for the North Sea) and capturing temporal and spatial variability. |
| **SDG 15 – Life on Land** | | |
| **EU 15_10** – Share of forest area | Romania | Definition of a well-defined and reproducible method based on freely-accessible EO data, allowing for: harmonisation of forest inventory, comparability over time, detection of gradual change, high spatial resolution and high frequency of dissemination (currently: 3-4 years; SDGs-EYES: monthly). Results will be validated against ground truth. |
| **EU 15_50** – Estimated soil erosion by water | Romania | Improvement of RUSLE-based workflow provided by JRC, with better spatial resolution (currently: 100 m; SDGs-EYES: 10 m) and frequency of dissemination (currently: aperiodic; SDGs-EYES: monthly or quarterly). Improved computation of RUSLE factors, accounting for: i) a more dynamic assessment of rain erosivity, representing the temporal climate variability and changes in rainfall intensity; ii) modification of soil properties after wildfires; iii) phenological variations of land cover; iv) presence of anthropic artefacts to dampen erosion in agricultural areas and v) an improved computation of geomorphological features. |
| **Cross – goals** | | |
| **UN 13.1.1** – No. affected persons attributed to disasters per 100'000 population | Sahel | Definition of an easy-replicable methodology based on globally available datasets and innovatively employing machine learning to examine compound climate hazards. Computation in a quasi-real-time way on the basis of registered disasters. Estimation of the number of victims at the event scale. |

The Project is approaching the intermediate stage, and preliminary results are available concerning all the indicators in Table 1, although with different completion levels. Under an overall agile approach, a demo version of the integrated platform will be released next year, with the future ambition to include other indicators also concerning different SDGs, such as SDG 6. Main results will be presented at the Conference.

**Acknowledgements**

"SDGs-EYES: A Copernicus driven service for monitoring UN SDG indicators" (https://sdgs-eyes.eu/ - Grant Agreement No. 101082311) is funded by the European Commission under the Programme HORIZON.2.4.10 - Space, including Earth Observation. Views and opinions expressed are however those of the authors only and do not necessarily reflect those of the European Union or the European Health and Digital Executive Agency (HADEA). Neither the European Union nor the granting authority can be held responsible for them.

# Water Balance Modeling of The Nile River Behind Aswan High Dam and The Future Expectation

Mohamed SOLIMAN[1,2]

[1] Civil and Environmental Department, Faculty of Engineering, Beirut Arab University, Lebanon
[2] Irrigation Engineering and Hydraulics Department, Faculty of Engineering, Alexandria University, Egypt
m.soliman@bau.edu.lb

ABSTRACT

Today, Egypt has a great stress on the available water resources. The quantity of available water is inversely affecting the national economic development. Various studies indicated that recent high population growth (2%) along with moderate industrial growth (+1%) and agriculture expansion will require about 90 BCM of water by 2050 under different scenarios. Moreover, the natural freshwater resources of Egypt (Nile River) may be influenced by upstream countries developments and climate change impact. Egypt usually overcomes the water imbalances between water supply and demand (about 20 BCM in 2017) using water recycling that increases the total water efficiency to 88%. Furthermore, the water quality is degraded which limits its use for specific purposes. Therefore, the government started to release different water infrastructures projects with expected investments estimated at 900 billion Egyptian pounds to build new desalination plants and huge wastewater treatment plant to increase unconventional water resources, which is expected to be 40% of the total resources. In this study, a vision for the future water status in Egypt through numerical modeling is presented. This vision is standardized by the current status of the available water resources. Recommendations to overcome anticipated water challenges and to optimize the available opportunities are provided. With the surface water resources of Egypt currently fully exploited, the need of alternative water resources has never been of profound urgency as it is nowadays.

## 1. Introduction

Since the 1970's, Egypt water uses have exceeded its natural resources. About 98% of Egypt's freshwater resources originate outside of its borders, such as the Nile River and groundwater aquifers. Egypt will be influenced by developments the upstream basin countries. This is considered to be one of the main challenges for water policy and decision-makers. On the other hand, the non-traditional water resources represent 20% only of the total water resources in Egypt. Climate change is expected to have an impact on the water sector, resulting in more demand especially in the agricultural sector in addition to the impact of high sea level on groundwater reservoirs in the Nile Delta, which increases its salinity and makes it non-consumable. Egypt is already below the amount needed for being able to be food self-sufficient. Many researchers predicted the water balance situation by 2050 including different scenarios. They concluded that water share per capita will be less than 350 $m^3$/capita/yr that may classify Egypt as a poor-water country (Eldin, 2013). Moreover, (Omar & Moussa, 2016) assessed three scenarios of water resources situation for Egypt in the year 2025 using the Water Evaluation And Planning model (WEAP). The findings indicated that water shortage in 2025 would be 26 BCM/yr in case of continuation of current policies. However, to the best of the author knowledge, none of the recent studies simulated the Egyptian water balance using decomposed governorates in order to provide greater accuracy as well as allowing more factors to be taken into consideration, which allows the government to take better decisions and long-term sustainable developments.

## 2. Materials and methods

In the current study, temporal and spatial model using WEAP is developed to represent the logical sequence in water resources management of Egypt. The model shown in Fig. 1 is calibrated by the present demand of water for all purposes, for the year 2017. The main purpose of the model is to determine how the demand in

various sectors will be affected by growth then to project what the water demand will be in short and long-term future, 2030 and 2050, respectively. The used system consists of a network of nodes, both storage (i.e., reservoirs, groundwater basins, and storage right accounts) and non-storage (i.e., diversion points, demand locations, return flow locations, etc.), and links (i.e., canals, river reaches) connecting these nodes. On the basis of a set of simulations, usually made for management strategies, the performance of the basin is evaluated in terms of water allocation, shortages, overall basin water balance, etc.

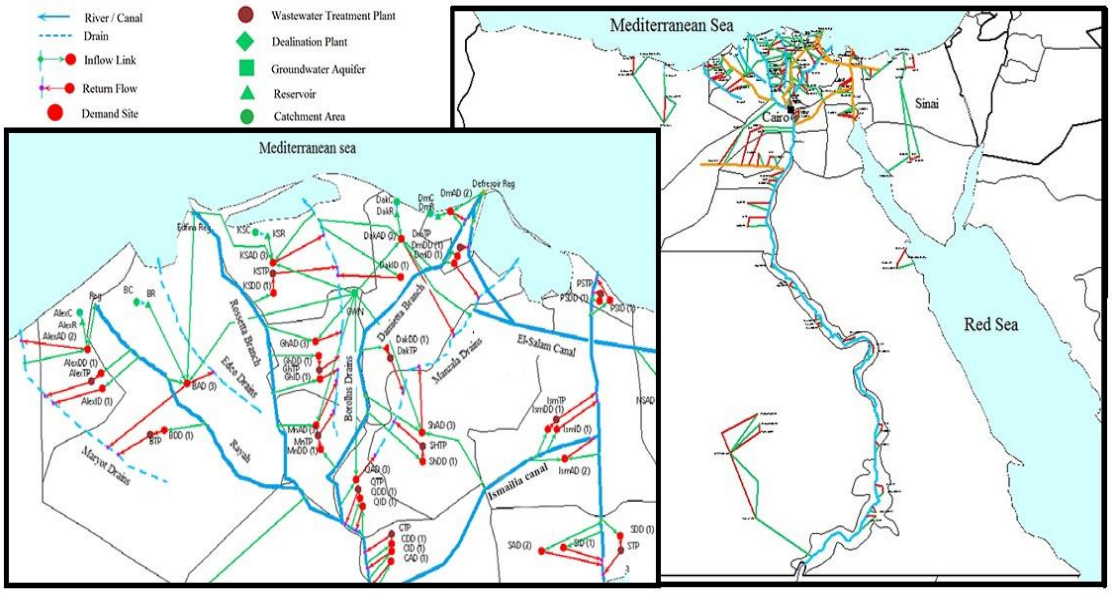



**Fig. 1.** The developed WEAP model developed for Egypt water resources and closeup for the Nile Delta

## 3. Results and Conclusions

Based on WEAP model, Fig. 2 illustrates the predicted total water delivered and required by 2050. It is expected, by 2050, a population of 175 million capita will consume about 12.1 BCM (rate 180 L/day/capita), 76.52 BCM of water will be used to irrigate 12.6 million feddan with efficiency 80% and about 7.92 BCM will used in the industry sector. The total water demand is expected to increase based on overpopulation and agricultural land necessities increase to be 100 BCM in 2050 instead of 80 BCM in 2017. Therefore, the total water supply is essential to increase as a response to water requirements with the same amount. By, 2050, total conventional water inflow will be 63.64 BCM, including 55.5 BCM of Nile water, 1.57 BCM of rainfall, deep groundwater abstractions of 4 BCM and 2.56 BCM of desalinated water. The deep groundwater will be used to irrigate new agricultural lands at Owinat, Toshka and Moghra. While total non-conventional water supply (recycled water) will be 36.9 BCM with a ratio of 37% of fresh water. Finally, the drainage water to sea will decrease from 12 BCM to 10.14 BCM. These results depend on improving the water use efficiency, preserving natural resources and protecting the environment in order to support achieving sustainable development in Egypt.

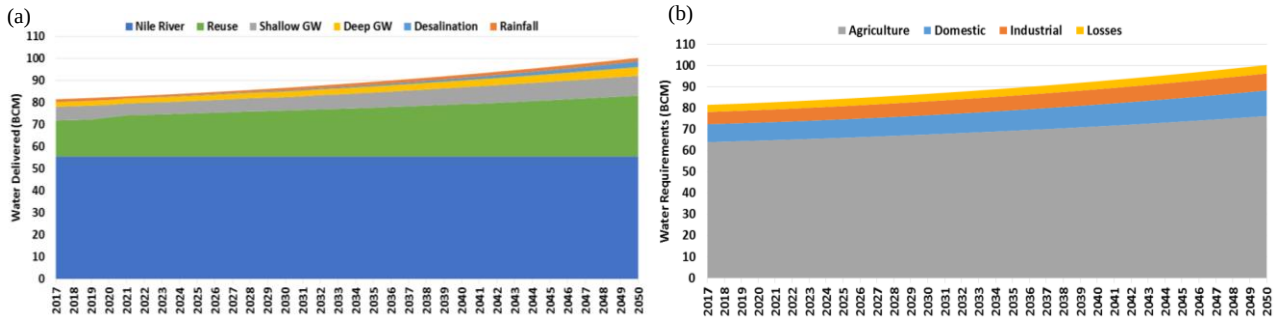



**Fig.2.** (a) Total water delivered by 2050 and (b) Total water requirements by 2050

**References**

Eldin, M.N. (2013) Climate Change Risk Management In Egypt: Proposed Climate Change Adaptation Strategy For The Ministry Of Water Resources & Irrigation In Egypt. Cairo: Unesco.
Omar, M., Moussa, A. (2016) Water Management In Egypt For Facing The Future, Journal Of Advanced Research, 7, 403–412.

# Integrated approach to evaluate the role of floating farming for addressing disaster risk management and nexus between water-food-health-economy-human wellbeing

Pankaj KUMAR[1*], Md Nasif AHSAN[2], Yasuo TAKAHASHI[1], Koji MIWA[1]

[1] Institute for Global Environmental Strategies, Japan 2400015
*kumar@iges.or.jp; yasuo.takahashi@iges.or.jp; k-miwa@iges.or.jp

[2] Economics Discipline, Khulna University-9208, Bangladesh
nasif.ahsan@econ.ku.ac.bd

ABSTRACT

In the face of triple environmental crisis (climate change, biodiversity loss, and pollution) plus land degradation, the urgency for collective action considering nexus between its possible implications to forge a sustainable future has never been greater (Kumar, 2019). This is even more urgent in case more vulnerable regions like coastal area, small island countries, for example Bangladesh (Khatun et al., 2022). This study strives to evaluate the importance of climate smart agriculture to address the nexus between water-food-health-human well-being in South Coastal Region of Bangladesh. Questionnaire survey (n=341) based endogenous switching regression (ESR) model is used to examines the determinants and impacts of adopting climate smart agricultural practices based on floating farming, considering the behaviors of adopters and non-adopters (Di et al., 2011). Study findings suggest that approximately 79% of the sampled farm households adopted floating farming as an adaptation strategy in the presence of climatic extreme events, namely, waterlogging, hazard effects, and erratic rainfall. Moreover religion, hazard effect, training, and previous knowledge of floating farming were the determinants of adopting floating farming. Considering the profit of the farm households, the result implies that the farm profit of adopters increases by 42% compared to non-adopters, where different farm supports such as cooperative membership, technical, credit, and training positively affected farms' profit. Estimates from ESR model exert that adoption of floating farming resulted in better wellbeing when compared with counterfactual situation. Analysis reveals that adopters of floating farming experienced a significant gain of US$ 15.30/decimal as farm profit compared to control mean (US$ 36.38/decimal), whereas non-adopters would have gained US$ 6.81/decimal if they have adopted floating farming, indicating the missed opportunity for enhanced profitability. Research findings has high policy relevance to enhance farmers' profitability and resilience to climatic shock in the wetlands of southwestern Bangladesh.
Keywords- Climate risk; nexus; human well-being; floating agriculture

## Introduction

Climate change and its induced extreme weather conditions like cyclone, flood has significant impact on the agriculture and livelihood especially in developing nations with limited adaptive capacity both in terms of skilled human and financial resources (Boudiaf et al., 2020; Khatun et al., 2022). According to the Intergovernmental Panel on Climate Change (IPCC), a changing climate might cause a 2% loss in GDP and 30% reduction in agricultural crop productivity (results in food security related issues) in South Asia by 2050 (IPCC, 2022). Farmers in developing nations, who are anticipated to suffer the most effect of climatic variability, should pay particular attention to this (Chen & Gong, 2021) and hence enhancing upland farmers' ability to implement sustainable livelihood strategies (such as cultivars, agricultural inputs, cultivation techniques etc.) to naturally adapt to climate change and ensure food security is critical (Khanal et al., 2021). Bangladesh one of the most vulnerable countries towards climate change, are facing the heat as these extreme weather conditions (flooding and persistent waterlogging) have significantly harmed the lives of people and their property and had a negative impact on their livelihood, agriculture, healthcare, and education (Al-Maruf

et al., 2020). With above background, this research tries to assess the impact of adopting floating farming on farmers' welfare, considering the behavior of both adopters and non-adopters of floating farming.

## Study area and methodology

Two districts, Gopalganj and Barishal, in Bangladesh, were selected as study area based on three criterias (presence of persistent waterlogging even during the dry season; inhabitants' dependence on available natural resources for their livelihood, directly or indirectly; and high susceptibility of the area to natural hazards, such as tropical cyclones, floods, and salinity intrusion). For methodology, a multistage sampling technique (literature review, lottery, and systematic random sampling) was utilized to select 341 respondent households from 16 villages. The questionnaire, consisting of 48 closed-ended questions, was developed to address water-related aspects, such as water quantity, water quality, water security, and water stress-related issues. Pilot survey followed by detailed survey was conducted between November 2022 to January 2023. Endogenous switching regression model (ESR), which is a two-stage estimation-based parametric approach that can control the effects of all observed and unobserved variables that influence both adoption and outcome variables, was used to examines the determinants and impacts of adopting climate smart agricultural practices based on floating farming, considering the behaviors of adopters and non-adopters.

## Result and discussions

Climatic change and its induced extreme events such as erratic rainfall, flooding, waterlogging (2/3$^{rd}$ of surveyed farmlands are waterlogged for 101 days in average) have serious impacts on traditional farming activities. Study findings suggest that approximately 79% of the sampled farm households adopted floating farming as an adaptation strategy in the presence of climatic extreme events, namely, waterlogging, hazard effects, and erratic rainfall. Moreover religion, hazard effect, training, and previous knowledge of floating farming were the determinants of adopting floating farming. Considering the profit of the farm households, the result implies that the farm profit of adopters increases by 42% compared to non-adopters, where different farm supports such as cooperative membership, technical, credit, and training positively affected farms' profit. Estimates from ESR model exert that adoption of floating farming resulted in better wellbeing when compared with counterfactual situation. Analysis reveals that adopters of floating farming experienced a significant gain of US$ 15.30/decimal as farm profit compared to control mean (US$ 36.38/decimal), whereas, non-adopters would have gained US$ 6.81/decimal if they have adopted floating farming, indicating the missed opportunity for enhanced profitability.

## Conclusion

This study strives to assess the impact of floating farming as a means of climate-smart adaptation strategy on farmers' well-being in flood-affected and water-logged low-lying districts of Gopalganj and Barishal districts of Bangladesh. The evidence from this study implies that farmers should be provided with need-based training related to floating agriculture. Hence, enhanced and adequate support from government, non-government, and international organizations is needed to strengthen the capacity of the poor farmers practicing floating farming and increase their resilience in the wake of climate change. For instance, amenities such as providing technical knowledge, training, input support, and financial support from the initial stage (bed preparation) to the final marketing of crop products may motivate farmers to sustain this practice. The government should also develop necessary arrangements to assist other non-government and international bodies involved in introducing and promoting floating farming in the flood-prone regions of Bangladesh.

**Acknowledgements**

This study was financially supported by SRF-NEXUS project from Institute for Global Environmental Strategies (IGES), Japan. The usual disclaimer applies.

**References**

Al-Maruf, A. (2020) 24. Floating gardening in coastal Bangladesh: Evidence of sustainable farming for food security under climate change. Journal of Agriculture, Food and Environment (JAFE)| ISSN (Online Version): 2708-5694, 1(4), 161-168.

Boudiaf, B., Dabanli, I., Boutaghane, H., Şen, Z. (2020). Temperature and precipitation risk assessment under climate change effect in northeast Algeria. Earth Systems and Environment, 4(1), 1-14.

Chen, S., Gong, B. (2021) Response and adaptation of agriculture to climate change: Evidence from China. Journal of Development Economics, 148, 102557.

Di, Falco, S., Veronesi, M., Yesuf, M. (2011) Does adaptation to climate change provide food security? A micro-perspective from Ethiopia. American journal of agricultural economics, 93(3), 829-846.

IPCC. (2022) Climate Change 2022: Mitigation of Climate Change. https://www.ipcc.ch/report/ar6/wg3/.

Khanal, U., Wilson, C., Rahman, S., Lee, B. L., Hoang, V. N. (2021). Smallholder farmers' adaptation to climate change and its potential contribution to UN's sustainable development goals of zero hunger and no poverty. Journal of Cleaner Production, 281, 124999. https://doi.org/10.1016/j.jclepro.2020.124999

Khatun, F., Ahsan, M, N., Afrin, S., Warner, J., Ahsan, R., Mallick, B., Kumar, P. (2022) Environmental non-migration as adaptation in hazard-prone areas: evidence from coastal Bangladesh. Global Environmental Change, 77, 102610.

Kumar, P (2019) Numerical quantification of current status quo and future prediction of water quality in eight Asian megacities: challenges and opportunities for sustainable water management. Environ. Monit. Assess. 191.

# DPSIR analysis of the closure of water resources in Axarquía region (southern Spain)

Julio BERBEL[1], Esther DÍAZ-CANO[2], Nazaret M. MONTILLA-LÓPEZ[3], Antonio R. HURTADO[4]
[1,2,3,4] WEARE- Water, Environmental and Agricultural Resources Economics Research Group,
Universidad de Córdoba (Spain)
[1]berbel@uco.es; [2]edcano@uco.es; [3]g02molon@uco.es; [4]es2rohuc@uco.es

ABSTRACT

Axarquia region (36°50′00″N 4°10′00″W) Southern Spain is the main producer of avocado and mango in Europe, crops that are suffering the consequences of a long drought. The combination of population growth and the increase of the cultivated area with subtropical crops is leading to groundwater overexploitation. This work applies the European Environment Agency's DPSIR (drivers, pressures, state, impact, and response model of intervention) framework to analyze closure process in this region. The water crisis has impacted citizens (urban supply), farmers (losses of yields and crops) and environment (decreasing water reserves). Supply has increased by incorporating reclaimed wastewater, and the upcoming building of a desalination plant, but demand control and proper governance are required to reach sustainability.

## 1.- Axarquia region and water resources closure

Axarquia is a region located in Southern Spain, limited by a range of mountains at the north, east and west, and by the Mediterranean Sea at the south. Annual sunshine is around 2.600 hours, and the annual average temperature is 19ºC. The plain and the coastal area make subtropical crops possible, and tourism is present all year round. Our case study applies the European Environment Agency's DPSIR (drivers, pressures, state, impact, and response model of intervention) framework to analyze closure process in Axarquia.

### *1.1 Driving forces*

Two driving forces explain the increase in water demand. First, population has grown from 140.000 (1998) to 220.000 (2020) (around 2,5% annually). Besides resident population, tourism (secondary residences, hotels, etc.) increases urban demand pressure. The second driving force is the search for agricultural profitability as the low income obtained from traditional cultivation of rainfed pasture and herbaceous forces farmers to look for alternatives. Thus, the irrigated area in the region has increased from 5.200 ha (1999) to 13.300 ha (2021). Most of this growth is due to avocado and mango, which account for 9.500 ha (71% of irrigated area).

### *1.2 Pressures*

Urban demand of water in the area is very high compared to Spanish standards, with inhabitants consuming 322 L/person·day, i.e., 2,5 times the Spanish average (132 L/person·day). Part of this excessive consumption is due to huge losses in the water distribution networks (40%) and part is due to seasonal tourism.

The most important pressure in quantitative terms is water for irrigation, which has grown from 34 $hm^3$ (1999) to 97 $hm^3$ (2021), according to our estimations based on standard irrigation doses and the crop cultivated area, which implies supplying crops below maximum need. This estimate is lower than the 111 $hm^3$ resulting from the application of FAO's irrigation water needs formula (FAO assumes maximum yield and related irrigation needs). Furthermore, the estimated irrigation water use of 97 $hm^3$ is higher than the 78 $hm^3$ of irrigation water rights established in the region's hydrological plan indicating a water supply that forces deficit irrigation practices similar to neighboring Guadalquivir River (

### *1.3 Status*

Following a typical closure trajectory, public response to scarcity in the 80's was the construction of the "La Viñuela" dam (capacity160 $hm^3$) coming into operation in 1998. However, the high demand combined with a

long drought (2018-present) has produced a water crisis in the region. Figure 1 shows the estimated abstraction from different sources and the piezometric level in the aquifer.

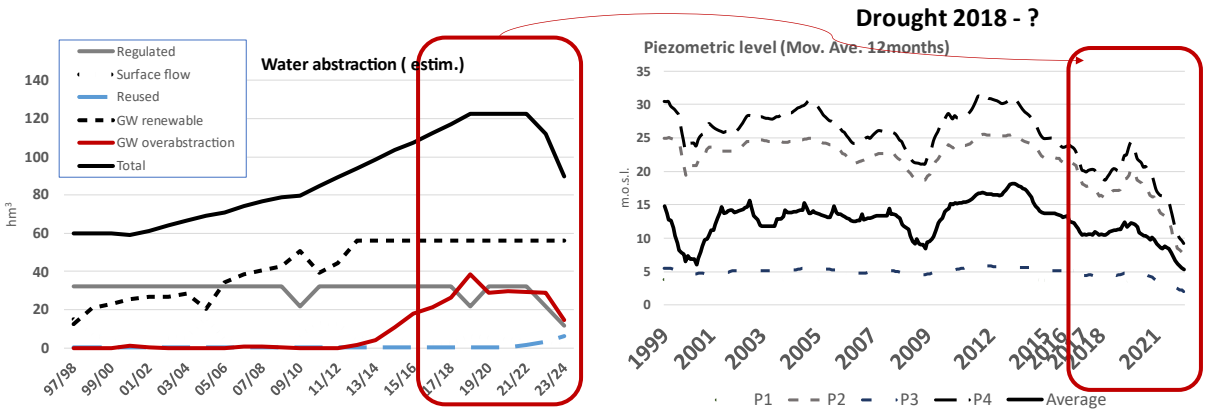



**Fig. 1.** Estimated water abstraction (1996-2023) and piezometric level in the Velez-Malaga aquifer.

### *1.4 Impact*

The current conditions have led the "La Viñuela" reservoir with 7% of its capacity (Jan 2024) and water authority has reduced urban water supply and limited irrigation. The lack of surface water has driven farmers to resort to both legal and illegal groundwater abstraction, and the piezometric levels (Fig. 1 right) show the existence of high abstraction rate, with the risk of seawater intrusion and subsequent impact in groundwater dependent ecosystems. Farmers have seen trees die and are resorting to 'radical pruning' (leaving almost no leaves in the tree) or even to uprooting. Regional mango and avocado yields in 2023 decreased to 20-30% of annual average, while other crops such as olive trees adapt better to deficit irrigation (Expósito et al., 2016).

### *1.5 Responses*

Private sector response to crisis has involved reducing water supply to crops and even eliminating subtropical crops area. Some projects are now in place to implement precision irrigation and reduce water use. Public response has included the investment in urban wastewater reclamation plants, with around 20 $hm^3$ of reclaimed water entering the system from the Axarquía municipalities including reclaimed wastewater from Malaga city (neighbor basin). In addition, the construction of a desalination plant has recently been approved.

## 2.- Conclusions and future actions

The process of water closure in Axarquia region shows a typical 'closure' trajectory where increased supply has not been able to meet growing demand. This scenario is due to a combination of population growth and a three-fold increase of the area cultivated with water-intensive subtropical crops, which is leading to groundwater overexploitation. The public-private response of increasing non-conventional water supply (currently through reclaimed wastewater, and a desalination plant coming soon) will not solve the problem unless demand control and proper governance schemes are implemented. DPSIR framework is a useful tool to understand the dynamic of socio-hydrological systems and attempt to adequate public and private responses to avoid perverse effect that eliminate in the long term the gains obtained at short term. To support the transition to a scenario of sustainable governance in the region. Additionally, our team is developing hydro-economic models, building a database, and conducting analyses of wastewater reclamation costs, we hope that this improves long term sustainability and governance in the region.

**Acknowledgements**

The authors acknowledge the financing received under the projects PRIMA-BONEX (Grant Number 2141) GOVAQUA project (HE-CL6-GOV-2022-RIA-101086578) and CYCIT (PID2019-107127RB-I00 BHYEM):

**References**

Expósito A, & Berbel J (2016) Microeconomics of deficit irrigation and subjective water response function for intensive olive groves. *Water*, 8(6), 254. Doi/10.3390/w8060254

Molle F, Wester P, Hirsch, P (2010) River basin closure: Processes, implications, and responses, Agricultural Water Management, 97(4), 569-577.

Tocados-Franco, E., Berbel, J., & Expósito, A. (2023). Water policy implications of perennial expansion in the Guadalquivir River Basin (southern Spain). Agricultural Water Management, 282. Doi: 10.1016/j.agwat.2023.108286

# Stakeholder-based WEFE System Sustainability Assessment: A SWOT Analysis Application on an Agricultural Mediterranean Area

Dimitrios MALAMATARIS[1], Anna CHATZI[1], Konstantinos Babakos[1], Vassilios PISINARAS[1], Evangelos Hatzigiannakis[1], Andreas PANAGOPOULOS[1]

[1] Soil and Water Resources Institute, Hellenic Agricultural Organization "DEMETER", 57400 Thessaloniki, Greece
d.malamataris@swri.gr
a.chatzi@swri.gr
k.babakos@swri.gr
v.pisinaras@swri.gr
e.hatzigiannakis@swri.gr
a.panagopoulos@swri.gr

ABSTRACT

The global security of the WEFE (Water-Energy-Food-Ecosystems) nexus is increasingly worrisome due to the impacts of population growth, unsustainable resource consumption, non-concerted management of the nexus sectors, and climate change. Considering that trade-offs within complex challenges often result in disputes among the research community, it becomes essential to establish a consensus among stakeholders supported by scientific evidence to achieve sustainable societies. This paper presents the findings of a stakeholders' workshop concerning the WEFE nexus characteristics of a highly intensive agricultural Mediterranean area, namely Pinios River Basin (PRB) situated in central Greece.

## 1. Introduction

Sustainability is essentially determined by the interplay of three core elements: environmental, economic, and social. Often, we over-evaluate the environmental element while at the same time overlooking the social one. The simultaneous address of all three elements in an equitable way is a prerequisite for attaining long-term sustainability. In addition, achieving and ensuring nexus sustainability requires the oversight and evaluation of all nexus sectors along with their interconnections, as well as the recognition and resolution of diverse management viewpoints among stakeholders. Overall, developing an effective nexus sustainable strategy is a particularly formidable challenge.

Active stakeholder participation is widely recognised as a key component of effective sustainable planning since it offers dependable insights that make research more robust (Baccar et al., 2021). Its importance is acknowledged by both the European Union and the United States legislation which have mandated public involvement, including deliberation, in the formulation and execution of nexus policies (Alfredo et al., 2016). Engaging a representative and active group of stakeholders in nexus mapping and management processes seems to offer a promising solution for fostering shared perspectives on uncertainty, enhancing transparency, and capitalizing on stakeholder expertise. There are several means of incorporating the social element into complex systems, being interviews and workshops the most widespread participatory approaches.

The SWOT (Strengths, Weaknesses, Opportunities, and Threats) analysis represents a strategic tool aiming at outlining complex systems while assessing their limitations and potential through the recognition of related internal and external environments. It has also been extensively used for exploring decision-making possibilities and establishing strategic development processes.

## 2. Materials and Methods

### *2.1. Stakeholders' workshop*

In the Pinios River Basin (central Greece), a workshop was structured to collect useful data for understanding its WEFE nexus system. It took place on 17th May 2022, in Larissa city, with the participation of around 50 stakeholders. The whole group of stakeholders was divided into two trans-sectoral Working Groups, which were requested to fill in particular fields in different posters, each representing an individual challenge. The whole procedure was managed by facilitators. Rehearsal and role-playing had taken place in the previous days, while supporting maps of each nexus sector were prepared. Stakeholders provided their answers using posters of different colours each standing for a different nexus sector ("water"-blue, "energy"- yellow, "food" - pink, and "ecosystems"- green) (Figure 1).



**Fig. 1.** Filled posters after the completion of the Pinios River Basin stakeholders' workshop.

### *2.2. SWOT Analysis*

The SWOT analysis was built upon four quadrants, with the upper two encompassing the internal factors (strengths and weaknesses), and the lower two comprising the external factors (opportunities and threats). The most widespread responses among stakeholders per each nexus sector are presented in Fig. 2.

| | *Helpful* | *Harmful* |
|---|---|---|
| *Internal* | **STRENGTHS** | **WEAKNESSES** |
| | Plenty of water-related studies | Limited availability of water resources |
| | Land of high productivity | High production cost |
| | Suitable geomorphological and climate conditions | Difficulties in installation of new Renewable Energy Sources |
| | Extended natural protected area | Difficulties in maintenance of rivers environmental flow |
| *External* | **OPPORTUNITIES** | **THREATS** |
| | Integrated Rural Development Infrastructure Program "HYDOR 2.0" | Desertification of agricultural areas |
| | CAP 2023-27 | Abandonment of agricultural sector |
| | Completion of water and energy-related projects in the upstream part of Acheloos river | Expansion of photovoltaics to agricultural land |
| | Special Environmental Assessment and Management Plan for Natura 2000 areas | Biodiversity reduction |

**Fig. 2.** SWOT analysis results from the Pinios River Basin stakeholders' workshop.

The interlinked WEFE sectors are grappling with worldwide and local challenges resulting from climate change. These sectors are intricately connected and have interdependent benefits and bottlenecks, underscoring the importance of managing natural resources to promote sustainability. The findings of the analysis offer policymakers valuable insights into key considerations when compiling policies for the nexus system. Sustaining resources, fostering synergies, and enhancing collaboration across WEFE sectors can help Improve resource resilience in the pilot area.

**Acknowledgements**

This research was funded by European Union's Horizon 2020 research and innovation program under grant agreement No 101003632, project REXUS.

**References**

Alfredo, K, Montalto, FA, Bartrand, T, Wolde-Georgis, T, Lall, U (2016). Using a participatory stakeholder process to plan water development in Koraro, Ethiopia, Water, 8(7), 275.
Baccar, M, Bergez, JE, Couture, S, Sekhar, M, Ruiz, L, Leenhardt, D (2021). Building climate change adaptation scenarios with stakeholders for water management: A hybrid approach adapted to the South Indian water crisis, Sustainability, 13(15), 8459.

# Application and testing groundwater sustainability indicators for stressed semi-arid regions

Nicolás García SALAZAR[1], Nuno BARREIRAS[2], Luís COSTA[3], José Paulo MONTEIRO[4]

[1] Instituto Superior Técnico, Portugal

nicolasgarciasalazar@outlook.com

[2] CERIS, Instituto Superior Técnico, Portugal
nuno.barreiras@tecnico.ulisboa.pt

[3] Agência Portuguesa do Ambiente, Portugal
luis.ricardo.costa@apambiente.pt

[4] FCT, Universidade do Algarve, Portugal
jpmontei@ualg.pt

## ABSTRACT

Despite Portugal's relative water resource abundance, the southern Algarve region, with its semi-arid climate, has variable rainfall patterns that challenge stable and sustainable water supply management. The region has been witnessing recurrent droughts over the past two decades, which, coupled with increasing water demands, have increased groundwater stress and threatened its sustainability. Additionally, declines in groundwater levels, saline intrusion, and increased nitrate concentrations have all been linked to over-exploitation of the area's karstic aquifers.

Against this backdrop, and in the pursuit of sustainable groundwater management, the study endeavours to test diverse groundwater sustainability indicators on three critical Algarve groundwater bodies: Almádena-Odeáxere (PTM2), Mexilhoeira Grande-Portimão (PTM3), and Querença-Silves (PTM5). Almost no studies of water management using a comprehensive set of groundwater sustainability indicators have been conducted in Portugal before. Therefore, this study offers a new method to assess sustainability by employing different indicators that provide valuable support to policymakers and managers.

This research ultimately identifies 14 indicators combining survey-based and computation-based methodologies to assess environmental, socio-economic, and resource management aspects. The study culminates in the development of a Groundwater Sustainability Index (GWSI), an innovative approach that enables a multi-dimensional sustainability analysis consolidating diverse data into a single value (Fig. 2). The GWSI categorizes Querença-Silves as nearly unsustainable, signalling an urgent need for interventions to avoid deterioration. Almádena-Odeáxere and Mexilhoeira Grande-Portimão exhibit moderately sustainable levels, presenting opportunities for less immediate yet important measures.

Indicators assessing groundwater quality indicate that intensive agriculture poses a major pollution risk due to nitrate contamination, particularly in Querença-Silves. Sea water intrusion risk is significant in Mexilhoeira Grande-Portimão, requiring monitoring and management efforts to safeguard groundwater sustainability and protect economically valuable areas. Indicators assessing groundwater quantity underscore unsustainable over-exploitation in the Querença-Silves aquifer. However, credibility issues arise from conflicting recharge estimates, highlighting the need for unified and comprehensive groundwater models for the region. Lastly, survey-based indicators denote weaknesses in control mechanisms, economic instruments and institutional capacity, affecting sustainability efforts. Public participation mechanisms are deemed insufficient, and societal awareness of groundwater sustainability is lacking.

This study serves as a vital step towards fostering sustainable groundwater management in the Algarve region. The integration of sustainability indicators and the GWSI into regional policies and programs promises to enhance resource management and set the path for a more secure and resilient water future in the face of evolving climate and socio-economic dynamics in the region.

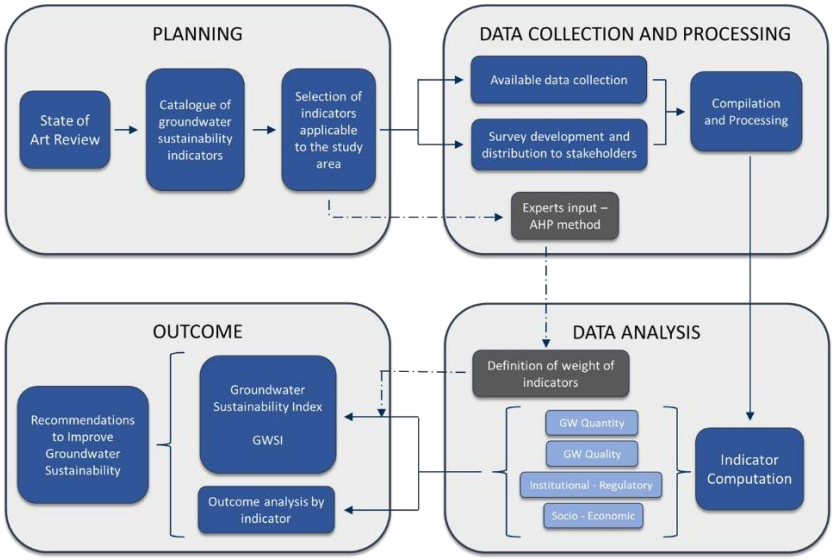



**Fig. 1.** Research methodology used for the study.

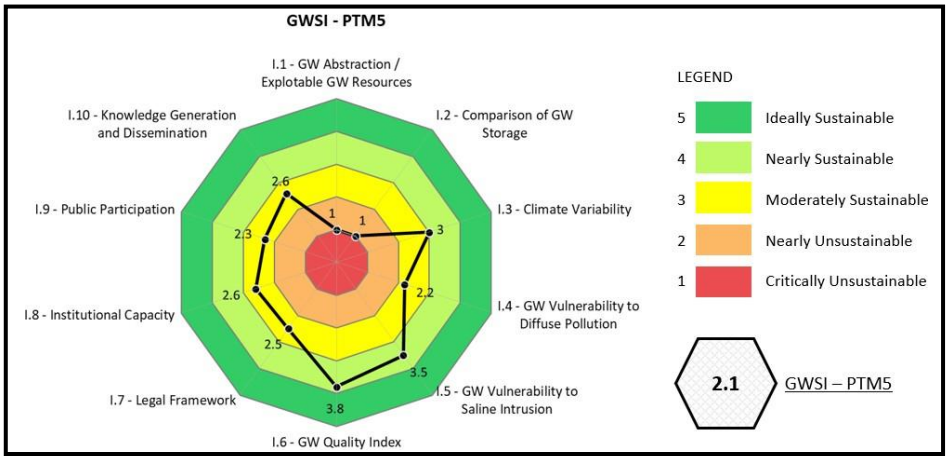



**Fig. 1.** Groundwater Sustainability Composite Index of Querença-Silves (PTM5)

**Acknowledgements**

This work was carried out at Instituto Superior Técnico and Civil Engineering Research and Innovation for Sustainability (CERIS), and has been funded by the Joint Master Degree Programme on Groundwater and Global Change - Impacts and Adaptation (acronym GroundwatCh), and by Fundação para a Ciência e a Tecnologia (FCT) in the framework of project UIDB/04625/2020. The authors also would like to extend their acknowledgements to Edite Reis and ARH Algarve for their collaboration and the data provided.

**References**

APA. (2020) Plano Regional de Eficiência Hídrica - Região do Algarve. Volume I - Memória descritiva, APA

ARH Algarve. (2022) Plano de Gestão das Bacias Hidrográficas das Ribeiras do Algarve - 3° Ciclo -Caracterização e Diagnóstico - Parte 2: Volume A., APA

Costa, L. C. (2022) PhD Thesis: Numerical Modelling applied to the understanding of groundwater flow and mass-transport in south Portugal - A perspective of regional hydrogeological problems affecting groundwater status. University of Algarve.

Karimi, D., Bahrami, J. & Taheri, K. (2022) Groundwater sustainability assessment based on socio-economic and environmental variables. Hydrogeology Journal, 30(7), 1963–1988. https://doi.org/10.1007/s10040-022-02512-6

Majidipour & Missimer, T. M. (2021) Index-based Groundwater Sustainability Assessment in the Socio-Economic Context: a Case Study in the Western Iran. Environmental Management, 67(4), 648–666. https://doi.org/10.1007/s00267-021-01424-7

Pandey, V. P., Shrestha, S., Chapagain, S. K., & Kazama, F. (2011) A framework for measuring groundwater sustainability. Environmental Science and Policy, 14(4), 396–407. https://doi.org/10.1016/j.envsci.2011.03.008

Stigter, T. Y., Ribeiro, L., & Carvalho Dill, A. M. M. (2006) Application of a groundwater quality index as an assessment and communication tool in agro-environmental policies - Two Portuguese case studies. Journal of Hydrology, 327(3–4), 578–591. https://doi.org/10.1016/j.jhydrol.2005.12.001

Vrba, J., Lipponen, A., Girman, J., Van Der Gun, J., Haie, N., Hirata, R., Lopez -Gunn, E., Neupane, B., Shah, T., & Wallin, B. (2007). Groundwater resources sustainability indicators; IHP-VI series on groundwater; Vol.:14; UNESCO, IAEA, IAH, 2007

# The State of European River Network Connectivity

Tamara LEITE[1], Gonçalo DUARTE[1], Pedro SEGURADO[1], Maria Teresa FERREIRA[1], Paulo BRANCO[1]

[1] Associate Laboratory TERRA, Forest Research Centre, School of Agriculture, University of Lisbon Lisboa, Portugal,

tamaraleite@edu.ulisboa.pt, goncalo.f.duarte@gmail.com, psegurado@isa.ulisboa.pt, terferreira@isa.ulisboa.pt, pjbranco@isa.ulisboa.pt

## 1. Introduction

Humans greatly modify riverscapes by altering stretches, and watersheds, and accelerating climate changes. As a consequence of damming and channelization, longitudinal and lateral connectivity of rivers have been severely compromised, and most rivers are disconnected from their floodplains. The dramatic effects of dams on water, sediment transport and fish movements have made them a common subject of fluvial research. However, most research lacks the distinction between the independent effects of natural pre-existing barriers -waterfalls- and the artificial ones. Most studies have considered the dam as the principal or only barrier impairing longitudinal fish movements. However, the upstream water reservoir itself represents a strong ecological barrier because it creates completely different hydrological and limnological conditions. Furthermore, lateral fragmentation is also a significant threat to ecological functions in the river landscape, negatively affecting the development of side-channel habitats, floodplain evolution, riparian ecosystem processes, and biodiversity. Roads and railroads are even more abundant features in riverscapes than dams. Additionally, navigation in heavily developed waterways may impact diversity of fish assemblages, contributing to the effects of migration barriers, pollution, expansion of invasive species, and habitat destruction.

## 2. Materials and Methods

As a baseline for the natural fragmentation calculations, we compiled and verified the locations of natural barriers within European river systems Waterfalls (www.europeanwaterfalls.com/, 2020; *World Waterfall Database*, Swan and Gross, 2012). Spatial analyses were based on the Catchment Characterisation and Modelling – River and Catchment database v2.1 (CCM2), developed by the Joint Research Centre (JRC) (De Jager and Vogt, 2007). The geographic location of the natural barriers was automatically allocated to the respective CCM2 basin and closest segment, and later visually verified and corrected. To characterize anthropogenic disturbance in longitudinal and lateral connectivity of European rivers, we mapped these ecological barriers, by identifying the river network segments affected by dams and their reservoirs, roads, and railroads, and waterways. The information about the location of artificial barriers higher than 5 meters within European rivers was collected from AMBER Barrier Atlas (AMBER Consortium, 2020), the Georeferenced Global Dams And Reservoirs (GeoDAR v1.1, Wang et al., 2021), and the GlObal geOreferenced Database of Dams (GOODD v1, Mulligan et al., 2020). The geographic location of the dams was automatically integrated and manually verified with the respective Catchment Characterisation Model (CCM2) basin and segment (De Jager and Vogt, 2007). We also used the GeoDar database (GeoDAR v1.1, Wang et al., 2021) to obtain the reservoir area created by each large dam. Additionally, we used the Global Roads Inventory Project (GRIP) database (Meijer et al., 2018) to determine river segments intersected by roads and railroads, as well as the Navigational Waterways data provided by the United Nations Economic Commission for Europe (UNECE) to determine river stretches used as navigable water. In this analysis, to quantify the longitudinal connectivity within river networks we calculated the Dendritic Connectivity Index at the basin level, which can be calculated for potamodromous or diadromous fish species (DCIp and DCId respectively, Cote et al., 2009).

## 3. Preliminary Results

We retrieved a total of 1343 waterfalls for European River networks (Fig.1A). We compiled a total of 12 656 artificial barriers in Europe, 9 212 of which affect the river network at the CCM2 resolution (Fig. 1B). Considering the water storage created by these large dams, reservoirs affect 79 393 Km of the river upstream of the physical barriers. An estimated 18 594 Km of rivers are used as navigational waterways. Finally, at least 7 052 Km of rivers are affected by roads and railroads, either by being intersected by these infrastructures or through disturbance of the river margins and floodplains. Regarding the connectivity calculations, results clearly show

that, on average, basins have a natural longitudinal connectivity of 80% regarding the type of movements of potamodromous and diadromous species, and not the usually assumed 100%. Reservoirs are responsible for 9% decrease in longitudinal connectivity. Overall, most of the larger European basins are extremely fragmented, with less than 50% connectivity values.

## 4. General Conclusions

To perform a realistic longitudinal connectivity study, we argue that the starting point of the analysis should not be "total connectivity", but the natural connectivity of the systems that predates the construction of any artificial barrier. Reservoirs and the segments affected upstream of dams act as ecological barriers and are dramatically impactful to fish movements. Longitudinal connectivity is the most relevant dimension for fish species, nonetheless, lateral disconnection is recognized as a significant impact on ecological function in riverscapes, negatively affecting the development of side-channel habitats, floodplain evolution, riparian ecosystem processes, and biodiversity. Aggregating these metrics allows the classification of the sub-basins regarding the overall effect on lateral connectivity. Assessing the extent of these disturbances is relevant in attaining goals placed by environmental policies like the Water Framework Directive or the Nature Restoration Law.

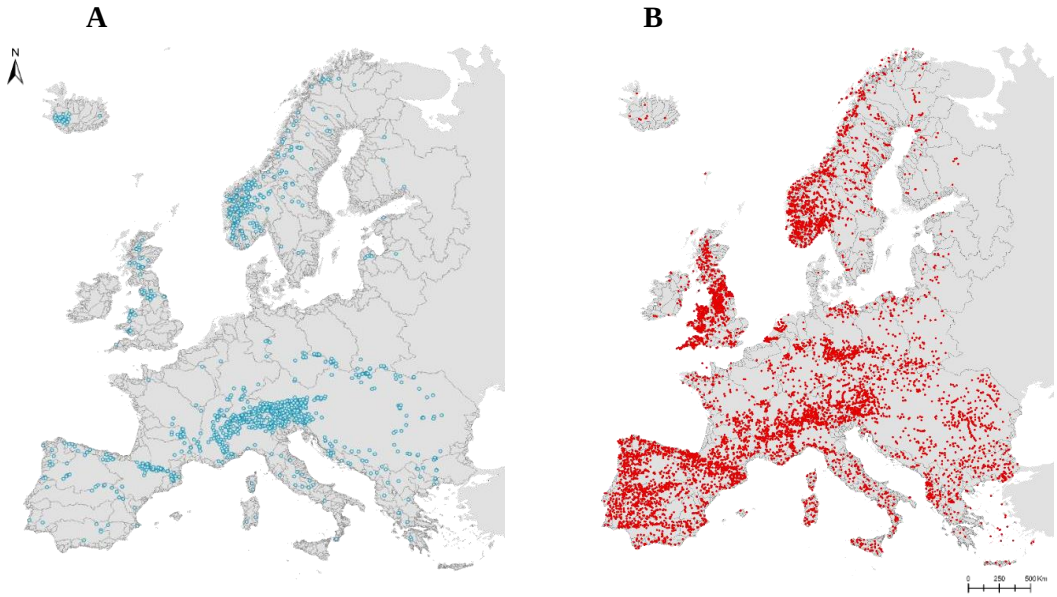



**Figure 1.** Maps of natural (A) and artificial barriers (B) in Europe.

**Acknowledgements**

This research was funded by the project Dammed Fish (PTDC/CTA-AMB/4086/2021), and the MERLIN project (H2020–101036337). Tamara Leite was supported by a Ph.D. grant from the FLUVIO–River Restoration and Management programme funded by Fundação para a Ciência e a Tecnologia I. P. (FCT), Portugal (UI/BD/15052/2021- DOI 10.54499/UI/BD/151052/2021). Gonçalo Duarte has been financed by FCT within the project PTDC/CTA-AMB/4086/2021 and via UIDP/00239/2020. Paulo Branco was financed by national funds via FCT (LA/P/0092/2020). Forest Research Centre (CEF) is a research unit funded by Fundação para a Ciência e a Tecnologia I.P. (FCT), Portugal (UIDB/00239/2020). The Associate Laboratory for Sustainable Land Use and Ecosystem Services (TERRA) is also funded by FCT (LA/P/0092/2020-DOI 10.54499/LA/P/0092/2020).

**References**

AMBER Consortium, 2020. The AMBER Barrier Atlas. A Pan-European database of artificial instream barriers. Version 1.0 June 29th, 2020. https://amber.international/european-barrier-atlas/.

Belletti, B., Garcia de Leaniz, C., Jones, J., Bizzi, S., Börger, L., Segura, G., Castelletti, A., van de Bund, W., Aarestrup, K., Barry, J., Belka, K., Berkhuysen, A., Birnie-Gauvin, K., Bussettini, M., Carolli, M., Consuegra, S., Dopico, E., Feierfeil, T., Fernández, S., Fernandez Garrido, P., Garcia-Vazquez, E., Garrido, S., Giannico, G., Gough, P., Jepsen, N., Jones, P.E., Kemp, P., Kerr, J., King, J., Łapińska, M., Lázaro, G., Lucas, M.C., Marcello, L., Martin, P., McGinnity, P., O'Hanley, J., Olivo del Amo, R., Parasiewicz, P., Pusch, M., Rincon, G., Rodriguez, C., Royte, J., Schneider, C.T., Tummers, J.S., Vallesi, S., Vowles, A., Verspoor, E., Wanningen, H., Wantzen, K.M., Wildman, L., Zalewski, M., 2020. More than one million barriers fragment Europe's rivers. Nature 588, 436–441. https://doi.org/10.1038/s41586-020-3005-2

Cote, D., Kehler, D.G., Bourne, C., Wiersma, Y.F., 2009. A new measure of longitudinal connectivity for stream networks. Landscape Ecol 24, 101–113. https://doi.org/10.1007/s10980-008-9283-y

De Jager, A., Vogt, J., 2007. Rivers and Catchments of Europe - Catchment Characterisation Model (CCM) European Commission, Joint Research Centre (JRC) [Dataset] PID: http://data.europa.eu/89h/fe1878e8-7541-4c66-8453-afdae7469221.

European Waterfalls https://www.europeanwaterfalls.com/ [WWW Document], 2020.

Meijer, J.R., Huijbregts, M.A.J., Schotten, K.C.G.J., Schipper, A.M., 2018. Global patterns of current and future road infrastructure. Environmental Research Letters 13. https://doi.org/10.1088/1748-9326/aabd42

Mulligan, M., van Soesbergen, A., Sáenz, L., 2020. GOODD, a global dataset of more than 38,000 georeferenced dams. Sci Data 7, 1–8. https://doi.org/10.1038/s41597-020-0362-5

Swan, B., Gross, D., 2012. World Waterfall Database.

Wang, J., Walter, B., Yao, F., Song, C., Ding, M., Maroof, A., Zhu, J., Fan, C., Xin, A., McAlister, J., Sikder, S., Sheng, Y., Allen, G., Crétaux, J.-F., Wada, Y., 2021. GeoDAR: Georeferenced global dam and reservoir dataset for bridging attributes and geolocations. Earth System Science Data Discussions 1–52. https://doi.org/10.5194/essd-2021-58

# Adaptive agreements on benefits sharing for managed aquifer recharge in the Mediterranean region

Anika CONRAD[1], Ronjon HEIM[1], Rafael BERGILLOS[2], Joaquín ANDREU[2], Charlotte ROHDE[1], Catalin STEFAN[3], Constantinos PANAGIOTOU[4], Anis CHEKIRBANE[5], Teresa LEITÃO[6], Syrine GHANNEM[2], Abel SOLERA[2], and Javier PAREDES[2]

[1] adelphi research gGmbH, Germany
conrad@adelphi.de, heim@adelphi.de, rohde@adelphi.de

[2] Universitat Politècnica de València (UPV), Spain
rbermec@upv.es, ximoand@upvnet.upv.es, sghanne@upv.es, asolera@upvnet.upv.es, jparedea@hma.upv.es

[3] Technische Universität Dresden (TUD), Germany
catalin.stefan@tu-dresden.de

[4] ERATOSTHENES Centre of Excellence (ERATOSTHENES CoE), Cyprus
constantinos.panagiotou@eratosthenes.org.cy

[5]Institut National Agronomique de Tunisie (INAT), Tunisia
a.chkirbene@ecopark.rnrt.tn

[6] Laboratório Nacional de Engenharia Civil (LNEC), Portugal
tleitao@lnec.pt

## ABSTRACT

Managed aquifer recharge (MAR) is a globally recognized solution for sustainable management of water resources in the water-stressed Mediterranean region addressing water scarcity and enhancing groundwater resources. However, diverse stakeholder interests, the complex and dynamic nature of aquifer recharge systems and of associated societal, ecological and hydrogeological conditions as well as an overabundance of decision support tools, present major obstacles for an equitable and sustainable management of MAR systems. Reliable governance mechanisms of guaranteeing benefits are required for a good functioning of the system and for proper exploitation of its potential. This contribution introduces the concept of adaptive agreements developed for fostering the wider implementation of MAR in the Mediterranean countries. The format and scope of the agreements are flexible and responsive to changing hydrological, environmental, and socio-economic conditions. They empower stakeholders to collaboratively initiate and manage MAR projects, while reducing the risks for future conflicts, addressing power imbalances and cost disparities, and ensuring equitable sharing of MAR benefits such as improved water quality, increased water availability, and ecological restoration. Drawing on four case studies from the Mediterranean region, the authors showcase the diverse mechanisms and strategies used to establish, adapt, and manage agreements.

Moreover, this contribution emphasizes the pivotal role of effective governance and stakeholder engagement through participatory workshops and civil assemblies in shaping adaptive agreements for MAR. Engaging local communities, governments, water authorities, and environmental organizations is essential for building trust and ensuring the sustainability of MAR projects. Alongside stakeholder engagement (Conrad 2022), the integration of decision support tools for scientifically substantiating agreements is also discussed, encompassing MAR feasibility criteria and mapping (Panagiotou 2022), water resource systems impact assessment with the AQUATOOL DSS (Andreu et al., 1996), and modeling techniques (Glass et al., 2022) for predicting the impact of MAR on groundwater systems. By considering the unique challenges of Mediterranean region, the study provides valuable insights into designing flexible and equitable agreements that can promote sustainable water management and support climate change adaptation.

## 1. Views of local stakeholders on MAR agreements – first results from stakeholder interviews and workshops

In four different demonstration sites in Spain, Portugal, Cyprus, and Tunisia, stakeholders from policy, research, and practice related to MAR projects have been consulted about the specific requirements they expect MAR agreements to fulfil. The review of interviews revealed that MAR agreements are expected to:

- Ensure fair distribution of water recovered from MAR systems and associated benefits among beneficiaries involving stakeholders from different sectors.
- Provide clear information on the impact, costs, and benefits of the MAR system (including an assessment of ecosystem services).
- Promote sustainable and environmentally friendly MAR management.
- Define the operation mode of the MAR system (incl. infiltration and abstraction patterns) based on scientific results of groundwater models.
- Ensure adequate engagement of relevant stakeholders in the management of the MAR system. Promote stakeholder engagement formats to reduce future conflicts as best as possible.
- Clearly define the roles and responsibilities of authorities and other stakeholders.
- Clearly define the financing of the MAR system (incl O&M). Preferably O&M costs are covered by beneficiaries and revenue streams based on a cost-benefit analysis.
- Ensure the production and exchange of relevant data and information on the MAR system is available to all stakeholders in a transparent manner to increase trust and raise awareness.
- Be in line with the existing legal framework and support its implementation.
- Ensure adequate capacity building formats for stakeholders related to MAR management are offered, adapted to the specific local challenges and needs.
- Promote and facilitate future MAR projects.

Regarding the format of the MAR agreements, stakeholders stressed that the agreements should reflect the perspective and interest of all relevant stakeholders, especially those using groundwater resources. Further, the agreements should not be legally binding but rather in form of a Memorandum of Understanding between key stakeholders. The need was also expressed for local and regional water authorities to coordinate and promote the agreements to ensure their adequate implementation.

## 2. Adaptive method for creating MAR agreements

The steps towards adaptive MAR agreements are embedded in a general governance framework. This framework serves as a voluntary assessment tool to evaluate the performance of MAR systems and their governance. It guides decision-makers in identifying necessary improvements and equips them with tools for effective planning, implementation, and operation of MAR systems. The framework is designed to be applicable across various MAR typologies that include technical, social, legal, policy, economic and environmental aspects. In this context, the MAR governance framework: (1) Define what can be understood as effective, efficient, and inclusive MAR systems, (2) Guide decision-makers on how to assess the current status of their MAR system and identify information gaps, and (3) Provide instruments, formats, and guidelines empowering MAR decision-makers to fill these gaps.

**Acknowledgements**

The AGREEMAR project is funded by National Funding Agencies from: Germany (Bundesministerium für Bildung und Forschung – BMBF, grant no. 02WPM1649), Cyprus (Research & Innovation Foundation – RIF, grant no. 0321-0024), Portugal (Fundação para a Ciência e a Tecnologia – FCT, grant no. PRIMA/0004/2021), Spain (Agencia Estatal de Investigación, Ministerio de Ciencia e Innovación – MCI, grant no. PCI2022-133001) and Tunisia (Ministère de l'Enseignement Supérieur et de la Recherche Scientifique – MESRSI, grant no. PRIMA/TN/21/07). The project is funded under the Partnership for Research and Innovation in the Mediterranean Area (PRIMA). This programme is supported under Horizon 2020 by the European Union's Framework for Research and Innovation.

**References**

Andreu, J., Capilla, J., & Sanchís, E. (1996). AQUATOOL, a generalized decision-support system for water-resources planning and operational management. Journal of hydrology, 177(3-4), 269-291

Glass, J., Junghanns, R., Schlick, R., Stefan, C. (2022) The INOWAS platform: A web-based numerical groundwater modelling approach for groundwater management applications. Environmental Modelling & Software, 155, 105452. http://dx.doi.org/10.1016/j.envsoft.2022.105452

Conrad, A.; Heim, R.; Helling, Leo. 2022. AGREEMAR Deliverable D1.1: Stakeholder engagement strategy and plan. Available online at https://www.agreemar.inowas.com/deliverables.

Panagiotou, C.F., Chkirbene, A., Stefan, C., Martins, T.N., Leitão, T.E. 2022. AGREEMAR Deliverable D2.1: Matrix of feasibility criteria for managed aquifer recharge. Available online at https://www.agreemar.inowas.com/deliverables.

# Assessment of the impact of drought management protocol in the Guadalquivir River Basin applying hydro-micro-macro-economic modelling

Ángela VALLE-GARCÍA[1], Nazaret M. MONTILLA-LÓPEZ[2], Julio BERBEL[3], Carlos GUTIÉRREZ-MARTÍN[4]

[1,2,3,4] WEARE-Water, Environmental and Agricultural Resources Economics Research Group, Universidad de Córdoba (Spain)

[1]g22vagaa@uco.es, [2]g02molon@uco.es, [3]berbel@uco.es, [4]carlos.gutierrez@uco.es

ABSTRACT

Hydro-economic modelling combines biophysical and socioeconomic factors for water management. At best, the economic effects in hydro-economic models only take into account the microeconomic scale, ignoring the changes that the general economy of the region may have. The main objective of this work is to develop a link between a hydro-economic model and Computable General Equilibrium (CGE) model, using the Guadalquivir River Basin (GRB) in Spain as a case study. We apply the drought management plan of the GRB at micro and macro-economic scale in drought situation. Our results show that the economic impact of droughts decreases when macroeconomic effects are considered due to the increase in crop prices when crop area is reduced.

## 1. Introduction and objectives

In regions characterized by persistent water scarcity, droughts worsen water shortages, largely due to the increasing global demand for water, driven by a growing world population and rising affluence (Wada et al., 2016). This heightened demand for water coincides with the closure of certain river basins, which is defined as the inability to meet the growing demand for water for different uses, where it is no longer possible to increase the conventional water supply (Molle et al., 2010). To address this, effective demand-side policies are crucial, as they can limit choices for users and encourage adaptive responses, especially in the agricultural sector, with significant economic implications. The allocation of water rights plays a crucial role in managing water resources in closed basins with limited water availability, necessitating careful oversight and regulation of water usage.

Hydro-economic modelling is a sophisticated tool that combines biophysical and socioeconomic factors to provide insights for water management decisions, contributing to better water resource planning. This model has become essential for examining water-human systems, predicting management scenarios, formulating policies, and improving water-related infrastructure operations. However, few hydro-economic models incorporate economic agents capable of adapting and making decisions in the face of water scarcity. Moreover, to the best of our knowledge, none of them take into account effects on the economy that would cause prices to be altered when the crop area changes significantly.

The main objective of this work is to analyse the effects of linking a hydro-micro-economic model and a macro-economic model. This is achieved by developing a hydro-economic model applied to the Guadalquivir River Basin (GRB) in southern Spain and a macro-economic (Computable General Equilibrium) model of the region of Andalusia economy to understand the feedback between the agroeconomic sector and the regional economy.

## 2. Methodology

The hydro-economic model (Martínez-Dalmau et al., 2023) consists of a network of nodes and links representing the hydrological system and agricultural and urban water demands representing the economic agents. The agricultural demands are calibrated with Positive Mathematical Programming (Dagnino and Ward, 2012) so that farmers react to water scarcity by adapting crop distribution. A CGE model (Bosello and Standardi, 2015) calibrated at a regional level is developed for the macroeconomic aspect. These models are

interconnected through the land-use component and exchange information on commodity prices, water availability, and water allocation changes (Fig. 1). The Drought Management Protocol of the GRB has been applied when water availability of agricultural agents is reduced by 25% to demonstrate the effect of the coupling between micro- and macro-economic models.

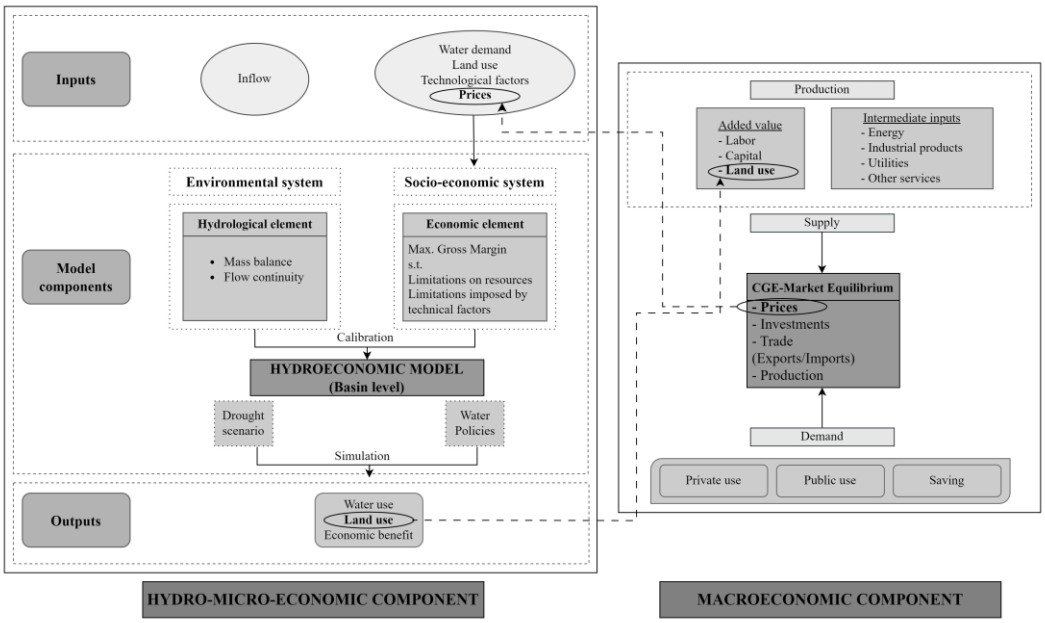



**Fig. 1.** Modelling framework

## 3. Results

The results show that the effects of the reduction in crop area (in the hydro-economic model) due to drought are dampened by the macroeconomic model because it leads to an increase in prices. That is, some crops reduce their area less due to higher prices. When models converge (no further changes in crop area and no more price changes in the feedback between the two models), there is a new crop distribution compared to the results obtained with the hydro-economic model alone. Wheat recovered a 5% of its lost area when taking into account the price increase. Other cereals recover 16% and olive groves 2%, while vegetables and fruits decreased by an additional 1%, fibers and other crops by 2% and rice and beets remained unchanged. The economic gain from the price increase effect is greater than the loss from the quantity effect (loss of crop area), leading to a final situation with a higher average gain than the situation without drought.

## 4. Conclusions

We have developed a coupling between a hydro-economic model and a macro-economic model capable of taking into account changes in commodity prices when crop areas decrease due to drought. This has mitigated the economic impacts of the drought due to the price effect, even allowing for higher profits. It must be understood that the total net gain is not evenly distributed, with winners and losers among farmers.

Accounting of a single hydro-micro-economic model provides more robust results than consideration of separate hydrological and microeconomic models, which rely on soft links between models.

**Acknowledgements**

This research is part of the project TED2021-131066B-I00, funded by MCIN/AEI/10.13039/501100011033 and by the European Union "NextGenerationEU"/PRTR.

**References**

Bosello F, Standardi G (2015) Working Paper Nº RP0274, CMCC Research Papers. CMCC, Lecce (Italy).
Dagnino M, Ward FA (2012) Economics of agricultural water conservation: empirical analysis and policy implications, International Journal of Water Resources Development, 28(4), 577-600.
Martínez-Dalmau J, Gutiérrez-Martín C, Kahil T, Berbel J (2023) Impact of alternative water policies for drought adaptation in the Guadalquivir Mediterranean river basin, southern Spain, Journal of Hydrology: Regional Studies, 47,101444.
Molle F, Wester P, Hirsch P (2010) River basin closure: processes, implications and responses, Agricultural, Water Management, 97(4), 569-577.
Wada Y, Flörke M, Hanasaki N, Eisner S, Fischer G, Tramberend S, Satoh Y, Van Vliet MTH, Yillia P, Ringler C, Wiberg D (2016) Modeling global water use for the 21st century: The Water Futures and Solutions (WFaS) initiative and its approaches, Geoscientific Model Development, 9(1), 175-222.

# The right to the city as lens for a multifaceted analysis of Managed Aquifer Recharge

Keyla ALPES[1], João Lutas CRAVEIRO[1], Teresa E. LEITÃO[1]

[1] National Laboratory for Civil Engineering, Portugal
kalpes@lnec.pt, jcraveiro@lnec.pt, tleitao@lnec.pt

ABSTRACT

## 1. Introduction and methodology

The French sociologist Henri Lefebvre, author of the well-known work “the right to the city”, presents the conception of space in three dimensions: through its apprehension (through the senses, and instruments, which account for its materiality), through its planning (through professionals and techniques) and their appropriation (which goes back to emotions, desires, needs, life stories, belonging and spatial identity ties). This conception of the space makes it possible to consider not only the so-called objective components, but also the subjective components. Those components are essential in the analysis and proposition of successful solutions to complex problems (wicked problems), namely socio-environmental problems. In the field of complex problems, worsening water scarcity stands out, in a close relationship with other factors such as the human densification of urban spaces, soil contamination or loss of water quality, or even the variations and disturbances in the precipitation regime, among other climate change impacts.

This paper aims to address the relationships of interdependence between social and environmental systems, exploring the expansion of the right to the city, implying a right to life, under the essential availability of water resources, in adequate quantity and quality, in the sense of authentic development, human, sustainable, which, unlike elements that can be measured by quantitative indicators of consumption and economic growth. It calls for a change in lifestyles, categorizations and indicators that take into account other ways of being, transforming and being in the world, as well as their narrow connection with social, environmental and economic sustainability.

Following what was said in the previous paragraphs, this work seeks to introduce and promote the relevance of using this conception of space in the analysis of socio-environmental issues, such as Managed Aquifer Recharge (MAR). It leads to the ethics of development from the perspective of Human Ecology (especially using authors such as Lefebvre, Goulet, among others). Following such ethics principles, in the case of water management, requires an adequate selection of representativeness scales for decision makers. It should not be too small or with localized representation, where the focus on the fair management of a common essential resource could be lost in the midst of particular interests, and not too wide as to make it difficult to make decisions in line with the specific needs of each place. This takes up the third dimension of space, of its appropriation, which leads to a deeper reflection returning to perverse or complex problems. Jacquinet, citing Horst Rittel - who formalized wicked problems for the first time - explains that there would be no definitive scientific test to mitigate wicked problems, because they are human creations (anthropic) and science exists to understand natural phenomena. So, if the wicked problems are human creations, and based on Human Ecology (study of the relationship between mankind and nature), it would not be enough to seek solutions to the wicked problems based solely on nature, there must also be an intervention on Man, the first generator of perverse problems. To do so, the question would be as to what would characterize a human being; what would differentiate it from an animal. The answer is already well established by philosophy and would be conscious, and its ability to develop and cultivate values, virtues, and wisdom. The main human

input is gained by acting on this essence where perverse or complex problems can and should be mitigated. Making technological solutions effective and sustainable is important but contemplating cultural adaptation that complements technical adaptation is also necessary for the survival of the human species. And with that we come to Goulet, for whom ethical values would be the basis of a sustainable development. In other words, space is not just its materiality, it is not just its planning, but it is its life.

Regarding an integrated and participatory management of water resources, especially in the face of scarcity problems, some technical solutions have been developed, including managed aquifer recharge. MAR has already been used in some countries on several continents, including Europe. To introduce this solution in Portugal, some projects have been developing a technique that induces recharge of an aquifer through infiltration, allowing the subsequent extraction of that water in a controlled and monitored manner. Infiltration water may come from surplus water or reused water, among other sources. This technique is being applied in Comporta, Portugal, a case study of the AgreeMAR project ("Adaptive agreements on benefits sharing for managed aquifer recharge in the Mediterranean region", https://agreemar.webspace.tu-dresden.de/), which counts the National Laboratory for Civil Engineering (LNEC) among its partners. The project proposes and applies participatory and integrative methodologies, where the third dimension of space (according to Lefebvre), the human, the living component, is being accounted for.

The methodology used in this research consisted, primarily, of a bibliographic review.

## 2. Concluding remarks

The aim of this communication is to elicit the notion of a dialectical three-dimensionality when analysing spaces, considering their so-called objective and subjective aspects. It intends to make the apprehension of reality clearer and more complete, facilitating the analysis and search for solutions to impasses between mankind and nature that we face today. The article is based and inspired by the theory of sociologist Lefebvre and, citing the example of water scarcity addressed through MAR. MAR technique applications, where human adaptation is perceived through the use of technology capable of apprehending and transforming reality by impacting it, can also be a possibility of fostering a positive adaptive process from a social, cultural and political point of view, through which the human component is duly considered, as well as indicators capable of accounting for the complexity of this component. Both technological and cultural adaptations are fundamental in the achievement of any human project sustainable, to overcome wicked problems and guarantee the survival of the human species.

**Acknowledgements**

The AGREEMAR project is funded under the Partnership for Research and Innovation in the Mediterranean Area (PRIMA), supported under Horizon 2020 by the EU's Framework for Research and Innovation, and by the National Funding Agencies (FCT, grant no. PRIMA/0004/2021).

**References**

Denis, G (2008) Denis Goulet and the project of Development Ethics: Choices in Methodology, Focus and Organization. Available online at http://doi. Org/10.1080/1464988080.

Glass J, Stefan C (2023) AGREEMAR Deliverable D6.4b: Minutes of the AGREEMAR mid-term meeting. Available online at https://www.agreemar.inowas.com/deliverables.

Jaquinet, M (2021) Complex problems (Wicked Problems) and management challenges, Lisbon, Universidade Aberta. Available online at http://hdl.handle.net/10400.2/5129.

Schmid, D (2012) Lefebvre`s Space Production Theory: Towards a Three-Dimensional Dialectic. Available online at https://www.revistas.usp.br/geousp/article/view/74284.

Ribeiro W C, Santos C L S, Silva L P B (2019) Conflict over water, between scarcity and abundance: Theoretical frameworks. Available online at https://e-revista.unioeste.br/index.php/ambientes/article/view/23619.

# Water reuse in the context of water planning: challenges of the transnational Guadiana River Basin

Maria Carolina SOUSA[1], Manuel Victor MATOS[2], Ana Catarina MIRANDA[3], Andreia CARDOSO[4], Teresa FIDELIS[5]

[1,2,3,5] Department of Environment and Planning, University of Aveiro
mary.carolina@gmail.com
manuelvictor16@hotmail.com
anacatarinammiranda@gmail.com
teresafidelis@ua.pt
[4] BIOPOLIS Program in Genomics, Biodiversity and Land Planning, University of Porto
andreiasaavedra@cibio.up.pt

ABSTRACT

The Guadiana River Basin, located in the Iberian Peninsula, is an area of shared water that is prone to experiencing water scarcity and drought. This study analyses the integration of water reuse into the water resources plans and river basin management plans of Portugal and Spain in a transnational context. The legal frameworks for water management in both countries are similar, but Portugal has a more extensive set of planned measures for water reuse. Issues strengthening the connections between planning systems for land use and water resources are not a principal apprehension in these water policies and plans, and the implementation of the measures in the legislation are the challenges for the management of is transnational river basin.

## 1. Introduction

The water tensions and conflicts tend to become more frequent due to the scarcity events and the implications of climate change and inefficient use of water resources in different world regions. Water governance compels the establishment of policies, regulations, and agreements for the efficient management of water and its reuse. Water management in the Iberian Peninsula presents an additional factor to the challenge of water resource management, which is a significant number of rivers that Portugal and Spain share, i.e., the Guadiana River. Throughout its entire length, the basin receives several pressures on its water bodies, including agriculture, extractive industry, and urban and recreational activities. The water demand is likely to surpass its availability in many river basins of Southern Europe, systematically more affected by droughts, where lower levels of water on rivers and streams are expected to be reduced by 40% due to climate change (Alcalde-Sanz et al., 2014). The objective of this study is to analyse if and how water reuse is being integrated in the scope of the water resources plans of the Guadiana River Basin District.

## 2. Research approach and methodology

The research database contained for both countries guiding documents for decisions and investments, considering the significance of strategic action papers (Table 1). From the database, document analysis is carried out by following a deductive method of inquiry, using qualitative content analysis and comparative case study analysis.

Table 1. Database of documents from Portugal and Spain

| Type of document | Portugal | Spain |
|---|---|---|
| Water, efficient water use, and drought plans | National Water Plan (Decree-Law n. 76/2016)<br>National Programme for Efficient Water Use (Resolution of the Council of Ministers n. 113/2005)<br>Prevention, Monitoring and Contingency Plan for Drought Situations | National Hydrological Plan (Law 10/2001)<br>National Plan for Purification, Sanitation, Efficiency, Saving and Reuse (Order TED/801/2021)<br>Special Drought Plan for the Guadiana River Basin |

| | | |
|---|---|---|
| Water reuse regulation | Legal Framework of Production of Water for Reuse (Decree-Law n. 119/2019) | Legal Framework for the Reuse of Treated Water (Royal Decree n. 1620/2007) |
| Guadiana river basin plans (Program of Measures) | Guadiana Hydrographic Region Management Plan 2016 – 2021 (Resolution of the Council of Ministers n. 52/2016)<br>Guadiana Hydrographic Region Management Plan 2022 - 2027 (in progress) | Hydrological Plan of the Spanish Part of the Hydrographic Demarcation of Guadiana 2016-2021 (Royal Decree 1/2016)<br>Hydrological Plan of the Spanish Part of the Hydrographic Demarcation of Guadiana 2021-2027 (in progress) |

## 3. Results and Discussion

Water reuse is recognized in Portugal and Spain as a means to improve water efficiency, combat water scarcity, and enhance environmental conditions. However, Spain's strategy for the Guadiana basin lacks precise measures. Both countries incorporate water reuse in their drought contingency plans, mostly for agriculture and industry, with Spain implementing its plan nationwide. Portugal has a more extensive framework for water reuse, incorporating risk assessments and compensation mechanisms, whereas Spain's regulations are more general in nature. To conclude, the Guadiana river basin plan in Portugal prioritises water reuse across all water bodies and presents more concrete elements to execute the water reuse measures foreseen, in contrast with the concise and generic forecasts that the Spanish Guadiana plan offers, limiting it to the Upper Guadiana subsystem to tackle water deficits.

For provisions to become possible, it is necessary to comprehend the status of the existing water treatment and distribution infrastructure and what needs to be done or revised in financial, technical, and temporal terms (Molinos-Senante et al., 2013). Although the legal provisions and approval for water production facilities are already in place (APA, 2023), the measures devised in the Guadiana River Basin Management have not yet been fully implemented. Investment is still being made in large amount of water abstraction (Dias, 2023) and the inter-basins water transfers (Lusa, 2024) during critical drought.

The successful implementation also requires due attention to the articulation between land use planning with water resources conservation and efficiency planning, within a water-land use nexus (Fidélis et al., 2020), not just the legislation content (Fidélis & Roebling, 2014). Spain is more developed than Portugal in what concerns land-water management regulations over water quantity; however, this concern is not the object of the main worries with water planning and management documents in the countries.

## 4. Conclusions

Considering the international Guadiana basin has a scarcity index classified as severe, water reuse is an important measure to encourage the use of non-conventional water sources. Portugal and Spain have action plans and specific measures for integrating water reuse into water resource planning; however, the management challenges include complying with current regulations and improve integrating themes on the water-soil nexus in future revisions or formulations of water resource plans and policies to Guadiana river basin.

**Acknowledgments**

**T**his work was supported by the "Project O - Demonstration of planning and technology tools for a circular, integrated and symbiotic use of water", Research Project funded from the European Union's Horizon 2020 - grant agreement No 776816. Thanks for the financial support are also due to the Research Unit on Governance, Competitiveness and Public Policy (GOVCOOP), to FCT/MCTES through national funds, and the co-funding by the FEDER, within the PT2020 Partnership Agreement and Compete 2020.

**References**

Alcalde-Sanz, L, Gawlik, BM, European Commission. Joint Research Centre. (2014). Water reuse in Europe: relevant guidelines, needs for and barriers to innovation. Publications Office. https://doi.org/10.2788/29234

APA. (2023). Licenças emitidas. Agência Portuguesa do Ambiente. https://apambiente.pt/agua/licencas-emitidas

Dias, C. (2023). Seca: Espanha e Portugal querem tirar mais água do Guadiana e a pressão aumenta. PÚBLICO. https://www.publico.pt/2023/06/04/azul/noticia/seca-espanha-portugal-querem-tirar-agua-guadiana-pressao-aumenta-2052038

Fidélis, T., Abrantes, J., Cardoso, A., Miranda, A. C., Riazi, F., Teles, F., Roebeling, P., Lopes, M., & Capela, I. (2020). Policy and planning settings for the transition to circular economy - Barriers and drivers in place. https://www.eu-project-o.eu/wp-content/uploads/2022/04/D3.2-Policy-design-for-the-transition-to-circular-economy-barriers-and-drivers-in-place.pdf

Fidélis, T., & Roebeling, P. (2014). Water resources and land use planning systems in Portugal—Exploring better synergies through Ria de Aveiro. Land Use Policy, 39, 84–95. https://doi.org/10.1016/j.landusepol.2014.03.010

LUSA. (2024). Andaluzia em "situação extrema" de seca insiste em transferência de água desde Portugal. Agência de Notícias de Portugal. https://www.lusa.pt/international/article/2024-01-18/42171641/andaluzia-em-situa%C3%A7%C3%A3o-extrema-de-seca-insiste-em-transfer%C3%AAncia-de-%C3%A1gua-desde-portugal

Molinos-Senante, M., Hernández-Sancho, F., Sala-Garrido, R., & Cirelli, G. (2013). Economic feasibility study for intensive and extensive wastewater treatment considering greenhouse gases emissions. Journal of Environmental Management, 123, 98–104. https://doi.org/10.1016/j.jenvman.2013.02.044.

# Uncertainties in Hydrological-Hydrodynamic Catchment Flood Modeling

Leon Frederik DE VOS[1], Nils RÜTHER[1], Karl BROICH[1]

[1] Technical University Munich, Germany
frederik.de-vos@tum.de
nils.ruether@tum.de
karl.broich@tum.de

ABSTRACT

With rising computational resources, small catchments can now be fully modeled with a hydrodynamic model incorporating the hydrological processes and do not need an external coupling to a hydrological model. In this study, the 2D Finite Element solver of the openTELEMAC system is used to model the resulting flood event of a 100-year rainfall with a duration of four hours in an ungauged German catchment with an area of approximately 58 km². For the rainfall-runoff process, the included SCS-CN method is applied. A small sensitivity analysis shows that the CN values are very sensitive, and the Strickler roughness values are less sensitive.

## 1. Introduction and Methods

The study area is a catchment of around 58 km² in middle Germany with elevations from around 170 m at the confluence into the Main River to 370 m at the upstream catchment borders. These types of catchments can be completely modeled by a 2D-hydrodynamic model, which incorporates the rainfall-runoff process. This omits the external coupling of a hydrological model upstream of the hydrodynamic model. Therefore, the complete catchment area is solved by the full 2D shallow water equations (SWE), so that the hydrological and hydrodynamic processes are determined within one model (David et al., 2023). The simulation time for an event can be kept manageable by coarsening the computational mesh in the overland regions and refining the mesh only in the streams. In the overland, the edge length of a mesh element increases to up to 25 m, while the mesh elements in the streams have an edge length of 1 m. Topographical thalwegs outside of bathymetrically surveyed streams are resolved with an edge length of 4 m to ensure water routing towards the streams.

This study uses the openTELEMAC system (EDF, 2022) to model flood formation and propagation. The incorporated SCS-CN model for the rainfall-runoff process and the Manning-Strickler model for the friction term of the SWE. This method has been validated in previous studies (e.g., Broich et al., 2019).

The catchment study area is ungauged; therefore, a validation of the model is hindered. Instead, a sensitivity analysis is conducted to assess the impacts of the rainfall-runoff model and the friction model for a 100-year rainfall with a duration of four hours (Euler II distribution, 61 mm in total). The sensitivity of the SCS-CN method is investigated by increasing and decreasing the CN-values by 5 % and 10 %. For the Manning-Strickler model the Strickler coefficient $k_{st}$ (equal to $1/n$, with $n$ the Manning coefficient) is varied. The sensitivity of the $k_{st}$ is separated into the stream channels and the overland. For both regions, the $k_{st}$ is increased and decreased by 20 %.

## 2. Results and Discussion

Fig. 1 shows the resulting hydrographs at the catchment outlet for the sensitivity of the different tested cases. Table 1 lists the maximum discharge for every test case and the relative difference of the maximum discharge for each test case compared to the base case. Increasing the roughness in the model (which implies decreasing the $k_{st}$ values) reduces and delays the flood peak. The reduction amounts to 4 % for the overland, and for the channel to 2 %. Decreasing the roughness increases the flood peak by 4 % for the overland and 2 % for the

channel. The flood peak also arrives earlier. The roughness in the overland is, therefore, slightly more sensitive than the roughness in the channel.

The CN values show an extremely high sensitivity for the model. By increasing the CN-values by 5 %, the flood peak already increases by 50 %. Reducing the CN-values by 5 % decreases the flood peak by 32 %.

The SCS-CN method shows a significantly higher sensitivity than the friction model, as it directly influences the volume of water in the model and not just the flow dynamics. Therefore, the flood model and its uncertainties are more impacted by the hydrological model than by the hydrodynamic model.

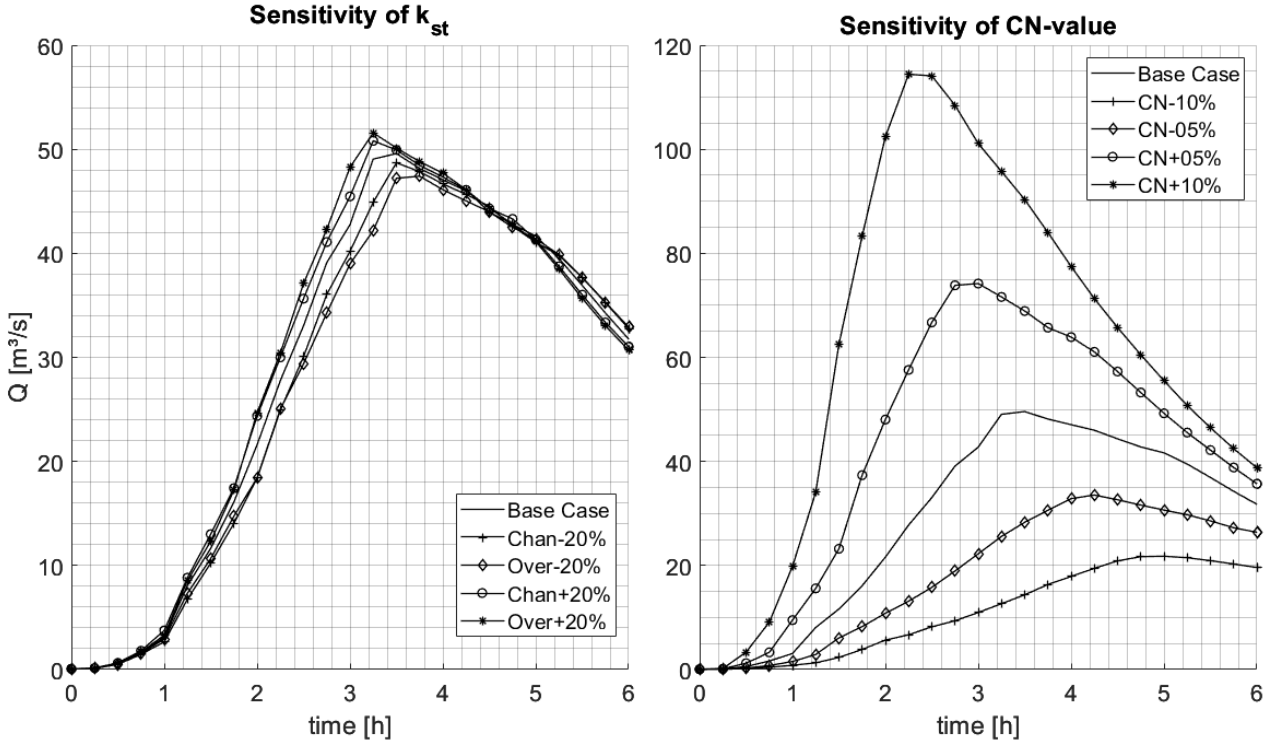



**Fig. 1.** Comparison of the sensitivity of the friction model (left) and SCS-CN model (right) using the hydrographs at the catchment outlet.

## 3. Conclusion and Outlook

This study shows the high sensitivity of the SCS-CN model on a hydrological-hydrodynamic flood model in a small catchment. Different hydrological models that include a temporal infiltration will be tested in the future to further address the rainfall-runoff process. Additionally, field measurements in the study area are planned for a better representation of drainage infrastructure and to assemble baseflow discharge data of the different streams.

**Table 1.** Max. discharges at the catchment outlet and relative difference from the base case for each case.

| Case | Base Case | Chan-20% | Over-20% | Chan+20% | Over+20% | CN-10% | CN-5% | CN+5% | CN+10% |
|---|---|---|---|---|---|---|---|---|---|
| Max. discharge [m³/s] | 49.6 | 48.6 | 47.4 | 50.8 | 51.6 | 21.8 | 33.5 | 74.2 | 114.4 |
| Relative Difference from Base Case [-] | - | 0.98 | 0.96 | 1.02 | 1.04 | 0.44 | 0.68 | 1.50 | 2.30 |

**References**


Broich, K., Pflugbeil, T., Disse, M., & Nguyen, H. (2019). UsingTELEMAC-2D for hydrodynamic modeling of rainfall-runoff. XXVIth Telemac User Conference.

David, A., Rodriguez, E. R., & Schmalz, B. (2023). Importance of catchment hydrological processes and calibration of hydrological-hydrodynamic rainfall-runoff models in small rural catchments. Journal of Flood Risk Management, 16(3), e12901. https://doi.org/10.1111/jfr3.12901

EDF (2022): TELEMAC-2D. User Manual. Version v8p4.

# Flood analysis in a small catchment following the July 2021 events in Belgium: respective contributions from runoff and overflowing

Sandra SOARES-FRAZÃO[1], Yves ZECH[1], Robin MEURICE[1], Nathan DELPIERRE[1], Pierre-Yves GOUSENBOURGER[1]

[1] Institute of Mechanics Materials and Civil Engineering, UCLouvain, Belgium
sandra.soares-frazao@uclouvain.be
yves.zech@uclouvain.be
robin.meurice@uclouvain.be
nathan.delpierre@uclouvain.be
pierre-yves.gousenbourger@uclouvain.be

ABSTRACT

In July 2021, an intense precipitation event has hit Belgium severely. While most of the damages occurred in the Eastern part of Belgium along the Vesdre valley, other catchments also endured severe floods. This is the case for the municipality of Aiseau-Presles located in the Biesme catchment, a tributary of the Sambre River, illustrated in Fig. 1.

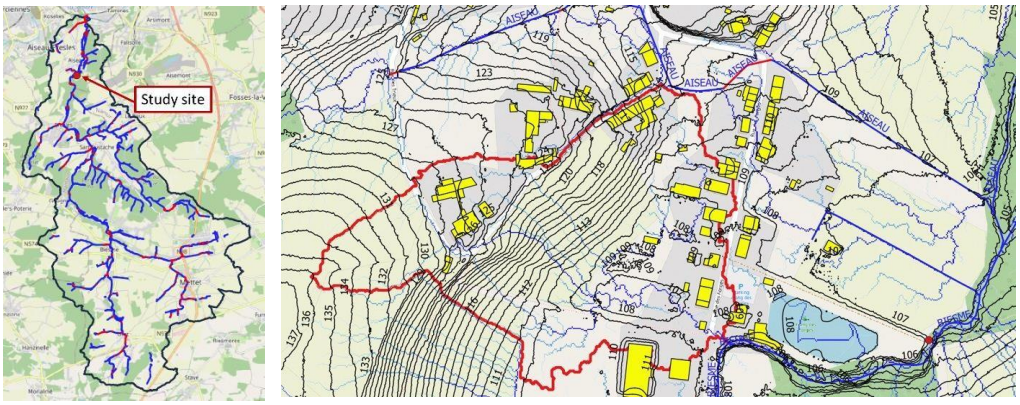



**Fig. 1.** Left: Biesme catchment and location of study sites where the main flooding occurred; Right: zoom on the study area

As can be seen in Fig. 1, the subcatchment relative to the study site (51 840 m²) presents a local steep slope and a series of houses are located close to the Biesme River. During the July 2021 event, water depths up to 2 m were observed around the houses located along the Rue Lambot. The question raised by the municipality concerned the causes of these inundations: were these mainly due to excessive runoff along the steep slopes or to overflowing of the Biesme river?

## 1. Hydrological modelling

A gauging station is available in the Biesme river close to the study area, and this was used to calibrate a hydrological model based on the Athys software (http://www.athys-soft.org/). The results are presented in Fig. 2, where a very good agreement can be observed. A model was then established for the study area subcatchment, to evaluate the possible contribution of runoff to the total discharge. Results show this contribution is negligible, which was confirmed by simulation results performed using HEC-RAS that showed that runoff in the area could only be responsible for water depth about 10 cm with peak discharge and volume that can be evacuated by the existing sewer network after of some adaptations.

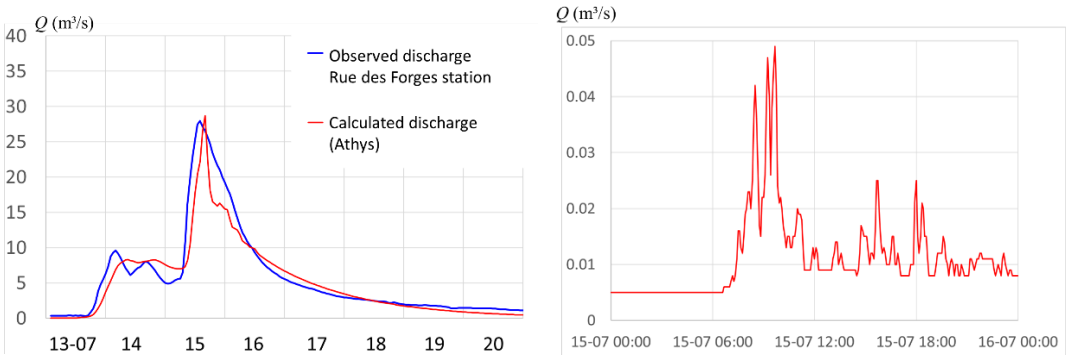



**Fig. 1.** Left: Comparison between observed and calculated discharge at the Aiseau station;
Right: Runoff hydrograph relative to the study area

## 2. Hydraulic modelling

A hydraulic model of the study area including the Biesme River was established using the Watlab (https://sites.uclouvain.be/hydraulics-group/watlab/) software developed at UCLouvain and verified using a combined hydrological and hydraulic modelling using HEC-RAS. As illustrated in Fig. 3, these simulations showed that the main cause of the inundation was overflowing of the Biesme river starting at the southern end of the Rue des Forges. The calculated water depths are in good agreement with the field observations.

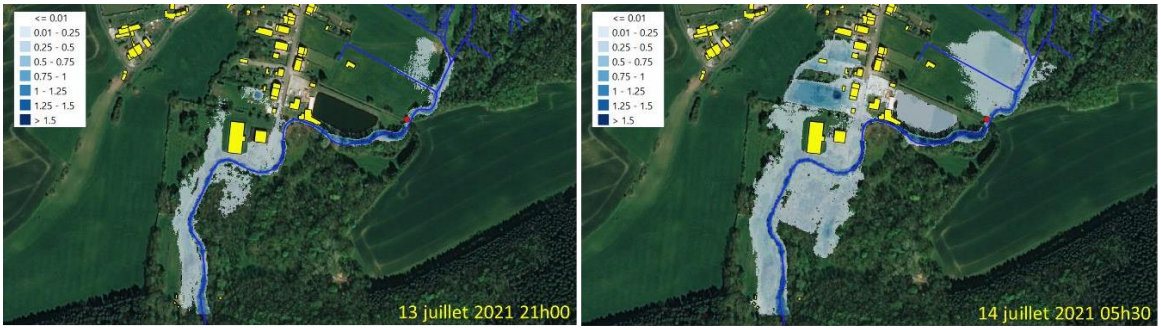



**Fig. 3.** Progressive inundation of the study area by overflowing of the Biesme river

## 3. Conclusions

The simulations allowed to determine that overflowing was the main cause of inundation, and to identify a series of sills in the Biesme river that cause the increase of the water level at the origin of the inundations. Discussions are ongoing with the municipality to find the best possible solutions, i.e. either removing some of the sills or building a small dike along the river.

**Acknowledgements**

The authors wish to thank IGRETEC and especially Sylvie Van Goethem, as well as the municipality of Aiseau-Presles for providing the data.

**References**

Bouvier, C., Delclaux, F. (1996): ATHYS: A Hydrological environment for spatial modelling and complig with a GIS. Proceedings of the HydroGIS 96, Vienna, Austria, pp. 19-28. AIHS publication no 235.

# Performance of Water Delivery by Direct Pumping System at Farm Level: Case Study of Abu-Gabal Tertiary Canal, Egypt

Shimaa MELEHA[1], Ahmed ALY [2], Ahmed EL-ANSARY [1], Mohamed SOLIMAN [1, 3]

[1] Irrigation Engineering and Hydraulics Department, Faculty of Engineering, Alexandria University, Egypt
shomeleha@yahoo.com
elansaryezzat@yahoo.com
m.soliman@bau.edu.lb

[2] Water Management Research Institute, National Water Research Centre, Egypt
email: dr.ahmedmohsenaly@gmail.com

[3] Civil and Environmental Department, Faculty of Engineering, Beirut Arab University, Lebanon

ABSTRACT

The Ministry of Water Resources and Irrigation (MWRI) initiated a national program to improve the existing irrigation system of agricultural lands in the Nile River Delta during the past five decades. The program implemented series of interventions in irrigation delivery system. Eventually, electric pumps are used to directly supply irrigation water (direct pumping system) instead of using an open stand tank. The main objective of this paper is to evaluate the direct pumping system for irrigation improvement project in El-Baslaqoun command area, Abu-Gabal Tertiary Canal (at farm level canal), as a model example in Kafr El-Dawar area, Egypt. The results of water delivery performance reveal that efficiency, equity, and dependability were evaluated as "poor" according to the performance standards. Using MATLAB code, different scenarios were explored to improve water delivery performance. It is found that when the riser diameter mostly modified to be four inches for all valves, the system does not only deliver the adequate amount of water required to crops without excess flow but also gives a fair share of water among farmers.

## 1. Introduction

Since 1970's, MWRI launched many programs to improve the irrigation water efficiency such as Egypt Water Use and Management Project (EWUP) and the Regional Irrigation Improvement Program (RIIP) in 1989. Then a series of irrigation improvement projects were achieved; the first phase of the irrigation improvement project (IIP1) implemented from 1996 to 2007 and the second phase of irrigation improvement project IIP from 2007 to 2009. Eventually, the Integrated Irrigation Improvement and Management Project (IIIMP) started in 2009 as a successor of the IIP projects with an integrated improvement package that tackles irrigation and drainage improvement. The project replaces the individual pumps and open stand tank by the direct pumping system that installed at the head of each Tertiary Canal. Teaima et al. (2013) studied the feasibility of using the direct pumping system and concluded that it can be used without any risk where reasonable cost reduction is remarked. However, there is no solid conclusion that evaluates the farmers' practices using the direct pumping system. Therefore, the main objective of this study is to evaluate direct pumping system in El-Baslaqoun command area, as a case study to understand the farmers' practices in their farms. Set of performance indicators proposed by (Molden and Gate., 1990) (adequacy, efficiency, equity, and dependability) are used in this evaluation. Moreover, a mathematical model (MATLAB) is developed for further understanding the hydraulic behavior of the system in order to propose reasonable modifications to the system.

## 2. Materials and Methods

### *2.1. Determination of performance indicators*

Successful irrigation water delivery system is important to achieve the objectives of delivering the accurate amount of water to users who served by the system. Therefore, (Molden and Gate., 1990) were concluded four

effective indices for assessing distribution system performance (Adequacy (PA), efficiency (PF), dependability (PD), and equity (PE). The values of these indicators are classified as "good", "fair", "poor" according to performance standards.

$$PA = \frac{1}{T}\sum_{i=1}^{n} a_i \frac{Q_{Di,t}}{Q_{Ri,t}} \quad (1)$$

$$PF = \frac{1}{T}\sum_{i=1}^{n} a_i \frac{Q_{Ri,t}}{Q_{Di,t}} \quad (2)$$

$$PE = \frac{1}{T}\sum_{t=1}^{T} CV_R\left(\frac{Q_{Di,t}}{Q_{Ri,t}}\right) \quad (3)$$

$$PD = \frac{1}{R}\sum_{i=1}^{n} a_i . CV_T\left(\frac{Q_{Di,t}}{Q_{Ri,t}}\right) \quad (4)$$

where, $Q_{Di,t}$ is the amount of water delivered, and $Q_{Ri,t}$ is the amount of water required in sub-region *i* with area $a_i$ during a certain time (t), while *n* is the number of sub-regions in the irrigation system, T is the time period, as well as *R* is the total irrigated area.

### *2.2. Mathematical modeling*

A mathematical model developed by MATLAB code is used to simulate Abu-Gabal Tertiary Canal shown in Fig.1 (a), as well as, to further investigate the actual hydraulic behavior of the system. All elements of the irrigation network (Tertiary Canal) that applied in this model are described in the form of nodes and reaches. Nodes contain the connection points between marwa and Tertiary Canal while reaches represent each pipeline connecting any two nodes. The model is a successive iterative to solve energy and conservation equations. The model is calibrated by tuning the minor loss coefficient. Fig. 1 (b &c) represent comparison between measured and simulated results (riser flow rate and total head) for different operation cases for Abu-Gabal Tertiary Canal. The coefficient of determination between total head simulated and measured ($R^2$) in the first and second cases is equal to 0.83 and 0.95, respectively.

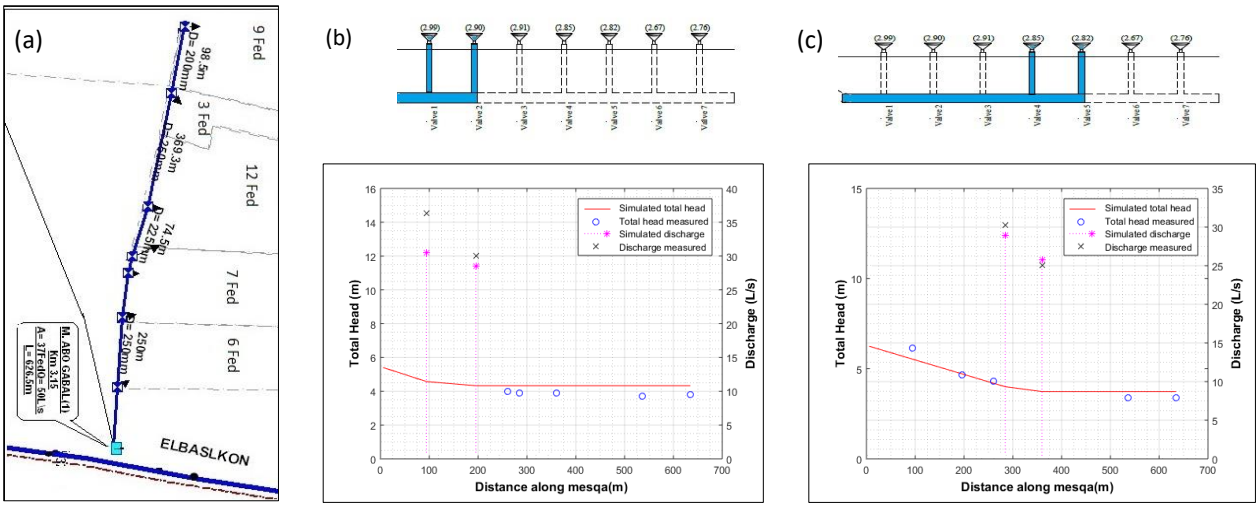



**Fig. 1.** (a) Layout of Abu-Gabal Tertiary Canal, (b) model calibration Case 1 – (valves 1 & 2 opened) and (c) Case 2 – (valves 4 & 5 opened)

## 3. Results and Conclusions

According to performance standards, PA, PF, PE and PD in Abu-Gabal Tertiary Canal are computed to be 0.97, 0.66, 0.31 and 0.4, respectively. All indicators show "poor" performance except PA which shows "good" performance. It is indicated that the amount of water delivered by the system to Tertiary Canals was considered to be enough but above the required amount, which causes a drop of value PF. Moreover, it reveals the randomness and inequality of water distribution of water supply between farmers. The developed mathematical model is used to generate operation scenarios. To achieve high water delivery performance, valves diameter should be mostly modified to be 4 inches for all valves. The expected theoretical water saving by applying this modification ranges from 8-20% per Acres.

**References**

Molden D, Gates G (1990) Performance measures for evaluation of irrigation water delivery system, Journal of Irrigation and Drainage Engineering, 116(6), 804.

Teaima R, Gharib A, and Younes M (2013) Feasibility of direct pumping for irrigation Improvement Project, International Journal of Mechanical Engineering and Technology (IJMET), 4, 494- 511.

# Indicators to Promote Sustainable and Climate Resilient Water Management at Urban Natural Spaces

Maria Adriana CARDOSO[1], João Nuno FERNANDES[2], Ana Estela BARBOSA[3]

[1] National Laboratory for Civil Engineering, Portugal
macardoso@lnec.pt; jnfernandes@lnec.pt; aestela@lnec.pt

ABSTRACT

The Horizon Europe project NATURELAB – *Nature Based Interventions for improving health and well-being* proposes an integrative and innovative approach to contribute to resilient communities with a focus on health and care prevention. The project established a portfolio of key indicators and guidelines to characterize, design, protect and manage different types of nature spaces. The indicators focus on the characteristics of the nature site and its context, comprising not only the variables that can affect health and well-being but also the settings and resources that ensure that people can have comfort, and their basic needs attended to. The indicators will be tested and validated through its application to 15 experimental sites, located in Europe and Peru. The project aims at contributing to the sustainability of the territory and the resilience to extreme events – such as intense precipitation and heat waves.

This study introduces the NATURELAB indicators proposal, aiming to guarantee sustainable and climate-resilient water management in urban natural spaces. These indicators were developed based on prior knowledge, findings from other projects funded by the EU, and tailored to meet specific needs.

## 1. Introduction

Societies have faced unprecedented challenges, above all in cities, where approximately 55% of the global population is gathered. Living in urban areas presents several opportunities, but can lead to some drawbacks, such as a lack of sense of belonging and the absence of attachment to nature. The contact with natural elements in cities allows the acknowledgment of the fact we are not separate from the ecosystems. Exposure to Nature-based Solutions (NbS) also provides other numerous benefits, especially for health, including mental and physical well-being. In this context, NATURELAB – *Nature Based Interventions for improving health and well-being* has an innovative approach to contribute to resilient communities, by enhancing the green and blue areas' benefits, as the resilience to climate change and urban water management. Therefore, the project directly attends the UN SDG 3, SDG 6, SDG 11 and SDG 13. In its research, NATURELAB established indicators designed to ensure sustainable and climate-resilient water management in urban natural spaces. This portfolio will be validated through application to 15 Sites in Portugal, Greece, The Netherlands, Germany, and Peru.

## 2. NbS supporting water sustainability and urban resilience under climate change

NbS are emerging as sustainable solutions that contribute to urban resilience and to the maintenance, enhancement, and restoration of biodiversity and ecosystems, while addressing societal challenges and promoting sustainable and resilient urbanization (Beceiro et al., 2020; Wendling et al., 2018). Blue green infrastructure, which is part of the urban water infrastructure, has a potential value for climate change mitigation and adaptation. Additionally, this type of infrastructure plays a key role in enhancing circularity, optimising the water-energy-materials nexus (Fu and Butler, 2021). There are many co-benefits provided by urban green spaces in addition to improved public health, when good planning, design and management is assured (Ward Thompson and Silveirinha de Oliveira, 2016). NbS had gained visibility in urban planning and development, with several European cities incorporating green infrastructure, such as parks, green roofs, and urban forests, into their strategies to address urban challenges like heat island effects and air pollution. Taking into account this importance, several regulations and policies were developed by the EU or with its support. Multiple benefits for society, the economy, the environment, and human well-being are brought by NbS. As

with consideration of any health outcomes associated with an environmental exposure, how the exposure is measured is important in determining what relationships are apparent, and what causal pathways and mechanisms can be inferred (Nieuwenhuijsen et al., 2015). Studies of green space and health to date have used a variety of measures and indicators.

## 3. Guidelines to support urban NbS contribution towards water and communities' sustainability

The attributes of green spaces play a crucial role in determining the potential for human activities and reflect the sustainability of water usage and management. The NATURELAB project considers the following steps towards the evaluation of the urban natural spaces: (i) Characterization of the context and activities to be carried out; (ii) Characterization of the water availability and needs; iii) Definition of the system to assess water sustainability, based on indicators; (iv) Development of a diagnosis and sustainability targets definition; (v) Identification and characterization of the measures to be implemented. The proposal of indicators to promote sustainable and climate resilient water management at urban natural spaces is presented in Table 1.

**Table 1.** Indicators to promote sustainable and climate resilient water management

| Indicator | Description | Metrics and ease of determination | Recommendation |
|---|---|---|---|
| Water sources available | Water availability in the site | Which types of water supply sources exist? | Explore lakes, rivers, abundant nature, serene water |
| Impervious area | Surface imperviousness | Percentage of impervious area (%) | Minimize concrete, prioritize green spaces; foster biodiversity, preserve natural drainage. |
| Water needs | Water related facilities availability and needs | Water supply needs (total, toilet equipment, water supply points, irrigation, washing) | Assess water needs; enhance facilities for conservation and access |
| Physical access to water supply | See Silva et al. (2023) | N. of operational physical access points to water supply in the area | Ensure easy access; promote safety around water bodies |
| Wastewater disposal | See Cardoso et al. (2020) | Wastewater disposal exists and is adequately used? | Monitor, maintain wastewater systems for environmental and public health |
| Stormwater management | | Solutions for stormwater management are adequately used? | Invest in green infrastructure; mitigate floods, protect ecosystems. |
| Drinking water consumption | B-WaterSmart Silva et al. (2023) | Water supply consumption | Promote conservation; ensure safe, sustainable drinking water practices. |
| Drinking water in non-potable uses | See Cardoso et al. (2020) and Silva et al. (2023) | Is drinking water being significantly used for non-potable uses? | Implement greywater systems; optimize non-potable water usage wisely. |
| Water use from alternative sources | | Is being used for non-potable uses? | Explore diverse sources; reduce reliance, ensure sustainable water use. |
| Redundancy in Water supply sources | See Cardoso et al. (2020) | Which types of water supply sources are being used? | Establish backup sources; ensure resilience for water supply. |
| Redundancy in stormwater storage capacity | | Is there a volume to store rainwater or stormwater? | Increase storage capacity; bolster resilience against fluctuating precipitation levels. |
| Risk of Water supply interruption | | Water supply interruptions occurrence | Assess risks, diversify sources, ensure contingency plans for interruptions. |
| Risk of Flooding | | Flooding incidents | Implement floodplain management; safeguard areas prone to inundation |
| Risk of Wastewater discharges | | Wastewater discharges to ecosystem services | Monitor, regulate wastewater discharge; protect ecosystems from harmful contaminants |
| Risk of Water quality compliance | | Is the water quality compliant with the legal requirements for its use? | Ensure standards met; monitor, maintain water quality for environmental health. |

**Acknowledgements**

This project has received funding from the European Union's Horizon Europe Research and Innovation Programme under Grant Agreement number 101083857 and co-funded by the UK Research and Innovation Grant Award No. 10067111.

**References**

Beceiro, P., Brito, R. S., & Galvão, A. (2020). The Contribution of NBS to Urban Resilience in Stormwater Management and Control: A Framework with Stakeholder Validation. Sustainability, 12(6), 2537. https://doi.org/10.3390/su12062537

Cardoso, M. A., Brito, R. S., Pereira, C., Gonzalez, A., Stevens, J. R., & Telhado, M. J. (2020). RAF Resilience Assessment Framework—A tool to support cities' action planning. Sustainability, 12(6), 2349. https://doi.org/10.3390/su12062349

Fu, G., & Butler, D. (2021). Pathways towards sustainable and resilient urban water systems. In IWA Publishing eBooks (pp. 3–24).

Nieuwenhuijsen, M., Donaire-González, D., Rivas, I., De Castro, M., Cirach, M., Hoek, G., Seto, E., Jerrett, M., & Sunyer, J. (2015). Variability in and Agreement between Modeled and Personal Continuously Measured Black Carbon Levels Using Novel Smartphone and Sensor Technologies. Environmental Science & Technology, 49(5), 2977–2982. https://doi.org/10.1021/es505362x

Silva, C., Cardoso, M. A., Rosa, M. J., Alegre, H., Ugarelli, R., Bosco, C., Raspati, G., Azrague, K., Bruaset, S., Damman, S., Koop, S., Muranetto, S., Conceição, M. M. S., Gomes, C. M., Rosell, L. F., Schmuck, A., Strehl, C., & Doss, P. M. (2023). D6.3 Final version of the water-smartness assessment framework (V2). EU B-WaterSmart project.

Ward Thompson, C. & Silveirinha de Oliveira, E.M. (2016). Evidence on health benefits of urban green spaces. in A Egorov, P Mudu, M Braubach & M Martuzzi (eds), Urban Green Spaces and Health: A Review of Evidence. WHO, Copenhagen, pp. 3-20

Wendling, L., Huovila, A., Castell-Rüdenhausen, M. Z., Hukkalainen, M., & Airaksinen, M. (2018). Benchmarking Nature-Based Solution and Smart City assessment schemes against the Sustainable Development Goal Indicator Framework. Frontiers in Environmental Science, 6. https://doi.org/10.3389/fenvs.2018.00069

# Water Demand and Usage Trends among Group Water Schemes: Implication for Water Conservation.

Sarpong Hammond ANTWI[1], David GETTY[1], Alec ROLSTON[2] , Suzanne LINNANE[1] , Róisín Dowd SMITH[3]

[1] Centre for Freshwater and Environmental Studies, Dundalk Institute of Technology, Dundalk, Co. Louth A91K584, Republic of Ireland.
Hammond.sarpong@dkit.ie
David.Getty@dkit.ie
Suzanne.Linnane@dkit.ie
[2] Goyder Institute for Water Research, SA 5005, Adelaide, South Australia.
director@goyderinstitute.org
[3] National Federation of Group Water Schemes, 24 Old Cross Square, Co. Monaghan, H18NX30 Republic of Ireland.
roisin@nfgws.ie

ABSTRACT

Over the past two decades, the Group Water Scheme (GWS) sector in the Republic of Ireland has undergone significant changes by moving beyond providing water access and equity to rural consumers to become a leading example of best practices in drinking water provision. This transformation has been achieved through a range of policies and measures to address water leakages, water quality and demand, and conservation; however, the scale of this reduction and its implications on the sector have not yet been adequately assessed. This study uses a structured online survey questionnaire to examine the impact of water conservation initiatives implemented by GWS and underscores the critical role of accurate data collection and the need for GWS to adopt long-term initiatives to enhance water quality and access.

## 1. Introduction

The Group Water Scheme (GWS) sector in the Republic of Ireland (RoI) has significantly improved water availability and equity for rural consumers over the past seven decades, despite challenges such as E.*coli* contamination and faecal coliform contamination (EPA, 2022), which impacts water quality. These issues are exacerbated by poor regulatory compliance, leaks in distribution mains and consumer connections, and high nitrogen and phosphorus concentrations from agricultural activities (Bresnihan et al., 2021). Various strategies have been implemented, including expanding the water supply network, repairing aging pipes and universal water meters, and promoting water conservation measures. While these initiatives have reduced water demand over the past two decades, the full extent of this improvement remains unclear due to varying success among the schemes. More so, few studies (see, e.g., Bresnihan et al., 2021; Deane & MacDomhnaill, 2021; Rolston & Linnane, 2020) have evaluated the significant contributions of GWS to water policy and management in the RoI.

## 2. Methodology

The study used a survey questionnaire to solicit data from 102 GWS representatives in RoI on water demand and usage from 2008 to 2020 to draw inferences on consumption trends. Unaccounted-for Water (UFW) rates were also calculated from schemes' water demand and usage records using the equation below:

$$\text{UFW} = (SUM(MR - MU). \text{ UFW Rate} = \frac{SUM(MR-MU)}{MR} \times 100.$$

*Where MR = Meter Reading and MU = Meter Usage*

Various reports on the National Federation of Group Water Schemes (NFGWS) legislation and policies, newsletters and reports from GWS, scientific publications, and key governmental reports were also reviewed.

*2.1 Water demand and usage trend*

A total of 102 respondents reported improvements in their daily water demand. Comparing 2018 to 2019, 30% saw a decrease, 53% reported similar levels, and 17% experienced an increase. In 2019, average daily water demand ranged from 5.1m³ to 1000m³, with only seven schemes exceeding 1000m³. An earlier study by Rolston & Linnane (2020) found that most GWS supply less than 1500m³ daily, consistent with our findings. Although the variation in daily water demand among GWS aligns with the national average (148 to 368 litres per person), some schemes have reduced their demand while others have seen increases (CSO, 2020). These variations are due to conservation measures, meter installations, leakage detection from 2008 to 2020, and late monitoring and recording. Ballingate Water Scheme only began collecting water readings in 2018, and usage was recorded in 2016, while Ballinabranana (Co. Carlow) maintained up-to-date records from 2018 to 2020 (Fig 1).

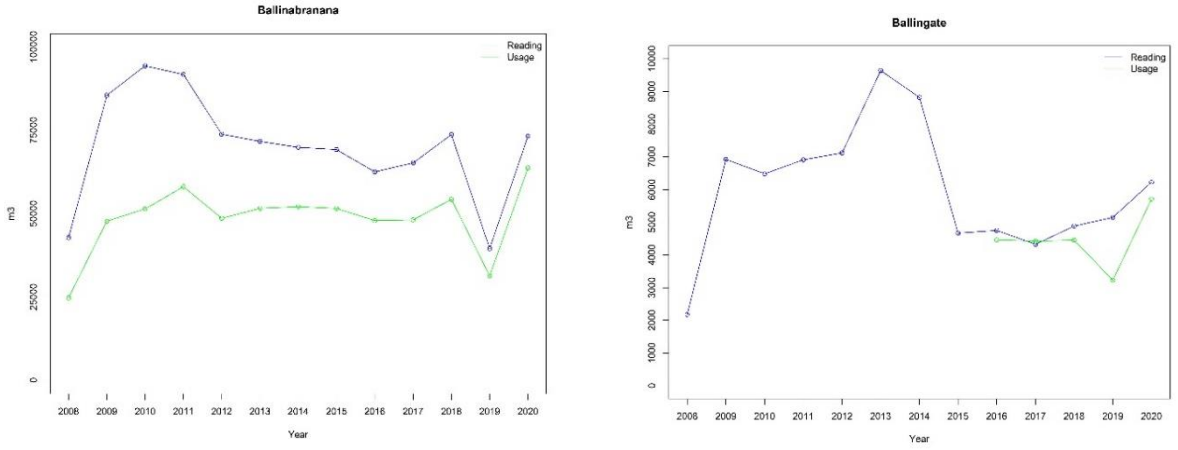



Fig. 1. Yearly water demand and usage trend

## 3. Conclusion and recommendations

In the past two decades, the GWS sector in the RoI has evolved from merely ensuring water availability and equity for rural consumers to becoming a model for best practices in drinking water provision. Through various policies and measures, the sector has addressed water leakages, improved water demand and quality, and enhanced conservation efforts. Survey responses and secondary data from various GWS indicate the significant progress made by the NFGWS to ensure that schemes fulfill their roles in protecting water sources and delivering clean drinking water. Despite this progress, recording meter readings and usage gaps remain a challenge. This study recommends training and ongoing engagement to help scheme representatives record and input data in standardized formats approved by the NFGWS, improving data clarity over time. Enhanced communication between the NFGWS, scheme representatives, and consumers should leverage modern methods such as social media, regular online updates, webinars, and collaborations with local community groups alongside traditional channels like emails and physical meetings. With growing water connection demands, increasing capacity within scheme networks should be part of rural development plans and infrastructure repairs. Schemes serving more than 50 people, as stipulated in the Drinking Water Regulations (Statutory Instrument No 439 of 2000), could be encouraged to merge or restructure to ensure proper data collection, water quality, and regulatory compliance.

## References

Antwi, S. H., Linnane, S., Getty, D., & Rolston, A. (2021). River Basin Management Planning in the Republic of Ireland: Past, Present and the Future. Water 2021, https://doi.org/10.3390/W13152074

Bresnihan, P., Hesse, A., & Merricks White, J. (2021). Learning from Group Water Schemes: Community Infrastructures for Sustainable Development. https://www.epa.ie/publications/research/water/Research_Report_364.pdf.

CSO. (2020). Domestic Metered Public Water Consumption 2018. https://www.cso.ie/en/releasesandpublications/er/dmwc/domesticmeteredpublicwaterconsumption2018/

Deane, B., & MacDomhnaill, B. (2021). The Alliance of Community-Owned Water Services in Europe: Opportunities and Challenges Based on the Irish Perspective. https://doi.org/10.3390/W13223181

EPA. (2022). Drinking Water Quality in Private Group Schemes and Small Private Supplies in 2020. https://www.epa.ie/publications/compliance--enforcement/drinking-water/annual-drinking-water-reports/DWQinPrivateGroupWaterSupplies-2022-02-21.pdf

Rolston, A., & Linnane, S. (2020). Drinking Water Source Protection for Surface Water Abstractions: An Overview of the Group Water Scheme Sector in the Republic of Ireland. https://doi.org/10.3390/W12092437

# How Can We Adapt Together? Bridging Water Management and City Planning Approaches to Climate Change

Vítor VINAGRE[1], Teresa FIDÉLIS[2], Ana LUÍS[3]

[1] Department of Environment and Planning, Campus de Santiago, University of Aveiro, 3810-193 Aveiro, Portugal
vcvinagre@ua.pt

[2] Research Unit on Governance, Competitiveness and Public Policies (GOVCOPP), Department of Environment and Planning, Campus de Santiago, University of Aveiro, 3810-193 Aveiro, Portugal
teresafidelis@ua.pt

[3]AdP Valor, Rua Visconde de Seabra, 3, 1700-421 Lisboa, Portugal
analuis@adp.pt

## 1. Introduction

The global trend of urbanization is progressing rapidly. Between 1950 and 2020, the urban population surged from 0.8 billion (29.6%) to 4.4 billion (56.2%), and projections indicate it could further climb to 6.7 billion (68.4%) by 2050.

Simultaneously, urban areas are experiencing observable impacts of climate change on human health, livelihoods, and critical infrastructure systems. These systems become increasingly vulnerable if their design does not account for evolving climate conditions. Managing water resources, crucial for human life, economic activities, and ecosystem functioning, faces significant challenges in a changing climate, given the uneven distribution of water availability across territory and time. Frequent extreme hydrological events, such as prolonged droughts and floods, create substantial uncertainty regarding cities' water security.

While numerous studies have addressed various aspects of the relationship between climate change, spatial planning, and the water cycle in recent years, there appears to be a gap in research that identifies, catalogues, and integrates consolidated expertise in these fields. Specifically, this study aims to explore the key factors contextualizing cities' adaptation to climate change, emphasizing the symbiotic relationship between the urban water cycle and urban planning.

## 2. Methodology

We opted for a systematic literature review to comprehensively identify, analyze, and interpret all available research in this domain. Following the Preferred Reporting Items for Systematic Review and Meta-Analysis (PRISMA) guidelines ensured the review process's reproducibility, traceability, and transparency. In total, 79 articles were taken into consideration.

## 3. Results and discussion

After considering the selected articles, they were categorized and systematized, revealing that literature addresses these challenges across various vectors: operational, organizational, institutional, behavioral, economic, technological, and urban planning, as illustrated in Figure 1.

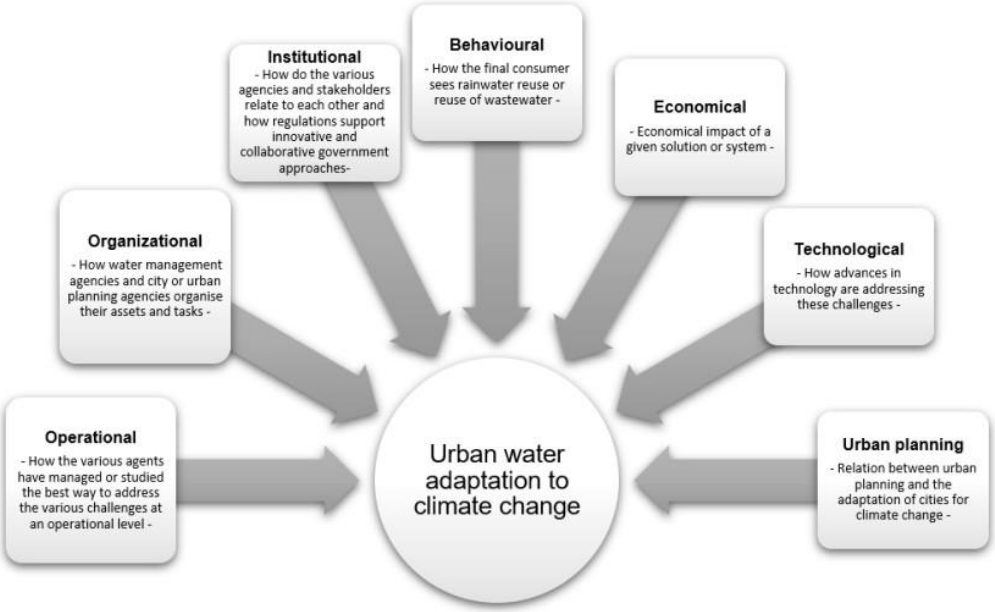



Figure 1 - Main vectors contributing to the urban water management adaptation to climate change (Vinagre et al., 2023)

Bearing in mind the dispersion of scientific communications and the diverse approaches presented, one initial conclusion is that the most significant innovations or the need for innovation primarily lie in organizational and economic aspects and in the relationships among various stakeholders, citizens/consumers. The emphasis is not so much on technological development, as the primary drivers for change stem from the shift in paradigm from centralized to decentralized systems and how to collaboratively manage them with other stakeholders, including territorial management entities.

While literature trends towards responding to climate change through decentralized systems, some of the most successful examples of adapting to climate change in the water supply sector, especially regarding water reuse, are found in the implementation of concepts from centralized systems. Notable instances include Singapore, Israel, and Southern California in the US.

It is evident that the planning of water infrastructures tends to be subordinate dweller to the planning of the territory, in a way that, in addition to being technically challenging, has also demonstrated other types of problems. The need to adapt to a changing climate will necessarily bring the disciplines of spatial planning and urban water supply management together.

## 4. Conclusions

The findings emphasize the importance of conducting technical and economic assessments for the comprehensive concept of sustainable urban water management (SUWM) systems. This involves integrating values beyond financial considerations. It highlights the necessity to tackle water scarcity not only from the supply side but also from a demand perspective. Additionally, there is a need to strengthen the connection between emerging water sources, like reuse, and city planning in the context of climate change. However, the current lack of attention to collaboration strategies remains a significant challenge. The insights and gaps identified in the analysis point towards new avenues for research and practical application in the field.

**Acknowledgements**

The authors are grateful to Águas de Portugal Group and the University of Aveiro for supporting this research.

**References**

Vinagre, V.; Fidélis, T.; Luís, A. How Can We Adapt Together? Bridging Water Management and City Planning Approaches to Climate Change. Water 2023, 15, 715. https:// doi.org/10.3390/w15040715

# Impact of implementation of efficiency targets in public water supply

Esther DÍAZ-CANO[1], Julio BERBEL[2], Antonio R. HURTADO[3]
[1,2,3] WEARE- Water, Environmental and Agricultural Resources Economics Research Group,
Universidad de Córdoba (Spain)
[1]edcano@uco.es;[2]berbel@uco.es; [3]es2rohuc@uco.es

ABSTRACT

This study investigates the establishment and impact of efficiency targets in the municipal water supply sector, emphasizing the importance of minimizing water losses for urban water resource management. Using energy consumption as an indicator, it illustrates the potential impact of reducing water leakage on various negative factors. The examination relies on a simple model demonstrating how minimizing losses affects energy consumption. With the EU's current average distribution losses at around 23%, and the proposed leakage targets for public water supply by January 2028, the paper explores the effect of reducing EU leakage to a possible target of 15%. The study suggests a synergistic approach, combining loss reduction with decreased final consumption, and concludes by highlighting the policy significance of minimizing distribution losses and proposing target levels.

## 1. The policy of efficiency targets setting in water sector

Performance targets are a common feature in the European environmental policy framework, illustrated by initiatives such as the Farm2Fork target aiming to reduce EU-level fertilizer use by 25% by 2030. Within the water sector, the EU Urban Wastewater Treatment Directive establishes varying deadlines based on population size (European Union, 1991). This research specifically concentrates on the decision-making process regarding the leakage threshold set forth in the recast Drinking Water Directive (DWD-Dir. EU 2020/2184), scheduled for January 2028 stating, “leakage reduction is performed using the infrastructural leakage index (ILI) rating method or another appropriate method” (European Union, 2020). The use of a common methodology in the EU to report leakage is critical as apparent losses refer to metering billing or unauthorized consumption, while real losses are physical losses in the distribution system. In this paper we will focus on real losses.

## 2. State of the art of efficiency targets in municipal water supply sector

There are large variations in how much freshwater different EU Member States abstract for public supply, from Greece (179 m³/person/year) to Malta (31 m³/person/year). EU public supply leakage is estimated to be an average of 23% at EU27, with many countries over 30% (EUREAU, 2021).

Some EU member states and regions combat water leakage through policy measures, including a) Direct Limitation with Specific Targets: Luxembourg, Denmark, and regions like Galicia (Spain) set specific leakage reduction targets including penalties at national or regional levels; b) United Kingdom (OFWAT) and Portugal (ERSAR) use national regulatory frameworks to incentivize water companies to achieve water loss targets; c) France incorporates water leakage into a performance index, determining penalties and incentives to encourage efficient management and finally, d) subsidies leakage targets (Italy).

The impact of such regulations might be seen in the case of Denmark where water losses are estimated at 7.8% on average, as since 1994, water firms with distribution losses higher than 10% must pay a penalty fee. Bjørner (2021) analyses the evolution of water leakage showing that the price cap introduced year 2011 has not affected to leakage performance in Denmark.

## 3. Impact of leakage targets in municipal water supply sector

### *3.1. Social and environmental impact of distribution water losses*

Urban water losses can lead to adverse environmental effects, including: a) Over-extraction of water, where the conservation of saved water can enhance quantitative conditions and bolster resilience against drought; b) Increased energy consumption, as water losses like leaks or distribution system inefficiencies contribute to higher overall energy usage; c) Depletion of resources and water pollution due to the use of chemicals for water treatment; d) Economic costs incurred when losses surpass the Economic Level of Leakage (ELL). These detrimental impacts validate the policy importance of establishing specific targets.

### *3.2. Estimation of impact of reducing water efficiency (leakage)*

Addressing losses has the potential to mitigate the previously mentioned interconnected negative impacts, leading to reductions in energy consumption, chemical usage, and water extraction. We will use energy consumption as an indicator of the environmental benefits associated with loss reduction. The current EU public water supply scenario shows average distribution losses of 23% and energy usage for water supply at 0.50 kWh/m$^3$ (Eureau, 2021). Figure 1 illustrates the energy needed per person served, demonstrating a decline as water leakages decrease. The figure depicts the energy variation to supply final volumes of 80, 100, or 120 L/p·day at different levels of leakage reduction aligning with most Member States statistical use (EUROSTAT).

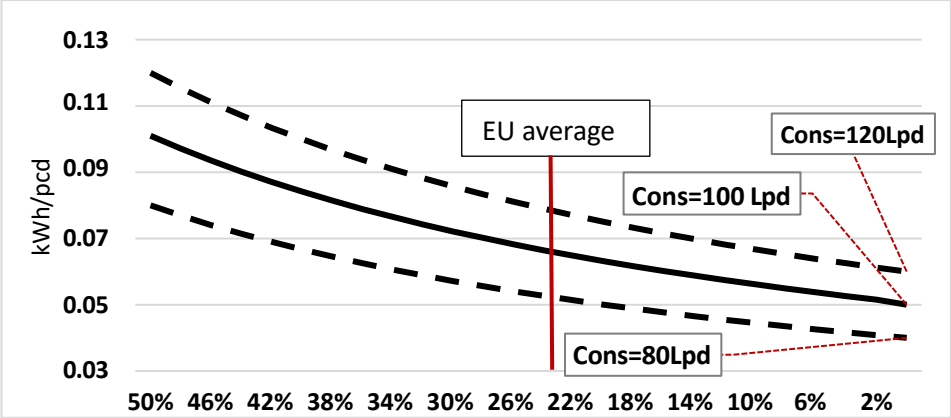



**Fig. 1.** Estimated impact of water efficiency (leakage) on per capita energy consumption in public water supply. Current leakage losses (23%) and energy use (0.50 kWh/m$^3$) from EUREAU, 2021. Own elaboration.

As depicted in Fig. 1, lowering water losses from the EU average decreases per capita energy consumption. Another viable and mutually beneficial strategy involves reducing final consumption, such as transitioning from the 100 L/p·d to the 80 L/p·d curve. The reduction of losses and the reduction of final consumption are complementary and synergistic, forming a foundation for future policies in public water supply.

## 4. Conclusions and future actions

The existing level of distribution losses in the EU, standing at 23%, poses avoidable environmental consequences. Minimizing these losses holds significance for climate change adaptation by preserving non-abstracted water for future droughts and enhancing the quantitative condition of water bodies. Furthermore, the reduction of losses is intricately connected to energy and chemical consumptions, contributing to climate change mitigation. Consequently, utilities are encouraged to adopt a target for reasonable distribution losses, such as 10% (the current legal level in DK) or 15% (proposed by some regions as an economically achievable goal). Regardless, the task of reducing losses is anticipated to be a key component of the policy agenda in the upcoming years, and the consensus regarding a common index such as ILI (Lambert, 2002) maybe convenient.

**Acknowledgements**

The authors acknowledge the financing received under the projects PRIMA-BONEX (Grant Number 2141) GOVAQUA project (HE-CL6-GOV-2022-RIA-101086578) and CYCIT (PID2019-107127RB-I00 BHYEM):

**References**

Bjørner, T. B., Hansen, J. V., & Jakobsen, A. F. (2021). Price cap regulation and water quality. Journal of Regulatory Economics, 60(2-3), 95-116.
EUREAU (2021) Europe's Water in Figures. An Overview of the European Drinking Water and Wastewater Sector. Edition 2021. July 2021.
European Union (1991) Council Directive 91/271/EEC of 21 May 1991 concerning urban waste-water treatment.
European Union (2020) Directive (EU) 2020/2184 of the European Parliament and of the Council of 16 December 2020 on the quality of water intended for human consumption (recast).
Lambert, A. O. & McKenzie, R. D. (2002, November). Practical experience in using the Infrastructure Leakage Index. In Proceedings of IWA Conference–Leakage Management: A Practical Approach. Lemesos, Cyprus.

# Impacts of the implementation of efficiency targets at river basin scale

Esther DÍAZ-CANO[2], Julio BERBEL[1], Alfonso EXPOSITO[3]
[1,2,3] WEARE- Water, Environmental and Agricultural Resources Economics Research Group,
[1,2] Universidad de Córdoba and [3] Universidad de Málaga (Spain)
[1]edcano@uco.es;[2]berbel@uco.es;[3]aexposito@uma.es

ABSTRACT

The purpose of this study is to assess the impacts derived from the application of EU-wide water efficiency targets at river basin scale. Specifically, it aims to determine their potential in achieving the objectives outlined in the Water Framework Directive (WFD) and addressing issues related to water scarcity and resilience to the impacts of climate change. The EU Blueprint for Water suggests the development of basin-specific efficiency targets by river basin authorities, emphasizing the importance of considering the broader impacts of individual measures at the river basin level in addition to sector-specific targets. The analysis leads to the conclusion that the impact of basin efficiency targets on reducing basin-wide water consumption is uncertain. Water managers can benefit from concentrating their efforts on attaining WFD objectives at specific water bodies to regulate excessive local water consumption. This perspective aligns with establishing efficiency goals in key sectors, including agriculture, industry, and urban water usage.

## 1.- The policy of water efficiency targets at basin level

The EU Blueprint for Water suggests the development of basin-specific efficiency targets by river basin authorities, emphasizing the importance of considering the broader impact of individual measures at the river basin level, in addition to sector-specific targets. Recently the revised Drinking Water Directive (Dir. EU 2020/2184) proposed to define efficiency targets (i.e., leakage reduction) for public water supply services as an example of sector target.

## 2.- Water efficiency at basin level

### *2.1.- Feasibility and constraints of water efficiency targets at basin level*

The cascading water use in river basins is one of the main constraints for the setting and practical implementation of water efficiency targets at the basin level. Usually, in river basins, the return flows from upstream water users (back to the river basin, lake or groundwater body e.g., due to water infiltration) are used as an input resource for downstream users. In consequence, a river basin system often has a different water use efficiency than its individual components, and low efficiencies in upstream areas ensure water flows in downstream water bodies. Figure 1 shows a hypothetical cascade use in a basin with various users with low efficiency (50% of withdrawal are not consumed and returned to the basin), but the overall basin efficiency achieves 87.5% as a consequence of the cumulative reuse of return flows by downstream users.

### *2.2-Wastewater reuse*

Another relevant issue regarding water basin-wide efficiency is wastewater reuse. In 2020, the EU 2020/741 wastewater reuse regulation entered into force. The new rules apply from 26 June 2023 and are expected to encourage and facilitate water reuse in the EU. Nevertheless, the wastewater reuse in a stressed basin is only positive in terms of alleviating water stress and improving water body status if return flows are not required by downstream users. Therefore, this non-conventional resource needs to be considered within the integrated water resources management.

### *2.3.- Estimation of impact of increasing individual user efficiency*

Figure 1 illustrates a hypothetical case when all three agents improve efficiency individually from IE=0.5 to IE=0.8. If the consumed fraction is unchanged, the basin overall efficiency increases from 0.875 up to 0.966.

The impacts on the environment will be: a) real water savings will account for 11.25 units (e.g., $Hm^3$), which remains in the source (e.g., reservoir, aquifer) to be allocated to environmental uses or to be reserved for drought prevention; b) we can assume with a certain level of uncertainty that return flows will export fewer chemicals and salts from agents (some authors have measured 80% reduction after the modernization of irrigation schemes, though additional research is required); c) The system requires unused water (not affected by diffuse pollution) to be abstracted to complement the former return flows so that downstream users are not negatively affected; d) The 'real savings' (11.25 units) may be seen as a quantitative improvement of the water bodies (i.e., aquifer, river, reservoir); e) Water consumption (evapotranspiration) does not change by the improvement in efficiency.

Our hypothetical example also illustrates that in a connected river with reused downstream return flows, the basin efficiency can be very high even if individual agents are not very efficient (see previous situation when agents with individual low IE=0.5 lead to an overall basin efficiency of 0.875).

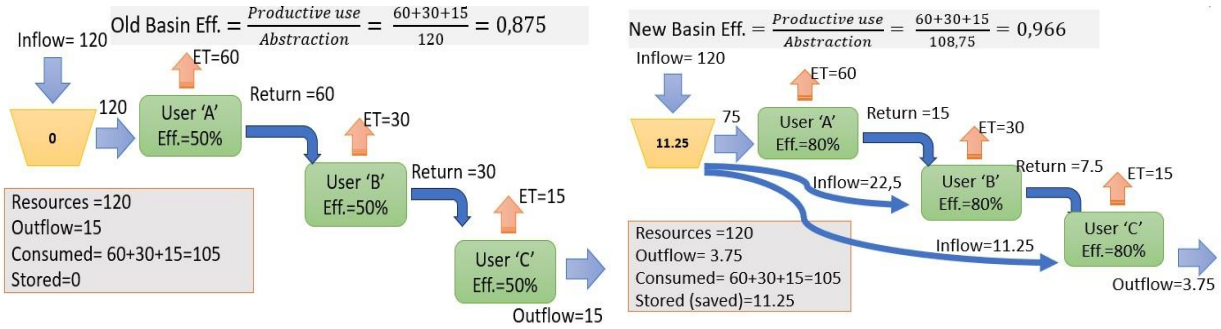



***Fig. 1.*** *Hypothetical case when users improve efficiency (EFF). Old basin Vs New Basin with 'modernization' (improved user efficiency)*

Successful cases of good governance regarding the implementation of irrigation efficiency measures are scarce. An example of bottom-up governance is the investment in water saving irrigation equipment in two adjacent aquifers where self-regulation controls reduced abstraction in one of them but produced increased depletion in the other, thus leading to a rebound effect (Zwickle et al., 2021). As example of 'top-down' approaches, water-stressed basins in southern Spain (e.g., Guadiana, Guadalquivir, Segura) include a norm in the hydrological plans that forces any water-saving investment to be accompanied by a reduction of around 25% in previous water rights and no further augmentation of irrigated areas, thus avoiding the rebound effect (MITECO, 2023). Despite these few examples, uncertainty still remains regarding the impacts assessment of efficiency measures and further research is required regarding the impacts on water quality, water body status and water supply guarantee at the basin level.

## 3.- Conclusions and future actions

The lack of consideration of return flows in the system has driven many examples of rebound effects as farmers either increase irrigated areas or intensify cultivation (more demanding crops or double cropping). Although the presented case is an ultra-simplified version of a basin, it clearly shows the link between individual agents and basin efficiency. Additionally, it illustrates the need for governance ensuring that "water savings" from efficiency gains do not result in reduced return flows.

Our team is currently developing hydro economic models at basin scale (Martínez-Dalmau et al., 2023) where we will test it in a real case study with the aim to identify the pros and cons of setting basin efficiency targets. Further, results will contribute to the discussion on this issue and its potential to inform water policy and improve water management at basin scale. Final version will be ready before congress presentation.

**Acknowledgements**

The authors acknowledge the financing received under the projects PRIMA-BONEX (Grant Number 2141) GOVAQUA project (HE-CL6-GOV-2022-RIA-101086578) and CYCIT (PID2019-107127RB-I00 BHYEM):

**References**

European Commission (2012) A blueprint to safeguard Europe's water resources. Brussels, 14.11. 2012, 2012.
MITECO, Basin Hydrological Plans https://www.miteco.gob.es/es/agua/temas/planificacion-hidrologica/planificacion-hidrologica/planes-cuenca/default.aspx (accessed Feb 2024)
Martínez-Dalmau, J., Gutiérrez-Martín, C., Expósito, A., & Berbel, J. (2023). Analysis of water pricing policy Effects in a Mediterranean Basin through a Hydroeconomic Model. Water Resources Management, 37(4), 1599-1618.
Zwickle, A. et al. (2021) Sustainable irrigation through local collaborative governance: Evidence for a structural fix in Kansas. Environmental Science & Policy, 124(4), 517-526.

# Financing Water Stewardship: Introducing Impact Investments to Address Water Impacts of Food Production Value Chains

Liisa SAIKKONEN[1]; Soile OINONEN[2]; Suvi SOJAMO[3] ; Outi PENTTILÄ[4]; Esther DÍAZ-CANO[5]
[1,2,3,4] SYKE, Finnish Environment Institute, Finland
[1]liisa.saikkonen@syke.fi
[2]soile.m.oinonen@syke.fi
[3]suvi.sojamo@syke.fi
[4]outi.penttila@syke.fi
[5] WEARE- Water, Environmental and Agricultural Resources Economics Research Group, Universidad de Córdoba (Spain)
[5]edcano@uco.es

ABSTRACT

This study delves into the burgeoning field of impact investments, focusing on their potential to mitigate the water-related impacts of production value chains. Given the escalating global concerns regarding water scarcity and the pivotal role of the agricultural sector in water consumption and pollution, the research offers a timely exploration of how impact investments can be harnessed for water stewardship. The study comprises of three primary components: a literature review, an analysis of the barriers and enablers for impact investments in water stewardship, and a living lab focusing on piloting impact investment schemes to fund water stewardship efforts in the Archipelago Sea catchment area in southern Finland.

## 1. Background

Growing populations and economies, changing lifestyles and global climate change are putting increasing pressure on our water resources. Major water using businesses, governments, cities and citizens all recognize the urgent need to work together to ensure the sustainability of this vital resource on which we all depend. Water stewardship - typically referring to sustainable and responsible practices of business - can be defined as the use of water that is socially and culturally equitable, environmentally sustainable and economically beneficial, achieved through a stakeholder-inclusive process that includes both site- and catchment-based actions (AWS, 2023). Some EU Member States have included water stewardship policies, e.g, Spain proposes a 'Water Observatory' that will issue 'water sustainability certifications' as part of the policy implementation (MITECO, 2023) and Finland has set a target for Finnish companies to become responsible water stewards by 2030 (Sojamo et al. 2019), identified water stewardship as a key approach to support sustainable practices along the food chain (Sojamo et al. 2021), and launched an inter-ministerial water stewardship action plan (Finnish Government, 2023).

Impact investments are traditionally defined as financial contributions aimed at generating both measurable social or environmental impacts and financial returns (Clarkin and Cangioni, 2016). However, we propose expanding this definition to encompass donations and payments made without the expectation of direct financial returns. When these contributions fund activities that yield measurable environmental improvements, they effectively serve as investments. These activities not only benefit the broader community but also provide indirect returns to the donor or payer, thus aligning with the core principles of impact investing.

## 2. Literature review

The literature review establishes a foundation by exploring the current scope and scale of impact investments and their historical application in addressing environmental impacts within production value chains. It particularly highlights instances where these investments have successfully contributed to water stewardship initiatives, offering a crucial context for their potential expansion into the realm of food production. The

body of academic literature in the field of impact investing, while historically limited, has seen notable growth in recent years (Singhania and Swami, 2023). In addition to peer reviewed literature, we expand the review to other relevant literature such as publications by OECD, World Bank and The Nature Conservancy.

### 3. Barriers and enablers of implementing impact investment

Based on the literature and their case examples, the study conducts an in-depth assessment of various barriers and enablers that influence the efficacy and adoption of impact investments in water stewardship. This analysis is critical in understanding the complex interplay of economic, institutional, and social factors that either facilitate or hinder the integration of impact investments in this sector.

### 4. Living lab: Archipelago Sea catchment area

The core of the study is the application of these findings to a specific Finnish Living Lab, namely the Archipelago Sea catchment area. It has been identified by HELCOM (Helsinki Commission, Baltic Marine Environment Protection Commission) as one of the agricultural water pollution hotspots in the Baltic Sea area, and the only one still existing in Finland. The objective of the Living Lab is to develop a financing scheme to support water stewardship initiatives. This scheme will enable the implementation of practical and cost-effective water conservation measures along the food production value chains, as identified in the agricultural water protection roadmap for the Living Lab case area (Laurila et al., 2022).

The Living Lab approach allows the consideration of local characteristics, such as institutional context, stakeholder dynamics, and governance structures, shaping the feasibility of impact investing mechanisms. The study identifies and evaluates potential impact investment strategies tailored to the unique environmental and socio-economic contours of this region. These strategies are aimed at enhancing sustainable water use and quality in the food production value chains, aligned with both environmental objectives and economic viability.

### 3. Conclusions and future actions

This research contributes to the evolving discourse on sustainable finance, specifically within the nexus of water management and food production. By providing a detailed, context-sensitive analysis of impact investments tailored to a specific geographical setting, the study offers valuable insights and a general scheme that can be adapted and applied to other regions facing similar challenges. It underscores the potential of innovative financial mechanisms to drive meaningful environmental stewardship while maintaining economic growth and sustainability in the agricultural sector.

This work is part of the Horizon Europe project GOVAQUA, which aims to identify, assess, develop and validate innovative governance instruments and approaches to support and accelerate a transition towards sustainable and equitable water use in Europe. Such a transition is urgently required to reconcile water uses and environmental needs and to reach the aims of the EU WFD, the EU Green Deal and the UN SDGs. With putting innovative approaches into test in altogether six newly established Living Labs in collaboration with key stakeholders, the project aims to come up with good practices with European wide scaling up potential.

**Acknowledgements**

The authors acknowledge the financing received under the projects GOVAQUA project (HE-CL6-GOV-2022-RIA-101086578)

**References**

AWS, Alliance for Water Stewardship (2023) https://a4ws.org/about/ .
Clarkin, J. and Cangioni, C. (2016) Impact Investing: A Primer and Review of the literature. Entrepreunership Research Journal 6(2), 135-173.
Finnish Government (2023) National advancement of water stewardship - Action plan 2023–2025. Ministry of Agriculture and Forestry, Ministry of Econmic Affairs and Employment, Ministry of the Environment, Ministry for Foreign Affairs, Finnish Environment Institute. (in Finnish). Available at: https://julkaisut.valtioneuvosto.fi/bitstream/handle/10024/164955/VN_2023_48.pdf
Laurila, E., Kulmala, A., Luostarinen, S., Keto, A. and Jaakkola, M. (2022) Saaristomeriohjelma – Maatalouden vesiensuojelun tiekartta. Varsinais-Suomen Elinkeino-, liikenne- ja ympäristökeskus.
MITECO (2023) “Proyecto de real decreto por el que se aprueba el reglamento de reutilización de las aguas”. Madrid. Nov 2023
Singhania, M and Swami, D. (2023) Impact Investing: Scientometric review and research agenda. Bus. Ethics Environ. Responsib.
Sojamo, S., Salminen, J., Puharinen, S-T., Belinskij, A., Halonen, M., Heikinheimo, E., Saari, P., Airaksinen, J., Illman, J., Behm, K., Reinikainen, A. & Usva, K. (2021) Water responsible Finland 2030 – best practices, steering methods and stewardship approaches (Waterstewardship2030). Final report (in Finnish). Available at: https://julkaisut.valtioneuvosto.fi/bitstream/handle/10024/163047/VNTEAS_2021_26.pdf
Sojamo, S., Usva, K., Wessman-Jääskeläinen, H. & Hohentahl, C. (2019) Finnish companies the most responsible water stewards in the world – roadmap for 2019–2030. Finnish Ministry of Agriculture and Forestry 2019:18. Available at: https://julkaisut.valtioneuvosto.fi/bitstream/handle/10024/161800/Suomalaisyrityksist%C3%A4%20maailman%20vesivastuullisimmat.pdf?sequence=4.

# The Axarquía (SE Spain) as Living Lab for testing governance innovations aiming at a sustainable management of water resources

Damián SÁNCHEZ-GARCÍA[1] and Suvi SOJAMO[2]

[1] Cetaqua Andalucía, Spain
damian.sanchez@cetaqua.com
[2] Finnish Environment Institute (Syke), Finland
suvi.Sojamo@syke.fi

ABSTRACT

Water governance refers to a series of political, institutional and administrative processes through which administrations and stakeholders articulate their interests, concerns and needs, in order to implement decisions to achieve a sustainable and equitable use of water resources. EU Member States encounter different water difficulties, which comprise water scarcity, hydro-morphological alterations, and diffuse origin contamination. These issues are projected to worsen due to climate change, increasing demands for development, and structural transformations in associated sectors such as agriculture and energy. In this context, innovative instruments regarding water governance can play a key role in accelerating a path to sustainability transition in water management. The objective of this contribution is to present the first stages taken for the setting-up of a Living Lab where two innovative instruments to support and accelerate a transition towards sustainable and equitable water use in Europe will be tested. The Living Lab is located in the Axarquía region (SE Spain), where the scarcity of water resources, cyclic droughts and the existence of two high-demanding water sectors (agriculture and drinking water production) leads to unsustainable water resources management. The two assessed instruments are a water accounting hydroeconomic tool, and a digital tool based on integrated water management and users' participation. This contribution shows the preliminary results achieved in the Axarquía living lab as well as the foreseen next steps.

## 1. Introduction

European Union (EU) Member States face various water challenges, including water scarcity, hydro-morphological pressures, and diffuse source pollution (EEA, 2021). These challenges are expected to be exacerbated by climate change, growing development needs, and structural changes in sectors beyond water such as agriculture and energy. Overuse and depletion of water resources causes ecological debt, threatens livelihoods and weakens the European economy – and must be urgently addressed in view of the systemic transition to a sustainable and equitable water use (EC, 2019).

The GOVAQUA project (funded by the European HORIZON programme) supports and accelerates a transition towards sustainable and equitable water use in Europe by identifying, assessing, developing and validating innovative water governance approaches. These approaches are tested and validated through participatory processes in 6 Living Labs, one of which is located in the Axarquía region (SE Spain).

## 2. Axarquía region

The Axarquía region is located in Eastern Málaga, Western Granada (228,000 inhabitants, SE Spain) (Fig. 1). It faces challenges in water management due to its semi-arid climate and limited water resources. It receives low annual rainfall, making it one of the driest areas in Europe. The scarcity of water poses a significant challenge for agricultural activities and the supply of drinking water for the population. To alleviate water shortages, the region has built the reservoir 'La Viñuela' (capacity 165 $hm^3$), which supplies

water for irrigation and domestic use. Total water resources are estimated at 92 $hm^3$/year whereas total demands are 103 $hm^3$/year, resulting in 11 $hm^3$/year of deficit (CMA, 2021).




**Fig. 1.** Location of the Axarquía region.

The Axarquía is known for its cultivation of subtropical crops due to its mild climate. Avocados, mangoes, papayas, chirimoyas (custard apples), and lychees are some of the main crops grown in the area (10,000 ha out of 15,000 ha total cultivated area; CMA, 2021).

## 3. Governance innovations

The main water governance challenge in focus in the Axarquía is the control of over abstraction and the re-allocation of scarce water resources and competition between users. This will be addressed through a new digital tool serving as a key element to implement a new governance model based on integrated water management and users' participation, integrating water reuse, managed aquifer recharge and financial tools as key elements of integrated water management. The tool will consist of 6 modules: Water resources availability, Water demands, Alternative water resources (MAR and reclaimed water, 20 $hm^3$; and desalinated water, forecasted 25 $hm^3$), Ecological flows, Water governance and Economic analysis. Prediction tools based on machine learning techniques will be included to anticipate drought or scarcity scenarios. The water governance assessment will allow the identification of critical points to improve water management. The platform will also include dynamic responses from users to avoid future rebound effects (the dynamic response of users after efficiency improvement that generates higher consumption in comparison to 'expected savings').

## 4. Living labs

A living lab can be defined as "an innovation ecosystem where societal stakeholders and researchers collaboratively explore, experiment with and evaluate one or more water governance innovations" (Sojamo et al., 2023). In the framework of the GOVAQUA project, a four-phases methodology has been developed for the testing of the innovative governance approaches/tools in each of the living labs, based on the sequencing of Malmberg et al. (2017) and Rădulescu et al. (2022): (i) Initiation and preparation; (ii) Exploration; (iii) Experimentation; (iv) Evaluation and feedback phases.

## 5. Next steps

The critical foreseen steps of the living lab process implementation in the Axarquía are the following:

- Detailed characterisation of the current hydrological (water resources and demands) and economic statuses at the living lab.
- Organisation of the first workshop with local stakeholders and water users aiming at understanding and benchmarking the current water governance setting, defining the desired future state and co-designing the innovative instruments to be tested.

**Acknowledgements**

This is a contribution to the project "Governance innovations for a transition to sustainable and equitable water use in Europe (GOVAQUA)", co-funded by the European Commission (Horizon Europe project number 101086578).

**References**

CMA (2021). Hydrologic Plan of the Andalusia Mediterranean Basins.
EC (2019) Towards a sustainable Europe by 2030. European Commission, Directorate-General for Communication.
EEA (2021) Drivers of and pressures arising from selected key water management challenges. A European overview. EEA Report No 9/2021. European Environment Agency.
INE (2023). Spanish National Statistics Institute. Agricultural Census. https://www.ine.es/
Malmberg, K., Vaittinen, I., Evans, P., Schuurman, D., Ståhlbröst, A. and Vervoort, K. (2017) Living Lab Methodology Handbook.
Rădulescu, M.A., Leendertse, W. and Arts, J. (2022) Living Labs: A Creative and Collaborative Planning Approach. In: Franklin, A. (eds) Co-Creativity and Engaged Scholarship. Palgrave Macmillan, Cham.
Sojamo, S, Sánchez-García, D., Vinke-de Kruijf, J. and Özerol, g. (2023) Process Design for GOVAQUA Living Labs of Water Governance Innovations. GOVAQUA Deliverable 6.1.

# Occurrence and Distribution of Per- and Polyfluoroalkyl Substances in San Francisco Bay Area Drinking Water

Sudarshan KURWADKAR[1], Emma HOFFMAN-DAVIES[2]

[1] Department of Civil and Environmental Engineering, California State University, Fullerton, California, USA
skurwadkar@fullerton.edu

[1,2] Engineering Geologist, San Francisco Bay Regional Water Board, San Francisco, California, USA
ehoffman@csu.fullerton.edu

ABSTRACT

In recent years, there has been a growing concern regarding the occurrence of per– and polyfluoroalkyl substances (PFAS) in the aquatic environment. Their widespread detection, long-term persistence, and associated human health and ecological risk have renewed the emphasis on mitigating adverse impacts through material substitution, voluntary phaseouts, and regulatory measures. Despite these measures, PFAS are routinely detected in inland, coastal, marine, and subsurface environments. In this study, we have documented the occurrence of PFAS in groundwater that serves as a source of potable drinking water in the San Francisco Bay Area (SFBA). This study was undertaken as part of the U.S. Environmental Protection Agency's (USEPA) requirement for sampling and monitoring PFAS in drinking water wells to determine their occurrence, magnitude, and vulnerability of water resources. Careful analysis of several years of data suggests that many drinking water wells in the SFBA have elevated levels of various PFAS. Chronic exposure to PFAS-contaminated drinking water has serious human health implications. Analysis of existing PFAS remediation technologies, indicates the effectiveness of adsorption, reverse osmosis, and ion exchange technologies. Our findings suggest that these technologies are effective for the treatment of five PFAS compounds – perfluorooctanoic acid (PFOA), perfluorooctane sulfonate (PFOS), perfluorobutane sulfonate (PFBS), perfluorononanoic acid (PFNA), and perfluorohexane sulfonate (PFHxS).

# On the generalization of image-based river turbidity monitoringunder different hydrological conditions

Domenico MIGLINO[1], Khim Cathleen SADDI1[4,5], Francesco ISGRO[3], Seifeddine JOMAA[2], Michael RODE[2], and Salvatore MANFREDA[1]

1 Dipartimento di Ingegneria Civile, Edile e Ambientale (DICEA), Università degli Studi di Napoli Federico II, Italy
domenico.miglino@unina.it

2 Dep. of Aquatic Ecosystem Analysis and Management, Helmholtz Centre for Envir. Research - UFZ, Magdeburg, Germany

3 Dip. di Ingegneria Elettrica e delle Tecnologie dell'Informazione (DIETI), Univ. degli Studi di Napoli Federico II, Italy

4 Istituto Scuola Superiore Pavia (IUSS Pavia), Pavia, Italy

5 Department of Civil Engineering and Architecture, Ateneo de Naga University, Naga, Philippines

## ABSTRACT

Digital cameras could provide significant advantages to existing river monitoring techniques, enhancing the temporal and spatial resolution of observations. In this work, an image processing procedure for estimating river turbidity was tested in a real-scale experiment carried out in Germany, along the Selke River, within the Bode catchment, instrumented and managed by the Helmholtz Centre for Environmental Research (UFZ), Germany. The field campaign was conducted using different tracers, camera models and installation settings to understand the full potential of the camera systems in operational water quality monitoring. The gathered data were compared to the measurements of the turbidimeters installed in the river cross-section. The results prove that this procedure can properly represent the water turbidity trends employing an RGB camera in a real case study under natural conditions. Nevertheless, further investigations are necessary to select the best camera setup and to detect the most fitting spectral indexes for a reliable long-term image-based river turbidity monitoring system.

## 1. Introduction

Turbidity is a key optical property of water. High turbidity values can be a proxy for the presence of suspended organic and inorganic matter in rivers. The on-site experiment of June 2023, represented in Figure 1, aimed to change, within the river, both the duration and intensity of three synthetic turbidity events, generated by adding different natural clay tracers, as suspended solids with varying reflectance properties.

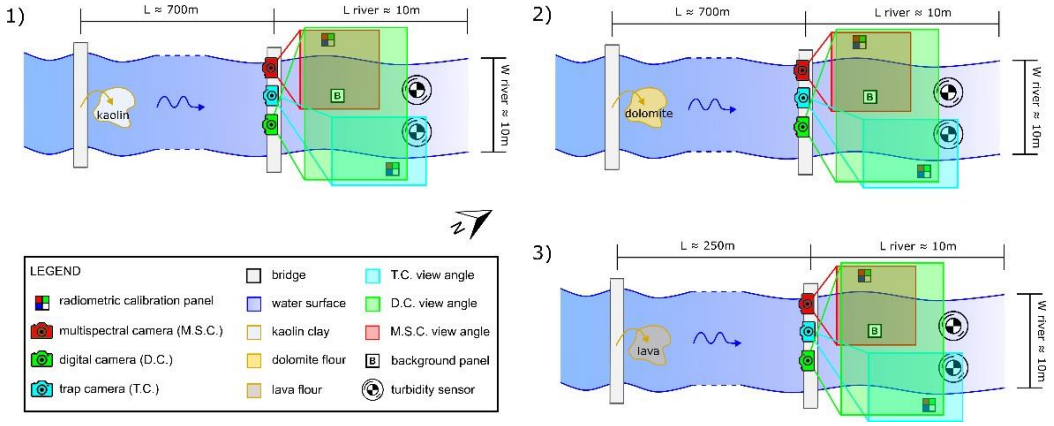



**Figure 1.** Plan of the monitored river section during the experiment of 30/06/2023, showing the generated synthetic turbidity events, using three different natural clay tracers: kaolin (**1**), dolomite (**2**) and lava (**3**) flours.

The main objective of this field campaign was to generalize, as much as possible, the camera monitoring methodology recreating many real river pollution events, also for minimizing the long-term effects on lighting and hydrological conditions of the experimental site, better described in Miglino et al. 2022.

## 2. Methods

During the experiment, three different cameras were installed on the bridge: one trap camera, Ceyomour CY50, with a frame rate of 15 seconds; another multispectral camera (MSC), Tetracam ADC Snap, with a frame rate of 2 seconds; a third camera, Nikon Coolpix P950, with a frame rate of 6 seconds. At the same time, the turbidimeter was installed on-site and had a frame rate of 2 seconds. The results were homogenized, considering all the sensors and camera measurements recorded simultaneously. River flow velocity was around 0.3 meters per second and the water depth was approximately 25 centimeters, while the clay tracers was poured far enough from the monitoring cross-section, to ensure the complete mixing between clay and water. The generated turbidity events allowed us to explore the image-based procedure potential by varying water optical characteristics and suspended solids concentration, simulating the real river conditions.

## 3. Results and discussion

As shown in some preliminary results in Figure 2, there is a good matching between camera bands reflectance and measured turbidity, especially considering the RED band, for all three turbidity peaks.

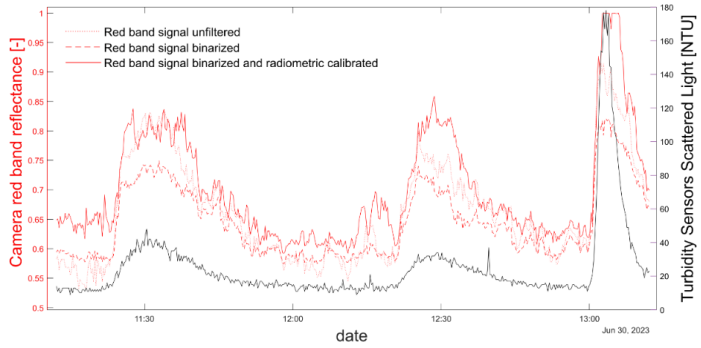



**Figure 2.** Comparison between the reflectance of the trap camera red band and the turbidity measurements of the sensor installed on site, during the short-term experiment of 30/06/2023.

Besides, it is essential to consider the issue of background reflectance, particularly in shallow waters, as those of the experiment, to fully understand the range of applications of the procedure. The removal of the background component from the total water-leaving reflectance can lead to a better estimate of the real water turbidity level. Finally, for single short-term monitoring (hours) the RED band reflectance seems to be the most reliable index for turbidity monitoring, better than spectral indexes (Table 1) coming from existing bands ratios in literature (e.g., R/G, NDTI, NDWI, etc.).

**Table 1.** Spectral indexes, used to compare camera bands reflectance and turbidity measurements, and their $R^2$ values of coefficientsof determination, considering trap camera and multispectral (MS) camera results.

| | M.S. CAMERA | TRAP CAMERA |
|---|---|---|
| SPECTRAL INDEX | $R^2$ | $R^2$ |
| RED BAND | 0.93 | 0.87 |
| GREEN BAND | 0.68 | 0.83 |
| NDTI | 0.48 | 0.59 |
| NDWI | 0.41 | |

On the other hand, considering long-term monitoring (days, months), the single bands reflectance tends to bemore influenced by different light and flow conditions, which is even more true using low quality cameras. Hence, it is better to use indexes and multiple bands in this case.

## 4. Conclusions

In conclusion, it is necessary to find the best spectral indexes to properly detect the water turbidity variations for changing light conditions and river flow characteristics, while factoring different camera capabilities. As future research directions, additional experiments will test the method under different hydrological and environmental conditions. The final goal of this work is to provide a new monitoring solution for inland water security and water resources management practices.

### References

Miglino, D., Jomaa, S., Rode, M., Isgro, F., & Manfreda, S. (2022) Monitoring Water Turbidity Using Remote Sensing Techniques,Environmental Sciences Proceedings, 21(1), 63.



# Posters

8th IAHR EUROPE CONGRESS
LISBON - PORTUGAL
4-7 JUNE 2024
WATER - ACROSS BOUNDARIES
IAHR AIRH
Hosted by Spain Water and IWHR, China

# Preliminary results of the monitoring of the insect community in a periurban section of the Manzanares River (Madrid, Spain)

S. Ibarra MELLADO[1], M.R. García SÁNCHEZ-COLOMER[2], A.D. Young Sánchez MATEOS[1], J.L. Viejo MONTESINOS[1]

[1] Department of Biology, Faculty of Science, Universidad Autónoma de Madrid (UAM); [2]Centre for Studies and Experimentation in Public Works (CEDEX)

## Motivation

The goal of this study is to evaluate the recovery of the river ecosystem. **We plan on monitoring changes in insect communities in relation to climate and human intervention before, during and after construction work**.

**This study evaluates insect communities as part of a monitoring campaign that started in 2023 to assess the recovery of the ecological and hydrological continuity of a section of the Manzanares River (Madrid, Spain) (Fig. 1).**

The study contributes to the project "Recovery of the fluvial ecosystem Manzanares-Gavia-Bulera. Green and blue infrastructure Metropolitan Forest of Madrid", supported by the Biodiversity Foundation (Ministry for Ecological Transition and the Demographic Challenge), under NextGenerationEU's Recovery, Transformation and Resilience Plan (PRTR). The group responsible for the project is formed by the Madrid City Council, the Centre of Studies and Experimentation of Public Works (CEDEX) and the Conama Foundation.

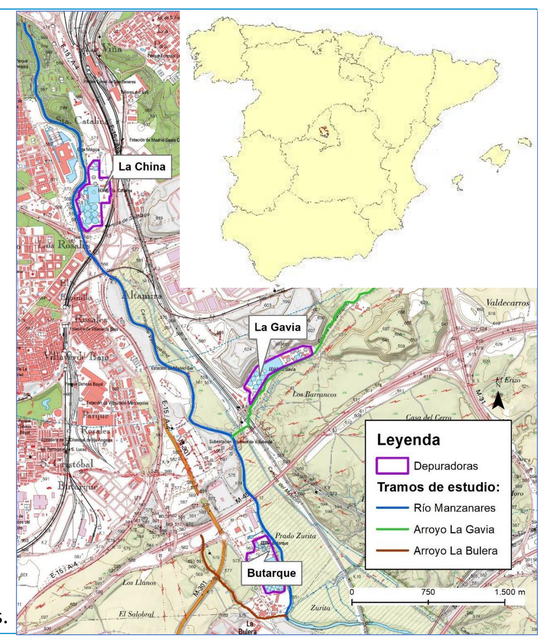



Fig. 1. Location of the study sections.

## Results

Although the projected works have not yet begun, we can advance preliminary results of the previous situation.



Fig. 2. Eleven percent of the flying insects captured are pollinators.

**We collected a total of 935 flying insects belonging to 8 different orders, 99 individuals were important pollinators (11%).** November was the month with the highest abundance: 440 captures. In August, on the contrary, only 12 insects flew into the trap. Pollinator abundance peaked in April, with 53 captures, more than 50 percent of all pollinators. Individuals of the black fly *Simulium erythrocephalum* were captured in July and November. 21 different invertebrate orders were observed on the plants and soil of the two transects. During the summer diversity dropped, especially in July when only 3 invertebrate orders were detected.

**There is a strong correlation between diversity of flying insects and pollinator diversity (*p < 0,001*) and flying insect biomass *vs* pollinator biomass (*p < 0,001*). Biomass of flying insects is strongly correlated with maximum temperature (*p < 0,001*) as well.** Diversity and abundance in the transects are inversely correlated to maximum temperature and positively correlated to relative humidity, Moisture index and NDVI values.

## Methodology



Fig. 3. Vehicle-mounted insect collector

**We introduce an innovative sampling method: a vehicle-mounted box as a trap for airborne insects (Fig. 3).** The device is a reinforced acrylic 50 x 50 cm cube strapped onto the roof rack of an SUV. A tilting acrylic lid opens on its own once the car is in motion allowing air to flow through the box and out of a 2 mm mosquito net on the back pane (Fig. 4). This study presents the results of 11 months of sampling before the construction began.

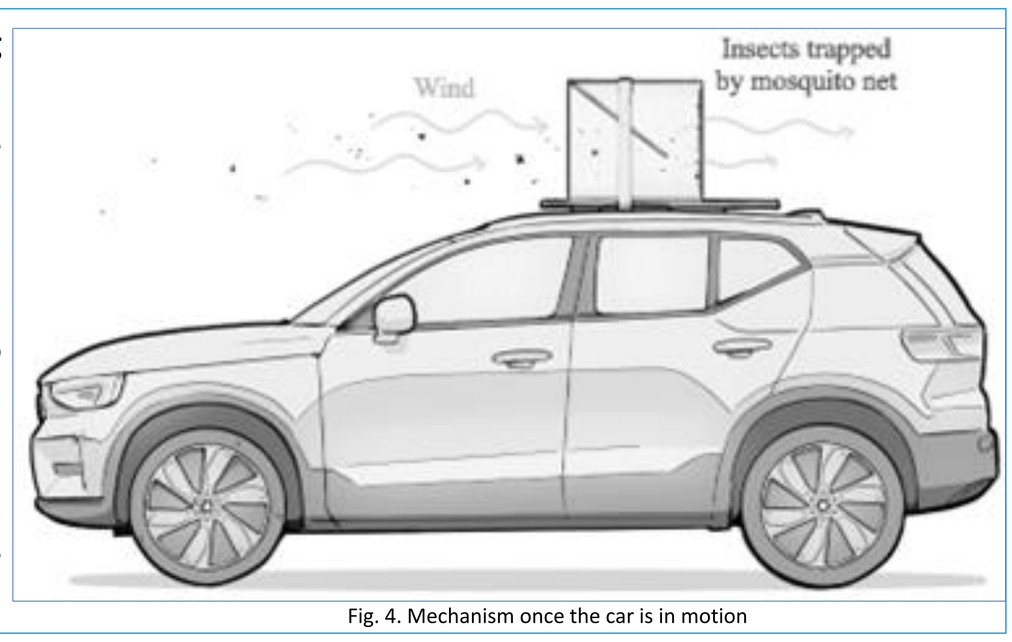



Fig. 4. Mechanism once the car is in motion

## Conclusions

**The most shocking finding is that insects were more abundant during fall and winter months (September to January). Our main hypothesis is that air humidity is the limiting factor for small insects but heat benefits heavier flying insects such as bees, wasps, or hoverflies (Syrphidae) which are pollinators and were present independently of air humidity**. Black flies are significant for public health as they feed on human blood, can cause allergic reactions and are prone to be a vector of disease (Kim, 1987).

Diversity in ground transects appears to be very dependent on humidity and less so on temperature, plants offer shelter, nourishment, and a humid microclimate to many invertebrates like springtails (Collembola) or snails, and herbaceous vegetation was notably more abundant during the winter months.

**We hope to monitor how the construction sites affect these insect populations in the future**. Our predictions are that epigean arthropods inhabiting the transects will be negatively impacted by debris from construction work. Dust will affect plant cycles can be which can modify pollinator interactions and numbers.

Contacts: M.R. GARCÍA SÁNCHEZ-COLOMER (manuel.colomer@cedex.es), J.L. VIEJO MONTESINOS (joseluis.viejo@uam.es)

References: Kim KC, Merritt RW (Eds.) Black flies, ecology, population management, and annotated world list, University Park, London, 1987. ISBN 0-271-00417-7

Acknowledgments: Felipe García Matas has contributed with numerous improvements to the sampling system.

8th IAHR EUROPE CONGRESS
LISBON - PORTUGAL
4-7 JUNE 2024
WATER - ACROSS BOUNDARIES

IAHR AIRH
Hosted by Spain Water and IWHR, China

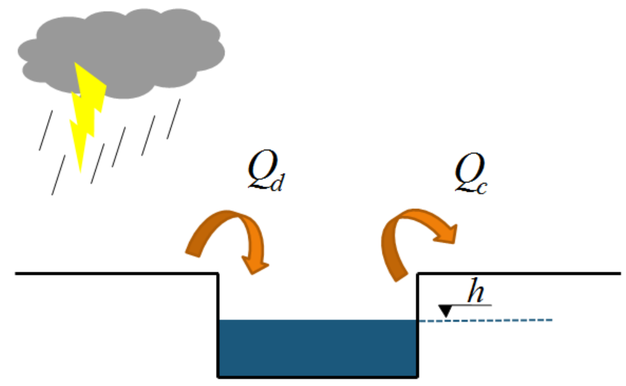
# Development of a simple reservoir water level controller

Filipa N. Nogueira, José L.S. Pinho
CTAC - Center for Territory, Environment and Construction,
Department of Civil Engineering, University of Minho,
4800-058 Guimarães, Portugal.

## Model

$$h(k+1) = h(k) + BQ_c(k) - BQ_d(k)$$

$B=-T/A$,
$A$ is the average storage area ($m^2$),
$T$ is the control time step ($s$),
$k$ is a positive integer, and $h(k) < 0$.




## Control description

$$Q_c(k) = \max(0, \tilde{Q}_c(k))$$

$$\tilde{Q}_c(k) = 0.99\, B^{-1}(h^* - h(k)) + Q_d(k)$$

$$h \longrightarrow h^*$$

## Results

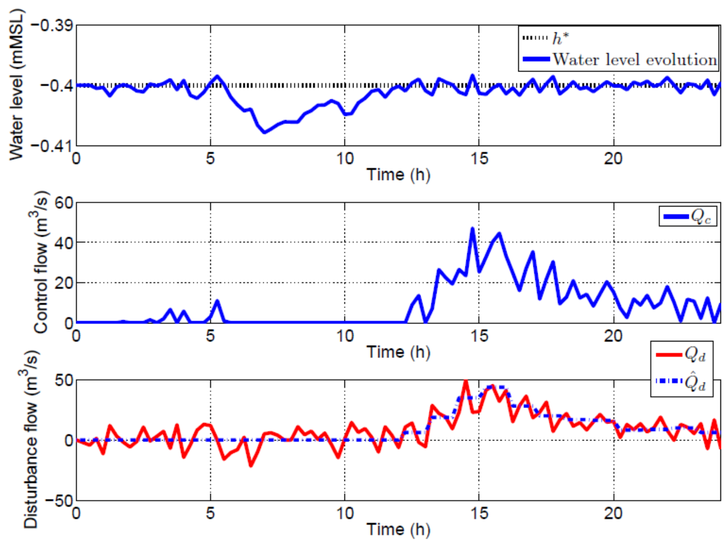



Fig.1 - The evolution of the water level is illustrated on the top graph, where the dashed black line corresponds to the desired reference value. The pump control flow is represented on the second graph. On the bottom graph the rainfall-runoff inflow, $Q_d$, is marked in solid red line, whereas the estimated disturbance is marked in dashed blue line.

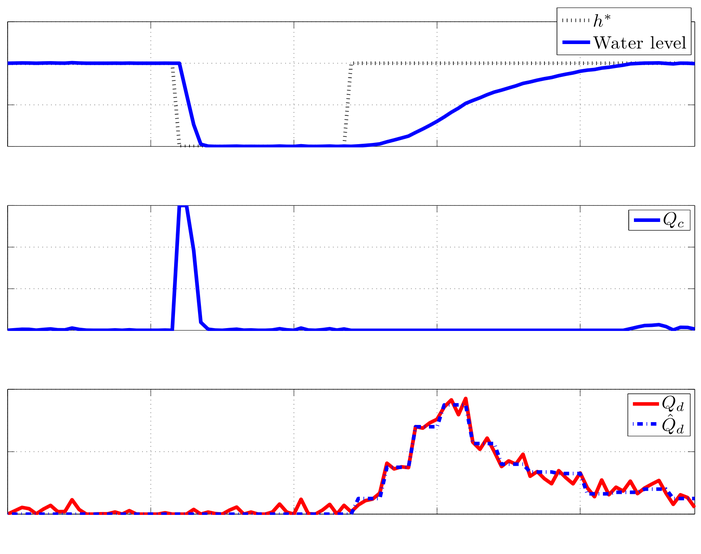



Fig.2 – The control of the reservoir water level assumes changes in the reference level during the control period ($h^*$ = -0.40 m from the beginning until t = 6 hours, $h^*$ = -0.42 m from t = 6 hours until t = 12 hours, and $h^*$ = -0.4 m from then on). The evolution of the water level is illustrated in the top graph, where the dashed black line corresponds to the desired reference value. The pump control flow is represented in the second graph. In the bottom graph, the rainfall-runoff inflow, $Q_d$, is marked with a solid red line, whereas the estimated disturbance is represented by a dashed blue line.

## Conclusions

- A control law was designed and implemented for the operational management of a pumping system, intended to maintain a reference level in a reservoir, based on a state-space representation and subject to a rainfall-runoff inflow event.

- This controller has the advantage of:
  - being simple to implement,
  - its performance is not very time-consuming,
  - It allows the changing of the desired reference values during the whole control process.

Contact: filipan@civil.uminho.pt

**References:**
J. M. Lemos, L. F. Pinto, L. M. Rato, M. Rijo, *Multivariable and distributed lqg control of a water delivery canal*., Irrigation and Drainage Engineering 139(10) (2013) 855–863.
J. M. Maestre, P. J. van Overloop, M. Hashemy, A. Sadowska, E. F. Camacho, *Human-in-the-loop model predictive control of an irrigation canal*., IEEE control systems 35(4) (2015) 19–29.
A. Lacasta, M. Morales-Hern´andez, P. Brufau, P. Garcia-Navarro, *Simulation of pid control applied to irrigation channels*., Proceedings of the 12th International Conference on Computing and Control for the Water Industry, Procedia Engineering 70 (2014) 978–987.
P.J. van Overloop. *Model predictive control on open water systems*. Ph.D. dissertation. Delft University of Technology, The Netherlands., 2006.

**Acknowledgments:** This work was financed by FCT/MCTES through national funds (PIDDAC) under the RD Unit The Centre for Territory, Environment, and Construction (CTAC), with the reference UIDB/04047/2020 (doi.org/10.54499/UIDB/04047/2020)

8th IAHR EUROPE CONGRESS
LISBON - PORTUGAL
4-7 JUNE 2024
WATER - ACROSS BOUNDARIES

IAHR AIRH
Hosted by Spain Water and IWHR, China

# Stormwater Attenuation & Enhanced Infiltration System to Mitigate Flood and Drought Conditions in Urban and Rural Environments: Part II

Stephen THOMAS[1], George FRENCH[1], Joseph O'MEARA[2], Matthew DALE[2], Bruno CASAL[3]
[1] OGI Groundwater Specialists, Durham, UK
[2] Groundwater Dynamics Ltd, Leamington Spa, UK
[3] Sondagens Casal Lda, Sintra, Portugal
stephen.thomas@ogi.co.uk

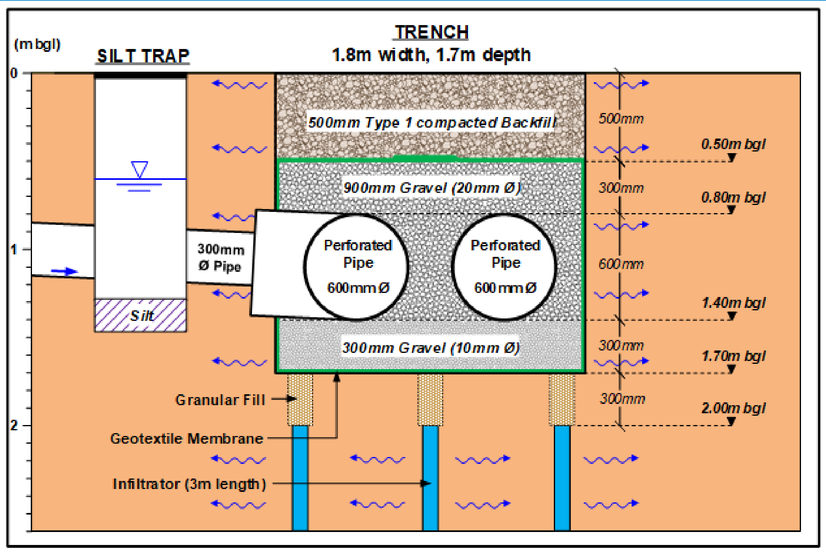



**Figure 4**. Attenuation and Enhanced Infiltration section.

The combination of the nonwoven geotextile of a green fibre structure, with the pea gravel backfill, adds treatment for hydrocarbon contamination by promoting the growth of a microbic biofilm which absorbs and digests hydrocarbon that may have entered the gravel filled attenuation trench.



**Figure 5**. Perforated pipes installed within gravel filled attenuation trenches.



**Figure 6.** Final backfilling of attenuation trench and wrapping with green nonwoven geotextile.

**Rainwater infiltration theory into unsaturated ground**

Rainwater infiltration into unsaturated ground above water-table is complex to simulate. When water fills the attenuation volume in the trenches, water also fills the infiltrators beneath. This results in a high differential pore water pressure between the water-filled infiltrators, together with natural suction pressure in the surrounding unsaturated ground.

The pressure in the infiltrators will be governed by the elevation of the water head in the attenuation storage (Figure 7).

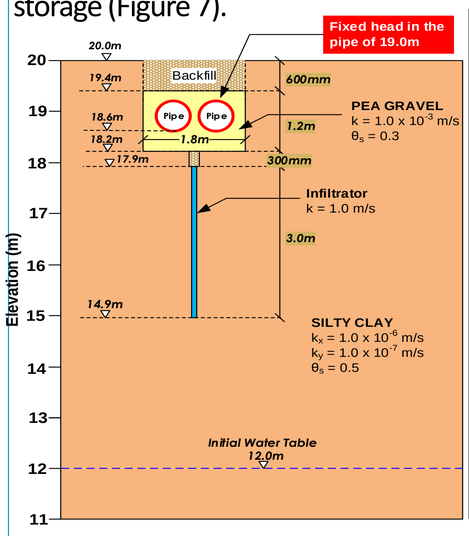



**Figure 7. I**nfiltrator with ground properties used in the mathematical modelling.

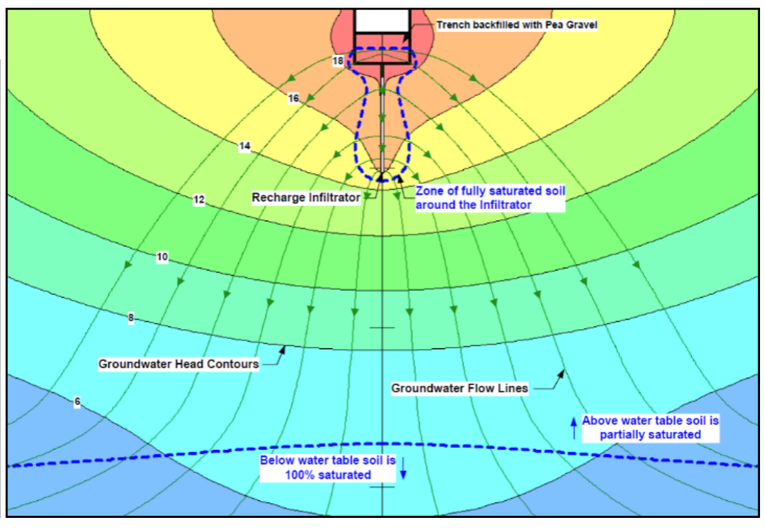



**Figure 9**. Simulated head contours and flow paths.

If the water level rises to 600 mm above the trench base and the infiltrators are 3.3 m below this base, the pressure at the infiltrator tip will be approximately 38 kPa. The initial negative pore water pressure in the surrounding unsaturated ground, or soil suction, can reach -50 kPa in fine-grained soils. This results in a differential pore-water pressure of about 88 kPa, driving water from the infiltrator into the ground. Validated by mathematical models, stormwater attenuation and enhanced infiltration systems outperform traditional soak away trenches and are increasingly accepted in the UK construction industry, despite some resistance.

**Finite element modelling of enhanced infiltration**

The movement of the collected stormwater through the infiltrator into the ground has been modelled by French and Thomas (Authors) using the GeoStudio finite element software SEEP/W (Geostudio, 2012). The finite element model requires "discretisation" of the ground domain surrounding the infiltrators into tens of thousands of smaller zones called "elements" to geometrically simulate the groundwater behaviour using the radial version of the equation below:

$$\frac{\partial}{\partial x_i}\left(k_{rw}\, K_{ij}\, \frac{\partial h}{\partial x_j}\right) = \left(S_w S_s + \varphi \frac{\partial S_w}{\partial \psi}\right)\frac{\partial h}{\partial t} - Q_w$$

where $k_{rw}$ is relative permeability, $K_{ij}$ is Hydraulic Conductivity Tensor, h is hydraulic head, $\varphi$ is porosity, $S_w$ is water saturation, $S_s$ is Specific Storage, ψ is pressure head, and $Q_w$ point recharge. The non-linear functions used in the modelling for (i) Volumetric Water Content, and (ii) Hydraulic Conductivity, which are dependent on soil suction, are presented in Figures 8a and 8b.

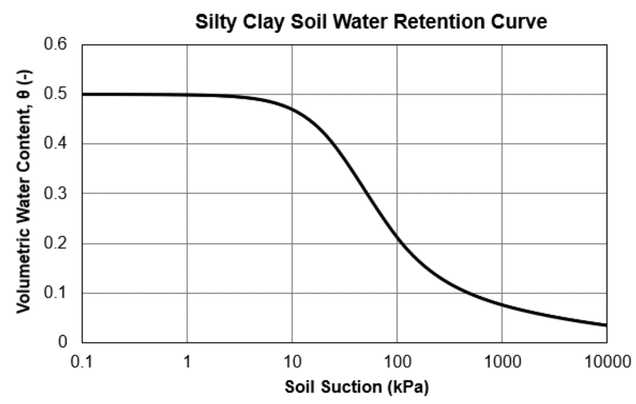



**Figure 8a.** Soil-water retention function curve

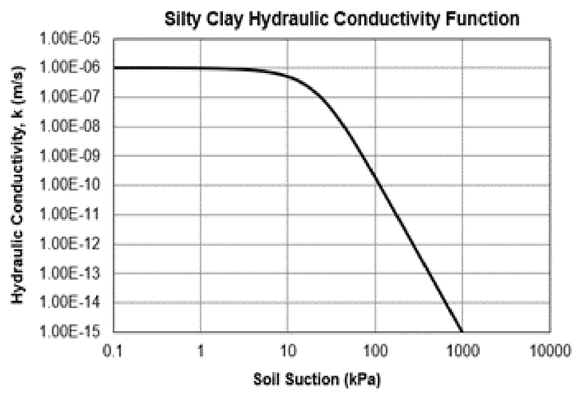



**Figure 8b**. Hydraulic conductivity vs soil suction

The finite element model then enables different properties and boundary conditions to be input in a range of locations for which the governing flow equation is solved, and heads output. From these outputs, other information can be calculated such as pore pressure, degree of saturation and groundwater velocity. An axisymmetric finite element computer model has been utilised to simulate two-dimensional radial steady-state flow of collected water into the vadose (unsaturated soil) zone surrounding an infiltrator. For this scenario, a saturated sump and infiltrator have been simulated using SEEP/W. The simulated soil is based on a typical UK anisotropic silty clay.

Input horizontal permeability is 1.0 x $10^{-6}$ m/s and vertical permeability 1.0 x $10^{-7}$ m/s. To simulate the unsaturated behaviour of the soil, SWRC (Soil Water Retention Curve) along with a hydraulic relative conductivity function have been selected based on typical functions for silty clays, (Figures 8a and 8b). A fixed head boundary condition is applied to the sump, and a high permeability infiltrator is specified to simulate the flooded sump and infiltrator. Figure 9 illustrates simulated groundwater head contours (18m to 6m) and flow lines (green arrows). The dashed blue line indicates the water table position, where pore water pressure is 0.0 kPa and saturation is 100%.

Groundwater flow is driven by a gradient of hydraulic head (Darcy's Law); which explains the pattern of groundwater flow that can be seen in Figure 9. The head changes from 19.0m at the sump to 15.0m at the bottom of the infiltrator. This 4.0m head differential drives the water down through the vertical infiltrator, as depicted by the green arrows.

In the unsaturated zone above the water table, negative pore pressure creates a significant differential head between the positive pressure in the infiltrators and the negative pore-water pressure so enhancing infiltration. Water enters the soil at depth and flows horizontally into more permeable silt or sand layers, creating a fully saturated zone around the infiltrator (Figure 9). This saturation increases groundwater flow & permeability. Figure 10 illustrates stormwater attenuation and enhanced infiltration, showing how collected stormwater is directed to drains and attenuation trenches, eventually percolating down to replenish aquifers. Combining the pressure head of the collected stormwater in the attenuation trenches, with the negative suction pressure in the unsaturated vadose zone, increases the differential pressure to force the water into the ground via these infiltrators. By installing vertical infiltrators, ground of higher permeability is regularly encountered.

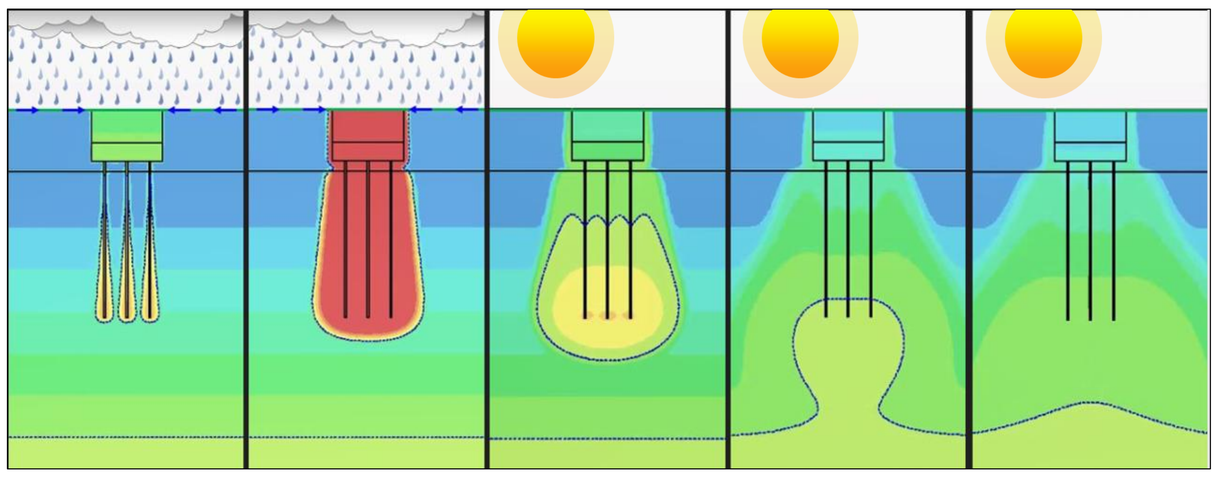


**Figure 10.** Various stages of attenuation and enhanced infiltration during and following a storm event.



**Figure 11.** The images above depict a test project between Birmingham and Manchester, where a steady rate of over 2000 $m^3$/day of infiltration to the ground was achieved from 78 infiltration wells

Stormwater Attenuation & Enhanced Infiltration Systems (SAEIS) are utilized in the UK to alleviate flooding and recharge groundwater. Given Portugal's declining groundwater and increased flooding, implementing these systems would benefit its hydrogeology and weather. Mathematical modelling is presented which simulates the water flow through the infiltrator system, and into the unsaturated soil strata. Combining the storage capacity of the attenuation trenches with a large number of infiltrators, produces a highly efficient attenuation and infiltration system that not only mitigates the impact of flooding but has no requirement for ongoing energy consumption. SAEIS also aids in drought mitigation by replenishing aquifer water resources. These systems align with low-carbon sustainability and contribute to UN Sustainable Development Goal 6: Ensure availability and sustainable management of water and sanitation for all.

**Contacts**: Stephen.Thomas@ogi.co.uk; jomeara@groundwaterdynamics.co.uk; bruno.casal@sondagenscasal.pt

# Impact of beaver activity on water resources in the catchment and water quality

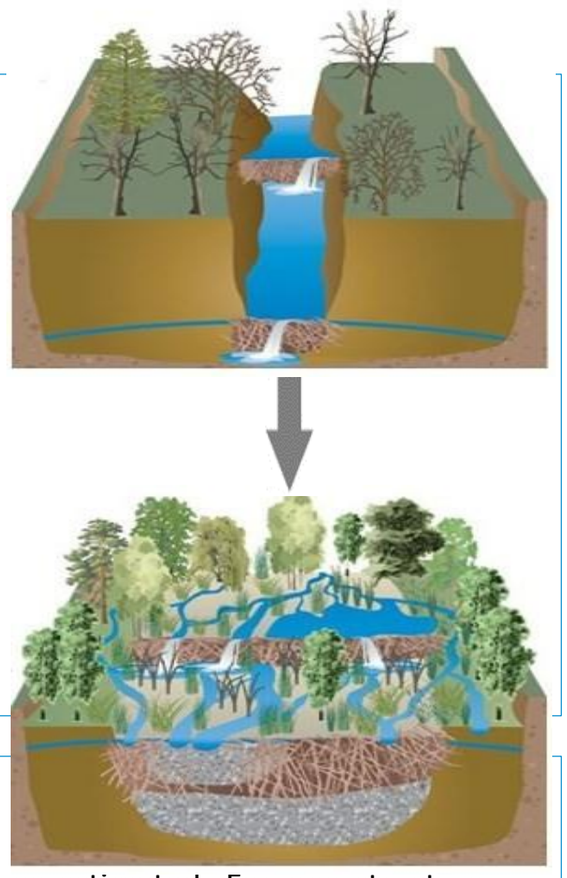
Stanisław Zaborowski[1], Tomasz Kałuża[2], Paweł Strzeliński[3], Mateusz Hammerling[4]

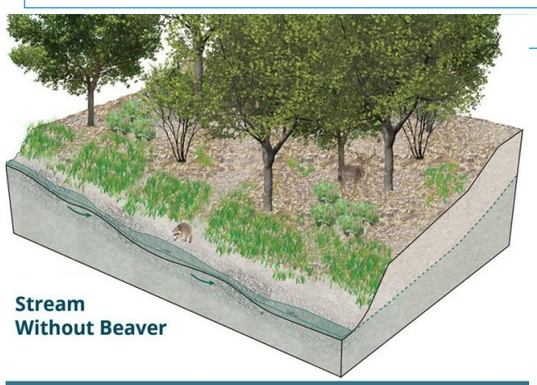
[1, 2, 3, 4] Poznań University of Life Sciences

8th IAHR EUROPE CONGRESS
LISBON - PORTUGAL
4-7 JUNE 2024
WATER - ACROSS BOUNDARIES
IAHR AIRH
Hosted by Spain Water and IWHR, China

## Motivation

As a result of ongoing climate change and environmental transformation, there are greater and more intense water shortages in many places. Conventional solutions involving the construction of large reservoirs do not fully solve this issue. In the case of small-scale retention which includes the construction of small but numerous and dispersed reservoirs and the restoration of wetlands, the available funds, technical and administrative possibilities are inadequate. Beavers have always been helpful in this matter. In the 19th and 20th centuries, beavers were almost non-existent in Europe. As a result of a number of programmes, their population has increased significantly and their activities have resulted in the creation of many wetlands, beaver ponds and thus make a noticeable contribution to the retention of the water we are lacking. Although the impact of their activities is evident, the actual environmental impact of beavers is not fully recognised. This has motivated me to investigate and understand the phenomena surrounding beaver activity and determine their impact on the environment.



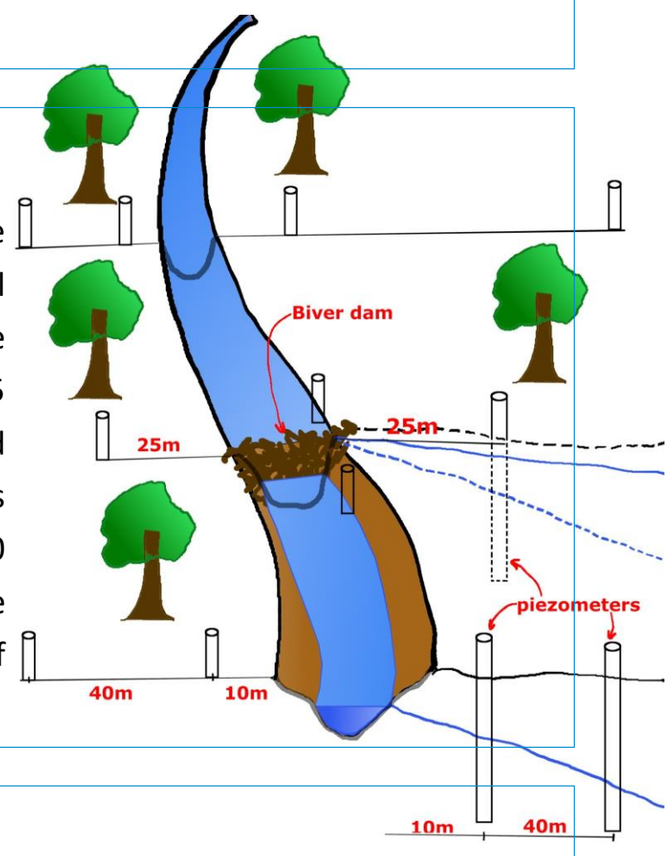



## Results

Based on the measurements, the amount of both riverbed and soil retention was estimated. For one structure with an impoundment height of 0.7 m, the amount of retained water was 4,200 m3 in the riverbed and valley alone. The extent of the dam's impact reached 300 m upstream of the dam. The system of the water level in the ground significantly depended on the shape of the river valley and the soil parameters. With steep valley banks, a very small range of impact and thus elevation of the groundwater level curve was observed. On the other hand, for a watercourse with a flat valley, a noticeably greater impact of damming was observed for changes in the groundwater system and resources. At one site, an rise in the water level of up to 0.40 meters was observed in the range of installed piezometers. It is worth adding that it was often asymmetric due to the river course in the plan. On the basis of water quality studies, a significant improvement in water quality was determined downstream of the dam compared to samples taken upstream of the dam.

## Methodology

The paper presents the impact of beaver activity on the formation of water resources and water quality in the catchment area. In addition to channel retention gained from the construction of dams by beavers, water is still stored in the soil profile. The resources and quality of this water have not yet been estimated. Field studies were carried out on 10 objects (beaver dams), among which can be identified 5 dams in the forest environment and 5 dams in other areas. All beaver dams were located in Great Poland Province (Poland). Measurements included inventory of beaver dams (e.g., width, height and length), building material, riverbed and valley geometry, species composition of nearby flora, and water table system in the riverbed (above and below the dam) and in 10 piezometers located in an area of about 1000 m2. During the measurements, physicochemical parameters were checked and heavy metals were ordered to be determined in the bottom sediments upstream and downstream of the dams. The inventoried objects were characterized by a width of 3 – 10 m and a height of no more than 0.9 m.




## Conclusions

Beaver activity in the form of building their dams is extremely beneficial. The increase in natural retention of trough as well as soil in the catchment area is very important in times of water scarcity. The resources thus secured provide a valuable source for nearby animals and allow nearby plants to survive. Slowing of the flow in the resulting floodplains (beaver ponds) contributes to sedimentation of pollutants and improvement of the quality of retained water, and the water overflowing on the surface dam becomes oxygenated, improving its physicochemical properties. In addition, the hydromorphological changes occurring in the watercourse contribute to the creation of new habitats for flora and fauna. The impact of rising groundwater levels on the forest stands growing in river valleys is inconclusive. On the one hand, trees growing in the close vicinity of watercourses were often in worse condition or felled by beavers. However, within the river valleys, the increase in retention and raising of the groundwater level, positively affected the remaining tree stands (especially riparian forests). It is worth adding that many times there are several dams on the watercourse (cascade of structures), which multiplies the retention effect.

Contacts: stanislaw.zaborowski@up.poznan.pl

References: Macfarlane WW, Wheaton JM., Bouwes N, Jensen ML, Gilbert JT, Hough-Snee N, Shivik JA. (2017) Modeling the capacity of riverscapes to support beaver dams, Geomorphology, Volume 277, 15 January 2017, Pages 72-99
McKinstry, M. C., Caffrey, P., & Anderson, S. H. (2001). The importance of beaver to wetland habitats and waterfowl in Wyoming, Journal of the American Water Resources Association, 37(6), 1571–1577. https://doi.org/10.1111/j.1752-1688.2001.tb03660.x. Omelczuk Ł, Kozieł M (2017) Wpływ działalności bobra europejskiego Castor fiber L. na zmiany stosunków wodnych na Polesiu Zachodnim, WPTPN, Badania Fizjograficzne, Seria A, Tom 68, 2017, s. 99-113
Pollock M, Beechie T, Wheaton J, Jordan C, Bouwes N, Weber N, Volk C (2014) Using Beaver Dams to Restore Incised Stream Ecosystems, BioScience, Volume 64, Issue 4, April 2014, pp. 279–290, doi.org/10.1093/biosci/ Puttock A, Graham HA, Ashe J, Luscombe DJ, Brazier RE (2020) Beaver dams attenuate flow: A multi-site study, Hydrological Processes. 2021; 35:e14017.
Westbrook CJ, Ronnquist A, Bedard-Haughn A (2020) Hydrological functioning of a beaver dam sequence and regional dam persistence during an extreme rainstorm, Hydrological Processes, 34(18), 3726–3737. http://dx.doi.org/10.1002/hyp.13828.

Acknowledgments: The research was co-founded by the National Science Centre of Poland within the PRELUDIUM project (No. 2021/41/N/ST10/02490): "Evaluation of anthropogenic factor"

# Assessment of Dam Inflow Forecasting by Blending Ensemble NWP Rainfall with Radar Prediction

Wansik YU[1], Jinhyeog PARK[1] , Shinuk KANG[1],
Kyoungpil KIM[1] , Mieun KIM[1]
[1] K-water

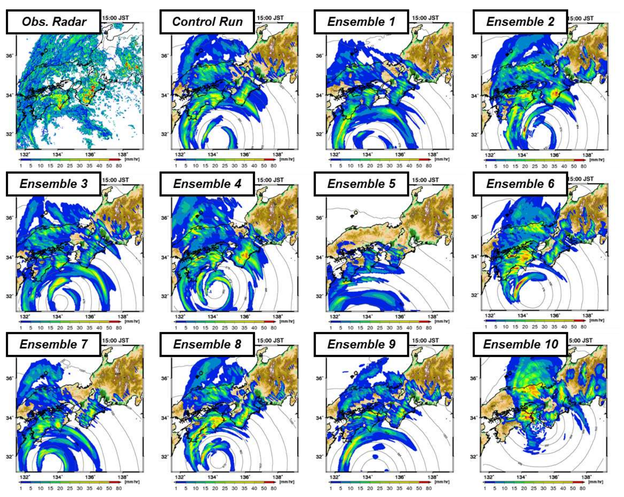
8th IAHR EUROPE CONGRESS
LISBON - PORTUGAL
4-7 JUNE 2024
WATER - ACROSS BOUNDARIES
Hosted by Spain Water and IWHR, China

## 1. Introduction

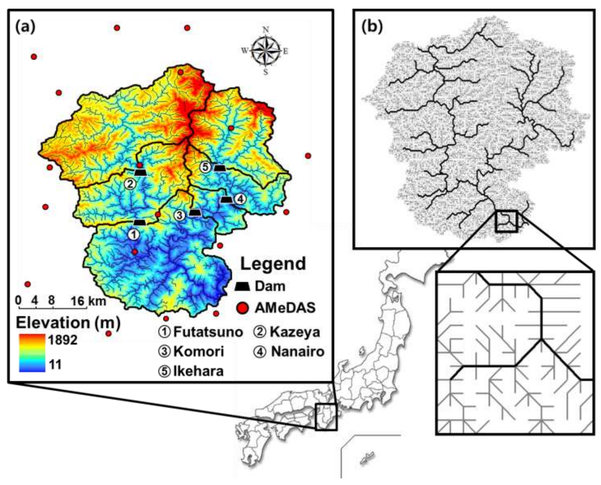
The main objective of this study is to blend the advantages of ensemble information of radar based prediction with NWP rainfall for the accuracy improvement of dam inflow forecasting in viewpoint of the hybrid forecast. Improved radar based prediction proposed by Nakakita et al. (2012) and updated NWP rainfall by error field scheme are merged with changing weight function through CSI and RMSE indexes of previous 3 hours lead time. The proposed blending method is verified through 2011 largest rainfall event for Typhoon Talas, and is applied into the hybrid dam inflow forecasting on sub-catchment, which is Futatsuno (356.1km$^2$) dam catchments.

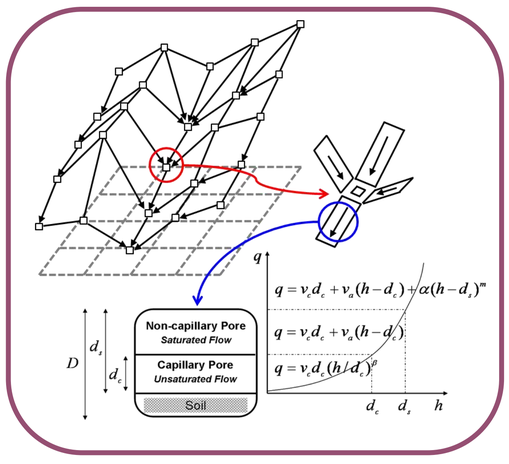
## 2. Data and Methodology

### Ensemble NWP rainfall of Typhoon




### Target area and a hydrologic model



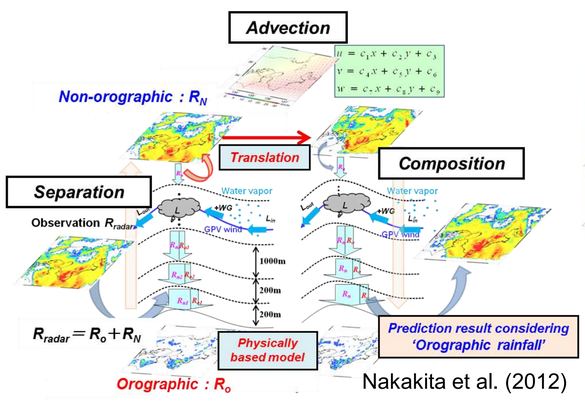




### Methodology

- In this study, the ensemble surface precipitation (Psrf) from NWP model with 30h forecast time and 2km resolution was utilized.
- We used the grid-based one-dimensional kinematic wave method for subsurface and surface flow simulation, which was enhanced by Tachikawa et al. (2004).
- We focused on sub-catchment, which is Futatsuno dam catchments (No. 1), for the accuracy improvement of the dam inflow forecasting in small catchment.

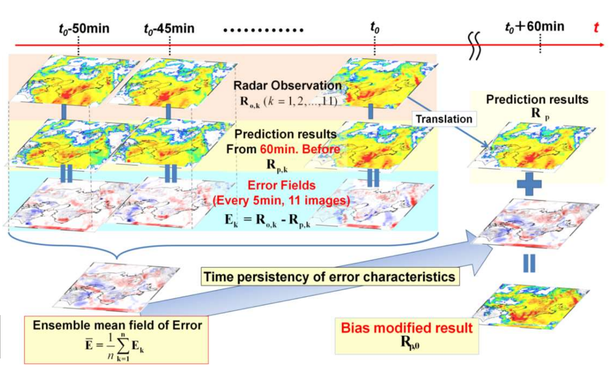
## 3. Improved Radar Image Extrapolation Method

### 1. Orographic Rainfall Identification Scheme




Nakakita et al. (2012)

### 2. Error Field Scheme




Kim et al. (2009)

## 5. Blending of NWP Rainfall with Radar Prediction

- The blending method with radar prediction and updated NWP rainfall using error filed scheme is configured to start a blend forecast after 6 hours (to+6h) until 3 hours ahead.

$$R_{blend,i} = C_{radar,i} \times R_{radar} + C_{nwp,i} \times R_{nwp,i}$$

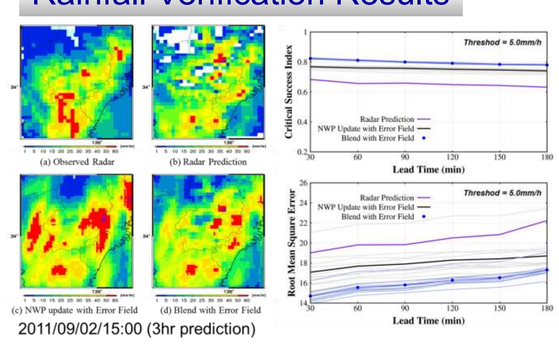
$$C_{radar,i} + C_{nwp,i} = 1$$

$$\begin{bmatrix} R_{blend,1} \\ R_{blend,2} \\ R_{blend,3} \\ \vdots \\ R_{blend,10} \end{bmatrix} = \begin{bmatrix} C_{radar,1} \\ C_{radar,2} \\ C_{radar,3} \\ \vdots \\ C_{radar,10} \end{bmatrix} \times R_{radar} + \begin{bmatrix} C_{nwp,1} \\ C_{nwp,2} \\ C_{nwp,3} \\ \vdots \\ C_{nwp,10} \\ C_{nwp,11} \end{bmatrix} \times \begin{bmatrix} R_{nwp,1} \\ R_{nwp,2} \\ R_{nwp,3} \\ \vdots \\ R_{nwp,10} \\ R_{nwp,11} \end{bmatrix}$$

$$C_{nwp,i} = \frac{w_{nwp,i,1} + w_{nwp,i,2}}{2}, \quad w_{nwp,i,1} = \frac{CSI_{nwp,i}^2}{CSI_{radar}^2 + CSI_{nwp,i}^2}, \quad w_{nwp,i,2} = 1 - \frac{RMSE_{nwp,i}^2}{RMSE_{radar}^2 + RMSE_{nwp,i}^2}$$

$$C_{radar,i} = \frac{w_{radar,i,1} + w_{radar,i,2}}{2}, \quad w_{radar,i,1} = \frac{CSI_{radar}^2}{CSI_{radar}^2 + CSI_{nwp,i}^2}, \quad w_{radar,i,2} = 1 - \frac{RMSE_{radar}^2}{RMSE_{radar}^2 + RMSE_{nwp,i}^2}$$

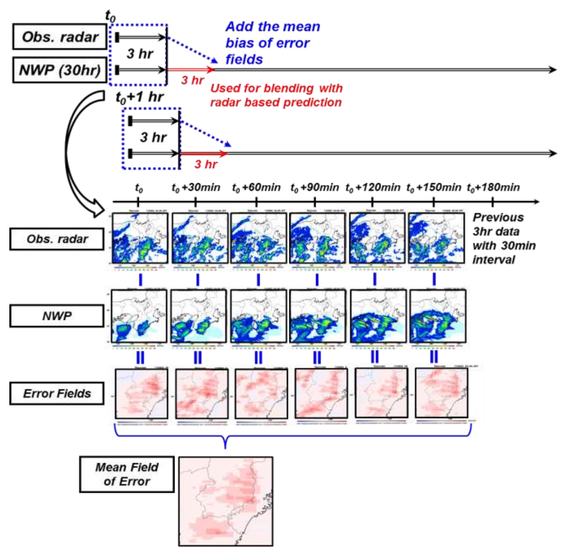
### Rainfall Verification Results




2011/09/02/15:00 (3hr prediction)

## 4. NWP Updating with Error Field Scheme

### Error Field Scheme

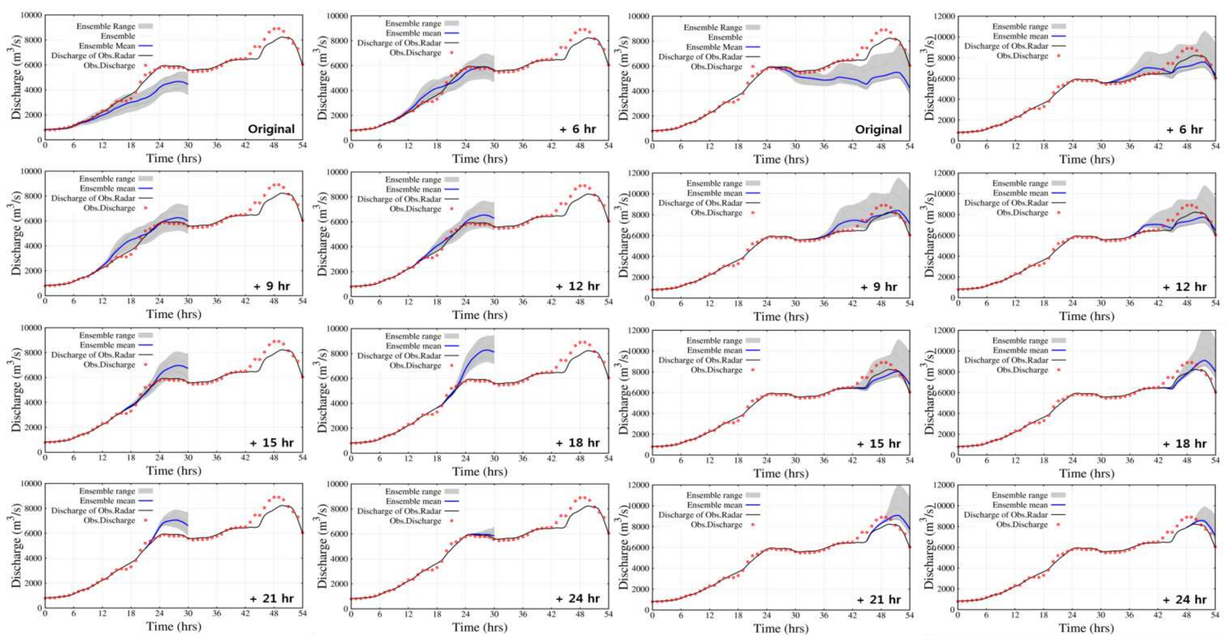



- The mean bias of error fields is calculated using 6 consecutive previous observed radar images and original ensemble NWP rainfall outputs.
- Then mean bias of 3 hours error fields gives the information to post ensemble NWP rainfall forecasting.
- These updated 3 hours in ensemble NWP rainfall are then used to run the blending method, which merges with radar rainfall prediction from improved radar image extrapolation method

## 6. Application into Hybrid Dam Inflow Forecast

### 1st Forecasting (Rising limb period)

### 2nd Forecasting (Peak discharge period)




## 7. Conclusions

- The proposed blending method improved the rainfall prediction accuracy than the results of radar prediction and updated NWP rainfall by the interactive influence of merging weights from radar prediction and updated NWP rainfall.
- Hybrid dam inflow forecasting with combination of blending method and updated NWP rainfall could improve the under-predicted part of original ensemble NWP rainfall, and also could represent the peak value and cover the observed discharge in first and second forecast periods over the two catchments.

Contacts: Wansik YU (yuwansik@gmail.com)

Acknowledgments: This work was supported by Korea Environment Industry & Technology Institute(KEITI) through Water Management Program for Drought, funded by Korea Ministry of Environment(MOE)(RS-2023-0023194)

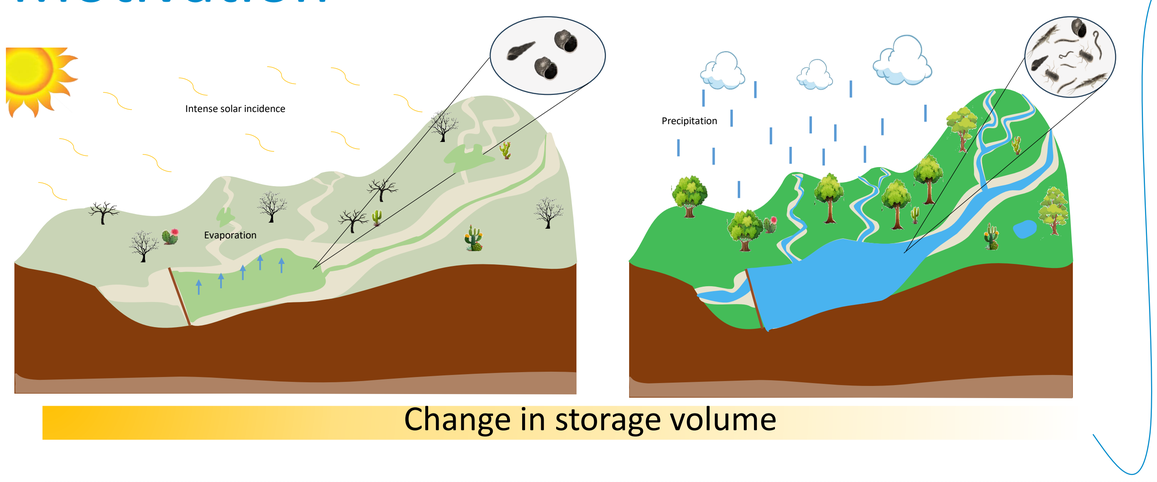
# Reducing storage volume causes loss of water quality in semi-arid reservoirs and reduces the diversity of benthic macroinvertebrates

Carlinda MEDEIROS[1], Lucianna FERREIRA[2], Laisa COSTA[1], Rodolfo NÓBREGA[3], John CUNHA[1], Joseline MOLOZZI[2], Carlos GALVÃO[1]

[1] Federal University of Campina Grande, Campina Grande, PB, Brazil
email: carlinda.rodrigues@professor.ufcg.edu.br
[2] State University of Paraíba, Campina Grande, PB, Brazil
[3] School of Geographical Sciences, University of Bristol, Bristol, United Kingdom

8th IAHR EUROPE CONGRESS
LISBON - PORTUGAL
4-7 JUNE 2024
WATER - ACROSS BOUNDARIES
IAHR AIRH
Hosted by Spain Water and IWHR, China

## Motivation



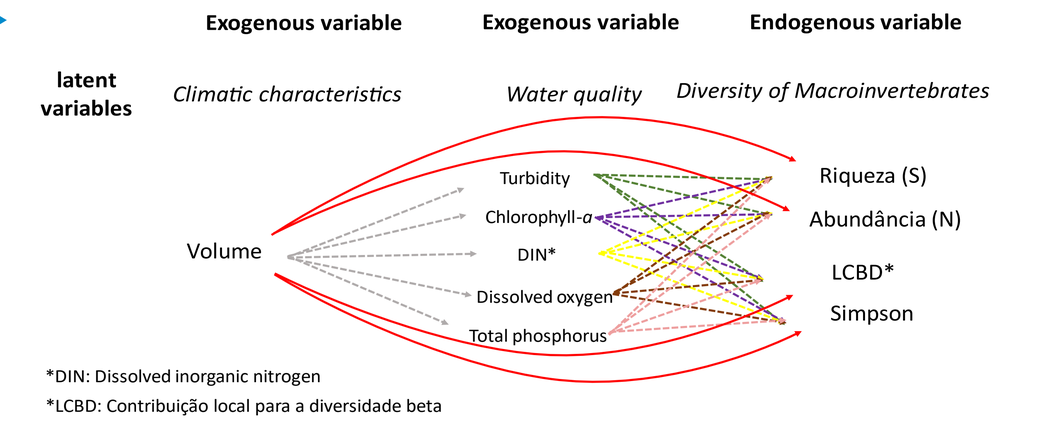




**Figure 1.** Hypothetical causal relationship between storage volume of semi-arid reservoirs, water quality and community diversity of benthic macroinvertebrates.

This study aims to analyse hierarchical effects and unravel the complex relationships between the storage volume of semi-arid reservoirs on water quality and the diversity of benthic macroinvertebrates.

## Methodology

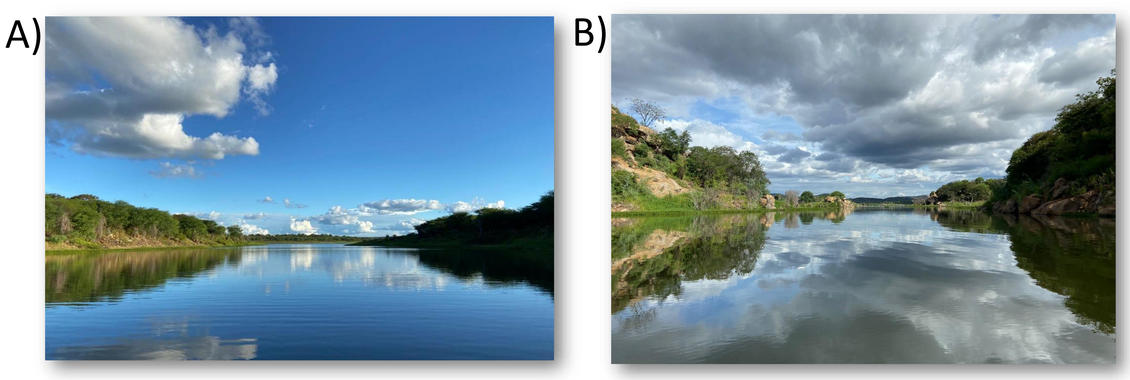



**Figure 2.** Sumé (A) and Cordeiro (B) reservoirs, located in the Paraiba river basin, Brazilian semi-arid region.

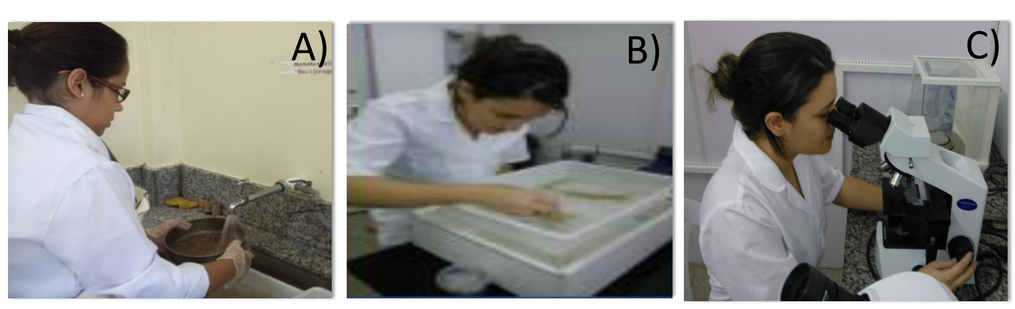



**Figure 3.** Sample processing in the laboratory: A) Sample washing, B) Material sorting and, C) Identification of the organisms.

## Results

- Reduced storage volume in reservoirs increases nitrogen and phosphorus concentrations in water (Figure 3).
- Total phosphorus mediated a positive effect on the Simpson's index, indicating an increase in the dominance of tolerant individuals, such as the exotic species *Melanoides tuberculatus* and *Corbicula largillierti*.
- The negative relationship between nitrogen and richness indicates that this nutrient in water can cause a reduction in the variability of different genres that provide different ecological functions in reservoirs.
- These results demonstrate that the change in storage volume alters the environmental conditions of the reservoirs, and these act as a filter, selecting only species that have functional and morphological traits to survive in adverse conditions, favoring the establishment of exotic species.

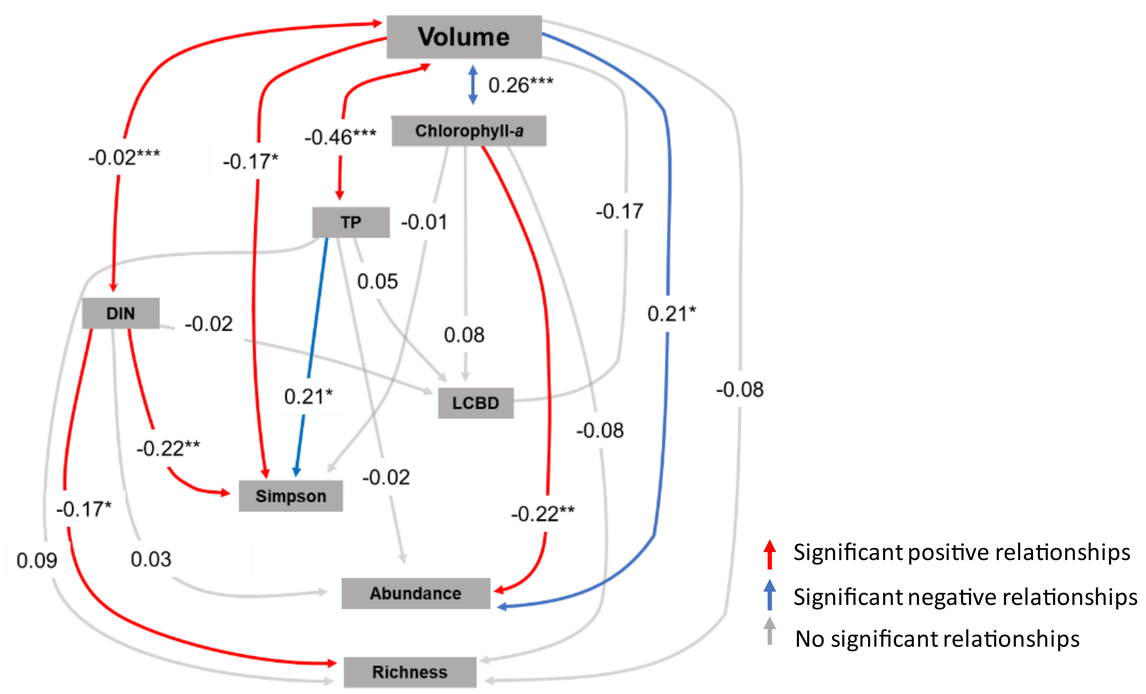



**Figure 4.** Path diagram of SEM with the causal relationships between storage volume, water quality, and diversity of benthic macroinvertebrates. Values of standardized regression coefficients and covariances are presented for each causal relationship.

## Conclusions

The causal model demonstrates that increasing volume increases chlorophyll-a but decreases nitrogen and phosphorus concentrations in the water. In turn, chlorophyll-a and nitrogen reduce the abundance and richness of species, respectively, while total phosphorus favours the establishment of dominant species. These results provide insights for water resource managers regarding decision-making and maintaining adequate minimum volumes of water to promote the health and integrity of semi-arid reservoirs and their sustainable use.

Contacts: carlindarailly@gmail.com

Acknowledgments:
CAPES
CNPq Conselho Nacional de Desenvolvimento Científico e Tecnológico
UEPB
UFCG Universidade Federal de Campina Grande

8th IAHR EUROPE CONGRESS
LISBON - PORTUGAL
4-7 JUNE 2024
WATER - ACROSS BOUNDARIES
Hosted by Spain Water and IWHR, China

# Streamflow Predictions in Ungauged Basins Using Remote Sensing Information and Artificial Intelligence

Sangdan Kim[1], Jeongeun Won[1], Jiyu Seo[1]
[1] Pukyong National University, Busan 48513, Korea

## Motivation

Predicting streamflow in ungauged basins is one of the major challenges in hydrology. In this study, the aim was to investigate the potential performance enhancement in streamflow predictions that can be achieved by training artificial intelligence using remote sensing information obtained from artificial satellites. Specifically, artificial intelligence models were developed using satellite-based information for 25 basins in South Korea and their performance in daily streamflow predictions was compared with models developed using basin feature data obtainable on the ground. To achieve this, an integrated approach combining recurrent neural network (RNN) and decision tree (DT)-based algorithms was employed. The second curiosity addressed in this study is the examination of performance differences between relatively easy-to-construct RNN models and DT-based algorithms. By testing common RNN models (Long Short-Term Memory (LSTM) and Gated Recurrent Unit (GRU)) and DT-based algorithms (Random Forest, XGBoost, LightGBM), the goal is to explore the most suitable combination of model architectures for South Korea.

## Results

The performance of streamflow predictions by models trained using scheme MRG for 25 ungauged basins was examined. A comparison of model NSE performance with scheme MG is presented in Fig. 1.

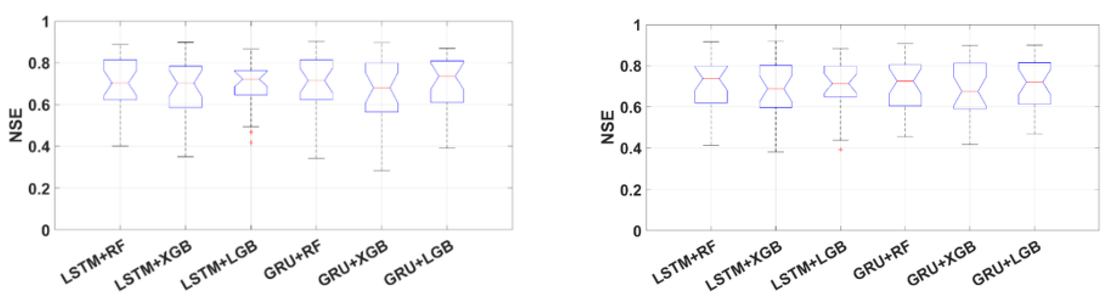



**Fig. 1.** Performance of scheme MG(left) and MRG(right).

- Scheme MG: Learning using meteorological data and geographical information of basin
- Scheme MRG: Learning using meteorological data, geographical information, and additionally incorporating remote sensing information
 * Geographical information (basin area, curve number, saturation hydraulic conductivity, imperviousness ratio)

1) The predictive performance obtained for ungauged basins using models trained on data from multiple gauged basins consistently exceeded a specific threshold, regardless of the two training approaches employed in this study.

2) These findings highlight the efficacy of data-driven models in forecasting streamflow in ungauged basins.

3) It is essential to acknowledge, however, that these outcomes rely on the assumption that data from basins with analogous climatic and geographical characteristics were utilized during model training. Thus, it is recommended to employ these models for ungauged basins that align with the conditions within which they were originally trained.

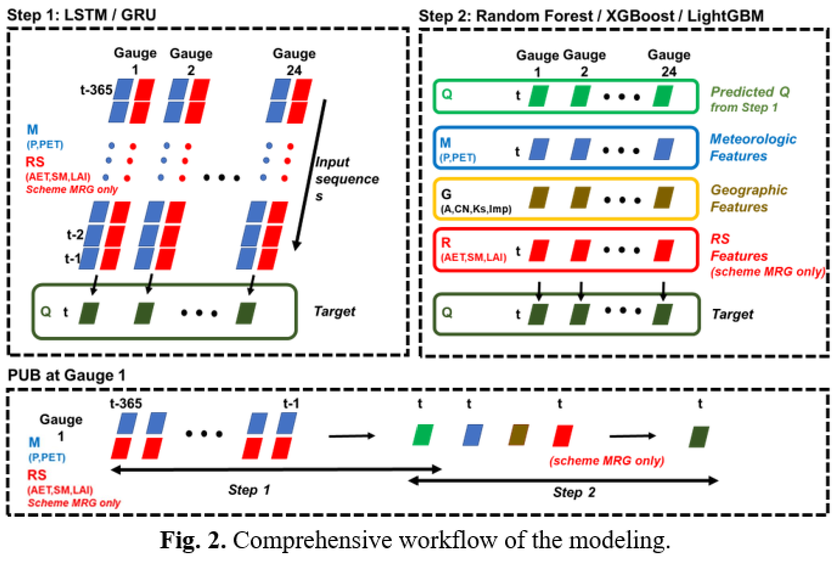



**Fig. 2.** Comprehensive workflow of the modeling.

## Methodology

In this study, a Leave-one-out cross-validation (LOOCV) method is applied using all 25 basins. Among the 25 basins, one specific basin is assumed to be an ungauged basin, and the model is trained using data from the remaining 24 basins. Then, the trained model is used to assess the predictive performance of the assumed ungauged basin's streamflow. This procedure is repeated until all basins have been tested. Consequently, 25 models are constructed, and performance evaluations are conducted for 25 ungauged basins. To examine the impact of training data on the performance of data-driven models in prediction in ungauged basins (PUB), we established two major training strategies : (1) Scheme MG: Learning using meteorological data and geographical information of basin (basin area, curve number, saturation hydraulic conductivity, imperviousness ratio); (2) Scheme MRG: Learning using meteorological data, geographical information, and additionally incorporating remote sensing information. Through these approaches, we aimed to investigate the extent to which the input of remote sensing information influences the performance of data-driven models, addressing our first curiosity.

In recent times, there has been a surge in various machine learning and deep learning algorithms that are not only proposed but also actively implemented in practical applications. As users, it is crucial to discern which of these promising machine learning or deep learning techniques are best suited for our specific dataset. In this study, for the first-step RNN modeling phase, we opted for LSTM and GRU, while in the second-step DT-based modeling phase, we selected Random Forest, XGBoost, and LightGBM. This allowed us to evaluate the performance of each model combination, resulting in an examination of the PUB performance for a total of 2×3 = 6 model combinations. The comprehensive workflow of the modeling conducted in this study is depicted in Fig. 2.

## Conclusions

In this study, the additional utilization of remote sensing information did not significantly improve the prediction performance for ungauged basins, and the importance of the added remote sensing information within the model prediction process was found to be relatively low. However, it provided a slight improvement in predicting dry season streamflow. Nevertheless, the combination of recurrent neural networks and decision tree-based algorithms applied in this study still exhibited limitations in predicting dry-season streamflow in ungauged basins. Considering that basin hydrological processes differ between dry and wet seasons, future research could benefit from strategies that separately train models for these distinct periods. Furthermore, there is a growing availability of larger sample datasets, including remote sensing information, for model training. This presents an opportunity to advance the use of data-driven models in PUB applications, and more research in this direction is needed. Additionally, research on appropriate hyperparameter estimation for data-driven models will be essential for future developments.

Acknowledgments: This work was supported by the National Research Foundation of Korea (NRF) grant funded by the Korea government (MSIT) (No. NRF-2022R1A2B5B01001750). This work was also supported by Korea Environmental Industry&Technology Institute (KEITI) through Wetland Ecosystem Value Evaluation and Carbon Absorption Value Promotion Technology Development Project, funded by Korea Ministry of Environment (MOE). (2022003640001). Contacts: skim@pknu.ac.kr

# Understanding the Impacts of River Network Fragmentation on Freshwater Fish Species

**Tamara Leite** [1], Florian Borgwardt [2], Paulo Branco [1]

[1] Forest Research Centre, Associate Laboratory TERRA, School of Agriculture, University of Lisbon, Lisboa, Portugal; [2]University of Natural Resources and Life Sciences, Vienna; Institute of Hydrobiology and Aquatic Ecosystem Management (IHG); Vienna; Austria

8th IAHR EUROPE CONGRESS
LISBON - PORTUGAL
4-7 JUNE 2024
WATER - ACROSS BOUNDARIES

Hosted by Spain Water and IWHR, China

**Longitudinal connectivity** of freshwater systems allows upstream/downstream movements of aquatic migratory species. Multiple obstacles, partially or totally blocking upstream movements, promote cumulative non-additive impacts on freshwater fish. **There are at least 1.2 million instream barriers in 36 European countries.** It is important to assess the impacts of barriers on the **structural and functional longitudinal connectivity of riverine systems**, and the consequences for fish species, assemblages, and diversity, to improve conservation measures and ecosystem management to halt biodiversity loss.

## Objective

Understand the impacts of riverine longitudinal connectivity loss, regarding potamodromous and diadromous fish species across Europe.

## Tasks

### 1. River Network Connectivity in Europe

Determining connectivity loss caused by large dams in Europe, using graph theory analysis.

Compiled databases:

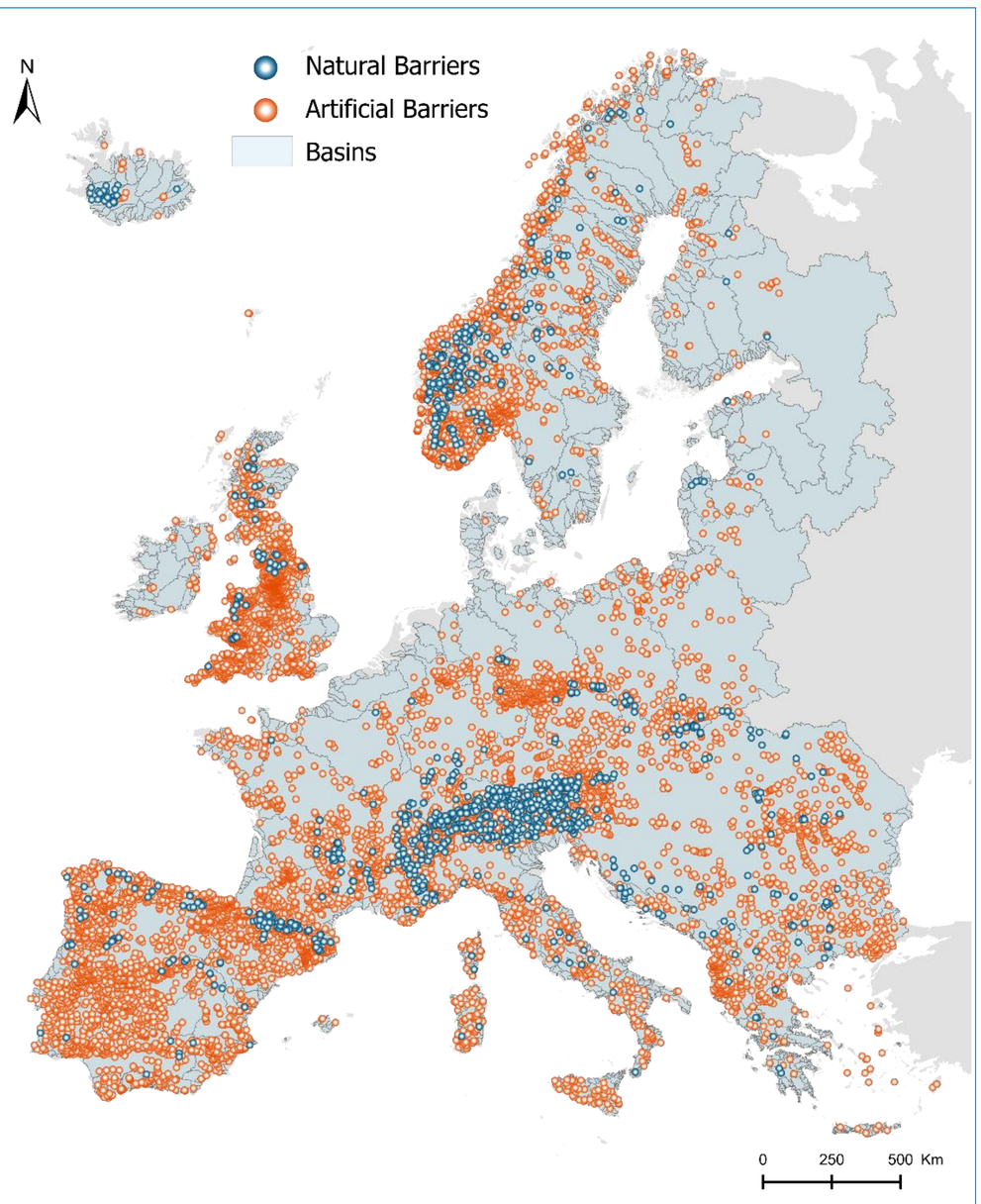
- ✓ **AMBER Barrier Atlas** (Belletti et al., 2020)
- ✓ **Georeferenced Global Dams And Reservoirs** (GeoDAR v1.1, Wang et al., 2021)
- ✓ **GlObal geOreferenced Database of Dams** (GOODD V1) (Mulligan et al., 2020)

### 2. Natural Vs. Artificial Fragmentation in Europe

*Are we underestimating the effects of artificial barriers?*

Compare the effects of natural to artificial fragmentation – regarding waterfalls, dams and the upstream water reservoir.

Determine **natural fragmentation** of the systems, since most research on river network fragmentation discards the effects of natural pre-existing barriers, such as waterfalls, only accounting for the constructed artificial ones, such as **dams**. Moreover, studies on the impacts of dams have considered the dam as the principal or only barrier impairing longitudinal fish movements. However, the **upstream water reservoir** itself represents an ecological barrier.




**Geographic location of dams and waterfalls** automatically integrated and manually verified with the respective Catchment Characterisation Model (CCM2) basin and segment (De Jager and Vogt, 2007).

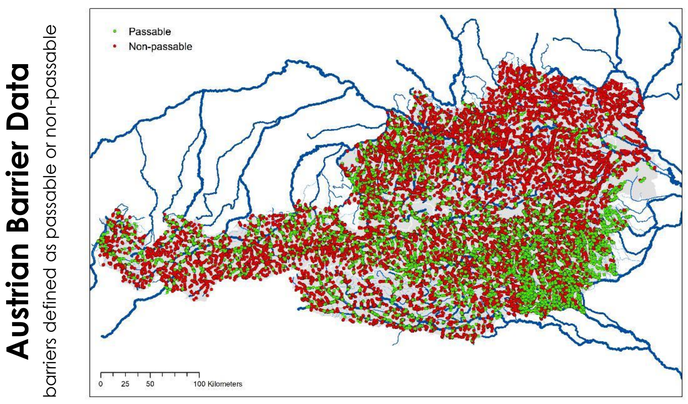
**Connectivity** calculated using **Dendritic Connectivity Index (DCI)** (Cote et al., 2009), regarding potamodromous and diadromous species (DCIp and DCId, respectively), to quantify longitudinal connectivity of each river network.

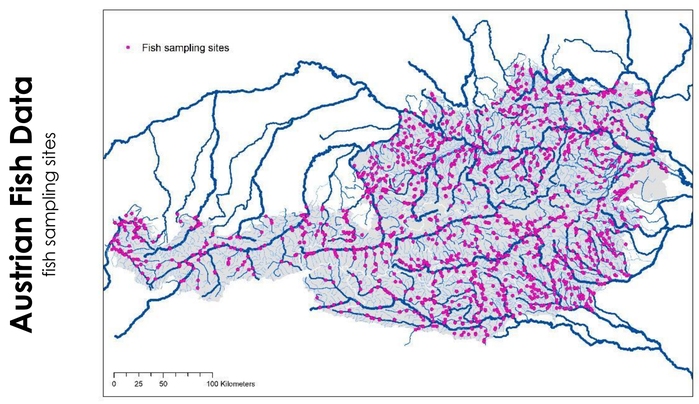
### 3. Partial River Connectivity (Austria)

What are the impacts of different barriers on fish community structure and diversity?

Classify barriers by type and determine their effects on river network structural connectivity.

Determine impacts of different barrier on fish diversity and community composition




### 4. Could Functional Resilience Be Improved by Restoring Connectivity?

Identify fish diversity hotspots in Europe.

Determine consequences of fragmented river systems for functional diversity.

Model management and restoration plans to enhance connectivity in barrier fragmented systems.

## Take Home Message

**Fragmentation of freshwater systems** will greatly reduce structural and functional longitudinal connectivity within river basins, which will ultimately have effects on fish species and communities, leading to a **decrease in functional resilience**.

Contacts: **tamaraleite@edu.ulisboa.pt**

**References:** Belletti, B., Garcia de Leaniz, C., Jones, J., Bizzi, S., Börger, L., Segura, G., Castelletti, A., van de Bund, W., Aarestrup, K., Barry, J., Belka, K., Berkhuysen, A., Birnie-Gauvin, K., Bussettini, M., Carolli, M., Consuegra, S., Dopico, E., Feierfeil, T., Fernández, S., Fernandez Garrido, P., Garcia-Vazquez, E., Garrido, S., Giannico, G., Gough, P., Jepsen, N., Jones, P.E., Kemp, P., Kerr, J., King, J., Łapińska, M., Lázaro, G., Lucas, M.C., Marcello, L., Martin, P., McGinnity, P., O'Hanley, J., Olivo del Amo, R., Parasiewicz, P., Pusch, M., Rincon, G., Rodriguez, C., Royte, J., Schneider, C.T., Tummers, J.S., Vallesi, S., Vowles, A., Verspoor, E., Wanningen, H., Wantzen, K.M., Wildman, L., Zalewski, M., 2020. More than one million barriers fragment Europe's rivers. Nature 588, 436–441. https://doi.org/10.1038/s41586-020-3005-2; Cote, D., Kehler, D.G., Bourne, C., Wiersma, Y.F., 2009. A new measure of longitudinal connectivity for stream networks. Landscape Ecol 24, 101–113. https://doi.org/10.1007/s10980-008-9283-y ; De Jager, A., Vogt, J., 2007. Rivers and Catchments of Europe - Catchment Characterisation Model (CCM) European Commission, Joint Research Centre (JRC) [Dataset] PID: http://data.europa.eu/89h/fe1878e8-7541-4c66-8453-afdae74692211.; Mulligan, M., van Soesbergen, A., Sáenz, L., 2020. GOODD, a global dataset of more than 38,000 georeferenced dams. Sci Data 7, 1–8. https://doi.org/10.1038/s41597-020-0362-5; Wang, J., Walter, B., Yao, F., Song, C., Ding, M., Maroof, A., Zhu, J., Fan, C., Xin, A., McAlister, J., Sikder, S., Sheng, Y., Allen, G., Crétaux, J.-F., Wada, Y., 2021. GeoDAR: Georeferenced global dam and reservoir dataset for bridging attributes and geolocations. Earth System Science Data Discussions 1–52. https://doi.org/10.5194/essd-2021-58

**Acknowledgements:** This research was partially funded by the project Dammed Fish (PTDC/CTA-AMB/4086/2021). Tamara Leite was supported by a Ph.D. grant from the FLUVIO–River Restoration and Management programme funded by Fundação para a Ciência e a Tecnologia I. P. (FCT), Portugal (UI/BD/15052/2021). Paulo Branco was financed by national funds via FCT (LA/P/0092/2020). Florian Borgwardt was financed by the MERLIN project (H2020 - 101036337). Forest Research Centre (CEF) is a research unit funded by Fundação para a Ciência e a Tecnologia I.P. (FCT), Portugal (UIDB/00239/2020). The Associate Laboratory TERRA (LA/P/0092/2020) is also funded by FCT.

8th IAHR EUROPE CONGRESS
LISBON - PORTUGAL
4-7 JUNE 2024
WATER - ACROSS BOUNDARIES
IAHR AIRH
Hosted by Spain Water and IWHR, China

# Implementation of Finite Element Techniques for the Displacement Control of Constructed Dams

M.T. Yubero[1], E. Bonet[1], LI. Sanmiquel[1], M. Bascompta[1]
[1]Manresa School of Engineering. EPSEM, UPC, Spain

## Motivation

Taking into account that Spanish dams were built between 1950 and 1990, it is understood that more than 50% of them are 50 years old or even older.

In this context, on 13 April 2021, the Spanish Ministry for Ecological Transition and the Demographic Challenge approved RD 264/2021. In it, the technical safety standards for dams and their reservoirs stipulate that these dams must be monitored due to the state and age of the infrastructures and also due to the poor control provided so far. A clear example of a dam with low control is:

The **Santa Fe dam**, located in the Catalan town of Fogars del Monclús, in Montseny (Barcelona). This is a **gravity arch dam**, **built in 1920 with very heterogeneous granite material**.

This is the main motivation for this work, which aims to do the following:

(1) To monitor a masonry dam more than 50 years old.

(2) Modelling and calibrating the behaviour of the dam condition in 3D with the FEM program KRATOS, and also with topographic measurement points deployed by the dam.

(3) Improving decision-making with respect to anomalous situations.




## Results

The results obtained from the modelling are quite similar to the topographic field measurements.

There are limitations due to the fact that it is a masonry dam, with granite blocks and mortar between blocks, whose Young's modulus values are high and low respectively. In addition, there are leaks in some areas of the face dam.

Finally, after the construction of the dam, the right abutment was enlarged, which also affects the value of the resistance.

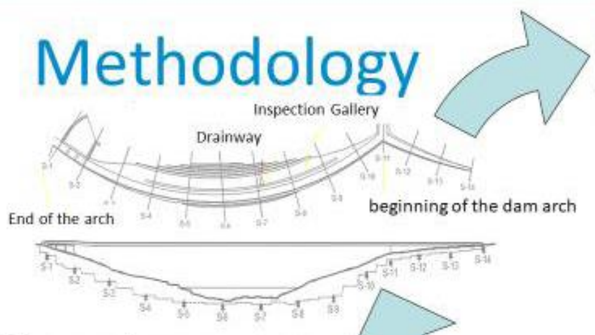
Then, taking into account all these considerations, the Young's modulus results correctly satisfy the real values in Zone 1 (left abutment and central zone), where a Young's modulus around 36.6 MPa has been obtained. In Zone 2 (right abutment) a Young's modulus of 31.6 MPa has been obtained, which is slightly lower due to the enlargement conditions and the leaks mentioned above.








## Methodology




Measured movements at topographic points along the length of the dam



Meshing (tetrahedrons) used for dam in 3D calibration

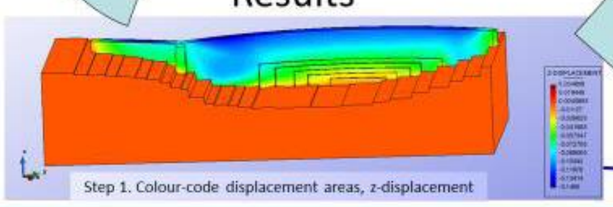
GiD SIMULATION

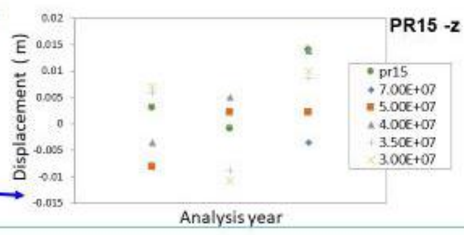
KRATOS MULTI-PHYSICS

| | Dam body | Foundations |
|---|---|---|
| Constitutive Law | Linear elastic plane strain | Linear elastic plane strain |
| Density (kg/m3) | 2600 | 3000 |
| Elastic Modulus (MPa) | Variable | 3e10 |
| Poisson Ratio | 0.25 | 0.25 |

KRATOS (Dam Application) allows to solve a coupled thermo-mechanical problem (Bofang formulation (1997), and Dirichlet conditions).

Results




| Water Level (m) | E= 70 MPa | E=50 MPa | E=40 MPa | E=35 MPa | E=30 MPa |
|---|---|---|---|---|---|
| 23.2 | -0.0587 | -0.0838 | -0.1029 | -0.1159 | -0.13 |
| 18.2 | -0.0669 | -0.0919 | -0.1064 | -0.1098 | -0.1229 |
| 20.4 | -0.0645 | -0.0897 | -0.1014 | -0.1182 | -0.1336 |
| 9.7 | -0.0679 | -0.0876 | -0.0876 | -0.1098 | -0.1236 |

*Dam displacements in z-direction for different water levels (m) and different modulus of elasticity, E (MPa)*

## Conclusions

The intricacy of the body of the Santa Fe Dam required a 3D calibration of the dam, subdividing the body into two zones due to a different behaviour characterised by the topographic points.

Zone 1 was calibrated from PR-15 and zone 2 from PR-16, which represent the points with the greatest movements because of their position in the dam. In addition, the two zones were verified with the remaining topographic points.

With the calibration of the displacements in the x, y and z directions, a modulus of elasticity was obtained for Zones 1 and 2 of 36.6 MPa and 31.6 MPa, respectively. Obtaining a model able to establish the stresses that the dam must withstand for any scenario.

Regarding the inaccuracies of the model obtained, various simplifications have been done that lower the quality of the results, such as, for example, the assumption of a stationary regime, the elimination of the galleries zone, the non-consideration of the effect of the material joints or even the consideration of the Bofang boundary condition for a dam of less than 30 m in height.

Contacts: maria.teresa.yubero@upc.edu , enrique.bonet@upc.edu

References:
**Bofang, Z. 1997.** *Prediction of water temperature in deep reservoir.* 1997.
**CIMNE. 2019. GiD**. *The personal pre and post processor. [On line]. https://www.gidhome.com.*
**Kratos Multiphysics. 2019**.*[On line] http://www.cimne.com/kratos/about_whatiskratos.asp.*

Acknowledgments: Polytechnic University of Catalonia, Operating company of the Santa Fe Dam Cimne (International Centre for Numerical Methods in Engineering).

8th IAHR EUROPE CONGRESS
LISBON - PORTUGAL
4-7 JUNE 2024
WATER - ACROSS BOUNDARIES
IAHR AIRH
Hosted by Spain Water and IWHR, China

# Assessing Shoreline Changes using Satellite and UAV Imagery: A Kinmen Coast Case Study in Taiwan

Wei-Po HUANG[1], Jui-Chan HSU[1], Chun-Jhen YE[1] , Sin-Hong LIN[1]
[1] National Taiwan Ocean University, Taiwan

## Motivation

Kinmen is one of the island close to China coast. Compared to Taiwan, these small islands have fewer survey data and are less developed. Under the threats of climate changes, coastal erosion is occurring on these small islands. With the growing population of islands and the increasing demand for coastal land, the analysis of shoreline change trends has become a crucial coastal management tool. However, as previously stated, there is a notable scarcity of monitoring data for these small islands, rendering a precise assessment unfeasible. Due to its affordability and the abundance of historical information, satellite imagery is one of the most valuable data sources for the assessment. In order to improve the use of satellite imagery for shoreline acquisition, shoreline identification and tide level correction must be automated. It should be noted that satellite imagery only provides the rate of coastal line change in two dimensions, while topographic volume changes cannot be estimated. Instead, UAV-mounted cameras are used to generate 3D topography using photogrammetry, a technique that is becoming more popular due to its efficiency and comprehensiveness. Both methodologies can be integrated to gather comprehensive historical data and can also be employed for future monitoring to ascertain the complete trend of coastal topography alterations.

## Results

In order to derive the 0m isobaths, the detected shoreline was altered using the in-situ measured beach slopes and tidal elevations. Figure 1 illustrates the differences in 0m isobath change rates estimated from the satellite images and the measured results within the same period. The satellite-derived 0m isobaths change rates are consistent with those derived from in-situ surveys. Figure 2 shows the change in 0m isobaths along the coast from 2018 to 2021 derived from Satellite images. In the summer, the 0-meter isobaths exhibited a receding pattern, whereas in the winter, they advanced towards the sea. In order to understand the change volume of the beach, photogrammetric surveys with UAV-mounted camera were conducted during the winter season of 2023 (Jan.-Apr.). The change of the topography is shown in figure 3. The results demonstrate notable accumulation along the beach face, aligning with the observed trend derived from the satellite images.

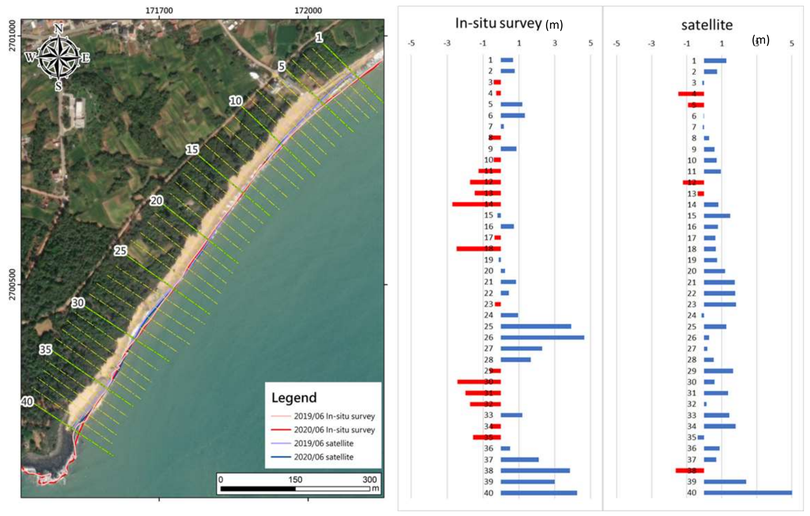



Figure 1. Comparison of 0m isobath displacements estimated by in-situ surveys and satellite images (2019-2020).




Figure 2. The 0m isobath displacements along the beach derived from satellite images from 2018 to 2021.

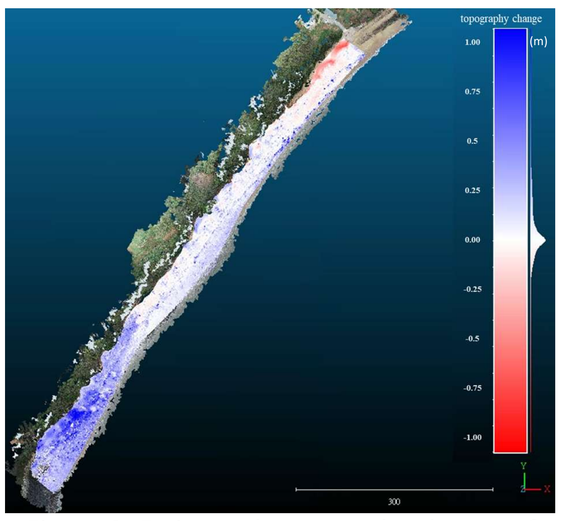



Figure 3. Estimated topography change of the beach by UAV imagery in 2023.

## Methodology

In this study, the annual and the seasonal trends of beach topography changes by using satellite imagery and aerial photographs were assessed. The coast with sea cliffs in Kinmen, one of the islands, is used as a case study. An open-source software toolkit, CoastSat, is used to obtain time-series shoreline position from satellite images. The historical shorelines can be determined by using the multilayer perceptron of a Neural Network classifier to supervise the classification. Each pixel in the image is classified into the following four categories: 'sand', 'water', 'white-water', and 'other land features'. In order to derive the 0m isobaths, the trigonometric relationships is used to alter the instantaneous waterline based on the measured coastal slope and water level elevation. In addition, Structure from Motion (SfM), a practical photogrammetric technique is used to derive three-dimensional surface reconstructions from overlapping photographs captured by the UAV's camera. A high-density point cloud of 3-D positions is then created by automatically detecting thousands of matching object and texture features in multiple, overlapping images of the ground surface.

## Conclusions

This approach enables historical changes to be supplemented by satellite imagery. Furthermore, in future endeavors, photogrammetric surveys can be employed to ascertain the volume of these changes, thereby furnishing comprehensive data for enhanced coastal management and informed risk assessment.

Contacts: Wei-Po HUANG email: a0301@mail.ntou.edu.tw

References:

Acknowledgments: This work was partly supported by the National Science and Technology Council, Taiwan, Project no. NSTC 112-2625-M-019-003-. Their support is deeply appreciated.

8th IAHR EUROPE CONGRESS
LISBON - PORTUGAL
4-7 JUNE 2024
WATER - ACROSS BOUNDARIES

IAHR AIRH
Hosted by Spain Water and IWHR, China

# Reduction of microplastic pollution in shipbuilding industry

Ivana Lučin[1], Marta Alvir[1], Siniša Družeta[1], Bože Lučin[2]
[1] Faculty of Engineering, University of Rijeka, Croatia ; [2]FlowTech d.o.o., Rijeka, Croatia

## Motivation

Microplastic (MP) particles in marine environment can act as carriers for toxic chemicals, heavy metals, and specific bacterial communities, potentially harming marine life and posing risks to human health. Antifouling paints on ship hulls are known sources of MP. However, the increased use of plastic pipes in the shipbuilding sector has intensified the problem. The process of cutting and installing plastic pipes near the sea facilitates the entry of MPs into marine ecosystems. This overlooked issue requires further investigation to quantify the amount of plastic debris it produces and to motivate industry to adopt effective measures for MP reduction.

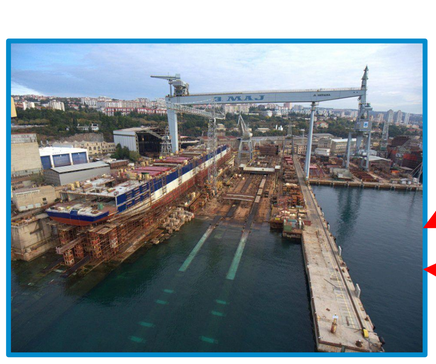


Foto: Shipyard Uljanik, Croatia

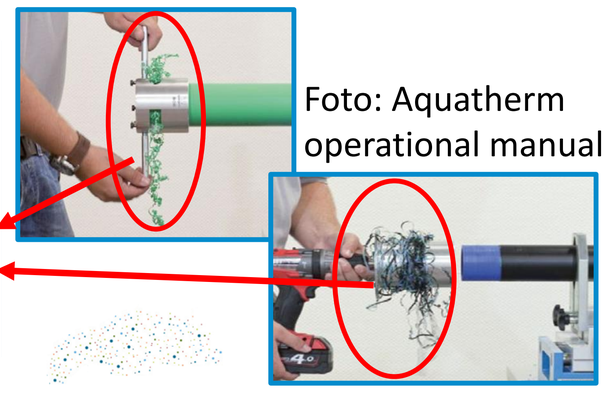


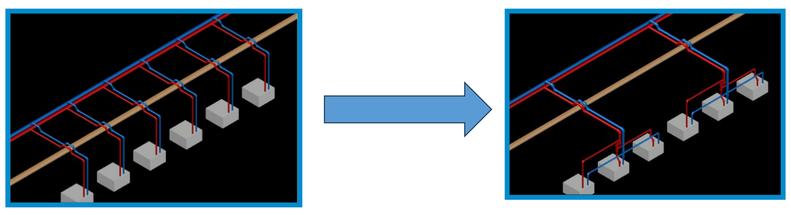
Foto: Aquatherm operational manual

airborne microplastic particles

## Results

Green 3D modelling practices, which aim to reduce cutting operations [2], can help reduce plastic debris. Based on guidelines from the plastic pipe producer for the preparation of pipe endings [1], a rough estimation of plastic debris pollution for the chosen case is presented.

Green 3D modelling practices



Plastic debris pollution reduction estimation:



14 Cola bottles – 500 ml



7 Cola bottles – 500 ml

**For the industry to adopt green strategies, exact calculations of microplastic emissions during standard operations in shipbuilding must be determined.**

Reducing operations with plastic pipes and shifting work to the pre-outfitting stage [3] can also lower the total cost of work and, consequently, reduce $CO_2$ emissions.



Design cost ↑ 6-10%

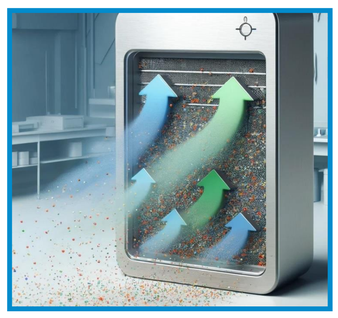


Credit: shutterstock.com

Production cost 20-30% ↓
$CO_2$ emissions ↓
Microplastic emissions ↓

A pre-designed warehouse for pre-outfitting stage, equipped with an appropriate ventilation system for capturing microplastics particles, can contribute to containing MP particles. Such solutions should be investigated in more detail using CFD simulations to determine the optimal equipment and locations for the most efficient particle capture.





Source: Generated using AI

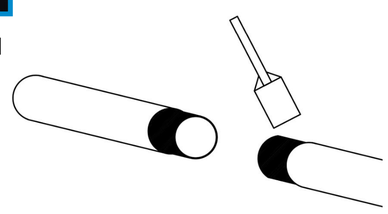
## Methodology

To the authors' knowledge, only one paper [4] has investigated the amount of particles produced by cutting pipes in open area. In shipbuilding, additional preparation of pipe endings is required, which also generates plastic debris.

One scenario was chosen with the distribution of hot and cold water to consumers. Based on the guidelines from the plastic pipe producer [2] for preparation of pipe edges, estimations of plastic debris were made based on the estimated weight of the material that needs to be removed .



Source: Generated using AI



Pipe ending preparation

## Conclusions

The adaptation of the shipbuilding industry to novel ecological demands can require a substantial amount of time. This may be due to the significant investments and time required to implement new procedures. To accelerate this process, scientists must establish proper quantification methods, allowing the industry to see the exact impact they are having on the environment and how adopting new solutions can help reduce this negative impact. **Future work should focus on estimating microplastic particle emissions during the cutting of various pipe sizes and materials , using equipment common in shipbuilding to replicate real operating conditions as closely as possible.**

Contact: ivana.lucin@riteh.uniri.hr

References: [1] AG, G.I.S. Application technique, Geberit HDPE/Silent-DB20, 2022. Available online: https://cdn-geberit-country- 619sg.prod.web.geberit.com/

[2]Lučin, B., et al.(2023). Strategies for Green Shipbuilding Design and Production Practices Focused on Reducing Microplastic Pollution Generated during Installation of Plastic Pipes. Journal of marine science and engineering, 11(5), 983.

[3] Kunkera, Zoran, Tihomir Opetuk, Neven Hadžić, and Nataša Tošanović. "Using digital twin in a shipbuilding project." Applied Sciences 12, no. 24 (2022): 12721.

[4] Luo, Y., Al Amin, M., Gibson, C. T., Chuah, C., Tang, Y., Naidu, R., & Fang, C. (2022). Raman imaging of microplastics and nanoplastics generated by cutting PVC pipe. Environmental Pollution, 298, 118857.

8th IAHR EUROPE CONGRESS
LISBON - PORTUGAL
4-7 JUNE 2024
WATER - ACROSS BOUNDARIES

IAHR AIRH
Hosted by Spain Water and IWHR, China

# Unbalanced sediment flux caused by tidal pumping and residual circulation in the meso-tidal Yeosu Bay

Ho Kyung Ha[1*], Su In Kim[1], Jun Young Seo[1], Jae-Hun Park[1], Pyeong Joong Kim[2]
[1] Department of Ocean Sciences, Inha University, Incheon, Republic of Korea
[2] Underwater Survey Technology 21, Incheon, Republic of Korea

## Abstract

In the western (M1) and eastern (M2) channels of Yeosu Bay, two mooring systems with acoustic Doppler current profilers were installed to investigate the transport processes of suspended sediments. Over the mooring period, the currents (M1: -1.10–0.80 m $s^{-1}$; M2: -0.85–0.85 m $s^{-1}$) were mainly dominated by ebb tides. Two-layered residual currents developed by the freshwater discharge at M2 (< 0.24 m $s^{-1}$) were higher than that at M1 (< 0.16 m $s^{-1}$). Even if the same current-induced shear stress as M2 was applied to the bed, M1 could be resuspended with higher SSC (max: 233 mg $l^{-1}$) to reach the water surface. This is because the bed sediments at M1 have relatively low cohesive sediment (mud) content and shell fragments. These differences in current and sediment resuspension created an unbalanced sediment flux. The seaward sediment flux at M1 was mainly driven by tidal pumping, whereas the landward flux at M2 was mainly driven by residual currents. Although the sediment fluxes tended to be compensated and balanced mutually by tidal cycles over the entire period, the sediment flux at M2 was about twice higher than that at M1. Suspended sediments exhibited an influx pattern into the bay.

## Study area

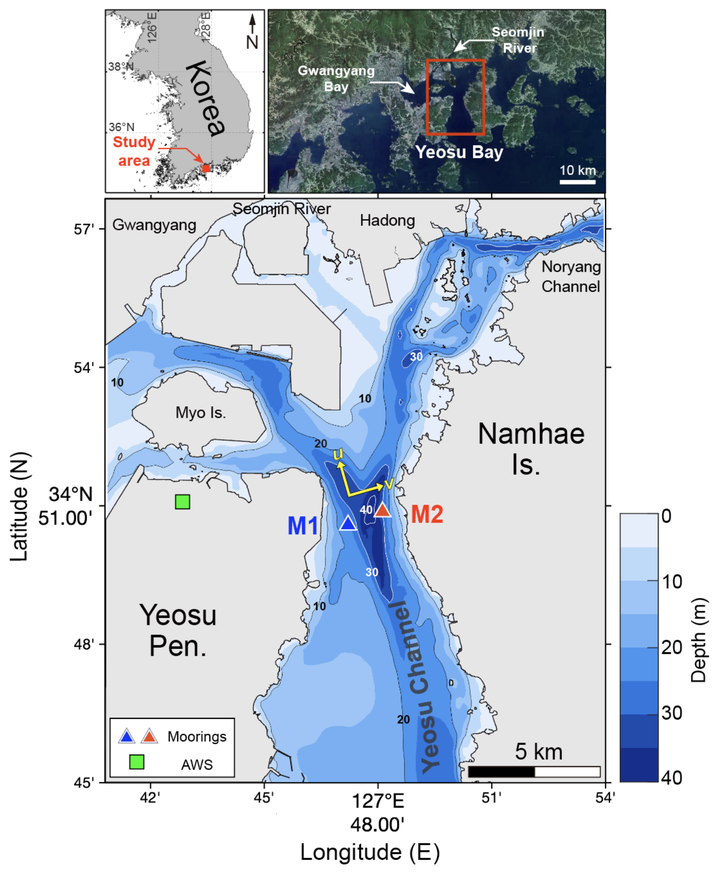



**Figure 1.** Map of study area. Two acoustic Doppler current profilers (ADCPs) were deployed at western (M1) and eastern (M2) parts of Yeosu Bay, Korea.

## Sediment dynamics

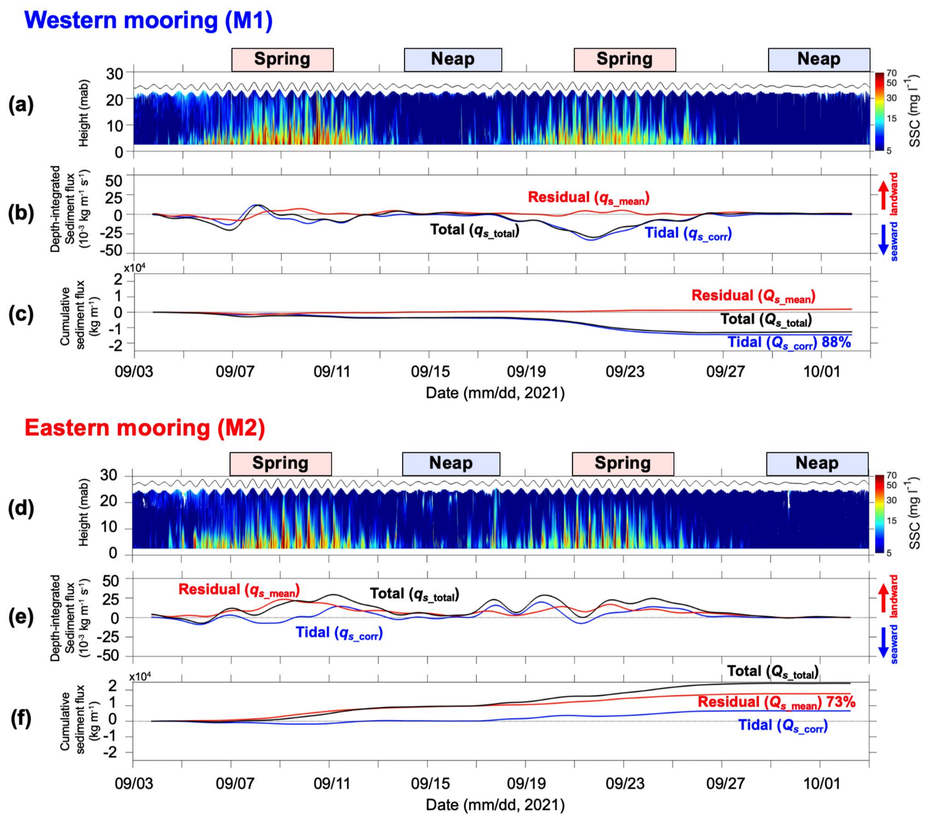



**Figure 3.** Time series of (a and d) SSC profiles, (b and e) decomposed sediment fluxes, and (c and f) cumulative sediment fluxes. $q_{s_total}$ is the depth-integrated sediment flux (kg $m^{-1}$ $s^{-1}$) from the bottom to the water surface and $Q_{s_total}$ is the total sediment flux (kg $m^{-1}$) over four weeks.

## Hydrodynamics

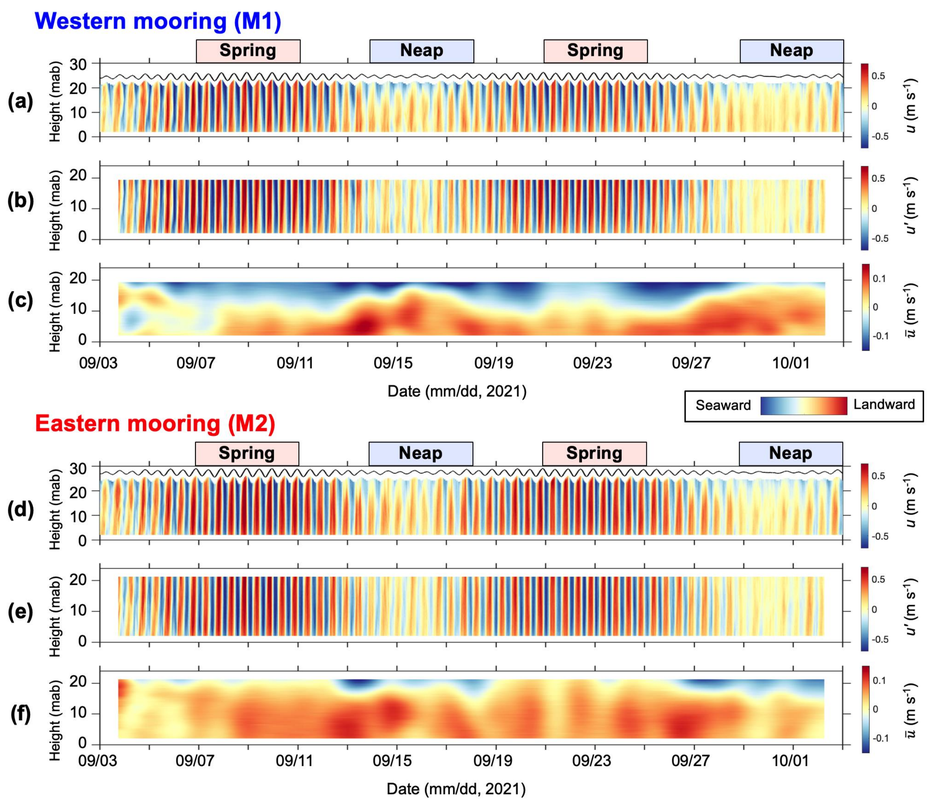



**Figure 2.** Time series of (a and d) along-channel current velocity ($u$), (b and e) tidal current velocity ($u'$) and (c and f) residual current velocity ($\bar{u}$) during the mooring period.

## SSC asymmetry during flood and ebb

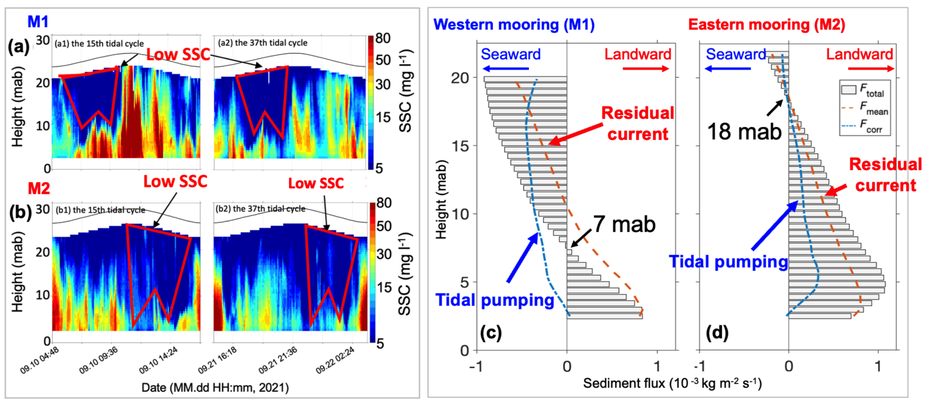



**Figure 4.** Examples of remarkably low SSCs in upper water column during (a) 15th and (b) 37th tidal cycle. (c and d) Tide-averaged suspended sediment flux ($F_{total}$). The red and blue dashed lines indicate the advective flux ($F_{mean}$) and tidal pumping flux ($F_{corr}$), respectively.

## Conclusions

- The seaward sediment flux at TM01 was mainly driven by tidal pumping (88%), whereas the landward flux at TM02 was mainly driven by residual currents (73%).
- SSC variation in TM01 was primarily influenced by local sediment resuspension, while in TM02, it was predominantly influenced by the advection.
- This study highlights the important roles of tidal pumping and residual currents in controlling sediment transport in meso-tidal bay system.

**Contacts:** *hahk@inha.ac.kr (H.K. Ha)

**Acknowledgments:** This research was supported by “Development of 3-D Ocean Current Observation Technology for Efficient Response to Maritime Distress” (20210642) of Korea Institute of Marine Science and Technology Promotion (KIMST) funded by the Ministry of Oceans and Fisheries, Korea.

8th IAHR EUROPE CONGRESS
LISBON - PORTUGAL
4-7 JUNE 2024
WATER - ACROSS BOUNDARIES
Hosted by Spain Water and IWHR, China

# Machine Learning Analysis of Elemental Variation in Sediment Cores of the Boka Kotorska Bay – Adriatic Sea

Vaso MANOJLOVIĆ[1], Milena RADOMIROVIĆ[1], Bojan TANASKOVSKI[2], Chiara CANTALUPPI[3], Sandro DEGETTO[3], Slavka STANKOVIĆ[1]

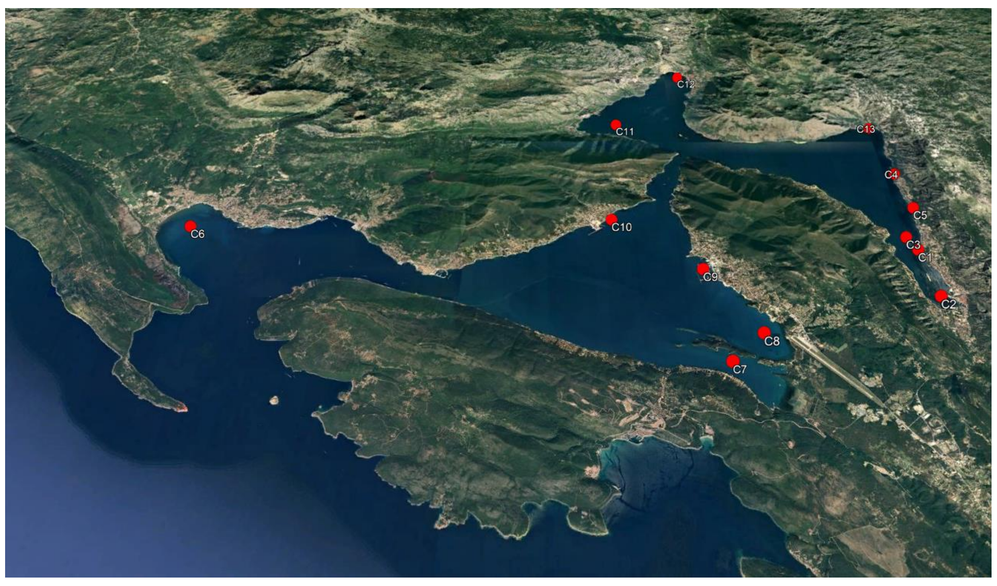
[1] University of Belgrade, Faculty of Technology and Metallurgy, Serbia
email: v.manojlovic@tmf.bg.ac.rs; mradomirovic@tmf.bg.ac.rs; slavka@tmf.bg.ac.rs
[2] Military Technical Institute, Serbia, email: bojantanaskovski@yahoo.com
[3] Italian National Research Council, Italy, email: chiara.cantaluppi@cnr.it; sandro.degetto@alice.it

## Motivation

Marine sediments represent a critical component of coastal ecosystems and serve as indicators of environmental change. Human activities have caused negative changes in the natural state of sediments, especially in the 20th century, due to reflexive interactions between humans and the environment. Through the analysis of sediment cores with the application of statistical and numerical model simulations, it is possible to ascertain the occurrence and magnitude of events caused by anthropogenic factors. Trace element contamination, which is directly related to numerous human activities and perturbations, has been a serious environmental issue in coastal areas, as well as in river basins, since the 1980s. Understanding the elemental composition, origin, and properties that affect the complex biogeochemical and sedimentological composition of bottom marine sediments is essential for determining the trajectories and sources of elements and their anthropogenic inputs within the ecosystem.

## Results

Concentration profiles of the analyzed elements in sediment cores demonstrated their temporal distribution pattern at different section depths. The Extra Trees (Extremely Randomized Trees) Regression method was employed to predict the average age of sections in undated sediment cores based on the different elemental distributions and other related features. Using the results of 137Cs and 210Pb dating, elemental composition of sedimentary layers, and machine learning model predictions, an approximate 95-year record of element deposition in sediment cores was determined. The analysis showed the simultaneous relative importance of each input to the model results, with an $R^2$ on the test set of 0.93 and a mean absolute error in year units of 8.11, demonstrating the model's excellent predictive ability. This integrated approach and comprehensive analysis increased the knowledge of geochemical processes in the sedimentary system over the last 100 years.



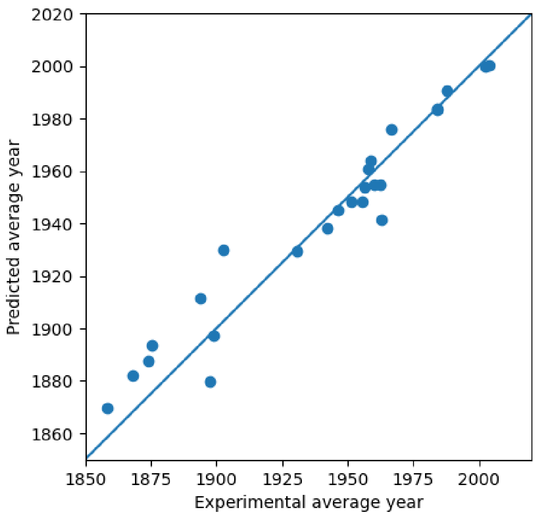




**Fig.** a) Sampling sites in the Boka Kotorska Bay (Montenegro), Adriatic Sea; b) The relationship between the experimentally obtained values (outputs) and calculated parameters using the obtained model (target)

## Methodology

This paper presents data obtained by the analysis of 13 sediment cores (C1-C13) collected from the coastal areas of the Bay in 2005 (C1-C5) and 2007 (C6-C13) using a core sampler with an inner diameter of 8.2 cm. After sampling, the cores were carefully sliced into 9 to 15 sections, with a total of 181 sections obtained from all core samples. Energy dispersive X-ray fluorescence spectroscopy (ED-XRF) was used to quantify major (Al, Ca, Cl, Fe, K, Mg, Mn, Na, P, S), minor, and trace elements (As, Ba, Br, Cd, Ce, Cr, Cs, Cu, Ga, Hg, I, La, Nb, Nd, Ni, Pb, Rb, Sb, Sn, Sr, Th, U, V, Y, Zn, Zr). High-resolution gamma-ray spectrometry was used for the determination of activity concentrations of radionuclides (137Cs, 210Pb). The experimental dataset included variables such as sampling dates and locations with corresponding coordinates, average section depths of analyzed sediment cores, average section ages of dated cores, and elemental content of each layer of the analyzed sediment cores. The Extra Trees (Extremely Randomized Trees) Regression method was employed to predict the average age of sections in undated sediment cores based on the different elemental distributions and other related features used for predictive modeling.

## Conclusions

The proposed methodology demonstrated the utility of machine learning for the interpretation of geochemical data. The integration of a predictive machine learning approach to investigate depositional changes in down-core chemistry and elemental variations in undated sediment cores in the Boka Kotorska Bay successfully predicted the average age of sediment core sections with high accuracy. The analysis results showed the simultaneous relative importance of each of the inputs to the model results, demonstrating the model's excellent predictive ability. This comprehensive analysis increased the knowledge of geochemical processes in the sedimentary system over the last 100 years. The findings provide a useful basis for future research that will address the determination of local background concentrations from uncontaminated core layers, as well as the chronological accumulation and deposition of metals in the sediments of the Boka Kotorska Bay.

Contacts: Vaso Manojlović, email: v.manojlovic@tmf.bg.ac.rs , phone: +381643531622

Acknowledgments: This work was supported by the Ministry of Education, Science and Technological Development of the Republic of Serbia (Contract No. 451-03-47/2023-01/200287)

# AQUABREAK: An Innovative Nature-Based Solution for Coastal Resilience

Raylton Bendô[1], Bárbara Proença[1], Andreia Gomes[1], Ivana Bosnic[1], Lénia D. Rato[1], Diogo Mendes[2], Diogo Fonseca[1]

[1] HAEDES; [2]CERIS - IST

8th IAHR EUROPE CONGRESS
LISBON - PORTUGAL
4-7 JUNE 2024
WATER - ACROSS BOUNDARIES
IAHR AIRH
Hosted by Spain Water and IWHR, China

## Motivation

Coastal protection measures against natural hazards are usually achieved through seawalls and breakwaters, which are rigid structures that require ongoing and expensive maintenance. In addition, these have high initial costs that do not always represent an effective protective measure, such as the case in Furadouro (Ovar) (Tavares et al. 2021).

Several studies have previously addressed the effectiveness of submerged aquatic canopies in mitigating wave energy attenuation. For instance, Mork (1996) reported a wave energy reduction ranging from 70% to 85% across 258-meter-long kelp natural kelp forests. Thus, a nature-based solution (NBS), based on a seaweed aquaculture field appears as a potential alternative or complement to coastal protection, both in economic and ecological perspectives. However, the documented wave conditions under testing do not allow to understand the effectiveness of such biologically based floating structures (floating breakwater – FBW) to apply them as coastal resilience solutions . Here, with the AQUABREAK project, we aim to assess this subject and contribute to filling this apparent research gap and contribute to future applications.

## Methodology

### Physical Model Experiment

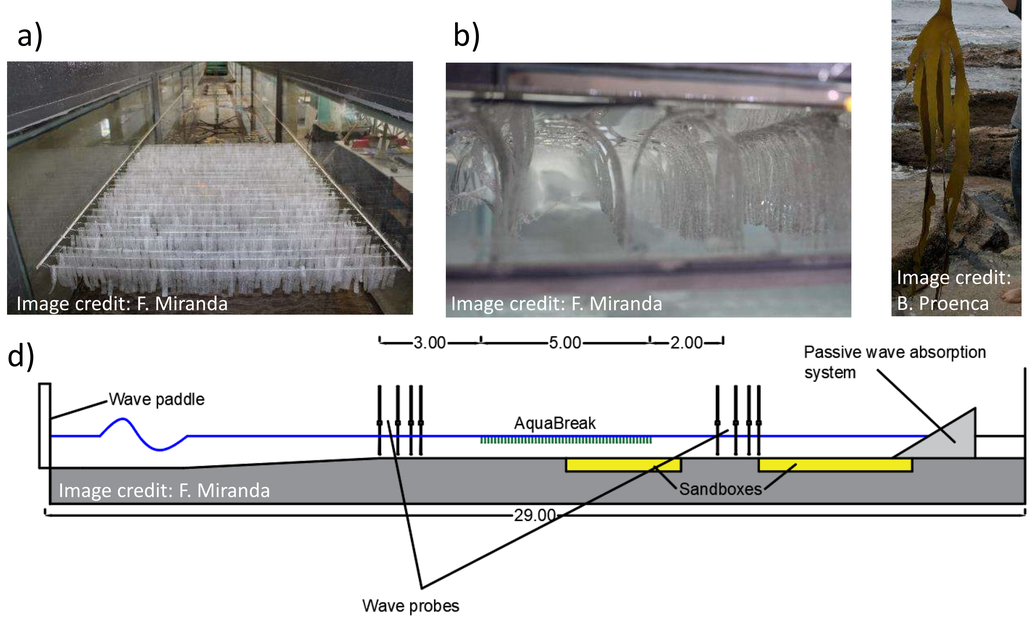



**Fig.1** (a) Physical Model Experiment; (b) Mimicking algae; (c) Example of real algae; (d) Wave flume scheme.

56 Experiments
- 2 water levels;
- 7 wave conditions (*Hm0* and *Tp*)
- 3 FBW length + 1 without FBW

### Numerical Modelling

SWASH
*Simulating WAves till SHore*

Vegetation module:
- Morison Eq. (rigid cylinder)
- Height - $hv$ = 0.075 m
- Diameter - $dv$ = 0.007 m
- Density - $Nv$ = 1600 stems/m$^2$
- Drag Coef. - *Cd* variable

## Results

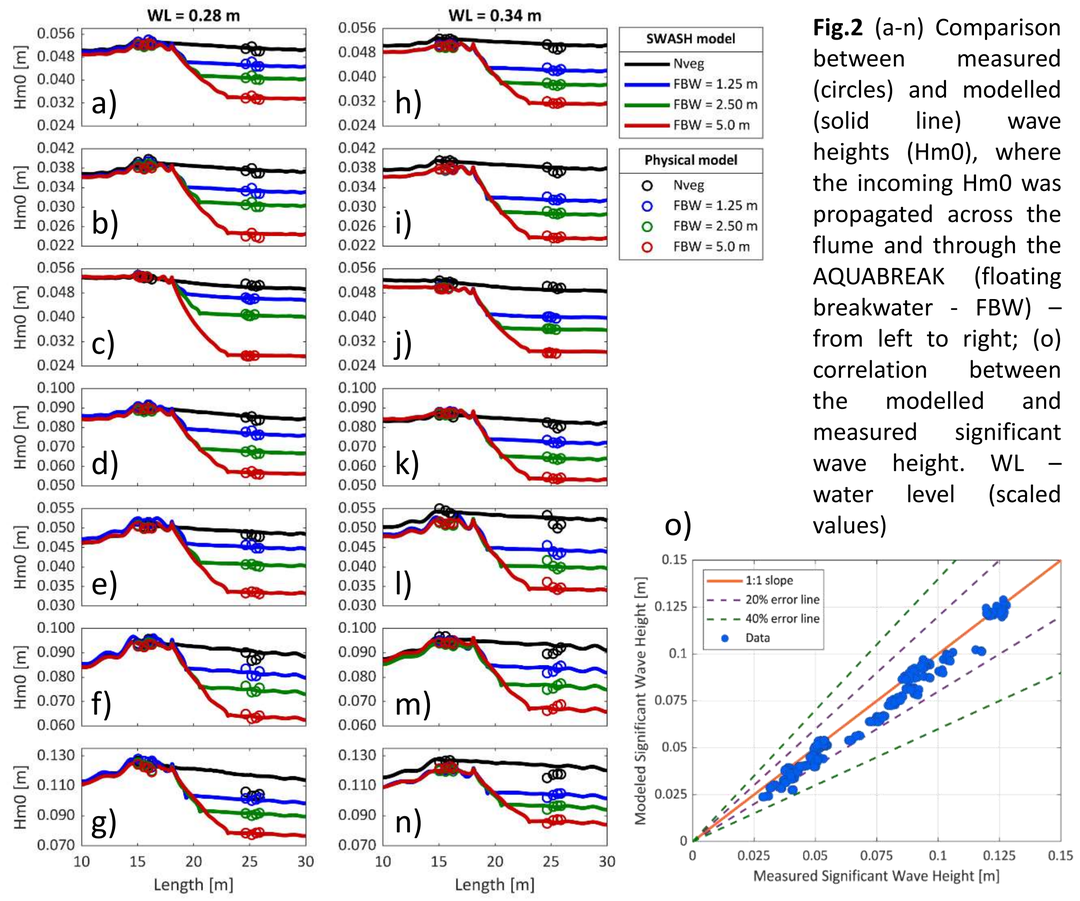



**Fig.2** (a-n) Comparison between measured (circles) and modelled (solid line) wave heights (Hm0), where the incoming Hm0 was propagated across the flume and through the AQUABREAK (floating breakwater - FBW) – from left to right; (o) correlation between the modelled and measured significant wave height. WL – water level (scaled values)

Statistical metrics show small errors and a strong correlation coefficient:

- Root Mean Square Percentage Error (RMSPE) of 3.97%.
- BIAS of 0.023.
- Correlation coefficient close to 1.
- Wave attenuation of 11%, 20% and 33% for 50 m, 100 m and 200 m of FBW length.

## Conclusions

Nature-based solutions represent innovative approaches to coastal protection measures using submerged canopies. This study showed the effectiveness of a living floating breakwater to induce wave attenuation for 14 wave conditions. These results are relevant to support the design features such as the field length and its relative positioning to the coast. These parameters are essential for an optimized wave energy dissipation system and consequent coastal inundation reduction in coastal implementations. In addition, NBSs represent a step toward achieving the EU's CO2 emissions targets.

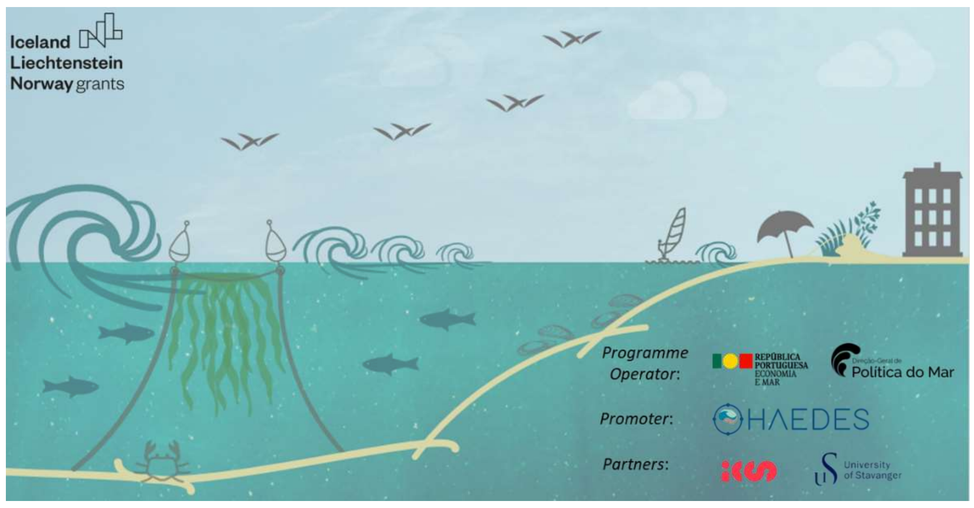



**Fig.3** AQUABREAK – Aquaculture Living Breakwater for Coastal Protection and Sea Decarbonization.

**Contacts:** raylton.bendo@haedes.eu; barbara.proenca@haedes.eu; diogo.fonseca@haedes.eu

**References:** Miranda, F., Proença, B., Fonseca, D., Haerens, P., Bento, A.M., Siriwardane, S., Pavlou, D., Rosa Santos, P., Taveira Pinto, F. and Fazeres Ferradosa, T. (2024). AquaBreak Project: A Nature-Based Solution Towards Food Demand and Coastal Protection. In Analytical and Experimental Methods in Mechanical and Civil Engineering. DOI: 10.1007/978-3-031-49723-0_7

Mork, M. (1996). The effect of kelp in wave damping. Sarsia, 80(4), 323–327. https://doi.org/10.1080/00364827.1996.10413607

Tavares, A. O., Barros, J. L., Freire, P., Santos, P. P., Perdiz, L. and Fortunato A. B. (2021) A coastal flooding database from 1980 to 2018 for the continental Portuguese coastal zone. Applied Geography, 135, 102534

**Acknowledgments:** This work was performed in the scope of the AQUABREAK – Aquaculture Living Breakwater for Coastal Protection and Sea Decarbonization project, Grant code PT-INNOVATION-0093, funded by the "Blue Growth" Program of the EEA Grants Portugal 2014-2021

8th IAHR EUROPE CONGRESS
LISBON - PORTUGAL
4-7 JUNE 2024
WATER - ACROSS BOUNDARIES
Hosted by Spain Water and IWHR, China

# The coastal challenge of climate adaptation: systemic approaches

**Marion PERNEY** [1,2], Bruno BARROCA[1], Maria Fabrizia CLEMENTE[2], Charlotte HEINZLEF[3], Mattia Federico LEONE[2] , Isabelle THOMAS[4], Damien SERRE [3]
[1] UGE, Lab'Urba, France; [2]UNINA,DiARC, Italy; [3]UPS, UVSQ, CEARC, France; [4]UdeM, Canada

## Motivation

The number of climate-related natural disasters, and especially floods, has more than doubled over the past decade, according to the United Nations Office for Disaster Reduction. Among these disasters, the risk of flooding appears to be the most "damaging". During the period 2000-2019, these disasters cost the lives of more than one million people and caused almost 3,000 billion dollars of economic losses (UNDRR, 2020). Also, the increasing complexity of sociotechnical systems makes flood risk management difficult.

Human concentration (37 per cent of the world's population lives within 100 km of the coast at a population density twice the global average (UNEP, 2017), and urban population contribute to increase flood risk in such areas. The need to innovate in risk management approaches is explained by the awareness of the lack of consideration of vulnerable territories.

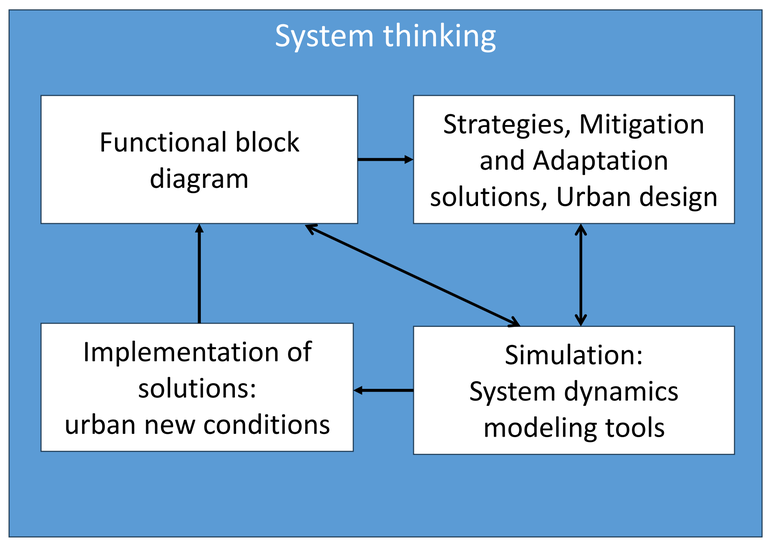
There is a need to provide a **conceptual framework** and to present **practical applications** concerning the development of **dynamic tools and methods** for **assessing the relevance of territorial adaptation measures** in urban coastal areas.

## Methodology

The methodology leading to an operational implementation of adaptation solutions in a systemic perspective in coastal areas is, first, based on a **functional analysis** of technical systems and urban components. Then, this analysis is carried out using a **functional block diagram** representing and modelling the urban systems to identify eventual disruptions under coastal flooding events.

In terms of simulation, to assess adaptation measures, this functional approach is deployed using two "tools" approaches:

- **spatial analyses based on GIS processes**, generalized from open-source data,
- **system dynamic analyses** with the development of a stock and flow model to simulate the effectiveness of technical measures in them ability to contrast flood risks under different climate event scenarios.




## Results

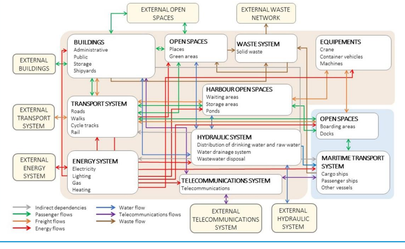
Tools' approaches used on diverse case studies, selected because of their location in particularly vulnerable areas: coastal submersion

| Case study | Spatial analyse | Functional block diagram | Simulation System Dynamics | Mitigation and Adaptation solutions | Implementation |
|---|---|---|---|---|---|
| Naples | x | x | x | x | x |
| Le Havre | x | x | | x | |

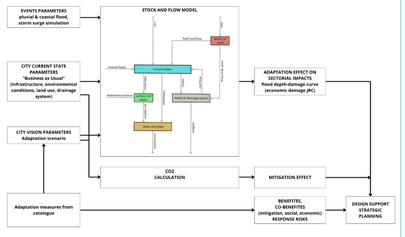
Spatial analyse

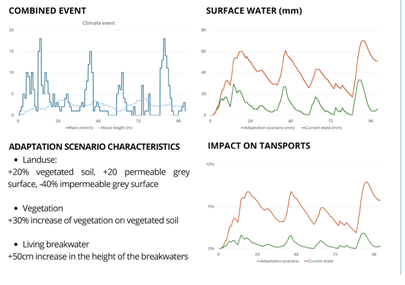



Functional block diagram




Simulation

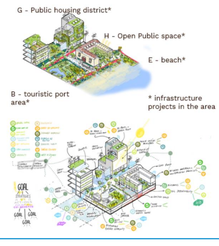



Adaptation solutions




Implementation




## Conclusions

**Port cities** play a strategic role in the transportation of goods and people, acting as **catalysts for the development of urban and regional economies** but are areas **highly vulnerable to climate change impacts**. Transformation of port infrastructures is essential to reduce physical impacts on facilities and logistics activities.

This methodology highlights the need to address the issue of **climate adaptation process** at several stages in the design of a **resilient coastal city**, from the study of vulnerability, the identification of the sectors and urban systems impacted, the identification of related adaptation and mitigation solutions, their effectiveness in countering risks, and finally, the opportunity to **generate urban renewal**. The method and the tools presented can be invaluable in helping **urban planners** in their **decision-making**.

Contacts: bruno.barroca@univ-eiffel.fr, mariafabrizia.clemente@unina.it, marion.perney@unina.it

References:
Clemente, M. F. and Barroca, B.: Integrating Natural Hazards into the Planning and Design of Critical Infrastructures in Urban Coastal Areas. A Case Study in Le Havre, France, EGU General Assembly 2023, Vienna, Austria, 23–28 Apr 2023, EGU23-12732
Perney, M., Moreno, M., Giannino, F., and Leone, M. F.: System dynamics for water management in coastal cities under multi-risk scenarios, EGU General Assembly 2024, Vienna, Austria, 14–19 Apr 2024, EGU24-15592

Acknowledgements: The research, is central subject of a PhD thesis and linked to the Horizon Europe project "KNOWING Framework for defining climate mitigation pathways based on understanding and integrated assessment of climate impacts, adaptation strategies and societal transformation" (2022-2026) is funded by the European Union under the Horizon Europe programme (GA 1011056841).

8th IAHR EUROPE CONGRESS
LISBON - PORTUGAL
4-7 JUNE 2024
WATER - ACROSS BOUNDARIES

IAHR AIRH
Hosted by Spain Water and IWHR, China

# Occurrence of Microplastic in Thai Aquatic Environment

Sudarshan Kurwadkar[1], Grace Natalia[2], Suwanna Boontanon[2], Somchai Pathomsiri[2]
[1] California State University, Fullerton, USA; [2]Mahidol University, Salaya, Thailand

## Motivation

Microplastics are ubiquitous, as evidenced by their frequent detection in various environmental matrices, including lakes, rivers, marine, estuarine, and freshwater environments. Numerous studies have highlighted the occurrence, size, type, form, and chemical composition of microplastics. However, most of this research originated from developed countries, which have dedicated resources. Conversely, there's a noticeable gap in the literature concerning the occurrence of microplastics in the aquatic environments of developing countries, particularly within South Asian regions like Thailand. This study aims to fill that gap by documenting the occurrence and concentration of microplastics in both water and sediment within Thailand's coastal zones. Microplastic pollution of water bodies in Thailand is largely due to inadequate waste management practices, including improper disposal of plastics, insufficient recycling efforts, and the release of untreated sewage, particularly from transient coastal populations. Our motivation is to identify and document the occurrence and abundance of microplastics in key locations such as the Gulf of Thailand, the Chao Phraya River Estuary, Bandon Bay, the Songkhla Lagoon, Tapi-Phumduang River System, Nonthaburi and Rayong. This work is vital in understanding the extent of microplastic pollution in Thailand and may drive improvements in waste management and environmental protection strategies.

## Results

Results shows that surface water, sediments, and wastewater in Thailand have varying amounts of microplastics, with highest mean concentrations ranging from 48 ± 8 x$10^3$ pcs/L, >2 x$10^5$ pcs/kg, and 76-192 pcs/L, respectively (Figures 1&2).

Sediments in the coastal areas, specifically the Eastern Gulf of Thailand, appear to be highly impacted by microplastic compared to the Western Side (Fig 1). Very high microplastic concentration was detected in the Rayong area in sediment and water samples. Chao Phraya River Estuary has a high microplastics concentration (Fig. 2)

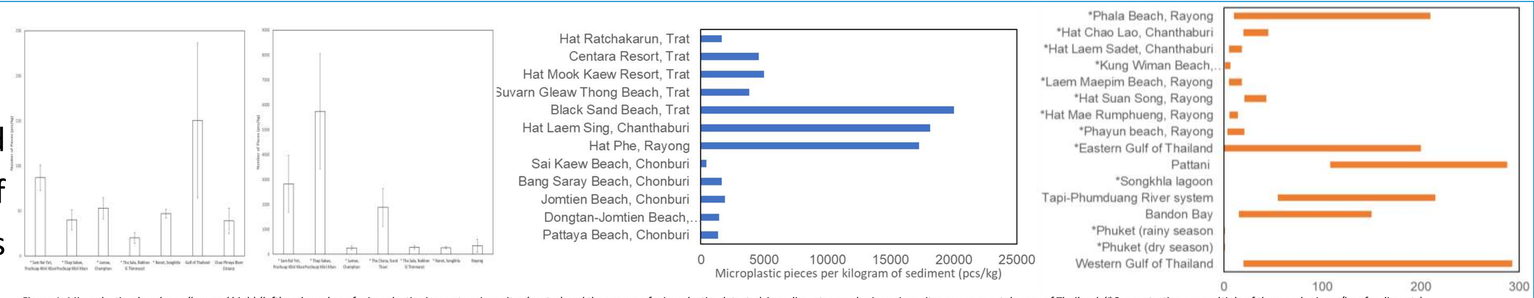



*Figure 1: Microplastic abundance (low and high) (left) and number of microplastic pieces at various sites (center) and the ranges of microplastics detected in sediments samples in various sites across coastal areas of Thailand. (*Concentration are multiple of thousands pieces/kg of sediments)*

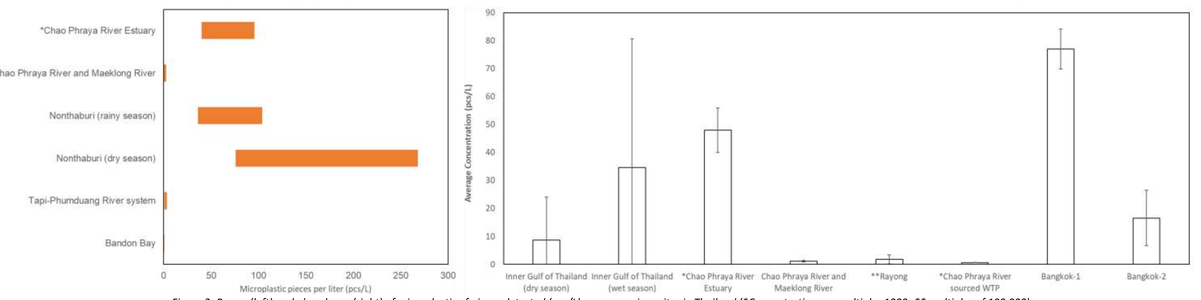



*Figure 2: Range (left) and abundance (right) of microplastic of pieces detected (pcs/L)s across various sites in Thailand (*Concentration are multiples 1000; ** multiples of 100,000)*

## Methodology

Extensive data on the type and size of the microplastics in water and sediment samples was collected from across the coastal areas of Thailand. The objective is to understand the magnitude and abundance of microplastic pollution in the Thai aquatic environment. Figure 3 shows the locations of various sampling sites with data tabulated and analyzed. These sites represent coastal areas frequented by seasonal tourists, and the likelihood of microplastic pollution is high due to the use of disposable plastic. These sites also include the areas that include sewage treatment plant outfalls and river discharges, specifically from the major rivers such as Chumphon, Tapi, Pumduang, and Pakphanang. The sampling sites were selected based on the ocean surface circulation critical for the distribution and accumulation of microplastics.

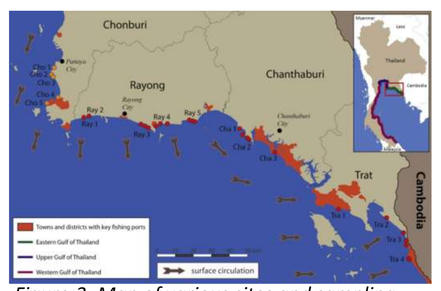



*Figure-3: Map of various sites and sampling locations (Source: Bissen and Chawchai, 2020)*

Various data was collected from the selected sites, including surface water, wastewater, drinking tap water, and sediments. The data was carefully tabulated based on the types of plastics and their respective size ranges observed in water and sediment samples. The data for sediment samples was recorded as the number of pieces per kilogram of sediments, while the microplastic concentration was recorded in pieces per liter of the water sample.

## Conclusions

Analysis of the compiled data shows widespread occurrence of microplastics of varying sizes and types throughout the Thai coastal areas. Most plastics are not biodegradable due to their chemical resilience; they grow brittle over time and disintegrate into tiny pieces. In addition to natural weathering, physical forces, such as the long-term effect of waves, further break down plastics into varying shapes and sizes. In Thai coastal areas, tiny plastic fragments of varying sizes ranging from 0.05 to 5 mm were abundantly detected in water and sediments. Specifically, the coastal areas frequented by seasonal tourists coupled with industrial complexes and illicit dumping of plastics of various forms have significantly impacted the Thai coastal areas. The continued occurrence of microplastics in the aquatic environment will adversely affect the aquatic food web since marine biotas often confuse microplastics with food, leading to their bioaccumulation. Ingestion of significant amounts of varying sizes and types of microplastic may adversely impact marine life due to their bio-accumulative potential, thus serving as a primary pathway to the food web. Ingestion of microplastic-laden seafood may adversely affect human health. This study has shown the extent, type, and size of microplastic pollution in Thai aquatic resources for the first time, justifying the need to protect and preserve Thailand's water resources.

Contacts: Professor Sudarshan Kurwadkar (skurwadkar@fullerton.edu); Professor Suwanna Boontanon (suwanna.boo@mahidol.ac.th)

References:

1. Bissen, R., Chawchai, S. (2020). Microplastics on beaches along the eastern Gulf of Thailand – A preliminary study, Marine Pollution Bulletin, 157,111345, https://doi.org/10.1016/j.marpolbul.2020.111345
2. Thepwilai, S., Wangritthikraikul, K., Chawchai, S., Bissen, R. (2021). Testing the factors controlling the numbers of microplastics on beaches along the western Gulf of Thailand, Marine Pollution Bulletin, 168, 112467, https://doi.org/10.1016/j.marpolbul.2021.112467.

Acknowledgments: Professor Sudarshan Kurwadkar was supported through the Short-term Visiting Scholarship Program (Fiscal year 2023) sponsored and managed by the Mahidol University, Salaya Campus, Thailand.

8th IAHR EUROPE CONGRESS
LISBON - PORTUGAL
4-7 JUNE 2024
WATER - ACROSS BOUNDARIES

IAHR AIRH
Hosted by Spain Water and IWHR, China

# A surrogate-based optimization of urban-roofing strategies for flash flood control

JiHyun Kim[1], Suyeon Choi[1], Mahdi Panahi[1], and Yeonjoo Kim[1]
[1] Department of Civil and Environmental Engineering, Yonsei University, Seoul, South Korea

## Motivation

The ongoing climate change is expected to increase urban climate risks substantially, therefore various efforts have been made to mitigate such hazards, such as installation of green or cool roofs on the urban buildings. Considering the costs required for the installation, prior to any actual execution, it is necessary to figure out the optimal configuration of roofing strategies (i.e., roof type and distribution). Such prior assessment can be performed using a statistical or numerical model with various scenario implementations, yet requires high computational power and time. In this study, we developed a deep learning-based surrogate model to optimize roofing strategies for urban flash flood control.

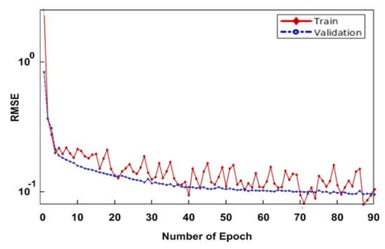
## Results

### Base framework (WRF-UCM) evaluation

Overall acceptable performance when the outputs of monthly $T_{avg}$ , $P_{total}$, and $R_h$ during 2000-2009 were compared against KMA-ASOS

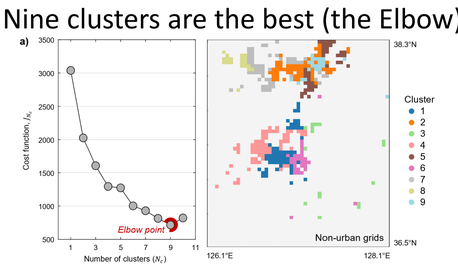
| Station | | Temperature | | Precipitation | | Relative Humidity | |
|---|---|---|---|---|---|---|---|
| ID | °N, °E | r | RMSE (°C) | r | RMSE (mm) | r | RMSE (%) |
| 98 | 37.90, 127.06 | 0.83 | 1.3 | 0.60 | 158.9 | 0.78 | 8.0 |
| 102 | 37.97, 124.63 | 0.75 | 1.5 | 0.61 | 41.1 | 0.56 | 10.0 |
| 108 | 37.57, 126.96 | 0.81 | 1.3 | 0.55 | 152.0 | 0.76 | 7.2 |
| 119 | 37.27, 126.98 | 0.82 | 1.3 | 0.55 | 183.4 | 0.69 | 7.7 |
| 202 | 37.48, 127.49 | 0.86 | 1.2 | 0.58 | 174.6 | 0.83 | 7.2 |

### Multi-ResNet accuracy: 73%



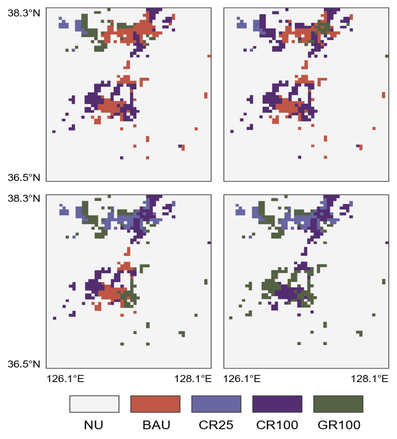

### Urban clustering

Nine clusters are the best (the Elbow)




### Multi-type roof scenarios

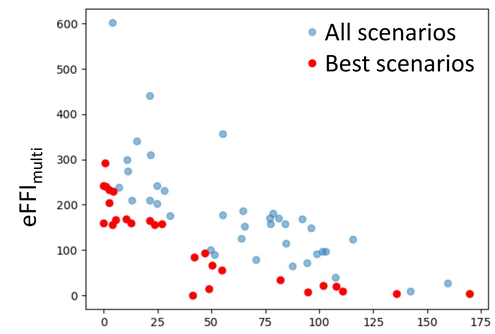
Four roof schemes on nine clusters, therefore total of 262,144 scenarios




Example of roof scenarios

### Optimal roof configuration

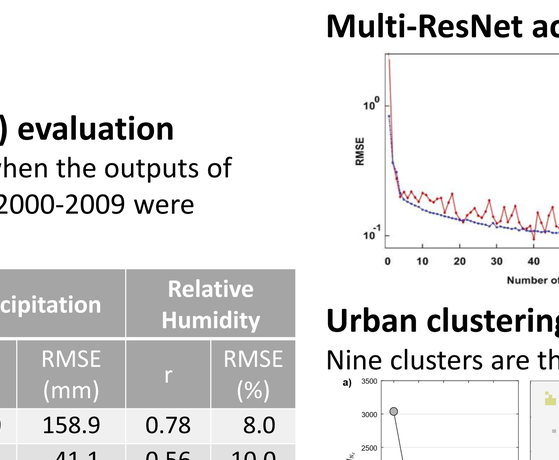
Costs of the roof scenarios with lower flash floods were generally higher. Based on the Pareto surface, best roof scenarios were decided as below.



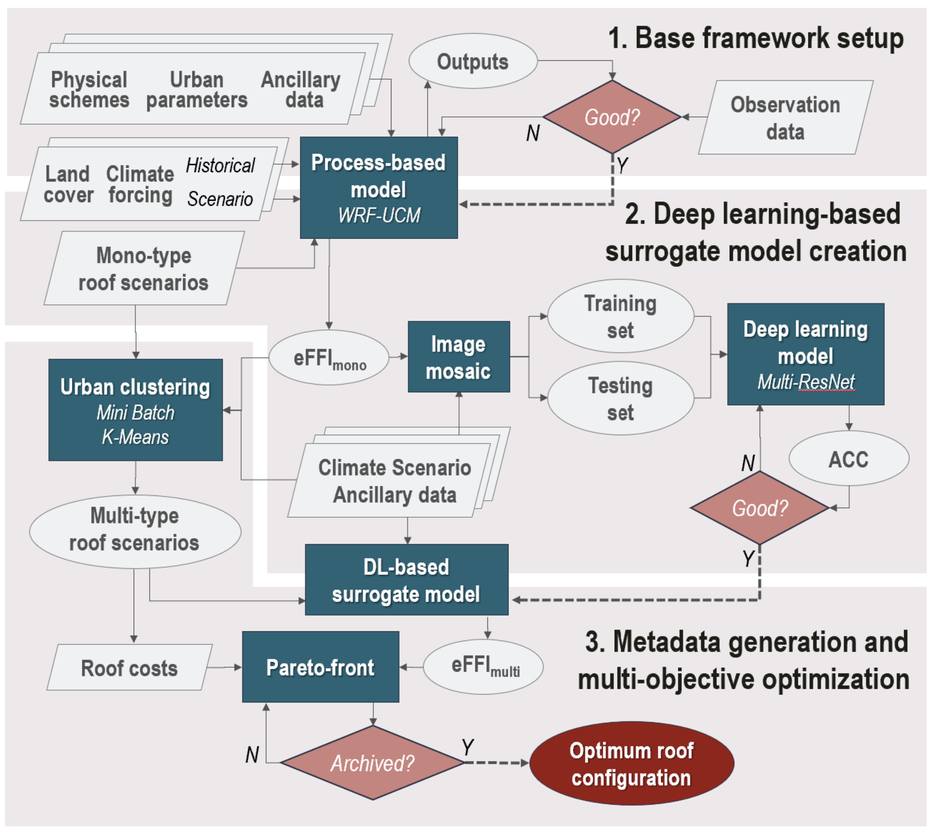

## Methodology

### Study site

- Seoul and surrounding areas
- Area of 2.4 Mha
- Population of 26 M
- Urbans (4.7%), forests (56.9%), and others
- Annual $T_{avg}$ of 12.4 °C
  Annual $P_{total}$ of 1286.6 mm



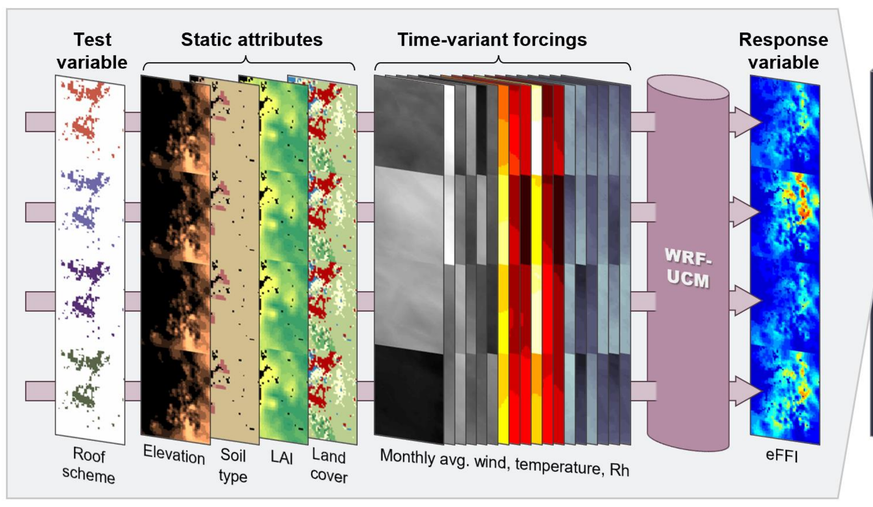

### Work flow




### Base framework (WRF-UCM) setup

- Weather Research and Forecasting (WRF) regional climate model coupled with the single-layer Noah urban canopy model (UCM) (Kusaka and Kimura, 2004)
- Initial and boundary conditions: 18 bias-corrected CMIP6 and ERA5 dataset (Xu et al., 2021) with SSP5-RCP8.5 scenario, rescaled to 1.25° × 1.25°

### Deep learning-based surrogate model




**Multi-residual networks** (Abdi and Nahavandi, 2016)

a deep learning algorithm using multiple residual functions in each block in parallel, or hierarchically, to capture different levels of features, allowing to handle complex data

| Roof scheme | Setting |
|---|---|
| Business as usual (BAU) | Default albedo value |
| 25% cool roof (C25) | Albedo value of 0.37 |
| 100% cool roof (C100) | Albedo value of 0.88 |
| 100% green roof (G100) | Green roof option |

**Objective index**: eFFI (effective flash flood index)

$$eFFI_{mono} = \sum_{h=1}^{N} \left(P_{mono,h} - \theta_{FFI}\right)$$

$P_{mono,h}$: 3-hrly precipitation from WRF-UCM with mono-roof scheme
$\vartheta_{FFI}$: flood-inducing rainfall in Seoul (37 mm/h, Dao et al., 2020)
$N$: the number of data points (i.e., 736 during three months)

### Urban clustering

- 1.52e228 roof scenarios to explore all the cases of four roof schemes on 379 urban grids
- To reduce the number of roof scenarios, clustering urban grids using the Mini Batch K-means method (Chavan et al., 2015) with nine variables (lat, long, temperature, relative humidity, wind speed, and the object ($eFFI_{mono}$)
- Best cluster number was decided based on the Elbow method (Syakur et al., 2018)

### Pareto surface

- Optimal roof configurations were decided based on the trade-offs among multi-objects, i.e., costs (installation, maintenance, environmental benefits, Peng and Jim, 2015) and the $eFFI_{multi}$ from the surrogate model

## Conclusions

Process-based models are computationally demanding to explore various urban planning scenarios, which is required to explore the optimum strategy to mitigate urban climate risks. Our results suggest that DL-based surrogate models could provide an useful framework for urban planning and management.

Contacts: kim.jk237@gmail.com and yeonjoo.kim@yonsei.ac.kr
References: Chavan et al. (2015) Int. J. Sci. Eng. Technol. Res. 04, 1356–1358 Kusaka and Kimura (2004) J. Appl. Meteorol. 43, 1899–1910 Syakur et al. (2018) IOP Conf. Ser. Mater. Sci. Eng. 336 Peng and Jim (2015) Urban Green. 14, 554–561 Xu et al. (2021) Sci. Data 8, 293
Acknowledgments: National Research Foundation of Korea (NRF) grants funded by the Korean government (MSIT) (2020R1A2C2007670 , 2020R1C1C1014886, and 2022R1C1C2009543 ) and Korea Environment Industry & Technology Institute (KEITI) through the R&D Program for Innovative Flood Protection Technologies against Climate Crisis funded by the Korean Ministry of Environment (No. RS-2023-00218873)

# Decentralized management of urban wastewater through the implantation of artificial wetlands for the renaturalization of the Carraixet ravine

Enric GIL-MARTÍNEZ[1], Carmen HERNANDEZ-CRESPO[1], Mª Eugenia RODRIGO SANTAMALIA[2], Luís LIDON CEREZUELA[1], Enrique Javier ASENSI DASI[1], Miguel MARTÍN MONERRIS[1], Vicent BENEDITO DURÁ[1]

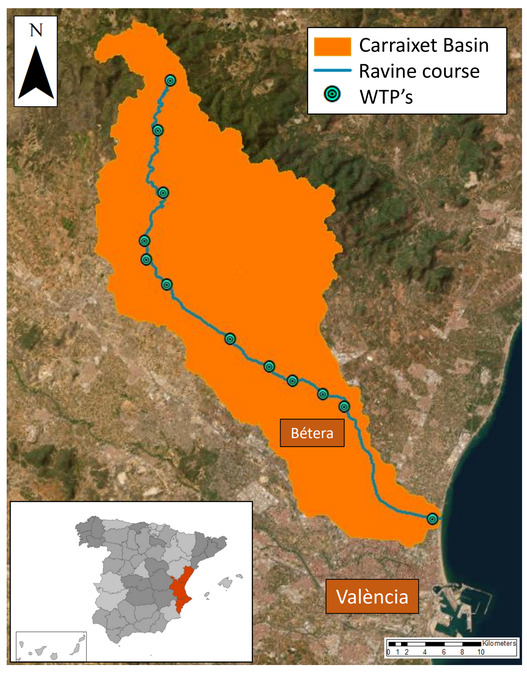
[1] Instituto Universitario de Ingeniería del Agua y Medioambiente (IIAMA) – Universitat Politècnica de València (UPV), València, Spain

[2] Instituto Agroforestal Mediterraneo – Universitat Politècnica de València (UPV)

8th IAHR EUROPE CONGRESS
LISBON - PORTUGAL
4-7 JUNE 2024
WATER - ACROSS BOUNDARIES
IAHR AIRH
Hosted by Spain Water and IWHR, China

## Motivation

The Carraixet, is a ravine with intermittent regime in the most part of its course that is under different anthropogenic pressures. The fact that its territorial environment lacks natural habitat for 75% of its length, gives it even greater ecological value necessitating the restoration of ecological functionality to improve its biodiversity and especially to act as an ecological corridor. (Harris et al., 2006). This aquatic ecosystem relies in some stretches on wastewater treatment plants (WTP), the management of which poses major challenges, such as non-compliance with quality standards and periodic sewer overflows not treated. Addressing these challenges involves adapting wastewater management to climate change, ensuring standards compliance, and adopting decentralized, nature-based solutions. The objective of this study is to improve effluent quality and mitigate the impact of sewer overflows on the ecosystem, to improve biodiversity, ecological functionality of the ravine and carbon sequestration.





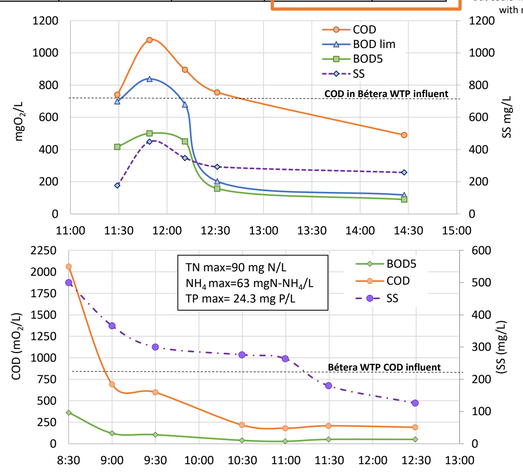

## Results

In the Carraixet basin, there are 12 WTP's most of them serving less than 2,000 equivalent inhabitants. The treatment plant located at the end of the ravine and the systems in Bétera are the most significant, serving 16,000 and 160,000 equivalent inhabitants (ae), respectively. Our focus will be on the results from Bétera.

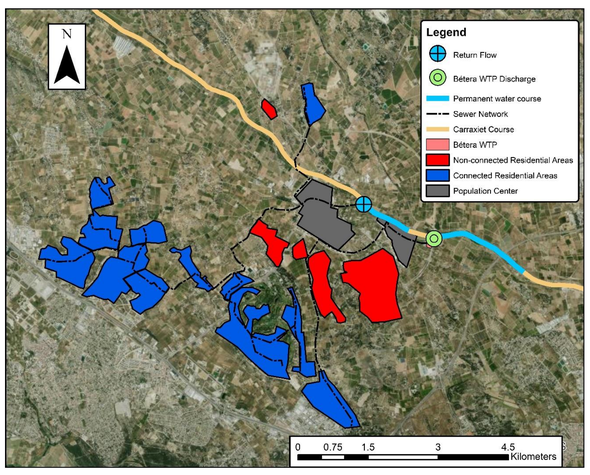
### Discharge/ Overflow Characterization

| SS(mg/L) | COD($mgO_2$/L) | BOD$_5$ ($mgO_2$/L) | TN(mg N/L) | TP (mg P/L) |
|---|---|---|---|---|
| 7,44±4,93 | 30,87±13,17 | 8,69±4,29 | 42,9±10,39 | 5,3±3,06 |

The treated discharge complies with the legislation RD 509/1996. But could we do something with nutrients?

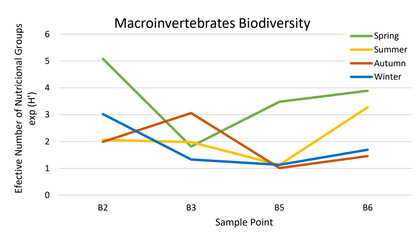


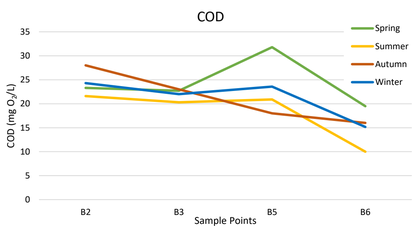

### Distribution of the sewer network in Bétera




The criteria for identifying suitable areas for disconnection from the existing network and proposing in-situ treatment will be based on management costs per equivalent inhabitant. For residential areas without a treatment system, the direct design and implementation of wastewater treatment through artificial wetlands are proposed.

### Distribution of the sewer network in Bétera

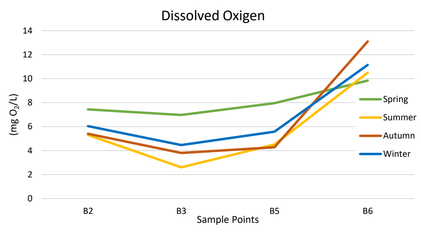



The aquatic biodiversity of invertebrates indicates that the first sampling point, located near the discharge of the treated effluent, does not exhibit the worst biologic indices. Contrary to expectations, it shows greater biodiversity than other points further from the discharge site.

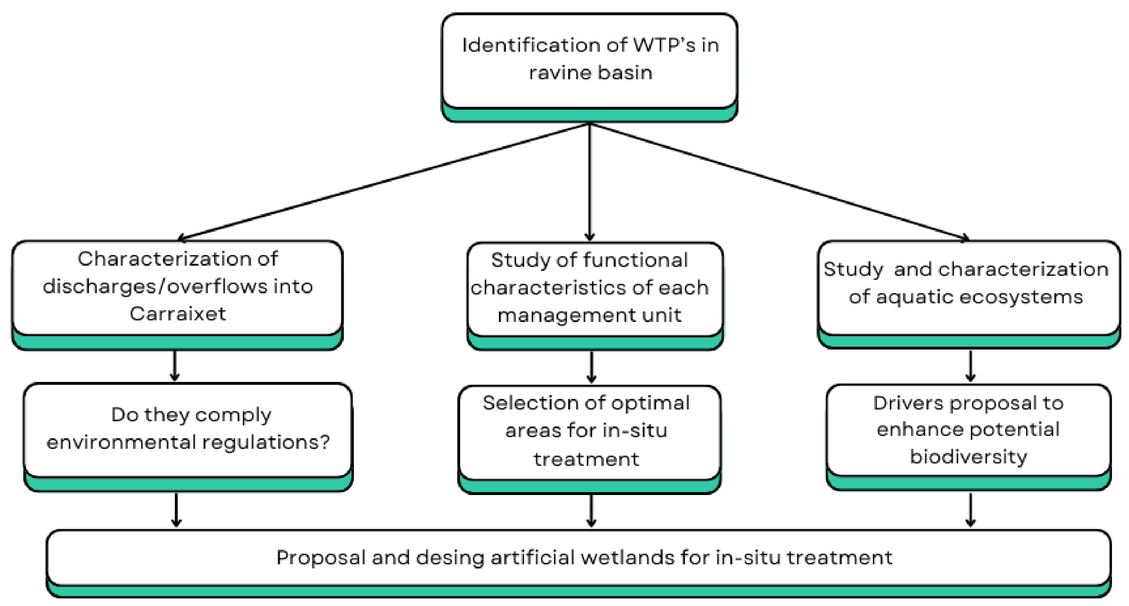
The data suggest a recovery of aquatic biodiversity along the wetland downstream, which is also associated with improved water characteristics.

Although more exhaustive analyses are necessary, these results suggest that habitat heterogeneity (indirectly represented by the presence of a regenerating flow), may be of equal or greater importance than the variables defining water characteristics.




## Methodology

Given the extensive scope of this project, spanning the entire basin and the existence of urban areas characterized by complex infrastructure and significant wastewater management systems, it is imperative to employ a structured methodology which is schematized in the flow path diagram. This framework examines the Carraixet ravine basin from three interconnected perspectives: urban wastewater management systems, discharge and overflow points over the ravine, and the aquatic ecosystems within the Carraixet in sections fed with natural waters.




## Conclusions

- In the highly anthropized Carraixet basin and given forecasted climate scenarios, it is crucial to preserve the ravine's unique natural environment and enhance its biodiversity by controlling the quality of incoming water.
- Improving sewage treatment plant discharges and network overflows can be achieved with nature-based technologies like artificial wetlands.
- Residential wastewater far from treatment plants can be treated on-site in constructed wetlands, reducing pumping and maintenance costs, and enabling local water reuse if needed.
- In residential areas with septic tanks but no treatment systems, constructed wetlands can provide local water treatment and reuse.
- In all cases, whether near or at a short distance from the ravine, water can be reused for irrigation or discharged into the ravine for revegetation and biodiversity enhancement, depending on seasonal needs.
- Revegetating the ravine and creating constructed wetlands also act as carbon sinks, essential under current environmental conditions.

Acknowledgments: The GARBIOFICAR project is funded by the European Union-Next Generation EU (TED2021-130907B-I00). Competitive research projects, Recovery, Transformation, and Resilience Plan, State Research Agency

8th IAHR EUROPE CONGRESS
LISBON - PORTUGAL
4-7 JUNE 2024
WATER - ACROSS BOUNDARIES

IAHR AIRH
Hosted by Spain Water and IWHR, China

# Stormwater Attenuation & Enhanced Infiltration System to Mitigate Flood and Drought Conditions in Urban and Rural Environments: Part I

Stephen THOMAS[1], George FRENCH[1], Joseph O'MEARA[2], Matthew DALE[2], Bruno CASAL[3]
[1] OGI Groundwater Specialists, Durham, UK
[2] Groundwater Dynamics Ltd, Leamington Spa, UK
[3] Sondagens Casal Lda, Sintra, Portugal
stephen.thomas@ogi.co.uk

## SUMMARY

A Stormwater Attenuation & Enhanced Infiltration System enables collection, attenuation and infiltration of stormwater back to the ground, thus mitigating surface flooding. Here we describe how innovative attenuation and infiltration systems function in practice, and demonstrate by mathematical modelling how water flows through the system and infiltrates water into an anisotropic soil of medium horizontal permeability.

Mathematical modelling conducted by the authors demonstrates that infiltration systems can be effective in both medium and low permeability ground, benefitting from the anisotropy of the ground where horizontal silt and sand bands exist within otherwise clay soil, as it enables the infiltration of stormwater at depth into more permeability soil layers.

Where stormwater has traditionally been sent to watercourses and sewers, the application of effective infiltration systems has a significant benefit by mitigating the risk of localised flooding, together with replenishing water resources. Stormwater attenuation and enhanced infiltration exemplify true low-carbon sustainability, contributing to the United Nations Department of Economic and Social Affairs for Sustainable Development Goal 6:

***Ensure availability and sustainable management of water and sanitation for all.***

## Introduction

Climate change is leading to more extreme weather events globally (Stott, 2016). In the UK, this manifests as hotter periods and frequent high-intensity rainfall (Kay et al., 2011; Schaller et al., 2016), compounded by urban development reducing natural infiltration areas (Charlesworth and Booth, 2016). Consequently, less water is recharged into major aquifers, prompting the UK Government to mandate Sustainable Drainage Systems (SUDS) to mitigate peak flooding from impermeable surfaces (Fletcher et al., 2015).

Building Regulations Part H (2015) prioritize rainwater drainage to adequate soakaways or infiltration systems. In response, a Stormwater Attenuation and Enhanced Infiltration System (SAEIS) was developed to infiltrate water at depths of 3-12 metres, suitable for low permeability anisotropic soils like laminated sandy and silty clays (Jarvis et al., 1984). This system reduces local surface water flooding and peak river levels post-storm by infiltrating water into deeper soil layers (Figure 1).

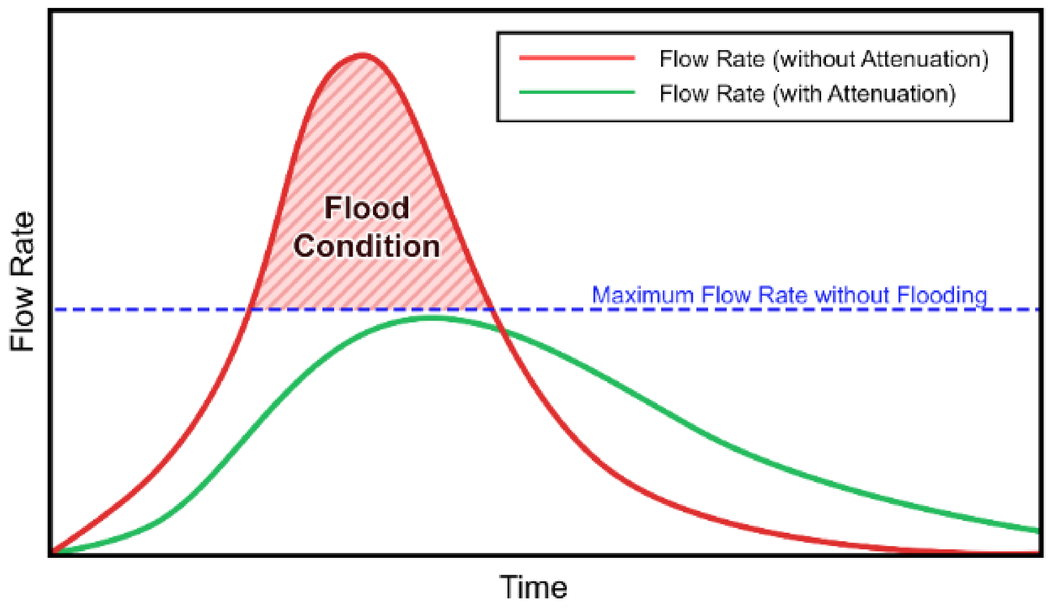



**Figure 1**. Illustration of two storm event hydrographs for non-attenuation and attenuation conditions.

This paper describes the mathematical modelling applied to demonstrate the impact of attenuation and enhanced infiltration systems, by simulating the seepage of stormwater from the infiltrators into the surrounding anisotropic strata of mixed medium and low permeability, common in the UK.

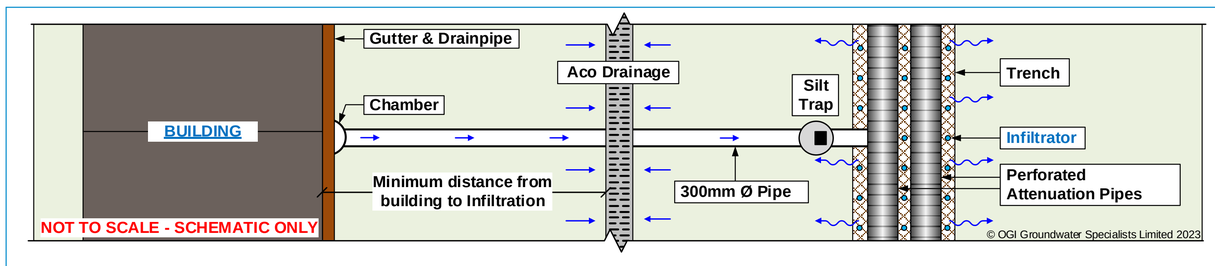
With storm flood conditions also occurring more frequently in areas of Portugal over recent decades, enhanced infiltration techniques have the potential to mitigate the worst impact of such flooding events. Furthermore, the resulting enhanced infiltration of storm rainwater back to the unsaturated vadose zone will also serve to contribute to the mitigation of drought conditions, as the infiltrated rainwater will eventually find its way downwards to the water table.

### Storm water attenuation and enhanced infiltration system

The enhanced infiltration system has been designed to attenuate and infiltrate large volumes of rainwater following storm events. The schematic in Figure 2 depicts how the system collects stormwater, and then how it is attenuated and infiltrated into the ground.

Stormwater that lands on buildings and paved surfaces such as car parks, then enters the drainage system through a series of gutters and drains. Water then flows through a series of underground drains towards a silt trap where fine particles can settle out from the water to mitigate clogging of the infiltration system. Water then flows into a series of attenuation trenches set a minimum of 5.0m away from buildings. The trenches are typically in the order of 1.8m wide and 1.7m deep (Figure 3).

Each trench normally contains one or two large diameter perforated pipes, designed to provide a high storage volume to attenuate collected rainwater following a storm event. The trench is backfilled around the perforated pipes with gravel or angular stone. At the base of each trench, the pipes typically sit on a layer of 10 mm pea gravel. Gravel or stone is then backfilled around the pipes and typically to 300 mm above the crown of the pipes. Surrounding this gravel & pipe attenuation structure is a specialist nonwoven green geotextile developed to promote the growth of a microbic biofilm to absorb and digest hydrocarbon that may have entered the gravel filled trenches.



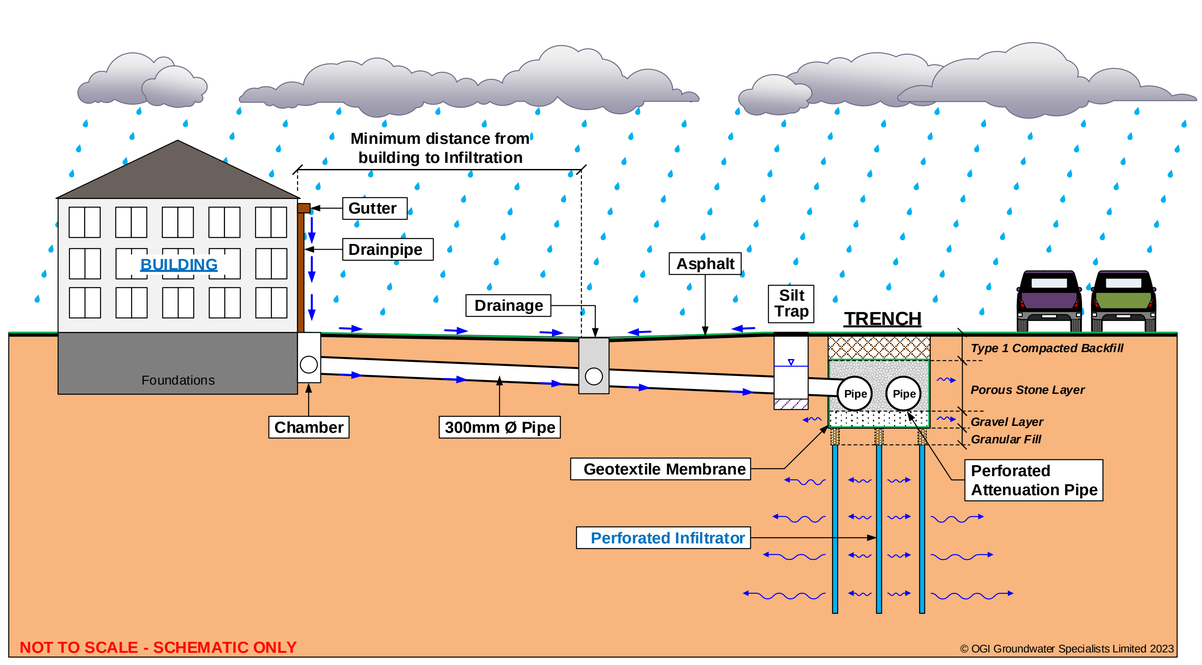




**Figure 2**. Stormwater Attenuation and Enhanced Infiltration System.

Nonwoven geotextile also provides stabilizing of the sub-base construction. Above the attenuation structure is placed graded stone, compacted to provide greater bearing capacity, for a road surface.

Pre-drilled beneath the attenuation trenches are a series of specially designed vertical infiltrators (Figures 2 and 4), which aid the infiltration of water into the soil. Each infiltrator comprises a 90mm drilled borehole, then installed with a device that is designed to accelerate the transmission of water into the ground. The top of each infiltrator is set normally 300 mm below the trench base (Figure 4).

The length of infiltrators normally varies between 3m and 12m, depending on the geology and volume rate of water that needs to be infiltrated.

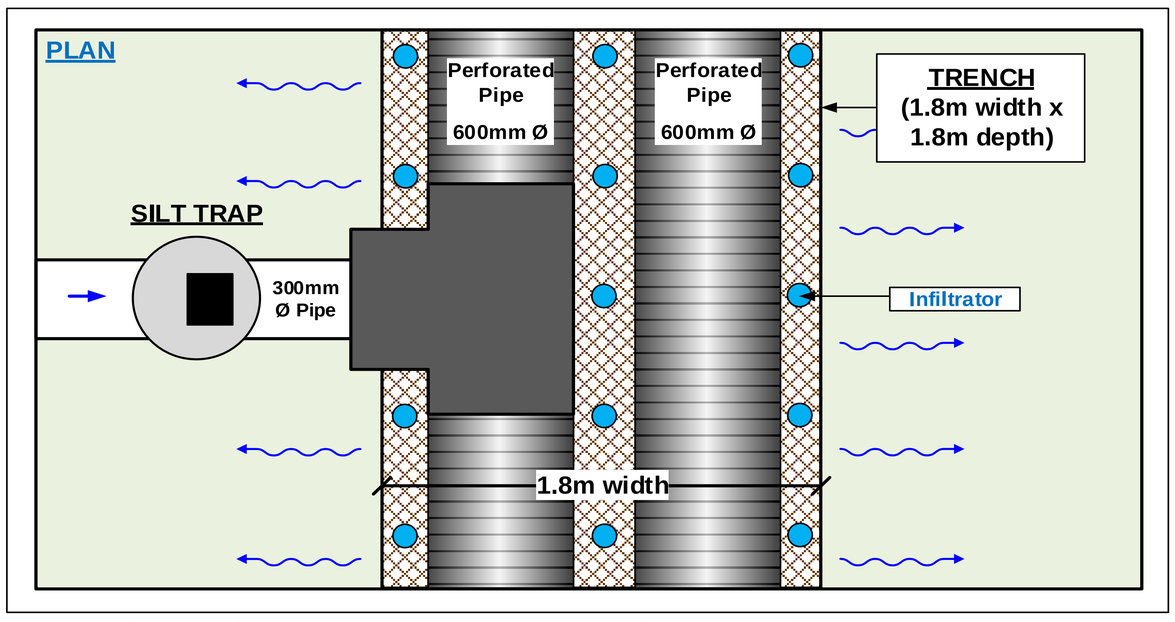



**Figure 3**. Schematic of the Attenuation and Enhanced Infiltration system in plan.

The attenuation and enhanced infiltration system depicted above has been successfully implemented to discharge collected water at over 500 sites in the UK. The system provides an elegant and energy-efficient solution to the flooding challenges at each location.

The system has proved particularly successful in draining waterlogged sports fields, including rugby fields, cricket pitches and horse racing tracks. However, the main area of growth currently is for new-build housing and commercial construction, where city councils are legislating for 100% of the collected rainfall to be reintroduced back to ground.

To illustrate the application of this attenuation and enhanced infiltration system, Figures 5, 6 and 7 present the application at an industrial unit and car park in the northeast of England. The silty-clay ground was initially considered to be unsuitable to soak away stormwater; but after installation, the 180m of trench, together with circa 500 infiltrators, was sufficient to manage the rainwater over 4 Ha.

Two horizontal perforated pipes are installed and then backfilled with gravel to 300 mm above the crown of the pipes. Nonwoven green geotextile wrapping of the gravel is then completed before a graded stone is infilled and compacted on top of the geotextile to provide greater bearing capacity before the construction of an asphalt finish for vehicle use.

To mitigate the potential of silts from entering the trench attenuation system, there are many silt traps and chambers constructed to intercept the silts. These structures are regularly cleaned as part of a planned maintenance program.

To degrade any possible hydrocarbon collected, the attenuation trench, comprising pipes and gravel is wrapped with specialist green nonwoven geotextile (Figure 6) before compaction of the grading layer.

**Contacts**: Stephen.Thomas@ogi.co.uk; jomeara@groundwaterdynamics.co.uk; bruno.casal@sondagenscasal.pt

8th IAHR EUROPE CONGRESS
LISBON - PORTUGAL
4-7 JUNE 2024
WATER - ACROSS BOUNDARIES

IAHR AIRH
Hosted by Spain Water and IWHR, China

# Hydraulic Modeling of the Wastewater Subsystem (SAR) of Serzedo

Ribeiro, V.[1], Silva,C.[2], China, H.[3] , Carraco dos Reis, F.[4]
[1] CTGA, Lda.; [2]CTGA, Lda.; [3]CTGA Lda., [4]ENVIMAN, Lda.

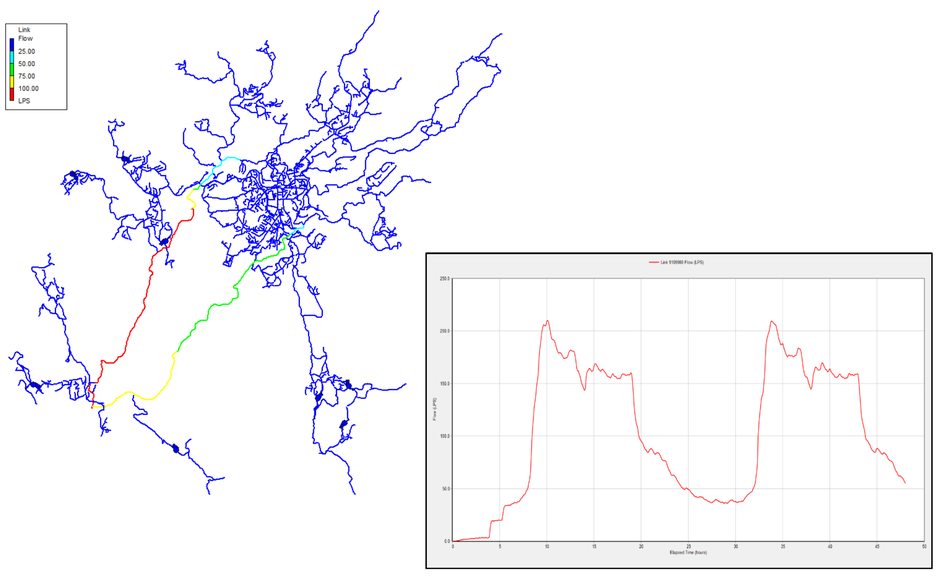
## Motivation

The complexity of large drainage systems, which integrate combined and separate networks, makes the control of inappropriate inflows, flood risks, and pollution of receiving environments particularly challenging. The main challenge possibly consists of controlling these risks in a rational and transparent manner, in sustainable terms, with minimal costs in economic, social, and environmental terms.

Whitin the scope of providing services for the "Hydraulic Modeling of the Wastewater Subsystem (SAR) of Serzedo", efforts where made to provide the management entity of the sanitation system under study (**Águas do Norte, S.A.**) with a tool that allows evaluating the subsystem's performance, particularly regarding the presence of inappropriate inflows in its networks. In this scenario, a hydraulic model was developed using Storm Water Management Model (SWMM) simulation software, a *freeware* from the Environmental Protection Agency (EPA), with the goal of providing a framework for analyzing optimization scenarios of the hydraulic behavior of the subsystem and, additionally, developing an Action Plan for stormwater control.

## Results

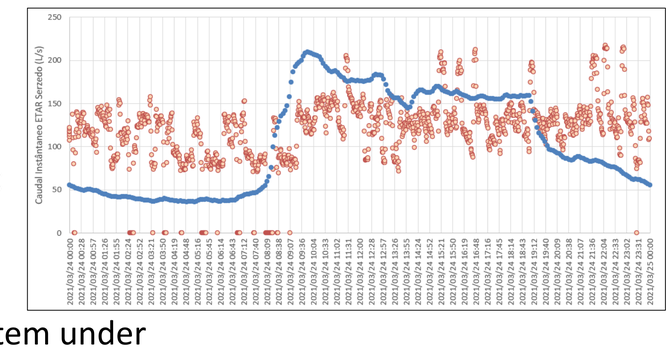
In general, it was possible to develop a hydraulic model of the wastewater drainage system under study, which allowed for the analysis and prediction of its hydraulic behavior based on the characteristics of its components, it's operational mode, and the flows it carries. This made it possible to quickly and effectively conduct sensitivity analyses and simulate various scenarios with sufficient accuracy, without needing to interfere with the system in question or expose it to unknown operational conditions. Thus, it constitutes a fundamental tool in decision support with a wide range of applications, including strategic planning, project support, system operation and maintenance, operator training, and even rehabilitation action planning.




## Methodology

The elaboration of the hydraulic model involved several steps and considerations:

1) Data collection and Analysis – gathering relevant data (maps, plans, topographic surveys, "as-builts");
2) System Characterization – identifying and mapping out the components of the drainage system;
3) Model Development – input collected data into the hydraulic modeling software;
4) Simulation and Analysis – simulations were run to analyze the hydraulic behavior of the drainage system under different scenarios, including normal conditions, peak flow events, and system failures;
5) Sensitivity Analysis and Optimization – assess the impact of changes in parameters such as pipe diameter, slope, roughness coefficient, and boundary conditions;
6) Validation and Verification – Validation of the model by comparing simulated results with field measurements and observed system behavior.




## Conclusions

With the "Hydraulic Modeling of the Serzedo SAR," the aim was to provide the management entity of the sanitation system under study with a tool that allows them to assess the performance of the subsystem, particularly concerning the existence of inappropriate inflows.

The hydraulic modeling process of the Serzedo SAR included several stages that allowed obtaining the final simulation model (base version). The next steps should focus on measures to acquire information and knowledge about the inflows to the SAR, enabling the calibration and development of the hydraulic simulation model of the hydraulic behavior of the system.

After calibrating the model, it will be possible to identify the critical points of the system and define flow control solutions to implement, as well as develop a plan for the rehabilitation/remodeling of the infrastructure components of the drainage system.

Contacts: [1]vitor.ribeiro@ctga.pt (Eng.º), [2]carlos.silva@ctga.pt (Eng.º), [3]hugo.china@ctga.pt (B.SC in Industrial Chemistry) [4]filipecarraco@ctga.pt (Eng.º)

References: Águas do Norte, "Estudo de Desvio de Caudais da Rede em Baixa no Concelho de Fafe";
Almeida, M. C. e Cardoso, M. A. (2010). Série Guias Técnicos 17 – Entidade Reguladora dos Serviços de Águas e Resíduos, LNEC.

Acknowledgments: Águas do Norte, S.A. (Grupo Águas de Portugal)

# Cadastral Survey, Cleaning, and Video inspection of Collectors – SAR Lever Gaia

André Fonte[1], Pedro Nogueira[2], Hugo China[3], Filipe Carraco dos Reis[4]

[1] B.Sc. In Geography, Geomatics Division, CTGA, Lda., andre.fonte@ctga.pt; [2]B.Sc. In Chemistry, Waste Management Division, ENVIMAN, Lda., pedro.nogueira@ctga.pt; [3]B.Sc. In Industrial Chemistry, Executive Director, CTGA, Lda., hugo.china@ctga.pt; [4]Civil Engineer, Management, ENVIMAN, Lda., filipecarraco@ctga.pt

## Motivation

As part of the public tender for the acquisition of services for "***Cadastral survey, cleaning, and video inspection of interceptors in Lever-Gaia***" promoted by SIMDOURO – Saneamento do Grande Porto, S.A., the management entity presented several activities leading to the creation of a preventive maintenance plan. A set of tasks was carried out with the aim of supporting the decision to draw up a maintenance and rehabilitation plan for the systems.

The benefits of the geographical representation of the date, as well as its compilation with the observations of the video inspection systems, present benefits in terms of asset management of wastewater drainage systems, showing effectiveness in maintaining the functional state of the drainage networks.

This assessment provides a view of the degradation of infrastructure components and the impact of their failure, helping to prioritize interventions in the system in terms of future investments, leading to a strategy of economic and financial sustainability in the medium and long term.

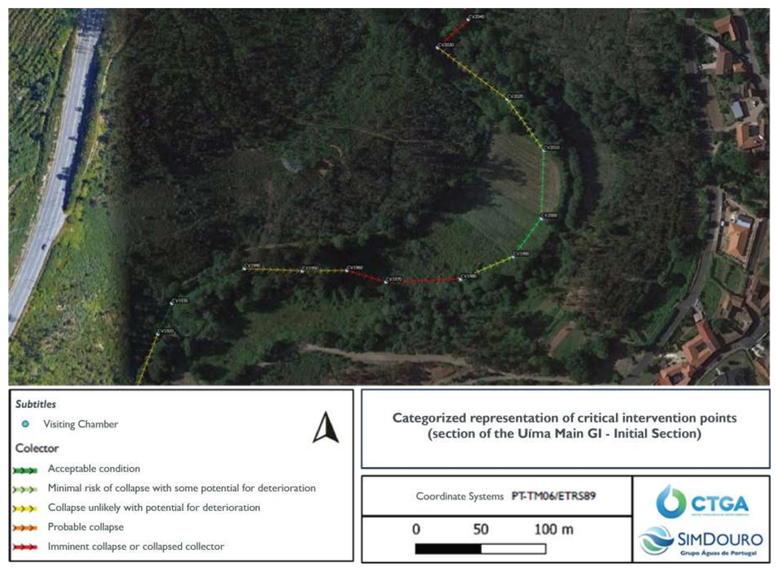
## Results

Categorization and graphical representation of anomalies detectable by the video inspection system;

Relationship between structural condition, WRc score and probability of collapse.

| Collection ID | Verified anomalies (Coding) | WRc score (range) | Scale | Description | Criteria |
|---|---|---|---|---|---|
| COLI I | **BAAA** - Vertical deformation<br>**BDDB** - Turbid effluent, water level 50%<br>**BDA** - Crushed duct, loss of visibility | ≥165 | 5 | Imminent collapse or collapsed collector | ✓ Collapsed or imminently collapsing pipework.<br>✗ Collapse or imminent collapse.<br>✓ Urgent rehabilitation of the pipeline is recommended, measures should be taken to limit the movement of vehicles and pedestrians (if applicable). |






## Methodology

- **Topographical survey of the drainage system, with the previous creation of a support network** (PT-TM06/ETRS89);
- **Cadastral survey of the system** (GIS: information storage, geographical representation of data and spatial analysis);
- **Total/partial cleaning of drainage systems, with removal of waste, its transportation and disposal in an appropriate final destination** (aims to maintain the systems, safeguarding their physical and functional conditions) and **Flow detour**;
- **Video inspection** (report generator with coding of detected anomalies and observed collector profiles; WRc method to determine the structural conditions, based on a scoring system. Observations relevant to the structural conditions of the collectors, coded according to EN 13 508-2:2003, are assigned a certain score for a given anomaly. The total score for each collector inspected is calculated based on the sum of the scores associated with each anomaly. The total score is then converted into structural condition classes and, consequently, into collapse probability classes (categorization)).

## Conclusions

The main objective of using the services presented was to carry out a thorough diagnosis in order to collect reliable data that would support a preventive maintenance strategy to be carried out later by SIMDOURO – Saneamento do Grande Porto, S.A.

According to the anomalies detected, it was possible to apply the categorization methodology to the spatial data, thus creating priority areas for intervention. This categorization allows the management entity to optimize costs in intervention/rehabilitation programming, revealing effectiveness in maintaining the functional state of drainage networks, revealing effectiveness in maintaining the functional state of drainage networks.

The application of these techniques shows results in terms of the company's economic and financial sustainability, thanks to the effectiveness of this system in supporting decision-making, creating the conditions for an internal strategy of economic and financial sustainability in the medium and long term.

Contacts: [1] andre.fonte@ctga.pt (B.Sc. In Geography), [2] pedro.nogueira@ctga.pt (B.Sc. In Chemistry), [3]hugo.china@ctga.pt (B.SC in Industrial Chemistry) [4]filipecarraco@ctga.pt (Eng.º)

Acknowledgments: SIMDOURO – Saneamento do Grande Porto, S.A

# Roof-harvested rainwater health risk assessment: A case study in Lagos, Nigeria

John Chukwuemeka Kingsley [1], Pu, Jaan Hui (Supervisor)[1]
[1] University of Bradford, UK

8th IAHR EUROPE CONGRESS
LISBON - PORTUGAL
4-7 JUNE 2024
WATER - ACROSS BOUNDARIES
IAHR AIRH
Hosted by Spain Water and IWHR, China

## Motivation

- Shortage of safe drinking water is a significant issue experienced in economically less developed countries.
- Around 2 billion people worldwide lack access to services that safely manage drinking water.
- QMRA models are used to evaluate the likelihood and extent of adverse health consequences from pathogen exposure.

## Study Area

- The study area is the Ikorodu Local Government Area of Lagos. Ikorodu is in Lagos' northern region.
- Significant reliance on rainfall in the area, particularly during the rainy season.

## Results

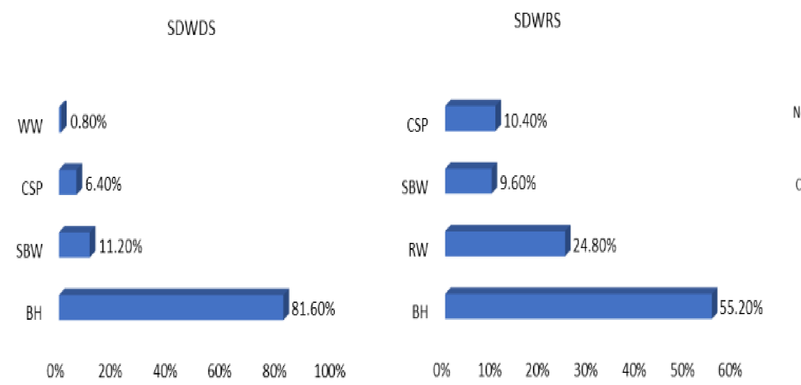



Figure 2: Proportion of the sources of drinking water in the dry and rainy season, respectively. SDWDS and SDWRS denote sources of drinking water in the dry season and sources of drinking water in the rainy season respectively). CSP, SBW, WW, RW and BH denote Community stand up pipes, Sachet and bottle-water, well water, rainwater and boreholes, respectively.

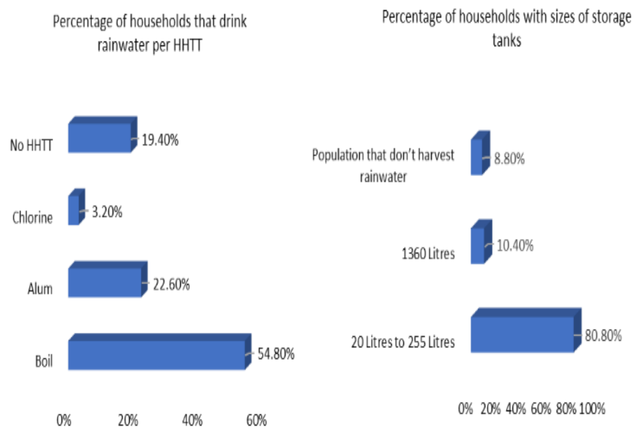



Figure 3: Proportion of households that drink rainwater per HHTTs and sizes of storage tanks respectively.

Table 1: Infection risk for those exposed to contaminated rainwater in the four scenarios

| S/N | HHTTs applied | *E. coli* Dose (MPN/100 mL) | *E. coli* Dose in 2000 mL (MPN) | P(i) % | N | Number of events per year, E | Maximum Py (%) | Maximum Ry |
|---|---|---|---|---|---|---|---|---|
| 1 | Alum | 0.78 | 15.54 | 0.0118 | 0.118 | 281 | 0.00964 | 96 |
| 2 | Alum + Chlorine | 0 | 0 | 0 | 0 | 281 | 0 | 0 |
| 3 | Boil | 0 | 0 | 0 | 0 | 281 | 0 | 0 |
| 4 | Chlorine | 0 | 0 | 0 | 0 | 281 | 0 | 0 |
| 5 | No HHTTs | 1.55 | 31.08 | 0.0234 | 0.234 | 281 | 0.00999 | 100 |

## Methodology

- A well-detailed survey involving 125 households of the study area has been conducted.
- The HHTTs used includes boiling, alum, chlorination and the combination of chlorination and alum and this was obtained in the questionnaire

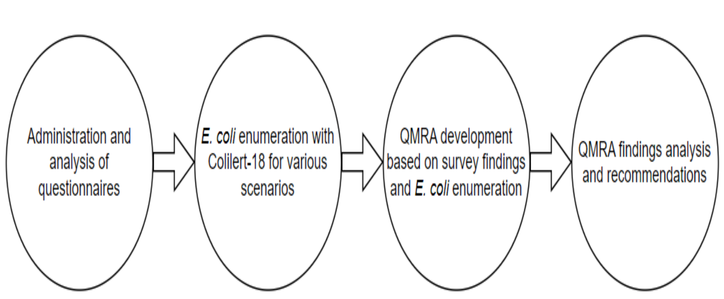



Figure 1: Flowchart of the methodology

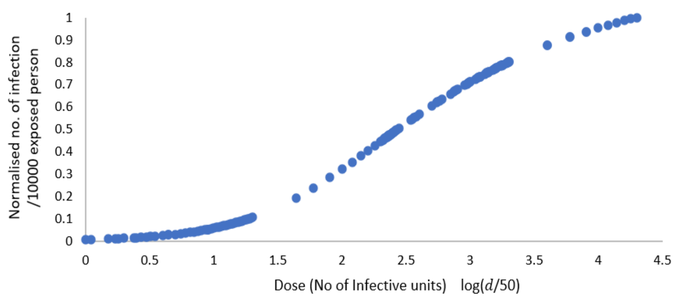



Figure 5: The dose-response relationship of beta-Poisson. The dose-response relationships correlate N to P(i)

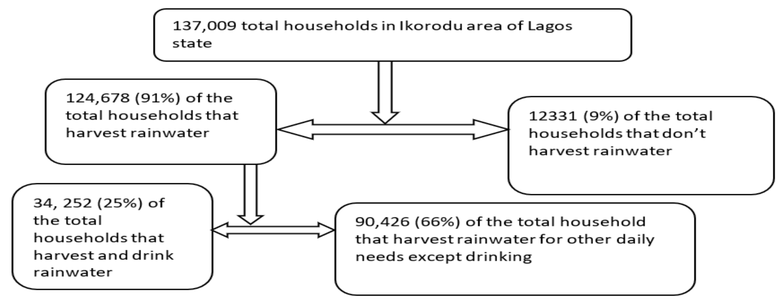



Figure 4: Estimation of the proportion of households using rainwater (the percentages in the Figure were calculated using the survey results)..

## Conclusions

- The proportion of respondent that use boreholes reduced from 82% in the dry season to 55% in the rainy season.
- High dependence on rainwater since 114 households (out of the 125) harvest rainwater (either to drink or use).
- 25% of the total respondent's drink rainwater in the rainy season.
- 6 of the 31 rainwater drinkers admitted drinking the untreated rainwater.
- Alum reduced the turbidity and total suspended solids (TSS) while combination of alum and chlorine and boiling remove Total coliform and E.coli.
- It is imperative that a disinfectant is applied to rainwater, especially if it is to be consumed.
- The combination of alum and chlorine and the alum alone have significant effect on turbidity and TSS; while boiling and chlorination have the much less effect towards these physical parameters.
- The results showed that the pathogenic E. coli exposure risk from ingesting RHRW without HHTT was 100 and 96 per 10,000 exposed households per year, respectively, showing the need of disinfecting collected rainwater

References: John, C.K. and Pu, J.H. (2023) Household Reusable Rainwater Technology for Developing and Under-Developed Countries. Taylor and Francis Limited. London. DOI: 10.1201/9781003392576
John, C.K.; Pu, J.H.; Moruzzi, R.; Pandey, M. and Azamathulla, H. (2021a) Reusable rainwater quality at Ikorodu area of Lagos, Nigeria: Impact of first-flush and household treatment techniques. Journal of Water, Sanitation and Hygiene for Development,
John, C.K.; Pu, J.H.; Moruzzi, R. and Pandey, M. (2021b) Health-risk assessment for roof-harvested rainwater via QMRA in Ikorodu area, Lagos, Nigeria. Journal of Water and Climate Change. jwc2021025. https://doi.org/10.2166/wcc.2021.025.

# Roof-Top Sediment Deposition and Microbial Analysis in Various Sanitation Environments

John Chukwuemeka Kingsley [1], Pu, Jaan Hui (Supervisor)[1]
[1] University of Bradford, UK

## Motivation

- Shortage of safe drinking water is a significant issue experienced in economically less developed countries.
- The deposition of particulate matter in places with varying hygiene levels, and the bacteria linked with their deposits were identified.
- The primary goal of this study was to estimate the amount of particulate matter that drops from the atmosphere

### Study Area

- The study area is the Ikorodu Local Government Area of Lagos. Ikorodu is in Lagos' northern region.

## Results

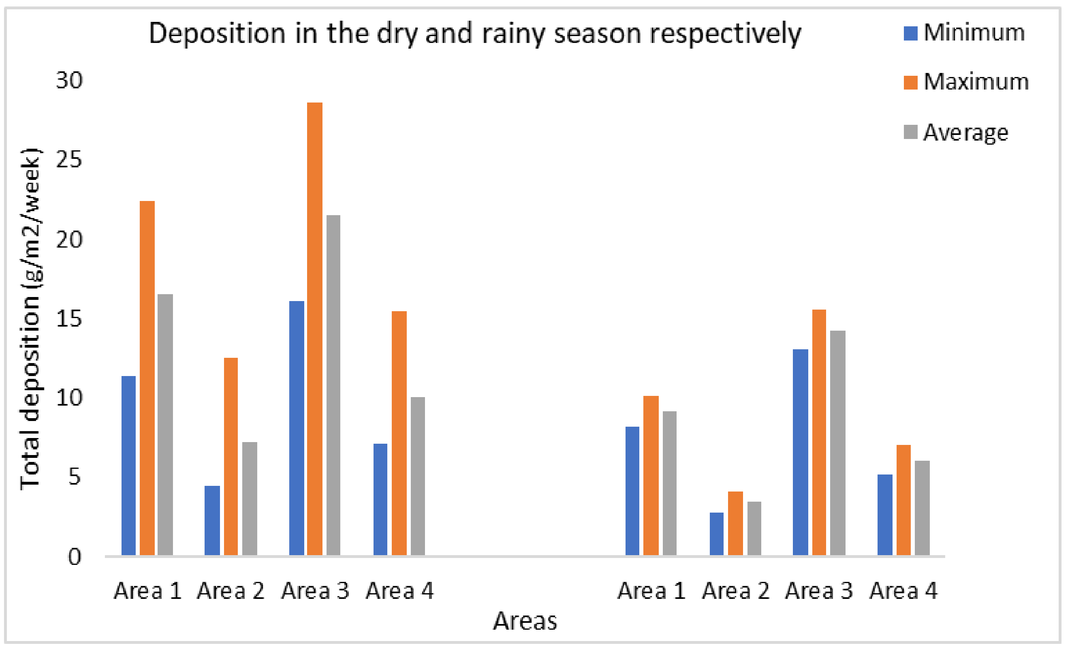



Fig 3: Depositions in the four areas in the dry and rainy season (Areas 1 to 4 on the left was done in the dry season while the ones on the right was done in the rainy season).

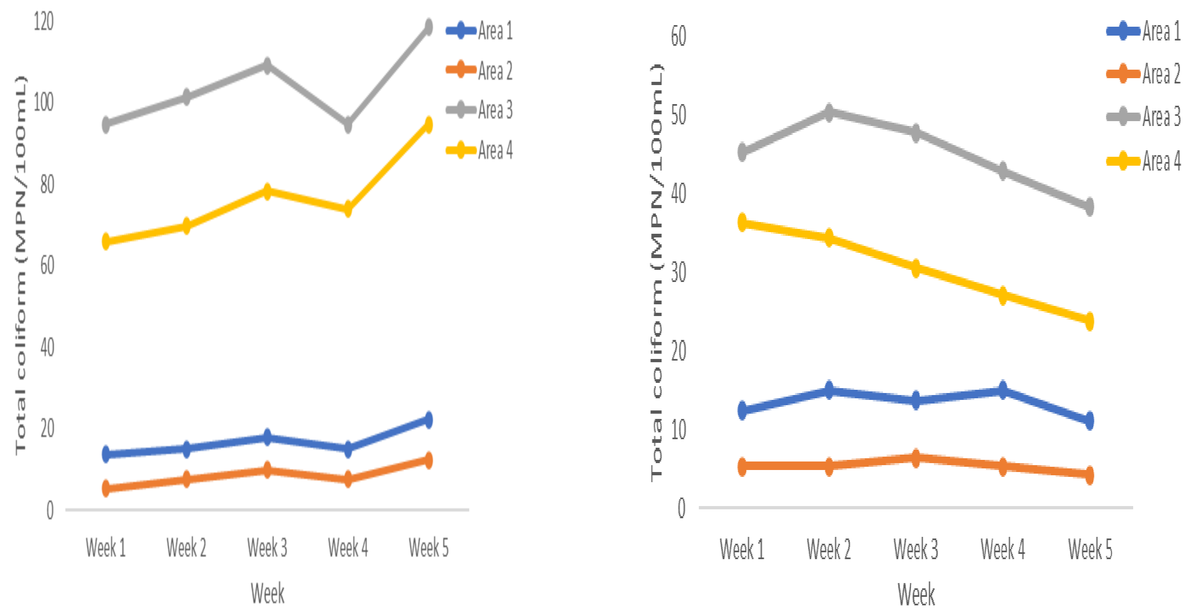



Figure 5: Plot of Total coliform (MPN/100 mL) in the four areas in the dry and rainy season, respectively.

## Methodology

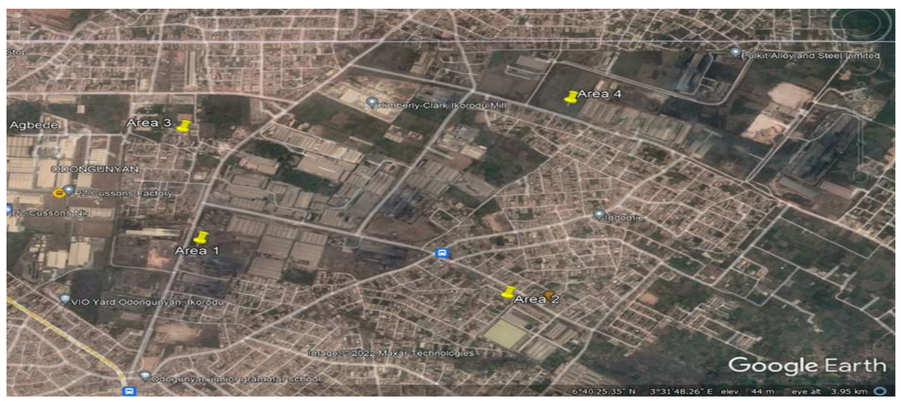



Fig 1: Location of the four study areas on Google map (Google Earth, 2023



Fig 2: 10-inch funnel attached to a 5 L plastic container for measuring total deposition

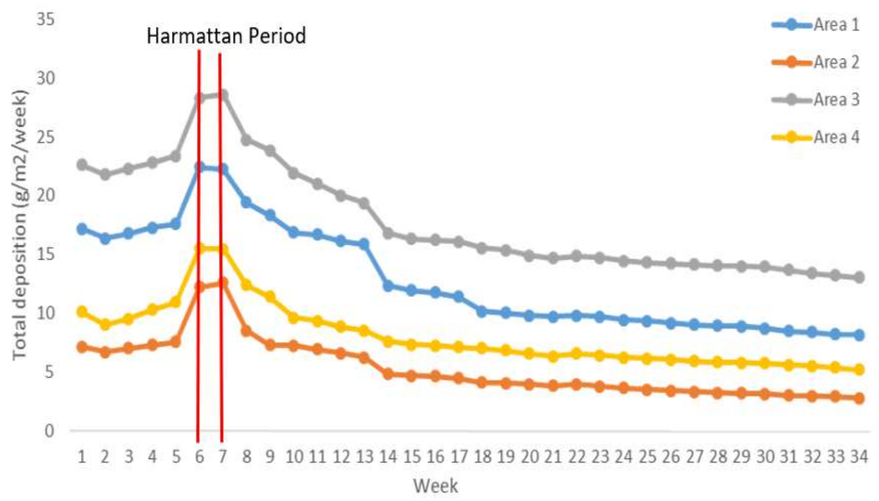



Fig 4: Total depositions in the four areas in both seasons (Week 1 to 17 is the dry period while week 18 to 34 is the rainy period).

## Conclusions

- Results the data revealed that locations with poor drainage infrastructure and low cleanliness had greater bacterial counts on their roofs than those with good sanitation, and that unpaved and unvegetated areas created more deposits than paved and vegetated areas.
- The deposition of particulate matter and microbes on building roofs moves into rainwater storage tanks.
- The findings revealed that enumerated microorganisms and total suspended solid (TSS) depositions were lower in the rainy season compared to the dry season, with the largest deposition occurring during the Harmattan period.

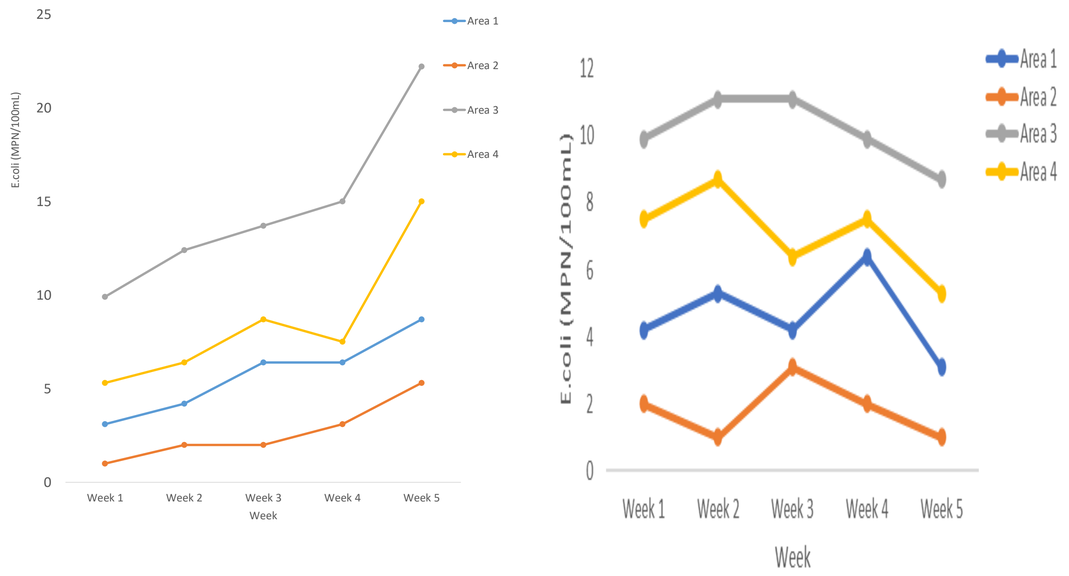



Figure 6: Plot of E.coli (MPN/100 mL) in the four areas in the dry and rainy season, respectively

References: John, C.K.; Pu, J.H., Pandey, M., Hanmaiahgari, P.R., Moruzzi, R., Zang, S. and Jamei, M. (2023) Deposition and microbial analyses from roof-top sediments within different environments. Topics in Catalysis. 10.1007/s11244-023-01856-x
John, C.K. and Pu, J.H. (2023) Household Reusable Rainwater Technology for Developing and Under-Developed Countries. Taylor and Francis Limited

8th IAHR EUROPE CONGRESS
LISBON - PORTUGAL
4-7 JUNE 2024
WATER - ACROSS BOUNDARIES

# URCA!: climate change scenarios, design storms and participatory approach to improve urban resilience

Anna PALLA[1], Ilaria GNECCO[2], Francesca PIRLONE[3], Giovanna GROSSI[4], Michèle PEZZAGNO[5], Antonella PIETTA[6], Arianna DADA[7], Marco MAGLIONICO[8], Alberto Paolo CAMPISANO[9], Patrizia PIRO[10], Ruggero ERMINI[11], Carmen FATTORE[12], Carlo GIUDICIANNI[13], Sara TODESCHINI[14], Enrico Fortunato CREACO[15]

[1,2,3] DICCA-Università degli Studi di Genova, [4,5,6,7] DICATAM-Università degli Studi di Brescia, [8] DICAM-Università di Bologna, [9] DICAR- Università di Catania, [10] DINCI-Università della Calabria, [11,12] DICEM-Università della Basilicata, [13,14,15] DICAr-Università degli Studi di Pavia

## Motivation

The Italian national research project named **URCA!** (Urban Resilience to Climate change: to activate participatory mapping and decision support tool for enhancing the sustainable urban drainage) is aiming at promoting the resilience of the cities to climate change by favouring the distributed implementation of Sustainable Urban Drainage (SUD) systems. The main objectives of the project are three: i) to provide innovative guidelines for the SUDs design, ii) to show the implementation of a participatory approach and iii) to develop a new Decision Support System (DSS).

## Methodology

Aiming at testing approaches and strategies in different urban and climatic conditions in Italy, several case studies are being considered that are spread over the Italian territory.

The structure of the project consists of the following Work Packages (WP):

WP1 – project coordination;
WP2 – climate change impact analysis;
WP3 – environmental impact mitigation;
WP4 – participatory approach for the intervention planning;
WP5 – SUD design;
WP6 – Decision support system development;
WP7 – Dissemination.

Besides the project management and dissemination activities, research efforts have been focused so far on WP2, WP3 and WP4, respectively dedicated to define the design of SUD systems, to evaluate/mitigate their environmental impact and to favour their insertion in urban planning tools. The last objective will be pursued through the engagement of stakeholders in participatory mapping aiming at increasing the awareness of citizens, students, experts, local authorities and enterprises on the hydraulic risk – also linked to climatic risk – and on potential mitigation measures.

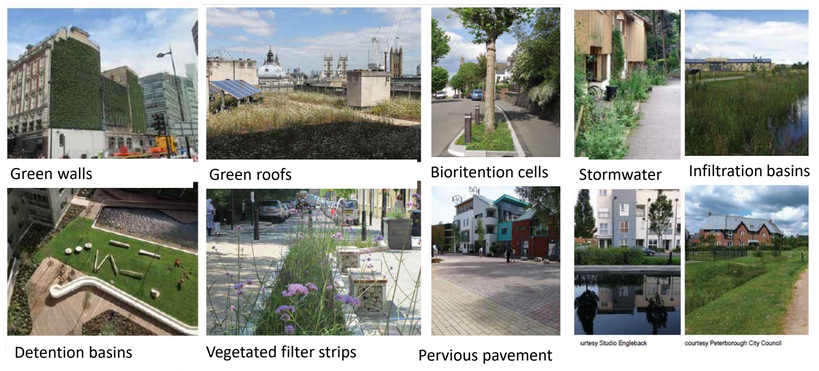


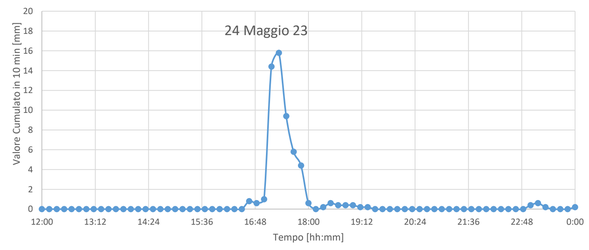
Figure 1: Examples of SUDs, source: The SUDS Manual, CIRIA C573.

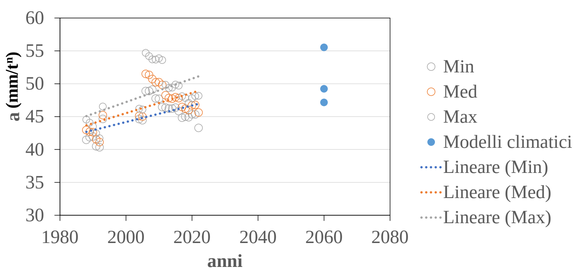

Figure 2: Green roof site Genoa


Figure 3: Green roof site Rende

## Climate Change – future scenarios and design storms

The analysis carried out so far in WP2 aims at the definition of climate change scenarios tailored on SUDs, that is at the local scale, suitable for the evaluation of climate change scenarios on the sizing and performance of several devices. Climate projections provided by regional climate models for the half and the end of the current century were taken from the CORDEX (www.cordex.org) database. Statistical analysis of meteorological observations (precipitation and temperature) and climate projections led to the definition of climate change scenarios suitable for testing the performance of SUDs also in the future climate for several case studies.. Reliability of 2- and 3- parameter DDF curves to provide estimates of rainfall volumes for design storms of short duration was finally tested for several sites. For the same sites also the shape of a representative design hyetograph was investigated, accounting for more recent observed heavy storms.




## Case studies for the implementation of participatory strategies

In WP4 reference target groups were set for each case study and different participatory strategies were implemented according to site features, to develop guidelines for the engagement of several actors at the local scale.

-> 56 investigated areas – Municipality of Brescia
-> Sampierdarena, urban neighborhood – Municipality of Genoa
-> Ex Barilla industrial area, Municipality of Matera



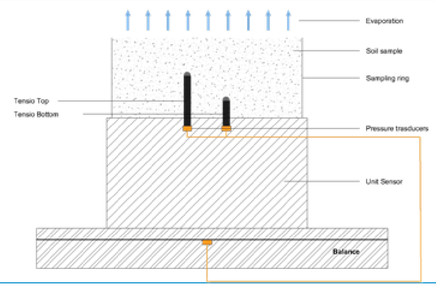




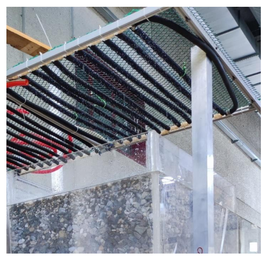
## Experimental activity

In WP5 the hydraulic behaviour of some SUDs is investigated:

- Draining layers
- Pervious pavement
- Blue roofs



Scheme of the HYDROPO device used in Cosenza for the retention curve definition


Rainfall simulator Bologna test-bed

Contacts: giovanna.grossi@unibs.it

References: URCA! Project Deliverables (https://prinurca.wordpress.com/)

Acknowledgments: the URCA project is funded by the Italian Ministry of University and Research (call RPIN2020)

8th IAHR EUROPE CONGRESS
LISBON - PORTUGAL
4-7 JUNE 2024
WATER - ACROSS BOUNDARIES
Hosted by Spain Water and IWHR, China

# Sensitivity Analysis of the Distributed Hydrological Model SWAT to the Curve Number (CN2) Parameter

Kaline GOMES [1], Jonathan SILVA [2], Sandra SAAD [3]
[1,2] Federal University of Rio Grande do Norte, Brazil; [3]Federal University of Campina Grande

## Abstract

This work presents a sensitivity analysis of the Soil and Water Assessment Tool (SWAT) hydrological model to the Curve Number (CN2) parameter on the surface runoff in the Maxaranguape River Basin, located in the Northeast of Brazil (NEB). The CN2 is based on soil hydrological class, land use and land cover (LULC) and Antecedent Moisture Condition (AMC). This parameter was varied by -30%, -10%, +10% and +30 of its initial prescription. These variations in CN2 caused considerable changes in surface runoff ranging from -79% to 107%, which shows the attention that must be given when prescribing this parameter in SWAT.

## Introduction

A simple and widespread method for determining the approximate volume of surface runoff of a rain event is the Curve Number method. The method was developed by SCS (Soil Conservation Service – 1957), is widely used in several countries, and uses as input only rainfall and CN, based on the hydrological soil class, LULC and Antecedent Moisture Condition (AMC). The AMC is divided into three groups, according to the amount of rain that occurred on the five days prior to the day of analysis. AMC 1 is the dry soil condition (represented by CN1); AMC 2 is the average moisture condition (represented by CN2) and AMC 3 is the saturated soil condition (represented by CN3). The Model used in this paper is the Soil and Water Assessment Tool Model, which uses CN2 in the hydrological component. Nowadays, this model has been used in studies around the world, with the aim of understanding hydrological processes (Abbaspour, et. al., 2015) and how changes in the LULC impact water resources (Li et. al., 2024), as these changes are capable of altering the CN and runoff values in a basin.

The study area was chosen because it is considered a water reserve for the public water supply in the capital of Rio Grande do Norte (RN), and because there are intense processes of change in LULC, which drives to the need of analyzing how the variation in CN2 impacts on the flow of the basin. Therefore, the objective of the paper is to test the sensitivity of the hydrological model SWAT, to the CN2 parameter on the flow in the Maxaranguape River Basin, like area of study.

## Methodology

The study area is the Maxaranguape River Hydrographic Basin, located in the NEB and the location is illustrated in Figure 1. The Basin has a climate that varies between rainy tropical and dry summer, with average annual precipitation of around 1,300 mm at the mouth. Semiarid with an annual average of 900 mm at the head of the basin in the extreme west and has a drainage area of 990km²

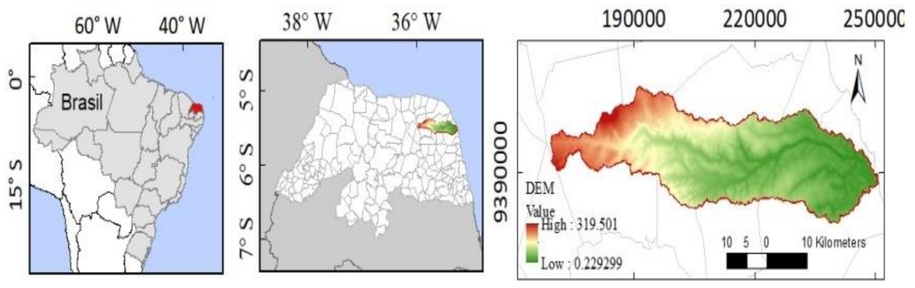



Fig. 1. Location of the Hydrographic Basin

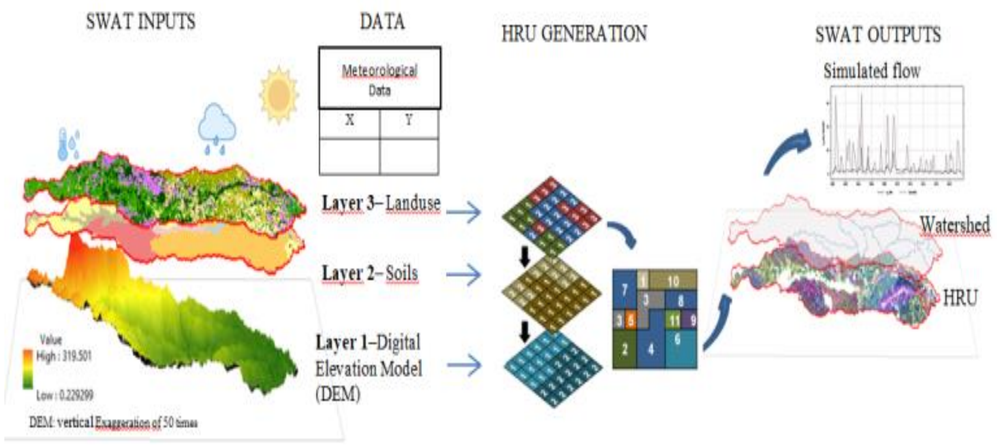



Fig. 2. Illustration of how SWAT works integrated with ArcGis.

SWAT is a mathematical model that uses physical and conceptual equations to simulate the hydrological cycle. The Model was running with daily, monthly or annual outputs, being capable of simulating long periods, to estimate the effects of variations in the physical characteristics of the basin, predicting the hydrology in each Hydrological Response Unit (HRU). The area was discretized containing 15 sub-basins and 104 HRU (Fig.2), generated with the Digital Elevation Model (DEM), from the NASA Shuttle Radar Topography Mission Global (SRTM) with a spatial resolution of 30m, LULC, from MapBiomas and Solos, from Radam. Brazil, which were grouped into four classes of hydrological soils, considering the potential for generating surface runoff: Low (Latosol), Medium (Argisol), High (Neosols, Vertisols, Cambisols and Gleisols) and floodplain soils (alluvial and hydromorphic soils ). The climatic data used to force the model are as described: Rain, Temperature, Solar Radiation, Relative Humidity and Wind. To make up for the lack of data available for the area, the database by Xavier *et. al.* (2022) was used, with a georeferenced grid of 0.1ºx0.1º and daily values. DEM: with Exaggerationvertical50 times In the sensitivity analysis, SWAT was integrated into the period from 01 Jan 1997 to 31 Dec 2019 (3 Initial years for the warm up) and was run 5 times. The first simulation was called initial and the remaining 04 simulations, according to the change in the CN2 parameter, for all Land Use and Land Cover, for the following variation: -30%, -10%, +10% and + 30 in relation to the CN2 of the initial simulation

## Results and Conclusions

The average annual surface runoff (SURQ) in the initial simulation (without changing CN2) was 334 m³/s. For simulations with an increase in CN2 by 10% (502 m³/s) and 30% (690 m³/s), there was an increase in relation to the initial SURQ of 50% and 107%, respectively. For the simulations in which CN2 decreased -10% (214 m³/s) and -30% (69 m³/s), the average annual surface runoff corresponded to a decrease of 36% and 79%, respectively. We noticed that CN2 has a significant control on the surface runoff pattern and that modifications to this parameter generated percentage changes much higher than the percentages prescribed in the tests. As expected, an increase in CN2 increases surface runoff, just as a reduction in it reduces surface runoff. The effects of this change alter the water balance, mainly modifying evapotranspiration, which is better the greater the surface runoff. Given the sensitivity of CN2 in SWAT with respect to surface runoff, we conclude that this parameter must be prescribed with considerable attention

Contacts: [1]kmuriel2001@gmail.com, [2]jonathan.mota@ufrn.br, [3]sandraisaad@gmail.com

References:

ABBASPOUR, K.C.; S., ROUHOLAHNEJAD; VAGHEFI, S; SRINIVASAN, R.; YANG, H.; KLØVE, B. A continental-scale hydrology and water quality model for Europe: Calibration and uncertainty of a high-resolution large-scale SWAT model. Journal of Hydrology. 2015. DOI: https://doi.org/10.1016/j.jhydrol.2015.03.027.

LI, Wuhua; CHENG, Xiangju; Zhu, Dantong. Towards the hydrological effects of land use change in karst area, a case study in Lijiang River Basin, China. Journal of Hydrology. 2024. DOI: https://doi.org/10.1016/j.jhydrol.2024.130629

XAVIER, Alexandre C.; KING, Carey W.; SCANLON, Bridget R. New improved Brazilian daily weather gridded data (1961–2020). International Journal of Climatology, 2022. DOI: 10.1002/joc.7731.

8th IAHR EUROPE CONGRESS
LISBON - PORTUGAL
4-7 JUNE 2024

WATER - ACROSS BOUNDARIES

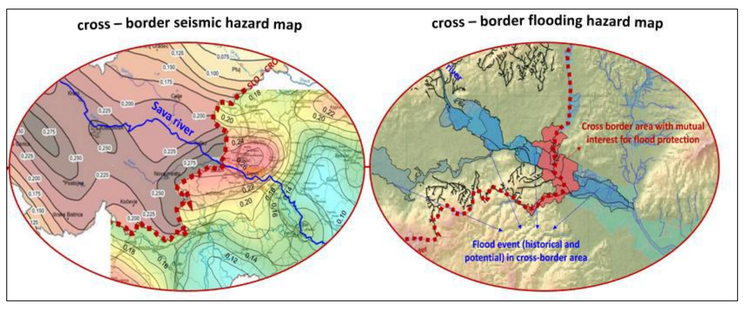
IAHR AIRH
Hosted by Spain Water and IWHR, China

# Cross border cascading hazard scenarios in Sava River Basin – results of the CROSScade project

Rak G.[1], Novak G.[1], Četina M.[1], Žižmond J.[2], Anžlin A.[3], Kosič M.[3]
[1] University of Ljubljana, [2]SPEKTRAL d.o.o., [3]ZAG (all from Slovenia)

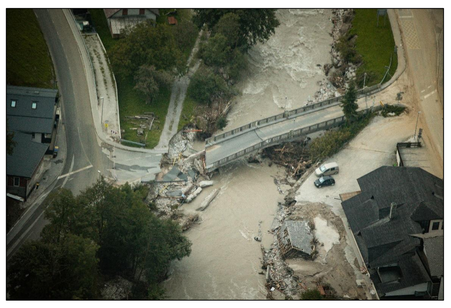
## Motivation

Severe earthquakes in Croatia (2020) and floods in Slovenia (2023) → Project CROSScade (Cross-border cascading risk management for critical infrastructure in the Sava River Basin): investigation of risks caused by earthquakes, floods, and their possible cascading sequence of events in the cross-border region of Slovenia and Croatia.







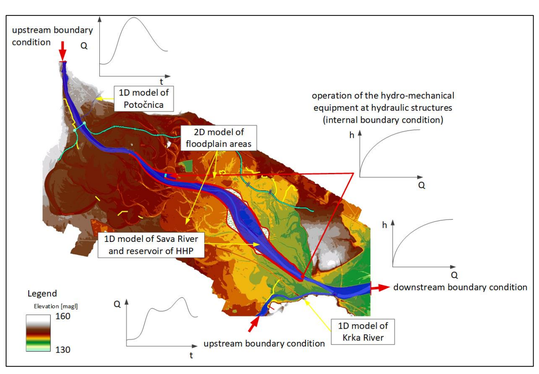



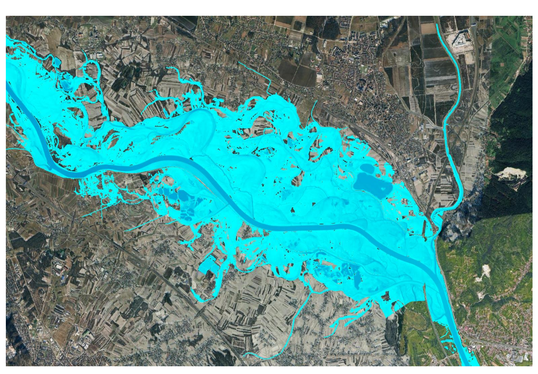
## Methodology

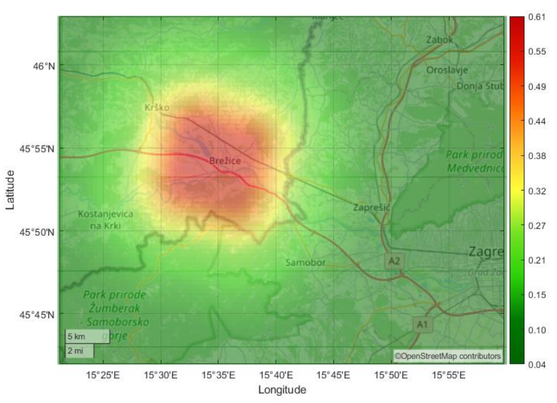
| Hydraulic models | Seismic models |
|---|---|
| Sections: Brežice – SLO and CRO border – Zagreb; 70km$^2$ | Two seismic scenarios examined → historic events |
| MIKE Flood + HEC-RAS; 1D+2D approach; HPP operating | Scenario 1: $M_w$ = 5.7 earthquake near Brežice (Slovenia) |
| Geometry: LIDAR + profiles + HPP design/operation data | Scenario 2: $M_w$ = 6.0 earthquake near Zagreb (Croatia) |
| Calibration: water gauging stations, field measurements | Simulations based on ESHM2020 prediction equation |
| 5 scenarios of HPP malfunctioning and gate(s) breakage | Area divided into 500 m x 500 m cells |
| 3 flood wave scanarios: $Q_{10}$, $Q_{100}$, $Q_{500}$ + levee breaching | Each scenario: 500 simulations |

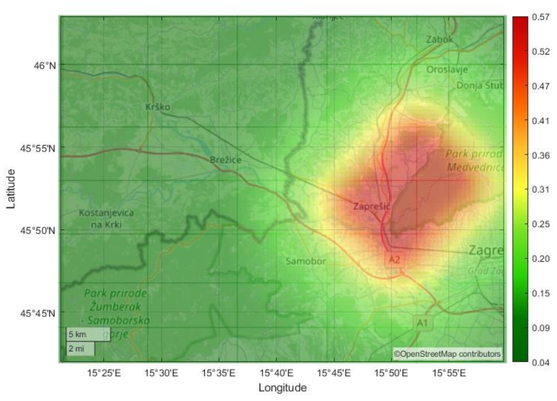
## Results

- Hydraulic models: Q(t), h(t), v(t) at locations of critical infrastucture, and flood maps
- Seismic models: Spatial distribution of peak ground acceleration (PGA) on the rock surface






## Conclusions

1) Selected 5 most relevant scenarios of HPP Brežice malfunction and breaching → showed no serious damage to critical infrastructure → additional simulations of $Q_{10}$, $Q_{100}$ and $Q_{500}$ floods → investigation of critical levees.
2) Seismic simulations showed the largest PGAs above the fault rupture zone; individual simulations showed significant variability in PGA values → potentially different consequences & larger cross-border impacts.
3) Hydraulic and seismic modelling results formed the basis for a detailed vulnerability analysis of critical infrastructure.
4) The conclusions point to the importance of developing cross-border harmonised hazard scenarios that go beyond the limitations of national studies, which are often restricted to specific geographical boundaries.

Contacts: gasper.rak@fgg.uni-lj.si; gorazd.novak@fgg.uni-lj.si; matjaz.cetina@fgg.uni-lj.si; jure.zizmond@spektral.si; mirko.kosic@zag.si; andrej.anzlin@zag.si

References: Deliverables of the CROSScade project - available for download at https://crosscade.eu/

Acknowledgments: Project CROSScade (Cross-border cascading risk management for critical infrastructure in the Sava River Basin) was co-funded by European Union, Grant Agreement Number 101048395

8th IAHR EUROPE CONGRESS
LISBON - PORTUGAL
4-7 JUNE 2024
WATER - ACROSS BOUNDARIES
IAHR AIRH
Hosted by Spain Water and IWHR, China

# Depth determination in coastal regions using a Machine Learning model and a time-series of PlanetScope images

Rúben Santos[1,2], Rui Quartau[1,2]
[1] Instituto Hidrográfico – Marinha
[2] Universidade de Lisboa, Faculdade de Ciências, Instituto Dom Luiz

## Motivation

The objective of this study, conducted in Tavira, Portugal, is to **demonstrate the capability to determine depths in shallow water regions without depending on in-situ data**, **particularly in areas where acquiring acoustic data is cost-prohibitive in coastal monitoring programs**. To achieve this goal, a model previously trained with depth data and multispectral images from 2018 was used. This model enables depth determination for any period by providing multispectral images. In this investigation, 9 satellite images sourced from the PlanetScope (PS) constellation, with a spatial resolution of 3.0 m and four spectral bands (blue, green, red, and near-infrared), were employed. Despite the relatively diminutive size of these satellites (0.1 x 0.1 x 0.3 m), their optical sensors yield images of lesser quality compared to those captured by Sentinel-2 satellites, thereby posing challenges in the context of depth determination. Overcoming the uncertainty introduced by this limitation is achievable through the adoption of a high temporal resolution strategy, such as daily image acquisition. Leveraging this time series enables the mitigation of noise, outliers, and other dynamic factors that fluctuate over time, influencing the accurate calculation of depth values. These factors include turbidity, suspended matter concentration, and chlorophyll-a levels along the water column.

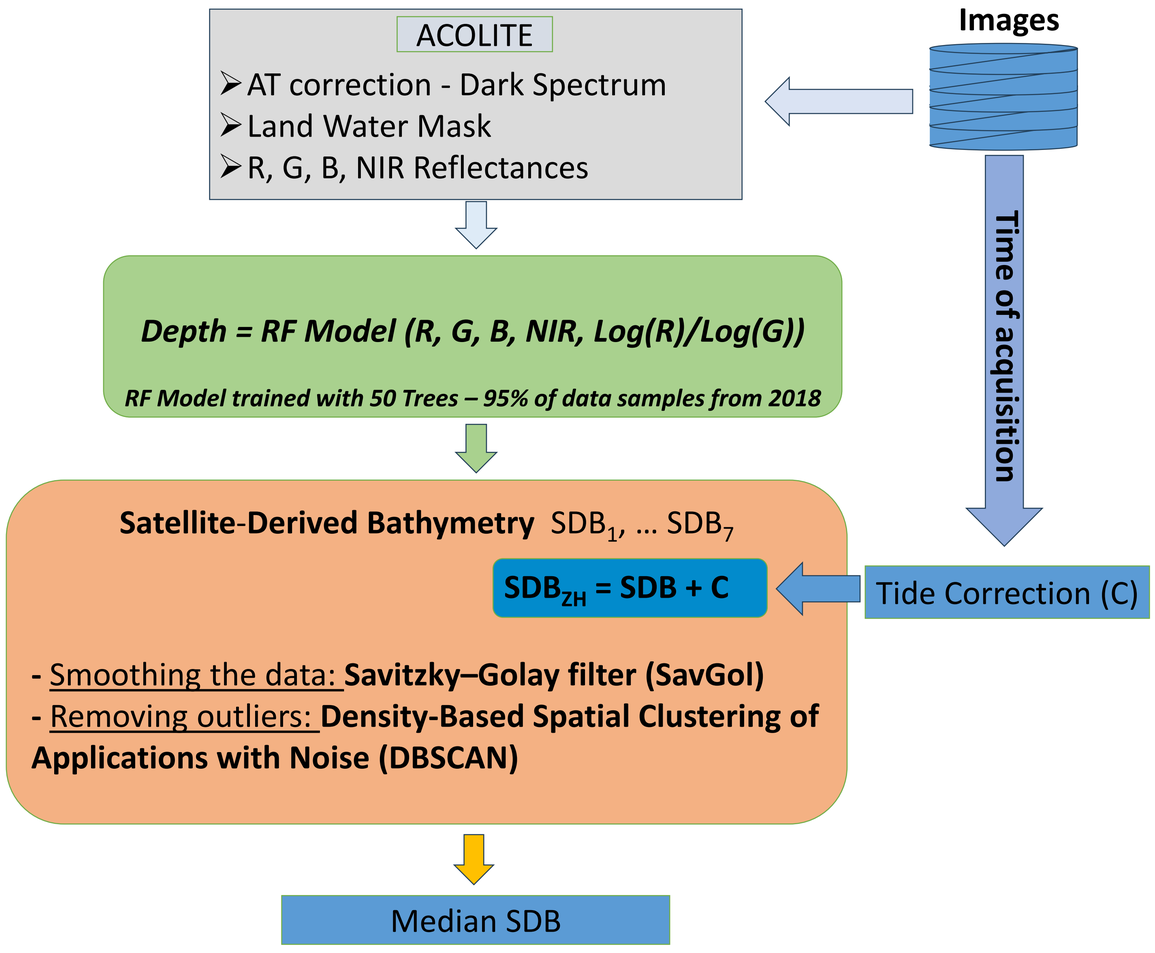
## Methodology

Random Forest (RF) model (2018) allowed the Satellite-Derived Bathymetry (SDB) for 9 PS images, acquired between August and October 2019. The 9 PS images were processed by Dark Spectrum to remove the atmospheric effects, the band reflectances were determined and the Water-Land mask was applied.

The tidal height for each acquisition time was removed from the depths determined by the RF model, obtaining all SDB surfaces in relation to the same vertical reference. The Savitzky-Golay filter was applied to smooth the results, followed by the application of the DBSCAN (Density-Based Spatial Clustering of Applications with Noise) algorithm to eliminate outliers and noise. Subsequently, the median value for depth (Median SDB) was derived.

A vertical cross-section was computed, spanning from the shallow to the deep regions, utilizing the 9 SDB and Digital Elevation Model Reference (DEMR).

Quality verification involved measuring the differences between the Median SDB and DEMR surfaces. The analysis included determining the histogram, mean, median, and standard deviation of those differences.




## Results

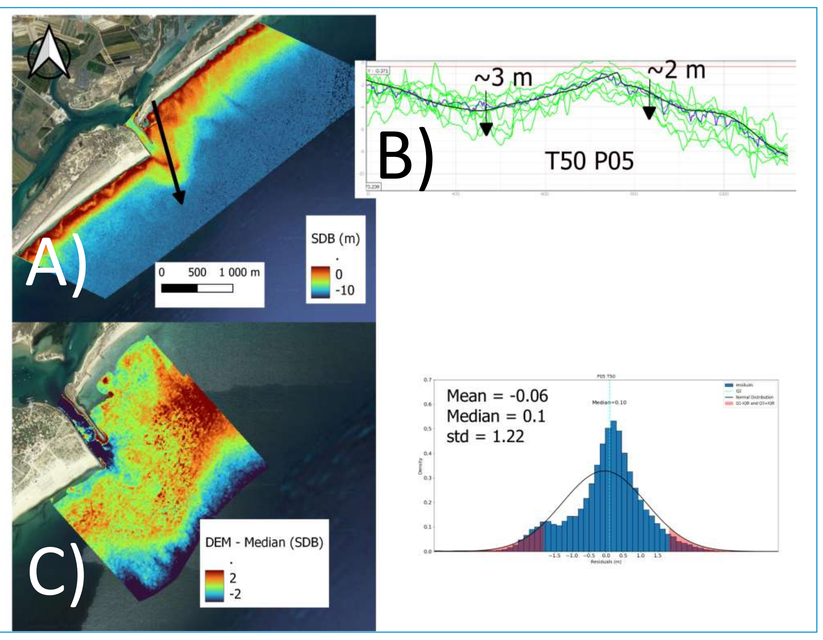
A) The final depth results are represented by Median Satellite-Derived Bathymetry Surface (Median SDB) that aligns closely with the morphological features observed in the Digital Elevation Model – 2019 Reference (DEMR, black line in cross-section of Figure B).

B) The 9 SDB (green lines in cross-section of Figure B) that originated the final result, reveals a vertical variation of 2-3 m (cross-section location is represented by black arrow in Figure A).

C) The differences between the Median SDB and DEMR provides the following insights (Figure C and graph):

- Median of 0.1 m; Mean of -0.06 m; Standard deviation of 1.22 m

- The histogram of the differences follows a normal distribution with its central tendency positioned at the median value.




## Conclusions

The results obtained in this study are promising for obtaining depths in coastal regions through multispectral images without the need for in-situ data. However, we are aware that improving the current model is important to reduce the median and standard deviation of the differences between the determined depth and the reference. Enhancing the model will lead to more accurate results, enabling the determination of seasonal variations and changes caused by extreme events or climate alterations without in-situ data.

Contacts: ruben.santos@hidrografico.pt

Acknowledgments: This work was funded by the Portuguese Fundação para a Ciência e a Tecnologia (FCT) I.P./MCTES through national funds (PIDDAC) – UIDB/50019/2020. Planet - Education and Research Program. COSMO – Agência Portuguesa do Ambiente

8th IAHR EUROPE CONGRESS
LISBON - PORTUGAL
4-7 JUNE 2024
WATER - ACROSS BOUNDARIES

IAHR AIRH
Hosted by Spain Water and IWHR, China

# Impact of the RF algorithm parameterization on the determination of depth in coastal regions using PlanetScope images

Rúben Santos[1,2], Rui Quartau[1,2]
[1] Instituto Hidrográfico – Marinha
[2] Universidade de Lisboa, Faculdade de Ciências, Instituto Dom Luiz

## Motivation

This study was conducted in a region where the acquisition and updating of bathymetry are quite expensive through conventional methods, leading to the lack of knowledge about more than 50% of the seafloor morphology in these coastal areas. In recent decades, the scientific community has developed algorithms capable of determining depth from satellite-acquired images to obtain updated information of the coastal regions. The Hydrographic Institute (IH) has been developing methodologies to improve information for these regions, employing empirical, physical, and statistical algorithms. Empirical models are simple to apply and produce results with residuals between 1.5 and 2.0 m when compared to acoustic data. On the other hand, implementing physical models is a complex task, requiring substantial computational resources and a comprehensive set of parameters for the water column. However, these models provide more accurate results with residuals between 0.7 and 1.2 m. Statistical models, including Machine Learning algorithms, also require significant computational resources but yield results with residuals in the range of 0.4 to 1.0 m, which are interesting for depth determination. The present study aims to analyze the influence of parameterization of the Machine Learning algorithm, Random Forest (RF), in determining Satellite-Derived Bathymetry (SDB) in the coastal region of Tavira.

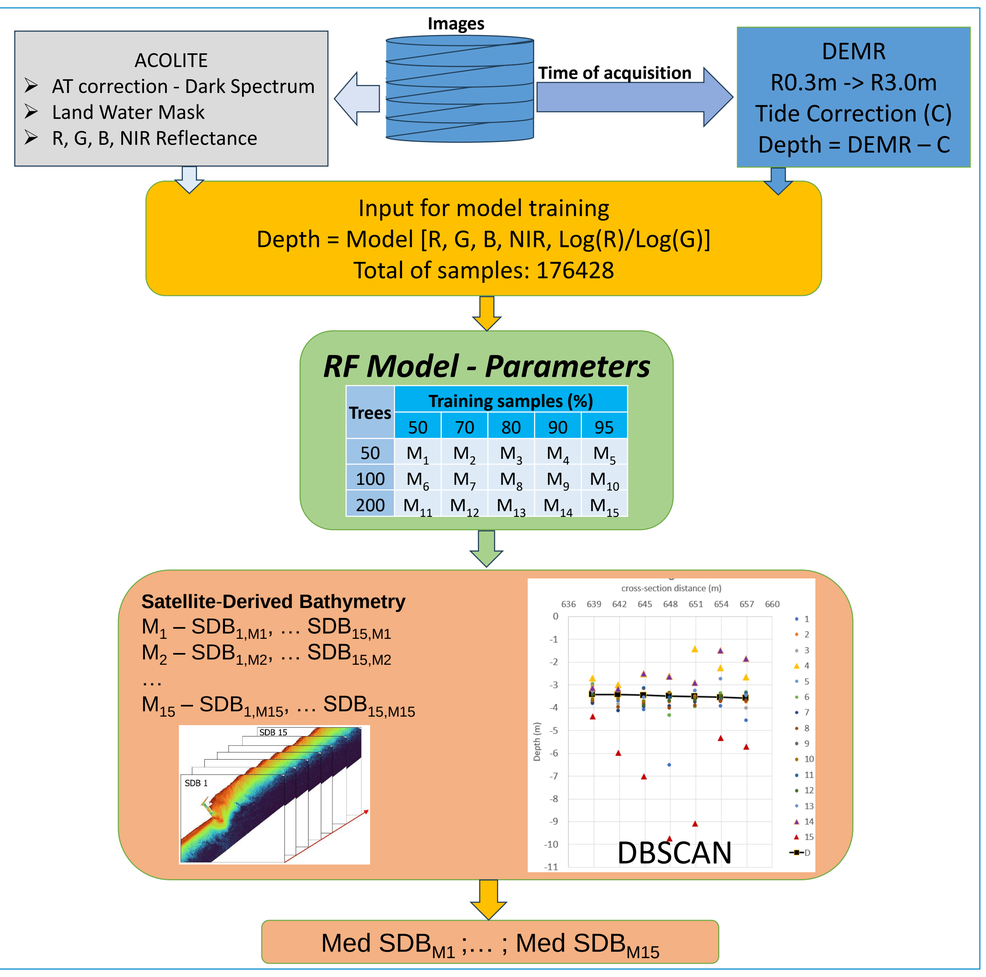
## Methodology

15 PlanetScope (PS) images were selected with 4 spectral bands: blue (B1), green (B2), red (B3), and near-infrared (B4), acquired between August and October 2018 to cover the topographic-hydrographic survey that was the source for the Digital Elevation Model of Reference (DEMR) with a spatial resolution of 0.3 m and then the resolution was decreased to 3.0 m. The tide height at acquisition time of each image was determined using modeled data for the tide gauge of Faro provided by the IH. PS images were processed by Dark Spectrum to remove the atmospheric effects; the band reflectances were determined and the Water-Land mask was applied.

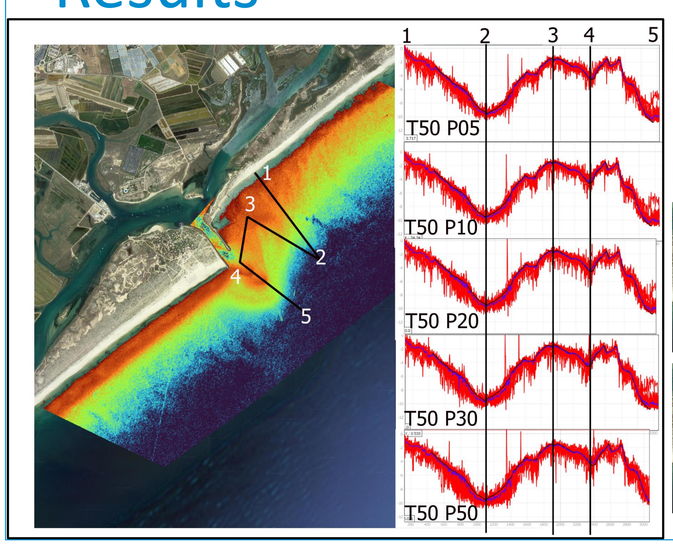
The input dataset for the model training was the depths corrected for the tide height at the time of image acquisition, the reflectances of spectral bands B1, B2, B3, B4, and the ration of log(B3)/log(B2). This allowed us to study the impact of parameterization on the depth determination by varying the number of decision trees (50, 100, 200) and the percentage of data used in model training (50, 70, 80, 90, 95). Each model was applied to all 15 satellite images, resulting in 15 SDB for each model.

Density-Based Spatial Clustering of Applications with Noise (DBSCAN) was applied to the 15 SDB to remove outliers and noise, then a median SDB was determined.

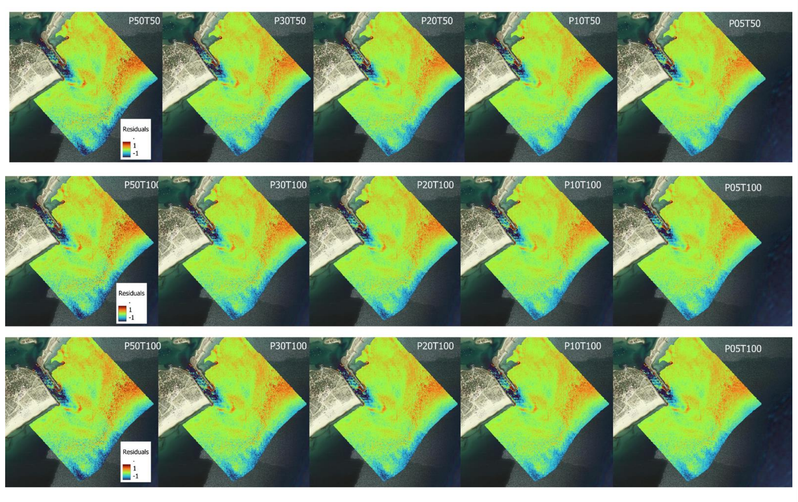
The median SDB for each model parameters was compared with DEMR for analyzing the impact of parameters in the final SDB.

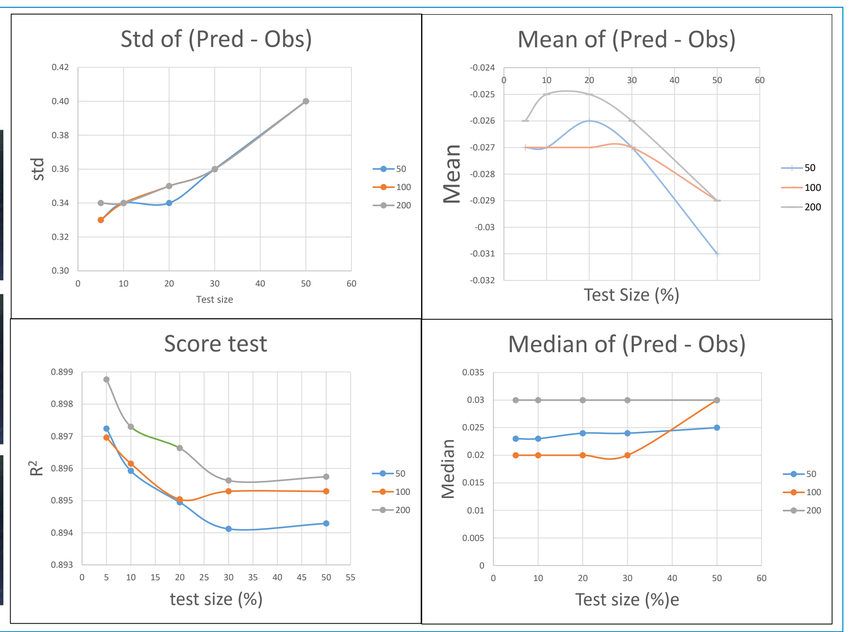



## Results




Residuals = Med SDB - DEMR




## Conclusions

The standard deviation of residuals between Median SDB and DEMR varied between 0.33 and 0.40 meters. The best results were obtained for models trained with more samples. The number of decision trees had no impact on these results. The score test (R2) allowed observing a high efficiency of the model adjustment to the test data. All test values ranged between 0.89 and 0.90, concluding that the model parameterization had no impact on these results. These results are promising as they suggest that it may be possible to apply these models to images of different years without the need of in-situ depth surface. In future could be study the noise removal process and explore the model's transferability to diverse coastal environments.

Contacts: ruben.santos@hidrografico.pt

Acknowledgments: This work was funded by the Portuguese Fundação para a Ciência e a Tecnologia (FCT) I.P./MCTES through national funds (PIDDAC) – UIDB/50019/2020. Planet - Education and Research Program. COSMO – Agência Portuguesa do Ambiente

WATER - ACROSS BOUNDARIES

8th IAHR EUROPE CONGRESS
LISBON - PORTUGAL
4-7 JUNE 2024

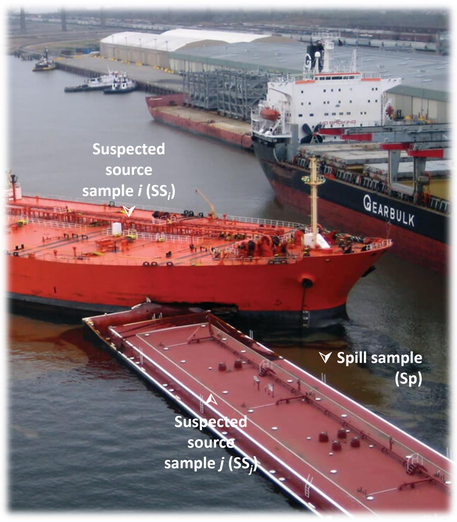
IAHR AIRH
Hosted by Spain Water and IWHR, China

# Statistically sound approach to compare oil patterns and assess the accuracy of the forensic findings

A. C. Rocha[1,2], C. Palma[1], R.J.N. Bettencourt da Silva[2]

[1] Division of Chemistry and Pollution of Marine Environment, Hydrographic Institute
[2] Center for Strutural Chemistry, Faculty of Science of the University of Lisbon

## Motivation




- Oil spills in marine environments are common and represent a significant environmental concern.
- The findings obtained from chemical analyses of spill (Sp) and suspected sources (SS) samples are used to identify the polluting source and presented in court to assign legal liability.
- The evidence's weight conferred by the chemical analysis findings can be expressed as likelihood ratio (*LR*) and should also be presented to support the defendant's guilt or innocence verdict in court.
- In oil spill source assessment, the *LR* is represented by the ratio of the probabilities of observing compositional equivalence between Sp and two competing suspected spill sources, ($SS_i$ and $SS_j$) given that the spilled oil and the oil from the suspected sources *i* and *j* are and are not the same, respectively. The higher the *LR* value, greater is the ability to distinguish oil compositions from different suspected sources.
- The chemical composition of oil samples, *i.e.*, oil fingerprints, are characterised by a set of ratios between abundances of oil-discriminating compounds, known as diagnostic ratios (*DR*).
- To identify the spill source, the oil fingerprints have been compared using the Student-*t* test (S-t) or a single criterion (SC) applied to the comparison of all *DR* of the fingerprint, recommended by the Nordtest method [1] and the EN 15522-2 standard [2], respectively.
- The S-t and SC approaches are supported on assumptions (*i.e.*, normality of the *DR* probability distributions and a relative standard deviation based on the empirical knowledge experts) which can lead to a higher probability of inaccurate polluting source identifications.

**It is necessary to develop new methods for interpreting results that are based on suitable statistical approaches to guarantee the quality of the identification, as well as to present the evidence in court in an intelligible way.**

**This work presents:**

- **a new approach, that provides statistically sound criteria for *DR* comparison, simulates *DR* used to estimate the probabilities of true and false compositional equivalence claim and calculate *LR*;**
- **the assessment of the performance and the identification quality obtained by the new approach and the conventional ones;**
- **an uncertainty-based strategy to report the chemical analysis findings for oil spill source identification.**

## Results

Composition of SS3 more similar to Sp1 and Sp2 than SS2 (higher $P_{FEq}$, in particular the $P_{FEq}$ estimated by the MCM and S-t approaches)

- $P_{TEq}$, $P_{FEq}$ and, consequently, *LR* are affected by the number of *DR* compared, the compositional similarity degree between Sp and SS and the number of *DR* comparison trials considered to declare compositional equivalence of Sp and SS.
- Higher $P_{TEq}$ and $P_{FEq}$ were found when the compared fingerprints were characterised by a reduced number of *DR* (Sp2 *vs.* SS1/SS2/SS3).

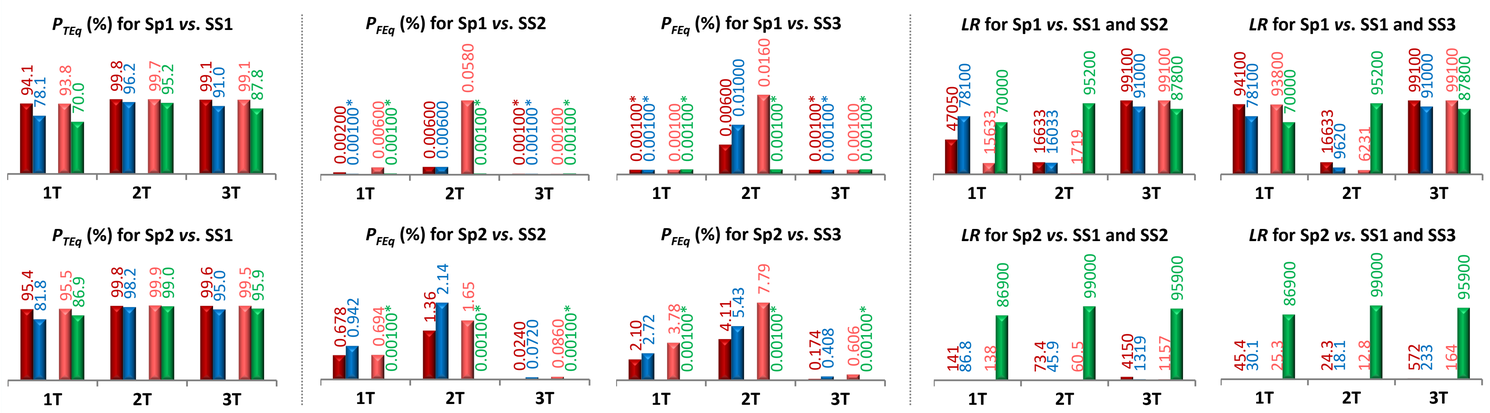



**Fig. 1:** Likelihood ratios (*LR*) and probabilities of true ($P_{TEq}$) and false ($P_{TEq}$) compositional equivalence claim, determined by MCM, S-t and SC approaches, considering the assessment of compositional equivalence using a different number of DR comparison trials (*x*T, with *x* as the number of trials): ■ MCM approach (Nordtest scenario); ■ MCM approach (EN 15522-2 scenario); ■ S-t approach (Nordtest scenario), and ■ SC approach (EN 15522-2 scenario). (*) $P_{FEq}$ = 0; for *LR* determination purpose, the worst case of a half of a compositional equivalence claim in 50,000 analised DR sets was assumed.

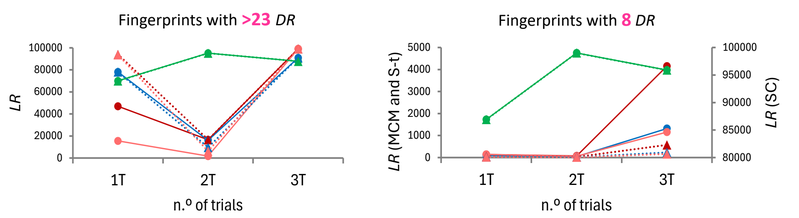
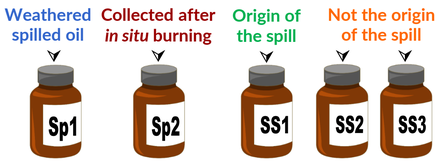



**Fig. 2:** Evolution of the likelihood ratio value (*LR*) with the number of *DR* comparison trials considered (*x*T, with *x* being the number of trials) for the fingerprints comparison: ● Sp1 *vs.* SS1 and SS2 and ▲ Sp1 *vs.* SS1 and SS3, both by MCM approach (Nordtest scenario); ● Sp1 *vs.* SS1 and SS2 and ▲ Sp1 *vs.* SS1 and SS3, both by MCM approach (EN 15522-2 scenario); ● Sp1 *vs.* SS1 and SS2 and ▲ Sp1 *vs.* SS1 and SS3, both by S-t approach (Nordtest scenario); ● Sp1 *vs.* SS1 and SS2 and ▲ Sp1 *vs.* SS1 and SS3, both by SC approach (EN 15522-2 scenario).

- When the MCM and S-t approaches are used to evaluate the compositional equivalence of Sp1 or Sp2 and the competing SS considering the outcomes from two trials, the *LR* decreases due to an increase in $P_{FEq}$, despite an important rise in $P_{TEq}$. The introduction of a 3rd trial in the evaluation of the compositional equivalence of the compared samples results in an increase in the *LR*, owing mainly to the substantial reduction in $P_{FEq}$.
- The determined *LR* for SC approach reflect only the $P_{TEq}$ variation with the number of trials considered (null $P_{FEq}$ estimated).
- A relevant increase in *LR* is achieved when a 3rd trial is considered in the comparison of Sp with SS that is not the spill source (benefit in reducing $P_{FEq}$), while only two trials can be considered when comparing Sp and SS that is the spill source (benefit in increasing $P_{TEq}$), unless a defined threshold value is not met.

## Methodology

1. Samples from a Round Robin Test were analysed:




2. Sample preparation, GC-MS analysis and *DR* selection according to EN 15522-2 [2].




3. *DR* simulation: performed applying the chromatographic data of each Sp and SS to a developed and available computational tool [3], under the *DR* comparison conditions recommended by the Nordtest method [1] and the EN 15522-2 [2] (MCM and S-t confidence intervals determined for 98% of confidence level);

**Nordtest scenario** applied to MCM and S-t

$$n_{Sp} = n_{SS} = 3 \quad ; \quad DR = \frac{A}{(A+B)}$$

**EN 15522-2 scenario** applied to MCM and SC

$$n_{Sp} = n_{SS} = 2 \quad ; \quad DR = \frac{A}{B}$$

$n_{Sp}$ and $n_{SS}$- n.° of replicates applied to simulation; *A* and *B* – abundances of compound *A* and *B*.

4. Estimation of the probabilities of true ($P_{TEq}$) and false ($P_{FEq}$) compositional equivalence claim used to determine *LR* as described in Fig. 3:

- **Combination of the outcomes from *x* *DR* comparison trials:** false difference claims are less likely when the compositional equivalence are evaluated using the *DR*s' match results from other *DR* comparison trial that apply different GC-MS analyses of Sp and/or SS [3; 4].
- **Equivalence of $\overline{DR}_{Sp}$ and $\overline{DR}_{SS}$:** assigned when the zero is included in the confidence intervals.
- **Compositional equivalence of Sp and SS:** declared if each $\overline{DR}_{Sp}$ is equivalent to the respective $\overline{DR}_{SS}$ in at least one or two out of two and three *DR* comparison trials, respectively.

MCM $\left(\overline{DR}_{Sp} - \overline{DR}_{SS}\right) \pm t(0.02;2) \cdot s$ S-t $\left(\overline{DR}_{Sp} - \overline{DR}_{SS}\right) \pm t(0.02;|\xi|) \cdot s_d$ SC $\left(\overline{DR}_{Sp} - \overline{DR}_{SS}\right) \pm 0.14 \cdot \overline{DR}_d$

$s$ - standard deviation of the $\left(\overline{DR}_{Sp} - \overline{DR}_{SS}\right)$
$s_d$ - standard deviation of the $\left(\overline{DR}_{Sp} - \overline{DR}_{SS}\right)$ [3]
$|\xi|$ - degrees of freedom of the $\left(\overline{DR}_{Sp} - \overline{DR}_{SS}\right)$ [3]
$\overline{DR}_d$ - mean value of $\overline{DR}_{Sp}$ and $\overline{DR}_{SS}$ [3]

$\left(\overline{DR}_{Sp} - \overline{DR}_{SS}\right)$: mean value of three $\left(\overline{DR}_{Sp} - \overline{DR}_{SS}\right)$ simulated
$\left(\overline{DR}_{Sp} - \overline{DR}_{SS}\right)$: difference between mean values of three $\overline{DR}_{Sp}$ and three $\overline{DR}_{SS}$ simulated
$\left(\overline{DR}_{Sp} - \overline{DR}_{SS}\right)$: difference between mean values of three $DR_{Sp}$ and three $DR_{SS}$
Considered 98% of confidence level

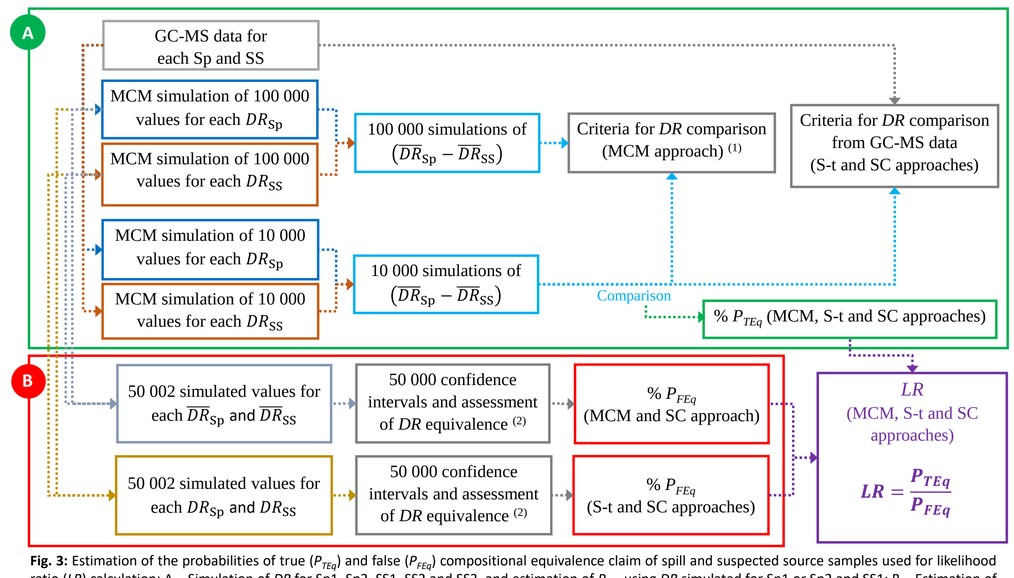



**Fig. 3:** Estimation of the probabilities of true ($P_{TEq}$) and false ($P_{FEq}$) compositional equivalence claim of spill and suspected source samples used for likelihood ratio (*LR*) calculation: A – Simulation of *DR* for Sp1, Sp2, SS1, SS2 and SS3, and estimation of $P_{TEq}$ using *DR* simulated for Sp1 or Sp2 and SS1; B – Estimation of $P_{FEq}$ using *DR* simulated for Sp1 or Sp2 and SS2 or SS3. (1) Determination described by Rocha et al. [3]; (2) Determination described in the poster.

## Conclusions

- Conventional approaches revealed limitations in presenting the findings of chemical analysis, identifying the polluting source with greater uncertainty (<$P_{TEq}$) despite, in general, reliably distinguishing the oil compositions from competing suspected sources. However, when a small number of *DR* is compared and/or both SS are very similar to Sp, the MCM and the S-t approaches showed a weaker distinction of chemical compositions of competing SS, needing a 3rd *DR* comparison trial to increase the *LR* value. The MCM approach prove to be more promising in comparing oil fingerprints, as it is the approach that ensures identifications with reduced uncertainty (>$P_{TEq}$) and appropriate discrimination between the oil patterns of the suspected sources, particularly characterised by an adequate DR set. Moreover, the MCM approach's identification criteria are the only ones that are statistically sound and appropriately adjusted to the performance of the *DR* determination. If the experts use the Nordtest or EN 15522-2 methods, they should be aware of the drawbacks, which can be lessened by conducting multiple DR comparison trials—a step that these methods do not advise.

- The variations in $P_{TEq}$ and $P_{FEq}$ observed in the study allowed us to establish a strategy for reporting the findings from chemical analyses performed on Sp and SS. The strategy (Fig. 4) improves the ability to discriminate between oil compositions from competing suspected sources by increasing the *LR* value, as well as to grant a sound conclusion about the spill origin by increasing the probability of the compositional equivalence claim of Sp and SS most likely to be the polluting source. The *LR* are determined using probabilities of compositional equivalence claim from the two most probable spill sources ($P^{xT}_{Sp|SS_\alpha}$ and $P^{xT}_{Sp|SS_\beta}$). A minimum threshold values are needed to identify the spill source and to assess the discrimination of competing SS compositions: $P^{xT}_{Sp|SS_\alpha} \geq 95.0\%$ and a $LR \geq 190$ (an $LR > 100$ leads to a moderately strong support according to ENFSI guidelines [5]). The *DR* equivalence assessment from other *DR* comparison trial is included in the estimation of $P^{xT}_{Sp|SS_\alpha}$ and/or $P^{xT}_{Sp|SS_\beta}$ if the defined criteria are not met.

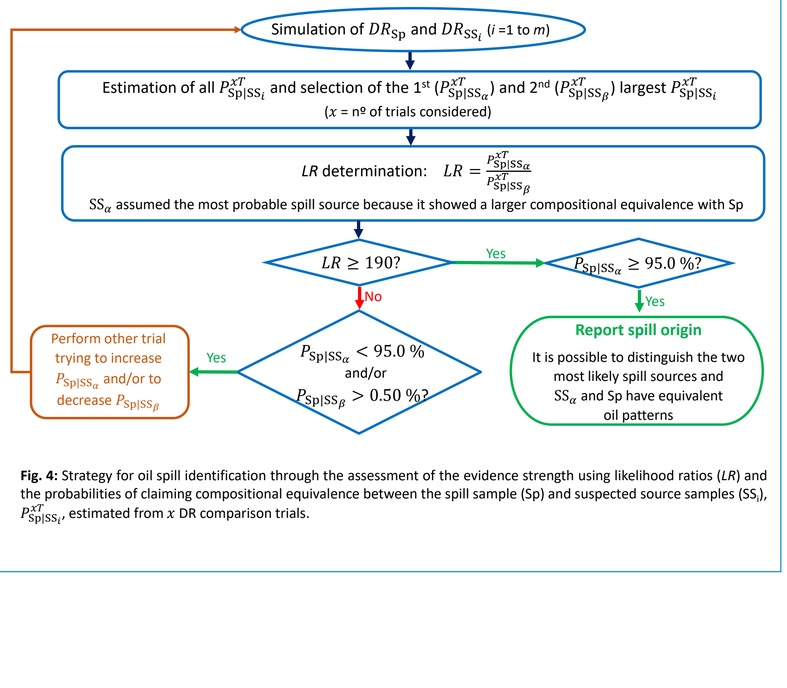



**Fig. 4:** Strategy for oil spill identification through the assessment of the evidence strength using likelihood ratios (*LR*) and the probabilities of claiming compositional equivalence between the spill sample (Sp) and suspected source samples ($SS_i$), $P^{xT}_{Sp|SS_i}$, estimated from *x* DR comparison trials.

**Acknowledgments:** The authors are thankful for the volunteer organisation of Round Robins Tests on the identification of oil spills by the Oil Spill Identification Network of Experts within Bonn Agreement (Bonn-OSINet).

## References:

[1] [2] [3] [4] [5]

## Contacts:



**Ana Catarina Rocha**
catarina.rocha@hidrografico.pt



**Ricardo Bettencourt da Silva**
rjsilva@ciencias.ulisboa.pt



**Carla Palma**
carla.palma@hidrografico.pt

8th IAHR EUROPE CONGRESS
LISBON - PORTUGAL
4-7 JUNE 2024
WATER - ACROSS BOUNDARIES
Hosted by Spain Water and IWHR, China

# Air Characteristics During Rapid Filling of Long Distance Water Transmission Pipes

Rui-lin Feng[1], Ling Zhou[2], Mohsen Besharat[3] , Yanqing Lu[4] , Qian-xun Chen[5] , Yinying Hu[6] , Yunjie Li[7]

[1] College of Water Conservancy and Hydropower Engineering, Hohai University, 1 Xikang Road, Nanjing, China; [2] School of Civil Engineering, University of Leeds, Leeds, LS2 9JT, UK

## Motivation

The long-distance water transmission system has a complex pipeline layout, during changes in operating conditions, maintenance and repairs, it faces the challenge of dealing with large volumes of trapped air in the pipeline during air-water two-phase flow. Trapped air pockets can mitigate pressure wave impacts or cause severe and damaging pressure. Current numerical models used to study air content in pipelines are the rigid water column model proposed by Martin (1976), which has undergone continuous improvement by many scholars to consider factors such as water elasticity, water column length change, steady and dynamic friction of pipelines, and so on.

Despite this progress, most existing models assume air changes uniformly, although simplifying the solution, but neglecting the significance of pressure wave transmission during compression and expansion of air, especially for large-scale long-distance water transport systems. Therefore, it is essential to establish a precise model of the rapid filling process that considers air dispersion and assesses the influence of air in large-scale engineering to address this research gap and provide guidance for engineering design. .

## Results

The experimental setting established by Zhou (Zhou et al., 2023). And a virtual long pipe system is constructed after the accuracy of the numerical simulation results is verified by the experiment.

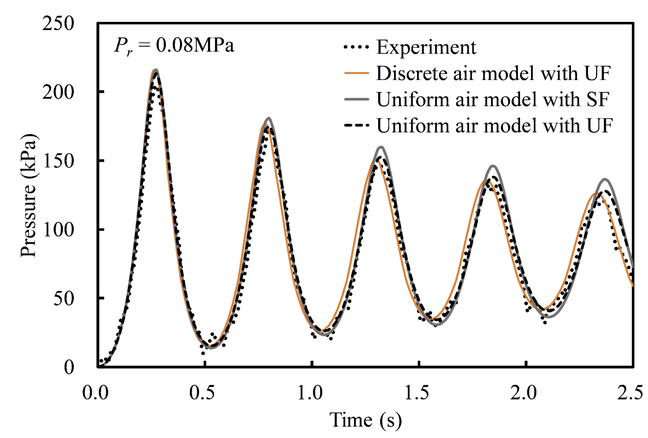



Fig. 1. Comparison of results simulated by discrete air model with uniform air model and Zhou's experiments at $P_r$ = 0.08 MPa

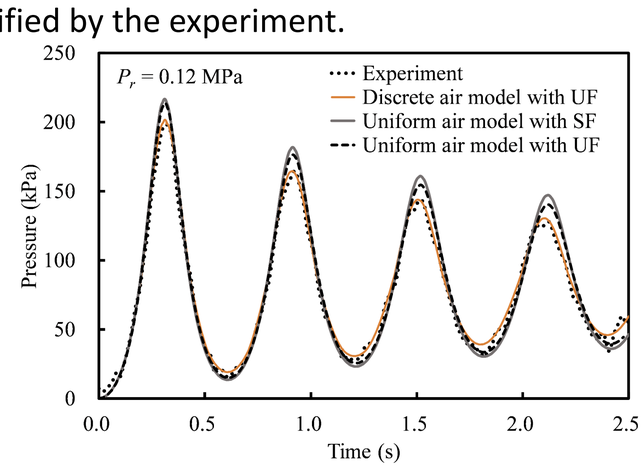



Fig. 2. Comparison of results simulated by discrete air model with uniform air model and Zhou's experiments at $P_r$ = 0.12 Mpa

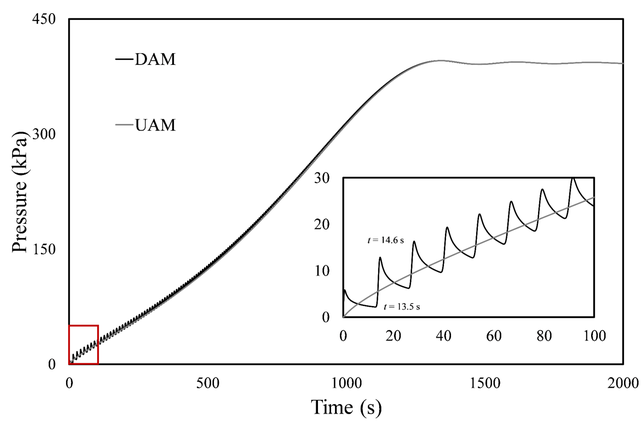



Fig. 3. Comparison of results simulated by discrete air model with uniform air model in a 2400m long pipe system

## Methodology

Mathematical models include: (1) continuity and momentum equations for water, (2) continuity and momentum equations for air, and (3) continuity and pressure equilibrium equations for interfaces. The Godunov scheme of Finite volume method (GTS) is used to solve the process.

(1) The equations for the filling water region

$$\frac{\partial H}{\partial t}+\frac{a^2}{g}\frac{\partial V}{\partial x}=0$$

$$\frac{\partial H}{\partial x}+\frac{1}{g}\frac{\partial V}{\partial t}+J_Q+J_U=0$$

(2) The equations for the air region

$$\frac{\partial \rho}{\partial t}+\frac{\partial(\rho u)}{\partial x}=0$$

$$\frac{\partial(\rho u)}{\partial t}+\frac{\partial(\rho u^2+P)}{\partial x}=0$$

(3) The equations for the air-water interface

$$L_w=L_{w0}+\int_0^t V_{inter}\,dt$$

$$H_{inter}=\frac{P}{\rho_w g}+Z_{inter}$$

## Conclusions

(1) The air continuity equation and momentum equation are derived, which are combined with the water control equation and the air-water interface control equation, and the rapid filling model considering discrete air is established.

(2) The discrete air model considering the basic characteristics of the air is established to simulate the rapid filling process. The simulation results of the proposed model are compared with the uniform air model and experimental results, and it is proved that the model is more accurate in the simulated pressure phase and amplitude.

(3) The propagation process of air pressure waves can be shown, and the internal relation between the wave propagation process and system pressure fluctuation is explored. The pressure wave propagates from the air-water interface to the end of the air and back to the interface, causing a small fluctuation in pressure with each propagation.

(4) The model is applied to a virtual large-scale water pipeline to investigate the scale effect of air pressure waves. The peak pressure is higher than that of the uniform air model over long distances system.

Contacts: rl.feng@hhu.edu.cn

References: such as Zhou, L., Feng, R. L., Pan, T., Li, Y., Liu, D., & Che, T. C. (2023). Coupled Second-Order GTS-MOC Scheme for Transient Pipe Flows with an Entrapped Air Pocket. Journal of Hydraulic Engineering, 149(9), 04023030.

Acknowledgments: The writers gratefully acknowledge the financial support for this research from the National Natural Science Foundation of China (Grant Nos. 51839008 and 51679066) and China Scholarship Council (Grant No. 202306710100) .

8th IAHR EUROPE CONGRESS
LISBON - PORTUGAL
4-7 JUNE 2024
WATER - ACROSS BOUNDARIES

IAHR AIRH
Hosted by Spain Water and IWHR, China

# The comparison of a mechanistic model with a machine learning model for microplastic modelling in Gediz River Basin, Türkiye

Yiğithan KAZANCI[1], Nefise ALYÜRÜK[2], Orhan GÜNDÜZ[1,3], Neval BAYCAN[2]
[1] Izmir Institute of Technology, Department of Environmental Engineering, İzmir, TÜRKİYE;
[2]Dokuz Eylul University, Department of Environmental Engineering, İzmir, TÜRKİYE;
[3]Izmir Institute of Technology, Department of International Water Resources, İzmir, TÜRKİYE

## Motivation



In response to the complexities of microplastic (MP) dispersion, researchers have pursued innovative modeling approaches to predict the behavior of these pollutants. Notably, mechanistic models and machine learning (ML) models have emerged as prominent methodologies. Mechanistic models utilize physical and chemical principles to simulate microplastic fate and transport, while ML models leverage algorithms to discern patterns from available datasets. This study aims to contribute to the evolving field of MP research by conducting a rigorous comparison between mechanistic and ML models in the Gediz River Basin, Türkiye. By evaluating the strengths and limitations of each approach, this research seeks to enhance our understanding of MP distribution in freshwater systems and improve the accuracy of predictive models.



## Methodology

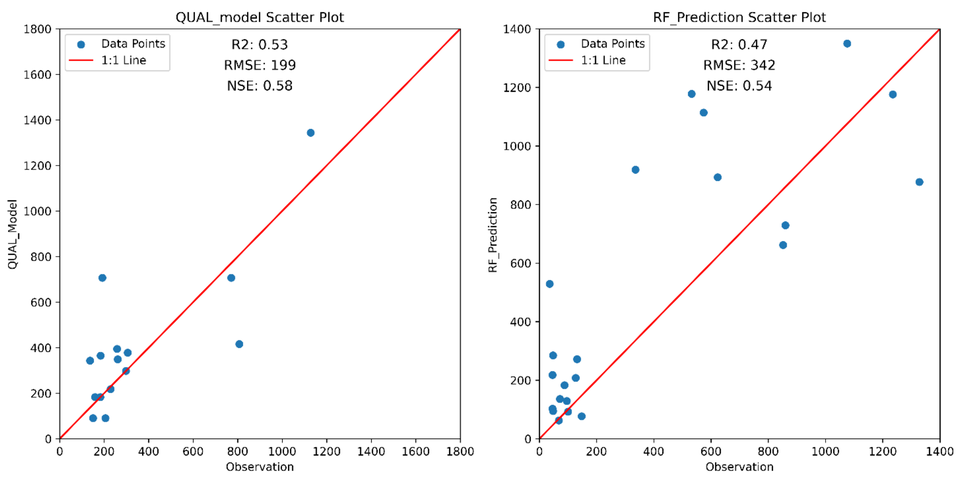
| Feature | | QUAL2K Model | Random Forest Regression Model |
|---|---|---|---|
| **Data Utilization** | | Averages of data from 80 sampling points | All data from 125 sampling points (raw data) |
| **Sampling Period** | | Data from 4 different months | Data from 7 different months |
| **Data Types** | **Hydrodynamical & Hydraulic** | ADCP & Field measurements for streamflow and Manning coefficients | Hydrodynamical, Physicochemical, Microplastic Quantity |
| | **Physicochemical Properties** | Field measurement with multimeters | Field measurements with multimeters |
| | **Microplastics** | Microscope + FTIR Polymer Analysis | Microscope + FTIR Polymer Analysis |
| **Model Type** | | Steady-state simulation (Solution of ADE with backward finite difference scheme) | Regression model (supervised learning, scikit-learn) |
| **Purpose** | | Simulate steady-state response of river microplastic & Determine the spatial distribution of MP | Predict microplastic levels at different times & locations over the Gediz River. |
| **Data Partition** | | Not applicable (N/A) | Training: 80%, Testing: 20% |



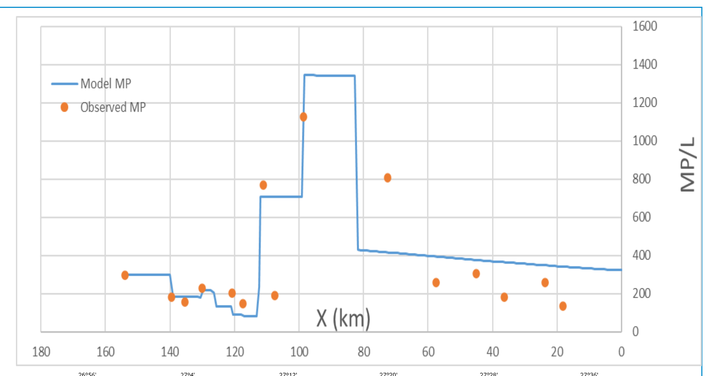


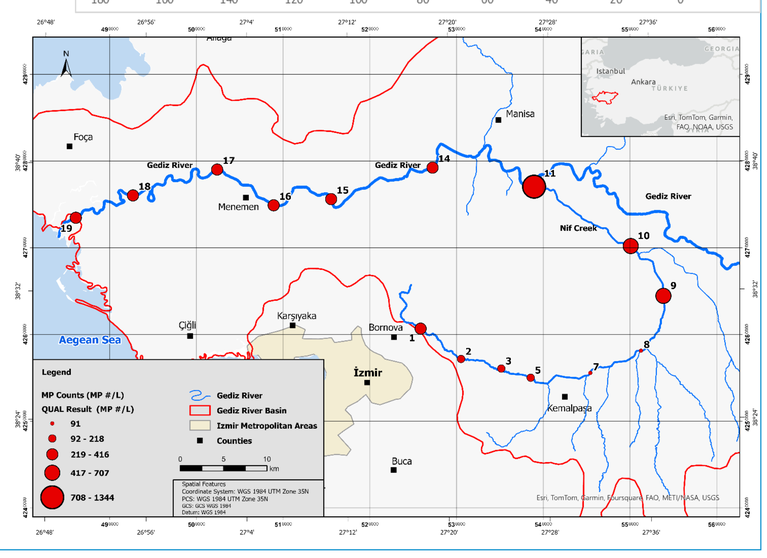
## Results

- A significant outcome of the QUAL2K model highlighted the impact of the Nif River, showing an increase in microplastic concentration until its confluence with the Gediz River, indicating point and diffuse source impacts.
- Both models showed moderate predictive capabilities with R2 values of 0.53 for QUAL2K and 0.47 for RF, indicating a potential for representing microplastic distribution.
- The Nash-Sutcliffe efficiency coefficients were 0.58 for the QUAL2K model and 0.54 for the RF model, suggesting the need for richer datasets and improved site characterizations for enhanced model performance.
- The spatial distribution of microplastics observed in the study exhibits fluctuations that reflect the combined influence of multiple sources along the river, as depicted in the model versus observed data graph.




- The study underscores the potential of combining mechanistic and ML models to offer robust tools for countries with limited access to continuous and diverse data.
- Ongoing research aims to refine both the QUAL2K and RF models, with the ultimate goal of improving the management and mitigation of microplastic pollution in freshwater systems.




## Conclusions

The study conducted in the Gediz River Basin highlights the critical need for determining baseline levels of microplastics in inland rivers through advanced modeling techniques. By integrating the mechanistic QUAL2K model with the data-centric Random Forest model and rigorously cross-checking their performances, we are better positioned to understand and predict microplastic distribution. This dual-model approach not only facilitates more accurate assessments of microplastic pollution but also serves as an essential step in developing targeted strategies for the mitigation and management of microplastics in freshwater systems. Such collaborative modeling efforts are vital for the protection and preservation of inland water bodies from the pervasive threat of microplastics.

Contacts: Yiğithan Kazancı, yigithankazanci@iyte.edu.tr

References: Pedregosa et al., JMLR 12, pp. 2825-2830, 2011, Chapra, S. C., Pelletier, G. J., & Tao, H. (2003). Qual2K. A Modeling Framework for Simulating River and Stream Water Quality (Beta Version): Documentation and User's Manual, Civil and Environmental Engineering Department, Medford, Tufts University.

Acknowledgments: This study was supported by Scientific and Technological Research Council of Turkey (TÜBİTAK) with project number of 121Y460.

8th IAHR EUROPE CONGRESS
LISBON - PORTUGAL
4-7 JUNE 2024
WATER - ACROSS BOUNDARIES

IAHR AIRH
Hosted by Spain Water and IWHR, China

# Coastal Risk Assessment and Application of the small islands: case study on Green Island and Orchid Island in Taiwan

Chun-Jhen YE[1], Wei-Po HUANG[1], Jui-Chan HSU[1]
[1] National Taiwan Ocean University, Taiwan

## Motivation

Green Island and Orchid Island are two islands under Taiwan's jurisdiction, accounting for only 0.04% and 0.13% of Taiwan's total area, respectively. With rich natural ecological resources and Austronesian culture (Figure 1), the length of the natural shoreline accounts for more than 80%, bringing an average of hundreds of thousands of tourists visiting every year. However, because Green Island and Orchid Island are located in the area affected by typhoons in the northwest Pacific Ocean, they are often affected by storms and swell. Therefore, the coastal protection facilities have been built in many places under the petitions of the local people. At the same time, coastal protection facilities are in conflict with adjacent natural landscapes. Thus, through the coastal risk assessment, this study clarifies the risk level and vulnerability of each coastal protection facility section and then discusses feasibility such as reducing the elevation of coastal protection facilities or decommissioning them. The result will feed back to the competent authorities for the sustainable development of coastal areas and coping with climate change.



Figure 1. The vessels of the Yam's aborigines in Orchid Island.

## Results

### (A) Risk Identification

According to the results of the anonymous FDM-based questionnaire, representative hazard/vulnerability factors include:

| | |
|---|---|
| Hazard | (a)Geophysical properties; (b)Storm wave; (c)Wave; (d)Width of the buffer zone; (e)Historical event; (f)Overtopping; (g)Shoreline change rate; (h)Structural inspection |
| Vulnerability | (a)Population; (b) Land use; (c)Warning system; (d) Emergency shelter |

### (B) Risk Classification and the Risk Evaluation

The scores of the hazard and vulnerability indexes are divided into five degrees with an interval of 0.2. According to the hazard and vulnerability assessment, the hazard indices are of low-to-moderate low grades and the vulnerability indices are of low-to-moderate high grades. The coastal risks are shown to be of low-to-moderate grades in the risk matrix. The coastal risk maps are shown in Figure 2.

### (C) Risk Treatment- Adaptive strategy

According to the risk assessment, the vulnerability properties obviously dominate the coastal risk. The extensive reef buffer zone reduces the hazard risks of the facilities. The residential buildings and infrastructures are mostly located behind the coastal protection facilities, which induces relatively high vulnerability risk. Hence, they are recommended to promote hazard resilience ability, including warning systems and emergency shelters for climate change. Although the hazard risks are relatively low in the study area, the overtopping analysis indicates the sectors of study areas still have the circumstances of overtopping under the protection standards. Consequently, it is not suggested to modify the structural properties of the facility, but the visual landscape conflict can be substantially mitigated by precise environmental governance.

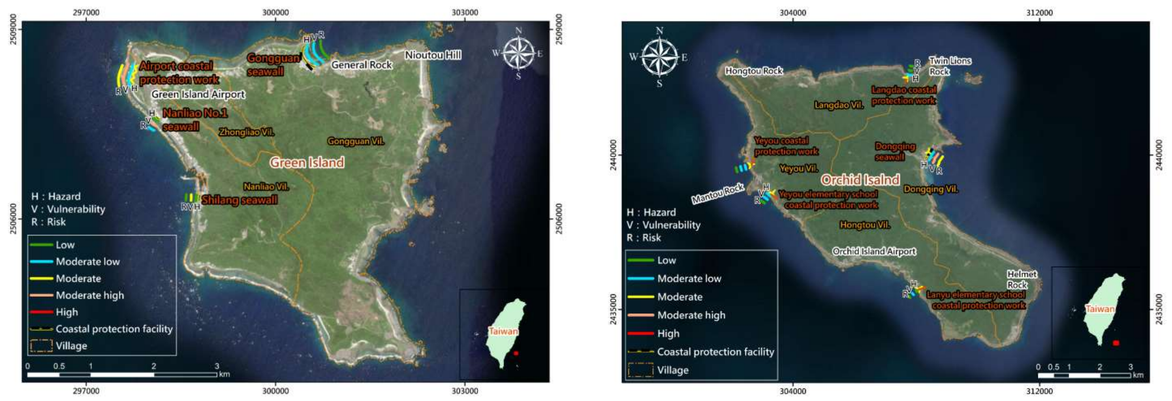



Figure 2. The coastal risk maps of Green Island and Orchid Island.

## Methodology

In terms of risk assessment, this study considers risk identification, risk classification, and risk evaluation to quantify the integrated hazard and vulnerability index. The illustrations of the assessments are following below:

**Risk Identification**

The Fuzzy Delphi Method is employed to calculate the consensus value and the importance of each hazard and vulnerability factor to select the representative factors by the anonymous questionnaires from the experts and the stakeholders. The consensus value of representative significance 6 is taken as the threshold to adopt the representative factors.

**Risk Classification**

The step of risk classification aims to build up the classification rule of the representative factors. The analyses are shown below:

- Qualitative analysis
- Quantitative analysis
- semi-quantitative analysis

**Risk Evaluation**

This study calculates the weight relationships between representative factors via the Analytic Hierarchy Process to generate the grades of hazard and vulnerability index. The risk matrix is composed of the hazard and vulnerability index.

The risk matrix of the coastal risk assessment

| Hazard \ Vulnerability | Low | Moderate-Low | Moderate | Moderate-High | High |
|---|---|---|---|---|---|
| High | Moderate | Moderate-High | High | High | High |
| Moderate-High | Moderate-Low | Moderate | Moderate-High | High | High |
| Moderate | Low | Moderate-Low | Moderate | Moderate-High | High |
| Moderate-Low | Low | Low | Moderate-Low | Moderate | Moderate-High |
| Low | Low | Low | Low | Moderate-Low | Moderate |

Figure 3. The interactions of hazard and vulnerability on the risk matrix.

**Risk Treatment**

According to the division of authority department, the adaptive strategy is proposed to improve the hazard and vulnerability risk respectively. Simultaneously, the governance countermeasures are discussed based on the risk assessment, including reducing the elevation of coastal protection facilities or decommissioning them.

## Conclusions

This study quantifies the hazard and vulnerability risks and discusses the feasibility and the countermeasures of modifying the structural properties of the facility with the risk levels, which is the first implementation in these two small islands. All in all, the results are informative for hierarchical management and practical sustainable governance for climate change.

Contacts: Chun-Jhen YE. E-mail: 20852006@email.ntou.edu.tw

References:

Acknowledgments: This work is supported by the Eighth River Management Branch, Taiwan, Project no. 112-B-001-01-001-031. Their support is deeply appreciated.

WATER - ACROSS BOUNDARIES

8th IAHR EUROPE CONGRESS
LISBON - PORTUGAL
4-7 JUNE 2024

IAHR AIRH
Hosted by Spain Water and IWHR, China

# Effective Flood emergency response: rapid deployment solutions

Diogo FREITAS [1], Laura MOLANO2[2], Diego GARCÍA[3], Ginna TORRES[4]

[1,2,3,4] A. Bianchini Ingeniero, S.A. (Maccaferri), Spain

## Motivation

Climate change has affected the frequency and scale of natural disasters. In recent years, floods, storms, droughts, wildfires, and extreme temperatures have become more frequent and the occurrence of a disaster affects people and economies. Over the last five years, climate-related disasters have had a very high recurrence rate, and floods were the most frequent type of disaster, as illustrated in Fig. 1.

A successful strategy for disaster management is the combined methodology of monitoring and mapping to forecast a potential risk. Current technology, such as satellite remote sensing, provides timely and accurate geospatial information for risk reduction and rapid response coordination.

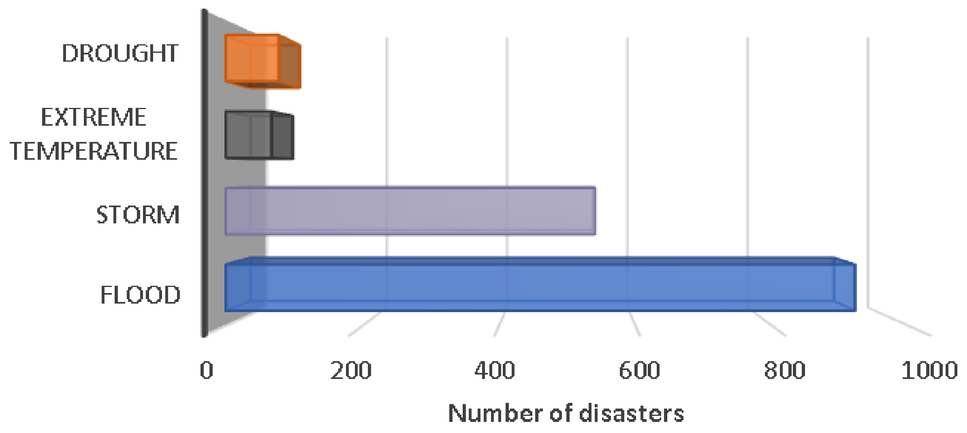



***Fig 1.*** *Occurrence of climate-related disasters between 2018 and 2022 as recorded by EM-DAT (CRED, 2023)*

## Methodology

The emergency flood works require versatility to allow easy deployment, therefore protecting assets from rising flood water on time. The system is supplied in folded units that can be easily connected to rapidly build large barriers without requiring skilled labor. The system showcased is a multicellular structure made of hexagonal double-twisted wire mesh internally lined with a geotextile sleeve. The geotextile lining enables the system to be filled with locally available materials such as sand or general fill.

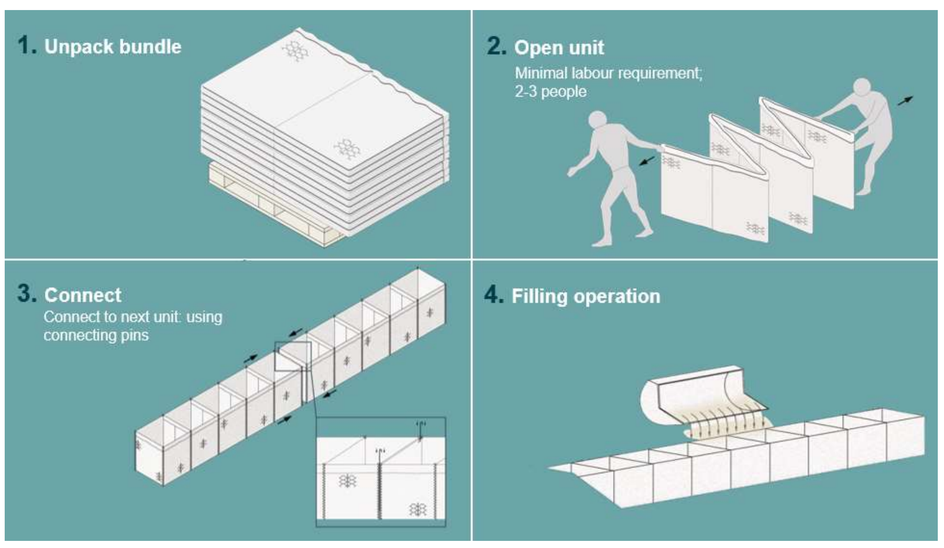



***Fig 2.*** *Multicellular system installation procedure*

## Results

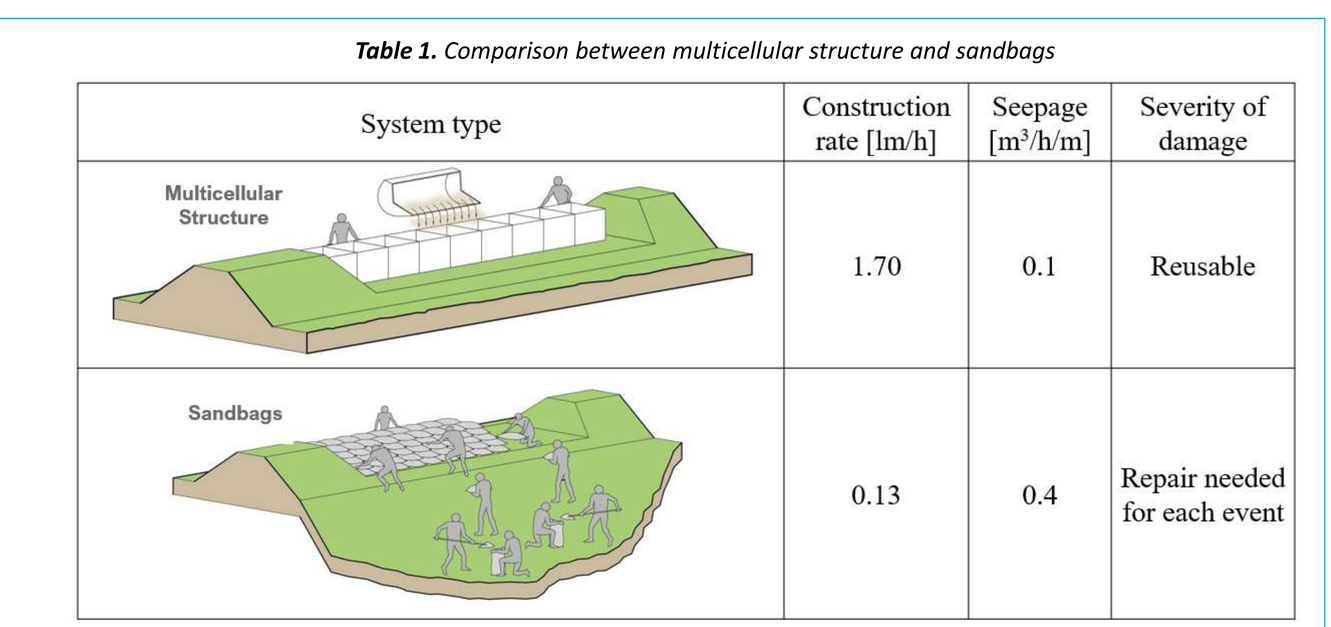
The great advantage of this multicellular system is the quick and easy assembly compared with traditional sandbags. Below, a comparison of the construction rate of a straight-line barrier with the two solutions is shown in Table 1, where the sandbag requires more intensive labor. It was noted that the seepage rate is registered for a water depth of 0.9 m is higher for sandbags and for most cases has damage to repair.

***Table 1.*** *Comparison between multicellular structure and sandbags*

| System type | Construction rate [lm/h] | Seepage [m³/h/m] | Severity of damage |
|---|---|---|---|
|   | 1.70 | 0.1 | Reusable |
|   | 0.13 | 0.4 | Repair needed for each event |

## Conclusions

Implementation of the multicellular system allows the deployment of faster flood emergency response plans. As a temporary solution, the units will be folded up and efficiently stored for another emergency. The system also can be designed as a permanent solution to protect land developments in floodplains. When used as a permanent solution after an emergency, the structure can be covered and revegetated in harmony with the environment.




**Contacts:** [1]d.freitas@maccaferri.com; [2]l.molano@maccaferri.com; [3]dg.gordo@maccaferri.com; [4]g.torres@maccaferri.com

**References:** CRED (2023). Disasters in numbers 2022. Centre for Research on the Epidemiology of Disasters (CRED).
Dottori, F., Kalas, M., Salamon, P., Bianchi, A., Alfieri, L., & Feyen, L. (2017). An operational procedure for rapid flood risk assessment in Europe. Natural Hazards and Earth System Sciences, 17(7), 1111-1126.
UNDRR (2015). Sendai Framework for Disaster Risk Reduction 2015-2030. United Nations.

8th IAHR EUROPE CONGRESS
LISBON - PORTUGAL
4-7 JUNE 2024
WATER - ACROSS BOUNDARIES
IAHR AIRH
Hosted by Spain Water and IWHR, China

# Dam-break flood risk assessment and response actions within self-rescue zone

Anderson Matheus de Sousa Lima[1], Carlos de Oliveira Galvão[1]
[1] Federal University of Campina Grande (UFCG), Department of Civil Engineering, Brazil

## Motivation

The Self-Rescue Zone (SRZ) is usually defined as a dam downstream side whose time or distance until the flood wave reaches it is equal to a prescribed time or distance, respectively, assuming the shorter length. The Emergency and Action Plan (EAP) for the SRZ contains the description of land use and occupation, their vulnerabilities, and alert and evacuation responses. The response actions are driven by the dam status and possibility of disruption. The response actions are not usually related, in the EAP, to the flood hazard magnitude and vulnerability levels of the population and infrastructure within the SRZ. We propose the risk associated to the flood hazard and vulnerability levels as a better indicator of the response actions, than the current guidelines in the EAP.

## Methodology

The methods are described in Table 1. A high-resolution digital terrain model, made available by the Pernambuco Three-dimensional Program (PE3D), was used, with an altimetric accuracy better than 25 cm (Silva et al., 2022). The data has excellent accuracy and quality for the flood simulation, performed using HEC-RAS 2D hydrodynamic model. Data on the dams and downstream region included technical and inspection documentation of the dams, as well as their EAP, population census data, satellite images, and field surveys.

**Table 1.** Summary of methods

| Phases | Descriptions |
|---|---|
| Hazard Levels | The hazard was calculated using the proposal of Stephenson (2002) for a given point in the flooded area, with IA = h.v, where h corresponds to the depth of the water (m) and v, the flow speed ($m.s^{-1}$). |
| Vulnerability Levels | The vulnerability level was determined through the application of the Vulnerability Index, proposed by Viseu and Almeida (2008), to assess the risk in valleys downstream of a dam, which considers four sub-indices: Household Physical Vulnerability Sub-Index, Sub-Index of economic vulnerability, Demographic Vulnerability Sub-Index and the Preparedness Vulnerability Sub-Index. |
| Flood Risk Levels | The risk was determined as a product of hazard and vulnerability. |
| Response Levels | The level of response in a potential emergency situation in a dam self-rescue zone was based on the "Entrepreneur's Manual on Dam Safety" (ANA, 2016), and related to the risk assessment levels. |

The product between hazard and vulnerability results in the assessment of flood risk levels and corresponding response actions, indicated by colours for easy communication (Figure 1).

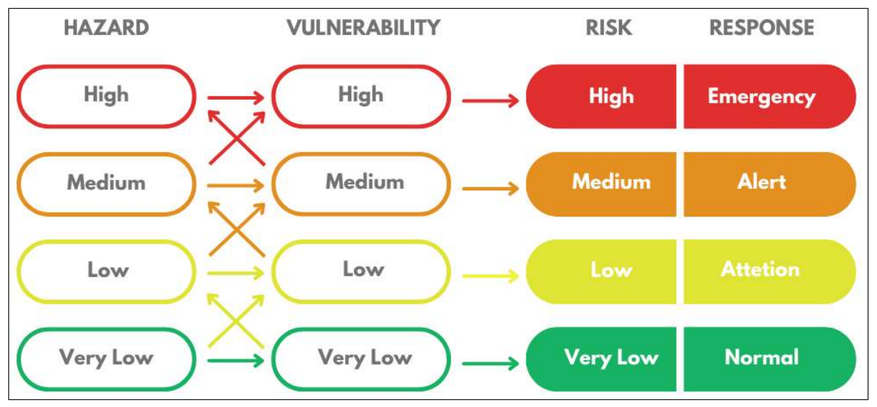



**Fig. 1.** Relationship between hazard and vulnerability levels in determining the flood risk and response actions.

## Results

The methods were applied to two cascade dams in the State of Pernambuco, Brazil, used as a case study: the Guilherme Azevedo and Jaime Nejaim Dams. The results show that the hazard levels vary within the SRZ (Fig. 2a). However, the vulnerability is High in the whole SRZ, resulting in a High risk level and corresponding response for the entire zone.

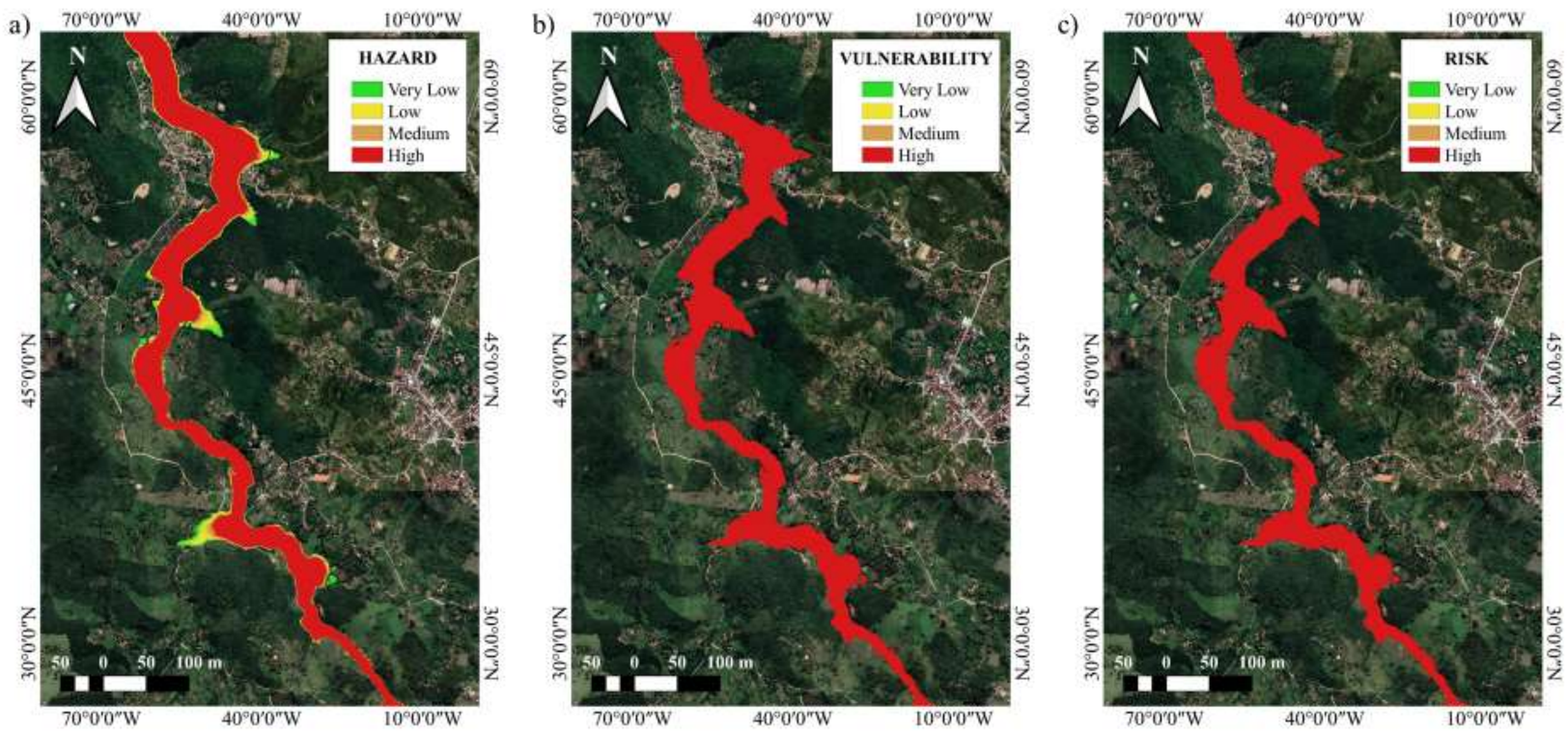



**Fig. 2.** SRZ flood patch: a) hazard, b) vulnerability, and c) risk.

## Conclusions

The joint consideration of the flood hazard magnitude and population and infrastructure vulnerability, spatially distributed within the SRZ, has the potential to better inform the response actions in the event of a dam disruption. The proposed guidelines, if included in the EAP, can motivate improved updating in flood hazard estimation and human occupation in the SRZ.

**Contacts:** anderson.m.sousa@estudante.ufcg.edu.br; carlos.galvao@ufcg.edu.br

**References**: National Water and Basic Sanitation Agency (ANA) (2016) Entrepreneur's Handbook on Dam Safety. / Silva JPN, Bello MIMCV, Silva TB, Silva WMP (2022) Rupture Simulation of São Bento do Unas's Dam using HEC-RAS Software, Revista Brasileira de Geografia Física, 15, 856-871. / Stephenson D (2002) Integrated flood plain management strategy for the Vaal, Urban Water, 4, 425-430. / Viseu T, Almeida AB (2008) Vulnerability index for risk evaluation: an approach for safety on dam`s downstream valleys, Proceedings da "Sixth International Conference in Computer Simulation Risk Analysis and Hazard Mitigation", Cefalónia, Grécia, Maio.

**Acknowledgments:** The authors acknowledge the funding from the Paraíba State Research Foundation (FAPESQ), grant 016/2023, from the National Council for Scientific and Technological Development (CNPq), and from the Brazilian Ministry of Science, Technology and Innovation's National Institutes of Science and Technology: Climate Change and Observatory of Water Security and Adaptive Management.

# The Evaluation of Water Supply Capability for Drought Management

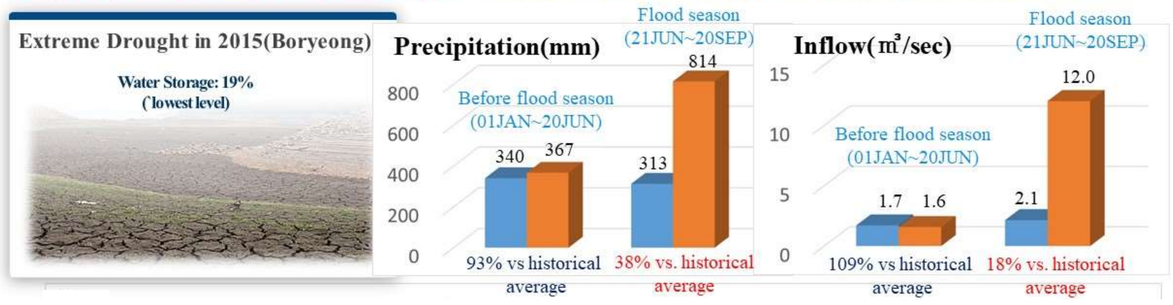
Jin Hyeog PARK[1], Shin Uk KANG[2], Hyun Gu CHOI [3], Wan Sik Yu[4]
[1] K-water; [2]K-water; [3]K-water ; [4]K-water

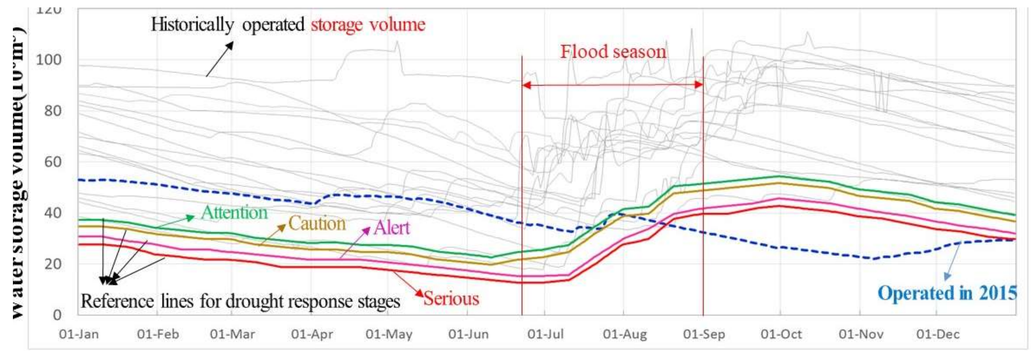
8th IAHR EUROPE CONGRESS
LISBON - PORTUGAL
4-7 JUNE 2024
WATER - ACROSS BOUNDARIES
IAHR AIRH
Hosted by Spain Water and IWHR, China

## Motivation

- The average frequency of significant droughts in KOREA is about 5 to 7 years since 1970's, but it was found out that it occurred almost every year since 2006. **(fluctuation in reginal rainfall ↑, rainfall patterns and peak patterns ↕ )**

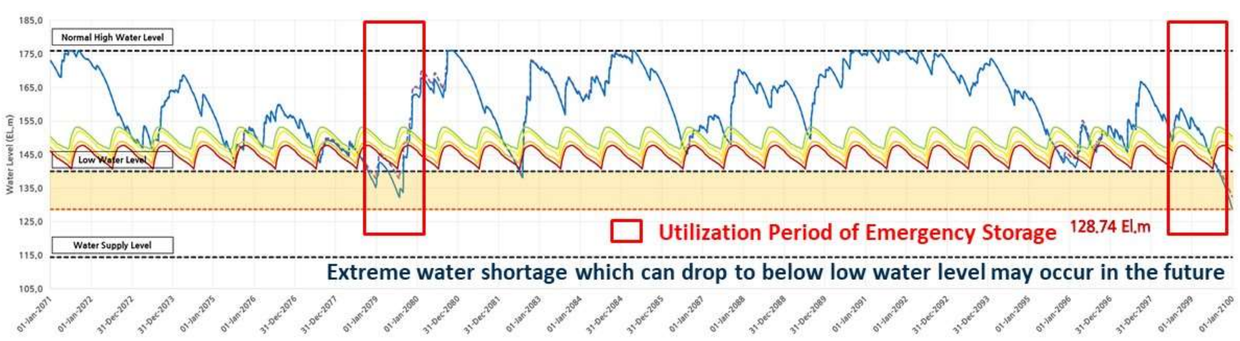
**The water supply from multi-purpose dams during the dry season has been too much dependent on the inflow volume during the flood season → Reservoir operation rule's revision(drought response plans)**




## Results

- Reservoir Reserve for Hapcheon Reservoir



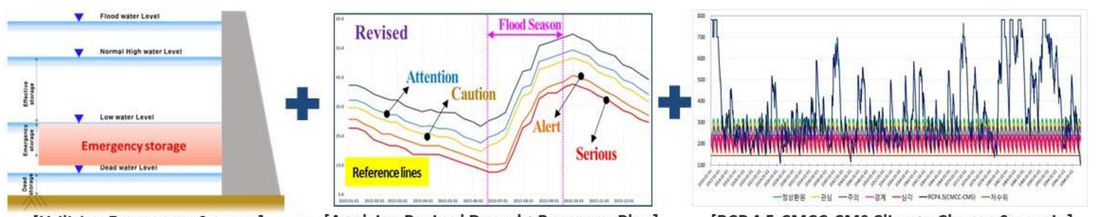

[Reservoir Simulation Result for End of 21st Century - No Reduction for Domestic and Industrial Water Supply]

**Shortage of water supply doesn't occur utilizing emergency storage with revised reservoir operation rules**

| Division | Elevation (EL.m) | Storage ($10^6m^3$) | Emergency Storage ($10^6m^3$) | Ratio (%) |
|---|---|---|---|---|
| Early 21C (2011-2040) | 133.03 | 95.34 | 55.73 | 42.9% |
| Middle 21C (2041-2070) | 132.59 | 88.66 | 62.41 | 48.0% |
| End 21C (2071-2100) | 128.74 | 64.53 | 86.54 | 66.6% |

* Emergency Storage : 130.0($10^6m^3$)

## Methodology

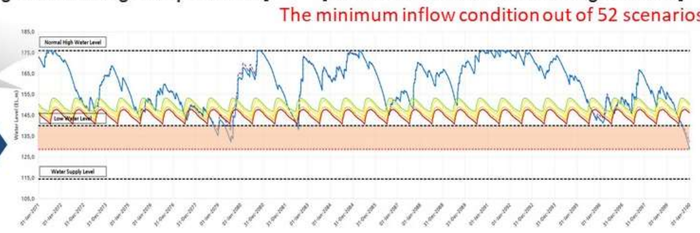



[Utilizing Emergency Storage] [Applying Revised Drought Response Plan] [RCP 4.5 CMCC-CMS Climate Change Scenario]

The minimum inflow condition out of 52 scenarios




[Reservoir Operation Simulation Model]



[Estimation of the Optimal Reservoir Reserve Storage and Evaluation Water Supply Capability]

➢ **Evaluation Index :** Reliability(Period, Supply) ➢ **2 Cases Simulation**

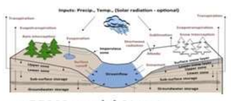
$$Rel_t = \frac{Number\ of\ failure}{Total\ number} \times 100 \qquad Rel_s = \frac{Q_s}{Q_n} \times 100$$

Resiliency $Res_1 = \frac{1}{M}\sum_{i=1}^{M} d_i$ Vulnerability $Vul_H = \frac{1}{M}\sum_{j=1}^{M} d(j)$

| CASE | Operation Method |
|---|---|
| I | Do not use emergency storage & Drought response plans |
| II | Use emergency storage & Revised Drought response plans |

### ▶ AR5 RCP Climate & hydrology scenarios

- Total 52 Scenarios : 26 GCMs and 2 RCP(4.5&8.5) Scenarios (by APCC)
- Statistical Downscaling(considering uncertainties) : **SDQDM** (APCC, 2016)
- Baseline Period: 1976~2005, Projection Period: 2011~2100(each 30years: early, mid, end of the 21st century)
- Daily Hydrological Scenario(Flow Discharge) : **PRMS(Rainfall-Runoff Model)**(1976~2100)



<PRMS model Structure>

| No. | Model | No. | Model | No. | Model | No. | Model |
|---|---|---|---|---|---|---|---|
| 1 | CMCC-CM | 8 | MIROC5 | 15 | MPI-ESM-LR | 22 | IPSL-CM5B-LR |
| 2 | CCSM4 | 9 | HadGEM2-AO | 16 | MPI-ESM-MR | 23 | BCC-CSM1-1 |
| 3 | CESM1-BGC | 10 | HadGEM2-CC | 17 | FGOALS-s2 | 24 | CanESM2 |
| 4 | CESM1-CAM5 | 11 | HadGEM2-ES | 18 | NorESM1-M | 25 | MIROC-ESM-CHEM |
| 5 | BCC-CSM1-1-M | 12 | INM-CM4 | 19 | GFDL-ESM2G | 26 | MIROC-ESM |
| 6 | MRI-CGCM3 | 13 | IPSL-CM5A-MR | 20 | GFDL-ESM2M | | |
| 7 | CNRM-CM5 | 14 | CMCC-CMS | 21 | IPSL-CM5A-LR | | |

## Conclusions

- Drought response plans for multi-purpose dams are revised to satisfy the water supply reliability of 95% for water demand at each drought response stage and can be fully utilized to secure additional water storage volume during dry season.
- Reservoir reserve storage concept is introduced to respond the **extreme drought** utilizing revised drought response plans, emergency storage based on AR 5 GCM**(CMCC-CMS)** RCP 4.5 scenarios and evaluated water supply capability for extreme drought risk management.
- It is expected that a complex application such as the **emergency storage with revised reservoir operation rules** can highly improve water supply capability and secure water supply more effectively in the future considering climate change.
- We expect to contribute to provide a reliable water supply by developing standardized new reservoir operation rules based on climate change scenarios and reserve storage technologies to prevent extreme droughts in advance.

Contacts: Jin Hyeog PARK(park5103@kwater.or.kr)

Acknowledgments: This work was supported by Korea Environment Industry & Technology Institute(KEITI) through Water Management Program for Drought, funded by Korea Ministry of Environment(MOE)(RS-2023-0023194)

# Cascading effects and scenario risk assessment for damaging geohydrological events

Daniela BIONDI[1], Sara BLOISE[1] , Pasquale VERSACE[1]

[1] Department of Computer Engineering, Modelling, Electronics and Systems, University of Calabria, Italy

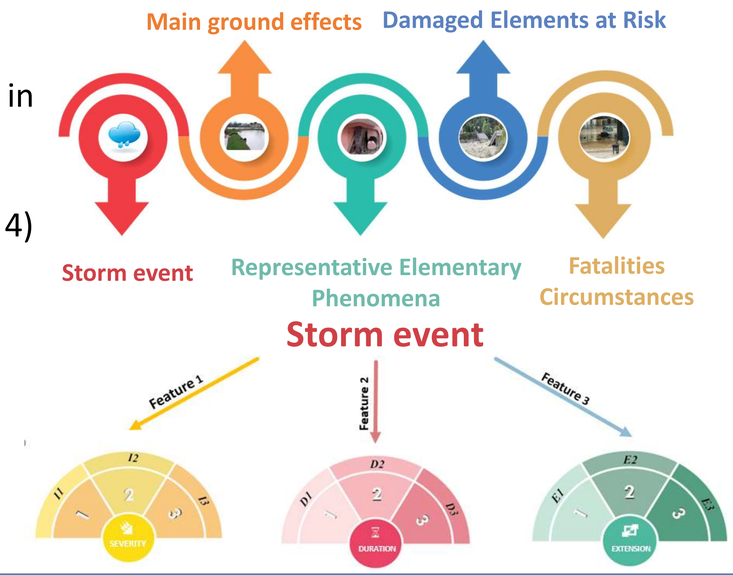
## Motivation

Building multiple, complex risk scenarios is a priority for the improvement of the effectiveness of early warning systems and technical countermeasure designs to mitigate impacts associated with severe weather events, such as floods and landslides. This study outlines the extension of CERCA (Cascading Effects in Risk Consequences Assessment), an approach developed for rainfall-induced geohydrological and hydraulic hazards, with the aim of characterizing event scenarios by evaluating potential cascading effects and consequences while maintaining consistency with the Italian Civil Protection Guidelines for the national warning system. . The framework comprises a chain, resembling an event tree, beginning with the characterization of the triggering rainfall event and subsequently connecting various ground effects and phenomena that either interact or are independently generated by the same forcing storm event. Explicit focus has been placed on identifying the key characteristics of the rainfall event, including critical duration, extent, and severity (i.e., return period), in order to reveal potential dependencies with the consequent scenario. Severity diagrams are used as a simple tool, allowing for a synthetic visualization of storm severity while considering the complexity related to rainfall spatial variability and duration. In contrast, the classical procedure of associating a unique return period with an event, hides a great part of the storm complexity by neglecting spatial variability. Several destructive storm events observed in the Calabria region (south Italy) were chosen as examples for the analysis.

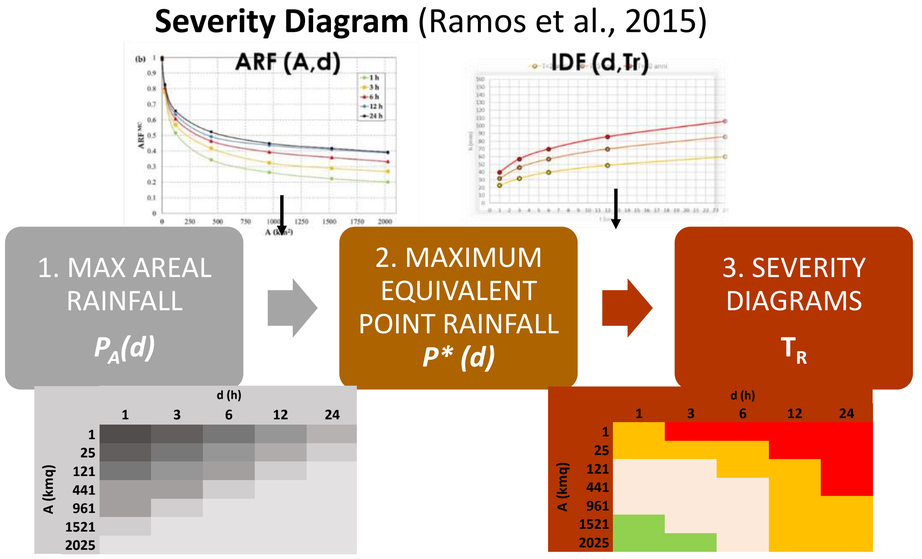
## Methodology

CERCA provides a framework for an integrated scenario assessment for strategic risk management in Italy, divided into five stages, which involve the assessment of: 1) Storm event; 2) Main ground effects; 3) Representative elementary phenomena; 4) Cascading effects in terms of damaged elements at risk; 5) Circumstances leading to fatalities. Severity diagrams, representing storm severity in terms of return period, mapped as a function of area and duration of rainfall accumulation, are employed at stage 1) to identify the key characteristics of triggering storm events.

### Characterization of the storm event




**Severity Diagram** (Ramos et al., 2015)




### CERCA (Cascading Effects in Risk Consequences Assessment): operational tool for geo-hydrological scenario risk assessment and cascading effects evaluation

**Main ground effects** → **Representative Elementary Phenomena** → **Damaged Elements at Risk** → **Fatalities Circumstances**

| Main ground effects |
|---|
| TE01: Flash flood and other rapid onset flood |
| TE02: Medium onset flood |
| TE03: Slow onset flood |
| TE04: Pluvial flood |
| TE05: Deep-seated slope failure |
| TE06: Shallow landslides |
| TE07: Debris flow |
| TE08: Sinkhole |
| TE09: Thunderstorm |

Biondi et al. (2023)

***Erosion and landslides***
**REP1**: Erosion
**REP2**: Soil slip
**REP3**: Slope instability, locally deep
**REP4**: Rockfall
**REP5**: Debris flow
**REP6**: Sinkhole

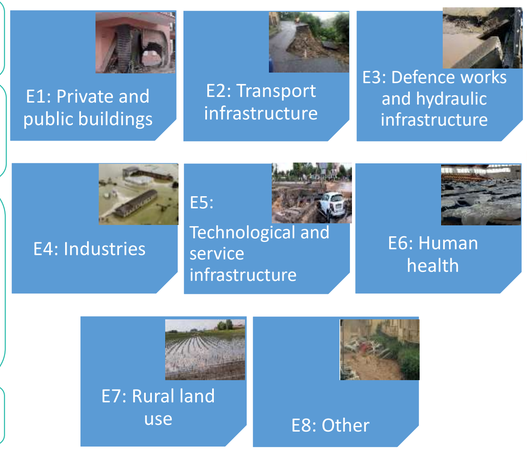
***Riverbed phenomena***
**REP8a/b**: Partial or total occlusion of bridges/riverbed narrowing/buried streams (major/minor rivers)
**REP9a/b**: Raising water levels (major/minor rivers)
**REP10a/b**: Bank erosion (major/minor rivers)
**REP11a/b**: Sediment transport (major/minor rivers)
**REP12**: Wandering channel
**REP13**: Meander cut-off

***Drainage***
**REP7**: Flooding due to inadequate drainage or sewage systems, surface water flow

***Flooding***
**REP14a/b**: Flooding of areas close to streams (major/minor rivers)
**REP15a/b**: Widespread flooding (major/minor rivers)

***Overflow***
**REP16a/b**: Overflow of river banks (major/minor rivers)
**REP17a/b**: Bridges and infrastructures overtopping (major/minor rivers)
**REP18**: Levee piping
**REP19a/b**: Levee damage/failure (major/minor rivers)

***Thunderstorms***
**REP20**: Hailstorm **REP21**: Lightning **REP22**: Wind




**R01:** People inside buildings in flooded rooms at or below the street level

**R02:** Vehicles or motor-vehicles in flooded roadways

**R03:** Pedestrian dragged by water or people who have fallen/ have been swept into river

**R04:** Vehicles or motor-vehicles in underpass or tunnel

**R05:** Weather-induced fatal vehicles incidents

**R06:** People involved in partial or total collapse of buildings caused by landslides or dragged/buried by mud or debris flow

**R07:** Vehicles hit by landslides or dragged/buried by mud or debris flow

**R08** People outdoors hit by landslides or dragged/buried by mud or debris flow

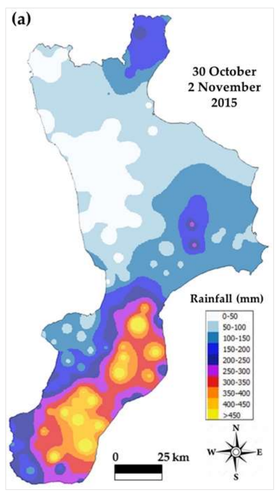
**R09:** People outdoors involved in collapse of embankments, bridges, etc.

**R10:** Side effects (heart attacks, infectious diseases, wind related deaths)

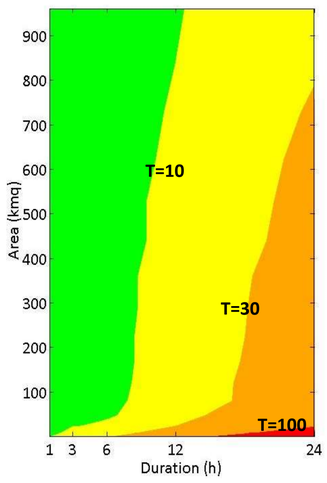
## Results

a) 30th October – 2nd November 2015

Cumulated rainfall

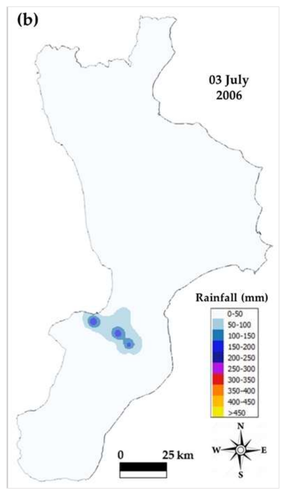



Severity Diagram

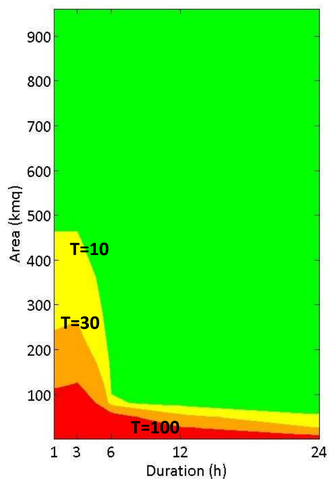



(b) 3rd July 2006

Cumulated rainfall




Severity Diagram






**TE01: Flash floods and other rapid onset floods**



**TE06: Shallow landslides**

**REP7:** Flooding due to inadequate drainage or sewage systems, surface water flow → **E2**: Transport infrastructure

**REP8b:** Partial or total occlusion of bridges/riverbed narrowing/buried streams (minor rivers) → **E1**: Private and public buildings; **E2**: Transport infrastructure; **E4**: Industries

**REP9b:** Raising water levels (minor rivers) → **E1**: Private and public buildings; **E2**: Transport infrastructure; **E4**: Industries

**Rep10b:** Bank erosion (minor rivers) → **E1**: Private and public buildings; **E2**: Transport infrastructure; **E4**: Industries; **E5**:Technological and service infrastructure; **E6c**:Human health - Evacuated population; **E6a**: Human health - Deaths/missing → **R02**; **R03**

**REP11b**: Sediment transport (minor rivers) → **E4**: Industries; **E5**:Technological and service infrastructure; **E6c**:Human health - Evacuated population; **E6a**: Human health - Deaths/missing → **R02**; **R03**

**REP15b**: Widespread flooding (minor rivers) → **E6c**:Human health - Evacuated population; **E6a**: Human health - Deaths/missing → **R02**; **R03**

**REP16b**: Overflow of river banks (minor rivers) → **E6c**:Human health - Evacuated population; **E6a**: Human health - Deaths/missing → **R02**; **R03**

**REP2**: Soil slip → **E2:** Transport infrastructure

## Conclusions

Severity diagrams are employed to identify critical characteristics of triggering storm events, highlighting the coexistence of extreme and ordinary (non-extreme) rainfall intensities over the affected area. The entire proposed framework is effective in processing post-disaster information, offering the capability to identify site-specific dependencies based on hazard proneness, exposure, and vulnerability conditions. It also brings attention to risks from cascade effects that are rarely predicted with the traditional 'decomposition' approach relying on Hazard-Vulnerability-Exposure multiplication through simple map overlays. Furthermore, the link to characteristics of the forcing rainfall provides a comprehensive view of possible hazard/impact scenarios, that can be valuable in the forecasting phase.

Contacts: daniela.biondi@unical.it; sara.bloise@dimes.unical.it; linoversace@libero.it

References:


- Biondi D, Scarcella GE, Versace P (2023) CERCA (Cascading Effects in Risk Consequences Assessment): An operational tool for geo-hydrological scenario risk assessment and cascading effects evaluation, Hydrology Research, 54 (2), 189–207.
- Ramos MH, Creutin J-D, Leblois E (2005) Visualization of storm severity, Journal of Hydrology, 315,. 295-307

8th IAHR EUROPE CONGRESS
LISBON - PORTUGAL
4-7 JUNE 2024
WATER - ACROSS BOUNDARIES

Hosted by Spain Water and IWHR, China

# A Framework and Indicators for Global Water Security Assessment

Joo-Heon LEE[1], Seo-Yeon PARK[1], Young-Jun KIM[1], Jong-Suk KIM[3]
[1] Joongbu University; [2]Wuhan University

## Introduction

UN-Water (2013) defines water security as 'the capacity of a population to safeguard sustainable access to adequate quantities of acceptable quality water for sustaining livelihoods, human well-being, and socioeconomic development, for ensuring protection against waterborne pollution and water-related disasters, and for preserving ecosystems in a climate of peace and political stability'.

The Asian Development Bank's definition is, 'the availability of adequate water to ensure safe and affordable water supply, inclusive sanitation for all, improved livelihoods, and healthy ecosystems, with reduced water-related risks toward supporting sustainable and resilient rural-urban economies… ' (ADB, 2020a).

Water security can be assessed by a variety of methods and concepts, but the underlying objectives are similar. The most important thing to be cautious about when evaluating water security is to set appropriate indicators and secure reliable data to evaluate all countries in the world. The purpose of this study is to establish an evaluation framework for reasonable assessment within the range of available data.

## Assessment Framework and Indicators




**Fig 1. 5 Core areas for Water security assessment framework**

The framework for assessing water security can vary according to the purpose and intent of the assessment. Since the limitations of available data increase depending on the spatial scope (Basin, Country, Continent, Global) for water security assessment, it is very important to set available indicators along with the composition of the assessment framework for Global Water Security Assessment.

**Table 1. 15 Indicators and data sources of 5 Core areas to assess the Global Water Security**

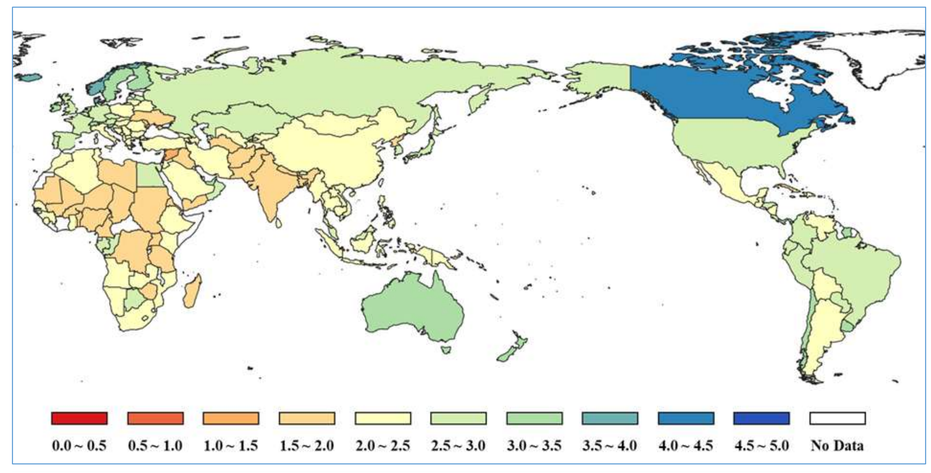
| Core area | Indicators | Temporal Scales | Definition | Data Sources |
|---|---|---|---|---|
| **Core area 1.** Social equity | Improved drinking water supply rate | 2017 | Total population with access to improved drinking-water source (JMP) | WHO · UNICEF (JMP) |
| | Renewable water resources per person | 2017 | Total renewable water resources per capita ($m^3$/inhab/year) | AQUASTAT |
| | Sewerage rate | 2015 | Improved sanitation facilities (% of population with access) | INDEX MUNDI |
| | Diarrheal diseases | 2017 | Diarrheal diseases death rates in children under 5 | Our World in Data] |
| **Core area 2.** Economic efficiency | Value of industrial water consumption | 2000:2017 | Industrial production/ Industrial water withdrawal | OECD /AQUASTAT |
| | Value of agricultural water consumption | 2000:2017 | Value of Agricultural Production/Agricultural water withdrawal | FAO /AQUASTAT |
| | GDP (Gross Domestic Product) | 2019 | GDP per Capita | World Bank |
| **Core area 3.** Resilience to water-related disasters | Drought frequency | 1979:2018 | SPI (Standardized Precipitation Index) < -1 or less occurrence frequency SPI(3) for Meteorological Drought | NOAA |
| | Areas of vulnerable to drought | 2013:2017 | % of Crop Cultivation Area to Total country area | AQUASTAT |
| | Flood frequency | 1969:2018 | Flood occurrence (WRI) | AQUASTAT |
| | Areas of vulnerable to flood | 2017 | Urban population/ Total population | AQUASTAT |
| | Ratio of Irrigated area | 2012 | Area equipped for irrigation: total/ Cultivated Area | AQUASTAT |
| | Flood control capability | 1950:2018 | Reservoir Capacity/Total Area | ICOLD / AQUASTAT |
| **Core area 4.** Environmental sustainability | River Health Index | 2010 | Biodiversity Threat | RIVERS IN CRISIS |
| | | 2000:2017 | Human Water Security Threat | |
| **Core area 5.** Government Competency | Government Capacity | 2018 | Voice and Accountability | World Bank |
| | | | Political Stability and Absence of Violence | |
| | | | Government Effectiveness | |
| | | | Regulatory Quality | |
| | | | Rule of Law | |
| | | | Control of Corruption | |

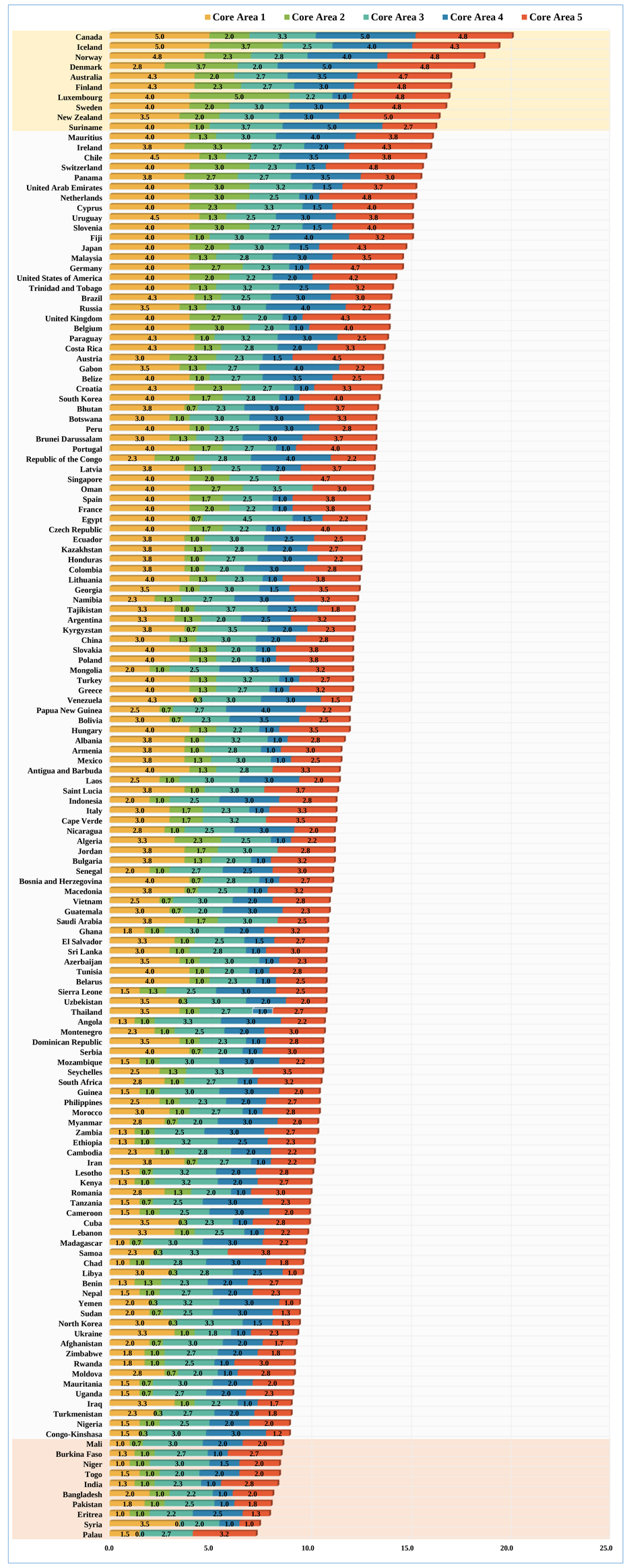
This study defines water security as the ability of countries or societies to provide clean water and adequate sanitation services to all members of society, ensure an economic value of water, protect human life and the environment from pollution and water-related disasters, and achieve ecosystem conservation and recovery based on desirable governance that includes appropriate institutions and sufficient financing capacity(Park et al. 2022).

## Global Water Security Assessment

The Water Security Index (WSI) was calculated to fall into the range from 1 to 5 using Eq. (1). The figure and chart on the right shows the water security assessment results for 150 countries where detailed indicator data for each of the five core areas can be obtained.

$$\text{WSI(Water Security Index)} = \frac{\text{Core area } (1 + 2 + 3 + 4 + 5)}{5} \qquad \text{Eq. (1)}$$




References:

Acknowledgments: This work was supported by Korea Environment Industry & Technology Institute(KEITI) through Aquatic Ecosystem Conservation Research Program Program(or Project), funded by Korea Ministry of Environment(MOE)(2022003050007)

8th IAHR EUROPE CONGRESS
LISBON - PORTUGAL
4-7 JUNE 2024
WATER - ACROSS BOUNDARIES

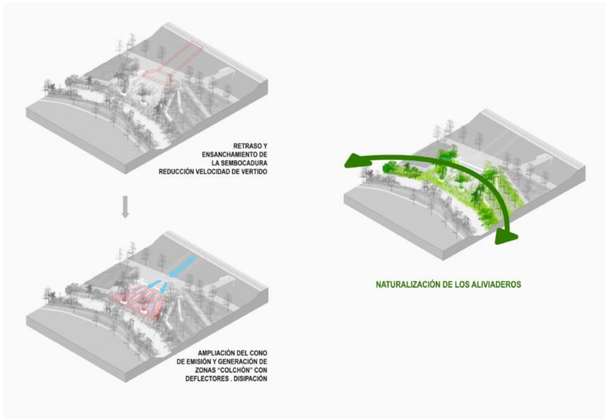
Hosted by Spain Water and IWHR, China

# Does sampling frequency matter? Comparative analysis of physicochemical quality elements in the Manzanares River (Madrid, Spain)

**F. M. Cortés** [1*], M. Díaz-redondo[1], M. García[1]
[1] Centre for Studies and Experimentation on Public Works (CEDEX), Spain.
Francisco.M.Cortes@cedex.es

## Motivation

The "***Recovery of the fluvial ecosystem Manzanares-Gavia-Bulera. Green and blue infrastructure Metropolitan Forest of Madrid***" project focuses on the recovery of the riverine vegetation corridor through a nature-based proposal for the adaptation of drainage systems' outlets. It is carried out by the Madrid City Council in association with the Centre for Studies and Experimentation on Public Works (CEDEX) and the CONAMA Foundation.




Basic schema of the main idea behind the project.

In this context, among other parameters and indicators, CEDEX is analysing the physicochemical data gathered from the sampling points networks either from **Tagus River Basin Authority (TRBA)** and the **Madrid City Council (MCC)**.

→ The *TARB network* follows European and Spanish guidelines (WFD, & RD 817/2015), that is, a minimum frequency of 3 months (4 samples per hydrological year) for physicochemical quality elements (PCQE).

→ The *MCC network* is much more ambitious, collecting between 104 – 160 samples per hydrological year, far more than the recommended monthly control.

Given that each network has different sampling frequencies, and some of the control points are coincident, the opportunity to evaluate whether the sampling frequency could influence the assessment of PCQE status classification has arisen**.**

## Results

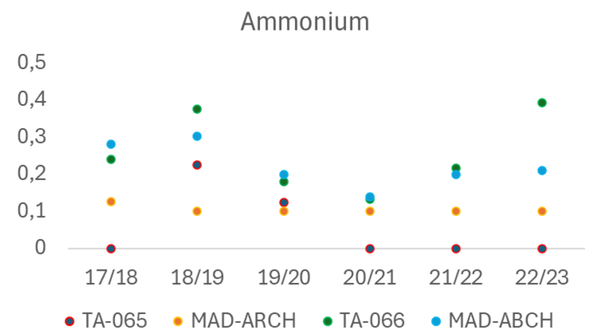
- **Discrepancies** in the status classification between TARB & MCC control points have been **detected for Phosphates**.
- Since it is a *'Heavily modified' water body*, the discordances are attenuated. The maximum potential in this type of WB is 'Good or better' (there is no chance for 'High' status).
- For a *'Natural' WB*, discrepancies are even higher, especially for Phosphates, with up to two status classes apart between TARB & MCC control points.

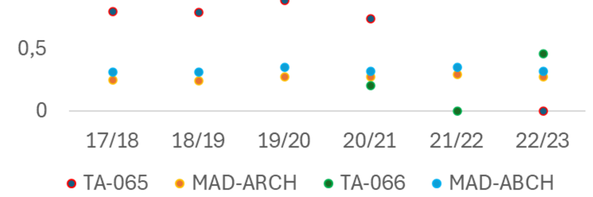
Status classification for each indicator in the four sampling points for the aggregate period 2017/2018 – 2022/2023. The numeric value represents the median of the medians for the six-year period

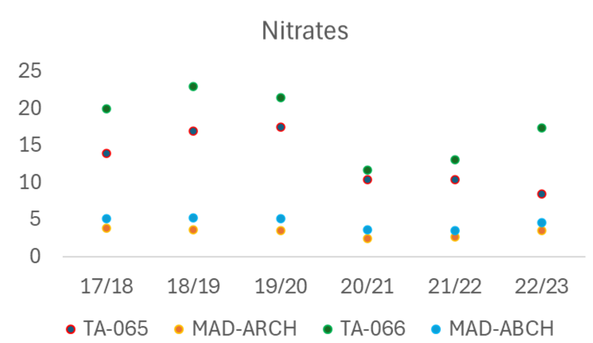
| Status classification | TA-065 | MAD-ARCH | TA-066 | MAD-ABCH |
|---|---|---|---|---|
| *Ammonium* | 0,00 | 0,10 | 0,23 | 0,20 |
| *Phosphates* | 0,81 | 0,28 | 0,73 | 0,33 |
| *Nitrates* | 12,25 | 3,59 | 18,70 | 4,92 |

Status classification in case the water body would have been defined as 'Natural' instead as 'Heavily modified' (as it is currently).

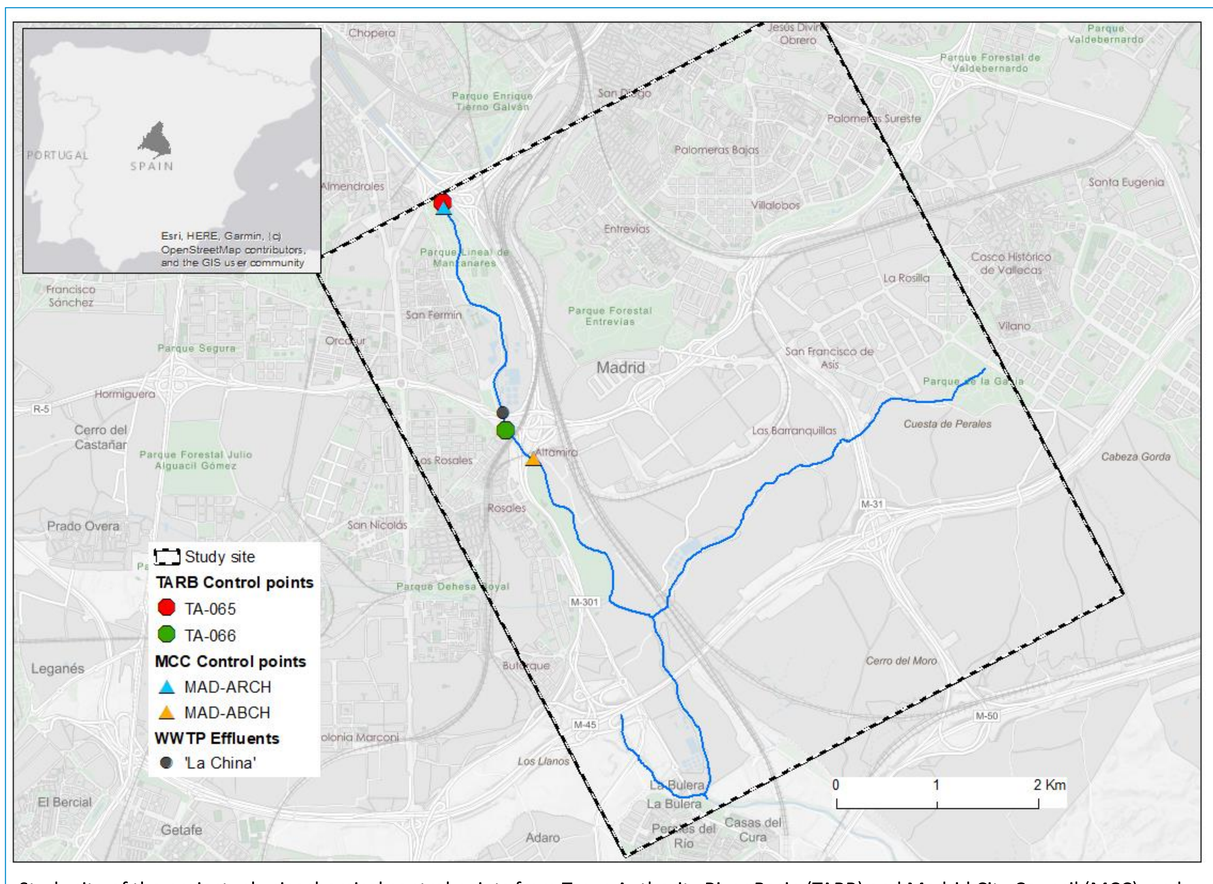
| Status classification | TA-065 | MAD-ARCH | TA-066 | MAD-ABCH |
|---|---|---|---|---|
| *Ammonium* | 0,00 | 0,10 | 0,23 | 0,20 |
| *Phosphates* | 0,81 | 0,28 | 0,73 | 0,33 |
| *Nitrates* | 12,25 | 3,59 | 18,70 | 4,92 |




Medians of the annual observations per hydrological year in the four sampling points




Study site of the project, physicochemical control points from Tagus Authority River Basin (TARB) and Madrid City Council (MCC), and the effluent from La China WWTP.

## Methodology

- Within the study area of the project there exist two coincident physicochemical sampling points (**TA-065** & **MAD-ARCH**) upstream of the effluent from 'La China' WasteWater Treatment Plant (WWTP), and two more sampling points (**TA-066** & **MAD-ABCH**) close enough to compare downstream the effluent.
- To determine whether the sampling frequency could affect the assessment of the physicochemical status, the analysis has been focused on nutrients (Ammomium, Phosphates and Nitrates) for the period 2017/18 – 2022/2023.
- According to the Spanish criteria (MITERD, 2021), the assessment unit is the hydrological year, so the evaluation has been made both individually, and then, in an aggregate way for the six-year period.
- The value per assessment unit and variable has been obtained using the medians of the annual observations. For the aggregate evaluation (multi-year) the median of the medians has been used.

Thresholds for status classification of nutrients for the Spanish river type 15. RD 817/2015.

| R-T15 - Poorly mineralized continental Mediterranean river axes | | | Thresholds for status classification | |
|---|---|---|---|---|
| **Quality element** | **Indicator** | **Units** | *High/ Good* | *Good/ Moderate* |
| *Nutrients* | Ammonium | mg $NH_4$/L | 0,2 | 0,6 |
| | Phosphates | mg $PO_4$/L | 0,4 | 0,5 |
| | Nitrates | mg $NO_3$/L | 10 | 25 |

## Conclusions

❑**Yes, it does** to some extent.

❑ There are no differences in status classification for Ammonium and Nitrates. However, this is because it is a '*Heavily modified' WB*, and only applies the threshold between 'Good or better/ Moderate'

❑ For **Phosphates,** the status classification is 'Moderate' in **TARB** points versus the 'Good' status for **MCC** points. If it was a 'Natural' WB, the difference would be even higher, up to two classes.

❑ Anyway, the median values of the six-year period for Phosphates and Nitrates are quite different comparing TARB & MCC sampling points.

❑ **Sampling frequency** – that is, the sample size – and probably the **timing of the year** when the sample is taken could have some influence in the assessment of the ecological status.

❑ Given that the assessment follows the WFD "One out-all out" criteria, smaller sample sizes for parameters like nutrients, that vary greatly among months and even daily, could lead to misclassify their status, and hence limit the achievement of a better ecological status.

❑ To that regard, although the study presented here is very modest, it seems advisable to review sampling frequency for some parameters and indicators that, maybe, are leading to an incorrect assessment of WBs.

**Selected references:**

✓ European Commission (2000). *Directive 2000/60/EC of the European Parliament and of the Council of 23 October 2000 Establishing a Framework for Community Action in the Field of Water Policy*.

✓ Ministerio de Agricultura, Alimentación y Medio Ambiente (MAGRAMA) (2015). *Real Decreto 817/2015, de 11 de septiembre, por el que se establecen los criterios de seguimiento y evaluación del estado de las aguas superficiales y las normas de calidad ambiental*.

✓ Ministerio para la Transición Ecológica y Reto Demográfico (MITERD) (2021). *Guía para la evaluación del estado de las aguas superficiales y subterráneas*.

**Acknowledgments:**

This study is developed within the project "***Recovery of the fluvial ecosystem Manzanares-Gavia-Bulera. Green and blue infrastructure. Metropolitan Forest of Madrid***", with the finantial support of the Biodiversity Foundation (Ministry for Ecological Transition and the Demographic Challenge), under the NextGenerationEU's Recovery, Transformation and Resilience Plan (PRTR).

8th IAHR EUROPE CONGRESS
LISBON - PORTUGAL
4-7 JUNE 2024
WATER - ACROSS BOUNDARIES
Hosted by Spain Water and IWHR, China

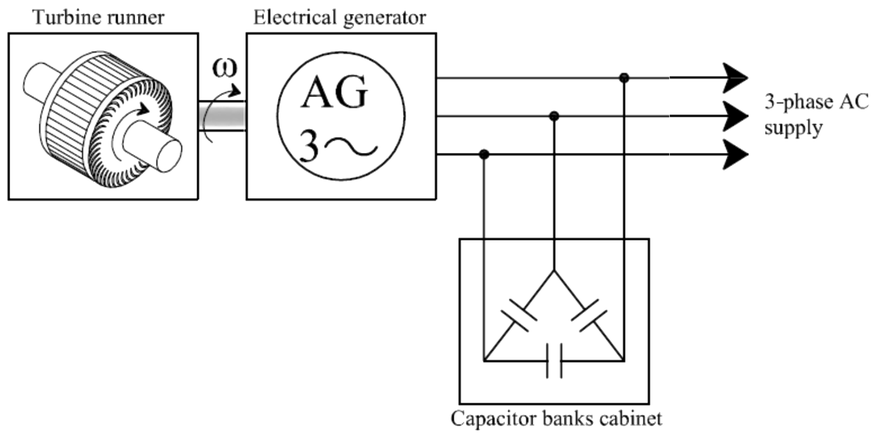
# Management of electric network failure in mini-hydro plants

Marco SINAGRA[1], Calogero PICONE[1], Angelo ACCETTA[2], Marcello PUCCI[2], Tullio TUCCIARELLI[1]

[1] Università degli Studi di Palermo, Italy; [2]National Research Council of Italy - INstitute of Marine engineering, Italy

## Introduction

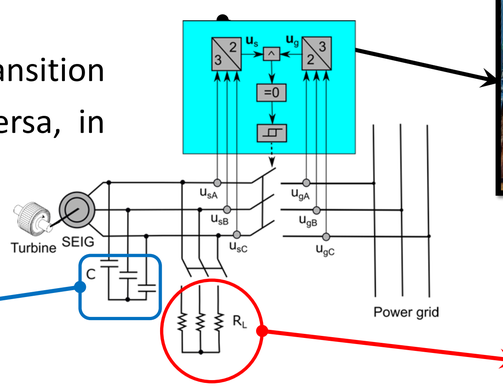
Small hydropower plants are usually connected directly to the national electricity grid to ensure the stability of the hydraulic turbine and of the water flow in the pipeline. In case of failure of the electricity grid, the balance between the power produced by the turbine and the power delivered to the grid is immediately lost. This imbalance leads to transient phenomena that can damage both the turbine and the water pipeline. The problem is even more relevant when the turbine is installed in water transport network for energy recovery, as the length of the upstream pipeline may be several kilometres. In this work, a low-cost methodology is studied for the continuity of the electricity production in case of power grid failure and reconnection in parallel without shutdown of the turbine.

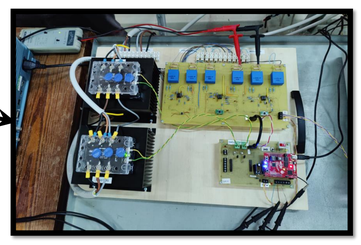



*Block diagram of the SEIG connection scheme*

## Methodology

Experimental set-up of the SEIG connection for smart transition from stand-alone to grid-connected system and vice versa, in mini-hydro turbines.



Smart system with microcontroller board based on a 32-bit ARM core and three-phase solid-state relays with faster turn-on **(0.1 ms)** and turn-off times (10 ms).



Capacitor bank cabinet (10, 50, 60 µF)



Resistive load cabinet (up to 5 kW)

To minimize the electromechanical transient occurring when the SEIG is connected back to the power grid, two conditions must be satisfied:

- ❑ the gap between the SEIG and the power grid frequency and voltage amplitude must be very low;
- ❑ the gap between the SEIG and the power grid voltage angles must be very low.

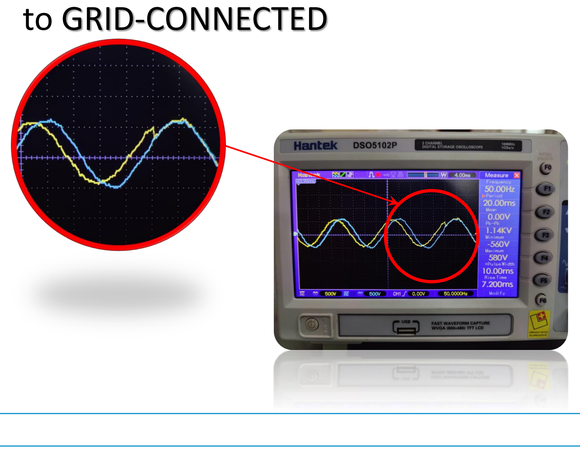
The first condition can be satisfied by a proper design of the system in terms of resistive and capacitive loads connected values.

The second condition can be satisfied by continuously monitoring the vector product between the SEIG and the power grid. The SEIG is connected back to the power grid only when the vector product is null.

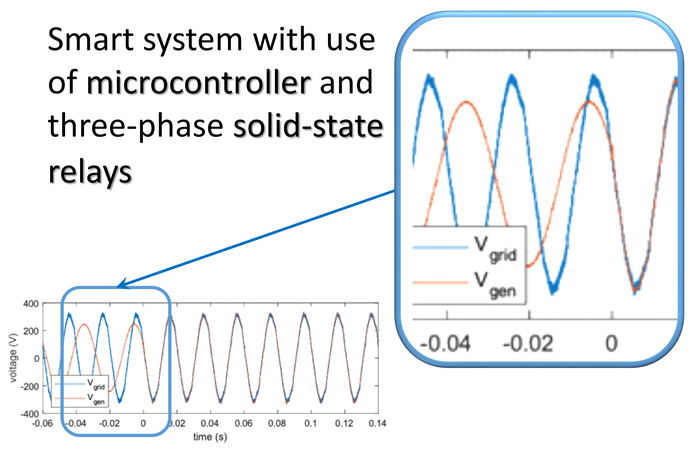
## Results

**TESTING ON LAB SCALE OF THE HYDROPOWER MANAGEMENT SYSTEM:**

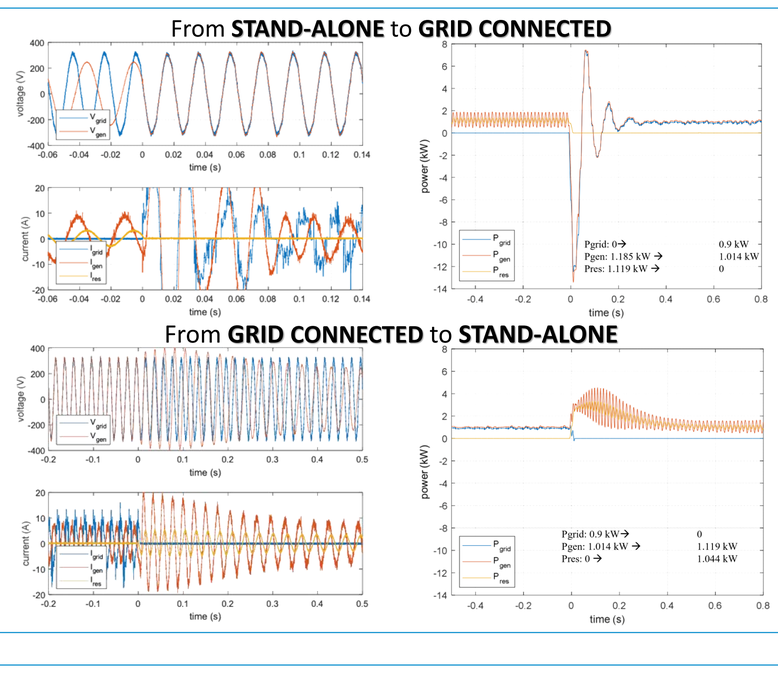
Manual switching from STAND-ALONE to GRID-CONNECTED




Smart system with use of microcontroller and three-phase solid-state relays




From **STAND-ALONE** to **GRID CONNECTED**




From **GRID CONNECTED** to **STAND-ALONE**




## Conclusions

The experimental tests have the purpose of validating the developed low-cost technological solution, which allows to minimize peaks and oscillations of the stator currents, electromagnetic torque and speed occurring when the SEIG is connected back to the power grid.

A proper choice of resistive and capacitive loads is very critical to guarantee low differences between the SEIG and the power grid frequency and voltage amplitude, for different working points of the hydraulic turbine coupled with the SEIG.

Contacts: marco.sinagra@unipa.it; calogero.picone@unipa.it; angelo.accetta@cnr.it; marcello.pucci@cnr.it; tullio.tucciarelli@unipa.it

References: Dai J., Wu S., Han G., Weinberg J., Xie X., Wu X., Song X., Jia B., Xue W., Yang Q. (2018) Water-energy nexus: A review of methods and tools for macro-assessment, Appl. Energy, 210, 393–408.

Oikonomou K., Parvania M. (2019) Optimal Coordination of Water Distribution Energy Flexibility with Power Systems Operation, IEEE Trans. Smart Grid, 10, 1101–1110.

Lundin, U., Jonsson, P., Facciolo, L.(2023. Using hydropower turbine discharge as a complementary spillway (2023) Journal of Applied Water Engineering and Research, 11(1),117-126.

Acknowledgments: This research was funded by Ministero dell'Università e della Ricerca, PNRR-M4C2, ECS_00000022, title of research project: "SiciliAn MicronanOTecH Research And Innovation CEnter SAMOTHRACE" (MUR, PNRR- M4C2, ECS_00000022), spoke 3—Università degli Studi di Palermo"S2-COMMs—Micro and Nanotechnologies for Smart & Sustainable Communities".



AV DO BRASIL 101 • 1700-066 LISBOA • PORTUGAL
tel. (+351) 21 844 30 00
lnec@lnec.pt www.lnec.pt